Association for Research in Otolaryngology

38TH Annual MidWinter Meeting

Saturday, February 21 –
Wednesday, February 25, 2015

Baltimore
Marriott Waterfront

Baltimore, Maryland

ARO OFFICERS FOR 2015-2016

PRESIDENT:

Ruth Anne Eatock, PhD (14-15)
University of Chicago
Department of Neurobiology
947 East 58th Street, Mail Code 0928
Chicago, IL 60637 USA

PRESIDENT ELECT:

Lawrence R. Lustig, MD (14-15)
Columbia University Medical Center
Department of Otolaryngology-HNS
Harkness Pavillion, Suite 818
180 Fort Washington Ave.
New York, NY 10032 USA

PAST PRESIDENT:

Jay T. Rubinstein, MD, PhD (14-15)
University of Washington
Virginia Merrill Bloedel Hearing
Research Center
Box 357923
Seattle, WA 98195 USA

SECRETARY/ TREASURER:

Elizabeth S. Olson, PhD (14-17)
Columbia University
Otolaryngology & HNS
630 West 168th Street
New York, NY 10032 USA

EDITOR:

Linda J. Hood, PhD (12-15)
Vanderbilt University
Department of Hearing and Speech Sciences
1215 21st Ave S, MCE S Tower, Room 8310
Nashville, TN 37232-8242 USA

HISTORIAN:

David J. Lim, MD
UCLA Geffen School of Medicine
Dept of Head & Neck Surgery
2100 West Third Street
Los Angeles, CA 90057 USA

COUNCIL MEMBERS AT LARGE:

Barbara Canlon, PhD (12-15)
Karolinska Institute
Department of Physiology & Pharmacology
Von Eulers Vag 8
Stockholm 171 77
SWEDEN

Howard Francis, MD (13 – 16)
Johns Hopkins School of Medicine
Department of Otolaryngology – HNS
601 North Caroline Street
Baltimore, MD 21287-0910 USA

Sharon G. Kujawa, PhD (14-17)
Massachusetts Eye and Ear Infirmary
Department of Otology and Laryngology
243 Charles Street
Boston, MA 02114 USA

ARO Executive Director:

Haley Brust
Talley Management Group
19 Mantua Road
Mt. Royal, NJ 08061 USA
(856) 423-7222 ext: 103
(856) 423-0041
hbrust@talley.com
headquarters@aro.org

ABSTRACTS OF THE 38TH ANNUAL MIDWINTER MEETING OF THE

Welcome to the 38th ARO Midwinter Meeting, our fifth visit to the Baltimore Marriott Waterfront. Our 2015 program includes over 1,178 submitted presentations, 17 symposia – three featuring young investigators - three workshops and exhibitors.

At daily **Mentoring Sessions** for young investigators (*4-5 pm Saturday and Sunday* and *12:30-1:30 pm Monday and Tuesday* - bring your lunch), mentors and peers exchange ideas on different topics in navigating careers.

The **Presidential Symposium** *(Saturday 8 am - noon)*, "Diverse Ears Serving Diverse Tasks: Communicating, Moving, Learning, Deciding", samples the breadth and innovation in current ear-related research. Six speakers illustrate the imaginative application of model systems and new technologies to a wide range of questions, from the development of the vestibular periphery to decision-making and vocalization.

At the **ARO Business Meeting** *(Sunday, 6-7 pm)*, we update the state of the Association, transfer leadership from the 2014 Council to the 2015 Council, including the new President, Larry Lustig, and hand out prizes – you can enter the prize draw when you visit the **exhibits**.

The inaugural **ARO Public Lecture** (*Monday 8 pm, National Aquarium in Baltimore*) features complementary presentations on navigation by sound in blind humans (Daniel Kish) and in animals (Cindy Moss), in a beautiful setting just a half-mile from the meeting hotel.

At the **Awards** ceremony *(Monday 6- 7:30 pm)* and reception *(7:30-8:30 pm)*, we celebrate the people and work that merited several awards, including the **Geraldine Dietz Fox Young Investigator Award** and the **ARO Award of Merit**: **Dr. Tom Friedman** (NIDCD), for pioneering research in the genetics of hearing and deafness. This year's awards ceremony includes special recognition of **Geraldine Dietz Fox** for her long and substantial support of hearing researchers.

A **memorial** *(Tuesday 3:30-5:30 pm)* is being held for David Mountain, who died in November 2014. David was an expert in cochlear mechanics and Professor of Biomedical Engineering at Boston University, with many friends, colleagues, and students in the ARO.

Rollex Band returns to the **Hair Bal**l (*Tuesday 8 pm – midnight*). This popular event began in 2006 as an offsite "Patch-Clampers Ball" instigated by those hair cell and dance enthusiasts Bill Roberts, Mark Rutherford and Paul Fuchs.

Each MidWinter Meeting depends on the hard work and innovative contributions of many ARO members in various committees, especially the Program Committee, with energetic and thoughtful assistance from Talley Management. Thanks to all. To help us continue to improve, please respond to a survey you will be sent after the meeting, and consider joining a committee - see "About Us" at www.aro.org for the options and contact headquarters@aro.org to volunteer.

Best wishes for a productive and fun meeting,

Ruth Anne Eatock
ARO President, 2014-2015

CONFERENCE OBJECTIVES

At the conclusion of the MidWinter Meeting, participants should be better able to:

- Explain current concepts of the function of normal and diseased states of the ear and other head and neck structures
- Recognize current controversies in research questions in auditory neuroscience and otolaryngology
- Describe key research questions and promising areas of research in otolaryngology and auditory neuroscience

REGISTRATION

The 2015 MidWinter Meeting Registration Desk is located in the Grand Ballroom Foyer and will be open and staffed during the following hours:

Friday, February 20	4:00 PM-7:00 PM
Saturday, February 21	7:00 AM-6:00 PM
Sunday, February 22	7:00 AM-7:00 PM
Monday, February 23	7:00 AM-7:00 PM
Tuesday, February 24	7:00 AM-6:00 PM
Wednesday, February 25	7:30 AM-12:00 PM

SPEAKER READY ROOM

The 2015 Program Committee is committed to providing attendees cutting edge technology and coordinated presentations at the MidWinter Meeting. To be fully prepared for your session, each presenter is requested to visit the Speaker Ready Room at least 24 hours prior to your presentation. The Speaker Ready Room is located in the **Falkland Room** and will be open the following days and times:

Saturday, February 21	7:00 AM-6:00 PM
Sunday, February 22	7:00 AM-6:00 PM
Monday, February 23	7:00 AM-6:00 PM
Tuesday, February 24	7:00 AM-6:00 PM
Wednesday, February 25	7:00 AM-10:00 AM

ADMISSION

Conference name badges are required for admission to all activities related to the 3th Annual MidWinter Meeting, including the Exhibit Hall and social events.

PROGRAM AND ABSTRACT BOOKS

A limited supply of the abstract will be available for purchase at the ARO MidWinter Meeting Registration Desk. Electronic copies of the books are also available online at www.aro.org.

MOBILE DEVICES

As a courtesy to the speakers and your fellow attendees, please switch your mobile device(s) to silent while attending the sessions.

RECORDING POLICY

ARO does not permit audio or photographic recording of any research data presented at the meeting.

BREAKS

Complimentary coffee and tea will be available in the morning and at selected breaks.

ASSISTED LISTENING DEVICES

A limited amount of assisted listening devices are available at the ARO MidWinter Meeting Registration Desk, courtesy of Phonak.

A SPECIAL NOTE FOR THE DISABLED

ARO wishes to take steps that are required to ensure that no individual with a disability is excluded, denied services, segregated or otherwise treated differently than other individuals because of the absence of auxiliary aids and services. If you need any auxiliary aids or services identified in the American with Disabilities Act, or any assistance in registering for this course please contact ARO Meetings Department at meetings@aro.org; via telephone at 856-423-0041, option 2; or write to ARO Meetings Department, 19 Mantua Road, Mt. Royal, NJ 08061.

FAMILY ACTIVITIES / CHILD CARE

Please contact the Hotel Concierge for information about off-site activities and tourism needs. Subsidized onsite day care is being offered through an experienced, accredited company, KiddieCorp. The child care room is located in **Dover BC Room**.

2015 ARO MIDWINTER MEETING

PROGRAM COMMITTEE

Ruth Y. Litovsky, PhD, *Chair* (3/14-2/17)
Carolina Abdala, PhD (3/14-2/17)
Kumar Alagramam, PhD (3/13-2/16)
Jianxin Bao, PhD (3/12-2/15)
Jennifer Bizley, PhD (3/14-2/17)
Alan Cheng, MD (3/13-2/16)
Erick Gallun, PhD (3/14-2/17)
Richard Hallworth, PhD (3/12-2/15)
Larry Hoffman, PhD (3/12-2/15)
Philip X. Joris, MD, PhD (3/13-2/16)
Jeff Lichtenhan, PhD (3/13-2/16)
Su-Hua Sha, MD (3/12-2/15)
Barbara Shinn-Cunningham, PhD (3/14-2/17)
Jennifer Stone, PhD (3/13-2/16)
Xiaoqin Wang, PhD (3/14-2/17)
Council Liaison: Ruth Y. Litovsky, PhD
spARO Representative: Chang Liu

Animal Research Committee
Claus-Peter Richter, MD, PhD, *Chair* (3/13-2/16)
Esperanza Bas Infante, PhD (3/12-2/15)
Wei Dong, PhD (3/14/-2/17)
James Fallon, PhD (3/14-2/17)
Rudolf Glueckert, PhD (3/14-2/17)
Andrej Kral, MD, PhD (3/13-2/16)
Amanda Lauer, PhD (3/12-2/15)
Stéphane Maison, PhD (3/14-2/17)
Charidrakala Puligilla, PhD (3/1-/16)
Suhrud Rajguru, PhD (3/14-2/17)
Maike Vollmer, MD, PhD (3/13-2/16)
Council Liaison: Sharon Kujawa, PhD (3/15-2/17)
spARO Representative: Lukas Landegger

Award of Merit Committee
Eric D. Young, PhD, *Chair* (3/13-2/16)
Catherine E. Carr, PhD (3/14-2/17)
David P. Corey, PhD (3/13-2/16)
Charley Della Santina, MD PhD (3/12-2/15)
Stefan Heller, PhD (3/14-2/17)
John Middlebrooks, PhD (3/14-2/17)
Brian C. J. Moore, PhD (3/12-2/15)
Karen P. Steel, PhD (3/13-2/16)
Steve D. Rauch, MD (3/13-2/16)
Council Liaisons: Past-President Jay Rubinstein, MD (2/14-3/15) and David Lim (2/14-3/15)

Diversity & Minority Affairs Committee
Avril Genene Holt, PhD, *Chair* (3/13-2/16)
Deniz Baskent, PhD (3/13-2/16)
Gail S. Donaldson, PhD (3/12-2/15)
Michael Hoa, MD (3/14-2/17)
Mirna Mustapha, PhD (3/14-2/17)
Diana Peterson, PhD (3/14-2/17)
J Tilak Ratnanather, DPhil (3/13-2/16)
Shurud Rajguru, PhD (3/13-2/16)
Khaleel Razak, PhD (3/12-2/15)
Lina Reiss, PhD (3/13-2/16)
Council Liaison: Howard W. Francis (3/13-2/16)
spARO Representative: Hormira Osman

External Relations Committee
Anne E. Luebke, PhD, *Chair* (3/11-2/15)
Julie Bierer, PhD (3/13-2/16)
Jonathan Fritz, PhD (3/13-2/16)
Corne Kros, PhD (3/12-2/15)
Hainan Lang, MD, PhD (3/12-2/15)
Cynthia Morton, PhD (3/14-2/17)
George Pollak, PhD (3/12-2/15)
Pamela Roehm, MD, PhD (3/12-2/15)
Debara Tucci, MD (3/14-2/17)
Beverly Wright, PhD (3/13-2/16)
Jinsheng Zhang, PhD (3/13-2/16)
Council Liaison: Sharon Kujawa, PhD (2/15-2/17)
spARO Representative: Becky Lewis

Finance & Investment Committee
Paul Fuchs, PhD, *Chair* (3/13-2/16)
John P. Carey, MD (3/14-2/17)
Matt Kelley, PhD (3/14-2/17)
Sharon G. Kujawa, PhD (3/12-2/15)
Robert Raphael, PhD (3/12-2/15)
Christopher Shera, PhD (3/14-2/17)
Ex-officio: Secretary/Treasurer,
Elizabeth S. Olson, PhD (3/14-2/17)

International Committee
Benedikt Gröthe, PhD, Germany, *Chair* (3/12-2/15)
Karen Banai, PhD, Israel (3/12-2/15)
Alan Brichta, PhD, Australia (3/14-2/17)
Byung Yoon Choi, MD, Korea (3/12-2/15)
Alain Dabdoub, PhD, Canada (3/13-2/16)
Andy Forge, PhD, UK (3/13-2/16)
Bo Hong, Ph.D., China (3/12-2/15)
Juichi Ito, MD, PhD, Japan (3/14-2/17)
Andrej Kral, MD, PhD, Germany (3/13-2/16)
Christian Lorenzi, PhD, France (3/13-2/16)
Jan Wouters, PhD, Belgium (3/13-2/16)
Council Liaison: Barbara Canlon, PhD (3/14-2/15)
spARO Representative: Yilai Shu

JARO Editorial Board
Paul B. Manis, PhD, *Editor-in-Chief* (2011-2016)
Christian Chabbert, PhD (2012-2015)
Bertrand Delgutte, PhD (2013-2016)
Mark Eckert, PhD (2013-2016)
Ana Belén Elgoyhen (2013-2016)
Donna Fekete, PhD (2012-2015)
Andrew Grifith, M.D., Ph.D. (2011-2015)

Robert Funnell (2013-2016)
Ruth Litovsky, PhD (2013-2016)
Manuel Malmierca, MD, PhD (2012-2015)
Shawn Newlands, MD, PhD (2012-2015)
Donata Oertel, PhD (2013-2016)
Dominik Oliver, PhD (2012-2015)
Christopher Plack, PhD (2013-2016)
Christoph Schreiner, MD, PhD (2012-2015)
Susan E. Shore, PhD (2012-2015)
Xiaorui Shi, MD, PhD (2013-2016)
George A. Spirou, PhD (2014-2017)
Marianne Vater, PhD (2013-2016)
Marcel van der Heijden, PhD (2014-2017)

Long Range Planning Committee
Steven H. Green, PhD, *Chair* (3/14-2/17)
Karina Cramer, PhD (3/14-2/15)
Amy Donahue, PhD NIDCD Rep.
Lisa Goodrich, PhD (3/14-2/17)
Troy Hackett, PhD (3/12-2/15)
KC Lee, ScD (3/13-2/16)
Tobias Moser, MD (3/14-2/17)
Sunil Puria, PhD (3/13-2/16)
George Spirou, PhD (3/12-2/15)
Doris Wu, PhD (3/12-2/15)
Council Liaison: President-Elect: Larry Lustig (3/14-2/15)
Chair, International Cmte: Benedikt Gröthe, PhD (3/14-2/17)
spARO Representative: Anna Diedesch

Membership Committee
Chris J. Sumner, *Chair* (3/12-2/15)
Eric Bielefeld, PhD (3/12-2/15)
Sam Gubbels, MD (3/14-2/17)
Colleen Le Prell, PhD (3/14-2/17)
Glenis R. Long, PhD (3/12-2/15)
Dan Polley, PhD (3/14-2/17)
Tianying Ren, MD (3/12-2/15)
Council Liaison: Barbara Canlon (3/14-2/15)

Nominating Committee
Jay Rubinstein, *Chair* (3/14-2/15)
Julie Bierer, PhD (3/14-2/15)
Charley Della Santina, MD, PhD (3/14-2/15)
Tony Ricci, PhD (3/14-2/15)
Dan Sanes, PhD (3/14-2/15)

Publications Committee
Anil K. Lalwani, MD, *Chair* (3/13-2/16)
Yuri M. Agrawal, MD (3/13-2/16)
Maria Chait, PhD (3/14-2/17)
Elisabeth Glowatzki, PhD (3/14-2/17)
Charles J. Limb, MD (3/13-2/16)
Erick Xi Lin, PhD (3/12-2/15)
Xue Z. Liu, MD, PhD (3/12-2/15)
John S. Oghalai, MD (3/12-2/15)
Chris Stecker, PhD (3/13-2/16)
Daniel Tollin, PhD (3/12-2/15)
Kelly L. Tremblay, PhD (3/13-2/16)
JARO Editor: Paul B. Manis, PhD, ex officio
Springer Representative: Gregory Baer, ex officio
Secretary/Treasurer: Elizabeth S Olson, PhD (3/14-2/17)
Council Liaison: Linda J. Hood, PhD (3/13-2/14)
spARO Representative: David Morris

Travel Awards
Ronna Hertzano, MD PhD, *Chair* (3/14 2/17)
Jin Woong Bok, PhD (3/12-2/15)
Mike Bowl, PhD (3/14-2/17)
Benjamin Crane, MD PhD (3/14-2/17)
Angelika Doetzlhofer, PhD (3/12-2/15)
Elizabeth Driver, PhD (3/14-2/17)
Robert Froemke, PhD (3/12-2/15)
Matt Goupell, PhD (3/14-2/17)
Samuel Gubbels, MD (3/12-2/15)
Michael Hildebrand, PhD (3/12-2/15)
Chandrakala Puligilla, PhD (3/14-2/17)
Felipe Santos, MD (3/13-2/16)
Jong Ho Won, PhD (3/13-2/16)
Li Xu, MD, PhD (3/12-2/15)
James F. Battey, MD, PhD, NIDCD Dir ex officio
Council Liaison: Howard W. Francis (3/13 2/16)
spARO Representative: Jeremy Duncan

EXECUTIVE OFFICES
ASSOCIATION FOR RESEARCH IN OTOLARYNGOLOGY
19 Mantua Road
Mt. Royal, New Jersey 08061
Phone: (856) 423-0041
Fax: (856) 423-3420
E-Mail: headquarters@aro.org
Meetings E-Mail: meetings@aro.org

AWARD OF MERIT

2015 Award of Merit Recipient
Thomas B. Friedman, PhD
National Institute on Deafness and Other Communication Disorders
National Institutes of Health

Award of Merit Lecture Abstract

"Science, my boy, is composed of errors, but errors that it is right to make, for they lead step by step towards the truth." Jules Gabriel Verne

A book by Jules Gabriel Verne, a 1960s movie titled "Inherit the Wind" and a Scientific American paper by Theodosius Dobzhansky influenced me as teenager to pursue biomedical research as a career. What did Verne have in mind when in his 1864 novel "*Journey to the Center of the Earth*" he stated that errors can point to truth? This novel was written at the same time there was debate about Charles Darwin's publication "*On the Origin of Species*", which ultimately led to the issues explored in "Inherit the Wind". Was Verne's use of the "error" concept a reference to magical thinking, to deceit when truth is expected, or to unintentional error when difficult problems and complex questions are tackled?

AWARD OF MERIT BIOSKETCH

Thomas B. Friedman is the recipient of the 2015 Award of Merit. The ARO has chosen to honor Tom for his groundbreaking work on the genetics of human hearing loss. Tom has contributed to the discovery and characterization of a large number of genes underlying syndromic and nonsyndromic hearing loss. The work is noted for combining gene identification in human families using positional cloning, meticulous phenotypic evaluations, seminal genetic epidemiologic observations, generation and characterization of mouse models, and elucidation of protein function via a variety of cell and molecular biological techniques. The importance and creativity of this work has led the ARO to honor Tom with this Award of Merit.

Tom received his B.S. and Ph.D. degrees in Zoology from the University of Michigan. He completed a fellowship in the NIMH/NIH intramural research laboratory of Dr. C.R. Merril, where he worked on galactosemia. Also in 1974, Tom launched his independent career as an Assistant Professor at Oakland University, Rochester, Michigan. Rochester was close to Tom's birthplace of Detroit, Michigan where his two children's grandparents lived. He continued his upward trajectory with a major publication on cell-autonomous timing of urate oxidase expression in *Drosophila melanogaster* Malpighian tubules.

In 1978, Tom moved to Michigan State University where he continued working on *Drosophila melanogaster*. In the late 1980's, Tom shifted his research focus toward the molecular genetics of human deafness. It is the rare senior scientist who significantly and successfully changes their model organism and focus at the mid-point of their independent career. This was an extremely fortunate turn of events for the embryonal field of deafness genetics. Tom began his efforts by positional cloning of the Waardenburg syndrome type I (WS1) locus. He, James H. Asher and Robert J. Morell authored a series of publications on the mapping and positional cloning of *PAX3* as the gene underlying WS1. (The mapping papers were published as part of a consortium but the positional cloning papers arose primarily from his collaborative effort with his Michigan State colleagues.) In 1995, Tom published the genetic map location of nonsyndromic recessive deafness DFNB3. This study was particularly notable as the first genome-wide linkage analysis, of any human disease or disorder, to successfully use homozygosity mapping.

In 1996, he was recruited to the NIDCD intramural research program in Bethesda. Several years later he identified the Myosin 15A gene as the cause of DFNB3 nonsyndromic deafness, which was published as one of a pair of partner papers with Sally Camper in 1998. Sally, her MD/PhD student Frank Probst, and Tom used a novel and clever paradigm utilizing bacterial artificial chromosome (BAC) transgenes to rescue hearing in the orthologous mouse mutant (shaker 2). They used this information to refine and sequence the critical interval and ultimately identify *MYO15* as the causative gene in shaker 2 mice and in humans with DFNB3 deafness. Tom has subsequently contributed to and, in most cases, led studies identifying approximately 30 genes underlying hearing loss. Three of these genes also underlie Usher syndrome type I, a devastating disorder that causes congenital deafness and progressive blindness. This remarkable number of discoveries is attributable to over 15 years of collaboration with his colleague and friend Sheikh Riazuddin in Lahore, Pakistan. Professor Riazuddin has ascertained nearly 1500 large families segregating deafness, providing an unparalleled resource for the mapping and cloning of human deafness genes.

Tom could easily have limited his research program to gene mapping and identification but, luckily for our field, he did not. He has elucidated the functions of at least six deafness genes through elegant and rigorous molecular and cellular studies of mouse models of these disorders. Most of these genes encode proteins required for normal structure or function of the hair bundle that resides on the apical surface of each hair cell. Working with his fellow, Zubair Ahmed, and in collaboration with Guy Richardson, Tom demonstrated the protein product of an Usher syndrome type I gene, protocadherin 15, to be a component of the hair cell stereociliary tip link. Among a number of Tom's contributions to the literature on myosin 15, he reported that myosin 15 is located at the tips of stereocilia and is required for the development of the

staircase morphology of the hair bundle. In a spectacular cell biology study, Inna Belyantseva, a staff scientist in Tom's laboratory, and their collaborator, Gregory Frolenkov, showed that this staircase morphology requires an Usher syndrome gene product called whirlin, which is itself transported to the tips of stereocilia by myosin 15. Most recently in 2014, his postdoctoral fellow, Jonathan Bird, published the successful purification of large amounts of biologically active myosin 15 in Sf9 cells. The clever co-expression of chaperones to assist proper folding in combination with two different unexpected light chain-binding partners resulted in active unconventional myosin 15. This was a major accomplishment that numerous myosin labs across the world had been unable to achieve.

Tom has also made seminal discoveries of genes and their protein products that are present at the base of hair cell stereocilia. Saima Riazuddin, a fellow with Tom, identified mutations in the *TRIOBP* gene as the cause of human deafness DFNB28. Tom and his colleagues subsequently demonstrated that the TRIOBP protein, which is present at the base of stereocilia, tightly bundles F-actin and is required for the formation of rootlets that anchor stereocilia in the hair cell cuticular plate. Tom also described a novel protein called taperin that is present at the tapered bases of stereocilia. Importantly, this study by Atteeq Rehman, who was the first author, was one of the first to use targeted capture and next-generation sequencing to identify a mutant gene for a Mendelian disorder.

Tom has uncovered predominant mutations causing isolated deafness and Usher syndrome in Ashkenazi Jews. Two of these studies were published in 1998 and 2003. Testing for these mutations was rapidly incorporated into routine diagnostic screens available to relevant patients. He has produced several other observations phenomena that have been of wide interest in human genetics. One example was a discovery by Saima of a dominant modifier of DFNB26 deafness that prevents profound congenital deafness in homozygous carriers of mutations at the DFNB26 locus. Another genetic first was Tom's description of a novel fusion gene with alternative reading frames in which mutations cause nonsyndromic deafness in humans. In collaboration with Dr. William Newman, Tom, Meghan Drummond, and Atteeq uncovered a mutation of *CLPP*, a mitochondrial protease, as one of the causes of Perrault syndrome, a hearing loss syndrome associated with ovarian dysgenesis.

In addition to his love of science, Tom has two other passions: his family and Squash. Wife Penelope is a master clinician and internal medicine consultant in the NIH Clinical Center. Tom's son Joshua is a pediatrician in Auckland, New Zealand with special expertise in and dedication to the identification and care of battered children. Tom's daughter Martha is a sculptor with a productive studio in Brooklyn, NY, and a sculpture faculty member of the Princeton University Visual Arts Department. Tom's devotion to the sport of Squash provides multiple restorative physical and psychological forms of release and respite.

– David P. Corey and Andrew J. Griffith

Past Presidents

1973-74 David L. Hilding, MD
1974-75 Jack Vernon, PhD
1975-76 Robert A. Butler, PhD
1976-77 David J. Lim, MD
1977-78 Vicente Honrubia, MD
1978-80 F. Owen Black, MD
1980-81 Barbara Bohne, PhD
1981-82 Robert H. Mathog, MD
1982-83 Josef M. Miller, PhD
1983-84 Maxwell Abramson, MD
1984-85 William C. Stebbins, PhD
1985-86 Robert J. Ruben, MD
1986-87 Donald W. Nielsen, PhD
1987-88 George A. Gates, MD
1988-89 William A. Yost, PhD
1989-90 Joseph B. Nadol, Jr., MD
1990-91 Ilsa R. Schwartz, PhD
1991-92 Jeffrey P. Harris, MD, PhD
1992-93 Peter Dallos, PhD
1993-94 Robert A. Dobie, MD
1994-95 Allen F. Ryan, PhD
1995-96 Bruce J. Gantz, MD
1996-97 M. Charles Liberman, PhD
1997-98 Leonard P. Rybak, MD, PhD
1998-99 Edwin W. Rubel, PhD
1999-00 Richard A. Chole, MD, PhD
2000-01 Judy R. Dubno, PhD
2001-02 Richard T. Miyamoto, MD
2002-03 Donata Oertel, PhD
2003-04 Edwin M. Monsell, MD, PhD
2004-05 William E. Brownell, PhD
2005-06 Lloyd B. Minor, MD
2006-07 Robert V. Shannon, PhD
2007-08 P. Ashley Wackym, MD
2008-09 Paul A. Fuchs, PhD
2009-10 Steven Rauch, MD
2011-12 Karen B. Avraham, PhD
2012-13 Debara L. Tucci, MD
2013-14 John C. Middlebrooks, PhD
2014-15 Jay T. Rubinstein, MD, PhD

Award Of Merit Recipients

1978 Harold Schuknecht, MD
1979 Merle Lawrence, PhD
1980 Juergen Tonndorf, MD
1981 Catherine Smith, PhD
1982 Hallowell Davis, MD
1983 Ernest Glen Wever, PhD
1984 Teruzo Konishi, MD
1985 Joseph Hawkins, PhD
1986 Raphel Lorente de Nó, MD
1987 Jerzy E. Rose, MD
1988 Josef Zwislocki, PhD
1989 Åke Flóck, PhD
1990 Robert Kimura, PhD
1991 William D. Neff, PhD
1992 Jan Wersäll, PhD
1993 David Lim, MD
1994 Peter Dallos, PhD
1995 Kirsten Osen, MD
1996 Ruediger Thalmann, MD & Isolde Thalmann, PhD
1997 Jay Goldberg, PhD
1998 Robert Galambos, MD, PhD
1999 Murray B. Sachs, PhD
2000 David M. Green, PhD
2001 William S. Rhode, PhD
2002 A. James Hudspeth, MD, PhD
2003 David T. Kemp, PhD
2004 Donata Oertel, PhD
2005 Edwin W. Rubel, PhD
2006 Robert Fettiplace, PhD
2007 Eric D. Young, PhD
2008 Brian C. J. Moore, PhD
2009 M. Charles Liberman, PhD
2011 Robert V. Shannon, PhD
2012 David P. Corey, PhD
2013 Karen P. Steel, PhD
2010 Ian Russell, PhD
2011 Robert V. Shannon, PhD
2012 David P. Corey, PhD
2013 Karen P. Steel, PhD
2014 H. Steven Colburn, PhD
2015 Thomas B. Friedman, PhD

2015 TRAVEL AWARD RECIPIENTS

Yassan Abdolazimi
Kelsey Anbuhl
Nicolas Barascud
Tanaya Bardhan
Robert Baumgartner
Elliott Brecht
Brian Buechel
Annalisa Buniello
Axelle Calcus
Elise Cheng
Lauren Chessum
Soyoun Cho
Alexander Claussen
Laura Corns
Joseph Crew
Hugo Cruces Solis
Angela Dixon
Seham Ebrahim
Erica Ehlers
Alexander Ferber
Katharine Fitzharris
Philippe Fournier
Christopher Gouveia
David Goyer
Chul Han
Sriram Hemachandran
Ariel Hight
Clarke Jeanne
Courtney Jernigan
Alyson Kaplan
Hanin Karawani
Alexander Kell
Fatemeh Khatami
Kyunghee Kim
Grace Kim
Jong Sei Kim
Astrid Klinge-Strahl
Tal Koffler
Elliott Kozin
Bradley Kushner
Lukas Landegger
Charlsie Lemons
Gaven Lin
Hsin-Wei Lu
Iva Macova
David Maidment
Pranav Mathur
Jameson Mattingly
Richard McWalter
Golbarg Mehraei
Anahita Mehta
Frances Meredith
Ian Mertes
Aditi Mohankumar
Maria Morell
Joanna Mulvaney
Vidhya Munnamalai
Anthony Myint
Christopher Neal
Jennifer Olt
Erol Ozmeral
Clarisse Panganiban
Lauren Poppi
Heather Porter
Paul Ranum
Rajamani Rathinam
Stefan Raufer
Amrita Ray
Jennifer resnik
Francesca Rocchi
Steven Rosenblatt
Sarah Rotschafer
Rony Salloum
Zafar Sayed
Zachary Schwartz
Parth Shah
Yilai Shu
Max Siegel
Suzanne Smart
Meirav Sokolov
Omotara Sulyman
Kirupa Suthakar
Ilmar Tamames
Zhengquan Tang
Pei-Ciao Tang
Elaine Thompson
Anna Tinnemore
Hiroko Torii
Kristy Truong
Eleni Vlahou
Yanli Wang
Rachel Wayne
Sonia Weimann
Karessa White
Matthew Winn
Maria Geraldine Zuniga

ISSN-0742-3152

The *Abstracts of the Association for Research in Otolaryngology* is published annually and consists of abstracts presented at the Annual MidWinter Research Meeting. A limited number of copies of this book are available, after the meeting this publication will be added to the electronic library on the ARO website (1978-2014). Please address your order or inquiry to Association for Research in Otolaryngology Headquarters by calling (856) 423-0041 or emailing headquarters@aro.org.

This book was prepared from abstracts that were entered electronically by the authors. Authors submitted abstracts over the World Wide Web using Omnipress Abstract Management System. Any mistakes in spelling and grammar in the abstracts are the responsibility of the authors. The Program Committee performed the difficult task of reviewing and organizing the abstracts into sessions. The Program Committee; Program Committee Chair, Dr. Ruth Litovsky; the President, Dr. Ruth Anne Eatock; and the Editor, Dr. Linda J. Hood constructed the final program. Omnipress electronically scheduled the abstracts and prepared Adobe Acrobat pdf files of the Program and Abstract Books. These abstracts and previous years' abstracts are available at www.aro.org.

Citation of these abstracts in publications should be as follows: **Authors, year, title, Assoc. Res. Otolaryngol. Abs.: page number.**

Table of Contents

SYM-1

Evolutionary Perspectives on Solving the Cocktail Party Problem: A Frog's-Ear View

Mark Bee
University of Minnesota

In large social groups, listeners experience increased difficulty with speech perception due to energetic and informational masking and impaired source segregation. This difficulty is often compounded for listeners with hearing loss. While we humans call this the "cocktail party problem," it is really a human problem in name only. Many nonhuman animals – from cicadas to cetaceans – also communicate acoustically in large and noisy social groups. While a substantial body of literature focuses on the human cocktail party problem, relatively few studies have investigated how nonhuman animals may be evolutionarily adapted to solve biologically analogous problems. As a result, we still have a limited understanding about the potential diversity of evolved strategies nature has discovered to solve cocktail-party-like communication problems. This talk will describe recent and ongoing work aimed at testing hypotheses about signal processing strategies that enable frogs to communicate vocally in noisy "breeding choruses." Individual male frogs commonly produce loud (e.g., 90-100 dB SPL at 1 m) vocalizations to attract females for mating. Sustained high levels of background noise and acoustic clutter from overlapping signals characterize frog choruses, which can often be heard by humans over long distances (e.g. > 2 km). Frogs differ from humans and other mammals in having internally-coupled middle ears, extra-tympanic sound transmission pathways through the lungs and shoulders, and inner ears with two separate sensory organs (only one of which is tonotopically organized) that encode different frequency ranges of airborne sound. After briefly outlining several functional constraints on frog communication posed by the acoustic environment of frog choruses, this talk will report results from recent studies of auditory masking and sound source perception aimed at uncovering how treefrog listeners may be adapted to cope with such constraints. Specifically, this talk will cover research on the acoustic cues for auditory grouping, spatial release from masking, and dip listening. The talk aims to illustrate how broad-scale, comparative studies of carefully considered animal models may ultimately uncover evolutionary diversity in signal processing strategies for solving cocktail-party-like problems in communication. This work was supported by NIDCD R03 DC008396 and R01 DC009582 and by NSF IOS 0842759.

SYM-2

Neuronal Encoding of Sound and Gravity in the Fruit Fly

Azusa Kamikouchi
Nagoya University

How does the brain process sound and gravity information? Understanding the organization of neural circuits that process these signals is indispensable to answer this question. The fruit fly *Drosophila melanogaster*, with its small brain size and a rich repertoire of genetic tools, is ideally suited for exploring the neural-circuit basis of information processing in the brain. To unravel the neural mechanism how the fruit fly processes acoustic and gravity information in the brain, we systematically analyzed sensory neurons in the antennal ear of the fly, and then their downstream neural circuits. By mapping the projection of all sensory neurons in the fly ear, which receives sound and gravity information, we identified five zones in the brain that receive input from distinct subgroups of sensory neurons in the fly ear. Activity imaging revealed that these five zones can be categorized as three functionally distinct groups: (1) a primary vibration center (auditory zones A and B), (2) a primary deflection center (gravity zones C and E), and (3) a primary vibration and deflection center (auditory and gravity zone D). A fly brain thus could encode sound and gravity information by expanding the complex movements of the fly's antennal receiver into 5-dimensional space in the primary center. To elucidate the neural substrates for further information processing in the brain, we performed a large-scale analysis to identify neurons downstream of each zone. Whereas neurons downstream of primary auditory zones project mostly within the brain, those of primary gravity zones directly descend to the thorax in most cases. We thus focused to analyze the auditory neural circuit in the brain, and established a projection map comprised of 40 types of secondary auditory neurons. By analyzing the connections of these neurons, we found several anatomical similarities between auditory neural circuits in flies and mammals, such as parallel ascending pathways, binaural interaction, and multimodal pathways. Such similarities predict that the basic principle of acoustic information processing could be shared between mammals and flies.

SYM-3

Circuits Underlying Cortical Decisions

Anthony Zador
Cold Spring Harbor Laboratory

To study how animals use sensory information to make decisions, we have developed a rodent model of auditory discrimination. We previously found that a subset of neurons in auditory cortex, those that project to the auditory striatum, play a central role in propagating information beyond the cortex. In my talk I will discuss recent experiments indicating that plasticity at corticostriatal synapses plays an essential role in the acquisition of the association between the sound and the action in this task.

SYM-4

Development of the Zebrafish Vestibular System

Tanya Whitfield
Bateson Centre and Department of Biomedical Science, University of Sheffield, Sheffield S10 2TN, UK

The zebrafish provides a particularly tractable model system for studying development and function of the vestibular system of the inner ear. Although it lacks a cochlea, the anatomy of the fish ear is otherwise highly conserved with mammals, consisting of three semicircular canals and three otolithic organs.

Fish otoliths are the counterparts of mammalian otoconia; in the fish, they are used to detect sound in addition to gravity and linear accelerations. We have studied the earliest phases of otolith formation in the zebrafish embryo. Otoliths adhere to the tips of the kinocilia of the first hair cells to appear in the otic vesicle, the tether cells. Surprisingly, loss of ciliary axonemes or ciliary motility does not disrupt otolith formation completely. A loss of hair cells, however, results in failure of the initial otolith seeding and tethering step. This early stage in otolith formation is critically dependent on Otogelin function. At later stages, tethering of the saccular otolith to its sensory patch is dependent on a -Tectorin function: in fish mutant for *tecta*, the otolith becomes detached. Mutations in human *OTOG* and *TECTA* genes are known to be causative for deafness and/or vestibular dysfunction in humans.

The topological arrangement of the semicircular canal system is established during day 2-3 of embryogenesis in the zebrafish, and involves the movement, fusion and rearrangement of otic epithelia. Extracellular matrix production drives epithelial projections into the otic vesicle lumen, where they fuse to form pillars that become the hubs of the canal ducts. We are studying mutant fish in which formation of one, two or all three canal ducts in the ear are disrupted. In the *gpr126* mutant, the otic epithelial projections over-express extracellular matrix components, overgrow, and fail to fuse, resulting in defects in all three canals. In other mutant lines (*otx1b, cloudy*), individual canal ducts fail to form. We are using confocal and light sheet microscopy to image canal morphogenesis in real time in transgenic embryos and adult fish, and are correlating morphological abnormalities in the ear with specific behavioural abnormalities. Mutants with ear abnormalities display hyperactivity and circling behaviour, consistent with vestibular deficits.

SYM-5

Motor-auditory Interactions for Listening and Learning

Richard Mooney
Duke University School of Medicine

A classical view is that sensation begets movement, which implies a flow of information from sensOlY to motor regions of the brain. However, the flow of information from motor to sensory regions also is critical to perception and motor learning. Motor to auditory interactions are especially important to hearing, because they can serve to suppress responsiveness to self-generated sounds while boosting sensitivity to unexpected sounds arising from sources in the environment. Motor to auditory interactions are also thought to fac ili tate the learning of soundgenerating behaviors, such as speech and musicianship, by conveying a motorrelated prediction of the auditory consequences of the ensuing movement. The brain can then compare this predictive signal to movement-related auditory feedba ck to generate an error signal that can guide motor learning. The circuit, cellular and synaptic mechanisms that mediate such motor to auditory interactions in the vertebrate brain are poorly understood. I will discuss research from our group in both songbirds and mice that use a variety of methods, including in vivo cellular imaging, electrophysiology, viral gene transfer and optogenetics, to map, monitor and manipulate motor to auditory interactions important to auditory processing and vocal motor learning. These studies reveal features of central brain organization that are likely to be relevant to human auditOlY function, especially in the context of speech perception and learning.

SYM-6

Functional Neuroimaging of Speech Perception in Cochlear Implant Recipients

John Oghalai
Stanford University

Understanding speech is arguably the most important function of the human auditory system. Cochlear implants (CIs) are a standard therapy for deafness, yet the ability of implanted patients to understand speech varies widely for unknown reasons. To better understand this variability in outcomes, we have been translating the technique of functional near-infrared spectroscopy (fNIRS) to study brain responses to speech in deaf subjects after cochlear implantation. We also study normal-hearing controls. We imaged activation patterns within the auditory cortex in response to speech stimuli of varying intelligibility, and correlated the patterns to behavioral measures of speech perception. Similar to normal-hearing controls, implanted subjects with good speech perception abilities exhibited greater cortical activations to natural speech than to unintelligible speech. In contrast, implanted subjects with poor speech perception had similarly large cortical responses to all stimuli. Turning off the implant reduced cortical activation in all implanted subjects. Thus, this translational research demonstrates that fNIRS provides an objective measure of speech perception in deaf subjects hearing through a CI. Furthermore, these results indicate that although implanted subjects with poor speech perception are receiving stimulation to their auditory pathway, and the information reaches the brain, these subjects are unable to discriminate speech from that signal. Because it is a relatively easy-to-use test that provides novel objective data critical to CI functionality, fNIRS may serve as an important adjunct to behavioral speech perception measures in the clinical practice of CI programming.

PS-1

Vestibular Hair Cell Regeneration Induced by Math1 Gene Transfer Following Gentamicin Ototoxicity in Mouse Utricle Epithelium

Dong-Dong Ren[1]; Rui Ma[2]; Xiao-Yu Yang[3]; Wen-wei Luo[3]; Juan-mei Yang[3]; Fang-lu Chi[3]
[1]Uinversity of Fudan,Shanghai,China; [2]Eye,Ear,Nose and Throat Hospital, Research Center; [3]Eye,Ear,Nose and Throat Hospital, Department of Otolaryngology

Objectives

The toxic effects of inner ear caused by gentamicin and other aminoglycosides can be manifested through hearing loss and balance dysfunction because of damage of hair cells. We and other researches have demonstrated that over-expression of Atoh1/Math1 in the mouse utricle could induce the ectopic hair cell-like cells(HCLCs).In our study, we explore the role

of Atoh1/Math1 in the vestibular hair cell regeneration after gentamicin ototoxicity in mouse utricle epithelium in vitro.

Methods
z Ad5-EGFP-math1 and/or gentamicin were used to over-express math1 and/or damage the epithelium in the utricle of neonatal mice in vitro. We compared the number、position and proliferation of new HCLCs between in sensory regions and the ectopic non-sensory regions using immunofluorescence technique, laser scanning confocal microscope and SEM scan.

Results
The morphological and statistical studies have shown that after the treatment of gentamicin, the stereocilia bundle of Type I hair cells in striolar region was damaged at first. The sensory precursor cells labeled by Sox2 and EDU(+) cells were increased. But the proliferation of cells gradually decreased with the increase of gentamicin dose. The number of proliferating cells co-cultured in Ad-Math1 and gentamicin was more than a simple addition of Ad-Math1 or gentamicin in sensory region, especially in striolar region.

Conclusion
The destruction of utricular hair cells after gentamicin treatment was began with stereocilia bundle and gradually spread to cell body in Type I hair cells, especially in the striolar region. Over-expression of Atoh1/Math1 induced new hair cell-like cells in sensory region and nonsensory region after gentamicin treatment mainly underwent cell division of supporting cells first and then trans-differentiated into HCs.

PS-2

DAPT enhances Atoh1 Activity to Generate New Hair Cells In Situ Following Neomycin Ototoxicity in Rat Cochleae In Vitro

Juan-mei Yang; Wen-wei Luo; Zhao Han; Fang-lu Chi; Haibin Sheng
Eye & ENT Hospital of Fudan University

Previous studies showed that adenovirus-mediated Atoh1 overexpression or the pharmacological inhibition of Notch signaling by γ-secretase inhibitors could induce new hair cell formation in mammals. However, both of these methods have limitations for the recovery of hearing loss. The stimulation of in situ formation of hair cells after hair cell loss is a promising approach to hearing recovery. Increasing the viral infection rate and the rate of conversion of supporting cells to hair cells in situ is a difficult problem that needs to be solved. To develop an effective and efficient therapy for hearing recovery, we used a higher concentration of fetal bovine serum (FBS) in the culture medium and prolonged the duration of culture to increase the supporting cell gaps. Simultaneously, we applied a human adenovirus serotype 5 vector that encoded Atoh1 and the reporter gene EGFP (*Ad5-EGFP-Atoh1*) in combination with the γ-secretase inhibitor N-[N-(3,5-Difluorophenacetyl)-L-alanyl]- S-phenylglycine t-butyl ester (DAPT). Increasing the FBS concentration and prolonging the duration of culture increased the supporting cell gaps and thereby increased the virus infection rate, which, when combined with the application of DAPT and *Ad5-EGFP-Atoh1,* increased the rate of conversion of supporting cells to hair cells and thus produced more hair cells. Thus, Atoh1 overexpression induced in situ formation of hair cells via trans-differentiation, and DAPT enhanced Atoh1 activity, leading to the production of more new hair cells. The concurrent application of DAPT and *Ad5-EGFP-Atoh1* could be an effective and efficient therapy for recovery of hearing loss in the future.

PS-3

Changes in the Notch Signaling Pathway during Spontaneous Hair Cell Regeneration in the Neonatal Mouse Cochlea

Melissa Trone; Sumedha Karmakar; Brandon Cox
Southern Illinois University, School Of Medicine, Springfield

The Notch signaling pathway has been implicated in the developmental regulation of the inner ear sensory epithelium as well as in non-mammalian hair cell regeneration. During development, Notch signaling mediates lateral inhibition which allows some progenitor cells to differentiate into hair cells while neighboring cells are inhibited from a hair cell fate and instead become supporting cells. Many studies have shown that inhibition of Notch signaling allows mammalian supporting cells to convert into hair cells in the normal, undamaged cochlea and in the drug damaged cochlear explant. This mechanism is also implicated during the spontaneous hair cell regeneration process in non-mammalian vertebrates. However, it is currently unknown whether the Notch pathway plays a role during spontaneous hair cell regeneration that was recently observed in the neonatal mouse cochlea *in vivo*. In this model, hair cells were killed *in vivo* using Atoh1-Cre^{ER}+;Rosa26-loxP-Stop-loxP-$DTA^{+/f}$ mice (Atoh1-DTA) and tamoxifen administration at postnatal day (P) 0 and P1. This produced hair cell ablation by Cre-mediated expression of diphtheria toxin fragment A (DTA) specifically in hair cells. Subsequently supporting cells were able to either directly transdifferentiate into hair cells or mitotically regenerate hair cells. We investigated the Notch signaling pathway in the Atoh1-DTA model as a potential mediator for the regenerative capacity observed with the hypothesis that Notch signaling is reduced in supporting cells of the Atoh1-DTA damaged cochlea, allowing them to transdifferentiate and regenerate hair cells. In a gene expression array from P2 cochlear tissue, the expression of Jagged1, a Notch ligand, and Hey1, a downstream Notch effector, were reduced in Atoh1-DTA cochleae compared to control cochleae. Using the Hes5-nlsLacZ reporter mouse, we also found that the number of cells expressing Hes5, another downstream Notch effector, was reduced in Atoh1-DTA cochleae at P2 while the supporting cell population was maintained. Additional studies are underway using *in situ* hybridization and real time qPCR to further investigate the Notch signaling pathway in the Atoh1-DTA model. From our preliminary data we expect to find that Notch signaling is reduced after hair cell damage in the neonatal mouse cochlea.

PS-4

In Vivo Hair Cell Ablation Recruits Lgr5+ Progenitor cells to Mitotically Regenerate Hair Cells in Neonatal Mouse Utricle

Renjie Chai[1]; Grace Kim[2]; Tian Wang[2]; Nicole Pham[2]; Duc-huy Nguyen[2]; Alan Cheng[2]

[1]Southeast University, Nanjing, China; [2]Department of Otolaryngology-Head and Neck Surgery, Stanford University School of Medicine, Stanford, CA, 94305, USA.

Background

Tissue injury activates endogenous stem/progenitor cells to regenerate lost cells. The inner ear utricle requires mechanosensory hair cells (HCs) to detect linear acceleration. The utricle consists of two types of HCs (Type I and II); after damage, non-mammalian utricles mitotically regenerate HCs, and both types of HCs are replenished. In adult mammalian utricles, supporting cells (SCs) nonmitotically regenerate HCs, which are predominantly extrastriolar Type II HCs. Recent studies have revealed that the neonatal utricles can mitotically regenerate HCs after damage. The current study aims to identify and characterize these damage-recruited progenitor cells.

Methods:

We used the Pou4f3-DTR mice, where the human diphtheria toxin receptor is driven by Pou4f3 expression, to ablate HCs. Diphtheria toxin was injected on postnatal day (P)1 and tissues were examined from P3 to P30. To detect Lgr5 expression, we used the Lgr5-EGFP-CreERT2 reporter mice. In parallel, we fate-mapped Lgr5+ progenitors and Plp1+ SC in this neonatal HC damage model using Pou4f3-DTR;Lgr5-EGFP-CreERT2;ROSA26R-tdTomatoor Pou4f3-DTR;Plp1-CreERT;ROSA26R-tdTomato mice.

Results:

After DT injection at P1, ~27% of HCs were present in utricles from P15 Pou4f3-DTR mice in comparison to age-matched, wildtype controls. At P30, normalized HC number increased to 55%, suggesting HC regeneration. Without damage, Lgr5 is absent from the postnatal utricle. After HC ablation, Lgr5 expression is found predominantly in striolar supporting cells at P4. Lineage tracing of Lgr5+ cells revealed that they contributed to the striola, Myosin+ HCs at P30. These fate-mapped HCs displayed abnormal-appearing f-actin+, espin+ stereocila and Ctbp2+, Shank1+ synapses. Quantification of Calbindin, Sox2, and Tuj1+ calyx expression in fate-mapped, Myosin7a+ HCs showed that ~50% regenerated HCs were Type I. In contrast to Lgr5 whose expression, tracing of Plp1+ cells identified traced Myo7a+ HCs in both the striolar and extrastriolar regions. Without damage, no Edu+, Myo7a+ HCs, ~1-2 Edu+, Sox2+ SCs, (per 20,000 μm^2) were detected in the striola or extrastriolar of P30 utricles. After damage, ~14 Edu+, Myo7a+ HCs, ~96 Edu+, Sox2+ SCs were found in striolar and ~6 Edu+, Myo7a+ HCs, ~28 Edu+, Sox2+ SCs were found in extrastriolar region. Lineage tracing of Lgr5+ cells revealed that ~23% of traced HCs and ~48% of traced SCs were also labeled with Edu.

Conclusions:

HC ablation induces Lgr5 expression in striolar SCs, which contribute to regeneration of Type I and II striolar HCs in the neonatal utricle. Lgr5+ SCs can re-enter cell cycle to mitotically regenerate HCs.Thus, Lgr5+ SCs act as facultative HC progenitors.

PS-5

Morphological and Functional Analyses of Vestibular Hair Cell Loss and Replacement in Adult Pou4f3DTR Mice After Treatment with Two Different Doses of Diphtheria Toxin

Jennifer Stone[1]; James Phillips[1]; Tot Nguyen[1]; Jay Gantz[1]; Clare Gamlin[1]; Caitlyn Trullinger-Dwyer[2]; Remy Pujol[3]; Edwin Rubel[1]

[1]University of Washington School of Medicine; [2]College of Wooster; [3]INSERM France

Adult mice have a small capacity for vestibular hair cell (HC) replacement after injury. In a prior study, we examined utricular HC loss and replacement in adult Pou4f3$^{DTR/+}$ mice (C57Bl/6 background) after administration of 50 ng/g diphtheria toxin (DT). This dose of DT killed 94% of utricular HCs in 2 weeks, and nearly 20% of HCs were replaced in 2 months. Here, we expanded this study to compare effects of two DT doses (low = 25 ng/g, and high = 50 ng/g) and to analyze lateral ampullae as well as utricles. We studied adult wildtype and Pou4f3$^{DTR/+}$ mice on a CBA/CaJ background up to 170 days post-DT. We examined temporal and dose-dependent changes in supporting cell numbers, synapses between HCs and the vestibular nerve, and numbers of vestibular ganglion neurons, and we tested lateral crista function by measuring the horizontal vestibulo-ocular reflex (VOR).

DT killed HCs in utricles and lateral ampullae in Pou4f3$^{DTR/+}$ mice (but not wildtype controls). At 14d post-DT, HC numbers were reduced to ~8% of controls in the high-dose group and 20% of controls in the low-dose group, in both organs. Over time post-DT, HC numbers increased in the high-dose group but did not change significantly in the low-dose group, in both organs. Higher numbers of total HCs, and a higher proportion of type I HCs, were seen at all times in the low-dose group, but it is not clear if this difference was due to greater HC survival or HC replacement. Supporting cell numbers did not change over time at either DT dose. By 14 days, dramatic reductions in ribbon synapse component density and peripheral fiber density were detected and found to vary with dose. Replacement hair cells had ribbon synapse components, as assessed by Ctbp2 immunolabeling and TEM, but there was a dramatic loss of ribbon synapse components and peripheral nerve fibers at later times (170 days) post-DT. Current experiments are assessing cell bodies in the vestibular ganglion. Mice that received high-dose DT demonstrated complete loss of VOR at 14d post-DT, with no improvement over time. By contrast, low-gain VORs were evoked in mice at 70d and 170d post-DT after low-DT, suggesting that surviving or replacement HCs were functional in these animals. This study demonstrates dose-dependent variation in loss of vestibular HCs and vestibular function following DT administration to

Pou4f3$^{DTR/+}$ mice. Current experiments address if hair cell replacement and recovery vary with DT dose.

PS-6

Distinct Ways of Sensory Hair Cell Regeneration in Zebrafish Lateral Line

Dong Liu[1]; Yuting Wu[2]; Yuanhe Zhang[2]; Guozhu Tang[2]; Xiaoxiao Mi[2]; Hong Guo[2]
[1]Peking University; [2]Peking University School of Life Science

In zebrafish, the hair cell (HC) regeneration in the inner ear and lateral line (LL) neuromast is achieved through induction of support cell proliferation, from which nascent HCs are differentiated. In this study, we intended to test whether 'trans-differentiation' or non-proliferative mechanism is also present in LL HC regeneration. In the EdU tracing experiments, we observed that non-proliferated cells became HCs upon different ototoxic damages within 24 hours post HC damage (24hp) and the number of EdU negative HCs was not increased over time. After 24hp, all nascent HCs were EdU labeled, suggestive of proliferative regeneration. Thus, in the damaged neuromasts, non-proliferative and proliferative regeneration operate sequentially. Among different known cell proliferation inhibitors used, the damaged neuromasts could fully regenerate HCs only in the presence an anti-leukemia drug, and the nascent HCs were all EdU negative. It appeared that the anti-leukemia drug treatment could continuously keep high *atoh1a* expression, a HC progenitor marker, while the intrinsic Notch inhibition, due to ototoxic damage, transiently elevated *atoh1a* expression.

By blocking Notch signaling before and after the ototoxic damages, both non-proliferative and proliferative regenerations were enhanced, suggesting that they may share a common HC progenitor pool, or they use distinct progenitor populations that are regulated by Notch signaling. Therefore, 'trans-differentiation' is a natural means of HC regeneration in zebrafish LL system. In addition to be an acute response to HC damages, 'trans-differentiation' could also serve as an alternative once proliferative regeneration process is blocked.

PS-7

3-D Gradient Culture of Human Vestibular Nerve

Fredrik Edin; Hao Li; Wei Liu; Helge Rask-Andersen
Uppsala University

Background

Currently there is great interest in regenerating SG nerves to reduce or close the gap between the SG and cochlear implants (CI) to improve frequency discrimination and improve the hearing experience for patients [1, 2]. To attract the neurons requires making a gradient of neurotrophins, e.g. BDNF [3] inside the cochlea. This approach also requires a 3-D matrix to be inserted into the cochlea to allow the neurons to cross the scala typmani and attach to an electrode. To study the effect of gradients on inner ear neurons we have used a microfluidic system creating a stable gradient over time.

Material and Methods

The human vestibular ganglion (VG) is collected with ethical and patient consent during surgery to remove vestibular schwannoma using a translabyrinthine approach The regenerative capacity of the vestibular nerve has been demonstrated in rodents [4] and humans [5]. As the VG is embedded in Matrigel™ inside a closed microfluidic device different media can be introduced on either sides of the gel. By continually changing the media on both sides introducing the neurotrophin of interest on one side letting, the other side acts as a sink a gradient is formed through the gel.

Results

When cultured in Matrigel™ human VG is capable of re-sprouting neural extensions within 6 days. Gradients of BDNF, GDNF and Netrin-1 could be formed inside the culture chamber which influenced neurite outgrowth. Other models of gradient culture were also evaluated. 3-D visualization of outgrowth showed that neurons could interact with cochlear implants *in vitro*.

References

1. Xie, J., et al., *Neurotrophins differentially stimulate the growth of cochlear neurites on collagen surfaces and in gels.* Neural Regen Res, 2013. 8(17): p. 1541-1550.
2. Brors, D., et al., *Interaction of spiral ganglion neuron processes with alloplastic materials in vitro.* Hearing Research, 2002. 167(1–2): p. 110-121.
3. Glueckert, R., et al., *Deafferentation-associated changes in afferent and efferent processes in the guinea pig cochlea and afferent regeneration with chronic intrascalar brain-derived neurotrophic factor and acidic fibroblast growth factor.* J Comp Neurol, 2008. 507(4): p. 1602-21.
4. Travo, C., S. Gaboyard-Niay, and C. Chabbert, *Plasticity of Scarpa's ganglion neurons as a possible basis for functional restoration within vestibular endorgans.* Frontiers in Neurology, 2012. 3.
5. Edin, F., et al., *3-D gel Culture and Time Lapse Video Microscopy of the Human Vestibular Nerve.* Acta Otolaryngologica, 2014. Submitted.

PS-8

Nestin-Expressing Cells in the Adult Murine Cochlea

Cynthia Chow; Parul Trivedi; Madeline Pyle; Jacob Matulle; Xinyu Zhao; Samuel Gubbels
University of Wisconsin-Madison

Background

The adult mammalian inner ear does not regenerate cochlear hair cells following auditory insult. Inner ear stem cells have been found to be present in the cochlea of young adult mice; however, there has been little evidence for their existence into adulthood. Nestin is an intermediate filament found in neural progenitor cells during early development and adulthood, and is a multi-potent and neural stem/progenitor cell marker. Nestin expression has been described in the postnatal and young adult rodent cochlea; however, there are discrepancies be-

tween these reports in the spatial distribution and identity of nestin expressing cells. We sought to 1) evaluate nestin expression in the adult mouse cochlea and 2) characterize the subpopulation of cells expressing this progenitor marker and their progeny using a lineage tracing approach.

Methods

Nestin-CreER^{T2}/tdTomato-reporter mice were used to identify putative stem cells and their progeny in the organ of Corti of adult mice. Tamoxifen was administered to nestin-CreER^{T2}/tdTomato-reporter mice at 2 months of age and analysis performed at days 1, 7, 14, 35 and 56. Cochlear tissue was analyzed via immunohistochemistry and the tdTomato-positive cell population was quantified throughout the length of the organ of Corti and compared between time points.

Results

Cells expressing nestin and their progeny persist into adulthood in the murine inner ear on the neural (medial) aspect of the inner hair cell layer. Quantitative analysis suggests these cells do not proliferate over time. Immunohistochemisty revealed tdTomato-positive cells co-localize the supporting cell markers Sox2 and Sox10; however, they do not co-localize Krox20, GFAP or NF200.

Conclusions

Cells expressing nestin, a marker of a stem cell fate, appear to persist into adulthood in the murine inner ear. TdTomato-positive cells co-localize the supporting cell markers Sox2 and Sox10, suggesting they may be a type of supporting cell within the organ of Corti. Although the cellular identity of the population of nestin-expressing cells and their descendants remains unclear, our results suggest that cochlear nestin-expressing cells do not appear to be part of the spiral ganglion nor Schwann cell populations. Additional studies are needed to elucidate whether tdTomato-positive cells retain stem/progenitor qualities and whether they are supporting cells at the medial aspect of the organ of Corti or alternatively peripherally located elements of the spiral ganglion cell population.

PS-9

Macrophage Recruitment and Epithelial Repair Following Hair Cell Injury in the Mouse Utricle

Mark Warchol[1]; Tejbber Kaur[1]; Edwin Rubel[2]; Keiko Hirose[1]
[1]Washington University School of Medicine; [2]University of Washington

Introduction

Resident macrophages are associated with most hair cell epithelia, but their function is poorly understood. In many tissues, macrophages participate in the removal of cellular debris after injury and often promote tissue repair. We have used a novel transgenic mouse model to examine the activity of vestibular macrophages in response to hair cell lesions.

Methods

Studies used transgenic mice in which the gene for the human diphtheria toxin receptor (huDTR) was inserted under regulation of the Pou4f3 promoter. Hair cells in such mice can be selectively lesioned by systemic treatment with diphtheria toxin (DT). These mice were crossed with a second transgenic line, yielding animals in which one or both alleles of the fractalkine receptor CX3CR1 were replaced with a GFP construct. Such mice expressed GFP in all macrophages. In addition, mice that were Pou4f3-huDTR:CX3CR1$^{GFP/+}$ possessed normal fractalkine signaling, while mice that were Pou4f3-huDTR:CX3CR1$^{GFP/GFP}$ lacked fractalkine signaling. Animals received a single injection of diphtheria toxin (25 ng/gm) and utricles were fixed and examined after 7-56 days of recovery.

Results

DT treatment resulted in the death of ~70% of utricular hair cells within 7 days. Although cellular junctions in the uninjured utricle are supported by thick bundles of F-actin (e.g., JC Burns et al., J Comp Neurol 511: 396, 2008), we found that initial epithelial repair after hair cell loss was often mediated by much thinner actin cables. Enhanced numbers of macrophages were present near and within the sensory epithelia of DT-lesioned utricles, and numerous macrophages appeared to be actively engulfing hair cell debris. We observed no apparent difference in macrophage numbers in the DT-lesioned utricles of CX3CR1$^{+/GFP}$ mice vs. CX3CR1$^{GFP/GFP}$ mice, suggesting that fractalkine signaling does not play a critical role in macrophage recruitment after injury. We also observed actin basket-like structures (putative phagosomes) in the sensory epithelia of all specimens. However, the numbers of such baskets was not enhanced by DT-mediated hair cell injury.

Conclusions

Hair cell death attracts macrophages toward the sensory epithelium of the utricle, and such macrophages participate in the removal of hair cell debris. The chemoattractant that mediates this response is not known, but it is unlikely to be fractalkine. Epithelial injury following hair cell loss is initially repaired by thin actin fibers. Utricular supporting cells also form actin baskets that might remove hair cell debris. In contrast to macrophages, however, the numbers of these structures is the same in lesioned vs. control utricles.

PS-10

Providing a Cell Culture Controlled Milieu for the Generation of Spiral-Ganglion Like Neurons from Human Embryonic Stem Cells

Augusta Fernando; Kazuaki Homma; Bula Bhattacharyya; Abdelhak Belmadani; Chaoying Zhang; Tammy McGuire; Omotara Sulyman; Himanshi Desai; Richard Miller; John Kessler; Akihiro Matsuoka
Northwestern University

Background

Recent studies have shown that the use of stem cell based therapies can possibly direct to recover the damaged auditory network. The purpose of this study was to use human embryonic stem cells (hESCs) to direct the generation of otic neural progenitors like cells (ONPs) in a controlled culture milieu with instructive growth factors and later regulate the differentiation of the precursor cells to spiral-ganglion like neurons.

Methods

Cell culture: Undifferentiated hESCs (H7) were seeded on matrigel coated culture dishes in medium containing N2B27. To generate ONPs, the medium was first supplemented with bone morphogenic protein, its antagonist and transforming growth factor inhibitors. The ONPs were then generated using Wnt, sonic hedgehog and neurotrophins. These cells were further differentiated into neurons with neurotrophins, dibutryl cAMP and notch signaling inhibitor.

RT-PCR: RNA was extracted from ONPs and RT-PCR was performed for the expression of transcription factors at the development of the pre-placodal ectoderm such as SIX1 and SIX4.

Immunocytochemistry: hESCs were cultured in the specific medium with growth factors and screened for the presence of preneural and neuronal markers for ONPs and spiral- ganglion like neurons (SGNs).

In vitro electrophysiology: The stem-cell derived ONPs were cultured on glass coverslips coated with polyornithine and laminin and treated with differentiating medium containing Dibutryl cAMP. Coverslips were transferred to a recording chamber fitted to an AxioExaminer D1 microscope for electrophysiological recordings.

Results

PCR results showed the expression of the early embryonic development transcription factors, SOX2, p75, SIX1 and SIX4. Immunofluorescence images demonstrated the presence of nestin, FOXG1 in the ONP population and SGN-like cells demonstrated the presence of beta III tubulin, Trk B, Trk C and vGlut1/2. There are stem-cell derived viable neurons present in the culture as demonstrated by calcium imaging. The physiological function of stem cell–derived neurons assessed showed resting membrane potential and also exhibited significant inward currents upon depolarization.

Conclusion

Our results demonstrate the possibility of generating hESC-derived ONPs and SGN like cells with diffusible-ligand treatments and physiologically active neurons can further advance our stem cell replacement therapy of human SGNs.

PS-11

Neuronal Differentiation of Human Embryonic Stem Cell-derived Otic Neuronal Progenitors following Co-culture with Rat Auditory Brainstem Slices

Omotara Sulyman[1]; Augusta Fernando[2]; Tammy McGuire[2]; Christopher Gouveia[2]; Zafar Syed[2]; John Kessler[2]; Akihiro Matsuoka[2]

[1]Northwestern University, Feinberg School of Medicine; [2]Northwestern University

Introduction

Cochlear implantation has become the standard of care for patients with severe to profound sensorineural hearing loss. However there is a degree of variability in patient outcomes which can be conceivably attributed to several factors including; the number and integrity of surviving spiral ganglion neurons (SGNs), the health of their central synaptic connection and the proximity of the electrodes to the SGNs. Therefore, regeneration of SGNs is crucial in enhancing the efficacy of cochlear implants and future hair cell generation therapy. In our previous experiments, we have consistently demonstrated that human embryonic stem cell-derived otic neuronal progenitors (hESC-derived ONPs) almost uniformly expressed specific markers for ONPs. Yet, it would remain to be determined whether these cells could establish a synaptic connection to the cochlear nucleus. To address this issue, we performed an ex vivo model organotypic co-culture of brainstem slices. The purpose of this study, therefore, was to evaluate whether our hESC-derived ONPs could establish a synaptic connection with the cochlear nucleus.

Methods

HESC-derived ONPs were generated as previously described. Organotypic rat auditory brainstem slices were generated using the previously described Stoppini interface method. Postnatal Sprague-Dawley rat pups (P12-P15) were decapitated after carbondioxde overdose. The skulls were then opened and the area of the cochlear nucleus was labeled using CM-Dil tissue labeling paste (Molecular probes, Eugene OR). The brainstem was placed onto a sterilized plastic sheet and placed on the tissue chopper. Three hundred µm thick transverse sections of the brainstem containing the cochlear nucleus were obtained and individual slices were then transferred onto polyester membranes with 0.4µm pore size and 24 mm in diameter (Corning) for interface cultures. The hESC-derived ONPs were deposited at 500 µm away from the edge of the brainstem slice. Immunohistochemical analyses were performed on the tissue against using synapsin1, synaptotagmin1, synaptophysin1, bassoon and SV2A markers.

Results

Our preliminary result indicated that after engraftment, hESC-derived ONPs gradually integrated into the brainstem slices. The engrafted ONPs expressed some of the neuronal markers and synaptic markers indicating the co-culture with the brainstem slices appeared to accelerate neuronal differentiation.

Conclusion

The organotypic cultures with brainstem slice containing the cochlear nucleus are suitable models for evaluating host and graft interaction for hESC-derived ONPs.

PS-12

Engineering Hair Cells Through Reprogramming of Human Wharton Jelly Cells

Adam Mellott[1]; Heather Shinogle[1]; Jenny Nelson-Brantley[1]; Michael Detamore[1]; Hinrich Staecker[2]

[1]University of Kansas; [2]University of Kansas School of Medicine

Introduction

The inability of hair cells to regenerate within the human cochlea is a major challenge in restoring hearing. Several strategies have explored the potential of delivering nucleic acids

to the site of injured hair cells, and the possibility of differentiating stem into hair cells. However, few strategies have looked at the combinational evaluation of manipulating both the intracellular and extracellular signaling simultaneously in stem cells. We hypothesized that mesenchymal stem cells isolated from Wharton's jelly of the human umbilical cord (hWJCs) could be pushed toward a hair cell phenotype by up-regulating Atoh1 while seeding transfected hWJCs on decellularized cochleas isolated from C57BL/6 mice. The current study is the first study to use the cochlea as a tissue scaffold to drive hair cell development in hWJCs while simultaneously over-expressing Atoh1 for the purpose of engineering an *ex vivo* model of inner ear epithelium.

Methods

hWJCs were isolated from three separate human umbilical cords (*n* = 3*)* according to protocols approved by the KU IRB, and expanded to P5. Cochleas were isolated from C57BL/6 mice carcasses, and decellularized with 1% SDS in DI water over three days followed by decalcification in 10% EDTA in DI water for an additional three days. Cochleas were soaked in a 5% antibiotic-antimycotic PBS solution for 24 hrs. One of three groups of hWJCs were then seeded onto the decellularized cochleas or plated statically in 6-well plates: (1) untreated hWJCs, (2) GFP-transfected hWJCs, or (3) Atoh1-trasnfected hWJCs. Cells were cultured for up to seven days then collected for analysis. Gene expression regarding IEHC specific genes, neuronal precursor genes, and early developmental genes were assessed via RT-qPCR. Protein expression was assessed via immunocytochemistry. hWJCs were stained with FM 1-43.

Results

In our preliminary studies, *Atoh1* positive cells have shown a morphological shift away from hWJC phenotypes (**Fig. 1**). We have detected distinct differences in the gene expression of hair cell specific genes, neuronal precursor genes, and early developmental genes between *Atoh1* transfected hWJCs and untreated hWJCs in static culture. Immunocytochemistry revealed positive expression of *Myosin 7a* in *Atoh1* transfected cells. Data pertaining to the culture of treated hWJCs seeded on decellularized cochleas are still being collected and quantified, and are not yet available for presentation.

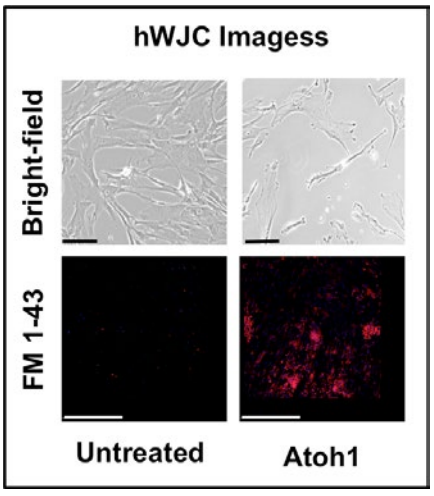

Figure 1 Legend: Images of untreated hWJCs and Atoh1-transfected hWJCs after seven days in static culture. Atoh1-transfected cells display a slight elongated morphology in the bright-filed images and stain positive for FM 1-43 whereas untreated hWJCs appear fibroblastic and are negative for FM 1-43 staining. Black Scale Bar = 50 µm. White Scale Bar = 500 µm.

Conclusions

Atoh1-transfected hWJCs seem to be capable of developing early hair cell phenotype markers according to preliminary gene expression data and immunocytochemical imaging.

PS-13

Cross Species Expression of Prestin in Rodent, Primate, and Human Choroid Plexus Epithelium

Dongguang Wei[1]; Brent Wilkerson[1]; Sona Santos[2]; Kiarash Shahlaie[1]; **Rodney Diaz**[1]

[1]University of California, Davis; [2]California National Primate Research Center

Background

Irreversible loss of cochlear hair cells (HCs) leads to hearing loss and affects the quality of life of millions of people worldwide. Restoring damaged HCs to the inner ear remains a major challenge. Biological implants with key molecular and morphological characteristics of inner ear HCs may be implanted into the cochlea and can serve to replicate HC form and function. Prestin, a member of the SLC26A/SulP transporter family, functions as a molecular motor in outer hair cells (OHCs), converting auditory stimuli to length changes in OHCs and is responsible for amplification and frequency tuning along the cochlear spiral. Expression of prestin is therefore critical for any proposed biological cochlear implant. Here we demonstrate expression of prestin both outside of the cochlea and conserved across species, in the choroid plexus (CP) epithelium of the mouse, rhesus monkey, and human.

Methods

Mouse CP tissues are quickly harvested and dissected from whole mouse brain. Rhesus monkey CP tissues are obtained from wild type rhesus monkeys that have undergone scheduled necropsy for unrelated purposes and that have no demonstrated neurological deficits. Human CP tissues are obtained from banked neurosurgical samples. CP epithelial sheets are processed for immunofluorescent staining, reverse transcriptase polymerase chain reaction, and scanning electron microscopy.

Results

Rodent, non-human primate, and human CP cells show strikingly similar morphological characteristics as polarized columnar epithelia. All tissues express prestin both at the RNA and protein level. All tissues exhibit an enriched, stereocilia-like appliance on their apical surface, similar in appearance to the apical structural identity of HCs. CP cells also express a variety of other HC biomarkers, including myosin VIIa and myosin VI.

Conclusion

Cross species and cross lineage expression of prestin in rodent, non-human primate, and human CP cells suggests prestin as an evolutionarily conserved functional molecule. If gene expression is evolutionarily conserved among different cell lineages and different species, this suggests a biological process with shared similarities. CP cells share strikingly similar molecular and morphological characteristics with co-

chlear HCs and may serve as potential autologous biological implants for the repopulation of hair cell depleted cochlear sensory epithelium.

PS-14

Survival and Neuronal Differentiation of Human Embryonic Stem Cell Derived-Otic Neuronal Progenitors in X-linked Severe Combined Immunodeficiency (X-SCID) Rats

Christopher Gouveia[1]; Zafar Sayed[1]; Augustina Fernando[1]; Miho Matakasu[1]; Omotara Sulyman[1]; Himanshi Desai[1]; Tammy McGuire[1]; Tomoji Mashimo[2]; Claus-Peter Richter[1]; Samuel Stupp[1]; Jack Kessler[1]; Akihiro Matsuoka[1]
[1]Northwestern University; [2]Kyoto University

Background

One of the major current limitations of translational *in vivo* studies in regeneration of spiral ganglion neurons (SGNs) is the lack of a suitable animal model. A previous *in vivo* transplantation of hESCs in the Mongolian gerbil used cyclosporine to prevent immune rejection of transplanted cells. Cyclosporine, however, often causes significant dehydration that precludes it from being used long-term. Instead an immunodeficient animal is ideal for the xenotransplantation of human tissues or human stem cells. Among these, a SCID mouse model is the most widely used animal model in regenerative medicine. SCID mice are perfect hosts for allogeneic and xenogeneic stem cell transplantation *in vivo*, However, it would be extremely challenging to perform stem cell transplantation into the modiolus of the SCID mouse model due to its small size. Recently, a knockout rat with X-SCID using zinc-finger nucleases has become available for research use. The X-SCID rat model will allow transplantation of hESC-derived ONPs into the modiolus without concerns of long-term rejection. The purpose of this study was to use the X-SCID rat for transplantation of ONPs into the modiolus to evaluate for the survival and neuronal differentiation.

Methods

The SCID rats were deafened with ouabain. Four weeks later, deafening was confirmed by ABR. Human ESC-derived ONPs suspended into brain-derived neurotrophic factor (BDNF)/neurotrophin-3 (NT-3) loaded isoleucine-lysine-valine-alanine-valine peptide amphiphile (IKVAV-PA) aligned gels were then be injected into the modiolous of the SCID rat with the aid of a micromanipulator and microinjection. The X-SCID rats were allowed to recover for 1 month. The brain stem was cut at 300 mm, and slices containing the cochlear nucleus were transferred to a humidified chamber, where they were allowed to recover for at least 45 min. These slices were used to perform immunohistochemistry for synaptic markers. Additionally, temporal bones from these animals were harvested, post-fixed over night, and decalcified by EDTA. The tissue was then sectioned in a cryostat for immunohistochemical analysis to detect ONP's with neuronal markers.

Results

Our preliminary results indicate that transplanted ONPs in deafened X-SCID rats survived after one month. The transplanted ONPs expressed positive mature-neuronal makers such as TUJ1, indicating that the ONPs had differentiated into neurons.

Conclusions

X-SCID rats offer a promising research tool for inner-ear stem cell behavior by overcoming research limitations encountered by cyclosporine in large rodent models, and small size of X-SCID mouse models. Our preliminary results show that these animals are a viable alternative.

PS-15

Nanofibrous Scaffolds for the Integration of Human Embryonic Stem Cells into the Cochlea

Sandra Hackelberg[1]; Arjun Rastogi[2]; Samuel J. Tuck[1,2]; Christina White[1,2]; Liqian Liu[1]; Diane Prieskorn[1]; Joseph M. Corey[1,2]; Josef Miller[1]; R. Keith Duncan[1]
[1]University of Michigan; [2]VA Ann Arbor Healthcare Center

The restoration of hearing by means of cochlear implants relies on the presence of functional spiral ganglion neurons (SGN). However, age, genetics, infection, noise, blast exposure, and skull fractures can lead to progressive auditory neuron loss with or without associated hair cell loss. Since mammalian SGNs do not spontaneously regenerate, methods to promote regeneration and guide integration are of paramount importance. While considerable strides have been made in directing cell fate, functional, organized integration of stem cells with host tissue remains a major hurdle. Nanofibrous scaffolds have the potential to both guide integration and open avenues toward novel biohybrid cochlear implants. We have previously utilized nanofibrous scaffolds to promote the neurodifferentiation of mouse embryonic stem cells. Here, we extend those studies using human embryonic stem cells (hESCs) and polycaprolactone (PCL) nanofibrous scaffolds. PCL could reproducibly generate uniform fibers with average diameters below 1 µm. hESCs were predifferentiated to derive neuronal precursor cells (NPC) capable of adopting a glutamatergic fate. Briefly, hESCs were used to form embryoid bodies using BMP-inhibitors and plated to form rosettes in presence of small molecule morphogens. The NPCs were plated on plasma treated PCL fibers and control films and different coatings tested for adhesion. Terminal differentiation progressed for 2-6 weeks in Neurobasal-based medium. At different time points in culture, cells were fixed and examined for lineage, maturation, and transmitter phenotype. Both aligned and unaligned scaffolds promoted the growth of human NPCs. The cells preferred Matrigel or fibronectin coating over laminin and poly-l-lysine for optimal adhesion. The growth of cellular extensions was observed alongside as well as across single fibers. Consistent with findings on other cell types grown on this material, we could not find signs of toxic effects interfering with cell viability. Further analysis will be required to fully understand the impact of structure and material on the differentiation and functional abilities of neurons grown on nanofibers. To study the integration of the neurons with the cochlear tissue, the nanofibrous scaffolds have to be modified prior to insertion in the auditory periphery. Methods

will be described for forming nanofiber conduits in bundled and rolled configurations along with surgical strategies for implantation.

PS-16

Evaluating the Effect of Human Pluripotent Stem Cell Maintenance Platforms on Otic Differentiation

Parul Trivedi; Sofiya Reshetylo; Rebecca Brodziski; Cynthia Chow; Su-Chun Zhang; Samuel Gubbels
University of Wisconsin

Background

Human pluripotent stem cells (hPSCs) have a number of applications for improving our understanding and ability to treat hearing loss. These include disease modeling using patient-derived iPSCs for developmental studies, discovery of novel deafness-causing genetic mutations, and potentially a cell-based therapy for hearing loss. We and other investigators have defined methods to generate otic progenitor cells from hPSCs. To facilitate translation of hPSC-based applications relevant to hearing loss, outlining feeder-free stem cell maintenance conditions in order to generate otic progenitor cells is of critical importance. Experience in hPSC differentiation in other model organ systems (CNS, cardiac) has demonstrated that transitions from feeder to feeder free differentiation conditions can dramatically alter the gene and protein expression profile of the resultant target progenitor or differentiated cell type. The present study was undertaken to compare the ability of hPSCs to generate otic progenitor-like cells with or without the use of a MEF feeder cell layer during hPSC maintenance.

Method

H9 human embryonic stem cells and IMR90-4 human induced pluripotent stem cells were maintained on 1) a mouse embryonic fibroblast (MEF) feeder layer or 2) feeder free conditions (no feeder cell layer nor serum) using established protocols. Cells were then differentiated to an otic fate using the same differentiation protocol. Differentiating cells were tested for the presence of transcriptional factors after 7, 14 and 30 days of differentiation. Analysis was then performed using qPCR and immunohistochemistry for gene and protein markers of the pre-placodal region and otic placode.

Results

Human PSC maintained on MEF expressed gene and protein markers of an otic fate in a sequence consistent with that seen during development. When hPSC were maintained in feeder free conditions and then differentiated using an identical protocol, there was a lower level and altered pattern of expression of pre-placodal and otic progenitor markers.

Conclusions

Maintenance using a feeder free platform alters the ability of hPSC to differentiate towards an otic progenitor-like fate. Modification of cell maintenance protocols to enable feeder layer free handling of hPSC will be necessary to allow the generation of robust populations of otic progenitor-like cells from hPSC for translational purposes.

PS-17

Atonal Adenoviral Gene Delivery Regenerates Sensory Hair Cells in Adult Mouse and Human Vestibular Explants Ex Vivo

Susan Stevenson[1]; Chi Hsu[1]; Lloyd Klickstein[1]; Douglas Brough[2]; Hinrich Staecker[3]
[1]Novartis Institutes of BioMedical Research, Inc.; [2]GenVec, Inc.; [3]University of Kansas Medical Center

Background

Sensorineural hearing loss and balance dysfunction result from loss of inner ear sensory hair cells and/or auditory nerves. Sensory cells can be damaged by pharmacological agents, loud noises, infections or aging; loss of these cells is permanent as they do not regenerate. No pharmacologic agents exist to restore hearing and balance function. The atonal gene, ATOH1, is a basic helix-loop-helix (bHLH) transcription factor required for differentiation of sensory hair cells. Adenoviral vectors expressing the ATOH1 mouse homolog (Math1) have been evaluated in rodent models and reported to result in regeneration of hair cells and restoration of hearing or balance function. The objective of this study was to characterize an adenoviral vector expressing the ATOH1 human homolog (Hath1) for its ability to regenerate sensory hair cells in isolated vestibular macular organ cultures from adult mice and humans.

Methods

Ad5.GFAP.Hath1 is an E1, E3, E4deleted adenovirus 5 (Ad5) vector engineered to express Hath1 under the control of the GFAP (glial fibrillary acidic protein) promoter, which will limit expression to supporting cells. Adult C57BL/6 mouse vestibular organ cultures were used to profile Ad5.GFAP.Hath1 for its ability to regenerate sensory hair cells after chemical ablation. Utricles were harvested and exposed to neomycin (10^{-3}M) for 72 hrs, then transduced with Ad5.GFAP.Hath1 for 24 hrs and maintained in culture for 14 days. The number of myosin VIIa (myoVIIa) positive sensory hair cells was determined by Immunofluorescence. A range of vector concentrations was explored from $2.75x10^8$ down to 2.75 vp/µL.

Results

The feasibility of Ad5.GFAP.Hath1 to regenerate sensory hair cells in human macular organ cultures was explored using inner ear vestibular epithelia harvested from patients undergoing labyrinthectomy. Sensory hair cells were ablated by exposure with neomycin and then transduced with Ad5.GFAP.Hath1 for 24 hours and maintained in culture for 14 to 28 days and then stained for the presence of myoVIIa positive cells by immunofluorescence. In Ad5.GFAP.Hath1 treated mouse utricles, there was a ~60% recovery of myoVIIa positive cells at $2.75x10^8$ to $2.75x10^5$ vp/µL, which dropped to background levels at $2.75x10^4$ vp/µL. In two independent human utricles samples, Ad5.GFAP.Hath1 was able to effectively recover myoVIIa positive cells and regenerate sensory hair cells in these human utricle explants after neomycin exposure.

Conclusion

These results with Ad5.GFAP.Hath1 using *ex vivo* model systems support the therapeutic hypothesis to treat patients

with sensorineural hearing loss using atonal adenoviral gene therapy.

PS-18

Adenoviral-mediated expression of Atoh1 in Adult Mouse Vestibular Organs Efficiently Converts Supporting Cells into Hair Cells In Vitro.

Joseph Burns; Matthew Kelley
NIH

Introduction

When mechanosensitive hair cells (HCs) within the inner ear die, adult mammals fail to replace sufficient numbers, resulting in permanent auditory and vestibular deficits. Since neighboring supporting cells (SCs) are more resilient than HCs, reprogramming SCs into HCs by targeted activation of genes that regulate HC differentiation, such as the transcription factor Atoh1, is a promising regenerative strategy. However, recent data suggests that SCs in the adult mammalian cochlea are highly resistant to Atoh1-mediated reprogramming, and the SCs that do convert remain immature. Compared to the cochlea, the effects of Atoh1 over-expression in the vestibular organs have not been thoroughly characterized. Limited evidence indicates that Atoh1 can reprogram adult vestibular SCs into HCs; however, it is unclear what percentage of vestibular SCs is amenable to reprogramming.

Methods

To test whether ectopic Atoh1 expression can convert vestibular SCs into HCs at adult ages, we explanted utricles from mice older than postnatal day 60 (>P60) into organ culture and transduced them overnight with an adenovirus that co-expresses murine Atoh1 and cyan fluorescent reporter protein (CFP) under control of a CMV promoter (*Ad-CMV-Atoh1-2A-CFP*). The CMV promoter shows activity in all SCs. For controls, we transduced utricles with an adenovirus that expresses only CFP (*Ad-CMV-CFP*) using the same promoter as for the Atoh1 vector.

Results

Less than 4% of CFP-expressing control cells labeled with antibodies against the HC marker Myo7a in control cultures at 2, 7, 10, or 14 days post-infection (DPV). Similarly, only 3% of CFP-positive cells were Myo7a-positive at 2 DPV in utricles overexpressing Atoh1. However, this number increased to 79% at 7 DPV, and then plateaued at 90% by 10 DPV (n=4 utricles per time point). SCs from all regions of the sensory epithelium converted into HCs, and reprogramming efficiency did not appear to depend on age or vestibular organ as robust conversion was still observed in utricles, saccules, and cristae from P484 mice. Characteristic of HCs, the CFP-positive/Myo7a-positive cells had flask-like shapes and lacked attachment to the basement membrane. However, no hair bundles or cuticular plates were visible in CFP-positive HCs, suggesting that these cells remained immature during the culture period.

Conclusion

These results indicate that most, if not all, SCs in adult mouse vestibular organs remain amenable to Atoh1-mediated conversion into HCs, at least in vitro. However, replacement HCs failed to express markers of maturity, suggesting that Atoh1 expression may be insufficient to induce fully differentiated HCs.

PS-19

Regulation of Synaptic Ribbon Formation by Intracellular Calcium Stores in the Sensory Hair Cell

Hiu-Tung Wong[1]; Katie Kindt[2]
[1]NIDCD/NIH and Johns Hopkins University; [2]NIDCD/NIH

Background

The ribbon synapse structure allows reliable transmission of both timing and intensity information from the auditory and vestibular sensory hair cells to the central nervous system. The synaptic ribbon is a specialized presynaptic structure of the ribbon synapse and tethers glutamate-filled vesicles and coordinates as well as facilitates rapid and sustained vesicle release. Previous studies have shown that synaptic ribbon structure is sensitive to local calcium concentration during a critical period of development. Within the cell, several sources of calcium including endoplasmic reticulum (ER) and mitochondria may actively modulate calcium concentration during this developmental window. We aim to investigate how sensory activity is spatially and temporally regulated in order to properly form synaptic ribbons that are required for controlled vesicular release in the sensory hair cell.

Methods

To study the effects of calcium stores on ribbon synapse development, we examined hair cells in the zebrafish lateral line. Lateral line hair cells resemble mammalian vestibular hair cells in structure and are easy to access for pharmacology, stimulation and visualization. Our work utilizes transgenic zebrafish lines that express mitochondria or ER targeted, fluorescent calcium sensors to visualize calcium dynamics in developing hair cells. In addition, our work uses pharmacology to disrupt ER-mitochondrial calcium cycling in the developing zebrafish hair cells.

Results

Preliminary results show that heightened mitochondrial calcium transport occurs during the period of synaptic ribbon formation in the basal ends of the sensory hair cell, and that this behavior is restricted to immature hair cells. This result is consistent with previous findings that synaptic ribbon size can also be influenced by $Ca_v1.3$ mediated calcium influx.

Conclusion

We predict that synaptic ribbon formation may be modulated spatially and temporally by mitochondrial calcium or ER-mitochondrial calcium cycling, and may ultimately shape mature ribbon synapse function.

PS-20

Using Zebrafish to Monitor Vesicle Release at Hair Cell Ribbon Synapses

Suna Li[1]; Katie Kindt[2]; Teresa Nicolson[3]
[1]National Institutes of Health; [2]NIDCD/NIH; [3]Vollum Institute, Oregon Health & Science University

Background

Synaptic ribbons are electron-dense presynaptic structures composed mainly of the protein Ribeye. They are found in hair cells, photoreceptors, and bipolar cells, which must be capable of sustained, fast rates of vesicle release to faithfully transmit sensory information. Fine filaments tether glutamate-loaded vesicles to the ribbon bodies near L-type Ca^{2+} channels ($Ca_v1.3$). Graded changes of the cell's membrane potential trigger vesicle exocytosis from the ribbon synapses and glutamate release. Ribbon body size and shape vary depending on cell type and species, although the effects of these morphological differences on vesicle release dynamics and postsynaptic activity are unclear. Furthermore, the molecular requirements for hair cell vesicle release in our system remain unknown.

Methods

To monitor vesicle release at ribbon synapses with *in vivo* confocal microscopy, we used transgenic zebrafish larvae that express a genetically encoded, pH-dependent vesicle exocytosis indicator (SypHy) localized to posterior lateral line hair cells. We also examined Ca^{2+} mediation of vesicle release at presynaptic ribbons by pharmacologically modulating Ca^{2+} influx at L-type calcium channels.

Results

We have established the characteristics of vesicle release at individual synaptic ribbons within our transgenic line. Surprisingly, although previous data suggest Ca^{2+} influx at presynaptic ribbon bodies is homogenous within a hair cell, vesicle release is not. Acute pharmacological treatment with isradipine and S-(-)Bay K8644, which respectively block and activate L-type calcium channels, appeared to significantly affect the magnitude of the SypHy response.

Conclusion

Our data sheds light on the complex relationship between presynaptic Ca^{2+} influx at ribbon synapses and vesicle exocytosis. Future work will determine the molecular requirements for vesicle release and proper ribbon synapse development in lateral line hair cells.

PS-21

Multivesicular Exocytosis During Moderate Depolarization of Auditory Hair Cells

Owen Gross; Henrique von Gersdorff
Oregon Health & Science University

Background

Amplitudes of miniature excitatory postsynaptic currents (mEPSCs) recorded from an auditory afferent nerve fiber become larger and exhibit greater variance when the membrane of the presynaptic hair cell is depolarized to the threshold for L-type calcium channel opening (-60 mV). This phenomenon has previously been interpreted as a sign of calcium-dependent multivesicular exocytosis, i.e. the coordinated, simultaneous fusion of multiple synaptic vesicles. An alternative model suggests that a dynamic fusion pore provides a better explanation for the observed properties of neurotransmitter release at hair cell synapses, though the different interpretations might reflect physiological differences across species. Here we present data suggesting that large amplitude events observed in bullfrog (*Rana catesbeiana*) afferent nerve fibers result from multivesicular release.

Methods

Whole cell calcium currents and EPSCs were recorded from paired auditory hair cells and afferent nerve fibers in the bullfrog amphibian papilla as previously described (Cho et al., 2011). The change in hair cell membrane capacitance (ΔC_m) due to synaptic vesicle fusion during exocytosis was measured using a simulated lock-in amplifier. A deconvolution algorithm with high temporal resolution (~100 µs) was employed to calculate the instantaneous release rate during afferent fiber EPSCs lasting for several seconds.

Results

Moderate depolarization of the hair cell from a holding potential of -90 mV to values between -55 mV and -45 mV produced exocytosis rates spanning a range of 100–3,000 vesicles per second, while the individual fusion event rate was typically 1.5–3 fold smaller. Deconvolution analysis revealed that the average quantal content per event was larger during stronger depolarizations. The total number of vesicles released during each evoked EPSC was compared with the corresponding hair cell ΔC_m, providing a single vesicle capacitance estimate of 38 aF, under the assumption that 80% of release events are detectable in the EPSC. This result is largely consistent with recent anatomical measurements.

Conclusions

Analysis of EPSC statistics, combined with ΔC_m measurements, provides strong evidence that large amplitude events observed during periods of moderate hair cell depolarization reflect synchronized fusion of multiple vesicles. Because the single vesicle capacitance estimate agrees closely with independent measurements, there appears to be minimal saturation of postsynaptic glutamate receptors during sustained periods of relatively strong release (>1,000 ves/s). Furthermore, synaptic vesicle endocytosis makes negligible contributions to measurements of ΔC_m on the time scale of 2–3 s.

PS-22

Actin Filament Network Regulates Exocytosis at the Hair Cell Ribbon Synapse

Marie Guillet; Gaston Sendin; Jean-Luc Puel; **Régis Nouvian**
INSERM

Background - Introduction

Inner hair cells transduce sound stimulation into the release of glutamate onto the auditory nerve fibers. Glutamate secretion is achieved through the coupling between calcium channel and synaptic glutamate-filled vesicle. The molecular machinery involved into the regulation of exocytosis is not

fully identified. Here, we probed whether the actin filament network regulates the synaptic vesicle exocytosis at the inner hair cell ribbon synapse.

Methods
To assess the influence of actin filament on calcium-triggered exocytosis, patch-clamp recordings of voltage-gated Ca2+ influx and exocytic membrane capacitance changes were performed. Inner hair cells were infused during 10 min with drugs known to depolymerize or stabilize the actin filament through the patch-pipette.

Results
Infusion of latrunculin A, known to depolymerize the actin filament, elicited an increase of exocytosis. While phalloidin, which promote the actin filament nucleation, had no effect on glutamate release, its infusion prevents the increase of exocytosis induced by latrunculin A. In addition, we also observed an increase of exocytosis in cells poisoned with cytochalasin D, another toxin promoting actin de-polymerization. The increase of secretion was, however, restricted to the 20 ms step depolarization. Cytochalasin D infusion did not affect exocytosis evoked either by short depolarization (from 5 to 10 ms duration) or by long depolarization (beyond 20 ms). Because the exocytosis plot against the stimulus duration is cumulative, the limited effect (at 20 ms pulse duration) suggest that a fraction of vesicle, normally recruited with 50 ms pulse duration, becomes available for shorter pulse (20 ms) after the actin filament disruption.

Conclusion
Our results suggest that actin network disruption increases exocytosis and that actin filament may spatially organize a sub-fraction of synaptic vesicle with respect to the calcium channel.

PS-23

Regulation of BK Channel Phosphorylation with Akt1 Inhibition

Yoshihisa Sakai; Bernd Sokolowski
University of South Florida, Morsani College of Medicine

Background
The phosphorylation of proteins is an important event for cell function, since it can determine their activation, translocation and degradation. Protein phosphorylation can occur in a signaling cascade that links to cell survival/death, in response to stimulation from endogenous and/or exogenous factors. Serine (S) and threonine (T) demarcate phosphorylation sites by Protein Kinase A (PKA), Protein Kinase B (Akt), and Protein Kinase C (PKC). The large conductance Ca^{2+}-activated K^+ channel (BK) has many putative phosphorylation sites by these kinases and can play a role in the proliferation and apoptosis of cells. However, little is known as to how BK behavior changes in response to phosphorylation. Using phospho- and dephospho-mimetic BK mutants, we examined BK regulation by these kinases.

Methods
Myc tagged human BK-*wt* and BK mutants, BK-A (S869A) and BK-D (S869D), dephospho- and phospho-mimetics, respectively, were stably transfected into HEK293 cells. These BK stable cell lines were transiently transfected with Akt1 siRNA or scrambled RNA. Western blots and proliferation assays were used to measure the effects of decreased Akt1 expression on HEK293 cells lacking BK, and HEK cells expressing BK-*wt* or BK phospho- and dephospho-mimetics. Expression was measured by band densitometry with β-actin serving as a control.

Results
Silencing Akt1 by ~45% results in a 10% downregulation of BK-*wt* and BK-A, whereas BK-D, the phosphorylated form, upregulates by ~50%. In the absence of Akt silencing, proliferation/viability assays show that BK-*wt* and BK-A show greater proliferation/viability than HEK293 cells lacking BK, whereas BK-D shows no difference. Moreover, BK-A proliferation is significantly greater than BK-*wt.* When these cells are subjected to Akt1 siRNA, the results show that BK-D proliferation/viability increases by ~10%, whereas both BK-*wt* and BK-A show a decrease of ~14% and 28%, respectively. Additional analyses of GSK3β, a direct target of Akt in the signaling cascade, downregulates by ~38% with Akt1 silencing. In contrast, PKA expression in BK-*wt* HEK cells upregulates by ~21% with Akt1 silencing. The results suggest PKA may initiate the phosphorylated form (BK-D) of BK through amino acid site 869.

Conclusions
Akt1 plays a significant role in the signaling cascade for cell death/survival. Our results show that both BK-*wt* and its dephosphorylated form decrease with decreased Akt1 expression. In contrast, the phosphorylated form of BK increases and is likely the form that is expressed at the cell membrane, leading to an increase in cell proliferation/viability despite a decrease in Akt1.

PS-24

Mining for BK Channel Partners

Lancia Darville; **Bernd Sokolowski**
University of South Florida, Morsani College of Medicine

Background
Large conductance Ca^{2+}-activated K^+ (BK) channels are highly expressed in the central nervous system (CNS) and are important modulators of intracellular signaling. Although BK has been studied in the CNS, there are a limited number of studies of BK protein networks in the cerebellum. The cerebellum plays a key role in motor control and learning and is involved in cognitive and behavioral processes as well as a number of neurological diseases. Hence, the cerebellum may provide insights into BK-associated proteins (BKAPs) involved in cochlear signaling. Coimmunoprecipitation (coIP) with mass spectrometry is a proteomic approach that allows for enrichment of target proteins and associated partners.

Methods
The immunocomplex-capture technique was used to coIP BKAPs using 30-day old mouse cerebellum lysate. We performed CoIPs using anti-BKα polyclonal antibody, while using ChromPure IgG antibody as a negative control. One-dimensional electrophoresis was used to fractionate samples,

followed by excising and digesting gel bands and analyzing their content using nano LC-MS/MS. CoIPed proteins were validated using Scaffold and annotated using the UniProt Gene Ontology (GO) program. Protein networks were determined using Ingenuity Pathway Analysis (IPA).

Results

We identified 61 BKAPs, some of which were previously reported, such as ATP1A1 and DNM1. Other identified partners were not linked previously to the BK channel, such as 2',3'-cyclic-nucleotide 3'-phosphodiesterase (CNP), which is located in the cytoplasm and mitochondrial inner membrane. GO annotations showed that 39% and 54% of BKAPs are in the plasma membrane and cytoplasm, respectively. IPA revealed that 18 BKAPs function in nervous system development, while 22 are involved in organismal survival. Four major networks were identified using a maximum of 35 molecules for analysis. The highest scoring network contained 23 BKAPs associated with molecular transport, developmental disorder, and hematological disease. This network contained 35 nodes and 101 edges. There were seven hub proteins including, NSF, which is located in the cytoplasm, as well as ATPase and SNAP25, which are found in the plasma membrane. IPA analysis also showed that CNP interacts directly with tubulin and indirectly with ERK1/2. Interestingly, ERK1/2 is a key player in normal cochlear development and hearing.

Conclusions

Our study shows that BKAPs function in neurological disease and ~20% are expressed in the inner ear with some related to hearing loss. Our data provide insights into BK cerebellar function, while revealing a potential roadmap in the cochlea.

PS-25

A Differential Sensitivity to Nifedipine Reveals the Implication of Two Pools of Ca2+ Channels in IHC Exocytosis: A Nifedipine-Insensitive Pool Triggering the RRP and a Nifedipine-Sensitive Pool Controling Vesicular Recruitment to the Ribbon

Philippe Vincent; Didier Dulon
University of Bordeaux

Introduction

Exocytosis at IHCs' ribbon synapses involves L-type CaV1.3 channels and is composed of two components: first, a fast component reflecting the fusion of a RRP (Readily Releasable Pool) of vesicles attached to the ribbon and a secondary slow component corresponding to the recruitment of distant vesicles to replenish the ribbon. Both exocytotic mechanisms have been suggested to be otoferlin and Ca^{2+}-dependent but we still don't know their respective Ca^{2+} sensitivity and whether they use the same pool of Ca^{2+}-channels.

Methods

Ca^{2+} currents and real-time changes in membrane capacitance were here recorded in mouse IHCs (P15-P17) in whole-cell voltage-clamp configuration. We used the property of UV-sensitivity of the dihydropyridine compound nifedipine, which can be transformed into an ineffective nitroso-compound, to instantaneously restore Ca^{2+} currents in cells incubated with 20 µM nifedipine. Brief UV-flashes were delivered with a Mic-LED 365.

Results

The vesicular RRP fusion and recruitment were assessed by stimulating IHCs with a train of 100 ms-repetitive voltage-steps from -80 mV to -10 mV, each stimulation separated by 100 ms. In presence of active nifedipine, the first exocytotic response was systematically comparable to controls (23.2 ± 2.5 fF and 20.5 ± 6.6 fF, $p > 0.05$; control and nifedipine, respectively), even with a Ca^{2+} current decreased by 80 % (-234.9 ± 14.2 pA and -49.7 ± 4.6 pA, $p < 0.001$; control and nifedipine, respectively). The second and following stimulations did not generate significant exocytotic responses in presence of active nifedipine, indicating that the vesicular recruitment process was inhibited. UV-flash inactivation of nifedipine, producing a fast threefold increase in Ca^{2+} current (-49.7 ± 4.6 pA and -141.8 ± 8.4 pA, $p < 0.001$, before and after UV-flash inactivation, respectively) did not instantaneously rescue exocytosis. The exocytotic recruitment capability of IHCs was only restore after the fourth 100 ms stimulation following the UV flash, suggesting the need of a deep diffusion of Ca^{2+} into the cell for an efficient recruitment of distant vesicles.

Conclusions

Our findings argue for an important role of nifedipine-sensitive Ca^{2+} channels in the vesicular recruitment process at the ribbon while a small pool of nifedipine insensitive Ca^{2+} channels essentially controls RRP vesicular fusion

PS-26

Purinergic Modulation of Acetylcholine Release through P2Y and A1 Receptors at the Efferent-Inner Hair Cell Synapse in the Developing Inner Ear

Facundo Alvarez Heduan[1]; Eleonora Katz[2]; Juan Goutman[2]; Ana Belen Elgoyhen[2]
[1]INGEBI (CONICET-UBA); [2]INGEBI

Before the onset of hearing (postnatal day (P) 12 in mice) inner hair cells (IHCs) are transiently innervated by medial olivocochlear (MOC) efferent fibers. Acetylcholine released by these fibers activates α9α10 nicotinic receptors coupled to SK2 calcium-activated potassium channels, leading to inhibitory post synaptic currents (IPSCs). During this developmental period, IHCs fire spontaneous sensory-independent action potentials that are required for normal development of the auditory pathway. Recent studies suggest that this spontaneous activity is driven and/or modulated by ATP released from cochlear supporting cells and that ACh released from efferent fibers would also contribute to this regulation. The main goal of this study is to investigate the role of ATP and their products of hydrolysis such as adenosine in modulating the MOC-IHC synapse.

IHC from Balb/c mice at P9-11 were recorded in the whole-cell patch-clamp mode while applying different agonists and antagonists of purinergic receptors. Neurotransmitter release

was evoked by electrical stimulation of the efferent axons. 100 double pulse (interval: 25 ms) stimuli protocols were applied at a frequency of 1 Hz. The quantal content (*m*) was estimated as the ratio between the mean amplitude of evoked synaptic currents and the mean amplitude of spontaneous synaptic currents.

ATP reversibly decreased *m* in a concentration dependent manner compared to control (1 µM: 15±7 %, 10 µM: 52±14 %; 50 µM: 57±11 %, 100 µM: 51±6 %). Suramin, a non-specific P2 antagonist, abolished the effect of ATP. PPADS, an antagonist with a preferential effect on P2X receptors, and TNP-ATP, a specific P2X antagonist, did not modify ATP-induced inhibition. Furthermore, α,β-MeATP, a specific P2X agonist, had no effect on *m*. Both non-hydrolyzable ATP analog ATPγS, and the specific P2Y agonist 2-MeSADP, mimicked the effect of ATP (39±9 % and 58±7 % compared to control, respectively). Similar effects of ATP and ATPγS were observed during trains of stimuli. Adenosine decreased *m* in a reversible and concentration dependent manner (1 µM: 42±8 %, 10 µM: 70±5 %, 100 µM: 72±4 %). CGS15943, a specific P1 receptor antagonist, abolished the effect of adenosine, while NECA, a specific P1 agonist, decreased *m* (10 µM: 74±0.5 %).

Our results show that both ATP and adenosine inhibit ACh release at the MOC-IHC synapse through the activation of P2Y and A1 receptors, respectively. These results suggest that ATP may have multiple roles in the developing cochlea.

PS-27

BK Channels are not the Target of the NO-cGMP Signaling Cascade in Mouse Inner Hair Cells

Isabelle Lang; Barbara Fell; Stefan Münkner; Jutta Engel
Saarland University

Introduction

The big conductance, voltage and Ca^{2+}-activated K^+ (BK) channel is widely expressed and serves many functions, e.g. controlling smooth muscle tone and neuronal excitability. In mature mammalian inner hair cells (IHCs), BK channels underlie the fast-activating outward K^+ current, $I_{K,f}$, which is responsible for fast repolarization of the receptor potential and for the small time constant of the IHC. Recently, the NO-cGMP signaling pathway involving cGMP-dependent protein kinase type I (cGKI) has been found to protect IHCs from noise trauma (Jaumann et al., Nature Medicine 2012) but the targets of cGKI in IHCs are unknown. In smooth muscle cells, elevated cGMP levels activate cGKI, which phosphorylates and activates BK channels, thereby counteracting cellular depolarization (Lu et al., 1998). We therefore analyzed whether cGMP increases whole-cell BK currents in mature IHCs in a similar way.

Methods

Patch-clamp recordings of BK currents were performed on whole-mounts of the organ of Corti dissected from mature mice (P20). The patch-pipette contained the non-hydrolyzable analogue 8-bromo-cGMP. Because of an intrinsic Ca^{2+} dependence of PKGI, three intracellular free Ca^{2+} concentrations ($[Ca^{2+}]_i$), 1.8 nM, 22 nM and 209 nM, were used in the pipette. Further, the subcellular distribution of BK channels were analyzed using immunofluorescence labeling and image acquisition with two different excitation intensities.

Results

BK currents were isolated by their fast activation kinetics at 1.2 – 1.3 ms after depolarization, when other voltage-activated K^+ channels had not yet opened. Effects of 3 µM 8-bromo-cGMP on IHC BK current amplitudes and activation kinetics were subtle and showed a non-monotonic dependence on $[Ca^{2+}]_i$. Biophysical parameters such as $V_{1/2}$ and steepness obtained from fitting I-V curves to the product of a Boltzmann function times driving force were unaltered at the three $[Ca^{2+}]_i$ concentrations. Immunolabeling of BK channels revealed the known large BK channel clusters at the IHC neck and a smaller pool of BK-positive puncta at the synaptic pole of the IHCs.

Conclusion

Taken together, BK channels are not a major target of the NO-cGMP-cGKI pathway in IHCs. The subcellular distribution of BK channels suggest that the two subpopulations may follow different activation mechanisms, which remains to be determined.

Supported by the DFG (International Research Training Group 1830).

PS-28

Differences in Acetylcholine Response Characteristics between Inner and Outer Hair Cells of Neonatal Mice

Michael Evans[1]; Helen Kennedy[2]
[1]Keele University, UK; [2]University of Bristol

In the cochlea the conversion of sound into nerve activity is subject to inhibitory feedback from the medial population of olivocochlear efferent neurons which directly inhibit the outer hair cells (OHCs). During neonatal development, these cholinergic neurons first target the inner hair cells (IHCs) before reaching the OHCs prior to the onset of hearing. This differential innervation is interesting since it suggests that inhibitory feedback is required before and after cochlear maturation where it is likely to perform different roles. The acetylcholine receptor (AChR) on the hair cells is formed of alpha 9 and alpha 10 subunits producing a cation channel of high calcium permeability, so that channel opening induces a calcium influx which activates SK2 potassium channels resulting in inhibition. We have performed whole-cell recording experiments at room temperature using cesium-BAPTA based internal solutions to investigate the properties of the AChR current in IHCs and OHCs in the excised apical cochlear turn from neonatal mice (P7-P12).

In response to topical ("puff") applications of ACh (0.1-0.5 mM) current-voltage curves reverse at 0 mV and show inward and outward rectification in both hair cell types. Current onsets are fast for OHCs, peaking after about 0.2s, and show evidence of desensitisation over the 0.6 -1.0s application. For

IHCs, currents are generally larger and activate more slowly over about 0.5s. They also show a slower desensitization. For IHCs, the currents are dependent on the level of external calcium, showing a bell-shaped curve with a peak at 0.5 mM calcium, as has been found previously (Gomez-Casati et al, 2005). These preliminary data indicate some clear kinetic differences in the response characteristics of the AChRs in IHCs and OHCs which might underlie different roles played by the efferents' during their developmental progression from targeting IHCs to OHCs.

Reference
Gomez-Casati ME, Fuchs PA, Elgoyhen AB & Katz E (2005). J Physiol 566, 103–118.

PS-29

The Role of Otoferlin in Synaptic Function, Auditory Fatigue and Temperature Sensitive Auditory Neuropathy

Nicola Strenzke; Gulnara Yamanbaeva; Elisabeth Auge; Ellen Reisinger
Göttingen University

The hair-cell specific protein Otoferlin is essential for transmitter release at the inner hair cell ribbon synapse. Otoferlin knockout mice and human patients with hair cells deficient for this protein are profoundly deaf, hindering a further dissection of the underlying synaptic mechanisms. A role for otoferlin in synaptic vesicle replenishment and a late step for exocytosis has been suggested based on *in vivo* and *in vitro* electrophysiological data from the "*pachanga*" mouse line which has reduced otoferlin expression in inner hair cells.

We now analyzed auditory systems responses in a new mouse mutant carrying the I515T point mutation which in humans causes a temperature-sensitive auditory synaptopathy/neuropathy phenotype. Auditory brainstem response (ABR) wave I amplitude was reduced and thresholds were only moderately elevated, enabling further systems physiology analysis in these mice. Hearing loss was more severe in mutants carrying one I515T and one knockout allele. Together with immunohistochemical and cell physiological data, this suggests that the severity of the phenotype in otoferlin mutant mice scales with the amount of otoferlin expression. Heat exposure appears to further reduce otoferlin protein levels and led to a linear decrease of ABR wave I amplitude in both wildtype and mutant mice.

Sound-induced spiking in single auditory nerve fibers from otoferlin I515T mutants was well-preserved when low stimulus rates were used, but showed a dramatic reduction in spike rates at higher stimulation rates. Adaptation was increased and recovery from adaptation was delayed, resulting in a deficit in gap detection performance in prepulse inhibition of the startle response and in an operant conditioning behavioral task. In line with the normal single neuron response thresholds, subjective hearing thresholds appeared normal.

Our data suggest an expression-dependent severity of the phenotype in otoferlin mutants which is dominated by enhanced auditory fatigue, These findings are consistent with the human phenotype.

PS-30

α2δ2 Controls the Function and Trans-synaptic Coupling of Cav1.3 Channels in Mouse Inner Hair Cells and is Essential for Normal Hearing

Barbara Fell[1]; Stephanie Eckrich[1]; Dietmar Hecker[1]; Gerald J. Obermair[2]; Veit Flockerzi[1]; Bernhard Schick[1]; Jutta Engel[1]
[1]Saarland University; [2]Medical University Innsbruck

Voltage-gated calcium channels (VGCCs) are protein complexes composed of an α_1 pore-forming subunit and auxiliary subunits β and $\alpha_2\delta$. VGCCs of cochlear inner hair cells (IHCs) are mainly composed of the subunits $Ca_v1.3$ (Platzer et al., Cell 2000) and β2 (Neef et al., J. Neurosci. 2009), and lack of either $Ca_v1.3$ or β2 causes deafness. So far, expression and contribution of the four $\alpha_2\delta$ subunits $\alpha_2\delta1$-4, which assist in channel trafficking and can modulate I_{Ca} gating properties, are unknown.

Inner hair cells (IHCs) expressed $\alpha_2\delta2$ mRNA at pre-hearing and hearing age as shown by quantitative RT-PCR. Therefore we analysed hearing and IHCs of ducky mice ($\alpha_2\delta2^{du/du}$), a mouse line with a mutation in the CACNA2D2 gene encoding a non-functional $\alpha_2\delta2$ protein. Elevated auditory brainstem response (ABR) click and frequency-dependent hearing thresholds were found in the ducky mice. Moreover, averaged ABR waveform 40 dB over click threshold showed a significant delay of wave II (discharge of auditory nerve fibers) and distortion of wave IV. Otoacoustic emissions were not impaired pointing to a normal outer hair cell (OHCs) function.

Immunolabeling showed normal expression of IHC presynaptic $Ca_v1.3$ and $Ca_v\beta2$. Peak Ca^{2+} and Ba^{2+} current densities of IHCs were reduced by 29% and voltages for half-maximum activation of Ca^{2+} and Ba^{2+} currents were shifted by 5 mV and 7 mV. As a result of the reduced calcium currents, exocytosis of IHCs in ducky mice was significantly reduced between -15 and -5 mV. These results are in accordance with the classical role of $\alpha_2\delta$ subunits in surface expression and gating modulation of VGCCs. Quantification of double-immunolabeled presynaptic $Ca_v1.3$-clusters and postsynaptic AMPA/PSD-95 receptor complexes by line scan analyses revealed impaired trans-synaptic coupling of pre- and postsynaptic proteins at the IHC synapse in ducky mice. The number of both, separated $Ca_v1.3$ clusters and PSD-95 clusters was significantly increased whereas the total number of these clusters was unchanged.

We here show that $\alpha_2\delta2$ plays a crucial role in the composition of IHC Ca^{2+} channels and forms VGCC complexes at an excitatory synapse together with $Ca_v1.3$ and β2. These findings implicate a novel role for the $\alpha_2\delta2$ subunit, which is localized extracellulary and contains protein-protein interaction domains, for optimal positioning of the presynaptic release site and the postsynaptic receptor complex in ultrafast synaptic transmission.

PS-31

A History of Temporary Threshold Shift (TTS) Research

Rickie Davis[1]; Christa Themann[2]
[1]National Institute for Occupational Safety and Health; [2]NIOSH

We all have experienced the loss of hearing sensitivity upon exposure to loud sounds that resolves over hours or days. It is probable that those during the early days of man also experienced temporary threshold shifts. The advent of electronics in the early 20th century allowed for reproducible presentation of a sound stimulus. This sound stimulus level could be manipulated allowing for reliable measurement of Temporary Threshold Shifts (TTS) and Permanent Threshold Shifts (PTS) and ultimately led to the clinical audiometer. Electronics also allowed for noise exposures to be presented in the loudness range where TTS and PTS could be carefully studied in the laboratory.

As purposely creating PTS in humans is unethical, studies of TTS and Asymptotic Threshold Shift (ATS, a TTS that grows over 6-12 hours of noise exposure) became the foundation for rules and regulations designed to prevent Permanent Threshold Shift. This research was later used to develop occupational and environmental noise limits. Later studies indicated that TTS was not a good predictor of PTS, and the research fell out of favor. Recently, TTS research has experienced a resurgence, as advanced imaging techniques allow study of specific underlying mechanisms and challenge previous assumptions about threshold shift. This poster will review seminal research on TTS beginning with World War II.

PS-32

Variation Analysis of Transcriptome Data Reveals Candidate Genes for Further Investigation of Individual Variation in Cochlear Responses to Acoustic Trauma

Bohua Hu[1]; Shuzhi Yang[1,2]; Qunfeng Cai[1]; Robert Vethanayagam[1]; Youyi Dong[1]; Jonathan Bard[1]; Jennifer Jamison[1]
[1]State University of New York at Buffalo; [2]The First Affiliated Hospital of Chinese PLA General Hospital

Introduction

Individuals display different susceptibility to acoustic trauma. Although this variation has been linked to multiple biological events, its molecular basis is still not clear. One strategy to address this question is to identify the genes that contribute to the individual variation. Given the presence of a large number of genes expressed in the cochlea, selecting candidate genes for an in-depth investigation is a research challenge. In this investigation, we analyzed the expression variation of cochlear genes using RNA-sequencing (RNA-seq) data to identify the genes that potentially contribute to individual variation.

Methods

C57BL/6J mice were exposed to a broadband noise at 120 dB SPL for 1 hour. The cochlear sensory epithelia were collected at 1 day post-noise exposure for RNA-seq. The RNA-seq data were analyzed to identify the genes showing an increased expression variation after the acoustic trauma. The functional relevance of these identified genes were defined using two bioinformatic tools: the database of annotation, visualization and integrated discovery (DAVID) and Ingenuity pathway analysis (IPA). To verify the results, we examined the change in expression of 84 genes responsible for mitochondrial function using qRT-PCR in animals showing different levels of cochlear dysfunction after acoustic overstimulation.

Results

Control samples without acoustic trauma displayed diverse levels of variation in FPKM values across individual genes. This variation was significantly increased for some genes, but remained unchanged or decreased for others after acoustic trauma. Bioinformatics analyses revealed that the genes with increased variation were related to the molecular pathways of apoptosis, cell damage and defense. By contrast, the genes that were stable were functionally related to basic biological processes. Further screening of the genes responsible for mitochondrial function revealed three genes showing a damage-level dependent expression change. All these genes displayed increased individual variation in their expression levels measured by RNA-seq after the noise injury, suggesting that the genes with the increased expression variation are likely to contribute to individual variation in the cochlear response to acoustic trauma.

Conclusion

Variation analysis of RNA-seq data is a valuable strategy for identification of candidate genes for further investigation into the molecular basis of individual variation in the cochlear response to acoustic overstimulation.

PS-33

9-methyl-beta-carboline: Protection against Cisplatin-Induced Toxicity in vitro and Pharmacokinetics following Intratympanic Injection

Catrin Wernicke[1]; Jacqueline Hellwig[1]; Nicole Gottschalk[1]; Florian Theden[2]; Rachael Ward[2]; Tomasz Zygmunt[2]; Stefan Plontke[3]; Hans Rommelspacher[2]
[1]The Technical University of Applied Sciences Wildau; [2]AudioCure Pharma GmbH; [3]ENT Clinic of the University of Halle (Saale)

Previous studies have demonstrated that 9-methyl-beta-carboline (9MßC) promotes cell survival and neuroregeneration through mechanisms that include: 1) increased performance of the respiratory chain; 2) increased transcription and expression of the neurotrophins; 3) reduced levels of ROS; 4) decreased apoptosis and; 5) the reduced expression of inflammatory modulators. We hypothesized that these properties may also protect hair cells from the burden of ototoxicity caused by a range of chemicals including the chemotherapeutic agent cisplatin. Therefore, we investigated the effect of 9MßC in an *in vitro* model of cisplatin-induced toxicity in the human neuroblastoma cell line SH-SY5Y.

Cells were pre-treated for 2, 4 and 7 days with 9MßC and subsequently treated with different concentrations of cisplatin for 3 days. Cell viability was determined with the MTS assay and caspase activation was measured. Furthermore, we used real-time RT-PCR to investigate the expression of the apoptosis regulating factors Bax and Bcl2 and of several factors known to be involved in cell survival and protection. Pre-treatment with 9MßC for 4 and 7 days significantly reduced cisplatin-induced apoptotic cell death. This was accompanied by an enhanced transcription of the anti-apoptotic Bcl2. Treatment of SH-SY5Y cells with 9MßC induced up-regulation of several neurotrophic factors including brain derived neurotrophic factor (BDNF), neurotrophin factor 3 (NT3) and the neuroprotective factors cerebellin, leukemia inhibitory factor (Lif), B-cell translocation gene 2 (BTG2) and inhibitor of DNA binding 2 (ID2). In contrast, the Bax/Bcl2 ratio was down-regulated.

This *in vitro* data prompted us to begin developing 9MßC for the treatment of hearing loss *in vivo.* The pharmacokinetic profile of 9MßC formulated in a thermo-reversible polymer gel (poloxamer 407) was investigated following intratympanic administration in the guinea pig. The gel formulation led to a sustained release of drug within the perilymph up to 48 hours after administration with an elimination half-life of 3.4 hours and limited systemic exposure. Functional analysis with brainstem-evoked response audiometry (BERA) and histological examination revealed no adverse effects of the poloxamer 407 vehicle.

These results demonstrate that 9MßC significantly protects against cisplatin-induced cell death by mechanisms that include a reduction in apoptosis and the increased expression of a range of neuroprotective factors. Moreover, when delivered in a poloxamer gel, 9MßC is released into the inner ear in a slow, sustained manner that could be suitable for clinical application. Studies investigating the functional effects of 9MßC in a guinea pig model of noise trauma are underway.

PS-34

Cilia Mutants Confer Resistance to Neomycin-Induced Hair Cell Death

Tamara Stawicki; Liana Hernandez; Robert Esterberg; Tor Linbo; Kelly Owens; Edwin Rubel; David Raible
University of Washington

Hearing loss as a result of hair cell death is a dose limiting side effect of multiple therapeutic drugs, including aminoglycoside antibiotics and chemotherapeutics. Our goal is to identify novel genes involved in hair cell death and survival in response to these medications. We have used the zebrafish lateral line system to screen for mutations that confer protection against hair cell death in response to neomycin. Through this screening we have identified a mutation in the *dynein cytoplasmic 2 heavy chain 1 gene (dync2h1). dync2h1* has been implicated in other systems in retrograde intraflagellar transport in cilia. *dync2h1* mutants show the curved body phenotype typically seen in zebrafish cilia mutants. *dync2h1* is the second cilia gene identified through this screen, the first being the transition zone gene *cc2d2a* (Owens et al, PLOS Genetics, 2008). Hair cells of the lateral line in *dync2h1* mutants appear to initially develop normally, however, by 5 days post fertilization (dpf) their kinocilia are dramatically shortened and there is a reduction in total hair cell number. These phenotypes are similar to what has previously been reported in the anterograde intraflagellar transport gene *ift88* (Tsujikawa & Malicki, Neuron, 2004) and indeed we find that *ift88* mutants show a similar degree of protection against neomycin as *dync2h1* mutants. In contrast to the loss of kinocilia seen in *dync2h1* and *ift88* mutants, *cc2d2a* mutants show grossly normal kinocilia morphology. *cc2d2a* mutants also show less protection against neomycin-induced hair cell death then *dync2h1* and *ift88* mutants. Using neomycin conjugated to Texas Red we investigated neomycin uptake in our cilia mutants. We found that *dync2h1* mutants showed a reduction in neomycin uptake whereas *cc2d2a* mutants showed no difference in neomycin uptake when compared to their wild-type siblings. Therefore, while both cilia genes are involved in neomycin-induced hair cell death they appear to function via different mechanisms. Future experiments will look at other cilia mutants to further delineate the cilia signaling pathways responsible for modulation of aminoglycoside-induced hair cell death.

PS-35

Overexpression of X-linked Inhibitor of Apoptosis Protein Protects Against Neomycin-Induced Hair Cell Loss in the Apical Turn of the Cochlea During the Ototoxic-sensitive Period

Shan Sun[1]; Mingzhi Sun[1]; Yanping Zhang[2]; Muhammad Waqas[3]; Huiqian Yu[2]; Yingzi He[2]; Shankai Yin[4]; Jian Wang[4]; Renjie Chai[3]; Huawei Li[2]
[1]University of Fudan; [2]Fudan University; [3]Southeast University; [4]the Sixth Hospital Affiliated to Shanghai Jiao Tong University

Background

Aminoglycoside-induced cochlear ototoxicity causes hair cell (HC) loss and results in hearing impairment in patients. Previous studies have developed the concept of an ototoxicity sensitive period during which the cochleae of young mice are more vulnerable to auditory trauma than adults. However, the mechanisms involved in the ototoxicity-sensitive period are not well understood.

Methods

Here, we first used wild type mice to compare the neomycin-induced ototoxicity at four developmental ages in mice postnatal day (P)1–P7, P8–P14, P15–P21, and P60–P66. We then measured the expression levels of apoptosis-related genes in response to neomycin administration in mice at different developmental stages with qPCR. Last, we used the X-linked inhibitor of apoptosis protein (XIAP) overexpression transgenic mice where the XIAP is overexpressed in this transgenic mouse; neomycin was injected from P8 to P14 to ablate HC, ABR was measured and tissues examined at P30.

Results

In this study, we compared neomycin-induced ototoxicity at four developmental ages described as above and found that

when neomycin was administrated during from P8 to P14, the auditory brainstem response threshold increase was significantly higher at low frequencies and HC loss was significantly greater in the apical turn of the cochlea compared to neomycin administration during the other age ranges. qPCR data revealed that the expression of apoptotic markers, including *Casp3* and *Casp9*, was significantly higher when neomycin was injected from P8 to P14, while the expression of XIAP gene was significantly higher when neomycin was injected from P60 to P66. Because XIAP expression was low during the neomycin-sensitive period, we overexpressed XIAP in mice and found that it could protect against neomycin-induced hearing loss at low frequencies and HC loss in the apical turn of the cochlea.

Conclusion

Our findings demonstrate a protective role for XIAP against neomycin-induced hearing loss and HC loss in the apical turn of the cochlea during the ototoxic-sensitive period. These results also provide *in vivo* evidence that apoptotic factors are involved in the sensitive period of neomycin-induced ototoxicity. Overexpression of XIAP, therefore, might serve as a novel therapeutic target for reducing aminoglycoside-induced HC damage and hearing loss.

PS-36

Role of Spiral Ligament Fibrocyte-derived CXCL2 in Cochlear Inflammation

Jeong-Im Woo; Sung-Hee Kil; Yoo Jin Lee; David Lim; Sung Moon
University of California, Los Angeles

Cochlear inflammation is critically involved in the pathogenesis of various cochlear diseases such as meningitis-associated hearing loss, cisplatin ototoxicity and acoustic trauma. Previously, we have shown that the spiral ligament fibrocytes (SLFs) play a pivotal role in cochlear inflammation through recognition of pro-inflammatory molecules and release of various chemokines such as CCL2 and CXCL2. Since neutrophils are known to contribute to tissue damage in a variety of human diseases, we aimed to determine the molecular mechanism involved in the CXCL2/CXCR2 axis in cochlear inflammation. Migration assays showed that lysozyme M-positive PMNs are attracted by the conditioned medium of rat SLF cell line (RSL) cells exposed to the lysate of nontypeable *H. influenzae* (NTHi). It was found that mouse bone marrow-derived cells and splenocytes are attracted by the conditioned medium of the IL-1β-exposed RSL cells. Quantitative RT-PCR analysis showed that RSL cells up-regulate CXCL2 upon exposure to pro-inflammatory cytokines such as IL-1β. Luciferase assays showed that NTHi-induced CXCL2 up-regulation is inhibited by a chemical inhibitor of p90RSK, BRD7398. CXCR2-deficient PMNs were less attracted by the conditioned medium of the NTHi-exposed RSL cells than wild-type PMNs. A selective CXCR2 inhibitor, SB225002, appeared to suppress migration of HL-60 cells (a human acute promyelocytic leukemia cell line) in response to the conditioned medium of the IL-1b-exposed RSL cells. Flow cytometric analysis with Fluo-3 showed that calcium is mobilized by the conditioned medium of the IL-1b-exposed RSL cells. Calcium assays with Fura-2 showed that SB225002 inhibits calcium mobilization by the conditioned medium of the NTHi-exposed RSL cells. Taken together, we suggest that SLFs up-regulate CXCL2 via p90RSK signaling, resulting in cochlear infiltration of neutrophils through CXCR2-mediated calcium mobilization.

PS-37

Apoptotic and Necrotic Cell Death in Cochlea Treated With Kanamycin or Kanamycin Plus Ethacrynic Acid

Dalian Ding; Haiyan Jiang; Peng Li; Kelei Gao; Hong Sun; Richard Salvi
University at Buffalo

Background

Cell death generally occurs by apoptosis or necrosis. Apoptosis, a carefully orchestrated intracellular death program, is triggered by a wide range of stimuli that regulate a network of proapoptotic and antiapoptotic proteins that leads to the removal of damaged or excess cells. The major morphological characteristics of apoptosis are blebbing, cell shrinkage, nuclear fragmentation, chromatin condensation and chromosomal DNA fragmentation. In contrast, necrosis is triggered by external factors that results in cell swelling, membrane rupture and the uncontrolled release of the cell's contents into the extracellular. Here we identified the cochlear cell death pathways in an acute cell death model in which adult rats were treated with co-administration of kanamycin (500 mg/kg, I.M.) plus ethacrynic acid (40 mg/kg, I.V.) and a chronic cell death model in which adults rats were treated for seven consecutive days with daily injection of kanamycin (500 mg/kg, I.M.).

Methods

Cochlea hair cell death was identified using an Apoptosis-Necrosis Quantification Kit. Apoptotic cells were identified by annexin V conjugated with FITC (green fluorescence) which specifically binds to the phosphatidylserine exposed on the outer membrane leaflet. Necrotic cells were identified by labeling (red fluorescence) with ethidium homodimer III (EthD-III), a highly charged nucleic acid probe. Healthy cells were labeled with the membrane-permeant blue fluorescent DNA dye, Hoechst 33342.

Results

In acute damage induced by kanamycin plus ethacrynic acid, hair cell death occurred exclusively by apoptosis (green fluorescence); necrotic cell death (red fluorescence) was not detected. In contrast, chronic damage induced by seven consecutive days of kanamycin treatment was characterized by a mixture of apoptotic and necrotic hair cell death.

Conclusions

Chronic hair cell death from kanamycin can occur either by an apoptotic or necrotic route; potential intervention strategies to promote hair cell survival will likely only rescue those dying by apoptosis. Since acute hair cell death from the combination of kanamycin plus ethacrynic acid occurs predominantly by apoptosis, interventions to rescue these cells would seem to

be more favorable provided that the intervention is potent and occurs early enough to block the cell death cascade.

PS-38

The Middle Ear Muscle Reflex in the Diagnosis of Cochlear Neuropathy

Michelle Valero; M. Charles Liberman
Massachusetts Eye and Ear Infirmary

Introduction

Cochlear neuropathy, i.e., loss of cochlear nerve fibers without loss of hair cells, is an important problem in age-related hearing loss (ARHL), in noise-induced hearing loss (NIHL), and possibly in other types of acquired sensorineural hearing loss. Cochlear neuropathy does not elevate behavioral thresholds until ~90% of the cochlear nerve fibers are lost, but even more moderate pathologies may cause significant perceptual and physiological deficits. Therefore, there is a need for new approaches to diagnose this condition in humans. The subset of cochlear nerve fibers with high thresholds and low spontaneous rates (SRs) are the most vulnerable in both ARHL and NIHL, and they may be particularly important in driving the middle-ear muscle reflexes (MEMR). Because one role of the MEMR is to protect the inner ear from high-level sounds, low-SR neuropathy can lead to a vicious cycle wherein the ear becomes more vulnerable and damaged as its protective mechanisms deteriorate. Thus, an early diagnostic tool would be of great value.

Methods

We induced low-SR cochlear neuropathy by exposing young mice to a 1-octave (8 – 16 kHz) band of noise at ~98 dB for 2 hours. Auditory brainstem responses and distortion-product otoacoustic emissions (DPOAEs) were used to verify temporary threshold shifts and recovery. We then measured 1) the modulation of high-level DPOAEs by contralateral acoustic stimulation (CAS) or 2) the modulation of chirp spectra by CAS. The second paradigm was employed to temporally separate the OAE from the stimulus. Here, we focus only on the changes in the ear-canal sound pressure due to CAS. For both paradigms, measurements were taken before and after administration of α-D-tubocurarine to block the MEMR followed by strychnine to block the olivocochlear efferent reflex. Synapse counts were measured in cochlear whole mounts to confirm the neuropathy.

Results

We found that CAS-modulation of high-level DPOAEs is dominated by the MEMR in anesthetized mice, with a smaller contribution from the olivocochlear efferent pathway. CAS modulation of the chirp spectra was fully mediated by the MEMR. CAS modulation in both experimental paradigms was greatly attenuated in subjects with temporary threshold shifts and a permanent low-SR-specific neuropathy.

Conclusions

The magnitude of the MEMR is attenuated and its threshold elevated in mice with low-SR cochlear neuropathy. Therefore, the MEMR may be valuable in the early detection of this important pathology.

PS-39

Protective Effect of Astaxanthin Nano Emulsion in Vestibular Hair Cells

Kazuma Sugahara[1]; Yousuke Takemoto[2]; Makoto Hashimoto[2]; Yousuke Takemoto[2]; Hiroaki Shimogori[2]; Hiroshi Yamashita[2]
[1]Yamaguchi University Graduate School of Medicine; [2]Department of Otolaryngology, Yamaguchi University Graduate School of Medicine

Introduction

It was known that aminoglycoside induced hair cell death was related with the free radical generation. Many kinds of molecules can protect hair cells against aminoglycoside ototoxicity. Astaxanthin is a kind of carotenoid and provides the red color of **salmon** meat and the red color of cooked **shellfish**. Astaxanthin has the strong antioxidant activity. Therefore, the dietary supplement and cosmetics which contain astaxanthin were manufactured in many countries. However, Astaxanthin was difficult to transit to the living tissue, because the molecule is a lipophilic material. Nano nano emulsion of astaxanthin was developed in Fuji film company (Japan). The nano emulsion can diffuse into water and transit to the living tissue.

In the present study, we evaluated the protective effect of nano emulsion of astaxanthin on the inner ear sensory cells against neomycin ototoxicity.

Materials and Methods

Cultured utricles of CBA/N mice were used. Cultured utricles were divided to three groups (Control group, Neomycin group, Neomycin + Astaxanthin group). In the Neomycin group, utricles were cultured with neomycin (2 mM) to induce hair cell death. In Neomycin + Astaxanthin group, utricles were cultured with neomycin and Astaxanthin (100 – 1 μM). Twenty-four hours after exposure to neomycin, the cultured tissues were fixed with 4% paraformaldehyde. To label hair cells, immunohistochemistry were performed using anti-calmodulin antibody. The rate of survival vestibular hair cells was evaluated with the fluorescence microscope. In addition, immunohistochemistry against 4-hydroxy-2-nonenal was performed to evaluate the product of hydroxy radical.

Results

The survival rate of hair cells in Neomycin + Astaxanthin group was significantly more than that in Neomycin group. The signals of 4-hydroxy-2-nonenal were inhibited in neomycin + Astaxanthin group.

Discussion

As the clinical effects of astaxanthin, the inhibition of diabetic complications, eye diseases, cancer prevention, and anti-fatigue action has been reported. In this study we showed that nano emulsion of astaxanthin protects sensory hair cells against neomycin-induced death in mammalian vestibular epithelium. The nano emulsion of astaxanthin can be used as the protective drug in the inner ear.

PS-40

Interleukin-6 Hyperpolarizes Strial Capillary Endothelial Cells by Activation of Stretch-Gated Chloride Channels

Yuqin Yang; Hongzhe Li; Peter Steyger; **Zhi-Gen Jiang**
Oregon Health & Science University

Background

In murine models of aminoglycoside ototoxicity with bacterial sepsis, endotoxemia elevates systemic and cochlear proinflammatory cytokine levels, enhances cochlear uptake of aminoglycosides, and exaggerates ototoxicity. The underlying mechanisms are poorly understood. We hypothesized that endotoxemia-induced cytokines alter the electrophysiology of endothelial cells of strial capillary networks to facilitate aminoglycoside trafficking within the cochlea.

Methods

We tested whether selected interleukins (ILs) alter whole-cell membrane potential and currents in endothelial cells (ECs) of dissociated capillaries from the guinea pig cochlear strial vascularis.

Results

We found that (1) capillary ECs *in vitro* can be distinguished from pericytes (PC) morphologically and electrophysiologically. The ECs normally showed a higher input resistance (1 – 4 GΩ) with mild outward rectification but no inward rectification in I/V curves. PCs typically displayed a Ba^{2+}-sensitive inward rectification. (2) In ECs, but not PCs, 5 -10 min application of IL-6 (0.1 nM) or IL-10 (1 nM) slowly activated a robust long-lasting (>1 h) and partially reversible outwardly rectifying current with a reversal potential between -30 and -62 mV, causing a 5–18 mV hyperpolarization. In contrast, IL-1α (10-100 nM) and LPS (20-100 µg/ml) had no such effect. (3) This IL-activated current was suppressed by the Cl^--channel blocker niflumic acid (30 µM), also by the classic Cl^--channel blockers 300 µM DIDS or DPC, and by phospholipase A2 inhibitor cyclosporine (300 µM), but not sensitive to K^+-channel blockers TEA, 4-AP and Ba^{2+} (all 1 mM) or cation channel blockers La^{3+} (100 µM) and Gd^{3+} (30 µM) or opioid receptor antagonist naloxon (10 µM). (4) Hypotonic solution (200 mOsm/l) activated a current with a voltage- and time-dependency, dynamics and pharmacological profile similar to those of the IL-activated current. (5) The actions of hypotonicity and the ILs had a reciprocal masking rather than additive or facilitating effect when applied one after another separated by a ~30 min interval. (6) Application of either the effective ILs or the hypotonic solution often caused visible swelling of the recorded and adjacent ECs.

Conclusions

At least two interleukins activate a chloride current with biophysical and pharmacological profiles similar to those of volume-gated Cl^- channels, resulting in hyperpolarization. This hyperpolarization increases the electrophoretic driving force for aminoglycosides entering the endothelial cells and will promote trafficking of the circulating drug into the intrastrial space. These data indicate that specific cytokines such as IL-6 and IL-10 contribute to enhanced aminoglycoside ototoxicity in endotoxemia.

PS-41

Cochlear Hair Cell Damage Activates Type II Afferent Neurons

Chang Liu; Elisabeth Glowatzki; Paul Fuchs
Johns Hopkins University School of Medicine

The mammalian cochlea is innervated by two groups of cochlear afferents – larger caliber, myelinated type I afferents contact inner hair cells for high fidelity transmission of acoustic information. In contrast, the function of sparse, unmyelinated type II afferents has been mysterious for decades. Here we asked whether type II afferents, in addition to glutamatergic excitation by outer hair cells (OHCs), also may detect damaged tissue, as during acoustic trauma. We performed intracellular giga-ohm seal recordings from type II afferents near their terminal arbors under OHCs in excised cochlear turns from young rats (P7 – P9), then ruptured individual OHCs with a sharp glass needle. Strikingly, upon hair cell rupture, action potentials are elicited in type II afferents. In voltage clamp, hair cell damage induces a large inward current, composed of a fast component likely carried by potassium ions and a slow component eliminated by the ATP receptor blocker, PPADS. The slow component also was reduced by the connexin hemichannel blocker carbenoxolone, suggesting the damage response may involve ATP release from cochlear outer sulcus cells. We characterized the intrinsic purinergic responses of type II afferents. Both ATP and UTP (a P2Y receptor agonist) depolarized all tested afferents, as shown previously (Weisz et al., 2009 Nature 461:1027). ATP-evoked currents reversed at 0mV and could be blocked by the P2X antagonist PPADS, suggesting the opening of ionotropic P2X receptors. On the other hand, UTP-evoked currents reversed near -80mV and could be antagonized by XE-991, an inhibitor of KCNQ channels, suggesting that UTP activates metabotropic P2Y receptors to close KCNQ channels through second messenger mediated pathways. Moreover, we found that the KCNQ channel opener retigabine prevented excitation of type II afferents when hair cells were damaged, consistent with the role of KCNQ channels in regulating neuronal excitability. Our results suggest that type II cochlear afferents could respond to tissue damage which might occur under noxious levels of sound. The mechanism involves ATP acting through ionotropic P2X receptor and metabotropic P2Y receptors.

PS-42

Analysis of Preferred Listening Levels from an MP3 Player: Effects of Earphone Type, Music Genre, and Listening Duration

Miseung Koo[1]; **Hyun-Yong Shim**[2]; Jinsook Kim[3]
[1]Graduate School of Hallym University, Chuncheon-si; [2]Hearing Research Laboratory of SMC-SEC, Department of Otorhinolaryngology Samsung Medical Center; [3]Division of Speech-language Pathology and Audiology, College of Natural Sciences, Hallym University

The Improper use of personal listening devices causes hearing loss by two potential elements: individual's preferred listening levels (PLLs) and exposure duration (Portnuff et al., 2011). In the literature, the following factors have been generally discussed as affecting the PLLs: background noise, a music genre and an earphone type (Keppler et al., 2010; Kim, 2013). With the two factors, the longer listening duration has been considered to affect the PLL. This study investigated the effects of the earphone types (earbuds or over-the-ear earphones), the music genre (ballad or dance), and the listening duration (30 or 60 minutes) on sound pressure levels (SPLs) and PLLs from an MP3 player. The PLL data was used to find whether there was a frequency characteristic of Korean pop music. The experiment was carried out in a quiet room designed to be under the provisions of ANSI s3.1 (1999) and OSHA (1996). Twenty-two normal hearing young adults participated in the study. Each participant was asked to select his or her most PLLs. One earphone was connected to the participant's better ear and the other was linked to a sound level meter via a 2 cc-coupler or an artificial ear to measure the SPLs. Repeated analysis of variance (ANOVA) was used to analyze data with an earphone type, a music genre, and listening duration as an independent factor, and the loudness A-weighted equivalent continuous noise level (LAeq) in dBA as a dependent variable. And a paired sample t-test was used to compare the PLL of the two music genres. There was no significant main effect on the PLLs and no significant interactions among the three factors. Overall SPLs and PLLs of the earbuds were about 10 dBA and 1.78 dBA greater, respectively, at maximum volume setting, than those of the over-the-ear earphones. The average PLLs for ballad were higher than dance music. The PLLs, for both music genres, were greatest at 500 Hz followed by 1,000, 250, 2,000, 4,000, 125, 8,000 Hz. At the four frequencies of 250, 2,000, 4,000, and 8,000 Hz, the PLLs were significantly different ($P < 0.05$). The PLLs for Korean pop music was similar to other genres' in the tested factors. The result of the earphone type suggested that supra-aural (over-the-ear) type earphones seemed to be more suitable to prevent NIHL as lower PLLs for the over-the-ear earphones, possibly due to isolation from the background noise.

Table 1: SPLs (LAeq, LAFmax) of both genres on various volume levels

Volume (%)	LAeq (dBA)				LAFmax (dBA)			
	Earbuds		Over-the-ear earphones		Earbuds		Over-the-ear earphones	
	Ballad	Dance	Ballad	Dance	Ballad	Dance	Ballad	Dance
10(25)	70.9	73.4	57.3	60.7	80.6	82.9	68.2	70.7
20(50)	85.9	88.4	72.1	75.3	95.7	97.9	83.0	85.2
30(75)	100.9	103.4	89.3	92.7	110.5	112.6	101.0	103.1
40(100)	115.5	117.9	104.3	107.5	124.1	126.2	115.9	116.1

Table 2: Data of the PLLs selected by each participant

Ballad					Dance			
$LAeq_{,30mins}$ (dBA)		$LAFmax_{,30mins}$ (dBA)		Volume	$LAeq_{,30mins}$ (dBA)		$LAFmax_{,30mins}$ (dBA)	
earbuds	over-the-ear earphones	earbuds	over-the-ear earphones		earbuds	over-the-ear earphones	earbuds	over-the-ear earphones
57.9 (1)		78.1		**1**	60.9 (3)		77.2	
	52.2 (1)		66.6	**2**	60.9 (2)	54.6 (2)	72.7	68.8
60.6 (1)		69.7		**3**	63.6 (4)		76.6	
62.5 (8)	54.3 (2)	72.6	64.6	**4**	64.6 (5)	51.7 (2)	74.2	64.2
64.3 (3)		78.1		**5**	65.1 (3)	54.7 (2)	74.0	72.2
65.0 (1)	55.9 (2)	74.9	73.5	**6**		55.5 (2)		64.2
65.9 (3)	52.9 (1)	75.9	68.2	**7**	69.1 (1)	60.3 (2)	78.6	70.7
	61.3 (1)		71.9	**8**		60.0 (1)		73.5
	60.3 (1)		72.1	**9**		60.1 (1)		70.0
71.2 (2)	57.4 (1)	80.8	68.5	**10**		66.2 (4)		76.9
	58.3 (1)		69.0	**11**	74.8 (1)		84.2	
	63.1 (1)		75.6	**12**				
				13		68.0 (1)		78.4
	67.5 (2)		79.2	**14**	79.2 (2)	73.1 (1)	88.9	82.8
81.5 (1)		91.4		**15**				
	68.4 (1)		78.4	**16**				
81.6 (1)	68.9 (2)	91.5	81.4	**17**		68.9 (1)		77.9
	75.3 (1)		79.2	**18**		76.0 (1)		84.8
	78.4 (1)		88.9	**20**				
	76.1 (1)		86.4	**23**				
	83.5 (1)		94.6	**24**		79.6 (1)		89.1
				25	95.5 (1)		105.2	
	83.8 (1)		94.8	**27**				
				30		93.2 (1)		101.7
94.9 (1)		106.1		**32**				
	98.8 (1)		109.4	**36**				

Table 3: Average PLLs regarding the three variables

Music Genre		Ballad		Dance	
Listening Duration		30 min.	60 min.	30 min.	60 min.
Earphone Type	Earbuds	67.00	66.00	67.03	65.61
	Over-the-ear earphones	66.49	65.17	63.50	63.53

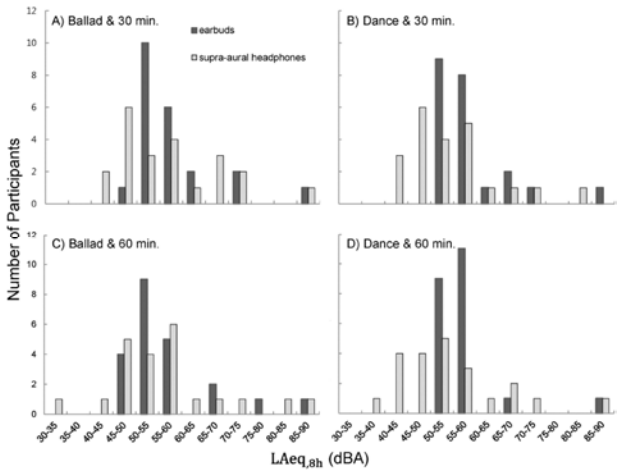

Figure 1: Distribution of the PLLs ($LAeq_{,8h}$) with earbuds and over-the-ear earphones

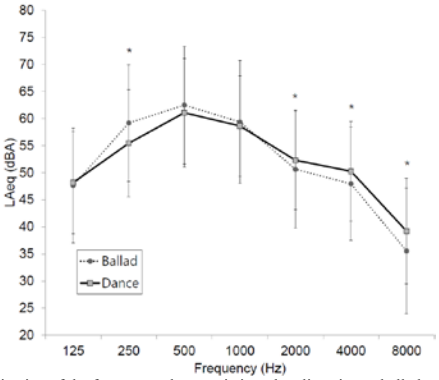

Figure 2: Schematization of the frequency characteristics when listening to ballad and dance music. At 250 Hz, the PLLs of dance music were significantly lower than those of dance. On the other hand, at the frequencies of 2,000 Hz and greater, the PLLs of dance music were significantly greater.

PS-43

Spiral Ganglion Neurons in Postnatal Day 3 Rats Are More Vulnerable than Their Mature Counterparts

Kelei Gao[1]; Dalian Ding[1]; Peng Li[2]; Haiyan Jiang[1]; Hong Sun[3]; Richard Salvi[1]

[1]University at Buffalo, SUNY; [2]Sun Yat-Sen University; [3]Central South University

Background

Aminoglycoside antibiotics are widely used clinically to treat life threatening bacterial infections; however, ototoxicity is one of its severe dose-limiting side effects. The prevailing view in the literature is that the sensory hair cells are the primary ototoxic target of aminoglycoside antibiotics and that spiral ganglion neurons only begin to degenerate weeks or months after the hair cells have died off due to lack neurotrophic support from hair cells and/or supporting cells, also known as delayed spiral ganglion neuron death.

Methods

To investigate the time course hair cell and spiral ganglion neuron death in early postnatal life, we prepared cochlear organotypic cultures from postnatal day 3 (P3) rat pups and adult rats and treated them with various concentrations of kanamycin (0.1-1 mM) for different period of time.

Results

In both adult and P3 rats, the cochlear hair cell damage began at the base of the cochlea and progressed towards the apex in a dose dependent manner. Spiral ganglion neurons in adult rats were resistant to kanamycin damage even at the highest concentration. In contrast, spiral ganglion neurons in P 3 rat pups were rapidly destroyed by kanamycin. The superoxide radical and caspase-3 were highly expressed in damaged type I spiral ganglion neurons in P3 pups. In contrast, type II spiral ganglion neurons in P3 rats were resistant to kanamycin.

Conclusions

Adult spiral ganglion neurons are resistant to kanamycin in vitro, consistent with in vivo models of delayed spiral ganglion neuron degeneration. But kanamycin was found to cause direct damage to type I spiral ganglion neurons in P3 cochlear organotypic cultures. The neurotoxic damage appears to be initiated by superoxide oxidative stress followed by an apoptotic chain reaction. These developmental differences in toxicity may be related to the development of anti-oxidative stress systems or myelin development in adults. The different susceptibility of type I and type II spiral ganglion neurons to kanamycin ototoxicity is puzzling and deserves further study.

PS-44

Ototoxic Effects of Cobalt in Cochlear Organotypic Cultures Vitro

Peng Li; Dalian Ding; Kelei Gao; Haiyan Jiang; Richard Salvi; Jerome Roth

University at Buffalo

Background

Cobalt, a trace, dietary element required in minute amount for normal health, is active in cobalamin coenzymes such as vitamin B12. However, excessive cobalt commonly leads to three major sensory toxicities sensorineural hearing loss, optic atrophy, and peripheral neuropathy. The mechanisms underlying cobalt neurotoxicity are believed to involve oxidative stress, hypoxic injury, and mitochondrial dysfunction leading to apoptosis. However, since the pathways through which cobalt damages the sensory hair cells and spiral ganglion neurons in the inner ear are poorly understood, we investigated the mechanism of cobalt ototoxicity in cochlear organotypic cultures.

Methods

Cochlear organotypic cultures from postnatal day 3 rat pups were treated with various concentrations of cobalt (0.01-1 mM) for durations from 24 to 72 h. The pathological changes in the cochlear sensory hair cells and spiral ganglion neurons were evaluated qualitatively using immunocytochemistry and histological stains to identify stereocilia, nuclei, superoxide, caspase-3 and auditory nerve fibers and spiral ganglion neurons. Damage to hair cells, auditory nerve fibers, and spiral ganglion neurons was related to cobalt concentration.

Results

In all experimental conditions, increases in cobalt concentration caused a dose and time dependent increase in spiral ganglion neuron degeneration. In contrast, the stereocilia of cochlear hair cells were just disarranged or desquamated at higher concentrations and longer durations, but there were few missing hair cells. Cobalt-induced spiral ganglion degeneration was characterized by an increase superoxide labeling, an indicator oxidative stress, nuclear fragmentation, a morphological feature of apoptotic cells death, and caspase-3 labeling, a caspase-mediated cascade of programed cell death.

Conclusions

Surprisingly, cobalt-induced damage to postnatal day 3 cochlear organotypic cultures was primarily confined to the spiral ganglion neurons and auditory nerve fibers. However, the cochlear hair cells were relatively resistant to cobalt injury. Thus, cobalt induces an auditory neuropathy, rather than sensory cell damage, in postnatal day 3 cochlear cultures. Further studies are needed to characterize the damage patterns

in older animals to determine if cobalt neurotoxicity continues to be the dominant form of damage.

PS-45

D-methionine (D-MET) Administration, Delayed Up to 36 Hours Post-Noise, Significantly Rescues from Permanent Steady State or Impulse Noise-Induced Hearing Loss

Daniel Fox; Robert Meech; Tim Hargrove; Steven Verhulst; Kathleen Campbell
Southern Illinois University School of Medicine

Background

Noise-induced hearing loss (NIHL) is the most common cause of hearing loss worldwide and costs billions of dollars in the US alone. D-methionine (D-met) significantly reduces NIHL when administered before and/or after steady state or impulse noise exposure. D-met is currently in our FDA-approved Phase 3 clinical trials to prevent NIHL and tinnitus. However, dosing and dose timing require further optimization for NIHL rescue i.e. initially administering D-met after, rather than prior to, noise exposure. The overall purpose of this study was to determine maximum time delay for effective D-met post-noise rescue protection from permanent NIHL.

Methods

Fourteen groups of 3-year-old male chinchillas laniger (n = 10/group) were used for this study. Seven groups were exposed to steady state noise (105 dB SPL centered at 4 kHz for 6 hours) and seven groups were exposed to impulse noise (155 dB SPL at 2/second for 75 seconds). For each group, intraperitoneal (ip) D-met (200 mg/kg) was delivered every 12 hours starting 7, 9, 12, 18, 24, 36, or 48 hours after noise cessation and then another 48 hours twice daily for a total of 5 ip D-met injections per animal. A control group received placebo starting 7 hours after noise cessation. ABR threshold was measured at baseline and 21 days post-noise exposure to determine threshold shift. Cytocochleogram analysis quantified remaining cochlear outer hair cells.

Results

D-met provided significant protection ($p \leq 0.01$) from steady state or impulse noise compared to placebo controls even when administration began up to 36 hours post-noise exposure. Optimal protective dosing delay time occurred up to 24 hours post-noise exposure for both noise types with gradually diminished, but significant, protection up to 36 hours. A significant effect between ears was noted for the impulse but not steady state exposures, consistent with our previous impulse noise experiments. Cytocochleogram analysis is currently in progress.

Conclusions

The study demonstrates significant and effective D-met rescue dosing with delays up to 36 hours post-steady state or -impulse noise exposure. Results may have significant clinical impact for optimal effective D-met protection from NIHL, particularly for unexpected noise exposures. Further, the long-term D-met rescue observed in the study may suggest alternative protective mechanisms beyond D-met's established direct and indirect antioxidant characteristics.

Funding

These studies were funded by DoD Army Research and Materiel Command, #11342008; PI Kathleen Campbell, PhD.

PS-46

Involvement of Mitochondrial Small Molecule Transport Genes in Cochlear Responses to Acoustic Injury

Weiping Yang[1]; Qunfeng Cai[1]; Shuzhi Yang[1,2]; Youyi Dong[1]; Robert Vethanayagam[1]; Bohua Hu[1]
[1]State University of New York at Buffalo; [2]The First Affiliated Hospital of Chinese PLA General Hospital

Introduction

Mitochondria play an essential role in the maintenance of cell function. Mitochondrial dysfunction, including the decrease in mitochondrial membrane potential and the increase in mitochondrial membrane permeability, has been documented after acoustic trauma. However, the molecular mechanisms for these functional changes are still unclear. The current study was designed to determine how genes related to mitochondrial function respond to acoustic overstimulation.

Methods

C57BL/6J mice (male and female, 4-8 weeks) were used. These animals were exposed to a broadband noise at 120 dB SPL for 1 hour. At 1 day post noise exposure, the organ of Corti tissues were collected for expression analyses of 84 mitochondrial function genes. To determine the differential changes of gene expression in response to different levels of acoustic trauma, we divided the samples into either a mild-damage group or a severe-damage group based on the levels of ABR threshold shifts of the cochleae from which the samples were collected. The expression patterns of these genes were then compared between the normal and the mild-damage group and between the normal and the severe-damage group. Protein expression patterns of selected genes were analyzed using immunohistochemistry to determine the spatial distribution of the genes expressed in the organ of Corti.

Results

The noise exposure caused an average of 34.4 ± 12.1 dB and 54.1 ± 16.0 dB threshold shifts for the mild- and the severe-damage group, respectively. A total of 10 genes displayed changes in expression after the acoustic trauma. Among these genes, four genes (Sfn, Bid, Slc25a24, Slc25a15) were up-regulated and three genes were down-regulated (Bcl2, Slc25a30 and Cpt1b) in both the mild- and severe-damage groups. Noticeably, expression changes of three genes (Slc25a13, Slc25a22 and Cox18) were damage-dependent. These genes were up-regulated in the mild-damage group only. Bioinformatic analyses revealed that these genes are involved in multiple mitochondrial/cellular functions, including apoptosis and mitochondrial membrane transport. Among the genes showing a damage level-dependent change, Slc25a22 and Slc25a13 are glutamate carrier genes and Cox18 is a

cytochrome C oxidase assembly factor. Further immunolabeling revealed that Slc25a22 and Slc25a13 were expressed in Deiters cells, suggesting a role for supporting cells in regulation of glutamate metabolism.

Summary
Genes important for mitochondrial small molecule transport and apoptosis respond to acoustic overstimulation. Genes related to the glutamate metabolism in mitochondria are likely to contribute to individual susceptibility to acoustic trauma.

PS-47

Electrode Insertion Trauma-Initiated Changes in Gene Expression Levels of Inflammatory Pathway and Fibrosis Genes and their Response to Dexamethasone

Thomas Van De Water; Esperanza Bas Infante
University of Miami Miller School of Medicine

Cochlear implantation can result in initiation of an inflammatory cascade which can affect conservation of a patient's residual hearing and initiate a fibrosis reaction. In animal models of cochlear implantation trauma-induced hearing loss, local treatment of traumatized cochlea with dexamethasone has been demonstrated to protect hearing and sensory receptor cells. However little is known about changes in gene expression that occur in response to electrode insertion trauma (EIT) and what are the effects of dexamethasone treatment on EIT-initiated changes in gene expression.

A mouse model of EIT was used to study changes in the expression levels of inflammatory and fibrosis associated genes using PCR gene arrays at seven days post-EIT. Unoperated contralateral cochleae were used as controls for gene expression. The threshold for over-expression was 2-fold and for gene repression ½-fold. To study the effect of dexamethasone on EIT-induced changes in gene expression our EIT-organ of Corti + Lateral Wall Tissue (EIT-OC+LW) explants were used and compared to control cochleostomy only control OC+LW explants. Isolated leucocytes were interacted with explants. Gene expression levels were determined by quantitative RT-PCR.

In vivo: Implanted mouse cochleae showed up-regulation of pro-inflammatory cytokines (IL-1α, IL-1β, IL-4, IL-6, IL-13 & IFN-γ); cell-cell or cell-matrix interaction molecules (integrins, thrombospondin), chemokines (Ccl-3 and Ccl-12), fibrogenic molecules (TGFβ-1 and CTGF), remodeling factors (Dlk1, cyclins, collagens, IGF, FGF, TIMP1 & 2, MMPs and BMP4), and apoptosis-related, Fas-ligand. Anti-fibrotic genes (TGFβ3, TGFR2, Smad6 and Smad7) and anti-apoptotic molecules, i.e. Bcl-2, were down-regulated. In vitro- EIT-OC+LW explants demonstrated an inflammatory response that was characterized by increases in inflammatory cytokines (i.e. TNFα & IL-1β), inducible enzymes (i.e. iNOS & COX-2), cell adhesion molecules (I.E. VCAM1 & E-Selectin) in the explants and ICAM1 & L-Selectin in leukocytes and chemokines (CCL-2, in both explants and leukocytes). The EIT-OC+LW explants next enter in a proliferative-fibrosis phase with increases in the growth factors CTGF and TGF-β1 in both explants and leukocytes. DXM inhibited increases in inflammatory gene over-expression initiated by EIT in both the explants and in reacted leukocytes and an increase in cytokine IL-10 gene expression in leukocytes that were indirectly co-cultured with DXM pre-treated OC+LW explants.

DXM treatment of traumatized cochlear tissues protect against many deleterious changes in gene expression that are initiated by EIT and initiates changes in gene expression that down-regulated the expression of genes involved in both the inflammatory cascade and cochlear fibrosis.

PS-48

Wnt Signaling in Cochlear Implant-Induced Fibrosis

Esperanza Bas Infante; Thomas Van De Water
University of Miami Miller School of Medicine

Although atraumatic surgical techniques are being implemented, early trauma to the delicate structures of the inner ear still occurring. Electrode insertion trauma (EIT) triggers a wound healing process in which there is cross-talk between cellular, extracellular, vascular, and cytokine-related components and can result in hair cell and spiral ganglion neuron apoptosis and loss of residual hearing. This uncontrolled inflammatory process can lead to foreign body reaction, fibrosis around the electrode, and new bone formation. Increased levels of Tissue Growth Factor (TGF)-beta 1 have been reported during wound healing. TGF-ß1 is a pro- fibrotic cytokine, which plays a major role in development, fibrosis, and wound remodeling. Wnt signaling has been associated with wound healing. TGF-ß1-mediated fibroblast proliferation and hyperplastic wound formation has been shown to be dependent on ß-catenin expression. This study investigates co-operation between Wnt and TGF-ß1 signaling pathways in fibrous tissue formation after a CI electrode insertion trauma (EIT) in a mouse model. A series of PCR arrays for Wnt target genes 7 days post-EIT and histological examinations were made at different days post-EIT. Gene expression analyses show up-regulation (>2 fold compared to control) of genes involved in development and differentiation: growth factors (Angptl4, Bmp4, Ctgf, Fgf20, Gdnf, Igf1, Il6, Jag1), Antxr1, Ccnd1&2, Cdh1, Dab2, Dlk1, Egfr, Fn1, Fst, Gja1, Id2, Nrcam, Nrp1, Twist1; Calcium Binding and Signaling (Ccnd1, Egfr, Ptgs2), Adhesion and Migration (Cd44, Cdh1, Ctgf, Egfr, Fgf7, Fn1, Gdnf, Igf1, Il6, Jag1, Nrcam, Nrp1, Twist1) and Cell Cycle (Ahr, Ccnd1&2, Cdkn2a, Egfr, Id2, Igf1, Ptgs2). Signal transduction genes involved in WNT signaling (Dkk1, Sfrp2, Tle1, Wisp1, Wisp2), TGFß Signaling: (Bmp4, Fst, Id2) and Jag1 from the Notch pathway were up-regulated. Transcription Factor Tcf7l2 from WNT Signaling was upregulated, while Tcf7l1 as well as Cebpd and Ppard were down-regulated (>0.5 fold). Immunohistology shows a significant increase in co-localised pAkt and ßGal (reporter expressed in the presence of the LEF/TCF and activated ß-catenin) at 3 days post-EIT in the organ of Corti and cells encapsulating the electrode. Our results suggest that upon EIT, the TGF-ß1/phosphatidylinositol 3-kinase (PI3K) signaling pathway is activated and col-

laborates with Wnt/ ß-catenin pathway through GSK-3 in the profibrotic and/or new-bone formation in the scala tympani.

PS-49

Ototoxicity-Induced Loss of Hearing and Inner Hair Cells is Attenuated By HSP70 Gene Transfer

Yohei Takada[1]; Donald Swiderski[1]; Tomoko Takada[1]; Min Young Lee[1]; Lisa Kabara[1]; David Dolan[1]; Lindsey May[2]; Lisa Cunningham[2]; Yehoash Raphael[1]
[1]University of Michigan; [2]NIH

The most common reason for sensorineural hearing loss is death of hair cells (HC) from diverse stressors. Heat shock proteins (HSPs) are molecular chaperones, participating in folding, targeting and degrading proteins in all cells. In addition, HSP expression is increased in response to various environmental stresses to protect cells from damage. One common HSP, HSP70, inhibits apoptosis caused by heat shock and other stresses. Previous studies showed that cultured mouse utricles exposed to HSP70 from conditioned media or adenovirus (Ad) mediated over-expression were protected from HC loss caused by aminoglycosides. Here we test whether Ad.*HSP70* gene transfer protects against a systemic ototoxic insult in the guinea pig cochlea, in vivo.

Guinea pigs were deafened by administration of kanamycin (SC, 400 mg/kg) and furosemide (IV, 100 mg/kg) to induce a severe ototoxic lesion. The viral vector Ad.*HSP70*-mCherry (1.5µl) was injected into the scala media of the left (experimental) cochlea via basal turn cochleostomy 4 days before deafening. Control animals received an identical ototoxic insult after injection with Ad.mCherry. Hearing thresholds were measured by ABR before deafening and prior to sacrificing the animals, 14 days following deafening. Cochlear tissues were prepared for fluorescence microscopy as whole mounts stained for Myosin VIIa (experimental ear) or Myosin VIIa and phalloidin (contralateral ear). HC were quantified in both ears in both groups.

Injection of Ad.*HSP70*-mCherry resulted in mCherry fluorescence in non-sensory cells of the organ of Corti. The ototoxic insult eliminated both outer HCs (OHC) and inner HCs (IHC) in the basal turns of both control (Ad.mCherry-injected) ears and contralateral (non-injected) ears. Ad.*HSP70*-mCherry-treated ears exhibited a less severe lesion with more IHC survival than Ad.mCherry-injected ears. OHC were not protected. ABR thresholds were significantly better in Ad.*HSP70*-mCherry treated ears than in control ears and contralateral ears. Because injection into the scala media involves a traumatic loss of some HCs, the degree of protection by HSP70 we observed may underestimate of its true protective effect.

Our data show attenuation of severe ototoxic trauma by HSP70 over-expression in supporting cells after injecting Ad.*HSP70*-mCherry into the scala media of the guinea pig cochlea. Compared to controls, ABR thresholds were improved in treated ears and IHC were protected in the basal turn. HSP70 augmentation may represent a potential therapy against ototoxicity and other cochlear traumas. It is currently unknown whether HSP70 acts on the supporting cells and prevents elimination of damaged HC, or acts directly to protect the HC.

PS-50

The Role of Extracellular Matrix Versican in the Maintenance of Mouse Auditory Sensitivity after Cochlear Injury

Yazhi Xing[1]; LaShardai Conaway[1]; Kenyaria Noble[1]; Jianning Zhang[2]; Xin Liu[1]; Clarisse Panganiban[1]; Richard Schmiedt[1]; Jeremy Barth[1]; Corey Mjaatvedt[1]; Hainan Lang[1]
[1]Medical University of South Carolina; [2]Shanghai University of Traditional Chinese Medicine Yueyang Hospital

Background

Versican, a large extracellular matrix (ECM) proteoglycan, is found in various mammalian tissues and has been implicated in angiogenesis, wound healing and inflammation. In the central nervous system, versican is expressed by glial cells and plays important roles in the guidance of axonal growth during development and in nerve tissue regeneration after injury. Here, we examined the role of versican in auditory sensitivity after injury by 1) investigating spatiotemporal expression of versican in the cochlea and auditory nerve, and 2) assessing effects of noise exposure in a versican-deficient mouse model.

Methods

Cochlear specimens of postnatal and young-adult CBA/CaJ mice were used to characterize spatiotemporal expression patterns of versican with multiple protein and gene expression assays. Versican V0/V2 deficient (*Vcan*^{tm1Zim}, Dours-Zimmermann et al., 2009) and wild type (WT) mice were exposed to octave band noise at 106 dB SPL for 2 hours. Consequences of noise exposure were evaluated by auditory brainstem response (ABR) measurement and morphological examination of the cochlea and auditory nerve.

Results

Gene microarray and immunohistochemistry assays revealed that versican was highly expressed in the auditory nerve at postnatal day 0 (P0) and down-regulated with age from P3 to the young-adult stage. Quantitative RT-PCR analysis of adult CBA/CaJ cochlear tissues indicated that isoforms V0, V1 and V2 were expressed in the auditory nerve and isoforms V0 and V1 were expressed in the cochlear lateral wall. Young-adult WT and *Vcan*^{tm1Zim} mice had similar ABR wave I thresholds. However, after noise exposure, WT mice had larger ABR threshold shifts and recovered after 2-4 weeks, whereas *Vcan*^{tm1Zim} mice had smaller threshold shifts and less capacity to recover. Ultra-structural observation revealed several abnormities in *Vcan*^{tm1Zim} cochleas including 1) disorganization of the interdigital processes between marginal and intermediate cells in the stria vascularis, and 2) distortion of satellite cells and myelin sheaths surrounding cochlear neurons.

Conclusions

Versican exhibits dynamic expression patterns in cochlear tissues during postnatal development and in the adult. Ver-

sican is required for structural and cellular integrity of the cochlea, it influences the severity of noise-related damage, and is required for full recovery from noise injury. Taken together, these findings indicate the important role for versican in the maintenance of auditory sensitivity in response to noise trauma.

This work has been supported by National Institutes of Health Grants R01DC012058, P50DC00422, P30GM103342, P20GM103499 and R25 GM072643.

PS-51

Human Audiometric Thresholds do not Predict Specific Cellular Damage in the Inner Ear

Lukas Landegger[1]; Demetri Psaltis[2]; Konstantina Stankovic[1]

[1]Massachusetts Eye and Ear Infirmary, Harvard Medical School; [2]Optics Laboratory, School of Engineering, Swiss Federal Institute of Technology Lausanne (EPFL)

Introduction

As otology enters the field of gene therapy with first human studies underway, the question arises if audiograms - the current gold standard for the evaluation of hearing function – predict cellular damage within the human inner ear and thus should be used to define inclusion criteria for future trials. Although several authors have tried to draw conclusions from the analysis of small groups of human temporal bones *post mortem* or from the psychophysical identification of cochlear "dead regions" *in vivo*, a comprehensive study demonstrating or refuting a correlation between audiometric thresholds and cellular damage within the cochlea is lacking. We have performed such a study using a large and diverse cohort of individuals.

Methods

A total of 131 human temporal bones from 85 adult individuals (ages 19-92 years, median 69 years) with sensorineural hearing loss due to various etiologies were analyzed. Cytocochleograms – which quantify loss of hair cells, neurons, and strial atrophy along the cochlear length – were compared with the latest available audiometric tests prior to death (time range 5 hours to 22 years, median 24 months). The Greenwood function was used to infer, from cytocochleograms, locations corresponding to frequencies tested in clinical audiograms. For each center frequency, the equivalent rectangular bandwidth of 0.9 mm was assumed. Correlation between audiometric thresholds at clinically tested frequencies and cell-type specific damage in those frequency regions was tested by calculating Pearson correlation coefficients.

Results

Similar audiometric profiles reflected widely different cellular damage in the cochlea. In our diverse group of patients, audiometric thresholds tended to be more influenced by hair cell loss than by neuronal loss or strial atrophy. However, this trend was not statistically significant: Pearson correlation coefficients across frequencies ranged from 0.60 for inner hair cells to 0.18 for stria and 0.15 for neurons.

Conclusion

Audiometric thresholds do not predict specific cellular damage in the human inner ear. Our study highlights the need for better non- or minimally-invasive tools, such as cochlear endoscopy, to establish cellular-level diagnosis and thereby guide therapy and monitor response to treatment.

PS-52

On the Origin of the Tympanic Electrical Noise in Humans

Javiera Pardo; Constantino D. Dragicevic; Macarena P Bowen; Paul Delano

Universidad de Chile

Introduction

The functional status of the auditory nerve is essential for the perceptual outcome of cochlear implant patients. Nowadays, there is no good electrophysiological measure of the auditory nerve of deaf patients that are candidates for a cochlear implant. Interestingly, in guinea pig studies, the power spectrum of the spontaneous activity recorded with an electrode located in the round window of the cochlea shows a broad energy peak centered around 800 to 1000 Hz. This signal is called round window noise or ensemble background activity. The proposed origin of this component is the unitary spontaneous activity of auditory-nerve fibers, as each action-potential, lasting 1-2 ms approx., contributes to the signal in that frequency band. Here, we used a non-invasive method to record -for the first time in humans- this neural noise by means of a tympanic wick electrode (Intelligent Hearing Systems®).

Methods

We recorded a total of 26 volunteers, referenced to vertex or to the contralateral earlobe. Recordings were performed under silent or in response to stimuli of different modalities, including auditory, vestibular, gustatory, somatosensory and motor activity.

Results

Although all subjects showed a peak of spontaneous activity at 1000 Hz, there was a considerable variability between individuals, which depended on electrode impedance. We performed several controls to discard electromyographic and electrocardiographic origin. In addition, we also discarded facial, trigeminal and chorda tympani nerve origin. The most reliable responses were obtained with vestibular stimulation by either high (air flow at 49ºC) or low (24ºC) temperature, which produced an increase in the magnitude of the energy at 1000 Hz. On the other hand, only in one subject (out of 12) we obtained an auditory response to a broad-band noise which displayed a peak around 800 Hz.

Conclusions

These results demonstrate that the electric noise from the tympanic membrane is originated from a biological source, suggesting that the 1000 Hz component has a mixed origin, probably including vestibular brainstem networks. However, it still remains unknown whether the 800 Hz peak response reflects the auditory-nerve activity.

PS-53

Aquaporin 4 Expression in the Ear is Essential for Sustaining the Endocochlear Potential

Jinhui Zhang[1]; Ahmed Hassan[2]; Manfred Auer[2]
[1]Oregon Health & Science University; [2]Lawrence Berkeley National Laboratory

Mice with genetic deficiency in aquaporin 4 (AQP4) have profound hearing loss. Although the mechanism relating AQP4 and hearing loss is not yet known, a clue is provided by the finding that AQP4 expression in brain astrocytes is critical for ion homeostasis. AQP4 expression in the inner ear is predicted to mediate water and potassium ion transport necessary for endocochlear potential (EP) and hearing function. Normal blood-labyrinth barrier integrity in the stria vascularis requires a high degree of structural and functional integration between the endothelial cells (ECs), pericytes, and perivascular resident macrophages (PVMs, cochlear microglia) in the barrier. In this study, we report that AQP4 (M23 isoform) is richly expressed in the PVMs that surround vessels in the stria vascularis. Suppression of AQP4 with siRNA dramatically changes the cellular interaction between ECs and PVMs. The silencing affects PVM morphology and down-regulates connexin 43 (Cx43) expression between PVMs and ECs. Normally elongated PVMs change morphology and become star-shaped (or stellate) following down-regulation of AQP4. AQP4 suppression also has significant effects on expression of Kir4.1, a critical channel for the production of EP. Down-regulated expression of Kir4.1 may be responsible for the observed drop in the EP and subsequent hearing loss. Overall, our study suggests that AQP4 in PVMs is important for controlling PVM structure, facilitating communication with ECs, and sustaining the EP essential for hearing function.

PS-54

Gap Junction Pannexin 1 (Panx1) Hemichannels Dominate ATP Release in the Cochlea

Hong-Bo Zhao; Yan Zhu
University of Kentucky Medical School

Background

Gap junction channels posses a relatively larger pore size (~ 10 A) and are permeable to small molecules, such as ATP. Pannexin is a newly-identified gene family to encode gap junctional proteins in mammals. Different from connexins, pannexins mainly form hemichannels on the cell surface to provide an intracellular-extracellular conduit, which can release ATP. In previous study, we reported that pannexins also extensively expresses in the inner ear. Pannexin 1 (Panx1) is a predominant isoform (Wang et al., J. Comp. Neurol. 2009). We also found that ATP release in the cochlea is mainly dependent on gap junction hemichannels (Zhao et al., PNAS, 2005). However, the detailed mechanism remains undetermined. ATP is an energy molecule and also is an important signaling molecule in extracellular space. ATP-mediated purinergic signaling has a critical role in hearing. It has been reported that purinergic P2X2 receptor mutations can induce nonsyndromic hearing loss and increases susceptibility to noise. To further elucidate ATP-purinergic function in the cochlea, in this study, the Pannexin-mediated ATP release in the cochlea was investigated.

Methods

Panx1, Cx26. and Cx30 deficient mice were used. The cochlea was isolated. ATP release was measured by a bioluminescence-based, luciferin-luciferase assay.

Results

Different from connexin hemichannels, which close at physiological level of extracellular Ca^{++} (2 mM), Panx1 hemichannels can open to release ATP under the physiological Ca^{++} concentration. ATP release was 10.58±0.42 fmoles in the WT mouse cochlea at 2 mM extracellular Ca^{++} level. Unser application of 0.1 mM carbenoxolone, which can block pannexin hemichannels, the ATP release was significantly reduced to 1.71±0.41 fmoles ($P<0.001$, ANOVA). The ATP release was also reduced in Panx1 knockout (KO) mice. ATP release in the Panx1 KO mice was 1.28±0.23 fmoles at 2 mM extracellular Ca^{++} level. In comparison with WT mice, the ATP release was significantly reduced by ~ 8-fold ($P<0.001$, ANOVA). However, there was no ATP release reduction in Cx26 KO and Cx30 KO mice. Cx26 and Cx30 are predominant connexin isoforms in the cochlea. The measured ATP release at 2 mM extracellular Ca^{++} concentration in Cx26 KO mice and Cx30 KO mice was 10.87±0.32 and 10.21±0.41 fmoles, respectively, similar to that measured in WT mice ($P=0.89$ and 0.91, respectively, ANOVA).

Conclusions

Panx1 hemichannels rather than connexin hemichannels dominant ATP release in the cochlea under physiological conditions. Panx1 deficiency can reduce ATP release in the cochlea, which can reduce endocochlear potential generation leading to hearing loss.

PS-55

Utricular Hair Cells and Transitional Cells Reciprocally Regulate Endolymphatic Cation Transport Via Purinergic Stimulation

Bo Gyung Kim[1]; Sung Huhn Kim[2]; Jin Young Kim[2]; Young Joon Seo[2]; Gyu Rin Hwang[2]
[1]Soocheonhyang University; [2]Yonsei University

This study was performed to identify how the utricular transitional cells and hair cells reciprocally act to regulate inner ear cation movement to protect vestibular hair cells via purinergic regulation. The temporal bone of C57BL/6 mouse was dissected and the transitional cell and hair cell area of utricle was exposed. Vibrating probe was used to measure transepithelial current from the area and purinergic agonist, antagonist and various cation absorbing channel inhibitors were used to identify the function of the area. Minimal cation absorption current (5.0 ± 1.5 μA/cm^2) was detected in the transitional cell area and large cation absorption current (20.5 ± 3.4 μA/cm^2) was detected in the hair cell area of the utricle. The cation absorption current of utricular transitional cell area was transiently increased with the application of ATP (100 μM). However, cation absorption current was changed to large cation

secretion current with the application of ATP (100 μM) in the utricular hair cell area. The current in \ The each EC_{50} value of ATP-induced current from the both area was 15 μM and 18 μM respectively and the current was inhibited by suramin (100 μM), PPADS (10 μM), and 5-BDBD (5 μM).This result implies that utricular hair cells secret cation and transitional cell absorb cation via P2X2 and P2X4 receptor mediated purinergic stimulation. This is likely to happen to protect utricular hair cells in the stressful condition by providing a shunt for cation from hair cells to transitional cells.

PS-56

Lipid Droplets from Guinea Pig Hensen Cells are Protein-Storage Organelles Sensitive to Glucocorticoids

Gilda Kalinec[1]; Gwen Lomberk[2]; Pru Thein[1]; Arya Parsa[1]; Channy Park[1]; Raul Urrutia[2]; **Federico Kalinec[1]**
[1]University of California, Los Angeles; [2]Epigenetics and Chromatin Dynamics Laboratory, Mayo Clinic

Introduction

The cytoplasm of guinea pig Hensen cells (HCs) is filled with numerous lipid droplets (LDs). The molecular components as well as the function of these LDs are still unknown, although it has been suggested that they could be associated with immunological responses in the organ of Corti, acting as cytoplasmic reservoirs of important anti-inflammatory molecules.

Methods

We investigated the proteome of LDs isolated from guinea pig HCs untreated or treated with the synthetic glucocorticoid dexamethasone for 5 min and 15 min. We performed nano-LC-ESI-MS/MS, and the data was analyzed by searching a guinea pig protein database with ProteinPilot, spectral counting-based quantification with QSpec, gene ontology classification, and KEGG (Kyoto Encyclopedia of Genes and Genomes) pathway analysis. The localization of selected proteins was further investigated with confocal and electron microscopy

Results

In LDs of control cells, and after eliminating resident proteins from other organelles, we identify a total of 309 LDs-associated proteins. We recognized 23 of them (7.4%) as associated with LD metabolism, 23 (7.4%) related to protein folding and processing, 71 (23.0%) to vesicular formation and maintenance, 111 (36.0%) to vesicular transport, and 81 (26.2%) to the cytoskeleton. The proteome of LDs from dexamethasone-treated cells showed quantitative and qualitative differences, probably associated with a decrease in the number of LDs per HC as well as functional changes.

Conclusions

Our results led us to conclude that: i) LDs have resident proteins and others that are cargo, with some of them probably being recycling products of other membranous compartments (e.g.: ER, endosomes, mitochondria); ii) some of these cargo proteins are in the surface but others are actually stored inside the lipid core of the droplets; iii) LDs are tightly associated with cytoskeletal as well as vesicular maintenance and transport proteins; iv) binding of the glucocorticoid dexamethasone to mineralocorticoid receptors in the surface of HCs would induce signals that change the biophysical properties of the LDs surface, facilitating both their fusion and/or fragmentation and the release of cargo proteins. These responses could be crucial, among other functions, for immunological responses in the organ of Corti.

PS-57

CaBP1/Caldendrin Regulates the Development of High-Frequency Hearing

Tian Yang; Elizabeth Scholl; Barbara Robinson; Ning Hu; Steven Green; Marlan Hansen; Amy Lee
University of Iowa

CaBPs are a family of EF-hand containing Ca^{2+}-binding proteins with high homology to calmodulin (CaM). While their physiological roles are just being defined, CaBPs are known to regulate voltage-gated Ca_v1 Ca^{2+} channels. For $Ca_v1.3$ channels, which regulate exocytosis from inner hair cells, CaBPs prolong channel opening by inhibiting Ca^{2+}-dependent inactivation (CDI). The limited CDI of $Ca_v1.3$ Ca^{2+} currents in inner hair cells is thought to be important for normal sound coding. CaBPs can compete with CaM to inhibit CDI of $Ca_v1.3$ channels, but whether they do so in inner hair cells, or have other cellular functions, is unknown. Therefore, we analyzed the expression and potential function of CaBPs in the mouse cochlea. We compared the expression levels of four CaBPs (CaBP1, CaBP2, CaBP4, and CaBP5) by quantitative PCR, which showed that CaBP1 was present at the highest levels. CaBP2 was expressed at comparatively low levels, with CaBP4 and CaBP5 nearly beyond detection. We also examined the expression pattern of the three splice variants of CaBP1 (Caldendrin, CaBP1-L, and CaBP1-S) by *in situ* hybridization. Caldendrin, which is the main CaBP1 variant expressed in the cochlea, is highly expressed in the spiral ganglion, while CaBP1 –S and/or CaBP1-L are expressed in the both inner and outer hair cells. In contrast, CaBP2 is expressed exclusively in outer hair cells. We then analyzed hearing in CaBP1/caldendrin knockout (KO) mice with acoustic brainstem response (ABR). KO mice have lower ABR threshold at 32 kHz at P15. However at P30, the 32 kHz threshold of KO became indistinguishable from the wild-type mice. ABR thresholds at lower frequencies (8 kHz and 16 kHz) were similar between KO and wild-type mice at all ages. Histologically, hair cells, and synapses in KO mice were relatively normal. We conclude that CaBP1 and Caldendrin are expressed in distinct cell-types in the cochlea and delay the development of high-frequency hearing.

PS-58

Sensory Transduction in Outer Hair Cells does not Account for the Hearing Loss Caused by Haploinsufficiency of Transcription Factor Gata3

Tanaya Bardhan; Walter Marcotti; Matthew Holley
The University of Sheffield

Introduction

Gata3 regulates the development of the cochlear sensory epithelium and spiral ganglion neurons. Haploinsufficiency leads to ~30dB of hearing loss in mice (Van der Wees et al., 2004, Neurobiol Dis.16:169-78), and accounts for hypoparathyroidism, hearing loss and renal anomaly in human HDR syndrome (Van Esch et al., 2000, Nature 406:419-22). Hearing loss in heterozygous gata3 mice has an early onset and is thought to originate primarily from functional defects in the outer hair cells (OHCs; Van Looij et al, 2005, Neurobiol Dis. 20:890-7) although defects in the inner hair cells (IHCs) may also be possible. We recorded the physiology of hair cells to identify potential functional deficits that could explain the observed hearing loss.

Methods

Whole cell voltage clamp recordings were used to measure basolateral membrane and mechanoelectrical transducer currents in OHCs and IHCs from wild type and gata3 heterozygous mice from postnatal days P6 to P60. Whole cell current clamp recordings were used to measure voltage responses and resting membrane potential. Recordings were performed at room temperature (20-25°C) using the Axopatch 200B amplifier.

Results

We found that the size of the K^+ currents measured at 0mV was similar between wild type and heterozygous mice both at both prehearing stages and mature stages. Resting membrane potentials of OHCs in adults were also comparable. Maximal mechanoelectrical transducer currents at -121mV in heterozygous OHCs were normal. Interestingly, we observed a ~25% reduction in the number of apical OHCs in heterozygous cochleae as early as P4.

In immature IHCs, basolateral membrane currents elicited at 0mV were not significantly different between wild type and heterozygous mice. However, from P16, the BK current $I_{k,f}$ measured at -25mV appeared to be reduced in heterozygous IHCs, and this was more pronounced at P28-30. Resting membrane potentials of IHCs at this age were comparable. IHC numbers in heterozygous animals were unaffected.

Conclusion

We conclude that the physiological differentiation of hair cells is not influenced by gata3 haploinsufficiency. While IHCs seem to progressively be affected by reduced expression of gata3, OHCs remained viable until adult stages, indicating that hair cells are unlikely to explain the hearing loss in heterozygous mice. Functional deficits could, however, be related to electromotility and/or innervation. The premature degeneration of hair cells is accompanied by degeneration of supporting cells and spiral ganglion neurons, which reflect a more general developmental deficit in heterozygous mice.

PS-59

Co-localization of the Atrial Natriuretic Peptide Synthesizing Enzyme Corin and Natriuretic Peptide Receptor A in the Cochlea

Janet Fitzakerley[1]; **Jill LaBine[2]**; Sara Prince[1]; George Trachte[1]
[1]University of Minnesota Medical School; [2]University of Minnesota Duluth

Atrial natriuretic peptide (ANP) and its receptor, NPR-A, regulate fluid and electrolyte balance in many tissues. Previous work in our laboratory has shown that administration of ANP significantly improves thresholds in normal mice and that NPR-A knockout mice exhibit an early onset, high frequency hearing loss. NPR-A has been shown to be expressed in several cells of the cochlear potassium recycling pathways, as well as in spiral ganglion neurons. One interpretation of those localization experiments is that ANP may act in an autocrine or paracrine manner in the cochlea, in addition to functioning as a circulating hormone. The experiments in this study were designed to test the hypothesis that ANP is made in the cochlea by determining the location of its synthesizing enzyme, corin, and contrasting corin and NPR-A expression in the cochlea. NPR-A and corin were localized within the cochlea using standard immunohistochemical techniques. CBA/J mice under 100 days old with normal hearing were perfused with a 4% paraformaldehyde/0.05% picric acid solution and cochlear sections were cut at a thickness of 10 microns on a cryostat. Commercially available antibodies against NPR-A, corin and Kir4.1 (a marker for intermediate cells) were used and visualized via confocal microscopy. Kidney and heart tissue were used as a positive control for both NPR-A and corin, while skeletal muscle acted as a negative control. Corin and NPR-A were both found in the spiral limbus, the spiral ligament, the stria vascularis and in the spiral ganglion. In most cochlear regions, corin and NPR-A were co-expressed in the same cells (e.g., fibrocytes of the spiral limbus and spiral ligament, type I spiral ganglion neurons). However, in the stria vascularis, corin was found only in the intermediate cells, while NPR-A was expressed by basal and marginal cells, but not intermediate cells. Based on these results, ANP is in position to work in a paracrine fashion in the stria vascularis, but as an autocrine messenger elsewhere in the cochlea. In addition, the presence of corin in cells critical to the potassium recycling pathways further supports the hypothesis that ANP is a critical regulator of inner ear fluid and electrolyte balance.

PS-60

Intra-Tympanic Injection of Isosorbide for Endolymphatic Hydrops in Guinea Pig

Minbum Kim; Kyu-Sung Kim
Inha University College of Medicine

Objectives

The aims of this study were to investigate intracochlear isosorbide concentration in perilymph after intra-tympanic injection of isosorbide (IT-ISB) and its feasibility for endolym-

phatic hydrops in guinea pig model. **Methods.** Twenty-four male guinea pigs were used. Isosorbide, an osmotic diuretic, was administered via IT-ISB vs. PO. (1) To compare the drug concentration after IT versus that after PO of 100% of ISB, perilymph was aspirated at 3 and 6 h after administration. (2) And intracochlear concentration was checked after intratympanic injection of isosorbide with different concentration (100, 50 and 25%). (3) In normal animals, change of middle ear mucosa was microscopically observed after IT injection with different concentration of ISB. (4) Finally, improvement of endolymphatic hydrops was observed histologically after intratympanic injection (IT) in animal model with surgically induced hydrops (12 weeks). Intracochlear concentration of isosorbide was analyzed by high-performance liquid chromatography coupled to refractive index detection. **Results.** Isosorbide rapidly passed through the round window membrane into perilymph after IT-ISB. (1) The intracochlear concentration after IT- ISB for 30 min was higher than that after PO at both 3h and 6h (p = 0.02 and 0.03, respectively). While isosorbide concentrations in perilymph were 28.88 and 12.67 mM at 3 and 6 h after PO, the corresponding concentrations after IT-ISB were 117.91 and 75.03 mM, respectively. (2) Similar intracochlear concentration was measured between 50% and 100% ISB at 3h and 6h, however, significantly lower concentration was observed after IT of 25% ISB (Kruskal Wallis test, p = 0.004, 0.005) . (3) In some animals, middle ear mucosa was grossly swollen 1 week after 100% IT-injection (2 out of 5), in which thickness of mucosa was higher than both normal control and those after 50% IT-injection.(4) In animal model with hydrops, IT of isosorbide reduced endolymphatic hydrops histologically. **Conclusion.** Isosorbide can rapidly pass through the round window membrane after IT, and IT can deliver higher concentrations of isosorbide into perilymph than those achieved with PO. Intratympanic injection of 50% ISB could be appropriate for following animal study about efficacy and safety of IT-ISB. In the animal model with surgically-induced hydrops, improvement of hydrops was observed after IT of isosorbide.

PS-61

Differences in Corticocollicular Projection Patterns between Primary Auditory Cortex and Ventrorostral Belt to the Inferior Colliculus in Guinea Pig

Malgorzata Straka[1]; Robert Hughes[2]; Patrick Lee[2]; Hubert Lim[2]

[1]Johns Hopkins University; [2]University of Minnesota

The inferior colliculus (**IC**) receives many corticofugal projections, which can mediate plastic changes such as the IC's frequency tuning. While the strongest projections are found in the IC's external cortices, fibers originating from the primary auditory cortex (**A1**) have been observed throughout the IC's central nucleus (**ICC**), and these projections have shown to be organized tonotopically. There is less or conflicting evidence for projections to the ICC from non-A1 cortical regions. Particularly in guinea pig, there exists a ventrorostral belt (**VRB**) region that has primary-like properties and often been mistaken for A1, with its clearest differentiating characteristic being VRB's longer response latencies. We sought to investigate if there are projections from VRB to the ICC and if they exhibit a different projection pattern to those from A1 to the ICC. In this study, we performed experiments in ketamine-anesthetized guinea pigs, in which we positioned 32-site electrode arrays within A1, VRB, and ICC. We identified the monosynaptic connections between A1-to-ICC or VRB-to-ICC using an antidromic stimulation method, and we precisely analyzed their locations across the midbrain using three-dimensional histological techniques. Compared to the corticocollicullar projections from A1, there were fewer projections to the ICC from VRB, and these projections had a weaker tonotopic organization. The majority of VRB projections were observed in the caudal-medial versus the rostral-lateral region along an isofrequency lamina of the ICC, which is in contrast to the A1 projections that spanned throughout an ICC lamina. These findings suggest that the VRB directly modulates sound information within the ascending lemnsical pathway with a different or complementary role compared to the modulatory effects of A1.

PS-62

Subcortical Effects of Auditory Cortex Microstimulation in the Alpha-9 Knock-out Mice.

Cristian Aedo[1]; Alex León[1]; Paul Delano[2]

[1]University of Chile; [2]Universidad de Chile

Introduction

The auditory efferent system comprises descending projections from the auditory cortex to the cochlear receptor, including the olivocochlear system, which is a mandatory pathway to the sensory epithelium. The olivocochlear reflex can be activated by contralateral acoustic stimulation, suppressing bilateral cochlear responses.

Methods

Here, we measured the effects of contralateral noise (CN) in auditory brainstem responses (ABR, Waves I to V), previous, during and after auditory-cortex microstimulation (MS) (1 to 4 μA, 32 Hz rate) in anesthetized wild type (WT) mice and in the α9 nicotinic receptor knock out (KO) mice, in response to tones of frequencies between 10 and 20 kHz.

Results

The latencies of cortical evoked potentials varied between 7 and 34 ms (WT) and from 8 to 22 ms (KO). In 16 experiments (8 WT and 8 KO) auditory-cortex MS produced an increase of the suppressive effect of contralateral noise stimulation in wave I and V of the ABR. Larger effects were accompanied of auditory-cortex increased latencies in both cases (WT and KO). The difference between the effect of contralateral noise without cortical MS and with cortical MS ranged in WT mice from 0.6 to 6.6 dB in wave V and from 0.1.to 4.9 dB in wave I, while in KO mice from 0.1 to 1.6 dB in wave I and from 0.9 to 3.7 dB in wave V.

Conclusions

These results suggest that the activation of descending projections from the auditory cortex to subcortical nuclei, en-

hances the strength of the olivocochlear reflex on subcortical responses.

PS-63

Bi-directional Thalamic Gain Control via Layer 6 Corticothalamic Spike Patterning

Amanda Clause[1]; Kevin Sikah[2]; Kenneth Hancock[1]; Daniel Polley[1]

[1]Harvard Medical School, Massachusetts Eye and Ear Infirmary; [2]Harvard University

Background

Beginning with the early descriptions of Ramon y Cajal, anatomists have noted the massive and specific network of corticofugal projections that originate in layers (L) 5 and 6 of the cerebral cortex and innervate nearly every level of the central nervous system. Corticothalamic (CT) projections are the largest component of the auditory corticofugal system, yet their functional role in hearing is poorly understood. L5 and L6 projections differ in nearly every respect – from axon morphology and synaptic physiology to inter-areal targeting within the medial geniculate body (MGB). Thus, to explore the contribution of CT feedback to thalamic sound representations we used an optogenetic approach to selectively manipulate a single component of the CT projection – the so-called 'modulator' input originating in L6.

Methods

A cre-dependent channelrhodopsin viral construct was injected into the auditory cortex of the Ntsr1-cre transgenic mouse line, where Cre recombinase is expressed only in L6 CT neurons. MBG single units were recorded extracellularly in awake, head-fixed mice via a chronically implanted multichannel silicon probe. L6 activity was manipulated with millisecond precision using a diode laser.

Results

Activating L6 CT projections had mixed effects on MGB units, presumably reflecting the contribution of direct glutamatergic input versus indirect inhibition through the thalamic reticular nucleus. This suggests that L6 activity can either enhance or suppress the salience of thalamic sound representations, depending on the relative timing between CT feedback and the ascending auditory signal. We explored this idea by using a genetic algorithm to tailor the pattern of L6 activation based on real time spike feedback from MGB units. Using these optimized stimulation strategies, we observed that L6 CT input could clearly suppress or enhance the firing rate of MGB units to a fixed auditory stimulus. In some cases, bi-directional modulation could be observed in the same unit, depending on the stimulation pattern employed.

Conclusions

These findings suggest that the long-standing search for a singular effect of CT feedback on thalamic sound representations is ill-posed. We found that L6 stimulation could either amplify or attenuate thalamic sound representations, and could even directly elicit spikes in MGB units. These effects varied between MGB units, but also depended on the rate, duration, and relative timing between L6 activation and the sound stimulus. This raises the intriguing possibility that L6 neurons can bi-directionally modulate the gain of thalamic sound representations according to how spiking is temporally organized.

PS-64

Selective Attention to Visual Stimuli in α9-Nicotinic Acetylcholine Receptor Knock-out Mice.

Gonzalo Terreros[1]; Pascal Jorratt[1]; Ana Belen Elgoyhen[2]; Paul Delano[1]

[1]University of Chile; [2]Universidad de Buenos Aires, Argentina

Background

The auditory efferent system comprises descending pathways from the auditory cortex to the cochlea, allowing modulation of sensory processing even at the most peripheral level. This modulation is exerted by medial olivocochlear neurons that make synapses with outer hair cells through a particular nicotinic cholinergic receptor constituted by α9/α10 subunits. The role of the efferent system is still debated, but one of the proposed functions is to reduce cochlear sensitivity in tasks that require selective attention to visual stimuli. We compared the behavioral performance of α9-nicotinic acetylcholine receptor (α9-nAChR) knock-out (KO) and wild type (WT) mice, in the presence of auditory distractors during selective attention to visual stimuli.

Methods

Wild type and KO mice between P50 and P65 days, were trained in a two-choice visual discrimination task to respond by pressing a lever after a target light was presented. Correct responses were rewarded with food pellets. During experimental period, mice were food deprived, maintaining 85 to 92% of their free-feeding weight. The experimental period began when they reached a criterion of 70% accuracy for target lights of 500 ms. This period consisted of 12 days with 110 trials per session, including (i) three basal days (visual discrimination), (ii) three days with tones and clicks distractors, (iii) three days with a broad-band noise distractor, and (iv) three days only with visual discrimination.

Results

We found a significant decrease in the number of correct responses in KO mice (n=5) with the broad-band noise distractor (WT= 79.20 ± 13.72, KO = 57.13 ± 17.69; p=0.0317). In addition, an increase in the number of omitted responses in KO mice was observed in the presence of auditory distractors (tones and clicks: WT=17.0 ±5.12, KO= 37.13 ± 18.13 and broad-band noise: WT= 18.27± 13.86, KO=39.20 ± 16.31; t-test, $p<0.05$), compared to WT mice. In order to study sustained attention in WT and KO mice, we divided the behavioral performance in five blocks of 22 trials. Data show that differences in correct and omitted responses in KO mice appeared in the last three blocks of trials.

Conclusions

α9-nAChR KO mice perform poorly in a selective attention to visual stimuli paradigm. Moreover, our data suggest that KO mice might compensate the behavioral performance during

the first trials of each session by central mechanisms, and that an intact MOC efferent-OHC synaptic transmission is needed to reduce cochlear sensitivity during sustained attention to visual stimuli.

PS-65

Neuronal Responses to Acoustic Stimuli in the Orbitofrontal Cortex of the Mouse

Kevin Donaldson[1]; Shihab Shamma; Jonathan Fritz[2]
[1]University of Maryland, College Park; [2]University of Maryland

Neurons in auditory cortex can show rapid task-related changes in receptive fields when animals are engaged in sound detection and discrimination tasks (Fritz et al,, 2003). One likely source of topdown signals to A1 that could trigger these changes are frontal cortical areas (Fritz et al., 2010), which have both direct monosynaptic and also multiple indirect polysynaptic projections to A1 (e.g. via Nucleus Basalis, Amygdala, Claustrum, or higher auditory cortical areas). In favor of a direct pathway, an earlier 2-photon study in the mouse (Winkowski et al., 2013) showed that pairing orbitofrontal cortex (OFC) stimulation with tones caused rapid changes in sound driven activity within A1. These OFC-induced influences on auditory responses resembled behavior-induced influences on auditory responses and demonstrated that orbitofrontal cortical activity could play a causal role in shaping rapid, dynamic changes in A1. These results raised the question of whether there were reciprocal auditory inputs to frontal cortex and neuronal responses to acoustic stimulation in OFC. To answer this question at a functional level, we recorded neurophysiologically from the OFC of passively-listening, head-restrained awake mice. Mice were habituated to the holder and presented with a variety of synthetic acoustic stimuli including tones, bandpassed white noise, rippled noise, FM sweeps and also natural animal vocalizations (all at ~60-65 dB SPL). Using tungsten and silicon probes, we recorded multi-unit activity in response to these acoustic stimuli from 135 sites in the OFC (LO/VO) of 19 mice (CBA and C57BL/6J strains). We found that 89/135 (65%) sites in the OFC showed responses to acoustic stimuli, 78/89 of which were excitatory (88%) and 11/89 inhibitory (12%). Auditory responses spanned a range of latencies ranging from 40-260 ms. Electrolytic lesions were placed at recording sites where acoustic responses were observed, and subsequent histology confirmed the location of recordings in LO/VO. In linear array recordings we observed auditory responses in multiple depths, throughout all cortical layers of OFC. Auditory responses were also found in the supplementary motor cortex (M2) that lies just dorsal to OFC. Four of the mice were behaviorally naïve, and fifteen were trained to behavioral criterion on either classical (n=5) or instrumental (n=10) conditioning tasks before OFC recording. We shall describe the effects of training on OFC responses and discuss the implications of auditory responses in OFC on topdown modulation of auditory cortical plasticity.

PS-66

Trial-to-trial Variation of Mismatch Negativity and Band-specific Power of Auditory Evoked Potential in Rat Auditory Cortex

Tomoyo Shiramatsu; Hirokazu Takahashi
The University of Tokyo

Background

Mismatch Negativity (MMN) refers to a negative deflection in auditory evoked potential (AEP) in response to sound changes. We have reported that MMN in rats is not a mere effect of stimulus-specific adaptation (SSA), while middle latency potential (P1) exhibited strong SSA. On the other hand, some recent studies pointed out the possible relationship between the MMN and alpha band power of EEG. In this study, we investigated whether MMN amplitude depends on SSA of P1 or on alpha band power, based on single trial analysis.

Methods:

A surface microelectrode array with a grid of 10×7 recording sites epipially recorded AEPs during an oddball paradigm from the right auditory cortex of anesthetized rats (8 - 10 postnatal weeks, 250 - 310 g). The test stimuli were 60-dB SPL, 100-ms-duration tone bursts. The test frequencies were either 10 or 12 kHz. In each block, 1620 standards (90%) and 180 deviants (10%) were delivered every 700 ms, and the single-trial responses of standard and deviant AEP were obtained.

Results:

In the single-trial AEPs, the amplitudes of deviant P1 and MMN were quantified. P1 amplitude was defined as the maximum potential within 50 ms from the stimulus onset. MMN amplitude was defined as the maximum within 50 - 150-ms post-stimulus latency in the subtraction waveform of the deviant response from standard response. We also extracted alpha band power from the single-trial AEPs, as the root mean square of the 100-ms band-pass filtered AEPs (8 - 13 Hz).

First, amplitudes in single-trial responses did not exhibit correlation between P1 and MMN waves. More interestingly, MMN amplitude exhibited a bimodal distribution while P1 amplitude showed a unimodal distribution, suggesting that MMN is generated only in some trials (‘on trials’) but not in other trials (‘off trials’). Furthermore, after the deviant sound onset, alpha band power in the on trials was larger than the off trials. On the other hand, 900 to 600 ms before the deviant sound onset, alpha band power was larger in off trials.

Conclusions:

These results suggest that generation of MMN is independent of SSA of P1, but mediated by the brain state before sound stimuli, such as alpha band power.

PS-67

Topographic Distribution of Stimulus-Specific Adaptation in the Rat Auditory Cortex

Javier Nieto[1]; Blanca N. Aguillon[2]; Manuel Malmierca[2]
[1]University of Salamanca; [2]Institute of Neuroscience of Castilla y León. INCYL

Neurons in the auditory cortex (AC) show stimulus-specific adaptation (SSA), a specific decrease in response to repetitive stimulation (Ulanosvky et al., 2003). SSA has also been found subcortically at the inferior colliculus and medial geniculate body, where it is strong only in the non-lemniscal subdivisions (Malmierca et al., 2009). SSA has been shown to be widespread and strong in the primary AC (A1), but its distribution in other cortical fields remains unexplored. The main goal of the present study was to characterize the topographic distribution of SSA within the five tonotopic fields of the rat AC as defined in Polley et al. (2007).

Experiments were performed on adult female rats anesthetized with urethane. Multiunit activity to pure tone stimulation was collected from different locations across the whole AC under an oddball paradigm (deviant probability: 10%, frequency contrast: 0.5 octaves, interstimulus interval: 300 ms), using two stimuli that evoked strong and similar neural responses. SSA was quantified using the common SSA index (CSI). Stereotaxic coordinates relative to bregma were carefully determined for each electrode penetration, and the limits between the putative fields were outlined for each animal using the BF gradient as the main reference landmark (Figure 1A).

Data collected so far (608 recording sites in 9 animals) show unequivocally that SSA is topographically distributed throughout the AC (Spearman distance correlation, $p<0.01$). Specifically (Figure 1C), CSI levels in A1 (99 recordings, median±IQR, **0.52**±0.35) and the anterior auditory field (93 recordings, **0.60**±0.35), which form the core (lemniscal) auditory cortex in the rat, were significantly lower than those in the two tonotopic belt fields of the rat, namely the posterior auditory field (54 recordings, **0.75**±0.23) and suprarhinal auditory field (71 recordings, **0.73**±0.27); CSI levels in the ventral auditory field (119 recordings, **0.65**±0.34), also in the core, were intermediate and statistically different from A1 only (Kruskal-Wallis one way ANOVA by ranks, Dunn-Sidak multiple comparison method, $p<0.01$). Interestingly, low CSI levels seem to be confined to the center of the core fields, getting gradually higher towards their periphery, where they show a sharp increase in the boundaries between core and belt fields (Figure 1B).

These results are in general agreement with the well established distribution of SSA in lower auditory relay stations; even though SSA is ubiquitous within the whole AC, the core fields feature low to medium levels of SSA, whereas in the belt fields SSA levels are high to extreme.

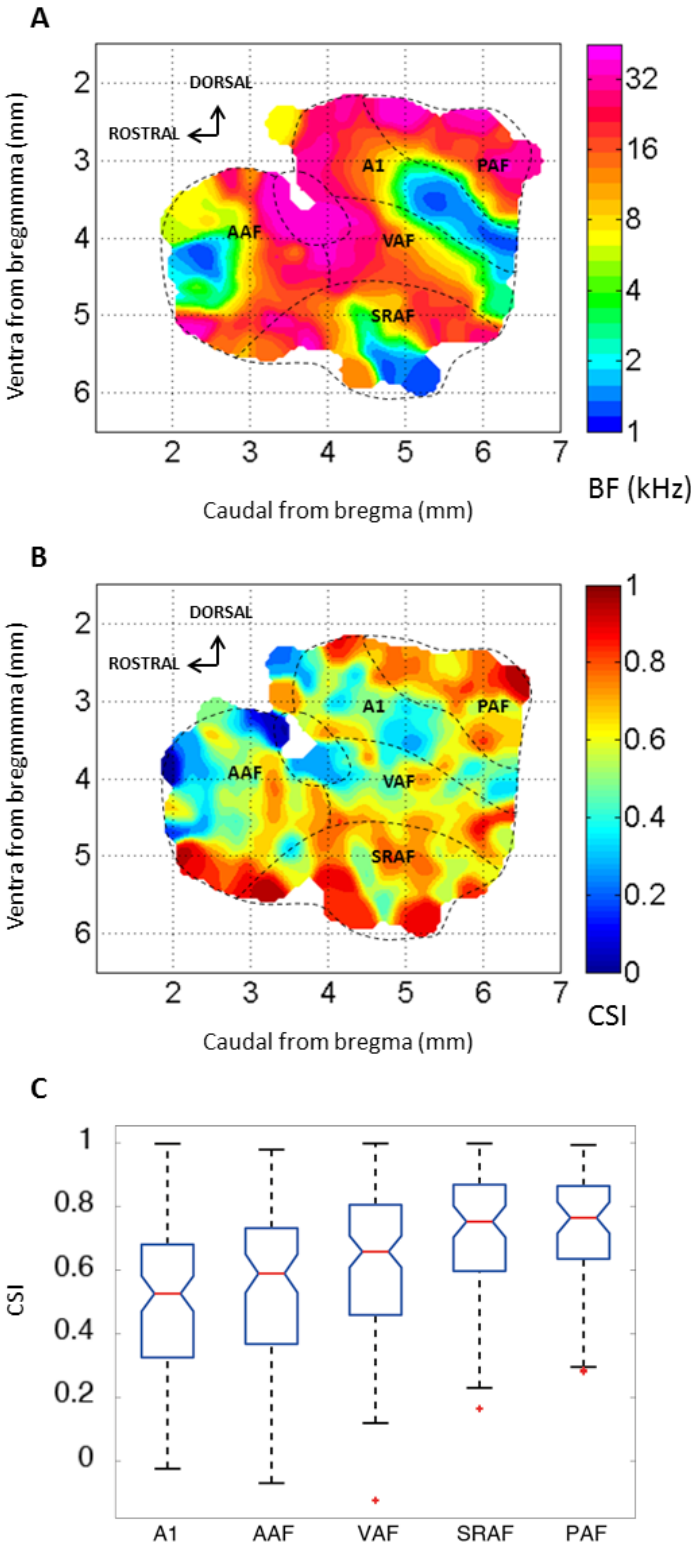

PS-68

Understanding the Network for Top-Down Control of Auditory Representation

Zachary Schwartz; Stephen David
Oregon Health & Science University

Introduction

The internal brain state that influences hearing combines multiple variables, such as selective attention, listening effort, and prior experience, including reward associations. Previous work (e.g. David, et. al. PNAS 2012; Atiani, et. al. Neuron 2009) has shown effects of attention and task difficulty on the representation of sound in primary auditory cortex. However, our understanding is limited by analyses that do not compare the effects of multiple aspects of behavioral state. We hypothesize that two behavioral state variables - attention and effort - have distinct influences on neural activity.

Methods

To contrast the influence of different internal state variables on auditory representations, we developed a discrimination task that controls attention and effort separately. Head-fixed animals were rewarded for responding to a pure tone target embedded in a continuous stream of vocalization-modulated noise (narrow-band noise modulated by the amplitude envelope from a natural vocalization). On each trial, two noise streams were presented simultaneously, centered at different frequencies and from different spatial locations. To manipulate effort, the level of the target relative to noise (SNR), but not its location or frequency, was varied between blocks. To manipulate attention, the frequency and location of the target tone was changed between trial blocks, holding SNR constant. During the attention task, the animal was trained not to respond to catch stimuli whose location and frequency differed from the target, verifying that attention was directed to the target. We trained two ferrets to perform the task and recorded activity of single neurons in primary auditory cortex (A1) using extracellular electrodes.

Results

When attention was directed away from the neuron's best frequency (BF), the response to noise distractor increased relative to when attention was directed to the BF. Spontaneous spike rate did not change. During the manipulation of effort, on the other hand, we observed changes in spontaneous but not evoked activity. Spontaneous activity decreased when the animal engaged in the high-effort task. Filter-based models indicate that attention modulated the gain of auditory responses, while effort modulated overall firing rate, independent of the stimulus.

Conclusion

These two aspects of behavioral state influence neural activity differently, suggesting they are controlled by distinct top-down circuits. A complete understanding of auditory processing requires an understanding the effect not only of stimulus features but also the structure of behavioral tasks.

PS-69

Neuronal Activity in Primate Auditory Cortex During the Performance of Audiovisual Tasks

Michael Brosch; Henning Scheich
Leibniz Institut für Neurobiologie

It is well established that engaging in a task affects neuronal activity in auditory cortex (for recent review see Scheich and Brosch, 2012, SHAR, Volume 45, edited by Cohen, Popper, Fay). To further determine which cognitive and motivational aspects of tasks modify auditory cortical activity we trained two macaque monkeys to be able to perform two tasks on the same audiovisual stimulus and to do this with two reward sizes. The monkeys had to touch a bar after a tone had been turned on together with an LED, and to hold it until either the tone (auditory task) or the LED (visual task) was turned off. An instruction presented before the audiovisual stimulus informed the monkeys about which of the two tasks had to be performed in a trial and about the reward size (large or small) that could be earned. Among the 399 multiunits recorded from the auditory core during task performance there many multiunits that exhibited a phasic response to the auditory and to the visual stimuli, or that slowly changed their firing (either ramped up or down) between task elements. These phasic and ramping responses were seen both during the performance of the auditory and the visual task, with generally weaker responses during the auditory task. Reward size had no effect on the firing during any phase of the task, except after its delivery. At this time many multiunits responded more strongly to the large rewards. Our study confirms and extends previous reports on the emergence of tonic/ramping activity in auditory cortex as subjects become engaged in a task, and in the task dependence of auditory cortical neuronal activity.

PS-70

Processing in Auditory Cortex Depends on the Characteristics of the Discrimination Task: fMRI Study

Teemu Rinne[1]; Suvi Talja[1]; G. Christopher Stecker[2]
[1]University of Helsinki; [2]Vanderbilt University

Auditory two-tone discrimination tasks can be accomplished via two potential strategies or "processing modes". In the first, a direct "sensory-trace" comparison of the tones is made on each trial. In the second, "context-coding" mode, listeners make a categorical judgment based on implicit knowledge. Previous behavioral studies suggest that experienced listeners adopt the more efficient context-coding strategy when possible, but that random trial-to-trial variation can force listeners to make sensory-trace comparisons (Hafter and Bonnel, *Percept. Psychophys.* 1998; Nahum et al., *J. Neurosci.,* 2010).

Our recent studies have investigated the role of human auditory cortex (AC) and inferior parietal lobule (IPL) in auditory discrimination and categorical memory-based (n-back) tasks using functional magnetic resonance imaging (fMRI). Several studies have consistently demonstrated greater AC activation

during discrimination tasks, and greater IPL activation during memory tasks. Thus, in the present fMRI study, we hypothesized greater activation in AC regions during discrimination in the sensory-trace mode, and in IPL when listeners utilized the context-coding mode.

Pairs of sounds differing in interaural time-difference (ITD) were presented in three task conditions: discrimination, 2-back and visual task. During the discrimination task, within-pair ITD difference was 0 or ±300 μs and pair structure depended on condition: (1) fixed 0 μs reference presented first, (2) fixed 0 μs reference presented second, (3) random pairs (ITD of each sound ±300 or 0 μs), and (4) random pairs (ITD ±300, ±225, ±150, ±75, or 0 μs). Subjects pressed a button when the parts of a sound pair matched in ITD. During the 2-back task, subjects indicated when a sound pair (no within-pair ITD difference) matched in ITD with the one presented two trials ago. In the visual task, subjects ignored the sounds and detected orientation changes in Gabor gratings.

Preliminary results suggest that auditory performance during these task conditions was associated with distinct brain activation patterns. IPL activation, in particular, was modulated consistent with a greater role in context-coding than in sensory-trace mode.

PS-71

Top-Down Attention Modulates the Frequency of the 40-Hz Auditory Steady State Response during Gap-Induced Resets

Brandon Paul; Larry Roberts; Ian Bruce; Daniel Bosnyak; David Thompson
McMaster University

Background

The auditory steady state response (ASSR, localizing to A1) is an electrical brain potential evoked by amplitude modulated (AM) sounds reaching its amplitude maximum at AM rates near 40-Hz. Perturbing the AM stimulus by inserting a brief gap in the AM train desynchronizes ("resets") the ASSR followed by a recovery period within 250 ms after stimulation resumes. Although this process is reported to be attention-sensitive – revealing how cognitive factors shape network synchrony – the time course of ASSR power and frequency modulations during the reset, as well as their frequency specificity, are unknown under attention. The current study investigates these variables.

Methods

15 normal-hearing participants were presented with 40-Hz AM tone bursts with either a 400 Hz or 5 kHz carrier frequency to the left ear. Each tone burst was 2 seconds in length and contained 3 gaps interspersed every 550 ms. Gaps were 12.5 ms (short) or 62.5 ms (long) in duration. In an active attending condition, participants listened to the tone bursts and reported if 1 or 2 long gaps were present in the tone burst. In a passive listening condition, participants were instructed to ignore the stimuli and not respond. We recorded the 128-channel electroencephalogram for all trials. Frequency modulations of the ASSR reset were estimated by computing the spectral centroid (the "center of mass" of the power spectrum) for each window of the short-time Fourier transform. ASSR power over this time period was also calculated.

Results

The centroid during the 50-250 ms recovery period was compared against the centroid of the 200 ms pre-gap baseline. For all gaps in both carrier frequencies, the centroid frequency decreased during the recovery period under active attending. In contrast, the centroid frequency increased during recovery under passive listening for the 5 kHz carrier and was unchanged at 400 Hz. ASSR power was not modulated at any time under attention.

Conclusions

Active attending leads to lower frequency modulations during ASSR recovery following a gap-induced reset while power remains unchanged. Low frequency shifts under attention may arise due to the synchronization of a distributed attention network to ASSR sources in A1. Communication between these centers would unfold over longer distances, resulting in a lower-frequency signal.

PS-72

State-Dependent Behavioral Changes in Ferret Higher Order Auditory Cortex in the Ventral Posterior Ectosylvian Gyrus

Diego Elgueda[1]; Stephen David[2]; Susanne Radtke-Schuller[3]; Shihab Shamma[1]; Jonathan Fritz[1]
[1]University of Maryland, College Park; [2]Oregon Health and Science University; [3]Ludwig-Maximilians-Universität

We have shown previously that neurons in ferret primary auditory cortex (A1) enhance their ability to encode task-relevant stimuli through rapid spectrotemporal receptive field (STRF) plasticity during auditory tasks requiring discrimination between classes of reference and target sounds, leading to enhanced representation of behaviorally relevant sounds. Recent work reveals that such contrast is further heightened in non-primary auditory cortical areas lying ventral to A1 in fields PSF/PPF in the dorsal Posterior Ectosylvian Gyrus (dPEG). Recordings in dorsolateral frontal cortex (dlFC) are consistent with a model in which plasticity in auditory cortex is controlled by feedback from dlFC. However, the pathways by which top-down signals from dlFC reach auditory cortex are not fully known. In order to better understand top-down attentional modulation in higher order auditory cortical processing, we investigated responses in a newly described auditory region - ventral-anterior PEG (vaPEG), which includes areas pro-PPF, VPr, and the adjacent bank of the pseudo-sylvian sulcus cortex (PSSC). Six ferrets were trained on go/no-go conditioned avoidance tone-detection (spectral) and click-rate discrimination (temporal) tasks, in which they had to refrain from licking water when presented with a target stimulus. We recorded >200 single-unit responses in awake, head-fixed ferrets during passive listening and active listening while performing auditory discrimination tasks. Compared to A1 and dPEG, neurons in vaPEG were weakly responsive to tonal stimuli, more broadly tuned, and displayed longer response latencies and durations. Also, vaPEG neurons had

weaker phase locking to the envelope of rippled noise stimuli, making it difficult in most cases to compute STRFs. Often, these neurons displayed more robust responses to ferret vocalizations than to synthetic stimuli. During auditory task performance, we observed modulatory effects in both spectral and temporal tasks, with a general tendency to selectively enhance responses to target sounds, suppress responses to non-target sounds, or enhance the difference between responses to target and reference stimuli. Similar to dlFC, some vaPEG neurons showed behaviorally gated, selective responses to target stimuli. Although most behavioral effects were transient and rapidly recovered to baseline firing rates, there were also cases of post-behavioral persistent effects, consistent with our previous observations in ferret A1 and dlFC. Preliminary neuroanatomical studies suggest vaPEG may be comparable to some parabelt auditory areas in the primate. The striking behavioral modulation in vaPEG observed in this area, suggests that it lies in a pivotal position in the processing hierarchy between purely sensory encoding and the encoding of sound meaning.

PS-73

Single-Unit Physiological Characterization of Putative Auditory Parabelt Cortex in the Marmoset Monkey

Darik Gamble[1]; Xiaoqin Wang[2]
[1]Johns Hopkins School of Medicine; [2]Johns Hopkins

The current working model of primate auditory cortex comprises the hierarchical arrangement of a series of functionally distinct information processing stages: a primary 'core' region, a secondary 'belt' region, and a tertiary 'parabelt' region. Combined anatomical, physiological, and imaging data have subdivided core and belt into multiple tonotopic subfields (Kaas & Hackett 2000, Petkov et al. 2006). In contrast, there currently exists no physiological characterization of parabelt, and its subdivision into distinct rostral and caudal fields rests solely on anatomical grounds.

We report here preliminary single-unit extracellular recording data from a region tentatively identified as parabelt, based on distance from the lateral sulcus medially, and the presence of visually responsive units laterally. Recording was performed in a head-fixed chronic preparation, in both passive and behaving conditions. Video monitoring allowed classification of the passive state as either 'quiescent' (eyes closed) or 'alert' (eyes open). While effects of animal state varied widely between units, a majority of units fit best either a multiplicative- or additive-gain model, suggesting that even though firing rates varied significantly with animal state, stimulus preferences in this cortical region remained relatively stable between quiescent, alert, and behaving conditions.

While many units in parabelt responded to broadband stimuli, approximately half also responded to narrowband stimuli and could be characterized in terms of their best frequency (BF). The spatial arrangement of BFs showed a tonotopic organization, with a high-frequency reversal located near the expected border between rostral (RPB) and caudal parabelt (CPB). Using this apparent delineation between RPB and CPB, we compared response properties between these two fields. Response latencies in both fields were significantly longer than in the more medial core and belt regions in the same animal. Furthermore, latencies in RPB were significantly longer than in CPB, consistent with a caudal to rostral increase in latency observed elsewhere in primate auditory cortex (Bendor & Wang 2008, Camalier et al. 2012). A majority of units in both fields exhibited facilitation to sinusoidal amplitude modulation, but units in CPB had higher best modulation frequencies and narrower modulation tuning functions. We discuss these findings in relation to further refinements of functional models of auditory cortex and future research directions for characterizing parabelt.

PS-74

Temporal Dynamics of Cortical Activity during Performance of the Mini-Mental Status Exam: An Intracranial Electrophysiology Study

Mitchell Steinschneider[1]; Kirill Nourski[2]; Ariane Rhone[3]; Hiroyuki Oya[2]; Hiroto Kawasaki[2]; Matthew Howard[2]
[1]Albert Einstein College of Medicine; [2]University of Iowa Medical Center; [3]University of Iowa

Multiple studies have demonstrated increased activity in auditory cortex during active listening and suppression of activity in response to self-generated vocalizations (e.g. Eliades & Wang, 2005, Cereb Cortex 15:1510-23). These findings have been extended to include suppression of high gamma activity in the electrocorticogram (ECoG) during self-generated speech (e.g. Greenlee et al., 2013, PLoS ONE 8:e60783). Activity in lower ECoG frequency bands has also been shown to be prominent in auditory cortex (e.g. Schroeder and Lakatos., 2009, Trends Neurosci 32:9-18). Interactions between higher and lower ECoG frequency bands during dialog-based experimental paradigms are unknown. This study examined these interactions by recording ECoG activity while subjects performed components of the mini-mental status examination.

Subjects were neurosurgical patients undergoing chronic invasive monitoring for medically refractory epilepsy. Studies were approved by the University of Iowa Institutional Review Board and NIH, and subjects could rescind their consent for participation at any time without affecting their clinical evaluation. Recordings were made simultaneously from multiple brain regions, including superior temporal gyrus (STG), temporoparietal junction and prefrontal cortex. The ECoG was filtered into frequency bands (theta, alpha, beta, gamma and high gamma) using FIR filters implemented in MATLAB. Responses in each frequency band were related to listening to the instructions of the interviewer and to the subject's verbal responses.

In auditory cortex on the lateral surface of STG, gamma and high gamma bands tracked the speech envelope and were suppressed during self-initiated speech. This relationship began to break down in the beta band. Alpha activity was generally suppressed during listening and increased during brief quiet periods separating syllables and words spoken by either the interviewer or the subject. Patterns of theta activ-

ity were similar to those seen in the alpha band. Response patterns at the temporoparietal junction were similar to those seen at more anterior locations in STG. Activity in prefrontal cortex was more complex and appeared to reflect task difficulty, effort and performance. We are currently examining additional auditory-related brain regions to identify their activity associated with different tasks in the mini-mental status exam (e.g. short-term memory, arithmetic calculation).

We conclude that activity in low and high frequency bands within the ECoG reflects different complementary functions in auditory- and auditory-related cortex, resulting in a rich mosaic of dynamic power changes engaging multiple cortical areas and associated with distinct aspects of sound processing and action.

PS-75

Role of Myelination in the Dynamics and Regional Distribution of Na+ Entry at Nerve Terminals in the Auditory Brainstem

Jun Hee Kim; Emmanuelle Berret; Sei Eun Kim
University of Texas Health Science Center, San Antonio

Myelin increases axonal conduction velocity and is responsible for high frequency impulse propagation in the mammalian auditory nervous system. Axon myelination is also important in ion channels clustering at axon nodes and paranodes in auditory nerve fibers. However, there is little known about the role of myelination in expression of ion channels and their kinetics at axon heminodes (last axonal nodes) and nerve terminals, which is critical for action potential firing and neurotransmitter release. Our published studies have shown that myelination is required for maintaining both presynaptic excitability and the temporal fidelity of synaptic transmission in the auditory brainstem (1Kim et al., 2013; 2Kim et al., 2013). Here we have investigated underlying mechanisms whereby loss of myelination alters presynaptic excitability and temporal fidelity of synaptic transmission in the auditory nervous system. We examined the expression of Na+ channels and subsequent Na+ dynamics along the axon and at terminals using the Long Evans shaker (*LES*) rats, which lack condensed myelination due to a genetic deletion of myelin basic protein (MBP). Immunohistochemistry data showed that loss of myelination disrupted the cluster of Na+ and K+ channels at axon heminodes and terminals, whereas nodal Na+ and K+ channels kept their clusters along demyelinated axon fibers in the *LES* rat. Using presynaptic whole-cell recording and Na+ imaging at the calyx of Held axon and terminal, we found that dispersed Na+ channel expression at heminodes resulted in reduced resurgent and persistent Na+ currents in the *LES* rat. In control rats, intracellular Na+ rise and decay were faster at the axon heminode (where Na+ channels are clustered) than at presynaptic terminals. In contrast, in the *LES* rat, Na+ rise during action potential firing was smaller and slower at demyelinated axon heminodes than at presynaptic terminals. These results suggest that myelination is critically required for the clustering of Na+ channels at axon heminodes and terminals, in order to maintain the fidelity and reliability of Na+ dynamics and action potentials at myelinated axon terminals in the auditory nervous system.

1. Kim SE, Turkington K, Kushmerick C and Kim JH. Central dysmyelination reduces the temporal fidelity of synaptic transmission and the reliability of post-synaptic firing during high-frequency stimulation. *J Neurophysol.* 110(7): 1621-1630. 2013.

2. Kim JH, Renden R and von Gersdorff H. Dysmyelination of auditory afferent axons increases the jitter of action potential timing during high-frequency firing. *J Neurosci.* 33(22): 9402-9407, 2013.

PS-76

Identification of Two Differing Sources of Glutamatergic Excitation in Principal Cells of the Ventral Cochlear Nucleus.

Xiao-Jie Cao; Donata Oertel
University of Wisconsin

What integrative tasks are carried out by the principal cells of the ventral cochlear nucleus (VCN) depends on how the synaptic currents that converge on the cell sum and on how the intrinsic properties of neurons convert synaptic currents into voltage changes. Much is known about how type I auditory nerve fibers affect the principal cells of the ventral cochlear nucleus of the mouse. They excite their targets with glutamatergic EPSCs whose convergence and magnitudes vary with the target and which consistently show synaptic depression (Cao and Oertel, 2010, J Neurophysiol 104, 2308-2320; Yang and Xu-Friedman, 2009, J Neurophysiol 102, 1699-1710). Principal cells of the VCN also receive other excitatory inputs, including from type II auditory nerve fibers (Brown et al., 1988, J Comp Neurol 278, 581-590; Berglund and Brown, 1994, Hear Res 75, 121-130). Two approaches are used to increase the likelihood that we record responses to type II fibers with whole-cell patch recordings from principal cells in slices of the VCN. First, shocks were presented to the granule cell lamina, an area that contains terminals of type II but not type I fibers. Second, 1 mM ouabain was applied to the round window to reduce the number of type I auditory nerve fibers (Lang et al., 2005, J Assoc Res Otolaryngol 6, 63-74; Fu et al., 2012, Neurotox Res 22:158-169). Four to seven days after treatment, auditory brainstem responses (ABRs) on the treated side were compared to the contralateral control side to assess the efficacy of the treatment. We found that thresholds of responses to clicks were elevated at least 10 dB in 13/17 animals, and thresholds to tones were elevated by 10-20 dB at one or more of four frequencies tested in 17/17 animals. In T stellate cells responses to trains of shocks at 100 Hz to the granule cell lamina (n=5) and responses to trains of shocks of fibers in the magnocellular regions of the VCN of ouabain-treated animals (n=2) were facilitating. We conclude that T stellate cells have two distinct sources of excitation that differ in their short term plasticity. Type I fibers produce trains of EPSCs that show synaptic depression while another source of excitation produces trains of EPSCs that show facilitation. The latter source of excitation could arise from the activation of type II auditory nerve fibers.

PS-77

Cholinergic Signalling in the Gerbil AVCN Modulates Spherical Bushy Cells Membrane Potential, Excitability and Temporal Precision on Different Time Scales

David Goyer; Richard Sinzig; Stefanie Kurth; Thomas Kuenzel
RWTH Aachen University

Low frequency spherical bushy cells (SBC) receive direct input from the auditory nerve via the Endbulbs of Held. Recent data have shown that inhibition changes SBC input-output function by tuning excitability in a stimulus-dependent manner. Furthermore, the existence of cholinergic projections into the cochlear nucleus has been shown before, formed by collaterals from the olivocochlear bundle as well as a pathway coming from the tegmentum, projecting in a top-down fashion into the CN. We hypothesize that this modulatory system plays an additional role in fine-tuning of SBC input-output function.

In frontal and parasagittal auditory brainstem slices of P14-26 gerbils (Meriones unguiculatus), whole cell patch clamp recordings from SBC were obtained in the presence of Glycine and GABA receptor antagonists. First, 1mM Acetylcholine or 500µM Carbachol was locally applied onto the SBC with a Picospritzer to investigate the principal effect of ACh on the cells. This experiment was repeated in the presence of blockers specific to nicotinic (D-Tubocurarine, Methyllycaconitine) and muscarinic Acetycholine receptors (Atropine). To assess changes in SBC's excitability, pharmacological stimulation with ACh was combined with electrical stimulation of auditory nerve fibers to evoke Endbulb inputs onto SBC. Immunohistochemical staining with α-Bungarotoxin (BTX) and against Choline Acetyltransferase (ChAT) were done to further localize cholinergic signaling in the AVCN.

We show that ACh caused a transient depolarization of 3.23 mV (+/- 1.7 mV), relaxing back to rest with a weighted-tau of 282 ms (+/- 311ms, n=7). This was due to activation of α7 subtype containing nicotinic receptors. Additionally, repeated ACh applications (10sec interval) tonically shifted the RMP towards depolarized values from **RMP ± std** to **RMP+1.34** mV (+/- 1.66mV, n=18), which was driven by muscarinic ACh-Receptors and lasted minutes. Additionally, the cells hyperpolarized under Atropine influence. Immunohistochemical staining revealed colocalizing ChAT and BTX staining in the neuropil surrounding SBC. The combined electrical and pharmacological stimulation revealed an increase in SBC's firing probability while under ACh influence. We assessed the impact of cholinergic modulation on sound encoding in a SBC model.

With this work we have shown that SBCs can be modulated by Acetylcholine, impacting their membrane potential und firing probability. The cholinergic projections originating in the tegmentum could be modulating the SBCs input-output function independent of the already established stimulus dependent modulation.

PS-78

Influence of Small Dendritic Excitatory Inputs on Temporal Precision in a Compartment Model of Low Frequency Spherical Bushy Cells

Thomas Kuenzel
RWTH Aachen University

Anatomical studies in the AVCN reported small excitatory dendritic inputs consisting of either bouton terminals formed by auditory nerve fibers or synaptic dyads by giant terminals contacting adjacent somata. The function of these small dendritic inputs is unknown. Low-frequency spherical bushy cells (SBC) often receive only a single somatic input from the auditory nerve via the Endbulb of Held terminal. Still, it was observed in juxtacellular recordings performed in gerbils that low-frequency SBC improve the precision of phase-coupling from input to output. It was hypothesized that tonic inhibition sets the EPSP threshold in a stimulus dependent manner, allowing only the largest and most rapidly rising EPSP to elicit an output spike. These remaining EPSP thus must have better timing than smaller, more slowly rising EPSP.

We tested this assumption in a model of SBC contacted by a large somatic input and realistic inhibitory contacts. Excitatory synaptic events were bestowed with a phase-dependent conductance to match the observation from the in vivo experiments. A distinct increase in output vector strength occurred when these phase-dependent events interacted with tonic inhibition. However, the source of the phase-dependency of the endbulb conductance remains elusive.

Thus, we next created a compartment model of SBC that included a representation of the dendritic tree. We asked whether coincident excitatory events of small synaptic contacts might augment the endbulb events in a phase-dependent manner. Geometrical parameters of the SBC dendrite were derived from reconstructions of SBC filled with fluorescent dye during slice recordings. Varying numbers of excitatory synaptic mechanisms with a mean individual conductance of 1nS were connected to the dendritic compartment. All synaptic inputs were driven by phase-coupled spiking activity produced by an auditory periphery model in response to pure tone stimuli.

The dendritic inputs alone elicited a depolarizing but subthreshold membrane potential deflection that resembled the response shape of the auditory nerve fibers. In addition, a shallow (<1mV) but phase-coupled modulation of the membrane potential during ongoing responses occurred. In total, endbulb EPSP had a significantly steeper slope when endbulb and dendritic inputs interacted. During the onset stimulus response, endbulb events now more robustly caused output spiking. In total, vector strength of output events was slightly increased, but to a lesser amount than in the phenomenological implementation.

We therefore conclude that small dendritic inputs can at least contribute to the improvement of temporal precision in low frequency SBC.

PS-79

Slow Inhibition Improves Temporal Precision in Sphercial Bushy Cells.

Christian Keine; Tamara Radulovic; Rudolf Rübsamen
University of Leipzig

The anteroventral cochlear nucleus (AVCN) is part of the first processing station of the central auditory system. Spherical bushy cells (SBCs) located in the rostral pole of the AVCN are constituents of the brainstem sound localization circuitry. These cells receive their main excitatory input directly from auditory nerve fibers (ANF) by giant synaptic terminals, the endbulbs of Held. In addition to ANF input, SBCs receive acoustically triggered inhibitory input mediated by γ-aminobutyric acid (GABA) and/or glycine, the physiological role of which is still elusive. This inhibition shows remarkably slow dynamics in slice recordings.

In this study, we aimed for an in vivo characterization of acoustically evoked inhibition and their potential contribution to temporal precise signal transmission. Juxtacellular in vivo recordings in P25-P32 gerbils were performed and the input-output function analyzed using varying acoustic stimulation. The temporal precision of the ANF input and the SBC output was quantified by analyzing the phase-locking to low-frequency sound stimuli. While acoustically evoked inhibition does not change the ANF input to the cells, it considerably reduces the success rate of postsynaptic AP generation in a stimulus intensity dependent manner. Additionally, inhibition reduces the EPSP rising slope and prolongs the EPSP-to-AP transition time. For low-frequency stimulation, the SBCs show an increased phase-locking compared to their ANF input. This improvement is achieved by a two-step process: (i) selection of large, well-timed EPSPs to evoke postsynaptic action potentials and (ii) variability in EPSP-to-AP transition time additionally enhancing the temporal precision of SBC output.

We suggest that tonic inhibition in conjunction with convergence of excitatory inputs plays a major role in the improvement of temporal precision in SBCs.

PS-80

A Model of Acoustically Evoked Inhibition in Spherical Bushy Cells

Jörg Encke[1]; **Christian Keine[2]**; Meenakshi Asokan[3]; Rudolf Rübsamen[2]; Werner Hemmert[1]
[1]Technische Universität München; [2]University of Leipzig; [3]Indian Institute of Technology, Madras

Introduction

Spherical bushy cells (SBCs) are the principal neurons of the anteroventral cochlear nucleus. They receive a limited number of supra-threshold excitatory inputs from auditory nerve fibres via endbulbs of Held, so that their response mostly resembles that of the auditory nerve. In addition, SBCs receive glycinergic and GABA-ergic inhibitory inputs which have a significant impact on their output. In vivo recordings in the gerbil have shown that the strength of inhibition in SBCs strongly depends on the stimulus frequency being strongest 1-2 octaves above the SBCs characteristic frequency (CF). Also, the impact of acoustically evoked inhibition shows a stimulus intensity dependent increase.

Methods

We used extracellular recordings in the gerbil as a basis to fit the inhibitory inputs of a computational model. Input spike trains for the model were generated by one high spontaneous rate fibre of the Zilany auditory periphery model [1]. Sideband inhibition was implemented with a set of inter-neurons with different CFs and a varying strength of inhibitory inputs to the SBCs.

Results

The measured receptive field of a spherical bushy cell could be reproduced in the model using frequency dependent synaptic weights for the inhibitory inputs. The weight dependency was chosen to be Gaussian shaped with a center frequency at about an octave above CF and a half width of about 200Hz. A good fit to the spiking rate data was obtained while the failure fraction of the model was too low during weak stimulation.

Summary

This newly developed model is able to reproduce the measured, level dependent excitation and inhibition at CF by assuming inhibition from an inhibitory sideband positioned about an octave above CF.

[1] M. S. A. Zilany, I. C. Bruce, and L. H. Carney, "Updated parameters and expanded simulation options for a model of the auditory periphery.," *The Journal of the Acoustical Society of America*, vol. 135, pp. 283–6, Jan. 2014.

PS-81

Synaptic Plasticity Interacts with Postsynaptic Membrane Kinetics in the Chick Cochlear Nucleus

Stefan Oline; R. Michael Burger
Lehigh University

Auditory stimuli are processed in parallel frequency-tuned circuits, beginning in the cochlea. Auditory nerve fibers (nVIII) share this topographic pattern, known as tonotopy, and impart frequency tuning onto their postsynaptic targets in nucleus magnocellularis (NM). Though all NM neurons perform similar functions, specializations exist along the tonotopy that reflect the characteristic frequency (CF) of their nVIII inputs, and may confer computational specificity. High CF neurons receive few (1-3) large inputs. Low CF neurons receive more than eight small inputs, yet are more excitable with a higher input resistance. Unlike high CF NM cells, which may relay information with 1 output spike per input, low CF NM neurons improve spike timing relative to their inputs, putatively by averaging the input time of many inputs through synaptic integration. We therefore asked if the tonotopically distributed postsynaptic membrane differences contribute to the apparent difference in computational strategy.

An efficient way to evaluate membrane properties is by examining responses to injected current. We used two current clamp protocols, ramps of varying slopes, and frequency modulated sine waves that sweep across a broad range of frequencies (ZAP currents). Ramps create systematically changing PSPs, from which spike responses can be evaluated. Alternatively, ZAP currents allow evaluation of a neuron's membrane frequency response, which may contribute to synaptic integration.

Low CF neurons, compared with their high CF counterparts, exhibited longer integration times in response to ramp currents with spikes following less steep and more prolonged stimuli. In tandem, responses to ZAP currents varied by CF. We classified almost all low CF neurons as low-pass**,** and nearly a third of high CF neurons were band-pass. These responses were strikingly adaptive to input conditions. Although low CF neurons remained characteristically low-pass regardless of holding potential, mild depolarization shifted frequency selectivity of high CF neurons via a several-fold increase in peak response frequency (*f*0). This suggests that, when depolarized, low-voltage gated K^+ channels in high CF neurons shunt slow input stimuli, while maintaining a band-pass region for faster inputs. Preliminary evidence to support this conclusion is shown, where *f*0 predicts peak spike entrainment to trains of current pulses presented at a range of frequencies.

Together, these data suggest that computational strategy for spike initiation in NM may depend on both input conditions and tonotopic position. Interestingly, the ability for high CF neurons to alternate between low- and band-pass filtering may indicate a stimulus-dependent switch, between relay and integrate-and-fire strategies.

PS-82

Differential Effects of Background Noise and Reverberation on Periodicity-Tagged Neural Segregation of Intonated Concurrent Vowels in the Ventral Cochlear Nucleus

Mark Sayles; Arkadiusz Stasiak; Ian Winter
University of Cambridge

Background

Psychoacoustic studies demonstrate differential effects of noise and reverberation on "cocktail-party" listening. We previously identified neural correlates of impaired ΔF0-based intonated concurrent-vowel segregation under reverberant conditions in the ventral cochlear nucleus (VCN). Here we examine the differential effects of background noise and reverberation on VCN segregation of concurrent vowels.

Methods

Spike times were recorded from VCN single units in urethane-anesthetized guinea pigs, using tungsten-in-glass microelectrodes. Units were classified as primary-like (PL), primary with notch (PN), transient chopper (CT), sustained chopper (CS), onset chopper (OC), onset-L (OL), onset-I (OI), and low-frequency (LF). Stimuli were synthetic vowels /a/ and /i/, presented monaurally, either alone, or as a "double vowel". F0 was either static (125 Hz, or 250 Hz for /a/, and 100 Hz, or 200 Hz for /i/), or sinusoidally modulated at 5 Hz, by ± 2 semitones around these values. Reverberation was added by convolution. Background noise (5-kHz bandwidth) was added at signal-to-noise ratios of {10, 3, 0} dB. Spike trains were analyzed in terms of their short-term inter-spike-interval distributions, pitch-template contrast, and a harmonic-cancellation model of double-vowel segregation.

Results

We recorded responses to single and double vowels in quiet, anechoic conditions and in quiet, reverberant conditions from 129 single units with best frequencies (BFs) between 0.1 and 6 kHz (36 PL/PN, 47 CT/CS, 24 OC/OL/OI, 19 LF, 3 unusual). From 52 of these units we recorded responses to the vowel sounds under anechoic conditions in background noise (17 PL/PN, 26 CT/CS, 6 OC/OL/OI, 3 LF). There is a strong interaction between F0 modulation and reverberation on template contrast. Conversely, there is no interaction between F0 modulation and signal-to-noise ratio on template contrast. The effects of noise on double-vowel segregation are strongly BF-dependent, due to increasing cochlear-filter bandwidth with increasing BF resulting in more total (masking) noise power passed by higher-BF filters. In contrast, reverberation impairs neural segregation of intonated double-vowels independent of BF. A harmonic-cancellation scheme can exploit residual periodicity in low-BF units in the region of the first formant for intonated double-vowel segregation in noise.

Conclusions

The effects of background noise and reverberation on double-vowel segregation in the VCN are not equivalent. Reverberation impairs neural exploitation of periodicity information when F0 is modulated. Background noise attenuates periodicity representations (and therefore periodicity-based segregation) in higher-BF units but does not interact with F0 modulation to impair speech segregation.

PS-83

Spectral-Temporal Receptive Fields in the Cochlear Nucleus Estimated Using Dynamic Moving Ripples

Arkadiusz Stasiak[1]; Monty Escabi[2]; Stefan Bleeck[3]; Jessica Monaghan[3]; Matthew Wright[3]; Ian Winter[1]
[1]University of Cambridge, UK; [2]University of Connecticut, Storrs, USA.; [3]University of Southampton, UK

Background

Spectro-temporal receptive fields (STRFs) have been used to characterise neuronal responses at higher stages of the auditory pathway, e.g. the cortex, thalamus or inferrior colliculus. However, there is less information on how spectro-temporal modulations are processed or transformed between the auditory nerve and the different unit types in the cochlear nucleus (CN). Such information is also valuable for understanding the functional trasnformation between the CN and inferior colliculus. To address this issue we have selected two broadband stimuli, DMR (dynamic moving ripple) and RN (ripple noise), commonly used for characterizing neuronal spectro-temporal

processing at higher stages of auditory pathway (Rodriguez *et al.,* 2010).

Methods
The DMR and RN stimuli (bandwidth 1-20kHz) were presented to the left ear of normal hearing, urethane-anaesthetised, pigmented guinea-pigs at 3 different sound levels (with intervals of 20 dB) for 180 seconds. Spectral and temporal modulations were varied independently in order to densely probe the response space between 0-4 cycles per octave (spectral) and 0 – 500 Hz (temporal), respectively. Single units in the CN were isolated and recorded extracellularly with low impedance glass-coated tungsten microelectrodes.

Results
We have recorded from 10 chopper units (CH); 5 primary-like with a notch units (PN), 8 onset units (ON), 14 units from the DCN. 11 units were classified as unusual. There are distinct STRF patterns and ripple transfer functions for different unit types in the CN e.g. Primary-like with a notch units phase-lock to the fastest modulations and thus have a higher temporal modulation frequency upper cut-off. Onset units (ON), by comparison, responded to a restricted range of spectral modulations and thus have a lower upper cut-off in their spectral modulation frequency tuning. On average chopper, onset and PN units consistently exhibited temporal band-pass tuning irrespective of unit BF and a weak, but systematic, progression from low-pass to band-pass spectral tuning with increasingly higher levels of sound stimulation. Single units recorded from the dorsal cochlear nucleus and classified as type II, type IV or pause-build show the most diverse spectrotemporal response patterns.

Conclusions
There are significant differences in the spectro-temporal response properties between different unit types in the cochlear nucleus. Such patterns may ultimately contribute to the range and diversity of spectro-temporal sensitivities observed in inferior colliculus. However, due to our limited sample we are currently unable to determine whether the range of responses found the CN can account fully for those observed in the inferior colliculus.

PS-84

Neural Correlates of Context-Dependent Enhancement in the Dorsal Cochlear Nucleus

Bertrand Fontaine; Tom Franken; Philip Joris
KU Leuven

Introduction
A sound can be perceived differently, depending on the presence of other stimuli. In perceptual enhancement, a multitone complex presented in isolation is perceived as a single object. If a target tone is deleted from the complex (the conditioner) and then reintroduced (the test), it will perceptually "pop out". We hypothesize that perceptual enhancement emerges in the Dorsal Cochlear Nucleus (DCN). No correlates of enhancement were found in the auditory nerve, one synapse before the DCN, but were in the Inferior Colliculus, one synapse after the DCN. DCN output cells have responses that exhibit strong lateral inhibition. This feature is critical to implement the mechanisms that have been postulated to underlie enhancement: during the conditioner, the broadband lateral inhibition adapts but the narrow band excitation does not. During the test, the firing rate will be higher than without a preceding conditioner.

Methods
We performed extra-cellular recordings in Mongolian gerbils under general anesthesia using experimental protocols similar to psychoacoustic experiments. To quantify enhancement we compared statistics of the neural response with and without a conditioner. Different parameters of the stimulus protocol were changed such as spectral notch width, overall level, delay between conditioner and test, and frequency of the target tone. We also performed in vivo patch clamp recordings to study the statistics of the subthreshold signals.

Results
In 83% of the cells that were physiologically classified as DCN, the presence of the conditioner with a given spectral notch induced an increase in the firing rate compared to the case without conditioner. Temporal properties were also altered by the presence of the conditioner: the response to the enhanced condition exhibited a shorter latency and a higher temporal precision. Enhancement could persist several hundreds of milliseconds and was higher when the target tone was at the best frequency of the neuron. Enhancement was also reflected in the mean of the membrane potential.

Conclusion
Many properties of the DCN responses parallel psychophysical measures of perceptual enhancement, including the dependence on the spectral notch width surrounding the target, the overall level of the complex, and the delay between the conditioner and the test. More intracellular recordings need to be performed to test the hypothesis of adaptation of inhibition.

PS-85

Somatosensory Influences on Spectral Feature Detection in the Cochlear Nucleus

Calvin Wu; Susan Shore
University of Michigan

The cochlear nucleus (CN) decodes spectral information for early processing of sound localization cues. The filtering properties of the head and pinna create directional-dependent transfer functions that contain frequency-specific notches and rising edges, both detected by the principle output neurons of the dorsal cochlear nucleus (DCN), fusiform cells (FCs). Coding of these sharp spectral features in FCs relies on basal dendritic inputs from wide-band inhibitors in the ventral CN and narrow-band inhibitors in the deep DCN. FCs also process concurrent multisensory information via their apical dendrites, but it is not known whether these inputs influence spectral feature detection. In the present study, coding of spectral cues in the guinea pig CN was confirmed by single-unit spectral notch and edge responses. Pairing notch and edge stimuli with somatosensory stimulation of the neck (C2–C5 region) resulted in short-term, cell-specific alterations in notch and edge sensitivity. These alterations were

stimulus-timing dependent, and especially prominent when spectral stimuli preceded somatosensory signals. These results suggest that CN integrates proprioceptive information, such as that generated during orienting head movements, to modulate spectral response sensitivity, and may participate in active sound localization.

PS-86

Modulation of Extrasynaptic NMDA Receptors by Synaptic and Tonic Zinc in the Dorsal Cochlear Nucleus

Charles Anderson[1]; Robert Radford[2]; Daniel Zhang[2]; Ulf-Peter Apfel[2]; Stephen Lippard[2]; Thanos Tzounopoulos[3]
[1]University of Pittsburgh; [2]MIT, Dept. of Chemistry; [3]University of Pittsburgh, Depts. of Otolaryngology and Neurobiology

Many excitatory synapses contain high levels of zinc within glutamatergic vesicles. Although synaptic zinc and glutamate are co-released, it remains controversial whether zinc diffuses away from the release site (phasic release) or whether it remains bound to presynaptic membranes or proteins after its release. Here we show that synaptic zinc is phasically released during action potentials. In particular, in response to short trains of presynaptic stimulation, synaptic zinc diffuses outside the synaptic cleft to inhibit extrasynaptic NMDA receptors (NMDARs) in the dorsal cochlear nucleus. During higher rates of presynaptic activity, glutamate activates additional extrasynaptic NMDARs that are not inhibited by synaptic zinc diffusion, but these NMDARs are inhibited by ambient (tonic), non-synaptic zinc. Previous studies revealed that zinc modulates synaptic NMDARs and that extrasynaptic NMDARs are functionally distinct from synaptic NMDARs. In this context, the present results reveal the novel physiological role for zinc in modulating extrasynaptic NMDAR-mediated signaling and establish zinc as a neurotransmitter in the auditory system.

PS-87

Modifications in Stimulus-Timing Induced Plasticity of DCN Fusiform Cell Responses Following Muscarinic Acetylcholine Receptor (mAchRs) Blockade.

Roxana Stefanescu; Susan Shore
University of Michigan

The dorsal cochlear nucleus (DCN) receives auditory input from the cochlea and somatosensory input from the trigeminal ganglion and spinal trigeminal nucleus (Sp5) via parallel fibers. Stimulus-timing dependent plasticity (StTDP), the macroscopic correlate of spike-timing dependent synaptic plasticity (SpTDP), can be induced in DCN following a bimodal (auditory-somatosensory) stimulation protocol in which auditory and facial electrical stimulation are presented at various onset difference intervals (Martel et al., ARO 2015). In vitro studies (Tzounopoulos et al. Nat Neurosci., 7(7):719-25, 2004) showed that changes in the neural responses following SpTDP stimulation take the form of a Hebbian "learning rule" in DCN fusiform cells but are anti-Hebbian in cartwheel cells. Physiological activation of muscarinic acetylcholine receptors (mAChRs) converts postsynaptic Hebbian long term potentiation to anti-Hebbian long term depression in fusiform cells, via activation of the endocannabinoid system and other mechanisms including activation of NMDA receptors and G-protein coupled receptors (Zhao et al. J Neurosci., 31(9):3158-3168). In cartwheel cells, in addition to these mechanisms, activation of the mAChRs suppresses large-conductance calcium-activated potassium channels (BK), which increases the amplitude of the postsynaptic potentials evoked by parallel fiber activation (He et al. J Neurosci 34(15):5261-5272). The interplay between these complex mechanisms is likely to alter *in vivo* fusiform cell responses. In this study, we investigate the effects of mAChR blockade on StTDP induced learning rules in the fusiform cells of the DCN.

In vivo, sound-evoked and spontaneous activity was recorded from single fusiform cells in the guinea pig DCN before and after bimodal stimulation to determine the StTDP learning rule for each cell. The learning rules were evaluated again after mAchR blockade using 2µl of 80 µM atropine solution delivered to the fusiform cell layer. Changes in plasticity were assessed by comparing the learning rules evaluated before and after mAchR blockade.

Significant changes were observed following mAchRs blockade including inversion of the learning rule profiles, preservation of the initial profile with changes for specific bimodal intervals as well as suppressive or enhancing characteristics. Pause build-up units showed an overall increase in the number of Hebbian learning rules, while build-up units showed an increase in the number of anti-Hebbian learning rules following mAchR blockade.

We conclude that mAchRs contribute significantly to bimodal plasticity in the DCN. Rather than a dominant enhancing or suppressive effect in stimulus-timing induced plasticity, blocking mAchR results in a redistribution of the plasticity inducing properties of the DCN circuitry.

PS-88

Spontaneous Spiking Gates Effective Size of a Convergent Inhibitory Network in the Dorsal Cochlear Nucleus

Hsin-Wei Lu; Laurence Trussell
Oregon Health & Science University

Introduction

In many neurons, spontaneous action potential activity may lead to short-term synaptic depression at a neuron's terminals, thus reducing the efficacy of transmission to postsynaptic targets. However, in microcircuits, multiple neurons often respond in concert to a stimulus, and together affect a common target cell. This convergence would be expected to offset the effects of depression at any one synapse; conversely, reduction in spontaneous activity would tend to enhance the potency of single presynaptic cells.

Methods

The dynamic relationship between convergence and plasticity was explored by combining paired recording, modeling, and optogenetic approaches in a microcircuit made by inhibi-

tory cartwheel interneurons of the mouse dorsal cochlear nucleus in brain slices.

Results
Paired patch-clamp recordings showed that spontaneous spiking in the cartwheel cell induced profound synaptic depression and greatly reduced its efficacy of inhibiting the postsynaptic neuron. A computational model suggested transmission during low and high frequencies is mediated by different vesicle pools. By selectively stimulating channelrhodopsin-expressing cartwheel interneuron populations with different light intensities, we estimated the number of convergent inputs required for inhibiting target neuron spiking under various background spiking levels. Effective inhibition required a critical number of inputs, and this number increased as spontaneous spiking was enhanced.

Conclusions
The level of spontaneous spiking controls the effective size of interneuron population needed to achieve inhibition. More generally this work suggests that by modulating spontaneous activity, neural circuits can titrate the impact of information carried by small vs large numbers of neurons.

PS-89

3D Characterization and Quantitative Morphometric Analysis of Ultrastructural Features that Determine the Strength and Polarity of Synapses on Fusiform Cells in the Dorsal Cochlear Nucleus

Rony Salloum[1]; Grahame Kidd[1]; Christopher Yurosko[1]; Manick Saran[2]; Anthony Lytle[1]; **James Kaltenbach[1]**
[1]Cleveland Clinic; [2]John Carroll University

Introduction
Fusiform cells represent the major class of principal cells of the dorsal cochlear nucleus. The synaptologies of these neurons is central to their function. Despite much attention to the origin and pharmacological identities of their synapses, the ultrastructural features determining the strength and functional polarity of fusiform cell synapses have not been quantitatively analyzed in 3 dimensions. We performed such an analysis of fusiform cell soma synapses, focusing on synaptic terminals and their mitochondria and active zones, as well as the post-synaptic densities (PSD), all key components participating in the energetics of synapses and the release and binding of neurotransmitter.

Methods
Sections were cut and imaged using a serial block face scanning electron microscope into 6 stacks of 500-800 sections (70 nm thick) and spanning a volume of 150 x 210 x 50 mm. Features selected for analysis included synaptic terminals and their active zones and mitochondria. Each structure was traced through the image stack over the entire surface of the soma then reconstructed in 3D, providing the basis for quantifying the volume of synaptic terminals and the number of active zones and mitochondria they contain. Synapses were then categorized as asymmetric (Gray Type I) or symmetric (Type II) based on the presence or absence of well-defined PSDs.

Results
Terminals were widely spaced on the soma surface. Their volumes fell along a continuum from small to large allowing examination of the relationship between terminal size and the number of active zones or mitochondria. We found that the number of both active zones and mitochondria were strongly correlated with the size of the terminal. Most axo-somatic synapses were symmetric, although terminals of different sizes, shapes and symmetry were often found to be interconnected by different branches of a common axon. Tracing axons retrogradely over short distances revealed extensive linkages, with an average of three terminals/axon (range 1-10).

Conclusion
The results suggest that larger synapses possess larger numbers of active zones and mitochondria consistent with the interpretation that they exert stronger influence on the postsynaptic cell than smaller terminals. The wide spacing between terminals may be a means by which synaptic influence on cells is spatially optimized with the smallest number of terminals. Caution should be exercised in inferring that different sizes, shapes and symmetries of synapses indicate different sources, as our results demonstrate that such differences can be found among terminals from the same axon.

PS-90

Circuitry between the Dorsal Cochlear Nucleus and the Inferior Colliculus in the Mouse

Giedre Milinkeviciute[1]; Michael Muniak[2]; Tan Pongstaporn[2]; Annie Cho[2]; David Ryugo[2]
[1]University of New South Wales, Garvan Institute of Medical Research, Australia; [2]Garvan Institute of Medical Research

Background
The central auditory system is comprised of numerous auditory nuclei that are connected by ascending and descending projections. The cochlear nucleus (CN) and inferior colliculus (IC) are two major structures with complementary interconnections, much of whose detailed nature remains to be elaborated. In order to infer mechanisms of signal processing at this early stage, it is essential to establish how these structures are connected. This project is focused on the synaptic connections between the dorsal cochlear nucleus (DCN) and the IC.

Methods
A cocktail of anterograde and retrograde tracer dyes was injected into the DCN of CBA/CaH mice in the awake animal after determining multiunit best frequency and threshold. Brains were processed using standard histologic methods for visualization and examination of neuronal tracer dyes using fluorescence, bright field, and electron microscopy (EM), and axons and cells were traced.

Results
Some if not all of the ascending DCN fibres that terminate in the ipsilateral IC reach this location by traveling through the

contralateral IC and crossing over via the commissure. Terminal fields were observed in the dorsal (DCIC) and external cortices (ECIC) of the IC. Preliminary data suggest reciprocal contralateral connections between the IC and the DCN that establish feedback and feedforward loops. EM analysis seeks to confirm synapses between labelled endings and retrogradely filled cells in the IC. There are numerous retrogradely filled cells in the ipsilateral IC. The ratio between labelled cells in the ipsilateral and contralateral sides is 3:1, respectively. Although the majority of labelled cells seem to be contained within the central nucleus of the IC (CNIC) bilaterally, cells in the ipsilateral side are found in other IC subdivisions as well. It is yet to be determined whether cells in the CNIC are contained within the same frequency band.

Conclusions
The multiple pathways between the DCN and the IC emphasize considerable complexity in how auditory signals are processed. A frequency-specific enhancement of acoustic signals is implied through the reciprocal contralateral circuit. Feedback from the ipsilateral IC might strengthen the signal through additional reverberant excitation, lateral inhibition, or even both. These findings would implicate a role for the DCN-IC circuit in signal enhancement in noisy backgrounds. Moreover, ascending DCN terminals in the DCIC and ECIC might be synapsing onto the cells that receive descending input from the auditory cortex, creating a circuit for cortical modulation of sound processing through links to memory and emotion.

PS-91

The Effect of Selective Elimination of A1-MGBv Corticothalamic Neurons on Mistuning Detection in Ferrets

Natsumi Homma[1]; Max Happel[2]; Fernando Nodal[1]; Victoria Bajo[1]; Andrew King[1]
[1]University of Oxford; [2]Leibniz Institute for Neurobiology

Recent evidence suggests that corticothalamic feedback can sharpen the spectral receptive fields of thalamic neurons and modulate the temporal precision of their responses. In this study, we aimed to investigate the role of the corticothalamic feedback system in the perception of spectral and temporal modulations by using a mistuning detection task with complex sounds.

We evaluated the behavioural effects of selective elimination by chromophore-targeted laser photolysis of corticothalamic neurons, projecting from the primary auditory cortex (A1) to the ventral division of the medial geniculate body (MGBv), in adult ferrets trained to carry out a mistuning detection task. Bilateral injections of fluorescent microbeads conjugated with the light-sensitive chromophore chlorin e6 were made in MGBv following electrophysiological recording. After allowing sufficient time for the beads to be transported to the cortical cell bodies, apoptosis was induced by infrared (670 nm) laser illumination of A1.

Mistuning detection was measured using a positive conditioned go/no-go task design. Complex harmonic tones composed of 16 harmonics with a fundamental frequency (F_0=400 Hz) were presented as a reference sound, while in the target sound the 4th harmonic was shifted (0.03-12%) to a higher frequency so that it was no longer an integer multiple of F_0. The microbead injections were made in the thalamus once the animals had been trained, and mistuning detection performance was tested before and after bilateral laser illumination of A1. Postmortem histology revealed that injection sites were located in MGBv. The cell densities of NeuN-positive layer VI neurons were measured using the optical fractionator stereological probe in the anterior, middle (where A1 is located) and posterior ectosylvian gyrus. A reduction in cell density by approximately 30% was observed in the middle ectosylvian gyrus relative to controls, supporting the selective elimination of corticothalamic neurons in A1.

Based on signal detection theory, behavioural performance was quantified by the animals' d' scores, an index of detection sensitivity, and by psychometric analysis. Corticothalamic lesion resulted in poorer mistuning detection performance, as indicated by decreased d' values, a shift of the psychometric curves towards higher frequencies with a threshold increase, and a trend for shorter reaction times at small mistuning frequencies. The behavioural impairment seemed to correlate with the degree of corticothalamic cell loss. These results support a role for A1-MGBv corticothalamic feedback in the accurate recognition of complex auditory stimuli.

PS-92

Beneficial Effect of Frequency-dependent Response Latency on Frequency Integration in Guinea Pig Primary Auditory Cortex

Masataka Nishimura; Wen-Jie Song
Kumamoto University

Frequency-dependent shortening of response latency has been demonstrated in the primary auditory cortex (A1) in a number of laboratories (Heil, 1997; Mendelson et al, 1997). The functional significance of the change in latency, however, remains unknown. From spatial representation of frequency in A1 and cortical lateral inhibition, we envisaged that frequency-dependent latency change may play a role in spectrum integration. Here we directly tested this notion by manipulating the relative presentation timing of two narrowband noises, while recording cortical activity with an in vivo optical imaging technique.

First, we quantified the frequency-latency relationship in the guinea pig A1, by recording responses evoked by 20–80 dB SPL of narrowband noises centering at 1, 2, 8, and 16 kHz (± 0.25 octave). In agreement with previous reports in other species (Heil, 1997), response latency in guinea pig A1 was level- and frequency-dependent, in a manner that louder and/or higher frequency sounds evoked earlier cortical activity than smaller and/or lower frequency sounds. Specifically, 16-kHz-noise evoked responses 3 ms earlier than 1-kHz-noise at the same intensity of 60 dB SPL (mean ± SEM: 14.2 ± 0.5 ms for

1-kHz-noise, 11.3 ± 0.3 ms for 16-kHz-noise); 1-kHz-noise at 70 dB SPL and 16-kHz-noise at 40 dB SPL evoked responses at the same latency in spatially separated positions (12.9 ± 0.5 ms for 1-kHz-noise, 13.1 ± 0.6 ms for 16-kHz-noise). To examine whether the latency difference of a few milliseconds can affect cortical integration, we measured responses evoked by 1-kHz-noise and/or 16-kHz-noise in the A1, presented either simultaneously or with one sound systematically delayed at 4-ms steps. Suppressive effect was observed over all locations in A1 for all delays. At the best-frequency position for 16 kHz, the suppressive effect was significantly stronger when 16-kHz-sound was delayed for 4 ms than other cases. This result suggests that the shorter latency of the response to 16-kHz-noise may function to make the response resistant to suppression by lower frequency components, thereby facilitating spectrum integration in A1. Such a mechanism might be particularly important in cortical representation of natural sounds, because higher frequency components of natural sounds typically have relatively lower intensity compared with lower frequency components.

PS-93

A Computational Model for the Disorganized Tonotopy and Pitch Cells of the Auditory Cortex: Analogy with the Visual Cortex

Hiroki Terashima[1]; Masato Okada[2]
[1]NTT Communication Science Laboratories / The University of Tokyo; [2]The University of Tokyo / RIKEN BSI

Background

The tonotopy of the primary auditory cortex (A1) has been revealed more disorganized than the retinotopy of the primary visual cortex (V1). Does this discrepancy suggest that the two functional areas employ distinct computational strategies? Theories for V1 have linked its retinotopy to learning of natural image statistics. Since V1 and A1 share basic structural features, we hypothesized that their dissimilar topographies emerge from a single learning principle with distinct input statistics. The present study attempted to demonstrate that a single computational model can reproduce both an ordered retinotopy and a disordered tonotopy depending on inputs. In addition, we investigated behaviours of “complex cells” that the model constructed from natural sounds.

Methods

To show distinct statistics of natural sounds and natural images, we used human narratives of the Handbook of the International Phonetic Association and van Hateren natural image database. The sounds were pre-processed into cochleogram.

The V1 computational model we used is Topographic Independent Component Analysis (TICA). It is a neural network consisting of two layers: neurons of the first and second layer correspond to the simple and complex cells of V1, respectively, following learning of natural images. Instead of natural images, we applied this model to natural sounds.

Results

The first analysis is a simple comparison of natural sound statistics and natural image statistics using correlation matrices. In the frequency domain, natural sounds exhibit not only local correlation but also non-local, typically harmony-related, statistics. This contrasts with natural image statistics, which have only a local correlation pattern.

We tested how this distinct input statistics affect learning results of the TICA model. When applied to natural images, the model learned a smooth, V1-like topography; however, with natural sound inputs, the learned tonotopy exhibited some non-smooth jumps between neighbouring units, whereas the global tonotopic tendency still appeared. Thus, the smoothness discrepancy can emerge from different natural stimulus statistics even through a single learning principle.

Finally, we investigated how “complex cells” of the model respond to complex sounds. We found that some of them are pitch-selective similarly to pitch cells reported in the marmoset auditory cortex [Bendor & Wang, 2005], which suggests a computational analogy.

Conclusion

We demonstrated that a disordered tonotopy can emerge from natural sound statistics through a learning model that was originally proposed for V1. Moreover, the model suggests that pitch-selective cells of the auditory cortex are computationally analogous to the V1 complex cells.

PS-94

Neural Correlates of Relative Sound Location in Ferret Auditory Cortex

Katherine Wood[1]; Stephen Town[2]; Huriye Atilgan[2]; Gareth Jones[2]; Jennifer Bizley[2]
[1]University College London; [2]UCL Ear Institute

The brain uses the limited cues available to it to calculate the location of sounds. Two main localisation cues are available, monaural cues, which arise at the ear due to interaction of sound with the pinna, and binaural cues; the difference in time and difference in level it takes a sound to travel between the two ears. Many studies have investigated the ability of human listeners to localise sound sources to an absolute location (e.g. Stevens and Newman, 1936). Other studies have determined the minimum discriminable difference in spatial location that a listener can reliably detect; the minimum audible angle (Mills, 1958). However, very few studies have investigated relative sound localisation, i.e. reporting the relative position of two sequentially presented sources. Determining the relative location of two sound sources or the direction of movement of a source are ethologically relevant tasks. Here we report behavioural data and multi-unit activity from auditory cortex of ferrets performing a relative localisation task.

Ferrets were trained in a positively conditioned 2AFC task to report whether a target sound originated from the left or right of a preceding reference. In standard testing, the target and reference stimuli were 150 ms noise bursts separated by a 10 ms gap. The reference was presented from one of 6 locations in the frontal 180° and the target was presented from a speaker 30° to the left or right. We recorded using 32 individually moveable tungsten electrodes, in a 4x4 array on each side of the head.

A total of 1359 recordings showed sound-evoked activity ($p<0.05$, t-test of mean firing rate in 50 ms before and after stimulus onset) from 194 unique recording sites in 2 ferrets. Of the 1359 unit recordings, 28% (380/1359) of recordings showed significant tuning to reference sound location ($p<0.05$ Kruskall-Wallis test on firing rate during reference sound presentation and reference location). Overall, 66% of unit recordings were tuned to contralateral space, 23% tuned to midline locations, and 11% were ipsilaterally tuned.

On-going analysis is exploring the contribution of ILD and ITD cues to spatial tuning through the use of band-pass stimuli, and to investigate the relationship of other response measures a pattern classifier approach is being used to determine whether neural responses are informative about the location of the reference/target, the direction of movement and/or the response of the ferret.

PS-95

Exploring the Role of Synchrony in Spatial and Temporal Auditory-Visual Integration

Gareth Jones[1]; Stephen Town[2]; Katherine Wood[2]; Huriye Atilgan[2]; Jennifer Bizley[2]
[1]University College London; [2]UCL Ear Institute

Animals and humans integrate sensory information over time, and combine this information across modalities in order to make accurate and reliable decisions in complex and noisy sensory environments. Little is known about the neural basis of this accumulation of information, nor the cortical circuitry that links the combination of information between the senses to perceptual decision making and behaviour. Most previous examples of multisensory enhancement have relied on synchrony dependent mechanisms, but these mechanisms alone are unlikely to explain the entire scope of multisensory integration, particularly between senses such as vision and hearing, which process multidimensional stimuli and operate with vastly different latency constraints.

Presented here are two audio-visual behavioural tasks, one spatial, one temporal (adapted from Raposo, et. al. 2012), requiring subjects (ferrets and humans) to accumulate evidence from one or both senses over time. In the temporal task subjects estimated the average rate of short auditory and/or visual events embedded in a noisy background (20 ms white noise bursts or flashes) over a defined time period (1000 ms). Instantaneous event rates throughout this time period varied, meaning the accuracy with which the event rate could be estimated increased over time. Similarly, in the spatial task, subjects were required to report whether a greater event rate was presented to the left or right of space. Discrimination was assessed in both unisensory auditory and visual conditions as well as in synchronous and asynchronous multisensory conditions, and subject performance improved under each multisensory condition in both tasks. In the temporal task, accuracy and reaction times for humans were improved in both synchronous and asynchronous multisensory conditions (accuracy: 71% and 72%, reaction times: 275±9 and 300±10 ms, mean ±SE, respectively), relative to the auditory and visual unisensory performance (accuracy: 64% and 62%, reaction times: 345±14 and 338±10 ms, respectively). In the spatial task, overall accuracy for humans was improved in both synchronous and asynchronous multisensory conditions (66% and 68%, respectively), relative to the auditory and visual unisensory performance (accuracy: 61% and 62%, respectively). To investigate how the additional information available in the multisensory conditions leads to optimised listening performance, these data are being analysed in the context of previously published drift diffusion models. Lastly, to better understand how such signals are represented in the brain, recordings are being performed form auditory and visual cortex of anesthetised ferrets.

PS-96

Auditory Responses In The Mouse Frontal Cortex

Hemant Srivastava[1]; Madhur Parashar[2]; Sharba Bandyopadhyay[2]
[1]Duke University; [2]IIT Kharagpur

An important function of the orbitofrontal cortex (OFC) is to assign value to different sensory inputs based on their contextual or behavioral relevance. Among other functions of the OFC, it also directs attention to salient features of the sensory environment and further is involved in inhibiting or allowing motor responses to sensory stimuli depending on context. The mechanisms by which sensory stimuli are represented in the different divisions of OFC and how values are determined is not clearly understood. This study is a first attempt to decipher such questions from a purely sensory aspect. Usually important stimulus aspects in a dynamic environment occur as deviant stimuli in the midst of similar ongoing stimuli. Occurrence of a rare stimulus is one way to think of a stimulus that is of high value. We used such an auditory stimulus paradigm where a deviant stimulus occurs in a train of similar/same stimuli. We use local field potentials in the OFC and responses of single neurons in the OFC to such stimuli. Responses clearly show OFC responding strongly to deviant stimuli. Further with retrograde tracers in OFC we show that there are direct inputs in OFC from the primary auditory cortex (A1) as well as secondary regions. This shows the possibility of direct sensory inputs underlying such deviant detection capability. Based on our observations we use a network model with integrate and fire neurons and depressing synapses to show that such a network is capable of showing selective responses to deviant stimuli. We further extend the model to include feedback from OFC to A1, in accordance with other neuroanatomical data, to show that responses following deviant stimuli along with other inputs, depending on the context (aversive or rewarding), can cause plasticity of neuronal receptive fields in A1 that has been previously observed during behavior.

PS-97

Mechanisms of Cortical Suppressions Evoked by the Reversed Form of a Damping Natural Sound

Junsei Horikawa[1]; **Hisayuki Ojima[2]**
[1]Toyohashi University of Technology; [2]Tokyo Medical and Dental University

Introduction

Transient natural sounds tend to start with a large-amplitude attack followed by a gradually damping tail. Such sounds are perceived different when they are played reversely in time. Previously, it was behaviorally shown that the guinea pig innately discriminated a time-reversed version from its original forward sound. Voltage sensitive dye imaging have revealed that activation of the primary auditory cortex (AI) was strong when it was played forward, while the activation was extremely reduced if the same sound was reproduced backward. We analyzed what portions of the damping natural sound were responsible for this reduction in the AI activation when it was reproduced backward.

Method

The natural sound used was a footstep sound (FSS or FW), a train of 10 identical sound segments, each being about 80 ms long and separated by about 600 ms. It was temporally characterized by a 1-ms high-amplitude attack portion followed by a 80-ms gradually damping tail and spectrally by a noise-like wide bandwidth with a few prominent energy peaks. The backward version (BK) was reproduced by reversing the FSS on a sound editing software and then divided into 3 portions for test sounds. For the first test sound (S1), the early 43 ms portion was removed from the BK. For the second (S2), the short click-like high-amplitude end was removed from the BK. The third test sound (S3) was this click-like end portion itself. Voltage sensitive dye imaging was carried out under the anesthesia of a mixture of Xylazine and Ketamine followed by a muscle relaxant (approved by local animal committee).

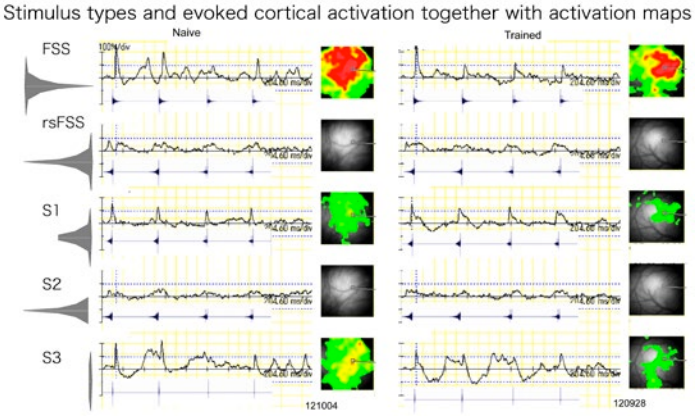

Results and Conclusion

Compared to the activation with the forward version (FSS), the full BK (srFSS) evoked much reduced activation, as shown in figures below. The S3 evoked the strong cortical activity comparable in strength to that evoked by the full FW. The S1 evoked the cortical activation that was weaker than that evoked with the S3 or the FW but stronger than that evoked by the S2. This S2 is longer in duration than the other test sounds but evoked the minimum activation comparable to that evoked with the full BK. A damping envelope of the FW turns to the ramping envelope when it is time-reversed. Therefore, the decaying portion of the FW would suppress the cortex strongly when its reversed form (i.e, ramping) comes earlier than the powerful sound component.

PS-98

Nicotinic Enhancement of Sound-Evoked Responses in Auditory Cortex Involves Phosphorylation of Extracellular Signal-Regulated Kinase and GluA1 Subunit of AMPA Receptors

Kenichi Yamasaki; Kiyonobu Inakuma; Takahiro Nagayama; Hideki Kawai
Soka University

Systemic nicotine administration facilitates sound-evoked responses in mouse primary auditory cortex (A1) (Kawai, et al., 2011, J.Neurosci. 272,123-129). This facilitation peaks at ~10 min after nicotine injection and lasts for at least half an hour. Pharmacological studies indicated that this nicotine-induced long-term potentiation (nicotinic LTP) is mediated by nicotinic acetylcholine receptors containing α4 and β2 subunits (α4β2*-nAChRs) and activation of extracellular signal-regulated kinase 1/2 (ERK1/2) (Intskirveli and Metherate, 2012, J. Neurophysiol., 107, 2782-2793). How α4β2*-nAChRs and ERK1/2 activation leads to nicotinic LTP remains unclear. One possible mechanism will be an enhancement of synaptic transmission at excitatory synapses by increasing the number and/or conductance of synaptic AMPA receptors (AMPARs). Such changes could occur via NMDA receptor (NMDAR)-dependent phosphorylation of GluA1, an AMPA receptor subunit, at Ser845 by protein kinase A (PKA) and/or at Ser831 by PKC or aCaMKII. Ser845 phosphorylation leads to facilitation of exocytosis at extrasynaptic sites followed by ERK1/2-dependent transport of the receptors to postsynaptic density (PSD). Ser831 phosphorylation increases channel conductance. Here we biochemically examined whether GluA1 and ERK1/2 are phosphorylated by systemic nicotine and/or sound stimulation, and whether NMDAR is necessary for the phosphorylation using synaptoneurosomes prepared from the upper layers of auditory cortex stimulated *in*

Systemic nicotine exposure, but not white noise (WN) stimuli, promoted Ser845 phosphorylation, and pairing nicotine and WN stimuli had a similar effect. Nicotine, WN, or their pairing did not affect Ser831 phosphorylation of GluA1. Meanwhile, nicotine exposure alone or pairing stimuli increased synaptic ERK1/2 activation to a similar extent in most cases, suggesting that nicotinic activation alone promotes ERK1/2 phosphorylation. We then examined if nicotine-induced phosphorylation of Ser845 or ERK1/2 is mediated by NMDARs. Systemic exposure of CPP, a NMDAR blocker, did not affect nicotine-induced Ser845 and ERK1/2 phosphorylation. Ser845 phosphorylation by pairing stimuli was also not affected, suggesting its independence from NMDAR activation and a direct role of postsynaptic α4β2*-nAChRs in the phos-

phorylation. Interestingly, however, pairing stimuli enhanced ERK1/2 phosphorylation in the presence of CPP more than in its absence, suggesting that NMDAR activation normally opposes postsynaptic nicotinic signaling to ERK1/2.

These data overall suggest that nicotinic LTP appears to involve activation of postsynaptic, not presynaptic, α4β2*-nAChRs and subsequent phosphorylation of Ser845, not Ser831. Nicotinic activation of synaptic ERK1/2 appears to be regulated by NMDAR activation. Future studies will reveal interplay among α4β2*-nAChR-mediated signaling to Ser845 and ERK1/2 and NMDAR-mediated control of ERK1/2 phosphorylation.

PS-99

Neural Circuitry Underlying Contrast Gain Control in Primary Auditory Cortex

James Cooke; Benjamin Willmore; Jan Schnupp; Andrew King
University of Oxford

While sensory environments can vary dramatically in their statistics, neurons have a limited dynamic range with which they can encode sensory information. In sensory cortex, this problem is in part resolved by the systematic adjustment of neural gain in accordance with the contrast of sensory input. This computation also results in contrast invariant representations in cortex that are also more resilient to static background noise. The biophysical basis of contrast gain control (CGC) is currently unknown but shunting inhibition by parvalbumin positive (PV+) interneurons is a likely candidate. We aim to investigate the mechanistic basis of CGC using mice as our model organism, given that optogenetic methods for the circuit level interrogation of the nervous system are well established in that species. First, we characterised CGC in the anaesthetised mouse by performing large scale extracellular recordings across all layers of A1. We found that CGC is present in units recorded in all layers of mouse A1. In order to test the involvement of PV+ interneurons in CGC, we expressed the light-driven neural silencer Archaerhodopsin (Arch) in these cells using a transgenic approach. This allowed us to optogenetically reduce the activity of PV+ interneurons while presenting sensory stimuli that elicit CGC. We find that this manipulation produces a multiplicative disinhibition in pyramidal cell responses, indicative of a change in neuronal gain. This is in keeping with the hypothesis that CGC in pyramidal cells is produced by shunting inhibition provided by contrast driven changes in PV+ activity.

PS-100

Altered Development of the Auditory Cortex in a Mouse Model of Fragile X Syndrome

Teresa Wen; **Sarah Reinhard**; Harpreet Sidhu; Khaleel Razak; Iryna Ethell
University of California, Riverside

Fragile X Syndrome (FXS) is a genetic cause of autism and a leading cause of intellectual disability, affecting 1 in 4000 males and 1 in 8000 females. Humans with FXS show significant auditory processing deficits, most notably hyperacusis and reduced habituation. The Fmr1 knockout (KO) mouse demonstrates similar deficits, including impaired critical period plasticity, hyper-responsiveness to tones, increased response variability, and broader receptive fields. Delayed auditory cortical development may lead to deficits in higher auditory functions, but the underlying mechanisms are unclear.

In this study we examined structural changes in the developing auditory cortex that may underlie abnormal auditory cortex development in Fmr1 KO mice. We analyzed the development of dendritic spines in excitatory neurons as well as the association of perineuronal nets (PNN) – a component of extracellular matrix – with inhibitory parvalbumin (PV) positive interneurons in wild-type (WT) and KO mouse auditory cortex. The developmental changes in FMRP (Fragile X Mental Retardation Protein) expression and Matrix Metalloproteinase-9 (MMP-9) levels were also characterized. FMRP has been shown negatively regulate MMP-9 levels. MMP-9 levels are elevated in FXS and could affect dendritic spine and PNN development, whereas genetic deletion of MMP-9 in Fmr1 KO mice show recovery of some FXS-associated behaviors.

Dendritic spines were labeled with the diolistic approach. Immunohistochemistry was used to label PV+ interneurons and PNNs. FMRP and MMP-9 levels were quantified using Western blotting and gel zymography.

Our studies show that FMRP levels peaked during the second postnatal week and decreased into adulthood. MMP-9 levels were also developmentally regulated in the auditory cortex and their decrease coincided with PNN accumulation and maturation of dendritic spines at the end of critical period of plasticity window. In Fmr1 KO mice the development of PV/PNN and spine maturation was delayed, and MMP-9 levels remained high in Fmr1 KO mice at P18.

These data suggest that structural changes that occur during the auditory critical period may underlie auditory hypersensitivity in FXS. Overexpression of MMP-9 may lead to excessive cleavage of PNN and elongation of dendritic spines. While these processes are necessary for inducing activity-dependent, plastic changes within developing circuits, permitting responsiveness to environmental stimuli, in FXS auditory cortex we find these same mechanisms are perturbed during early auditory development, likely leading to a hyper-excitable and more broadly tuned system.

Funded by NIH Grant 1U54HD082008-01.

PS-101

The Role of Myelin in Temporal Aand Spectral Processing in the Auditory System

Livia de Hoz[1]; Klaus-Armin Nave[1]; Sharlen Moore[2]
[1]Max Planck Institute of Experimental Medicine, Goettingen, Germany; [2]IMPRS and Max Planck Institute of Experimental Medicine, Goettingen, Germany

This project aims to understand better the role of fast and reliable conduction speed on sensory processing. Myelin plays

a crucial role in speeding up action potential propagation and axonal maintenance. Since the auditory system is highly optimized for the processing of stimuli that are encoded in time, we tested auditory processing in a mouse model (*shiverer*) with abnormal myelination in the absence of axonal degeneration. We recorded acutely from the primary auditory cortex of *shiverer* and wild type (wt) mice, while presenting auditory stimuli aimed to test frequency coding, frequency discrimination and temporal processing.

Tuning curves were used to determine frequency coding. For the assessment of frequency discrimination we used stimulus-specific adaptation (SSA). SSA occurs when two frequencies, one highly repeated and one rarely presented, are different enough that adaptation to the constant one can occur in the absence of adaptation to the other. SSA is reflected in a larger response to the rare frequency and decreases with ΔF, the rate of stimulus presentation, and higher repetition of the rare frequency. Temporal processing was assessed using standard protocols of gap detection (for temporal acuity) and different click rates (for temporal reliability).

Shiverer mice had longer stimulus response latencies in all protocols as expected. Temporal processing was also impaired: *shiverer* had higher gap detection thresholds and could not follow click rates as well as *wt.* In addition, responses in shiverer mice were larger in the absence of an obvious difference in hearing threshold or jitter. Frequency coding and discrimination were, however, normal. Therefore, temporal processing is severely affected in the absence of myelin, while spectral processing is spared. This is presumably because the former is dependent on precisely timed responses within a given fibre path, while the spectral processing depends on the comparison between responses across different fibre paths.

PS-102

Neuronal Responses in the Ferret Auditory Cortex during a Multisensory Localization Task

Amy Hammond-Kenny; Victoria Bajo; Andrew King; Fernando Nodal
University of Oxford

Our unified perception of the world relies on the ability to integrate information obtained from different sensory modalities. Such integration was once thought to take place in so called higher or associative cortical areas, but has latterly been described even at the level of primary sensory cortices. Here we explore multisensory integration in the ferret auditory cortex by recording neural activity while animals perform a multisensory localization task, thereby enabling correlation of behavioural performance with neural activity. Ferrets were trained by positive operant conditioning, using water as a reward for correct responses, to trigger a stimulus while standing on a platform at the centre of a circular arena and then to approach the source of the stimulus, which was presented from 1 of 7 peripheral sites separated by 30° intervals around the frontal hemifield. Stimuli were either unisensory (auditory or visual) or multisensory (audio-visual) of varying durations (20-2000 ms) and, for auditory stimuli, of different intensities (56-84 dB SPL). Behavioural measurements included latency and accuracy of both approach-to-target and head orienting responses. Following collection of baseline behavioural measurements, neural activity was recorded during performance of the task via multi-electrode arrays implanted bilaterally in the auditory cortex. Analysis of behavioural data showed that ferrets responded more accurately and rapidly to multisensory stimuli as compared to either unisensory stimuli. We observed a significant increase in the percentage of correct approach-to-target responses for stimulus durations ≥100 ms and a decrease in both approach-to-target and head orienting response times. In addition, race model inequality analysis of approach-to-target response times showed significant violations of the model, suggesting that the observed results cannot be attributed to probability summation alone, thus supporting the existence of a multisensory integration mechanism. Analysis of electrophysiological recordings identified 174 driven units from a total of 224 recording sites. Our results show that activity in the auditory cortex can be modulated by concomitant visual stimuli, with 76 units (43%) responding to both auditory and visual stimuli. In addition, >90% of these bisensory units demonstrated sub-additive interaction to combined audio-visual stimuli presentation. Together, these results indicate that multisensory responses are quite widespread at the level of the auditory cortex, although the magnitude of the observed interactions also suggests a potential role for further higher cortical areas in multisensory integration.

PS-103

Dynamical Integration of Statistical Auditory Information in Behaving Ferrets

Yves Boubenec[1]; Bernhard Englitz[2]; Shihab Shamma[1]
[1]École Normale Supérieure; [2]Donders Centre for Neuroscience

Many natural sounds have spectrotemporal signatures which can best be defined statistically, examples include wind, fire or rain. While their local structure is highly variable, their spectrotemporal statistics are stationary and provide humans with sufficient information for classification. In the present study we investigate the neural basis of the detectability of *changes* in the statistical representations of sounds. The experiments focus on the dynamical properties of change detection during ongoing exposure, and hence were designed with stimuli of a minimal sound texture - a modified cloud of tones - which retained the central property of auditory textures: statistical predictability. At a random time, the marginal probability of the tone cloud was changed, which had to be detected by behaving ferrets. This constrained animals to gather information about the ongoing stimulus before making a decision about a potential change. The change occurred with a high probability in a specific frequency band, and with a lower probability in other channels. Animals were trained to detect the change, and were only given a limited time to make this choice after the change. Single- and multi-unit recordings of neuronal activity were collected in primary and secondary auditory cortex of trained animals.

We investigated how performance was affected by the probability of the change occurring in a specific frequency channel, as an indication of the animal's attentional focus on the frequency region where the change was likely. Specifically, we used reconstruction techniques to contrast stimulus encoding in the attended and non-attended frequency channels, both in passive and active animals. Furthermore, by varying the difficulty, we observed that the animals' performance (computed with Hit and Miss rates) greatly depended on the size of the change. This was further explored by examining the system trajectory in the PCA-reduced neuronal space as a function of (a) the outcome (Hit/Miss) and (b) the size of the change (Small/Large). Finally, we also investigated how the precursor interval (i.e. the duration of time interval before the change) influences both the animal's performance and the neural representation of the ongoing stimulus. The precursor interval was found to be crucial in a similar psychophysics experiment (see accompanying Poster "Integration of statistical information in complex acoustical environments").

PS-104

Stimulus-Dependent Multiple Sound Feature Encoding in the Songbird Auditory Forebrain

Gunsoo Kim; Allison Doupe
University of California, San Francisco

Introduction

Understanding neural mechanisms underlying the processing of complex communication sounds remains a major challenge. With their rich vocal communication behaviors, songbirds can offer insights into this question. In the primary auditory cortical area field L of zebra finches, we asked whether a single field L neuron can encode multiple spectrotemporal features and investigated how the multiple feature encoding might adapt to changing sound stimuli.

Methods

Single unit recordings were made using chronically implanted electrodes in unanesthetized adult zebra finches. Field L neurons were probed with stimuli rich in spectral and temporal modulations and effective in driving these neurons. To investigate effects of stimulus statistics, neural responses were compared between low and high intensities (low vs high mean conditions) or between low and high contrasts in intensity (low vs high variance conditions). Neural receptive fields and gain functions were obtained using the technique of maximally informative dimensions (MID).

Results

We found that a significant subset of field L neurons (n=19, 33, and 13 neurons for low mean/variance, high variance, and high mean conditions, respectively) were tuned for 2 spectrotemporal features (or MIDs), revealing a second feature that cannot be seen with spike-triggered averaging. The second MIDs tended to be more broadband and to have a symmetric gain function, indicating a form of phase invariance. The 2 MIDs together jointly carried more information (23% on average) about the neural response than the first MID alone. In the high mean and high variance conditions, the impact of the second MID was significantly greater than in the low mean/variance condition (by 93% and 166%, respectively). In the high mean condition, both first and second MIDs shifted toward higher temporal (but not spectral) modulation frequencies, indicating that neurons become more sensitive to temporal changes in intensity than absolute intensity. In contrast, in the high variance condition, MIDs tended to contain lower spectral modulation frequencies, indicating a reduced spectral sensitivity.

Conclusions

Our results demonstrate a further spectrotemporal sensitivity that was not revealed by spike-triggered averaging in songbird cortical neurons and suggest that the two features dynamically adapt to changing stimulus statistics.

PS-105

The Role of Cochlear Hair Cells and Spiral Ganglion Neurons in the Infrared Laser Stimulation

Bingbin Xie; Chunfu Dai
Eye and ENT Hospital, Fudan University, Shanghai, China

Introduction

Optical technologies play an increasingly important role in neuroscience and the development of treatments for neurological, psychiatric, and cardiovascular diseases. Importantly, optical technologies afford many advantageous features compared to electrical stimulation, namely greater spatial resolution along with accuracy and no stimulation artifacts [1-3]. Infrared lasers have been applied to directly evoke physiological responses in neuronal and other excitable cells both *in vivo* and *in vitro* without any prior genetic or chemical manipulation [4-5]. The advantage of direct infrared excitation makes it attractive for a variety of applications in basic and clinical research, ranging from hearing restoration to optical pacing [2].Previous studies demonstrated that laser-evoked optical auditory brainstem responses (oABRs) and compound action potentials (CAPs) could be recorded in both normal hearing and deafened animals [6]. Pulsed infrared radiation also activates sensory hair cells of the semicircular canal crista ampullaris of the toadfish *in vivo* [7]. To confirm if either cochlear hair cells or SGNs are the targets of pulsed infrared stimulation oABRs, further investigation is required. In the current study, we compared the differences between the oABRs in both normal hearing and deafened guinea pigs, and compared the variation of the distortion product otoacoustic emission (DPOAE) after infrared laser stimulating, to determine the role of the cochlear hair cells in the infrared laser stimulation.

Methods

We used pulsed infrared lasers to study evoked optical auditory brainstem responses (oABRs) in normal hearing and deafened animals. We also compared the morphology and anatomy of SGNs in normal hearing and deafened guinea pigs.

Results

By recording oABRs evoked by varying infrared laser pulse durations, we discovered that degeneration of SGNs in deaf-

ened guinea pigs was associated with an elevated oABR threshold and with lower amplitudes. Moreover, as we prolonged pulse duration in both normal hearing and deafened animals, oABR threshold decreased while amplitudes increased. Electron microscopy revealed that SGNs from deafened guinea pigs had swollen and vacuolar mitochondria, and that SGN soma and axons were demyelinated. Additionally, different results in the same normal hearing animal could be recorded while changing the orientation of the optical fiber, only the fiber pointed to the Rosenthal's canal directly, can the oABR be recorded.

Conclusion

Deafened guinea pigs have elevated thresholds and smaller amplitude responses, likely a result of degenerated SGNs. SGNs are the real target of the infrared laser stimulation in the process of recording oABR, the cochlear hair cells did not involve in.

PS-106

Signal Modulation for Optical Stimulation of the Peripheral Auditory System

Patricia Stahn[1]; Hubert Lim[2]; Marc Kannengiesser[1]; Christoph Andres[1]; Dietmar Hecker[1]; Edgar Janunts[1]; Benjamin Hoetzer[1]; Marius Hinsberger[1]; Achim Langenbucher[1]; Bernhard Schick[1]; Gentiana Wenzel[1]
[1]Saarland University; [2]University of Minnesota

Introduction

To code complex acoustic signals, such as speech, controlled modulation of different frequency channels of the auditory system is necessary. Laser light with specific parameters can be used to activate the peripheral hearing organ at different levels (Wenzel et al, 2010). However within the duration of a word, it is not possible to switch between different laser wavelengths with current laser systems. Hence, the objective of our project is to investigate methods for achieving frequency-specific modulation using monochrome laser pulses. We analyzed the firing patterns of neurons across the central nucleus of the inferior colliculus (ICC) in response to varying laser pulse parameters in anesthetized guinea pigs.

Methods

We positioned a 16-site electrode array (NeuroNexus Techonlogies, Michigan, USA) across the tonotopic axis of the ICC. We then inserted a 105 µm diameter optic fiber into the outer ear canal and directed it towards the ear drum. We recorded and analyzed optically-induced ICC spike activity in response to stimulation with 10 ns laser pulses using a 532 nm Q-switched, INCA-laser system (Xiton Photonics, Kaiserslautern, Germany). We varied the level (0-40 µJ/pulse) and pulse rate (100-4000 pps; 1-3 pulses) of stimulation. The animals were then sacrificed immediately after each experiment and their temporal bones were harvested for further analysis.

Results

The best frequencies of the recorded neurons in each animal typically spanned 2 to 20 kHz. Stimulation of each parameter elicited activity in the ICC that increased in spike rate and spanned a greater number of recording sites as the optical energy was increased in level. Interestingly, stimulating with different pulse rates between 100 and 4000 pps generally activated similar frequency regions of the ICC: the maximum activity occurred on neurons most sensitive to 4-8 kHz and a second maximum occurred for 16-20 kHz. We also observed that varying temporal patterns of activity could be achieved using different numbers and rates of pulses. Consistent with previous findings using noninvasive neural recordings (i.e., auditory brainstem responses), increasing the laser repetition rate above 1000 pps led to superposition of activity across pulses.

Conclusions

The results demonstrate that different temporal patterns or modulation of activity in the auditory system is possible with varying optical stimulation parameters using a monochrome laser. However, adjusting pulse rate alone may not be sufficient to achieve frequency-specific activation, at least for ear drum stimulation. Studies investigating the effects of other laser parameters on frequency-specific modulation are in progress.

PS-107

Neural Response Patterns Recorded from the Guinea Pig Inferior Colliculus to Speech

Claus-Peter Richter; Xiaodong Tan; Nan Xia; Petrina LaFaire; Hunter Young
Northwestern University

Introduction

The maximum achievable repetition rate of action potentials recorded from single units in the central nucleus of the inferior colliculus (ICC) to trains of infrared laser pulses is lower than those evoked by trains of acoustic clicks or electrical pulses. Although the maximum following rate of INS is lower than that of acoustic clicks and electrical current pulses, high repetition rates may not be necessary for cochlear implant coding. Here we demonstrate that the repetition rates for selected units in the inferior colliculus evoked by speech signals are well below 100 Hz for each channel and that the achieved pulse repetition rates with optical stimulation are sufficient to code the acoustic information.

Methods

Word lists obtained from the speech in noise (SIN) test were played to the ear of a guinea pig and corresponding neural responses to the each word were recorded in the contralateral ICC. Recordings were made either with multichannel electrode arrays or with single tungsten electrodes. Spectrograms and peri-stimulus raster plots were created and compared.

Results

Acoustic stimuli increased the rate of action potentials when the frequency in the spectrogram was close to the best frequency of the selected unit. Average repetition rates were typically below 100 Hz even at sound levels above 80 dB SPL. Loudness is well reflected by the sum of the action potentials across the channels.

Summary

In normal hearing animals, average pulse repetition rates in the ICC during speech are lower than 100 Hz in single unit

level. The dynamics of optical stimulation appears to be sufficient to encode speech. Loudness seems to be coded by the sum of the activity across the channels rather than the rate increase within a channel.

PS-108

Multichannel Optrode for Optical Stimulation

Nan Xia[1]; Xiaodong Tan[1]; Hunter Young[1]; Matthew Dummer[2]; Mary Hibbs-Brenner[2]; Claus-Peter Richter[1]
[1]Northwestern University; [2]Vixar Inc

Background

Optical stimulation, such as optogenetics or infrared neural stimulation (INS), has been proposed as a novel method to stimulate neurons. These stimulation methods are generally using optical fibers or single optical chips, such as micro Light Emitting Diodes (µLEDs), to deliver the radiation to the target tissue. At present, stiff optical fibers have been used to deliver the radiation for optical stimulation of auditory neurons, during the insertion of the optical fiber(s) into scala tympani, the inner ear might be damaged. It might be beneficial to directly insert the optical sources into the cochlea.

Method

Blue µLEDs (wavelength 470nm for optogenetic approach), red Vertical Cavity Surface Emitting Lasers (VCSEL, wavelength 680nm for functional testing and wavelength 1850nm for INS) were used as light sources for the multi-channel optrodes. To fabricate the optrode, conductive silver epoxy was used to connect all cathode of VCSELs or µLEDs to the uninsulated part of a 125µm diameter Teflon coated silver wire. This wire also serves as the heat sink. The anode of each VCSEL or µLEDs was connected with epoxy to a 25 or 75µm diameter Teflon coated platinum/silver wire. The optrode was then moved to a semi-cylindrical mold with diameter of 0.8 mm, and was embedded into silicone. For functional testing, the optrode was placed into a physiological saline bath on a shaking table and was agitated for 24 hours, 7 days per week. The function of each channel was tested daily and overall appearance of the optrodes was visually inspected. After the *in vitro* test, the 4-channel red or an infrared optrode was implanted into a cat cochlea. Acoustic ABRs thresholds were tested before and every other week after the implantation.

Results

In the saline bath, the longest test series lasted more than 3 months without any changes in optrode appearance or function. For the red VCSELs, the ABR responses were absent one month after implantation above 10kHz, and ABR thresholds were elevated on average by 32dB at frequencies below 10kHz. Changes in threshold were stable after the implantation. Moreover, stimulation with the infrared optrode evoked an ABR.

Conclusion

We successfully fabricated implantable multichannel cochlear optrodes for INS and optogenetics. The current results show that it is feasible to insert multichannel optrode into the cat cochlea and that cochlear damage does not progress beyond the damages caused by the insertion of the optrode.

PS-109

Towards Optogenetic Stimulation of the Auditory Pathway: Implementing the Fast Channelrhodopsin Chronos and Multichannel microLED Arrays

Daniel Keppeler[1]; Victor H. Hernandez[2]; Anna Gehrt[3]; Marcus Jeschke[3]; Christian Wrobel[3]; Gerhard Hoch[3]; Christian Goßler[4]; Ulrich T. Schwarz[5]; Patrick Ruther[4]; Michael Schwaerzle[4]; Roland Hessler[6]; Tim Salditt[7]; Nicola Strenzke[8]; Sebastian Kügler[9]; Tobias Moser[10]
[1]University of Göttingen Medical Center; [2]InnerEarLab, Dept. of Otolaryngology, University of Göttingen Medical Center, Göttingen, Germany; Bernstein Focus for Neurotechnology, University of Göttingen, Göttingen, Germany; Department of Chemistry, Electronics and Biomedical Engineering, Division of Sciences and Engineering, University of Guanajuato, Guanajuato, Mexico.; [3]InnerEarLab, Dept. of Otolaryngology, University of Göttingen Medical Center, Göttingen, Germany; [4]Department of Microsystems Engineering (IMTEK), University of Freiburg, Freiburg, Germany; [5]Fraunhofer Institute for Applied Solid State Physics (IAF), Freiburg, Germany; Department of Microsystems Engineering (IMTEK), University of Freiburg, Freiburg, Germany; [6]MED-EL, Innsbruck, Austria and MED-EL Germany, Starnberg, Germany; [7]Department of Physics, University of Göttingen, Göttingen, Germany; Center for Nanoscale Microscopy and Molecular Physiology of the Brain, University of Göttingen; [8]Auditory Systems Physiology Group, Department of Otolaryngology, University Medical Center Göttingen, Göttingen, Germany; [9]Department of Neurology, University Medical Center Göttingen, Göttingen, Germany; [10]InnerEarLab, Dept. of Otolaryngology, University of Göttingen Medical Center, Göttingen, Germany; Bernstein Focus for Neurotechnology, University of Göttingen, Göttingen, Germany; Collaborative Research Center 889, University of Göttingen Medical Center, Göttingen, Germany

Cochlear implants are by far the most successful neuroprostheses implanted in over 300,000 people worldwide and enable open speech comprehension in a majority of users. However, patients suffer from low frequency resolution due to wide current spread from stimulation contacts, which limits the number of independently usable channels and compromises speech comprehension in noise, music appreciation or prosody understanding. Our goal is to overcome these drawbacks by pursuing an optogenetic approach: Optical cochlear implants activate spiral ganglion neurons genetically modified to spike upon light stimulation. Optical stimulation can be spatially confined and thus promises lower spread of excitation in the cochlea. Accordingly, an increased number of independent stimulation channels is expected to enhance frequency resolution and intensity coding.

We investigated optogenetic cochlea stimulation employing various transgenic rodent models as well as virus-mediated expression of channelrhodopsin variants in spiral ganglion neurons. Blue light stimulation of the spiral ganglion via fiber-coupled lasers activated the auditory pathway, as

demonstrated by recordings of neuronal population responses along the auditory pathway. Auditory brainstem response thresholds were found to be around 1 mW/mm² - similar to thresholds for cortical neuron stimulation. Expression of Chronos, a channelrhodopsin variant with high light sensitivity and ultrafast gating properties was established. Our preliminary data suggest reduced light required for responses and allowed reliable neuronal spiking for stimulation up to at least 80 Hz. Therefore, Chronos-mediated cochlear optogenetics may help to achieve high spike rates in spiral ganglion neurons as required for efficient coding of auditory information.

Towards multichannel optical implants we, in collaboration with semiconductor experts, have implanted rodent cochleae with flexible µLED arrays accommodating approximately 100 µLEDs per 1 cm. Measurement of cochlear space and positioning of cochlear probes were assessed in 3D models derived from x-ray tomography.

Ongoing experiments to further characterize optogenetic stimulation of the cochlea will be presented and discussed. Taken together, our experiments demonstrate the feasibility of optogenetic cochlea stimulation to activate the auditory pathway and lay the groundwork for future applications in auditory research and prosthetics.

PS-110

Comparison of Virally-Mediated Transfer of ChR2 to Transgenic Expression of ChR2 in the Cochlear Nucleus: Implications for Development of an Optical Auditory Brainstem Implant

Elliott Kozin[1]; A. E. Hight[2]; Xiankai Meng[1]; Alyson Kaplan[1]; Ashton Lehmann[1]; Ed Boyden[3]; Albert Edge[1]; M. Christian Brown[1]; Daniel Lee[1]

[1]Massachusetts Eye and Ear Infirmary; [2]Program in Speech and Hearing Bioscience and Technology, Harvard Medical School; [3]Massachusetts Institute of Technology

Introduction

Auditory brainstem implant outcomes vary widely across users. One possible explanation for this variability may be limited auditory selectivity due to the spread of electrical stimulation and channel cross talk. An optogenetic-based auditory brainstem implant may be able to increase the number of independent channels. Previous work has demonstrated feasibility of transferring channelrhodopsin-2 (ChR2) to the cochlear nucleus (CN) using gene transfer techniques. However, the ideal promoter and mechanism for gene delivery for tissue selectivity in the CN is unknown. Herein, we compare virally mediated gene transfer of ChR2 in CBA/CaJ mice to two different strains of transgenic mice that express ChR2 in the auditory system.

Methods and Materials

Viral Transfer Model: CBA/CaJ mice age 6–8 weeks were anesthetized, a left craniotomy was performed, and an adeno-associated viral vector carrying a CAG promoter for the ChR2 gene promoter was injected into the CN. After 4-6 weeks recovery, the left CN (CN) and right inferior colliculus (IC) were exposed via craniotomy. Transgenic Model: We employed two transgenic lines: 1) mouse in which ChR2 expression is driven by a VGLUT-2 promoter and 2) a novel ChR2 mouse generated with a Cre-FloxP system driven by a CAG promoter. Light stimulation and neural recording: A 16-channel probe placed in the IC recorded multi-unit activity evoked by either acoustic stimulation or optical stimulation via a blue-light laser fiber placed on the surface of the CN. At the conclusion of the experiment, the brainstems were extracted and the extent of opsin expression was evaluated.

Results

Confocal microscopy demonstrated the three strains were similar in terms of wide expression of ChR2 in neurons and subdivisions of the CN. Neurophysiology recordings found all three strains had an auditory brainstem response (ABR) upon stimulation with blue light. ABR morphology varied between the three strains of mice. Light stimulation evoked strong activity in the IC in both the viral-mediated (max 300 spikes/s) and the CAG-ChR2 transgenic model (max ~300 spikes/s), but not the VGlut2-ChR2 transgenic model (0 spikes/s). No light-driven responses were demonstrated in control cases.

Conclusion

Our study highlights the variability of light-evoked neural activity due to differential expression among cell types in the CN. We identify the potential upper limits of temporal resolution in the central auditory system using ChR2 transgenic mice. Finally, we illustrate the importance of tissue specificity in the development of auditory implants based on optogenetic stimulation.

PS-111

Plasmonic Stimulation of Neurons and its Implications for Cochlear Implant Technologies

Parveen Bazard; Robert Frisina; Joseph Walton; Venkat Bhethanabotla

University of South Florida

Introduction

Cochlear implants work on the principle that electrical current can stimulate auditory nerve fibers (ANFs) via implantable electrodes. Implants use a set of electrodes to deliver pulses to ANFs in such a way that the stimulation mimics tonotopic features of the cochlea. Unfortunately, electrical stimulation results in current spread, resulting in low spatial resolution. Recent research has shown that infrared laser stimulation can also invoke responses from ANFs, and can give better spatial resolution than electrical stimulation. However, infrared light has the disadvantage of heating the surrounding tissue along with auditory nerve.

Metal nanoparticles can be designed to tune their localized surface resonance (LSPR) peak to a specific wavelength, and to have a desired ratio of their radiative to non-radiative decay rate. Non-radiative decay leads to localized heating. In this work, such localized heating is utilized to stimulate neurons using a visible wavelength to achieve high spatial and temporal specificity. In particular, we show for the first

time that small gold (Au) nanoparticles (< 20 nm in diameter) can stimulate neurons using a visible wavelength light of 532 nm. This finding has the potential to replace current electrode stimulation of peripheral and central neurons, including stimulation of ANFs for cochlear implants.

Methods

Au nanoparticles and a 532 nm wavelength green visible laser were used to excite the electrically excitable SH-SY5Y, human neuroblastoma cell lines, which can be differentiated like neurons. The Au nanoparticles approx. 20 nm size were synthesized using the standard citrate methods that involve addition of a 1% solution of sodium citrate solution to 0.01 M boiling gold salt solution. For stimulation of SH-SY5Y neurons, nano-electrodes were fabricated by coating Au nanoparticles on glass micropipettes. The coating of particles involves functionalization of glass surface with γ-(aminopropyl) triethoxysilane and finally, coating of Au nanoparticles onto the functionalized glass surface. The electrophysiological measurements were made using the patch-clamp technique in whole cell configuration. All the experiments were performed at room temperature without perfusion.

Results

When the nano-electrode was placed in the proximity (approx. 2 µm) of a patched neuron and the 532 nm laser was focused on the tip of the nano-electrode using a 50 µm inner diameter optical fiber; an instant change in cell resting potential (10-30 mV) was observed. Further experiments are underway to optimize the laser parameters (power/pulse width) to establish reliable thresholds for inducing action potentials.

PS-112

Optogenetic Control of Cochlear Nucleus Neurons using Spatially Focused Beams from a Laser Collimator

A. E. Hight[1]; Elliott Kozin[2]; Xiankai Meng[2]; Amélie Guex[3]; Alyson Kaplan[2]; Stéphanie Lacour[3]; Albert Edge[1]; M. Christian Brown[1]; Daniel Lee[1]

[1]Harvard University Medical School; [2]Massachusetts Eye and Ear Infirmary; [3]Ecole Polytechnique Fédérale de Lausanne

Introduction

The auditory brainstem implant (ABI) is a neuroprosthesis that provides sound sensations to deaf individuals who are not candidates for a cochlear implant (CI). Overall performance among ABI patients is modest compared to users of the CI. Optogenetics provides an alternative mode of stimulation that may circumvent the limitations of conventional ABIs, including electrical current spread and broad activation along the tonotopic axis (Verma et al. 2014). Here, we use a laser collimator to deliver a narrow beam of light to the photosensitized cochlear nucleus (CN) and examine the corresponding upstream activation of responses along the tonotopic axis in the inferior colliculus (IC).

Methods

We use a transgenic mouse expressing blue light-sensitive ChR-2 in spiral ganglion neurons and their central processes located in the CN (Meng 2014). Surgical access to the CN for optical stimulation is as previously described (see JoVE article, Kozin et al. 2014). One of two light sources were used to deliver blue light: 1) a 400 µm diameter fiber optic cable placed directly on the CN surface or 2) a 10 µm single mode fiber connected to an adjustable laser collimator delivering converged beams of light. Laser light delivered by either laser source was pulsed for 1 ms at a rate of 28 pulses/s. Responses were multi-unit activity in the inferior colliculus (IC) acquired from a 16 channel recording probe placed along the tonotopic axis as confirmed by acoustic stimulation (8-45.7 kHz, 0.5 octave steps, 20 ms duration).

Results

Optical stimulation by either light source evoked strong neural activity (~250 spikes/s at ~2 mW laser intensity), comparable to driven rates from acoustic stimulation (~300 spikes/s). Preliminary data show variability in the extent of neural activity from broad versus narrow, even with the collimator. Shifting the collimated light in the CN from the medial (high CF) to the lateral (low CF) border produced a shift in the center of IC activity along its tonotopic axis.

Conclusion

Restricted widths of evoked activity along the tonotopic axis suggest that effective light beam diameters are at least smaller than the exposed surface of the CN (~600 µm). Additionally, the center of evoked activity along the tonotopic axis can be controlled by focusing the light at three positions along the CN surface, indicating a resolution of at least 200 µm, a dimension that is smaller than the diameter of a single human ABI electrode (550 or 700 µm).

PS-113

Generation of a Novel Transgenic ChR2 Mouse for Optogenetic Control of the Cochlea

Xiankai Meng; A. E. Hight; Elliott Kozin; Yen-fu Cheng; Jingrong Lu; M. Christian Brown; Daniel Lee; Albert Edge

Massachusetts Eye and Ear Infirmary

Introduction

We generated a mouse model in which channelrhodopsin-2 (ChR2) is expressed in neurons of the auditory system to test the utility of optogenetics for development of an auditory prosthesis. Activation of neurons by light should have increased frequency resolution due to tissue-specific selectivity, thus addressing channel cross talk due electrical current spread in current cochlear implants. Herein, we describe: 1) generation of a transgenic mouse expressing ChR2+ in spiral ganglion cells (SGC), and 2) auditory responses to optical stimulation of the cochlea in the ChR2+ mouse.

Methods

We obtained three types of offspring by crossing Bhlhb5-Cre male mice with female mice containing a flox-stop cassette upstream of the ChR2 gene in frame with an eYFP gene: wild-type (Bhlhb5-ChR2-/-), heterozygous (Bhlhb5-ChR2+/-), and homozygous (Bhlhb5-ChR2+/+) mice. Confocal microscopy was used to determine eYFP localization and Western blot quantified ChR2 expression levels. Blue light laser (473nm wavelength) was introduced through a cochleostomy in the

lateral wall of the cochlea. Optically-evoked auditory brainstem responses (oABRs) and inferior colliculus (IC) multi-unit recordings were recorded.

Results

1) ChR2-eYFP expression was found in SGC in heterozygous and homozygous mice. The ChR2-eYFP was observed in the soma, and the peripheral and central axons of almost all SGCs. Expression of ChR2-eYFP was not observed in other cochlear cell types. The CAG promoter drove expression for at least 7 months in the transgenic mice. No ChR2-eYFP was observed in the wild-type mice.

2) A pulse of blue light evoked oABRs with peak magnitudes up to 40 uV and latencies as short as 1 ms in both heterozygous and homozygous mice. Evoked multi-unit activity (~180 spikes/second) in the IC had a synchronization index of up to 0.9 to a light pulse train at 28 Hz applied to the ChR2+ cochlea.

3) ChR2-eYFP expression level in homozygous mice cochleae was almost two-fold that of the heterozygous mice. Amplitudes of the first peak of the oABR were higher in homozygous as compared to heterozygous littermates. The slope of the amplitude growth function showed a positive linear correlation with the expression level of ChR2.

Conclusion

We generated and characterized a novel Bhlhb5-ChR2+ transgenic mouse line that was sensitive to light-based stimulation in the peripheral auditory system. Our study demonstrates the feasibility of using optogenetic technology for stimulation of cochlear neurons.

PS-114

Harmonic Fusion and Pitch Affinity: Is There a Direct Link?

Laurent Demany; Damien Bonnard; Rene Dauman; Catherine Semal

CNRS and Universite de Bordeaux

Introduction

Simultaneous pure tones with harmonic frequency ratios (FRs) tend to be perceptually fused. Deviations from harmonicity decrease fusion and can be detected on this basis. However, negative deviations (compressing the FRs) are better detected than positive deviations (Demany et al., JASA 1991; Borchert et al., JEP-HPP 2011). This asymmetry is reminiscent of the "octave enlargement" phenomenon observable with tones presented consecutively (Ward, JASA 1954), and may therefore suggest that the fusion of simultaneous pure tones with harmonic FRs is directly related to the perceived affinity of their pitches. We tested this hypothesis here.

Methods

Each stimulus consisted of three simultaneous (in condition "S") or consecutive (in condition "C") pure tones. The FRs of adjacent tones varied across stimuli between 0.96 and 1.04 octaves, taking eleven possible values. The frequency of the lowest component of each stimulus was selected randomly between 200 and 400 Hz. The tones were presented at about 15 dB SL in threshold-equalizing noise. This ruled out the possibility of cochlear interactions between the tones in condition S. Hence, the peripheral representation of a given tone was presumably identical in the two conditions. On every trial, the subject was presented with two stimuli defined by different FRs, and had to choose the better-tuned stimulus. Each of the eleven FRs was compared in this way to the other ten ones. Twenty subjects were tested.

Results

Except for two of the twenty subjects, the individual functions relating choice rate to FR magnitude in each condition could be well fitted by two regression lines forming an inverted V. On average, the apex of this inverted V was reached for an FR of 1.0016 octave in condition S and 1.0063 octave in condition C. The difference was statistically significant [$t(17)=3.165$, $P=0.0057$]. In addition, the inverted Vs showed a significantly different asymmetry in the two conditions: In condition S, the slope of the regression lines was steeper below the apex than above it; in condition C, the opposite was found.

Conclusions

Under the hypothesis that the fusion of simultaneous pure tones approximately one octave apart is determined by the perceived affinity of their pitches, similar results were expected in our two experimental conditions. The failure of this prediction suggests that harmonic fusion is in fact not determined by relations between pitches. In the auditory system, harmonic fusion may take place below the level at which pitch is extracted.

PS-115

Binaural Pitch Fusion is Broader in Hearing-Impaired Listeners than Normal-Hearing Listeners

Lina Reiss[1]; Corey Shayman[2]; Keri O'Connell-Bennett[1]; Jennifer Fowler[1]; Jennifer Fowler[1]

[1]Oregon Health & Science University; [2]University of Illinois at Urbana-Champaign

Background

Previously, we showed that cochlear implant users experience abnormally broad pitch fusion between ears, i.e. fuse sounds that differ by as much as 3-4 octaves in pitch between ears (Reiss et al., JARO 2014). The goal of this study was to determine whether hearing-impaired listeners without cochlear implants (e.g. bilateral hearing aid users) also experience broad binaural pitch fusion, and whether the fusion range size is related to either the degree of hearing loss or interaural pitch mismatches due to diplacusis. Normal-hearing listeners were also tested for comparison of fusion ranges measured using the same procedure.

Methods

Twelve hearing-impaired listeners and nine normal-hearing listeners were recruited. Subjects performed two tasks: 1) *Interaural pitch matching*, in which a reference tone in one ear was pitch-matched to sequentially presented comparison tones in the contralateral ear; 2) *Dichotic fusion range mea-*

surement, in which a reference tone was presented simultaneously in one ear with a tone in the contralateral ear, and the contralateral stimulus varied to find the frequency range that fused with the reference tone. Only frequencies above each subject's upper frequency limit of sensitivity to interaural phase differences were tested in the fusion task.

Results

Hearing-impaired listeners had binaural pitch fusion ranges that varied in size from 0-3.5 octaves, with an average of 1.1 octaves. These fusion ranges were broader than the average of 0.024 octaves seen in normal-hearing listeners. Fusion range widths were significantly correlated with interaural pitch mismatch in normal-hearing listeners, but not hearing-impaired listeners. Instead, for hearing-impaired listeners, fusion range was significantly correlated with poorer hearing thresholds.

Conclusions

Hearing impaired listeners can exhibit broader binaural pitch fusion ranges than those seen in normal-hearing listeners, and this seems to depend on the amount of hearing loss. As in bimodal cochlear implant users, the broadened fusion may account for some cases of speech perception interference observed with binaural compared to monaural hearing aid use.

PS-116

Pitch Dominance within Harmonic Complexes in Hearing-impaired Listeners

Ian Mertes; Erin Wilbanks; Marjorie Leek
VA Loma Linda Healthcare System

Introduction

The perception of complex pitch is important for the ability to hear individual voices in the presence of background noise. In normal-hearing (NH) listeners, complex pitch perception may be dominated by the energy at specific harmonic components (Moore et al., *JASA*, 1985) or at specific frequency regions (Dai, *JASA*, 2000). In hearing-impaired (HI) listeners, pitch dominance may be altered because energy at these harmonics may be attenuated and/or distorted. Differences in pitch dominance between these groups may be a factor in the increased difficulty HI listeners experience when listening in background noise. The purpose of this study was to compare pitch dominance in NH and HI listeners as assessed using harmonic complexes. The perceptual weight of each harmonic component and the relative influence across components were compared between groups.

Methods:

On each trial, subjects listened to two harmonic complexes and selected the interval they perceived as having the higher pitch. Each complex included the first 12 harmonics of one of four fundamental frequencies (100, 200, 300, and 600 Hz). Trial presentations were blocked according to fundamental frequency. Complexes were 200 ms in duration and were presented under earphones to one ear at an overall level of 80 dB SPL. On each presentation, the frequencies of each harmonic component were randomly perturbed by up to ±4% and all phases were selected randomly. Following Dai (2000), and Richards and Zhu (*JASA*, 1994), for each harmonic, a correlation was computed between the subject's responses and the differences in amount of perturbation between intervals on each trial. A larger correlation coefficient, or weight, suggested a greater influence of that harmonic on complex pitch perception because frequency changes at that harmonic were associated with the subject's response.

Results:

Preliminary results indicated that the first 3-4 harmonics were generally the most influential, regardless of fundamental frequency. Considerable variability across individuals was seen in terms of the strength of correlations at each harmonic. However, correlations tended to be greater in NH subjects relative to HI subjects.

Conclusions:

NH and HI listeners demonstrated similar patterns of pitch dominance in harmonic complexes, but the component weights were generally weaker in HI listeners. The results will be discussed in light of previous studies of pitch dominance, and with respect to the impact of hearing loss on complex pitch perception. [Work supported by NIDCD].

PS-118

Possible Origins of Human-Like Pitch Perception Mechanisms

Xindong Song; Michael Osmanski; Yueqi Guo; Xiaoqin Wang
Johns Hopkins University

Pitch perception of harmonic complex sounds is a crucial feature of human audition, especially in music and speech perception, auditory stream segregation, among others. Yet the evolutionary origins of pitch perception, and whether its underlying mechanisms are unique to humans, is unknown. Based on estimates of frequency resolution at the level of the auditory periphery, psychoacoustic studies have revealed several primary features of pitch perception in humans, for example, (1) Pitch strength of a harmonic tone is dominated by resolved harmonics; (2) Pitch of resolved harmonics is sensitive to the quality of spectral harmonicity; (3) Pitch of unresolved harmonics is sensitive to the salience of temporal envelope cues. Here we show that, for a standard musical tuning fundamental frequency of 440Hz (ISO 16), the marmoset (*callithrix jacchus*), a highly vocal non-human primate species, has capabilities comparable to humans in terms of how many individual frequency components can be resolved in a harmonic complex sound. Furthermore, we show that marmosets exhibit all primary features of pitch perception demonstrated in humans. Previous studies have identified a specialized pitch processing region in both marmoset and human auditory cortex. Thus marmosets and humans appear to share the same or similar pitch perception mechanisms. The observations obtained from marmosets suggest that neural mechanisms for pitch perception are not unique to humans, but likely originated earlier than the separation of Old World and New World monkeys in primate evolution.

PS-119

Effects of Musical Training on Pitch Discrimination of Resolved and Unresolved Complex Tones

Federica Bianchi; Sébastien Santurette; Dorothea Wendt; Torsten Dau
Technical University of Denmark

Musicians typically show enhanced pitch-discrimination ability compared to non-musicians, consistent with the hypothesis that musicians are more sensitive to some acoustic features critical for both speech and music processing. It has been debated whether this perceptual enhancement, so far mainly observed for complex tones containing resolved harmonics, can be ascribed to higher peripheral frequency selectivity, increased sensitivity to spectro-temporal features due to finer representations at a cortical level, or an enhanced ability to attend to and extract such features. The present study investigated whether musical training enhances pitch-discrimination performance for complex tones containing resolved vs. unresolved harmonics to the same extent, and whether this enhancement can be ascribed to increased frequency selectivity or to a higher effort in performing the task.

A behavioral pitch-discrimination experiment was performed in 8 musically-trained and 6 non-musically-trained listeners. Fundamental frequency (F0) difference limens were obtained for harmonic complex tones with F0s between 100 and 500 Hz, filtered in either a low or a high frequency region, leading to variations in the resolvability of audible harmonics. In a second experiment, listeners' pupil dilations were measured as an indicator of the required effort in performing the same pitch-discrimination task for conditions of varying resolvability and task difficulty.

Musically-trained listeners obtained smaller behavioral pitch-discrimination thresholds than non-musicians by a factor of about 2 in both resolved and unresolved conditions, indicating that the presence of resolved harmonics is not necessary for enhanced pitch discrimination following musical training. Additionally, the transition point between unresolved and resolved harmonics derived from the obtained thresholds was similar for musicians and non-musicians, suggesting similar peripheral frequency selectivity for the two listener groups. Musicians' pupil dilations indicated an increase in task-induced effort with increasing difficulty of the task and decreasing resolvability of the stimuli. Non-musicians' pupil dilations also indicated an increase in effort from easy-to-medium task-difficulty conditions, but effort significantly decreased during a pitch discrimination task comprising unresolved complex tones and high task difficulty. Thus, musicians showed a larger effort than non-musicians when discriminating the pitch of unresolved complex tones.

Overall, these findings indicate a similar perceptual benefit for resolved and unresolved complex tones following musical training, which may not be ascribed to sharper peripheral filtering in musicians. Higher task-induced effort may partly explain the enhanced performance of musicians for unresolved complex tones.

PS-20

A New Method for Assessing the Time Course of Auditory Enhancement

Lei Feng; Andrew Oxenham
University of Minnesota

Introduction

A target tone becomes more audible and may 'pop out' from a simultaneously presented multi-tone masker if the masker, termed precursor, is presented first without the target. This phenomenon, known as "auditory enhancement," reflects the general perceptual principle of contrast enhancement, and may help in the detection of new acoustic events and in the perceptual constancy of speech under varying and noisy acoustic conditions. Previous studies often used two-interval procedures, where the masker in one interval could act as a precursor to the masker in the second interval, and/or fixed signal or masker frequencies, which may have affected estimates of enhancement. Here we tested a new one-interval pitch comparison task with frequency roving to measure the enhancement of a supra-threshold target as a function of precursor duration and gap between precursor offset and target onset.

Methods

Fourteen normal-hearing (NH) listeners were tested. In each trial, a seven-component inharmonic complex, including six masker tones and one target tone, was followed by a pure-tone probe. Listeners were asked to judge whether the target and probe tone had the same pitch (present-absent task), or the direction of pitch change (up-down task).Threshold target level was measured adaptively, and enhancement was defined as the difference in threshold between precursor-absent and precursor-present conditions. Three precursor durations (62.5, 250, and 1000 ms) and three precursor-complex gaps (10, 100, and 1000 ms) were measured for a total of nine conditions. Control conditions involving notched-noise and bandpass-noise precursors were also tested.

Results

The mean data revealed a maximum of over 24 dB enhancement with the longest precursor and shortest gap. Enhancement decreased with decreasing precursor duration and increasing precursor-complex gap. Enhancement was slightly larger in the up-down task than in the present-absent task, but there were no significant interactions between task type and stimulus variables. Notch noise and bandpass noise were not as efficient as the masker precursor, although they still showed some enhancement with long precursors and short gaps.

Conclusions

The new enhancement paradigm can be used to determine the effective increase in the gain of supra-threshold targets, while reducing possible longer-term effects associated with previous paradigms. This method will be used to test cochlear-implant (CI) users in the future. The results may help in developing signal-processing techniques which could compensate for some perceptual differences between CI users and NH listeners.

PS-121

Auditory Perceptual Filters in Macaque Monkeys

Jane Burton; Corey Mondul; Margit Dylla; Ramnarayan Ramachandran
Vanderbilt University

The auditory system is thought to utilize overlapping bandpass filters for the detection and resolution of complex sounds. All acoustic energy that falls within such an auditory filter will contribute to the ability to perceive a stimulus using that filter. The critical band is a measure of frequency resolution that represents the bandwidth of noise at which signal threshold ceases to change and can be derived directly from auditory filter shape. The critical band has been well quantified in humans and other mammalian species, but little work has been done to examine critical bands in monkeys. A previous study measured critical bands in macaques, but the band widening methods employed were not ideal. The purpose of this study was to investigate the auditory perceptual filters of macaque monkeys using a notch-widening paradigm.

Two monkeys (*Macaca mulatta*) were trained to detect pure tone signals in the presence of a broadband noise masker in a reaction time Go/No-Go task using the method of constant stimuli. Thresholds were measured for tones at frequencies covering the entire audible range for macaques. Noise was notched around the signal frequency symmetrically and asymmetrically to examine overall filter shape and the upper and lower edges of the auditory filters. Thresholds decreased with increasing notch widths and approached thresholds to tones alone at the widest notchwidths. These thresholds were fit with a rounded exponential function and integrated to determine auditory filter shape. The critical band was determined as the bandwidth at the half power point of this filter. Macaque critical bands were found to be comparable to human data, when derived from both critical ratio estimates and the notch-widening procedure. Critical bandwidths increased with frequency in a sublinear fashion, yielding narrower auditory filters in the highest frequencies (16-32 kHz), but did not change as a function of noise level. Macaque auditory filters were also asymmetric at high noise levels (≥ 50 dB SPL) with a broader lower edge and narrower upper edge, which is consistent with human auditory filters. These results provide further support for the use of macaques as a model for human hearing. These behavioral data form a basis for neurophysiological investigations of the peripheral vs. central mechanisms underlying auditory perceptual filters. Additionally, these results serve as a normative baseline for future studies of noise-induced hearing loss.

PS-122

The Battle of the Sexes Continues: Who "wins" in a Frequency Discrimination Task?

Liat Kishon-Rabin; Yael Zaltz; Daphne Ari-Even Roth
Tel-Aviv University

Background

The male and female auditory system differs in many aspects including the physical dimensions of the ear, brain anatomy, the exposure to androgens, and exposure to environmental factors. Whether these differences result in an advantage in hearing performance of one sex over the other is of continuous debate. In adults, physiological evidence showed some advantage for females although psychophysical data tended to show greater sensitivity for males in auditory tasks primarily related to temporal processing. In children the results of the few studies were equivocal. The lack of a significant sex effect has been attributed primarily to small sample size and the influence of confounding factors such as age and cognition. The purpose of the present study was to examine the effect of sex in a large sample of 109 children and adults using an auditory frequency discrimination (FD) task.

Methods

64 children (6.9-9 years old, 31 males and 33 females) and 45 adults (18-34 years old, 21 males, 24 females) with normal hearing and no musical training participated in this retrospective study. FD threshold estimations at 1 KHz were obtained for all listeners and additional six were obtained for 85 (45 adults and 40 children) using an adaptive forced-choice procedure. Cognitive measures were obtained for the children.

Results showed that when age was held as a covariate, males performed better than females. In a regression analysis sex explained 4.8% and 9.6% of the variance in children and adults' performance, respectively (effect size $\geq$ 0.5). In children, age, sex and auditory cognition explained 32.1% of the variance in the first three thresholds with sex remaining significant. Additional analysis confirmed that the sex difference was limited to the first three thresholds.

Conclusions

Based on the hypothesis that at low frequencies FD is mediated by temporal processing, our results are in keeping with previous data showing that these abilities are superior in males. The diminishing effect with increasing auditory experience may suggest that other factors eventually override this initial sex difference. This study further emphasizes the many factors that influence the outcome of what is considered a basic auditory task and contributes to our knowledge regarding sex-related differences in auditory processing.

PS-123

Effect of Distractor Saliency on Amplitude-modulation Detection Task

Shunsuke Kidani; Hsin-I Liao; Makoto Yoneya; Makio Kashino; Shigeto Furukawa
NTT corporation

Salience sounds are assumed to capture attention and distract listeners from performing a task that is irrelevant to the sounds. This study aimed to test this hypothesis by examining sensitivity of an amplitude-modulation (AM) detection task while distractor sounds with various subjective salience were presented.

The stimuli were presented dichotically via a headphone. An auditory sequence which consisted of 8-kHz tone bursts (200-ms duration; 65-dBA level) with 2000-ms intervals and was presented to the listener's left ear. The listener's task

was to detect a 20-Hz sinusoidal AM target imposed on the tone bursts as soon as possible by button press. Task difficulty was manipulated as a within-subject factor. The AM depth was determined for individual listeners in a preliminary test, in which the resulting detection sensitivity (d') was adjusted around 1 and 3 for the difficult and easy tasks, respectively. Six types of distractors were used including abstract sounds (e.g. white noise, tone) and environmental sounds (e.g. bird's singing). Each distractor had a level of 71 dBA and was presented for 300 ms. The subjective salience of the distractors had been estimated in terms of the Thurstone scale derived in our earlier study [Kidani et al., ARO2014 abstract]. The distractors were presented to the ear opposite to the target, i.e., the right ear, in random order. When the distractor was presented, the temporal center of the distractor was synchronized to that of the target. The distractors were low-pass filtered (6-kHz cutoff frequency) to avoid spectral crossover between the distractor and the target.

The sensitivity (d') was significantly impaired by the presence of the distractor only in the easy task condition ($p < .001$) but not in the difficult task condition ($p = 0.12$). The sensitivity varied among the distractors (ANOVA; $F(5,42) = 2.44$, $p < .05$). However, there was no significant correlation between the sensitivity in the AM detection task and the subjective salience of the distractor ($p = 0.87$).

The study showed the distraction effects of the task-irrelevant sound. However, we did not find evidence for the contribution of subjective salience to the distraction effect. The results cannot be explained by low-level sensory factors such as peripheral interaction since the target and distractors were presented to opposite ears and did not overlap in spectrum, or modulation masking interference since certain distractor sounds which contained no AM impaired performance. Unknown high-level factors may be involved in the observed phenomenon.

PS-124

Assessing Temporal Fine Structure Processing Indirectly: An AM/FM Interference Task

Nihaad Paraouty; Nicolas Wallaert; Daniel Pressnitzer; Christian Lorenzi
Ecole Normale Superieure - Paris & LSP - UMR 8248 CNRS, France

It is believed that auditory sensitivity to amplitude modulation (AM) reflects the use of temporal-envelope (E) cues, whereas sensitivity to slow frequency modulation (FM) primarily reflects the use of temporal-fine structure (TFS) cues for carrier frequencies up to 1 kHz. Several psycho-acoustical studies have demonstrated that hearing-impaired listeners show poorer-than-normal sensitivity to FM, and normal or even better-than-normal sensitivity to AM, consistent with the notion that cochlear damage alters neural phase locking to TFS cues while sparing (or even enhancing) processing of E cues. However, the perceptual deficit observed for FM detection may partly result from reduced "processing (central) efficiency", rather than from alterations in neural phase-locking to TFS cues. We developed an interference paradigm in order to address this issue. Importantly, the paradigm was designed such that poor sensitivity to TFS should lead to better perceptual performance. This paradigm was based on a pilot study showing that AM detection worsens when the tonal carrier is frequency modulated at the same rate as the AM. Detection thresholds were measured for a 5-Hz sine AM applied to a 0.5-kHz tone carrier. The latter was either unmodulated or frequency-modulated at 5 Hz at increasing FM depths. It was reasoned that listeners with poor TFS sensitivity (and thus, poor FM sensitivity) should show better AM detection thresholds than listeners with good TFS sensitivity when the pure-tone carrier is modulated in frequency. For each listener, psychoacoustic measures of TFS sensitivity (i.e., thresholds for detecting a change in interaural phase, IPD) and frequency selectivity (i.e., thresholds for detecting a pure tone in notched noise using 2 notch widths: 0 and 150 Hz) were also obtained at 0.5 kHz. It was reasoned that the magnitude of the interference effect between AM and FM should be predicted by IPD scores only, if this interference effect reflects the use of TFS (neural phase-locking) cues rather than the conversion of FM into AM (E cues) at the output of cochlear filters. Data collected on young and elderly normal-hearing listeners will be presented and discussed. Preliminary results obtained in young normal-hearing listeners indicate that as expected, AM detection thresholds increase (become poorer) systematically when the carrier is frequency modulated, and the magnitude of this interference effect increases systematically as a function of FM modulation depth. We plan to extend the study with data from hearing-impaired listeners, with a particular focus on patients suffering from acoustic trauma.

PS-125

The Use of Slow and Fast Temporal Envelope Cues in Phonetic Discrimination at 3 Months Of Age

Laurianne Cabrera; Lynne Werner
University of Washington

Introduction

Speech perception requires efficient auditory mechanisms to track differences in the spectro-temporal cues differentiating phonetic contrasts. In adults, slow (<16Hz) temporal envelope cues (or amplitude modulation, AM) play the most important role in speech identification in quiet. The fast AM cues and the temporal fine structure (or frequency modulation, FM) play a more important role in noise. The present study aims to explore the role of AM cues on two different time scales (below and above 8 Hz) in phonetic discrimination in 3-month-old infants. Previous studies showed that the detection of AM may be mature around 3 months of age. Thus, 3-month-old infants may be able to discriminate phonetic contrasts on the basis of slow and fast AM cues. However, it is not clear whether infants are able to switch between slow and fast AM cues in different listening conditions.

Method

English syllables with different stop consonants are processed by two tone-excited vocoders. These vocoders selectively replace the original FM cues with pure tones in 32

frequency bands. The AM cues are extracted in each frequency band with two different cut-off frequencies: 256 Hz or 8 Hz. Participants are 3-month-olds (N=54) and 18-30-year-old adults (N=17) with no risk factors for hearing loss. An observer-based testing method is used. Each participant has to detect a change in a repeating syllable from a non-target phonetic category to a target category: voiced, unvoiced, labial, coronal or velar (see Table 1). Discrimination is tested in quiet or in a speech-shaped noise (SNR= -5dB). When participants reach 80%-correct criterion in the AM-256Hz condition, discrimination is assessed in the AM-8Hz condition.

Table 1. Phonetic contrast conditions. Each participant is exposed to one phonetic contrast condition. Participants listen to the background syllables played repeatedly. There are two trial types that occurred with equal probability during testing: change and no change trials. During change trials, one target syllable (chosen randomly) is played once. During no-change trials a background syllable is played.

Phonetic contrast condition	Target syllables	Background syllables
Voiced	ba, da, ga	pa, ta, ka
Unvoiced	pa, ta, ka	ba, da, ga
Labial	pa, ba	da, ta, ga, ta
Coronal	da, ta	ba, ta, ga, ka
Velar	ga, ka	ba, pa, da, ta

Table 2. Three-month-old infants and adults who passed the 80%-correct response criterion in each vocoder condition in quiet or noise. The chance level to pass the 80%-correct criterion within 2 or 3 sessions is about 4% in AM-256Hz and 1% in AM-8Hz.

	AM-256 Hz	AM-8Hz
Quiet: 3-month-olds	25/30 (83%) in an average of 2 sessions	12/25 (48%) in an average of 3 sessions
Noise: 3-month-olds	23/24 (93%) in an average of 2 sessions	9/23 (39%) in an average of 2 sessions
Quiet: Adults	17/17 (100%) in an average of 1.4 sessions	17/17 (100%) in an average of 2 sessions

Results/Conclusions

The findings suggest that 3-month-old infants are able to use slow and fast AM cues to discriminate phonetic contrasts in quiet and in noise. However, results also suggest that phonetic discrimination is easier when fast AM cues are available in both noise and in quiet (see Table 2). It is thus unlikely that infants' performance is limited by immature temporal resolution. Nevertheless, more experience with the native language—and thus, with the acoustic cues related to syllabic rate—may improve the use of the slow AM cues for phonetic perception.

PS-126

Effects of Carrier Intensity on Amplitude Modulation Detection using High and Low-fluctuating Noises

Ali Almishaal; Skyler Jennings
University of Utah

Effective processing of the speech envelope is essential for speech understanding. Fluctuations in the speech envelope can be simulated using amplitude modulation (AM). Processing of AM may be influenced by cochlear compression. Specifically, compression may reduce the "effective" contrast between AM high-intensity peaks and low-intensity valleys. The proposed perceptual experiments are designed to test the hypothesis that AM detection deteriorates at high carrier levels due to compression. AM thresholds were measured for a 20-Hz modulation imposed on a narrow-band noise (NBN) carrier as a function of carrier level. The carrier duration was 500-ms. A notched-noise, centered on the carrier, was used to restrict off-frequency listening. High-fluctuating (GN: Gaussian) and low-fluctuating (LNN: low-noise noise) noise carriers were used to examine the influence of inherent noise fluctuations on AM thresholds, and how these fluctuations interact with compression. The results show that thresholds obtained with GN were higher than those obtained with LNN carriers; however, this difference was strongly dependent on carrier level. For GN carriers, AM thresholds worsen and then improved with carrier level. In contrast, thresholds obtained with LNN carriers improved markedly with carrier level. Poorer AM thresholds in GN carriers may originate from the relatively greater degree of inherent fluctuations in GN than LNN, resulting in a form of modulation masking. The effect of level seen with GN carriers is consistent with greater compression at mid-levels. The differential effects of carrier level in GN and LNN carriers may be consistent with linearization of the cochlear input-output (I/O) function. This linearization would result in greater effective contrast in the experimentally imposed AM stimulus. With GN carriers, contrast would also increase for inherent noise fluctuations, leading to greater potential for modulation masking. Conversely, a lack of inherent fluctuations in LNN carriers, in conjunction with a linearized I/O function, may result in greater effective contrast in the AM stimulus, but with little competing fluctuations inherent in the noise. A potential mechanism for this linearization of the I/O function is the medial olivocochlear (MOC) reflex, which reduces outer hair cell gain when elicited. If such is the case, these results suggest that the MOC reflex may increase the contrast between peaks and valleys of AM stimuli.

PS-127

Improved Decrement Detection with Decrement Location may Result from Efferent Processing

Jessica Chen; Skyler Jennings
University of Utah

The ability to understand speech in background noise may be partially facilitated by the medial olivocochlear reflex (MOCR), in normal-hearing individuals. The MOCR is elicited by moderate-to-high level sounds and reaches its full strength after ~100 ms, following the onset of an acoustic elicitor. The main effect of the MOCR is to reduce outer hair cell (OHC) gain in response to sound. A reduction in OHC gain may lead to a better signal-to-noise ratio (SNR) at the output of the cochlea. This change in gain may also increase the contrast between high-intensity peaks and low-intensity dips in a speech envelope. This hypothesis is tested by inserting a decrement in an otherwise steady-state signal to simulate the abrupt intensity dips occurring in speech, such as gaps between words and sentences, and voice-onset time. Decrement thresholds were obtained at the onset and the temporal center of a narrow-band, low-fluctuating noise pedestal centered on 2-kHz and 4-kHz. With the sluggish start of the MOCR, detection of the decrement at the pedestal onset is assumed to occur while the MOCR is in its latent state. Detection of the decrement at the temporal center of the pedestal is assumed to occur

when the MOCR is fully active. Preliminary results indicate that decrement thresholds are lower when the decrement is located at the temporal center of the pedestal compared to a decrement near the onset. This finding is consistent with the hypothesis that eliciting the MOCR improves the post-cochlear contrast between steady-state and decrement portions of the pedestal. Alternative hypotheses, such as neural adaptation and perceptual confusion, may also account for these findings. As part of a larger project, mechanisms behind decrement detection are being evaluated using a computational model of the auditory system.

PS-128

The Effects of Masker Fluctuation on Overshoot Measured with Narrowband-Noise Maskers

Skyler Jennings; **Kayla Hirschmugl**
University of Utah

The detection of a short probe in a noise masker improves when the probe is moved from the onset of the masker to the temporal center of the masker. This improvement (called overshoot) may be due to a regulation of cochlear gain via the medial olivocochlear (MOC) reflex. For Gaussian noise (GN) maskers, the magnitude of overshoot depends on masker bandwidth, where greater overshoot is associated with larger bandwidths. This result is consistent with physiological findings in laboratory animals, which suggest that the MOC reflex is only weakly elicited by narrowband stimuli. An alternative hypothesis for reduced overshoot in narrowband noise is the presence of relatively greater temporal fluctuations in band-limited stimuli. The present study tests this hypothesis by comparing overshoot measured with high and low-fluctuating noise. Detection thresholds were measured for a 6 ms probe presented 2 ms or 198 ms after the onset of a simultaneous narrowband-noise masker. The probe frequency was either 2000 Hz or 4000 Hz, and the masker spectrum was centered on the probe frequency with a bandwidth of 0.5 equivalent rectangular bandwidths. GN and low-noise noise (LNN) maskers were used to produce a high or low degree of inherent fluctuation, respectively. Overshoot was not observed with GN maskers. Conversely, large (8-20 dB) overshoot was observed in all subjects with LNN maskers. These results suggest that overshoot obtained using narrowband-noise maskers is primarily dependent on the degree of inherent masker fluctuation, rather than the strength of the MOC reflex to narrowband stimuli.

PS-129

Assessing Temporal Fine Structure Processing Indirectly: A Modulation Detection Interference (MDI) Task

Dorit Enja Jung[1]; David Timothy Ives[2]; Christian Lorenzi[2]
[1]University of Groningen, University Medical Center Groningen; [2]Dept d'Etudes Cognitives, Ecole normale superieure

Background

Aging and cochlear hearing loss seem to impair the processing of temporal fine structure (TFS) cues while sparing the processing of slow temporal envelope (E) cues. Here, we present a feasibility study to establish whether TFS-processing capacities can be assessed indirectly through an E detection task. This novel task was aimed to limit the contribution of high-level (cognitive) factors when elderly and hearing-impaired process TFS cues.

Methods

All stimuli were presented binaurally. Participants had to detect slow envelope changes in the form of sinusoidal amplitude modulation (SAM) applied to a high-frequency pure-tone carrier. This target stimulus was always presented diotically. This E detection task was performed in the presence of an "interfering" low-frequency pure tone that was sinusoidally amplitude modulated at the same modulation rate as the target tone. This low-frequency tone was always masked by a narrowband or broadband noise. The low-frequency tone's audibility (and thus, the audibility of the superimposed SAM) was altered by changing its interaural phase (i.e., its binaural TFS). It was reasoned that good TFS sensitivity in the low-frequency region would result in large binaural masking level difference (BMLD); this, in turn, would result in strong modulation detection interference (MDI) and thus, poor SAM detection in the high-frequency region.

Results

Data of six young, normal-hearing listeners will be presented. Changes in binaural TFS (interaural phase) generally led to an increase in E detection thresholds (i.e., a MDI effect). However, this effect reached significance only for one of five tested signal-to-noise ratios. Also, large intersubject variability was observed.

Conclusions

This data suggest that TFS processing can influence E processing indirectly, and that future implementations of the present E / TFS interaction paradigm could be used to assess TFS-processing abilities. It is expected that in future implementations of this task, elderly and hearing-impaired populations will outperform young, normal-hearing controls, thus controlling for a potential decline in "processing efficiency".

PS-130

Inherent Fluctuations in Forward Maskers: Effects of Masker-Probe Delay for Listeners With Normal and Impaired Hearing

Adam Svec[1]; Judy Dubno[2]; Peggy Nelson[1]
[1]University of Minnesota Twin Cities; [2]Medical University of South Carolina

Background

In a previous study (Svec *et al.,* 2014), forward-masked thresholds were higher for maskers with maximal than minimal inherent fluctuations, and these differences were similar for normal-hearing (NH) and hearing-impaired (HI) adults. The slope of recovery from steady-state forward maskers is typically shallower in HI listeners than NH listeners due to loss of cochlear nonlinearities, whereas the time constant for recovery is less affected by hearing loss; it remains unclear if similarly distinctive patterns will be observed for forward

maskers with inherent fluctuations. Based on previous results, we hypothesized that the effectiveness of fluctuating maskers is related to both recovery from forward masking and recovery from inherent fluctuations. To test this hypothesis and assess the extent to which recovery from inherent fluctuations is affected by loss of cochlear nonlinearities, forward masked thresholds were measured for maskers with maximal and minimal inherent fluctuations as a function of the delay between the masker and the probe in NH and HI listeners.

Methods
Forward-masked detection thresholds were measured for NH and HI listeners for a 10-ms, 4000 Hz probe and either a Gaussian noise masker (GN, maximal fluctuations) or low-fluctuation noise masker (LFN, minimal fluctuations) centered at 4000 Hz and presented at masker-probe delays of 25, 50, and 75 ms.

Results
For NH listeners, forward masked thresholds were higher in GN than in LFN at shorter masker-probe delays but were similar at longer delays, resulting in steeper slopes of recovery for highly fluctuating forward maskers. In contrast, forward masked thresholds for HI listeners were higher in GN than in LFN at all masker-probe delays, resulting in slopes of recovery that were independent of masker fluctuations. At the longest masker-probe delay, amount of masking (masked threshold – quiet probe threshold) with minimal masker fluctuations was similar for NH and HI listeners, but highly fluctuating maskers yielded higher masked thresholds for HI listeners, suggesting that the time course of recovery from inherent fluctuations may be greater in HI than NH listeners.

Conclusions
HI listeners showed increased masking from random masker fluctuations even at longer masker-probe delays. Because slopes of recovery were affected by inherent fluctuations in NH listeners but were independent of masker fluctuations in HI listeners, these results may not be fully explained by the peripheral loss of cochlear nonlinearities.

PS-131

Listener-Specific Sound-Localization Performance: A Matter of Better Ears?

Piotr Majdak; Robert Baumgartner; Bernhard Laback
Austrian Academy of Sciences

Background
The ability to localize sound sources in sagittal planes (top, down, front, back) varies considerably across listeners. However, the reasons for being a better or poorer sound localizer are unclear yet. The directional acoustic spectral features, described by head-related transfer functions (HRTFs), also vary considerably across listeners. Here, we investigated whether the listener-specific quality of directional cues provided by the HRTFs contributes to the listener-specific sound-localization performance.

Methods
Sound localization in conditions corresponding to listening with others' HRTFs was tested under the assumption of complete re-calibration to the others' HRTFs. To this end, a model of sagittal-plane localization (Baumgartner et al., 2014 JASA 136:791-802) was used to simulate the re-calibration of the listener to the tested HRTFs. As input, the model requires the HRTFs of the target sounds, the template HRTFs the listener is calibrated to, and the sensitivity parameter representing the listener's efficiency in processing localization cues. The sensitivity parameters of 23 listeners were adjusted to best match the actual experimental performance obtained for Gaussian white noise bursts with a duration of 500 ms. The localization performance was measured in terms of quadrant error rates and the root-mean-square of local polar errors. Then, the HRTF sets and the sensitivity parameters were systematically permuted across the members of the listener group. The state of complete re-calibration was simulated by using the same HRTF set for the template and targets. The impact of the two model parameters was estimated by the correlation of the actual with the predicted localization performance.

Results
The listener-specifically calibrated model predictions yielded a correlation between actual and predicted performance of 0.91. The permutation of HRTFs yielded a correlation of 0.82. The permutation of the listener-specific sensitivity substantially reduced the correlation to approximately 0.22.

Conclusions
The permutation of the listener-specific sensitivity affected the predicted localization performance much more than the permutation of the HRTF sets. This suggests that the across-listener variability in sagittal-plane localization ability is only marginally attributable to the quality of directional cues in human HRTFs. Rather, the sensitivity parameter, supposed to represent the listeners' efficiency in processing directional cues (e.g., spectral-shape sensitivity) appears to be more important. This finding might be relevant for developing non-spatial experimental measures serving as predictors of listener-specific sound-localization performance.

PS-132

Listeners'Confidence in their Responses in a Front/Back Discrimination Task Assessed by Reaction Time.

Guillaume Andéol; Jean Christophe Bouy; Clara Suied
Institut de recherche biomédicale des armées

Background
Listeners sometimes localize auditory targets behind when they are actually ahead and reciprocally. Those front/back reversal vary with the eccentricity of the auditory targets. It is not clear whether the listeners are aware or not of their difficulty to distinguish front from back. Previous studies have suggested a relationship between reaction time (RT) and confidence. In the present study, we use a reaction time paradigm in a front/back discrimination task to assess listeners 'confidence in their response.

Methods
Listeners sat on a chair placed at the center of a 12-loudspeakers ring (Azimuth: 0 to 360 by 30°step), inside an anechoic room. A wideband noise target was presented at 70 dB SPL with a 10 dB roving range. Listeners had to indicate whether the target was in front of or behind them by pushing a switch. They were asked to respond as quickly and as accurately as possible. We also measured the individual listener's detection time of the noise emitted by the 12 loudspeakers.

Results
The auditory target position had no impact on detection time. RTs varied with the eccentricity of the auditory target. Most listeners had longer RTs for lateral targets (60° of eccentricity). Independently of the eccentricity, RTs were longer for positions with higher front/back discrimination errors.

Conclusion
These results suggest that the listener's confidence in the response is related to target eccentricity and front/back errors.

PS-133

The Reliability of Contralateral Spectral Cues for Sound Localization in Sagittal Planes

Robert Baumgartner; Piotr Majdak; Bernhard Laback
Austrian Academy of Sciences

Introduction
Monaural spectral cues are essential for sound-source localization along sagittal planes. Psychophysical studies have shown that the human auditory system applies variable relative weights to the monaural cues at the two ears depending on the perceived lateral angle. In particular, the contribution of the contralateral ear decreases with increasing lateral eccentricity. It remains unclear, however, whether the lower weighting of the contralateral ear is a consequence of less pronounced spectral cues or whether the auditory system increasingly ignores the spectral cues provided by the contralateral ear.

Methods
We investigated this question by simulating sound localization experiments with 23 human listeners. Gaussian white noise bursts with a duration of 500 ms were presented at azimuths all around the listeners and elevations ranging from -30° to 80°. For the simulation, we used a sagittal-plane localization model that has been evaluated previously for a large range of lateral angles and various modifications of head-related transfer functions (Baumgartner et al., 2014 JASA 136:791-802). The model allows to continuously modify the contribution of the ipsilateral and contralateral signals. We compared the localization performance between three weighting configurations, namely, ipsilateral only, contralateral only, and binaural weighting according to the perceived lateral angle.

Results
The predicted localization performance, measured in terms of quadrant error rate (QE) and the root- mean-square of local polar errors (PE), was similar to that usually measured in localization experiments. For the ipsilateral and binaural conditions, the QEs were 9.2% and 9.4%, respectively. In the contralateral condition, the QE was 10.6%. The PEs were nearly the same for all conditions (32.6°±0.1°).

Conclusions
The similar performance predicted for the ipsilateral ear only and for the contralateral ear only indicates that the spectral cues provided by the contralateral ear are similarly pronounced as those provided by the ipsilateral ear. Hence, the experimentally observed larger ipsilateral weighting does not seem to be a consequence of less reliable spectral cues at the contralateral ear. The applicability of our findings in the context of real-life situations is discussed.

PS-134

Human Perception of Reverberation Incorporates Environmental Statistics

James Traer; Joshua McDermott
Massachusetts Inst. of Technology, Department of Brain and Cognitive Sciences, MIT

Background
-- Human sound recognition is remarkably robust to the distortion introduced by reverberation in everyday environments. Our lab has been exploring the hypothesis that this robustness is rooted in the ability to decompose the acoustic input into the contributions of the sound source and the reverberation, the latter of which can be described by a linear filter. Because the separation of source and filter (given only their convolution) is inherently ill-posed, any such capacity must depend on prior assumptions about the nature of filter and/or source. We have estimated the distribution of environmental impulse responses (IRs) encountered by human listeners in daily life, and are exploring the degree to which it constrains perception.

Methods
We obtained over 400 locations by randomly querying volunteers about their locations many times a day over the course of two weeks. We then measured the IR of the space at each location (offices, city streets, bathrooms, elevators etc.). To test the perceptual sensitivity to any environmental regularities, we generated synthetic IRs that were either faithful to the observed distribution of real-world IRs, or that deviated from it in various ways. We assessed a) the sense of reverberation conveyed by different types of IRs, b) recognition and discrimination of sound sources in reverberation, and c) discrimination of IRs given only their convolution with a sound source.

Results
IR measurements suggested that the diffuse tails of real-world IRs decay exponentially, with decay rates that are frequency-dependent. Moreover, the dependence of decay rate on frequency varied systematically with overall decay rate (i.e. room size). These properties were observed across a broad range of indoor and outdoor environments. Our psychophysical experiments indicate that human perception is strongly dependent on whether reverberant energy decay maintains this form. Rated realism, the ability to recognize sound sources in reverberation, and the ability to discriminate properties

of the IR all degraded when the IR deviated from the measured distribution of real-world environmental IRs.

Conclusion
Naturally occurring environmental IRs have stereotyped properties that have evidently been internalized by the auditory system over the course of development or evolution. Human listeners have some ability to separately estimate the source and filter in reverberant conditions, and are strongly constrained by whether the filter conforms to the naturally occurring distribution.

Funding
NIH NRSA post-doctoral fellowship awarded to JAT, McDonnell Scholar Award to JHM.

PS-135

A Rapid and Objective Sound Localization Test for Infants and Young Children

Filip Asp; **Erik Berninger**; Åke Olofsson
Karolinska Institutet

Introduction
The ability to locate the source of a sound has a survival value and thus exists in many species. Assessment of the immature human sound localization (SL) ability during infancy includes subjective observation of infants' behavior (e.g. head turns). We have developed a rapid method for SL measurements in infants from 6 months of age, where children's perception is studied by objectively observing their gaze in relation to spatially distributed auditory and visual events.

Methods
Twelve children aged 7 – 39 months who passed the neonatal newborn hearing screening and eight normal-hearing adults aged 18 – 40 years participated in the study. SL was measured in sound field by presenting a cartoon movie at 63 dB SPL_{Ceq} from 1 of 12 equidistantly placed loudspeaker/display-pairs spanning a 110 degree arc in the frontal horizontal plane. During shifts of the continuous sound to randomly assigned loudspeakers, subjects' pupil positions (i.e. their gaze) relative to the loudspeaker/display-pairs were sampled using an objective corneal reflection eye-tracking technique. We analyzed the gaze during 1.6 seconds sound-only periods, immediately after a loudspeaker shift with the visual stimuli paused, to determine SL accuracy, which was expressed as an Error Index (EI, ranging from 0 to 1, where 0 corresponds to perfect SL accuracy and 1 corresponds to random performance), reflecting the variance in SL ability. The aim was to study if gaze may be used for the study of SL accuracy during infancy and early childhood.

Results
Pupil positions were successfully recorded in all participants in a mean (SD) elapsed time of 168 (50) seconds and 162 (28) seconds, in children and adults respectively. Preliminary results indicate and age-related improvement of SL accuracy during infancy and early childhood (EI = 0.62 – 0.003 × Age (weeks), r = -0.68, p = 0.015, n = 12). Adults showed high SL accuracy (mean EI (SD) = 0.054(0.021)) and high reliability (mean test-retest (SD) = 0.013 (0.039)).

Conclusions
Gaze may be used as a fast and objective measure of perceived sound-source location already from 7 months of age.

PS-136

Toward a Deployable Stereo-Hearing Test Package

Lincoln Gray[1]; Kristin Boulier[2]; Jared Christophel[2]; **Sophia Ganev**[1]; Brittany Harwell[1]; Bradley Kesser[2]; Brandon Lancaster[1]; Robert Nagel[1]
[1]James Madison University; [2]University of Virginia

Prompted by a need for long-term follow-up on aspects of binaural processing following various forms of ear surgery, a multidisciplinary team developed a small packaged system to test sound localization and speech perception in noise. The system costs about $800, and can be delivered to post-operative patients in the United States for about $50 to $100 (round-trip). Initial testing during system design has demonstrated that the system can be unpacked, set up, and used by lay persons without professional supervision. Eight speakers unpack on a 'table-cloth' mat into precise locations, 180 degrees around the front of a laptop (see Figure). The system currently evaluates accuracy of horizontal sound localization and understanding of speech with noise at different locations. The sound localization test presents 48 250-ms broadband noises at random locations with an average intensity of 70 dB randomly roved by 10 dB; the listener clicks a button to indicate the perceived location. The speech in noise test adaptively varies broadband noise based on the accuracy of a button click to the Coordinate Response Measure Corpus command "Ready [Call-sign] go to [Color] [Number] now". The system is currently in use in a quiet room in an ENT clinic. Data show the system is sensitive (with 'very large' effect sizes, ES) to asymmetric hearing between unilateral and bilateral listeners in localization accuracy (ES, Cohen's d = 1.9; p < .001) and speech in noise tests(ES, $_p\eta^2$=.43; $F_{1,9}$=6.8, p=.029) and is sensitive to small changes in pinna cues (ES, Cohen's d=1.1, t_{10}=3.7, p=.004, in repeated measures ANOVA of errors in localization with and without pushing the helix back against the temporal bone with a small headband in normal-hearing adult volunteers). Before unsupervised deployment, automatic, continuous measurement of background noises and image-detection confirmation of stable head position during test trials will be implemented into the system.

PS-137

Sound Localization in Horizontal Plane Through the Bilaterally Applied Bone-Conducted Ultrasonic Hearing Aids: The Effect of Real-Time Correction of Binaural Parameters

Takuya Hotehama; Seiji Nakagawa
National Institute of Advanced Industrial Science and Technology

Background

Ultrasound can be perceived via bone-conduction not only by the normal hearing but also by the profoundly hearing impaired. Thus, we have developed a novel hearing-aid using the bone-conducted ultrasonic (BCU) perception (BCU hearing aid: BCUHA) for the profoundly hearing impaired, in which an ultrasonic carrier is amplitude-modulated (AM) by collected external sound and presented through a bone-conduction vibrator onto the mastoid portion. If sound localization is capable by the bilaterally applied BCUHAs, it can introduce the benefit of the "binaural hearing" to the BCUHA users. However, in the pilot study, we found that it was difficult to localize sounds with the simply (separately) bilaterally applied BCUHAs. So, it was needed to find out the effective "binaural" presentation methods for bilaterally applied BCUHAs.

Methods

Sound localization tests for BCUHAs were conducted to verify the effectivity of correction of inter-lateral parameters (ITD_{env} and IID) of the output of the BCUHAs in which the Double Sideband Transmitted Carrier (DSB-TC) modulation and "Transposed" modulation were employed as the amplitude-modulation methods, on accuracy of sound localization of horizontal direction.

Results

Subjects hardly lateralized when the BCUHAs were simply applied bilaterally with the double-sideband modulation method. On the other hand, the localization performances were improved when the inter-lateral intensity and time differences of presenting signals of BCUHAs were enhanced on the basis of those of the collected external sounds, and when the "transposed modulation" was employed as the modulation method.

Conclusion

Our results suggest the necessity of the inter-lateral cooperative system to modify the spatial parameters of the output signal for accurate sound localization through the BCUHAs.

PS-138

The Vestibular Origins of Airborne Hearing Determined the Evolutionary Path for Spatial Hearing and Neural Specializations

Mark Riggle
Causal Aspects, LLC

Evolutionary constraints on the origins of hearing suggest an alternative neural architecture for spatial hearing. The constraints begin with the development of tympanic membrane hearing (TMH) which occurred about 100 million years after mammals and archosaurs (bird ancestors) had separated. Before TMH, because any sound perception could only arise from skull vibrations, there could be no sensory specialization for hearing (a cochlea), no ITD, no ILD, and no spectral information. Because prior to TMH would be severe deafness, it is *not* parsimonious to assume neural specialization for hearing would evolve. Additionally, because the cochlea descended from a vestibular organ and because TMH would have caused sounds to produce vibrations in a vestibular fluid, that therefore, at the origin of TMH, external sounds would have been encoded in the vestibular neural signals. However, because evolution requires that TMH be immediately useful, initial hearing must then have occurred without auditory neural specialization. We show how that perhaps occurred.

Method

The construction of a model where, at the origin of TMH, other neural systems (specifically visual orientation, vestibular, and tactile somatosensory) would together process that sound-encoding vestibular signal and then spatially localize the sound source into eye-targets of the optic-tectum(OT). From this initial hearing capability, evolution will develop the auditory cochlea and neural specializations.

Results

A capable model for initial sound localization arises from the following (diverse supporting evidence also provided):

1. Sound sources can be accurately localized by a simple and biologically implementable (without ITD) mathematical operator;

2. Because that operator for sound localization exactly parallels some vestibular processing, the sound signal encoded on the vestibular signal can be spatially localized by the vestibular cerebellum;

3. To utilize that spatial location for eye-targeting in the OT (which needs retinal coordinates), sound localization reused the same neural circuitry as used by the OT for localizing a somatosensory touch. That localization (which requires a transformation from body-space into retinal coordinates) may be partially computed in the oculomotor cerebellum;

4. An additional pathway from the vestibular nuclei through the trigeminal system may provide the sound signal to the somatosensory cortex for cortical awareness.

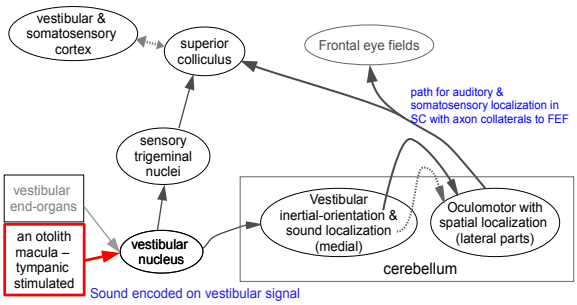

Figure 1. At initial tympanic hearing (middle-ear bone development), the new sound signal (encoded in the vestibular output) can be processed by reusing the combination of vestibular orientation and somatosensory localization (targeting into retinal spatial coordinates). Thus, without requiring initial auditory neural specializations, neural plasticity can provide useful spatial hearing

Summary
At the origin of TMH (and thus independently in mammals and archosaurs), this vestibular-somatosensory processing combined with neural plasticity would enable basic spatial hearing. Thereafter, evolution will rapidly develop the specialized, modern auditory systems - however, this means that the later evolved ascending pathways must have other auditory functions.

PS-139

Effect Of Auditory Cues On Spatial Orientation

Adham Karim; Kavelin Rumalla; Timothy Hullar
Washington University in St. Louis

Postural stability is a result of the collaborative efforts of the vestibular, proprioceptive, and visual neural inputs. Recent work suggests that auditory input may also contribute to maintaining balance. Here, we tested the hypotheses that this process depends on using external auditory stimuli as spatial landmarks, and that sound localization is central to its success.

The Unterberger test was used to assess how auditory inputs affect balance and orientation. Seven auditory conditions were used; all were performed in darkness. Condition was silence, condition two was the presence of a white-noise stimulus presented through ear buds under ear defenders ("head-fixed"), and condition three was a white noise source at ear level 1 meter in front of the subject. Conditions 4-7 were similar but with the auditory source at 45, 90, 135, and 180 degrees relative to the anteroposterior direction. Performance was measured by the amount of angular deviation from starting position after completing 50 paces.

8 subjects participated. Angular deviation in silence was an average of 31 deg and when sound was presented through ear buds ("head-fixed condition") was 34 deg. This was not statistically significant (p=0.94). Performance worsened with increasing angle of the sound source, with a local maximum of 40 deg deviation with the sound source at 135 deg; this improved slightly at 180 deg.

We found that non-directional sound offered no benefit over silence, whereas a directional sound source provided a valuable external auditory landmark for improving orientation. Performance corresponded closely to sound localization ability in the azimuthal plane, which worsens with increasing angle but improves slightly when approaching 180 degrees. This suggests that auditory stimuli improve orientation by functioning as earth-fixed landmarks and that this benefit is mediated by the ability to localize sound.

PS-140

Non-linear Viscoelastic Models for Middle-ear Ligaments and Tendons

Hamid Motallebzadeh; W. Robert J. Funnell
McGill University

Mathematical models of the middle ear help in interpreting and predicting its sound-transmission function and ultimately can be used to design new diagnostic tools and therapeutic techniques. Modelling the components of the middle ear and defining their material properties are challenging. Experimental measurements of the mechanical properties of the tympanic membrane, stapedial annular ligament, anterior mallear ligament, tensor tympani tendon, stapedial tendon and incudostapedial joint have been reported by R.Z. Gan's group. They performed both standard uniaxial tensile tests (stress-stretch relationship measured with displacement-ramp loading and unloading) and stress relaxation tests. The mechanical behaviour of each structure displays both non-linearity and viscoelasticity. However, finite-element models of the middle ear and its components were either non-linear or viscoelastic, but not both, until we developed a nonlinear viscoelastic model for the tympanic membrane based on the measurements by that group. In this study, nonlinear viscoelastic models are developed based on the measurements for the ligaments and tendons. The constitutive equation of each model is a convolution integral composed of a non-linear elastic part, represented by an Ogden hyperelastic model, and an exponential time-dependent part, represented by a Prony series. The material parameters of the tissues are identified by comparing the model outputs with the experimental data. Our approach allows us to model both the loading and unloading curves, and the associated hysteresis, with a single set of parameters for each middle-ear component. In addition, a frequency-domain analysis is performed based on the obtained material parameters, and the effect of strain rate is explored.

PS-141

The Middle Ear as an Impedance-Matching Device

Taylor Fields; Lucia Schnetzer; Robert Withnell
Indiana University

Introduction
The role of the middle ear is to transmit acoustic energy in the ear canal to a fluid-filled cochlea. Conventionally, a hydraulic system analogy is employed to describe how gain is provided to overcome the reflection of energy that would otherwise occur at an air-water interface. This mechanism does not minimize the amount of reflected energy, but instead provides gain to the transmitted energy. Conversely, as first suggested by Fletcher and Thwaites (1979), the conical shape of the eardrum may enhance sound transmission by impedance matching. In this case, the reflection of sound is reduced in favour of sound transmission. Fay et al. (2006) modelled the conical shape of the eardrum including a flexible toroidal outer region using a finite element model and demonstrated the capacity of the eardrum to act as an impedance matching device.

Methods
We have modelled the middle ear using an electrical circuit analogy with the ear canal modelled as a one-dimensional lossy transmission line and the eardrum acting as (i) a conical horn, and (ii) a conical horn with a toroidal perimeter. The model was fit to acoustic input impedance data from healthy human ears.

Results
A model of the acoustic input impedance of the ear, with the eardrum modelled as a conical horn, provided a good fit to data. The reflectance of the ear showed a frequency-dependence inconsistent with a hydraulic system mechanism.

Conclusion
The results support replacing the hydraulic system analogy with an impedance matching mechanism for the description of how the middle ear transfers acoustic energy to the cochlea.

PS-142

Electromyography (EMG) Measurement of Chinchilla Middle Ear Muscle Reflex

Zachary Yokell; Don Nakmali; Rong Gan
University of Oklahoma

Background
The stapedius is one of two muscles in the middle ear and is triggered when the ear is exposed to high intensity sound. The stapedius muscle reflex damps the stapes' motion and provides a protective mechanism to mitigate the high ossicular motion transmitted into the cochlea. The lowest sound stimulus that triggers the response is known as the acoustic reflex threshold. The reflex threshold corresponds to the middle ear muscle protection function and relates to the development of hearing protection devices for people working in high intensity noise environments and soldiers on the battlefield. This paper reports our preliminary study on stapedius muscle reflex in chinchillas using the electromyography (EMG) measurement when the animal was exposed to high intensity sound or blast overpressure. The muscle reflex threshold was determined and compared with the conventional tympanometric measurement.

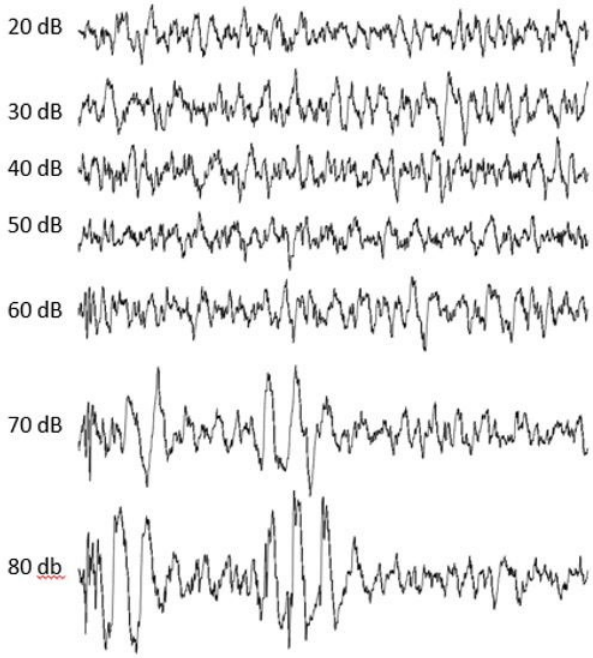

Figure 1. EMG results with acoustic stimulation from 20-80 dB.

Methods
Healthy adult chinchillas were used in this study. After sedation, the stapedius muscle was surgically exposed in one ear. Care was taken to ensure that the tympanic membrane and ossicular chain remained intact. Two electrodes were inserted into the muscle while a third was inserted into the animal's leg as a ground. Data was acquired using TDT System 3 and BioSig software. The electrical activity of the muscle in response to increasing acoustic loads was measured through EMG while the animal was lightly anesthetized. The animal was then moved to our anechoic chamber and exposed to blast overpressure produced by a compressed air (nitrogen)-driven blast apparatus. Muscle activity was measured through EMG during the blast.

Results
Results were obtained using both acoustic loading and blast exposure. Acoustic loading showed an average threshold of 65±6 dB. Figure 1 depicts the acoustic stimulus results from one animal. Blast exposure was at an overpressure of 5 psi which is below the chinchilla tympanic membrane rupture threshold. The amplitude and latency of the EMG signals of the stapedius response to the blast stimulus were recorded.

Conclusions
The novel EMG measurement of acoustic reflex in chinchillas based on exposure to acoustic loading and blast overpressure are reported in this study. The results demonstrate that the approach is feasible for further study on middle ear muscle protection mechanism.

(Supported by NIH R01DC011585 and DOD W81X-WH-14-1-0228)

PS-143

The Role of Resonance in Middle Ear Transmission

Elizabeth Olson[1]; Nina Kumar[1]; Jason Lei[1]; Christopher Bergevin[2]
[1]Columbia University; [2]York University

The rodent middle ear transmits sound pressure to the inner ear with high fidelity: in the frequency domain middle ear transmission is broad-band with a delay-like phase-frequency relationship, and in the time domain the time waveform is preserved. High fidelity transmission occurs despite the presence of pronounced mechanical resonances in the tympanic membrane (TM) and acoustic resonances in the middle ear space. We present two studies that probe the role of these resonances in middle ear transmission, both performed in the gerbil ear. In one study, a click stimulus (acoustic duration ~ 30 microsec) was applied open field to the ear canal and the motions at many locations on the TM, and the lateral process of the malleus were measured. The motion time-waveform of the lateral process was quite similar to the acoustic click. In contrast, the TM responded with prolonged oscillatory responses of various frequencies at different locations. However, the *average* of the TM response waveforms was quite click-like. This finding suggests that the "Discordant Eardrum" view of the TM proposed by Fay, Puria and

Steele (PNAS, 2006), in which many discordant resonances produce high-fidelity and broad-band sound transmission, is a meaningful way to conceptualized TM operation. In the other study (reported in Bergevin and Olson, JASA 2014) pure tone stimuli were delivered open field to the ear canal and the pressure responses in the middle ear cavity were measured at several locations, via a small opening in the bony wall of the bulla. While a large pressure drop existed across the TM (~10-30 dB, varying in frequency), the motion of the TM produced significant pressure within the cavity, and reflections from the bony wall of the bulla gave rise to pressure maxima and minima within the cavity. These reflections will modify the pressure difference across the TM that drives its motion, and in particular, will increase the pressure drive when a minima occurs at the TM. However, overall these reflections seemed to have a small effect on the pressure at the TM, and this is likely due to the multi-phasic motion of the TM (related to the first study above), and the irregular shape of the bulla walls.

PS-144

Sensitivity of a middle-ear finite-element model to material properties

Nima Maftoon[1]; W. Robert J. Funnell[1]; Sam J Daniel[1]; Willem F. Decraemer[2]
[1]McGill University; [2]University of Antwerp

Finite-element models of the middle ear depend on the material properties of its structures. Many studies have been dedicated to measurement or estimation of these material properties, yet for most properties we are far from having good estimates. Inter-subject variability adds to the uncertainty of material parameters. It is important to know which parameters have the strongest effects on the model results, in order to concentrate efforts on reducing their uncertainties. In this study we present a finite-element model of the gerbil middle ear reconstructed based on a microCT dataset, supplemented by histological images and orthogonal-plane fluorescence optical sectioning images. The model includes the pars tensa, pars flaccida, malleus, incus, stapes, anterior mallear fixation, posterior incudal and annular ligaments, and incudomallear and incudostapedial joints. The eardrum was modelled using second-order shell elements with variable thickness measured using confocal microscopy. The ossicles were modelled using second-order solid elements and the ligaments and joints were modelled using second-order incompressible solid elements with a mixed pressure-displacement formulation. The cochlea was modelled as a purely resistive discrete element. A baseline set of model parameters, primarily based on *a priori* estimates from the literature, was established. Each model parameter was changed ±10% of its baseline value and the effects on various features of the model results were determined. These feature included the magnitudes at low frequencies and at the resonance peak of the umbo and pars tensa responses; the pars-flaccida-induced feature in the umbo response; the low-frequency lever ratio; the middle-ear resonance frequency; and the break-up frequency of the pars tensa. The sensitivity analysis showed that the parameters that have the strongest effects on the model results are the Young's modulus, thickness and density of the pars tensa; the Young's modulus of the stapedial annular ligament; the Young's modulus and density of the malleus; and the Poisson's ratios of the incudomallear and incudostapedial joints. The large effects of the Poisson's ratios of the joints suggest that more sophisticated joint models would be beneficial.

PS-145

A Hybrid Ear Canal and Middle Ear Model Approach for Neonates

Shinji Hamanishi[1,3]; Michio Murakoshi[2]; Charles Steele[3]; Hiroshi Wada[4]; Sunil Puria[3]
[1]Sendai National College of Technology; [2]Kagoshima University; [3]Stanford University; [4]Tohoku Bunka Gakuen University

Introduction

In infants, conventional single-frequency tympanometry often indicates an abnormal middle ear in otherwise normal middle ears (Keefe *et al*., 1996) and thus there is a need to develop new measures for the neonatal population.

A Sweep Frequency Impedance (SFI) meter for screening of neonatal middle-ear diseases was recently developed (Murakoshi *et al*., 2013). It measures dynamic behavior of the middle ear by sweeping frequency tone from 100 to 2000 Hz.

Computational models can help improve our understanding of the sensitivity and specificity of the SFI for clinical use. Many publications have shown that the neonatal tympanic membrane and middle-ear ossicle morphometry is nearly adult like (Dahm *et al*., 1993). Our working hypothesis is that a hybrid model consisting of a neonatal ear canal coupled to an adult tympano-ossicular chain can be physiologically similar to the normal neonatal ear. We test this hypothesis by using the Finite Element (FE) modeling approach and comparing simulations and measurements of middle-ear admittance (Y_{ME}), power reflectance (PR), and SFI.

Methods

Geometries of neonatal ear canal and adult middle ear were constructed based on FE models by Qi *et al*. (2006), and Cai *et al.* (2013), respectively. The model is validated with Y_{ME} and PR from the literature. Simulated SPL curve, which is obtained by applying constant volume displacement equivalent of 80 dB SPL at the ear canal entrance, is compared with SFI in 10 ears of 9 neonates. Simulation is also compared with chronologically measured SFI in neonate from 6 to 92 days of age by increasing the Young's modulus of soft tissue of the ear canal (E_{EC}).

Results

In the SFI test, two resonances at approximately 260 and 1130 Hz were observed. FE simulations show that only lower resonance frequency moves to higher frequencies by increasing E_{EC}. Chronological simulations indicate that the neonatal ear canal walls begin to develop rapidly after 2.5 months of age.

Conclusions

The lower and higher frequency resonances in SPL curve may be related to soft wall surrounding ear canal and mid-

dle-ear resonance, respectively. The proposed hybrid FE model is consistent with measurements of Y_{ME}, PR, and SFI and is thus a viable representative model for the neonatal ear. Further measurements of middle-ear output at the stapes are needed in order to test this hybrid approach.

Funding
Grant number R01 DC05960 from the NIDCD of NIH and Fellowship for Research Abroad from Institute of National Colleges of Technology, Japan.

PS-146

Sound-induced In-plane and Out-of-plane Motion of Human Tympanic Membranes

Morteza Khaleghi[1]; Jeffrey Tao Cheng[2]; Cosme Furlong[1]; John Rosowski[3]
[1]Worcester Polytechnic Institute; [2]Massachusetts Eye and Ear Infirmary; [3]Harvard Medical School

Background
The acousto-mechanical-transformer behavior of the Tympanic Membrane (TM) is determined by its geometry (shape and thickness) and mechanical properties. The questions of "How the TM couples acoustic energy to the ossicles?" and "How TM shape and vibration affect this series of events?" have yet to be fully answered. Holographic studies of 1D vibrations of the TM have been reported by several groups; however, 3D measurements of TM motions are few. In this study, we use full-field-of-view holographic techniques to measure near simultaneously the shape and 3D sound-induced displacement of cadaveric human TMs. Combinations of shape and 3D displacement measurements are used to characterize motions tangent and normal to the TM plane.

Methods
We developed a digital holographic system capable of full-field measurements of shape and three-dimensional sound-induced motion of the TM. The spatial resolution of the measuring system is >1,000,000 points per the 70 mm2 TM area, and the temporal resolution is determined by the 50kHz limit of the acousto-optic modulator used to strobe the phasic illumination. The method of dual-wavelength holographic contouring was used to measure the shape of the TM with a spatial sensitivity of 10-30 micrometers. The 3D motion at each location on the TM was determined within an accuracy of 10-20 nm using the method of multiple sensitivity vectors in stroboscopic holographic interferometry. A numerical rotation matrix is used to rotate the original camera-based coordinate system of the measuring system, to a local TM coordinate system enabling characterization of motion components normal to the local TM surface (out-of-plane) and tangential to the local surface (in-plane). FFT algorithms are used to quantify the magnitude and phase of the motion components.

Results
In-plane and out-of-plane sound-induced motion components of three human TM samples are quantified at frequencies between 1 and 10 kHz, a range that covers low, mid, and high auditory frequencies. Results indicate that (1) the phase of in-plane motion components are greatly affected by the dimensional shape gradients, and (2) the magnitudes of local in-plane motion components are at least 10 to 20 dB smaller than the magnitude of motions normal to the local TM surface.

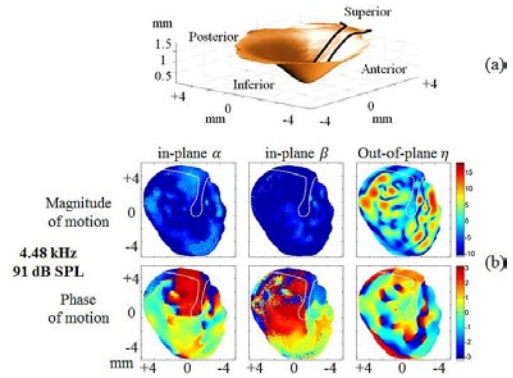

Figure 1. Shape and 3D sound-induced motion of a human TM measured with holographic interferometry: (a) 3D shape of the TM; and (b) the in- and out-of-plane sound-induced motion components (magnitude and phase) of the TM excited with a tone of 4.48 kHz at 91 dB SPL, normalized by the out-of-plane motion of the Umbo at each frequency. The motion colorbars are in logarithmic magnitude scale, and phases are in radians. The handle of the malleus, the manubrium, is outlined in all the figures.

References

1. J.J. Rosowski, I. Dobrev, M. Khaleghi, W. Lu, J. T. Cheng, E. Harrington, and C. Furlong, "Measurements of three-dimensional shape and sound-induced motion of the chinchilla tympanic membrane," *Hear. Res.*, 301:44-52, 2013.

2. M. Khaleghi, W. Lu, I. Dobrev, J. T. Cheng, C. Furlong, J. J. Rosowski, "Digital holographic measurements of shape and three-dimensional sound-induced displacements of tympanic membrane," *Opt. Eng.*, 52(10):101916-101916, 2013.

Conclusions
The fact that the in-plane components are much smaller than out-of-plane components is consistent with modeling the kinematics of TM by a thin-plate, in which the direction of motion vectors are restricted to the direction of corresponding normal vectors to the TM surface with no tangential motion.

PS-147

Where is the Energy Stored? Energy Flow in the Eardrum Can Account for Long Transmission Delays in the Frog

Peter Narins[1]; Sebastiaan Meenderink[1]; Marcel van der Heijden[2]; Christopher Bergevin[3]
[1]University of California, Los Angeles; [2]Erasmus MC; [3]York University, Canada

Background
Transmission from the external ear to auditory nerve can introduce appreciable delay, given the cascade of transduction and transmission processes that occur. Much of this lag can be attributed to filtering by the frequency-selective elements in the ear. That is, resonance takes time: the sharper the tuning, the longer the delay. However, one vertebrate group has proved to be an outlier: anuran amphibians' (frogs and toads) ears exhibit comparatively long delays (several milliseconds), yet relatively broad tuning. These delays have been partially attributed to the middle ear (ME), though their biomechanical origins remain unclear.

Methods
The present study used scanning laser doppler vibrometery to map surface velocity over the tympanic membrane (TyM) of anesthetized adult bullfrogs (*Rana catesbeiana*). Three fe-

males and one male were studied. Stimuli consisting of constant-voltage frequency sweeps (duration: 700 ms; sweep range: 0.2-8.0 kHz) repeated once every second were delivered via a loudspeaker placed 18 cm away from the TyM. Stimulus generation and data acquisition were controlled by Polytec software; subsequent analysis was done using customized software written in MATLAB. We also investigated TyM motion by measuring the pressure ratio across the TyM, the effects of ossicular interruption, and changes due to physiological state of TyM ('dry-out').

Results

Mechanical responses showed varying degrees of radial symmetry in a frequency-dependent fashion. Our main finding is the general observation of a circularly-symmetric inward-traveling wave at intermediate frequencies on the TyM surface, starting at the outer edges and propagating inward with decreasing amplitude towards the center (the site of the ossicular attachment). For low stimulus frequencies (~0.5 kHz), the entire membrane vibrates in a simple (0,1) mode. At higher frequencies (> 2.5 kHz), intermediate nodes become apparent, suggestive of standing waves. A large pressure drop was apparent across the TyM, and ossicular interruption appears to have had relatively little effect on the measured responses.

Conclusion

The delays we observed on the bullfrog TyM, approximately an order of magnitude longer than those observed for gerbil, appear to arise from a slow, mechanical inward-traveling wave. These motions can account for a substantial fraction of the relatively long delays previously observed in the anuran inner ear, and can help inform models of mammalian TyM biomechanics.

PS-148

A New Method to Measure 3D Tympanic Membrane Motion with Multi-View Digital Holography

Jérémie Guignard[1]; **Jeffrey Tao Cheng[2]**; Ivo Dobrev[3]; Payam Razavi[4]; Morteza Khaleghi[4]; Cosme Furlong[4]; John Rosowski[2]

[1]Massachusetts Eye and Ear Infirmary; [2]Eaton-Peabody Laboratory, Massachusetts Eye and Ear Infirmary, Boston MA; [3]University Hospital Zurich, Switzerland; [4]CHSLT, Worcester Polytechnic Institute, Worcester MA

Background

The complexity of sound-induced tympanic membrane motion, in particular at frequencies above a few kilohertz, calls for improved metrological methods. Previous work from our group showed that digital holography achieved high spatial- and temporal-resolution quantification of tympanic membrane motion. It has been shown that, at frequencies less than about 8 kHz, the 3D motion of the tympanic membrane can be derived from its shape and a one-dimensional measure of motion. At higher frequencies, however, it may be necessary to measure the 3D motion directly, which can be achieved by using multiple sensitivity vectors.

Methods

We present a new method to measure tympanic membrane motion along several sensitivity vectors to reconstruct its 3D motion. The relative orientation of the holographic system and the measured membrane was varied to obtain motion measurements along several directions. We used a planar marker and a camera calibration algorithm to compute the relative orientation of the camera and the measured membrane to deduce the sensitivity vector. The resulting motion vectors were summed to obtain the 3D motion.

Results

The sensitivity vector estimate was found to be accurate down to 0.5 degree, resulting in a theoretical displacement measurement error of less than 10%. We validated the present method by comparing its results to those of an existing, documented method for 3D membrane motion measurement. We show preliminary results on a human cadaveric temporal bone preparation.

Conclusions

The multi-view digital holographic system is a novel tool for characterization of the 3D motion of the full surface of the tympanic membrane. The method provides a cost-effective alternative to other 3D systems for hearing research, while minimizing hardware requirements.

PS-149

3D Vibrational Measurements and Principal Axes of Rotation of Middle Ear Ossicles in the Mouse

Peter Gottlieb; Sunil Puria

Stanford University

Background

The presence of three distinct ossicles in the middle ear is a ubiquitous and uniquely mammalian trait, yet the benefits conferred by this complicated anatomy are still debated. One hypothesis contends that this system allows multiple modes of rotation to minimize the effects of ossicular inertia at higher frequencies of vibration. The mouse middle ear provides a particularly interesting test of this theory. The malleus includes a relatively massive prominence known as the orbicular apophysis, which causes the first principal axis of the malleus to lie almost orthogonal to the manubrium and the anatomical axis defined by the gonial attachment and the short process of the incus. A previous 1D study (Dong et al., Hearing Research 2012) suggested that despite the orbicular apophysis, the ossicles vibrated primarily about the anatomical axis. In the absence of true 3D measurements, however, it is difficult to draw strong conclusions about this motion.

Methods

The 3D velocity of 12-15 points along the ossicular chains of adult wild-type CD-1 mice was measured using a Polytec CLV-3D laser Doppler vibrometer. SyncAv was used to generate pure-tone stimuli while pressure within 1mm of the tympanic membrane was synchronously recorded using an ultrasonic probe tube microphone. The ossicular transfer function, or the velocity divided by the pressure at the tym-

panic membrane, was calculated for each point. 3D models of the ossicles were reconstructed from a μCT scan, and the principal axes of rotation were calculated. The 3D motion of the ossicles was then calculated using a least-squares fitting algorithm.

Results
The magnitude of the ossicular transfer function at all points rose steeply from low frequencies up to above 10kHz, after which it generally remained flat. While the ossicles moved primarily together as a rigid body at low frequencies, there was considerable slippage between the malleus and incus at higher frequencies. The angle between the calculated rotational axes of the ossicles and their first principal axes varied with frequency.

Conclusion
Our measurements are consistent with previous results in finding the ossicular transfer function in mice to act like a high-pass filter. These 3D measurements demonstrate more complex modes of vibration, however, with frequency-dependent rotational axes that depart from the anatomical axis.

PS-150

High-Speed Digital Holographic Method (HDHS) for Transient Acoustic Measurements of the Human TM

Payam Razavi[1]; Ivo Dobrev[2]; Michael Ravicz[3]; Jeffrey Tao Cheng[3]; Cosme Furlong[1]; John Rosowski[3]
[1]Worcester Polytechnic Institute; [2]University Hospital Zurich; [3]Massachusetts Eye and Ear Infirmary

Background
Our research is focused on the Tympanic Membrane (TM) and its role in transforming sound energy in the ear canal into mechanical vibrations of the ossicles. Past work has concentrated on the TM response to continuous tonal stimuli. Here we investigate the response of the TM to acoustic transients, i.e. the response of the TM evoked by a single click.

Methods:
We use a High-Speed Digital Holographic System (HDHS) with a high speed camera to capture up to 80,000 frames per second, which enables us to record and analyze the transient response of the TM with a temporal resolution of 20 ms for the duration of the TM response. An improved local phase correlation method based on a single phase shift for all frames allows us to resolve the full-field response of the membrane to a single excitation. Each HDHS image consists of >100k simultaneous independent data points, which allows observations and quantification of temporally-varying spatially-dependent motion parameters such as modal frequencies, time constants, damping ratios, etc.

Results:
We measured displacements of human cadaver TMs in response to an acoustic click (50ms square wave excitation, flat spectrum 0.5–8 kHz). The response decay time constants were in the 200-700ms range. Dominant modal frequencies were at 0.8, 1.8 and 3.6 kHz**.** Our preliminary results show spatial differences in the tuning of various regions of the TM (natural frequencies) and also in the damping (rate of decay).

Conclusions:
The HDHS is a new and versatile means to quantify the transient dynamics of the TM. Because of the high rate of image acquisition and the short duration of the measurement, the measurements are less affected by subject-based variations in position due to breathing or head motion so that the system can be potentially used in-vivo applications. Different parts of the TM have different responses to transient stimuli, which could be due to local variations in mechanical properties.

PS-151

Measurement of Intra-cochlear Pressure Differences using a Commercial Pressure Sensor

Martin Grossöhmichen; Rolf Salcher; Thomas Lenarz; Hannes Maier
Hannover Medical School

Background
The difference in pressure at the scala vestibuli (SV) and scala tympani (ST) is known to correlate with cochlear excitation. Measurement of this pressure difference can therefore be used to estimate cochlear excitation in response to acoustic stimulation at the tympanic membrane, or in response to mechanical stimulation of the inner ear or middle ear structures, and to compare the two. In order to establish this measurement of pressure difference as a new standard method for characterizing output of middle ear implants or direct acoustic cochlear stimulators, to replace ASTM F2504-05 where its method is not applicable, it is necessary to first demonstrate that the measurement is feasible with commercially available sensors. Here, the feasibility of differential pressure measurement was investigated using a commercially available pressure sensor.

Methods
All TBs used in the study fulfilled the modified acceptance criteria of ASTM F2504-05 given by Rosowski et al. (2007). Sound pressures in SV (P_{SV}) and ST (P_{ST}) were measured in cadaveric human temporal bones (TBs) with commercially available fiber-optic Fabry-Pérot pressure sensors (Samba Preclin 420 LP) when the TM was stimulated acoustically between 0.1 and 10 kHz (sequence of sine wave signals with a resolution of ~1/3 octave). Simultaneously the vibration response at the stapes footplate (SFP) was determined with a laser Doppler Velocimeter (LDV, Polytec) and the sound pressure level at the TM was recorded with a probe microphone, while the differential pressure across the cochlear partition was determined by two intra-cochlear optical pressure sensors in the SV and ST. Different sealing techniques of the probe to the bone were tested.

Results
In both scalae sound pressures were measurable between 0.1 and 8 kHz with signal-to-noise ratios (SNRs) > 12 dB. The complex pressure difference ($P_{SV} – P_{ST}$) was calculated relative to the outer ear canal sound pressure level and relative

to the SFP velocity. Results were comparable to experiments with a custom-made pressure sensor (Olson et al. 1998) published by Nakajima et al. (2009), Pisano et al. (2012) and Stieger et al. (2013). When using a silicone rubber ring for sealing, results were similar to measurements performed with a sealing made of alginate.

Conclusions

The results demonstrate that the commercially available Samba pressure sensor is usable for simultaneous measurements of intra-cochlear sound pressures in SV and ST.

PS-152

Influence of AAV.Ntf3 in the Cochlea on Deafness Related Changes in Auditory Nerve Terminals

Noel Wys; Donald Swiderski; Deborah Colesa; Brett Slajus; Breanne Miller; Bryan Pfingst; Yehoash Raphael; Richard Altschuler

University of Michigan

There has been considerable interest in the influence of neurotrophic factors on survival of the auditory nerve and regeneration of peripheral processes following inner hair cell loss. There has been less attention on their potential influence on central processes in the cochlear nucleus. The present study used vesicular glutamate transporter 1 (VGlut1) immunostaining, a relatively selective marker for auditory nerve terminals in the cochlear nucleus (Zhou et al, 2007) to examine central connections. Guinea pigs were bilaterally deafened with 5% Neomycin, followed by unilateral intrascalar inoculation with adeno-associated virus (AAV) containing the *Ntf3* gene insert. This was followed by placement of a cochlear implant in the inoculated ear. Animals were tested in psychophysical and electrophysiological experiments for 5 to 14 months and then euthanized for histological evaluations. Animals received electrical stimulation during test sessions lasting about 2 hours each day, 4 to 5 days/week. Immunofluorescent labeling for VGLUT1 was carried out in sections through the ventral cochlear nucleus (VCN). A region of interest in the high frequency portion of the magnocellular region of the VCN was identified and digital images acquired using laser scanning confocal microscopy. Images were imported into a Metamorph Image Analysis workstation and thresholded to determine the density of labeling. There was a significant decrease in VGLUT1 labeling in the VCN following deafening regardless of treatment when compared to non-deafened controls. There was a significantly greater density of VGLUT1 immunolabeling in the VCN ipsilateral to the AAV.*Ntf3* treated cochleae versus the VCN ipsilateral to deafened untreated cochleae. This could be due to increased survival of spiral ganglion neurons from NT-3 treatment and/or their electrical stimulation. Co-immunolabeling with antibody to VGLUT1, antibody to the post-synaptic glutamate receptor (GLUR2/3) and/or antibody to GAP-43, a growth cone marker was also examined. Co-labelling was found in the VCN of deafened animals, and was not present in the VCN of normal hearing untreated animals. This suggests new auditory nerve connections in VCN are occurring in deafened animals with some but not complete loss of spiral ganglion neurons. Comparison between VCN ipsilateral to NT-3 treatment versus no treatment in an initial survey from a subset of animals did not show a significant influence of peripheral NT-3 and the relatively brief electrical stimulation on density of GAP-43 immunolabel.

PS-153

Encapsulated Cell Device Releasing Neurotrophic Factors Protects Spiral Ganglion Neuron from Degeneration in Guinea Pig

Anette Fransson[1]; Jens Tornoe[2]; Lars Wahlberg[2]; Mats Ulfendahl[1]

[1]Karolinska Institutet; [2]NsGene

Using a novel encapsulated cell (EC) device providing long-term release of neurotrophins would be an important tool for a damaged inner ear. The EC device contains a genetically modified human cell line enclosed within a semi-permeable membrane that allows for the outflow of the active factor(s) and the influx of nutrients. In this study we investigated the effect of implanted EC devices, releasing either BDNF or GDNF, in deafened guinea pigs. Two groups served as control, one group was implanted with empty devices containing no cells and one group received devices containing only the parental cell line not releasing any neurotrophins. The EC-device was placed in the scala tympani in the basal turn of the cochlea. At the same time an electrode was inserted through the round window to elicit electrically-evoked auditory brainstem responses (eABR). EABR were measured once a week during the four-week treatment period. At the end of the experiment, the cochlea was processed for morphological analysis. The eABR measurements showed that there was a statistical difference between the BDNF and GDNF treated groups compared to the control group. Structural analysis is ongoing. The results demonstrate that the BDNF or GDNF releasing EC devices effect the spiral ganglion neurons in a manner similar to what has previously been shown in animals treated with neurotrophic factors administered to the inner ear through a cannula connected to an osmotic pump. Compared to the osmotic pump, the EC device offers a much more long-term therapeutic approach (beyond 12 months).

PS-154

Attenuation of Progressive Hearing Loss in DBA/2J Mice by Epigenetic-Modifying Reagents Is Associated with Up-Regulation of the Zinc-Importer Zip4 /Slc39a4

Hideki Mutai[1]; Fuyuki Miya[2]; Masato Fujii[1]; Tatsuo Matsunaga[1]

[1]National Hospital Organization Tokyo Medical Center; [2]RIKEN

Background

Hearing loss can be caused by a combination of multiple environmental and genetic factors. Various factors for preventing hearing loss have been discussed, including serum level of zinc (Shambaugh, 1985 Am J Otol). DNA methyltransferases (Dnmts) and histone deacetylases (Hdacs) are major

components of epigenetic regulatory pathways and interact to change chromatin conformation and modulate gene expression. Genes involved in epigenetic pathways such as *DNMT1*, *MECP2*, and *HDAC8* are associated with multiple symptoms including hearing loss. We have studied the role of epigenetic regulatory mechanisms in the postnatal rat auditory epithelium (Mutai et al., 2009 Dev Neurobiol). In this study, we investigated whether epigenetic regulatory pathways could modulate a mouse model of progressive hearing loss.

Methods

BA/2J mice, models for progressive hearing loss, were injected subcutaneously with one or combination of following reagents: l-methionine (MET) as a methyl donor, valproic acid (VPA) as a pan-Hdac inhibitor, folic acid, and vitamin B12. The mice were treated for 4 to 12 weeks (N ≥ 5) and ABR threshold shifts were measured at 8, 16, and 32 kHz. Microarray analyses (MouseGenome430-2.0, Affymetrix), and quantitative RT-PCR were performed using total RNA from the left cochlea. Immunostaining was performed using the right cochlea. Finally, the mice were treated with epigallocatechin gallate (EGCG), a *Zip4/Slc39a4* inducer. Statistical significance was determined by one-way ANOVA.

Results

RT-PCR detected *Dnmt* and *Hdac* expression in the postnatal as well as adult mouse auditory epithelium. Subcutaneous treatment of DBA/2J mice with a combination of MET and VPA (M+V) significantly reduced the ABR threshold shift at 32 kHz. Treatment with MET, VPA, folic acid, or vitamin B12 alone did not result in such an effect. Microarray analyses detected 299 probes significantly up- or down-regulated in the cochleae treated with M+V compared with the control vehicle-treated mice. Quantitative RT-PCR confirmed significant up-regulation of a zinc importer, *Zip4,* in cochleae treated with M+V. Immunohistochemistry demonstrated an intense Zip4 signal in cochlear tissues such as the lateral wall, organ of corti, and spiral ganglion. EGCG-treated DBA mice had a significantly reduced ABR threshold shift at 32 kHz and up-regulation of *Zip4* expression.

Conclusion

This study suggests that epigenetic pathways can modify auditory function and that zinc intake in the cochlea via Zip4 mediates the maintenance of mammalian hearing.

PS-155

Molecular and Structural Characterization of Nodes of Ranvier in the Auditory Nerve of Postnatal, Young-adult, and Aged Mouse Ears

Clarisse Panganiban; Yazhi Xing; LaShardai Conaway; Nancy Smythe; Bradley Schulte; Jeremy Barth; Hainan Lang

Medical University of South Carolina

Background

Canonical nodes of Ranvier and nodal junctions are integral for rapid axonal conduction throughout the auditory nerve. Mouse auditory nerve fibers refine and mature during early postnatal development, with the onset of hearing occurring at postnatal (P) days 10-12 followed by significant improvement of auditory brainstem response (ABR) thresholds from P12 to P14, reaching thresholds near those of mature mice. Mouse strains also display age-related auditory functional declines, and these can serve as models for human age-related hearing loss. Here we examined the temporal relationships between 1) molecular and structural maturation of nodes of Ranvier and ABR thresholds and 2) age-related abnormalities and degeneration of nodal segments and declines in auditory function.

Methods

The CBA/CaJ mouse strain was used because it has relatively late-stage, age-dependent hearing loss and cochlear degeneration. Microarray analysis was performed on total RNA samples collected from auditory nerve at P0, 3, 7, 10, 14, and 21. Nodal function-related genes were assembled by querying the Gene Ontology Database. Gene expression patterns were evaluated using dChip. Ultrastructural and immunohistochemical characteristics of nodal structure were examined and correlated with ABR threshold measurement in postnatal, young-adult (1-3 month-old), and aged (1.5-2 year-old) mice.

Results

Node-related genes exhibited temporal mRNA expression patterns during development, which distinguished nodal segment identities and complemented hearing onset. Coordinately regulated groups included: 1) node of Ranvier-associated genes showing peak expression during P0-P3; 2) paranode- and myelination-related genes with peak expression beginning at P7 and extending through P21; and 3) up-regulation of a subset beginning at P10, including $Na_v1.6$, the sodium channel implicated in saltatory conduction of mature nodes. Immunohistochemistry indicated that the paranodal and nodal structural proteins, contactin and Nrcam respectively, were fully assembled at P10, whereas $Na_v1.6$ showed robust expression by P14, correlating with the periods of hearing onset and significant gains in ABR. In young-adults, most paranodes closely flanked the nodes, whereas slight gaps between paranodes and nodes were detected in aged mice, with some paranodes exhibiting longer segments, or less compact and more disordered pairs. Ultrastructural analysis of auditory nerve from aged mice also revealed disorganization of paranodal septate junctions and node elongation.

Conclusions

Specific node segment types form at different periods during development encompassing the period of hearing onset. The integrity and organization of nodal segments, specifically the paranodes, appear to deteriorate with age. Correlational analysis between pathological alterations of nodal segments and age-related auditory function declines are ongoing.

PS-156

Effect of Cell Permeable Analog of cAMP on GluA2 Receptor Subunit Trafficking in the Spiral Ganglion Neurons

Sriram Hemachandran; Steven Green
The University of Iowa

Introduction

Cochlear Inner hair cells (IHC) transmit sound stimuli by releasing the neurotransmitter glutamate onto the afferent nerve fibers (type 1 Spiral Ganglion neurons (SGN)). SGNs have AMPA receptors on their post synaptic surface which is the major receptor involved in calcium influx, when there is excess sound (noise) the IHCs release a lot of glutamate and this leads to increased influx of Ca^{2+} in the SGN. This leads to excitotoxic trauma and the destruction of the synapse. An AMPA receptor is made of 4 subunits; they mix and match to form the ionotropic channel. The receptors will be calcium impermeable if one or more GluA2 subunits are present. The efferent nerve releases CGRP, a neuropeptide which activates Adenyl cyclase. This increases the cAMP concentration in the cell. cAMP is known to promote AMPA receptor trafficking in the central nervous system. One thing to study is, whether same process occurs in SGN and owing to its importance in noise related trauma, more important question is, will cAMP promote trafficking of GluA2 subunits?.

Method

The dissociated spiral ganglion neurons were cultured on an 8 well plate, some wells were treated with cell permeable cAMP for 120 min and other wells were used as untreated controls**.** The comparison of subunit trafficking between the control cells and the cells treated with cpt-cAMP was quantified by calculating the ratio of the intensity of surface labelled GluA2 subunits to the total GluA2 subunits by fluorescence microscopy.

Result and Summary

There was a significant increase in the surface concentration of GluA2 subunits in the cell permeable cAMP treated cells when compared to the untreated controls. This indicates that under the influence of CGRP the GluA2 subunits are trafficked to the surface. This means that either GluA2 is specifically trafficked to the surface as a compensatory mechanism or all subunits get trafficked to the surface and the net Ca^{2+} will be analogous to the number of surface AMPA receptors with no GluA2 in it.

PS-157

Spatial Irregularities of Compound Action Potential Origination in Individual Cochleae

Jeffery Lichtenhan[1]; James Dornhoffer[2]; **Kaitlyn Kennedy**[3]; Alec Salt[1]
[1]Washington University School of Medicine in St. Louis; [2]University of Arkansas for Medical Sciences; [3]Missouri State University

We previously demonstrated that injection of ototoxic pharmaceuticals from a pipette sealed into the guinea pig cochlear apex can be used to identify origins of various cochlear responses, such as those in response to infrasound and the Auditory Nerve Overlapped Waveform (Salt et al. 2013, Lichtenhan et al. 2014). Controlled apical injections are far more precise than round-window delivery of pharmaceuticals. Injected solutions are slowly driven towards the cochlear aqueduct in the base of scala tympani, resulting in a progression of solution from the apex to base over a period of 30-35 min. In our most recent experiments, injection rates were adjusted once each minute (25 – 626 nl/min) to compensate for cross sectional area gradations along scala tympani so the drug moves down the cochlea at 0.5 mm/min. Kainic acid (2.16 mM) in artificial perilymph was injected, and a battery of measurements was repeated at ~90 sec. intervals to allow comparison of time courses for abolition of compound action potentials (CAPs) evoked from finely spaced tone burst frequencies (8 – 16 per octave).

Otoacoustic acoustic emissions were largely unaffected, demonstrating that cochlear mechanics were not impaired by the injection procedure. The rate of abolition for CAPs to near-threshold 1 – 2.8 kHz was similar and suggests common spatial origins, while the rate of abolition for CAPs to near-threshold 4 – 16 kHz tone bursts was systematic in low to high frequency order. But, the rate of abolition for CAP fine structure showed a clustering that varied across individual ears. The rate of abolition for CAPs to stimuli that vary from low to moderate levels demonstrates that responses at a given frequency systematically spread towards the most sensitive mid-frequency (8 kHz) region of the guinea pig cochlea: As level increases, responses to low-frequency stimuli spread towards higher frequency cochlear regions while responses to high-frequency stimuli spread towards lower frequency cochlear regions. The rate of abolition for CAP level series varied across individual ears, reflecting individual differences in regions of sensitivity. As expected, CAPs to the highest stimulus levels at frequencies spread toward high frequency regions. These results demonstrate that slow injection of ototoxic solutions into the cochlear apex provides novel insight to the irregular spatial origins of cochlear responses, and thus the frequency-place map, in individual ears.

PS-158

Factors Released by the Organ of Corti Support Survival of Spiral Ganglion Neurons and Promote Neurite Outgrowth in Culture

Claudia Frick[1]; Marcus Mueller[2]; Hubert Loewenheim[2]
[1]University of Tübingen Medical Center; [2]University of Oldenburg

In mouse cochleae, the number of spiral ganglion neurons (SGNs) innervating sensory hair cells is reduced during the first postnatal week. This developmental refinement was attributed to a decline in neurotrophin expression of hair cells in the organ of Corti (OC). Loss of the OC results in retraction of SGN dendrites and, at least in rodent models, in fast degeneration of SGN. Exogenous application of BDNF and NT-3 can prevent SGN degeneration *in vivo* and stimulates neuronal survival and outgrowth *in vitro*. To examine whether BDNF is sufficient to safeguard survival and neurite out-

growth in SGNs, we investigated neuronal death and neurite outgrowth in a spiral ganglion (SG) explant culture. SG explants from the apical cochlear turn of postnatal mice were cultured and analyzed. Neurons were stained for NF200 and nuclei were stained with DAPI. Cell death and dying neurons were quantified. Neurite outgrowth was quantified using a modified Sholl-analysis. Neurite outgrowth in SG explants was compared for three conditions: SG explant alone, OC co-culture, and BDNF supplement. Least neurite outgrowth was observed when SG explants were cultured alone. Co-culturing with the OC significantly increased neurite outgrowth. Supplement of 25 ng/ml BDNF increased neurite outgrowth significantly, showing that BDNF is a very potent factor for stimulating neurite outgrowth. The proportion of neurons in explants in OC co-culture condition was twice the number of neurons in explants cultured alone or with BDNF supplement. Comparison of the proportion of dying neurons for the three conditions disclosed a prolonged neuronal survival for the OC co-culture which was not observed when BDNF was supplemented. While BDNF was shown to significantly stimulate neurite outgrowth, BDNF was insufficient to safeguard neuronal survival to the same extend as factors released by the OC. The OC co-culture strongly supported survival of SGNs in culture. This indicates the existence of yet unidentified factors, which are released from the OC and support the survival of spiral ganglion neurons.

PS-159

Beyond Hearing: The Potential Use of Low Frequency Tones to Identify Outer Hair Cell Loss

Aryn Kamerer; Marcello Peppi; Francisco Diaz; Mark Chertoff
University of Kansas Medical Center

Introduction

As biologic treatment for cochlear hearing loss advances, there is a growing need for diagnostic techniques to identify and discern underlying physiologic damage or dysfunction. Our previous studies have successfully used the cochlear microphonic (CM) to locate regions of outer hair cell loss along the basilar membrane. The CM is an electrophysiologic response traditionally attributed to current flow through hair cells. Our previous study, in agreement with recent literature, has shown that the auditory nerve (AN) can significantly contaminate the CM, complicating interpretation of results. The purpose of the current study was to attempt to circumvent the AN response of high-frequency fibers by using stimuli with frequencies beyond the range of high-frequency AN turning curves while simultaneously evoking current flow through hair cells to allow us to measure the CM independent of the AN component.

Methods

Mongolian gerbils were assigned to either an experimental group, whose cochleae were treated with 1mM of a neurotoxin, ouabain, or a control group treated with artificial perilymph placed in the round window niche. The CM was recorded to 45 Hz and 85 Hz tone bursts embedded in 18 high-pass filtered noise conditions. CM amplitudes were plotted as a function of distance along the cochlear partition, creating a cumulative amplitude function (CAF). Compound action potentials (CAPs) and distortion-product otoacoustic emissions (DPOAEs) were additionally obtained before and after the application of ouabain.

Results

Ouabain was effective in eliminating the AN from the 8-24 kHz test conditions and reducing the response at 1-4 kHz, as reflected in CAP measurements. DPOAEs were unaffected by ouabain, with the exception of a small drop in amplitude at 24 kHz. The CM response to the tones without noise was not reduced by the application of ouabain, although some post-treatment amplitudes significantly increased. Similarly, the CAF curve did not change with ouabain treatment.

Conclusions

This study shows that the low-frequency (45-85 Hz) CM does not include neural contamination from basal regions of the cochlea. Therefore, low-frequency tones may be used as appropriate stimuli to obtain the CAF, and to ensure a sensitive measure of outer hair cell function.

PS-160

The Effects of Carboplatin Induced Ototoxicity on Temporal Coding in the Auditory Nerve

David Axe; Michael G. Heinz
Purdue University

Sensorineural hearing loss (SNHL) and temporal coding within the auditory nerve (AN) is often discussed in terms of threshold shift and changes in tuning. In most cases, these changes are attributed to dysfunction of outer hair cells (OHCs). However, in many pathologies, including noise induced hearing loss (NIHL), inner hair cells (IHCs) are disrupted as well and may affect temporal coding. The chemotherapy drug carboplatin, administered in chinchillas, has been shown to selectively damage IHCs while leaving OHCs unaffected across much of the cochlear partition. Here, we have used this model to evaluate effects of IHC dysfunction on temporal coding without the confound of broadened tuning. Distortion-product otoacoustic emissions (DPOAEs) and auditory-brainstem-responses (ABRs) were measured before and at least three weeks after a single IP injection of carboplatin to characterize the degree and configuration of hearing loss, and to confirm the lack of effect on OHC function. Single-unit spike-train responses were recorded from barbiturate-anesthetized chinchillas, and compared between the normal-hearing control group and the carboplatin-exposed group. Tuning curves, rate-level functions, and post-stimulus-time histograms were used to characterize all auditory-nerve fibers. Quantitative analyses were performed on recorded spike trains, with temporal coding evaluated in terms of both fine structure and envelope coding. Temporal responses to sinusoidally amplitude-modulated (SAM) tones of varying modulation frequency, modulation depth, and background-noise levels were measured. We estimated the ability of each nerve fiber to detect and discriminate between varying levels of amplitude modulation in quiet and in varying levels of background noise. Consistent with our ABR and

DPOAE measurements, AN-fiber thresholds were only slightly elevated in the carboplatin group and there was no significant change in tuning-curve bandwidth. Rate-level functions demonstrated an average reduction in both spontaneous and stimulus-driven firing rates, such that the average slope of the rate-level functions did not change. In general, synchrony to the envelope and temporal fine structure of the stimuli was not significantly affected. However, estimated modulation detection thresholds based on phase locking were worse in the carboplatin group than in the normal-hearing control group. This result appears to be due largely to the reduced number of spikes in the carboplatin-group responses, which decreases the statistical detectability of the modulation. These results suggest that, although IHC damage does not degrade cochlear tuning, it often reduces the number of spikes available in the AN response and thus can degrade the representation accuracy of the temporal structure of perceptually relevant complex sounds.

PS-161

Fractalkine (CX3CL1) Signaling Regulates Macrophage Recruitment into the Cochlear Sensory Epithelium and Influences the Survival of Spiral Ganglion Neurons After Hair Cell Lesion

Tejbeer Kaur[1]; Keiko Hirose[1]; Edwin Rubel[2]; Mark Warchol[1]
[1]Washington University; [2]University of Washington

Background

Fractalkine receptor (CX3CR1) is expressed by circulating monocytes, by microglia in the CNS, and by tissue macrophages. The chemokine fractalkine (CX3CL1) is the exclusive ligand for CX3CR1. Studies in the central nervous system have demonstrated that absence of fractalkine signaling result in neurotoxicity. Spiral ganglion neurons (SGNs) are necessary for transmitting information from the cochlea to the auditory brainstem, but the factors that influence SGN survival after hair cell injury are not fully understood. We have used a novel mouse model to examine the role of cochlear macrophages and of fractalkine signaling following the selective ablation of hair cells.

Methods

Double heterozygotes (*CX3CR1*$^{+/GFP}$*:Pou4f3*$^{DTR/+}$) mice expressing human diphtheria toxin receptor (DTR) under the control of Pou4f3 were crossed to CX3CR1$^{GFP/GFP}$ (homozygous) mice, which express GFP in macrophages and lacks fractalkine signaling. Mice transgenic for DTR and either heterozygous or homozygous for CX_3CR1 (*Pou4f3*$^{DTR/+:CX_3CR1^{+/-}}$ and *Pou4f3*$^{DTR/+:CX_3CR1^{-/-}}$) were used as experimental mice and mice wild type for DTR and either heterozygous or homozygous for CX_3CR1 (*Pou4f3*$^{+/+:CX_3CR1^{+/-}}$ and *Pou4f3*$^{+/+:CX_3CR1^{-/-}}$) served as controls. Mature mice were given a single injection of diphtheria toxin (DT, 25ng/gm). After 1-56 days recovery, cochleae were fixed and processed for immunohistochemistry or plastic sectioning.

Results

Single DT injection resulted in nearly-complete ablation of both inner and outer hair cells within 7 days. Despite the elimination of all hair cells, we observed no loss of spiral ganglion neurons, up to 56 days. Loss of cochlear hair cells was associated with increased numbers of macrophages in the spiral ganglion, beginning at 7 days post-DT; this number remained elevated at 56 days post-DT. Immunofluorescence labeling confirmed the expression of CX3CL1 in the cochlear sensory epithelium and somas of SGNs. Deletion of CX3CR1 (the specific receptor for the CX3CL1) reduces macrophage recruitment in the sensory epithelium (~60%) and spiral ganglion (~30%) after cochlear injury. Also, beginning at 56 days after DT, we observed a significant loss of SGNs in CX3CR1$^{-/-}$ mice than CX3CR1$^{+/-}$ littermates controls.

Conclusions

Our results suggest that the selective death of hair cells is sufficient to recruit macrophages into the cochlea. Deletion of CX3CR1 reduces macrophage numbers in the sensory epithelium and spiral ganglion, and also leads to the reduced survival of SGNs after hair cell death. These results suggest that injury-evoked macrophage recruitment is associated with the long term survival of target-deprived SGNs, but the precise role of fractalkine signaling in this process remains to be determined.

PS-162

Spoken Word Recognition in Saudi Children with Cochlear Implants: Effects of Lexical and Demographic Factors

Nada Alsari; Andrew Faulkner
University College London (UCL)

Introduction

The current study aimed at examining the effects of Lexical characteristics, age at implantation, and length of implant use on spoken word recognition in Arabic speaking children using multichannel cochlear implants (CI) through the application of the Lexical Neighbourhood Test (ALNT). The newly developed ALNT takes account of the lexical properties of word frequency and neighbourhood density (i.e. number of phonemically similar words). These lexical characteristics are incorporated from the Neighbourhood Activation Model (NAM) which assumes that words are organized in the mental lexicon according to word frequency and neighbourhood density.

Design

The study comprised three sessions. The first session included 44 paediatric CI users aged between 5 and 13.5 years with a mean of 8.5 years. Age at cochlear implantation ranged from 1.7 to 11 years with a mean of 4.33 years and duration of cochlear implant use ranged from 6 months to 9.5 years with an average of 4.3 years. In the second session, 36 of the 44 children were included while only 26 of the 44 children participated in the third session. In all three sessions, word recognition was assessed using the ALNT. Effects of lexical properties, age at implantation and length of CI use were investigated using Linear mixed model analysis (LMM) and regressional models.

Results
The average percent-correct scores for the easy words for sessions 1, 2, and 3 were 68.63%, 74.85%, and 76.33% respectively while for the hard words was 46.73%, 51.33%, and 58.87% respectively. In all three sessions, the percentage of words correctly identified in the easy lists was higher than the hard lists. Multiple regression analysis revealed that neighbourhood density was a significant predictor of word recognition but word frequency did not play a role in word recognition on the ALNT. Age at implantation had significant effects on word-recognition performance on the ALNT while length of implant use did not.

Conclusions
Arabic speaking pediatric CI users' open-set word recognition on the ALNT was influenced by the lexical characteristics of word frequency and neighbourhood density and scores were higher for easy than for hard words. Age at implantation had significant effects on word recognition performance as early implanted children exhibited better performance than children implanted later. Length of implant use however, did not significantly affect word recognition in the current study. This may be related to sample size or that these effects tend to diminish overtime with increased experience.

PS-163

Atypical Audio-Vocal System Regulation in Autism Spectrum Disorder

I-Fan Lin[1]; Takemi Mochida[1]; Kosuke Asada[2]; Masaharu Kato[1]
[1]NTT Communication Science Laboratories; [2]The University of Tokyo

Introduction
Individuals with autism spectrum disorder (ASD) suffer from impairment in social interaction and communication, which may be caused by their difficulties in speech control. A previous study found increased vocal responses to pitch-shifted auditory feedback in a subgroup of individuals with ASD, which indicates that they may have abnormal audio-vocal system regulation. To investigate how the audio-vocal system regulation responds to internally and externally perturbed auditory feedback in individuals with ASD, we examined their vocal behaviors when they were exposed to delayed auditory feedback (DAF) and loud background noise.

Methods
Ten adults with ASD (two males) and thirteen age- and IQ-matched neurotypical adults (five males) joined this study. In the first experiment to examine how participants responded to DAF, participants said 'ma-mi-mu-me-mo' repeatedly under 0.05-, 50-, 100-, 200-, or 400-ms auditory feedback delay for the voiced condition and for the whispered condition. Pink noise was sent with the altered auditory feedback through headphones to mask the air-conduction of their own speech. In the second experiment to examine the background noise-induced Lombard effect, either no noise or 68.8-dB SPL pink noise was mixed with their own speech and fed back without delay through headphones when they said numbers randomly displayed on the computer screen.

Results
The results show that the ASD group was more influenced by DAF than the control group in syllable error, phonation duration, and speech rate for the voiced condition. Nevertheless, there was no such group difference for the whispered condition due to the increased influence of DAF on the control group. On the other hand, the observed Lombard effect, measured by phonation duration and loudness, was smaller in the ASD group than in the control group.

Conclusions
Our findings show that for internally perturbed auditory feedback, the audio-vocal system had larger responses in the ASD group than in the control group. On the other hand, for externally perturbed auditory feedback, the audio-vocal system had smaller responses in the ASD group than in the control group. Taken together, it is suggested that the audio-vocal system in the ASD group in our study was susceptible to auditory feedback error associated with their own speech act but not to degraded speech intelligibility caused by background noise.

PS-164

Does Working Memory Training Improve Speech-in-Noise Performance in Older Adults?

Rachel Wayne[1]; Cheryl Hamilton[1]; Julia Huyck[2]; Ingrid Johnsrude[3]
[1]Queen's University; [2]Kent State; [3]University of Western Ontario, Queen's University

Difficulty understanding speech in background noise is a chief complaint of older adults. Although amplification devices improve hearing sensitivity, hearing speech in background sound remains challenging. Speech comprehension in noise appears to depend on working memory and executive-control processes, and training may augment such functions and offer an alternative strategy for age-related hearing loss rehabilitation. Cogmed Working Memory Training (Pearson) is an adaptive, computerized working memory training program that has been shown to generalize to related working memory tasks in older adults (Brehmer et al., 2012), but generalization to speech-in-noise tasks has not been assessed. We examined whether Cogmed training in older adults generalized to related working-memory tasks (near-transfer) and to other cognitive domains (far-transfer) using a neuropsychological test battery. We also assessed far-transfer to two measures of speech-in-noise performance: a closed-set sentence identification task (Kidd et al., 2008), and word report for semantically coherent (e.g. "her new skirt was made of denim") and anomalous (e.g. "her good slope was done in carrot") sentences. Stimuli for both tasks were presented with a two-talker masker at +3 and +6 SNR. We tested 24 subjects between 59-73 years of age, and hearing loss ranged from mild (<40 dB) to severe (70-90 dB). Following standard Cogmed procedures, subjects completed five weeks of adaptive working memory training, as well as five weeks of placebo training (with span of working memory tasks limited to three items), in a counterbalanced cross-over design. Neuropsychological

and speech testing was conducted at three time points: prior to the start of training, and following each of the five-week training blocks. Subjects' scores on the adaptive working memory training tasks improved. However, training did not generalize to other cognitive domains, or even to other working-memory tests. We did not observe any training-related improvement in speech-in-noise performance. However, we observed a significant correlation between each of two working-memory measures and speech-in-noise-performance (anomalous/coherent sentence task). Although working memory training did not improve speech-in-noise performance, our results are consistent with a growing literature suggesting that working memory is important for speech understanding under difficult listening conditions.

Brehmer et al. 2012. *Front Hum Neurosci, 6,*(63).

Kidd et al., 2012. J *Acoust Soc Am, 124*,(6).

PS-165

Listening Difficulties and Sustained Attention: Is It Specifically Auditory?

Hettie Roebuck; Johanna Barry
Institute of Hearing Research

Recent research has suggested that some of the listening difficulties associated with developmental disorders like Auditory Processing Disorder (APD) or specific language impairment derive from underlying difficulties in the ability to sustain attention (1). The evidence available suggests these difficulties are specific to the auditory modality (2,3), with some evidence further arguing that in fact the deficits are actually specific to speech processing (4). Studies assessing sustained attention however have used a wide range of stimuli and procedure. Differences in conclusions about the nature and specificity of the attention deficits may reflect these differences in paradigm designs.

In this study, we systematically assessed the modality and type of specificity of the deficits in sustained attention in APD in two groups of children (typically developing (C-TD) and Referred for APD (C-refAPD)). All participants had normal audiograms and were aged between 8 and 12 years. Inattention was measured using a continuous performance task where participants responded to an infrequent target (n = 72) among more frequent non-targets (n = 252) over a sustained period of time (11 mins). Three stimulus conditions were included, namely: two shapes/letters (X, O; visual condition), two pure tones ('C' 261.6 Hz; 'G' 392Hz (auditory non-linguistic condition), and two speech sounds ('Ex' and 'Oh'; auditory linguistic condition). These latter two stimuli were chosen to be maximally perceptible, while having minimal linguistic content. All stimuli (regardless of modality) were presented for 200ms with an inter-stimulus interval (ISI) of 2000ms. Participants were instructed to press the button as soon as they saw/heard the target stimulus only. Inattention was defined as 'targets missed' and errors were compared for each of the three conditions for the two groups of children.

The C-refAPD made more errors across all tasks than the C-TD group. This confirms previous research suggesting an underlying deficit in sustained attention in this group. The preliminary results also suggest both groups made more errors on the auditory non-linguistic condition compared to the visual and auditory linguistic conditions. Performance on these latter two conditions was similar. Overall, the poorer performance on the tonal condition suggests that the deficits in sustained attention, rather than being simply auditory specific, may actually depend on the nature of the processing demands placed on the listener. These findings may potentially contribute to understanding more about why poorer frequency discrimination deficits is commonly reported for children with listening difficulties.

References

1. Moore, D.R., Ferguson, M.A., Edmondson-Jones, A.M., Ratib, S., & Riley, A. (2010). The nature of auditory processing disorder in children. Pediatrics, 126, e382-390.

2. Noterdaeme, M., Amorosa, H., Mildenberger, K., Sitter, S., & Minow, F.(2001). Evaluation of attention problems in children with autism and children with a specific language disorder. European Child & Adolescent Psychiatry, 10, 58-66.

3. Spaulding, T. J., Plante, E., & Vance, R.(2008). Sustained selective attention skills of preschool children with specific language impairment: Evidence for separate attentional capacities. Journal of Speech, Language, and Hearing Research, 51,16-34.

4. Ebert, K. D., & Kohnert, K. (2011). Sustained attention in children with primary language impairment: A meta-analysis. Journal of Speech, Language, and Hearing Research, 54(5), 1372-1384.

PS-166

Self–reported Hearing Difficulties Among Adults with Normal Audiograms: The Beaver Dam Offspring Study.

Kelly Tremblay[1]; Alex Pinto[2]; Mary Fischer[2]; Barbara Klein[2]; Ron Klein[2]; Sarah Levy[3]; Ted Tweed[2]; Karen Cruickshanks[2,4]
[1]University of Washington; [2]University of Wisconsin, School of Medicine and Public Health, Department of Ophthalmology and Visual Sciences, Madison, WI 53726; [3]University of Washington, Dept of Speech and Hearing Sciences. Seattle, WA. 98105; [4]University of Wisconsin, School of Medicine and Public Health, Department of Population Health Sciences, Madison, Wisconsin.53726.

Introduction

The purpose of this study was to identify how often, on a population-basis, people with normal audiometric thresholds report experiencing hearing difficulties (HD) in noise and which factors (cognitive, behavioral, mental health, socioeconomic, vision, etc.) are associated with such HD.

Methods

This was a cross-sectional investigation of participants in the Beaver Dam Offspring Study (BOSS). BOSS includes adult offspring of participants (21-84 years of age) in the population-based Epidemiology of Hearing Loss Study. Questionnaire information about education, income, behaviors, envi-

ronmental factors and medical history (including tinnitus) was collected. Tests of cognition, vision, and hearing were also conducted. Audiometric data were available on 2783 of the BOSS participants.

Results

682 participants had audiometric thresholds that fell within normal limits, and 12.0% (82/682) self-reported having HD. Therefore, the prevalence of self-reported HD with normal audiometric thresholds in the entire cohort was 2.9% (82/2783). Multivariable models controlling for age and gender revealed HD, in the presence of normal hearing thresholds, to be associated with self-reported neuropathy type symptoms (e.g., numbness, tingling and loss of sensation, and vision difficulties) accompanied by self-report of a history of noise exposure. People who reported having HD were more likely to have seen an ear doctor for hearing loss than the non- HD group even though performance on audiological tests (audiograms, DPOAEs, word recognition in quiet and in competing message) did not differentiate the two groups.

Conclusions

This study identified a group of people who reported experiencing HD yet had normal audiometric test results. Auditory as well as non-auditory risk factors were identified. Examples include: noise exposure, visual disturbances, and signs of neuropathy (numbness/tingling/ temporary loss of sensation).

PS-167

Unrecognized Hearing Loss and its Association With Health and Cognitive Declines

Paul Mick[1]; Kathleen Pichora-Fuller[2]

[1]University of British Columbia; [2]University of Toronto

Introduction

The 2012 United States Preventive Services Task Force concluded they could neither recommend for or against screening for hearing loss (HL) in older adults because it is unclear if screening improves health outcomes for people who are unaware they have HL. Epidemiological studies have shown associations between HL and cognitive decline, dementia, depression, social isolation, falls, hospitalizations, physical and mental burden of disease.

Objective

The objective of our study was to determine if cross sectional associations between audiometric HL and cognitive decline, dementia, depression, social isolation, falls, hospitalizations, physical and mental burden of disease are also observed when samples are restricted to participants who have audiometric HL but report that their hearing is “excellent” or “good”, and those with normal hearing.

Methods

United States population-based data from the 1999-2010 National Health and Nutrition Examination Survey (NHANES) cycles were used. The sample was restricted to participants who had a 500, 1000, 2000 and 4000 Hz pure tone average (PTA) ³ 25 dB and answered that their hearing was “good” or “excellent” or had normal hearing (PTA < 25 dB). The age range differed for each outcome because different variables were measured in different age groups. In analyses of hospitalizations, burden of disease, and depression participants were 70 or older. For cognition, participants were 60-69, and for falls, 40-69. The analysis of social isolation included individuals aged 60-69 and 70+ (survey sample weights could not be combined for both age groups). Multivariable regression models were used to assess cross-sectional associations adjusting for demographic and cardiovascular confounders. We accounted for the complex sampling design in all analyses by using sample weights according to National Center for Health Statistics guidelines.

Results

In the restricted sample, greater HL was associated with lower scores for cognition (digit symbol substitution test score difference of -2.1 [95% confidence interval: -3.9, -.25] per 10 dB of HL), and social isolation in the 60-69 year old group (odds ratio of 1.58 [95% CI: 1.2, 2.1] for social isolation index score > 2 per 10 dB of HL) in the fully adjusted models. HL was not associated with the other outcome measures.

Conclusion

Audiometric HL is independently associated with lower cognitive scores and greater social isolation among people with HL who report that their hearing is “good” or “excellent.” Further research is needed to determine if screening programs to identify such people might lead to better cognitive and social outcomes.

PS-168

Challenges In Designing And Developing An Auditory Training iPad App For Adults With Hearing Loss

Rohit Bhattacharya; Margo Heston; Jo Eun Song; Lindsey Fernandez; Tilak Ratnanather

Johns Hopkins University

Introduction

There is an increasing need for auditory training from deaf adults with cochlear implants or digital hearing aids. While several desktop programs are available, mobile applications are few; this is compounded by time or financial constraints giving adults limited opportunities to benefit from auditory training. To address the need for a portable, inexpensive form of auditory training, we have developed an iPad app called Speech Banana based on the book “Auditory Training for the Deaf” by Monsees and Whitehurst published in 1952.

Method

The app consists of 38 lessons, reflecting the scheme presented in the original book. Each lesson is comprised of a passive exercise where both visual and auditory stimuli are provided, and an interactive quiz where sentences with these words are presented in auditory form only. The user types the sentence heard using the native keyboard and receives feedback that determines correctness of the answer. The chapters may be used in any order, allowing the user to focus on challenging sounds as needed. Users may also customize gender of the voice and the volume of the background

noise. Challenges of the design and implementation process included readability of text and ease of typing, storage of high quality sound files, and production of stimuli through the iPad speakers.

Results
Speech Banana was released to the general public via the JHU Apple App Store in October 2014. Announcements were made via several social networks as well as national and international organizations. Possible users were invited to complete a survey and provide suggestions for improvement such as options for multiple speakers, retroactive compatibility and exportability to other platforms such as web or Android.

Conclusion
Speech Banana has the potential to be a resource used by adults with cochlear implants or digital hearing aids hopefully in conjunction with fewer, more productive visits with an auditory therapist. Feedback provided by the app may be used to focus more closely on challenging sounds, and users will remain more quantitatively informed about their progress. The next steps of development include a Korean version, implementation of adaptive learning techniques, a web application and spoken input capabilities.

PS-169

Face and Content Validity of a Web-Based Otoscopy Training Simulator

Brandon Wickens[1]; Jordan Lewis[2]; Sumit Agrawal[3]; **Hanif Ladak[2]**
[1]Dalhousie University; [2]Western University; [3]London Health Sciences Centre

Background
Otoscopy is an important and widely used diagnostic tool for identifying ear pathology. Despite being a common tool, accuracy rates in otoscopic examinations are low. A web-based training simulator (*OtoTrain*) was developed at our institution to enhance the otologic education of health professional students and residents. This simulator teaches the principles and technique of otoscopy; it also provides an introduction to common otologic diseases through an interactive 3D simulator, pictures, summary text and a testing platform.

Objective
Our goal is to assess the face and content validity of this novel simulator.

Methods
The web-based otoscopy simulator was designed and distributed to 15 world-renowned experts. After viewing an instructional video, unlimited access to the simulator was provided until experts felt comfortable with the interface and its content. Feedback was then solicited through an online survey. The survey assessed expert agreement to statements describing the simulator, and asked experts to compare the simulator efficacy to the current standard in otoscopy education. Qualitative feedback through open-ended questions was then used to modify and enhance the simulator in preparation for further study and distribution.

Results
Eleven surveys were collected and descriptive statistics were used to assess responses. Responses demonstrated approval of the module interface, content and applicability to medical education. Experts were supportive of this novel otoscopy trainer when compared with classic education tools. Overall, they indicated that this method of otoscopy training is equivalent or superior to traditional training methods. Insightful qualitative feedback was used to enhance the simulator and its content.

Conclusions
The web-based otoscopy simulator *OtoTrain* shows sufficient face and content validity for application to training in otoscopy.

PS-170

Correction Factors for Multiple Auditory Steady-State Responses in Normal Hearing Adults: the Effect of Modulation Frequency

Zahra Ghasemahmad[1]; Saeid Farahani[2]
[1]Kent state University, Northeast Ohio Medical University, Tehran University of Medical Sciences; [2]Tehran University of Medical Sciences

Background
Multiple Auditory Steady-State Response (MASTER) is a kind of evoked potential that is used to objectively get an estimate of hearing thresholds by simultaneously presenting amplitude-modulated tones at 4 carrier frequencies in both ears. When using this technique, correction factors, defined by the manufacturing company are applied to ASSR thresholds. These correction factors are applied in the same manner for 40HZ and 80HZ modulation frequency and for subjects with normal hearing or hearing loss. However, modulation frequency and the amount of hearing loss affect the thresholds to a large extent. In this study by comparing ASSR and Pure tone audiometry (PTA) thresholds at different modulation frequencies, we aimed to examine the reliability of the correction factors and determine the effect of modulation frequency on these factors.

Methods
24 normal hearing subjects (aged 20-40 years old) including15 females and 9 males with hearing thresholds at or better than 20dB underwent PTA and ASSR in three different modulation frequencies (20, 40 and 80 HZ). MASTER was compared with PTA thresholds and correlation of the correction factors and difference scores were measured in all modulation frequencies.

Results
Correction factors that are defined for the instrument, matched the difference scores obtained for 80 Hz ASSR much better than other modulation frequencies. In addition, for carrier frequency of 500Hz at all tested modulation frequencies, correction factors were significantly different from the difference scores obtained in our study. The smallest differences between ASSR and PTA thresholds were observed at 80 Hz multiple ASSR at 2000 and 4000 Hz. While at 500 Hz and

1000Hz, 40 Hz Multiple ASSR demonstrated the smallest difference scores. Also, correlation coefficients revealed poor relationships between ASSR and PTA at most carrier and modulation frequencies (r=0.2-0.58).

Conclusion
By applying the correction factors for MASTER suggested by the manufacturing company, we demonstrated an unreal hearing loss especially at lower frequencies. These correction factors are a better predictor of hearing thresholds at 80 Hz ASSR rather than at 40 Hz. As the relationship between MASTER and PTA thresholds does not seem to follow a consistent rule, cautions need to be taken when using this technique without a golden standard for predicting hearing thresholds in normal hearing subjects and non-organic hearing loss.

PS-171

Optimizing Pure-Tone Audiometry Using Gaussian Processes

Dennis Barbour; Brittany M. Wallace; Jacob R. Gardner; Noah M. Ledbetter; Mitchell S. Sommers; Kilian Q. Weinberger; Xinyu D. Song
Washington University

Background
Pure-tone audiometry (PTA) has long been established as a reliable measure of hearing loss. Though procedures have been standardized over the years, they have never become automated in standard practice, leading to a substantial labor cost for hearing health professionals. Attempts to automate PTA have generally duplicated the steps of manual procedures, which is suboptimal for an automated algorithm where ease of implementation is not a factor. A novel approach that is both automatic and optimally delivered for each subject has the potential to simultaneously improve audiometric estimates while also freeing audiologist time for more complex procedures.

Methods
We have designed a psychometric algorithm incorporating Gaussian process (GP) classification that automatically selects and delivers appropriate pure tones in succession. Each new tone is selected to contribute the most information to subsequent threshold estimates. Additional tones are delivered in the same fashion until the overall threshold estimate confidence meets or exceeds a preset minimum value.

This algorithm was tested on normal-hearing and hearing-loss individuals. Pure-tone air conduction thresholds were evaluated using 1) the GSI-61 standard manual audiometer, 2) a manual computer-based PTA protocol, and 3) an automated GP-based PTA protocol. The GP-based protocol was conducted twice for each subject. Accuracy of the GP-based protocol was evaluated using relative deviation from pure-tone thresholds obtained from manual PTA, and reliability was evaluated using relative deviation between the two separate GP runs.

Results
The GP-based protocol achieves accuracy comparable to other automated audiogram methods and test-retest reliability comparable to standard manual approaches. Furthermore, the GP algorithm automatically provides threshold estimates for frequency ranges typically omitted from standard PTA, as well as a confidence estimate on the accuracy of the result. Time of execution was comparable to other PTA methods.

Conclusion
GP-based PTA appears to be well-suited for testing hearing thresholds. Benefits of this approach include no need for direct audiologist supervision, accuracy and reliability comparable to other methods, execution time comparable to other methods, automatic sampling of the most informative frequencies, confidence values of threshold estimates, and logging of data for electronic recordkeeping. This automated algorithm has the potential to reduce the manual labor associated with PTA, potentially freeing up the thousands of workdays hearing healthcare professionals spend annually performing PTA.

PS-172

Test-Retest Reliability of Word Recognition Score (WRS) Using Korean Standard Monosyllabic Word Lists for Adults (KS-MWL-A) as a Function of the Number of Test Words

Junghak Lee[1]; Jinsook Kim[2]
[1]Hallym University of Graduate Studies; [2]Hallym University

Objective
Word recognition score (WRS) is one of the most frequently used measures for speech audiometry. Korean monosyllabic word lists for adults (MWL-A) were recently developed and selected as a Korean standard (KS) for WRS test of speech audiometry. The purpose of this study was to establish the test-retest reliability of WRS obtained using the KS-MWL-A based on the international standard for speech audiometry (ISO 8253-3:2012).

Methods
Subjects consisted of 167 adults aged to 18 to 25 years with normal hearing sensitivity for octave frequencies from 250 Hz to 8000 Hz. Four lists of recorded KS-MWL-A were used for measuring WRS which consisted of 200 monosyllabic words. WRSs were obtained in 2 dB steps from the level of speech recognition thresholds (SRTs) to the level of 86% correct responses or greater. After one or two weeks, retest of WRS was performed with the same condition as the first test. To establish the test-retest reliability, correlation, confidence interval (CI) and prediction interval (PI) were calculated for five WRS bands from 50% to 90%, recommended by the international standard, which consisted of 45~55%, 56~65%, 66~75%, 76~85%, and 86~100% respectively. If WRS was greater than 50%, the presentation level descended to the level below 45% correct responses and then ascended from 2 dB above the SRT to the level up to 86% or greater in 2 dB steps. From these data, the percentage of correct responses was computed for 10, 25, and 50 test words at each test level as a psychometric function for each subject.

Table 1. Korean standard monosyllabic word lists for adults (KS-MWL-A) and international phonetic alphabets

List 1			List 2			List 3			List 4		
귀	글	꽃	난	코	양	국	십	당	산	한	돈
gwi	gɯl	k'ot	nan	ko	yaŋ	gug	sib	daŋ	san	han	don
남	용	연	위	숯	회	마	열	매	두	포	엿
nam	yoŋ	yʌn	wi	sut	hɸ	ma	ʌl	mɛ	du	po	yʌt
해	겉	달	죽	오	겁	봄	쥐	신	공	의	꿀
hɛ	gʌt	dal	ʧug	o	gyʌb	bom	ʧwi	sin	goŋ	ui	k'ul
밀	다	혀	더	강	인	이	또	뼈	말	셈	막
mil	da	hyʌ	dʌ	gaŋ	in	i:	t'o	b'yʌ	mal	sum	mag
옷	뚤	녹	값	외	답	농	파	낫	넋	은	비
ot	t'l	nog	gab	ɸ	dab	noŋ	pa	nat	nʌg	ɯn	bi
잔	피	김	모	장	노	학	너	교	방	때	궁
ʧan	pi	gim	mo	jaŋ	no	hag	nʌ	gyo	baŋ	t'ɛ	guŋ
댁	상	악	금	대	불	들	맛	발	힘	사	단
deg	saŋ	yag	gɯm	dɛ	bul	dɯl	mat	bal	him	sa	dan
겁	네	덕	효	욕	목	간	끼	저	야	집	요
gʌb	ne	dʌg	hyo	yug	mog	gan	k'i	jʌ	ya	ʧib	yo
시	별	조	성	미	계	컵	틀	굴	짐	배	뺨
si	bʌl	ʧo	suŋ	mi	gye	kʌb	tl	gul	ʧim	bæ	b'ŋ
병	추	군	빛	솔	실	새	나	피	그	솜	늪
byʌŋ	ʧʰu	gun	bit	sol	sil	sæ	na	k'ɸ	gɯ	som	nɯb
소	만	잎	서	벼	애	등	곳	살	차	화	옥
so	man	ib	sʌ	byʌ	ɛ	dɯŋ	got	sal	tʃa	hwa	ok
점	죄	폐	날	담	널	개	운	님	옴	절	재
ʧʌm	ʧɸ	pye	nal	dam	nul	gɛ	un	nim	ɯb	ʧʌl	ʧɛ
키	일	꿈	깨	져	안	징	덤	왕	수	뇌	탈
ki	il	k'um	k'ɛ	tʃʌ	an	ʧiŋ	dʌm	waŋ	su	nɸ	tal
앞	구	터	잠	강	쑥	손	주	곰	돌	귤	기
ab	gu	tʌ	ʧam	gaŋ	s'ug	son	ʧu	gom	dol	gyul	gi
무	삼	샘	표	띠	종	유	침	면	넷	여	멋
mu	sam	sɛm	pyo	t'i	ʧoŋ	yu:	tʃim	myʌn	net	yʌ	mʌt
논	도	능	눈	전	음	밤	역	열	검	칼	우
non	do	nɯŋ	nun	ʧʌn	ɯm	bam	ʌg	yʌl	gʌm	kal	u:
자	알		길	놀		예	후		놀	씨	
ʧa	al		gil	nɯl		ye	hu		nol	s'i	

Table 2. Means, standard deviations, correlations, standard errors and 95% confidence intervals of word recognition score (WRS) tested by Korean standard monosyllabic word lists for adults (KS-MWL-A) as a function of the number of test words

No. of test words	M1 (SD1)	M2 (SD2)	Md (SDd)	r	SE	95% CI (±2SE)
10	72.94 (15.80)	74.94 (18.81)	-2 (16.82)	.54 p=.00	1.82	±3.64
25	72.46 (14.29)	74.67 (14.53)	-2.21 (10.98)	.71 p=.00	1.12	±2.24
50	70.15 (14.53)	71.74 (14.24)	-1.59 (9.48)	.78 p=.00	.91	±1.82

*M1: means of WRSs at test
*M2: means of WRSs at retest
*Md: means of the differences between WRSs at test and retest
*SD1: standard deviations of WRSs at test
*SD2: standard deviations of WRSs at retest
*SDd: standard deviations of differences between WRSs at test and retest

Results

The Pearson correlation coefficients between WRSa at test and retest were 0.78 for 50 test words, 0.71 for 25 and 0.54 for 10 words. Results also showed that 95% CIs and 95% PIs were narrower for 25 and 50 test words than those for 10 test words.

Conclusion

Based on the aforementioned results, Korean WRS test using the KS-MWL-A has high reliability for 25 and 50 test words, but relatively low for 10 test words. It is suggested that 95% CIs for each test words be criteria for meaning significant differences between test and retest WRSs for groups and 95% PIs at each band of WRS for each test words be utilized for a considerable difference between test and retest for each individual.

Table 3. Means, standard deviations, standard errors, 95% confidence intervals, 95% prediction intervals for each band of word recognition score (WRS) tested by Korean standard monosyllabic word lists for adults (KS-MWL-A) as a function of the number of test words

No. of test words	WRS correct response	Difference of correspondence				SEM	95% PI
		M	SD	SE	95% CI	(SD/√2)	(±2SEM)
50	46~55	-2.13	13.77	1.56	6.21	9.74	±19.47
	56~65	-2.59	11.51	1.30	5.18	8.14	±16.28
	66~75	-1.43	12.23	1.24	4.9	8.65	±17.30
	76~85	0.31	9.11	0.99	3.93	6.44	±12.88
	86~100	3.11	7.62	0.60	2.37	5.39	±10.78
25	46~55	-5.50	15.70	5.55	26.26	11.10	±22.20
	56~65	-5.22	13.83	2.88	11.96	9.78	±19.56
	66~75	-4.00	12.65	3.07	13.00	8.94	±17.89
	76~85	-3.50	10.50	2.14	8.88	7.42	±14.85
	86~100	0.64	7.63	1.53	6.30	5.40	±10.79
10	46~55	6.92	20.57	5.70	24.86	14.55	±29.09
	56~65	-7.22	21.37	5.04	21.25	15.11	±30.22
	66~75	-5.00	17.57	4.14	17.48	12.42	±24.85
	76~85	3.33	18.79	4.43	18.69	13.29	±26.57
	86~100	3.14	12.55	2.12	8.62	8.87	±17.75

*SEM: standard error of the measurement

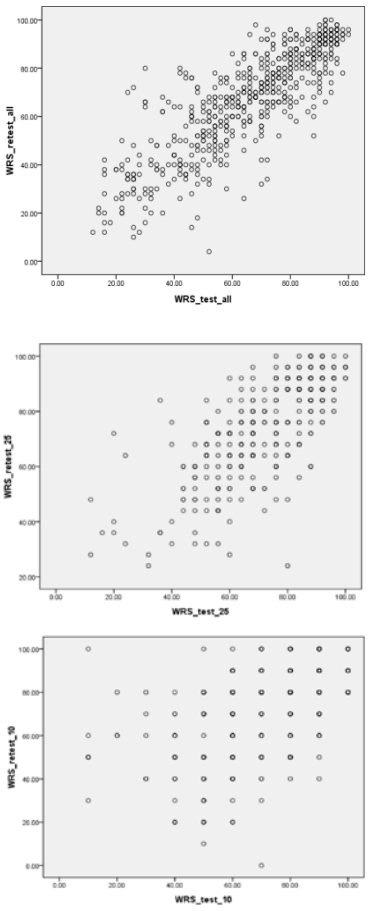

Figure 1. Scatter plots of WRSs at test and retest for 50(Top), 25(Middle) and 10(Bottom) test words

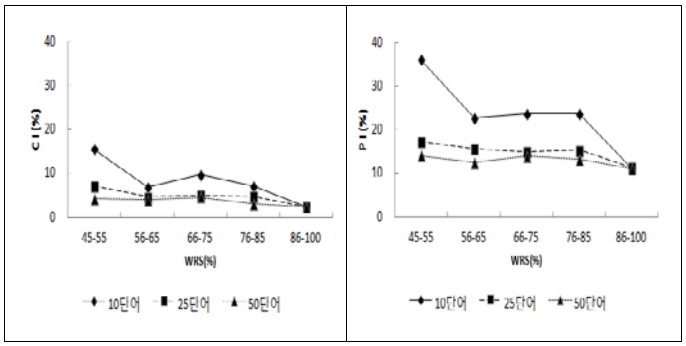

Figure 2. Confidence intervals(CIs, Left) and prediction intervals (PIs, Right) of 95% for each band of WRS as a function of the number of test words

PS-173

Development of Word Recognition in Mandarin Chinese-Speaking Children with Early Cochlear Implantations

Xin Liu[1]; **Li Xu**[2]; Haihong Liu[3]; Cuncun Ren[4]; Ying Kong[4]; Beier Qi[4]; Sha Liu[1]

[1]Beijing Tongren Hospital, Capital Medical University,Beijing Institute of Otolaryngology, China; [2]Communication Sciences and Disorders, Ohio University,US; [3]Beijing Children's Hospital, China; [4]Beijing Tongren Hospital, Capital Medical University, China

Introduction

Early implantation has been shown to contribute to better speech and language development in prelingually-deafened children. Word recognition development of Mandarin Chinese-speaking children who have received cochlear implants early in life has not been studied extensively. The purpose of this study was to examine the development of word recognition in Mandarin Chinese-speaking children who received multichannel cochlear implants (CIs) prior to age of 3 years and to compare their development with that of children with normal hearing (NH).

Method

Two groups of children, aged 3 to 6 years, participated in this study: (1) 130 children with CIs who received cochlear implantation before the age of 3 years and (2) 107 typical developing children with NH. The ability of word recognition was evaluated using the Standard-Chinese version of the Lexical Neighborhood Test (LNT) that included the monosyllabic and the disyllabic LNT. These two test components were further divided into disyllabic easy (DE), disyllabic hard (DH), monosyllabic easy (ME), and monosyllabic hard (MH) lists. The ANOVA was performed to analyze the effects of age and word category on the open-set word recognition in children with CIs. LNT scores from the two groups were compared using independent samples t-tests.

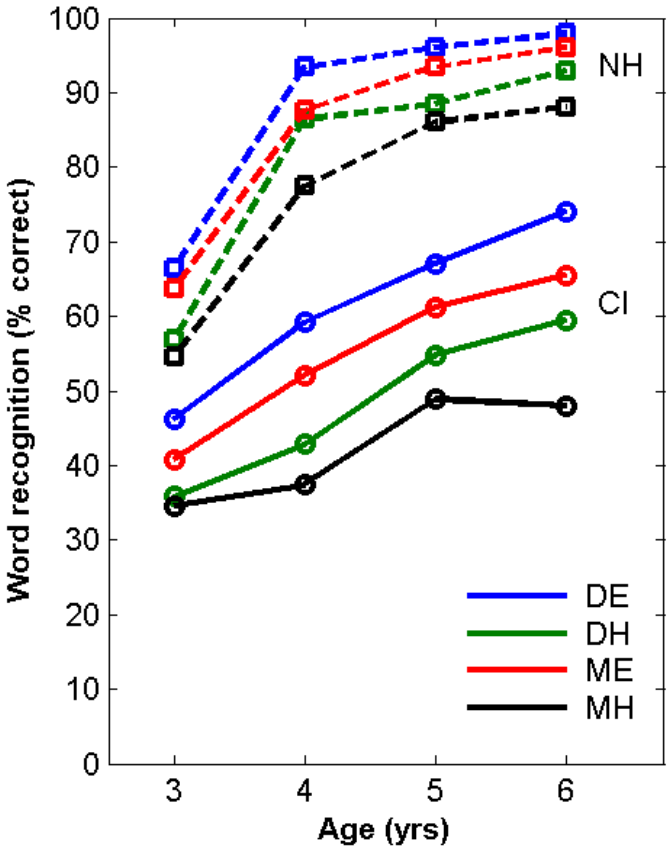

Results

The results of the open-set word recognition test are shown in Figure 1. The CI group had significantly lower LNT scores than their NH peers at 3, 4, 5, and 6 years of chronological age, respectively (all $P<0.05$). Nevertheless, children in the CI group exhibited steady improvements in the speech perception as the age increased and displayed a trend approaching the scores of the NH group after 4 years of age. The lexical characteristics of the word stimuli had significant influences on the recognition scores for both groups of subjects. That is, the scores were higher for easy words than for hard words and were higher for disyllabic words than for monosyllabic words.

Conclusion

This study demonstrated that prelingually-deafened, Mandarin-speaking children who were implanted prior to 3 years of age exhibited steady improvements in their speech perception as their age increased and that the gaps between the CI and the NH groups showed a trend to narrow after 4 years of age.

PS-174

Development of Early Vocal Production Pattern and rehabilitation format in Korean Normal Hearing Infants

Eunbith Cho[1]; Jinsook Kim[2]
[1]*Graduate School of Hallym University, Chuncheon.;*
[2]*College of Natural Sciences, Hallym University, Chuncheon, Korea*

The purpose of this study was to analyze pre-linguistic vocalization patterns in Korean infants with normal hearing (NH), ranged from birth to 18 months, and to develop a rehabilitation program for the Korean infants having difficulties in the vocalization development due to hearing loss. The vocalization during the first two years of life is generally considered as a foundation for the phonological development, coordination of the articulation mechanism, and the meaningful speech. Twenty NH infants ranged from 1 to 18 months of age. The participants were divided into the 6 groups based on their ages; 0~2 months, 3~5 months, 6~8 months, 9~12 months, 13~15 months, and 16~18 months. Data were recorded with 3 video cameras (Sony, model SOC-HDR-XP100, SOC-HDR_XR150, SOC-HDR-XR300) transcribed by the research of pediatric audiology laboratory then compared with the Stark Assessment of Early Vocal Development-Revised (SAEVD-R). In order to elicit representative vocalization, four recording situations were applied including free play with parent and/or toys, a feeding period, solitary play, and etc. The results showed that early vocal development of 1~18 months infants with normal hearing produced a little higher level of SAEVD-R such as vowels, consonants, and monosyllables as the age increased. When the consonants produced by the NH infants were classified according to the place of articulation, the bilabial sounds appeared first followed by labiodental and velar sounds. Specially, the unique /ŋ/ sound, which means 'yes' in Korean, was appeared between 7 to 8 months of age. Based on the results of this study, a structured aural rehabilitation program for Korean infants were presented. This program will include 'Short Fun Stimulation for Inducing Imitation (SFSII)' and Korean traditional child care method 'Dan Dong Sip Hun'. Further, more normal and hearing impaired infant's data should be included for more systematic plans of aural rehabilitation of that age.

Level	Vocalization Type
Level 1. Reflexive (0–2 months)	VEG(vegetative sounds), CR, Q(quasi-Resonant nuclei), Q2
Level 2. Control of Phonation (1–4 months)	F(Fully-Resonant Nuclei), F2,cv,cv2,CH
Level 3: Expansion (3–8 months)	V(vowel), V2, Vg(Vowel Glide), IN, SQ, MB(marginal babling)
Level 4: Basic Canonical Syllables (5–10 months)	CV, CB, WH,CV-C, CVCV
Level 5: Advanced Forms (9–18 months)	CMPX, JN(jargon), DP(diphongs)

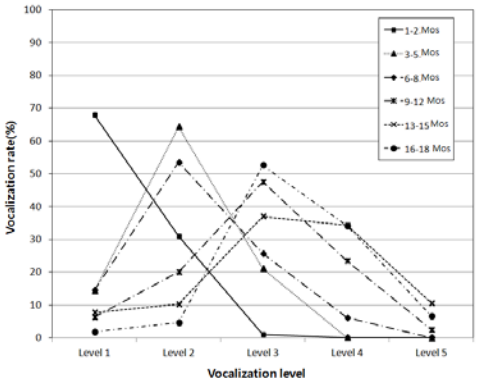

Figure1. Mean proportion of speech-like and non speech-like utterances across ages

PS-175

Healthy People 2020 Hearing and Other Sensory or Communication Disorders: Methods, Data Resources, and Prevalence Estimates for Measuring Progress towards Achieving Objectives

Howard Hoffman[1]; Chuan-Ming Li[1]; Katalin G. Losonczy[1]; May S. Chiu[1]; Christi L. Themann[2]
[1]*National Institute on Deafness and Other Communication Disorders (NIDCD), National Institutes of Health (NIH);*
[2]*National Institute for Occupational Safety and Health (NIOSH), Centers for Disease Control and Prevention (CDC)*

Introduction

Healthy People (HP), sponsored by the U.S. Office of the Assistant Secretary for Health, provides a national health agenda based on quantifiable objectives to improve the Nation's health. Only objectives tracked using reliable national data sets are included. Nine goals to improve hearing health were included in the HP 2010 Chapter 28--Vision and Hearing Health. HP 2020 retained these original nine hearing health objectives but expanded the topic area to include health objectives for other communication disorders, adding targets for tinnitus, balance (vestibular), smell, taste, voice (swallowing), speech and language.

Objective

Report on HP 2020 objectives and describe innovative assessment procedures for tracking objectives in the "Hearing and Other Sensory or Communication Disorders" topic area.

Methods
Hearing healthcare goals include assessing rates of: newborn hearing screening, evaluation, and intervention; use of hearing aids, assistive listening devices, and cochlear implants; timely hearing evaluations; and use of hearing protection to guard against noise-induced hearing loss. Some objectives required setting up new databases (CDC EHDI Program), while others relied on innovative design of new questions for the National Health Interview Survey (NHIS), including combining NHIS questions with hearing exam data from the National Health and Nutrition Examination Survey (NHANES); still others required extracting information from the Healthcare Cost and Utilization Project (HCUP) in order to track annual cochlear implant (CI) surgeries.

Results
CI surgeries nearly doubled from 2001–2010. The largest increase and highest prevalence for CI surgeries was for severe-to-profound hearing-impaired preschool-aged children, increasing from 9.0% in 2001 to 13.0% in 2009. Hearing aid use among older adults (aged 70+ years) with hearing loss of moderate or greater severity increased from 25.2% to 30.1%, 2001–2012. Among younger adults (20–69 years) with moderate or greater hearing loss, prevalence remained unchanged around 16%. Baseline estimates of adults (aged 20–69 years) having a hearing examination in the past 5 years are 28.6%, and for older adults (70+ years) 38.5%. Ever use of hearing protective devices for adults with noise exposure history is estimated as 53.1%, while noise-induced hearing loss among adolescents is estimated as 4.1%, increasing to 10.9% among working-age adults.

Conclusion
The goal of HP is to redirect U.S. health policy towards prevention and health promotion based on the "new" public health, a.k.a. the "third epidemiological revolution". This report describes new methods, baseline measures, and resulting estimates that are being used to track HP 2020 objectives for hearing and other sensory or communication disorders,

PS-176

One Possible Electrophysiological Method for TEN Test: A Preliminary Report of acoustic Change Complex (ACC) and Threshold-Equalizing Noise (TEN)

Soojin Kang[1]; Il-Joon Moon[2]; Heesung Park[2]; Jihwan Woo[3]; Sung Hwa Hong[2]
[1]University of Ulsan, Ulsan; Samsung Medical Center, Sungkyunkwan University School of Medicine, Seoul; [2]Department of Otorhinolaryngology-Head & Neck Surgery, Samsung Medical Center, Sungkyunkwan University School of Medicine; [3]School of Electrical Engineering, Biomedical Engineering, University of Ulsan

Background
Damage to the inner hair cells and/or spiral ganglion neurons results in hearing loss with poor speech discrimination, where is called the cochlear dead region (CDR). If a hearing-impaired person has CDR(s), amplification with hearing aid may not be beneficial to the patient. Recently, a pure-tone test in the presence of threshold-equalized noise (TEN) was introduced to identify CDR. However, this subjective and behavioral method cannot be used for uncooperative persons, so there is a need to develop the objective measurement of the cochlear dead region. The acoustic change complex (ACC) is an evoked potential elicited by changes in an ongoing sound. In this study, we developed TEN-ACC test aimed to present preliminary TEN-ACC data and to evaluate the use of TEN-ACC as an objective tool for detection of CDR.

Methods
Thirty normal-hearing subjects participated in this study. The tests were approved by the Samsung Medical Center Institutional Review Board. The acoustic stimulus, i.e., the first 1 s consisted of only TEN, while the next 1 s consisted of TEN and 1- or 4-kHz pure tone, was provided via an inserted earphone. The pure-tone level was varied from 0–15 dB SNR in 3 dB steps in order to identify the TEN-ACC threshold. The ACC was recorded from Cz and averaged at 120-repeated responses. The behavioral TEN test based on the study by Moore et al (2012) was performed to get the detection thresholds of pure tones over the TEN noise. Then, these two thresholds, behavioral (B) and electrophysiological (EP), were compared.

Results
Robust TEN-ACCs could be collected in all 30 patients. As the pure-tone level over the TEN noise increased, the ACC amplitude increased and the ACC latency decreased. The mean thresholds of 1- and 4-kHz TEN-ACC were 5.9 and 8.1 dB SNR, while those of the behavioral TEN tests were -0.2 and -0.93 dB SNR, respectively. The results demonstrate a positive correlation between the behavioral and electrophysiological thresholds.

Conclusion
Although thresholds of two different measurements were not quite similar (EP thresholds > B thresholds), a significant correlation was found. With these preliminary results, it is assumed that TEN-ACC in the cochlear dead region detection would be possible. Increased validation with hearing-impaired participants is further required.

PS-177

Tone-Language Speakers Show Hemispheric Specialization and Differential Cortical Processing of Contour and Interval Cues for Pitch

Gavin Bidelman; **Weilun Chung**
University of Memphis

Electrophysiological studies demonstrate that the neural coding of pitch is modulated by language experience and the linguistic relevance of the auditory input; both rightward and leftward asymmetries have been observed in the hemispheric specialization for pitch. In music, pitch is encoded using two primary features: contour (patterns of rises and falls) and interval (frequency separation between tones) cues. Recent evoked potential studies demonstrate that these "global" and "local" aspects of pitch are processed automatically (but bi-

laterally) in trained musicians. Here, we examined whether alternate forms of pitch expertise, namely, tone-language experience, influence the early detection of intervallic and contour deviations within ongoing pitch sequences. Neuroelectric mismatch negativity (MMN) potentials were recorded in Chinese speakers and English-speaking nonmusicians in response to continuous pitch sequences with occasional local (interval) or global (contour) deviations in the ongoing melodic stream. This paradigm allowed us to explore potential cross-language differences in the hemispheric weighting for contour and interval processing of pitch. Chinese speakers showed larger MMNs for both pitch interval and contour deviants than English speakers across the board. However, Chinese speakers also showed differential pitch encoding between hemispheres not observed in English listeners; Chinese speakers' MMNs revealed a leftward hemispheric laterality for interval processing but a rightward bias for contour processing. In contrast, no asymmetries were observed in English speakers. Collectively, our findings suggest tone-language experience (i.e., Chinese) sensitizes auditory brain mechanisms for the detection of subtle local/global pitch changes in the auditory stream and exaggerates functional asymmetries in pitch processing between cerebral hemispheres.

PS-178

Hemispheric processing asymmetries in auditory and audio-visual speech perception

Van Summers[1]; Ashley Zaleski[2]
[1]Walter Reed National Military Medical Center; [2]Gallaudet University

Introduction

Since the identification of Wernicke's and Broca's areas in the nineteenth century, speech processing at the level of the cortex has been viewed as primarily lateralized to the left-hemisphere (LH) for most listeners (with the asymmetry reversed in about 20% of left handers and about 5% of right handers). Little is known about whether hemispheric asymmetries and the degree of LH dominance in speech perception are altered when visual speech cues are available. Given the important role of the right hemisphere (RH) in visual processing, and in processing faces in particular, the RH may play a greater role in audio-visual (AV) than audio-only (AO) speech recognition. Experiments were conducted to examine whether experimental manipulations aimed at emphasizing left- or right-hemisphere cortical processing may differentially influence performance in AO and AV speech tasks.

Methods

Right-handed subjects identified consonants (C) in sequences of nonsense syllables (/a/-C-/a/-C-/a/-C-/a/) spoken by a male talker. Target stimuli were masked by speech-shaped noise in AO and AV listening conditions. Increased LH or RH processing was primed by having subjects flex and contract either the right or left hand while attending to the speech stimulus. Similar techniques have been shown to influence responses in decision tasks, with the left hand movements priming more holistic responses (associated with the RH) and right-hand activity associated with more analytic decisions (associated with the LH). Target stimuli were presented diotically at 65 dB SPL. Adaptive tracking was used to determine the noise level supporting ~70%-correct consonant recognition.

Results

As expected, consonants were more easily recognized in AV than AO conditions regardless of which hemisphere was primed. For AO conditions, flexing/contracting the right hand (presumably increasing the relative influence of LH processing on consonant responses) led to improved consonant recognition relative to flexing/contracting the left hand. For AV listening, this pattern was reversed: left hand movements (presumably increasing the relative influence of RH processing on responses) were associated with improved consonant recognition relative right hand flexing/contracting.

Conclusions

The results are consistent with parallel and partially-independent speech processing occurring in the right and left hemispheres. The relative accuracy of processing in the two hemispheres may depend on whether visual cues are available in the listening environment. Right or left hand motor activity during stimulus presentation appears to have increased the influence of processing in the contralateral hemisphere on consonant responses.

PS-179

Event-Related Potential (ERP) Effects of Neighborhood Density of Spoken Words in Young and Older Adults

Cynthia Hunter
State University of New York at Buffalo

Words that sound similar to many other words, or have high *neighborhood density,* are recognized more slowly and less accurately than words that sound similar to few other words. Larger decrements in recognition for high-density words have been observed in older than in young adults. The *neighborhood density effect* is believed to reflect activation and competition among a spoken word and its similar-sounding *neighbors* as the sounds of a word unfold over time. However, density effects are typically investigated with measures of behavior after a word is recognized, and have rarely been investigated with continuous measures. The current experiment used event-related potentials (ERPs) as well as behavioral measures of response time and accuracy to examine the time course of density effects for words and nonwords. Data were collected from both young and older adults in order to examine age differences. Behavioral results showed equivalent density effects in the lexical decision task across age groups as well as main effects of age, with older adults responding more slowly and less accurately than young adults. ERP results in young adults showed modulation of the amplitude of the N400 ERP by neighborhood density, such that N400 amplitude was larger for high- than low-density items. Similar modulation of N400 amplitude by density has been reported for visual words and may reflect spreading activation to semantic representations of neighbors. Older adults did not show this density effect. In addition, older

adults had reduced N400 amplitudes compared to young adults. Reduced N400 amplitudes with older age have been consistently reported in the literature. Age differences in the N400 ERP may reflect age-related changes in lexical access, including activation and competition among lexical neighbors. Older adults showed a late ERP effect of neighborhood density for words only. Specifically, older adults showed larger positive amplitude for high- than low-density words between 800-1400 ms after word onset. The functional significance of this effect is unclear, although it may potentially reflect compensatory processes involved in lexical access. Overall, the results are consistent with findings from previous ERP studies and provide new insights into the time course of lexical access in both young and older adults.

PS-180

Processing of English /r/ and /l/ by native Korean, Japanese, and American English listeners using the Acoustic Change Complex

Lee Jung An; Brett Martin; Glenis Long
The Graduate Center, City University of New York

Background

Native language influences the perception of non-native speech sounds. Perception of English liquids /r/ and /l/ is challenging for native Korean and Japanese adult listeners because these sounds are not phonemic in these languages. The Korean language, however, has a partial phonetic model available (intervocalic [ɾ]-[ll]) that could potentially facilitate processing of English /r/ and /l/. The effects of native language on the neurophysiological processing of English intervocalic /r/ and /l/ by native Korean, Japanese and American English listeners was examined using the acoustic change complex combined with behavioral identification and discrimination data.

Methods

Eight participants from each language group participated. Stimuli were a synthetic continuum generating percepts in American English listeners ranging from /iri/ to /ili/. Stimuli were presented at 70 dB SPL via insert earphones using a 1200 ms interstimulus interval. The acoustic change complex was recorded using a 64-channel Neuroscan system. Behavioral testing included a 2-alternative forced choice identification and a 3-alternative forced choice oddity discrimination tasks.

Results

Behavioral data indicated that English medial /r/ and /l/ were perceived in a categorical manner by Americans, in a categorical-like manner by Koreans and in a non-categorical manner by Japanese. P1-N1-P2 acoustic change complex responses at the midline-central electrode site (FCz) did not differ significantly between language groups, suggesting little effect of native language on the primary cortical encoding of these sounds. In contrast, the ACC T-complex measured over lateral-temporal electrode sites (T7 and T8) differed significantly between language groups suggesting that native language impacts secondary cortical processing of these sounds. Differences between groups included Ta morphology, Ta latency, and Tb latency. In addition, regional dipole source analysis revealed that the Japanese group had greater variability of individual source locations and significantly superior (the z coordinate) source location compared to the other language groups.

Conclusion

The partial phonetic model available to Koreans appears to provide a processing advantage not available to the Japanese. The ACC T-complex showed significant effects of language group providing a potential index of the influence of native language on /r/ and /l/ processing.

PS-181

Does the Auditory System Efficiently Code All Languages or Just American English?

Christian Stilp; Lily Assgari
University of Louisville

Background

Independent Component Analysis (ICA) is a powerful method for uncovering statistical structure in natural stimuli. Lewicki (2002, *Nature Neuroscience*, 5(4):356-363) used ICA to examine statistical properties of environmental sounds, animal vocalizations, and human speech. Statistically optimal filters for encoding each sound class were generated, and the relationship between filter center frequency and sharpness (Q_{10}) for each was compared to that measured in the mammalian auditory nerve. Filters that optimally encoded speech best matched physiological measures, leading Lewicki to suggest speech makes efficient use of the coding properties of the auditory system. However, these analyses only examined American English, which is not representative of the world's languages. Different languages vary considerably in their phonemic inventories and acoustic properties, and this variability may produce ICA solutions that challenge the proposed fit between speech and auditory nerve tuning. This was tested by using ICA to examine the statistical structure of a variety of languages found worldwide.

Methods

Recordings of 14 languages (Dutch, Flemish, Greek, Javanese, Ju|'hoan, Norwegian, Swedish, Tagalog, Tahitian, Urhobo, Vietnamese, Wari', Xhosa, Yeyi) were collected, mostly from the UCLA Phonetics Lab Archive (http://archive.phonetics.ucla.edu/). All recordings were at least one minute long and contained clear speech tokens from a native speaker without any background noise. Recordings were divided into 8-ms samples and analyzed using maximum likelihood ICA, following Lewicki (2002). The unmixing matrix (*i.e.*, statistically optimal filters) was iteratively updated by stochastic gradient descent across 20,000 epochs. Center frequency and Q_{10} were measured for each filter (row) in the unmixing matrix. Linear regressions were calculated on Q_{10} as a function of center frequency, then compared to regressions for American English and physiological measures in cat auditory nerve (Evans, 1975; Rhode & Smith, 1985).

Results

Languages produced a range of ICA solutions, as expected, but statistically optimal filters were broadly consistent with

those for American English and physiological measures. The only notable deviations were languages with slightly higher regression intercepts (sharper overall frequency tuning of ICA filters; Greek, Tahitian, Vietnamese) or a shallower regression slope (lower frequency sharpness and higher temporal precision in ICA filters; Ju|'hoan).

Conclusions
Results validate Lewicki's (2002) proposal that speech is well-aligned with response properties in the auditory nerve by extending this fit to a wide range of languages. This supports the efficient coding hypothesis, that sensory systems adapt and evolve to capture structure and regularity in the environment.

PS-182

Reliable Spectral Properties Elicit Contrast Effects in Perception of Noise-Vocoded Speech

Christian Stilp
University of Louisville

Background
The auditory system is highly sensitive to stable aspects of the acoustic environment. When acoustic frequencies are reliable across time (*i.e.*, relatively stable or recurring in the acoustic spectrum), the auditory system adapts to these frequencies and maximizes sensitivity to changes in the input (*i.e.*, unadapted frequencies). These changes are perceptually enhanced, resulting in contrast effects. Stilp, Anderson, and Winn (under review) found that when a 300-Hz-wide region in a preceding sentence was amplified by as little as +5 dB, contrast effects were observed in identification of subsequent vowel targets. Amplifying frequencies near the first formant of [ɪ] ("ih") in the precursor produced more [ɛ] ("eh") responses to the target, and *vice versa*. It is widely appreciated that reliable spectral properties influence speech perception by normal hearing listeners, but their role in speech perception by listeners with atypical or impaired hearing is unclear. The present experiment utilized noise vocoding to investigate sensitivity to reliable spectral properties in the perception of spectrally degraded speech.

Methods
Normal-hearing listeners labeled vowels from a 10-step series varying primarily in the first formant (F_1) center frequency, varying perceptually from [ɪ] to [ɛ]. Vowels followed a precursor sentence. Spectral properties in the sentence were made reliable by amplifying a 300-Hz-wide band near the target vowel's F_1 (100-400 Hz, near F_1 in [ɪ], or 550-850 Hz, near F_1 in [ɛ]) by 20 dB using a finite impulse response filter. Sentences and target vowels were then processed by a noise vocoder, with frequencies between 100-5000 Hz divided into 6-32 spectral channels according to Greenwood's formula. Listeners responded by clicking the mouse to indicate whether the target vowel sounded more like "ih" or "eh".

Results
Listeners responded "ih" more often following sentences with reliable spectral properties consistent with [ɛ] and *vice versa*, indicating contrast effects in identification of noise-vocoded speech. Contrast effects were observed at all spectral resolutions, and were at least as large as those produced using non-vocoded materials with similar amplification (Stilp *et al.*, under review). Even when stimuli lacked sufficient spectral resolution to accurately distinguish [ɪ] from [ɛ], responses were biased away from (contrastive with) the reliable spectral property in the preceding sentence.

Conclusions
Perception is sensitive to reliable spectral properties in spectrally degraded speech. Results suggest listeners who use cochlear implants may similarly attune to stable spectral properties in the acoustic environment.

PS-183

Perception of Noise-Vocoded Speech Matures during Adolescence

Julia Huyck
Kent State University

Noise-vocoded (NV) speech is a form of speech that bears key similarities to speech as transduced through a cochlear implant; the temporal envelope is largely preserved while the spectral structure is substantially reduced. Adults initially have difficulty comprehending NV speech, but are able to improve their comprehension dramatically within the first 30 sentences of exposure. Much less is known about the perception of NV speech in younger listeners. Here we were interested in how adolescents initially perceive and subsequently learn to understand NV speech. Younger adolescents (11-13 years), older adolescents (14-16 years) and adults (18-23 years) with normal hearing listened to 40 meaningful English sentences that had been vocoded using six band-limited noises. After hearing each sentence, the participants were asked to report as many words as they could from that sentence. No feedback about the accuracy of their responses was provided. Preliminary data suggest that percent correct word report improved over the course of training (main effect of time $p<0.001$, mean improvement = 11.8 percentage points) and that all three age groups learned at a similar rate (age x time interaction *n.s.*). However, the younger adolescents had generally poorer word report scores (mean = 71.2%) than either the older adolescents ($p < 0.01$, mean difference = 7.8%) or the adults ($p = 0.05$, mean difference = 8.4%), and the two older groups did not differ from one another (*n.s.*). The results suggest that the ability to understand vocoded speech, at least in meaningful sentences, continues to develop into adolescence. As such, this result may have implications for individuals who receive cochlear implants late in childhood or adolescence.

PS-184

Effects of Speech Rate Context on Speech Comprehension

David Weintraub; Joel Snyder
University of Nevada, Las Vegas

Introduction

It is well known that perception of small units of speech is influenced by the rate of pre- and post-speech. This effect occurs on multiple timescales. At long timescales, in particular, perception of function words (e.g., *or*, *the*) is sensitive to the average rate of a conversation-length period of speech (Baese-Berk et al., 2014). The purpose of the current study is to examine whether larger units of speech, namely sentences, are similarly sensitive to the average rate of speech at long timescales.

Methods

Speech stimuli consisted of sentences with the final word of each sentence spliced out. Speech rate was manipulated using time compression. Sentences were presented in two blocks of trials, which differed in their average compression rate. Sentences in the *fast context* block were compressed to 25%, 30%, or 35% of their original duration. Sentences in the *slow context* block were compressed to 35%, 90%, and 110% of their original duration. At the end of each sentence, a printed word appeared that either was or was not the original ending to the spoken sentence. Participants reported whether the printed word was the original ending, not the original ending, of if they did not know. Correct performance was taken as a measure of comprehension of the spoken sentence.

Results

Speech comprehension decreased as a function of increasing compression rate. More importantly, speech comprehension was higher for 35%-compressed sentences within the fast context block compared to the same sentences in the slow context block. This effect did not occur immediately, instead emerging after several minutes of exposure to the average speech rate within a block.

Summary and Conclusions

The results of this study suggest that comprehension of large units of speech (i.e., sentences) is affected by the average rate of a conversation-length period of speech. These results may reflect a contrastive context effect on the comprehension of speech, such that sentences spoken at relatively slow rates, compared to the average rate of sentences within a long-term context, are easier to understand. It is of note, however, that the 35%-compressed sentences were more similar to the average rate of speech in the fast context block. Therefore, these results may reflect perceptual learning of sentences compressed to the average within-block speech rate, which is more likely to generalize to 35%-compressed sentences in the fast context block.

PS-185

Noise-band Vocoding Interferes with Auditory Statistical Learning in Adults

Tina Grieco-Calub[1]; Hillary E. Snyder[1]; Paul N. Reinhart[1]; Casey Lew-Williams[2]
[1]Northwestern University; [2]Princeton University

Introduction

Auditory statistical learning refers to the ability to extract structure (e.g., consistent syllable sequences) from patterned auditory input (e.g., language) and has been widely proposed as a foundation for early language development (Saffran, Aslin, & Newport, 1996). Critically, successful segmentation of speech into its constituent parts hinges on the ability to hear: listeners not only need to discriminate individual speech units (e.g., phoneme, syllables), but also track relations between units over time. How spectral degradation of speech interferes with listeners' ability to track these relations is currently unknown. This is a clinically relevant issue when considering that individuals who use cochlear implants (CIs) must acclimate to spectrally degraded electric hearing and – in the case of infants – break into speech for the first time. The purpose of this study is to determine the role of spectral resolution in auditory statistical learning in adults by manipulating an artificial language with noise-band vocoding.

Methods

Young adults listened to an artificial language consisting of a monotone stream of trisyllabic nonsense words that lacked pause-related cues to word boundaries (Lew-Williams & Saffran, 2012). The artificial language was either unprocessed (i.e., full spectral resolution) or processed with an 8-channel noise-band vocoder. Following exposure, adults were tested with a 2-AFC task on their ability to distinguish trisyllabic sequences with perfect vs. weak vs. novel syllable transition statistics (respectively, words vs. part-words that spanned word boundaries vs. unfamiliarized nonwords). Adults then participated in a syllable identification task (CV) to determine if errors in statistical learning were attributable to specific errors in phoneme identification.

Results

Adults were significantly less accurate at identifying words and part-words (vs. nonwords) when exposed to the 8-channel vocoded language (51.8%) than to the unprocessed language (76%; $p<0.001$). These results suggest that spectral degradation disrupts adults' ability to segment the syllabic structure of the artificial language. Consistent with these findings, phoneme identification was significantly worse for adults tested in the 8-channel condition (59%) than for adults tested in the unprocessed condition (98%, $p<0.001$). Information transmission analysis of phonetic features suggests that initial consonant voicing was confused most frequently in the 8-channel condition.

Conclusions

Spectral degradation interferes with auditory statistical learning. One potential source of this interference appears to be confusion among the constituent consonants of the speech signal. This experiment motivates a planned investigation

exploring statistical learning abilities in individuals with CIs, with the goal of improving aural habilitation/rehabilitation programs.

PS-186

Top-down Repair of Speech: F0 Contours

Jeanne Clarke; Etienne Gaudrain; Deniz Baskent
University Medical Center Groningen

Introduction

Top-down cognitive processes can enable a listener to perceptually repair degraded speech for better comprehension. In phonemic restoration, the repair mechanisms can be shown by the improvement of interrupted speech intelligibility when silent interruptions are filled with noise bursts. The success of such top-down repair can be influenced by bottom-up acoustic cues such as spectral resolution. Another important acoustic cue for speech perception in adverse listening conditions that may also be involved in repair mechanisms is voice pitch (F0). However, in a previous study, we showed that disrupting the average F0, with alternation between speech segments up to one octave, had no effect on intelligibility of interrupted speech and on phonemic restoration benefit. These results suggested that listeners could overcome mismatched indexical cues to favor linguistic cues. This study aims to investigate the effect of another indexical cue, namely F0 contours (independently of the average F0 value). We hypothesize that having the wrong information would be worse than having no information about F0 contours.

Methods

Sentences interrupted with periodic silent intervals (with or without filler noise) were manipulated in four F0 contours conditions, and the intelligibility was compared to that of the original F0 contours. The modifications of F0 contours consisted of (i) compressing the magnitude of F0 around its median value, thus flattening the F0 contours, (ii) expanding the magnitude of F0 by exaggerating the F0 contours with a factor 1.5, and (iii) with a factor 1.75, (iv) misrepresenting the dynamic F0 information by inverting the F0 contours (within the same range). All stimuli were resynthesized using TANDEM-STRAIGHT.

Results

The global intelligibility decreased only for the inverted F0 contours. The phonemic restoration effect was observed in all F0 contour conditions, indicating that the top-down repair of interrupted speech was not impaired by any F0 contour manipulation.

Conclusion

Modifying the magnitude of F0 contours (all conditions except the inverted contours) did not have any effect on interrupted speech intelligibility. However, the direction of the F0 contours seems to be a cue listeners relied on for intelligibility of interrupted speech. Indeed, not completely validating our hypothesis, having wrong dynamic information of F0 (inverted contours) impaired interrupted speech intelligibility, whereas having no dynamic information (flat contours) did not. However, even the wrong dynamic information of F0 did not impair the top-down repair of interrupted speech. It seems top-down repair of speech is based more on linguistic cues than on indexical cues.

PS-187

Concurrent Speech Perception in Musicians and Non-Musicians

Deniz Baskent; Michael Chesnaye; Nikki Tahapary; Etienne Gaudrain
University of Groningen, University Medical Center Groningen

Introduction

Musicians have been shown to have advantages in perception of a wide range of acoustic stimuli compared to non-musicians. Such advantage may be due to better processing of acoustic features, such as fundamental frequency (F0), which is also a primary dimension in music, or due to enhanced cognitive abilities, such as better attention abilities and better selection of streams based on acoustic cues. Evidence for a transfer of this advantage to better perception of speech has been mixed. However, previous studies have primarily used noise as background masker, and if the musician advantage is due to better processing of F0 or due to better segregation, a concurrent speech perception task may be a better tool to investigate the musician advantage for speech. Concurrent voices differ in terms of vocal characteristics, i.e., not only F0, but also the vocal tract length (VTL), which may be processed differently by musicians and non-musicians. Unlike F0, VTL, was shown to be less utilized by musicians in a previous gender categorization study. By testing musicians and non-musicians with concurrent speech where F0, VTL, or both varied between target and masker, we investigated whether there is a musician advantage for concurrent speech perception, and if so, what underlying factors may have contributed to this advantage.

Methods

The F0 and VTL of the concurrent voices were systematically varied and speech intelligibility was measured with musicians and non-musicians.

Results

The musicians showed overall better intelligibility performance than non-musicians. However, almost all the difference was attributable to the condition where the target and masker voices were identical. The two groups drew equivalent benefit from F0 differences between concurrent voices, while musicians seemed to benefit slightly less from VTL differences than non-musicians.

Conclusions

Musicians did show a systematic advantage over non-musicians for concurrent speech perception. Because most of the advantage was shown in a condition where there was no difference in the average vocal characteristics of the talkers, this musician advantage is unlikely to be related to the processing of these speaker-specific vocal characteristics. Alternatively, because the prosodic F0 contours of the concurrent voices differed, instantaneous F0 differences remained even when the average F0 were identical. The musician advan-

tage could also be derived from an enhanced ability to process and disentangle fast changing F0 differences.

PS-188

Selective Auditory Attention Through Cortical Entrainment Shows Frequency Dependency

Lucas Baltzell[1]; Cort Horton[1]; Yi Shen[2]; Virginia Richards[1]; Ramesh Srinivasan[1]

[1]University of California, Irvine; [2]Indiana University

Background

Cortical entrainment to the temporal envelope in speech aids in speech perception. This entrainment can be measured by cross-correlating the envelope of the speech stimulus with the neuro-electric response (EEG) recorded while the stimulus is heard. Recently, this technique has been used to study attention in a multi-talker environment. By measuring the effect of attention on cortical entrainment, it is possible to understand how attention changes the neural representation of the stimulus envelope. Using data originally collected by Horton et al. (2013), a retrospective analysis is presented. The question of interest was whether or not the effect of attention on the entrainment to the stimulus envelope was frequency dependent.

Methods

EEG was recorded while subjects attended to one of two different speech streams (i.e., attended and unattended streams) presented simultaneously from two loudspeakers separated spatially. The speech stimuli were passed through a gamma-tone filterbank and the envelopes of the filter outputs were cross-correlated with the EEG. This leads to a cross-correlation function for each peripheral filter and for each of the two types of speech streams.

Results

The results indicate that while both the attended and unattended cross-correlations were, at most lags, statistically greater than chance, the attended cross-correlation reached a maximum at ~800 Hz, while the unattended cross-correlations reached a minimum in this same frequency region.

Conclusions

The difference in the envelope-to-EEG correlation between the attended and unattended speech streams is frequency dependent. This frequency dependency likely reflects both the envelope coherence across the spectrum inherent to the speech stimuli, and a sensitivity to the spectral distribution of the information-carrying envelope cues in speech.

PS-189

Effect of Number of Masking Talkers on Speech-on-Speech Recognition for Children and Adults

Lori Leibold; Stephen Lockhart; Lauren Calandruccio; Emily Buss

University of North Carolina at Chapel Hill

Introduction

This study examined the effect of number of masking talkers on word recognition for children and adults in competing speech maskers composed of 1, 2, 3, 4, 6 or 8 talkers. A non-monotonic relationship between amount of masking and number of masking talkers has been observed for adults in the context of speech-on-speech recognition (e.g., Carhart et al. 1975; Freyman et al. 2004). For example, Carhart et al. (1975) observed an increase in masking for adults as the number of talkers increased from 1 to 3, followed by no further increases in masking as additional talkers were added. This pattern of results is thought to reflect a reduction in informational masking due to a decrease in target-masker similarity as additional talkers are added to the masker stream (e.g., Freyman et al. 2004). Pronounced child-adult differences in speech recognition have been observed for speech maskers composed of 1-2 talkers compared with relatively steady-state noise (e.g., Hall et al. 2002; Wightman & Kistler 2005), Thus, it was hypothesized that larger child-adult differences would be observed for maskers with <3 talkers than for maskers with >4 talkers.

Methods

Listeners were normal-hearing 8- to 12-year-olds and 19- to 35-year-olds. Speech recognition thresholds (SRTs) were estimated for male spondee words in a continuous 60-dB-SPL speech masker composed of 1, 2, 3, 4, 6, or 8 male talkers. The level of the target spondee words was adaptively varied to estimate the level associated with 71% correct spondee identification. The procedure was a four-alternative forced-choice with a picture pointing response.

Results and Discussion

SRTs were higher for children than adults in all maskers, with child-adult differences ranging from 3 dB in the 6- and 8-talker maskers to 7 dB in the 2-talker masker. The effect of number of masking talkers differed across the two age groups. For adults, a significant decrement in performance was observed as the number of masking talkers increased from 1 to 2 and from 2 to 3. Similar SRTs were observed for adults in maskers with 3, 4, 6, and 8 talkers. For children, a significant decrement in performance was observed as the number of masking talkers increased from 1 to 2, but SRTs were similar for maskers with 2 or more talkers. These results are consistent with the hypothesis that children experience less benefit than adults from temporal gaps in a speech masker composed of a small number of talkers.

PS-190

Modelling of Spatial Release from Masking in Simulated Cochlear Implanted and Electroacoustic Listeners

Ben Williges[1]; Volker Hohmann[2]; Mathias Dietz[2]; **Tim Jürgens[2]**

[1]Carl-von-Ossietzky Universität Oldenburg; [2]Medizinische Physik and cluster of excellence "Hearing4all", Carl-von-Ossietzky Universität Oldenburg

Introduction

Cochlear implant users, who can use an additional hearing aid in their implanted or non-implanted ear often show better speech intelligibility performance with than without the hearing aid. Many studies have assessed this "electroacoustic

benefit" using spatially co-located speech and noise. However, for normal-hearing listeners, it is well known that separating speech and noise also leads to improved speech intelligibility due to better-ear listening and binaural processing. The amount of this "spatial release of masking" depends on the acoustic condition and the individual hearing loss.

Goals of the study:
The goals of this study are to assess (i) the electroacoustic benefit and (ii) possible binaural cues for speech perception in different combinations of simulated electric and acoustic hearing and different spatial positions of speech and noise. Furthermore (iii), a model of binaural speech intelligibility is used to predict the results obtained from the speech recognition experiments.

Methods:
A headphone experiment with virtual acoustics was designed to assess speech-in-noise-performance (speech reception thresholds, SRTs) using a sentence test in German. A vocoder (mimicking closely the signal processing and physiology in electric hearing) and a low-frequency band pass were used to simulate 10 different forms of "hearing configurations" (bilateral CI, bimodal, hybrid monaural and others). SRTs were assessed for 3 noise azimuths with 10 normal-hearing listeners. A standard model of binaural speech intelligibility (BSIM) in combination with the same signal processing as used for the experiments was used for the predictions.

Results:
Electroacoustic benefit was found in monaural and symmetric binaural electroacoustic hearing for all three noise directions, and in bimodal hearing with additional acoustic hearing on the implanted ear. No electroacoustic benefit was found for bimodal hearing. Head shadow (around 10 dB) and binaural summation were found for bilateral cochlear implanted condition and bilateral electroacoustic condition; in addition, binaural squelch was found for the latter configuration. The model of binaural speech intelligibility showed considerable matches to almost all measured SRTs, when fitted to only two conditions. Electroacoustic benefits and quantitative amounts of binaural cues agreed with measurements.

Conclusion:
Acoustic hearing in combination with simulated cochlear implantation offers electroacoustic benefit in spatially co-located and spatially separated speech and noise conditions. These effects can be successfully modelled using a standard model of (normal) binaural speech intelligibility, which indicates that the interaction between the electroacoustic input and binaural processing is captured by the model.

PS-191

Localization and Speech Performance in Noise in Bone Anchored Implant vs CROS Hearing Aid Users

Hillary Snapp
University of Miami

Introduction
Individuals with a severe unilateral hearing impairment largely lose the ability to localize auditory events within the horizontal plane and experience difficulty in their ability to understand speech, particularly in reverberant or noisy environments. This is due to the loss of auditory cues provided through binaural hearing. Historically, unilateral sensorineural hearing loss (SNHL) was treated with contralateral routing of signal (CROS) hearing aids. However, CROS hearing aids were not well accepted due to complaints of occlusion in the better ear, poor sound quality, discomfort, etc. The introduction of bone anchored implants (BAI) resulted in a resurgence in treatment for unilateral SNHL, and several comparison studies of CROS and BAI devices emerged in the literature suggesting that the BAI system is superior to CROS technology for the treatment of unilateral SNHL. However, this research is now outdated and represents obsolete CROS hearing aid technology. New wireless systems overcome much of the previous acoustic limitations, which led to the earlier reports of limited benefit with CROS technology. We propose that non-invasive wireless CROS technology is capable of providing similar benefit to the more invasive BAI system for unilateral severe-profound hearing loss.

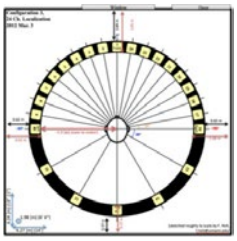

Figure 1. A schematic of the experimental setup with 24 loudspeakers in a circular array with a radius of 1.3 m.

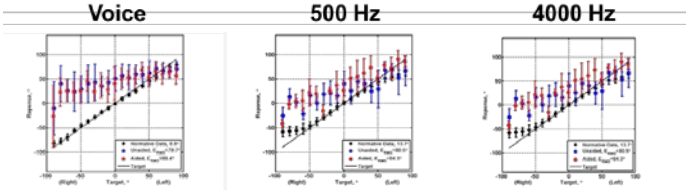

Figure 2. Localization performance average and standard deviations for normal hearing subjects for the voiced 'hey', 500Hz 1./3 oct., and 4kHz 1/3 oct. noise plotted against aided an unaided BAI users.

Methodology:
This clinical study is designed as a single-subject, repeated measures experiment. Localization ability and speech perception in noise was prospectively studied in adult monaural listeners utilizing either BAI or CROS hearing aid as a treatment solution for their hearing loss. All subjects were evaluated in the aided and unaided conditions using an array of 24

speakers emitting narrow and broad band signals, spatially separated by 10 degrees in the front and 30 degrees in the rear. A control group of 10 normal hearing subjects were included for comparison. Subjective outcomes were reported using the Speech, Spatial, and Qualities Scale.

Results
A comparison of localization performance between the outcomes in subjects with severe to profound unilateral hearing loss with BAI and CROS hearing aid users will be presented. Preliminary results indicate that the CROS hearing aid provides similar performance as compared to the BAI system for both localization and speech in noise performance. Objective benefit is correlated to subjective report post treatment

Conclusion
Monaural listeners receive significant improvements in speech in noise for both BAI and CROS hearing aid systems, but no improvement in localization. There is no quantifiable difference in performance between systems for the described outcome measures.

PS-192

Exposure to Consistent Room Reverberation Facilitates Consonant Perception

Norbert Kopčo[1]; **Eleni Vlahou[2]**; Ueno Kanako[3]; Barbara Shinn-Cunningham[4]
[1]P. J. Šafárik University; [2]Department of Psychology, University of California, RIverside; [3]School of Science and Technology, Meiji University; [4]Center for Computational Neuroscience and Neural Technology, Boston University

Background
An important aspect of real-world speech communication is the ability to adapt to reverberant listening environments that distort the speech signal. A few past studies show that consistent exposure to a particular room facilitates speech understanding, at least for a limited set of speech sounds [A. J. Watkins, 2005, J. Acoust. Soc. Am. 118:249–262.] and for sentences with rich lexical information [N. Srinivasan and P. Zahorik, 2013, J. Acoust. Soc. Am. 133: EL33-9]. Here, we present the results of two experiments investigating the effects of room consistency on phoneme perception using a wide range of consonants. Stimuli were nonsense syllables, allowing us to factor out lexical influences on perceptual compensation for reverberation.

Methods
Stimuli were VC syllables consisting of 16 consonants that were preceded by the vowel /a/ spoken by three different talkers, presented over headphones. Using room-related transfer functions, we simulated two different reverberant environments or anechoic space. On each trial, listeners heard an initial "carrier" phrase consisting of 0, 2 or 4 VC syllables, followed by a single target VC syllable. Listeners had to identify the consonant in the final target syllable. In some trials, the target and carrier had the same reverberation (matching), while in others the carrier syllables were simulated with either a different reverberant room (non-matching) or in anechoic space (anechoic). In Exp. 1 the carrier length was randomly varied from trial to trial; in Exp. 2 it was fixed within each block. We hypothesized that phoneme identification would be best in the matching condition, and that the benefit would increase with the length of the carrier phrase.

Results
Qualitatively, there was no difference between randomized and blocked trials. Reverberation hampered phoneme perception, with some consonants being particularly affected. Consistent with our hypotheses, exposure to consistent reverberation improved target consonant identification accuracy compared to when the carrier was anechoic. Relative to non-matching reverberation, the benefit of matching reverberation was less consistent: the benefit was significant for both 2-and 4-VC carrier phrases in Exp. 2 (blocked trials), but only reached significance for the 2-VC carrier phrase in Exp. 1 (randomized trials).

Conclusions
Short-term exposure to a consistent acoustic environment mitigates the detrimental effects of reverberation on phoneme perception, facilitating speech understanding in adverse conditions.

PS-193

Is it Periodicity That Makes Dynamic Harmonic Complexes Less Effective Maskers of Speech Than Noises?

Stuart Rosen; Tim Green; David Perry
UCL

There is much theoretical and practical interest in determining what makes a masker more or less detrimental to speech perception. One striking finding is that harmonic complexes are much less effective maskers than a noise with the same overall spectral envelope. There are at least two possible explanations. Firstly, harmonic complexes consist of discrete spectral components so that, at least at low frequencies where harmonics are resolved, there is the possibility of 'glimpsing' into frequency regions between harmonics where there is little masker energy. Secondly, the periodicity of the complex may allow it to be more effectively segregated or 'cancelled out'. Here we examine the role of periodicity by comparing the relative masking effectiveness of dynamic complexes in which the discrete spectral components form either a harmonic or inharmonic series. The harmonic dynamic complexes have modulations in fundamental frequency (F0) modelled on genuine F0 contours found in connected speech (interpolated through silence and voicelessness), but no other spectral or temporal modulations. Inharmonic complexes are created by spectrally rotating the harmonic complexes around a centre frequency near 2 kHz. This preserves the harmonic spacing but creates an inharmonic series, except when the rotation frequency is an exact multiple of the F0 of the original complex. Because the F0 is changing all the time, this will happen only rarely and fleetingly. In this way we create maskers that differ in periodicity, but are composed of equivalently spaced discrete spectral components and so provide equivalent opportunities for inter-harmonic glimpsing. Speech Reception Thresholds (SRTs) will be determined adaptively for sentences in the presence of maskers with the

same spectral envelope that are either noisy, harmonic or inharmonic through rotation. Comparing the SRTs for harmonic and inharmonic complexes will allow a quantitative assessment of the importance of periodicity in making a harmonic masker less effective than a noisy one.

PS-194

Effects on Sentence Recognition in Speech-Related Maskers of Masker Periodicity, Envelope Fluctuations, and Number of Fundamental Frequency Contours

Tim Green; Stuart Rosen
UCL

Speech is often perceived against a background of various numbers of competing voices. Many interrelated factors determine intelligibility in such circumstances. For example, masker fluctuations may allow glimpsing; fundamental frequency (F0) contours may help separate target and competing voices; informational masking (IM) may occur and both target and masker periodicity may be important. Here we attempt to isolate the contributions of certain key masker properties using novel unintelligible maskers that eliminate IM due to masker intelligibility but allow the independent manipulation of the number of F0 contours and availability of glimpsing opportunities. One set of maskers comprised speech-shaped noise (SSN), either unmodulated or amplitude modulated with one of the following: a 10-Hz square wave, a 10-Hz sinusoid, an envelope extracted from single-talker connected speech, an envelope extracted from two-talker babble. Each envelope manipulation was also applied to carriers consisting of pulse trains whose F0 tracked contours extracted from connected male speech. F0 contours were extrapolated through periods of silence and voicelessness. The number of independent F0-contour pulse trains within a masker was 1, 2, 3 or 4. Target speech consisted of IEEE sentences (male talker) passed through a 12-channel noise vocoder (30-Hz envelope filter). The vocoder eliminated periodicity and degraded spectral resolution in a manner similar to cochlear implant speech processing. Speech reception thresholds (SRTs) were measured adaptively for each of the 25 (unvocoded) masker conditions (5 carriers x 5 envelopes). There were significant main effects both of carrier and envelope, with no significant interaction. Performance with square wave modulation was significantly better than that in all other envelope conditions, which did not differ from each other. Thus, only square wave modulation produced better performance than unmodulated maskers, so that glimpsing did occur, despite the comparatively high SNRs required for understanding vocoded speech, but only with the most extreme form of envelope fluctuation. Envelope effects were consistent across carrier types, indicating no special role for periodicity in glimpsing, at least with these aperiodic targets. Performance was better for maskers with one F0 in the carrier than for all other carrier types and better for 2-F0 carriers than for SSN carriers. This indicates that masker periodicity contributes to better speech intelligibility and also that the presence of additional competing voices can have detrimental effects due to the presence of additional competing F0 contours, independent of changes in the availability of glimpsing opportunities. (Supported by the Medical Research Council, Grant Number G1001255).

PS-195

Interactions Between Spectral Resolution and Inherent Temporal-Envelope Noise Fluctuations in Speech Understanding in Noise

Evelyn Davies-Venn; Heather Kreft; Andrew Oxenham
University of Minnesota

Introduction

Recent studies using normal-hearing listeners have discovered that the inherent temporal-envelope modulation in noise, rather than the overall noise power, limits our ability to understand speech in noise (Stone and Moore, 2014, J. Acoust. Soc. Am. 135:1967-77). In contrast, cochlear-implant (CI) users' speech perception in noise seems unaffected by the inherent fluctuations (Oxenham and Kreft, 2014, Trends in Hearing 18:1-14). The current explanation for the lack of effect in CI users is that channel interactions, produced by poor spatial (spectral) resolution and current spread, result in noise temporal envelopes with less inherent modulation. The current study measured the effects of inherent fluctuations in vocoder simulations of CI processing as a function of channel separation, manipulated by varying the effective slopes of filtering (simulating more and less focused stimulation methods) and the spectral spacing between adjacent channels (simulating the distance between adjacent electrodes).

Methods

Speech recognition in noise was measured in young normal-hearing listeners for tone-vocoded AZBio sentence lists using pure-tone and Gaussian-noise maskers at various signal-to-masker ratios with speech presented at 65 dB SPL. Various degrees of current spread were simulated with filter slopes of 8, 16 and 24 dB/ octave, and different channel separations were tested by dividing the spectrum into 16, 8, and 6 channels.

Results

Overall performance improved with increasing number of channels and increasing filter slopes. In the 16-channel condition, performance improved as the filter slopes became steeper but, even with slopes of 24 dB/octave, listeners did not benefit from the lack of inherent fluctuations in the pure-tone maskers. In the 8- and 6-channel conditions, the additional spacing between adjacent channels reinstated some of the benefit of the pure-tone maskers, but only when the analysis filters were as narrow as in the original 16-channel condition. Wider analysis filters resulted in a reduced difference between the pure-tone and noise maskers, presumably because of the decrease in relative low-frequency modulation energy with increases in filter bandwidth.

Conclusions

The results suggest that even relatively steep filters, simulating reduced current spread in CI users, can still reduce or eliminate the effect of inherent noise fluctuations on speech intelligibility. The outcome suggests that dramatic improve-

ments in the spectral resolution of CI users and large spacing between adjacent electrodes would be needed to recreate the effects of inherent noise fluctuations on speech perception, as observed in normal-hearing listeners.

PS-196

The Cafeteria Study: Effects of Visual Cues, Hearing Protection, and Real-World Noise on Speech Recognition

Mary Barrett[1]; **Kerrianne Costantino**[1]; Julie Cohen[2]; Sandra Gordon-Salant[1]; Douglas Brungart[2]
[1]University of Maryland; [2]Walter Reed National Military Medical Center

Introduction

Previous studies that have examined the impact of interfering noise on speech understanding have used prerecorded speech stimuli played to individuals in a laboratory setting. These studies may not account for the acoustic and social factors that potentially impact a person's ability to communicate adequately in real-world settings. The purpose of this study is to investigate how well normal-hearing listeners can perform in an interactive communication task when in a noisy real-world environment.

Methods:

Groups of four native English speakers, ages 18-80, with normal hearing were tested in a college cafeteria. The group members performed the task in one of four conditions, which were semi-randomized across listeners for each block: a baseline condition, a surgical mask condition (no visual cues), and two conditions with hearing protection devices (3M Combat Arms earplugs, in the open and closed conditions). There were eight blocks of 52 trials. Each member had a hand-held tablet and wore a head-tracking device. During each trial, one talker said a phrase from the Modified Rhyme Test (e.g. "You will mark den please"), and the three listeners selected a key word from a closed set of six words on the tablet. A sound level meter measured the level of the ambient noise and the target speech. The percent correct, reaction time, and degree of head movement were measured for each listener.

Results:

Preliminary data were collected from 52 participants. The average level of background noise measured across all trials was 72 dBA. When visual cues were removed via the surgical mask, listeners performed more poorly than in the baseline condition. The performance of the listeners also declined when wearing the hearing protection devices, and this effect was more detrimental in the closed than the open condition. Reaction times increased compared to the baseline condition when visual cues were removed and when earplugs were worn. Additionally, reaction times were longer when the earplugs were closed compared to open. Listeners tended to move their heads more during more difficult listening conditions.

Conclusions:

The results of this preliminary study provide some valuable insights into the behaviors adopted by talkers and listeners when communicating in noisy real-world environments. The results also confirm that previous findings showing enhanced speech perception performance with visual cues and reduced speech communication with the use of hearing protection devices generalize to more realistic real-world listening environments.

PS-197

Line of polarization Reversal (LPR) is Located Lateral to the Striola in the Chinchilla Utricular Macula

Anna Lysakowski[1]; Steven D. Price[1]; Jay M. Goldberg[2]
[1]Univ. of Illinois at Chicago; [2]Univ. of Chicago

The striola is a region of the utricular macula (UM) recognized by the presence of pure-calyx afferents (Fernández et al. 1990), which are selectively stained by calretinin (Desmadryl and Dechesne, 1992). The UM consists of two zones separated by a Line of Polarity Reversal, or *LPR*. Traditionally, it was thought that the *LPR* ran down the middle of the striola (Lindeman, 1969). Recent studies in mice (Li et al., 2008) and rats (Schweizer et al., 2009), however, have shown that the *LPR* is located along the lateral edge of the striola. Here, we determine whether a similar arrangement holds in the Chinchilla laniger, a species from a different rodent suborder, which has been used in many of our physiological studies (e.g., Goldberg et al., 1990a,b). The chinchilla, like mice and rats, is a lateral-eyed mammal.

Individual endorgans were dissected and their hair bundles removed by sonication. Hair-bundle polarization was determined by the location of the kinocilium, indicated by a hole in the cuticular plate, which was otherwise labeled by spectrin. Calretinin marked the pure calyx afferents in the striolar region (Desai et al., 2005a,b).

As in the mouse and rat, the *LPR* in the chinchilla is located at the lateral edge of the utricular striola separating the utricular macula into two zones: 1) the medial extrastriolar and striolar regions; and 2) the lateral extrastriola.

Tract-tracing studies of the central projections of the various utricular zones done by Maklad et al. (2010) indicate that the first zone projects to the vestibular nuclei, whereas the lateral extrastriola projects to the cerebellum. Combining the central projections of the utricular macula with the hair-cell polarization of the various zones results in the various righting responses needed to maintain an upright posture of the head and body. The results have profound implications for sensory processing in that the pure calyx afferents, located medial to the *LPR*, may all project only to the vestibular nuclei, and not to the cerebellum.

PS-198

Otolith Organ Structures and Functions in Caspase-3-Deficient Mice

Naoki Shimizu[1]; Atsushi Tamura[1]; Rebecca Cook[1]; Scott Wood[2]; Adrian Perachio[1]; Tomoko Makishima[1]
[1]University of Texas Medical Branch; [2]Azusa Pacific University

Background

Caspase-3 (Casp3) is a universal cell death effector protease. Compared with the auditory phenotype in Casp3 mutant mice, details of the vestibular phenotype are not well known. Previously, we reported impaired vestibulo-ocular reflex (VOR) and semicircular canal malformations in the Casp3 deficient mice, showing caspase-3 plays an important role in the vestibular system. In the present study, we extended observations to the otolith organs revealing functional and histological characteristics of Casp3 mutant mice, focusing on age-related changes.

Methods

Functional studies of otolith organs were conducted by recording otolith-induced ocular responses using the counter rotation paradigm. We used two simultaneous yaw axis rotation centrifugations to generate a rotating gravity vector similar to an off-vertical axis rotation (OVAR) but with a larger resultant gravito-inertial force (pseudo-OVAR). Evaluation of hair cells was carried out in whole mount vestibular epithelia of the utricles and the saccules of the corresponding mice. To verify the effect of aging, mice in different age groups were compared.

Results

Similar to wild-type mice, we observed two components in the horizontal slow phase eye velocity in all *Casp3+/-* mice; unidirectional nystagmus, for which the velocity storage mechanism (VSM) is responsible, and oscillatory eye movements which arise through linear VOR. In contrast, robust nystagmus was rarely evoked, with reduction of horizontal modulations in most of aged *Casp3-/-* mice (>18M). Hair cells in the utricle remained intact throughout the age range studied (up to age 24M) in both *Casp3+/-* and *Casp3-/-* mice, whereas severe degeneration of hair cells in the saccule was frequently observed in aged *Casp3-/-* mice. These histological findings were not associated with functional observations, e.g. a Casp3-/- mouse with significant hair cell degeneration in the saccule still presented robust nystagmus.

Conclusions

The ocular performance was independent of the numbers of hair cells in the saccule, indicating that the responses during pseudo-OVAR arise largely through activation of utricular hair cells. The Casp3-/- mice could serve as a tool for selective evaluation of each otolith organ, the utricle and the saccule. The sparsely evoked nystagmus in aged *Casp3-/-* mice may attribute to inadequate peripheral inputs to VSM or altered central neural mechanism itself.

PS-199

Zonal Differences in Na+ Currents of Crista Ampullaris Calyx Afferent Terminals

Frances Meredith; Katherine Rennie
University of Colorado Denver

Introduction

Vestibular afferents form synapses with hair cells in central zones (CZ) and peripheral zones (PZ) of the crista. Pure calyx afferents contact CZ type I hair cells, whereas dimorphic afferents branch to form calyx and bouton endings that terminate on type I and type II hair cells respectively in both zones. Vestibular afferents show regular or irregular spontaneous firing, but the role of intrinsic ion channels in determining firing pattern is unclear. Interesting differences in Na^+ channel distribution within vestibular afferents have recently emerged. $Na_v1.5$ immunostaining was detected on the inner face of calyces and $Na_v1.6$ was seen at the heminode of dimorphic afferents, but was not found in pure calyx afferents (Lysakowski et al. 2011).

Methods

We recently developed a crista slice preparation to investigate regional differences in calyx properties. We used whole cell patch clamp to compare Na^+ currents in calyx-bearing afferents innervating type I hair cells of CZ and PZ in gerbil crista slices (100-120 µm; postnatal days 20-29). Recordings were made with K^+ or Cs^+-based intracellular solutions.

Results

In isolated calyces, tetrodotoxin (TTX, 500 nM) blocked 34 to 93 % of peak Na^+ current (n = 7), suggesting the presence of both TTX-sensitive and TTX-resistant Na^+ channels. In the slice preparation, Na^+ currents in CZ calyces showed slower activation and inactivation kinetics than PZ cells. Median time to peak was 0.26 ms in CZ calyces (n = 8), significantly longer than the value of 0.21 ms in PZ calyces (n = 8, $P<0.005$, Mann-Whitney Rank Sum Test). Median peak current in CZ calyces (n = 6) was -54 mV, significantly more hyperpolarized than -39 mV in PZ calyces (n = 6, $P<0.005$, Mann-Whitney Test). Half-inactivation of Na^+ currents averaged -85.8 ± 4.6 mV (SEM) in CZ calyces (n = 6) and -80.3 ± 2.7 mV in PZ cells (n = 10). Slope factor was 2.9 ± 0.8 in CZ cells (n = 6), significantly smaller than in PZ cells (5.5 ± 0.6, n = 10, $P<0.05$, t-test).

Conclusion

CZ calyx terminals have Na^+ currents with slower kinetics and different voltage sensitivities than PZ terminals. $Na_v1.6$-mediated currents, activating at more depolarized voltages and showing faster activation and inactivation kinetics, may predominate in dimorphic afferents. Other Na_v channel subunits may be important in CZ calyces.

PS-200

Determining Roles of Ionic Conductances in the Firing Characteristics of Vestibular Calyx Afferents

Matthew Kirk; Francis Meredith; Katherine Rennie; Tim Benke

University of Colorado

Introduction

Electrophysiological properties of vestibular afferents differ between central zones (CZ) and peripheral zones (PZ) of the crista and corresponding striolar and extrastriolar zones of the utricle and saccule. Centrally-located afferents typically have irregular firing, whereas peripheral afferents have more regular firing patterns. We incorporated Hodgkin-Huxley-style ionic conductances into a mathematical model to simulate zonal differences in firing properties of calyx-bearing afferents.

Methods

Whole cell patch clamp recordings were made from calyx afferent terminals in slices of gerbil crista. Channel blockers were applied to assess contributions of sodium and potassium currents. A mathematical model of the calyx terminal (Meredith et al. 2012) was modified to simulate firing as a distributed parameter model through an extended formulation of branched nerve equations (Hines 1984). Hodgkin-Huxley formulae were used to simulate membrane currents with sections of calyx membrane characterized with a constant capacitance and ionic currents representing Na+, hyperpolarization-activated cyclic nucleotide-gated (HCN), inactivating A-type K+, delayed rectifier (KCNQ) and leak currents respectively. Individual conductances were ascribed to the model from our experimental patch clamp recordings from central and peripheral zones and background literature.

Results

Whole cell recordings revealed large inward Na+ currents and outward K+ currents. Median inactivation of outward K+ currents was significantly greater in PZ calyces (9.4%, n = 66) than in CZ calyces (4.2%, n = 33; $P < 0.001$). Slowly activating inward HCN currents were observed in approximately 70 % of calyx terminals tested. Resting potential was similar in PZ and CZ calyx terminals (-58.4 ± 2.3 n = 10 CZ; -55.6 ± 1.1 n = 38 PZ; difference not significant). Approximately one quarter of cells showed spontaneous repetitive firing (range 1.3 to 63 Hz, mean 17.4 ± 3.4 Hz, n = 10 in CZ and 16.6 ± 4.0 Hz, n = 19 in PZ terminals). Firing pattern was most regular in PZ cells. Repetitive firing consistent with experimental data was evoked in calyx models in response to small depolarizing current steps.

Summary

We found a statistically significant difference in K+ current inactivation between CZ and PZ calyces. Underlying conductances were investigated by pharmacological and modeling approaches to assess regional variations.

PS-201

Effect of Brain-Derived Neurotrophic Factor, BDNF on TRPV1 and TRPA1 Channels in the Cultured Rat Vestibular Ganglia

Takefumi Kamakura[1]; Tadashi Kitahara[2]; Yusuke Ishida[3]; Yukiko Nakamura[3]; Takahiro Yamada[3]; Makoto Kondoh[3]; Yasumitsu Takimoto[3]; Takao Imai[3]; Arata Horii[4]; Hidenori Inohara[3]; Shoichi Shimada[3]

[1]Minoh City Hospital; [2]Nara Medical University; [3]Osaka University Graduate School of Medicine; [4]Osaka National Medical Center

Background

Transient receptor potential vanilloid (TRPV)-1and transient receptor potential ankyrin (TRPA)-1 are both cation channels co-expressed in sensory neurons such as dorsal root ganglia (DRG) and trigeminal ganglia (TG). TRPV1 is activated by noxious heat (>43°C), protons, capsaicin, and anandamide etc., while TRPA1 is activated by noxious cold stimuli (<17°C), alkaline pH (>8.5), cinnamaldehyde, mustard oil, allyl isothiocianate and icilin etc. In our previous study, TRPV1 and TRPA1 are expressed in the rat vestibular ganglia (VG) and it is suggested that these two channels in VG neurons might participate in vestibular function and/or dysfunction such as vertigo. On the other hand, brain-derived neurotrophic factor, BDNF is expressed in the VG neuron and BDNF and TrkB mRNA are upregulated by unilateral aminoglycoside (gentamycin) instillation into perilymph (Popper et al, Brain Research, 1999).

The objective of this study is to investigate the effect of BDNF on the functional expression of TRPV1 and TRPA1 channels in the cultured rat vestibular ganglion neurons.

Methods

To evaluate the effect of BDNF on TRPV1 and TRPA1, we cultured the rat vestibular ganglion neurons with and without BDNF treatment and examined their function by Ca^{2+} imaging experiments.

Results

We found that BDNF treatment of rat VG neuron significantly increased the fraction of capsaicin-sensitive (TRPV1-expressing) neurons and that of cinnamaldehyde-sensitive (TRPA1-expressing) neurons. Moreover BDNF treatment significantly increased the fraction of both capsaicin- and cinnamaldehyde-sensitive neurons.

Conclusions

In summary, our data showed evidence for a role of BDNF in regulating the pattern of expression of TRPV1 and TRPA1 channels, leading to increased co-expression of these two channels.

PS-202

5-HT3 receptor Expression in the Mouse Vestibular Ganglion

Yasumitsu Takimoto[1]; Yusuke Ishida[1]; Yukiko Nakamura[1]; Takefumi Kamakura[1]; Makoto Kondo[1]; Tadashi Kitahara[2]; Takao Imai[1]; Atsuhiko Uno[1]; Arata Horii[3]; Hidenori Inohara[1]; Shoichi Shimada[1]

[1]Osaka University; [2]Nara Medical University; [3]Osaka National Hospital

Introduction

The 5-hydroxytryptamine type 3 (5-HT_3) receptor is a ligand-gated ion channel and a member of the Cys-loop family of receptors. Previous studies have shown 5-HT_3 receptor expression in various neural cells of the central and peripheral nervous systems. Although the function and distribution of the 5-HT_3 receptor has been well established, its role in the inner ear is still poorly understood. Moreover, no study has yet determined its localization and function in the peripheral vestibular nervous system. To address this question, we investigate here the localization of the 5-HT_3 receptor in the mouse peripheral vestibular nervous system.

Methods

C57BL/6J wild-type (WT) and 5-HT_3 receptor knock-out (KO) mice were used in this study. We performed RT-PCR and *in situ* hybridization to examined 5-HT_3 receptor mRNA localization in the inner ear. Moreover, to confirm the presence of functional 5-HT_3 receptors channels in vestibular ganglion (VG) neurons, we studied the physiological effects of a selective 5-HT_3 receptor agonist (SR57227A) on freshly isolated VG neural cells from adult mouse using the measurement of intracellular calcium ion concentration (Ca^{2+} imaging).

Results

We found that both 5-HT_{3A} and 5-HT_{3B} receptor mRNA is expressed in VG neurons and also that 5-HT_3 receptor mRNA is localized in the VG of the inner ear. 5-HT_{3A} receptor mRNA is expressed in approximately 30% of VG (superior and inferior divisions) neurons, while 5-HT_{3B} receptor mRNA in VG neurons is expressed with a much lower signal. Our cell size analysis of 5-HT_{3A} receptor-expressing VG neurons showed that 5-HT_{3A} receptors are mainly expressed in medium or large sized cells. SR57227A induced increases in intracellular calcium in several VG cells from WT mice. However, SR57227A caused no change in intracellular calcium in VG neurons from 5-HT_{3A} receptor KO mice.

Conclusions

We have shown that 5-HT_3 receptor mRNA is localized in mouse inner ear VG neurons. Moreover, 5-HT_3 receptors expressed in VG neurons form a functional ion channel, as shown by a positive response to a selective 5-HT_3 receptor agonist. Together, these findings suggest that functional 5-HT_3 receptors are synthesized in VG neurons and might modulate the peripheral vestibular nervous system.

PS-203

Infrared Radiation Elicits Transient Plasma Membrane Depolarization in Cultured Neonatal Spiral and Vestibular Ganglion Neurons

Vicente Lumbreras; Esperanza Bas Infante; John Barrett; Suhrud Rajguru

University of Miami

Background

Infrared radiation (IR) allows direct stimulation of inner ear neurons without genetic or pharmacological manipulation. IR has been shown to elicit intracellular Ca^{2+} transients and electrical responses in neurons. These IR-evoked intracellular Ca^{2+} events are likely driven by Ca^{2+} transfer between the endoplasmic reticulum (ER) and mitochondria. The present study examines the potential contributions of IR-evoked intracellular Ca^{2+} release to the plasma membrane depolarization in cultured inner ear neurons.

Methods

Cultures of spiral and vestibular ganglion neurons isolated from p2-p3 rat pups were used in all experiments. Changes in plasma membrane potential ($\Delta\Psi_p$) were measured using FluoVolt™ Membrane Potential Kit. After incubation for 30 minutes, the dye was washed and replaced with artificial perilymph or Ca^{2+}-free DPBS. In specific experiments, the media temperature was cooled down to 4°C. A 140 mM potassium gluconate solution was added as a positive control to neurons pre-treated with valinomycin. IR stimulation (λ = 1863 nm) was delivered with a 400 µm diameter optical fiber connected to a Capella laser. A train of IR pulses (100 ms, 100 pps, 178 to 374 mJ cm^{-2}) was delivered to the neurons for 30 s while measuring changes in FluoVolt™ fluorescence. Pharmacological compounds targeting mitochondrial Ca^{2+} cycling (Ruthenium Red, CGP-37157), intracellular Ca^{2+} (BAPTA-AM), and Ca^{2+} extrusion from the ER (Ryanodine, Cyclopiazonic Acid) were used to study the contributions of IR induced intracellular Ca^{2+} release.

Results

Positive control responses in FluoVolt™ fluorescence could be elicited by adding potassium gluconate. Trains of IR stimuli delivered to the neurons resulted in a transient increase in FluoVolt™ fluorescence, suggesting IR-evoked $\Delta\Psi_p$ depolarization. The depolarization increased linearly with radiant exposure. Removal of extracellular Ca^{2+} and cold media temperatures did not alter the IR-evoked $\Delta\Psi_p$ depolarization. Pharmaceutical agents inhibiting the IR induced intracellular Ca^{2+} release significantly reduced the IR-evoked $\Delta\Psi_p$ depolarization with the response recovering following washout of the agents.

Conclusions

The results suggest that IR transiently depolarized $\Delta\Psi_p$ in the neurons. The observed depolarization does not seem to be driven primarily by acute extracellular Ca^{2+} influx or thermal effects on the plasma membrane. The pharmacological analysis suggests that the IR induced intracellular Ca^{2+} release may contribute to the IR-evoked $\Delta\Psi_p$ depolarization.

PS-204

Spontaneous Discharge in Mammalian Vestibular Afferents Modelled as Gamma-censored Poisson Processes

Larry Hoffman[1]; Michael Paulin[2]
[1]Gefgfen School of Medicine at UCLA; [2]University of Otago, Dunedin, New Zealand

Background

Vestibular afferents exhibit broad heterogeneity in spontaneous discharge interspike interval (ISI) distributions, and have been modeled by Gamma functions with shape (k) and scale (Θ) parameters. The Gamma model implies a fast Poisson process underlying spontaneous activity, whereby spikes are triggered by integrating Poisson events. However, the temporal characteristics of ISI distributions are inconsistent with simple Gamma models, requiring an offset parameter (d). This parameter is fundamentally different from k and q in that it represents a fixed offset, not a parameter of a formal stochastic process. Our goal was to generalize the Gamma model to account for temporal offsets in ISI distributions within an underlying stochastic model.

Methods

The Gamma-censored Poisson process (GCP) is the waiting time for k events in a Poisson process plus 1 event in another, independent Poisson process. The Gamma process functions to 'gate' events in the second process until a Gamma event occurs, enabling the next Poisson event to pass and the Gamma process is reset. We derived analytical forms of offset Gamma (OG) and GCP processes from spontaneous discharge of several hundred chinchilla horizontal and superior cristae afferents that represented broad ISI heterogeneity. This enabled us to compute parameters of OG (k,Θ,d) and GCP (k,Θ,τ) models directly from ISI data. The Kullback-Liebler divergences (KLD, representing differences between probability distributions) were computed between fitted models and ISI distributions.

Results

While OG models provided reasonable fits to spontaneous ISI distributions for all afferents, GCP models provided better fits for a large fraction of afferents. In no case was the OG model fit better than the GCP model. The associations between parameters of each subcomponent and the broad ISI heterogeneities were explored through regression analyses of model parameters and spontaneous discharge CV. We found that the Gamma subcomponent k was closely associated with ISI CV for afferents exhibiting CV≤0.1 (r^2=0.99). However, this association deteriorated for afferents exhibiting CV>0.1 (r^2=0.67). The parameter t of the GCP model's Poisson subcomponent was more closely associated with ISI CV for afferents with high CVs (i.e. CV>0.1; r^2=0.88) than those exhibiting low CVs (i.e. CV≤0.1; r^2=0.44).

Conclusions

The GCP model replaces the parameter d within the OG model by a Poisson rate parameter τ. The GCP model implies that vestibular afferent spontaneous discharge reflects a Poisson process gated by a separate Gamma process (sum of Poisson processes) which may be associated with synaptic events and dendritic integration, respectively.

PS-205

Pharmacological Characterization of the Synaptic Mechanisms Governing the Responses of Mammalian Vestibular Afferents to Efferent Stimulation

Joseph Holt; Paivi Jordan; Glenn Schneider
University of Rochester Medical Center

Background

Mammalian vestibular organs are endowed with a prominent cholinergic efferent innervation that gives rise to numerous varicosities abutting calyx terminals and hair cells. Responses of mammalian vestibular afferents to efferent stimulation are effectively excitatory and the resulting excitation often consists of fast and slow components differing in their activation kinetics and duration. Although a role for acetylcholine (ACh) has been suggested, the synaptic mechanisms underlying excitatory efferent actions in mammals are not well understood. To address this issue, we developed a mouse model to characterize the physiology and pharmacology of mammalian vestibular afferent responses to electrical stimulation of the efferent vestibular system (EVS).

Methods

C57Bl6 mice were anesthetized with urethane/xylazine, fitted with a tracheal cannula, and connected to a ventilator. A posterior craniotomy and cerebellar aspiration were performed to expose the right vestibular nerve branch and floor of the fourth ventricle. Glass microelectrodes were used to record the discharge of vestibular afferents in the anterior branch of CNVIII, visually identified just as it exits the otic capsule. Discharge regularity (CV*) of each afferent was computed from interspike intervals taken from background activity. To electrically stimulate the EVS, 5-s shock trains (333/s) were delivered to a four-electrode linear array lowered into the floor of the fourth ventricle along the rostrocaudal axis. Any muscle contractions resulting from efferent stimulation were subsequently blocked by IP administration of the paralytic d-tubocurarine.

Results

Mouse vestibular afferents were routinely excited by brainstem stimulation. Consistent with the projection of efferent neurons to the vestibular periphery, afferent excitation during EVS stimulation was abolished by sectioning the brainstem between the stimulating and recording electrodes. Like previous mammalian vestibular preparations, efferent-mediated excitation of vestibular afferents contained a fast perstimulus component (25-60 spikes/s) and a much slower component (10-15 spikes/s) persisting for 30-40 seconds after the stimulus. Efferent-mediated excitation of regularly-discharging afferents (CV*<0.1) consisted primarily of the slow component whereas EVS stimulation recruited both fast and slow excitation in irregularly-discharging afferents (CV*>0.2). Systemic administration of the muscarinic ACh receptor (mAChR) antagonists, atropine and scopolamine, blocked efferent-mediated slow excitation whereas the nicotinic ACh receptor (nA-

ChR) antagonist DHβE selectively blocked efferent-mediated fast excitation while leaving the efferent-mediated slow component intact. Systemic administration of the KCNQ channel antagonist XE991 also antagonized efferent-mediated slow excitation suggesting a role for M-currents.

Conclusion

Efferent-mediated fast and slow excitation of vestibular afferents is mediated by nAChRs and mAChRs, respectively. Ongoing work is focused on specifying receptor subtypes.

PS-206

Fast Cholinergic Responses in Cristae of Control and Alpha-9 subunit Knockout Mice

Lauren Poppi[1]; Hessam Tabatabaee[1]; Robert Callister[1]; Phillip Jobling[1]; Americo Migliaccio[3]; Joseph Holt[2]; Rebecca Lim[1]; Alan Brichta[1]

[1]The University of Newcastle; [2]University of Rochester; [3]Neuroscience Research Australia

Introduction

Acetylcholine (ACh) is the predominant neurotransmitter used by the mammalian peripheral efferent vestibular system (EVS). However, the precise cellular mechanisms underlying cholinergic EVS activation in mammals is unclear. Here we use a combination of 'control' (C57/Bl6 and CBA/129) and alpha-9 subunit knockout mice (alpha-9 KO; JAX strain 005696) to determine the cholinergic contribution to the activity of three major neuroepithelial components in the vestibular crista: type II hair cells, type I hair cells, and calyx afferent terminals. We used our semi-intact preparation of the mouse inner ear that preserves the cellular microarchitecture and allows us to record from individual cellular components in response to exogenously applied acetylcholine.

Methods

The semi-intact preparation of vestibular organs consisted of a vestibular triad including the horizontal and anterior cristae, and utricle. Whole-cell patch clamp recordings were made from hair cells and calyx afferent terminals using a KCl-gluconate internal solution. ACh (100 - 300 μM) was applied using a picospritzer to evoke cholinergic responses. Strychnine, apamin, and DHBE were used to block alpha-9 subunit containing nicotinic receptors (a9nAChRs), small-conductance calcium-activated potassium channels (SK), and alpha4-beta2 containing nAChRs (a4b2 nAChRs), respectively.

Results

Cholinergic activation has a complex and heterogeneous effect on the cellular components of the mouse crista. During brief ACh exposure (100 ms duration) in control mice, most type II hair cells displayed a triphasic current response; a brief, initial, depolarizing inward current, gated by the a9nAChRs (blocked by strychnine), and two distinct hyperpolarizing outward currents gated by SK channels (both blocked by apamin). The two outward currents were putatively identified as SK_2 and SK_3 based on kinetics, reversal potential, and sensitivity to apamin. The triphasic current was absent in alpha-9 KO mice. An inward current was also identified in calyx terminals from both control and alpha-9 KO mice suggesting a possible role for a4b2 nAChRs. In calyx afferent terminals and type I hair cells we also recorded long-lasting ACh-induced responses, which suggests the presence of muscarinic ACh receptors. We found no differences in ACh responses between C57/Bl6 and CBA/129 control mice.

Conclusions

As in outer cells of the cochlea, type II hair cells in the mammalian crista appear to be inhibited by ACh exposure through the combined activity of a9nAChRs and SK channels. In contrast, calyx afferent terminals are excited by presumed a4b2 nAChRs. The response of type I hair cells remains to be fully characterized.

PS-207

Distribution And Damage of Gentamicin in Vestibular Efferent System after Transtympanic Administration

Yi-Bo Zhang[1]; Qianru Wu[2]; Chunfu Dai[3]

[1]Fudan University, Shanghai, China; [2]Eye Ear Nose and Throat Hospital, Fudan University; [3]Department of Otology and Skull Base Surgery, Eye Ear Nose and Throat Hospital, Fudan University

Introduction

Transtympanic administration of gentamicin is an effective strategy in treating interactable vertigo. However, complications of hearing loss and disequilibrium are still troublesome when applying transtympanic administration of gentamicin. Disequilibrium associated with vestibular disorders depends on vestibular compensation. Vestibular efferent neurons may promote vestibular compensation by moderating the property of firing rate of vestibular afferents. We aimed to explore the distribution and damage of gentamicin in vestibular efferent system after transtympanic administration.

Methods

Six albino guinea pigs were transtympanically administrated with 100ul gentamicin (60mg/ml) and sarcrifaced at 3 days. Brainstems were fixed with trancardio perfusion of 4% paraformaldehyde-0.125% glutaraldehyde, harvested and then cut into 50um slices on vibratory microtomes. We selected slices of vestibular efferent neuron level and then immunostained with anti-gentamicin antibody, followed by DAB staining. Then we selected the region of vestibular efferent neurons with positive DAB staining for observation under transmission electron microscope.

Other 6 albino guinea pigs were transtympanically injected with 100ul gentamicin (5mg/ml) and sacrificed 3 days later. Vestibular semicircular ampulae were harvested after fixation of 4% paraformaldehyde-0.125% glutaraldehyde.Then we cut them into 50 nm ultrathin sections after embedding. Ultrathin sections were blocked with 1% BSA , immunostained with gentamicin antibody followed by 15nm colloidal gold, and then observed under transmission electron microscope.

Results

We found that intensive gentamicin located in vestibular efferent system bilaterally after transtympanic administration ipsilaterally at 3 days. Gentamicin located along the pathway of ipsilateral vestibular nerve trafficking from the vestibular

end organs to the vestibular efferent neurons. Vestibular efferent neurons with positive gentamicin particles showed significant damage through transmission electron microscope. Gentamicin was demonstrated in ipsilateral vestibular efferent synapse, along the vestibular efferent fibers and then into bilateral vestibular efferent neurons.

Conclusion

This study demonstrated that gentamicin was taken up by vestibular efferent synapses, trafficked along the vestibular nerve, and finally located in the vestibular efferent neurons after transtympanic administration.We also observed that 60mg/ml gentamicin resulted in damage of neurons under transmission electron microscope. It suggested that high dosage of gentamicin may result in vestibular disequilibrium after local injection. Using of low dosage of gentamicin may avoid the damage and further avoid disequilibirum.

PS-208

Does Gentamicin Directly Target on the Dark Cells following Intratympanic Gentamicin Injection

Chunfu Dai[1]; Feng Zhai[2]; Ru Zhang[3]; Peter Steyger[4]

[1]Eye Ear Nose and Throat Hospital, Fudan University; [2]Fudan University; [3]Tongji University; [4]OHSU

Objective:

To clarify whether gentamicin affects vestibular dark cells in guinea pigs, and relieves patients of aural fullness with intractable Meniere's disease (MD) following intratympanic administration.

Materials and Methods

Purified gentamicin-Texas Red (GTTR) was injected intratympanically in guinea pigs that were sacrificed at 1, 3, 7, 14 and 28 days. GTTR uptake was examined in hair cells, transitional cells and dark cells in vestibular end-organs were examined. Specific attention was paid to its distribution in dark cells under confocal microscopy, and the ultrastructure of dark cells using electron microscopy (EM), following intratympanic injection.

Results

Dark cells in the semi-circular canals showed weak GTTR uptake at 1, 3, 7, 14 and 28 days after intratympanic injection, with no significant differences at various time points after injection. However, the adjacent transitional cells demonstrate intense GTTR uptake that was retained for at least 28 days. Ultrastructural studies demonstrated negligible characteristics associated with apoptosis or necrosis in these dark cells. The tight junctions between dark cells showed no signs of disruption at 7 or 28 days after injection.

Conclusion

Intratympanic gentamicin has little direct impact on the vestibular dark cells.

PS-209

Histological and Functional Evaluation of the Vestibular System of Connexin 26 Null Mice

Min Young Lee[1]; Yohei Takada[2]; Lisa Beyer[2]; Donald Swiderski[2]; Shaked Shivatzki[3]; Karen Avraham[3]; Yehoash Raphael[2]

[1]University of Michigan; [2]Kresge Hearing Research Institute, Department of Otolaryngology, University of Michigan; [3]Department of Human Molecular Genetics and Biochemistry, Sackler Faculty of Medicine and Sagol School of Neuroscience, Tel Aviv University

Mutations of the GJB2 (connexin 26) gene cause significant hearing loss, but balance disorders are mild or absent. Mouse models for loss of connexin 26 function also demonstrate hearing loss and cochlear pathology but the extent of pathology and dysfunction in the vestibular system are less well characterized. To understand the outcome of connexin 26 mutations in the vestibular system, we evaluated the balance and histology of the vestibular sensory epithelium in a mouse with connexin 26 loss of function.

We compared transgenic C57BL/6 mice, in which cre-Sox10 drives excision of the connexin 26 gene from non-sensory cells flanking the sensory epithelium of the inner ear (Gjb2-CKO mice, designated CKO) to age-matched wild-types (WT). Vestibular function was tested at 4 months (3 WT and 3 CKO) using a rotarod and a spinning test in which stress induced by the spinning of a centrifuge-like apparatus is hypothesized to induce a measurable drop in core temperature of animals with a normal balance system. Animals were sacrificed at ages of 4 (n=2), 8 (n=2) or >12 weeks (n=10), and their cochlear and vestibular sensory organs harvested, dissected as whole mounts and labeled with phalloidin (F-actin) and antibodies against myosin VIIa (hair cells) and connexin 26.

Average time on the rotarod was not significantly different between WT and CKO animals, nor was the temperature drop induced by centrifugal spinning, suggesting that the balance of the mutants is normal or near-normal. Histological evaluation in 4 week-old animals showed that Connexin 26 immunoreactivity was prominent in the vestibular system of the WT mouse, but absent in the CKO specimens. At 8 weeks of age, the hair cell population in the cochleae of the CKO mice was severely depleted but in the vestibular organs it was intact, despite absence of connexin 26 expression. The vestibular organs appeared normal at the latest time point examined, 12 weeks.

In contrast to the progressive pathology in the cochlea, histology of the vestibular organs in Gjb2-CKO mice was relatively normal. Thus, these mutant mice mimic the human situation with respect to the impact of connexin 26 mutations on the vestibular system, which may facilitate studies on the difference between the auditory and vestibular systems in the roles of connexin 26 and the consequences of its absence.

PS-210

Medial Vestibular Nucleus Neurons Subdivided by Calcium Binding Protein Expression.

Thomas Wellings; Brett Graham; Robert Callister; Alan Brichta; Rebecca Lim
The University of Newcastle

Introduction

The medial vestibular nucleus (MVN) integrates multiple inputs, including those from the vestibular, visual, proprioceptive systems, and the cerebellum. The output of the MVN plays an essential role in the vestibulo-ocular reflex (VOR) and other vestibular functions such as *adaption* and *compensation*.

However, the precise organization of the MVN is unclear. While distinct subgroups of neurons within the MVN have been characterized neurochemically or electrophysiologically, few studies have combined the two methodologies to selectively characterize MVN subgroups. Two discrete subpopulations of MVN neurons have been identified by their expression of calcium binding proteins (CBPs): *calretinin* (*CR*) or *parvalbumin* (*PV*). Our objective was to electrophysiologically characterize these two neurochemical groups by using transgenic mice that co-expressed enhanced green fluorescent protein (eGFP) with either CR or PV.

Methods

Electrophysiology: Whole-cell patch clamp technique was used to record from fluorescently labelled eGFP-CR or eGFP-PV neurons in the MVN. Action potential profile, discharge properties, and miniature post-synaptic currents were examined in both populations of neurons. *Immunofluorescence:* Paraformaldehyde-fixed brainstems were immunolabelled using antibodies against GFP, calretinin, parvalbumin to determine co-expression levels and density of calbindin-positive cerebellar inputs.

Results

CR neurons are located in the juxtaventricular parvocellular MVN. These neurons have type B action potential profiles, consisting of a double afterhyperpolarisation (AHP). They have reduced excitability in response to depolarising current steps compared to control neurons (104 Hz/nA, n=31 vs 146 Hz/nA, n=30, $p<0.005$), and show little or no change in discharge rate following hyperpolarizing current steps (0.66 ± 0.22Hz, n=25 vs 5.98 ± 0.84Hz, n=23, $p<0.0005$). Synaptic inputs to CR neurons were GABAergic and glutamatergic, with very few glycinergic inputs.

PV neurons are located in the rostrolateral parvocellular MVN, and also have type B action potential profiles. They are less excitable than control neurons (124 Hz/nA, n=39 vs 170 Hz/nA, n=42, $p<0.05$). In contrast to CR neurons, PV neurons showed an increase in discharge rate after hyperpolarizing current steps that is no different to control (4.0 ± 0.5, n=32 vs 12.9 ± 4.9, n=36, NS). Inputs to PV neurons were comparable to CR neurons.

Conclusions

CR and PV neurons in the MVN have distinct and separate electrophysiological profiles. These different profiles suggest independent roles. The fidelity of discharge rate in CR neurons, and known increase in CR expression after labyrinthectomy suggests an important 'regulatory' role within the MVN. In contrast, PV neurons are more excitable than CR neurons and suggest a 'relay' function.

PS-211

Head Stability During Natural Locomotion: Quantitative Peripheral Vestibular Assessment in Rodents

Ashley Godin; Jonie Dye; Shannon Brewer; Takeda Yohei; Min Young Lee; Donald Swiderski; Yehoash Raphael; W Michael King
University of Michigan

We have developed a novel way to evaluate the peripheral vestibular system that is quantitative and easily implemented. We use a lightweight (< 1g) inertial motion sensor to measure angular head velocity and linear head acceleration while an animal moves freely in a 1 square foot experimental test chamber in the dark.

We hypothesize that the vestibulo-collic reflex (VCR), a 3-neuron arc comparable to the vestibulo-ocular reflex (VOR), is dependent on the vestibular periphery and can be evaluated by measurements of head motion during natural behavior.

Rodents are commonly used as animal models for genetic studies of inner ear physiology, ototoxicity and sensory cell regeneration. The auditory brainstem response (ABR), otoacoustic emission (OAE) and audiometric testing provide quantitative assessment of cochlear function in rodents, but there are no comparable methods to assess the peripheral vestibular organs, in part because of their diversity. For example, the vestibular evoked response is specific to the otolith organs and the VOR is specific to semicircular canal function (and requires technically difficult eye movement measurements). Other tests such as rota-rod and swim tests are not specific to the vestibular system.

Fourteen mice were prepared for vestibular testing by implanting a 1 cm post on their skull; the post provided an anchor for the inertial motion sensor. Head movement and orientation were evaluated by collecting data from the motion sensor while the mice moved freely in the experimental chamber for 5 minutes. After control data were obtained, the peripheral vestibular system was lesioned by injecting streptomycin directly into the posterior semicircular canal, first on one side, and several weeks later, on the other side. Following each injection, measurements of head movement and orientation were made over multiple days to determine the time course of vestibular loss and recovery due to peripheral regeneration or central compensatory mechanisms. Upon completion of the experiment, the mice were euthanized and the vestibular organs were dissected for histological analysis to determine the extent of hair cell loss and/or regeneration within each organ.

Head orientation and positional stability in space progressively changed after each lesion, with the amount of change correlated to the extent of hair cell loss assessed after sacrifice. These data confirm our hypothesis and validate the use of the motion sensor to measure the VCR. Measurement of the VCR is clinically relevant because vestibular evoked myogenic potential testing performed in the clinic (VEMP) also assesses the VCR reflex pathway.

PS-212

The Blood Labyrinthine Barrier in the Human Vestibular Endorgans

Ivan Iopez; Gail Ishiyama; Akira Ishiyama
University of California, Los Angeles

Introduction

The anatomical organization of the human inner ear vasculature is well documented at the light microscopy level. However, ultrastructural studies on the organization of the blood-labyrinth barrier (BLB) in normal human vestibular endorgans and from patients diagnosed with Meniere's disease (MD) are very limited.

Methods

We used vestibular endorgans obtained from autopsy (normal vestibular and auditory function, n=6), surgical specimens obtained from MD (n=6) and acoustic neuroma patients (n=6). The specimens were immersed in OsO4 and En block stained with uranyl acetate and lead aspartate. Tissue was dehydrated in ascending ethyl alcohols and embedded in resin (Epon®). Thin sections (100 um) were made with a diamond knife on an AO/Reichter Ultracut-E ultramicrotome. Transmission electron microscopic (TEM) observations and digital image capture were made using a FEI Tecnai TEM T20 (200 KV). Systematic analysis was be made by selecting sections containing blood vessels (BVs) through the stroma of the cristae and maculae. All sections were studied for the presence of caveolae in vascular endothelial cells (VECs), tight junction organization, perycites cytoarchitecture, thickening and disruption in the perivascular basement membranes.

Results

In MDs specimens, BVs of the stroma underneath the macula and cristae vestibular sensory epithelia showed differential degrees of atrophy from moderated to completely disrupted, i.e. BV lumen was narrow and the VECs were swollen. TEM high magnification examination shows increased transcellular vesicular transport across VECs and pericyte detachment. Tight junctions showed an almost normal organization. The perivascular basement membrane surrounding the blood vessels located in the stroma of vestibular endorgans showed morphological deterioration. The damage was reflected as edema in the perilymphatic space. Normal specimens or acoustic neuroma specimens showed no ultrastructural alterations.

Conclusions

The alterations of the BLB and the stroma located underneath the vestibular sensory epithelia suggests that the vestibular cells and supporting cells are affected by a pronounced disruption of fluid transport in the vestibular labyrinth. Vascular hyperpermeability, the excessive leakage of fluid and proteins from blood vessels to the interstitial space, commonly occurs in small BVs after traumatic and ischemic injuries. We hypothesize that damage to VECs and pericytes by oxidative stress results in loss of BLB integrity. Understanding the structural–functional relations between cellular components of the BLB in normal and pathological conditions in the human vestibular labyrinth can provide important information about the etiology of various inner ear conditions and aging and also help to elaborate new therapeutic approaches.

PS-213

Effects of Blast Overpressure Exposure on the Rotational and Translational Vestibulo-Ocular Reflex (VOR) in Rats

Yue Yu[1]; Jun Huang[1]; David Sandlin[2]; Courtney Jernigan[2]; Jerome Allison[1]; Hong Zhu[1]; **Wu Zhou[1]**
[1]University of Mississippi Medical Center; [2]PhD Program in Neuroscience

Background

It has been well-established that blast overpressure can induce mild to severe traumatic brain injuries (TBI). As an air-filled structure which directly exposed to the surrounding air, unprotected ears are among the most frequently damaged sites during blast exposure. Vestibular symptoms, such as dizziness and imbalance, are common complaints among patients with blast-induced TBI. In contrast to the blast-induced hearing loss and tinnitus that have been extensively studied over the past years, little is known about the mechanisms underlying blast-induced vestibular deficits. To fill this important knowledge gap, we recently established a rat model of blast-induced vestibular deficits which allows us to identify biomarkers of blast-induced TBI and to develop countermeasures for prevention and treatment. In previous studies, we have examined the blast exposure-induced changes in inner ear morphology and vestibular afferent neurophysiology. The goal of the present study is to investigate effects of blast-exposure on vestibular functions by measuring the gains and phases of rotational and translational vestibulo-ocular reflexes (VOR) in awake rats.

Method

Effects of blast exposure on rotational and translational VORs were studied in adult Long Evans rats. A head holder was surgically implanted on the skull for stabilization of a rat's head during head rotation and translation. Responses of the left eye to head rotations at 0.1, 0.2, 0.5 and 1Hz (60 degree/s peak velocity) and translations at 0.1, 0.2 and 0.5 Hz (0.1g peak acceleration) along the nasal-occipital (NO), inter-aural (IA) and 45 degrees from NO were measured by an ISCAN video-based eye tracker. VOR gains and phases were computed. After establishing a stable baseline response (3-5 days), animals were exposed to blast overpressure (peak intensity of 195 dB SPL) delivered to the left external ear canal under isoflurane anesthesia**.** Control rats received sham exposure. Gains and phases of the rotational and translational VOR were measured 4 hours after blast exposure and daily

to monitor the time course of blast exposure-induced vestibular deficits.

Results
Preliminary experiments showed that blast exposure delivered to the ear canal caused significant and long-lasting deficits in both the rotational and translational VOR.

Conclusions
These results indicate that the rotational and translational VOR can be used as biomarkers for assessing blast overpressure exposure-induced vestibular deficits in the rat model.

PS-214

Structural and Signaling Proteins Expressed in Human Hair Cells During Early Fetal Development.

Rebecca Lim; Hannah Drury; Melissa Tadros; Phillip Jobling; Robert Callister; Alan Brichta
The University of Newcastle

Background
During early fetal development, human hair cells of the vestibular system differentiate from morphologically and physiologically similar structures into distinct type I and type II hair cells (Lim et al., 2014). In this study we characterize a number of protein markers during a crucial developmental period, 12 to 14 weeks gestation (WG), when the morphological differentiation of human vestibular hair cells begins. These markers are not only associated with hair cells, but also structural proteins within hair bundles and synaptic machinery. In addition, since calcium is important for cell signaling during development and maturation, we also characterize the expression of the calcium binding protein, calbindin in the developing neuroepithelium.

Methods
All procedures were approved by the University of Newcastle Human Ethics Committee. Inner ear tissue was fixed in 4% paraformaldehyde overnight, washed, and sections cut (50 µM thick). Subsequently sections were incubated in a number of different antibodies including; myosin VIIa, phalloidin, acetylated alpha-tubulin, beta-tubulin, calbindin and CtBP2.

Results
Immunofluorescent labeling of proteins associated with hair cell bodies (MyoVIIa), structural proteins (beta-tubulin), hair bundles (phalloidin, acetylated alpha-tubulin), ribbon synapses (CtBP2), and calbindin were present in developing human vestibular hair cells by 12WG. At this stage of development, hair cells were beginning to morphologically differentiate into typical type I and type II hair cells. Some cells show a constricted neck in the apical region, consistent with a type I hair cell morphology. This morphological feature became more evident in cells by 14WG. At 12 WG both phalloidin and acetylated alpha-tubulin were expressed in recognizable hair bundles indicating hair bundle polarity was already established. Interestingly, a marker of ribbon synapses, CtBP2 was also present in hair cells by 12WG, indicating at least some of the machinery is in place for neurotransmission at this stage of development. The expression of calbindin was restricted to sub-populations of hair cells throughout the neuroepithelium.

Conclusions
During the crucial 12 to 14 WG period, human vestibular hair cells further differentiate and begin to exhibit morphological features of type I hair cells and type II hair cells. However many proteins associated with mature transduction and cell signaling pathways are already expressed in developing human hair cells before 12WG, suggesting protein expression occurs well in advance of morphological changes.

PD-1

Late-onset Hearing Loss Induced by Cx26 (GJB2) Deficiency Results from the Reduction of Active Cochlear Amplification

Jin Chen; Yan Zhu; **Hong-Bo Zhao**
University of Kentucky Medical School

Background
Deafness due to *GJB2* mutations is not always prelingual. A large group of these patients (~30%) demonstrate a progressive, late-onset hearing loss, starting from high frequency hearing loss in childhood. These individuals are good candidates for applying therapeutic interventions because they have normal hearing early in life. However, little is known about the underlying deafness mechanism. We previously reported that congenital deafness due to Cx26 deficiency results from cochlear developmental disorders rather than hair cell loss and endocochlear potential (EP) reduction. In this study, we investigated the deafness mechanisms underlying Cx26 deficiency induced late-onset hearing loss.

Methods
A time-controlled Cx26 conditional knockout (cKO) mouse model was established by an inducible gene knockout technique to define the deafness mechanisms underlying Cx26 deficiency induced late-onset hearing loss. Hearing function was examined by auditory brainstem response (ABR) and distortion product otoacoustic emission (DPOAE) measurements. Outer hair cell (OHC) electromotility was also recorded to further assess active cochlear amplification.

Results
We found that deletion of Cx26 after postnatal day 5 (P5) in mice could lead to late-onset hearing loss. The Cx26 cKO mice had normal hearing after mature. Then, the hearing loss appeared at high frequency range and progressively extended to the lower frequency range, similar to clinic observations. The hearing loss was moderate to severe. The ABR threshold was increased by 30-50 dB SPL. Different from congenital deafness induced by Cx26 deficiency, the cochlea appeared normal morphology and development under the light microscopy. Hair cells also had no apparent loss. However, consistent with our previous report (Zhu et al., Nat Commun., 2013), DPOAE was reduced, even though hair cells have no connexin expression and gap junctional coupling. The reduction was also progressive and severe at high-frequencies. Consistent with DPOAE reduction, OHC electromotility in Cx26 cKO mice was shifted to the right and the slope of voltage

dependence was reduced. The Cx26 cKO mice also had EP reduction but the reduction was not associated with progressive hearing loss.

Conclusions

Different from congenital deafness resulting from cochlear developmental disorders, Cx26 deficiency can reduce active cochlear amplification inducing late-onset hearing loss. Our study provides important information for developing newer protective and therapeutic interventions to this common non-syndromic hearing loss.

PD-2

A De Novo Functional Enhancer Eliminating Mitf-M Expression Results in Hearing Impairment and Depigmentation in Pigs and Mice

Wei-wei Guo[1]; Lei Chen[2]; Li-li Ren[3]; **Ning Yu**[3]; Li-dong Zhao[3]; Jia-nan Jia[3]; Ning Li[2]; **Shi-ming Yang**[3]
[1]Chinese PLA Medical School, Chinese PLA General Hospital; [2]State Key Lab of AgroBiotechnology, China Agriculture University, Beijing, China; [3]Dept Otolaryngology Head Neck Surgery, Institute of Otolaryngology, Chinese PLA Medical School, Chinese PLA General Hospital, Beijing, China

An enhancer is referred as a region of DNA that can be bound with transcriptional factor proteins to activate transcription of a gene. De novo enhancers can be generated with different patterns. Minor genetic changes in non-regulatory sequences were sufficient to generate new enhancers in fish. However, genetic variation drives either new genesis regulatory elements or phenotypic alteration has not been reported. Here we took advantage of a hearing loss model found in Rongchang pigs, studied the spontaneous mutation in a non-regulatory region of melanocyte-specific promoter of microphthalmia-associated transcription factor gene (Mitf). The mutation generated a novel repressor and eliminated the expression of Mitf-m. It consequently caused the early degeneration of intermediate cells of cochlear stria vascularis and a profound hearing loss, the typical phenotype of Waardenburg syndrome in humans. We confirmed that the mutation only exclusively affected Mitf-M, not other isoforms. The essential function of Mitf-M in hearing development was further validated using a knock-out mouse model. Taking together, our results demonstrated the sole dysfunction of Mitf-m isoform sufficiently causes deafness and depigmentation. To our knowledge, this study provides the first evidence of systemic functional de novo enhancer in mammal.

PD-3

Endothelin A Receptor Blockade has the Potential to Arrest both Glomerular and Strial Pathologies Associated with Alport Syndrome in Mice.

Dominic Cosgrove[1]; Michael Anne Gratton[2]; Daniel Meehan[1]; Duane Delimont[1]; Brianna Dufek[1]; Grady Phillips[2]
[1]Boys Town National Research Hospital; [2]Saint Louis University

Introduction

Alport syndrome is characterized by delayed onset glomerular disease associated with hearing loss. It is caused by mutations in type IV collagen genes and affects approximately 1 in 5000 worldwide. Our lab has discovered a mechanism underlying glomerular disease initiation involving induction of endothelin which acts on endothelin A receptors (ET_AR), activating the Rho GTPase CDC42 in glomerular mesangial cells. This culminates in the deposition laminin 211 in the GBM by mesangial filopodial processes. Laminin 211 activates focal adhesion kinase (FAK) in podocytes, which leads to pro-inflammatory responses that alter the GBM architecture and function. Blocking either FAK or the ET_AR ameliorates the glomerular disease in mice. The strial capillary basement membranes (SCBM) in Alport mice are also irregularly thickened, resulting in a reduced endocochlear potential and a hypoxic environment in the scala media. In this study we aimed to determine whether the mechanism of pathological onset in the ear is similar to that in the glomerulus.

Methods

The 129 Sv autosomal Alport mouse model and its wild-type littermates were analyzed for laminin 211 and $pFAK^{397}$ and for the distribution of ET_AR and endothelin-1 expression by immunofluorescence. Mice were administered Sitaxentan (ET_AR antagonist) from 2 to 7 weeks of age. The SCBM for vehicle-treated and sitaxentan-treated animals were morphometrically analyzed by transmission electron microscopy in mid-modiolar radially oriented thin sections. The SCBM thickness measures were analyzed as a function of group and apical-basal cochlear location.

Results

Laminin 211 and pFAK397 immunostaining were highly expressed in Alport stria, but not wild type stria, in the area surrounding strial capillaries. Endotheloin-1 and ET_RA were abundant in in Alport strial marginal cells, but not wild type marginal cells. Treatment of Alport mice with the ET_RA antagonist resulted in significant normalization ($p< 0.05$) of the SCBM architecture throughout the length of the cochlear duct approximating that of wild type mice.

Summary

These findings indicate that the molecular mechanism underlying glomerular basement membrane disease initiation in Alport mice is similar to that driving SCBM thickening. This work suggests that treatment of mice with ET_AR antagonists will ameliorate both the glomerular and strial pathogenesis in Alport mice. Additional work demonstrating improved strial function will be required to establish this point and to demon-

strate improved strial function in maintenance of lateral wall homeostasis.

PD-4

Virally-Mediated Gene Therapy Restores Hearing in a Mouse Model (Kcnq1 Null Mice) of Human Javell and Lange-Nielsen Syndrome

Qing Chang[1]; Jianjun Wang[1]; Qi Li[2]; Yeunjung Kim[1]; Binfei Zhou[1]; **Xi Lin[1]**

[1]Emory University School of Medicine; [2]Nanfang Hospital of Southern Medical University, Guangzhou 510515, P.R. China

Background

Mutations in the potassium channel subunit *KCNQ1* cause human congenital syndromic deafness, Javell and Lange-Nielsen (JLN) syndrome. No mechanism-base therapy is available now. We tested a gene therapy approach to treat the deafness phenotypes of JLN syndrome using *Kcnq1*$^{-/-}$ mice.

Methods

Virally-mediated *Kcnq1* expression was achieved by injecting a modified Adeno-associated virus (AAV) construct into the endolymph within two days of birth. For each animal only one side of the cochlea was injected and the other side was used as a control. Immunolabeling, histological and auditory functional examinations were performed to evaluate the treatment effect.

Results

Our gene therapy treatments resulted in transgene expression in most cochlear marginal cells where the native *Kcnq1* is exclusively expressed and transported to the apical membrane. Extensive ectopic expression in many other types of cochlear cells did not affect normal hearing in wild type (WT) mice. Examinations of cochlear morphology showed that the collapse of the Reissner's membrane, degeneration of hair cells and spiral ganglion neurons were corrected in *Kcnq1*$^{-/-}$ mice. Normal endolymphatic potential (EP) was restored. Auditory brainstem responses (ABRs) showed significant hearing improvements by an average of 20-40 dB in treated ears in a frequency range of 4-24 kHz, comparing to the untreated ear in the same animal. The best treated *Kcnq1*$^{-/-}$ mice showed ABR thresholds indistinguishable from the injected WT mice.

Conclusions

Results demonstrated the first gene therapy study in which gene defects specifically affecting the function of the stria vascularis (SV) were successfully treated. We have obtained consistent therapeutic effects using different batches of viral solutions and showed that extensive ectopic virally-mediated *Kcnq1* transgene expressions did not affect normal cochlear functions, both of which are significant components required by pre-clinical trials.

PD-5

Residual Hearing in DFNB1 Deafness and Its Clinical Implication in a Korean Population

So young Kim[1]; Ah Reum Kim[2]; Kyu Hee Han[3]; Min Young Kim[4]; Ja-Won Koo[4]; Seung Ha Oh[2]; Byung Yoon Choi[4]

[1]Seoul National University Bundang Hospital, Seoul National University College of Medicine; [2]Department of Otorhinolaryngology-Head and Neck Surgery, Seoul National University Hospital, Seoul National University College of Medicine, Seoul, Korea; [3]Department of Otorhinolaryngology-Head and Neck Surgery, National Medical Center; [4]Department of Otorhinolaryngology-Head and Neck Surgery, Seoul National University Bundang Hospital, Seoul National University College of Medicine, Seongnam, Korea

Introduction

The contribution of *GJB2* to the genetic load of deafness and its mutation spectra vary among different ethnic groups. In this study, the mutation spectrum and audiologic features of patients with *GJB2* mutations were evaluated with a specific focus on residual hearing.

Methods

An initial cohort of 588 subjects from 304 families with varying degrees of hearing loss were collected at the otolaryngology clinics of Seoul National University Hospital and Seoul National University Bundang Hospital from September 2010 through January 2014. *GJB2* sequencing was carried out for 130 subjects. Hearing loss, age, and inheritance patterns were evaluated in the *GJB2* mutants.

Results

Of the 130 subjects, 22 (16.9%) were found to carry at least one mutant allele of *GJB2*; c.235delC was the most common allele (40.0%), followed by p.R143W (27.5%) and p.V37I (10.0%). The p.V37I mutants showed significantly better hearing thresholds than other DFNB1 mutants without an in *trans* p.V37I allele. Moreover, among those probands without the p.V37I allele in a *trans* configuration who showed some degree of residual hearing, the mean air conduction thresholds at 250 and 500 Hz were 61.3 and 79.6 dBHL, respectively. The c.235delC mutation showed a particularly wide spectrum of hearing loss, from mild to profound, and relatively good residual hearing at low frequencies. In some cases, however, patients with identical genotypes showed different degrees of hearing loss.

Conclusions and Summary

Despite its reputation as the most frequent cause of severe to profound deafness, c.235delC, the most frequent DFNB1 mutation in our cohort, caused a wide range of hearing loss with significantly better hearing thresholds at 250 Hz and 2 kHz than in the non-p.V37I and non-235delC DFNB1 subjects. This finding highlights the importance of soft surgery for cochlear implantation in very young DFNB1 patients.

PD-6

Assembly and Disruption of Cochlear Gap Junction Macromolecular Complex are Regulated by Connexin 26

Kazusaku Kamiya[1]; Ichiro Fukunaga[1]; Kaori Hatakeyama[1]; Takashi Anzai[1]; Osamu Minowa[2]; Katsuhisa Ikeda[1]
[1]Juntendo University; [2]RIKEN, BioResource Center

Objectives

Hereditary deafness affects about 1 in 2000 children and GJB2 gene mutation is most frequent cause for this disease. GJB2 encodes connexin26 (Cx26), a component in cochlear gap junction. To elucidate the molecular pathway for the gap junction dysfunction, biochemical analysis of gap junction plaques (GJPs) with multiple Cx26 mutant mouse models are needed.

Methods

In this study, we analyzed macromolecular change of gap junction plaques with two different types of Cx26 mutation as major classification of clinical case, one is a model of dominant negative type, Cx26R75W+ and the other is conditional gene deficient mouse, Cx26f/fP0Cre as a model for insufficiency of gap junction protein.

Results

Gap junction composed mainly of Cx26 and Cx30 in wild type mice formed large planar GJPs. In contrast, Cx26R75W+ and Cx26f/fP0Cre showed fragmented small round GJPs around the cell border. In Cx26f/fP0Cre, some of the cells with Cx26 expression due to their cellular mosaicism showed normal large GJP with Cx26 and Cx30 only at the cell junction site between two Cx26 positive cells. These indicate that bilateral Cx26 expressions from both adjacent cells are essential for the formation of normal cochlear GJPs.

Here we demonstrate that Cx26-dependent gap junction plaque (GJP) disruption occurs as the earliest change during embryonic development, resulting in a drastic reduction in the GJP area, and is associated with excessive endocytosis with increased expression of Caveolin1 and Caveolin2 in models of two major forms of Cx26-associated deafness. GJP disruption with the functional defects was also clearly reproduced with human Cx26 and Cx30 clones in vitro (Kamiya et al., J. Clin. Invest., 2014, ;124(4):1598–1607).

Conclusions

In the present study, we demonstrated a new molecular pathology in most common hereditary deafness with different types of Connexin26 mutations, and this machinery can be a new target for drag design of hereditary deafness.

PD-7

Hearing Loss and Cochlear Pathology in a Type 2 Diabetic Mouse Models

Michael Anne Gratton; Dawei David Wang; Arya Namin Namin; Betty Yun Jin Chen
Saint Louis University

Introduction

Studies have investigated whether hearing loss (HL) is a complication of diabetes mellitus. Recent epidemiological investigations established a correlation specifically between T2DM and HL. T2DM is a global epidemic, affecting 312,000,000 people, 8.3% of the global population. The parameters and underlying mechanisms of T2DM-related HL have not been elucidated.

This project seeks to determine onset/progression of HL in two mice strains commonly used to model T2DM. The $Lepr^{db}$/$Lepr^{db}$ (Db/Db) mouse has a point mutation in the leptin receptor causing polyphagia, hyperglycemia, and obesity. In the second mouse (C57Bl6-DIO) a high-fat diet induces hyperglycemia, and obesity

Goal

The long-term goal is elucidation of the mechanism(s) of T2DM-induced HL. This portion of the overall project seeks to 1) determine onset and progression of HL in the Db/Db and C57-DIO mice strains via a systematic study of cochlear function and structure; and 2) to determine the extent that an animal model corroborates the hypothesis that microvascular changes are an important cause of cochlear and auditory nerve changes in T2DM.

Methods

Db/Db, C57-DIO and wild type mice from the C57Bl6 parent strain were followed from 5 to 20 or 30 weeks of age. Auditory brainstem response (ABR) measurements were performed followed by analysis of cochlear ultrastructure using scanning and transmission electron microscopy. Glycogen localization was demarcated via PATCH-SP. Measures of urinary and blood markers for diabetes were obtained.

Results

Blood and urinary data for the Db/Db mouse showed increased fasting glucose levels at 12 weeks of age with onset of a significant high frequency HL by 14 weeks. Structural analysis indicated decreased density of spiral ganglion cells and 8^{th} nerve fibers with only a mild loss of hair cells. Likewise, in the C57-DIO mouse fed a high fat diet from 6 weeks onward, elevated high frequency thresholds were evident by 20 weeks, as were elevations in fasting blood glucose. Histochemical staining to localize areas of glycogen storage indicated increased cellular glycogen in cell types throughout the scala media. Most striking was the increased glycogen content in Deiters cells, Reissner's membrane, strial marginal cells, vascular pericytes and satellite cells of the spiral ganglion. Interestingly, differences in the most reactive sites for glycogen were noted between the Db/Db and C57-DIO mice.

Conclusion
The Db/Db mutant and C57-DIO models of T2DM both show T2DM-associated HL and will be useful for investigation of the underlying mechanism of type 2 diabetes associated otopathology.

PD-8

HIV Transgenic Mice Have Sensorineural Hearing Loss

Pamela Roehm; Lifan He; Taha Mur; Kamil Amer
Temple University School of Medicine

Introduction
Clinical studies have shown that patients with HIV are more likely to have hearing loss compared with age-matched controls. However, in clinical studies it is impossible to determine if that excess hearing loss is due to the viral infection itself, highly active antiretroviral treatment, or opportunistic ear and/or brain infection due to immunosuppression. To definitively determine whether or not HIV viral infection itself causes sensorineural hearing loss (SNHL), we measured the hearing capacity of a murine model of congenital HIV infection. This model is known to develop HIV nephropathy.

Methods
We measured hearing thresholds in the Tg26 mouse model, a transgenic knock-in of the HIV DNA sequence other than the gag-pol genes, within a FVB/NJ genetic background. Auditory brainstem response (ABR) and distortion product otoacoustic emissions (DPOAEs) were measured at two and four months of age. ABR thresholds, ABR latencies and DPOAEs of Tg26 heterozygotes (Tg26+/-) and compared with levels in wild-type (wt) littermates.

Results
At 2 months of age the click ABR stimulus threshold for Tg26 +/- mice averages 16dB higher than that of wt littermates (35 dB SPL *v*. 19 dB SPL, p = 0.0093, Mann-Whitney U test), consistent with poorer hearing in the Tg26+/- animals. Similar findings were seen at 4 months of age, with an average ABR click stimulus threshold of 37 dB SPL in T26 +/- animals *v*. 19 dB SPL in wt littermates, p = 0.086. Tone ABR thresholds at 8000, 16000, and 24000Hz also showed a trend for worse hearing for Tg26+/- animals.

Conclusion
Click ABR results from the Tg26 model suggest that HIV viral protein expression directly induces SNHL. Our study will further help us understand the etiology of hearing loss in HIV-positive patients.

SYM-7

TMC Genetics in Mice and Humans

Andrew Griffith; Kiyoto Kurima; Yoshiyuki Kawashima; Hiroshi Nakanishi; Yukako Asai; Jeffrey Holt
National Institute on Deafness and Other Communication Disorders

The founding member of the mammalian transmembrane channel-like (*TMC*) gene family, *TMC1*, was discovered through linkage analysis and positional cloning of autosomal dominant nonsyndromic hearing loss DFNA36 segregating in a single North American family and autosomal recessive nonsyndromic hearing loss DFNB7/B11 segregating in multiple families from South Asia. The identification of human *TMC1* led to the identification and characterization of its mouse ortholog, *Tmc1*, and the demonstration that mutations of *Tmc1* cause dominant and recessive hearing loss in the Beethoven (*Bth*) and deafness (*dn*) mutant mouse lines, respectively. All of the reported dominant mutations of *TMC1* or *Tmc1* are missense amino acid substitutions clustered at two discrete locations within the *TMC1* gene. In contrast, the recessive mutations of *TMC1* or *Tmc1* include missense substitutions as well as a wide variety of genomic deletions, frameshift, nonsense and splice site mutations spanning the length of the gene. Thus the recessive alleles are presumed to act via a loss-of-function. Since heterozygous carriers of loss-of-function mutations have normal hearing, the dominant and semi-dominant mutations must act via a gain-of-function or dominant-negative mechanism, or a combination of these mechanisms. The *TMC1/Tmc1* mutant phenotypes are notable for the lack of an abnormal motor vestibular phenotype. The basis for this observation was revealed in studies of targeted deletion alleles of *Tmc1* and the closely related *Tmc2* gene in mice. Homozygous *Tmc2*-null mice have normal hearing and motor vestibular phenotypes, consistent with the observation that *TMC2* has not been implicated in any human auditory or vestibular disorders. However, double homozygous *Tmc1*-null;*Tmc2*-null mice are deaf, exhibit abnormal motor vestibular behaviors, and lack vestibulo-ocular reflexes. The basis for these observations was revealed in the spatiotemporal expression of *Tmc1* and *Tmc2* in the cochlea and vestibular end organs, where these genes are expressed in hair cells. Both *Tmc1* and *Tmc2* are expressed in mature vestibular hair cells, where they are required for normal mechanotransduction and may be a component of the mechanotransduction channel itself. The loss of function of one gene can be compensated for by the function of the other at the motor vestibular behavioral level. This compensation is incomplete at the level of the vestibulo-ocular reflex. In contrast, *Tmc1*, but not *Tmc2*, is expressed in the mature cochlea. Thus *Tmc2* is not available to compensate for the loss of *Tmc1* function in the auditory system, thus explaining the loss of hearing associated with mutations of *TMC1* or *Tmc1*.

SYM-8

Tmc Function in C. elegans Sensory Transduction

William Schafer; Marios Chatzigeorgiou; Yiquan Tang; Rhianna Knable
MRC Laboratory of Molecular Biology

C. elegans has an anatomically simple nervous system, but its sensory modalities parallel those in more complicated animals. Many known sensory transduction molecules are functionally conserved between worms and humans; we have therefore used worm genetics to identify receptors and channels involved in senses such as touch and taste and to study their function in vivo. Recent work has focused on the TMC

genes, which encode broadly-conserved multipass integral membrane proteins in animals. The human Tmc1 is a deafness gene required for hair cell mechantransduction; vertebrate genomes contain 7 additional TMC genes, many with unknown functions. *C. elegans* contains two members of the TMC family. One of these, TMC-1 forms a sodium-sensitive ion channel that functions in polymodal neurons as a sensor for salt taste chemosensation. The other, TMC-2 functions in touch neurons in mechanosensation. Interestingly, althought heterologous expression of TMC genes in mammalian cell culture has proven difficult, at least three mammalian TMC genes can be functionally expressed in *C. elegans* olfactory neurons. We have used transgenic nematodes expressing mouse TMC proteins to characterize the functional properties of mammalian TMCs and gain insight into their roles in human sensory biology.

SYM-9

TMC1 and TMC2 Localize at the Site of Mechanotransduction in Mammalian Inner Ear Hair Cell Stereocilia

Bechara Kachar[1]; Kiyoto Kurima[1]; Seham Ebrahim[1]; Bifeng Pan[2]; Hiroshi Nakanishi[1]; Bryan Millis[1]; Runjia Cui[1]; Yoshiyuki Kawashima[1]; Jeffrey Holt[2]; Andrew Griffith[1]
[1]National Institute on Deafness and Other Communication Disorders, NIH; [2]Boston Children's Hospital, Harvard Medical School

Mechanosensitive ion channels at stereocilia tips mediate mechanotransduction (MET) in inner ear sensory hair cells; however the identities of the MET channel complex components are unknown. Transmembrane channel-like 1 and 2 (TMC1 and TMC2) are essential for MET and are presumed to be components of the MET complex, but evidence that they localize at stereocilia tips is lacking. Using transgenic mice expressing TMC1-mCherry and TMC2-AcGFP, we determine that TMC1 and TMC2 localize along stereocilia early postnatally, and localize predominantly to stereocilia tips as hair cells mature. Both TMCs are absent from the tips of the tallest stereocilia, where tip links are absent and MET activity is not detectable. The distribution was confirmed for the endogenous proteins by immunofluorescence. Functionality of the tagged-proteins was verified by rescue of MET currents, and hearing and vestibular deficits in $Tmc1^{\Delta/\Delta};Tmc2^{\Delta/\Delta}$ mice expressing TMC1-mCherry and TMC2-AcGFP. These data are consistent with TMC1 and TMC2 being components of the stereocilia MET channel complex.

SYM-10

The Tip Link Protein PCDH15 Interacts with TMC1 and TMC2

Teresa Nicolson[1]; Reo Maede[1]; Katie Kindt[2]; Weike Mo[1]; Clive Morgan[1]; Timothy Erickson[1]; Hongyu Zhao[1]; Rachel Clemens-Grisham[1]; Peter Barr-Gillespie[1]
[1]OHSU; [2]NIH/NIDCD

Mutations in protocadherin 15 (PCDH15) cause deafness and vestibular dysfunction in fish, mice, and humans. As a central and conserved component of the mechanotransduction complex in hair cells, PCDH15 forms part of the tip link. To gain a better understanding of how PCDH15 is coupled to the transduction machinery, we performed a membrane-based yeast two-hybrid screen using zebrafish Pcdh15a as bait. We identified a positive interaction with Tmc2a, an orthologue of mammalian TMC2. *Tmc2* was recently implicated in deafness and vestibular dysfunction in mice, and its closely related gene, *Tmc1*, is associated with both recessive and dominant forms of hearing loss in mice and humans (DFNA36 and DFNB7/11). Using the yeast two-hybrid assay or a heterologous expression system, we also observed interactions among the orthologous mouse TMC isoforms and PCDH15 splice variants. To test the relevance of the Tmc2a-Pcdh15a interaction in vivo, we overexpressed the N-terminal fragment identified in yeast two-hybrid screen in zebrafish hair cells. We observed that the localization of Pcdh15a was no longer concentrated at the tips of stereocilia, and that mechanosensitivity was reduced. Our data combined provide a link between PCDH15 and TMC1 and TMC2, which is compelling evidence that TMC1/2 proteins are central players of the mechanotransduction complex in hair cells.

SYM-11

TMCs – Channels or Not?

Robert Fettiplace; Maryline Beurg; Kyunghee Kim
University of Wisconsin-Madison

Transmembrane channel-like (TMC) proteins have emerged as a likely component of the mechanotransducer (MT) channel complex in inner ear hair cells (Kawashima et al. 2011). However, their exact role in the complex remains uncertain. To address this problem, we characterized MT currents in cochlear coils isolated from Tmc1 mutants and Tmc1/Tmc2 double mutant mice, up to postnatal day (P) 10. Although Tmc1 mutant mice are deaf as adults, large MT currents can still be recorded in neonates up until P7. In the first post natal week, TMC2 is thought to substitute for TMC1 but is subsequently down-regulated. TMC1 deficiency before P7 is associated with changes in the calcium permeability and unitary conductance of the MT channel, and we and others have used these observations to propose that TMC1 must form part of the MT channel's ion conduction pathway (Pan et al. 2013; Kim et al. 2013). A significant finding was that the single MT-channel current of cochlear outer hair cells increased from apex to base in wild-type but not in two different Tmc1 null mutations, both of which largely abolished tonotopy. In Tmc1/Tmc2 double mutants, normal MT currents were absent, but mechanically-sensitive currents could still be evoked by negative displacements of the hair bundle. These, referred to as reversed stimulus-polarity currents, could be blocked by the same agents as those in wild-type (including FM1-43, amiloride, dihydrostreptomycin and external calcium), though often higher half-blocking concentrations were needed. A striking result was that severing the tip link by treatment with BAPTA did not abolish the reversed stimulus-polarity currents as it would have the normal MT current. Similar reversed stimulus-polarity responses have been reported in Pcdh15 Ames waltzer mutants (Alagramam et al. 2011), and are seen in wild-type after prolonged exposure of the hair bundles to BAPTA. We

suggest that the reversed stimulus-polarity currents flow though nascent MT channels that have been newly exported to the top of the hair cell, where they lack accessory subunits or attachment to extracellular links. In the absence of TMC1 and TMC2, MT channels still exist but are not connected to the tip link. We further propose that TMC1 is not the channel pore but may be an accessory subunit that constitutes part of an external vestibule influencing channel conductance and blocker affinity. If these suggestions are correct, the molecular identity of the pore-forming subunit is still unknown.

SYM-12

The Functional Contributions of TMC Proteins to Sensory Transduction in Auditory and Vestibular Hair Cells

Jeffrey Holt; Xiao-Ping Liu; Bifeng Pan; Yukako Asai; Kiyoto Kurima; Andrew Griffith; Gwenaelle Geleoc
Boston Children's Hospital / Harvard Medical School

Identification of the components of the sensory transduction channel in auditory and vestibular hair cells has eluded neuroscientists for many years. Recently, we have focused on Transmembrane channel-like proteins (TMC) 1 and 2 because they are necessary for sensory transduction in mammalian hair cells and may be components of the elusive transduction channel. *Tmc1* and *Tmc2* are expressed in hair cells and their protein products can be localized to the tips of hair cell stereocilia. Mice deficient in both *Tmc1* and *Tmc2* have complete loss of hearing and balance function and lack sensory transduction, despite intact hair bundles and tip-links (Kawashima et al., 2011). Mice that express only TMC1 or TMC2 have distinct single-channel conductances and calcium selectivity. A methionine-to-lysine substitution at position 412 in TMC1 causes deafness and reduces the single-channel current amplitude and calcium permeability (Pan et al., 2013). These results are consistent with the hypothesis that TMCs participate as essential components of the sensory transduction channel in auditory and vestibular hair cells, but the exact role of TMC proteins is not yet clear. They may form a vestibule at the mouth of the pore, the pore of the ion channel itself or both (Holt et al., 2014). However, these suggestions have proven controversial and alternate hypotheses have been presented including that TMCs may function as non-essential accessory subunits (Beurg et al., 2014).

For this symposium I will present the latest data from our lab and others and will discuss their implications for auditory and vestibular function. Current studies in our lab are focused on probing the structure and function of TMC1 and TMC2 by transfecting mutant TMC sequences into hair cells of *Tmc1/Tmc2* doubly-deficient mice and assaying for changes in the biophysical properties of sensory transduction. We find that the mutant constructs restore sensitivity to hair bundle deflections in virally-transfected hair cells and that the mutations have altered several biophysical properties of sensory transduction. The data provide further support for a direct role for TMC1 and TMC2 in sensory transduction in mammalian auditory and vestibular hair cells.

PD-9

Performance Evaluation of a Cochlear Implant Processing Strategy with Partial Tripolar Mode Current Steering

Xin Luo; Ching-Chih Wu
Purdue University

Introduction

In cochlear implants (CIs), partial tripolar (pTP) stimuli return part of the current to the two flanking electrodes (controlled by σ) to generate narrower excitation patterns than monopolar (MP) stimuli. To create additional spectral channels, current steering may be incorporated into focused pTP stimuli by varying the proportion of current returned to the basal and apical flanking electrodes (controlled by α and 1-α, respectively). Studies have shown that pitch generally decreased as α increased from 0 to 1 for steered pTP stimuli on the same main electrode. For subjects with relatively good pitch sensitivity, α varying from 0.4 to 0.6 may elicit continuous, non-overlapped pitch changes from one electrode to the next. This study compared the performances of three experimental CI processing strategies (MP, pTP, and pTP-steering) to evaluate the benefits of current focusing and current steering.

Methods

Four post-lingually deafened adult CI users were tested. The three strategies used the same signal processing as the HiRes-120 strategy and were matched in the number of main electrodes, phase duration, pulse rate, and loudness. The highest possible σ (0.625 or 0.75) that supported full loudness growth within the compliance limit was used for each subject. In the pTP-steering strategy, (1-α) varied from 0.4 to 0.6 for the main electrodes in the middle of the electrode array. The range of (1-α) was extended apically (0-0.6) or basally (0.4-1) for the most apical and basal main electrodes, respectively. The three strategies were tested in random order for speech perception in noise, melodic contour identification, vocal emotion recognition, pitch ranking, and spectral ripple discrimination. There was a 30-minute adaptation time for each strategy before testing.

Results

During the fitting of the pTP-steering strategy, the apical, middle, and basal channels created by pTP-mode current steering on each main electrode were generally ranked in pitch from low to high. Subjects described the sound quality of the pTP and pTP-steering strategies as crispy, hollow, and high-pitched. On average, performance in pitch ranking, spectral ripple discrimination, and vocal emotion recognition improved with current focusing (i.e., pTP > MP) but did not further improve with current steering (i.e., pTP ≈ pTP-steering). There were no clear benefits of current focusing and current steering to speech perception in noise and melodic contour identification.

Conclusions

The tested range of current steering (0.4-0.6) in pTP mode may not be sufficient to improve pitch ranking, spectral resolution, and speech perception with CIs.

PD-10

Selecting Cochlear Implant Channels Based on Focused Thresholds

Julie Bierer[1]; Emily Ellis[1]; Leonid Litvak[2]
[1]University of Washington; [2]Advanced Bionics

Introduction

Cochlear implant programming using focused electrical fields is under investigation for clinical devices. One previous study showed improved speech understanding in background noise when focused strategies were employed (Srinivasan et al., 2013). The hypotheses of the present study were that (1) focused stimulation will improve vowel and consonant recognition, and (2) speech perception can be further optimized by reducing the number of active channels based on the putative quality of the electrode-neuron interface. Channels with relatively high thresholds were presumed to have a poor interface as a result of poor neural health or electrode positioning (i.e., electrodes on the lateral wall or traversing through the basilar membrane).

Methods

Four experimental strategies were tested in 8 adult Advanced Bionic cochlear implant listeners using the BEPS+ software. The strategies were: 1) a 14-channel map with all channels programmed in the monopolar mode, or 2) in the partial tripolar mode (focusing parameter $\sigma > 0.675$); 3) a program based on the partial tripolar strategy (#2) with a subset of relatively high-threshold focused channels deactivated, or 4) an equal number of low-threshold focused channels deactivated. High-threshold channels were selected by first filtering the subject's threshold profile to enhance the peaks and troughs, and setting an exclusion/inclusion criterion based on the mean and standard deviation. All subjects had at least 6 months of experience with their cochlear implant. Listeners were given 20 to 30 minutes experience with each strategy. Speech perception abilities were measured in the sound field with medial vowel (hVd) and medial consonant (aCa) identification. Speech was presented at 60 dB SPL-A in the sound field in a sound-treated booth. If listeners performed better than 80% correct, testing was performed with multi-talker babble presented at a +10 signal to noise ratio.

Results

Subjects performed 2% better with focused stimulation strategies for vowel identification but not consonants. Performance on vowel identification was 30% better when high-threshold channels were deactivated compared to the low-threshold channels in quiet and 11% better in noise. Consonant identification was unchanged when tested in quiet and 8% better when tested in background noise.

Conclusions

These findings suggest that eliminating a subset of channels having elevated focused thresholds may lead to improvements in speech perception, supporting the motivating hypothesis that these channels have relatively poor electrode-neuron interfaces. Chronic experience with these strategies may lead to further improvements.

PD-11

Effect of Stimulus Polarity on the Spread of Excitation With Bipolar and Tripolar Stimulation in Cochlear Implants

Robert Carlyon[1]; Astrid van Wieringen[2]; John Deeks[1]; Jaime Undurraga[2]; Olivier Macherey[3]; Jan Wouters[2]
[1]Medical Research Council; [2]KU Leuven; [3]CNRS, Marseille

Animal experiments have shown more restricted excitation when cochlear-implant (CI) electrodes are stimulated in bipolar (BP) or tripolar (TP) mode, compared to monopolar (MP) stimulation. However there is only limited evidence on the benefits for human CI users.

BP stimulation results in equal opposite-polarity waveforms at each electrode, potentially leading to a bimodal excitation pattern. At least at moderately high levels, CI users are more sensitive to anodic than to cathodic current, suggesting that asymmetric BP pulses could selectively excite neurons near one electrode. We measured forward-masked PTCs, where 200-ms 1031-pps BP maskers consisted either of SYM or pseudomonophasic (PS) pulses ; for PS pulses both polarities were tested. The signal was three 97-μs/phase 344-pps SYM pulses, at a +3 dB sensation level, with masker-probe gap=6.8-ms. The first phase of each pulse had a duration of 97 μs, and, for PS pulses, was followed by an opposite-polarity ¼-amplitude 388-μs phase. For SYM pulses, several listeners showed the predicted bimodal PTCs. All except one of the 7 subjects showed a polarity effect: in most cases there was, as predicted, more masking when the short-high phase on the masker electrode closest to the probe was anodic compared to cathodic. One subject showed the opposite effect. As PTCs measure the masker level needed to mask a soft signal, this subject may be more sensitive to cathodic stimulation at soft levels.

Litvak (2007) reported that TP stimulation can sometimes produce broader excitation patterns than MP, due to activation produced by the flanking ("return") electrodes. If so, excitation patterns should be narrower for PS pulses where the short-high phase is anodic on the center electrode and cathodic on the flanking electrodes (PSA), compared to *vice versa* (PSC). We measured forward-masked excitation patterns for 200-ms 1031-pps maskers that were either PSA or PSC in partial tripolar (pTP) mode, or SYM in MP mode. The probe consisted of 4 symmetric TP pulses (rate=200 pps, masker-probe interval = 10ms). For all pulses the duration of the first phase was 97 μs. The level of all maskers was adjusted to produce the same amount of masking for a probe at the masker electrode. This level was higher for pTP-PSC than for pTP-PSA, consistent with greater masking by anodic than by cathodic stimulation. For each masker, thresholds were then measured for probes at a range of neighbouring electrodes, allowing us to identify any differences in the excitation-pattern width between maskers.

PD-12

Do Lower Stimulation Rates Improve Speech Understanding in Typically Low-Performing Groups of Cochlear-Implant Users?

Maureen Shader[1]; Nicole Nguyen[2]; Ronna Hertzano[2]; David Eisenman[2]; Samira Anderson[1]; Sandra Gordon-Salant[1]; Matthew Goupell[1]

[1]University of Maryland-College Park; [2]University of Maryland Medical School, Baltimore

Introduction

Cochlear-implant (CI) users performance on speech recognition tasks vary greatly, ranging from zero to near-perfect performance in quiet. Predictors of speech recognition performance include age of onset of deafness and duration of profound hearing loss, while age has not been established as a strong predictor. Audiologists often report a decline in older CI users' speech recognition with increasing age. Many audiologists also anecdotally report that programming with slower CI stimulation rates can improve objective and subjective speech understanding performance for groups of CI users who are low performers (e.g., older adults, individuals with early onset and prolonged duration of hearing loss). This study aims to investigate the effect of stimulation rate on speech recognition performance in CI users with early onset and prolonged hearing loss, as well as older CI users.

Methods

Speech recognition as a function of stimulation rate was measured in 25 CI users (one participant was tested in both ears) between 22 and 87 years of age (mean=61.6±15.1 yrs). Seven participants had early-onset hearing loss. Clinical software was used to set participant maps at 500, 720, 900, and 1200 pulses per second (pps). Speech recognition scores were measured monaurally at 60 dB SPL in the sound field in quiet and in 10-talker babble (+10-dB signal-to-noise ratio) using two sentence recognition tests. A brief cognitive battery was administered, consisting of a dementia screening, a working memory test, and two processing speed tests.

Results

Ten of 26 ears showed a significant effect of rate on speech recognition scores, where six of 10 ears were prelingually deafened. The majority of prelingually deafened ears showed significantly higher speech recognition scores (up to a 13.7% improvement) when mapped with slower rates (<900 pps) compared to faster rates (≥900 pps). Some of the participants in the older group (>75 years, N=5) had higher speech recognition scores with slow to moderate rates (720 and 900 pps) that were not apparent in the younger participants, especially in noise.

Conclusion

These results suggest that stimulation rate does affect speech recognition scores in some CI users. In particular, most prelingually-deafened adults benefited from slower stimulations rates. Results also indicate that stimulation rate may impact speech understanding scores in older adults differently than younger and middle-aged adults. These findings may influence clinical mapping procedures in order to optimize at least some low-performers' outcomes.

PD-13

Development of Electric-Acoustic Pitch Comparisons in Single-Sided-Deaf Cochlear Implant Users

Silke Klawitter[1]; Gunnar Geissler[2]; Andreas Büchner[2]; **Waldo Nogueira**[2]

[1]Hannover Medical School; [2]Medical University Hannover

Introduction

6 cochlear implant (CI) users with near-normal hearing in their non-implanted ear compared pitch percepts for pulsatile electric and acoustic pure-tone or harmonic tone stimuli presented to the two ears. 3 CI users were implanted with the 28mm MED-EL FLEX, 2 with the Cochlear CI24RE and 1 with the AB MidScala electrode. The experiments were performed right after activation of the CI for the first time and 2 or 3 months afterwards.

Method

After loudness balance the electric and acoustic stimuli, comparisons were performed between a 1000 pps pulse train and pure tones or between 12 pps electric pulse trains and bandpass-filtered acoustic pulse trains of the same rate. An interleaved adaptive procedure was used to obtain the match between the electric and the acoustic stimuli. In order to control for non-sensory biases potentially arising from the large range of acoustic stimuli presented during the pitch matching procedure sanity checks as proposed by [2] were applied.

Electrode positions for 2 subjects were taken from Cone Beam Computer Tomography data pre- and post- CI implantation. The cochlea length of each individual CI user was estimated pre- implantation. The longitudinal and angular positions of the intracochlear electrode contacts were determined postoperatively. The cochlear length and the electrode position estimations were then used to estimate the frequency corresponding to each CI user's electrode using Greenwood equation. Next the acoustic pitches matched to the electric pulse trains were compared to the Greenwood function estimations.

Conclusions

We observed that the 3 MedEL CI users matched the apical electrodes to lower frequencies than the Cochlear and AB CI users. The reason might be that the MedEl electrode array is inserted deeper in the cochlea. 3 CI users could perform reliable matches between acoustic and electric tones right after implantation, the other 3 could not obtain reliable matches. In two MedEl CI users we observed that the 12-pps electric pulse train was matched to the same frequencies than the 1000-pps right after implantation, however after 2 months of CI use the 12-pps electric pulse train was matched to lower frequencies than the 1000-pps pulse train. We hypothesize that this finding might be related to the accommodation of the CI users to the high stimulation rates delivered by their clinical strategy during the first month of device use. In general the

pitch elicited through electric stimulation deviated less than an octave with respect to Greenwood's estimate.

PD-14

Interaural Place Mismatches Persist for Long-Term Bilateral Cochlear Implant Users

Justin Aronoff[1]; **Justin Aronoff**[1]; Julia Stelmach[1]; Monica Padilla[2]; David Landsberger[2]

[1]University of Illinois at Urbana-Champaign; [2]New York University

Background

For cochlear implant (CI) users with a long electrode array in one ear and a short array in the opposite ear or a CI in one ear and a hearing aid in the other, there is a large initial interaural place mismatch. A number of studies have shown that such patients can adapt to this mismatch, although that adaptation is usually only partial, resulting in a smaller but persistent interaural place mismatch. With bilateral cochlear implant users with similar length arrays in each ear, insertion depth differences between ears is considerably smaller compared to those other populations. This would suggest that long-term bilateral CI users might completely adapt to these mismatches, removing the need to make any further adjustments to the mapping to perceptually align the two ears. To determine if that is the case, bilateral CI users were tested using a pitch matching task.

Methods

Nine bilateral CI patients with at least one year of bilateral experience were tested along with three bilateral CI patients with six months or less of bilateral experience. Participants were presented with stimulation on an electrode in one ear and asked to move the stimulation site on the opposite ear until the same pitch was perceived in both ears.

Results

For five out of the nine experienced bilateral users, the slope and/or intercept of the pitch matching results significantly deviated from a slope of 1 and intercept of 0, as would be expected if pitch matching was based solely on electrode number. Additionally, for new bilateral users, the deviation of their pitch matching data from what would be expected based on electrode number was twice as large as it was for experienced bilateral user.

Conclusions

The results suggest that despite long-term bilateral experience, interaural place mismatches still persist, although they may diminish with experience. This suggests that it is not sufficient to rely on adaptation to correct initial interaural place mismatches, but rather that this must be addressed with mapping techniques

PD-15

Discrimination of Vocal Characteristics in Cochlear Implants

Etienne Gaudrain; Deniz Baskent

University Medical Center Groningen / University of Groningen

Introduction

Listeners use vocal characteristics of speakers to identify and discriminate voices, which is particularly important for speech intelligibility in cocktail-party situations. Fundamental frequency (F0) and vocal-tract length (VTL) have been identified as the two main perceptual dimensions normal-hearing (NH) listeners rely on for this task. In cochlear implants (CIs), F0 perception mostly depends on temporal resolution, while VTL perception depends on spectral resolution. Previous studies on voice gender categorization have shown that CI users have more difficulties discriminating male and female voices than NH listeners. More recent data showed that while CI users are able to use gender-related F0 differences, they are unable to exploit VTL differences for this discrimination, unlike NH individuals. While F0 discrimination is widely studied with CI users, VTL discrimination is largely unknown. As a result, the source of the difficulty in CI VTL perception remains unclear; do CI listeners not use VTL cues because they cannot detect VTL differences at all, or, alternatively, because they cannot interpret the difference they hear as a change in VTL? The objective of the present study is to answer this question by characterizing VTL discrimination abilities in CI users, as compared to F0 discrimination abilities.

Methods

VTL and F0 of recorded (meaningless) CV sequences were manipulated using STRAIGHT, in order to measure just noticeable differences (JND) along these dimensions using an adaptive 3AFC method in postlingually deafened adult CI listeners.

Results

Although worse than in NH listeners, the F0 JNDs observed in CI users were consistent with the results of the gender categorization study, namely, these were found to be sufficient to support discrimination of male F0 from female F0. However, CI listeners did not perceive VTL differences typically found between male and female speakers.

Conclusions

Our results show that CI users cannot detect acoustic changes induced by gender-related VTL differences. More generally, these results indicate that present stimulation strategies do not allow CI users to benefit from VTL differences between male and female speakers. This may explain some of the difficulties CI listeners encounter in understanding speech in crowded environments. Furthermore, these suggest that F0 is not the only problematic voice cue in CIs, and that VTL may be even more negatively affected by the poor spectral resolution of the device. New stimulation methods must therefore be developed to improve the representation of not only F0, but also VTL, in the implant.

PD-16

Comparing Loudness Variability or Internal Noise Between High- and Low-Rate Pulse Trains

Mahan Azadpour[1]; Mario Svirsky[2]; Colette McKay[3]
[1]New York University; [2]New York University School of Medicine; [3]Bionics Institute

Recent cochlear implant processing strategies stimulate auditory nerve with high-rate pulse trains. Higher stimulation rates permit encoding of more rapid temporal envelope variations. However increasing rate of stimulation is detrimental to the detection of changes in stimulation level, in the sense that both intensity discrimination and modulation detection will require a larger change in the electrical currents to produce a detectable perceptual difference. Loudness of a sound can be described by a normal distribution determined by its average and its variance (related to internal noise or variability). According to signal detection theory, performance in an intensity discrimination task is proportional to the ratio of two factors: the amount of shift in the average loudness due to increased stimulation level, and the loudness variations or internal noise. The former (the numerator of the ratio) is smaller at higher stimulation rates (because of shallower current-to-loudness function resulting in a larger dynamic range), which might at least partially explain the larger level difference limens (LDL). Nevertheless it is not clear whether internal noise changes by stimulation rate, which would contribute to the effects of rate on LDLs.

It was hypothesized that because, at lower rates, neural responses phase lock more precisely to the individual pulses and are less scattered, perception would be less variable than at higher rates. Internal loudness variability was compared between high and low stimulation rates in a psychophysical approach based on signal detection theory.

Trains of 500 and 3000 pulses-per-second presented on a test electrode were loudness balanced to obtain reference stimuli. LDLs were obtained in 2-interval 3down-1up adaptive procedures in two conditions: 1) same rate for the variable and reference stimuli 2) for each reference rate, the variable stimulus at the other rate. Subjects' task was to point to the louder interval. The difference between LDLs obtained in conditions 1 and 2 using the same variable rate depended only on the relative relation of the internal noises at the two stimulation rates.

LDLs obtained in condition 1 were significantly larger at the higher rate. LDLs obtained in 1 and 2 with equal rate for the variable stimulus were not significantly different, suggesting that internal noise does not vary significantly by stimulation rate.

Larger LDLs at the higher rate are mainly caused by the shallower current-to-loudness functions. Hence the number of LDLs across the dynamic range should not differ among stimulation rates for the same subject and electrode position.

SYM-13

Physiologically-Based Modeling of the Mechanics of the Mammalian Cochlea

Julien Meaud[1]; Karl Grosh[2]
[1]Georgia Institute of Technology; [2]University of Michigan

The mammalian auditory system is an extremely complex sensory system. Invasive *in vivo* measurements are commonly used to directly characterize the physiology of the cochlea of animal models. Some indirect information about cochlear function can also be obtained using noninvasive otoacoustic emissions measurements, both in the case of animal models and humans. Computational models can help to better understand the physiology of the cochlea and the generation of otoacoustic emissions.

In this talk I will present results from a current effort on the development of a physiologically-based model of the mammalian cochlea. This computational model is based on first principles and includes a realistic biophysical model of the outer hair cells and a micromechanical model of the organ of Corti. Formulation of the model in the frequency-domain can be used to analyze the response of the cochlea to steady-state sounds while time-domain formulation can be used to simulate the response to transient stimuli.

With this computational framework, the response of the mammalian cochlea to sounds is simulated both in the case of normal conditions and in the cases of changes in the mechanics similar to what is observed in the $Tectb^{-/-}$ and $Otoa^{DENT/DENT}$ mutant mice. I will demonstrate that the model can help to explain the effect of these mutations on the mechanics of the cochlea. Using the same computational framework, I will show simulations of otoacoustic emissions of wild type animals. This computational model can then be used to predict the effect of tectorial membrane genetic mutations on otoacoustic emissions. These predictions will help to bridge the gap between noninvasive otoacoustic measurements and invasive in vivo data and will inform how changes in the physiological state of the cochlea that cause abnormal hearing affect otoacoutic emissions.

SYM-15

On the (Lack of a) Relationship Between Acoustic and Neural Temporal Fine Structure: Insights From Physiology-Based Modeling

Jayaganesh Swaminathan[1]; Louis Braida[2]; Steven Colburn[1]
[1]Boston University; [2]Massachusetts Institute of Technology

Fundamental questions about the perceptual importance of temporal fine structure (TFS) cues are often addressed using specialized acoustic stimuli, such as temporal-fine-structure speech. In this technique, sounds are initially split into several contiguous frequency bands. The "acoustic" TFS signal in each band is extracted either as the phase of the Hilbert analytic signal or by dividing the bandpass signal by the envelope magnitude (at each instant in time). Within the auditory system, the "neural" TFS is represented by the temporal patterning of the spikes for each neuron, typically referred to

as “phase locked” information. However, it is not entirely clear how the acoustic TFS signal is related to the “neural” TFS representation. This talk assesses the relationship between acoustic and neural TFS by examining the representation of different signals, from sine tones to speech. Neural TFS was quantified based on shuffled correlogram analyses of spike train data from a physiology-based auditory-nerve model. Preliminary results suggest that the relationship between acoustic and neural TFS is well defined for narrowband signals such as pure tones and much less straightforward for signals such as speech. Implications for speech representation in quiet and in noise and the predicted effects of sensorineural hearing loss will also be discussed.

Supported by NIH-NIDCD DC000117, DC004545 and AFOSR.

SYM-16

Model Predictions of How Cochlear Gain Loss and Neuropathy Interact

Sarah Verhulst
Oldenburg University

Cochlear gain loss and noise-induced cochlear neuropathy both affect the levels of scalp-recorded auditory-brainstem responses (ABRs). To yield more targeted diagnostics and tailored treatment, it is crucial to understand which stimulus configurations inform about either of both cochlear deficits. Whereas outcome measures such as psychoacoustics and brainstem response measures suffer from the inability to separate hearing deficits, models are able to control each component independently. Through hearing-impaired model predictions of brainstem responses, this study investigates which stimuli can differentially diagnose cochlear neuropathy in patients with an audiometric hearing loss.

A human auditory brainstem response model that is designed to capture level-dependent features of human click-evoked otoacoustic emissions and ABR wave-V is adopted. Cochlear gain loss was modeled through frequency-dependent auditory filter gain loss (and associated filter widening), and cochlear neuropathy through selective loss of all low- and medium spontaneous-rate auditory-nerve fibers. Both brainstem responses to transients and sustained responses were simulated for different combinations of hearing pathologies.

Model predictions show that the slope of the ABR wave-V latency as a function of stimulus level is only very little affected by cochlear neuropathy, but that it relates to the slope of the audiometric loss as a function of frequency. Amplitude-modulated stimuli are a good predictor for the degree of cochlear neuropathy in simulated envelope-following responses (EFR) when cochlear gain is intact. Simulated EFR strength was stronger for the 100 than 400 Hz amplitude-modulated noise of 75 dB SPL (m=-4 dB), and neuropathy reduced the EFR strength to the 100 Hz modulation frequency more so than to the 400 Hz modulation frequency. Cochlear gain loss affected both modulation frequencies equally, and did not add up linearly with how cochlear neuropathy reduced the responses. EFR strength in itself may thus not be a good predictor of the degree of cochlear neuropathy in listeners with audiometric losses. Rather, a difference measure between EFR strength to different amplitude-modulated stimulus configurations in the same listener may be able to circumvent the cochlear gain loss component to differentially diagnose the degree of cochlear neuropathy in these listeners. We plan on validating these model predictions using psychoacoustic and brainstem EEG correlates recorded in the same listeners.

SYM-17

Auditory Deafferentation and Temporal Processing Deficits

Frederic Marmel; Medardo A. Rodríguez-Mendoza; Enrique A. Lopez-Poveda
Universidad de Salamanca

Background

It is a common view that auditory impairments and aging lead to slower-than-normal auditory processing. A computational model (Lopez-Poveda & Barrios, 2013) recently proposed that deafferentation, i.e. a loss of auditory nerve fibers (ANFs), could account for this seemingly slower processing without postulating a change in the processing speed of individual fibers. In this model, the quality of the representation of a sound’s waveform in the population ANF response depends both on the probability of firing of individual fibers and on the number of available fibers. ANFs fire stochastically, with a higher probability for high-intensity than for low-intensity sounds and for sustained sound features than for brief transient sound features. A loss of ANFs thus deteriorates the quality of the representation of high-intensity and transient sound features. Here we asked whether this deafferentation model could explain temporal processing deficits typically observed in patients with auditory impairments and in elderly listeners.

Methods

We investigated the effect of deafferentation on the performance of young normal-hearing listeners performing temporal processing tasks. Temporal processing was investigated in a temporal integration task, a gap detection task, and an interaural phase differences detection task (IPD task, the phase differences being either in the envelope or in the temporal fine structure of the stimuli). Deafferentation was simulated in the model by varying the number of stochastic samplers that process the original signal (each sampler simulates an ANF and provides an undersampled representation of the original signal).

Results

For the temporal integration task, reducing the number of simulated ANFs resulted in higher detection thresholds for short-duration stimuli and consequently in an increase of the temporal integration effect. For the gap detection task, reducing the number of simulated ANFs resulted in higher detection thresholds. These findings are consistent with deficits associated with auditory neuropathy (Zeng et al., 2005) and, for the gap detection results, sensorineural hearing loss (Florentine & Buus, 1984) and aging (Schneider & Hamstra, 1999). Data acquisition for the IPD task is in progress.

Conclusion
Our results indicate that deafferentation - without any change in the phase-locking properties of individual fibers - can explain some of the temporal processing deficits associated with aging and auditory impairments. Computational approaches like ours could be all the more useful to clarify the role of deafferentation in temporal deficits, since it is a 'hidden' pathology, not easily incorporated in experimental setups.

SYM-18

Prediction of Behavioral Speech Intelligibility and Quality using a Computational Model of the Auditory System

Muhammad Zilany; Nursadul Mamun; Wissam Jassim
University of Malaya

Background
Assessment of speech quality and intelligibility based on listening tests (behavioral studies) is an expensive, time consuming, and complicated operation, because it relies on subject's feedback and laboratory test conditions. However, listeners' performance can be objectively predicted using a mathematical comparison of the features from the original (clean) and processed (degraded) speech (e.g., articulation index). Alternatively, subjective scores can be estimated by replacing the listeners with a reliable model of the auditory system (e.g., neurogram similarity index measure, NSIM). This study proposed a new objective speech quality and intelligibility metric, neurogram orthogonal polynomial measure (NOPM), in which orthogonal polynomials were applied on the auditory neurogram to extract features, referred to as orthogonal moments. Orthogonal moments have been widely used in image quality assessment.

Methods
In this study, a phenomenological model of the auditory periphery developed by Zilany and colleagues (J. Acoust. Soc. Am. 126, 283–286, 2014) was employed to simulate the responses of the auditory nerve fibers to speech signals. The output of a population of model AN fibers tuned to different characteristic frequencies can be visualized as a neurogram. Orthogonal moments, Tchebichef and Krawtchouk moments, were then extracted, and the correlation coefficient between normal and distorted moment neurograms was computed to produce NOPM score.

Results
Speech intelligibility: The effect of speech-shaped noise on recognition performance for listeners with normal-hearing and hearing loss was evaluated using the proposed metric, NOPM, and the predicted scores were compared to the subjective scores from behavioral studies using NU#6 word lists. The proposed method showed a good fit with the subjective scores for all cases. The predicted scores had a realistic dynamic range and were also well-separated as a function of hearing loss.

Speech quality: The proposed speech quality metric was used to predict the subjective scores from two standard databases, the NOIZEUS and the supplement 23 to the P series (P.Sup23) of ITU-T Recommendations. The estimated score was also compared to the score from some traditional objective quality measures (e.g., perceptual evaluation of speech quality). In general, the proposed neural-response-based metric yielded better results than most of the traditional acoustic-property-based quality measures.

Conclusions
NOPM showed a reasonably good quality of linear fitting between the predicted and subjective scores for all cases. The neural response-based proposed metric also showed a realistic and wider dynamic range compared to NSIM based on the responses from a model of the auditory periphery.

Supported by RP016B-13AET.

SYM-19

Predicting Forward Masking Data with Olivocochlear Efferent Effects in the Temporal Window Model

Elin Roverud; Elizabeth Strickland
Purdue University

Forward masking refers to the elevation of threshold for a signal when it follows a temporally non-overlapping sound. The underlying mechanisms responsible for forward masking are a matter of debate. The Temporal Window Model (TWM) proposes that the masker and signal are integrated within a temporal window. The temporal window can also account for the limited temporal acuity of the auditory system and improvement in threshold with increasing signal duration. It has been suggested that this integration process occurs centrally and reflects activity of neurons with long time constants (Oxenham, 2001). The medial olivocochlear reflex (MOCR), a sluggish, sound-evoked reflex that reduces gain of the cochlear amplifier, may also play a role in forward masking. However, how it may contribute to forward masking or manifest in psychoacoustical data is not well understood.

In a recent psychoacoustical study (Roverud and Strickland, 2014), we measured signal threshold in the presence of an off-frequency forward masker with a preceding on- or off-frequency precursor. Results showed differences in masking between on-frequency and off-frequency precursors *as a function of duration*, inconsistent with only temporal integration. The differences seen could reflect MOCR activity which reduces gain of on-frequency stimuli over a sluggish time course. Off-frequency stimuli presumably have no gain at the signal frequency place and therefore would be unaffected by the MOCR. To test this idea, we compared the predictions of two versions of the TWM, the standard TWM and a modified TWM that included gain reduction (TWM-GR). The standard TWM in this study consisted of four processing stages: a simplified filtering stage, compressive nonlinearity representing the basilar membrane input/output (I/O) function, a sliding integrating window, and a decision mechanism. In the TWM-GR, we added a history- and stimulus-dependent gain reduction module in the I/O function stage to simulate the MOCR. The gain reduction module considers the energy of on- and off-frequency stimuli over time and continuously feeds back

a gain reduction value that is applied to the I/O function after a delay.

The TWM-GR predicted differences between on- and off-frequency precursors as a function of duration. This was a result of the gain reduction module which predicted that on-frequency stimuli can reduce gain for themselves if they are sufficiently long. Implications of gain reduction for other forward masking data and limitations of the TWM-GR will be discussed.

Research support provided by grants from NIH (NIDCD): R01-DC008327, T32DC000030-21.

SYM-20

Efferent Control of Human Cochlear Tuning: Psychoacoustical Measurements and Computer Model Simulations

Enzo Aguilar[1]; Almudena Eustaquio-Martin[2]; Enrique A Lopez-Poveda[2]
[1]Universidad de Talca; [2]Universidad de Salamanca

Background

The brain has the capacity to modulate cochlear responses by means of medial olivocochlear efferents (MOC). MOC efferents can be activated in a reflexive manner by contralateral acoustic stimulation. Here, we investigated the effect of the contralateral medial olivocochlear reflex (MOCR) on human cochlear gain and tuning using psychoacoustical and computational modeling techniques.

Methods

It was assumed that the MOCR is activated by contralateral white noise (CWN) at 60 dB SPL. Psychophysical tuning curves (PTCs) were measured in forward masking for probe frequencies (f_P) of 500 Hz and 4 kHz, with and without CWN, in normal hearing listeners. Masker frequencies ranged from $0.5f_P$ to $1.3f_P$. PTCs were measured using short (2 ms) and long (10, 30, and 50 ms) masker-probe time intervals to assess cochlear tuning at near-threshold and supra-threshold conditions, respectively. Measured PTCs were mimicked using a computer model of forward masking with efferent control. In the model, the assumption was made that the MOCR reduces the cochlear gain to low- and moderate-level sounds. The model also accounted for off-frequency listening at low frequencies.

Results

The CWN affected PTCs and the effects were more evident at 500 Hz than at 4 kHz. PTCs measured with CWN showed lower masker levels and wider overall tuning than PTCs measured without CWN. The magnitude of CWN effects increased with increasing masker-probe time gap (or, equivalently, with increasing the masker level range in a PTC). For near-threshold PTCs, the CWN effect was obvious only for frequencies in the tails of the PTCs; for supra-threshold PTCs, by contrast, the CWN effects were obvious at all frequencies. The model reproduced qualitatively and quantitatively the PTCs measured both with and without CWN conditions.

Conclusion

Contralateral white noise affects PTCs, probably by activation of the contralateral MOCR. The analysis using the model suggested that the human MOCR reduces cochlear gain and this reduction is greater for apical than for basal cochlear regions (gain reduction was about 6 dB at 500 Hz and < 2 dB at 4 kHz). The model was crucial for explaining some seemingly paradoxical aspects of the behavioral data. These results are consistent with the previous physiological evidence. (Work supported by the Spanish MINECO to E.A.L.-P. (ref. BFU2009-07909) and by the Chilean CONICYT to E.A.).

PD-17

NIDCD Workshops

Amy Donahue
NIH

SYM-21

Why Do We Need Epidemiology, Anyway? The Use of Epidemiology for Prevention and Clinical Research

Javier Nieto
University of Wisconsin School of Medicine & Public Health

The goals of epidemiology are to understand how health and disease outcomes are distributed in the population and what are the determinants of such distribution. The target population of epidemiologic inquiry may be the general population (as in broad-based epidemiologic survey), but can also be clinical patients (a subfield known as “clinical epidemiology”). Similarly, the range of epidemiologic methods varies widely depending on the particular determinant of interest in the broad multilevel range of disease determinants (molecular/biological; behavioral/lifestyle; social and physical environment).

In this presentation, examples of the application of epidemiologic studies for the advanced of the understanding of disease causation and disease prevention are discussed, particularly in reference to cardiovascular disorders. Specifically, the development of research on three risk factors of atherosclerosis is discussed: hypercholesterolemia, inflammation, and obstructive sleep apnea. These examples are used to illustrate not only the application of different methodologies but also as case studies to discuss the strengths and limitations of the tools for causal inference in epidemiology.

The implications for research for prevention and treatment of aging-related disorders are also discussed.

SYM-22

Genetics of Age-related Hearing Loss

Paolo Gasparini[1]; Dragana Vuckovic[2]; Giorgia Girotto[2]
[1]IRCCS-Burlo Garofolo/University of Trieste; [2]University of Trieste

To date, very few environmental and genetics factors are known to contribute to Age-related Hearing Loss (ARHL) [1,2,3,4]. The lack of knowledge on ARHL molecular basis, prompted us to develop a combined multi-approach strategy using several thousands individuals from several populations

of Europe (Italy, Croatia, Finland and UK), Caucasus (Georgia, Armenia, Azerbaijan, Crimea) and Central Asia (Uzbekistan, Tajikistan, Kazakhstan, Kirghizstan). Starting from our past experience on GWAS meta-analysis combined with expression studies [5], the following strategy was designed: 1: GWAS meta-analysis for common tag-SNPs and functional variants, 2: replication in independent outbred cohorts, 3: gene-based for rare functional variants (i.e.SKAT), 4: Whole Exome Sequencing (WES) in a selected subgroup of 250 ARHL cases/controls, 5: Targeted Re-Sequencing (TRS) of 47 candidate ARHL genes (i.e. from GWAS Metanalyses, ENU mutagenesis) in a large series of cases and controls.

Research activities carried out at STEPS 1, 2 and 3 (in collaboration with K.Steel, and S.Dawson as well as part of the ongoing activities within the G-EAR Consortium) led to the identification of a series of new ARHL candidate genes: *ITFG2* ($p=6.92E^{-11}$), *PCDH20* ($p=4.71E^{-10}$), *SLC28A3* ($p=2.39E^{-09}$) and, with highly suggestive associations (ranging from $7.97E^{-06}$ to $1.90E^{-05}$) the genes *PTPRCAP, FN1, EAF1, METRNL, PDP2, ARRDC1, HDGF, TMOD1*. Some of these genes have been already replicated in large cohorts (i.e. *PCDH20* and *SLC28A3*) and part of them belong to gene-families already known as being involved in hearing loss and expressed in the cochlea. As regards to TRS, preliminary data carried out in 67 ARHL cases revealed the presence of at least one rare/predicted pathogenetic allele in approximately half of them. Mutations are present in 19 different genes. Research activities planned at STEPS 4 and 5 are in progress with WES, carried out in collaboration with CRG, Spain, now available to identify population disease-specific rare variants.

The strategy planned proved to be very useful and productive. *In vitro* and *in vivo* functional studies are now needed to confirm the role of the whole list of genes/variants identified through the above-described phases. Up-to-date results will be presented and discussed.

References

[1] Newman DL, et al. Hear Res. 2012; 294:125-32.
[2] Nolan LS, et al. Neurobiol Aging. 2013;34(8):2077.
[3] Bovo R, et al. Aging Clin Exp Res. 2011 Feb;23(1):3-10
[4] Vuckovic D, et al. Hearing, Balance and Communication 2014
[5] Girotto G, et al. 2014 PLoS One. 2014 Jan 14;9(1):e85352

SYM-23

Is Primary Prevention Possible? Findings from Longitudinal Cohort Studies

Karen Cruickshanks
University of Wisconsin School of Medicine and Public Health

Older people are at high risk for age-related hearing impairment, a chronic condition affecting communication and quality of life. Finding strategies for slowing or delaying the onset is important as there are no available treatments to reverse or stop this progressive disorder. Population-based longitudinal cohort studies are important for measuring incidence and relative risks, identifying modifiable risk factors, and translating experimental findings to the general population but there have been few cohort studies focused on understanding hearing impairment.

The Epidemiology of Hearing Loss Study (EHLS) which began in 1993 is an on-going population-based study of Beaver Dam, WI residents who were ages 43-84 years in 1987-88 (n=3753). The Beaver Dam Offspring Study (BOSS) is an on-going longitudinal study of their adult children ages 21-84 years which began in 2005 (n=3376). Each cohort has been examined at five-year intervals with standardized testing protocols including audiometric assessments of hearing, questionnaires, and laboratory measures. Examinations included measures of multiple cardiovascular risk factors.

These epidemiological studies have shown that the risk of hearing impairment is declining across generations, strong evidence that modifiable factors contribute to the pathogenesis of hearing impairment in adults. The findings from the EHLS and BOSS will be reviewed along with data from other longitudinal cohort studies with similar methods. Emerging evidence suggests that some cardiovascular risk factors, long-term chronic inflammation and atherosclerosis increase risk of hearing impairment. Therefore, aging changes in auditory function may be caused by systemic exposures and processes similar to some other age-related disorders. However, additional risk factors and pathways may be involved in this complex disorder. New directions from the current studies and future research needs will be discussed. The results from longitudinal studies suggest that primary prevention to maintain good sensory function in aging may be possible through interventions focused on multiple risk factors, an approach that has been successful in other chronic disorders of aging.

SYM-24

Risk Factors for Incident Hearing Loss: The Nurses' Health Study II and Health Professionals Follow-Up Study

Gary Curhan
Brigham and Women's Hospital/Harvard Medical School

Background

Large prospective cohorts with detailed information on a variety of relevant exposures can identify modifiable risk factors for hearing loss, which could lead to public health recommendations to help prevent this common condition.

Methods

Clinically and scientifically important findings on risk factors for hearing loss have been reported based on data from two large cohort studies: Health Professionals Follow-Up Study comprised of 51,529 men aged 40-75 at baseline in 1986 and Nurses' Health Study II comprised of 116,430 women aged 25-42 at baseline in 1989. Participants respond to biennial mailed validated questionnaires that collect extensive and detailed information on lifestyle, diet medical conditions and medication use. Biologic samples, including blood and DNA, have been provided by over 50,000 participants. Participation rates are high with follow-up exceeding 90% of eligible person-time. Two hearing related outcomes are being analyzed

in these cohorts: self-reported hearing loss (with date of onset) and audiometrically measured air conduction thresholds in a subset of 3300 NHS II participants. A detailed hearing study supplementary questionnaire was answered by over 40,000 participants, which provided information on family history of hearing loss, lifetime noise exposure, and evaluation and treatments. Cox proportional hazards regression is used to estimate relative risks for onset of hearing loss after adjusting for potential confounding factors.

Results

Our published findings to date have included over 14,000 cases of self reported HL in the two cohorts over 1.5 million person-years. More frequent use of aspirin, NSAIDs, or acetaminophen was associated with higher risk of self-reported HL. Moderate alcohol consumption was not associated with risk of hearing loss. In women, larger BMI and waist circumference were associated with increased risk, whereas higher level of physical activity was associated with lower risk. Also in women, higher intakes of fish and marine fatty acids were associated with lower risk of hearing loss. There was no association between vitamin intake and risk in men but preliminary data in women suggest a lower risk of hearing loss in those with higher intake of beta-carotene and folate.

Conclusions

Cohorts studies have identified modifiable risk factors for hearing loss, suggesting that the burden of hearing loss can be reduced. Future studies in these cohorts will examine additional modifiable potential risk factors including exogenous hormone use and other dietary factors. These important exposures will also be examined in the 3300 NHS II participants undergoing serial audiometric exams.

SYM-25

Hearing Health Disparities in Diverse Populations

David Lee
University of Miami Miller School of Medicine

The prevalence of hearing loss in adults varies as a function of many sociodemographic factors including age, gender, race/ethnicity, educational attainment, and occupation. Factors that underlie this variation are complex and include a mix of genetic and non-genetic factors that may interact to produce prevalence differences across these subgroups. Variations in the prevalence of modifiable risk factors associated with the development and progression of age-related hearing loss (e.g., occupational noise exposure, smoking, development of cardiovascular disease and diabetes) are important contributors to these variations. Finally, access to and the utilization of health care, including hearing health care, also varies across sociodemographic subgroups. This epidemiologic and healthcare access literature will be summarized and critical gaps in the literature will be outlined. Priority populations for intervention will be identified and a research agenda outlined which will inform efforts to advance the goal of preventing adult-onset hearing loss while simultaneously reducing hearing health disparities in the United States.

PD-26

Lungfish Hearing: Implications for the Evolution of the Tetrapod Middle Ear.

Jakob Christensen-Dalsgaard[1]; Christian Bech Christensen[2]; Peter Teglberg Madsen[2]
[1]University of Southern Denmark; [2]Aarhus University

Recent research has shown that tympanic middle ears evolved independently in the major vertebrate groups and represent independent experiments in terrestrial hearing. Furthermore, the tympanic ear emerged quite late – approximately 120 mya after the origin of the tetrapods and approximately 70 my after the first truly terrestrial tetrapods emerged. One of the major challenges is to understand the transitional stages from tetrapod ancestors to the tympanic tetrapod ear, for example how a non-tympanic ear functions in terrestrial hearing. Lungfish are the closest living relatives of the tetrapods, and the ear of lungfish may be similar to the ear of theearly tetrapods.

We have studied the sensitivity of African lungfish to air-borne sound, underwater sound and vibrations. We show that lungfish detect underwater sound pressure via pressure-to-particle motion transduction by air volumes in their lungs and that lungfish detect air-borne sound by sound-induced head vibrations, resulting in a limited sensitivity to low-frequency sound (lowest thresholds from 80 dB SPL). Adiditionally, lungfish are sensitive to substrate vibration with a sensitivity comparable to anurans and urodeles.

Based on ABR and vibration measurements also on amphibians, lizards, snakes and alligators we can outline scenarios for the initial adaptations of the middle ear to non-tympanic hearing and assess the selection pressures later adapting the middle ear for tympanic hearing. Hearing by bone conduction, sound induced vibrations of the skull, is found in snakes and some earless frogs, whereas urodeles and other earless frogs are more sensitive than predicted from sound-induced skull vibrations and may have specialized pathways to the inner ear. We propose four stages : 1) the unspecialized crossopterygian ear with immobile middle ear bone, 2) increased inner ear frequency ranges, 3) mobile middle ear structures and 4) the tympanic middle ear.

PD-27

Measurement of High Intensity Sound Pressure Transmission from the Ear Canal to Middle Ear

Rong Gan; Don Nakmali; Zachary Yokell
University of Oklahoma

Introduction

Exposure to high intensity sound or blast overpressure waves will result in damage of auditory system. However, there is a lack of knowledge on how the high intensity sound transmitted from the ear canal to middle ear and finally to cochlea. In this study, we report the experiments conducted in human temporal bones to monitor impulse sound pressure from the ear canal to middle ear. The goal is to characterize the trans-

fer function of the ear canal and middle ear in response to high intensity sound.

Methods
A compressed air (nitrogen)-driven blast apparatus located inside an anechoic chamber in our lab was used for this study. The fresh human temporal bone was mounted with two pressure sensors (PCB Piezotronics) inserted in the ear canal near the TM (P1) and inside the middle ear cavity behind TM (P2). Another sensor was placed at the entrance of the ear canal to measure sound pressure P0. The "head block" was setup vertically along the blast incident wave direction and horizontally perpendicular to incident wave. Eight temporal bones in vertical tests were in two groups: with and without pinna, and five temporal bones in horizontal tests were all with pinna. The pressure waveform was recorded and 5 exposures were performed for each setup of the temporal bone.

Results
The measurements obtained from all temporal bones show that blast overpressure P0 at the ear canal entrance induced the highest peak pressure P1 near the TM in the ear canal. The peak pressure was further transmitted through the TM into middle ear with a much lower value of P2. The average peak pressure ratio of P1 to P0 was 2.92 in the ears with pinna (N=4) and 1.34 in the ears without pinna (N=4) in vertical setup. This implies that the pinna enhances the impulse transduction in the ear canal. The overpressure level in horizontal setup was much higher than that in vertical test, and the peak pressure ratio of P1 to P0 was 1.25 (N=5) lower than that measured in vertical test.

Conclusions
This preliminary study demonstrates that the experimental setup for monitoring impulse wave transduction from the ear canal to middle ear is successful. The ear canal and TM play an important role for overpressure transmitted into the middle ear. (Supported by NIH R01DC011585 and DOD W81XWH-14-1-0228)

PD-28

Development of a Lumped Parameter Middle Ear Model for Gerbils and Comparison of Inter-Species Middle Ear Models

Charlsie Lemons; Julien Meaud
Georgia Institute of Technology

Measurements of otoacoustic emissions in the ear canal are affected by the forward and reverse pressure transfer functions and the reverse middle ear impedance. Thus, a comprehensive middle ear model should reflect each of these measurements of middle ear function using a single set of parameters. Due to the extensive set of experimental data, significant effort has been put forth in modeling the human middle ear: a lumped parameter model of the ossicular chain coupled with a transmission line model of the eardrum has been developed. This model fits experimental data very well and has low computational cost compared to finite element models; however, intracochlear measurements are generally restricted to rodents and models for rodent middle ears are limited. We adapted a lumped parameter middle ear model to represent the middle ear of gerbils, guinea pigs and mice using available experimental data. Non-linear least square fitting algorithms were used to fit model parameters to available data for the forward and reverse functions of the middle ear. The models for different species are compared to each other in order to (1) predict, if possible, what changes are necessary to model other mammals and to (2) draw conclusions about role of different components of middle ear. This research highlights how further data could be used to better characterize and model middle function in rodents. The models could be coupled to cochlear models in order to predict otoacoustic emissions in rodents.

PD-29

LPS Suppresses the Phagocytic Function of Macrophages by Down-regulation of SH3PXD2B Expression through TLR4 Pathway

Ping Zhu[1,3]; Shu-Yang Xie[2]; He-Ping Yu[3]; Xiaoling Zhang[2]; Luke Apisa[3]; Ping-Yu Wang[2]; Michael Roy Jacobs[3]; Qing Zheng[3]
[1]Sun Yat-sen University; [2]Binzhou Medical University; [3]Case Western Reserve University

SH3PXD2B (TKS4), a Src substrate and adaptor protein, is crucial to the formation of podosomes of macrophages and other cell types. This is an essential element in phagocytosis of pathogens. Lipopolysaccharide (LPS), a component of Gram-negative bacterial pathogens, is recognized by toll-like receptor 4 (TLR4) as a danger signal to initiate immune activation. Here, we found that LPS treatment decreased phagocytic function of macrophages through suppressing the expression of SH3PXD2B in LPS-treated peritoneal macrophages. In contrast, the expression of TLR4-related factors (TLR4, NF-κB and TNF-α) was increased in LPS-treated macrophages. LPS treatment yielded the same effects on the expression of SH3PXD2B and TLR4-related factors in cultured macrophages cultured from *Sh3pxd2b*$^{n/n}$-mutant mice, but not from *Tlr4*$^{-/-}$-mutant mice. This implies the TLR4 pathway takes part in LPS-stimulated down-regulation of SH3PXD2B expression. TNF-α treatment similarly reduced SH3PXD2B expression in cultured macrophages, an effect which was neutralized by TNF-α antibody. Moreover, LPS treatment of macrophage cultures disrupted formation of podosomes and phagocytosis of Chinese ink particles and of bacteria. SH3PXD2B expression in LPS-treated, cultured macrophages was rescued by ibuprofen. Ibuprofen also rescued macrophage function as measured by Chinese ink and bacterial ingestion assays. Our study reveals a novel pathway in which LPS decreases SH3PXD2B levels by a TLR4-related factor. This previously unappreciated pathogenic mechanism of Gram-negative bacteria may have important ramifications for understanding the pathogenesis of otitis media and other LPS-mediated infections and their treatment strategies.

PD-30

The Role of NFκB in the Pathogenesis and Recovery in Otitis Media

Brian Nuyen[1]; Xinwei Liu[2]; Kwang Pak[3]; Stephen Wasserman[1]; Allen Ryan[1]

[1]University of California, San Diego; [2]University of Central Florida College of Medicine; [3]VA San Diego Healthcare System

Background

Otitis media (OM), especially in its chronic forms, is a major contributor to global childhood morbidity and mortality, with consequences that include permanent hearing loss and speech and language development delays. Mechanisms of proneness to recurrent/chronic OM have been shown to involve mutations or polymorphisms in genes that subserve innate immunity as well as dysregulation of pathways that promote recovery from inflammation. Nuclear factor kappa-light-chain-enhancer of activated B cells complex (NFκB) is a dimeric transcription factor composed of NFκB1 and RelA subunits. It is a pleiotropic orchestrator of inflammation and operates downstream from several innate immune receptors. This suggests NFκB to be a critical potential regulator of pathogenesis and recovery in OM. We therefore evaluated its role in the middle ear (ME) response to bacterial infection *in vivo*.

Methods

48 NFκB1(-/-) mice and 48 wild-type (WT) mice were divided into sets of 6 mice, 1 for each of 8 time points (0, 1, 2, 3, 5, 7, 10, and 14 days after inoculation). Three mice per set were used for ME histopathology, and 3 were used for ME bacterial culture. The MEs of WT and NFκB1(-/-) mice were inoculated with transbullar injections of nontypeable *Haemophilus influenzae* (NTHi), with monitoring for ME infection and inflammation for the above time points. 0h animals were not inoculated, and served as controls.

Results

NFκB1(-/-) mice experienced prolonged ME mucosal thickening, enhanced inflammation, and delayed egress of neutrophils and macrophages from the tympanic cavity until day 10. Furthermore, WT mice generally cleared NTHi from the ME by day 5, while NTHi was recovered from NFκB1(-/-) mice until day 10. Interestingly, most NFκB1(-/-) ME cavities harbored an additional bacterial species besides NTHi during the course of OM disease, a species identified as *Klebsiella pneumoniae*. This pathogen was not observed in WT ME cavities.

Conclusions

In this mouse model of NTHi-mediated OM, NFκB-mediated signaling was important for the clearance of infection and resolution of inflammation. Also, NFκB1(-/-) mice apppeared to permit pathogens native to murine nasopharynges to participate in OM. This suggests a critical role for NFκB in limiting the passage of commensal bacteria through the Eustachian tube. Further studies may examine how NFκB influences the resolution of inflammation in chronic OM in children.

PD-31

Structural Changes of Tympanic Membrane in Acute Otitis Media Model of Chinchilla

Shangyuan Jiang[1]; Xiying Guan[2]; Brooke Hitt[1]; Rong Gan[1]

[1]University of Oklahoma; [2]Harvard University

Introduction

Acute Otitis Media (AOM) is the most commonly diagnosed disease in young children. Previous studies have revealed that the structural change of tympanic membrane (TM) contributes to the loss of TM mobility induced by AOM. However, how the microstructure of TM varies along the course of the disease has not been quantified in the literature. This study attempts to characterize the morphological changes of the TM through the middle ear infection course at various locations across the TM in the chinchilla AOM model using histological assessment.

Methods

Ten chinchillas were included in this study and divided into three groups: the control group of four animals, the 4 days AOM (4D) group of three animals, and the 8 days AOM (8D) group of three animals. AOM was created by transbullar injection of *Haemophilus influenza* in both ears. At the 4th or 8th day post inoculation, bullas were harvested and fixed after the animals were euthanized. The bullas were then decalcified and embedded in paraffin. Specimens were cut into sections at thickness of 8 μm from the superior to the inferior, and stained in H&E. The histological images were examined under a light microscope and thicknesses were digitalized for measurement of the membrane. The images at 10 locations of the TM were selected for measurement as shown in Fig. 1.

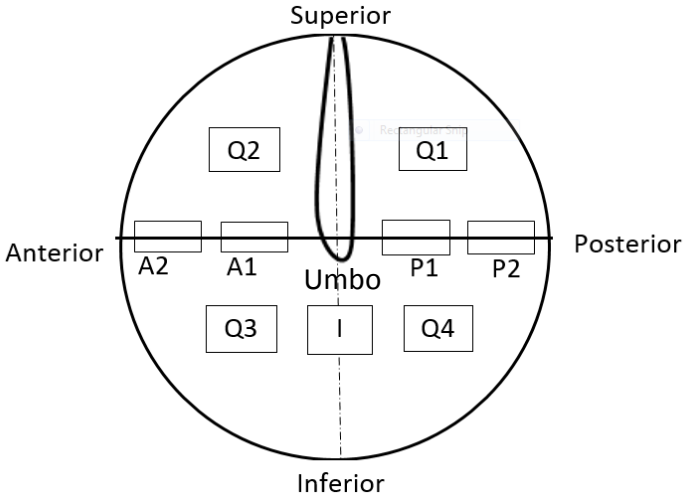

Fig. 1. Schematic of TM with 10 measurement locations.

Results

The TM thickness at different locations were measured and statically analyzed based on a sample size of N=4. The average TM thickness in 4 quadrants measured from 4D and 8D AOM ears is 15.7 μm and 24.0 μm in comparison with control ears of 12.4 μm. The thickness increase was mainly caused by edema and neutrophils infiltration in the sub-epithelial layers. The collagen fiber layers appeared intact without signif-

icant change. The anterior side and boundary regions of the TM were thicker than other locations in all control and AOM ears.

Conclusions
AOM resulted in TM thickness increase throughout the two phases of the disease with the measurement data over 10 locations. The thickness increases in anterior and boundary areas were more severe than other locations. The findings in this study provide evidences for understanding of TM mobility loss in AOM ears.

(Work supported by NIH R01DC011585)

PD-32

Drug Delivery to the Middle Ear Without Tympanostomy

Didier Depireux[1]; Maricel Cubangbang[2]; Mika Shimoji[1]; Mohammad Ahmed[1]; Amarel Tomney[2]; Stéphanie Val[2]; Benjamin Shapiro[1]; Diego Preciado[2]
[1]University of Maryland, College Park; [2]Children's National Medical Center, Washington DC

The standard-of-care for Acute Otitis Media (AOM) is systemic antibiotic administration. 42% of all antibiotics prescribed in the US are for the treatment of AOM. This pattern of systemic antibiotic use for AOM has contributed significantly to the appearance of resistant organisms, and to an increased incidence of antibiotic-related side effects. Puncture and tympanostomy tube placement through the ear drum *under general anesthesia*, for treatment of recurrent AOM or Chronic Otitis Media with Effusion (COME), is the most common pediatric surgical procedure requiring anesthesia in the United States. There is a critical public health need for better and less invasive strategies to treat AOM and COME, not only to minimize side effects and the development of resistant micro-organisms, but also to reduce the costly burden, pain, and attendant risks of surgical procedures and general anesthesia in young children.

We have recently developed a technology that uses magnet arrays to generate a force which atraumatically pushes drug-carrying nanoparticles across the tympanic membrane, from outer to middle ear. These biocompatible nanoparticles can be loaded with a variety of drugs, including steroids and antibiotics. In a rat model of otitis media with effusion, we have shown that delivery of sulfonamide-laden particles into the middle ear post-infection significantly reduces the duration of the otitis and associated inflammation when administered a day or several days post-onset. When administered in healthy rats, including negative and vehicle (nanoparticle alone) controls, with and without magnetic push, the particles caused no obvious long-term negative effects, as measured with auditory brainstem response, gap pre-pulse inhibition of the startle reflex and immunochemistry.

We will report on drug levels, nanoparticle concentration and cytokine levels, measured days and weeks following treatment, in the middle ear, cochlea, blood, brain, and other major organs. After administration and treatment with nanoparticles, we observe a transient but no permanent shift in hearing thresholds, probably because of a conductive hearing loss.

Thus, the use of magnetic nanoparticle-mediated delivery of antibiotics, steroids and other drugs is a non-toxic, safe and controlled method to achieve a sustained, clinically significant drug concentration in the middle ear, without the need for systemic administration and its associated development of antibiotic resistance, and will likely reduce the need for tympanostomy tube placement in children.

PD-33

Haptic Simulation of the Ossicles Palpation

Guillaume Kazmitcheff[1]; Hadrien Courtecuisse[2]; Yann Nguyen[3]; Mathieu Miroir[3]; Alexis Bozorg Grayeli[4]; Stephane Cotin[2]; Olivier Sterkers[3]; Christian Duriez[2]
[1]University Pierre et Marie Curie, Paris 6; [2]Shacra, INRIA, Université Lille 1, F-59650, Villeneuve d'Ascq, France; [3]Sorbonne Universités, UPMC Univ Paris 06, UMR S 1159, F-75005, Paris, France INSERM, UMR S 1159, F-75005, Paris, France AP-HP, Hôpital Pitié-Salpétrière, service ORL, F-75013, Paris, France; [4]CHU Dijon, service ORL, F-21000, Dijon, France

Palpation of the ossicular chain is delicate and essential during an ossicular surgery procedure. To provide a realistic surgical simulation design for training and rehearsal purpose, it is necessary to transmit a stable and credible forces feedback to the user. However, the strong heterogeneities of the biological tissues, such as the middle-ear components, involve stability and realism issues to simulate the deformation and the tactile rendering, particularly for a real-time application. Indeed, if the deformation model can be computed realistically at low frequency (30 Hz), the haptic rendering requires a refresh rate around 1000 Hz. This work is focus on the development of a haptic rendering method and its evaluation to design a real-time microsurgical simulator applied to the middle ear.

A mechanical model of the ossicular chain is developed in the medical simulation software SOFA (INRIA). We propose a new method for haptic rendering, which is based on a preconditioning algorithm to speed up the deformation computation coupled to an asynchronous approach to calculate the deformations and the haptic feedback. Scheduled interactions, between a surgical instrument and the ossicles, are performed to assess the quality of the force feedback rendering at high rate compared to the deformation computed at low frequency by the simulation for different simulation time step. Finally, a real-time simulation is performed allowing surgeons to interact with the ossicles while feeling the forces applied to the anatomical structures.

For the scheduled interaction, the forces computed at low frequency (48 Hz) by the simulation loop are 0.274 N ± 0.021 (n=4) and 0.270 N&± 0.013 (n=4) for our haptic rendering method at high rate (1000 Hz). This difference was not significant (paired-Student). Moreover, these forces are in good agreement with experimental measurements on human temporal bones during the palpation of the ossicles, ranging from

0.098 to 0.655 N [Bergin et al. 2014, OtolNeurotol]. During the real-time simulation of the palpation, the refresh rate is reported stable at 48Hz for simulation loop and at 1000Hz for the force feedback algorithm. The forces computed by the haptic process are consistent with those calculated in the simulation loop and the experimental data.

We assess that our method is able to compute the forces during interactions with non-linear and non-homogeneous materials. We successfully applied our method to an interactive simulation in real-time of a microsurgical intervention. Surgeons are able to interact realistically with our mechanical model of the ossicular chain.

PD-18

Repair of Mammalian Hair Cells via Sea Anemone Repair Proteins

Pei-Ciao Tang; Glen Watson
University of Louisiana at Lafayette

Sea anemones show an especially marked capacity to repair severely damaged hair bundles through a suite of repair proteins (RPs) that are secreted in the mucus overlaying the hair bundles. Previously, anemone-derived RPs were also found to enhance repair of hair cells in lower vertebrates, such as blind cavefish; therefore, their efficacy in repairing damaged hair cells in mammals, a taxon with a low capacity for hair cell repair, was explored herein. RPs were purified by blue native gel electrophoresis from the mucus of the model sea anemone *Nematostella vectensis*. Bands corresponding to RPs were excised from the gels and the polypeptides eluted in the culture media. Murine organ of Corti explants were traumatized by incubation in calcium-depleted HBHBSS for 15 min. Uptake of FM1-43 (30 sec) was used to examine the recovery of function of outer hair cells. Uptake of FM1-43 was compared among healthy controls, RP-treated explants, and traumatized controls. RP-treated explants were those that were allowed to recover for 1 hr in the presence of eluted RPs. Traumatized controls were explants that were allowed recover for 1 hr in culture media alone. FM1-43 uptake in RP-treated explants was comparable to that of healthy controls (p=0.498, n=15), and significantly greater than that of traumatized controls (p=0.010*, n=15). Furthermore, F-actin of the stereocilia was visualized with TRITC-phalloidin staining. Healthy controls had significantly more V-shaped (i.e., normally structured) hair bundles than either RP-treated explants or traumatized controls. However, the RP-treated explants had significantly more V-shaped hair bundles than the traumatized controls (p<0.001*, n=5). Normally, restoration of function in cochlear hair cells after Ca^{2+}-depletion trauma requires ~ 24 hr (Gale JE, Marcotti W, Kennedy HJ, Kros CJ, Richardson GP (2001) J Neurosci 21:7013-7025). Intriguingly, anemone RPs greatly shortened this recovery time to less than 1 hr. Collectively, these results indicate that anemone RPs significantly enhance the recovery of function and structure to experimentally traumatized hair bundles of outer hair cells in cochlea of mammals.

PD-19

Cochlear Supporting Cells are Regenerated After Ablation in Neonate Mice to Ensure Mature Hearing Function

Marcia Mellado Lagarde[1]; Guoqiang Wan[2]; Lingli Zhang[1]; Angelica Gigliello[3]; John McInnis[3]; Yingxin Zhang[4]; Dwight Bergles[4]; Jian Zuo[1]; **Gabriel Corfas[2]**
[1]St. Jude Children's Research Hospital; [2]Kresge Hearing Research Institute, University of Michigan; [3]Boston Children's Hospital; [4]John Hopkins University School of Medicine

Introduction

Supporting cells (SC) of the organ of Corti surround the sensory hair cells (HC) and dendritic terminals of primary afferent neurons providing physical scaffold and neurotrophic support, contributing to ionic balance and exchanging signals that are important for development and protection of the auditory organ. While loss of HC or primary auditory neurons results in sensorineural hearing loss, the consequence of SC loss on auditory function is largely unknown. In this study, we specifically ablated inner border and inner phalangeal cells (IBCs/IPhCs), the SCs surrounding the inner hair cells (IHCs), in mice in vivo and studied how this affected HCs, afferent neurons and hearing function.

Methods

We used the inducible Cre-loxP system in combination with a Cre-inducible diphtheria toxin transgene (DTA) to ablate specific SCs in the organ of Corti of mice in vivo in a time controlled manner. We used four different tamoxifen-inducible Cre lines: PlpCreER, Lgr5CreER, GlastCreER and Pou4f-3CreER to ablate IBCs/IPhCs alone or in combination with HCs or cells of the greater epithelial ridge (GER) at different ages. Organ of Corti were isolated, fixed and processed for whole mount or cross-sections followed by immunohistrochemistry and confocal imaging analysis. Auditory brainstem responses (ABR) were measured to assess hearing function.

Results

We found that after early neonatal ablation, IBCs/IPhCs are completely replenished within days. Regeneration of these SCs does not involve proliferation of surrounding cells but rather involves trans-differentiation of GER cells that requires the presence of IHCs. This plastic response of the neonatal cochlea preserves HCs and neurons, afferent innervation to IHCs and hearing sensitivity in adult mice. In contrast, the capacity for regeneration is lost after the onset of hearing when ablation of IBCs/IPhCs produces HC death and significant hearing impairment.

Conclusions

Our findings uncover a hitherto unrecognized capacity of the quiescent neonatal organ of Corti to efficiently replenish specific SCs after loss in vivo to guarantee mature hearing function. We show that this capacity exists in a limited time window and disappears after the onset of hearing. Better understanding of the developmental changes that occur in the organ of Corti at early postnatal ages, such as elimination of

the GER cells, are key to develop regenerative approaches to treat hearing loss.

PD-20

Toll-like Receptor 4 Signaling Contributes to Immune Cell Recruitment to the Cochlea After Acoustic Trauma

Robert Vethanayagam; Youyi Dong; Weiping Yang; Shuzhi Yang; Qunfeng Cai; Bohua Hu
University at Buffalo

Introduction

Noise overstimulation traumatizes the cochlea and causes sensory cell damage. This cell damage provokes the immune system to activate the inflammatory response. Previous studies have documented the influx of immune cells into the cochlea after noise exposure. However, the signaling pathway responsible for detection of sensory cell damage and recruitment of immune cells is not clear. Toll-like receptor 4 (TLR4) contributes to immune surveillance for endogenous molecules released from damaged tissues. In this study, we investigated the role of TLR4 signaling in noise-induced immune cell infiltration and production of inflammatory molecules in the mouse cochlea.

Methods

C57BL/6J (wild type) and TLR4$^{-/-}$ mice were exposed to a broadband noise at 120 dB SPL for 1 hour and the mice were sacrificed at 1, 4 and 7 days after noise exposure. Immune cells was identified by immunolabeling of CD45 and F4/80, commonly used markers for leukocytes. The number of positively-stained cells on the scala tympani side of the basilar membrane was counted. In addition, the transcriptional expression of TLR4-related genes was measured using qRT-PCR.

Results

CD45 is present on all bone marrow-derived white blood cells. Using CD45 as a marker, we found the presence of resident macrophages in the normal cochleae. Following acoustic trauma, the number of the immune cells, particularly macrophages, was slightly increased at 1 day post noise exposure, but the change was not statistically significant. By 4 day post-noise exposure, however, the number of the immune cells was significantly increased. This increase of immune cells was not detected in the TLR4 knockout mice, suggesting that TLR4 deficiency blocks the immune cell response in the cochlea. Moreover, the qRT-PCR analysis revealed up-regulation of the terminal protein Ap-1 (Jun) at 1 day (2.2 fold) and 7 day (3.5 fold) post-noise exposure in the cochlear lateral wall tissues of wild type mice. By contrast, this gene was down-regulated at 1 day and 7 day post-noise exposure in the lateral wall tissues of TLR4 knockout mice. Because Jun is a mediator of the TLR4 dependent production of inflammatory molecules, our result suggests that TLR4 signaling contributes the noise-induced inflammatory response in the cochlea.

Conclusion

TLR4 plays a role in regulation of immune cell recruitment and cochlear inflammation in noise-damaged cochleae. Modulation of TLR4 function holds promise for controlling cochlear inflammation and promoting tissue recovery.

PD-21

Use of the Zebrafish Lateral Line System to Model Afferent Neuron Damage Following Prolonged Glutamate Receptor Activation

Joy Sebe; Edwin Rubel; David Raible
University of Washington

Exposure to loud noise can cause temporary hearing loss, measured as an increase in the threshold required to elicit an electrical response from the brain or a behavioral response to auditory stimuli. Studies of TTS have demonstrated that while the hair cells remain intact, the postsynaptic terminals of spiral ganglion cells are damaged. Noise induced damage of spiral ganglion cell terminals and a transient elevation of hearing thresholds can be mimicked by perilymphatic perfusion of the glutamate receptor agonist, AMPA.. The inaccessibility of afferent neurons in the cochlea has made it difficult to examine afferent terminal damage and recovery in real-time. To visualize and record changes in afferent neuron morphology and function following AMPA application we have turned to the zebrafish lateral line system. The *objective* of these preliminary studies is to determine the extent to which the effects of afferent terminal damage and recovery that have been observed in the mammalian cochlea can be modeled in the zebrafish lateral line. We used a combination of *in vivo* time lapse imaging of afferent terminals and electrophysiological recordings of afferent neuron cell bodies using transgenic zebrafish larvae (6-7 days post fertilization). We established that afferent neurons respond to mechanotransduction by displacing hair cell stereocilia. A sinusoidal pressure wave (1Hz) was applied via a waterjet pipette. Afferent terminals expressing the fluorescent calcium indicator GCaMP5 exhibited increases in fluorescence intensity in response to waterjet-mediated stereocilia deflection. Loose patch recordings of afferent neurons also demonstrated that spike firing becomes phase-locked to the sinusoidal pressure wave. Using *neuroD:GFP* transgenic larvae, in which the afferent neurons express GFP, we found that bath application of AMPA leads to afferent terminal swelling. Recordings of phase-locked firing showed that afferent neurons lose the ability to fire in response to hair cell mechanotransduction within minutes of AMPA exposure. To determine whether spike firing recovers, we washed out AMPA. In a population of neurons, we found that spike firing resumed within 1 hour. These data support the use of the zebrafish lateral line to model afferent terminal damage and recovery following prolonged glutamate receptor activation. Future studies will examine the time course with which afferent terminal morphology and function recover after AMPA induced damage.

PD-22

Mitochondrial Dynamics in Aminoglycoside-Induced Hair Cell Loss

Jochen Schacht; Gao Wei; Ann Kendall
University of Michigan

Mitochondrial dynamics (fissions and fusion), the equilibrium between the generation of new organelles and the removal or repair of damaged ones, plays an important role in order to maintain the functionality of these organelles. Disruption of this process may cause developmental deficiencies or neurodegenerative disorders, and mediate the noxious actions of environmental stresses or neurotoxic agents.

An involvement of mitochondria in cochlear pathologies is well established, for example through ample documentation of intrinsic pathways of cell death. Furthermore, there is good evidence that the formation of reactive oxygen species (ROS), for which mitochondria are primarily held responsible, is a decisive factor in hair cell damage. In the case of aminoglycoside ototoxicity, metabolic studies have indeed shown direct effects of aminoglycosides on mitochondrial redox balance (Dehne et al., 2002; Jensen-Smith et al., 2012; Majumder et al., 2012). Our recent studies (Matt et al., Proc. Natl. Acad. Sci. US 109:10984-10989, 2012 & Shulman et al., J. Biol. Chem. 289:2318-2330, 2014) more specifically point to the mitochondrial ribosome as a target of aminoglycoside action, resulting in mitochondrial dysfunction and the well documented sequels of this failure, with ROS formation and cell death pathways among the options.

The present study attempts to elucidate the role of mitochondrial dynamics in aminoglycoside ototoxicity. The basic model is a 72-h culture of explants of the early postnatal murine organ of Corti in which micromolar concentrations of gentamicin cause a dose-dependent loss of outer hair cells in a base-to-apex gradient. We evaluate ROS generation, mitochondrial fusion and fission and hair cell death. Our salient findings are:

1. mitochondrial dynamics is disrupted by aminoglycoside antibiotics;
2. disturbance of mitochondrial dynamics precedes hair cell death;
3. mitochondrial permeability transition and ROS formation are upstream of disturbances of mitochondrial dynamics;
4. mitochondria-targeting scavengers and transition-pore blockers prevent cell death;
5. restoration of mitochondrial dynamics protects against gentamicin-induced hair cell death.

These results give new insights into the complexity of aminoglycoside actions and routes to cell death. They may also open new avenues to the design of protective strategies.

PD-23

Activation of CaMKKβ Signaling by Traumatic Noise Contributes to Outer Hair Cell Death

Kayla Hill; Xianren Wang; Hong-Wei Zheng; Su-Hua Sha
Medical University of South Carolina

Introduction

Noise-induced calcium (Ca^{2+}) influx in outer hair cells (OHCs) via voltage-gated Ca^{2+} channels (VGCC) has been well-documented in the pathogenesis of noise-induced hearing loss (NIHL). Ca^{2+}/calmodulin-dependent protein kinase kinases (CaMKKs) are serine/threonine-directed protein kinases that are activated by increases in intracellular Ca^{2+} concentration. CaMKKα and CaMKKβ are the two isoforms, of which CaMKKβ is the main activator of the AMP-dependent protein kinase (AMPK). We have previously reported that noise exposure activates AMPKα in OHCs. Here, we investigated noise-induced activation of CaMKKβ signaling in OHCs.

Methods

CBA/J mice at age of 12 weeks were exposed to one of two noise exposure conditions: broadband noise (BBN) from 2–20 kHz for 2 hours at 98 dB SPL to induce permanent threshold shifts (PTS) or 106 dB SPL to induce severe permanent threshold shifts (sPTS). In 7 week-old C57BL/6J CaMKKβ-knockout mice BBN from 2-20 kHz was applied at 94 dB SPL for 2 hours to induce PTS. An anti-phospho-CaMKI (T177) antibody was used on cochlear surface preparations to determine the activation of the downstream CaMKKβ signaling target in OHCs and in whole cochlear tissue homogenates. Auditory thresholds were determined by auditory brainstem responses (ABR). OHC losses were quantified from surface preparations labeled with myosin VII and then stained with DAB. CaMKKβ siRNA was delivered to the round window of CBA/J mice via intra-tympanic injection 72 hours before noise exposure to examine the role of CaMKKβ in NIHL. Furthermore, the physiological contribution of CaMKKβ to NIHL was elucidated in C57BL/6J CaMKKβ-knockout mice. Finally, treatment with the VGCC inhibitor verapamil via intra-peritoneal injection was utilized to assess potential protective effects of Ca^{2+}-influx inhibition on NIHL.

Results

Noise exposure resulted in an increase in the number of phosphorylated CaMKI-positive OHCs in the basal region of the cochlea, but did not alter the levels of pCaMKI in whole cochlear homogenates 1 hour after exposure. Pretreatment with CaMKKβ siRNA attenuated NIHL and OHC death. Consistent with these results, treatment with the VGCC blocker verapamil reduced the level of NIHL and OHC death. In contrast, CaMKKβ-knockout mice displayed no alteration in sensitivity to PTS noise exposure, although they exhibited normal baseline auditory thresholds.

Conclusions

These findings suggest that CaMKKβ signaling is involved in the pathogenesis of noise-induced OHC death. Pharmacological targeting of calcium signaling may protect against NIHL.

PD-24

The Role of a Newly Identified Mitochondrial-Stress Signaling Pathway ROS-AMPK-E2F1 in Hearing Loss

Lei Song[1]; Sharen McKay[2]; Wayne Yan[1]; Max Thormann[1]; Nuno Raimundo[3]; Jessica Nouws[1]; Abdul Khan[1]; Joseph Santos-Sacchi[1]; Gerry Shadel[1]

[1]Yale University School of Medicine; [2]Yale University School of Medicine University of Bridgeport; [3]Universitätsmedizin Göttingen Institut für Zellbiochemie

We recently described a transgenic mouse model of hearing loss induced by over-expression of the mitochondrial ribosomal RNA (rRNA) methyltransferase, TFB1M (Tg-TFB1M). TFB1 mice recapitulate maternally inherited deafness caused by the human A1555G mtDNA mutation, which results in increased methylation of the 12S rRNA in mitochondrial ribosomes and tissue-specific susceptibility to apoptosis (Raimundo et al, Cell 2012). The hearing loss measured by auditory brainstem response (ABR) in 9-12 month old mice is accompanied by reduction of the endocochlear potential (EP). Stria atrophy, as measured by the width of the stria at the middle turn using 5 um H&E stained FFPE histological sections through the cochlea, is not evident. Outer hair cells from TFB1 mice under whole cell clamp show motility and nonlinear capacitance parameters similar to controls.

As previously described the TFB1 activated ROS-AMPK-E2F1 pathway leads to apoptosis. Reduced expression of E2F1 abolished hearing loss in TFB1 mice (Raimundo et al, Cell 2012). In this study, we cross breed TFB1 mice with AMPK knockout mice and the reduction of ROS activated AMPK rescued hearing loss in 9-12 month old TFB1 mice. AMPK reduction alone does not compromise hearing.

To further explore the possibility of hearing loss rescue by removing ROS, we cross bred TFB1 mice with over expressed SOD2 and MCAT. The preliminary data suggest that there is partial rescue with MCAT and SOD2 over-expression. MCAT and SOD2 over-expression alone show low frequency hearing loss based on ABR.

PD-25

The Netrin-1 Receptors are Expressed in Sensory Epithelium and Spiral Ganglion Cells of the Cochlea

Kohei Yamahara[1]; Norio Yamamoto[2]; Takayuki Nakagawa[2]; Juichi Ito[2]

[1]Graduate School of Medicine, Kyoto University; [2]Department of Otolaryngology, Head and Neck Surgery Graduate School of Medicine, Kyoto University

Background

We have demonstrated that insulin-like growth factor - 1 (IGF-1) protects cochlear hair cells of neonatal mice against aminoglycoside (Hayashi et al. Molecular and Cellular Neuroscience 2013). We have identified two genes whose expressions were increased by IGF-1 treatment, using microarray and quantitative RT-PCR (qRT-PCR) (Hayashi et al. Neuroscience Letters 2014). One of such gene was netrin-1 (*Ntn1*). NTN1 is known to mediate an anti-apoptotic survival effect other than their conventional roles, axon guidance and cell migration through 6 different receptors, UNC5A, UNC5B, UNC5C, UNC5D, DCC, and NEOGENIN. Recent studies have indicated a crucial role for NTN1 receptors, especially UNC5B and DCC, in mediating survival effects of NTN1. We have demonstrated that administration of NTN1 resulted in the maintenance of both inner hair cells and outer hair cells numbers after aminoglycoside treatment just like IGF-1. These results indicated that NTN1 is the probable effector of IGF-1 signaling and that NTN1 can be the novel and potent treatment of sensorineural hearing loss. As a step to identify the effector cells of NTN1, we tried to identify the physiological expression of NTN1 rceptors in the cochlea using in situ hybridization for NTN1 receptors in the cochlea.

Methods

In situ hybridization was performed for each NTN1 receptor on 12 µm sections from mouse cochleae at P2. A partial length mouse cDNA sequence of each receptor was used to generate digoxigenin-labeled sense and antisense RNA probes. Corresponding sense probes were carried out in this experiment as controls and yielded little hybridization signal.

Results

Among these receptors, Only *Unc5b* is expressed in the sensory epithelium including hair cells as previously reported (Matilainen et al, Int. J. Dev. Biol 2007). But in spiral ganglion cells, much more receptors than previously reported are expressed including *Unc5b*, *Unc5d, Dcc* and *Neogenin*.

Conclusions

We found that NTN1 receptors are highly expressed in sensory epithelium and spiral ganglion cells of the cochlea in the physiological condition.

SYM-26

Sensitivity to Interaural Time Differences in the Inferior Colliculus of an Awake Rabbit Model of Bilateral Cochlear Implants

Yoojin Chung; Kenneth Hancock; Bertrand Delgutte

Massachusetts Eye and Ear Infirmary

Background

Although bilateral cochlear implants (CIs) provide improvements in sound localization and speech perception in noise over unilateral CIs, bilateral CI users' sensitivity to interaural time differences (ITD) is still poorer than normal. Single-unit studies in animal models of bilateral CIs using anesthetized preparations show a severe degradation in neural sensitivity to ITD at stimulation rates above 100 pps. However, temporal coding is degraded in anesthetized preparations compared to the awake state (Chung et al., J Neurosci. 34:218). Here, we characterize ITD sensitivity of single neurons in the inferior colliculus (IC) for an awake rabbit model of bilateral CIs.

Methods

Four adult Dutch-belted rabbits were deafened and bilaterally implanted. Single unit recordings were made from the IC over periods from 4 to 43 weeks after implantation. Stimuli were

periodic trains of biphasic electric pulses with varying pulse rates (20 – 640 pps) and ITDs (-2000 – 2000 μs).

Results
About 65% of IC neurons in our sample showed significant ITD sensitivity in their overall firing rates. ITD tuning curves were fitted to one of four templates: monotonic (sigmoid), peak, biphasic, and trough types. Monotonic was the most common type, followed by peak, biphasic and trough types (although 37% of units did not fit any of the templates). Across the neural sample, ITD sensitivity was best for pulse rates near 80-160 pps and degraded for both lower and higher pulse rates. Nevertheless, over 20% of the neurons showed significant ITD sensitivity at the highest rate tested (640 pps). The degradation in ITD sensitivity at low pulse rates was caused by the presence of strong background activity in many neurons; this background activity masked stimulus-driven responses. Selecting pulse-locked responses by temporal windowing revealed ITD sensitivity in these neurons. With temporal windowing, both the fraction of ITD-sensitive neurons and the degree of ITD sensitivity decreased monotonically with increasing pulse rate.

Conclusions
Similar ITD tuning shapes were observed in the IC of awake rabbits as in anesthetized cats, but there were more unclassified units in the rabbit. Using temporal windowing to suppress background activity, the dependence of ITD sensitivity on pulse rate in awake rabbit was in better agreement with perceptual data from human CI users than earlier results from anesthetized preparations. Such windowing might be implemented more centrally by coincidence detection across multiple IC neurons with similar response latencies.

Funding
NIH grants R01 DC005775 and P30 DC005209, and Hearing Health Foundation.

SYM-27

Mitigation of Informational Masking in Individuals With Single-Sided Deafness By Integrated Bone Conduction Hearing Aids

Bradford May[1]; Stephen Bowditch[1]; Yinda Liu[2]; Marc Eisen[2]; John Niparko[3]
[1]Johns Hopkins University; [2]Hartford Hospital; [3]University Southern California

Title: Mitigation of informational masking in individuals with single-sided deafness by integrated bone conduction hearing aids

Background
Individuals with single-sided deafness (SSD) find it difficult to communicate in situations that pose no challenge for normal listeners. For example, a conversational partner may be heard, but not understood in the presence of other talkers. This increased susceptibility to informational masking can be explained by an inability to separate competing sounds on the basis of binaural directional cues. We hypothesized that osseo-integrated bone conductors (IBCs) may re-create this directional information in SSD patients by delivering sounds with a unique vibro-acoustic signature to the functioning ear. Consequently, IBCs are expected to enhance communication in complex listening environments.

Methods
Informational masking was characterized in SSD patients with the coordinate-response measure. Target sentences were presented in free field accompanied by 0 – 3 distracting sentences. Target and distracting sentences were spoken by different talkers and originated from different source locations, creating two sources of information for sound separation. Increased susceptibility to informational masking was assessed by comparing the unaided error rates of SSD patients to normal controls. Mitigation of informational masking by IBCs was evaluated by comparing the aided and unaided performance of SSD patients. The acoustic basis of the IBC listening advantage was determined by correlating response errors with the voice pitch and location of distracting sentences.

Results
Unaided SSD patients produced significantly higher error rates than normal controls. Most errors involved confusions with the coordinates of distracting sentences. Errors were significantly reduced when SSD patients were tested with the IBC. The listening advantage was most strongly correlated with the availability of voice pitch cues, although performance was also influenced by the location of distracting sentences. Directional asymmetries appear to be dictated by location-dependent cues that are derived from the distinctive transmission characteristics of IBC stimulation.

Conclusions
These results suggest that informational masking is a significant source of communication impairment among SSD patients. Despite their extreme lateralization of auditory function, unaided SSD patients experience informational masking when distractors occur in either the deaf or normal spatial hemifield. Restoration of aural sensitivity in the deaf spatial hemifield enhances speech intelligibility under complex listening conditions, presumably by providing additional segregation cues that are derived from voice pitch and spatial location.

Funding
This research was supported by the Cochlear Corporation and National Institute on Deafness and Other Communication Disorders grant P30 DC005211.

SYM-28

Optimizing Interaural Cues for Bilateral CI Users

Ann Todd; Ruth Litovsky
University of Wisconsin-Madison

Listeners with bilateral cochlear implants (BiCIs) typically fail to show binaural release from masking for speech reception in free field environments. However, they can show binaural release from masking for signal detection when direct electrical stimulation is presented to a limited number of electrodes. The magnitude of binaural release from masking varies be-

tween listeners, and also within listeners across stimulation sites. We hypothesized that a contributing factor to the variability in binaural unmasking may be the ability of listeners to encode changes in amplitude in each ear. To address this issue, we examined whether variability in binaural unmasking, between listeners and also within listeners across stimulation sites, can be explained by the dynamic range and amplitude modulation detection thresholds measured in each ear individually.

Signal detection thresholds were examined in 6 BiCI users, for diotic (NoSo) and dichotic (NoSpi) conditions while stimulating individual pairs of electrodes. For each listener, NoSo and NoSpi stimuli were compressed between that individual's thresholds and maximum acceptable loudness levels. This followed adjustments in levels, aimed at achieving equal loudness across stimulation sites and approximately centered auditory images. In addition to the dynamic range, amplitude modulation detection thresholds were measured monaurally at each of the electrodes used for the binaural unmasking measures. For each participant, measurements were made at basal, middle, and apical stimulation sites.

All listeners showed some binaural release from masking. Within individuals, NoSpi thresholds were lower for stimulation sites at which NoSpi stimuli were compressed between a larger current range. NoSpi detection thresholds were better predicted by the smaller of the dynamic ranges of the two ears. Preliminary results showed that individuals with lower amplitude modulation detection thresholds had lower NoSpi detection thresholds.

The results thus far suggest that interaural differences for binaural release from masking are more usable given better abilities to encode monaural amplitude changes. Larger dynamic ranges and better amplitude discrimination may result in interaural level differences that are more salient due to a greater number of discriminable levels. Larger dynamic ranges may also result in interaural time differences that are more salient due to sharper slopes of amplitude modulations. Decreases in dynamic range that are necessary to achieve acceptable loudness levels with multi-electrode stimulation may play a role in reducing the ability of BiCI users to achieve binaural release from masking in free field environments.

Support provided by NIH-NIDCD R01DC003083 (Litovsky) and NIH-NICHD P30HD03352 (Waisman Center).

SYM-29

The role of combined electric and acoustic stimulation (EAS) for binaural summation, squelch, and spatial release from masking

Rene Gifford[1]; Timothy Davis[1]; Louise Loiselle[2]; Sarah Cook[3]; Timothy Davis[1]; Sterling Sheffield[1]; Michael Dorman[3]
[1]Vanderbilt University; [2]MED-EL Corporation; [3]Arizona State University

Background

There are a number of reports showing minimal estimates binaural hearing for individuals with cochlear implants (CIs). For CI recipients with acoustic hearing in the implanted ear, however, access to low-frequency interaural timing differences (ITDs) should theoretically offer greater availability to binaural cues resulting in greater estimates of squelch and spatial release from masking.

Methods

Speech understanding was assessed in a simulated restaurant environment as well as a cocktail party environment for 21 adult CI recipients with hearing preservation in the CI ear, 15 individuals with bimodal hearing, and 17 individuals with bilateral CIs. For the first set of experiments, speech was presented at 0 degrees and noise was either at 1) 0 degrees S_0N_0, 2) 0-360 degrees for the simulated restaurant environment $S_0N_{0\text{-}360}$ or 3) at 90 and 270 degrees for the cocktail party condition $S_0N_{90\&270}$. Using this experimental paradigm we were able to calculate the binaural unmasking benefit of adding acoustic hearing from the non-implanted ear, the implanted ear, as well as the spatial release from masking in each listening condition.

Results

For the simulated restaurant environment, the addition of acoustic hearing yielded an average benefit of 20- and 10-percentage points, for the non-implanted and implanted ears, respectively. For the cocktail party environment, the addition of acoustic hearing yielded an average benefit of 19- and 14-percentage points for the non-implanted and implanted ear, respectively. Little-to-no spatial release from masking was noted for any of the listening environments and conditions tested here.

Conclusions

Our two primary conclusions are as follows: First, for both the collocated and spatially separated noise conditions, adding acoustic hearing from either ear significantly improved speech understanding. We hypothesize that the EAS benefit as shown here can be attributed to i) binaural summation of low-frequency information in the collocated condition, and ii) binaural unmasking of speech resulting from the availability of masker ITDs with two acoustic hearing ears. Second, none of the tested hearing configurations resulted in a spatial release from masking. Though we do not yet have enough data to support a working hypothesis explaining the lack of spatial release, we believe that this may be related to the presence of noise at both ears directed immediately toward the ports of the HA and CI microphones.

SYM-30

Optimizing Binaural Cue Perception with Combined Cochlear Implant and Acoustic Stimulation

Tom Francart; Anneke Lenssen; Dimitar Spirrov; Jan Wouters
KU Leuven

Currently, bimodal listeners are normally fitted with a standard cochlear implant (CI) sound processor and hearing aid. This configuration has been shown to be advantageous compared to only the CI. We recently found that bimodal listeners with sufficient residual hearing can be sensitive to binaural cues:

interaural level differences and interaural time differences in the envelope and transients of the signal. However, with current clinical devices bimodal listeners do not appear to make advantage of binaural cues, due to poor cue transmission by the devices. We have developed two sound processing strategies to improve this: SCORE bimodal and MEnS.

The SCORE bimodal strategy aims to equalise loudness growth for both modalities using real-time application of models of loudness perception for acoustic and electric stimulation. As SCORE was found to improve loudness perception and not to interfere with speech perception and, it seems beneficial to implement it in clinical devices.

The MEnS strategy introduces temporal modulations on all stimulated electrodes, synchronously with modulations present in the acoustic signal, based on measurement of the peaks occurring at the rate of the fundamental frequency in voiced phonemes. Compared to the ACE strategy, interaural time difference detection and interaural-time-difference based lateralisation was significantly improved with just noticeable differences with MEnS well within the physically relevant range.

The application of these two strategies could lead to improved sound source localisation and binaural unmasking with bimodal stimulation.

SYM-31

Binaural Unmasking for Bilateral Cochlear Implantees

Matthew Goupell[1]; Joshua Bernstein[2]; Douglas Brungart[2]; Daniel Eisenberg[1]; Alan Kan[3]; Ruth Litovsky[3]
[1]University of Maryland-College Park; [2]Walter Reed National Military Medical Center; [3]University of Wisconsin-Madison

Introduction

Binaural unmasking benefits for speech presented in background noise can be substantial for normal-hearing (NH) listeners, but negligible for bilateral cochlear-implant (BICI) listeners. Two reasons were investigated as possible causes of the lack of binaural unmasking for BICI listeners. One possibility is that previous tasks were not optimized for demonstrating binaural unmasking. Increasing the amount of informational masking in a task typically increases the amount of binaural unmasking. Another possibility is that BICI listeners have asymmetrical ears. For example, there could be unequal neural degeneration or different array placements between the ears. Asymmetric inputs would diminish binaural benefits.

Methods

Masked speech understanding was measured for BICI and NH listeners. Binaural unmasking was measured by comparing performance for a monaural target and monaural masker (NmSm) to performance for a monaural target and diotic masker (NoSm). Both listener groups were presented with unprocessed speech. To vary the amount of informational masking, several masker types were tested: noise, one-, and two-talker maskers (either same or opposite gender). The speech corpus was also varied by using a closed set of five-word sentences with a low amount of informational masking and the coordinate-response-measure (CRM) corpus with a high amount of informational masking. The NH listeners were also presented with vocoded speech to examine the impact of asymmetric inputs. Asymmetric neural degeneration was simulated by having a different numbers of channels across the ears. Asymmetric insertion depths were simulated by imposing different amounts of frequency-to-place mismatch across the ears.

Results

Conditions with a low amount of informational masking produced nearly zero binaural unmasking for the BICI listeners. In contrast, a high-informational masking condition -- the CRM corpus with a one-talker masker -- produced substantial binaural unmasking for the BICI listeners. However, performance was still worse for the BICI listeners compared to the NH listeners. Asymmetric inputs in the vocoder conditions showed that speech presented to the ear with poorer resolution or more frequency-to-place mismatch was more difficult to understand in the presence of speech with a higher resolution or less mismatch.

Conclusion

BICI listeners demonstrate binaural unmasking if the task contains enough informational masking. However, they generally perform more poorly than NH listeners presented with unprocessed or vocoded speech. Differences between the ears of BICI listeners may be the cause of the reduced magnitude of binaural unmasking. CI device setting should consider these differences for BICI users, as well as single-sided deaf CI users.

SYM-32

Binaural Processing fdr Cochlear Implantees With Single-Sided Deafness

Joshua Bernstein[1]; Matthew Goupell[2]; Jessica Wess[2]; Gerald Schuchman[1]; Arnaldo Rivera[1]; Douglas Brungart[1]
[1]Walter Reed National Military Medical Center; [2]University of Maryland - College Park

Having two ears allows normal-hearing (NH) listeners to take advantage of head-shadow effects by selectively attending to the ear providing the best signal-to-noise ratio (the “better-ear” advantage) and provides access to binaural-difference cues for localizing sound and the perceptually segregating spatially separated sources. Cochlear implants (CIs) have been shown to improve speech perception in noise and sound localization for individuals with single-sided deafness (SSD; i.e., one deaf ear and one NH ear). However, most of the reported benefits appear to be attributable to better-ear advantages. Two studies investigated whether a CI can provide individuals with SSD with binaural-difference cues that are known to significantly enhance spatial hearing for bilaterally NH listeners.

The first study examined speech-on-speech masking for seven SSD CI users. Target speech and one or two masking talkers were presented to the NH ear. The CI ear was presented with silence or with a mixture containing only the maskers,

testing whether listeners could binaurally integrate the masker signals to better hear the monaural target. Presenting the maskers to the CI ear improved performance when the target and masking talkers were of the same gender, suggesting that a CI can provide binaural cues to facilitate speech-stream segregation when monaural cues are insufficient to do so.

The shorter length of the CI array relative to the cochlear duct tends to produce a mismatch between the places of stimulation in the NH and CI ears. Vocoder simulations presented to NH listeners suggest that this mismatch could limit the stream-segregation benefit provided by a CI for SSD. As a step toward evaluating and potentially reducing this mismatch, the second study employed a measure of interaural time difference (ITD) sensitivity to estimate the place of stimulation of a given CI electrode. Three SSD CI users were presented with bilateral acoustic pulse trains (100-Hz Gaussian-envelope modulated sinusoids) via insert earphone and auxiliary CI input. ITD sensitivity was characterized using lateralization judgments. Place of stimulation was manipulated by altering the carrier frequency in the NH ear and by activating only one electrode in the CI ear. For a given electrode, results showed a distinct performance peak, with maximum ITD sensitivity at a particular acoustic carrier frequency.

In summary, a CI has the potential to provide individuals with SSD with binaural-difference cues to enhance speech-stream segregation and sound localization. ITD sensitivity shows promise as a measure to evaluate and reduce spectral mismatch to improve binaural performance.

SYM-33

Field Tests of a Novel Sound Coding Strategy That Aims to Maximize ITD Sensitivity and Minimize Power Consumption in Cochlear Implants Recipients

Zachary Smith
Cochlear Limited

Understanding speech in complex listening environments remains a challenge for recipients of cochlear implants. While bilateral implantation improves the situation with the addition of a second ear, evidence suggests that much of the benefit can be attributed to monaural effects. A temporally sparse coding strategy, FAST, was developed with the aims of 1) delivering more salient interaural time difference (ITD) cues and 2) increasing power efficiency. In a series of studies, the commercial ACE strategy was compared with FAST. Results with the research coding strategy show significantly improved ITD sensitivity in some subjects and consistently longer battery life. Subjects with better ITD sensitivity were also able to take advantage of ITD to better understand a target talker in the presence of a masking talker. This suggests that improving ITD perception in recipients of cochlear implants may lead to better hearing outcomes in real-world listening situations.

PD-34

Robust Regulation of Stereocilia Length by the Redundant Functions of MYO3A and MYO3B and their Actin-Regulatory Cargos ESPN1 and ESPNL

Seham Ebrahim[1]; M'Hamed Grati[1]; Alanna Windsor[1]; Manmeet Raval[2]; Aurea de Sousa[1]; Runjia Cui[1]; Lijin Dong[1]; Michelle Baird[3]; Sherri Jones[4]; Christopher Yengo[2]; Bechara Kachar[1]
[1]National Institutes of Health; [2]Penn State University; [3]Florida State University; [4]University of Nebraska-Lincoln

Introduction

The precise regulation of stereocilia-length is essential for hearing and balance. The molecular motor myosin IIIa (MYO3A) traffics to stereocilia tips where it regulates stereocilia-length by transporting an actin-regulatory cargo, Espin1 (ESPN1). *MYO3A* and *ESPN* are associated with late-onset hearing loss (DFNB30), and with early onset hearing and vestibular deficits (DFNB36), respectively. Myosin IIIb (MYO3B), a MYO3A paralog, is thought to partially compensate for MYO3A function, delaying the onset of DFNB30. We aimed to investigate the distinct and overlapping roles of each protein in this complex to elucidate the molecular mechanisms underlying DFNB30 and DFNB36, and gain additional insights into the processes driving stereocilia-length regulation and molecular transport

Methods

Single-gene mouse knockouts for *Myo3a*, *Myo3b* and *Espn1* (*Espn* long isoform) were generated and null alleles verified by RT-PCR. Auditory function in each mutant was assessed by auditory brainstem response (ABR) recordings, stereocilia bundle morphology was characterized using confocal fluorescence microscopy, and vestibular function in the *Espn1*$^{-/-}$ mice was analysed through vestibular evoked potential (VsEP) measurements. Whole mount immunofluorescence, and biolistic over-expression of fluorescently-tagged proteins in organotypic explants of rat inner ear tissue, were used to determine their localization in stereocilia. Co-transfections of fluorescently-tagged proteins in COS7 cells and pull down assays of purified protein fragments were used to characterize protein-protein interactions.

Results

Neither *Myo3a*$^{-/-}$ nor *Myo3b*$^{-/-}$ mice presented abnormalities in stereocilia morphology or auditory function, but mice lacking both genes were embryonic lethal. *Espn1*$^{-/-}$ mice had stereocilia with misregulated lengths observed only in extrastriolar hair cells of the otolithic organs, suggesting the presence of a partial compensatory mechanism. We show here that espin-like (ESPNL), a molecular and structural homolog of ESPN1, also localizes to stereocilia tips, albeit in an inverse length-dependent concentration. Remarkably, ESPNL expression is enhanced in the striola. Heterologous expression assays show that both MYO3A and MYO3B transport ESPNL to the tips of filopodial actin protrusions. Biochemical analysis showed that, like ESPN1, ESPNL binds to the tail homolgy domain 1 (THD1) of both MYO3A and MYO3B. Fi-

nally, an inverse correlation between ESPNL concentration and MYO3 motility and localization to filopodia tips in COS7 cells provides evidence for a new cargo-mediated regulation of MYO3A function.

Conclusion
Collectively, these data demonstrate that ESPNL is a novel member of the MYO3/ESPN1 complex, with spatial complementary and compensatory function to ESPN1, providing additional insights into mechanisms underlying regulation of stereocilia-length and cargo transport, and the pathophysiology of DFNB30 and DFNB36.

PD-35

The CD2 Isoform of Protocadherin-15 is an Essential Component of the Tip-links in Mature Auditory Hair Cells

Elise Pepermans[1]; Vincent Michel[1]; Richard Goodyear[2]; Crystel Bonnet[3]; Samia Abdi[4]; Typhaine Dupont[1]; Souad Gherbi[5]; Muriel Holder[6]; Mohammed Makrelouf[7]; Paul Avan[8]; Sandrine Marlin[5]; Akila Zenati[7]; Guy Richardson[2]; Paul Avan[8]; Amel Bahloul[1]; Christine Petit[1]
[1]Institut Pasteur; [2]University of Sussex; [3]Institut de la Vision; [4]Centre Hospitalier universitaire de Blida; [5]Centre de référence des Surdités Génétiques, Hôpital Necker; [6]Service de Génétique Clinique, Hôpital Jeanne-de-Flandre; [7]Laboratoire de Biochimie Génétique, Université d'Alger; [8]Université d'Auvergne

Protocadherin-15 (Pcdh15) is a component of the tip-links, the extracellular filaments that gate mechano-electrical transduction channels of the inner ear hair cells. There are three Pcdh15 splice isoforms (Pcdh15-CD1, Pcdh15-CD2, Pcdh15-CD3), which only differ by their cytoplasmic domains. These three isoforms are thought to function redundantly in mechano-electrical transduction during hair-bundle development, but whether any of these isoforms composes the tip-link in mature hair cells was still unknown.

By immunolabeling we showed that Pcdh15-CD2 is correctly localized in mature auditory hair cells to form the lower tip-link component. We generated postnatal hair cell-specific conditional knockout mice that lose only Pcdh15-CD2 after normal hair-bundle development. Electrophysiological analysis of these mice indicated that mechano-electrical transduction is lost from P21 onwards. Morphological analysis of the auditory hair cells of these mice proved that the loss of mechano-electrical transduction is due to the loss of tip-links. We conclude that this isoform is an essential component of the tip-links in mature murine auditory hair cells. This conclusion could be extended to humans, since a frame-shift mutation in *PCDH15* (in the homozygous or compound heterozygous state) that only affects Pcdh15-CD2 was identified in profoundly deaf children from two unrelated families.These results provide key information for the identification of new components of the mature auditory mechano-electrical transduction machinery.

PD-36

Exposing the Varied Functional Roles of Hair Bundles with a Mechanical–Load Clamp

Joshua Salvi[1]; Dáibhid Ó Maoiléidigh[1]; Brian Fabella[1]; Melanie Tobin[2]; A. J. Hudspeth[1]
[1]The Rockefeller University; [2]Institut Curie

Hair bundles detect periodic stimuli in the auditory system and static or hydrodynamic stimuli in the vestibular and lateral-line systems. The mechanical properties of bundles and their accessory structures differ in accordance with these distinct physiological functions. Hair bundles range in height from 1 μm to 100 μm and in stiffness from 100 $\mu N \cdot m^{1}$ to 10,000 $\mu N \cdot m^{1}$. They possess stereocilia that vary in number from fewer than 20 to more than 300. Bundles may be cylindrical, fan-shaped, or Vshaped in configuration, and they may or may not possess a true cilium, the kinocilium. Hair bundles may be free-standing or they may be coupled to a tectorial membrane, otolithic membrane, sallet, or cupula. Because all bundles are otherwise built from similar molecular components, we hypothesized that their mechanical properties might regulate their distinct functions in different receptor organs.

We developed a mechanical-load clamp to systematically adjust both the load stiffness and constant force applied to a hair bundle, two parameters predicted to control a bundle's behavior. By controlling these properties and measuring a hair bundle's response, we mapped its state diagram. A typical diagram includes a central region within which the hair bundle oscillates spontaneously, surrounded by a domain of quiescence. The border between these regions constitutes a line of Hopf bifurcations. By delivering mechanical stimuli to hair bundles poised at different positions in the diagram, we ascertained that a bundle exhibits the sharpest tuning and greatest degree of entrainment near a supercritical Hopf bifurcation. Depending on its position in the state diagram, a particular hair bundle may oscillate or remain quiescent; it may or may not amplify periodic stimuli and the range of forces over which it is nonlinear can vary. We also found that, depending on the magnitude of the constant force, a bundle may rapidly twitch at the onset of a force pulse like an edge-detection system or may overshoot the motion of the stimulus fiber like a mammalian hair bundle. We conclude that a hair bundle's function depends fundamentally upon its mechanical load. Upon adjustment of only two mechanical parameters, a single hair bundle can exhibit a variety of mechanosensory behaviors, implying an essential similarity between the bundles from different organs and organisms.

PD-37

Modulation of Rat Auditory Hair Cell Mechanotransduction Channel Resting Open Probability Via an Adaptation Independent Mechanism

Anthony Peng[1]; Radhakrishnan Gnanasambandam[2]; Frederick Sachs[2]; Anthony Ricci[1]
[1]Stanford University; [2]University at Buffalo, The State University of New York

The auditory system is the most sensitive mechanosensory system known, able to detect movement down to atomic dimensions (Bialek. 1987. Annu. Rev. Biophys. Biophys. Chem. *16*: 455–478). This sensitivity is at least partly attributed to the mechanisms associated with gating of hair cell mechanotransduction (MET) channels, where at rest approximately 50% of the channels are open, positioning the channels at the steepest part of their activation curve (Johnson et al. 2011. Neuron *70*, 1143–1154). Previously, a calcium-regulated adaptation process was hypothesized to control the resting open probability of MET channels (Farris, Wells, and Ricci. 2006. J. Neurosci. *26*: 12526–12536). However, mammalian cochlear hair cell adaptation is not driven by calcium; low external calcium effects on resting open probability occur via an uncharacterized extracellular mechanism (Peng, Effertz, and Ricci. 2013. Neuron *80*: 960–972). Upon further investigation of the extracellular mechanism, we find that large radii divalent ions act similarly to calcium, intimating a nonspecific divalent ion mechanism. We show that hair cell depolarization also increases the resting open probability, and acts through a similar mechanism as external calcium. Finally, we find that a purported lipid-mediated stretch-activated channel modifier, GsMTx4, blocks both the voltage and the low external calcium effects on resting open probability with only a minor decrease in adaptation. These results suggest a new mechanism of calcium modulation of the hair cell MET channel that is independent of adaptation. This new mechanism further supports the conclusion that mammalian cochlear mechanotransduction adaptation is not driven by calcium, since an adaptation-independent mechanism accounts for the observed open probability changes.

PD-38

Probing the Central Anion Binding Site in Prestin

Dmitry Gorbunov[1]; **Dominik Oliver[2]**
[1]Philipps University; [2]Philipps University Marburg

Since the identification of prestin (SLC25A5), substantial efforts have been made to investigate the molecular mechanisms that generate its electromechanical ('piezoelectric') activity. The findings that non-mammalian orthologs of prestin are electrogenic anion transporters, the identification of functional protein domains, and the development of a structural model of prestin (1) pointed to mechanistic similarities between electromotility and transport.

We recently reported the overall 3D structure of mammalian prestin and non-mammalian homologs based on homology modeling, molecular dynamics simulations and experimental probing of the molecular architecture by cysteine accessibility scanning (1). This model delineates a central anion-binding site. In the transport-competent ortholog from chicken (cPres), this site is solute-accessible from extra- and intracellular sides, supporting an alternating access transport mechanism. Accordingly, mutations at this site disabled anion transport. In mammalian prestin, mutations at homologous positions abrogated electromotile activity as probed by nonlinear capacitance (NLC) recordings. We concluded that binding of monovalent anions into this site is required to enable the molecular rearrangements underlying electromechanical activity.

To further explore the relevance of anion binding to this site with respect to electromechanical function, we inserted fixed negative charges by site-directed mutagenesis. Replacement of a glutamate residue for an endogenous serine within the presumed binding site abrogated transport function of cPres, consistent with the proposed function of this site in accommodating the transport substrate. However, in mammalian prestin, this substitution entirely preserved wild type-like ability to generate NLC, even at high frequency stimulation. Strikingly, while wildtype prestin requires binding of intracellular monovalent anions, function of the glutamate mutant was entirely independent on intracellular anions. Thus NLC was unaffected by replacement of chloride by aspartate. Moreover, sensitivity to the competitive inhibitor, salicylate, was fully abolished.

These findings suggest that a fixed charge can functionally substitute for bound chloride, and thus directly support the requirement of a negative charge within the central binding site for prestin function. Specifically, this is additional evidence for the idea that small anions as well as the inhibitor, salicylate, bind to this site. The relation of a localized negative charge at this central position halfway through the membrane to the voltage sensor of prestin remains to be analyzed further.

(1) Gorbunov D, Sturlese M, Nies F, Kluge M, Bellanda M, Battistutta R, Oliver D (2014) Molecular architecture and the structural basis for anion interaction in prestin and SLC26 transporters. Nat Commun 5.

PD-39

Is Prestin Function Related to Oligomerization State?

Richard Hallworth
Creighton University

While prestin is likely a tetramer, and tetramerization is common throughout the SLC26 family of proteins, the role of oligomerization is unclear. Prestin non-linear capacitance (NLC) is well-described by equations derived from a first-order process, which suggests independent operation of monomers. Evidence for cooperative interactions is slight. The ubiquity of tetramerization in the SLC26 family, and the fact that many Slc26 proteins can hetero-oligomerize, suggests that oligomerization nonetheless serves some purpose.

Several prestin mutations demonstrate substantial changes in the membrane potential peak of NLC, both hyperpolarizing

(C1, D154N) and depolarizing (499, D342Q), without change in the unit charge transfer q. Using single-molecule imaging to determine stoichiometry, I here show that each of these four mutations separately reduces the oligomerization state of prestin from the tetramer to the dimer state. The observations suggest that tetrameric oligomerization is required for correct function of prestin.

PD-40

Anion-π Interaction is the Mechanism for the Voltage-Dependent Response of Prestin, the Motor Protein of Cochlear Outer Hair Cells.

David He; Sandor Lovas; Huizhan Liu; Marcus Hatfield; Jason Pecka; Kirk Beisel
Creighton University

Prestin is the motor protein of cochlear outer hair cells (OHCs). Its unique capability to perform direct, rapid and reciprocal electromechanical conversion depends on membrane potential and interaction with intracellular anions. How prestin senses the voltage change and interacts with anions is still unknown. Our three-dimensional model of prestin, using molecular dynamics simulations based on X-ray structures of the Glt_{Ph} protein as templates for homology modeling, predicts that prestin contains eight transmembrane spanning segments and that tyrosyl residues are the structural specialization of the molecule for the unique function of prestin. Using site-directed mutagenesis and electrophysiological techniques, we showed that the aromatic side chains of the four tyrosyl residues (Y367, Y486, Y501 and Y508) form non-covalent bonds with intracellular anions through anion-π interactions. Such weak interactions, sensitive to voltage and mechanical stimulation, confer prestin with a unique capability to perform electromechanial and mechanoelectric conversions with exquisite sensitivity. This novel mechanism is completely different from all known mechanisms seen in ion channels, transporters, and motor proteins.

PD-41

Prestin Anion Transporter Activity Demonstrated By Patch Clamp Analysis.

Iman Moeini-Naghani; **Jun-Ping Bai**; Joseph Santos-Sacchi; Dhasakumar Navaratnam
Yale University

Background

We have previously reported that prestin expressing cells exhibit formate uptake using C14 labeled formate. Anion transport with Cl-HCO3 exchange has also been demonstrated by Jonathan Ashmore's group. The ability to transport anions has implications to prestins voltage sensor in addition to raising the possibility of numerous compensatory mechanisms required for removing anions from the restricted subsurface cisterne in outer hair cells

Method

We performed whole-cell patch-clamp recordings to examine prestin current in an inducible prestin expressing HEK cell stable line. Currents were measured in the presence of 1mM extracellular chloride with and without 20mM formate.

Result

We confirm that prestin expressing HEK cells demonstrate a small but significant increased current when exposed to solutions containing 20mM formate with 1mM extracellular chloride (with 140mM intracellular (pipette) chloride). The current was most evident at hyperpolarizing voltages and inhibited by 0.2mM DIDS. In contrast, uninduced cells demonstrate a decrease in the inward current at hyperpolarizing voltages when perfused with 20mM formate. We interpret this current as due to prestin induced electrogenic anion transporter activity.

SYM-34

The Hearing Restoration Project: Overview

Peter Barr-Gillespie
Oregon Health & Science University

The plausibility of hair-cell regeneration serving as a treatment for hearing and balance disorders is growing each year. The Hearing Restoration Project (HRP) is a consortium of scientists who work collaboratively to advance knowledge and provide tools to the auditory and vestibular neuroscience community, with the hope of accelerating development of therapies for rehabilitation of hearing loss and balance dysfunction. Our consortium has identified major roadblocks that have stymied the field and designed approaches to overcome these barriers. We are working to identify targets for drug-based restoration of inner ear function, which will be necessary for eventual drug screening.

Two major confounding issues that have been addressed by the consortium are (a) only a small number of regulators of hair cell regeneration are known, and (b) little is known about how supporting cells change over time after hair cell damage. We have devised a strategic plan with three major phases: (I) understanding the response of supporting cells in species and organs that regenerate (chickens, fish) and those that do not (mice); (II) verification of pathways and development of regeneration strategies; and (III) identification of drugs that trigger hair-cell regeneration. In our first two years, the consortium has focused on Phase I and has carried out cross-species genomic profiling of supporting cell responses to injury (Ia), as well as tracking the supporting cell population after damage to determine the identity of cells to therapeutically target (Ib). Several new projects reflect our shift to Phase II of the project this year.

The goal of the symposium is to share with the ARO audience the HRP consortium's progress to date . We will first present the overall goals of consortium and introduce our Strategic Plan (Barr-Gillespie). Subsequent talks are segregated by the model systems we use—zebrafish and chickens, which are capable of hair cell regeneration, and mice, which are not. HRP investigators will discuss our genomics experiments (Piotrowski, Lovett, Segil), pathway testing approaches (Warchol, Groves), and fate mapping experiments (Oesterle, Heller).

SYM-35

Characterization of Support Cell Populations in Zebrafish Lateral Line Neuromasts

Tatjana Piotrowski; Linjia Jiang; Andres Romero-Carvajal Romero-Carvajal
Stowers Institute for Medical Research

A critical goal for the HRP is to determine why non-mammalian vertebrates are able to regenerate hair cells while mammals are not. Understanding the genetic regulation of supporting cell identity is a key step to achieving this goal, and is the focus of Phase I of the HRP Strategic Plan. The zebrafish lateral line has a number of advantages that aid in this cross-species comparison; for example, hair and support cells are readily accessible for manipulation and visualization, and are amenable to large-scale gene identification and expression analyses. Genes shown to be expressed in subsets of support cells in the zebrafish lateral line will likely show a similarly restricted expression pattern in chick or mouse and may serve as valuable candidate genes to aid in the identification of support cell subtypes in these model organisms.

In non-mammalian vertebrates, hair cells regenerate from support cells. Nevertheless, no systematic effort to study support stem cells in these model organisms has been executed; it is not known, for instance, where the stem cells reside, or if a specialized progenitor population exists. To study the molecular mechanisms underlying hair cell regeneration and to exploit this knowledge for the induction of hair cell regeneration in mammals, including humans, we need to understand the precise cell types responsible for producing the new hair cells and the precise changes in gene expression throughout this process. Our approach has been to characterize support cell populations in the zebrafish lateral line by performing large-scale gene expression analyses by in situ hybridization and RNA-Seq coupled with detailed lineage analysis of support cells during hair cell regeneration. Our studies set the stage for the identification of stem cells and progenitor cells and for determining at high cellular resolution which cells express particular signaling components and communicate with each other and are therefore crucial for hair cell regeneration. We have identified that, depending on the location in the neuromast, support cells either self-renew or differentiate and that this decision is controlled by signaling interactions between spatially restricted Notch and Wnt signaling.

The identification of spatially restricted progenitor populations allows us to search for additional genes expressed in these tissue compartments and perform a cross-species gene expression comparison. Genes expressed in different progenitor populations serve as candidates for inducing support cell renewal and regeneration in the mouse.

SYM-36

Chicken I. Genomic Profiling of the Regenerative Transcriptome in the Avian Cochlea after Aminoglycoside-Induced Damage

Michael Lovett
Imperial College, London

We recently described the first comprehensive transcriptome analysis of hair cell (HC) regeneration in the chick utricle. We have now completed a similar study of the regenerating chick cochlea. In alignment with Phase I of the HRP Strategic Plan, our aim is to identify pathways that may be useful in engineering human HC regeneration. We employed mRNA-seq of pure sensory epithelia from antibiotic-damaged *in vitro* organotypic culture systems. Samples were collected at 24hour intervals across a seven day regenerative time period and were compared to matched (undamaged) controls. Multiple replicates were carried out, and results were validated with multiple qRT-PCR reactions. The same filtering criteria were applied to both the utricle and cochlea datasets to identify significantly differentially expressed genes. This yielded ~3,600 genes in the utricle and ~4,600 across the cochlear time course. The overlap between the two regenerating sensory epithelia was ~1600 differentially expressed genes. We next filtered these for common HC-specific transcripts (~400 genes) and shared components of cell cycle regulation (~100 genes). The resulting set of 1100 is highly enriched for genes known to affect sensory function and neuronal development and is a rich new source of candidates, many as yet unexplored, for the core “regenerome” of HC replacement. The two time courses also reflect the different ways that these two sensory epithelia handle HC replacement. In the utricle, some supporting cells (SC) initially undergo phenotypic conversion to HC, while in a later phase many more additional HCs are produced from SC divisions. By contrast, in the cochlea cultures, the predominant method of HC replacement is phenotypic conversion. Analysis of *NOTCH* signaling components in our data clearly reflects these different programs and allowed us to cluster additional genes that show remarkable co-expression or reciprocal expression with genes such as *ATOH1*. These types of unbiased statistical pattern matching tools also allowed us to identify subgroupings of genes that are enriched for particular biological processes. Predominant among these are those encoding transcription factors (TFs). We have identified ~90 TFs that are shared parts of both regenerative programs and a group of ~20 that very specific to one or other of the two sensory epithelia. These prioritization methods have allowed us to identify a list of ~200 candidates that are now being tested by knockdown and over-expression analysis for their affects upon HC regeneration.

SYM-37

Chicken II. Pathway Testing

Mark Warchol[1]; Jennifer Stone[2]; Michael Lovett[3]; Stefan Heller[4]

[1]Washington University School of Medicine; [2]Virginia Merrill Bloedel Hearing Research Center and Department of Otolaryngology-HNS, University of Washington, Seattle, WA; [3]National Heart and Lung Institute, Imperial College, London, UK; [4]Department of Otolaryngology-HNS, Stanford University School of Medicine, Palo Alto, CA

The goal of the Hearing Restoration Project is to devise biological methods for inducing sensory regeneration in the mammalian inner ear. One promising approach is to identify the molecular signals that are permissive for regeneration in the ears of nonmammalian vertebrates, and then use such data as a 'blueprint' for initiating regeneration in the ears of humans. Toward that end, we have employed Illumina RNA-Seq methodology to profile the changes in gene expression that occur during hair cell regeneration in the chicken cochlea and utricle. The resulting data allow us to formulate hypotheses regarding the role of specific signaling pathways and molecules, which can then be tested in organotypic culture preparations.

Our data indicate that regeneration in the avian ear involves many of the same signaling pathways that mediate otic development, but also that the precise functions of those pathways are not always straightforward. Changes in the expression of Wnt ligands, receptors (FZD's), and pathway modulators (DKK3, SFRP's, WIF-1) were observed in the regenerating utricle. Application of exogenous Wnt's can stimulate proliferation of dissociated supporting cells, but pharmacological activation of Wnt signaling does not evoke cell proliferation in the undamaged utricle and does not enhance proliferation after hair cell injury. Moreover, sustained activation of canonical Wnt signaling leads to a reduction in the numbers of replacement hair cells. Such findings suggest the Wnt activation is involved in regeneration, but is not sufficient for triggering proliferation. Similar complexity is evident with FGF signaling. The uninjured utricle expresses several FGF ligands as well as FGFR1 and FGFR3. Expression of many FGF genes is reduced during the earliest phases of utricular regeneration, and is restored once replacement hair cells begin to differentiate. Application of exogenous FGF20 reduces regenerative proliferation in the utricle, suggesting that FGF signaling may terminate regenerative proliferation once adequate numbers of cells are produced. Finally, the Notch pathway is activated in both the regenerating utricle and cochlea. Pharmacological inhibition of Notch signaling (via inhibition of gamma-secretase) leads to increased hair cell differentiation in both sensory organs, but gamma-secretase inhibition also promotes proliferation in the utricle, but not in the cochlea. This finding suggests that either Notch or some other gamma-secretase-dependent pathway serves a critical role in regulating cell cycle entry.

SYM-38

Genome-wide Analysis of Supporting Cell Gene Expression and Epigenetics in the Perinatal Mouse Inner Ear.

Neil Segil[1]; Zlatka Stojanova[1]; Juan Maass[2]; Litao Tao[1]; Rende Gu[2]; Joanna Asprer[2]; Jennifer Stone[3]; Andrew Groves[2]

[1]University of Southern California; [2]Baylor College of Medicine; [3]University of Washington

As part of the HRP Consortium, we are tasked with collecting genome-wide data sets related to supporting cell transdifferentiation to hair cells (Phase Ia) and supporting cell responses to ototoxin-induced hair cell damage (Phase Ib). We and others have observed that prior to giving rise to new hair cell-like cells, supporting cells from the perinatal mouse organ of Corti (postnatal day 1; P1) are able to reenter the cell cycle and divide. Our labs also observed that supporting cells are able to directly transdifferentiate to hair cell-like cells following interruption of Notch signaling. The latent potential for cell cycle reentry and direct transdifferentiation are age-dependent, disappearing during the first few postnatal weeks. To understand the fundamental changes involved in supporting cell transdifferentiation, and the subsequent age-dependent loss of this response, we have undertaken to analyze the transcriptome of FACS-purified supporting cells by RNA-seq at P1 and P6, both under control conditions and in response to the Notch-inhibitor DAPT. Preliminary results indicate >900 genes change in abundance during the perinatal maturation of supporting cells. A subset of these are currently being validated.

In a second part of this experiment, we have begun an epigenetic analysis of several histone posttranslational modifications (μChIP-seq) that will help define the regulatory elements of genes involved in hair cell differentiation. We have analyzed the H3K9 acetylation status in hair cells and supporting cells genome wide, a mark considered to indicate "permissive" status for transcription, and compared it to gene expression profiles in P1 hair cells and supporting cells. We have observed that 82% of the genes that are co-expressed at a high level in both cell types are marked by H3K9Ac, while only 68% of hair cell-specific genes and 48% of supporting cell-specific genes contain H3K9Ac. This suggests that other epigenetic marks that are currently under study are likely to be involved in the regulation of the unique hair cell and supporting cell transcriptomes.

In the second project (Phase Ib), we have begun to analyze the transcriptome of FACS-purified mouse supporting cells before and after hair cell ablation by the aminoglycoside antibiotic gentamicin. This project was designed to dovetail with another HRP project, involving Mark Warchol, Jenny Stone, and Mike Lovett, in which transcriptome data from aminoglycoside-damaged chicken basilar papilla and utricle was collected over an extended time course. Our study focuses on P1 organ of Corti, and adult utricle.

SYM-39

Mouse II. Pathway Testing

Andrew Groves; Juan Maass; Rende Gu; Joanna Asprer; Martin Basch
Baylor College of Medicine

We currently know very little about the genetic networks that become active in supporting cells when hair cells die, nor about those that are activated in experimental models of hair cell regeneration. Understanding these networks will help guide mobilization of supporting cells in mammals in a similar manner to that seen during regeneration in birds, where supporting cells produce new hair cells. In the past few years, several studies have shown that supporting cells of neonatal mammalian cochleas have a limited capacity for regeneration, but can trans-differentiate into hair cells when the Notch signaling pathway is blocked. In experiments supporting Phase I of the HRP Strategic Plan, we now show that this ability of cochlear supporting cells declines precipitously after birth, such that supporting cells from six day old mouse cochleas are entirely unresponsive to inhibitors of the Notch pathway. We also show that this trend is present regardless of whether the Notch pathway is blocked with gamma secretase inhibitors or by direct blockade of the Notch1 receptor. The loss of responsiveness to inhibition of the Notch pathway is due in part to a down-regulation of Notch receptors and ligands during this six day period, a result that we have confirmed with RNA-seq analysis of control cultures, as well as those treated with gamma secretase inhibitors. Moreover, this down-regulation persists in the adult animal, even under conditions of noise damage. Our data suggest that the Notch pathway is used to establish the repeating pattern of hair cells and supporting cells in the organ of Corti, but is not required to maintain this cellular mosaic after the onset of hearing. Our results have implications for the proposed used of Notch pathway inhibitors in hearing restoration therapies.

SYM-40

Molecular Characteristics of Supporting Cells in Damaged Adult Organ of Corti

Elizabeth Oesterle[1]; Joerg Waldhaus[2]; Irina Omelchenko[3]; Robert Durruthy-Durruthy[2]; Danielle Lenz-Kasher[4]; Edwin Rubel[3]; Albert Edge[4]; Stefan Heller[2]
[1]University of Washington; [2]Department of Otolaryngology-HNS, Stanford University School of Medicine, Palo Alto, CA; [3]Virginia Merrill Bloedel Hearing Research Center and Department of Otolaryngology-HNS, University of Washington, Seattle, WA; [4]Massachusetts Eye and Ear Infirmary and Harvard Medical School, Harvard University, Boston, MA

Restoration of hearing in the aged, diseased, or damaged cochlea will likely require production of new sensory hair cells and supporting cells from the cells that remain, but little is known about the identity of the remaining cells. A better understanding of the changes induced by damage will provide a basis for developing therapies to trigger hair cell regeneration from cells remaining in the remnant organ of Corti. In support of Phase Ib of the HRP Strategic Plan, we are assessing the phenotypes and genotypes of cells that remain in the adult mouse organ of Corti after a variety of damaging insults. The hair cells of adult mice, including those from transgenic mouse strains in which specific supporting cell subtypes were permanently fate-labeled with a genetic marker, were damaged by aminoglycoside/loop diuretics, noise, or diphtheria toxin. The fate-labeled cells were studied at a variety of times after insult (6 weeks to 6 months post-insult) using immunohistochemical techniques with cell-specific markers and, in some instances, FACS sorting based on the red fluorescence of the genetic marker. FACS-isolated cells were examined with multiplex qRT-PCR to examine changes in expression of 96 genes relevant for inner ear cell identity and signaling pathways. With all damage paradigms, cochlear regions were seen where supporting cells remained, despite total or partial hair cell loss. Regions of flat epithelium were seen after aminoglycoside/loop diuretic administration or noise exposure; small patches of flat epithelium were interspersed between segments of damaged epithelium containing differentiated supporting cells. Fewer nuclei were present in the flat epithelium, and these cells expressed sulcus cell markers. Initial analysis of qRT-PCR results showed pillar and Deiters' cells remain largely unaffected 6 weeks following aminoglycoside/loop diuretic-induced hair cell loss.

Our studies indicate that differentiated supporting cells can survive for long periods despite total hair cell loss, and these cells largely retain cellular identity. In regions of flat epithelium, sulcus cells apparently migrate into the region formerly occupied by the organ of Corti. Even six weeks after damage, little change is seen in molecular profiles of cells from control and damaged organ of Corti.

SYM-41

Chicken III. Single Cell Trajectory Analysis of Hair Cell Regeneration

Mirko Scheibinger[1]; Robert Durruthy-Durruthy[1]; C. Eduardo Corrales[1]; Jennifer Stone[2]; Michael Lovett[3]; Mark Warchol[4]; and **Stefan Heller**[1]
[1]Department of Otolaryngology-HNS, Stanford University, Palo Alto, CA. [2]Virginia Merrill Bloedel Hearing Research Center and Department of Otolaryngology-HNS, University of Washington, Seattle, WA. [3]National Heart and Lung Institute, Imperial College, London, UK. [4]Department of Otolaryngology, Washington University School of Medicine, Saint Louis, MO.

Chickens regenerate sensory hair cells in response to ototoxic insults. Transcriptome analyses of cultured regenerating utricular and cochlear sensory epithelia at various time points after aminoglycoside-induced hair cell loss have already revealed candidate signaling events and pathways that might play important roles in the regenerative process. We do not know, however, the order of molecular/genetic/signaling events that initiate, execute, sustain, and terminate the different known modes of hair cell regeneration, information that is critical for Phase I of the HRP's Strategic Plan.

Here, we have established surgical streptomycin delivery to the postnatal day 7 chicken inner ear *in vivo* resulting in reli-

able 70-95% hair cell loss in the utricle when assessed 48h after surgery; a similar degree of damage is observed in the basilar papilla. We quantified cells entering S-phase at various time points after ototoxic insult, as well as the re-appearance of MYO7A positive cells with hair bundles, and established a time course of recovery. Using a 192-gene assay for quantitative RT-PCR at the single cell level, we assessed gene expression for all major and many minor signaling pathways previously confirmed as being active during regeneration. Hundreds of single cells at time points ranging from 6 h until 7 days after ototoxic insult were profiled. Cluster and principal component analyses allowed us to partition hair cells, supporting cells, invading macrophages, and supporting cells that initiated regenerative programs at various time points post-insult. Single cell trajectory analysis using mathematical modeling is being used to reconstruct the order of molecular events operative at the single cell level that controls hair cell regeneration. Our ongoing project has begun to reveal details about the possible interplay of genes and pathways that contribute to phenotypic conversion of supporting cells into hair cells, as well as the genetic regulation of regenerative cell cycle re-entry. The initial results of these analyses will be presented in the form of cell transition trajectories that describe changes in expression of genes as non-sensory cells initiate and execute regenerative responses.

PS-215

Transdermal-Induced Stimulus-Timing Dependent Plasticity in Dorsal Cochlear Nucleus is Altered with Noise Damage and Tinnitus.

David Martel[1]; Calvin Wu[2]; Susan Shore[2]
[1]University of Michigan, Ann Arbor; [2]University of Michigan, Kresge Hearing Research Institute

Introduction

Nearly eighty percent of tinnitus patients can modulate their tinnitus with somatic maneuvers of the face and/or neck (Levine et al, Prog Brain Res, 2007). This process is likely mediated by somatosensory connections to the cochlear nucleus (CN). The dorsal CN (DCN) integrates auditory inputs with somatosensory inputs from trigeminal and dorsal column systems. Fusiform cells of the DCN exhibit stimulus-timing dependent plasticity (STDP) in response to bimodal auditory-somatosensory stimulation: Hebbian-like plasticity occurs when neurons increase their activity in response to somatosensory- preceding auditory stimulation, but anti-Hebbian plasticity occurs when auditory- precedes somatosensory stimulation (Koehler and Shore, Plos One, 2013). In tinnitus animals, Hebbian-like rules invert to anti-Hebbian rules. Inverted STDP, along with elevated spontaneous rates, thus provide neural correlates of tinnitus (Koehler and Shore, J Neurosci, 2013). In the present study, bimodal stimulus-timing protocols used auditory and transdermal somatosensory stimulation in normal and noise-damaged animals with and without tinnitus to evaluate long-term alterations in DCN firing activity as a potential treatment for tinnitus.

Methods

Guinea pigs were either noise damaged with a 7 kHz-centered, half-octave noise band at 97 dB SPL for 2 hours to induce tinnitus, or served as normal controls. Gap detection was used to assess tinnitus. Transdermal electrodes were placed on the skin overlying the trigeminal ganglion or the C2 cervical vertebrae. Reference electrodes were placed on the nasal bridge or vertebrae. Two multichannel recording shanks were stereotaxically placed into the DCN fusiform cell layer. Somatosensory stimulation was achieved with current levels that did not evoke muscle contractions. Bimodal stimulus intervals of +\- 20ms, +\- 10ms, +\- 5ms were used to construct STDP timing rules. Comparisons were made with responses to unimodal electrical and auditory stimulation.

Results

Tinnitus animals showed elevated spontaneous activity at noise exposure and tinnitus frequencies, consistent with previous studies. Facial stimulation combined with sound produced Hebbian-like learning rules in normal animals, which were inverted in noise damaged and tinnitus animals, as shown previously with deep brain stimulation (Koehler and Shore, J Neurosci, 2013). Neck stimulation produced anti-Hebbian rules in normal animals, which were inverted in noise damaged and tinnitus animals.

Conclusion

This study demonstrates that long-term alterations of DCN firing rates through STDP can be achieved with non-invasive transdermal stimulation. This regulation of neural activity can be harnessed to treat tinnitus, especially in somatic tinnitus patients.

PS-216

Bats Cry Repeatedly for Help When Under Distress But These Calls Produce Strong Adaptation in Cortical Auditory Neurons

Julio Hechavarria-Cueria; Manfred Kössl
Goethe University (Frankfurt am Main)

Acoustic communication is widely used by animals as a mean of information exchange. Communication sounds carry information that has to be pieced together by the listener(s) to form meaningful “percepts”. Although the auditory cortex is regarded as the place where percepts are formed, at presently, the mechanisms by which cortical neurons cope with natural vocalizations remain controversial. To add to the current body of knowledge on the cortical processing of species-specific vocalizations, we studied the structure of the so-called distress calls of Seba’s short-tailed bat (*Carollia perspicillata*) and the response of cortical neurons to these calls. Distress calls are produced when the animals are under physical stress and previous studies have suggested these calls are optimized for attracting individuals from the same and from other species to help the emitter chase distress sources away. We found that distress calls emitted by *Carollia* are indeed optimally designed for maximizing their chance of being heard by fellow bats. *Carollia’s* distress calls are short (~ 3ms), broadband (13-100 kHz), with most of their energy at rather low frequencies (~ 20 kHz), and they are produced at high repetition rates

(intervals of ~ 15 ms). Calls that belong to the same distress phrase are similar to one another. The later make distress phrases rather monotonous but it also increases the chance that the broadcasted message (i.e. the repeated syllable) is heard by other bats. We also found that in anesthetized bats, neurons in the tonotopic fields of the auditory cortex adapt relatively fast in response to distress phrases. In other words, the response of the neurons is strong when the syllables of a phrase are played randomly and separated by 500ms from one another, but the response to the delayed syllables in a phrase is suppressed when the phrase is played in its natural form. This suppression is synchronized throughout the tonotopic cortex, that is, it occurs simultaneously in neurons tuned to different frequencies and it can be observed not only at the level of spike data but also in local field potentials recorded in distant electrodes. We suggest that adaptation (or forward suppression) in response to distress phrases represents an example of optimized neuronal processing of repetitive information.

PS-217

Homeostatic Gain Control Gradually Restores Neural and Perceptual Sensitivity to Sound Following Profound Cochlear Neuropathy

Jennifer Resnik[1]; Anna Chambers[1]; Yasheng Yuan[2]; Albert Edge[3]; Daniel Polley[3]

[1]Massachusetts Eye and Ear Infirmary; [2]Fu Dan University; [3]Massachusetts Eye and Ear Infirmary / Harvard Medical School

Background

Individuals on the auditory neuropathy spectrum can exhibit relatively normal cortical evoked potentials and hearing thresholds despite the absence of an auditory brainstem response (ABR). This discrepancy is commonly attributed to a dys-synchronization of action potential timing among surviving spiral ganglion neurons (SGN), though experimental support is lacking. Here, we propose an alternative explanation: Homeostatic plasticity enables higher levels of the CNS to partially compensate for profound SGN loss, thereby reinstating neural encoding and perceptual awareness of basic sound features.

Methods

We tested this hypothesis by recording from units in the central nucleus of the inferior colliculus (ICc) and primary auditory cortex (A1) of awake mice after ~95% of Type-I auditory nerve fibers were unilaterally eliminated via round window administration of ouabain. Unit responses to pure tones and chirp trains recorded at 7 days or 30 days following ouabain administration and compared to cochlear status, ABR, and behavior.

Results

ABR peak amplitudes dropped to the measurement noise floor within minutes of ouabain administration and showed no further recovery. However, psychometric tone detection functions were nearly normal when measured 7 or 30 days later. ICc recordings performed 7 days after denervation revealed an unmasking of responses to the intact ipsilateral ear and a near-complete loss of sensitivity to the denervated ear. A1 recordings also showed enhanced ipsilateral responses, yet 30% of recording sites maintained well-defined, low-threshold frequency response areas (FRAs) upon stimulation of the denervated ear. By 30 days after denervation, a minority of ICc units also recovered FRAs with relatively normal thresholds and tuning properties. By contrast to the progressive recovery of tone burst sensitivity, temporal encoding of broadband chirp trains recovered to a lesser extent at both 7 and 30 days.

Conclusion

Findings from our mouse model of auditory neuropathy suggest that the defining characteristics of this disorder can be explained by compensatory plasticity at higher levels of the CNS without the need to invoke mechanisms related to peripheral nerve dys-synchronization. These data further suggest that CNS compensatory plasticity supports the recovery of rudimentary sound features that can be encoded by spike rate (tone detection), though complex sound features that are encoded by precise spike timing (e.g., pulse train synchronization) do not recover to the same degree. Our ongoing studies examine the dynamic interplay between interneurons and excitatory neurons that enables homeostatic adjustment in the face of extreme afferent loss.

PS-218

Cross-modal and Intra-modal Plasticity in Visual Activity After Cochlear Implantation: Implication for Speech Perception Performance

Il Joon Moon[1]; Min-Beom Kim[2]; Ji Eun Choi[1]; Yang-Sun Cho[1]; Won-Ho Chung[1]; Sung Hwa Hong[1]

[1]Samsung Medical Center, Sungkyunkwan University School of Medicine; [2]Kangbuk Samsung Hospital, Sungkyunkwan University School of Medicine

Introduction

Visual-auditory cross modal plasticity has been reported and widely accepted in deaf individuals. The superior visual abilities of deaf individuals are reported as enhanced reactivity of visual events or enhanced spatial attention. Also, there are some reports with its association of speech outcome after cochlear implant (CI) in pre or postlingual deafness. However, the methods for identifying cross modal plasticity are limited in enhanced visual reactivity using PET or EEG study such as, visual evoked potentials in human. The purpose of our study was to investigate the association between visual-auditory cross modal plasticity and speech perception outcome in postlingual adult CI users by VEP response of auditory and visual cortex for visual reactivity and visual field test (VF) for spatial attention.

Methods

Postlingual deafness with adult cochlear implant users (N=12) and normal controls (N=12) were participated in this study. All CI users had their device implanted for more than 1 year, but obtained different levels of speech perception performance. We divided them into good (N=6) and poor performer (N=6) group based on word recognition scores. VEP

responses in auditory and visual cortex from all participants were obtained using Neuroscan. Goldmann perimetry was also administered for identifying visual field difference. The association between the amplitude of the N1 VEP response over the right temporal or occipital cortex in the three groups (control, good CI, poor CI) was analyzed. In addition, the association between VF by different stimuli and word perception score was investigated.

Result

In poor CI performer, N1 VEP amplitude in right temporal lobe was higher and N1 amplitude in occipital lobe was lower than the good performer group. Also, N1 VEP amplitude in right temporal lobe showed negative correlation with speech perception outcome and that in occipital lobe had positive correlation. In VF analysis, VF to low intensity stimuli was narrowed but VF to high intensity stimuli was not different in CI group as compared with those in controls. Of note, VF to low intensity stimuli was strongly correlated with speech perception scores.

Conclusion and summary

Persistent visual activation in right temporal cortex is associated with poor outcome following CI in postlingual deaf adults. Insufficient intra-modal (visual) compensation by occipital cortex also causes negative effect on speech perception after CI. Based on our results of visual field test, narrow visual field to low intensity stimuli could be novel behavioral evidence in CI users with poor speech outcome.

PS-219

Delayed Development of Cerebral White Matter in Children with Congenital Deafness

Kye Hoon Park[1]; Won-Ho Chung[2]; Hunki Kwon[3]; Jong-Min Lee[3]

[1]Soonchunhyang University College of Medicine; [2]Department of Otorhinolaryngology-Head & Neck Surgery, Samsung Medical Center, Sungkyunkwan University School of Medicine; [3]Department of Biomedical Engineering, Hanyang University

Removal of sensory receptors or changes in afferent activity have profound effects on the maturation of neuronal structure. Also, in congenital deaf children, it is supposed that a similar phenomenon would take place and that development delay of the white matter tract would be induced. However, the development of white matter has not yet been evaluated in the prelingually deaf children. The purpose of this study was to investigate the differences of white matter development in the congenitally deaf children as compared to normal hearing ones using tract-based spatial statistics (TBSS) method. Diffusion tensor imaging (DTI) was performed in 21 congenitally deaf (DEAF group) and 20 normal hearing subjects (HEAR group) from 1.7 to 7.7 years old. Using TBSS, we evaluated the regions of significant difference in fractional anisotropy (FA) values between groups. To evaluate the correlations between FA values and age in each group, we examined voxel-wise correlation analyses on the TBSS skeleton. Lower FA values at the white-matter tracts to Heschl's gyrus, inferior fronto-occipital fasciculus, uncinate fasciculus, superior longitudinal fasciculus, forceps major were found in DEAF group than in HEAR group less than 4 years old, but significant difference was not found between groups in subjects older than 4 years old. We also found the age-related development of the white-matter tract may continue until 8 years old in deaf children. These results suggest the delayed development of cerebral white matter tracts in the congenitally deaf children.

PS-220

Enucleation prevented CREB activation induced by auditory and tactile information in auditory cortex

Masaaki Nomura; Nobuhiro Yamamoto; Hideki Kawai

Soka University

Sensory loss in one modality leads to changes in the cortex of other sensory modalities. How such cross-modal changes occur is unknown, but could involve changes in cortical activities and structural reorganization. In this study, we used a mouse model of visual deprivation to investigate whether changes in cross-modal activities occur in auditory cortex. More specifically, by monitoring activation of cAMP response binding protein (CREB) – a transcription factor - in presumed A1 of enucleated mice, we investigated whether sound stimuli induce CREB phosphorylation and whether tactile stimuli and sound stimuli interact to activate CREB.

Mice (C57BL/J) were enucleated at both eyes at the time of eye-opening (postnatal day 14-15) and raised along with sham operated mice in regular 12-hour day-night cycles (8 am on/8 pm off). At 10 days after enucleation, anesthetized control (sighted) and blind mice were exposed to white noise (WN) stimuli (70 dB SPL, 1-20 kHz, 100 ms duration) for 15 min at 0.5 Hz in a sound-proof chamber. Immediately after stimulation, mice were stabilized with thumbtack on hands or with tapes on arms and perfused with 4% paraformaldehyde transcardially. Fixed brains were extracted and processed for immunofluorochemistry using antibodies against CREB. Stained sections were then imaged using an epifluorescence microscope. We analyzed distribution of cells that are immuno-positive for phosphorylated CREB (P-CREB) in divided layers of anatomically determined A1.

WN stimuli followed by pushing thumbtack in hands a few minutes later elevated fluorescence intensity of P-CREB immunopositive cells in layers II-IV about 1.7-fold over thumbtack stimulated control mice. Meanwhile, WN stimuli without tactile stimuli on hands did not significantly affect the intensity in sighted and blind mice. Interestingly, the combination of WN- and thumbtack-stimuli did not induce CREB phosphorylation in blind mice, suggesting that enucleation suppressed multisensory stimuli-induced cortical activities in A1.

This activation of CREB is likely mediated by calmodulin-dependent kinases (CaMKs) since a hemicortical injection of STO-609, a CaMK kinase inhibitor, reduced multisensory stimulated CREB phosphorylation in the upper layers of A1 in sighted mice.

These data suggest that auditory stimuli tag A1 for subsequent tactile stimuli to activate CREB via CaMKs in sighted control mice, while this tagging is prevented by enucleation. Future studies will reveal if enucleation reorganizes auditory as well as somatosensory cortex to isolate sensory modality.

PS-221

Searching the Physiological Correlates of Loudness Modulation After Transient Sound Deprivation and Enrichment

Philippe Fournier; Marianne Bélanger; Marc Schönwiesner; Sylvie Hébert
Université de Montréal

The relationship between intensity and loudness can be modified by acoustic conditions: Sound sensitivity increases after short-term sound deprivation whereas it decreases after sound enrichment. These shifts in sensitivity are mostly observable at high sound intensities, via changes in uncomfortable loudness levels. The central gain model proposes that modulation of neural activity after a deprivation or enrichment period is at the origin of the loudness modulation (to compensate for the lack or excess of stimulation). This model implies that the central nervous system activity should be affected by those procedures, but that cochlear measures should not. The present study tests this hypothesis by investigating changes in stapedial reflex thresholds (a brainstem measure) and growth of distortion product otoacoustic emissions (DP growth, a cochlear measure) before and after a week of sound deprivation and enrichment.

Methods

Young adults with normal hearing were assigned to either the Earplug or Noise generator group. Bilateral custom-fit musicians' earplugs and around-the-ear white noise generators produced about 25 dB of sound attenuation and stimulation, respectively, at 1kHz, 2kHz, and 4kHz. All participants were tested before and after seven days of continuous use of sound devices (24 hours a day). Hearing assessment included loudness growth functions (4 kHz frequency-modulated sweep), DP growth (4 kHz) and stapedial reflex thresholds (1 kHz and 4 kHz).

Results

Preliminary findings (N=7 and N= 8 participants in the Earplug and Noise generator groups, respectively) show no significant differences before and after deprivation or stimulation on loudness growth functions. In contrast, the Earplug group displays decreased reflex thresholds after deprivation (Mean Pre: 90 dB HL, Mean Post: 89 dB HL), whereas the Noise generator group displays the reverse effect (Mean Pre: 89 dB HL, Mean Post: 96 dB HL). No differences are observed in DP growth in either group.

Conclusions

These findings suggest that sensitivity is increased after sound deprivation and is decreased after sound enrichment. The stapedial reflex being a brainstem reflex, this indicate that sound deprivation and enrichment entail physiological modifications in the central auditory system. Our loudness growth task might lack sensitivity to capture the perceptual modifications of loudness. In contrast, the findings on DP growth might indicate that outer hair cells are not involved in loudness modulation. Further data collection on more participants, currently underway, will strengthen or refute these preliminary findings.

PS-222

BDNF-dependent Auditory Fibers Enhance Fidelity of Auditory Information Processing Within the Ascending Auditory Pathway

Marlies Knipper[1]; Tetyana Chumak[2]; Lukas Rüttiger[3]; Sze Chim Lee[3]; Dario Campanelli[3]; Annalisa Zuccotti[3]; Wibke Singer[3]; Jiří Popelář[2]; Katja Gutsche[4]; Hyun-Soon Geisler[3]; Sebastian Philipp Schraven[5]; Mirko Jaumann[3]; Jing Hu[6]; Thomas Schimmang[7]; Ulrike Zimmermann[3]; Josef Syka[2]
[1]University of Tuebingen; [2]Institute of Experimental Medicine, Academy of Sciences of the Czech Republic, Department of Auditory Neuroscience, Vídeňská 1083, 142 20 Prague, Czech Republic; [3]Department of Otorhinolaryngology, Hearing Research Centre Tübingen, Molecular Physiology of Hearing, University of Tübingen, Elfriede Aulhorn-Str. 5, 72076 Tübingen, Germany; [4]Instituto de Biología y Genética Molecular, Universidad de Valladolid y Consejo Superior de Investigaciones Científicas, E-47003 Valladolid, Spain; [5]Department of Otorhinolaryngology, Plastic, Aesthetic and Reconstructive Head and Neck Surgery, Comprehensive Hearing Center, University of Würzburg, Josef-Schneider-Straße 11, D-97080 Würzburg, Germany; [6]Centre for Integrative Neuroscience, Otfried-Müller-Straße 25, 72076 Tübingen, Germany; [7]Instituto de Biología y Genética Molecular, Universidad de Valladolid y Consejo Superior de Investigaciones Científicas, E-47003 Valladolid, Spain

The accomplishment of spatial and temporal cortical resolution in the central auditory system is a process that is assumed to be initiated by the first auditory experience. Experience driven activity has been suggested to trigger increased intrinsic inhibition towards shaping the central sound resolution in dependency of brain-derived neurotrophic factor (BDNF). The experience dependent driving force for this process has so far not been specified further. Using mice with conditional deletion of BDNF under the Pax2 promotor and the TrkC promotor, we here demonstrate that the deletion of BDNF in the cochlea ($BDNF^{Pax2}$-KO) but not in the auditory cortex ($BDNF^{TrkC}$-KO) or the inferior colliculus ($BDNF^{Pax2}$-KO, $BDNF^{TrkC}$-KO) severely reduced dynamic range of sound sensitivity and noise vulnerability. Extracellular sound-evoked responses from IC neurons in $BDNF^{Pax2}$-WT and $BDNF^{Pax2}$-KO mice before and after acoustic trauma, moreover revealed that a BDNF dependent auditory fiber activity drives short response latency, low sound thresholds, and the narrow tuning of IC neurons including the generation regulatory high-frequency inhibitory sidebands. Analysis of further characteristic features within the ascending pathway of the mice mutants suggests that driving force for BDNF dependent intracortical inhibition itself may be a BDNF dependent process. The loss of the BDNF dependent intracortical inhibition has se-

vere consequences for central sound processing. Data are discussed in the context of a novel role of cochlear BDNF for auditory processing and central auditory plasticity.

PS-223

Investigation of Auditory Cortex Response in the Audiologically Immature Rat with Single Side Deafness

Doo Hee Kim[1]; Yoon Chan Rah[1]; Min Young Lee[2]; Shin Hye Kim[1]; Jun Jae Choi[1]; Su Kyung Park[3]; Seung-Ha Oh[1]
[1]Seoul National University Hospital; [2]Kresge Hearing Research Institute; [3]Hallym University Medical Center

Background

Cortical plasticity of congenital single side deafness (SSD) patients might be different from that of prelingual SSD requesting for different rehabilitation strategies. The aim of this study was to investigate the development of the auditory cortex for the rats with prelingually induced SSD using single-unit recording and to compare the time series neuronal response with that of postlingually induced SSD rats.

Methods

Twelve Sprague-Dawley rats were used. Hearing deprivation was induced by cochlear ablation and kanamycin injection into the cochlear at the age of postnatal days 10 (prelingual group). The neuronal signal was obtained from the both auditory cortices at 2, 4, 6, and 8 weeks after deafening. Three rats allocated for the recording at each time point. After the wide exposure of auditory cortex, 4x4 microelectrode array was inserted into 4 spots for each hemisphere (depth of insertion: 500~900 μm). Sound stimulation (Gaussian white noise, 100 ms length) was generated and introduced every 685 ms during recording. The acquired data was sorted and peri-stimulus time histogram (PSTH) was generated. Averaged number of spikes, peak amplitude of PSTH and onset/peak latency were analyzed.

Results

At 2 weeks, greater number of action potential, greater peak amplitude, and longer peak latency were observed on contralateral side compared with that of ipsilateral side. The number of action potential and peak amplitude in contralateral were decreased rapidly after 4 weeks and slightly increased and maintained after 6 weeks. On the contrary, steady decrease of the number of action potential and peak amplitude were shown on the ipsilateral side and became reactionless at 8 weeks. The shortening of peak latency of both sides was shown at 4 weeks and they became almost the same between both sides. They were slightly increased and maintained stable thereafter. These results are different from that of SSD induced after auditory system maturation which showed rapid decrease and gradual recovery of neuronal response in both auditory cortices and gradual shortening of ipsilateral latency.

Summary

Different pattern of auditory system development was confirmed in preligual SSD group from that of postlingual SSD group or normal controls.

PS-224

Differential Effects of Noise Exposure on Auditory, Visual and Multisensory Cortical Areas

Ashley Schormans; Marei Typlt; Brian Allman
Western University

Introduction

Previous studies have identified that complete or partial hearing loss results in an increased responsiveness of neurons in the central auditory system to visual and/or tactile stimuli (i.e., crossmodal plasticity). At present, however, it remains relatively unknown how adult-onset partial hearing loss affects areas of the brain that already integrate multisensory information. In the present study, we investigated the effect of noise-induced hearing loss on neurons in the extrastriate visual cortex—an area known to integrate audiovisual stimuli, to determine whether crossmodal plasticity extends beyond the core auditory cortex.

Methods

Adult male Sprague-Dawley rats (n=7) underwent an auditory brainstem response (ABR) to determine their baseline hearing level, followed by a bilateral noise exposure (0.8-20 kHz at 120 dB for 2 hours). Two weeks later, hearing levels were reassessed, and an acute electrophysiological recording experiment was performed under ketamine/xylazine anesthesia. Using stereotaxic coordinates (5-6 mm caudal to bregma) and a dorsal/medial-to-ventral/lateral approach (40 deg), extracellular electrophysiological recordings were made with a 32-channel linear array electrode that was progressively inserted into the cortex to allow for the sampling of neurons spanning a predominately visual area (dorsal aspect of V2L), an audiovisual area (V2L), and a predominately auditory area (AuD). Computer-generated auditory (noise burst), visual (light flash) and combined audiovisual stimuli were delivered, and the associated spiking activity was used to determine the response profile of each neuron sampled (i.e., auditory, visual or multisensory). The same ABR + acute electrophysiology experiment was performed in age-matched control rats (n=7).

Results

Noise exposure increased the ABR click threshold 14±3 dB. In comparing noise exposed rats to controls, the proportions of visual and multisensory neurons were unchanged in the predominately visual area (dorsal V2L), whereas the proportion of visual neurons in the audiovisual area (V2L) increased 38%, and the proportion of multisensory neurons decreased (55% controls vs. 38% noise-exposed). This unexpected reduction in multisensory neurons in V2L was inconsistent with the crossmodal plasticity observed in the predominately auditory area (AuD), where the proportion of multisensory neurons nearly doubled (27% controls vs. 48% noise-exposed).

Conclusions

Overall, noise exposure increased the proportion of visually-responsive neurons encountered by ~20%; however, the degree and nature of crossmodal plasticity differed across the cortical areas, such that only the predominately auditory area, AuD, showed an increased proportion of neurons ca-

pable of processing multisensory information following the adult-onset partial hearing loss.

PS-225

Somatosensory-to-auditory Cross-modal Re-organization in Cochlear Implanted Children

Garrett Cardon; Anu Sharma
University of Colorado at Boulder

While many children with cochlear implants exhibit functional speech perception performance at, or above, expectation level, others do not. Poor performance often occurs despite an early age of implantation, appropriate device settings, and consistent device use. Studies aimed at elucidating the details of this variability in behavioral performance have only been partially successful. Mounting evidence suggests that the maturation and plasticity of the cerebral cortex may play a significant role in predicting behavioral performance in children with cochlear implants. For instance, it appears that a sensory system that experiences deprivation has the tendency to re-organize. This re-organization can occur by the recruitment of deprived sensory areas by intact modalities (i.e., cross-modal re-organization). Thus, the current study aimed to investigate whether the auditory cortex is recruited by the somatosensory system in deaf children who use cochlear implants, and whether the degree of cross-modal re-organization is related to the variability in these children's functional speech and language abilities. Using high-density EEG (128 electrodes), we evaluated cortical responses to both auditory and vibrotactile stimulation in children with cochlear implants and those with normal hearing between the ages of 5-13. Both waveform and cortical source localization analysis (i.e., current density reconstruction) were performed on these data. Current density reconstruction revealed that children with normal hearing presented with activation of the pre- and post-central gyri (i.e., somatosensory cortices) in response to vibrotactile stimuli. While children with hearing loss showed similar activation of the pre- and post-central gyri to vibrotactile stimulation, they also exhibited activation of auditory cortical areas. Our findings suggest that somatosensory stimuli were processed in areas of the cerebral cortex that typically deal with auditory stimuli in cochlear implanted children. These results point to possible cross-modal re-organization of the auditory cortex by the somatosensory system.

PS-226

Dark-Rearing Changes the Functional Connectivity of Supragranular Auditory Cortex

Xiangying Meng; Patrick Kanold
University of Maryland

Interactions between auditory and visual systems have been shown during sensory loss. For example, the cross-modal compensation in blind individuals leads to functional enhancement of the remaining senses, including enhanced frequency discriminations. Moreover, in mice brief (7 day) episodes if dark exposure (DE) after the critical period (P21) lead to altered auditory responses in auditory cortex (A1) (Petrus et al. 2014). In these studies A1 cells showed higher firing rates and frequency selectivity. While some of these changes can be accounted for by increases at the thalamocortical synapse (Petrus et al. 2014), increased frequency is likely due to refinement of thalamocortical or intracortical circuits. We thus hypothesized that DE leads to refinement of circuits within A1.

We here investigated this hypothesis by comparing the intracortical connections to Layer 2/3 neurons in DE mice to those from normally reared mice from P26 to P30. We use Laser-scanning photostimulation combined with whole cell patch clamp recordings in acute thalamocortical slices of auditory cortex to study the spatial pattern of excitatory and inhibition connections. We find that the spatial pattern of activation of neurons in A1 did not change after DE. However, we find layer specific changes in the spatial pattern of intracortical connections to layer 2/3 neurons after DE. Most prominently we find that the spatial pattern of excitatory ascending circuits as well as intralaminar circuits to layer 2/3 neurons are refined after DE compared to normally reared mice. Since layer 2/3 neurons integrate inputs from a large frequency (Chen et al. 2011) range the specific change in intracortical synaptic circuits after DE might contribute to the enhancement of frequency discrimination after DE. Together, our results demonstrate the powerful influence crossmodal influences have on the circuitry and sound processing in A1.

PS-227

Experience-dependent Enhancement Of Pitch Relevant Neural Activity in the Auditory Cortex is Limited to Native Pitch Acceleration Rates

Ananthanarayan Krishnan; Suresh Chandan; Jackson Gandour
Purdue University

Experience-dependent enhancement of pitch relevant information in the auditory brainstem has been shown to transfer to pitch acceleration rates beyond the pitch range of natural speech in Chinese listeners. These findings demonstrate that perceptually salient pitch cues in lexical tones shape brainstem pitch relevant neural activity not only in the speech domain, but also in auditory signals that fall outside the range of dynamic pitch that a native listener is exposed to. Since the brainstem and the auditory cortex represent components of a well-coordinated hierarchical processing network, our aim here is to determine if the experience-dependent sensitivity to changes in pitch acceleration, observed at the brainstem level, is shared by pitch processes in the auditory cortex. Cortical pitch responses (CPR), characterized by multiple transient components (Na, Pb, Nb) were recorded from Chinese and English participants in response to four, 250-ms dynamic iterated rippled noise stimuli with different rates of pitch acceleration ranging from low (0.3 Hz/ms; Mandarin Tone 2) to high (2.7 Hz/ms; 2 octaves). Peak latency of Na increased with acceleration rate for both groups, but the increase was greater for the English group at the faster acceleration rates. In contrast, Pb and Nb latency decreased with increasing acceleration rates for both groups with greater decrease observed for the Chinese group. Both Na-Pb and Pb-Nb, amplitude was greater for the Chinese, for acceleration rates

that fell within the range of natural speech. Finally, only the Chinese group showed a right hemisphere preference in the pitch related neural activity for all stimuli at the temporal electrode sites. These findings are qualitatively similar to the observations in the brainstem. However, the opposing changes in latency for Na (which marks pitch onset), and Pb, Nb (components strongly correlated with the dynamic portions of the pitch contour) suggest that these components, representing different temporal attributes of the pitch contour, are differentially affected by pitch acceleration. Specifically, Na latency changes may reflect decreasing pitch salience; and Pb, Nb latency changes may reflect the shortening time course of the pitch contour with increasing pitch acceleration. These findings are consistent with the notion that long-term language experience shapes processing of pitch relevant information in the auditory cortex with particular sensitivity to acceleration rates that occur in natural speech. The response asymmetry also highlights the emergence of early hemispheric preferences and their functional roles as related to sensory and cognitive properties of the stimulus.

PS-228

Cortical Pitch Response Components Reveal Experience-Dependent Sensitivity to Both Auditory and Linguistic Attributes of Lexical Tone

Ananthanarayan Krishnan; Chandan Suresh; Jackson Gandour
Purdue University

The aim of this study is to evaluate how pitch contours of varying shape influence latency and amplitude of cortical pitch-specific response (CPR) components (Na, Pb, Nb) as a function of language experience (Chinese, English). Stimuli included three dynamic, *curvilinear*, iterated rippled noise (IRN) pitch stimuli that differ in pitch direction and location of peak acceleration. Two are homologous to Mandarin lexical tones (Tone 2, T2; Tone 4 (T4); the third, a mirror image of T2 (T2'). By comparing stimuli, we can evaluate the effects of location of peak acceleration, pitch direction, and linguistic status. By comparing left/right frontal (F3/F4) and temporal (T7T8) electrode sites, we obtain a measure of hemispheric asymmetry. By comparing stimulus patterns at frontal and temporal sites we are able to assess experience-dependent, sensory and extra-sensory influences on pitch processing.

ANOVAs of latency and amplitude of CPR components by stimulus derived from the Fz electrode site revealed that peak latencies of Na elicited by T2'&T4 were longer in English than Chinese. As reflected by Na-Pb and Pb-Nb, Chinese exhibited larger amplitude than English across stimuli; T2 was greater than T4 across groups. For Na-Pb, within-group analyses showed that Chinese amplitude of T2&T4 was greater than T2'; English amplitude of T2 was greater than T2'&T4. For Pb-Nb, the same stimulus patterns were observed by group; by stimulus, Chinese amplitude was greater than English for T2&T4, but not T2'.

ANOVAs of amplitude of Na-Pb by stimulus derived from temporal electrode sites showed that native tones elicited a language-dependent, rightward asymmetry for the Chinese group, and that the group effect was circumscribed to the right temporal site. By hemisphere, stimulus comparisons yielded the same patterns across hemispheres. They varied by component (Na-Pb: T2 > T2', T4; Pb-Nb: T2&T4 > T2'). Na-Pb reflects sensory information; Pb-Nb, extra-sensory or linguistic information. At frontal sites, no evidence of hemispheric asymmetry is observed for either language group. Chinese amplitude was greater than English in response to native tones only. Stimulus comparisons yielded the same pattern (T2&T4 > T2') regardless of component or hemisphere. In contrast to temporal sites, both Na-Pb and Pb-Nb reflect the influence of linguistic information.

Our findings suggest that CPR components are modulated by experience-dependent, temporally distinct weighting of auditory and linguistic information at the right temporal site. More broadly, they are interpreted to be consistent with an interactive, parallel model of early pitch processing with discrete distributed cortical circuits.

PS-229

Synchronizing Bilateral Cochlear Implants: Preliminary Findings Using the UTD Cochlear Implant PDA (CiPDA) Research Platform in the Free-field

Heath Jones[1]; Alan Kan[1]; Ruth Litovsky[2]
[1]University of Wisconsin – Madison; [2]ahkan@wisc.edu

Background

Bilateral cochlear implants (BiCIs) provide significant spatial hearing benefits over a single implant, such as improved sound localization and speech-in-noise recognition. However, BiCI users still exhibit spatial hearing difficulties compared to normal hearing listeners. Deficits have been posited to result from the fact that the two implants function independently and that the lack of coordination between devices disrupts the ability to encode important acoustical cues used for spatial hearing. Recently, the UT-Dallas ciPDA device was developed to provide a real-time, portable research platform with synchronized stimulation across the ears, i.e., one time-clock is used to stimulate both implants. The current study evaluated spatial hearing abilities in BiCI users listening with the ciPDA device.

Methods:

Free-field sound localization and speech-in-noise testing was conducted in post-lingually deafened BiCI users fitted with Cochlear Freedom or N5 devices and had a minimum of 1 year bilateral experience. Localization performance was measured by calculating root-mean-square (RMS) errors between target and response angles. Speech reception thresholds (SRTs) were measured for two loudspeaker configurations: 1) Co-located; target/maskers presented from the center loudspeaker at 0°; 2) Symmetrically separated; target at 0° and maskers symmetrically distributed at ±90°. Spatial release from masking (SRM) was calculated as the difference between the SRTs for these two configurations. Performanc-

es with the ciPDA were compared to measures made using the patient's own clinical processors.

Results:
Results showed that acute listening with the ciPDA produced free-field spatial hearing performance comparable to the patient's own clinical processors. The across-subject average RMS errors were nominally lower in the ciPDA listening condition (27.6±3.2°) compared to the clinical condition (32.7±4.2°); however, this difference was not significant. In general, SRTs were lower for the clinical processors compared to the ciPDA. Some listeners exhibited larger SRM benefits (~3-6 dB) using the ciPDA, while others had either larger SRM with their clinical or equivalent SRM between conditions.

Conclusions:
Acute listening with a new hardware and software that synchronized stimulation between CIs in the two ears produced benefits in some but not all subjects. However, this work demonstrates that the UT ciPDA platform provides an effective means for testing novel algorithms and strategies in a CI users. In addition, although currently the device is only used in acute experiments, its success for free-field studies of spatial hearing may provide opportunity for further investigations.

PS-230

Pitch Ranking Using Different Current Focused Virtual Channel Stimulation

Monica Padilla; Natalia Stupak; David Landsberger
New York University

Introduction

Virtual channels (VCs) can be used to increase the number of sites of stimulation on a cochlear implant electrode array beyond the number of physical electrodes. However, because of the broad current spread from electrical stimulation, channel interaction limits the functional benefits of increasing the number of stimulation sites with traditional VCs produced with monopolar stimulation (i.e. MPVCs). Current focused VCs have the potential to increase the number of stimulation sites while reducing channel interaction and hopefully increasing the number of effective channels perceived. We originally proposed the Quadrupolar VC (QPVC; Landsberger and Srinivasan, 2009), which reduces the spread of excitation. However, unlike the MPVC, the QPVC theoretically produces an asymmetric spatial distribution. It is unknown how the asymmetrical spatial distribution of the QPVC would affect pitch ranking of different places of stimulation. Recently, we developed a new current steered VC (Virtual Tripole; VTP) to produce a symmetrical spatial distribution. In the following experiment, we pitch ranked MPVC, QPVC, and VTP stimuli to determine the effect of current focusing and the asymmetric spatial configurations on pitch perception.

Methods
Six post-lingually deafened users (one bilateral) of Advanced Bionics CII or HiRes 90K devices, participated in this study. Pitch ranking with MPVC, QPVC, and VTP stimuli was measured. The pitch of pulse trains presented at virtual electrode locations 4.5 to 7.5 were compared to a reference at electrode 6. Steps of $\alpha = 0.1$ (10% of the distance between two adjacent physical electrodes) were used between 5.5 and 6.5 and steps of $\alpha = 0.25$ for the remaining range. All stimuli were loudness balanced to the reference electrode. To reduce potential loudness cues, an amplitude jitter of 0.3dB was included. Subjects were asked to indicate which of two sounds was higher in pitch. A sigmoidal function was fitted to the data to find estimated slopes and crossing points.

Results
Preliminary analysis suggests that pitch percepts are shifted when stimulation is spectrally asymmetric (i.e. in QPVC mode). However, no overall difference in ability to pitch rank has been observed across the three different stimulation modes. A more thorough analysis of the results will be presented.

Conclusions
Although asymmetric stimulation may shift the pitch percepts, MPVC, QPVC, and VTP stimulation modes all provide good pitch information. Further analysis of the data is still required to determine the effects of stimulation mode on pitch perception. Conclusions from these analyses will be presented.

PS-231

Sound Quality Assessment Of Cochlear Implant Subjects with Short Med-El Implant Arrays

Richard Penninger[1]; Charles Limb[2]; Andreas Büchner[1]
[1]Medical University Hannover (MHH); [2]Johns Hopkins School of Medicine Peabody Conservatory of Music

Introduction
Despite remarkable success with language perception, music perception is typically poor for cochlear implant (CI) users (Limb & Rubinstein, 2012;Penninger et al, 2013). CI users subjectively report poorer musical sound quality following implantation compared to normal hearing (NH) subjects (Drennan et al, 2014). Musical sound quality is traditionally assessed via questionnaires or rating scales (Gfeller et al, 2002;Lassaletta et al, 2008).

The goal of the present study is to investigate how musical sound quality is rated on Med-El Flex 20 and 24mm electrodes.

Methods:
Five NH and five CI subjects participated in the experiment. Four CI subjects had a Med-El Flex 20mm electrode and one had a Med-El Flex EAS 24mm electrode. The subjects were asked to rate the sound quality of 25 altered musical stimuli in a Cochlear Implant MUltiple Stimulus with Hidden Reference and Anchor (CI-MUSHRA) test (Roy et al, 2012). The stimuli consisted of one unaltered stimulus and a 200, 400, 600, 800 and 1000Hz high-pass filtered version. One of the stimuli was a 1000-1200Hz band-pass filtered version (anchor).

Results:
Preliminary results show that NH subjects are able to rank the presented stimuli according to their sound quality. CI subjects performed a lot worse and were unable to discriminate

between the unaltered reference, the 200 and the 400 Hz high-pass filtered versions. The sound quality ratings of the CI subjects were overall a lot worse compared to the NH subjects.

Conclusion:
One of the reasons for the impaired sound quality ratings of the CI subjects could be their short implant array length.

Electrode number	1	2	3	4	5	6	7	8	9	10	11	12
Center Frequency (Hz)	149	262	409	602	851	1183	1632	2228	3064	4085	5656	7352
Reference												
200 Hz HPF												
400 Hz HPF												
600 Hz HPF												
800 Hz HPF												
1000 Hz HPF												
Anchor 1000-1200 BPF												

Figure 1 shows the activated electrodes for reach of the sound quality versions.

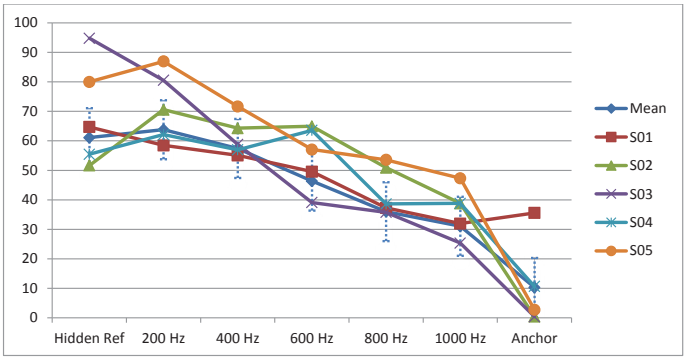

Figure 2 shows the sound quality ratings of the 5 CI subjects.

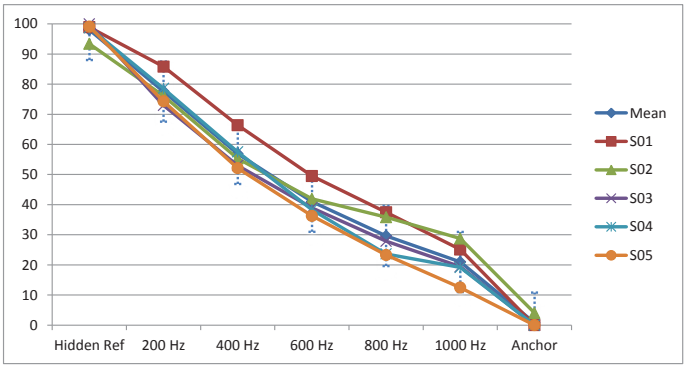

Figure 3 shows the sound quality ratings of the 5 NH subjects.

PS-232

Spectrotemporal Modulation Sensitivity as a Predictor of Speech Perception for Cochlear Implants Recipients

Il Joon Moon[1]; Jong Ho Won[2]; Yang-Sun Cho[1]; Won-Ho Chung[1]; Sung Hwa Hong[1]
[1]Samsung Medical Center, School of Medicine, Sungkyunkwan University; [2]University of Tennessee Health Science Center

Introduction
Reduced frequency selectivity due to the limited number of stimulating electrodes and channel interactions contributes to poor speech perception in noise for cochlear implant (CI) users. Previous studies demonstrated that CI users with better spectral resolution and temporal processing ability showed better speech understanding in noise. Speech signals present modulations both over time and frequency. This study examined CI users' performance on spectrotemporal modulation (STM) task and compared it to speech perception in quiet and in noise.

Methods
Ten normal-hearing (NH) listeners and twenty-three CI subjects participated. The minimum modulation depth required to detect STM was measured for combinations of temporal modulation rate (5 or 10 Hz) and spectral modulation density (0.5, 1, and 2 cycles/octave). Static ripple detection and temporal modulation detection (TMD) tests were administered. K-CID and K-HINT test were used to determine speech perception performance.

Results
Compared to NH subjects, STM detection thresholds were significantly elevated for CI users, especially for combinations of high density and rate. K-HINT scores were significantly correlated with STM sensitivity for three combinations of low density and rate: 0.5 c/o and 5 Hz, 0.5 c/o and 10 Hz, and 1 c/o and 5 Hz. Significant correlations were also found between the STM sensitivity and K-CID scores. Static ripple detection thresholds were only correlated with K-CID scores, and no correlations were found between TMD thresholds and both K-HINT and K-CID scores.

Conclusions
The present study demonstrates that CI users are partially able to perceive spectrotemporal modulation patterns that are critical for speech understanding. The STM sensitivity test, which is time efficient and a nonlinguistic measure, would be a useful tool to evaluate CI performance with different signal processing strategies that attempt to improve the delivery of temporal and frequency modulations.

PS-233

Loudness Recalibration in Normal-Hearing Listeners and Cochlear-Implant Users

Ningyuan Wang; Heather Kreft; Andrew Oxenham
University of Minnesota

Introduction
Auditory context effects, such as loudness recalibration and auditory enhancement, have been observed in normal auditory perception, and may reflect a general gain control of the auditory perceptual system. However, little is known about whether cochlear-implant (CI) users experience these effects. Discovering whether and how CI users experience loudness recalibration should provide us with a better understanding of the underlying mechanisms.

Methods
We examined the effects of a long-duration (1 s) intense precursor on the perception of loudness of shorter-duration (200 ms) target and comparison stimuli. The precursor and target were separated by a silent gap of 50 ms, and the target and comparison were separated by a silent gap of 2 s. For CI users, all the stimuli were delivered as pulse trains directly to the implant. The target and comparison stimuli were al-

ways presented to a middle electrode (electrode 8), and the position of the precursor was parametrically varied from electrode 2 through 14. For normal-hearing listeners, bandpass noise was used as a stimulus to simulate the spread of current produced by CIs. The center frequencies of stimuli were determined by a standard frequency map for16-channel CIs, corresponding to selected electrodes in the CI users.

Results
Significant loudness recalibration effects were observed in both normal-hearing subjects and CI users. As in previous studies, the effect size in normal-hearing listeners increased with increasing level difference between precursor and target. However, this trend was not observed in results from CI users.

Conclusions
The results confirm the effects associated with loudness recalibration in normal-hearing listeners. The differences between the results from CI users and normal-hearing listeners may be explained in terms of a "dual-process" hypothesis, which has been used to explain earlier data from normal-hearing listeners.

PS-234

Sensitivity to Interaural Level Differences are More Prevalent Than Interaural Timing Differences in Children Who Use Bilateral Cochlear Implants

Erica Ehlers; Shelly Godar; Ann Todd; Alan Kan; Ruth Litovksy
University of Wisconsin-Madison

Background
Binaural hearing provides access to inter-aural time and level differences (ITDs and ILDs), which are important for spatial hearing tasks. The provision of bilateral cochlear implants (BiCIs) to a growing population of children was motivated by possibility that they would be able to perform well on spatial hearing tasks. However, they are not exposed to ITDs on a daily basis through their processors, and ILDs are present but less robust than in the normal hearing system. Little is known about sensitivity of these children to ITDs and ILDs, under controlled conditions through research processors. Of particular interest in this study is the effect of place of stimulation along the cochlear array on ITD and ILD. Prior to establishing binaural testing, we also examined how well children are able to perceptually match the pitch of stimuli presented to binaural pairs of electrodes.

Methods
Children (ages 9-17) with bilateral Cochlear Nucleus CIs (N=16) participated in three experiments: (1) pitch magnitude estimation (PME) elicited from individual electrodes; (2) direct pitch comparison between electrodes in the two ears to find pitch-matched pairs; (3) discrimination of ITDs and ILDs for three different pitch-matched electrode pairs (basal, medial, and apical) using a two-alternative forced choice task. All stimuli were 100 pulses per second, constant amplitude electrical pulse trains, presented through synchronized research processors.

Results
PME results generally followed the tonotopic organization of the cochlea. Pitch comparison between ears showed similar pitch percepts within ±2 electrodes of the same number. For discrimination tasks, 15/16 subjects with BiCIs had measurable sensitivity to ILDs for the three electrode pairs. However, ITD sensitivity was only observed in 6/16 subjects, with 3/6 having sensitivity on all three electrode pairs.

Conclusions
Our results suggest that children with BiCIs show variability in binaural sensitivity at different places of stimulation. However, even when multiple places were tested, the majority of children did not show ITD sensitivity, though almost all children showed ILD sensitivity. It is likely that poor ITD sensitivity is due to the lack of transmission of this cue by clinical processors; in contrast, because ILDs can be transmitted in BiCIs, children grow up hearing those cues. These results suggest that long-term deprivation of binaural cues could result in degradation of neural circuitry mediating ITD processing. Thus, improving the coding of ITD cues in CI processors may be important for restoring ITD sensitivity in children with BiCIs.

PS-235

Interaural Differences in Firing Patterns between Coding Strategies for Unsynchronized Bilateral Cochlea-Implant Freedom and Nucleus Processors.

Francisco Rodriguez; Matthew Goupell
University of Maryland

Introduction
Bilateral cochlear-implant (CI) speech processors are not synchronized, which is generally assumed to distort interaural time and level differences (ITDs and ILDs, respectively) in the electrical firing patterns that are produced and propagated to the auditory system. The extent of these distortions has yet to be quantified in unsynchronized speech processors. The goal of this study is to quantify the changes to static and dynamic time and level interaural differences in behind-the-ear Cochlear Ltd. speech processors.

Methods
The extent of the distortions was measured in unsynchronized speech processors by comparing the ITDs and ILDs for a diverse group of acoustic stimuli consisting of pure tones, sinusoidal amplitude modulated (SAM) tones, Gaussian pink noise, SAM noise, words, and sentences. They were delivered to the processors via a custom 15 speaker array, each speaker is placed in the horizontal plane in 11.25 degree steps from +90 to -90 degrees. Speech processors were placed on the ears of a Knowles Electronics Manikin for Acoustic Research (KEMAR) in an anechoic chamber. Speech processors were set to either a 12-channel constant stimulation strategy (continuous interleaved simulation, CIS) or a 22-channel peak-picking strategy (advanced combination encoding, ACE). Both were configured to provide

900 pulses per second per electrode with a dynamic range of 40 dB. Automatic gain control (AGC) was enabled while the adaptive range optimization (ADRO) was disabled. Programs were set to everyday use to diminish the effects of microphone beam focusing. Each processor was connected to an implant-in-a-box and electrical train pulses were recorded from single electrodes for both sides simultaneously with 100-kHz sampling rate.

Results

The processors introduced distortions of ITDs and ILDs. The ITDs recorded from the CIs differs greatly from the ITDs obtained from the acoustic signal. On average, CIs ITDs were larger by approximately a factor of two when compared to the acoustic ITDs. Also, the CIs ITDs had a variance of about 650 μs while the variance of the acoustic ITDs was less than 0.1 μs.

Conclusion

The measure of the distortions caused by CIs show that ITD information is highly variable and distorted, possibly due to the effect of the dynamic range of the CIs (about 40dB). Therefore, to better present ITDs to CI users, bilateral synchronization that accounts for ILDs would be needed.

PS-236

Impaired Discrimination of Musical Consonance and Dissonance in Cochlear Implant Users

Meredith Caldwell; Patpong Jiradejvong; **Charles Limb**
Johns Hopkins University

Music perception is difficult for cochlear implant (CI) users due in large part to significant impairments in pitch perception. These impairments can significantly decrease the sense of enjoyment of CI users when listening to music. In normal-hearing (NH) listeners, dissonance in harmonic structure is typically perceived as unpleasant while consonance is perceived as pleasant. Here we sought to identify the level to which CI users are able to differentiate between musical dissonance and consonance. In light of previous research demonstrating the poor pitch perception in CI users, we hypothesized that they would not be able to discriminate between the two types of musical structure. A test battery of novel melodies was created that consisted of 8-bar melodies with choral accompaniment, using piano tones. Three permutations of varying levels of dissonance were created for each melody. The dissonance level was modified by changing the harmonic structure of the accompanying chords, with the least dissonant version consisting of consonant major triads and the most dissonant containing a dominant 7^{th} and a flatted 6^{th} in each chord. CI users and normal-hearing listeners were presented with each clip using free-field stimuli and asked to rate each on a Likert scale of -5 (very unpleasant) to +5 (very pleasant). Analysis of this data suggests that CI users are not able to differentiate between consonant and dissonant music. While the normal-hearing listeners consistently rated the more dissonant stimuli as “unpleasant”, the CI group’s ratings of the melodies were similar to one another regardless of the varying harmonic structure. CI users are not able to differentiate between consonant and dissonant music. These findings provide crucial information about the impact of poor pitch perception in CI users and the impact it has on their musical experience.

PS-237

Effect of Musical Characteristics and Processing Strategy on Music Perception of Cochlear Implant Users

Adam Schwalje[1]; Colleen Polite[1]; Anthony Spahr[2]; Lawrence Lustig[3]
[1]University of California, San Francisco; [2]Advanced Bionics; [3]Columbia University

Introduction

This prospective case-crossover study aims to elucidate the effect of musical texture, presence of vocal melody, and processing strategy on perception of listening quality and melodic prominence in cochlear implant (CI) users.

Methods

Participants completed a baseline questionnaire and then rated 35 samples, using a five point Likert-type scale, on the quality of their listening experience and the prominence of the melodic line. Music was chosen for the following attributes: monophonic, accompanied solo, or polyphonic texture; vocal or instrumental melody; and popular or classical style. In addition, new musical compositions were designed to isolate variables by using the same melody with different accompanying patterns. Samples were rated twice in each of four programming conditions: everyday, everyday with ClearVoice, music (using a standard music programming strategy), and music with ClearVoice.

Results

Four adult Advanced Bionics CI users were enrolled. One had bilateral CIs. Average age of participants was 48 years (range: 21 – 75 years). Average length of pre-implantation hearing loss was 13 years (range: 4 – 21 years); one subject was prelingually deafened. Average time since implantation was 17 months (range: 6 – 44 months). All reported some music education. One of the four patients had a music program on their CI.

Overall, monophony led to the highest quality listening experience (3.4 on a five-point scale), followed by accompanied solo (3.2) and polyphony (3.0, p=0.02). Melodies were significantly more difficult to discern in polyphonic settings (p=0.0002). Vocal accompanied solos were more highly rated for quality than were instrumental accompanied solos (3.3 vs 3.1, p=0.03).

Music programming strategies scored lower on quality than everyday programming (2.9 vs 3.2, p=0.01). Ratings of ClearVoice suggested a positive trend overall, but combined differences were not statistically significant (3.2 with ClearVoice vs 3.1 without, p=0.08). When analyzed for individual preferences, use of the ClearVoice processing strategy with the music program was associated with broadly significant improvements in quality, but not melodic prominence, for two of

four participants (average rating for these two subjects: music 2.6, music + ClearVoice 2.9, p=0.003).

Conclusions

Increasing complexity of musical texture led to decreased listening quality for a small group of CI users. Processing strategies like ClearVoice may improve the quality of the listening experience for some. An expanded understanding of which elements of music are most qualitatively challenging for CI users will help guide future inquiry.

PS-238

Feasibility of Flat Panel CT Imaging for Individualized Pitch Mapping in Cochlear Implant Users

Nicole Jiam; Monica Pearl; Courtney Carver; Charles Limb
Johns Hopkins University

For the past 50 years, advances in cochlear implant (CI) technology have capitalized on the tonotopic organization of the auditory system, particularly with respect to the cochlea. Greenwood's function has been used to describe the place-pitch frequency map of the cochlea, and theoretically describes an ideal logarithmic relationship between spatial location along the Organ of Corti and neural frequency response. Despite this relationship, cochlear implant users demonstrate significant impairments in pitch perception. Part of this difficulty may be attributed to the fact that implant insertions are performed blindly, and that frequency mapping takes place without incorporating the actual physical location of each electrode within the cochlea for each individual patient. Instead, a standard default map is typically applied to the frequency allocation for CI users, which does not account for the individual variability in cochlear lengths, electrode bending or kinking within the cochlea, or altered distances from the spiral ganglion neurons. Flat panel CT imaging is a new imaging tool that provides high-quality images and improved spatial resolution. In this study, we used post-operative flat panel CT (FPCT) imaging to analyze the individual variability in electrode contact placement and frequency mapping. We reported on 5 patients with 7 cochlear implants (Med-El standard 31.5mm arrays) who underwent FPCT imaging in 2013. Using DICOM image processing software and 3D curved planar reformation (CPR), we calculated theoretical frequencies based on each electrode contact location and compared those values to their actual maps. Our analysis revealed that individual FPCT information may allow improvements in CI mapping for preservation of pitch information for 75% (57/76) of the electrode contacts. The basilar electrodes (12, 11, 10, 4) rendered the greatest variance from the theoretical values, with a maximum of 12,000 Hz difference from expected value. To our knowledge, this is the first study that demonstrates the mathematical discrepancy between theoretical and actual cochlear implant placement with respect to pitch mapping. Further work is needed to examine the potential benefits of individualized pitch mapping for CI users, particularly with respect to speech perception, pitch perception, and sound quality.

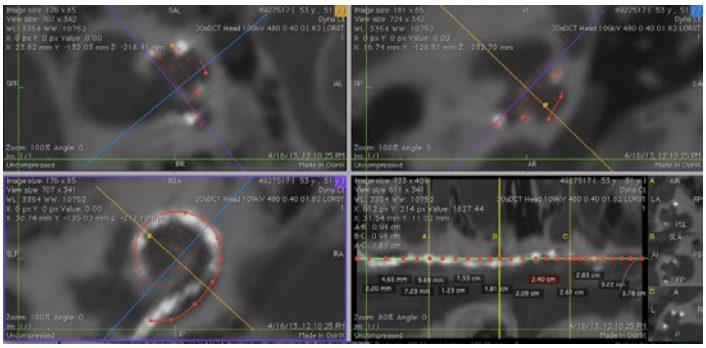

PS-239

Relationship between Multipulse Integration and Forward Masking Functions in Human Cochlear Implant Users

Ning Zhou[1]; Bryan Pfingst[2]
[1]East Carolina University; [2]University of Michigan

Introduction

The slopes of multipulse-integration (MPI) functions (threshold versus pulse rate functions) have been shown to correlate with the neural status in implanted guinea pigs, with shallower MPI functions predicting poorer neural health. MPI could be used in humans to non-invasively estimate neural health at specific stimulation sites along the electrode array. The hypotheses for the current study were that stimulation sites (electrodes) estimated by MPI slopes to have better neural status would show better place specificity of neural excitation and/or faster neural recovery from stimulation.

Methods

Subjects were implanted with the Nucleus® cochlear implants. For each tested ear, multipulse integration was measured by obtaining psychophysical detection thresholds for two pulse rates (80 and 640 pulses per seconds) and was surveyed across the electrode array. Two stimulation sites, one with the steepest and the other with the shallowest MPI functions, were identified in each ear. In Experiment 1, these sites were further assessed for place specificity of neural excitation in a forward masking paradigm, where the threshold for detecting a brief 20-ms stimulus on the site of interest (probe) was evaluated in the presence of a 300-ms forward masker with varying distance from the probe. In Experiment 2, the same sites were assessed for recovery from forward masking, where the masker was presented on the same location as the probe while the delay between the probe and masker was varied from 1 to 200 ms.

Results

Results of Experiment 1 showed that the slope of the masking curves was significantly correlated with the absolute detection threshold at 80 pps that mainly contributed to the steepness of the MPI functions. Higher thresholds at 80 pps predicted wider spread of neural excitation. Thresholds of the 80 pps stimuli were also highly correlated with the unmasked probe thresholds of the brief 20-ms stimuli. Results of Experiment 2 showed that the slope of the MPI functions was significantly correlated with the time constant of the for-

ward-masking recovery function, with steep MPI predicting shorter recovery time.

Conclusions

These results suggest that the MPI functions can be used to assess the condition of the surviving neurons such as refractoriness and adaptation to prior stimulation. Neural density might be estimated by absolute detection thresholds for low-energy pulse trains.

PS-240

Modulation Frequency Discrimination with Single and Multiple Channels in Cochlear Implant Users

John Galvin[1]; Sandy Oba[1]; Deniz Baskent[2]; Qian-jie Fu[3]
[1]University of California, Los Angeles; [2]Department of Otorhinolaryngology, Head and Neck Surgery, University Medical Center Groningen, University of Groningen, Groningen, The Netherlands; [3]University of Los Angeles, California

Introduction

Temporal envelope cues convey important speech information for cochlear implant (CI) users. Many studies have explored CI users' single-channel temporal envelope processing. However, in clinical CI speech processors, temporal envelope information is processed by multiple channels. In clinical fitting of CIs, single-channel current levels must often be reduced to accommodate multi-channel loudness summation. Amplitude modulation frequency discrimination (AMFD) thresholds have been shown to be better with multiple rather than single channels when there is no adjustment for multi-channel loudness summation. As such, it is unclear whether the multi-channel advantage in AMFD is due to the distribution of envelope cues throughout the cochlea or to the greater loudness associated with multi-channel stimulation. In this study, single- and multi-channel AMFD thresholds were measured with and without compensation for multi-channel loudness summation.

Methods

Multi-channel stimuli were comprised of three component electrodes that were either widely or narrowly spaced (i.e., relatively independent or overlapping channels). Single- and multi-channel stimuli were loudness-balanced to a single-channel reference presented at 50% of the dynamic range (DR); current levels for multi-channel stimuli were globally reduced in dB steps. AMFD was measured for equally loud single- and multi-channel stimuli using a method of constant stimuli. AMFD was also measured for single-channel stimuli at the same current levels used for the multi-channel stimuli; in this condition, the multi-channel stimuli were louder than the single-channel stimuli. The reference modulation frequency was 100 Hz; coherent modulation was applied to all channels. For equally loud single- and multi-channel stimuli, the modulation depth was between threshold and maximum acceptable loudness; for the reduced current single-channel stimuli, the same modulation depth was applied as a percentage around the reference amplitude.

Results

When single- and multi-channel stimuli were equally loud, there was no significant difference between single- and multi-channel AMFD thresholds. When the same current levels were used for single- and multi-channel stimuli, AMFD thresholds were significantly better with multiple channels than with any of the single component channels, consistent with previous studies. There was no significant difference in multi-channel AMFD thresholds when component electrodes were widely or narrowly spaced.

Conclusions

AMFD in CI users seems to depend more on the loudness of the stimulus, rather than the distribution of envelope information in the cochlea. As such, AMFD thresholds can be similarly improved by increasing the current of a single channel or by stimulating multiple channels.

PS-241

Prediction of Cochlear Implant Speech Intelligibility

Vahid Montazeri; Shaikat Hossain; Peter Assmann
The University of Texas at Dallas

Background

Cochlear implants (CIs) have been demonstrated to improve speech perception. However, CI users often experience great difficulties in the presence of background noise. The noise programs implemented in CIs do not provide adequate noise attenuation, a limitation that can be attributed to the absence of a model that accounts for different aspects of cochlear implant speech perception. Speech intelligibility models for listeners with normal hearing do not provide accurate predictions for CI users as the assumptions they are based upon are not valid for CI users. An envelope correlation based model was proposed by Yousefian and Loizou [J. Acoust. Soc. Am. 132(5), 3399-3405, 2012] which includes the CI users' MAP to predict their speech reception threshold (SRT). Good agreement between the observed and predicted SRT levels was reported (r=0.96). In the present study, an improved model is proposed to include individual differences into the predictions. In contrast with the original model, the corrected model is tested on pre-lingual as well as post-lingual CI users. The proposed model adjusts the predictions according to the individual's audiogram and reduces the computational complexity.

Methods

Nine adult CI users were recruited to participate in the speech perception experiments (mean age = 58 yrs, native English speakers). Three of the nine participants were pre-lingual CI users and six were post-lingual. Target sentences were taken from the IEEE corpus. Two types of noise - speech-shaped noise (SSN) and a female competing talker (taken from the AzBio corpus) - were used as maskers. The stimuli were played through a loudspeaker located in a sound-booth. Speech intelligibility was measured in the SNR range from -5 to 30dB in +5 dB steps. Audiograms were obtained using a two-alternative forced choice 2AFC protocol.

Results
The modified model utilizes the participant's audiogram to predict their SNR-Loss. Compared to the original model, results show a significant reduction in the prediction error for both speech-shaped and female talker maskers. For the collected data, the correlation between the true and predicted SRTs was found to be 0.89 for the modified model, compared to 0.51 for the original model.

Conclusion
Our findings suggest that including individual parameters into envelope correlation based models leads to improved performance. Further research is needed to evaluate the performance of the proposed model for short-length stimuli and other masker types.

PS-242

Neural Encoding of Interaural Time Differences - A Comparison Between Acoustic and Electric Stimulation in Normal Hearing Gerbils

Maike Vollmer; Armin Wiegner
University Hospital Wuerzburg

Background
Although bilateral cochlear implants (CI) provide benefits in directional hearing and speech understanding in noise, binaural performance of CI users involving interaural time differences (ITD) is typically below normal. To better understand these limitations, the present study directly compares the encoding of ITD for electric pulse trains and for acoustic stimuli that vary in their spectral content, onset slope and duration in the same neurons.

Methods
Normal hearing, adult gerbils were bilaterally implanted with round window electrodes, and earphones were sealed to the ear canals for acoustic stimulation. Electric stimuli were low-rate trains (10-40 pulses/s) of biphasic pulses. Acoustic stimuli were either pure-tones at the neuron's characteristic frequency or Gaussian noise bursts. To more closely mimic the instantaneous onset and short duration of electric pulses, we further used low-rate trains of acoustic clicks and chirps. ITDs were varied between +/-2000 µs. Responses were recorded extracellularly from single neurons in the dorsal nucleus of the lateral lemniscus and the inferior colliculus. We determined neural ITD sensitivity (ITD signal to total variance ratio) and ITD discrimination thresholds (just noticeable difference, JND) using a modified measure of standard separation (Sackitt, 1973). Rate-ITD-functions were fitted to calculate ITD tuning parameters (best ITD, halfwidth, ITD at maximum slope).

Results
When compared across acoustic stimuli, ITD JNDs were highest for noise stimulation, indicating poorest ITD discriminability. There were no differences in ITD sensitivity and discriminability between click and chirp stimulation. When compared across acoustic and electric stimulations, ITD sensitivities for pure tone, click and chirp stimulation were higher than those for electric and noise stimulation. However, ITD JNDs for electric stimulation did not differ from those for acoustic stimulation, independent of acoustic stimulus bandwidth, onset slope and duration. Moreover, ITD tuning functions for all broadband stimuli (electric pulse, noise, click/chirp) had narrower halfwidths than those for tonal stimulation. Otherwise, all ITD tuning parameters for electric stimulation were similar to those obtained for any of the acoustic stimuli tested.

Conclusion
In normal hearing animals, neural ITD discrimination for low-rate electric stimulation was not different from that for acoustic stimulation. These findings were independent of the spectral content, onset slope and duration of the acoustic signals. The results suggest that discrepancies between bilateral CI users and normal hearing listeners in ITD discrimination are based on deafness-induced changes in neural electric ITD coding.

PS-243

Neurofeedback As a Training Tool for Cochlear Implant Users

Annika Luckmann[1]; Jacob Jolij[2]; Etienne Gaudrain[1]; Deniz Baskent[1]
[1]University Medical Center Groningen; [2]University of Groningen

Cochlear implantees experience difficulties in pitch discrimination, which can lead to problems during daily speech communication and sound perception. Three factors related to pitch may influence this problem: fundamental frequency (F0) and vocal tract length (VTL), the two dimensions of voice characteristics in speech, as well as the musical pitch perception of the auditory stimulus. Earlier studies found that implantees rely almost entirely on F0 and do not use VTL cues when differentiating between male and female speakers (Fuller et al, 2013; Gaudrain, Baskent, 2014). In this study, we aimed to use neurofeedback as a training tool to both make VTL information more available to implantees, as well as to improve F0 and musical pitch perception. Neurofeedback is an online feedback method, in which neuronal oscillations, measured with EEG, are used to give real-time cues to individuals. These cues correspond to specific brain wave patterns. Through the real-time feedback, patients can be trained to regulate brain activity to match specific cognitive states. In a pilot study, 28 normal hearing participants were presented a pitch discrimination paradigm. Two stimuli were presented, which differed in either pitch, VTL or F0, fluctuating around threshold. The participants' task was to rate how much the second stimulus differed from the first. During this pilot, EEG was measured. Next to the behavioral data, we investigated both P300 and mismatch negativity (MMN), in order to understand the neural mechanisms of near threshold pitch perception. The P300 is a positive posterior brain evoked potential around 250-500 ms after stimulus onset, known to be an electrophysiological correlate of decision making, evaluation and categorization, commonly used in oddball paradigm studies. The mismatch negativity is also connected to changes in stimuli (such as pitch), but is thought of as a more unconscious process that appears 150-250ms post stimulus onset.

Preliminary results shows an MMN for VTL and F0 stimuli, but not for pitch stimuli. Behavioral data suggest that participants experience difficulties perceiving differences in melodic pitch in this paradigm, explaining the lack of an MMN.

Performing this paradigm with cochlear implant patients will give us more insight into the physiological basis of why they do not make use of the VTL and enables us to directly compare normal hearing subjects to cochlear implantees.

With this data, we will build a neurofeedback paradigm that aims at improving usage of pitch cues in implantees.

PS-244

AM Rate Discrimination by Cochlear Implant Listeners In On- and Off-Channel, Modulated Masking

Monita Chatterjee; Aditya Kulkarni
Boys Town National Research Hospital

Introduction

Amplitude modulation rate discrimination (AMRD) provides a measure of pitch processing in electrical hearing. In the present study, we measured effects of competing maskers on AMRD in adult cochlear implant (CI) users. Parameters of interest were target and masker AM rates, temporal offset between target and masker pulses, stimulation mode, and physical distance between target and masker electrodes. We hypothesized that conditions that promoted the greatest channel independence would cause the least interference.

Methods

Nine users of the Cochlear Coporation™ device were tested in monopolar (MP) mode; five of them were also tested in bipolar (BP) mode. Carrier stimuli were 300 ms long, 500 Hz trains of charge-balanced, 100 µs/phase biphasic current pulses. Psychophysical AMRD was measured using a 3-interval, forced-choice adaptive procedure. The target was always presented on El. 10 (middle of the array), while the maskers (loudness balanced to the 40% DR level on the target electrode) were either on the same electrode, or on electrodes located apically or basally from the target. The AM depth was fixed at a level 20% deeper than AM detection thresholds on individual channels. The target AM reference rate was fixed at 50 Hz; the masker AM rates were 27, 47, 50, or 67 Hz. In one condition, the masker was unmodulated with a level fixed at the peak amplitude of the modulated maskers (SS_{peak}).

Results

Results in MP mode showed a significant effect of masker envelope, with the condition in which the target reference rate equaled the masker AM rate (50 Hz) and the SS_{peak} condition, each producing the lowest AMRD thresholds. Electrode location and temporal offset did not impact the results. Similar results were observed in BP mode, and no significant effects of mode were observed. No significant differences were observed between the 27, 47, and 67 Hz masker AM rate conditions.

Conclusion

Factors designed to promote channel independence such as temporal offset, mode, and electrode location, did not influence the results. This underscores the large amount of channel interaction in CIs. We hypothesize that the low thresholds observed when the masker AM rate equaled the target reference rate, were due to charge summation at the neural membrane causing audible beats. Such summation effects can significantly impact auditory perception with CIs, as our results suggest that they persist even when channels are widely separated. Finally, no evidence for “modulation tuning” was observed in this study.

PS-245

Objective Evaluation of Spectral-Temporal Discriminability in Cochlear Implant Using a Computational Model

Hyejin Yang[1]; Jong Ho Won[2]; Sung Hwa Hong[3]; Jihwan Woo[1]
[1]University of Ulsan; [2]University of Tennessee Health Science Center; [3]Sungkyunkwan University

Sound processing strategies are vital to cochlear implant (CI) outcome improvements. In order to evaluate sound processing strategies, speech perception or psychoacoustic measures have been typically employed. However, such behavioral measures provide limited understanding on (1) the neural representations of electric stimulations set by each CI sound processing strategy, and (2) how such neural representations of the auditory-nerve fibers (ANF) affect behavioral outcomes. In this study, we developed a method for objective outcome measures using a computational biophysical model of electrically stimulated ANF responses.

Using a previously established ANF model (Woo et al., 2010, JARO), spectral-ripple discrimination (SRD) and Schroeder-phase discrimination (SPD) for two different sound coding strategies were simulated: HiResolution vs. CIS. First, 16 ANFs were linearly positioned at intervals of 36 mm, and 16 stimulating electrodes were set over the fifth central node of each ANF. Between every two ANFs, we positioned three more ANFs to observe the current steering effect. A neurogram was constructed using 61 ANF responses to the electric stimuli. The discrimination performance was evaluated using a neurogram similarity index (NSIM, Hines and Harte, 2012, Speech Commun.). Standard/inverted ripple and positive/negative phase stimuli were used to predict the SRD and SPD performance, respectively.

The discriminability estimated by the NSIM scores for both HiRes and CIS strategies increased with decreasing spectral-ripple densities and fundamental frequency. The model-predicted SRD and SPD threshold for both strategies are compared with the clinical outcomes.

An objective method of a computational model can be used to evaluate two different CI sound processing strategies. The results demonstrate that computational models may be a

valuable tool to evaluate the effectiveness of CI sound coding strategies.

PS-246

Modeling an Electrically Stimulated Human Cochlear Neuron to Simulate the Effects of Nerve Damage

Mohsen Hozan; Monita Chatterjee
Boys Town National Research Hospital

Introduction

A computational model of human cochlear neuron based on modified Hodgkin-Huxley (HH) equations was developed in the SIMULINK environment. While Simulink provides a graphical interface for the model to be easily manipulated, integrated MATLAB scripts will facilitate alterations in stimulus patterns as well as extracting and analyzing model outputs. The long-term objective of the model is to simulate effects of nerve damage on signal coding by electrically stimulated neurons.

Methods

Three major modifications suggested by Rattay et al. (*Hear. Res.* **153,** 43–63, 2001) were applied to the HH model to simulate the human neuron: 1) faster gating mechanisms to take into account the effect of increased temperature; 2) higher channel density in active compartments; 3) applying a white Gaussian noise current to simulate the low-amplitude fluctuations in membrane voltage. The entire model neuron consists a total of 47 compartments. Twenty one of these are passive resistive-capacitive internodal elements, and the rest, all actively involved in spike propagation, include: five peripheral and 15 central nodes, one peripheral unmyelinated terminal, three pre-somatic and one post-somatic segments and the cell body itself. Charge-balanced biphasic current pulses were injected at specific points of interest. The effects of nerve damage were investigated by manipulating the peripheral process, reducing the number of myelin layers, etc.. Unmodulated and sinusoidally amplitude-modulated pulse trains with variable carrier pulse rates were used to explore the temporal dynamics of the output spikes.

Results

Preliminary results suggest that reducing the number of myelin layers has a strong negative impact on spike propagation along the length of the central axon. Increasing the carrier pulse rate of the stimuli above a certain rate (depending on pulse duration and other parameters) also limited the neuron's ability to respond to all stimulus pulses, primarily due to refractoriness. Preliminary attempts to inject currents at even higher pulse rates resulted in complete loss of the neuron's ability to track the stimulus pattern, sometimes resulting in only an initial onset spike. All of these factors appear to interact in altering/distorting the neuron's coding of the input envelope.

Discussion

Temporal coding in cochlear implants is crucial for conveying speech information to the listener. Our results, although preliminary, confirm the importance of neural health in generating and carrying stimulus-driven action potentials along the central axon. In future work, besides expanding the stimulus parameter space, we aim to simulate the external potential field generated by electrodes surrounding the model neuron.

PS-247

Binaural Benefits for Speech Perception in Reverberated Environment by Bilateral Cochlear Implant Listeners

Moulesh Bhandary; **Yi Hu**
University of Wisconsin-Milwaukee

Introduction

Previous studies have examined speech recognition by bilateral cochlear implant users in a cocktail-party setting under anechoic listening conditions. However, in real-world listening environment, listeners always encounter problems of reverberation, which could significantly deteriorate speech intelligibility for all listeners, independent of their hearing status. The objective of this study is to investigate the effects of reverberation on the binaural benefits for speech recognition by bilateral cochlear-implant (CI) listeners.

Proposed Methods

Two groups of subjects – normal-hearing (NH) and bilateral CI (BiCI) were tested under different reverberant conditions. IEEE sentences were recorded from one male and one female talker. The male target speech was mixed with speech-shaped noise (energetic masking) or with a female competing speech (informational masking) at different signal-to-noise ratios. Simulations of spatial location and reverberations were performed using two sets of head-related-room-response-transfer-functions (HRRRTFs), with one simulating a slight reverberant environment and the other a more severe reverberant environment. The male target was from 0° azimuth, and the masker consisted of either one to two interferers. In listening conditions with one interferer, the interferer was placed either at 0°, −90°, or +90°. In listening conditions with two interferers, they were placed either in the front (0°, 0°), distributed on both sides (−90°, +90°), or from the same location on the right side (+90°, +90°). Stimuli were subjected to eight-channel noise-channel vocoding and were presented via headphones for NH subjects. Stimuli were presented via an auxiliary jack for BiCI subjects. Each subject was tested with individual ears and both ears.

Results and Conclusions

Interaction between masker types, spatial location and degree of reverberation will be discussed. We hypothesize that speech intelligibility decreases in reverberant environment compared to anechoic environment, and more reverberant environment produced significantly more masking than less reverberant environment did. The benefit of spatial hearing in reverberant environments will be revealed by comparing the results obtained from bilateral listening condition. We expect that reverberation differentially affects energetic and information masking, and that when the target and interferer(s) are spatially separated, reverberation has a greater detrimental effect on information masking than energetic masking; but when the target and the interferer(s) were co-located rever-

beration had a greater detrimental effect on energetic masking. The differences in performance between NH and CI listeners will allow us to understand whether the performance discrepancies across the two ears negatively affected binaural benefits in bilateral cochlear implants under reverberant listening conditions.

PS-248

Improved Neural Coding of ITD with Bilateral Cochlear Implants by Introducing Short Inter-Pulse Intervals

Brian Buechel; Kenneth Hancock; Bertrand Delgutte
Massachusetts Eye and Ear Infirmary

Background

Bilateral cochlear implant (CI) users have poor perceptual sensitivity to interaural time differences (ITD) of high-rate periodic pulse trains (>300 pps), but this sensitivity can be improved by jittering the inter-pulse intervals (IPIs) in a binaurally coherent manner (Laback and Majdak, Proc. Natl. Acad. Sci. 105: 814). Neural correlates of this effect have been found in the inferior colliculus (IC) of bilaterally implanted animals, where jitter could restore ongoing responses and ITD tuning in single units that otherwise gave only onset responses to high-rate pulse trains (Hancock *et al*., J. Neurophysiol. 108: 714). Specifically, spikes tended to occur soon after short IPIs in the jittered trains. In order to determine whether inserting short IPIs to an otherwise periodic pulse train could similarly improve neural ITD sensitivity, we investigated ITD tuning of IC neurons in an animal model of bilateral CIs

Methods

We recorded from single units in the IC of two unanaesthetized rabbits with bilateral cochlear implants. The stimuli were pulse trains of varying rate (320 to 1280 pps) with an extra pulse inserted every 5 to 80 ms so as to create short IPIs equal to 10 to 50% of the mean inter-pulse period. We measured mean firing rate for a wide range of ITDs (-2000 to 2000 µs) and compared the conditions with and without short IPIs.

Results

Inserting extra pulses at short IPIs increased firing rates for about half the neurons in our sample. Spikes tended to occur with short latencies after the extra pulses as indicated by phase locking to the short-IPI period. This effect was more pronounced at the higher rates tested (640 - 1280 pps), which by design had shorter IPI lengths at the extra pulse locations. Adding extra pulses also increased the number of ITD sensitive units from ~10 to 50%, comparable to the ~60% of units sensitive to ITD with low-rate periodic pulse trains.

Conclusion

The introduction of extra pulses to create short IPIs can increase firing rates and ITD sensitivity in IC neurons. These results are consistent with the effects seen with jittered pulse trains, with the added benefit of retaining control over the timing of the short IPIs. These findings support a novel CI processing strategy that would improve perceptual ITD sensitivity by introducing extra pulses at select times to the high-rate pulse train carrier.

Supported by NIH Grants DC005775 and P30 DC005209

PS-249

Development and In Vivo Characterization of a Novel Microfabricated Auditory Brainstem Implant Array

Amélie Guex[1]; A. E. Hight[2]; Nicolas Vachicouras[1]; Elliott Kozin[2]; M. Christian Brown[2]; Philippe Renaud[1]; Daniel Lee[2]; Stéphanie Lacour[1]
[1]*Ecole Polytechnique Fédérale de Lausanne;*
[2]*Massachussetts Eye and Ear Infirmary*

Background

The auditory brainstem implant (ABI) is a neuroprosthesis that provides hearing sensations to patients who are not candidates for the cochlear implant (CI). Clinical outcomes among ABI users vary among similar cohorts and this may be due to electrode design. The contemporary rigid ABI surface array design allows for limited spatial resolution of cochlear nucleus (CN) stimulation and is often associated with extra-auditory sensations due to electrical current spread to non-auditory neurons. Our study aims to improve spatial specificity of electric stimulation. We design, manufacture, and test a novel ABI design and compare it to acoustic stimulation in a rodent model.

Methods

The 14-channel microelectrode arrays (MEAs) are embedded in thin flexible polyimide films using standard microfabrication processes. The electrodes are coated with a conducting polymer, PEDOT, to increase their charge injection capacity. A three dimensional (3D) model of the CN guided the overall dimensions of the array so it covered the full tonotopic axis of the CN. The array is placed on the exposed surface of the CN in Sprague Dawley rats via craniotomy. Bipolar stimulation is induced (symmetric biphasic waveforms, 0.2ms phase duration, 23Hz frequency) and responses are assessed by auditory brainstem responses (ABR) and inferior colliculus (IC) recordings using a 16-site recording probe.

Results

A novel ABI array is successfully fabricated and ABRs and IC activity are elicited by electrical stimulation. Measurements of width of activity in the IC are larger with electrical stimulation compared to acoustic stimulation. Location of activation along the IC probe, measured with centroids and recording sites of maximal activity, vary with the lateromedial location of the stimulation pair on the CN, consistent with a shift along the tonotopic axis. The shift generated by electrical stimulation occurs along an average of 6.5 recording electrodes, smaller than the shift generated by acoustic stimulation. (12.2 electrodes, 1 to 46.5kHz stimulation)

Conclusions

Our novel electrode array elicits large responses in the auditory system. The distributed electrodes allow access the tonotopic axis of the CN, although the responses are on average wide. Wide activations may be due to stimulation of different cell types, including auditory nerve and parallel fibers at the surface of the CN traversing the tonotopic axis. Future

work includes selective targeting of tonotopically organized fusiform neurons located deeper in the CN, by specifically designed pulse waveforms or by cell-type specific optogenetic stimulation.

PS-250

Investigating Compensatory Mechanisms For Sound Localization: Visual Cue Integration and the Precedence Effect

Christopher Montagne; Yi Zhou
Arizona State University

Background

Sound localization can be difficult in reverberant environments. Fortunately listeners can utilize various compensatory mechanisms to improve their performance. For example, short latency echoes are perceptually fused into a single perceived direction of sound in a process called the precedence effect. Visual cues can also help compensate for auditory ambiguity during sound localization. Here we evaluate the combined effects of these auditory and visual compensatory mechanisms on sound localization.

Methods

Subjects localized sound in free field conditions. Two speakers were hidden behind an acoustic transparent curtain 45º to the left and right of the subject. In the experiment 15 ms broadband white noise bursts were used as sound stimuli and three high-powered LED lights were used as visual stimuli. The psychophysical method used was single-interval forced-choice. The listeners determined their perceived spatial locations of the sounds using a graphical user interface (GUI) displayed on a touch screen monitor.

Stimuli within randomized experimental blocks varied by an inter-stimulus interval (ISI) between the two speakers from 0 to 1 ms in Experiment 1 and from 0 to 3 ms in Experiment 2. Experiment 3 varied the level difference between the two signals (panning). Additionally, single speaker controls were included in each block to assess the subject's performance outside of ISI or panning conditions. All auditory stimuli were presented alone or in synchrony with one of the three LED lights.

Results

In Exp. 1 and 2 the localization range from left to right decreased by up to 20º in LED trials in comparison to the audio alone trials across the subject population. Probability density estimates indicate that the localization ranges shifted towards the locations of the LEDs, indicating visual capture. However in Exp. 3, the panning trials, the degree of visual capture found was negligible. In addition, visual capture was relatively small in single speaker control conditions for both ISI and panning trials, with probability density estimates not significantly differing from audio alone trials.

Conclusions

The influence of visual cues on spatial hearing increases as auditory cues become more ambiguous and require compensatory mechanisms like the precedence effect. These data support the notion that spatial hearing is fundamentally multisensory in realistic environments.

PS-251

Comparison of Forced-Choice and Auditory Localization Tasks For Assessing Spatial Audio-Visual Integration

Adam Bosen; Justin Fleming; Sarah Brown; Paul Allen; William O'Neill; Gary Paige
University of Rochester

A fundamental task in spatial perception is to assess the relationship between auditory and visual cues produced by objects in our environment, and, when appropriate, integrate those cues to form a unified estimate of object location. Previous experiments have used two distinct methods to probe audio-visual spatial integration. First, forced-choice judgments categorize the perceived unity between cues (i.e. "same location or not?"). Second, auditory localization assesses the graded influence of vision on auditory spatial perception. Previous research has indicated that when both tasks are performed concurrently they produce comparable measures of spatial audio-visual integration. However, this juxtaposition of tasks may confound performance, by forcing two distinct properties ('perceived unity' and 'target location') into congruence. Here, we compared these distinct tasks independently.

Young adults (n = 8) completed three experiment sessions. In each session, subjects were presented with concurrent auditory and visual targets (broadband noise bursts and LED flashes) and either made forced-choice judgments of spatial congruence between the two targets or localized the auditory target. Subjects performed one task type in sessions 1 and 3 (counterbalanced across subjects), and the other in session 2. Since responses are not directly comparable across tasks, a causal inference model of audio-visual spatial integration was used to estimate latent perceptual parameters (such as sensory accuracy, sensory uncertainty, and prior expectation) for each session. These parameters were compared to distinguish significant differences in subject perception across task types. Our subject population demonstrated variable agreement between the forced-choice and auditory localization tasks. The causal inference model indicated that when performance differed across tasks, it was due to the reduced prior expectation that targets originated from a common source in the localization task, indicating that these subjects adjusted their expectations (and subsequent performance) in a task-dependent manner. Results from sessions 1 and 3 (same task) were indistinguishable despite the interim shift to the other task in session 2. This indicates that task type, not time-dependent changes, determined this result. While spatial audio-visual integration can be assessed with both forced-choice and auditory localization tasks, these methods are not equivalent, and should not be interpreted interchangeably.

PS-252

Saccade-Related Modulation of Acoustic Activity Recorded From the External Ear Canal

Kurtis Gruters[1]; Christopher Shera[2]; Jennifer Groh[1]
[1]Duke University; [2]Harvard Medical School - Massachusetts Eye & Ear Infirmary

Saccadic eye movements can quickly and substantially change the relationship between eye-centered visual space and head-centered auditory space, a relationship that must be "known" by the brain in order to coordinate a unified sense of audio-visual space. Previous research has found that saccades can evoke activity in auditory neurons located in the inferior colliculus (Porter et al., 2007; Bulkin and Groh, 2012), the lateral/medial banks of the intraparietal sulcus (Mullette-Gillman et al., 2009), and superior colliculus (Lee and Groh, 2014). Presumably, this activity helps the auditory system calculate the hybrid reference frame that has been identified throughout the system (e.g. Mullette-Gillman et al., 2005; Porter et al., 2006; Lee and Groh, 2012). However, it is not clear at what level of the auditory system, or on what time scale, saccadic eye movement first influences auditory processes. We sought to test this question by determining whether acoustic signals recorded from ear canal display systematic peri-saccadic gain modulation.

We measured sound pressure level in the external ear canal of monkeys (n=3) and humans (n=7) as they made saccades from a central fixation point to various locations along the horizontal azimuth. Sound pressure measured in this fashion reflects oto-acoustic emissions generated by outer hair cells, activity of the middle ear muscles, and possible influences from muscles near, but not necessarily specific to, the ear. Both monkeys and humans exhibited statistically significant changes in the peri-saccadic acoustic signal within individuals and at the population level (Monte Carlo simulation and ANOVA, $p<0.05$).

These results indicate that eye movements influence auditory activity at the very periphery of the auditory system. Although the route by which such signals reach the ear is unknown, potential sources of proprioceptive or corollary discharge signals project to areas along the auditory pathway, and may in turn be transmitted to outer hair cells or middle ear musculature. Regardless of the source or route of transmission, eye movements systematically change the acoustic properties of the ear. Such changes are likely sufficient to pass eye position information throughout the entire auditory system and support a variety of interactions between vision and audition.

PS-253

An Audio-Visual Test of Dynamic Speech Recognition Using the Visually-Guided Hearing Aid (VGHA)

Gerald Kidd Jr.[1]; Virginia Best[1]; Joseph Desloge[2]; Christine Mason[1]; Elin Roverud[1]; Timothy Streeter[1]; Jayaganesh Swaminathan[1]
[1]Boston University; [2]Sensimetrics Corporation

Introduction

The VGHA uses eye tracking to steer a beam of amplification created by a head-worn microphone array. In this study, performance on an auditory-visual congruence task was compared for normal-hearing listeners using simulations (HRTFs) of the VGHA and natural binaural cues. The goal was to measure performance under conditions in which auditory and visual information must be compared concurrently for a target that changed location unpredictably over time in the presence of competing maskers.

Methods

The task was to track auditory and visual streams of words responding to instances when the words were congruent (defined as either an A/V exact word match or an A/V word syntactic category match). Competing streams of words were presented over headphones from different (virtual) locations. The "to be attended stream" was randomly presented from one of three positions (either straight ahead or +/- 30 degrees in azimuth) with a specified probability of switching. The visual stream of words was presented only from that location (via placement of the text in the corresponding position on a monitor) and the observer tracked the target visually by eye gaze which was recorded by the eye tracker. Performance in the VGHA condition (BEAM) was compared to conditions in which the sources were separated by natural binaural cues provided by KEMAR or were DIOTIC. Also, a combined BEAM-KEMAR condition was tested (BEAMAR) in which natural binaural cues were available at frequencies up to 800 Hz and the beamforming charactericstics, providing an advantageous SNR at the focus of the beam, were present above 800 Hz. In the BEAM and BEAMAR conditions the look direction determined the spatial filtering characteristics of the microphone array but had no influence on the acoustics in KEMAR or DIOTIC conditions.

Results

The congruence detection task was trivially easy in single-stream (unmasked) conditions but more difficult when other auditory streams were present and when the judgments were based on congruent syntactic categories compared to exact word matches. All three cases: KEMAR, BEAM and BEAMAR, yielded better performance than the DIOTIC control for these spatially separated sources. The ability to follow source location transitions was quite good in all cases although performance depended on the rate of presentation.

Conclusion

These findings indicated that the VGHA can effectively provide the benefit of a beamforming microphone array under

dynamic multi-source conditions requiring changes in the focus of attention along the spatial (azimuth) dimension.

[supported by NIH-NIDCD and AFOSR]

PS-254

An Objective Measure of Auditory Detection Threshold Based on a Light-Synchronized Tapping Task

Shigeto Furukawa[1]; Kazuki Onikura[2]; Shunsuke Kidani[1]; Masaharu Kato[1]; Norimichi Kitagawa[1]
[1]NTT Communication Science Laboratories; [2]Kyushu University

Introduction

In clinics, the audible threshold, often presented in the form of an audiogram, is the primary measure for assessing hearing ability. In standard measurements, audibility of a signal is assessed on the basis of the listener's subjective report. Thus, estimated detection thresholds would be inaccurate when the listener intentionally (or not) makes reports that are inconsistent with his/her perception (e.g., feigning; functional hearing loss). Here we attempted to develop a new method in which thresholds are estimated objectively on the basis of a synchronized tapping task. It is known that, in a task in which a listener is instructed to finger-tap synchronously with a regular-interval sequence of flashing light, the presentation of asynchronous sounds interferes with the listener's performance [e.g., Repp & Penel, Psychol Res, 2004]. Thus, the presence of auditory interference in the light-synchronization task can be considered to indicate that the auditory stimulus is audible.

Methods

Audiometrically normal-hearing adults participated in the experiment. The visual stimuli were red LED flashes (100-ms duration), presented in 640-ms intervals. The auditory stimuli, a sequence of 100-ms long tone bursts, varied in frequency (250, 1000, or 4000 Hz) and in level, were presented to the listener's right ear through an earphone. The level was varied between -15 and 45 dB relative to the listener's detection thresholds measured in advance using a standard two-alternative forced-choice method. The intervals of tone bursts were also 640 ms, but the relative phase of the tone bursts and light flashes was varied. Typically, a sequence consisted of 32 light flashes and tone bursts. The listeners were instructed to finger-tap synchronously with the light flashes.

Results

The phenomenon of the auditory interference in the light-synchronization task was confirmed: The presence of a sufficiently intense tone sequence modulated the tapping timing systematically with the relative phase of the tone sequence In most cases (frequencies and listeners), significant interference was detected when the tone level was more than 15 dB above the detection threshold estimated by a standard method.

Conclusions

The results indicate that this light-synchronized tapping task is sensitive to the audibility of acoustic signals and could therefore be used to estimate auditory detection thresholds with a certain degree of accuracy.

PS-255

Musical Features of Spontaneous Improvisation Associated with Emotional Cues

Malinda McPherson[1]; Monica Lopez-Gonzalez[1]; **Summer K. Rankin**[1]; Charles Limb[2]
[1]Johns Hopkins University School of Medicine; [2]Johns Hopkins University School of Medicine & Peabody Conservatory

Music is often described as the 'language of emotions', yet how music is able to both express and elicit emotions is poorly understood. While each component of music (e.g., key, mode, tempo, etc) contributes to the ability of music to convey emotion, no single feature of music sufficiently accounts for the vast emotional range of music. The novel production of complicated musical samples, such as improvisations, has never been studied. Instead, the bulk of knowledge about music and emotion comes from studies that examine the perception of music. These studies have established certain correlations between musical features and emotions. Previous studies have assumed that the connection between music and emotion can be accurately described using impoverished or greatly simplified musical stimuli, however the expression of emotion through music is almost certainly more complex. Here, we present the first ecologically valid examination of the production of novel emotional music.

We asked 14 professional jazz pianists (at least 5 years of professional experience; mean = 21±12 years) to improvise compositions based off of a visually presented emotional cue. The emotional cues consisted of 3 basic emotion categories (Happy, Ambiguous or Sad) within 2 different media types (cartoon faces and photographs); a white screen was used for the control condition. The pianists were instructed to improvise a 1 minute composition that matched the emotion expressed in the image. This emotional cue was the only constraint for the pianists. Musical data were collected with a MIDI (Musical Instrument Digital Interface) keyboard. Quantitative analyses were calculated on the key, durations, note density, range, and note overlap (staccato vs. legato).

The objective of this study was to explore whether during improvisation pianists use specific musical features to express different emotions. Our experimental design allowed us to examine emotional music performance in an artistically and ecologically valid setting. We found that the emotional cue and subsequent emotional intent of the performers greatly influenced all musical elements of their performance. Our results show that the general perception that particular emotions correlate with musical features (i.e., happy-major, sad-minor) does not explain the diversity of musical expression of emotion. Instead, there is a high amount of variety within each emotional category.

PS-256

Sensory-driven Predictions in Melodic Contour Processing: A Reaction Time Study

Narayan Sankaran; Simon Carlile
The University of Sydney

Introduction

The manner in which music instantiates and exploits listeners' expectations provides a conceptual framework for explaining how *affect* arises from sensory perception. Understanding this process can provide insight into musical emotion and other emergent phenomena such as speech prosody. Expectations may be cognitive, governed by syntactic knowledge. The current study, however, focused on low-level predictions stemming from the perceptual grouping of patterns in melodic contour. Though specific organizational principles have been proposed, empirical studies have employed retrospective paradigms in order to assess expectedness. Such methods may not accurately reflect bottom-up prediction, instead measuring effects associated with top-down reinterpretations that situate the melodic fragment within a broader musical context.

Methods:

Two reaction time experiments were performed with the presupposition that neural processing time inversely correlates with expectedness, and that the time-pressure of responding created an impediment to reinterpretation. In both experiments, three tone sequences were presented. Tones one and two constituted the implicative interval (II), the magnitude and direction of which established an anticipated continuation. Tones two and three comprised the continuation interval (CI), either realizing or denying the expected outcome. Upon hearing the final tone, listener's made a speeded decision regarding the direction of the CI (experiment 1) or detected whether any pitch change occurred within the CI (experiment 2). Ex-Gaussian functions were fit to response distributions, resulting in three descriptive parameters (μ, σ, τ) corresponding to the Gaussian mean, variance, and exponential decay respectively.

Results:

In both experiments, trends in μ and τ were consistently influenced by both the size (small vs. large) and relative direction of the preceding interval (II). Responses were faster for sequences in which the directions of the CI and II were congruent, and in which IIs were small. In experiment 1, this effect was most prominent in τ, with median-normalized values across the four permutations of small-large and congruent-incongruent contours ranging from 0.26 to 0.37. In experiment 2, this was most observable in μ, with values ranging from 0.72 to 0.78.

Conclusions:

Similar effects were present in both the *signed* directional and *unsigned* detection tasks. Evidence suggests that these two processes are functionally and anatomically independent, recruiting cortical and sub-cortical structures respectively. Results therefore highlight the potential influence of early processing mechanisms in governing melodic predictions. Sensitivity to certain melodic structures may reflect the auditory system's capacity for extracting long-term statistical regularities from the environment, or may constitute an automatic low-level facilitatory mechanism.

PS-257

Time vs. Space: Modality-Appropriateness and Cross-Modal Recruitment in Auditory and Visual Short-Term Memory

Abigail Noyce; David C Somers; Barbara Shinn-Cunningham
Boston University

Background

Many daily tasks require representation of spatial and temporal information in both the auditory and visual modalities. These two sensory systems have complementary affinities, with vision excelling in spatial resolution and audition excelling in temporal resolution. We examined short-term memory (STM) interactions between modality and information domain. Recent work from our laboratory shows that auditory STM tasks with high spatial demands engage visual-biased frontal lobe areas while visual STM tasks with high temporal demands engage auditory-biased frontal lobe areas. We suggest that STM recruits the frontal lobe network that is most appropriate for the information domain of the task, an idea we call the Domain Recruitment Hypothesis. Here, we investigate the memory processes driving this cross-modal recruitment of frontal executive control regions using a behavioral paradigm.

Methods

Subjects performed a change-detection task on short sequences of auditory or visual events. Auditory events were 50-ms complex tones. Visual events were an instantaneous change in a static image. Each event within a sequence had a unique azimuth location (set by interaural time difference or by screen position, respectively). Each adjacent pair of events had a unique stimulus onset asynchrony. In all tasks, subjects judged whether a probe sequence differed from a preceding sample sequence in either its spatial or temporal properties. Sample and probe sequences could each be either auditory or visual (four conditions). In a spatial task, subjects judged the sequence of event locations, ignoring event timing; in a temporal task, they judged the timing of the sequences, ignoring location.

Results

Performance on the spatial task was best when both sequences comprised visual events, and second-best when the sample sequence was visual and the probe auditory. Conversely, performance on the temporal task was best when both sequences comprised auditory events, and second-best when the sample sequence was auditory and the probe visual. Importantly, task-irrelevant information impaired performance only when the sample sequence modality was 'inappropriate' for the information domain of the task.

Conclusions
These results support the Domain Recruitment Hypothesis, as performance is best when stimuli are presented in the modality that is suited for the information domain of the task. Further, on cross-modal trials, modality-appropriate sample stimuli improve performance over modality-appropriate probe stimuli, suggesting that cross-modal domain recruitment occurs strongly during memory encoding. Finally, the influence of task-irrelevant information during modality-inappropriate encoding suggests that modality-appropriate information is obligatorily encoded and stored, regardless of task demands.

PS-258

Costs of Switching Spatial Attention in a Multi-Talker Conversation

Gaven Lin; Simon Carlile
University of Sydney

Background
Following a multi-talker conversation relies on the ability to rapidly and efficiently shift the focus of spatial attention from one talker to another. Previous studies have established the intelligibility costs associated with shifts in target spatial location[1] and spatial uncertainty[2] using short speech tokens. However, little is known about the impact of switching spatial attention on discourse comprehension, which involves the top-down filtering and integration of multiple semantic elements across time and across speech streams. This study aimed to i) isolate the costs of switching spatial attention during conversational turn taking and ii) identify possible cognitive factors which drive this process.

Methods
Sixteen normal hearing listeners participated in a novel sentence comprehension task. Three pairs of syntactically fixed but semantically unpredictable five word matrix sentences, recorded from a single male talker, were presented concurrently through an array of three loudspeakers (directly ahead and +/-30°). Subjects attended to one spatial location, primed by a tone, and followed the target conversation from one sentence to the next using the call-sign at the beginning of each sentence. Subjects were required to verbally recall the last three words of each sentence (echoic recall task) or answer a multiple choice question related to the target material (semantic task). The reading span test, attention network test, and trail making test were also administered to assess working memory, attentional control, and executive function respectively.

Results
There was a 10.9±1.4% decrease in word recall ($p<0.05$), a pronounced primacy effect, and a rise in masker confusion errors when the target switched spatial location between sentences. Switching costs were independent of the location, direction and angular size of the spatial shift. Increases in question difficulty resulted in a decline in semantic comprehension and an increase in the proportion of sentence attribution errors. Switching costs appear to be load dependent, only significant for complex questions which require multiple cognitive operations. Reading span scores were positively correlated with total words recalled ($p<0.05$) and negatively correlated with switching costs ($p<0.05$).

Conclusion
This study highlights i) the listening costs associated with shifts in top-down spatial attention and ii) the important role of working memory in maintaining goal relevant information and extracting meaning from dynamic multi-talker conversations.

References
[1] Best V, Ozmeral EJ, Kopco N, Shinn-Cunningham BG (2008) Object continuity enhances selective auditory attention. PNAS 105(35):13174-13177

[2] Brungart DS, Simpson BD (2007) Cocktail party listening in a dynamic multitalker environment. Percept Psychophys 69(1): 79-91

PS-259

Inviting Ferrets to the Cocktail Party: A Behavioral Model for Complex Sound Recognition and Selective Attention

Jennifer Bizley; Huriye Atilgan; Gareth Jones; Katherine Wood; Stephen Town
University College London

The aim of this study was to develop an animal model in which to examine the neural mechanisms of complex sound recognition and selective attention. Since our animal model, the ferret, has excellent low frequency hearing we chose to use human speech as stimuli for this task. We hope this will allow us to explore the neural processing of the acoustic cues underlying speech perception without the constraints of specialized language processing.

Two ferrets were trained to identify the word 'instruments' from a stream of speech tokens. The target word was a single instance spoken by one female talker whereas speech tokens (single words or short word pairs) were randomly drawn from >100 tokens to create a stream of words 3-6 seconds in duration. The target word was embedded within this stream somewhere between 1-4 seconds. On each trial a stream of speech always comprised words from a single talker and the whole stream was presented from a speaker positioned either to the animal's left or right. The ferret was trained to wait at a central spout until the target word was presented and was rewarded for then responding at a water-spout on the side from which the target stream came. Both ferrets learned this task over the course of 3-4 months. Ferrets were trained with a single female talker, and were able to accurately identify the target word, achieving excellent performance levels (d'>2.5). Without additional training subjects generalized identification behavior to 16 other male and female talkers (talker d' values ranged 2.3-3), despite considerable variation in voice pitch and target duration. One ferret has been tested in multi-talker babble with a threshold (d'=1) estimated to be at -12 dB.

In a dual stream variant of this task, two streams of speech were presented, one each from the left and right speakers (counterbalanced). The two streams were a single male and female talker. The identity / location of the target stream was

cued by starting this stream 1 second earlier than the distractor stream. Ferrets were required to respond to target words in the target stream while ignoring all words (including target words) in the distractor stream. The mean dual-stream d'-prime still exceeded 2. The ferret false-alarmed to the distractor side in only 20% of the trials in which a target was presented in the distractor stream indicating that she can selectively attend to one of two competing speech streams.

PS-260

Source Segregation and the Effects of Executive Function

Sara Misurelli[1]; Ruth Litovsky[2]
[1]*University of Wisconsin-Madison, Waisman Center;*
[2]*University of Wisconsin-Madison*

Background

In noisy environments, it is often difficult to attend to a talker of interest while simultaneously ignoring irrelevant auditory sources. Compared to adults, children are less able to extract target speech from interfering speech and noise, and they also demonstrate greater variability in performance on source segregation tasks. Little is known about why this variability occurs. The first goal of this study was to examine source segregation abilities across a large age range of NH listeners, and investigate the influence of various interferers and semantic content. The second main goal of this study was to examine the relationship between executive function and ability to segregate auditory sources.

Methods

Normal hearing (NH) participants, divided into four groups (7-10yrs, 11-14yrs, 15-17yrs and 18-22yrs) were tested on an open-set speech-in-noise task that was intended to elicit mechanisms of executive function. The auditory task consisted of participants repeating target sentences that were either semantically coherent or anomalous. Target speech was presented in quiet and with interfering speech or noise, either co-located or spatially separated, at four signal-to-noise ratios (SNRs) (-16, -8, 0, 8dB). Spatial release from masking (SRM), defined as improvement in performance due to spatial separation of sources, was calculated. Executive function tests assessed working memory and attention, and were administered through computer-interactive methods (NIH toolbox version 1.0). Expressive vocabulary and IQ were also measured.

Results

Results indicated that less masking and more SRM were shown with an increase in age. All participant groups showed the most benefit of spatial separation of sources at the negative SNRs and in conditions that contained the speech interferer. It was also found that semantic content had an effect on SRM. That is, in challenging conditions, coherent semantic content aided in release from masking. Lastly, executive function did not account for variability in SRM over other factors such as age and expressive vocabulary.

Conclusions

Our results coincide with previous research that shows children perform worse than adults on tasks of auditory source segregation, and that auditory source segregation continues to develop into adolescence. Consistent with adult data, semantically coherent sentences were more accurately reported and aided in release from masking above other cues, indicating semantic content influences intelligibility of target speech. In the future, it may be beneficial to compare the results of individuals with NH to clinical populations.

PS-261

Modeling Cocktail Party Processing in a Multitalker Mixture using Harmonicity and Binaural Features

Angela Josupeit; **Volker Hohmann**
Universität Oldenburg, Germany

Introduction

In a cocktail party situation with multiple talkers, human listeners are able to attend to one specific talker. This ability involves target talker identification, tracking of the target talker over time, and understanding his or her message in the presence of the distracting sounds. This study proposes an auditory model framework for performing these tasks and evaluates it using a call-sign-based multitalker listening task with spatially separated talkers [Brungart and Simpson, Perception & Psychophysics, 2007, 69 (1), 79-91].

Methods

The listening task involved (i) recognition of a target talker via a call-sign ("Baron") and (ii) understanding of a target phrase uttered by the target talker that consisted of a color and number word. Our proposed model framework consists of two main steps: First, the location and identity of the target talker is identified using a template matching procedure of harmonicity features [Ewert et al., Proceedings of the International Conference on Acoustics AIA-DAGA 2013, pp. 271-274] and binaural features [Dietz et al., Speech Communication 53, 2011, 592-605]. The template is based on multiple realizations of the target word "Baron". Second, the algorithm estimates a template of the color and number word based on the previously estimated target talker location and identity. Based on this template, the most likely color and number word spoken by the identified target talker is estimated. This contribution focuses on the first step, i.e, estimating the identity and location of the target talker.

Results

The template matching procedure is compared to an approach using the Ideal Binary Mask, and to the subject results from Brungart et al. (2007). Tests using a small set of sample runs with two spatially separated talkers show that the detection of target talker identity and the estimation of its location is possible with a high accuracy.

Conclusion

The proposed auditory model is able to detect the identity and location of the target speech token from a multitalker signal. It thus appears to be a good basis for estimating the target color and number tokens. Furthermore, the results achieved here on a small vocabulary are promising towards integrat-

ing harmonicity and binaural features into a complete CASA model that is based on a large vocabulary.

PS-262

Investigating the ear advantage using pupillometry

Alan Kan; Matthew Winn; Ruth Litovsky
University of Wisconsin-Madison

A dichotic digit span (DDS) task is commonly used as a diagnostic tool for central auditory processing disorder (CAPD). In this task, listeners are presented with a sequence of different digits in both ears simultaneously, and are asked to recall all the numbers they hear. For normal hearing listeners, a right ear advantage (EA) is typically observed, such that more numbers are recalled correctly from the right ear than for the left ear. One explanation for this effect is that the right ear might have stronger neural connections to the speech processing centers in the brain, because the left cerebral hemisphere is the primary site of language processing. However, variations in the EA can occur with shifts of attention, which means that the DDS task may not be sensitive enough to measure a stable right EA. Alternatively, because an anatomical explanation should lead to stable results, variable EA performance may suggest that the right EA is not due to anatomical asymmetry. One way of measuring a more stable EA may be through pupillary responses, which have been shown to be robust for resolving subtle differences in listening effort, and are consistent even in the presence of shifts in attention. The aim of this study is to determine whether measuring pupillary response in a DDS task will be a more robust method for establishing the presence of an EA.

Normal hearing subjects listened with headphones to dichotic pairs of digits presented to their left and right ears simultaneously, while seated in front of a Tobii T60XL eye tracker. Subjects were asked to verbally repeat either just the right ear digits, left ear digits, or all presented digits. Pupil dilation data was recorded in each trial and analyzed using established techniques to obtain an index of listening effort.

Subjects demonstrated differences in the amount of pupil dilation when recalling left vs right ear digits, indicating the presence of an advantage in one ear over another. Right EA was indicated by smaller pupil dilation for right-digit recall compared to left-digit recall, and this difference was variable across listeners. The results provide additional evidence for the existence of an EA, and suggest that pupillometry may be a more robust clinical tool than accuracy scores for measuring consistent EAs, which will aid in the diagnosis of CAPD.

PS-263

A Simple Vigilance Task Suitable For Measuring Auditory Attention in Animals

Thomas Brozoski; Donald Caspary; Carol Bauer; Kurt Wisner
Southern Illinois University School of Medicine

"Vigilance behavior, or watch keeping, involves the focusing of attention on the detection of subtle changes in the environment that occur over a long period of time" (Paus, et al., 1997). To investigate the role of brainstem and midbrain thalamic circuits in auditory attention, we developed a simple animal model using a vigilance paradigm. Rats were trained to lever press for food in operant test chambers in the presence of ambient sound. As long as sound was on, food was available, and could be obtained by lever pressing. Unpredictable periods of sound off (no sound) punctuated the ambient sound background. During sound-off periods, food was unavailable. Animals quickly learned to discriminate sound-on from sound-off, as indicated by cessation of lever pressing during sound off and resumption of lever pressing during sound on. Of interest was how rapidly the animals reacted to changes in sound level, in particular sound off. It was hypothesized that response latency would reflect aspects of auditory attention. The present experiments attempted to validate this hypothesis. It was shown that response latency, as indicated by response rate decay functions, was reliable and not directly dependent upon sound transition levels, at least over a 60 dB range. As expected, attention (i.e., response latency), but not sound-on lever press rate, of aged rats was compromised compared to that of young adult rats. Mirroring the results of human studies, old rat auditory attention was shown to improve with training. Dizocilpine, a glutamatergic n-methyl d-aspartate (NMDA) receptor antagonist, previously shown to degrade visual attention in rats (Rezvani, et al., 2013), was shown to degrade auditory attention in the present task. Cholinergic mechanisms have long been considered important in modulating attention. The present experiment examined the effects of a selective nicotinic and selective muscarinic antagonist, mecamylamine, and scopolamine, respectively. The nicotinic antagonist significantly interfered with attention performance while the muscarinic antagonist did not. The present vigilance method captured features of auditory attention mediated in part by nicotinic function and might prove useful for assessing thalamic, brainstem, and cortical circuits involved in auditory attention.

PS-264

The Representation of Unattended Sound can be Probed with Crowdsourcing

Kevin Woods[1]; Joshua McDermott[2]
[1]Harvard University; [2]MIT

Behaviorally relevant auditory stimuli often occur under conditions of inattention. However, it is difficult to probe the perception of unattended sounds in a laboratory setting, because once an unattended sound is queried, the subject is alerted to its relevance for the task. One solution is to run brief "one-shot" experiments in which an unattended sound is queried just once, but this approach is impractical in the lab due to the large number of subjects required. As a result, little is known about hearing under conditions of inattention, despite its prevalence in our lives. Here, we explore whether the challenges of studying inattention can be overcome by crowdsourcing-- remotely gathering small amounts of data from large numbers of subjects.

Crowdsourcing has become standard in other areas of psychology, but is rarely used in auditory research because it offers little control over sound delivery. We developed methods to partially control sound delivery and replicated experiments previously run in the lab, finding crowdsourced data to be of comparable quality. We then ran experiments that would not be feasible in the lab, using one-shot paradigms to probe unattended sound. In one experiment we measured salience (a sound's tendency to capture attention) by having subjects perform distractor tasks of varying difficulty and then afterward asking them about sounds that were present in the unattended background. When distractor tasks were difficult, unattended sounds were less accurately detected and identified. However, the size of this effect varied across sounds, suggesting a measure of salience: Highly salient sounds are heard largely independent of attentional load, while less salient sounds become much less likely to be detected as attentional load increases.

Our data suggest that crowdsourcing can be a useful tool in auditory psychophysics. The ability to test large numbers of subjects opens paradigms that are not feasible in the lab, including one-shot experiments that can be used to measure the salience of unattended natural sounds.

PS-265

Test of Attention in Listening (TAiL): Applicability, Validation and Test-Retest Reliability

Sygal Amitay[1]; Hannah Stewart[1]; Bronwyn Stirzaker[1]; Johanna Barry[1]; David Moore[2]; Yu-Xuan Zhang[3]
[1]MRC Institute of Hearing Research; [2]Cincinnati Children's Hospital Medical Center; [3]Beijing Normal University

Decades of research in attention have focused almost exclusively on visual attention under the presumption that attention is essentially supra-modal in nature. Current tests that include measures of "auditory" attention are all based on verbal processing, so little is known about attention to simple sounds. To address this we developed a novel Test of Attention in Listening (TAiL). The TAiL captures aspects of selective attention such as involuntary orientation (distraction by the unattended stimulus feature) and conflict resolution in addition to more general processing efficiency. It employs a simple two-tone paradigm, requiring a same-different speeded response based on either tone frequency or location (ear of presentation). For the TAiL to be accepted as a valid research and clinical tool we need to show that it is usable in a variety of populations, useful in taping into processes that impact on auditory performance, and its outcome measures are reliable across repeated application.

We present data showing that the TAiL measures are replicable in several independent adult samples, and that it is correlated with performance on psychoacoustic tasks. We further show that TAiL can be successfully used in children as young as 4 years of age, and that its measures are sensitive enough to enable us to trace their developmental trajectory in childhood, showing a decreased cost of conflict resolution arising from the unattended stimulus features compared to adults. Preliminary results suggest the TAiL can also be administered to older adults, including hearing-impaired elderly, provided the stimulus frequency range is limited to accommodate any existing hearing handicap.

We assessed the TAiL's validity by comparing it to other widely-used tests of attention (e.g. the Attention Networks Test). We present evidence that it taps into both modality-specific and domain-general processes. A factor analysis showed that attending to frequency is auditory-specific, while attending to location, together with aspects of visual attention and processing efficiency measures, loads on domain-general factors.

Finally, we present data showing that while reaction times reduced upon repetition of the TAiL, its reaction-time difference measures of involuntary orientation and conflict resolution remain unchanged when re-tested immediately, one week or three weeks later.

We conclude that the TAiL is a valid test capable of measuring several different aspects auditory-specific and supra-modal attention independently from verbal processing, is usable across a wide age range and is sensitive enough to enable an assessment of changes to attention measures over time within the same listeners.

PS-266

Adult-Like Auditory Object Processing in Children during Change Detection

Christina der Nederlanden; Erin Hannon; **Joel Snyder**
University of Nevada, Las Vegas

Introduction

Research on visual change detection suggests that 4-6 year olds do not use high-level knowledge about real-world objects and scenes to the same extent as adults and instead rely heavily on stimulus details. The goal of this study was to address the same issue about auditory objects and scenes by studying change deafness, the failure to notice large changes to complex auditory scenes. Previous change deafness studies found that adults had poorer change detection when they were unable to identify individual change-relevant sounds from scenes. Change detection was also poorer when change-relevant sounds were semantically related to each other (e.g., two different dogs barking). Together, this suggests that adults segregate scenes into objects and use high-level object knowledge to detect changes.

Methods

Six-, eight-, and ten-year-olds were presented with (1) four concurrent sounds (scene 1), (2) followed by the same four sounds or three of the same sounds plus a new sound (scene 2), and (3) finally a single sound from scene 1, scene 2, both scenes, or neither scene (object-encoding probe). Participants were asked to report on each trial whether scene 1 and scene 2 were the same or different and whether the final probe sound was in at least one of the prior scenes. On trials in which scene 1 and scene 2 were different, the two sounds

that were involved in the change could be semantically related or unrelated (e.g., a dog barking vs. a train whistle).

Results

Participants of all ages showed superior change detection on trials in which they were successful at encoding change-relevant sounds (i.e., a sound from only scene 1 or scene 2), compared to when they were not successful. This dependency of change detection on object encoding was largest when participants were asked about the scene 2 object, especially for the older participants. Furthermore, all age groups were better at detecting changes when the change-relevant objects were not semantically related.

Summary and Conclusions

Children in this study showed similar patterns of performance as adults, in particular showing superior change detection for real-world sounds when they were able to correctly identify change-relevant sounds and when a sound was replaced by a semantically-unrelated sound. These results suggest that by 6 years, children can individuate objects in complex auditory scenes and have substantial high-level knowledge about auditory object categories that can be applied to a challenging change detection task.

PS-267

Hearing Statistical Regularities in Fractal Tone Sequences

Benjamin Skerritt-Davis; Mounya Elhilali
Johns Hopkins University

The brain's ability to extract statistical regularities from sound is an important tool in auditory scene analysis, aiding in tasks such as stream separation, structural learning (e.g., for speech or music), and detecting new events in one's sound environment. Previous work on the brain's sensitivity to temporal statistics of sound has focused on lower-order statistics and pairwise transition probabilities; in this study, we are interested in processing of higher-order statistics. Using behavioral experiments, we tested human ability to detect changes in the statistical structure of tone sequences generated from random fractals, also known as power-law noise with $1/f^{\beta}$ spectrum, which occur in a variety of natural phenomena (e.g., plant structures, brain and heart signals, music). By varying the parameter β, the amount of long-range correlations can be manipulated while keeping lower-order statistics constant. In the training phase, naïve subjects listen to tone sequences generated with different β values and learn their own strategies for differentiating fractal structure. In the testing phase, stimuli are generated from a) two concatenated fractal sequences with differing β, or b) a single fractal sequence with constant β (control). Subjects are asked to detect changes in the structure of the tone sequences. By modifying the size of the change in β and sequence length before and after the change, results shed light on the degree of sensitivity to higher-order statistics, the time-scales involved in collecting these statistics, and the effect of experience on sensitivity.

PS-268

Integration of Statistical Information in Complex Acoustical Environments

Jennifer Lawlor[1]; **Yves Boubenec**[1]; Shihab Shamma[1]; Bernhard Englitz[2]
[1]Ecole Normale Supérieure; [2]Donders Centre for Neuroscience

Many natural sounds have spectrotemporal signatures which can best be defined statistically, examples include wind, fire or rain. While their local structure is highly variable, their spectrotemporal statistics can be used for recognition, as demonstrated recently (McDermott et al., 2011). This suggests the existence of a neural representation of these statistics, the properties of which are not well understood at this point. In the present study we investigated how the detectability of changes in the statistics of sounds is influenced by its general properties.

The present experiments focus on the dynamical properties of statistical representation during ongoing exposure. We therefore designed a minimal sound texture - a modified tone cloud - which retains the central property of auditory textures: statistical predictability. At a random time, the marginal probability of the tone cloud was changed. Subjects were asked to detect the change, and were given a limited time to make this choice.

We find that the size of change as well as the time needed to sample the original texture correlate positively with performance and negatively with reaction time, suggesting the accumulation of noisy evidence. Performance increases with the probability of tones' occurrence before the change in the frequency bins containing it, a result mirrored by the reaction times, which suggest an attentional effect. We further find that the change distribution along the frequency axis diminishes performance and increases reaction time. Finally, we perform a modified d' analysis, which indicates a shift in strategy from purely detecting the change to including a hazard rate about the timing of change. This is observed as the decision criterion changes a function of the time. In addition, we demonstrate that a modified drift-diffusion model can account for both the performance (as a function of integration time and amount of change) as well as the reaction time distributions. The model estimates a representation of the probabilistic structure of the texture (as given by the frequency marginal), and compares it against a more recent estimate.

In summary we quantify dynamical aspects of change detection in statistically defined contexts, and find evidence of the integration of statistical information. However, estimates of d' indicate that listeners change their response criterion during the task, inconsistent with pure integration. Finally, the present stimulus paradigm bears resemblance to previous research in auditory profile analysis, however, the present work considers explicitly the dynamics involved in integrating acoustic information and subsequent decision making.

PS-269

Around the World in 20 Scenes: An Exploration of Auditory Saliency through a Selection of Complex Natural Scenes

Nicholas Huang; Mounya Elhilali
Johns Hopkins University

Saliency is one of the key attentional mechanisms that facilitate parsing complex sensory information that impinge on our eyes, ears and the rest of our senses at every moment. While visual saliency has been extensively studied and modeled, there has not been as much tradition in studying the role of saliency in orienting neural resources to important events in a complex auditory scene. Most studies of auditory saliency have been confined to well-controlled or confined auditory stimuli that fail to capture the true complexities of real auditory scenes. The present study explores auditory saliency in a set of diverse natural scenes that represent the intricate nature of the soundscape in everyday settings. We collected a behavioral measure of saliency by having subjects listen to two concurrent scenes and indicate continuously which one attracted their attention. The behavioral saliency measure was used as marker to determine a set of salient events and explore the acoustic attributes associated with these events. Aside from certain expected correlates of saliency such as loudness, our analysis points to an interaction amongst various physical properties of the acoustic scene in controlling the degree of saliency of different sound events. This analysis was complemented with electrophysiological recordings while listeners attended away from the natural scenes. Markers based on Electroencephalography (EEG) indicate the engagement of an intricate neural circuitry during salient events.

PS-270

The Effect of Predictable Information on Listening Effort in Speech Perception, and the Role of Spectral Resolution

Matthew Winn; Sara Misurelli; Ruth Litovsky
University of Wisconsin-Madison

Introduction

Informative aspects of signals are those that are not predictable. Cognitive resources devoted to encoding predictable events are wasted, and potentially limit the resources available to encode unpredictable information.

In this study, we explored whether listeners can take advantage of semantic context and predictable events in speech signals by devoting less cognitive effort to encoding those events. Furthermore, we explored whether spectral degradation would limit the extent to which listeners could take advantage of such predictable events.

Methods

Listeners were presented with low-difficulty sentences of two types. First, predictability was *explicitly* controlled in five-word sentences such that 1) all five words were unpredictable, or 2) one of five words was entirely predictable (i.e. the same verb in every sentence). Second, predictability was controlled by using sentences with or without semantic predictability, using the R-SPiN sentence corpus. Stimuli were presented as unprocessed signals or through an 8-channel noise vocoder to degrade spectral resolution. Listening effort was gauged using pupil dilation, and verbal responses were also scored for accuracy. Pupillary responses were analyzed using multilevel growth curve analysis.

Results

For both the explicit (fixed-verb) and semantic context sentences, pupillary responses were smaller than those for sentences without any predictable information. For the explicitly coded stimuli, the benefit was spread across the entire stimulus rather than just the portion corresponding to the predictable word. Thus, listeners took advantage of the predictable components of the signal by committing less cognitive load to that component, thus making the entire sentence less difficult.

For vocoded signals, pupillary responses were elevated overall relative to those for unprocessed speech, consistent with previous work. Importantly, there was demonstrably smaller advantage to predictable information when the signal was degraded. That is, the reduction in effort corresponding to the predictable verb was smaller for vocoded signals than it was for regular speech. Word recognition accuracy was extremely high for all conditions.

Conclusions

Spectral resolution is known to affect speech perception at various levels, including overall accuracy, phonetic cue weighting, and listening effort. In this study, we show that spectral degradation also plays a role in the ability of a listener to exploit short-term predictability in a speech stream. Specifically, signal degradation interferes with the reduction in cognitive load that results from predictable aspects of clean signals. These results highlight the importance of spectral resolution not only in terms of speech intelligibility, but higher-level factors that impact the efficiency of processing.

PS-271

Correspondence between Pupillary Dilation Response and Subjective Rating of Sound Salience

Hsin-I Liao; Shunsuke Kidani; Makoto Yoneya; Makio Kashino; Shigeto Furukawa
NTT Communication Science Laboratories

Pupillary response is a potential physiological marker for auditory salience, underlaid by the neural substrate of the locus coeruleus–norepinephrine (LC-NE) system and/or superior colliculus. In our previous study, we found that pupillary dilation response (PDR) is evoked by deviated auditory stimuli, i.e., auditory oddballs (Liao et al., 2014, ARO). However, a direct link between PDR and subjective salience is lacking. The stimuli used in our previous study were limited to pure tone and noise. In the current study, we examined whether PDR reflects subjective salience by using a variety of sounds.

Ten types of sounds were used: synthesized sounds, such as pure tone, white noise, chirp, and beep, sounds selected

from a database, such as bird singing, dog barking, phone ringing, human crying and laughter, and self-recorded sound such as nail scratching across a blackboard. Each sound was presented for 500 ms with A-weighted sound pressure levels of 65 dB. An auditory sequence consisted of each type of sound presented 10 times. All 100 sounds were presented in random order with an inter-stimulus-interval of 10 sec. Participants listened to the auditory sequence diotically while their pupillary response was recorded using an infrared eye-tracker camera (Eyelink 1000 Desktop Mount) with a sampling rate of 1000 Hz. In separate sessions, participants performed subjective pairwise-comparison tasks based on the following aspects: salience, loudness, vigorousness, preference, beauty, annoyance, and hardness. The pairwise-comparison data were converted to the Thurstone scale to represent the relative subjective attitude in the aspects towards the sounds.

Results showed that pupil diameter increased gradually at stimulus onset, i.e., PDR, regardless of sound type. This PDR to sound was most effective during 1—2 s after sound presentation. Importantly, the PDR positively correlated with salience, loudness, and vigorousness and negatively correlated with beauty on the Thurstone scale. A marginal significance was also found in the positive correlation between PDR and annoyance and in the negative correlation between PDR and preference. In an analysis based on individual stimulus pairs and participants, the correlation between PDR and salience, as well as loudness, was further confirmed, but there was no correlation between PDR and other aspects. With the result that salience and loudness were highly correlated, the overall results suggest a common underlying mechanism of PDR to sounds in relation to auditory stimulation appraisal.

In summary, PDR reflects the subjective sound salience, including synthetized sounds and sounds that are recorded in natural environments.

PS-272

Inferring the Number of Objects from Collision Sounds

Max Siegel; Joshua McDermott
MIT

Background

Recognizing sounds is a difficult computational task; the same source may produce different sounds, and similar sounds can be produced by different sources. The human brain solves this problem effortlessly in most situations, but the underlying mechanisms are not well understood. One theory is template- or exemplar-based: sounds (and their labels) are stored and new sounds are recognized by choosing the closest stored example. Another theory is statistical: sound classes are represented via ensembles of low-level statistics, and new sounds are recognized by their statistical similarity to known classes. Here we propose a third alternative: that in some cases listeners recover physical parameters of the sound generation process. We introduce a task that provides evidence for this alternative.

Methods

We recorded the sounds produced by shaking different numbers (1 - 12) of marbles in a cardboard box. We asked subjects to either (a) estimate the number of marbles in single sound clips or (b) discriminate which of two clips had more marbles. We created several stimulus sets that differed only in the style of shaking (the motion trajectory of the box) and compared discrimination both within and across styles. The sounds from each stimulus set differed statistically and perceptually (e.g. vigorous shaking vs. light rocking).

Results

Subjects performed well in all tasks. In the estimation task (a), number estimates correlated well with the actual number; this was true for each shaking style., Estimate means increased approximately linearly with actual number, as did estimate variance, consistent with number estimation in other domains. In the discrimination task (b), performance was better for larger numerical differences (e.g. easier to discriminate 2 from 6 than 2 from 4), as expected. However, performance was remarkably equivalent for trials with two clips drawn from the same shaking style as from different shaking styles, despite the pronounced acoustic differences between styles.

Conclusion

Listeners are sensitive to subtle differences in the acoustic signal produced by different numbers shaken with the same style, yet can generalize across large variations in signal to compare number produced by different styles. The exemplar and statistical accounts described above are not well suited to explaining these results. We suggest that the brain recovers physical parameters from the sound source via a mental model; when one hears the sound of shaking marbles, one imagines physical scenarios that might produce the sound.

PS-273

Modelling the Dynamics of Decision Criterion in Ferrets Performing a Yes-No Detection Task

Robert Mill[1]; **Christian Sumner[2]**
[1]MRC; [2]MRC Institute of Hearing Research

In signal detection theory decisions about sensory stimuli are considered to be a product of a noisy internal representation of the stimulus, and a threshold decision criterion. An optimal placement of the criterion maximizes performance, whilst non-optimal choice of decision criterion reduces performance and results in responses that are biased to a particular choice that is unrelated to the stimulus. Optimal choice of criterion depends on context: a priori expectations of a particular stimulus, or of expected pay-off. Furthermore, in the natural environment at least, these task contingencies are subject to change on different timescales. Thus, optimizing of this decision criterion is a potentially challenging task.

Here a series of experiments was conducted, and a computational model applied, to investigate whether and how ferrets performing a psychophysical detection task were able to dynamically vary their decision criterion in response to changes in sound level at multiple timescales. Animals performed a yes-no signal-in-noise detection task, in which trials

were grouped into blocks that alternately contained easy- and hard-to-detect signals. During blocks of low-level tones (i.e. hard) decision criterion was low, and vice versa for higher-level (easy) tones. Additionally, the outcome of a given trial also had a strong influence on the decision in the following trial. Thus, ferrets exhibited both long- and short-term criterion dynamics.

We developed models of the decision criterion dynamics to account for the animals' behavior. In these models, decision criterion shifts solely on the basis of the outcome of the previous trial. Despite this, the models account reasonably well for changes in criterion from easy to hard blocks of trials. Furthermore, the best fitting models were those where decision criterion decayed rapidly back to a static baseline criterion. The apparent block-level stabilization of bias arises as the probabilities of outcomes and shifts on single trials mutually interact to establish equilibrium. This suggests that the animals employed very simple rules for optimizing criterion, which placed little burden on memory yet nevertheless were fairly effective in optimizing criterion at multiple timescales.

PS-274

Training Two Auditory Tasks at Once: Acquisition versus Consolidation

David Maidment; Emma Gill; Hi Jee Kang; Sygal Amitay
MRC Institute of Hearing Research

Investigating the mechanisms of auditory perceptual learning not only has implications for our understanding of the learning process and how to optimize it, but also to ways in which it can be applied to remediating auditory processing difficulties. Within this domain, current evidence provides a functional distinction between two phases of learning: (1) acquisition, the period of active practice, and (2) consolidation, the transfer of learning from short- to long-term memory. Support for this differentiation stems from findings that learning can be either enhanced or disrupted depending on the training schedule.

The present study examined the specific conditions under which a secondary auditory task will or will not disrupt learning of primary task. Namely, training on an amplitude modulation-detection (AMD) task was either interleaved in short, 60 trial blocks (acquisition) or presented consecutively following 360 trials (consolidation) by training of the same AMD task with a different modulation rate, the same AMD task with a different carrier frequency, or a different amplitude modulation-rate discrimination task (AMR) using the same modulation rate and carrier frequency as the primary AMD task.

Mixed training with the same AMD task during the acquisition phase of learning resulted in learning of both primary and secondary tasks – irrespective of whether the task-relevant (modulation rate) or task-irrelevant (carrier frequency) dimension differed. However, once consolidation had been initiated, learning was only observed for the secondary AMD task. By comparison, if AMD and AMR tasks were either interleaved or consecutively mixed within a training session, only the secondary AMR task was learnt. This pattern of results therefore provides additional support for a distinction between acquisition and consolidation phases of auditory perceptual learning. Furthermore, these findings may have critical implications for commercial training programs used in the treatment of hearing impairments, suggesting that the length of training and choice of tasks is crucial.

PS-275

The Time Course of a Refractory Period in the Benefits of Perceptual Training

David Little; Beverly A Wright
Northwestern University

Auditory skills improve with practice. Here we explore how training should be distributed within a day to get optimal improvement across days. Prior work indicates that listeners require sufficient training trials per session for across-day learning to occur and that additional training in a session beyond that amount yields no further improvement. These results suggest that trials must accumulate up to a threshold in order to consolidate in long-term memory and that after this threshold is reached there is a refractory period before further training can yield more improvement. This refractory period must be less than 24 hours because listeners benefit from each session when sessions are distributed across days, but the exact duration of this period is unknown. To further constrain this duration, we trained three groups of young adults with normal hearing on a frequency-discrimination task using three different 6-7 day training regimens. The standard stimulus was always two 1-kHz, 15-ms tones separated by 50 ms. Listeners practiced a sufficient-training regimen, with 360 trials/day, a long-training regimen, with 900 trials/day, or a practice-break regimen, with two 360-trial sessions each day, separated by a 30-minute break. Preliminary results suggest that the sufficient- and long-training groups learned the same amount, as in previous reports, consistent with the interpretation that a refractory period prevented the long-training group from benefiting from the additional daily training that they received. Crucially, the practice-break group showed greater learning than either the sufficient- or long-training groups, suggesting that the refractory period is less than 30 minutes. Furthermore, session-by-session the practice-break group (2 sessions per day) learned at the same rate as the sufficient-training group (1 session per day), indicating that these two groups received equal benefit from each session—as would be expected if the refractory period was over in 30 minutes. Distributed training (practice with breaks) yields greater improvement than massed training (practice without breaks) in a variety of learning domains. The present results suggest that one reason for this distributed-training advantage may be that distributing trials can place them outside of a refractory period that follows the induction of consolidation. The current data provide a potential formula for optimal training: Provide only enough trials per session to yield improvement across days, and separate those sessions by at least 30-minutes.

PS-276

Mouse Ultrasonic Vocalizations Augment Inhibition of the Acoustic Startle Reflex

Joshua Halonen; Holly McQuery; Nicole Wood; Joe Walton
University of South Florida

Background

The acoustic startle reflex (ASR) provides a behavioral assay that is comparable between humans and rodents. Utilizing prepulse inhibition paradigms, the ASR can be used to investigate the salience of stimuli preceding the startle elicitor. These stimuli are typically short tones or noise bursts. Measures of the resulting behavior provide information about how sound is processed in the ear and brain, including temporal processing. Woolley & Portfors (2013) discuss how the neural coding characteristics of species-specific vocalizations have similarities across a wide range of species (i.e. mice, bats, & finches). However, investigating the possible behavioral effects that vocalizations might have on the ASR is a relatively unexplored area. The aim of the present study is to investigate the effects of ultrasonic mouse vocalizations, as a novel prepulse stimulus. We hypothesized that this ethologically relevant stimulus would produce greater behavioral inhibition of the ASR compared to noise burst prepulses at the same intensity levels.

Methods

CBA/CaJ mice between 14 and 15 weeks (10 female and 18 male) were placed on top of a platform connected to piezoelectric transducers located inside sound attenuated chambers. Prior to the presentation of the acoustic stimuli, animals were allowed 5 minutes to acclimate to the testing context. Acoustic startle and noise burst stimuli were presented through Fostex speakers and ultrasonic stimuli (male vocalizations in response to female urine) were presented by Tucker-Davis Technologies ES1 free-field electrostatic speakers; both mounted ~25 cm from the base of the transducer platform. Vocalization and standard prepulse testing were counterbalanced. Prepulse inhibition testing consisted of random inter-trial intervals of 15 to 30 sec. Pre-pulse stimuli were either wideband noise or recorded mouse vocalizations 50 msec in duration, presented at 55 and 85 dB SPL. Thirty msec after the prepulse stimulus, the startle stimulus was presented at 100 dB SPL for 20 msec. Twelve trials were run at each intensity level.

Results

Initial data show a significant difference, in that the startle inhibition produced by the vocalization prepulse was 30% greater than the noise prepulse at 55 dB. So, the vocalization prepulse effectively increased startle inhibition.

Conclusion

The marked increase in inhibition with the vocalization prepulse suggests the delegation of a greater amount of neural processing and attention toward a naturalistic stimulus as compared to a non-ethologically relevant stimulus.

PS-277

Prepulse Inhibition of the Acoustic Startle Reflex for Behavioral Audiograms

Ryan Longenecker; Fuad Alghamdi; Merri Rosen; Alexander Galazyuk
Northeast Ohio Medical University (NEOMED)

Background

Current methods of assessment animal hearing performance are time consuming. It has been shown that prepulse inhibition of the startle reflex could be used to measure sensation thresholds at different sound frequencies in rats (Fechter et al. 1988). This study was designed to improve the accuracy of threshold assessment and to use this method for evaluation of hearing performance of individual animals across different days of testing.

Methods

24 CBA/CaJ mice were used for the study. The startle stimulus was a 20 ms white noise presented at 100 dB SPL, with a 1 ms rise/fall time. Prepulse stimuli consisted of a 20 ms pure tones (4 to 31.5 kHz) presented at 10 to 80 dB SPL 100 ms before the startle stimulus. The magnitude of the startle responses at different sound levels of the prepulse was measured and an inhibition function for a given frequency of the prepulse was constructed. Statistical analysis of this function was used to determine the threshold: the minimal level of the prepulse at which the startle response was significantly different than the startle without a prepulse. These thresholds were then used to plot audiograms for each mouse. Two groups of mice were studied: control (unexposed) and a group of mice exposed to a narrowband noise centered at 12.5 kHz presented at 116 dB SPL unilaterally for 1 hour under general anesthesia (Ketamine/Xylazine).

Results

All mice in the control group showed audiograms similar to those obtained with traditional conditioned avoidance paradigms (Heffner & Masterson 1980; Radizwon et al. 2009). Similarly, audiograms obtained in the present study showed the lowest thresholds for the frequencies 12.5 and 16 kHz. Sound exposed mice however showed elevated thresholds across a wide frequency range especially at 12.5 kHz and 16 kHz most likely reflecting damage at and around the frequency of the exposure.

Conclusions

Reflex modification audiometry could be a useful tool for fast and reliable assessment of animals' audiometry.

PS-278

Effects of Statistical Properties of Noise on Tone Detection by Non-Human Primates

Francesca Rocchi; Margit Dylla; Chaya Narayan; Justin Watson; Ramnarayan Ramachandran
Vanderbilt University

Detection of signals within natural environments requires the auditory system to accurately encode sound levels embedded in noisy backgrounds. However, the range of sound intensities that auditory neurons can reliably represent is rel-

atively narrow. This raises a fundamental question: how does neuronal activity reflect the variety of stimulus regularities in complex acoustic scenes? Previous studies addressed this issue by investigating the relationship between changes in neural firing rate and sound statistics, showing that neurons in the inferior colliculus (IC) of anesthetized guinea pigs adjust their responses to the mean of sound level distributions. These findings suggest that the dynamic range adaptation enhances the accuracy of the neural population coding. However, the absence of behavioral results leaves open the question on whether or not the mechanisms underlying sound detection might be based also on higher levels of information processing. Here we used a psychophysical approach (Go/No-Go task) to investigate how the auditory system of non-human primates (*Macaca mulatta* and *Macaca radiata*) encodes complex sound scenes. Monkeys were required to detected tones in a noise whose amplitudes changed every 50 ms. The amplitudes of noise were randomly sampled from a set of probability distributions similar to those designed by Dean et al. (2005). Each distribution was characterized by a high probability region of sound levels (centered at 10, 20, 30 or 40 dB SPL). According to previous work, the neuronal adaptation of the dynamic range to the mean distribution should determine a shift of the range of noise sound pressure levels encoded, improving coding accuracy with respect to the range of sounds presented. Thus, we hypothesized that a change in the mean of the distribution should not cause a shift in detection thresholds. Surprisingly, tone thresholds increased as the center of the high probability region of noise shifted towards higher noise levels, suggesting that the shift in the neuronal dynamic range might not impact behavior as expected. In addition, the slopes of the psychometric functions were consistently shallower for noise distributions characterized by high sound levels than for steady state noise. Preliminary investigations varying the range of the noise levels within the high probability region suggested that the variance of the distribution does not affect tone detection. These results form the basis of future neurophysiological studies in both the IC and the cochlear nucleus (CN) to understand the neuronal underpinnings of behavior in complex environments.

PS-279

Dependence of Nonlinear-Generation Distortion Product Otoacoustic Emission Components on Primary-Tone Levels

John Thiericke[1]; Dennis Zelle[2]; Anthony W. Gummer[2]; Ernst Dalhoff[2]

[1]University of Tuebingen; [2]University of Tuebingen Department of Otolaryngology

Introduction

Distortion product otoacoustic emissions (DPOAEs) are elicited when stimulating the inner ear with two simultaneously presented tones of frequencies f_1 and f_2. DPOAEs are reported to be of maximum amplitude and high sensitivity to noise-induced hearing loss, if they are evoked with optimal primary-tone levels to account for the different amounts of compression of the resulting traveling waves in the cochlea (Kummer *et al.*, 2000). However, existing studies have not considered interference between the nonlinear-generation and coherent-reflection components which contribute to the DPOAE. Here, we use a short-pulse stimulus paradigm (Zelle *et al.*, 2013) to extract the nonlinear-generation component in the time domain by means of onset-decomposition (Vetešník *et al.*, 2009) to obtain optimal primary-tone level ratios for the DPOAE contribution generated at the f_2-tonotopic place.

Methods

DPOAEs were recorded from five normal-hearing subjects for eight frequencies f_2 = 1 – 8 kHz with f_2/f_1 = 1.2. Primary-tone levels were selected in 5 dB SPL steps according to a modified scissor paradigm (Kummer *et al.*, 1998) with $L_1 = 0.4L_2+b$, L_2 = 25 – 75 dB SPL, and b = 34 – 59 dB SPL. The stimulus pairs were arranged as 120-ms long pulse trains with four f_1 pulses each of 30-ms duration and Hanning-shaped f_2 pulses with frequency-dependent half width. Onset decomposition yielded the amplitude of the nonlinear-generation component. For sake of comparison, measurements with continuous stimulus tones were performed. Primary-tone level pairs generating maximum DPOAE amplitudes were fitted with the equation $L_1 = aL_2 + b$ for each frequency.

Results

The DPOAE responses show typically a distinct maximum in DPOAE amplitude when varying L_1 for a fixed L_2 value. For both pulsed and continuous stimulation, the optimal primary-tone level ratio shows significant frequency dependence for fit parameters *a* ($p < 0.01$) and *b* ($p < 0.05$, one-sided t-test), with *a* = 0.57 ± 0.08, *b* = 31.88 ± 4.03 dB SPL (f_2 = 1 kHz) and *a* = 0.39 ± 0.03, *b* =52.83 ± 4.27 dB SPL, (f_2 = 8 kHz) for pulsed stimulation. The continuous data exhibits similar characteristics.

Conclusion

Optimal frequency-dependent primary-tone levels seem to increase the overlap of the two resulting traveling waves in the cochlea, thus, resulting in nonlinear-generation components with maximum amplitude for pulsed and continuous DPOAEs. The use of optimal stimulus levels may increase sensitivity of DPOAEs in evaluating the state of the cochlear amplifier.

PS-280

Optimizing Swept-Tone DPOAE Measurements in Adult and Newborn Ears

Carolina Abdala[1]; Ping Luo[1]; Christopher Shera[2]

[1]University of Southern California; [2]Eaton-Peabody Laboratories, Harvard Medical School

Introduction

Recording OAEs with swept (vs. discrete) tones has many advantages and is becoming more common. Rather than employing Fourier-based analyses, swept-tone algorithms fit a time-domain model of the measured waveform to the data using least-squares (LSF). As detailed by others (Long et al., 2008; Kalluri & Shera, 2013), the impact of changing sweep rate or analysis window on estimates of OAE magnitude and phase must be carefully considered. Likewise, application of swept-tone paradigms and LSF algorithms to newborns may require age-specific accommodations. Here, we present an

analysis of these methodological factors over an expanded frequency range in both adult and newborn ears.

Methods
DPOAEs were recorded from 15 adult and 8 newborn ears using primary tones swept upward at rates from 1 to 16 s/oct in two frequency segments: 0.5–4 kHz and 4–8 kHz. Analysis windows applied offline ranged from 31 ms to 4 s in duration. LSF analysis was applied to each sweep and the results averaged to obtain OAE estimates and their within-subject reliability. We quantified the impact of parametric changes on OAE magnitude and phase, noise floor, within- and across-subject variability and correspondence between swept- and discrete-tone evoked DPOAEs.

Results
Sweep rate and analysis window duration should be varied inversely to maintain a roughly constant analysis bandwidth (thus, the faster the rate, the shorter the analysis window). Maintaining this relationship is critical to capturing the total DPOAE (or removing reflection components if desired). Although fast sweep rates seem desirable, the use of shorter analysis windows often requires additional averaging to achieve adequate SNR. At high frequencies, the optimal sweep rate/analysis window relationship changes; windows must be shortened or the rate slowed to account for the increases in normalized delay of the reflection component. These trends were common to both newborns and adults. However, although longer analysis windows generally result in lower noise floors and better response stability in adult ears, this advantageous effect was reduced in newborns.

Conclusion
Swept-tone paradigms must be used with awareness of optimal interactions between sweep rate, analysis window duration, averaging time, and their various impacts on OAE estimates. Because optimal values are frequency dependent, we conclude that analysis windows ideally should vary continuously with frequency to most effectively estimate OAE phase and amplitude. While trends were similar in newborns and adults, heightened noise in neonatal recordings suggest adaptations may be warranted. These will be discussed.

PS-281

Characterizing the Combined Reflection-Distortion OAE Profile in Normal Ears

Radha Kalluri; Carolina Abdala
University of Southern California

Introduction
Different OAEs carry different information about cochlear function. Distortion-source OAEs gauge cochlear nonlinearity, whereas reflection-source OAEs are more sensitive to cochlear amplifier gain and sharpness of cochlear filters (Shera & Guinan, 1999). Using reflection- and distortion-source OAEs interchangeably or in isolation could dilute their distinct contributions and limit information about the cochlea. Here, we measure both emission types across a broad parametric area to define the combined profile of reflection- and distortion-source OAEs in normal ears. Our longer-term goal is to define deviations from this normal signature due to hearing loss.

Methods
Both stimulus-frequency (SF) and distortion-product (DP) OAEs were measured in 10 normal-hearing adults using rapid, swept-tone stimulus presentation across a broad range of stimulus frequencies and levels. OAE magnitudes and phases were extracted using least-squares techniques, and DPOAEs were unmixed to consider only the distortion component. For both OAE types, input/output functions were constructed at 4-6 frequencies and then normalized by stimulus level to create effective transfer functions from which three features were extracted: 1*) Peak strength* defined as the peak value of the effective transfer function, typically occurring at low stimulus levels and depicting strongest OAE growth (in normalized dB); 2) *Compression threshold* defined as the stimulus level at which the OAE begins to grow compressively (in dB SPL); 3) *Compression slope* defined as the rate of compressive growth (in dB/dB).

Results
As expected based on their distinct generation mechanisms, different patterns of level dependence emerged for each emission. The peak strength of SFOAEs was greater than the peak strength of DPOAEs in all normal ears and SFOAEs exhibited compression at lower stimulus levels than did DPOAEs. Analyses of peak strength and compression threshold reveal a cluster that may define the normal reflection-to-distortion energy and distinguish these ears from those with hearing impairment. Preliminary application of this SFOAE-DPOAE protocol to a small number of hearing-impaired ears has shown values falling outside of this normative cluster (Abdala & Kalluri, 2015).

Conclusions
The distribution of *combined* reflection-distortion OAE features (extracted over a broad parametric space) reveals a cluster in normal ears. We hypothesize that these same or similar features, obtained from reflection-distortion measurements in hearing-impaired ears will also form distinct clusters, possibly elucidating common underlying auditory deficits. The next step is a large-scale study including ears with hearing loss of varying origin to test this hypothesis. We are also continuing to augment our normative sample.

PS-282

Short-latency SFOAE Components Extracted with Different Methods

Karolina Charaziak[1]; Jonathan Siegel[2]
[1]Eaton-Peabody Laboratories; [2]Hugh Knowles Center, Roxelyn and Richard Pepper Department of Communication Sciences and Disorders, Northwestern University

Introduction
In healthy ears, the ear canal pressure response to low-level tones varied in frequency oscillates periodically around the intended stimulus value due to interference between the stimulus pressure and the delayed response from the cochlea–stimulus- frequency otoacoustic emissions (SFOAEs). Several methods have been used to separate the SFOAE

from the stimulus pressure. In one method SFOAE is extracted by means of two-tone suppression, where another tone (suppressor) is presented concomitantly with the probe to reveal the emission. In the case of complete suppression the change in pressure at the probe frequency corresponds to the total emission elicited by the probe. Because SFOAE is believed to originate predominately near the probe's tonotopic region in the cochlea, a suppressor tone close in frequency is usually used. However, suppressors with frequencies more than an octave higher can also reveal SFOAEs, although of different magnitudes and shorter latencies. While one interpretation of this result is that the high-frequency suppressor reveals emissions originating at cochlear locations basal to the probe's tonotopic place, another scenario assumes that the suppressor itself creates a new SFOAE at the probe frequency [Shera et al., 2004, Assoc. Res. Otolaryngol., Abstr. 27, 538]. This study evaluates these two possibilities by comparing SFOAEs revealed by suppressors to SFOAEs extracted with time-domain windowing of the ear canal pressure response to the probe tone.

Methods

The response to the probe tone stimulation measured in the ear canals of anesthetized chinchillas was transformed to the pseudo-time-domain (via Fourier analysis) where three components of different latencies were separated (estimates of the stimulus pressure, short-latency and long-latency SFOAEs). These components were then converted back to the frequency domain for comparisons with SFOAEs revealed with the suppression method utilizing either high-frequency or near-probe-frequency suppressors.

Results

The estimates of the stimulus pressure obtained with the windowing technique revealed curves of nearly constant level, suggesting successful separation from the OAE pressure. The long-latency SFOAEs matched well in both magnitude and phase the SFOAEs revealed with the near-probe suppressor. The short-latency SFOAEs had similar levels and phase slopes to SFOAEs revealed with high-frequency suppressors, however the match was imperfect in detail, plausibly due to limitations imposed by extraction methods.

Conclusions

The reasonable agreement between the SFOAEs revealed with the two methods suggests that high-frequency suppressors primarily suppress emission components evoked by the probe rather than creating new SFOAEs at the probe frequency.

PS-283

Micro- and Macrostructure of Stimulus-frequency Otoacoustic Emissions Evoked By Low-level Tones

James Dewey; Sumitrajit Dhar
Northwestern University

Stimulus-frequency otoacoustic emission (SFOAE) amplitude versus frequency curves often exhibit quasiperiodic fluctuations, or microstructure, superimposed on a more slowly-varying macrostructure. The microstructure is particularly pronounced for responses to near-threshold level probes, and is identical to the microstructure observed in SFOAE delays and behavioral hearing thresholds for a given ear (Dewey and Dhar, ARO Abstract #127, 2014). Here we further characterize and distinguish between the micro- and macrostructures of SFOAE responses to low-level tones. SFOAEs were evoked by discrete probe tones presented from 1.4-5.7 kHz in 1/100th-octave steps, using a single probe level of 18 dB forward pressure level (FPL). SFOAEs were extracted via the suppression method, with a 56 dB FPL suppressor placed 47 Hz below the probe frequency. Filtering and smoothing procedures were used to separate the microstructures in SFOAE amplitudes and delays from the respective macrostructures. Across 37 ears of female participants ages 18-26, SFOAE amplitude versus frequency curves were highly idiosyncratic. Responses were typically largest at lower frequencies, with patchier, low-amplitude responses often observed above 2 kHz. The microstructure common to SFOAE amplitudes and delays was evident throughout the frequency range tested, though its magnitude (typically < 15 dB in depth) was variable across frequency and ears. There was also no clear dependence of the microstructure depth on overall SFOAE amplitude. The correlation between SFOAE amplitude and delay microstructures was disrupted by the presence of deep (> 20 dB) notches in SFOAE amplitude, which could span either a relatively narrow or broad frequency range. These notches often separated a series of broad amplitude lobes, which comprised the macrostructure. In some ears, the spacing of these lobes also appeared to be quasiperiodic, with macrostructure peaks separated by 0.15-0.3 octaves, suggestive of an interference pattern between multiple cochlear sources. However, the sparseness of the responses from many ears precluded the observation of a common periodicity. In contrast, the microstructure periodicity (~10-20 cycles per octave) was highly related to the SFOAE phase gradient. This is consistent with the notion that microstructure arises via a cochlear resonance phenomenon initiated by the underlying SFOAE generation mechanism. Experimental manipulations of middle-ear transmission and cochlear properties may further elucidate the origin of the microstructure and its possible relationship to the macrostructure.

PS-284

Otoacoustic Estimates of Suprathreshold Auditory Filter Tuning

Stefan Raufer[1]; Sandra Tolnai[2]; Sarah Verhulst[3]
[1]Oldenburg University; [2]Center of Excellence "Hearing4all", Animal Physiology and Behavior Group, Department for Neuroscience, School for Medicine and Health Sciences, Carl von Ossietzky University Oldenburg, 26129 Oldenburg, Germany; [3]Cluster of Excellence "Hearing4all" and Medizinische Physik, Dept. of Medical Physics and Acoustics, Oldenburg University, 26129 Oldenburg, Germany

Frequency selectivity of the human auditory system has been studied in great variety over the past years. However, little is known about human auditory filter tuning above the auditory

threshold because of methodological limitations that require high suppressor tone levels (psychoacoustics) or an assumption of linearity (SFOAE group delays). Nonetheless, reliable estimates of suprathreshold filter tuning are necessary for studies explaining individual differences of supra-threshold coding of sound.

The proposed method is based on temporal suppression (or, forward masking) of click-evoked otoacoustic emissions (CEOAE), with the underlying thought that basilar-membrane impulse-response durations can be estimated from spectral peaks in an individual's CEOAE spectrum. Using temporal suppression, we determined the range of inter-click intervals (ICI) that kept a spectral peak in the CEOAE spectrum suppressed, as beyond a certain ICI, the forward masking effect disappears. We investigated the relationship between this ICI (i.e., the release of suppression) and that of the duration of the assumed underlying impulse response at that frequency. Using linear filter theory and the release-of-suppression values, we were able to find correlates of human auditory filter tuning.

Results from 11 subjects, recorded at 65 and 71 dB peSPL for ICIs between 0 and 8 ms, demonstrated a clear frequency-dependence of the release of suppression. High-frequency CEOAE peaks demonstrated suppression only for small ICIs, whereas longer ICIs were still capable of suppressing lower frequency CEOAE components. This frequency-dependence links to the basilar-membrane impulse-response duration that is shorter at higher frequencies than lower frequencies. When we derived tuning estimates from the OAE metric, both the 65 and 71dB peSPL conditions showed a strong frequency dependence of tuning, in agreement with near-threshold otoacoustic emission tuning estimates. Obtained by using a novel method, our data supports previous findings that Q values increase with increasing frequency in humans. Our OAE method may underestimate the tuning systematically, because release of suppression indicates the point in time where basilar-membrane impulse responses stop behaving nonlinearly, rather than estimating its full time course. Aside from this drawback, this method can be easily used to check whether a listener falls within "normal" ranges, and is much faster than deriving psychophysical measures tuning because tuning of all frequencies in the CEOAE spectrum can be investigated at once.

PS-285

The Ratio of MOC Inhibition of Stimulus Frequency Otoacoustic Emissions to MOC Inhibition of Auditory-Nerve Compound Action Potentials Varies with the Strength of MOC Stimulation

Maria Berezina-Greene[1]; John Guinan[2]
[1]Massachusetts Institute of Technology; [2]Mass. Eye & Ear Infirmary, Harvard Medical School

Introduction

The relationship between medial olivocochlear (MOC) efferent inhibition of stimulus frequency otoacoustic emissions (SFOAEs) and MOC inhibition of auditory-nerve compound action potentials (CAPs) is poorly understood. If both forward and backward traveling waves receive cochlear amplification and MOC activation reduces this amplification, then SFOAEs may show up to twice as much inhibition as CAPs when measured at sound levels where the cochlea is linear. Testing this hypothesis was a main motivation for this work.

Methods

MOC inhibition of SFOAEs and CAPs were compared at the same sound level (30-40 dB SPL) and frequency in anesthetized guinea pigs. MOC effects were quantified as shifts along the sound-level axis in sound-level functions obtained with and without identical MOC stimulation. SFOAEs were evoked by continuous probe tones (2-15 kHz) and were calibrated by suppressor tone bursts 50 Hz higher and 20 dB more intense than the probe tone. CAPs were evoked by tone pips at the SFOAE probe frequency. MOC activity was elicited by a midline brainstem electrode using 200/s shocks at low or high shock levels. The strength of MOC stimulation was measured by the shock-induced level shift in click-evoked CAP responses.

Results

The ratio of the MOC-induced SFOAE change to the MOC-induced CAP change (the "SFOAE/CAP inhibition ratio") was sometimes greater than 2 at the lowest shock levels, but decreased with shock level and was always less than 1 when the shock effects on click responses were >8 dB. Overall, the SFOAE/CAP inhibition ratio was strongly correlated with the shock inhibition of click responses, i.e., with the strength of the MOC stimulation ($p<0.001$).

Discussion

The dependence of the SFOAE/CAP inhibition ratio on the strength of MOC stimulation was unexpected. One hypothesis for this is that crossed and uncrossed MOC fibers do different things in the cochlea. At the lowest shock levels, the midline electrode excites predominantly crossed MOC fibers while at higher shock levels uncrossed MOC fibers are also excited (Gifford & Guinan, 1987, Hear Res. 29:179). If the hypothesis is true, then ipsilateral sound, which activates crossed MOC efferents, would produce a higher SFOAE/CAP inhibition ratio than contralateral sound, which activates uncrossed MOC efferents. More work needs to be done to understand why the SFOAE/CAP inhibition ratio depends on the strength of MOC stimulation and what this tells us about the gain received by backward traveling waves.

PS-286

Top-Down Modulation of DPOAEs in Gerbils

Katharina Jäger[1]; Manfred Kössl[2]
[1]Goethe University Frankfurt; [2]Institute for Cell Biology and Neuroscience

Background

The processing of auditory information along the ascending auditory system is well studied. Less known is the function and impact of cortical activity on the peripheral level. The descending corticofugal system contacts the outer hair cells via the medial efferent fibers, thus being in a position to modify afferent responses. Distortion-product otoacoustic emis-

sions (DPOAEs) are a suitable tool to assess outer hair cell function, as they are by-products of the nonlinear cochlear amplification process. The present project investigates the effects of cortical activity on DPOAEs in mongolian gerbils, *Meriones unguiculatus,* through cortical deactivation using the sodium-channel blocker lidocaine. As a second method it is planned to perform cortical deactivation using electrical stimulation.

Methods
Cubic and quadratic DPOAEs were evoked over a broad frequency range of f2=0.5-40 kHz at a given ratio of f2/f1=1.2 and levels of 60/50 dB SPL and 40/30 dB SPL, respectively. Emissions were recorded before and in a time range of up to 140 min after deactivation by lidocaine microinjections in the ipsilateral or contralateral hemisphere. In order to identify possible frequency-specific effects, neuronal responses at the site of injection were determined in form of neuronal tuning curves using extracellular recordings with carbon electrodes. As a control, in some animals saline was injected instead of lidocaine.

Results
Cortical microinjections of lidocaine induced reversible amplitude changes of DPOAEs in all tested animals. Across animals, a DPOAE amplitude decrease occurred as often as a DPOAE amplitude increase after injection. Effects were distributed across all tested frequencies and not restricted to the preferred frequency of the cortical site of injection. The DPOAE amplitude completely recovered after 88 minutes (Wilcoxon signed-rank test). When the injection was performed in the ipsilateral hemisphere, effects were of comparable magnitudes to those after injection in the contralateral hemisphere. In contrast, no significant changes in DPOAE levels were obtained after saline microinjections.

Conclusion
Results indicate that deactivation of auditory cortex activity through lidocaine has a massive impact on peripheral auditory responses in form of DPOAEs, probably through cortico-olivocochlear pathways. Effects seem to be wide-spread across frequencies, suggesting an ubiquitous influence of cortical activity on cochlear mechanics.

PS-287

Right Ear Advantage Drives the Link between Olivocochlear Efferent "Antimasking" and Speech in Noise Listening Benefits

Gavin Bidelman; Shaum Bhagat
University of Memphis

The human cochlea receives feedback from the medial olivocochlear (MOC) efferents arising in the caudal brainstem whose "antimasking" role enhances peripheral signal detection in adverse listening environments. In many aspects of audition, listeners show a right ear advantage, achieving superior behavioral performance with right- compared to left-ear stimulation. Here, we examined if a similar right-ear advantage extended to both speech-in-noise (SIN) listening and to contralateral suppression of transient-evoked otoacoustic emissions (TEOAEs), a proxy measure of MOC strength. We found that speech reception thresholds in noise, measured using the QuickSIN test, were lower in the right- (RE) compared to left ear (LE). TEOAE suppression with contralateral broadband noise was also greater in REs. A strong negative correlation was observed between performance on the QuickSIN and the amount of cochlear suppression in REs, indicating that lower speech reception thresholds in noise were associated with larger amounts of MOC-related cochlear feedback. This brain-behavioral correlation was not observed in LEs. The rightward bias in SIN abilities, contralateral suppression of TEOAEs, and stronger association between physiological and perceptual measures for RE stimulation is consistent with the brain's left hemisphere dominance for speech-language processing. We infer that corticofugal feedback from left cerebral cortex via the MOC efferent system may sensitize the right cochlea for signal-in-noise detection thereby facilitating figure-ground contrast and improving degraded speech listening abilities.

PS-288

Comparison Between the Degree of the Suppression of DPOAE and TEOAE Depending on the Frequency

Yeonkyoung Park[1]; Jinsook Kim[2]
[1]Hallym University; [2]Division of Speech-language Pathology and Audiology, College of Natural Sciences, Hallym University

It has been shown that the contralateral suppression of the EOAEs is an indicator for the MOC activation. The purpose of this study is to compare between the degree of the suppression of DPOAE and TEOAE across frequencies and to examine its correlations with the age, gender and the side of ear for the evaluation of the MOC function. In this study, data were collected from both ears of 97 subjects (42 men and 55 women) with normal hearing, grouping them by their age (20s, 30s, 40s and 50s or more) and gender. At the first session, the degree of DPOAE suppression across the 23 frequencies was measured using the white noise for the CAS. At the second session, the degree of TEOAE suppression were measured with the linear click stimulation at 80±2.8 dB SPL and 260 sweeps with the continuous BBN at 60dB SPL through the channel B (CAS). And then, the peak and the dip from the degree of DPOAE and TEOAE suppression over the frequencies were compared. Statistical analysis was performed using the SPSS Ver. 18.0 for windows (SPSS Inc., Chicago, IL). The results showed that The degree of DPOAE and TEOAE suppression at the peak and the dip was 1.60±1.02, -0.16±1.11 and 0.19±0, respectively. The degree of DPOAE suppression reached the highest level at a mean frequency of 1,091 Hz and the lowest level at a mean frequency of 4,757 Hz among the four sectors that we divided the frequencies into. Also, it was predominantly seen at the peak, while not seen nor changed at the dip. The degree of DPOAE suppression had no significant correlation with the gender, the age, while there was a significant correlation between the side of ears and the range of f2 ($F(3, 90)=4.099$, $P<0.05$). Likewise, the degree of TEOAE suppression reached the highest level

at a frequency of 1,000 Hz and the lowest level at a frequency of 4,000 Hz. However, the frequency had no significant effect on the degree of TEOAE suppression. The degree of TEOAE suppression had no significant correlation with the gender, the age and the side of ears. Conclusively, only the degree of DPOAE has a significant correlation with frequency. The results suggested that the degree of the contralateral suppression of DPOAE would be more clinically applicable as compared with that of TEOAE in consideration of the frequency, especially at the peak than at the dip.

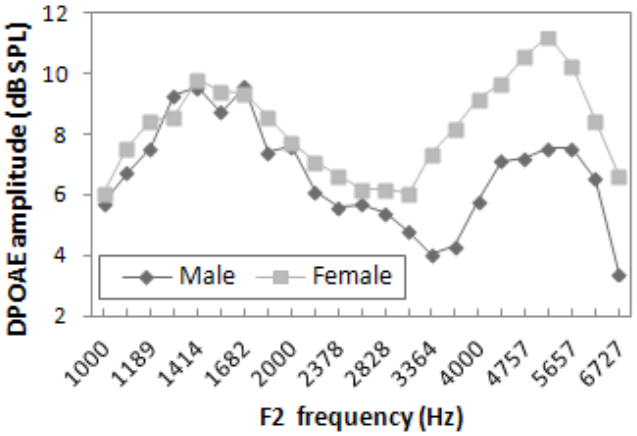

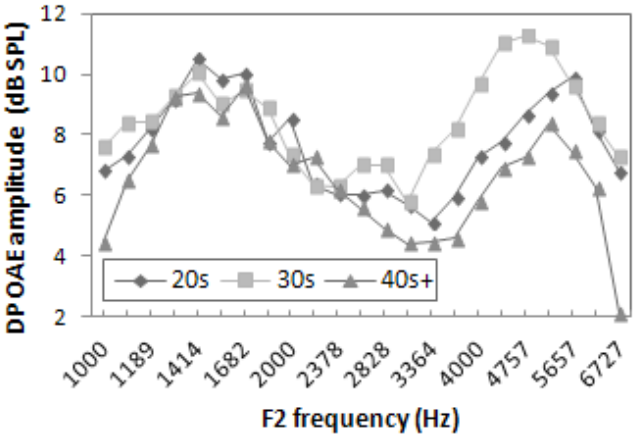

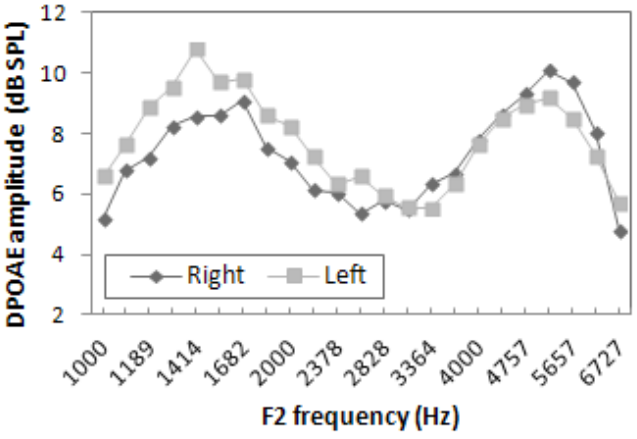

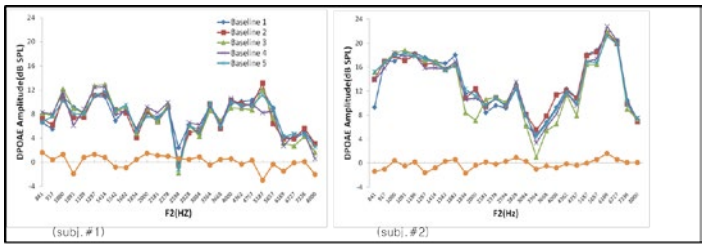

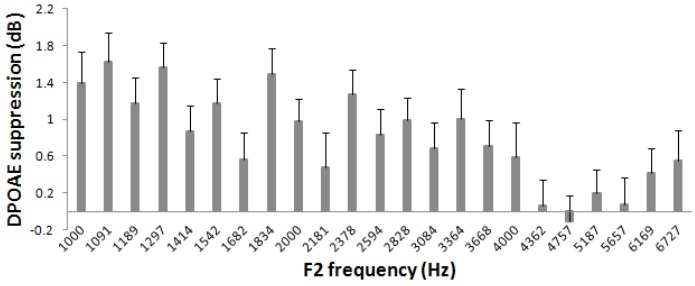

Type of frequency	Suppression (dB)	
	Mean	SD
Peaks for DPOAE	1.60	±1.02
Dips for DPOAE	-.16	±1.11
TEOAE	.19	±.43

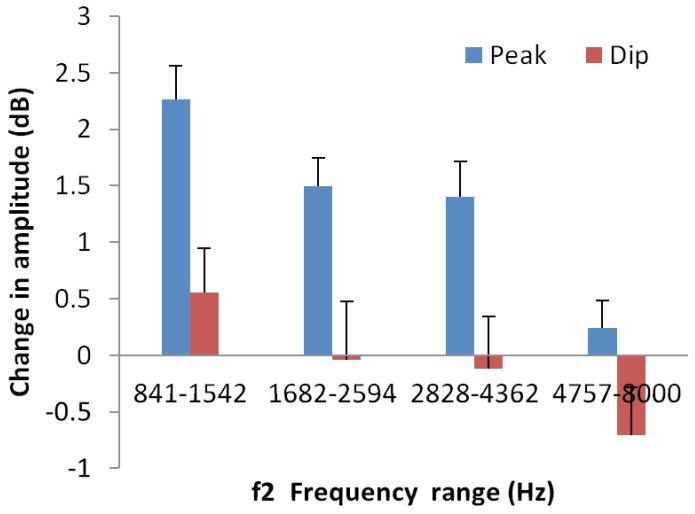

PS-289

The Level Effect of Contralateral Acoustic Stimulation (CAS) for the Distortion Product Otoacoustic Emission (DPOAE) Suppression

Jin bae Shin[1]; Jin sook Kim[1]; **Eui cheol Nam**[2]; **Ji yeon Kim**[1]

[1]Hallym University, S.Korea; [2]Kangwon National University, S.Korea

The purpose of this study is to identify the optimal Contralateral Acoustic Stimulus (CAS) level for measuring the DPOAE contralateral suppression. In order to do that, the effect of

gender, direction of ear, and the CAS level on the DPOAE suppression of normal hearing adults were tested in this study. Data were collected from the thirty five ears of the eighteen subjects (9 male, 9 female) with normal hearing in the both ears ranged from 21 to 26 years of age (mean 23.72 ± 1.56). The DPOAE was tested by ILO292 Otodynamics analyzer in the DP-gram function. The BBN was used for the CAS of DPOAE. The CAS was generated by an audiometer and delivered through a TDH 39 headphone placed on the participant's contralateral ear. The CAS was randomly presented at the level of 50, 60, 65, 70, and 80 dB SPL.

The results showed that, first, there was no significant effect of the direction of ear for DPOAE suppression ($p > .05$). The means (SDs) of the DPOAE suppression by the direction of right and left ears were 1.30(±1.09) and 1.07(±1.09), respectively. This result is inconsistent with other studies reporting that DPOAE suppression was larger on a right ear than left ear. Second, the DPOAE suppression was not significantly different between male and female. ($p > .05$). The DPOAE suppression from male and female were .98(±1.09) and 1.39(±1.09), respectively. However, Finally, Statistical analysis showed that as the CAS levels increased, the majority of the DPOAE suppression also increased ($p<.05$). The means(SDs) of the DPOAE suppression for the 5 different CAS levels, 50, 60, 65, 70, and 80 dB SPL, were .66(±1.20), 1.02(±1.23), 1.47(±1.73), 1.58(±1.70), and 1.21(±1.46), respectively. A significant interaction effect of CAS levels, gender, and direction of ear was also found ($p< .05$).

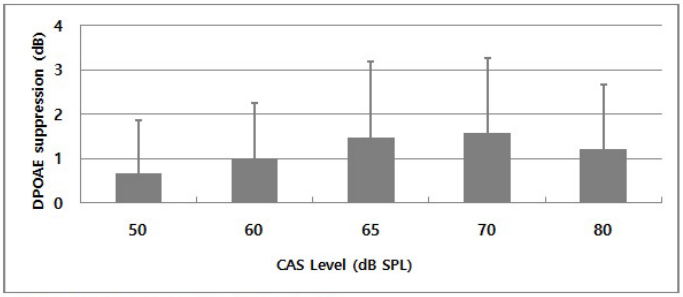

<Figure 1> DPOAE suppression by CAS levels

Taken together, the results of the current study showed that CAS at different levels induced mainly DPOAE amplitude suppression. The amount of suppression increased as the CAS level was increased with the rolling phenomenon at 80 dB SPL than 70 dB SPL in CAS level. Consequently, the 70 dB SPL or more level seems to generate the acoustic reflex in normal ears, and the 70 dB SPL or less CAS level seems to be efficient for observing decent DPOAE suppression.

PS-290

Identifying Acoustic Reflex and Medial Olivocochlear Effects on Transient Evoked Otoacoustic Emissions in Unanesthetized Mice

Yingyue Xu; Jonathan Siege; Mary Ann Cheatham
Northwestern University

Introduction

The descending neural pathway innervating outer hair cells, the medial olivocochlear (MOC) efferent pathway, is known to suppress cochlear responses such as otoacoustic emissions (OAEs). However, suppressive effects of the MOC reflex on OAEs are difficult to distinguish from middle ear muscle (MEM) contractions, which act not only on the energy delivered to the cochlea by changing the reflectance of the middle ear, but also on reverse transmission of OAEs. In the present study, we applied a time-domain measurement to detect MEM activation that may contaminate MOC effects on TEOAEs. Since anesthesia attenuates the MOC reflex (Chambers et al., 2012), we developed a protocol to perform measurements in unanesthetized mice.

Methods

Mice were given initial injectable or inhalational anesthesia for probe placements, and then measured during recovery periods. TEOAEs were measured using 50 dB peSPL tone pips gated by cosine ramps of 0.125 ms. Stimulus frequencies (22 +/- 4 kHz) produced maximal activation in the cochlear region where efferent innervation peaks in mice (Maison et al., 2003). MEM and potential MOC reflexes were activated by multiple levels of contralateral acoustic stimulation (CAS). The effect of CAS on TEOAEs was calculated by subtracting linear averages with and without CAS. Various methods were used to quantify changes in magnitude. Any detectable signal observed during the time interval of the stimulus reveals MEM effects, whereas delayed changes following the stimulus may indicate MOC effects. The lowest tested CAS levels that activated MEM or potential MOC reflexes was defined as reflex threshold.

Results

MEM and potential MOC reflexes could be activated by lower level CAS when mice were unanesthetized in the case of isoflurane or recovering from anesthesia in the case of ketamine/xylazine. MEM effects were seen in all unanesthetized mice, but only a few exhibited possible MOC effects. MEM thresholds ranged from 55-110 dB SPL, whereas MOC thresholds ranged from 50-100 dB SPL.

Conclusions

The method used in this study served as a sensitive indicator of contralateral MEM suppression that may contaminate MOC effects on TEOAEs. Results indicate that anesthesia suppresses the strength of both contralateral MEM and potential MOC reflexes, and that thresholds for reflex activation vary in unanesthetized mice as observed in humans (Marks and Siegel, 2011). Although potentially pure MOC effects were seen with CAS below MEM reflex thresholds, this behavior did not occur in the majority of cases because the two

descending neural pathways frequently have similar thresholds.

PS-291

Gentamicin Alters Molecular Function and Protein Profile in Cochlear Pericytes. Implications for Barrier Integrity and Cell-Cell Signaling in the Blood Labyrinth Barrier.

Elisa Ghelfi; Adam Bartos; Magda Bortoni-Rodriguez; Yohann Grondin; Emil Millet; Archana Swami; Rosalinda Sepulveda; Rick Rogers
Harvard School of Public Health

Background

Endothelial cells and pericytes constitute the functional unit of *stria vascularis* microvessels in the cochlear lateral wall and contribute to the formation of the Blood Labyrinth Barrier (BLB) of the inner ear. Endothelial Cells and pericytes regulate barrier permeability and signaling. We investigated the effect of Gentamicin on integrins and focal adhesion proteins in relation with the cell surface expression of caveolae in isolated cochlear pericytes. Caveolae are cholesterol and protein rich microdomains expressed on the cell surface, in cellular signaling and transcytosis. Caveolin-1, a constitutive protein of caveolae is involved in integrin-regulated caveolae trafficking and signalling at focal adhesions in migrating cells. Integrins associate with caveolin-1 and this interplay may contributes to the cell anchorage to the extracellular matrix.

Methods

Cochlear pericytes from the spiral ligament were isolated from Immortomouse® and cultured at 39 °C w/wo Gentamicin. Cell lysates were loaded in an Opti-Prep® gradient and ultra-centrifuged for 4 hr at 4 °C. Aliquots of caveolae-enriched fractions were selected by immunoblotting with anti-caveolin-1 antibody, proteins were separated on SDS-PAGE gel and analyzed by mass spectrometry. In parallel, confluent pericytes were incubated with Gentamicin at a concentration of 1, 5, 10 mg/mL for 2, 6, 12, and 24 hr. Whole-cell lysates were assessed for the expression of integrins, focal adhesion proteins and caveolae constitutive proteins caveolin-1 and 2, with immunoblotting and RT-PCR analysis.

Results

Cultured cochlear pericytes characterized by flow cytometry express αSMA, desmin and CD-13, a validated marker for brain pericytes. Untreated cochlear pericytes show a strong immunofluorescence labeling of caveolin-1. Enriched analysis of the Gene Ontology terms in a ranked gene list obtained with mass spectrometry analysis display a different profile of protein expression in caveolae from naïve cells' *vs* caveolae from Gentamicin-treated cells. In the enriched Gene Ontology analysis, integrin, focal adhesion and cell cytoskeletal proteins were significantly expressed in Gentamicin challenged cells. Immunoblotting analysis showed a decrease of α-actinin, vinculin and caveolin-1 expression in a concentration dependent manner with Gentamicin exposure.

Conclusion

Gentamicin treatment alters cytoskeletal and adhesion molecule protein profile in pericytes isolated from the cochlear microvasculature, potentially altering the BLB integrity and suggesting a new possible pathway for Gentamicin-induced ototoxicity.

Summary

Gentamicin administration in cochlear pericytes contributes to modify protein profile in caveolae and alters the adhesome complex.

PS-292

Chronic Conductive Hearing Loss Exacerbates Age-Related Loss of Afferent Synapses and Efferent Terminals in the Inner Hair Cell Area.

M. Charles Liberman[1]; Leslie D. Liberman[2]; **Stéphane F. Maison[1]**
[1]Harvard Medical School - Massachusetts Eye & Ear Infirmary; [2]Massachusetts Eye & Ear Infirmary

One function of the lateral olivocochlear (LOC) system may be to control the binaural balance of cochlear-nerve excitability that must underlie the use of bilateral intensity differences for sound localization (Darrow et al., 2006, Nature Neuroscience 9(12):10315). A prediction of such a hypothesis is that chronic unilateral changes in sound conduction should cause bilateral asymmetries in efferent tone.

To test the hypothesis, we removed the tympanic membrane unilaterally in 6-wk CBA/CaJ mice, and assessed cochlear function (ABRs and DPOAEs) ipsilaterally and contralaterally out to 64 wks of age, compared to age-matched controls, as well as to animals that were unilaterally de-efferented by stereotaxic lesion of the OC bundle. At 64 wks, cochlear afferent and efferent innervation was quantified by immunostaining for pre-synaptic ribbons (CtBP2), post-synaptic AMPA-receptor patches (GluA2) and a cholinergic marker found in OC terminals (VAT).

At 64 wks, control ears showed 15-25% loss of afferent synapses on inner hair cells (IHCs) and minimal (<10 dB) threshold shift. In de-efferented ears, threshold shifts were larger (20-30 dB) and IHC synaptic loss was worse (by as much as 55%) on the cut side, while the contralateral side was similar to controls. Outer hair cell (OHC) loss was worse on the de-efferented side compared to contralateral ear and to controls. In mice with chronic absence of tympanic membrane, IHC synaptic loss was also worse than that in control, indeed similar to that in de-efferented animals, and, correspondingly LOC density area was reduced by as much as 63% ipsilaterally compared to controls. OHC loss was similar to controls, as was the density of OC terminals in the OHC area.

Results suggest that chronic interaural sound-level differences modulate the LOC innervation density and confirm that LOC efferents are key to the long-term survival of cochlear nerve terminals. Results also suggest that chronic conductive hearing losses such as those produced by middle-ear infec-

tion, also lead to degenerative changes in the afferent and efferent innervation of the cochlea that are likely irreversible.

PS-293

Kinase Inhibitor Library Screen to Identify Targets Involved in Aminoglycoside-induced Ototoxic Damage to in Murine Organ of Corti

Matthew Ryals[1]; Kwang Pak[2]; Allen Ryan[2]

[1]Johns Hopkins University; [2]University of California San Diego

Background

Patients receiving ototoxic drugs including cisplatin or aminoglycosides can experience permanent sensorineural hearing loss. Although generation of reactive oxygen species and the activation of pro-apoptotic JNK signaling in hair cells have been implicated in the toxicity associated with aminoglycosides, the precise mechanism for the hair cell-specific toxicity has not been elucidated. A comprehensive inhibitory screen of signaling kinases may better define which pathways are involved in gentamicin toxicity to hair cells.

Methods

The mid-to-basal organ of Corti was dissected from transgenic mice aged P3-P5 with GFP expression in hair cells driven by a Pou4f3 promoter, divided into micro-explants, and plated in 96-well plates. Explants were pretreated for 24 hrs with a library of kinase inhibitors at 50, 100, and 500 nM concentrations, each performed in triplicate. 200 μM gentamicin was added after pretreatment, and explants were cultured for 72 hrs alongside untreated negative and gentamicin-alone positive controls. GFP-positive hair cells were imaged each day of treatment, and survival curves generated for each inhibitor treatment via hair cell counts (both inner and outer) in ImageJ.

Results

Protective inhibitors included those against epidermal growth factor receptor, general receptor tyrosine kinases (notably c-Src), PKR/PERK autophosphorylation, AMP-activated protein kinase A (AMPK), casein kinase 2 (CK2), cyclin-dependent kinase 4 (Cdk4), and p38 mitogen-activated protein kinase (p38-MAPK). Protective effects were strongest at 24 or 48 hours of gentamicin exposure. Enhanced toxicity was observed with the inhibition of Cdk2/4 (in contrast to the protective effect of inhibition of Cdk4 alone), or Chk1. In addition, NF-kB inhibition of was toxic to tissues during pretreatment, without gentamicin exposure.

Conclusions

The gentamicin dose and exposure time employed were substantially greater than in many previous mammalian studies, to identify strong positive hits. This may explain why inhibition of JNK signaling, previously been shown to be protective in murine organ of Corti, was not protective in this screen. In contrast, p38 MAPK inhibition has also been shown to be protective, and this was corroborated by our results. Our data also confirm previous studies showing a positive effect of c-Src inhibition against cisplatin ototoxicity in rat and noise-induced hearing loss in chinchilla. However, several kinase targets identified in this screen involve pathways not previously implicated in gentamicin toxicity. These pathways suggest additional cellular mechanisms of hair cell damage and survival, and may lead to novel therapies to prevent ototoxicity.

Protective Inhibitor	Strength/Day of Protective Effect	Best Inhibitory Concentration	Target/IC50 information
I5	Weak/Not Replicable	N/A	IC_{50} = 20 nM for HIV-1 and HIV-2[3]
I7	Medium D3	500 nM	IC_{50} <5 μM for Akt[1]
I26	Strong D2, D3	500 nM	IC_{50} = 21 nM, 63 nM, and 4 nM for EGFRwt, $EGFR^{L858R}$ and $EGFR^{L861Q}$, respectively
I35	Medium D2	500 nM	IC_{50} = 50 nM for Flt3[1] IC_{50} = 0.26, 0.91, 1.2, 2.1, 2.8, and 8.0 μM for c-Kit, KDR, c-Abl, Cdk1, c-Src, and Tie-2, respectively[1]
I38	Weak/Not Replicable	N/A	IC_{50} = 12μM for inhibiting autophosphorylation of IGF-IR in MCF-7 cells IC_{50} <1 μM for IGF-R1
I54	Strong D2, D3	500 nM	IC_{50} = 4.2 nM and 45 nM for PDGFR-β and PDGFR-α, respectively. IC_{50} = 22 nM for c-Abl. IC_{50} = 100 nM, 185 nM and 378 nM for Lck, c-Src, and Fyn, respectively. IC_{50} = 3.1 μM, > 10 μM, > 10 μM, 45.8 μM and > 100 μM for VEGFR, HER-2, Cdk's-1,-2,-4 &-7, bFGFR-1 and EGFR, respectively.
I55	Medium D2/Not Replicable D3	100 nM	IC_{50} = 4 nM in ligand-induced cellular PDGFR phosphorylation[1] IC_{50} = 7.6 nM for PDGFR kinase activity[1] IC_{50} = 434 for c-kit receptor phosphorylation[1] IC_{50} = 234 nM for c-kit receptor[1]
I56	Medium D2	500, 100 nM	IC_{50} = 210 nM for RNA-induced PKR autophosphorylation.[1] IC_{50} = 100 nM rescue PKR-dependent translation block.
I62	Medium D3	100 nM	IC_{50} = 2.7μM for EGFR

I68	Not Replicable	N/A	IC_{50} = 11.8 nM, > 10 µM, > 10 µM, 3.26 µM, 2.35 µM, and 2.57 µM for ROCKII, PKA, PKC, PKG, Aurora A, and CaMKII, respectively.[1]
II10	Strong D2	500 nM	K_i= 109nM in the presence of 5µM ATP and absence of AMP[1]
II23	Strong D2, Weak D3	500, 100 nM	IC_{50}= 110 nM for CK2[1]
II27	Strong D2, Weak D3	500, 100 nM	IC_{50}=200 nM for Cdk4/D1[1]
II29	Weak/Not Replicable	N/A	IC_{50}= 15 nM for mClk4[1] IC_{50}= 20 nm for mClk1[1] IC_{50}= 200 nM for mClk2[1]
II41	Strong D2, Medium D3	500, 100, 50 nM	IC_{50}= 350nM for Cdk4/D1[1] IC_{50}= 3.4 µM for Cdk6/D1[1]
II74	Weak D2, D3	100 nM	IC_{50}= 380 nM for p38a[1]
II75	Strong D2	500, 100 nM	IC_{50}= 35 nM for p38MAPK[1]
II77	Weak D3/Not Replicable	50, 100 nM	IC_{50}= 89 nM for p38 MAPK[2]
II80	Not Replicable	N/A	IC_{50}= 30 nM for GSK-3b[1]
II81	Weak D2, D3	50, 100 nM	K_i = 48 nM for PKA[2] IC_{50} = 270 nM for ROCK-II[3]
II83	Weak D3	500, 100, 50 nM	K_i = 16 nM for p38MAPK[2] IC_{50}= 350nM for p38b[3]
II95	Medium D2	50 nM	IC_{50}= 50 nM for Tpl2 Kinase
Toxic Inhibitor	**Strength of Toxic Effect**	**Most Toxic Concentration**	**Target/IC50 information**
II26	Wiped out post24hrs 200 uM Gent	500 nM	IC_{50}= 76 nM for Cdk4/D1[1] IC_{50}= 520 nM for Cdk2/E[1] IC_{50}= 2.1 µM for Cdk1/B[1]
II71	Wiped out after D0 pretreatment	500, 100, 50 nM	IC_{50}= 11 nM for the inhibition of NFKB activation in Jurkat cells transfected with pNFKB-Luc[1]
II88	Wiped out post24hrs 200 uM Gent	500 nM, 100 nM, 50 nM	IC_{50}=15 nM for Chk1[1] K_i= 15 nM for Chk1[2] K_i= 23 nM for CDK1[2] K_i= 5.6 nM for CDK2[2] K_i= 16 nM for CDK4[2]

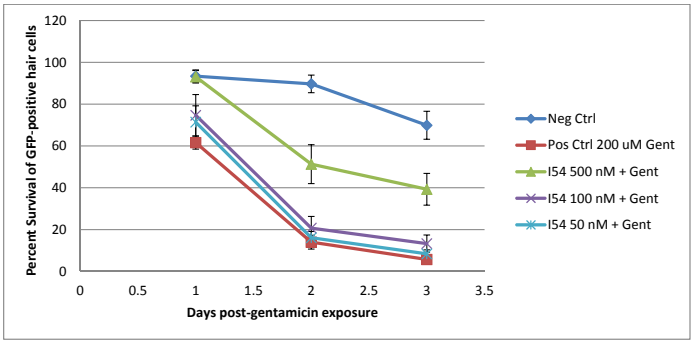

Sample Figure 1: Hair cell survival curves for each condition listed (500 nM inhibitor + 200 uM gentamicin (gent), 100 nM Inhibitor + 200 uM Gent, 50 nM inhibitor + 200 uM Gent, positive control of 200 uM Gent, negative control cultured in media + DMSO). Cells were counted at each time point (1 day after gent (D2), 2 days after gent (D3),and 3 days after gent (D4) with D1 representing the inhibitor pretreatment. This survival curve was performed for inhibitor 54, a general receptor tyrosine kinase inhibitor with activity against c-Src. Error bars represent SEMs.

References

1. Bielefeld, E.C., R. Wantuck, and D. Henderson, *Postexposure treatment with a Src-PTK inhibitor in combination with N-l-acetyl cysteine to reduce noise-induced hearing loss.* Noise Health, 2011. **13**(53): p. 292-8.
2. Bielefeld, E.C., et al., *An Src-protein tyrosine kinase inhibitor to reduce cisplatin ototoxicity while preserving its antitumor effect.* Anti-Cancer Drugs, 2013. **24**(1): p. 43-51 10.1097/CAD.0b013e32835739fd.
3. Chung, W.-H., et al., *A PI3K Pathway Mediates Hair Cell Survival and Opposes Gentamicin Toxicity in Neonatal Rat Organ of Corti.* Journal of the Association for Research in Otolaryngology, 2006. **7**(4): p. 373-382
4. Guthrie, O. n. W. (2008). "Aminoglycoside induced ototoxicity." Toxicology **249**(2–3): 91-96.
5. Harris, K.C., et al., *Prevention of noise-induced hearing loss with Src-PTK inhibitors.* Hearing Research, 2005. **208**(1–2): p. 14-25.
6. Wei, X., et al., *Minocycline prevents gentamicin-induced ototoxicity by inhibiting p38 MAP kinase phosphorylation and caspase 3 activation.* Neuroscience, 2005. **131**(2): p. 513-21.
7. Ylikoski, J., et al. (2002). "Blockade of c-Jun N-terminal kinase pathway attenuates gentamicin-induced cochlear and vestibular hair cell death." Hearing Research **163**(1–2): 71-81.

PS-294

Prostaglandin D2 May Mediate Aminoglycoside Induced Ototoxicity

Dongguang Wei; Hong Qiu; **Rodney Diaz**
University of California, Davis

Background

Aminoglycoside induced sensorineural hearing loss (SNHL) is frequently preventable and manageable. However, the molecular mechanisms underlying its pathogenesis remain to be fully addressed. Prostaglandin D2 (PGD2) is a mediator in various pathological processes. It is believed signifi-

cantly mediate inflammatory processes. However, recent studies have revealed that PGD2 can induce apoptosis via activation of the caspase-dependent pathway in various neoplastic cell lines. Our pilot study investigates whether PGD2 may mediate aminoglycoside induced ototoxicity by a similar caspase-dependent pathway.

Methods
Sprague Dawley rats were ototoxically deafened by an injection of 60% neomycin through the tympanic membrane. The middle ear cavity was filled with the neomycin solution, and the head of animal was kept for 60 minutes in the operation-side-up position for the drug to diffuse via the round window membrane into the cochlea. A subsequent intratympanic injection of 60% neomycin was performed on animals that did not show significant hearing loss. All animals were allowed to recover for 2-3 weeks following final ototoxic induction and their hearing losses were confirmed by auditory brainstem response (ABR). All animal intracochlear tissues were then harvested and processed for histology and immunohistochemistry studies.

Results
Type 2 PGD2 receptors (DP2) were weakly detectable in cochlear and vestibular sensory epithelia within the normal non-deafened cochleae. No DP2 receptors were detectable in spiral ganglion neurons and vestibular neurons. Starting the second week after deafening, strong DP2 receptor expression was detected within cochlear and vestibular sensory epithelia, which was correlated with neomycin induced ototoxic changes in cochleae. Interestingly, even at this stage, DP2 receptor expression was still barely detectable in spiral ganglion neurons and vestibular neurons.

Conclusion
Up-regulation of DP2 receptors correlates with ototoxic drug induced tissue changes, suggesting that prostaglandin D2 may play a role in mediation of aminoglycoside induced ototoxicity.

PS-295

Involvement of Interferon-Gamma Signaling in Autoimmune Inner Ear Disease

Hong Qiu; **Dongguang Wei**; Brent Wilkerson; Athena Soulika; **Rodney Diaz**
University of California, Davis

Background
Autoimmune inner ear disease (AIIED) is a syndrome of progressive sensorineural hearing loss and/or vestibular dysfunction caused by an autoimmune attack of the inner ear. Some cases resemble Meniere's syndrome, demonstrating bilateral attacks of hearing loss, tinnitus, and balance disorder. There are several potential pathways by which the immune system may cause hearing loss, including autoimmune provoked cytokine release which may elicit bystander damage, as well as cross-reactions induced by auto-antibodies which may cause peripheral damage to the inner ear due to shared epitopes with autoimmune-evoked antigens. Modulation of immune pathway signaling may provide opportunities for salvage of hearing function. Here we report that interferon-gamma (IFNγ) signaling may play a protective role in autoimmune hearing loss.

Methods
Murine experimental autoimmune encephalomyelitis (EAE), a well established animal model for multiple sclerosis, is induced in wild type (WT) mice and in interferon-gamma knockout (IFNγ -/-) mice. Auditory brainstem responses (ABR) are recorded prior to EAE induction and at D15-D19 after EAE induction, the timeframe at which hearing loss symptoms are manifest in both cohorts. Brainstem, cerebellar, and cochlear tissues are collected from WT and IFNγ-/- mice and analyzed for structural and neural cellular changes in central and peripheral auditory pathways.

Results
After EAE induction, hearing thresholds of WT mice are elevated 20±7.07dB at 32kHz, 27.5±17.7dB at 16kHz, 30±7.07dB at 8kHz, and 32.5±31.8dB at 4kHz. In IFNγ -/- mice, hearing thresholds are elevated at significantly higher levels compared to WT mice: 38.9±17.3dB at 32kHz, 38.5±17.9dB at 16kHz, 48±15.6dB at 8kHz, and 41.5±12.2dB at 4kHz (p<0.05). At the tissue level, intense infiltration by immune cells and activation of local microglia within the cerebellum and brainstem of the central nervous system and the cochlear modiolus was observed. On day 19 after EAE induction, some infiltration and accumulation of CD4 T cells, CD11b (macrophage/microglia), and IBA1 (activated microglia) positive cells was observed within the cochlear modiolus in WT mice, however significantly more abundant infiltration of the abovementioned immune cells was detected in the IFNγ -/- mice, the cohort of which demonstrated the more severe hearing loss.

Conclusion
IFNγ -/- mice display a greater degree of hearing loss and more significant immune cell infiltration in peripheral auditory pathways in the induced EAE model. This correlation suggests that the IFNγ signaling pathway may play an important protective role for hearing function in the pathogenesis of autoimmune induced inner ear disease.

PS-296

Neuronal Survival and Outgrowth for Cochlear Implant Optimization using a defined Growth Factor Combination

Jana Schwieger[1]; Athanasia Warnecke[1]; Thomas Lenarz[1]; Karl-Heinz Esser[2]; Verena Scheper[1]
[1]Hannover Medical School; [2]University of Veterinary Medicine Hannover, Foundation

Background
Cochlear implantion (CI) is nowadays the standard therapy for patients suffering from severe sensory neural hearing loss. In the last years, technical innovations like the development of novel speech processing strategies improved the benefits that patients can obtain with CI. The functionality of CI depends, among others, on the number of surviving primary auditory neurons, the spiral ganglion neurons (SGN). Additionally, the anatomical distance between the SGN, located in

the bony axis of the inner ear, and the CI, which is inserted in the scala tympani of the cochlea, results in suboptimal performance of CI patients and may be decreased by regeneration of the SGN fibers towards the arrays contacts. It is known that nerve growth factors can support neuronal survival and neurite outgrowth.

Since brain-derived neurotrophic factor (BDNF) is well known for its neuroprotective effect and ciliary neurotrophic factor (CNTF) increases neurite outgrowth, we evaluated if the combination of BDNF and CNTF leads to an enhanced neuronal survival with increased neurite outgrowth.

Methods
Dissociated postnatal rat SGN are cultivated in presence of BDNF and CNTF alone and in combination. The survival rate and neurite length of the auditory neurons is analyzed and compared to the negative control, which is SGN cultivation without addition of growth factors. Additionally, we examine the effects of the growth factors and their combination on the morphology of the SGN. Immunocytochemistry is performed to detect the presence and distribution of trkB-receptor and CNTF receptor-α in the SGN culture.

Results
The neuronal survival and neuritogenesis is significantly higher in SGN culture treated with the combination of the two nerve growth factors compared to treatment with each factor alone. Interestingly, the combination of BDNF and CNTF leads to a significantly higher number of bipolar neurons and a decreased number of neurons without neurites. The immunocytochemistry shows the presence of the receptors on the SGN but a lower CNTF receptor-α and a higher trkB-receptor expression at the supporting cells.

Conclusion
The combination of BDNF and CNTF might be a potential therapeutic tool to increase the SGN survival and to induce the regeneration of the nerve fibers into the direction of the CI. Further research has to be performed to determine the optimal concentration of the BDNF and CNTF combination and to evaluate directed outgrowth of neurites *in vitro* and *in vivo*.

PS-297

HPβCD Therapy in Humans with NPC1 Disease: Audiological Outcomes

Kelly King[1]; Chris Zalewski[1]; Nicole Farhat[2]; Lee Ann Keener[2]; Simona Bianconi[2]; Michael Hoa[1]; Forbes D. Porter[2]; **Carmen Brewer**[1]
[1]National Institute on Deafness and Other Communication Disorders, National Institutes of Health; [2]Eunice Kennedy Shriver National Institute of Child Health and Human Development, National Institutes of Health

Cyclodextrins are a family of cyclic oligosaccharides that enhance the solubility and bioavailability of hydrophobic compounds. They are commonly used in pharmaceutical applications and are generally considered safe. Recently, 2-hydroxypropyl-beta cyclodextrin (HPβCD) was shown to be an effective intervention in animal models for the neurologically devastating and lethal lipid storage disorder, Niemann-Pick type C1 (NPC1). In both the feline and mouse model, HPβCD has increased lifespan and ameliorated the neurodegenerative phenotype; however, significant and irreversible ototoxicity has occurred at effective dose levels. We present audiological data from the first human phase 1 trial of HPβCD for NPC1. Twelve patients (5 females, 7 males; ages 8-23 years) with genetically confirmed NPC1 enrolled in a dose-escalation study (50-400mg) and received monthly intrathecal infusions of HPβCD, with the first cohort starting in September 2013. Comprehensive monitoring for ototoxicity prior to each dose included behavioral assessments of hearing for standard test frequencies (.25-8kHz), extended high frequencies (9-20kHz), and distortion product otoacoustic emissions (DPOAEs). In addition to clinically significant changes in hearing, adverse events were categorized based on established criteria (Common Terminology Criteria for Adverse Events, CTCAE v4.03) intended to capture functional impact on daily living.

Eleven patients were able to participate in behavioral examinations of hearing. One patient (11 year old female) was too neurologically compromised to monitor hearing behaviorally, and DPOAEs were used as a proxy. Baseline hearing assessments prior to drug revealed pre-existing hearing loss in all patients (n=11) ranging from slight to severe in degree.

To date, three patients have had CTCAE grade one changes in hearing; two of these patients are siblings and experienced the toxicity following a single, low-dose exposure to the drug. Over half of those for whom extended high frequency audiometry could be measured (n=10) have shown decline in hearing for this test frequency range. The ototoxic effect appears to be rapid, and DPOAE data support a cochlear site of lesion, which is consistent with pre-clinical studies in feline, dog, and mouse models.

HPβCD is a promising therapy for NPC1 and evaluation in humans at higher doses will continue in order to determine efficacy. Ototoxicity is a likely outcome for patients treated with HPβCD, and these data, in combination with preclinical studies, lay a foundation for understanding the onset, severity, and mechanisms of hearing loss in humans, which will aid prognostic counseling, timely intervention, and potential otoprotective options.

PS-298

Autophagy-Related Gene Expression of Organ of Cortis in Aminoglycoside-Treated Rats

Yeon Ju Kim[1]; Chunjie Tian[1]; Jangho Kim[2]; Young Sun Kim[1]; Beomyong Shin[1]; Jong Joo Lee[1]; Hye Jin Lim[1]; You-Sun Kim[1]; Yun-Hoon Choung[1]
[1]Ajou University; [2]Seoul university

Background
Autophagy is a major intracellular degradation process, by which cytoplasmic material is degraded via fusion of the double-membrane compartment, autophagosome with lysosomes. This process is important for the maintenance of cell homeostasis. Previous our data showed that enhanced autophagic flux can delay the aminoglycoside-induced ototoxicity,

but the specific genes that are related with autophagy-dependent protective properties in hair cells have not been identified. To investigate the possible link between the autophagy process and hair cell protection against aminoglycoside-induced ototoxicity, we performed next generation sequencing (NGS) using *ex vivo* system.

Methods

Organ of Corti explants of Sprague-Dawley rats (postnatal day 7) were cultured on tissue culture plates. The explants were exposed to: (a) Distilled water, (b) 50 μM gentamicin and (c) 50 μM gentamicin + 50 pM rapamycin (as autophagy inducer) for 2 days. Transcriptome of organ of Corti cells were examined using RNA-sequencing. Differentially expressed genes were further verified for the organ of Corti with quantitative reverse transcription PCR (qRT-PCR).

Results

First, we evaluated hair cell loss in the apical, middle and basal turns of the organ of Corti in each group. Immunohistochemical findings of organ of Cortis showed that the loss of stereocilia was much more in the gentamicin-treated explants than in the gentamicin + rapamycin-treated explants. Then the RNA samples were extracted from each group and RNA sequencing was performed. We have shown the lists of differently expressed genes between samples. Results from the analysis are pending.

Conclusions

Autophagy may be closely connected with the aminoglycoside-mediated hair cell death and survival through the expression of specific genes.

PS-299

Protective Effects of Mild Therapeutic Hypothermia on Cochlear Implantation Insertion Trauma

Ilmar Tamames; Sonny Bao Huynh; Ramanamurthy V Mylavarapu; Suhrud Rajguru
University of Miami

Background

Prior literature has shown protective effects of mild therapeutic hypothermia on ischemic and traumatic injuries in neurons. Recent study by our group has extended the application of therapeutic hypothermia for conservation of auditory function following cochlear implantation surgery. Here we discuss the efficacy and safety of a novel portable device designed to provide localized hypothermia to the cochlea that avoids potential side effects from a systematic hypothermia.

Methods

In acute and chronic studies, the auditory brainstem responses (ABRs) were recorded from rats sedated with ketamine (44 mg/kg) and xylazine (5 mg/kg) to assess their hearing function before and after cochlear implantation surgeries. The changes in hearing with electrode insertion trauma were tested between 500 Hz to 32 kHz using pure tone pips. The hearing function was compared between three groups: control contralateral cochleae, cochleae that did not receive hypothermia during surgery and cochleae that received localized mild hypothermia to the middle turn of the cochlea for 20 minutes before and after induction of trauma. In acute experiments, ABRs were performed before and after implantation and the levels of reactive oxygen species (ROS) were measured at various time points. In the chronic experiments, ABRs were performed before surgery and at various time points up to 30 days following surgery. At the conclusion of the trials, inner ears were harvested for histology.

Results

The preliminary results from acute studies show that while electrode insertion trauma produced significant levels of ROS, mild hypothermia significantly reduced ROS generation. In chronic studies, we observed that there was an initial hearing loss of average 40 dB at 16kHz tested in the trauma only group. Comparatively, the function of cochleae receiving therapeutic hypothermia was conserved with an elevation on average of 10 dB and the hearing thresholds returned to pre-surgical levels rapidly. The results were confirmed by histology which showed a significant loss of hair cells in cochleae receiving surgical trauma compared to the hypothermia group.

Conclusion

Our results show that therapeutic hypothermia prevented significant functional loss from trauma induced during the cochlear implant surgery. Further experiments are underway to characterize the therapeutic benefits of localized hypothermia and develop a clinical device.

PS-300

Suppression of Oxidative Stress and Pro-inflammatory Cytokines in Cochlear HEI-OC1 Auditory Cells

Adam Bartos[1]; Yohann Grondin[1]; Magda Bortoni[1]; Elisa Ghelfi[1]; Rosalinda Sepulveda[1]; James Carrol[2]; Rick Rogers[1]
[1]Harvard School of Public Health; [2]THOR Photomedicine Ltd

Background

Noise, aminoglycoside antibiotics, or chemotherapeutic drugs can induce hearing loss through change in cellular metabolism leading to oxidative stress and cell death in cochlea. We investigated the mechanism of near infrared light (NIR) action on mitochondrial pathways in HEI-OC1 auditory cells exposed to oxidative stress conditions and found reduced oxidative stress and inflammation of NIR-treated cells, suggestive of a new approach to treat hearing loss. Near infrared light has been used for pain management, wound healing, and other therapeutic approaches. The efficiency and safety of non-invasive low-intensity NIR therapy make it suitable for new aspects in medical therapeutics, like noise induced hearing loss.

Objectives

We examined *in vitro* the effect of NIR on the oxidative stress and pro-inflammatory cytokine secretion due to gentamicin stress using HEI-OC1 auditory cells. We demonstrated that NIR induces a protective effect against oxidative stress through the down-regulation ROS, superoxide and Ca^{2+} level

resulting in the inhibition of oxidative stress and pro-inflammatory cytokine production.

Methods

Oxidative stress and inflammation measurements

HEI-OC1 auditory cells were stressed with 200 μM gentamicin antibiotic at non-permissive conditions for 3 hours. Oxidative stress characterization was performed *in vitro* with fluorescent cell-permeable dyes to measure ROS (2',7'-dichlorofluorescin diacetate) and specific marker for superoxide (dihydroethidium) and Ca^{2+} (Fluo-3). All fluorescent dyes were used at 1 μM concentration at non-permissive conditions for 20 minutes and were evaluated by flow cytometry (BD Accuri C6). Changes in pro-inflammatory cytokines (IL-1b, TNF-α) expression were determined by multiplex magnetic bead–based immunoassay (Bio-Rad MAGPIX) and flow cytometry.

NIR exposure

HEI-OC1 sensory cells were irradiated by a multiwell plate illuminator with 810 nm near-infrared light (Thor Photomedicine Ltd) for 100 seconds at power density 30 mW/cm^2 (3 J/cm^2), with or without gentamicin challenge. Cells were then incubated 10 minutes in non-permissive conditions prior to each experiment.

Results

Our data show that NIR suppresses inflammatory states in cochlear hair cells exposed to gentamicin through decreased expression of pro-inflammatory cytokines IL-1b (control: $p < 0.01$, gentamicin $p < 0.01$) and TNF-α (control: $p < 0.05$, gentamicin $p < 0.01$). Furthermore in gentamicin treated cells, NIR irradiation suppresses the release of ROS ($p < 0.01$) and reduces Ca2+ and superoxide levels ($p < 0.01$) 3h after exposure via a direct photochemical process.

Conclusions

Near infrared light suppresses oxidative stress and inflammation in cochlear HEI-OC1 auditory cells. NIR is a promising therapeutic candidate to address the problem of hearing loss.

PS-301

Epigenetic Changes in HEI-CO1 Auditory Cells following Cisplatin Challenge.

Archana Swami; Magda Bortoni; Yohann Grondin; Elisa Ghelfi; Adam Bartos; Rosalinda Sepulveda; Rick Roger
Harvard School of Public Health

Background

DNA methylation is a hallmark of epigenetic regulation and its role in the onset of hearing loss has been understudied. As a first step to assess the potential role for epigenetic cell regulation in hearing loss, we measured the change in global DNA methylation of HEI-OC1 auditory cells transiently exposed to cisplatin.

Objective:

To study changes in the global DNA methylation of auditory cells transiently exposed to cisplatin in vitro.

Methods:

HEI-OC1 auditory cells cultured in non-permissive conditions were transiently exposed for 4hr to 20 μM of cisplatin and allowed to recover for 24hr. Global DNA methylation was assessed by ELISA (5-mC DNA ELISA Kit Zymo Research) from DNA extracted using AllPrep® DNA/RNA/Protein Mini Kit from Qiagen and compared to non-challenged cells.

Results:

Our data shows global DNA methylation significantly decreased after transient exposure and 24 h recovery from cisplatin challenge ($P < 0.05$, two-tailed Student's t-test).

Summary:

In this study we show that brief exposure of HEI-OC1 cochlear hair cells to cisplatin alters the global DNA methylation. It is therefore likely that these epigenetic changes modify the cellular response to stress. Their significance at gene level and stress adaptation are currently under study.

PS-302

Adeno-associated Virus 1 Mediated Postnatal Gjb2 Expression in the Scala Media of the Cochlea Restored Hearing of Gjb6-/- Mice

Jianjun Wang; Qing Chang; Bei Chen; Binfei Zhou; Xi Lin
Emory University

Background

Non-sensory cells in the sensory epithelium of the cochlea are connected extensively by gap junctions (GJs) that facilitate intercellular ionic and biochemical coupling. Mutations in GJ genes coding for connexin 26 (Cx26, gene name *Gjb2*) and Cx30 (coded by *Gjb6*) are the most common causes of human nonsyndromic hereditary deafness. Currently no mechanism-based therapy is available for treatment. Here we performed gene-therapy using *Gjb6*$^{-/-}$ mice as the model.

Methods

Gjb2 or *Gjb6* with or without the GFP-tag was inserted into the adeno-associated virus (AAV) vector with the chicken-β-actin promoter. The AAV plasmids were packaged into AAV2/1 viruses with the titers of 1.0-1.5x10^{13}. About 1.0 μL solution of the recombinant viruses was injected into the scala media of one cochlea of *Gjb6*$^{-/-}$ mice (the other cochlea was used as a control) at P0 or P1. Whole-mount immunostaining of mouse cochlea and Western blotting were performed to determine the expression of AAV-mediated *Gjb2* after injection. Fluorescence recovery after photo-bleaching (FRAP) assay was performed to test the GJ-mediated intercellular communication. Endolymphatic potential (EP) and auditory brainstem response (*ABR*) were measured 1-2 months after injections to test the cochlear functions.

Results

GFP-labeling showed extensive puncta in the cell membrane of the Claudius, Outer Sulcus and Hensen's cells beginning from three days after injections. Strong ectopic expression in the cytoplasma of marginal cells, spindle-shaped cells was also observed. Stronger expression was observed over time and the viral-mediated Cx26 and Cx30 expressions lasted for at least 3 months. The functional recovery of the GJs was demonstrated by FRAP. *Gjb2*-mediated viral expressions did not damage morphology of hair cells and supporting cells, but restored the EP. The ABR thresholds of the ears injected

with AAV2/1-*Gjb2* was significantly lower than the non-injected control ears. The threshold improvements (in decibel (dB)) were about 30, 30, 30, 20 at 4, 8, 12 and 18 kHz respectively. However, postnatal injections of AAV2/1-*Gjb6* didn't yield similar functional hearing restoration.

Conclusions

Virally-mediated expression of Cx26 in *Gjb6*$^{-/-}$ mice restored the intercellular GJ-mediated communication and the EP in the cochlea. The ABR hearing thresholds were significantly improved, especially at low frequency range. These results are encouraging, and long-term effects are under investigation now.

PS-303

Identification of Immune/Inflammation Pathways in Acoustic Trauma Using Intra-subject Comparison of the Transcriptome of the Cochlear Sensory Epithelium

Bohua Hu[1]; Shuzhi Yang[1,2]; Qunfeng Cai[1]; Youyi Dong[1]; Robert Vethanayagam[1]; Bard Jonathan[1]; Jamoson Jennifer[1]
[1]State University of New York at Buffalo; [2]The First Affiliated Hospital of Chinese PLA General Hospital

Introduction

Acoustic overstimulation induces a complex biological response in the cochlea. This response includes the change in gene expression. In a previous study, we documented a global expression change of cochlear genes in noise-damaged cochleae. Because individuals display a large variation in their gene expression levels and because this variation is relatively less between the two ears of same subjects, we wanted to know whether an intra-subject comparison could revealed the genes or pathways that were not identified in our previous investigation.

Methods

C57BL/6J mice were exposed to a broadband noise at 120 dB SPL for 1 h. One ear of these mice was blocked before the acoustic overstimulation to attenuate the input sound level. At 1 day post-noise exposure, the sensory epithelium samples were collected from both the exposed ears and the protected ears for RNA-seq analyses to identify deferentially expressed genes. The functional reference of these identified genes was analyzed using two bioinformatics tools, DAVID and IPA. To determine the difference in the expression analyses between the intra- and the inter-subject comparison, we examined the expression patterns of a set of immune and inflammation genes using a qRT-PCR array analysis for additional mice exposed to the noise.

Results

A total of 58 genes displayed expression changes, with 51 being up-regulated and 7 being down-regulated. The DAVID analysis of these differentially expressed genes revealed the enriched pathways including cytokine-cytokine receptor interaction, NOD-like receptor signaling pathway, chemokine signaling pathway, cytosolic DNA-sensing pathway, and the Toll-like receptor signaling pathway. An upstream regulator analysis by IPA identified potential regulatory nodes, including TIL3, IFNG, TNF, TLR4, and IL1B. Further analyses of immune-related genes using qRT-PCR array revealed distinct patterns of expression changes between the intra- and inter-subject comparisons, suggesting that the current intra-subject comparison could identify genes that were missed by the inter-subject comparison. Interestingly, the protected ear, which had at least 40 dB attenuation of acoustic signals and displayed no detectable threshold shifts, displayed changes in expression of immune-related genes.

Conclusions

The immune/inflammatory response is a major cellular response to acoustic trauma.

PS-304

Pharmacological Mimic of Glutamate Excitotoxicity brings about Morphological Changes in Zebrafish Hair Cell Presynaptic Structures

Lavinia Sheets
Harvard Medical School

Introduction

One of the primary biological effects of noise exposure is excessive release of the excitatory neurotransmitter glutamate from hair cells. Previous studies examining afferent neurons innervating cochlear hair cells have shown postsynaptic nerve terminal swellings following noise exposure indicative of glutamate receptor overactivation and excitotoxicity. Yet whether high levels of glutamate also contribute to pathological changes in hair-cell presynaptic structures has not been directly examined. To address whether glutamate excitotoxicity contributes to morphological changes in hair-cell presynaptic structures, I examined ribbon synapse morphology in zebrafish lateral line hair cells exposed to drugs that mimic glutamate-induced excitotoxic trauma.

Methods

Pharmacological manipulation of larvae: 6-day-old zebrafish larvae were exposed to the ionotropic glutamate receptor agonist (S)-AMPA or the more potent excitotoxic agonist kainic acid (KA) diluted in Embryo Medium (E3) with 0.1% dimethylsulfoxide for 1 or 1.5 hours.

Immunohistochemistry and Image Analysis: Larvae were sedated on ice and transferred to fixative (4% paraformaldehyde), then processed for whole-mount immunohistochemical labeling of hair-cell synaptic proteins, including the synaptic ribbon protein Ribeye and the synaptic vesicle marker Vglut3. Z-stack images of neuromasts were acquired with a laser scanning confocal microscope. Quantitative image analysis was performed on raw images using Amira 3D Analysis software.

Live Imaging: Larvae were paralyzed with α-bungarotoxin and immobilized with a

thin layer of 0.8% low-melt agarose in an imaging chamber containing E3. Image z-stacks were obtained using a confocal microscope.

Results
Exposure to KA resulted in profound swelling of lateral-line afferent terminals analogous to that observed in KA exposed mammalian cochleae. Remarkably, I also observed changes in hair-cell presynaptic structures in larvae exposed to AMPA or KA; namely, significant changes in synaptic-ribbon size, an increase in the number of cytoplasmic aggregates of Ribeye, and changes in the intensity and localization of Vglut3. Moreover, larvae co-exposed to AMPA or KA and tricaine methanesulfonate (MS-222)—an anamniote anesthetic that blocks the activity of sensory and motor nerves, but does not affect the electrical activity of larval neuromast hair cells—showed significantly larger hair-cell synaptic ribbons and more intense Vglut3 immunolabel than larvae exposed to MS-222 alone, suggesting that excess glutamate may directly contribute to pathological changes in hair-cell presynaptic structures.

Conclusions
Cumulatively, these data indicate that glutamate excitotoxicity mediates damage to both presynaptic structures in hair cells and postsynaptic terminals, and suggest that excess glutamate resulting from noise exposure may damage hair-cell synaptic contacts through multiple signaling pathways.

PS-305

The Road to Reprogramming Leads to Protection

Wanda Layman; Shiyong Diao; Jennifer Dearman; Mario Sauceda; Jian Zuo
St Jude Children's Research Hospital

In the auditory field, ectopic expression of transcription factors such as *Atoh1* have been used to convert mammalian supporting cells into cells that express many endogenous hair cell markers. However, the reprogramming process of transforming supporting cells into hair cells may not be solely about genetic transformation, but also epigenetic transformation. Since HDAC inhibitors are commonly used to increase reprogramming efficiency of iPSCs, we hypothesized that an HDAC inhibitor may also increase cellular reprogramming in the organ of Corti. Adult *Fgfr3^{iCreER}; Atoh1-HA; tdTomato* mice were used to test whether systemic treatment of an HDAC inhibitor (SAHA) could improve hair cell regeneration *in vivo*. Mice treated Systemic SAHA treatment had no detrimental impact on hearing function compared to littermate vehicle treated controls. However, when kanamycin was administered to SAHA treated mice to induce damage, SAHA treated mice had little to no hair cell loss even 6 weeks post-kanamycin treatment, whereas vehicle treated controls lost >90% of their outer hair cells. Further analysis using wild type mice revealed that SAHA protection is dependent upon both SAHA dosage and kanamycin dosage. Interestingly, dosage dependent SAHA treatment has been reported to protect against cell death in mouse models of inflammation and neurodegeneration. Similarly, the protective effect of SAHA in the organ of Corti appears to be due to the activation of Nf-κB leading to an increase in the expression of the pro-survival genes, whereas littermate vehicle treated controls do not activate Nf-κB and up-regulate pro-apoptosis genes. Our data suggests that SAHA protects against aminoglycoside antibiotic ototoxicity by regulating multiple canonical and non-canonical HDAC targets.

PS-306

Protective Effect in Herbal Medicine "Shimotsuto" Using the Zebrafish Lateral Line and CBA/N Mice Vestibular Hair Cells

Yoshinobu Hirose; Kazuma Sugahara; Makoto Hashimoto; Hiroshi Yamashita
Yamaguchi University Graduate School of Medicine

Background
The zebrafish lateral line is a powerful system for studying hair cells and hair cell death. Hair cells can be easily labeled and imaged in vivo with fluorescence microscopy. We reported in 2014 ARO meeting that eight herbal medicines were screened for protective effects against aminoglycoside. All of them showed protective effect, especially in Shimotsuto, but there are no reports whether Shimotsuto can protect hair cells in Mammalians.

Methods
Zebrafish embryos were used in this study. Zebrafish larvae were exposed to Shimotsuto (1-1000 ug/ml) for 1 hour before 200 uM neomycin to induce hair cell death for 1 hour. After that, they were fixed in 4% paraformaldehyde, incubated with anti-parvalbumin, Alexa 488, and hair cell damage was assessed. Next, cultured utricles of CBA/N mice were used. Neomycin + Shimotsuto group, utricles were cultured with neomycin (2 mM) and Shimotsuto (1000 ug/ml). Twenty-four hours after exposure to neomycin, the cultured tissues were fixed with 4% paraformaldehyde.

Results
Both in zebrafish lateral line and mammalian vestibular epithelium, the survival rate of hair cells in Neomycin + Shimotsuto group was significantly more than that in Neomycin group.

Conclusion
The results indicated that Shimotsuto protects sensory hair cells against neomycin-induced death in zebrafish lateral line and mammalian vestibular epithelium. Shimotsuto can be used as the protective drug in the inner ear.

PS-307

Ototoxicity of Cisplatin Correlates with Changes in Blood Antioxidant Status

Pernilla Videhult Pierre[1,2]; Jakob Haglöf[1]; Birgitta Linder[1]; Mikael Engskog[1]; Torbjörn Arvidsson[1]; Curt Pettersson[1]; Göran Laurell[1]
[1]Uppsala University, Uppsala; [2]Karolinska Institutet, Stockholm

Background
Hearing loss is a dose-limiting side-effect of the anticancer drug cisplatin. According to animal studies, the ototoxicity involves DNA-adduct formation and oxidative stress. The aim

here was to investigate whether cisplatin-induced ototoxicity correlates with changes in blood antioxidant status.

Methods

After hearing assessment with ABR, anesthetized albino guinea pigs (weight: ~0.3 kg) were subjected to iv blood sampling and administration of either iv sodium thiosulfate (31 mg/ml; 1ml/0.3kg b.w.; n=7) or iv saline (9 mg/ml; 1 ml/0.3 kg b.w.; n=7). Half an hour later, they were given iv cisplatin (1 mg/ml; 8 mg/kg b.w.). After four days, the animals were reanesthetized, subjected to ABR assessment and iv blood sampling, and eventually decapitated. Blood samples were allowed to clot (~4 °C; 30 min) prior to centrifugation (1600×g; 4 °C; 15 min). The resulting serum was collected and stored at 80 °C until analysis. Prior to analysis, the serum samples were thawed on ice. Cold (~4 °C) acetonitrile was added at 3:1 (v/v) ratio for protein precipitation. After centrifugation (3000×g; 4 °C; 15 min), the supernatant was injected onto a UPLC-ESI-Q-TOF system with a HILIC-amide column running a 15 min gradient in both positive and negative mode. Acquired data were pre-processed using the freeware XCMS, normalized, and evaluated in SIMCA-P+.

Results

Cisplatin treatment caused elevated ABR thresholds in all guinea pigs. However, at high frequencies the elevations were significantly higher in saline-treated animals ($p<0.05$ at 20 and 30 kHz). Cisplatin treatment also resulted in a significant increase in reduced glutathione (GSH) in both sodium thiosulfate- ($p<0.01$) and saline- ($p<0.001$) treated animals. The increase was significantly larger in the saline-treated group ($p<0.01$). ABR threshold elevations and GSH increase were highly correlated ($R^2=0.73$; Figure 1).

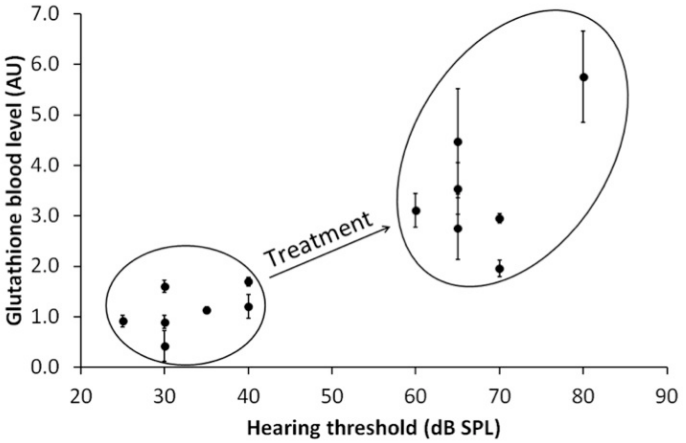

Figure 1. Blood levels of reduced glutathione versus ABR hearing thresholds at 30 kHz before and after treatment with cisplatin.

Furthermore, an antioxidant present in blood with association to the thioredoxin system, dihydrolipoic acid (DHLA), also showed increased blood levels ($p<0.05$). Additionally, and in line with elevated amounts of GSH, oxidized glutathione (GSSG) decreased ($p<0.01$) in both groups.

Conclusion

Cisplatin-induced ototoxicity appears to correlate with antioxidant levels in blood, notably increased levels of GSH. Iv administration of sodium thiosulfate prior to cisplatin seems to reduce ototoxicity and related antioxidant blood levels.

PS-308

ATM and DNA-PK Play Distinct Roles in Preventing Cisplatin-induced Cochlear Sensory Cell Death

Julien Menardo; François Florence; Jérôme Bourien; Régis Nouvian; Jean-Luc Puel; **Jing Wang**
INSERM

Introduction and Aims

Cisplatin (CDDP) is a widely used chemotherapy drug, but with significant ototoxic side effects, due to the death of the cochlear sensory hair cells. To date, the mechanism of CDDP-induced ototoxicity remains unclear, and hearing protection during CDDP-based chemotherapy in humans is lacking. This study is designed to examine the molecular pathway of CDDP ototoxicity from cellular up to the whole system level.

Methods

Here, we investigated the CDDP-poisoning pathway in CDDP intoxicated postnatal 3-day mouse cochleae *in vitro* and adult p53 knock-out or wild-type mice *in vivo*.

Results

Our results provide the first evidence that the activation of DNA damage response pathways governs the fate of hair cells subjected to CDDP intoxication, whilst oxidative stress, generally considered as a key mechanism, is only a later event. We demonstrate that the activation of ATM-mediated Chk2-p53 pathway conveys a pro-apoptotic signal to the cochlear hair cells, while activation of DNA-PK is cytoprotective for these cells. Surprisingly, pharmacological inhibition of ATM activation has contrasting effects in the different hair cell types. It promotes outer hair cell survival but increases inner hair cell loss, which hampers ATM manipulation as a strategy to prevent CDDP-induced ototoxicity. In contrast, targeting the downstream ATM pathway through genetic or pharmacological ablation of p53 causes attenuation of cochlear cell apoptosis, thus preserving hearing function.

Conclusion

These these findings underscore the need of considering the impact of DNA damage responses in cochlear cell death and propose pharmacological inhibition of p53 a**s** an attractive tool to prevent CDDP-induced ototoxicity in human chemotherapy.

PS-309

TrkB Regulation of the Circadian Clock in the Cochlea

Vasiliki Basinou; Christopher Cederroth; Inna Meltser; Gabriella Schmitz Lundkvist; Barbara Canlon
Karolinska Institute

Circadian rhythmicity is important for many bodily functions (e.g. metabolism, cell-cycle, sleep-wake cycle, reproduction, and hormonal regulation) and the central clock, found in the hypothalamus, the suprachiasmatic nucleus (SCN) synchronizes and coordinates rhythms to regulate various

physiological functions. Peripheral organs such as the liver, kidney, heart and pancreas also display prominent circadian rhythms. The central and peripheral clocks contain molecular oscillators organized as self-regulated feedback loops of core clock genes. To evaluate the presence of clock machinery in the cochlea, we first examined the temporal expression patterns of mRNAs encoding central clock components in the cochlea using the Nanostring nCounter technology. We found prominent circadian expression of the core clock genes in the cochlea (*Bmal1, Clock, Cry1, Reverb, Per1 and Per2*) as well as transcription factors regulated by these core clock genes that are involved in audiogenic seizures (*Dbp, Hlf, Tef*). Using a reporter mouse line in which luciferase was knocked-in to the *period 2* encoding sequence, we are able to show, in culture, Per2 protein oscillations illustrating the rhythmicity of the cochlea clock. Here we show that *bdnf* mRNA shows circadian rhythmicity peaking at night and is affected by noise trauma during the day but not during the night. By targeting the BDNF-receptor TrkB with the selective agonist 2,8 dihydroxyflavone (DHF) on cochlear explants, it was found that the amplitude of Per2 oscillations increased when treated during the day, but not during the night. *In vitro* application of DHF phase shifted and boosted the amplitude of cochlear PER2::LUC rhythms, which effects were blocked by the specific TrkB receptor antagonist, ANA12. The conclusions from this study provide an ensemble of knowledge on the circadian regulation of auditory functions and integrate the complex molecular interplay between neurotrophins and the clock machinery in the cochlea.

PS-310

High Quality RNA Extraction of the Mammalian Cochlea for qRT-PCR and Transcriptome Analyses

Kim Patil; Barbara Canlon; **Christopher Cederroth**
Karolinska Institutet

Molecular investigations of the hearing organ, the cochlea, have been hampered due to the difficulty of isolating pure RNA and in quantities sufficient enough for quantitative real-time RT-PCR or microarray analysis. The complex architecture of the cochlea, the presence of liquids, bone and cartilage tissue, in combination with the limited accessibility, are a major hurdle in obtaining contamination-free RNA to a level that does not affect downstream applications. Here, we present a protocol to extract RNA from the mouse cochlea, with yields and quality suitable for real-time RT-PCR or Affymetrix labeling. In contrast to current methods, such as TRIZOL or column-based extraction, this protocol combines the two and yields a high quantity of total RNA from a single pair of adult mouse cochleae. This protocol allows the isolation of RNA molecules from the mammalian cochlea providing access to whole-transcript expression analyses.

PS-311

Vestibular Changes in Chronic Otitis Media: A Human Temporal Bone Study

Mehmet Erdil[1]; Patricia Schachern[2]; Vladimir Tsuprun[2]; Mehmet Faruk Oktay[1]; Geeyoun Kwon[2]; Michael Paparella[2]; **Sebahattin Cureoglu[2]**
[1]Bagcilar Research Hospital; [2]University of Minnesota

Background

The effect of chronic otitis media (COM) on cochlear structures is studied in detail. Otitis media is considered the most common cause of vestibular disturbances and vertigo in children. However, the underlying causes of balance problems in COM are not extensively studied. One reason could be due to the technical difficulties involved in performing physiological studies in patients with middle ear pathologies and perforated eardrum. The aim of this study is to determine objectively the changes in hair cells of the vestibule, including saccule, utricle, and semicircular canals.

Methods

We defined COM as an inflammatory condition of the middle ear cleft containing intractable pathological changes such as cholesteatoma, granulation tissue, and tympanosclerosis. Excluded were subjects with a history of acoustic trauma, ototoxic drugs or otological surgery, and those with any other otological diseases, such as otosclerosis. Control group included normal human temporal bones, which are without any signs of middle and inner ear diseases using light microscopy.

Type I and Type II cells were counted separately under a differential interference contrast microscopy at x1250 magnification in 0.01 mm^2 surface area where the sections are perpendicular to maculae of saccule and utricle as well as the cupulae of the semicircular canals. Surface area was determined by multiplying the thickness of the section (20 μm) by the length of the sensory epithelium where the count was made. The results were expressed as density: number of cells per 0.01 mm^2 of surface area.

Results

Fifty human temporal bones from 38 cases (21 normal, 17 COM) ranging in age from 18 to 93 were included. The pathological changes in middle ears with COM were granulation tissues in 17, cholesterol granuloma in 5, and cholesteatoma in 1 temporal bone. There was a significant difference between normal and COM cases in the mean densities of saccular type I and type II, utricular type II, and posterior semicircular canal type I and type II cells. Mean density of lateral semicircular canal hair cells and utricular type I hair cells were not significantly different.

Conclusion

COM is associated with the loss of hair cells in the vestibular system. Although this is a pathologic study in human temporal bones from patients with COM, it may reflect the basis for vestibular symptoms such as dizziness and vertigo in cases with COM in clinical setting.

PS-312

Ototoxic Effects of Carbaryl in Rat Cochlear Organotypic Cultures

Vijaya Prakash Krishnan Muthaiah; **Vijaya Prakash Krishnan Muthaiah**; Peng Li; Kelei Gao; Dalian Ding; Jerome Roth; Richard Salvi
University at Buffalo

Introduction

Carbaryl, an organophosphorus insecticide marketed under trade name Sevin, is a reversible inhibitor of central and peripheral acetylcholinesterase. At the third most used insecticide in US, it has been detected at low levels in surface water and food. Since organophosphorus compounds have been reported to cause mild sensory neuropathy and since acetylcholine receptors are present in the cochlea, we speculated that carbaryl might be ototoxic. To test this hypothesis, we treated postnatal day 3 (P3) rat cochlear organotypic cultures with an organophosphorus pesticide with doses above the RfD set by the US Environmental Protection Agency.

Methods

Rat P3 cochlear organotypic cultures were prepared from Sprague-Dawley rat pups. A day later, the cochlear explants were treated with carbaryl at doses ranging from 50 µM to 500 µM for 48 h or 96 h. The degree of damage to hair cells, auditory nerve fibers and spiral ganglion neurons (SGN) was qualitatively and quantitatively analyzed. SGN and their radial processes were labeled with neurofilament-200 antibody. Phalloidin was used to label the F-actin that is heavily expressed in the stereocilia and cuticular plate of the hair cells. TOPRO-3 was used to stain nuclei.

Results

Carbaryl treatment resulted in a dose and duration-dependent loss of hair cells. In addition, carbaryl damaged the SGNs and peripheral nerve fibers projecting radially out to the hair cells. After 48 h of carbaryl treatment, hair cells started to degenerate at a dose of 200 µM. Increasing the dose to 500 µM for 48h resulted in a complete loss of cochlear hair cells along the entire length of the cochlea whereas 96 h treatment with 100 µM carbaryl destroyed 100% hair cells. In contrast to cochlear hair cell damage, SGN and auditory nerve fibers were only partially damaged after 48 h treatment with 500 µM carbaryl. Partial SGN destruction also occurred after 96 h treatment with 100 µM carbaryl. Carbaryl treatment resulted in the condensation and fragmentation of SGN, morphological features of apoptotic cell death.

Conclusion

Our results show for the first time that carbaryl, a widely used insecticide, can damage the cochlea. The hair cells are more susceptible to carbaryl ototoxicity than SGN. Studies are currently underway to more fully characterize the mode of carbaryl ototoxicity.

PS-313

Expression of the Hair Cell Survival Factor, Pou4f3, in Regenerated Hair Cells that Spontaneously Form in the Neonatal Mouse Cochlea Following Damage

Michelle Randle; Sumedha Karmarkar; Brandon Cox
Southern Illinois University School of Medicine

Background

Our lab has previously shown that the neonatal mouse cochlea spontaneously regenerates hair cells (HC) *in vivo* following damage. This occurs through mitotic regeneration and direct transdifferentiation of supporting cells (SCs) into HCs (Cox et al., 2014 *Development* 141:816-829). However, most regenerated HCs die between postnatal day (P) 7 and P15 from unknown causes. During embryonic development, HCs begin expressing the survival factor Pou4f3, a day before myosinVIIa. Pou4f3 knockout mice form partially differentiated HCs lacking stereocilia that undergo apoptosis shortly after differentiation (Erkman et al., 1997 *Nature* 381:603-606; Xiang et al., 1998 *Development* 125:3935-3946). Preliminary data indicate most HCs in our model (Atoh1-CreER^{T-M};ROSA26^{DTA} mice) lack Pou4f3 expression at P6, however no fate-mapping was performed thus we cannot distinguish between original/surviving HCs and regenerated HCs. The current study uses fate-mapping techniques to distinguish between these populations and we hypothesize that the majority of regenerated HCs lack Pou4f3 expression early after differentiation which causes premature cell death.

Methods

Mouse genetic CreER-loxP models were used to ablate HCs in neonates by expressing diphtheria toxin fragment A (DTA) and to fate-map original/surviving HCs with the tdTomato reporter. Tamoxifen administration at P0/P1 in Atoh1-CreER^{T-M};ROSA26$^{DTA/CAG-tdTomato}$ mice results in expression of DTA and tdTomato in HCs. The CAG promoter in the ROSA26$^{CAG-tdTomato}$ reporter allows for more robust expression (~99% HCs) than expression of DTA using the ROSA26^{DTA} allele (~80% HCs). Thus only original/surviving HCs are labeled with tdTomato since regenerated HCs weren't present when tamoxifen was given. Atoh1-CreER^{TM};ROSA26$^{CAG-tdTomato}$ mice given the same tamoxifen induction paradigm were used as controls. Cochleae were analyzed for Pou4f3 expression at P4, P7, and P15 by immunohistochemistry and confocal microscopy.

Results

Atoh1-CreER^{TM};ROSA26$^{LacZ/CAG-tdTomato}$ mice given the same tamoxifen induction paradigm were used to measure Cre efficiency with two floxed alleles. There was no difference in the percentage of tdTomato labeled HCs in Atoh1-CreER^{T-M};ROSA26$^{CAG-tdTomato}$ mice (1 floxed allele) compared to Atoh1-CreER^{TM};ROSA26$^{LacZ/CAG-tdTomato}$ mice (2 floxed alleles), validating our fate-mapping method. All HCs in controls expressed Pou4f3 at all ages tested. In Atoh1-CreER^{TM};ROSA26$^{DTA/CAG-tdTomato}$ mice, most regenerated HCs (tdTomato-negative) and original/surviving HCs (tdTomato-positive) expressed Pou4f3 at P15; while many regenerated HCs (tdTomato-negative) lacked Pou4f3 expression at P4 and P7.

Conclusion
This data indicates most regenerated HCs fail to express Pou4f3 correlating with their decreased survival rate. Further studies are needed to determine how the few regenerated HCs which survive until P15 are able to turn on Pou4f3.

PS-314

Comparisons of Cochlear Hair Cell Counts from Four Related Sound Damage Paradigms and Two Tissue Preparation Methods

Christopher Neal; Stefanie Kennon-McGill; Andresa Freemyer; Hinrich Staecker; Thomas Imig; Dianne Durham
University of Kansas Medical Center

Introduction
Tinnitus has multiple etiologies, including exposure to damaging acoustic stimuli. Acoustic trauma damages and kills cochlear hair cells (HC), and this loss of input to the CNS initiates a cascade of maladaptive changes. Here we quantify changes in HC number following exposure to one of four sound damage paradigms as part of work seeking to elucidate changes in the central auditory system in a rat model of tinnitus. We varied both sound intensity and duration. In addition we compared two common tissue preparation methods to determine their comparability in estimating HC loss.

Methods
We unilaterally exposed anesthetized, male Long-Evans rats to one of four 16 kHz sound damage paradigms (114 dB SPL for 1 hour; 114 dB SPL for 2 hours; 118 dB SPL for 1 hour; or 118 dB SPL for 4 hours). Animals recovered for three to four weeks prior to sacrifice and cochlea harvest. Cochleae were either (1) fixed, embedded in Araldite plastic, stained (toluidine blue) and sectioned parallel to the modiolar axis or (2) dissected into half turns, labeled (phalloidin, DAPI), and mounted on slides. Hair cell counts were performed without knowledge of exposure conditions. We constructed cochleograms using Greenwood's equation to transform percent distance to frequency (Hearing Res. 94, 157–162; 1996).

Results
One hour of sound exposure at either intensity resulted in fewer areas of statistically significant hair cell loss for both inner and outer hair cells, when compared to control animals, than either 2 or 4 hours of exposure. For longer duration sound exposures, HC loss was observed throughout the cochlea but most prominent in high frequency regions. We also compared counts of phalloidin-labeled HC to counts of DAPI-stained nuclei in the same tissue. We observed no significant differences in control animals, and only 2 areas of significant difference in sound exposed animals. Lastly, we compared counts from DAPI stained nuclei to counts from toluidine blue stained nuclei. We observed a greater discrepancy between counts in sound damaged animals than in control animals.

Conclusions
For our pure tone stimulus, increasing the duration of sound exposure created more HC loss than increasing intensity. Labeling cells with phalloidin or DAPI produced comparable results in estimating HC loss in whole mounts. The details of HC nuclear counts in damaged animals were more variable when comparing data from plastic sections and whole mounts. However, the pattern of HC loss revealed in these two preparations was similar.

PS-315

Mechanical Overstimulation Results in Decreased Stiffness of Inner Hair Cell Stereocilia Due to Actin Core Damage.

J Grossheim[1]; Ruben Stepanyan[2]; Gregory Frolenkov[1]
[1]University of Kentucky; [2]Case Western Reserve University

Background
While the actin paracrystalline core determines the rigidity of stereocilia proper, the arrangement of actin filaments in the rootlets allows the stereocilia to pivot at their base during hair bundle deflections. In chick auditory hair cells, mechanical stiffness of the hair bundle also depends on the extracellular links interconnecting stereocilia (Bashtanov et al., 2004). The extracellular link contribution to the hair bundle stiffness was found to be less significant in cochlear inner hair cells (IHCs) (Kitajiri et al., 2010), perhaps due to less mechanical coupling of IHC stereocilia. Mechanical overstimulation of mammalian auditory hair cells *in vitro* results in a decrease of the hair bundle stiffness (Saunders et al., 1986). We hypothesized that this decrease may be due to damage to the actin near the base of stereocilia, similar to that observed with transmission electron microscopy (TEM) in cats exposed to acoustic stimulation sufficient to cause permanent noise-induced hearing loss (Liberman, 1987).

Methods
We used a fluid-jet to deflect IHC stereocilia in cultured rat organ of Corti explants. We video recorded the bundle displacement to small stimuli before and after mechanical overstimulation with the fluid-jet. We estimated stiffness changes of the IHC bundle caused by overstimulation using frame-by-frame analysis of the bundle movement. We overstimulated all of the IHCs in a small region of the explant and demarcated it to distinguish this region from undamaged control IHCs in the same specimen. We then briefly fixed the tissue prior to cryoprotection for freeze substitution and embedding in HM-20 lowicryl resin for sectioning and TEM imaging. We used TEM to examine the actin filaments of stereocilia in rat IHC bundles with reduced stiffness from *in vitro* mechanical overstimulation.

Results
We found increased displacement in stereocilia bundles subjected to fluid-jet overstimulation indicating a decrease in bundle stiffness of nearly 50%. Subsequent examination of overstimulated stereocilia bundles via TEM revealed sub-micron breaks in the actin core of the stereocilia that were not found in unstimulated control IHC stereocilia nor in the unstimulated OHC stereocilia. The majority of these breaks (over 80%) were located within 500 nm of the cuticular plate, where the mechanical stress from the fluid-jet overstimulation would be greatest, and more than 40% were located within 100 nm of the cuticular plate.

Conclusion
The integrity of the actin filaments at the base of the stereocilia is likely to determine the stiffness of the IHC bundle.

PS-316

The Effects of Age and Hearing Loss on Neural Synchrony and Interaural Phase Difference Discrimination

Andrew King; Christopher Plack; Kathryn Hopkins
University of Manchester

Introduction
Hearing difficulties occuring in middle-age and later may be partly due to reduced neural synchrony to the temporal characteristics of sounds (e.g Ruggles, D., Bharadwaj, H. & Shinn-Cunningham, B. G. 2012. *Curr Biol*, 22, 1417-1422). Poor neural synchrony may affect sensitivity to interaural phase difference (IPD), which is used to locate and separate sounds from different azimuths. Neural synchrony can be recorded at the scalp as the electrophysiological frequency-following response (FFR). This study aimed to determine whether changes in IPD sensitivity associated with hearing loss and age (King, A., Hopkins, K. & Plack C. J. 2014. *J Acoust Soc Am* 134, 342-351) are related to poor phase locking as defined by FFR strength.

Methods
Listeners (N=37) varied in age (18-83 yr) and absolute threshold (−1 to 59 dB SPL at 250 and 500 Hz). In separate conditions, they discriminated IPDs in the temporal fine structure (TFS) and envelope of 20 Hz amplitude-modulated (AM) tones carried by either 250 or 500 Hz tones. Adpative tracks were used to estimate IPD discrimination thresholds. In a second session the FFR to four different AM tones was measured simultaneously (tones presented dichotically, two to each ear). AM rates of 16, 27, 115 and 145 Hz were used, with carrier tones of 307, 537, 357 and 578 Hz respectively.

Results
With absolute threshold partialled out, increasing age was correlated with poorer envelope-IPD discrimination, and to a lesser extent, TFS-IPD discrimination. FFR to the TFS components, and to the 145 Hz AM rate, deteriorated with age irrespective of absolute threshold. Correlations between TFS-IPD thresholds and FFR at the TFS components, and between envelope-IPD thresholds and 145 Hz envelope FFR, did not survive after age was partialed out. On the other hand, IPD thresholds still correlated with age when FFR strength was partialed out, suggesting that other age-related factors also affect IPD sensitivity. Absolute threshold was not correlated with either IPD discrimination or FFR phase coherence. This is inconsistent with King et al. (2014), but may be due to recruiting too few listeners with elevated thresholds to power the correlations.

Conclusions
Both FFR phase coherence and IPD discrimination deteriorate with age, but the age-related deterioration in IPD sensitivity does not seem to be strongly related to neural synchrony as measured by the FFR. It is possible that higher-level processes such as binaural integration or attention underlie the age-related deterioration in IPD sensitivity.

PS-317

A (Null) Effect of Age-Related Hearing Loss on Auditory Learning in Older Adults

Hanin Karawani[1]; Tali Bitan[2]; Joseph Attias[2]; Karen Babai[2]
[1]*University of Haifa and Rambam Health Care Campus;*
[2]*University of Haifa*

Introduction
Speech perception and communication in adverse listening conditions become more difficult as we age, particularly for individuals with age-related hearing loss (ARHL). What remains debated is whether those difficulties can be eased with auditory training. The aim of the current study was to compare the outcomes of training on speech perception under adverse conditions between normal-hearing older adults and those with ARHL.

Methods
56 listeners (60-70 y/o-33 F) participated in the study. A group of 25 participants with ARHL and 21 normal hearing adults received 14 sessions of home-based auditory training over the course of 4 weeks. Training was provided in three adverse listening conditions: (1) Speech-in-noise (2) time compressed speech and (3) competing speakers. Pre- and post-training sessions were completed by the trained participants and by 10 untrained listeners. On those sessions all listeners were tested on all of the trained conditions as well as on a series of untrained conditions designed to assess the transfer of learning to other, similar speech conditions.

Results
Significant improvements on all trained conditions were observed in both ARHL and normal-hearing groups over the course of training. Consequently, greater pre- to post-test changes were observed in trained than in untrained listeners on all three conditions. Nevertheless, learning did not transfer to any of the untrained conditions. Although normal hearing listeners outperformed ARHL participants across conditions both before and after training, the amount of learning was similar in the two groups. Untrained listeners showed minimal changes between the two test sessions.

Conclusions
Training-induced learning (but no generalization) was observed in both normal-hearing adults and those with ARHL. Despite the hearing loss, subjects with ARHL learned similarly to normal-hearing subjects over the course of training. Therefore, we conclude that ARHL does not interfere with the perceptual learning of speech in adverse listening conditions as assessed in the current study.

PS-318

The Role of Cognitive Abilities in Understanding Speech in Noise by Older Adults

Susan Teubner-Rhodes; Kenneth Vaden; Jayne Ahlstrom; Judy Dubno; Mark Eckert
Medical University of South Carolina

Background

Older adults report difficulty understanding speech in background noise, even after accounting for reduced speech audibility due to hearing loss. Tasks requiring selective auditory attention, such as speech in noise listening tasks, elicit elevated activity in frontoparietal and cingulo-opercular regions, which are hypothesized to reflect goal-directed inhibitory control and performance monitoring functions, respectively. Given that these attentional control functions can decline with age, we investigated the degree to which activity in these cortical regions and related cognitive abilities predicted word recognition in noise by older adults with relatively normal hearing (N=31, M_{age}=60.2).

Methods

fMRI was used to estimate neural activity for single words presented in continuous, multi-talker babble at 82 dB SPL with alternating blocks of +3 dB and +10 dB signal-to-noise ratio (SNR). We also collected behavioral measures of inhibitory control (Stroop) and attentional capacity (Wisconsin Card Sorting). Statistical analyses defined cortical regions that predicted correct word recognition on the next trial, thereby reflecting attentional indicators of trial-level performance; we then examined the extent to which inhibitory control and attentional capacity predicted the activity-performance relationship in these regions. A separate analysis identified regions where inhibitory control interacted with SNR, reflecting goal-directed responses to changing task demands.

Results

Trial-level Performance. Older adults with greater attentional capacity exhibited a stronger relation between dorsal paracingulate activity and trial-level performance (r=.59, p<.01). This suggests that the ability to process more information sources increases the benefit from performance monitoring.

Task Demands. Older adults with stronger inhibitory control demonstrated greater frontoparietal activity in the +3 dB SNR compared to the +10 dB SNR. In addition, greater frontoparietal activity for the +3 dB SNR was associated with higher accuracy in this condition (r=.47, p<.05) and with a smaller accuracy difference between the +3 dB and +10 dB SNR (r=-.41, p<.05). These effects remained significant even after controlling for variation in inhibitory control, suggesting that, across individuals, frontoparietal cortex facilitates word recognition under challenging listening conditions.

Conclusions

As listening difficulty increases, older adults with greater inhibitory control recruit frontoparietal regions that may suppress irrelevant information to benefit word recognition in noise. Additionally, older adults with greater attentional capacity demonstrated a greater performance benefit from cingulo-opercular activity. Thus, declines in inhibitory control and attentional capacity are expected to uniquely contribute to speech recognition difficulties in older adults.

PS-319

Age Related Shifts of Absolute Pitch Judgment and Their Relation to the Auditory Filter Bandwidths.

Minoru Tsuzaki[1]; Toshie Matsui[2]; Toshio Irino[3]; Chihiro Takeshima[4]
[1]Kyoto City University of Arts; [2]University of Tsukuba; [3]Wakayama University; [4]J. F. Oberlin University

Experiments recruiting absolute pitch (AP) possessors whose age was ranging from 20s to 50s has showed that pitch tends to be perceived higher than the “correct” standard pitch as the age is getting higher. The degree of this AP shift cannot properly be predicted either by the hearing level of each participant or by the level of otoacoustic emission.

To investigate further the contribution of changes in the mechanical characteristics of the auditory periphery by aging, the bandwidths of auditory filters were measured for a part of the participants and compared to their performance in the AP judgment.

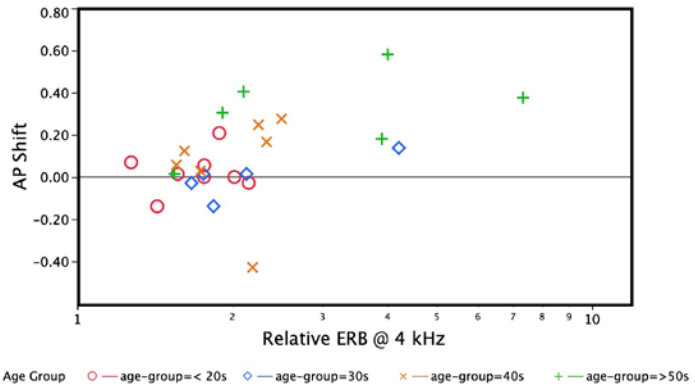

Twenty six participants were selected from a wide range of ages; their distribution was 8, 5, 7, and 6, respectively for, under 20s, 30s, 40s, and over 50s. The selection was not completely random. Participants who showed a clear tendency of the AP shift were selected with a higher priority for each age group. The measurement of the auditory filter bandwidth was performed with Rion Auditory Filter Measuring System HD-AF, which was developed to achieve a prompt measurement by applying the adaptive band-widening of notch noises. A session of measurements for five center frequencies, i.e., 250, 500, 1000, 2000, 4000 Hz, lasted about an hour.

The equivalent rectangular bandwidth (ERB) was estimated for each of the center frequencies, and its ratio relative to the standard value was calculated. A multiple regression analysis was performed for the degree of the AP shift with the five ERB ratios and the age as independent valuables. Only the ERB ratio at 4000 Hz showed a statistically significant correlation to the degree of AP shit. As the ERB ratio at 4000 Hz increased, the degree of the AP shift tended to increase.

It showed a significant correlation to the age, while the ERB ratios for the other center frequency did not.

The current result indicates that the widening of the auditory filter at 4000 Hz might lead to the upward AP shift. It is, however, difficult to hypothesize a rational mechanism why it should. The literatures on the psychophysics have told that the phase locked neural coding plays the major role to perceive the musical pitch while the place coding based on the mechanical characteristics of the basilar membrane is less important. Further investigations with more critical stimuli are necessary to explain the mechanism of age related AP shift.

PS-320

Age-Related Hearing Loss: Predicted Age-Specific Incidence, Based on Cross-Sectional, Age-Specific Prevalences, Compared with Observed Age-Specific Incidences from a Longitudinal Study

Howard Hoffman[1]; Howard J. Hoffman[1]; **Chuan-Ming Li[1]**; Christi L. Themann[2]; Hannes Petersen[3]; Mary Frances Cotch[4]; Lenore J. Launer[5]; Charles Della Santina[6]; Vilmundur Gudnason[7]

[1]National Institute on Deafness and Other Communication Disorders (NIDCD), National Institutes of Health (NIH); [2]National Institute for Occupational Safety and Health (NIOSH), Centers for Disease Control and Prevention (CDC); [3]University of Iceland and Landspitali University Hospital; [4]National Eye Institute (NEI), National Institutes of Health (NIH); [5]National Institute on Aging (NIA), National Institutes of Health (NIH); [6]Johns Hopkins School of Medicine; [7]Icelandic Heart Association and University of Iceland

Introduction

Prevalence is frequently measured in cross-sectional health surveys. While prevalence is important, so is incidence: the number of new cases observed (e.g., hearing impairment) within a specified duration. Because longitudinal studies are costly and time-consuming, statistical approaches have been used to convert age-specific prevalence into 'predicted' age-specific incidence for irreversible, nonfatal conditions (Leske, 1981).

Objective

Determine efficacy of using predicted, in lieu of observed, incidence for age-related hearing loss (ARHL).

Methods

Trained staff of The Age, Gene/Environment Susceptibility–Reykjavik Study, 2002–2006, conducted pure-tone, air-conduction audiometric exams on a population-based cohort of 5,172 adults aged 66–96 years. Repeat hearing exams were performed five years later (n=3,049). Hearing thresholds were measured in sound isolation booths at frequencies 0.5–8 kHz. We defined hearing impairment (HI) using the WHO-Global Burden of Disease classification: better ear (BE), pure-tone average (PTA) of thresholds at 0.5,1,2,4 kHz (PTA_{5124}) $\geq$35 dB hearing level (HL). The prediction method used logistic regression to smooth age-specific HI prevalences and transformed these with simple functional equations to convert smoothed prevalences into predicted 5-year HI incidences.

Results

For 3,049 older adults studied longitudinally, HI prevalence was 25.1% at initial exam and increased to 42.7% five years later. For women, age-specific, 5-year predicted incidence estimates were closely aligned with observed incidences at younger ages, 66–77 years, but diverged as age increased. The pattern was similar for men, although divergence occurred much earlier at age 70. After stratifying for reported noise exposure history prior to initial exam, the predicted incidence was significantly higher ($p<0.001$) than observed incidence. Men without noise exposure history had a pattern similar to women. With or without noise exposure history, the *observed* 5-year incidences for men were almost identical across all ages. However, the *observed* incidence for women was significantly increased compared to men; this results in convergence of HI prevalence for men and women past 85 years of age. For more extreme degrees of hearing impairment, *e.g.,* BE PTA_{5124} $\geq$50 dB HL, the predicted and observed incidences were nearly identical across the whole older adult age range.

Conclusions

Our results illustrate some drawbacks in predicting ARHL incidence from age-specific prevalence. Men who reported prior noise exposure had increased levels of predicted versus observed incidence, probably attributable to higher initial HI prevalence. Our finding of increased HI incidence for older women is significant. This study confirms other studies reporting no association between prior noise exposure and incident HI in older adults.

PS-321

Immunocytochemical Localization of NaKATPase in the Human Inner Ear and Changes with Age

Seiji Hoskawa; Kumiko Hosokawa; **Ivan Lopez**; Fred Linthicum; Gail Ishiyama; Akira Ishiyama

David Geffen School of Medicine, University of California, Los Angeles

Background

The ion transporter enzyme NaKATPase is the predominant factor for maintaining the osmotic gradient across the plasma membrane by providing the force for water transport. Its localization in the inner ear of several animal models has been well documented. We present a detailed study of its distribution in the normal human inner ear and changes in expression with age and disease.

Methods

The expression of NaKATPase in the human cochlea was investigated by indirect immunohistochemistry using formalin-fixed celloidin-embedded (FFCE) human temporal bone sections. A mouse monoclonal antibody against NaKATPase-alpha-1 subunit was used in this study. Temporal bones of 29 patients (12 male and 17 female) ranging from 42 to 97

years of age, with an average age of 75.5 years old (temporal bones with 11 normal auditory function, 4 Meniere's disease, and 21 other otological diseases) were used in this study. Image acquisition and quantitative analyses were made using micrographs acquired at 100x. NaKATPAse-immunoreactive area was quantified using the computer image analysis software ImageJ, version 1.48. Univariate analysis of variance analysis (ANOVA) was performed to test an association between the variables "Age <70 years-old Group" and "Age 70> years-old Group". Post-hoc individual univariate group comparisons were made for any significant results. A p-value of 0.05 was used in all statistical tests for establishing significance.

Results

NaKATPase-IR was detected in fibrocytes of the spiral ligament and the stria vascularis, in supporting cells of the organ of Corti but not in hair cells. In the spiral ganglia, NaKATPase-IR was seen in satellite cells but not in neurons. Mild expression of NaKATPase was detected in spiral limbus, and Reissner's membrane. NaKATPase-IR distribution was similar on the basal, middle, and apical turns of the cochlea. There was a significant increased of NaKATpase-IR in the spiral ligament of older age individuals. There was a statistically significant difference between the "Age <70 years-old Group" and "Age 70> years-old Group" (p=0.030). NaKATPase-IR was also present in nerve terminals of the vestibular sensory epithelia of the cristae and maculae.

Conclusion

The ubiquitous localization of NaKATPase in the human inner ear suggests an important role in homeostasis. Immunoreactive patterns in the human cochlea paralleled those seen in other animal models. The consistent and reliable detection of NAKATPase-IR in all temporal bone specimens suggest that this protein marker can be used to investigate the normal human inner ear cytoarchitecure and changes with age and/or disease.

PS-322

Preliminary Findings of Hear Here Alabama Project in West Central Alabama

Marcia Hay-McCutcheon; Adriana Hyams; Brianna Panasiuk; Sarah Ondocsin; Katie Palmer; Mary Margaret James; Forest Scogin

The University of Alabama

Introduction

Identifying adults with hearing loss and providing appropriate intervention could potentially improve the lives of many adults living in the state of Alabama. Considering that approximately 22% of the Alabama population is 55 years or older and that the state ranks 42nd in poverty levels, there could be a large percentage of the individuals that have both a hearing loss and have no resources to address the hearing loss. We need to understand the extent of hearing loss among this population and provide effective and appropriate assessment and intervention for these individuals. Currently, however, it is unknown how many people within Alabama have hearing losses and also have no access to hearing health care. The main goals of this study are: 1) to identify the prevalence of hearing loss of adults living in Alabama, and 2) to identify how hearing loss impacts the general physical and emotional health of these individuals.

Methods

A battery of tests was administered to adults 19 years of age or older. Pure-tone thresholds were obtained at 250 Hz, 500 Hz, 1000 Hz, 2000 Hz, and 4000 Hz. The Continuous Visual Memory Test (CVMT) required study participants to state whether or not a diagram shown to them was "OLD" if previously seen or "NEW" if never seen. Additionally, the SF-36 Health Survey (1992 Medical Outcomes Trust), which is designed to measure the health status from the client's point of view and the Charlson Comorbidity Index, which is designed to be used to evaluate the impact of comorbid conditions among study participants at the time of their enrollment into the study, were administered.

Results

Preliminary analyses using data from 193 adult study participants living in west central Alabama have suggested that hearing loss is associated with health status [$F(13, 149) = 31{,}270.16$, $p < 0.0001$], physical functioning [$F(13, 149) = 2.22$, $p = 0.034$], social functioning [$F(13, 149) = 3.023$, $p = 0.007$], and emotional role functioning [$F(13, 149) = 2.523$, $p = 0.018$]. Additionally, the degree of hearing loss was not associated with visual working memory skills.

Summary

Our results suggest that hearing loss is associated with other health issues in addition to the emotional well-being of individuals. This preliminary study is the first in a series of studies that will be conducted to improve the emotional and physical well-being of adults living in Alabama.

PS-323

Age Effects in Discrimination of Temporal Intervals Within Accented Sequences Differing In Sequence Rate and Type of Accent

Peter Fitzgibbons[1]; Sandra Gordon-Salant[2]

[1]University of Maryland, College Park; [2]University of Maryland

Background

Perceived stress or accent within speech or non-speech sound sequences can be introduced simply by elongating the duration of one or more sequence components. Earlier experiments have shown that the presence of accented components can diminish listener sequential temporal sensitivity (Hirsh et al., 1990), particularly for older listeners (Fitzgibbons & Gordon-Salant, 2010). The present study uses tone sequences to explore the relative influence of tonal accent and interval accent on temporal discrimination performance by younger and older listeners. The relative effects of sequence presentation rate and repetition of embedded target cues are also examined.

Methods

Reference stimulus sequences ("unaccented") consisted of six 40-ms 1000-Hz tone bursts, each separated equally by

silent intervals to create tonal inter-onset intervals (IOI) of 200ms or 100ms. These two IOIs established slower and faster sequence presentation rates, respectively. Accent within sequences was introduced by elongating the second tonal component by 100% (tone accent) or the second tonal IOI by 100 % (interval accent). For each discrimination condition, adaptive forced-choice procedures were used to measure a duration DL for increments of one or two successive targeted sequence intervals following the accented component. A total of 12 experimental sequences included 3 sequence types (unaccented, tonal accent, interval accent), 2 presentation rates, and 2 target-number conditions (one or two sequcnce intervals). Listeners included younger normal-hearing adults and two groups of older adults with and without hearing loss (N = 13/group). Stimuli were presented monaurally via insert earphone at 85 dB SPL.

Results

The duration DLs of the two older listener groups were equivalent, indicating that hearing loss did not influence discrimination performance. Younger listeners exhibited better target interval discrimination than older listeners for each stimulus condition. Discrimination performance was poorer for the accented sequences, compared to the unaccented sequences. Sequences featuring interval accents with the faster presentation rate produced the poorest discrimination performance in each listener group. Listeners also exhibited improved discrimination in conditions featuring two target intervals versus one, especially for accented sequences.

Conclusions

Sequence accent diminishes listener temporal discrimination performance, most notably for faster sequence rates. Older listeners have difficulty discriminating temporal intervals within accented sequences. However, repetition of a target interval improves discrimination performance, particularly for accented sequences. The results can be used to aid our understanding of sequential processing, and the specific age-related processing difficulties observed with samples of accented speech sequences.

PS-324

Effects of Age on Binaural Frequency Representation: Interaural Phase Differences and Frequency-following Responses

Christopher Clinard; Caitlin Cotter; Larissa Heckler; Mary Ellen Scherer

James Madison University

Background: Older adults, even with clinically normal hearing sensitivity, have difficulty understanding speech in the presence of background noise. This difficulty may be partly due to age-related declines in the neural representation of sounds.

Methods

Adults with clinically normal hearing sensitivity (thresholds ≤ 25 dB HL at octave frequencies 0.5 – 4.0 kHz) participated in this study. There were three groups of participants: younger (ages 21 – 25), middle-aged (ages 38-50), and older (ages 62-73). Two adaptive psychoacoustic tasks were used for testing perception of interaural phase differences (IPDs): IPD discrimination across frequencies and IPD discrimination for fixed frequencies. The across-frequency task determined the upper frequency limit of IPD discrimination using 180º, or π radian, IPDs. The fixed-frequency task assessed the ability to discriminate IPDs at four carrier frequencies: 500, 750, 1000, and 1125 Hz. Frequency-following responses (FFRs), which are dependent on phase-locked neural activity, were used to examine a neural representation of frequency; FFRs were elicited in monaural and binaural conditions by tone-bursts with carrier frequencies of 500, 750, 1000, and 1125 Hz. All stimuli were presented at 80 dB SPL. Analysis of FFRs included FFT-based measures of amplitude, stimulus-to-response correlations, and monaural-binaural differences.

Results

Behavioral interaural phase difference measures became poorer in middle-aged and older groups, for both the upper-frequency-limit task as well as the fixed frequency task. Age-related declines in FFR amplitude and stimulus-to-response correlations were observed, particularly at the higher frequencies.

Conclusions

These results suggest that binaural perception and binaural neural representation of frequency is negatively affected by age, even in the absence of significant hearing loss. Physiological findings are consistent with middle-aged and older adults having degraded phase-locked representations of frequency.

PS-325

Aging Affects the Perception and Subcortical Neural Representation of Musical Harmony

Oliver Bones; Christopher Plack

University of Manchester

Introduction

When two musical notes with simple frequency ratios are played simultaneously the resulting two-note musical chord (dyad) is pleasing and evokes a sense of *consonance*. Complex frequency ratios, on the other hand, evoke feelings of tension or *dissonance*. Consonance and dissonance form the basis of *harmony*, a central component of Western music. In earlier work we provided evidence that consonance perception is based on neural temporal coding in the brainstem (Bones et al., 2014, *Neuropsychologia*). Other work suggests that aging may be associated with a decline in temporal coding. Here we tested the hypothesis that, for listeners with clinically normal hearing, aging is associated with a decline in both the perceptual distinction of consonant and dissonant dyads and the distinctiveness of their neural temporal representations.

Methods

All participants had clinically normal hearing thresholds (≤ 20 dB HL) at octave frequencies between 250 and 2000 Hz. Participants were non-musicians. Forty-four (27 female) participants aged 18-81 (mean = 38.0, *SD* = 20.5) participated in the study. Dyads were created by combining each of eight

low notes with 11 high notes in the octave above, making 88 dyads in total. Behavioral methodology reported elsewhere (McDermott et al., 2010, *Current Biology*) was used to record individual pleasantness ratings for dyads and to calculate consonance preference scores. To control for a possible effect of age on general affect, participants also rated different categories of affective voice for pleasantness. The frequency-following responses (FFRs) to a consonant dyad and to a dissonant dyad were also recorded for each participant.

Results
Compared to younger listeners, older listeners rated consonant dyads as less pleasant and dissonant dyads as more pleasant. The effect of age interacted with type of stimulus (dyad or voice) and the association between age and perception of musical harmony remained when controlling for individual variation in voice preference. The distinctiveness of the neural temporal representation of consonant and dissonant dyads (neural consonance index; NCI) also correlated negatively with age. Furthermore NCI correlated with preference for consonance over the sample as a whole.

Conclusions
Aging is associated with a decline in the perception of musical harmony, and this decline is related to a deterioration in neural temporal coding.

PS-326

Association study on genetic factors contributing to age-related hearing loss

Hui Li[1]; Megan Kobel[1]; Brent Spehar[2]; Nancy Tye-Murray[2]; Robert Frisina[3]; Jianxin Bao[1]
[1]Northeast Ohio Medical University; [2]Washington University in St. Louis; [3]University of South Florida

Background
Age-related hearing loss (ARHL), also known as presbycusis, is a universal feature of mammalian aging and is characterized by a decline of auditory function, such as increased hearing thresholds and poor frequency resolution, starting at high frequency regions. In human, ARHL is contributed by a combination of genetic and environmental factors. Previous genome-wide association studies (GWAS) failed to identify genetic variations that account for the variability of hearing ability with age, suggesting that ARHL is caused by collective effect of many causative genetic elements with small influence. To identify these less significant genetic elements, more stringent sampling, more powerful technology to detect rare genetic variants and more robust statistical methods are required.

Method
We obtained a dataset including 636 subjects over 55 years old from the Rochester, NY greater metropolitan area. The hearing ability of each subject were measured by a battery of auditory tests: pure tone audiogram, supra-threshold Gap detection, speech recognition thresholds and Hearing in Noise Test. The subjects were classified into five groups based on pure tone audiogram: golden ear (GE), flat, high-frequency steep slope (HFSS), high-frequency gentle slope (HFGS) and mixed, each of which represents a unique audiogram configuration. The representative members from each group were selected for whole exome sequencing (WES), which is a powerful technology to detect both common and rare variants in the protein-coding regions of human genome.

Results
WES data from 106 subjects were collected with average 39,769 single-nucleictide polymorphism (SNPs) and 3531 insertion/deletion (indels) per subject. The attempt to identify SNPs associated with ARHL defined by pure tone thresholds didn't yield any genome-wide significant association, consistent with previous findings.

Conclusion
Our results confirmed that ARHL is a complex trait and contributed collectively by SNPs that fail to reach genome-wide significance. New statistical methods to identify ARHL-associated genetic patterns which represents a collection of genetic elements need to be developed.

PS-327

Targeted Deletion of Oncomodulin Changes Sensitivity to High Frequencies before causing Progressive Hearing Loss.

Dwayne Simmons[1]; Aubrey Hornak[1]; M. Charles Liberman[2]
[1]University of California, Los Angeles; [2]Mass. Eye and Ear Infirmary and Harvard Med. Sch.

Background
The tight regulation of Ca^{2+} is essential for cochlear function, and yet the role of Ca^{2+} binding proteins remains elusive. Oncomodulin (Ocm), a member of the parvalbumin family, is expressed in outer hair cells (OHCs), especially near the OHC lateral membrane in basal (high frequency) regions and more diffusely localized within OHCs from apical (low frequency) regions.

Methods
To study the role of Ocm in the cochlea, we generated a conditional Cre-lox knockout line driven by the β-actin promoter (*Ocm*$^{tm1.Ddsi}$) expressed at embryonic day 1. The absence of Ocm expression was confirmed by RT-PCR and immunocytochemistry. Cochlear function was assessed by auditory brainstem responses (ABRs) and distortion product otoacoustic emissions (DPOAEs). Hair cells were counted in cochlear wholemounts stained with anti-myosin VIIa, phalloidin (for actin) and DAPI.

Results
At 1 - 2 months Ocm mutants demonstrated enhanced thresholds (i.e., greater sensitivity) at frequencies above 8 kHz, by as much as 15 dB between 16 kHz and 45 kHz. Correspondingly, suprathreshold DPOAE amplitudes were enhanced at high frequencies. However, by 3 months, thresholds in Ocm mutants had begun to deteriorate, with threshold elevation of 5 - 10 dB above 16 kHz. By 4 months Ocm mutants showed a 50 - 60 dB threshold elevation at frequencies above 8 kHz. In contrast, wild-types at 7 months demonstrated little or no threshold elevation. There was no significant hair cell loss in either genotype prior to 2 months. However by 3 - 4 months, hair cell loss was more pronounced in Ocm mutants at 16 and

32 kHz regions, particularly in the first OHC row. OHC loss was patchy, with long stretches of normal appearing OHCs interrupted by short stretches with complete OHC loss. Some Ocm mutants with significantly elevated thresholds, had little or no OHC loss in corresponding cochlear regions. Inner hair cell loss was minimal.

Conclusions

The lack of Ocm leads to enhanced cochlear sensitivity at higher frequencies in young mice. However, this heightened sensitivity is associated with increased vulnerability such that mutant mice show accelerated hair cell damage and threshold elevation as the mice mature. Ocm may protect OHCs by decreasing the magnitude of Ca^{2+} transients, thereby decreasing OHC response magnitudes.

PS-328

Temperature Elevation During Endoscopic Ear Surgery: Understanding Contemporary Surgical Techniques and Limitations

Parth Shah; Elliott Kozin; Daniel Lee
Massachusetts Eye and Ear Infirmary

Introduction

Rigid endoscopes provide greater surgical access and superior visualization of the middle ear using a transcanal approach compared to the operating microscope. However, prior studies have suggested that the heat transfer from the light source to the tip of the endoscope can be associated with significant temperature elevations in a human temporal bone model as well as auditory threshold elevations in an animal model. Proposed methods to reduce temperature elevation during endoscopic ear surgery (EES) include removal of the endoscope at regular time intervals and co-application of suction. Herein, we aim to quantify the duration of middle ear exposure to endoscopic illumination during EES.

Methods

We retrospectively reviewed cases of endoscopic tympanoplasty from February 2014 to July 2014 (n=7). Measurements included time of exposure of the middle ear and promontory with the endoscope alone (Group A) and endoscope with suction (Group B). The number of times and duration that the endoscope was removed from the middle ear were also recorded. Descriptive analysis was performed.

Results

Mean patient age was 42 ± 7.6 (SD) years and average procedure length was 110.3 ± 30.0 (SD) minutes. After elevating the tympanomeatal flap, mean of total length of time that the endoscope was alone in middle ear without suction was 26.7 ± 13.2 (SD) minutes. Median time that the endoscope was placed alone in middle ear was 24 seconds and maximum time spent in middle ear was mean 240.3 ± 110.1(SD) seconds. Mean of total length of time that suction was placed in the ear alongside the endoscope was 4.5 ± 1.9 (SD) minutes. Median time that endoscope and suction were in the ear was 17 seconds with a maximum exposure of mean 46.9 ± 18.3 (SD) seconds. The median time that the endoscope was held outside the ear was 4 seconds.

Conclusion

We find that the endoscope resides in the middle ear without a cooling mechanism on average 26.7 ± 13.2 (SD) minutes throughout the procedure. Given previous human cadaveric and animal studies demonstrating significant heat transfer to the cochlea as well as elevation in auditory brainstem response thresholds, we recommend refinement of surgical techniques in EES to avoid prolonged thermal exposure. These data also have implications for further technical development of new instruments for endoscopic ear surgery.

PS-329

Pediatric Cochlear Implantation and Size of Cochlear Nerve Aperture

Maryanna Owoc; Elliott Kozin; Alyson Kaplan; Sid Puram; Rosh Sethi; Barbara Harrmann; Hugh Curtain; Daniel Lee; Michael Cohen
Massachusetts Eye and Ear Infirmary

Introduction

Previous studies demonstrate a relationship between sensorineural hearing loss (SNHL) and cochlear nerve aperture (CNA) diameter. However, it is unclear if CNA diameter changes with age, potentially confounding previous studies. Further, few studies have examined CNA diameter in cochlear implant (CI) recipients. Herein, we aim to 1) determine if size of CNA changes as a function of age in patients 0-4 years old, and 2) investigate CNA diameters and preoperative pure tone averages (PTA) in pediatric patients with CI.

Methodology

We retrospectively identified all subjects ages 0-4 years that visited our institution between 2009 and 2014. Inclusion criteria for SNHL study arm included patients with an ICD9 diagnoses of sensorineural hearing loss, as well as available audiogram and temporal bone computed tomography (TB-CT) scan (n=36 ears). Control subjects included patients undergoing TB-CT for reasons other than SNHL (n=50 ears) that also had an audiogram. CNA size was measured based on previously published methodology by two independent observers.

Results

Interobserver variability showed an intraclass correlation coefficient [R_i] = 0.949. Patients with SNHL had a smaller CNA diameter compared to control group (1.94 mm +/- standard deviation [SD] 0.83 vs. 2.35 mm +/- [SD] 0.22, p=0.001). There was no difference in CNA size in patients less than 2 (2.31 mm +/- [SD] 0.24) and patients 2-4 years old (2.40 mm +/- [SD] 0.19), p=0.158. Furthermore, no significant correlation was observed between CNA size and age (r=0.059, p=0.686). CI subjects were categorized into two groups based on CNA size. No difference in PTA (average threshold of hearing at 500, 1000, and 2000 Hz) was found between hypoplastic CNA (n=10 ears, 96.30 dB +/- [SD] 16.93) and normal CNA (n=15 ears, 96.73 dB +/- [SD] 14.61), p=0.946.

Conclusion

These results provide the largest analysis of CNA diameter and preoperative PTA in pediatric CI patients to date. The data confirms the relationship between CNA size and pro-

found SNHL. CNA size does not correlate with age in our study population. Further, there was no association between preoperative PTA and size of CNA in CI patients. These data have implications for preoperative evaluation of CI patients. Ongoing analysis includes correlation of CNA size and CI outcomes. A larger patient sample size is needed to confirm this initial analysis.

PS-330

Does the Anatomy of the Cochlea influences the Hearing Outcomes in Simultaneous Bilateral Cochlear Implanted Adults?

Daniele De Seta; Yann Nguyen; Evelyne Ferrary; Olivier Sterkers; Isabelle Mosnier
Université Pierre et Marie Curie, Paris

Objective

To investigate the influence of the differences of cochlear anatomy and electrode arrays position within the cochlea over the hearing outcomes in a group of bilateral simultaneous cochlear implanted adults (Med-El, Combi 40+) with 5 years follow up.

Material and Methods

Nineteen patients were followed up for 5 years in a prospective multicenter study; speech comprehension tests (disyllabic words) were performed before implantation, 3, 6, 12 months and 5 years after activation. Radiological analysis was performed on postoperative high-resolution CT scan. The major cochlear diameter and the cochlear height were calculated. The electrode to modiolus distance (EMD) for the electrodes at 180° and 360° and the angle of insertion of the array were measured.

Results

Bilateral performances tend to remain stable at 5 years follow-up after an initial improvement during the first year. Hearing tests at 5 years show that 'good performers' obtain lower scores in the better ear and in the bilateral hearing, on the other hand there is an improvement in the performance of the poorer ear (+18% in SNR +10, $p<.05$). On the contrary within the 'poor performers' there is a general tendency to improve the hearing performances for both ears tested alone and in bilateral condition, both in silence and in noise. Diameter and height of the cochlea resulted correlated ($r=.525$, $p=.01$). The mean angle of insertion for totally inserted arrays was 643° ± 93°. Major cochlear diameter resulted positively correlated to the EMD at 180°($r=.581$, $p<.001$), to the EMD at 360°($r=.471$, $p=0.003$) and negatively correlated to the angle of array insertion within the cochlea ($r=-.632$, $p=.001$). No correlation was found between the depth of insertion and hearing performances both at 1 year and at 5 years follow up, however EMD distance at 180° was correlated to the performances in silence and in noise at 1 year.

Conclusion

In the long term follow-up, bilaterally implanted patients with initial poor hearing performances improve their comprehension score especially in noise and the difference in hearing discrimination score between the two ears tend to reduce. The cochlear anatomy influences the hearing performances in the first year after implantation but this relationship is lost in the long term follow-up; the intraindividual differences between the two cochleas do not justify the different outcomes between the two ears.

PS-331

Auditory Brainstem Implant Candidacy in the United States in Children 0-17 Years Old

Alyson Kaplan; Elliott Kozin; Sid Puram; Maryanna Owoc; Parth Shah; A. E. Hight; Rosh Sethi; Aaron Remenschneider; Daniel Lee
Massachusetts Eye and Ear Infirmary

Introduction

Advances in neuroprosthetic technology have ushered in a new era for children with hearing loss. The auditory brainstem implant (ABI) is an option for hearing rehabilitation in profoundly deaf patients ineligible for cochlear implantation. No study has examined the potential unmet need for ABIs in the United States (US). Herein, we aim to quantify the potential number of pediatric ABI candidates.

Methods

A systematic literature review was conducted to identify studies detailing the prevalence of congenital cochlear and/or cochlear nerve (CN) anomalies. Absolute indications for ABI include bilateral cochlea or CN aplasia (Group A), and relative indications for ABI include bilateral cochlea or CN hypoplasia (Group B). Data was subsequently correlated to the US Census Bureau, the National Health Interview Survey, and the Gallaudet Research Institute to provide a rough estimation of pediatric ABI candidates.

Results

Twenty three studies with relevant radiographic data were identified. Rates of cochlear and CN anomalies varied widely. Out of children with known sensorineural hearing loss, cochlea aplasia was identified in 0-8.7% (median 0.21%), CN aplasia in 0-19% (median 3.57%), cochlea hypoplasia in 0-11.1% (median 3.55%), and CN hypoplasia in 0-14.3% (median 2.35%). Twelve studies documented rates of bilateral findings. Bilateral cochlea aplasia was identified in 0-8.7% of patients and bilateral CN aplasia in 0-4.76% of patients (Group A). Bilateral cochlea hypoplasia was identified in 0-8.7% of patients and bilateral CN hypoplasia in 0-5.4% of patients (Group B). Using population-level data on sensorineural hearing loss, we estimate a rate of approximately 1.56 per 100,000 children in the US with absolute indications for ABI and 2.62 per 100,000 children with relative indications for ABI.

Conclusion

Congenital cochlear and cochlear nerve anomalies are exceedingly rare, however there is clearly a distinct cohort of patients who may benefit from ABI technology. This study provides the first preliminary estimate of cochlea and CN aplasia/hypoplasia at the population level albeit with limitations based on available data. These data suggest the need for dedicated pediatric ABI centers to focus expertise and management.

PS-332

Short-Term-Effects of Compression of Temporal Lobe during Middle Fossa Acoustic Neuroma Surgery on Contralateral Speech Discrimination

Magnus Teschner[1]; Carl Lang[2]; Rolf Salcher[2]; Sabine Haumann[2]; Thomas Lenarz[2]

[1]Hannover Medical School; [2]Department of Otolaryngology, Hannover Medical School

Aim

Middle Fossa Acoustic Neuroma Surgery is associated with compression of the temporal lobe. The question arises weather this compression affects the functionality of the auditory cortex.

Material and Method

In patients, who underwent acoustic neuroma surgery, contralateral speech discrimination was tested pre- and post surgery using different speech discrimination tests. Results of patients with a middle fossa approach were compared with patients with a translabyrinthine approach.

Results

No major differences between the translabyrinthine and the middle fossa approach could be detected.

Conclusion

Compression of the temporal lobe during middle fossa approach acoustic neuroma surgery does not lead to short term impaired contralateral speech discrimination compared to translabyrinthine approach.

PS-333

Results on Laryngeal Pacing for Unilateral Vocal Fold Paralysis

Fangyi Chen[1]; Taiping zeng[1]; Zhiping Zhang[2]; Fei Zhang[1]; Yongbin Shi[3]

[1]South University of Science and Technology of China; [2]shihezi university, China; [3]Oregon Health and Science University

In this study, we developed an instrument system to test the feasibility of reactivating and synchronizing the unilaterally paralyzed vocal fold in a dog model. Unilateral vocal fold paralysis was induced by destruction of the left recurrent laryngeal nerve (RLN). Electromyography (EMG) activities from ipsilateral CT muscle during the breathing were recorded and used to trigger stimulation of ipsilateral vocalis muscles for synchronized adduction of the paralyzed cord. The EMG during breathing, rather than artificial electrical stimulation of vocal cord nerves (such as vagus nerve), was chosen to avoid the stimulus artifact in EMG recording. The vocal fold motion was continuous monitored during the experiment with an endoscope. During the intense breathing, the EMG signal was significantly above the noise level and sufficient to trigger the muscle stimulation. This signal was sampled and analyzed by a micro-controller-based system to generate the electrical pulse to stimulate the cricoarytenoid muscle. Different pulse parameters were tested and pulses of 2 mA intensity and 10 ms pulsewidth were chosen to induce proper vocal fold motion. With the closed loop of EMG recording and muscle stimulation, the vocal fold at the paralyzed side was reactivated and the motion was synchronized to that at the health side. This result demonstrated the feasibility of the ipsilateral laryngeal pacing for unilaterally paralyzed vocal fold.

PS-334

Increased Phosphatidylcholine (16:0/16:0) in the Folliculus Lymphaticus of Warthin Tumor

Yoshinori Takizawa[1]; Qian He[2]; Takahiro Hayasaka[3]; Noritaka Masaki[3]; Yukiko Kusama[4]; Jun Okamura[5]; Kunihiro Mizuta[5]; Hiroyuki Mineta[5]; Mitsutoshi Setou[3]

[1]Hamamatsu University school of Medicine; [2]Department of Otolaryngology-Head and Neck Surgery, First Affiliated Hospital of Guangxi Medical University; [3]Department of Cell Biology and Anatomy, Hamamatsu University School of Medicine; [4]Department of Diagnostic Pathology, Hamamatsu University School of Medicine; [5]Department of Otorhinolaryngology/Head & Neck Surgery, Hamamatsu University School of Medicine

Warthin tumor (War-T), the second most common benign salivary gland tumor, consists mainly of neoplastic epithelium and lymphoid stroma. Some proteins and genes thought to be involved in War-T were evaluated by molecular biology and immunology. However, lipids as an important component of many tumor cells have not been well studied in War-T. To elucidate the molecular biology and pathogenesis of War-T, we investigated the visualized distribution of phosphatidylcholines (PCs) by imaging mass spectrometry (IMS). In our IMS analysis of a typical case, 10 signals were significantly different in intensity ($p < 0.01$) between the War-T and non-tumor (Non-T) regions. Five specific PCs were frequently found in the War-T regions of all of the samples: $[PC (16:0/16:0) + K]^+$ (*m/z* 772.5) , $[PC (16:0/20:4) + K]^+$ (*m/z* 820.5), $[PC (16:0/20:3) + K]^+$ (*m/z* 822.5), $[PC (18:2/20:4) + K]^+$ (*m/z* 844.5) and $[PC (18:0/20:5) + K]^+$ (*m/z* 846.5). PC (16:0/16:0). PC (16:0/16:0) was increased specifically in the folliculus lymphaticus of War-T lymphoid stroma suggesting a different metabolism. Localization of PC (16:0/16:0) might reflect inflammation activity participating in the pathogenesis of War-T. Thus, our IMS analysis revealed the profile of PCs specific to the War-T region. The molecules identified in our study provide important information for further studies of War-T pathogenesis.

PS-335

Difference of TTSS effector gene genotypes and it's implication to antibiotics resistances in isolates of Pseudomonas aeruginosa from chronic otitis media

Min-Hyun PARK; So Young Kim; Eun Yun Roh; Ho Sun Lee

Boramae Medical Center, Seoul Metropolitan Government-Seoul National University, Seoul, Korea

Pseudomonas aeruginosa (P. aeruginosa) is one of the important pathogen in chronic otitis media (COM). In *P. aeru-*

ginosa infection, type 3 secretion system (T3SS) is most important virulence factor. To estimate the prevalence of T3SS genes, especially distribution of *exoU* and *exoU* genes and their association with antibiotics resistances in COM, we compared prevalence of T3SS genes between isolates from COM and pneumonia or bacteremia. The antibiotics susceptibilities were also examined in each isolates. As results, COM group manifested significantly more e*xoU* positive than control group, 70.6% in COM group, and 6.7% in control group (*P*<0.01). Furthermore, COM patients with *exoU* showed significantly more antibiotic resistances to ciprofloxacin and tobramycin (*p=0.035*), but no significant difference in control group. This high incidence of *exoU positive P. aeruginosa* and ciprofloxacin resistance can explain the chronicity and intractability of infection in COM, and elucidate this pathogenicity will pave the way to new treatment options for COM patients.

PS-336

Analysis of the Protein Expression Profile of Vestibular Schwannoma using MALDI-TOF-MS: Conflicting Roll of Apoptosis

Jae-Hyun Seo; Kyoung-Ho Park; Yong-Soo Park
The Catholic University of Korea

Introduction

Proteomic analysis by two-dimensional electrophoresis (2-DE) and matrix-assisted laser desorption and ionization time-of-flight mass spectrometry (MALDI-TOF MS) facilitates identification and characterization of specific proteins related to the pathogenesis of various diseases. In this study, we investigated the pathophysiology and mechanism underlying sporadic form of vestibular schwannoma by comparing vestibular schwannoma tissue with normal nerve tissue using proteomics.

Methods

Proteins were extracted from two vestibular nerve specimens and two vestibular schwannoma specimens and analyzed in parallel using 2-DE. We then analyzed 29 spots that were differentially expressed using MALDI-TOF MS. Upregulation of six proteins associated with apoptosis was confirmed by western blot analysis and immunohistochemistry.

Results

Twenty-nine proteins showing significant changes in the expression level between vestibular schwannoma tissue and normal nerve tissue were identified. Of these, seven proteins were related to apoptosis.

Conslusion

Our findings indicate that apoptosis is associated in a complex manner with the pathophysiology of vestibular schwannoma. The suppression of apoptosis is presumably involved in tumor occurrence and conversely, increased apoptotic expression contributes to the slow tumor growth rate and may be correlated with the Antoni type B area.

PS-337

The Safety and Efficacy of PF-04958242 in Age-Related Sensorineural Hearing Loss - A Randomized, Double-Blind, Placebo-Controlled, Single-Dose, Crossover Study

Martin Bednar[1]; Nick Demartinis[1]; Anindita Banerjee[1]; Laura Zumpano[1]; Francois Gaudreault[1]; Stephen Bowditch[2]; Frank Lin[2]
[1]Pfizer Inc; [2]Johns Hopkins

Introduction

AMPA (α amino-3-hydroxy-5-methyl-4-isoxazolepropionic acid) receptor mediated signaling plays a critical role throughout the neuroaxis of the auditory processing pathway. An approach that modulates activity dependent AMPA receptor mediated signaling at the ribbon synapse could plausibly enhance the ability of the limited population of spinal ganglion neuron synapses to transduce sounds. The action of AMPA potentiators to potentially amplify glutamate receptor signaling while preserving the spatial and temporal information encoded in endogenous synaptic activity may make this mechanism well suited to symptomatically improve deficits in sensorineural hearing loss.

Goals

To explore the potential for the AMPA potentiator mechanism to impact auditory function in subjects with mild to moderate age-related SNHL.

Methods

The trial was a single dose, double-blind, randomized, placebo-controlled, 3-way crossover study with two doses of PF-04958242 in 50 to 75 year old males and females with mild to moderate SNHL (N=44 randomized, N=41 received allocated treatment). The main outcomes and measures were pure tone average, speech discrimination score, and speech in noise testing change from baseline at one and five hours after a single dose of study treatment.

Results

The treatment was safe and well tolerated. Participants receiving PF-04958242 did not demonstrate a significant change from baseline in the study endpoints at 1 hour or 5-hours post-dose compared to placebo.

Conclusions

This clinical trial is the first-ever pharmacological study of a drug treatment for age-related SNHL and provides information with regard to study design, endpoints, variability, data characteristics, and operational feasibility to guide the design of future hearing loss trials.

PS-338

New Strategies and Methods to Prevent Reatresia / Restenosis of Reconstructed External Auditory Meatus (Re-EAMs)

Yihui Zou; Shiming Yang; Dong-yi Han
Institute of Otolaryngology

Objective

To explore new strategies and methods to prevent re- atresia / restenosis of reconstructed external auditory meatus (Re-EAMs) for congenital aural atresia / stenosis patients.

Methods

According to the reatresia / restenosis characteristics of Re-EAMs observed by the authors, a series of new prevention strategies, methods and relevant patent products are designed, measures include to improve the covering epithelium types and methods with all kinds of free skin & skin flap (207 ears), treat the junction area between tympanic membrane and Re-EAMs by artificial tympanic ring (our Patent No. ZL200820078991.5), support and expand the Re-EAMs with EAM expandor (our Patent No. ZL 720172847.3) and EAM modelbracket (our Patent No. ZL 200910242537.8).

Results

The restenosis / reatresia rate by using split thickness skin graft 16.9% (10/59) is significantly lower than those of Thiersch's skin graft in barrel-like 34% (17/50) ($P<0.05$) and mosaic 45.5% (15/33) ($P<0.01$), and there was no difference between the later two and other measures ($P>0.05$). The artificial tympanic ring improves the junction area morphology between tympanic membrane and Re-EAMs significantly. EAM expandor and EAM model bracket can support and expand the Re-EAMs well.

Conclusion

It is a new effective method to prevent restenosis/reatresia of the Re-EAMs) by mosaic grafting free thickness skin , implanting artificial tympanic ring, and supporting &. expanding Re-EAMs by EAM expandor and EAM model bracket, and worth of application .

PS-339

Vestibular Assessment in Children: Clinical Experience with Video Head Impulse Test

Angela Wenzel[1]; Karl Hoermann[2]; Manfred Huelse[2]; Roland Huelse[2]
[1]University Hospital Mannheim; [2]University Hospital Mannheim Department of Otolaryngology

Background

A standardized diagnostic protocol for children's vestibular assessment is still missing in daily clinical life. As rotatory chair testing and caloric test are usually not tolerated well by children, the aim of our study was to evaluate the importance and practicability of the video head impulse test performed in children.

Methods

65 children aged 3-16 years have been included in this prospective study. HVOR was assessed using a video-oculography system device (EyeSeeCam©). Gain at 40, 60 and 80msec has been measured. Furthermore it was evaluated how calibration of the system was tolerated by the participants, how the test itself was accomplishable in children and which difficulties arose during testing.

Results

Reproducible test results were accomplished in 49 children (75%). Median gain was 0.96 (+/- 0.37). A significant gain reduction between 40 and 80 msec was found ($p <0.05$). Catch-up saccades were found in 4 patients. Three of them were suffering from motoric retardation; one of them was later on diagnosed with bilateral semicircular canal aplasia. Performing the test approximately took 20 minutes, which is significantly longer than in adults ($p>0.05$). Calibration of the system with laser dots was easily doable in children aged 6 and older, whereas children between 3 and 5 years had more accurate calibration results using colorful little icons.

Conclusions

Video head impulse test is a sensitive and efficient vestibular test in children which is tolerated well by children aged 3-16 years. Therefore, video head impulse test can be easily used as a screening tool to detect vestibular dysfunction in the pediatric population.

PS-340

Utilizing System Identification Methods and Galvanic Vestibular Stimulation to Understand the Vestibular Contribution to Balance Control

Robert Peterka[1]; Adam Goodworth[2]
[1]Oregon Health & Science University; [2]University of Hartford

Introduction

Galvanic vestibular stimulation (GVS) provides a direct vestibular perturbation that can be used to investigate the vestibular contribution to balance control. However, the artificial nature of GVS needs to be understood when interpreting experimental results. The present study utilizes a model-based interpretation of experimental body sway responses to combinations of GVS and surface-tilt stimuli (STS) to identify how the vestibular contribution to balance changes as a function of test conditions and how GVS differs from natural vestibular stimulation.

Methods

Frontal-plane body sway of 9 young adults was evoked in 9 different eyes-closed test conditions using pseudorandom STS, GVS, and simultaneous mathematically uncorrelated STS and GVS. Sway angles of the lower (legs and pelvis) and upper (trunk and head) body segments were measured. Fourier analysis was applied to the stimulus and sway responses to compute frequency response functions (FRFs) that characterized the dynamic properties of balance control. Parameters of a multi-segmental balance control model [1] were identified that accounted for experimental FRFs. Different model structures were investigated to determine which accounted best for the unnatural vestibular stimulation provided by GVS.

Results
FRFs from the various test conditions were compared to identify differences in sway dynamics between responses to STS and GVS stimuli, stimulus amplitude-dependent changes, and interactions between simultaneously presented STS and GVS. When STS amplitude was increased while GVS amplitude remained constant, the STS FRFs changed indicating a coupled reweighting of proprioceptive and vestibular contributions to balance. The overall shapes of STS and GVS FRFs differed in ways indicating a lower bandwidth and an extended time delay for GVS responses. Modeling results showed that FRFs could be accounted for if we assumed that GVS perturbed only the vestibular angular velocity contribution to balance.

Conclusions
Responses to GVS suggest that GVS only influences vestibular angular velocity signals. This result is consistent with GVS evoking changes in semicircular canal afferent signals such that the vector combination from all 6 canals signals a net angular roll velocity [2]. Although otolith afferents are known to be sensitive to GVS, the wide directional distribution of otolith haircells results in no net GVS-evoked otolith angular position signal contributing to balance control. Understanding how humans respond to artificial vestibular stimulation in a variety of conditions is important for future work aimed at utilizing vestibular prostheses to improve balance control.

[1] Goodworth and Peterka, *J Neurophysiol*, 107:12-28, 2012.

[2] Fitzpatrick and Day, *J Appl Physiol*, 96:2301-2316, 2004.

PS-341

Subjective Visual Vertical Tilt Attraction to the Side of Rod Presentation: Effects of Age, Sex and vestibular disorders

Miche Toupet[1]; Christian Van Nechel[2]; Alexis Bozorg Grayeli[3]
[1]Dijon University Hospital, Dijon,Centre d'Explorations Fonctionnelles Otoneurologiques, and Institut de Recherche Oto-Neurologique (IRON), Paris, France; [2]Neurological Rehabilitation Department, Brugmann University Hospital, Brussels, Belgium; [3]Otolaryngology department, Dijon University Hospital, Burgundy UNiversity, and CNRS, UMR-6306, Electronic, Image and Computer Research Laboratory, Dijon, France

Introduction
The aim of this study was to evaluate the effect of initial rod position on the subjective visual vertical (SVV) tilt and to investigate the effect of sex and age on the SVV tilt induced by this initial position.

Materials and Methods
6420 consecutive patients with a large range of vestibular disorders and 315 control subjects underwent a complete clinical and instrumental work-up including SVV measurements. The mean age was 55 years (range: 3-97) and the sex ratio was 0.6. For SVV, the phosphorescent rod was presented in total darkness 12 times with a 45° deviation from the vertical alternatively on the right and the left. Each time, the patient was asked to place the rod at the vertical with a remote control.

Results
In average, each SVV measure was tilted to the side of the rod presentation. This effect gradually faded with the repetition of the measures. The visual attraction index defined by the sum of tilts after 12 measures, was higher in females than in males and greater in younger individuals (<20 years) and seniors (> 50) than in patients between 20 and 50 years old. This effect was independent from the type of the vestibular disorder.

Conclusion
The side of the rod presentation attraction influences the SVV tilt significantly influences the results regardless of the vestibular disorder. This effect is stronger in females, in children and in senior patients. It is probably related to the internal model of visual, otolithic and proprioceptive input processing.

PS-342

Serial cVEMP Testing is Sensitive to Disease Progression in Meniere Patients

Mark van Tilburg; **Steven Rauch**; Barbara Herrmann; John Guinan
Massachusetts Eye and Ear Infirmary

Introduction
Cervical vestibular evoked myogenic potentials (cVEMPs) are often used as a test in the diagnosis and follow up of Meniere's disease. In this study we evaluated whether progression of the disease can be monitored using the cVEMP. We also assessed whether peak-to-peak amplitude or threshold is more sensitive to change, and therefore better for monitoring Meniere's disease progression. Finally our pathological data are compared to data from healthy subjects.

Methods
All patients diagnosed with unilateral Meniere's disease between 2006-2013 and who had two cVEMP tests were included in this retrospective study. Patients with migraine-associated vertigo were excluded. The cVEMP was recorded at 4 frequencies and all 4 were included in our analysis. Both threshold and peak-to-peak amplitude assessments were made by one person using the normalized waveforms. Peak-to-peak amplitude was measured at 90 or 95dB HL. First and second test sessions and affected and unaffected ears were compared using t-tests. The results were compared with data obtained from healthy subjects using the same methods.

Results
29 patients with unilateral Meniere's disease met the inclusion criteria. The average time between tests was 28.3 months (SD 23.4 months). For the affected ear, thresholds from the second test were higher than those from the first test at all frequencies, and were significantly higher at 750 and 1000Hz. In contrast, the unaffected ear showed little difference in thresholds at any frequency between the first and the second test. At the first test Meniere patients showed a significant difference in interaural threshold difference at 500Hz, in the second test this difference was significant at all 4 frequen-

cies. Peak-to-peak amplitude measured at all frequencies showed very little difference between the first and second tests. Regardless of metric or frequency, the incidence of absent responses was substantially greater during the second test. Thresholds and PP amplitudes were worse in both ears of Meniere's patients than in normals.

Conclusion

cVEMP thresholds are sensitive to progression of Meniere's disease over time, showing elevation from first to second test. Peak-to-peak amplitude measures were far less sensitive to progressive change. The significant threshold difference between the first and second tests of the affected ear is interesting since it occurred mainly at high frequencies (i.e. 750 and 1000Hz). This supports the previous hypothesis that the resonance in the saccule changes as the disease progresses.

PS-343

Safe Direct Current Stimulator Valve Optimization for Vestibular Prosthesis

Evan Kararo; Kevin King; Yang Hong; Charles Della Santina; Gene Fridman
Johns Hopkins University

We showed previously that the range of head velocities encoded by the vestibular prosthesis can be nearly doubled if the spontaneous activity of the vestibular nerve afferents is suppressed by low amplitude anodic direct current. To avoid electrolysis and corrosion that occurs when direct current is delivered through a metal electrode, we designed a safe direct current stimulator (SDCS). The SDCS is a microfluidic system with saline filled fluid channels, two pairs of metal electrodes and valves. Alternating electronic current at the metal electrodes is converted into ionic direct current by modulating the valve states. A Nitinol wire opens and closes each valve by pinching a microfluidic channel when activated with electrical current. The longevity of Nitinol wire is a function of the stress and strain that it is subjected to and here we optimized both.

We examined how a reduction in the hardness of the silicone substrate affects the functionality of a valve. The valve consisted of a 100um diameter channel filled with electrolyte solution and embedded in a silicone substrate 150um below the surface. A Nitinol wire threaded through the silicone created an arch over the channel. Both ends of the wire were soldered to a circuit board below the substrate. We monitored 1kHz impedance of the channel as we applied current to the Nitinol wire to open and close the valve periodically at 1Hz. Lack of impedance change with wire compression indicated valve failure.

Our valve required 30g of pull force and 85mA to close a channel compared to previously published work on Nitinol pinch valves that required 140g of pull force and 200mA. The average time to close the valve was 0.348 ± 0.08s, the average opening time was 0.167 ± 0.06s, and the average cycle time was 0.515 ± 0.06s. The valve functioned for over 88,000 cycles before failure occurred at the solder site; an improvement over the previously reported 10,000 cycles before failure.

We found that reducing the hardness of the silicone reduces the power needed to operate the valve without reducing the functionality of the system. We are currently developing a system with reduced stress and strain on the Nitinol wire to further improve longevity of the system to implement it in an implantable vestibular prosthesis.

PS-344

Safe Direct Current Modulation of the Vestibular Labyrinth

Yu Zheng; Charles Della Santina; Gene Fridman
Johns Hopkins University

Background

Safe direct current stimulation (SDCS) technology has the potential to improve the fidelity of the vestibular prosthesis by being able to both excite and suppress the vestibular nerve afferent activity to encode head movements toward and away from the implant, respectively. To apply this new technology to vestibular prostheses, we need to characterize the VOR response to direct current (DC) modulation to understand how the vestibular afferents encode head rotation.

Methods

To emulate SDCS stimulation we delivered ionic DC to the vestibular labyrinth of chinchillas via microcatheter electrolyte-gel filled tubes implanted in each of the semicircular canals. We tested the vestibulo-ocular reflex (VOR) response to anodic and cathodic slowly modulating DC stimuli that ranged from 0 to 480μA anodic and 0 to -240μA cathodic. Each stimulus was offset in current amplitude such that it always returned to 0μA after every cycle.

Results

DC modulation delivered the sensation of sinusoidal head motion to each of the three canals at 0.5 - 10Hz in all animals as measured by their VOR responses. The responses in the four animals treated with gentamicin were similar in amplitude to those obtained from three animals not treated with gentamicin, implicating the vestibular afferents, rather than haircells as the neural target. Cathodic DC encoded head rotation toward the implanted labyrinth and maximum responses varied from 30deg/s to 250deg/s. Anodic DC encoded head rotation away from the implanted labyrinth with maximum responses varying between 25deg/s and 75deg/s. Anodic stimuli elicited VOR responses consistent with the inhibition of the vestibular nerve and cathodic stimuli elicited responses consistent with the excitation of the nerve.

Low selectivity is observed in the recorded VOR response (i.e. stimulation delivered to any canal evoked eye movements consistent with stimulation of the entire labyrinth).

The response from inhibition-to-excitation and excitation-to-inhibition reversed with the increased anodic and cathodic current amplitude respectively. This reversal of the response limited the maximum head velocity that could be encoded by DC.

Conclusion

Our results indicate that SDCS is applicable to deliver sensation to the vestibular nerves to modulate VOR response directions. We identified two challenges: low selectivity compromises the coding fidelity and the reversal of response constrains the encoded dynamic range. These two problems can potentially be addressed by modified electrode design with more focused current density and an optimized surgery protocol for higher proximity between the electrodes and target neurons.

PS-345

Quantitative Analysis of Slow Phase Component of Nystagmus by Original Video-Oculography, Revised HI-VOG.

Makoto Hashimoto[1]; Takuo Ikeda[2]; Kazuma Sugahara[1]; Hiroaki Shimogori[1]; Yoshinobu Hirose[1]; Hiroshi Yamashita[1]

[1]Yamaguchi University Graduate School of Medicine; [2]Tsuzumigaura Handicapped Children's Hosipital

Background

It is essential to use an infrared CCD camera in clinical examination of the vestibular system. Devices are currently available that can quite accurately record human eye movements, based on the principle of video-oculography (VOG). We devised an original video-oculography (HI-VOG) system using a commercialized infrared CCD camera, a personal computer and public domain software program (ImageJ) for the data analysis. The parameters of nystagmus (direction, velocity, and amplitude) have been quantified by analyzing quick phase.

Methods

The video image from the infrared CCD camera was captured at 30 frames per second at a resolution of 640*480 pl.. For analysis of the horizontal and vertical components, the X-Y center of the pupil was calculated using the original macro. For analysis of torsional components, the whole iris pattern, which was rotated by 0.1 degree, was overlaid with the same area of the next iris pattern, and the angle at which both iris patterns showed the greatest match was calculated.

Results

For quantitative analysis, the slow phase velocity of each occurrence of nystagmus, the average value of the slow phase velocity and the visual suppression value, were analyzed automatically. Analyses of the eye tracking test, as well as the test for optokinetic nystagmus were also applied in this system.

Conclusion

Using the revised HI-VOG system, it was possible to perform quantitative analysis of parameters of slow phase of nysgagmus from video images recorded with an infrared CCD camera.

PS-346

Prolonged Slow Phase Velocity Decay Time Constant is Associated with Worse Canal Function in Veterans with PTSD.

Yaa Haber[1]; Apollonia Fox[2]; Bishoy Samy[2]; Obatusin Mosadoluwa[2]; Helena Chandler[2]; Scott Wood[3]; Jorge Serrador[1,2]

[1]Rutgers University; [2]War Related Illness Injury Study Center East Orange, NJ VA Healthcare System; [3]Azusa Pacifica University Azusa, CA

Posttraumatic stress disorder (PTSD) is a chronic and disabling anxiety disorder occurring 3X more in veterans than civilians. Veterans seeking care for PTSD present with symptoms of dizziness, postural imbalance, and spatial disorientation. Such symptoms have also been identified in patients with impairments of their vestibular canals. Currently it is not known whether there is canal dysfunction in veterans with PTSD. We hypothesize that the symptoms of dizziness, postural imbalance and spatial disorientation may be due to imbalances of the semi-circular canals that may coincide with PTSD. Ten subjects, (5 with PTSD) sat in a motorized servo controlled chair in complete darkness while wearing 3D videooculography goggles (SMI, Denmark) which record eye movements. After recording a minute of baseline eye movement, the chair was accelerated by 10 deg/s^2 for a period of 40 seconds until a peak velocity of 400 deg/s was obtained. Angular acceleration in the yaw plane stimulates the horizontal semi-circular canals and this was evidenced by rapid nystagmus of the vestibular ocular reflex (VOR). This nystagmus is characterized by a rapid movement of the eye in the opposite direction of the acceleration force followed by a slow movement of the eyes in the same direction of the acceleration force. The slow component of eye movement results from vestibular neural input to the ocular muscles. The characterization of the slow phase of the VOR response can provide valuable insight into canal function during this per rotatory stimulation. Once acceleration is constant, the canals no longer sense angular acceleration and decrease their activation. This leads to a reduction in nystagmus which we are able to quantify using an exponential decay curve determined with a custom curve fitting method in MATLAB. Our analysis of these subjects indicates that veterans with PTSD have increased time constant decays. Shorter decays are affected by cupula return while longer delays concern the velocity storage mechanism. This increased time may be due to a prolonged activation of the signal within velocity storage mechanism of the vestibular system therefore leading to increased perception of the rotational stimulation in veterans with PTSD compared to the non PTSD group. Thus dizziness in patients with PTSD may also be exacerbated by this hyper responsiveness in central vestibular nuclei. Further work is needed to confirm these findings in a larger population. This work was supported by the VA Office of Public Health and a Congressionally Directed Medical Research Grant (Serrador).

PS-347

Ocular Torsion as a Measure of Otolith Function? Correlation of VEMPs and Static Ocular Counterroll.

Carolina Treviño Guajardo[1]; Jorge Otero-Millan[2]; Saverio Silipo[3]; John P. Carey[4]; Amir Kheradmand[2]
[1]Johns Hopkins University; [2]Johns Hopkins University- Department of Neurology; [3]University of Verona- Department of Clinical Neurology; [4]Johns Hopkins University- Department of Otolaryngology- Head & Neck Surgery

Introduction and Aims

Ocular vestibular evoked myogenic potentials (VEMPs) are believed to reflect the utricular-driven vestibulo-ocular reflex. Static ocular counterroll (OCR) refers to the compensatory torsional eye movement that occurs to counteract a static roll-tilt of the head or the body. This reflex is also mainly driven by the utricle. The principal aim of this study was to determine if VEMPs and static ocular counterroll (OCR) are correlated.

Methods

Eight healthy volunteers (n=16 ears) without history of neurotological complaints underwent both VEMP and OCR measurements. Ocular VEMPs were recorded in response to air conducted sounds (clicks and 500 Hz tone-bursts) delivered monaurally and to bone-conducted vibration (50 midline skull taps). Cervical VEMPs (cVEMPs) were recorded in response to monoaurally delivered 500Hz tone-bursts.

OCR was recorded during static roll tilt of the head 30 degrees to the left and righ shoulders. We used a commercial video-oculography system (Visual Eyes, Micromedical Technologies Inc.) controlled by custom made software to measure torsional position of the eyes by using a novel method. The software obtains images of both eyes with two high-speed infrared cameras at a rate of 100 frames per second. The iris pattern is then used to automatically measure the torsional rotation of the eyes in each frame.

Results

There was a significant correlation (Spearman's rank correlation) between OCR responses and oVEMPs to sound-evoked clicks (r_s=0.58, p =0.01) and tone-bursts (r_s =0.51, p =0.03). Neither midline skull tap oVEMPs (r_s =0.03, p=0.90) or cVEMPs (r_s =0.30, p=0.24) correlated with static tilt responses.

Conclusions

To our knowledge this is the first comparison of static ocular counterroll (OCR) with oVEMPs and cVEMPs. Our data show a correlation between static OCR and sound-induced oVEMPs but not between static OCR and cVEMPs. This is consistent with the notion that both static OCR and oVEMPs primarily measure utricular responses while cVEMPS measure saccular responses. Future work will assess both methods in patients with various degrees of vestibular hypo function. With the advent of high quality video goggle systems, the OCR test could easily be developed to clinically assess otolith function.

PS-348

Metrics of the Video Head Impulse Test (vHIT) of Semicircular Canal Function; Sensitivity and Specificity for Detecting Known Vestibular Loss and Age Dependent Norms for vHIT in Healthy Subjects

Ian Curthoys[1]; Leigh McGarvie[2]; Hamish MacDougall[1]; Ann Burgess[1]; Samanthi Goonetilleke[1]; Michael Halmagyi[2]; Elodie Chiarovano[3]; Catherine de Waele[3]
[1]University of Sydney; [2]Royal Prince Alfred Hospital; [3]Universite Paris Descartes

Background

Our Sydney team was the first to develop the new test of semicircular canal function – the video Head Impulse Test (vHIT) - as a fast simple test which is replacing the caloric test. But some basic metrics have not yet been reported – sensitivity and specificity for detecting objectively verified vestibular loss and age dependent norms. There have been reports comparing vHIT with calorics, but these cannot give the true sensitivity and specificity of vHIT for detecting known vestibular loss since both calorics and vHIT are tests of vestibular function- the caloric is **not** a definite indicator of vestibular loss since healthy people may have poor or even absent caloric responses.

Objectives

1. To measure the true sensitivity and specificity of vHIT in detecting known vestibular loss
2. To obtain normative values of vHIT gain in a large number of healthy subjects in decade age bands from 20 to 90years

Methods

The eye movement during small, abrupt, passive, unpredictable head turns were recorded by a high speed video camera, together with measures of head velocity, and software which gives objective measures of VOR gain for natural stimuli (MacDougall et al 2009; 2013).

Results 1. Sensitivity and Specificity of vHIT

We tested 37 patients within the first year after surgery for unilateral vestibular schwannoma (at Hopital Salpetriere, Paris), so they have objectively verified unilateral loss of vestibular function, together with 37 healthy people, with Otometrics Impulse system. The results show that vHIT is 100% accurate for detecting patients with known unilateral vestibular loss – sensitivity 1.0, specificity 1.0 - diagnostic accuracy 100%.

Results 2. Normative data

The one operator measured VOR gain of 85 healthy subjects aged between 20 and 93 across a range of head velocities and we report normative values for VOR gain (means +/- 2 standard deviations) of around 10 people in each decade of life. The clear result is that in healthy patients direct measures of VOR gain to these natural values of head acceleration remains close to 1.0 even into the ninth decade of life.

Conclusions

1. vHIT is an excellent test of semicircular canal function with sensitivity and specificity of 1.0, and diagnostic accuracy of 100% for detecting objectively verified vestibular loss

2. In healthy people directly measured horizontal VOR gain stays close to 1.0 at most tested velocities even in the 9th decade of life.

PS-349

Meniere´s Disease and Cochlear Implantation

Ioana Herisanu[1]; Peter K.[2]; Mark Praetorius[3]
[1]University Heidelberg Medical Center; [2]University Heidelberg Medical Center, Dept. of Otolaryngology; [3]University Heidelberg Medical Center, Dept. of Otolaryngology, Div. of Otology and Neurotology

Introduction

Since hearing loss over time is rather the rule then the exception in Meniere´s disease, we investigated the outcome of these patients receiving a cochlear implant in our institution.

Material and Method:

We did a retrospective study on eight patients with probable and definite Meniere´s disease out of 278 patients implanted between 2009 and 2013 in our cochlear implant program. Four cases had bilateral Meniere´s disease, one we excluded because of additional cochlear fibrosis and suspicion of capsular otosclerosis. Women to men ratio was 6/2. Mainly we aimed at the therapy of the vertigo symptoms first. Two patients received intratympanic application of Gentamicin, one an endolymphatic sac decompression surgery, one both, two had Betahistin therapy. After these treatments, no patient did report any vertigo episodes in the last three month prior to implantation. Four patients had a no responsive endolymphatic organ in the caloric test preoperative, two more after the implantation.

Results:

All patients profited from the implantation regarding the hearing function, mean values 70% speech understanding in Freiburger word recognition test with cochlear implant alone. Before the implantation no patient had any speech understanding at 85dB on the implanted ear. Six of seven patients had tinnitus before the surgery; four of them level 2 of 4. Three reported a tinnitus masking effect with the implant.

Conclusions:

The cochlear implant is a viable option for patients who have lost their hearing to Meniere's disease, but we recommend to control vertigo first. The implant can restore speech perception and improve the tinnitus, preparing the patient in case of additional contralateral ear deafness.

PS-350

Lower Bone Mineral Density in Weight-bearing Bones amongst Individuals with Generalized Vestibular Weakness

M. Geraldine Zuniga[1]; Travis R Ladner[1]; Guillaume Vignaux[1]; Howard Hoffman[2]; Chuan-Ming Li[3]; Florent Elefteriou[1]; Alejandro Rivas[1]
[1]Vanderbilt University Medical Center; [2]NIH/NIDCD; [3]NIH

Background

Work conducted by Vignaux et al (2013) showed that induction of bilateral vestibular lesions in rats results in significant bone loss in weight-bearing bones. This suggested that the process of bone remodeling has a vestibulosympathetic regulatory component.

While previous analysis of data from the National Health and Nutrition Examination Survey (NHANES) by Mendy et al (2014) suggested that demineralization of the temporal bone is associated with vestibular and auditory deficits, the present study further investigates if subjects with characteristics that resemble a bilateral or more generalized type of vestibular weakness present lower bone mineral density (BMD) in weight-bearing bones.

Methods:

All data was derived from the NHANES cycles 1999 through 2004. All participants who had information on balance questionnaires, standardized balance testing, bone mineral density (BMD), and relevant covariates available were included. Covariates included age, sex, diabetes, smoking history, use of beta blockers, and use of bisphosphonates. Subjects with balance difficulties referable to other medical conditions were excluded. In total 864 subjects were included. Subjects were classified as having generalized vestibular weakness (GVW), if in addition to failing condition four of the modified Romberg exam on the second attempt, they also reported balance and dizziness problems in the past year. Subjects were defined as not having GVW if they passed the Romberg exam on the second attempt. BMD between GVW groups was compared via Mann-Whitney U test. Presence of GVW and covariates were screened with univariate linear regression to assess relationship with pelvis and left leg BMD. Factors significant on univariate analysis at $p<0.10$ were entered into multivariate regression. Statistical significance was defined as $p<0.05$.

Results:

Pelvis BMD was lower in subjects with GVW (1.14 vs. 1.26 g/cm^2, $p<0.001$). Left leg BMD was also lower in this group (1.10 vs. 1.18 g/cm^2, $p<0.001$). On multivariate analysis, GVW correlated independently with pelvis BMD (Beta=-0.103, $p=0.001$). Overall model: $R^2=0.248$, $F(5,858)=56.653$, $p<0.001$. GVW also correlated independently with left leg BMD (Beta=-0.066, $p=0.012$). Overall model: $R^2=0.455$, $F(4,859)=179.161$, $p<0.001$.

Conclusions:

Participants with GVW had overall lower BMD in weight-bearing bones. This suggests that the vestibular system also contributes to bone remodeling in humans. Further investiga-

tion in individuals with true bilateral vestibular dysfunction is needed to describe the degree of this vestibulosympathetic component of bone remodeling and whether or not the use of bisphosphonates or beta-blockers can alter the course of this process.

PS-351

Interplay Between VEGF-A and cMET Signaling in Human Vestibular Schwannomas and Schwann Cells

Sonam Dilwali[1]; Daniel Roberts[2]; **Konstantina Stankovic[2]**
[1]Massachusetts Eye and Ear, Harvard-MIT Division of Health Sciences and Technology; [2]Massachusetts Eye and Ear, Harvard Medical School

Introduction

Vestibular schwannoma (VS), the fourth most common intracranial tumor, arises from the Schwann cells of the vestibular nerve. Although several pathways have been independently implicated in VS pathobiology, interactions among these pathways have not been explored in depth. We have investigated the potential cross-talk between hepatocyte growth factor (HGF) and vascular endothelial growth factor-A (VEGF-A) in human VS, an interaction that has been described in other physiological and pathological cell types.

Methods:

Freshly-harvested human specimens of sporadic VSs and great auricular nerves (GANs) were collected from indicated surgeries. The study protocols were approved by Human Studies Committee of the Massachusetts Eye and Ear and Massachusetts General Hospital. The specimens were divided for protein, RNA or culture work. Expression of VEGF and HGF pathway was measured in VSs versus GANs using qPCR and western blot analysis, and in VS and GAN secretions using cytokine array. Primary culture of Schwann cells and VS cells was treated with siRNA or pharmacologic reagents to interrogate cross-talk between HGF and VEGF-A pathway.

Results

We affirmed previous findings that VEGF-A signaling is aberrantly upregulated in VS, and established that expression of HGF and its receptor cMET is also significantly higher in sporadic VS than in healthy nerves. In primary human VS and Schwann cell cultures, we found that VEGF-A and HGF signaling pathways modulate each other. siRNAs targeting cMET decreased both cMET and VEGF-A protein levels, and siRNAs targeting VEGF-A reduced cMET expression. Additionally, siRNA-mediated knockdown of VEGF-A or cMET, and pharmacologic inhibition of cMET decreased cellular proliferation in primary human VS cultures.

Conclusions

Our data suggest cross-talk between these two prominent pathways in VS and highlight the HGF/cMET pathway as an additional important therapeutic target in VS.

PS-352

Histopathologic Changes of the Inner Ear in Rhesus Monkeys after Intratympanic Gentamicin Injection and Vestibular Prosthesis Electrode Array Implantation

Daniel Sun[1]; Lani Swarthout[1]; Mohamed Lehar[1]; Chenkai Dai[1]; Diana Mitchell[2]; John Carey[1]; Kathleen Cullen[2]; Charles Della Santina[1]
[1]Johns Hopkins University School of Medicine; [2]McGill University

Background

Bilateral vestibular dysfunction (BVD) due to gentamicin ototoxicity can have a significant impact on quality of life and result in large socioeconomic burdens. An implantable multichannel vestibular prosthesis (MVP) is a promising treatment approach that has been tested in animals and humans. However, uncertainty remains regarding the effects of both gentamicin ototoxicity and electrode implantation on temporal bone histopathology. Understanding the histological changes is important, as MVP-driven selective stimulation of semicircular canals (SCCs) is dependent on presence of primary afferents to each SCC crista despite previous ototoxic injury that led to BVD, and surgical trauma associated with MVP implantation. Retraction of primary afferents back toward Scarpa's ganglion would render selective stimulation difficult.

Methods

We investigated histopathologic changes of the inner ear associated with intratympanic gentamicin (ITG) injection and/or MVP electrode array implantation in 11 temporal bones from 6 rhesus macaque monkeys. Hematoxylin and eosin-stained 10 μm temporal bone sections were examined under light microscopy for 4 treatment groups: *normal* (3 ears), *ITG-only* (2 ears), *MVP-only* (2 ears), and *ITG+MVP* (4 ears). We estimated vestibular hair cell (HC) surface densities for each sensory neuroepithelium and compared findings across sensory end organs and treatment groups.

Results

In *ITG-only*, *MVP-only*, and *ITG+MVP* ears, we observed persistent ampullary innervation of SCC cristae despite ITG treatment and/or MVP electrode implantation. Furthermore, MVP electrode array implantation was not associated with injury to the auditory structures of the inner ear such as the oval window and cochlea, or the otolith organs except in 1 case, in which saccular injury occurred due to over-insertion of the posterior semicircular canal (PSC) electrode. Implanted electrodes reached to within 50–760 μm of the target cristae. Tissue reaction to MVP electrodes consisted of formation of a thin fibrotic capsule. Osteoneogenesis and a dense fibrotic reaction were each observed in only 1 of 6 electrode tracts examined. In *ITG-only* and *ITG+MVP* ears, neuroepithelial thinning and loss of type I HCs were attenuated in the maculae compared to the cristae, which were confirmed by semi-quantitative estimates of HC counts.

Conclusions

Consistent with physiologic studies that have demonstrated directionally-appropriate vestibulo-ocular reflex responses to

MVP electrical stimulation years after implantation, these histologic findings support an interpretation that although MVP implantation causes some inner ear trauma, it can be accomplished without destroying the distal afferent fibers an MVP is designed to excite, confirming the development of a canal-focused MVP to be a clinically sound goal.

PS-353

Evidence of Saccular Pathology in Human Diabetes Mellitus

Pelin Kocdor; Mehmet Erdil; Michael Paparella; Sebahattin Cureoglu; Meredith Adams
University of Minnesota

Introduction

The histopathologic changes that may underlie the association between diabetes mellitus (DM) and vestibular dysfunction have not been characterized in humans. This comparative human temporal bone (HTB) study aimed to compare the neuroepithelium and microvasculature of the saccule between subjects with and without DM.

Methods

The morphology of the saccule was compared between 40 subjects with DM (mean age at death 57 years) and 40 group age-matched controls without DM (mean age at death 56 years). The DM group included 16 subjects with type I DM (T1DM) and 24 subjects with type II DM (T2DM). Vessel wall thickness was measured from the most prominent arteriole in perpendicular section underlying the saccular macula in one HTB from each subject. Using differential interference contrast microscopy (Nomarski) at x1250 magnification, type I and type II vestibular hair cell counts were performed in HTBs with minimal autolysis in which the macula was oriented perpendicular to the plane of section. The vessel thickness (μm) and cell densities from each group (cells/mm2 surface area) were compared with t-tests assuming unequal variances.

Results

There were no qualitative differences in saccular morphology or in mean vessel wall thickness between subjects with DM and controls (2.16 μm vs. 2.00 μm, p = 0.20). The macula was oriented in a plane suitable for analysis in 14 HTB from 11 subjects with DM (4 T1DM, 7 T2DM) and in 31 HTB from 20 control subjects. There was no difference in mean age at death between the DM and control groups undergoing hair cell counts (54 vs. 55 yrs., p=0.80). The mean density of type 1 vestibular hair cells was significantly lower in the DM group compared to controls (24.7 vs. 27.2 cells/mm^2, p = 0.02). There was no difference between DM and control groups in type 2 vestibular hair cell density (21.9 vs. 21.0 cells/mm2, p=0.96).

Conclusions

Neuroepithelial pathology, manifested as a lower density of type I vestibular hair cells in the presence of a normal density of type II vestibular hair cells, was observed in the saccules of subjects with DM. Saccular microangiopathy, expressed as alterations in vessel wall thickness, was not observed. These findings are consistent with histologic observations in animals with experimentally induced diabetes and suggest that DM may have a deleterious effect on human vestibular sensory epithelia.

PS-354

Discrepancy Between Results on Video Head Impulse Test and Those on Caloric Testing in The Patients with Meniere's Disease.

Toru Seo; Katsumi Doi
Kinki University

Introduction

Video head impulse test (vHIT) was established in 2009 and has been widely performed for clinical examination. It was reported that the results of vHIT were different from those of the caloric testing in some cases with Meniere's disease. The aim of this study was to clarify whether the discrepancy exist.

Subjects and Method

The subjects consisted of 6 cases of unilateral Meniere's disease, 5 cases of vestibular neuritis and a case of Ramsay Hunt syndrome. The vHIT were examined using ICS Impulse. When VOR gain was lower than 0.8, we defined result as abnormal. CP% wase calculated from monotharmal caloric testing. When CP% exceeded 25%, we defined a result to be abnormal.

Result

While abnormal results in caloric testing were shown in 5 cases of vestibular neuritis, vHIT showed abnormality except one case of them. One case of Ramsay Hunt syndrome showed abnormality on both caloric testing and vHIT. On the other hand, abnormal results on caloric testing were shown in 4 cases of Meniere's disease and vHIT showed abnormal result on 1 case among them.

Conclusion

Discrepancy between the results on vHIT and those on caloric testing was confirmed. We suggested the following mechanism: endolymhatic hydrops causes the enlarged ampula portion, and then convection flow during caloric stimulation decrease. When sensory cell or cupula are not damaged, vHIT shows normal even in enlarged ampula portion.

PS-355

Difference of Autoantibody Between Meniere's Disease and Bilateral Sudden Hearing Loss: Is There a Different Autoimmunity Mechanism?

Sung Huhn Kim; Jae Young Choi; Hyun Ji Kim; Gyung Jin Noh
Yonsei University

This study was performed to investigate the difference of autoantibodies and their target tissues between Meniere's disease and bilateral sudden hearing loss. Ten patients with definite Meniere's disease, nine patients with bilateral sudden hearing loss, and ten controls were enrolled in this study. To identify serum circulating autoantibodies, Protoarray® analysis with patients' and controls' sera were performed. To detect Antigen-antibody reaction between circulating autoantibody and each cochlear and vestibular tissue, western blotting using mouse inner ear and patients' sera was performed. In ad-

dition difference of clinical features according to the presence of antigen-antibody reaction was investigated. Eighteen and twelve proteins had more than 2-fold greater signal intensity in the Protoarray® analysis of Meniere's disease and bilateral sudden hearing loss, respectively. The signal intensity of 8 and 2 proteins was more than 10-fold higher in the patients than in the controls in each disease entity (Meniere's disease and sudden hearing loss). None of them were commonly found in both diseases. Western blot analysis showed multiple Ag-Ab reaction between patients' sera and mouse inner ear tissues, and the band distribution was different between Meniere's disease and bilateral sudden hearing loss. Vertigo spells were more severe and treatment response was poorer in the Meniere's disease patients with the presence of Ag-Ab reaction, whereas hearing threshold was not significantly different between the sudden hearing loss patients' with and without Ag-Ab reaction. In conclusion, main pathologic mechanism of Meniere's disease and bilateral sudden hearing loss can be autoimmunity. There were multiple autoantibodies for each disease but their target antigen could be different between Meniere's disease and bilateral sudden hearing loss. Autoimmune reaction was correlated with the severity of vertigo symptoms and represented poor response to conventional medical treatment.

PS-356

Characterizing Vestibular Electrically Evoked Compound Action Potentials in Guinea Pigs

T. A. Khoa Nguyen[1]; Jack DiGiovanna[2]; Wangsong Gong[3]; Csilla Haburcakova[3]; Wigand Poppendieck[4]; Silvestro Micera[2]; Daniel M. Merfeld[3]

[1]École Polytechnique Fédérale Lausanne, Switzerland; [2]Translational Neural Engineering Laboratory, Center for Neuroprosthetics, École Polytechnique Fédérale Lausanne, Switzerland; [3]Jenks Vestibular Physiology Laboratory, Massachusetts Eye and Ear Infirmary, Boston, USA; [4]Department Medical Engineerg and Neuroprosthetics, Fraunhofer Institute for Biomedical Engineering, St. Ingbert, Germany

Patients with loss of vestibular function suffer from decreased physical and social well-being. Their symptoms may be treated with a vestibular implant that electrically stimulates peripheral afferents in the semicircular canals. Numerous studies with animal models and a few with human subjects demonstrated activation of the vestibular-ocular reflex (VOR) that provides a benchmark of vestibular function. To complement VOR, we measured peripheral neural function through vestibular electrically evoked compound action potentials (VECAP).

Four male guinea pigs were instrumented with a scleral search coil and an electrode array with eight sites – capable of stimulation and recording – inserted in one semicircular canal. A wire electrode placed into the neck muscle served as remote return electrode. A system consisting of PC, Med-El Research Interface Box II, transmitting coil and Pulsar cochlear implant was connected to the array. One electrode site and the remote electrode were used for monopolar stimulation, two other array sites were used for bipolar recording. VECAP was measured in response to single pulses, pulse trains and acute continuous pulses of varying current amplitude (25 µs/phase for all cases). VOR responses were measured with the search coil while the subject was alert and head-fixed in a dark room. All experiments were approved by the institutional animal care and use committee.

In all subjects, both eye movement and VECAP were evoked. However, few recording sites measured VECAP similar in shape to cochlear implant ECAPs with a negative (N) and a positive (P) wave (Fig. 1A). Correlation of VOR peak velocity and N-P voltage in response to single pulses revealed a piecewise linear function with a marked increase in peak velocity beyond a certain N-P voltage (Fig. 1B) and could represent a vestibular threshold. In response to pulse trains, N-P voltage was slightly reduced, but not significantly, while VOR responses increased and plateaued with pulse number (Fig. 1C-D), suggesting integration. After adaptation to acute continuous stimulation, modulation of current amplitude elicited VOR responses in both directions (e.g., left, right for horizontal canal stimulation); there were analogous changes in N-P voltage (Fig. 1E-F).

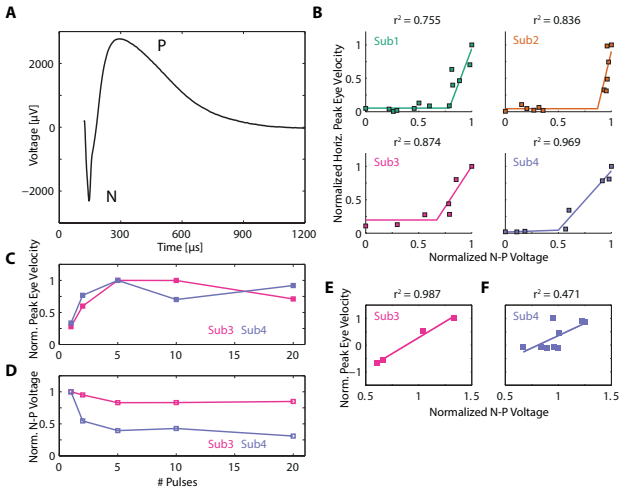

Figure 1. VECAP characterization in guinea pigs. **(A)** A typical VECAP measurement with negative (N) and positive (P) waves. **(B)** Mapping of N-P voltages and eye movement responses to single pulses showed piecewise linear relationships across all subjects. Starting from parameters in the linear region in (B), pulses were repeated for trains of various lengths; **(C)** and **(D)** show normalized VOR and VECAP responses, respectively. VOR responses increased up to five pulses then plateaued, VECAP decreased slightly after the first pulse and then stabilized. **(E)** With acute continuous stimulation, excitatory and small inhibitory responses were evoked by modulation of current amplitude that also modulated N-P voltage.

VECAPs can be recorded using a multi-site electrode that also stimulates the vestibular nerve. The mechanisms of VECAP warrant further research since it could only be recorded in ca. 20% of all recording configurations. Finally, the VECAP response to stimulation reflects physiological responses (VOR) and thus might be exploited in a vestibular implant for improved fitting.

PS-357

A Retrospective Chart Review Study of the Frequency and Patient Demographics of Gentamicin Antibiotic Use at University of Rochester Medical Center

Bradley Kushner; Paul Allen; Benjamin Crane
University of Rochester Medical Center

Aminoglycoside antibiotics are one of the most commonly prescribed antibiotics worldwide because of their antimicrobial efficacy, widespread availability and relatively low cost. The reported incidence of significant ototoxicity in the literature varies widely and usually ranges from 2% to 25%. Specifically, the incidence of cochleotoxicity has been reported to range from a few percent up to 33%, while balance can be affected in up to 15% of patients. Although the ototoxic and vestibulotoxic effects of gentamicin are well established, little research has been done to study their use in a hospital setting. The goal of our research is to retrospectively study the use of gentamicin in a hospital setting, to determine which hospital departments use these aminoglycosides most frequently, and to investigate the demographics of patients prescribed gentamicin. In addition, we will study the diagnoses most commonly linked with their use and the other antibiotics and medications used prior to and in combination with gentamicin (such as metformin or aspirin).

Using I2b2, an NIH funded open source system developed by Partners Healthcare and deployed at the University of Rochester, we performed analysis on all patients who have been prescribed gentamicin at the University of Rochester Medical Center since February 2011. Three (3) major populations of patients received gentamicin: 1) neonates 2) obstetrical women and 3) patients >55 with serious infections. Of the 3877 patients, 2597 (67%) were <2 years and 41% <1 year. 928 patients (24%) were between the age of 18-34 (813 of whom were female (88%)), and 865 were 55 years or older (22%). Additionally, patients receiving gentamicin had a long hospital course: 1747 patients (45%) had a stay longer than 10 days and 1477 patients (38%) had a stay between 5-10 days. Disorders associated with patients receiving gentamicin included: Perinatal complications (1564); sepsis (1399); acute/chronic renal disease (1287); labor, delivery, or neonatal complications (1250); diabetes (949); and UTI/pyelonephritis (775). The medications frequently administered concurrently with gentamicin included: Ampicillin (13,001 doses), cefazolin (3586), clindamycin (2941), vancomycin (2524), floroquinolones (2003), aspirin (1243), and metformin (307). Our demonstration that gentamicin is still widely used in a major medical health center suggests that the neonatal population and young adult women are at especially high risk for exposure. Further data analysis should focus strategies to protect these populations by avoiding unnecessary exposures and by possible concurrent administration of protective medications such as metformin and aspirin.

PS-358

Low-Frequency Cochlear Resonances below 100 Hz seen in Equal-Loudness Contours and Objectively Measured Middle-Ear Transfer Functions

Torsten Marquardt
University College London

Introduction

Utilising a distortion-product-otoacoustic emissions (DPOAE) suppression technique, Marquardt and colleagues (JASA, 2007) observed a pronounced resonance feature between 40 and 80 Hz inside the cochlea, which is presumably caused by an interaction of fluid inertia inside the helicotrema and apical basilar membrane (BM) compliance (Marquardt and Hensel, JASA 2013). This study investigates whether this resonance affects the perceived loudness of low-frequency tones.

Methods

Equal-loudness contours (ELCs) between 4 Hz and 125 Hz were measured monaurally using a custom-made infra-sound source and a novel maximum-likelihood tracking procedure that adjust the sound pressures of a large number tone pairs within this frequency region to subjective equality of their loudness. ELCs were derived from the obtained gradient field (pressure vs. frequency).

Middle-ear transfer functions (METFs) were measured from the same ears using the before mentioned DPAOE suppression technique. In short, the levels of a series of low-frequency tones (20-250 Hz) were adjusted so that they produce a DPOAE suppression pattern of constant depth. The adjusted levels describe the inverse frequency-transfer function of the sound pressure in the ear canal to the differential pressure across the BM at the location of DPOAE generation.

Results

Of the 16 tested subjects, four were unable to give repeatable loudness judgements and five had insufficient DPOAE levels to extract their METF. ELC and METF could be measured in nine subjects. METF of all 11 subject showed the previously observed resonance feature; in three cases just a step; in eight cases as a pronounced slope reversal in the otherwise rising METFs. One of these eight METFs showed two such resonances; one peaking at 55 Hz, the other at 90 Hz. Also the ELC of this subject featured these two humps. But in general, a single resonance was seen in almost all ELCs, which in most cased matched the one in of the same ear METF (if measurable). The resonance feature is most pronounced at higher sound levels (60 - 80 phon). It is therefore not expected that the resonance will be observed at hearing threshold.

Conclusion

The results demonstrate that the resonance observed in the METFs affects also the individual's perceived loudness of low-frequency tones. The standard ISO 226-2003 does not include this resonance so that the ELC of almost all subjects deviate significantly below 100 Hz from its isophon curves. Frequencies below the resonance (i.e. below ~50 Hz) are perceived louder than expected.

PS-359

Two Forms of Longitudinal Coupling in the Cochlea

Samiya Alkhairy[1]; Christopher Shera[2]
[1]MIT; [2]MEEI

In classical models of the cochlea, the organ of Corti is often idealized as a single partition consisting of an array of oscillatory elements coupled together solely by the inviscid fluid of the scalae. Recent studies, however, show that the viscoelastic properties of the tectorial membrane provide an additional form of longitudinal coupling that affects the behavior of the cochlea, including the motion of the basilar membrane (BM).

To help understand the role of this additional coupling in cochlear mechanics, we develop a single-partition model in which longitudinal coupling arises directly from the viscoelastic properties of the partition, rather than indirectly via the fluid. We study the behavior of this directly coupled (DC) model and compare it with that of the fluid-coupled (FC) classical model.

To explore how the different forms of coupling affect the BM response, we apply analytic methods (specifically WKB) to approximate traveling wave motion. We also apply inverse methods to BM velocity data to extract and compare effective BM impedances for both model types. Studying these two forms of longitudinal coupling in a simple (single partition) context is a step towards understanding the more complex mechanics of the organ of Corti, where both direct and indirect forms of coupling contribute to shaping its motion.

PS-360

Intracochlear Pressure Measurements from Scala Media

Sushrut Kale; Elizabeth Olson
Columbia University

Most models of passive cochlear mechanics assume a two-compartment model of the cochlea. These classical models suggest that the intracochlear pressure is roughly equal in magnitude and opposite in phase between scala tympani (ST) and scala vestibuli (SV). In these models, scala media (SM) is mechanically merged with SV. In contrast, another class of passive models assumes a multi-compartment cochlea suggesting more complex fluid-tissue interaction within SM. However, experimental data regarding the fluid-tissue interaction in the SM, even in a physiologically passive cochlea, did not exist. To this aim, we measured intra-cochlear pressure close to the sensory tissue in ST and SM, from the same animals to inform models of passive cochlear mechanics.

All the intracochlear pressure measurements were performed in-vivo in anesthetized, young adult Mongolian gerbils. A small cochleostomy was performed in the scala media (SM) in the first basal turn. A small hole (~90 μm diameter) was made in the strial wall using a small electric cautery. A miniaturized, fiber-optic pressure sensor (~80 μm diameter) was advanced through the SM hole in 1-μm steps and intra-cochlear fluid pressure was measured near the organ of Corti (OC) tissue in response to pure tones. Similarly, the intracochlear pressure was measured near the basilar membrane (BM) by advancing the sensor through a cochleostomy made in ST. All the SM pressure measurements were performed in physiologically passive cochlea.

Traveling wave was observed in both SM and ST pressure. Preliminary results supported the classical models to the first order in that the traveling wave mode of intra-cochlear pressure was roughly equal magnitude-opposite phase in the two scalae. In both SM and ST summation interference between two pressure modes, the traveling wave mode and the fast, compression pressure mode, was observed. The traveling wave pressure mode varied with frequency whereas the fast pressure mode was relatively independent of frequency. In SM the interaction between the two pressure modes was more complex than in ST and depended on the sensor location in the radial direction along the BM.

While to first order the data supported the classical models of passive cochlear mechanics, further experiments are needed to accurately determine the radial location of the sensors in order to interpret the relatively complex pressure patterns that could be observed in SM.

PS-361

Phase Difference Between Stapes and Round Window Motion as an Indicator of Inner-Ear Integrity

Kourosh Roushan[1]; Wade Chien[2]; Michael Ravicz[3]; John Rosowski[2]; Nakajima Hideko[2]; Christof Stieger[1]
[1]University Hospital Basel, Switzerland; [2]Department of Otology and Laryngology, Harvard Medical School, Boston; [3]Eaton-Peabody Laboratory and Department of Otolaryngology, Massachusetts Eye & Ear Infirmary, Boston

Introduction

In normal human temporal bones the phase of round window (RW) velocity differs from the phase of oval window (stapes) velocity by approximately –0.5 cycles (phase lag) at low frequencies – below approximately 1-2 kHz (Stenfelt et al. 2004). Our goal is to evaluate if this phase lag between stapes and RW velocity changes when there is an alternative inner ear path for volume velocity (third window) such as in superior canal dehiscence (SCD).

Methods:

We measured the velocities of stapes and RW with a single-point laser Doppler vibrometer in 13 fresh human temporal bones with acoustic sound stimulation. We also examined stapes and RW velocity phase data from 8 different fresh human temporal bones in a previous study (Chien et al. 2007) in which a superior canal dehiscence (SCD) was simulated.

Results:

In both sets of normal human temporal bones, we saw a relatively consistent 0.5-cycle phase lag of the round window velocity with respect to the stapes velocity at low frequencies (below about 1.5 – 1.8 kHz). In our first series of 13 normal human temporal bones the phase lag was generally at about

0.5 cycles in lower frequencies, started changing within a range of ±0.05 cycles between 0.7 kHz and 1.8 kHz and then increased up to 0.8 cycles at 5 kHz. In the second series of 8 human temporal bones before inducing a SCD, the phase lag was slightly less than 0.5 cycles between 0.5 and 1.2 kHz and increased above 1.5 kHz to approximately 0.75 cycles at 4 kHz. In each of the 8 bones, introducing an SCD decreased the lag significantly below 1 kHz to about 0.4 cycles. Above 1 kHz there was no significant difference in phase lag between SCD and the normal condition.

Discussion:
During air conduction in an intact inner ear, the phase of the RW motion lags the stapes by 0.5 cycles below about 1.5 kHz. This phase relationship, consistent with the two-window hypothesis, breaks down if a third window is introduced, as in the case of SCD. This study exemplifies how the relationship between stapes and RW phase can be used to determine whether an inner ear is intact without an abnormal third window.

PS-362

Generation and Transmission of Distortion Product Otoacoustic Emissions in the Mammalian Cochlea

Wei Dong
Loma Linda VA Healthcare System and Loma Linda University Healthcare

Background
Otoacoustic emissions (OAEs) are sounds originating from the active mechanics in the cochlea that travel back out to the ear canal (EC), thus holding the promise of providing a powerful non-invasive method for studying cochlear mechanics and a diagnostic tool for assessing cochlear impairment. However, OAEs are complex signals appearing as a sum of multiple components relating to different cochlear regions and different cochlear mechanisms. The question, of how to use the global DPOAE to explore and diagnose the pathology of local cochlear mechanics, has challenged OAE research for many years. The current study reviews the generation and propagation of distortion product OAEs (DPOAEs) via intracochlear observations.

Methods
Experiments were performed in anesthetized young adult gerbils. The care and use of the animals were approved by the Institutional Animal Care and Use Committee of Loma Linda VA Healthcare System (IACUC). The ear was stimulated with single-, two- or three-tones. Intracochlear pressure responses were mapped at locations close to or far from the basilar membrane (best frequency around 20 kHz) and at the base of the gerbil cochlea. Simultaneously, EC pressure responses close to the tympanic membrane were measured.

Results
When the ear was stimulated with two-tones, distortion products (DPs) were generated as the byproduct of the cochlear active signal processing. The characteristics of DPs in the time and frequency domain were consistent with the generation from a local nonlinearity. The generation region appeared to be spatially distributed from at least ~ 0.5 octave basal to the f2 peak when the f2/f1 ratio was 1.25. Once being generated, the DP appeared to travel independently of the primaries, both in the forward and reverse directions and passed through local cochlear filtering. The reverse propagation of the DP as a traveling wave was supported by the phase comparison of intracochlear pressures measured at two longitudinal locations simultaneously. The stapes appeared to be driven by the pressure of DP wavelets summed throughout the generation region and showed similar characteristics to those of the DPOAE measured in the EC.

Conclusions
Intracoclear observations suggested that DPOAEs were generated from a distributed nonlinearity, which appeared to be coincident with the location of the cochlear amplifier; the stapes was driven by pressure at the DP frequency propagating mainly through a reverse traveling wave.

PS-363

Radial and Axial Vibrations of the Organ of Corti in Live Guinea Pig Apex Measured Through Bone

Sripriya Ramamoorthy[1]; Yuan Zhang[1]; Tracy Petrie[1]; Anders Fridberger[2]; Tianying Ren[1]; Ruikang Wang[3]; Steven Jacques[1]; Alfred Nuttall[1]
[1]Oregon Health & Science University; [2]Linköping University, Sweden; [3]University of Washington, Seattle

Sound-induced mechanical response of the organ of Corti at the cochlear apex is relevant for speech perception. Past measurements in mammalian cochlear apex have been limited due to both difficulty in surgical access and changes to the hydrodynamics introduced by opening the otic capsule. Recently the measurement of axial (Gao et al., Journal of Neurophysiology 2014) and radial (Lee et al., Mechanics of Hearing 2014) vibrations of the organ of Corti through bone in the mouse apex without opening the capsule has become possible. A goal of this study is to determine the vibrations in both radial and axial directions in the same animal. The measurements were made using a phase-sensitive Fourier domain optical coherence tomography (PSFDOCT) and interferometry system we developed with center optical wavelength at 840 nm.

Young albino guinea pigs were surgically prepared and the bulla was widely opened to expose the cochlea with the otic capsule unopened. The vibrations in the radial direction were measured by pointing the OCT beam directly on the otic capsule at the apex turn. To measure the axial vibrations in the apex, the OCT beam was deflected by 90-degrees using a custom fixture with a small mirror placed inside the bulla at a 45-degree angle. Using this method, we measured the organ of Corti vibrations in the guinea pig apex in both radial and axial directions. The measured apex vibration data demonstrates significant compressive nonlinearity in live guinea pig that is absent postmortem. The magnitude of the vibrations in the radial direction are comparable to (same order of magnitude as) the vibrations in the axial direction. The compressive

nonlinearity, frequency response, and pattern of vibrations across the organ of Corti in the two directions will be presented.

PS-364

Interaction between Reticular Lamina and Basilar Membrane Vibration in Sensitive Cochlea

Tianying Ren; Wenxuan He
Oregon Health & Science University

Background

Remarkable sensitivity and sharp frequency selectivity of mammalian hearing depend on a functional cochlear amplifier, which uses the hair cell-generated force to boost the cochlear partition responses to soft sounds. In an intact cochlea, force generated by somatic and/or hair-bundle motility of the outer hair cells changes the shape of the organ of Corti, and disturbs surrounding cochlear fluid. However, the mechanism of how the hair cell-generated force drives the cochlear partition remains largely unknown.

Methods

After the cochlea was surgically exposed, the organ of Corti of the basal turn was electrically stimulated by passing a sinusoidal current through the cochlear partition. Using a purpose-built scanning low coherence heterodyne interferometer, electrically evoked reticular lamina and basilar membrane vibrations were measured through the intact round window membrane in the healthy mouse cochlea at the same longitudinal location as electrical stimulation. The reticular lamina location in the transverse direction was indicated by the carrier signal obtained by the vertical scanning. When the object light beam from the interferometer was focused on the reticular lamina or the basilar membrane, vibration magnitude and phase were measured as a function of frequency at different current levels.

Results

The magnitude of the reticular lamina vibration decreased with frequency at a constant rate and reached a minimum near 30 kHz. Above this frequency, the vibration magnitude increased and then decreased forming a response peak at the best frequency. The corresponding phase was approximately independent of frequency below 30 kHz and quickly decreased near the best frequency. The basilar membrane vibration magnitude was significantly smaller than that of reticular lamina vibration, and dominated by the tuned response. Despite significant phase difference between the reticular lamina and basilar membrane at the low-frequency side of the peak, there was no phase difference at the best frequency.

Conclusion

The current data indicate that the electrically evoked reticular lamina vibration constructively interferes with the basilar membrane vibration, resulting in high sensitivity and sharp tuning.

PS-365

Harmonic Distortion inside the Organ of Coti Measured Using a Scanning Heterodyne Low Coherence Interferometer

Wenxuan He; Tianying Ren
Oregon Health & Science University

Background

Mechanical harmonic distortion has been demonstrated in the basilar membrane vibration and in intra-cochlear fluid pressure near the cochlear partition. Since high sensitivity, sharp tuning, and large dynamic range of mammalian hearing depend on functional outer hair cells, these sensory cells are expected to play an essential role in the generation of harmonic distortion. Mechanical response at harmonic frequencies, however, has not been measured from microstructures near outer hair cells.

Methods

In the current study, a purpose-built scanning low coherence heterodyne interferometer was used to measure the reticular lamina and basilar membrane vibrations in the first turn of gerbil cochleae. The reticular lamina and basilar membrane locations in the transverse direction were determined by the carrier signal obtained by the vertical scanning at the radial location of the second row of outer hair cells. The magnitude and phase of the reticular lamina and basilar membrane vibrations were measured at primary and harmonic frequencies at different sound levels under sensitive and insensitive cochlear conditions.

Results

Harmonic distortion was observed in both reticular lamina and basilar membrane vibrations at intermediate and high sound levels in the sensitive cochlea. While basilar membrane harmonic distortion appeared near one-half of the best frequency, the reticular lamina harmonic distortion spread over a broad frequency range. The magnitude of reticular lamina harmonic distortion product was significantly higher than that of the basilar membrane distortion. Under the post-mortem condition, both reticular lamina and basilar membrane harmonic distortion disappeared at intermediate sound levels.

Conclusion

Due to direct mechanical coupling between outer hair cells and the reticular lamina, the current result implies that harmonic distortion is generated by the outer hair cells.

PS-366

Pressure-voltage-displacement Phase Shift Explains Active Cochlear Amplifier

Amir Nankali[1]; Julien Meaud[2]; Karl Grosh[1]
[1]University of Michigan; [2]Georgia Tech

Background

The pressure difference across the organ of Corti (OoC) produces a vibration of the micro-structures of the OoC. The OoC mechanical response ultimately gives rise to the sensation of sound. The vibration of the sensory epithelium is actively modified by stimulation of electromechanical forces of the cochlear outer hair cells (OHCs). A positive feedback

mechanism within the cochlea, called the cochlear amplifier, provides amplitude and frequency selectivity in the mammalian auditory system. The precise operating principle of cochlear active process is still under debate. One hypothesis is that OHC somatic motility converts electrical to mechanical power thereby enabling the nonlinear response of the cochlea. A model based on this hypothesis predicts that the frequency dependence of relative phase between OoC motion, intracochlear pressure, and extracellular potential in the scalae are related to the conversion of electrical to mechanical energy and to amplification. The purpose of this study is to test this hypothesis in a mathematical model of the cochlea and compare with experimental data.

Methods
We use a comprehensive three-dimensional model of the cochlea to test hypotheses of the cochlear function (described in Meaud and Grosh (2014)). The model is physiologically based and couples mechanical, acoustical (fluidic), and electrical features. The active process is explored by calculating pressure-displacement-voltage phase relation. The electrical output of the model is a prediction rather than a post-processing step. Hence, voltage predictions (along with basilar membrane (BM) displacement and fluid pressure) provide both insight into the operation of the cochlea and tests of model fidelity.

Results
We show a phase shift between voltage and BM displacement close to the characteristic frequency (CF) of a particular location along the cochlea. In our model we compute the mechanical power generated by the electrical process and show that the shift is correlated to generation of active power by OHC electromotility (voltage is nearly in phase with velocity). Moreover, our model predicts a voltage-pressure phase shift slightly below CF, consistent with the measurements of Dong and Olson (2013).

Conclusions
The conversion of electrical to mechanical power in the cochlea can be quantified not only by relating the local displacement to voltage but also by relating the voltage to pressure. The phase relation of both pressure and displacement to the voltage should be near 90 degrees for energy conversion to occur.

PS-367

A Second Resonator in the Organ of Corti Activated by Outer Hair Cell Motility

Yanju Liu; Sheryl Gracewski; Jong-Hoon Nam
University of Rochester

Background
One of classical views on cochlear mechanics is that the organ of Corti (OC) is a rigid frame to transform transverse vibrations of the basilar membrane into shear vibrations of the hair cell bundles (ter Kuile, 1900). Although this kinematic view seems still valid in passive cochlea, recent observations (Chen, et al., 2011) of the OC mechanics show that the OC vibrations are complicated at low sound pressure levels. The OC mechanics play an important role in active force transmission from the outer hair cell (Dong & Olson, 2013). Using a computational model, we investigated the complex modes of OC vibrations.

Methods
The model incorporates fluid dynamics, OC mechanics and outer hair cell motility. Cochlear fluid dynamics were solved using the 2-D finite difference method. Lumped parametric mechanics of the cochlear partition in classical models were replaced with a fully deformable 3-D finite element model of the OC complex (Nam & Fettiplace, 2012). The symmetry assumption of the cochlear fluid spaces was relaxed so that the top and the bottom fluid spaces interact with the top and the bottom surfaces of the OC, respectively. Assuming small stimulation, the outer hair cell's mechano-transduction is linearized and the model was solved in the frequency domain. The model was validated by comparing responses with known experimental data such as the frequency-place map and the traveling waves.

Results
The ratio of vibration amplitudes between the top and the bottom surfaces of the OC decreased from the basal toward the apical turn of the cochlea. This trend is consistent despite outer hair cell motility. The OC's top surface vibrations lead the bottom surface vibrations; however, they are in phase when there was no outer hair cell motility. In active OC, the outer hair cell membrane potential lags the basilar membrane displacement by 17(base), 34 (middle), and 25 (apex) degrees, whereas the phase lag became ~40 degrees throughout the length of cochlea when passive. The stiffness of the TM affected the sharpness of tuning, but did not affect overall frequency-place relation.

Summary
The OC complex responds as a single mechanical resonator when there is no active feedback from the outer hair cell. Outer hair cell active motility excites a second resonator of the OC complex in the basal turn. There exist qualitative differences between the apical and the basal responses that invite further investigation.

PS-368

A Canonical Nonlinear Cochlear Model

Karl Lerud[1]; Ji Chul Kim[1]; Felix V. Almonte[1]; Laurel Carney[2]; Edward W. Large[1]
[1]University of Connecticut; [2]University of Rochester

Nonlinear responses arise through active processes in the cochlea, which has exquisite sensitivity and a wide dynamic range that have been explained by critical nonlinear oscillations of hair cells. However, a single Hopf nonlinearity is insufficient to explain cochlear tuning at threshold levels. The question of how critical nonlinear oscillations interact with the basilar membrane and other organ of Corti components to determine tuning properties of the mammalian cochlea is a central issue. Here, we model cochlear dynamics using pairs of coupled canonical oscillators, each pair tuned to a distinct natural frequency corresponding to a specific place in the cochlear coil. A Hopf instability, which captures the nonlinear re-

sponses of outer hair cells and related organ of Corti components, is coupled to a linear basilar membrane that receives external input. We drive the system with a human middle ear model and determine cochlear parameters based on auditory-nerve tuning curves of macaque monkeys (Joris et al., PNAS, 2011). Finally, we perform a comprehensive dynamical analysis on the system, enabling us to understand its behavior in detail, and how this behavior accurately models the physiology. This leads us to a canonical computational model of the human cochlea as a tonotopically organized collection of oscillatory complexes, based on the principles of critical nonlinear oscillation and coupling dynamics.

PS-369

Electro-Acoustic Cochlear Implant Simulation Model

Attila Fráter[1]; Patrick Maas[1]; Jaime Undurraga[2]; Søren Riis[1]
[1]Oticon Medical; [2]University College London

Background

Atraumatic CI electrode technologies as well as improvements in surgical techniques have in recent years facilitated better preservation of residual low frequency (LF) hearing after CI implantation. For patients with residual LF hearing, hybrid electro-acoustic stimulation (EAS) devices show great promise for improved hearing performance. However, combining electric and acoustic hearing in the same cochlear is by no means trivial – information on stimulation interaction is limited. The goal of this work is to establish simulation model combining electrical and acoustic stimulation at the auditory nerve level. With such a model it is possible to simulate and study effects of e.g. timing between electrical and acoustic stimulation, aspects of acoustic versus electric compression as well as effects of temporal or frequency masking between the two stimulation modes.

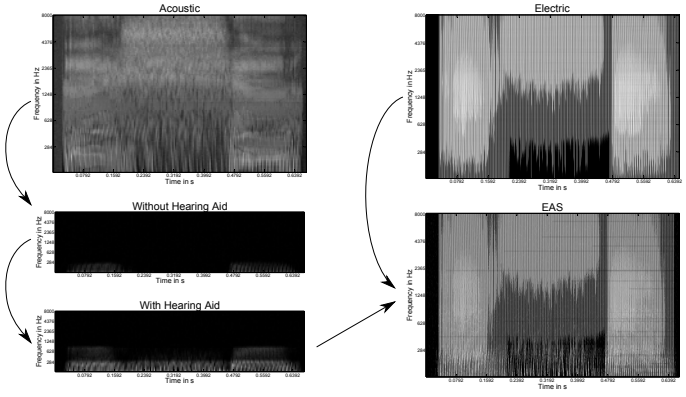

Methods

A computational model simulating EAS in CI users is built to mimic the neural response of auditory nerves. The Matlab Auditory Periphery (MAP) model is modified to account for impaired hearing and is furthermore extended to include a simple hearing aid (amplification) model. For the electric path, we use a model representing an Oticon Medical CI processor augmented by a model of the electric-to-auditory nerve interface. The phenomenological point process model of Joshua H. Goldwyn is used to generate auditory nerve firing patterns. This model also serves as a way of connecting acoustic and electric stimulation at the auditory nerve level by means of an inverse distribution function technique applied to the superimposed firing intensities.

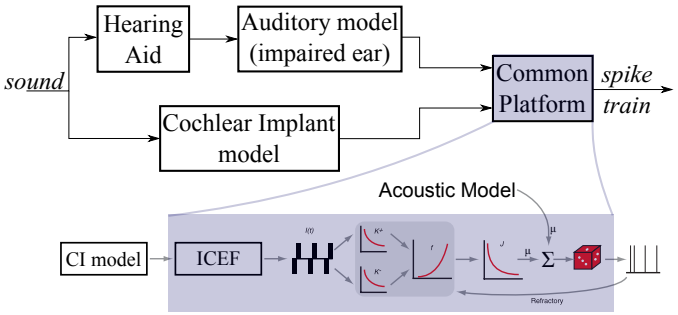

Results

For evaluation, the EAS model spike patterns are converted into neurograms in which the typical biophysical responses of the auditory system for acoustic and electric stimulation can be observed. Neurograms also serve as an input for a Neural Similarity Index Measure (NSIM), an objective measure by which neural activities evoked by different stimuli and model configurations can be compared. First results illustrate the importance of timing between electric and acoustic stimulation.

Conclusion

A model for simulating joint acoustic and electric stimulation at the auditory nerve spike pattern level has successfully been implemented. The model output has been verified to produce representative auditory nerve response patterns for different stimulation modes (acoustic, electric, EAS) on both artificial and VCV word stimuli. Moreover, it has been demonstrated how to apply NSIM as a measure between EAS model output and (normal hearing) acoustic model output to guide optimization of timing between acoustic and electric “N-of-M” CIS type stimulation.

PS-370

Contributions of Middle-Ear Inertia and Oval-Window Mobility on Bone Conduction Hearing

Xiying Guan[1]; Christof Stieger[2]; Rosemary Farahmand[1]; Brent Page[3]; Julie Merchant[3]; Defne Abur[3]; John Rosowski[1]; Hideko Nakajima[1]
[1]Harvard Medical School, Massachusetts Eye & Ear Infirmary, Boston, MA; [2]University Hospital Basel, University Bern, Switzerland; [3]Massachusetts Eye & Ear Infirmary, Boston, MA

Introduction

Although various BC mechanisms have been proposed, the relative contributions and details of these mechanisms have not been well characterized. One of the proposed contributors to BC is inertia of the middle ear that would have a frequency-dependent motion relative to the rest of the vibrating skull and temporal bone. Furthermore, a stiffened oval window (stapes footplate fixation) due to otosclerosis is clinically known to result in decreased BC sound transmission near 2 kHz, known as Carhart’s notch. The goals of this study are to quantify the contribution of the middle-ear inertia and to evaluate the effect of stapes fixation.

Methods
Intracochlear pressures in scala vestibuli and scala tympani of 6 fresh human specimens were measured with micro-fiber-optic sensors in the manner described in previous studies. The sensors were cemented to the bony cochlear surface allowing the sensors to vibrate together with the bone. Intracochlear pressures evoked by a Baha were measured under three experimental conditions: 1) intact ossicular chain, 2) the ossicles disarticulated at the incudo-stapedial joint to remove a majority of the middle-ear inertia, 3) and with the stapes footplate fixed.

Results
During BC stimulation, both the effects of ossiclar inertia and stapes fixation on intracochlear pressures were frequency-dependent. When the majority of the middle-ear mass was removed, on average the pressure magnitude in scala vestibuli (Psv) fell about 7 dB between 0.9-4 kHz. Stapes fixation resulted in 10-15 dB decrease in Psv over a similar frequency range (0.8-3 kHz). Scala tympani pressure (Pst) was smaller than Psv for all experimental conditions. Pst also decreased after each manipulation, but this reduction varied across specimens. The average decrease in Pst due to middle-ear disarticulation was 5 dB over 1-3 kHz, while oval-window fixation resulted in 10-15 dB reductions over 1-8 kHz. The effect on cochlear input drive, Psv-Pst, was similar to the effect on Psv for each condition.

Conclusion
The mechanism for Carhart's notch has been ascribed to the effect of middle-ear resonance. Our data is consistent with this idea in that removing most of the inertial effects of the middle ear has a significant effect on mid-frequency bone-conduction response. However, we find that preventing oval-window mobility has a greater effect at the same frequencies. Our data suggests that Carhart's notch depends more on the reduction in oval-window mobility than the loss of middle-ear resonance. This study is supported by NIH/NIDCD R01DC013303.

PS-371

Some Investigations into the Mechanisms of Bone Conducted Sound

Nathaniel Greene[1]; Jameson Mattingly[1]; Herman A Jenkins[1]; Daniel Tollin[1]; James R Easter[2]; Stephen P Cass[1]
[1]University of Colorado Anschutz Medical Campus; [2]Cochlear Boulder, LLC

Introduction
Bone-anchored hearing aids have gained considerable popularity in recent years for treatment of single-sided deafness, conductive hearing loss, or mixed hearing loss. Despite this success, the mechanisms underlying sound perception resulting from bone conducted sound remain unclear. Potential contributions include sound pressure generated in the ear canal or inner ear, ossicular or cochlear fluid inertia, cochlear compression, third window effects, and dynamic pressure transmission from the cerebrospinal fluid. Here, we investigate the mechanics of bone conducted sound in human cadavers by simultaneous measurement of ear canal SPL, stapes, round window, and cochlear promontory velocities, and scala vestibuli and tympani sound pressure during air and bone conducted sound stimulation.

Methods
Four whole cadaveric human heads were prepared by mastoidectomy and extended facial recess approach to expose the ossicular chain in both ears. Harmonic stimuli, with frequencies between 20 Hz and 2.5kHz, were presented via a calibrated closed-field earphone coupled to the ear canal, and by a bone conduction implant attached to the mastoid bone via a titanium abutment implanted ipsilateral to the measured ear. Pressure probes (FISO, Inc.) recorded sound pressure in the scala vestibuli (P_{SV}) and scala tympani (P_{ST}) concurrently with laser Doppler vibrometry (LDV) measurements of stapes, round window membrane, and cochlear promontory velocities ($V_{stap/RW/Prom}$), as well as the SPL in the ear canal. Responses were analyzed in both the time and frequency domains.

Results
Transfer functions were constructed from the FFT of each response. $V_{Stap/RW/Prom}$ were essentially identical for low frequencies (< ~700 Hz), while at higher frequencies (>1 kHz) V_{Prom} showed lower velocities. No substantial variation in phase was noted across the three locations. Similarly, P_{SV} and P_{ST} magnitude and phase were comparable (generally within 5 dB) at most frequencies, and showed lower responses with respect to stapes velocity for low and moderate frequencies (< ~5 kHz) when compared to air conducted sound.

Conclusions
These results suggest that multiple, frequency-dependent mechanisms likely contribute to the transmission of bone conducted sound to the cochlea, and in particular that ossicular motion likely contributes little to the mechanism of bone conducted sound input to the cochlea.

PS-372

Effects of Ipsilateral and Contralateral Placement of Bone-Conduction Systems on Cochlear Input Signal

Jameson Mattingly[1]; Nathaniel Greene[1]; Herman A. Jenkins[1]; Daniel Tollin[1]; James R. Easter[2]; Stephen P. Cass[1]
[1]University of Colorado-Denver; [2]Cochlear Boudler, LLC

Introduction
Bone-conduction (BC) implants have gained considerable popularity since their introduction in treating conductive hearing loss and single-sided deafness. Prior clinical studies have investigated the motion of the ossicular chain, skull, and round window in response to BC vibrations; however, little data exists measuring and comparing the difference in direct cochlear input with both ipsi- and contralateral stimulation. Here, we compare the velocity of the stapes, round window, and promontory ($V_{S/RW/Prom}$) and intracochlear pressures (P_{IC}) in human cadavers during presentation of BC sound ipsi- and contralateral to the measured ear.

Methods:
Both ears in four full cephalic human cadaveric temporal bones were prepared by mastoidectomy and an extended facial recess approach. P_{IC} was measured in the scala vestibuli and tympani with fiber optic pressure probes (FISO, Inc.) concurrently with $V_{S/RW/Prom}$ via laser Doppler vibrometry (Polytec, Inc.). Bilateral titanium implants were placed connected to an abutment. A BC transducer coupled to custom software provided pure tone stimuli between 20 Hz–15 kHz.

Results:
Transfer functions were generated from the fast-Fourier transform of each of the three measures. In all cases, magnitudes were comparable between ipsi and contralateral stimulation up to approximately 1 kHz, above which the measures decreased in response to contralateral relative to ipsilateral stimulation (by up to ~14 dB). Similarly, in each condition the slope of the phase above 1 kHz was steeper for contralateral than ipsilateral stimulation, suggesting an increased group delay from contralateral stimulation.

Conclusions:
Contralateral BC stimulation provides similar low-, and somewhat reduced magnitude high-frequency stimulation of the cochlea relative to ipsilateral BC stimulation. Likewise, contralateral stimulation produces a longer delay than ipsilateral stimulation. These results suggest the ipsilateral implant dominates the cochlear response, and differences in phase (timing differences) may provide sound localization cues in unilaterally implanted patients with single-sided deafness, as well as those with bilateral implants.

PS-373

A Sensorineural Hearing Loss Rat Model Based on Laser-Induced Shock Waves

Katsuki Niwa[1]; Kunio Mizutari[2]; Toshiyasu Matsui[3]; Takaomi Kurioka[2]; Takeshi Matsunobu[4]; Atsushi Tamura[5]; Satoko Kawauchi[6]; Shunichi Sato[6]; Yasushi Satoh[7]; Akihiro Shiotani[2]; Yasushi Kobayashi[3]
[1]National Defense Medical College, Saitama, Japan; [2]Department of Otolaryngology, Head and Neck Surgery, National Defense Medical College, Japan; [3]Department of Anatomy and Neurobiology, National Defense Medical College, Japan; [4]Division of Otolaryngology, New Tokyo Hospital, Japan; [5]Department of Otolaryngology, National Defense Medical College, Japan; [6]Department of Biomedical Information Science, National Defense Medical College, Japan; [7]Department of Anesthesiology, National Defense Medical College, Japan

Background
Sensorineural hearing loss caused by a shock wave is the most critical etiology relating to blast-induced hearing loss. We have already established small animal models of blast-induced traumatic brain injury and lung injury that are induced by laser-induced shock-waves (LISWs). The use of LISWs has many advantages to mimic traumatic injuries for organs, e.g., highly controllable shock wave energy, site-selectivity and reproducibility. We, herein, present a novel hearing loss model based on LISWs to replicate a blast-induced hearing loss.

Methods
Sprague-Dawley rats were used. LISWs were generated by irradiating a laser target with a nanosecond Nd:YAG laser pulse at three different laser fluences of 2.0, 2.25, and 2.5 J/cm^2. A set of LISW irradiation was applied to the right cochlear region via postauricular approach. The thresholds of auditory brainstem responses (ABRs) were measured continuously up to 4 weeks, and histological analysis was performed at 4 weeks after treatment. Hair cell and synaptic ribbon counts were conducted using whole-mount preparation of the organs of Corti, and spiral ganglion neuron (SGN) count was done by cross section of the cochleae.

Results
The ABR thresholds were elevated 1 day after treatment on all treatment groups. On the 2.0 J/cm^2 group, the threshold was recovered at pre-treatment level at 1 week after treatment. In contrast, the threshold shifts at high frequencies were remained up to 4 weeks after treatment on the 2.25 and 2.5 J/ cm^2 groups. Histological analysis revealed that the numbers of synaptic ribbon at the high frequencies area were significantly decreased on the 2.25 and 2.5 J/ cm^2 groups compared to the control group without LISW exposure, while the numbers of hair cells were preserved in each group. The numbers of SGNs at high frequencies were also significantly decreased on the 2.25 and 2.5 J/ cm^2 groups. All treated animals were survived after LISWs irradiation without any side injuries such as perforation of eardrum or cerebral hemorrhage.

Conclusion
Our rat model revealed that LISWs could generate gradient sensorineural hearing loss in shock wave energy dependent manner. Interestingly, significant hair cell loss was not observed even though the permanent threshold shifts occurred after LISW irradiation. These findings suggest that the cause of permanent threshold shifts on the high-power irradiated groups is dysfunction of synapses between the inner hair cells and the SGNs, or SGNs themselves. This model would replicate important characteristics of blast-induced hearing loss.

PS-374

Cochlear Fluid Dynamics as Revealed by Optical Coherence Tomography (OCT) : The Inside Story

Egbert de Boer[1]; Fangyi Chen[2]; Dingjun Zha[2]; Alfred Nuttall[2]
[1]Academic Medical Centre, University of Amsterdam, The Netherlands; [2]Oregon Hearing Research Center, Oregon Health & Science University

Introduction

Optical Coherence Tomography (OCT) allows us to measure movements of the basilar membrane (BM) and the Reticular Lamina (RL) separately. In a viable cochlea, the RL moves in the region of maximum response with an amplitude about

three times larger than the BM. This implies that during sound stimulation the volume of the fluid in the Channel of Corti (CoC) is not constant. We have observed only minor effects of the stimulus level on the (scaled) amplitude ratio and the phase relations at the two locations. We assume, therefore, that the effect of cochlear amplification on the difference between RL and BM movements is mostly a geometrical effect. This poster describes a few physical consequences of this idea.

We use a mathematical model. The geometry of the Channel of Corti is simplified to that of a rectangular box. On the upper and lower sides the fluid is excited by the movements of the Reticular Lamina (RL) and Basilar Membrane (BM), respectively. On one side the box has a solid wall, on the other side it is left open – that is where oscillating fluid can flow in and out. Appropriate boundary conditions are applied to the walls. The movements of the fluid in a cross-section of the channel are computed by solving the Poisson equation. In earlier work we considered the fluid-filled channel as an entity with an internal impedance, driven on the upper side from the stapes and loaded on the underside by the BM and the elements of the Organ of Corti connected to it. We now attempt to unite these two views. One conclusion can be drawn and one suggestion formulated. The conclusion is that effects of cochlear amplification on the RL-BM relation are (unexpectedly) small – and difficult to understand, and the suggestion: Many more especially directed and focused experiments are necessary to fill the gaps in our knowledge and understanding.

PS-375

Transmembrane Channel-like 1 and 2 are Localized at Stereociliary Tips of Mammalian Inner Ear Hair Cells

Kiyoto Kurima[1]; Bifeng Pan[2]; Seham Ebrahim[3]; Bryan Millis[3]; Taro Fujikawa[3]; Yoshiyuki Kawashima[3]; Hiroshi Nakanishi[3]; Runjia Cui[3]; Byung Yoon Choi[3]; Kelly Monahan[3]; Jeffrey Holt[2]; Andrew Griffith[3]; Bechara Kachar[3]
[1]National Institutes of Health; [2]Boston Children's Hospital, Harvard Medical School; [3]National Institute on Deafness and Other Communication Disorders, NIH

Background

Transmembrane channel-like 1 and 2 (TMC1 and TMC2) are essential for mechanoelectrical transduction (MET) in inner ear hair cell stereocilia, but conclusive evidence of their localization at the site of MET is incomplete.

Methods

To determine TMC protein localization in inner ear sensory hair cells, we generated bacterial artificial chromosome (BAC) transgenic mice expressing TMC1-mCherry and TMC2-AcGFP. The spatiotemporal expression and localization of the fluorophore-tagged TMC proteins in the hair cell stereocilia were observed by confocal microscopy. The localization of the native TMC1 and TMC2 were confirmed by immunofluorescence using specific antibodies.

Results

Expression of both TMC1-mCherry and TMC2-AcGFP restored the hair cell MET currents of homozygous *Tmc1* and *Tmc2* double mutant mice, and TMC1-mCherry alone rescued hearing and vestibular function, while TMC2-AcGFP alone rescued vestibular function only, consistent with the known expression and function of TMC1 and TMC2 in cochlear and vestibular hair cells. Both TMC1-mCherry and TMC2-AcGFP signals were observed as diffraction-limited puncta in stereocilia of inner ear hair cells. These fluorescent puncta were localized at the tips of shorter stereocilia, but absent from the tips of the tallest row of the stereocilia bundle where MET activity is thought to be absent. This distribution was confirmed for native TMC1 and TMC2 by immunofluorescence using specific antibodies. Consistent with the hypothesis that MET current in early neonatal cochlear hair cells of TMC1-deficient mice depends on the transient expression of *Tmc2*, TMC2 signals at cochlear hair cells were present at P3, but rapidly disappeared from stereocilia tips, first from outer hair cells (OHCs) and then from inner hair cells (IHCs) by P10. Conversely, TMC1 signal at the stereociliary tips persisted in both OHCs and IHCs to adulthood. When both TMC1-mCherry and TMC2-AcGFP were concurrently expressed, overlap of TMC1 and TMC2 fluorescence signals was often observed at the stereocilia tips of IHCs. The average intensities of TMC1-mCherry or TMC2-AcGFP fluorescent puncta at stereocilia tips were compatible regardless of whether these puncta comprise only TMC1-mCherry, only TMC2-AcGFP or both, suggesting that TMC1 and TMC2 do not exclude each other.

Conclusion

These data collectively establish the localization of TMC1 and TMC2 at stereocilia tips, consistent with the hypothesis that they are component of MET channel complex.

PS-376

Can TMC2 Compensate for TMC1 in Mature Cochlear Hair Cells?

Hiroshi Nakanishi[1]; Kiyoto Kurima[2]; Philine Wangemann[3]; Bifeng Pan[4]; Jeffrey Holt[4]; Andrew Griffith[2]
[1]NIH; [2]NIDCD, NIH; [3]Kansas State University; [4]Children's Hospital, Harvard Medical School

Background

Mouse TMC1 and TMC2 are required for mechanoelectrical transduction (MET) in cochlear and vestibular hair cells (HCs). Homozygous *Tmc1*$^{\Delta/\Delta}$ mice are deaf, *Tmc2*$^{\Delta/\Delta}$ mice have normal hearing, and double homozygous *Tmc1*$^{\Delta/\Delta}$;*Tmc2*$^{\Delta/\Delta}$ mice have deafness and profound vestibular dysfunction. These phenotypes are consistent with their different spatiotemporal expression patterns: *Tmc1* expression is persistent in cochlear and vestibular HCs, whereas *Tmc2* expression is transient in cochlear HCs but persisted in vestibular HCs. These results suggested that persistent *Tmc2* expression in vestibular HCs preserves vestibular function in *Tmc1*$^{\Delta/\Delta}$ mice. In this study, we hypothesized that persistent *Tmc2* expression in mature cochlear HCs could rescue auditory function in *Tmc1*$^{\Delta/\Delta}$ mice.

Methods:
We generated a bacterial artificial chromosome transgenic mouse line, Tg (P_{Tmc1}-*Tmc2*), in which *Tmc2* is expressed under the control of the *Tmc1* promoter so that it is expressed in mature cochlear HCs. We crossed Tg (P_{Tmc1}-*Tmc2*) and *Tmc1*$^{\Delta/\Delta}$ to generate Tg (P_{Tmc1}-*Tmc2*); *Tmc1*$^{\Delta/\Delta}$ mice for auditory and vestibular phenotypic analysis. FM1-43 uptake was evaluated as a proxy measure of MET in HCs.

Results:
The hearing thresholds of Tg (P_{Tmc1}-*Tmc2*); *Tmc1*$^{\Delta/\Delta}$ mice were approximately 80 dB SPL at postnatal day 16 (P16) and rapidly progressed to no responses at 90 dB SPL at P25. FM1-43 uptake was observed both in inner and outer HCs at P16. Outer, but not inner HCs took up FM1-43 at P25. Distortion product otoacoustic emission levels were nearly identical to those of *Tmc1*$^{\Delta/\Delta}$ mice at P16, indicating that active amplification by outer HCs was not rescued. Scanning electron microscopy of the organ of Corti demonstrated that HC stereocilia were intact in inner and outer HCs at P16. At P25, the stereocilia bundles were intact in inner HCs from the apical turn and in outer HCs from the apical to middle turns.

Conclusion:
The elevation of hearing thresholds were due to gradual disruption of MET channel function in inner HCs and disruption of the active amplification function of outer HCs. TMC2 expressed in mature cochlear HCs can partially rescue hearing in *Tmc1*$^{\Delta/\Delta}$ mice, but cannot fully compensate for TMC1.

PS-377

Functional Characterisation of Transmembrane Channel-Like Protein 1 and 2 Mutant Mice

Laura Corns; Walter Marcotti
University of Sheffield

Background
The mechanoelectrical transducer (MET) channel opens in response to stereociliary bundle deflection resulting in an inward current, the role of which is to depolarize hair cells and drive synaptic transmission at their basolateral membrane. There is strong evidence that transmembrane channel-like proteins 1 and 2 (TMC1 and TMC2) play a role in mechanoelectrical transduction (Kawashima *et al.,* J Clin Invest, 121:12; Pan *et al.,* Neuron, 79:1), however, the exact role is yet to be fully established. We showed that the amplitude of the MET current is unaffected in *beethoven mice* (*tmc1*$^{bth/bth}$), which have a single point mutation in *tmc1*, but the calcium reversal potential is reduced (Corns & Marcotti, ARO 2013, PS-774). TMC2 has been suggested to compensate for some loss of function observed in *tmc1* mutant mice (Kawashima *et al.,* J Clin Invest, 121:12). To further elucidate the relative roles of TMC1 and TMC2 we have investigated the MET current properties in *tmc2*$^{\Delta/\Delta}$;*tmc1*$^{bth/bth}$ mice.

Method
We performed whole cell patch clamp recordings from outer hair cells (OHCs) of the apical coil in acutely dissected organs of Corti from *tmc2*$^{\Delta/\Delta}$;*tmc1*$^{bth/bth}$ mice and littermate controls. MET currents were recorded from postnatal day 2 (P2) to P14. To elicit the MET current, a piezoelectric driven fluid jet was placed close to the hair bundles and 50 Hz sinusoidal stimuli applied.

Results
The amplitude of the MET currents recorded in apical OHCs did not differ between any of the combinations of *tmc1*$^{bth/bth}$ and *tmc2*$^{\Delta/\Delta}$ at any age investigated. The calcium reversal potential was significantly lower in *tmc2*$^{\Delta/\Delta}$;*tmc1*$^{bth/bth}$ and *tmc2*$^{\Delta/\Delta}$;*tmc1*$^{+/bth}$ mice compared to controls. Removing TMC2 alone did not have any effect on the calcium reversal potential in mice of all *beethoven* genotypes. In addition, the MET channel blocker, dihydrostreptomycin, was less effective at blocking the MET current in *tmc1*$^{bth/bth}$ mice than controls.

Conclusions
Our results suggest that TMC2 is not able to compensate for the defects associated with the *tmc1* mutation in *beethoven* mice. The role of TMC1 is still open to interpretation, with possibilities including it forming the pore of the MET channel, acting as an accessory subunit of the MET channel or trafficking essential MET components to the stereocilia tips.

PS-378

Lhfpl5 Mutation Alters the Conductance and Ca2+-selectivity of Hair-cell Mechanotransducer Channels

Maryline Beurg[1]; Wei Xiong[2]; **Robert Fettiplace[1]**
[1]University of Wisconsin, Madison; [2]The Scripps Research Institute

Introduction
Tetraspan membrane protein of hair cell stereocilia (TMHS, also referred to as LHFPL5), has been proposed as an integral component of the mechanotransduction machinery in cochlear hair cells, where it has been shown to interact with the tip-link constituent protocadherin-15 (Xiong et al. 2012). Mutation of *Lhfpl5* produces profound deafness in mice and in humans (Kalay et al. 2006; Longo-Guess et al. 2007), but its exact role in the transduction machinery is unknown.

Methods
Mechanotransducer (MT) currents were recorded in response to hair bundle deflections in patch-clamped cochlear outer hair cells of neonatal mice (post natal days 2 to 10) harboring an *Lhfpl5* null mutation. Comparisons were made with MT channel properties in *Tmc1* and *Tmc2* single and double mutants.

Results
Both the unitary conductance and Ca^{2+} selectivity of MT channels in the *Lhfpl5* mutant were reduced relative to wild-type. In addition, the tonotopic gradient in single MT-channel conductance, in which channels from the cochlear base have a conductance about twice those at the apex, was virtually absent in *Lhfpl5* mutants. In such mutants, the macroscopic MT current was strongly attenuated and the tonotopic gradient in its amplitude was also lost, though the current itself was not totally abolished. Besides this reduced conventional MT current, a larger-amplitude current could be evoked in the *Lh-*

fpl5 knockout by negative displacements of the hair bundle; this 'reversed-polarity' mode of stimulation was previously reported in hair cells of transmembrane channel-like protein (*Tmc1/Tmc2*) double mutants. The macroscopic MT current therefore possessed a two-harmonic structure. Several consequences of *Lhfpl5* mutation resemble those due to *Tmc1* mutation, implying that a component of the MT-channel conferring large conductance and high Ca^{2+}-selectivity is similarly disrupted in the absence of *Lhfpl5* or *Tmc1*. Immuno-labeling showed TMC1 was distributed throughout the stereociliary bundles in wild-type, but not in *Lhfpl5* mutants, raising the possibility that the effects of the *Lhfpl5* mutations may stem from down-regulation of TMC1. Localization of LHFPL5 to the stereocilia was unaffected in *Tmc1/Tmc2* double mutants.

Conclusion

We suggest that LHFPL5, similar to the tetraspan TARP proteins at glutamatergic synapses, may contribute directly as an accessory subunit of the MT channel and indirectly by targeting TMC1 and possibly other proteins to the channel complex. A variable amount of TMC1, as an accessory channel subunit, may account in the wild-type for the tonotopic gradient in single-channel conductance.

PS-379

Cadherin 23 Regulates Microtubule Structure in Receptor Cells of Cochlea and Retina via its Interaction with Marshalin

Jing Zheng; Vincent J. Mui; Jun Shi; Chongwen Duan; Mark F. Morel; MaryAnn Cheatham; Steven H DeVries
Northwestern University

Introduction

Cadherin 23 (CDH23) plays a crucial role in hearing, balance, and vision. In fact, Usher syndrome 1D is caused by mutation of CDH23. Besides forming the transient kinociliary links and the tip links in hair cells, CDH23 is also found around the centrosome and synaptic terminals of both hair cells and photoreceptor cells (Lagziel, et al., 2009). In order to define CDH23's various physiological role(s), we identified marshalin, a microtubule (MT) minus-end-binding protein, as a potential CDH23-associated protein (Zheng et al., 2009). Marshalin contains multiple protein interacting domains including a tubulin-binding domain called CKK. Marshalin stabilizes MTs through its binding to MT minus-ends, thereby protecting MTs from disassembly (Goodwin and Vale, 2010). As a rare MT minus-end-binding protein carrying several protein-protein interacting domains, marshalin may have a significant biological impact on the regulation of MTs that are known to play an important role in vesicle transport. The purpose of this study is to investigate the relationship between marshalin and CDH23, and explore its role in hearing and vision.

Methods

Plasmids encoding various marshalin and CDH23 isoforms or domains were transiently transfected into opossum kidney (OK) cells. Cytoskeleton changes induced by marshalin/CDH23 expression were investigated by immunocytochemistry. The physical association between marshalin and CDH23 was studied by co-immunoprecipitation (Co-IP). A Marshalin antibody was also used to reveal protein expression in both cochlea and retina.

Results

Marshalin is capable of dramatically organizing MTs into bundles in transiently transfected OK cells. However, CDH23 short isoforms, CDH23C1 or CDH23C, inhibit marshalin-induced MT bundle formation when CDH23 is co-transfected with marshalin into OK cells. This observation is consistent with Co-IP data indicating a physical association between CDH23 and marshalin. Our results also suggest that the N terminus of CDH23-C1/C2 binds to the CKK domain of marshalin. Immunohistochemistry also showed that labeling for marshalin, like that for CDH23 (Lagziel, et al., 2009), is found at the synaptic terminals of both hair cells and cone photoreceptor cells.

Conclusion

CDH23 binds to marshalin's CKK domain that is also a tubulin-binding site. By competing with tubulin for this CKK domain, CDH23 prevents marshalin binding to tubulin. Without the protection provided by marshalin binding, CDH23 indirectly facilitates MT depolymerization. These data suggest that CDH23 can regulate MT networks through its interaction with marshalin, thereby playing a role in synaptogenesis.

PS-380

Manipulation with Magnetic Tweezers of Mechanosensitive Ion Channels and Adaptation Motors in the Hair Cells of the Inner Ear.

Aakash Basu; Samuel Lagier; Maria Vologodskaia; Brian Fabella; A.J. Hudspeth
The Rockefeller University

Hair cells, ubiquitously found in the auditory and vestibular systems of vertebrates, transduce mechanical stimuli into electrical responses. The apical surface of each cell sports a hair bundle composed of numerous actin-filled stereocilia. Mechanical stimulation deflects the hair bundle and tenses filamentous cadherin tetramers called tip links that interconnect adjacent stereocilia. Tensing of the tip links is thought to open mechanosensitive ion channels to which the links are connected, leading to depolarization of the hair cell and the subsequent firing of afferent nerve fibers. A motor containing myosin 1c molecules readjusts the tension in the tip links, allowing transduction to adapt during sustained deflections. Because the channels and motors lie deep within the hair bundle, the direct experimental manipulation of the individual components has been challenging: experiments have heretofore been limited to deflections of entire hair bundles. We have devised a scheme for labeling tip links from the sacculus of the bullfrog's inner ear with paramagnetic particles through an epitope-specific anti-cadherin antibody and a long DNA tether. By measuring the potential difference across the tissue, we show that application of a magnetic field elicits inward transduction current—a result that directly confirms the hypothesis that tension in the tip links gates the mechanically sensitive channels. Future experiments that track the position

of the magnetic particle may demonstrate the opening and closing of transduction channels and the climbing and slipping of adaptation motors.

PS-381

Hair Bundle Coherence Dictates Response to Mechanical Stimulations

Jong-Hoon Nam[1]; Anthony Peng[2]; Anthony Ricci[2]
[1]University of Rochester; [2]Stanford University

Background

Hair cell sensitivity is represented by the mechanotransduction current-hair bundle displacement (I-X) relationship. A common technique for obtaining hair cell's I-X curve is to deliver mechanical stimulations to the hair bundle through a micro-probe and measure whole cell transduction current through a patch pipette electrode at the basolateral membrane. The sensory epithelium of the mammalian cochlea vibrates less than 100 nm even at high sound pressure levels. However, the measured operating range (OR, the range of hair bundle displacement corresponding to 10-90 percent activation) of cochlear hair cells *in vitro* ranges 100-1000 nm. Through computational simulations and experiments, we show that an experimental artifact (uneven stimulation) can explain the difference.

Methods

Computational: Two stereocilia bundles, one of outer hair cell and the other of inner hair cell, were modeled and simulated using finite element method. The profiles of different shaped probes were represented by rigid frames contacting individual stereociliary tips. The effect of different elastic and viscous couplings between stereocilia were simulated. Experimental: Different micro-probes were used to stimulate outer hair cell bundles and the I-X relations were measured. Inner hair cell stereociliary bundles were locally stimulated by a narrow-tipped fluid-jet, and Ca^{2+} flux into the stereocilia was visualized.

Results

Unlike natural situation where the hair cell stereocilia are evenly stimulated by the tectorial membrane, micro-probe deformed the stereociliary bundle unevenly. As a result, the OR in the micro-probe stimulation case was increased by a factor of 2-8 depending on the probe shapes. The uneven deformation of the stereocilia was more prominent between columns than between rows. According to our computational analysis, the elastic coupling between the stereocilia was more effective in binding the stereocilia together than the viscous coupling. Experiments also showed that the micro-probe tip that fitted better with the bundle profile resulted in narrower OR. The Ca^{2+} imaging of the stereocilia demonstrated that the mechano-transducer channels in a hair bundle do not respond in unison when the hair bundle was locally stimulated.

Conclusions

In the mammalian cochlear hair cells, the splay of a hair bundle due to uneven stimulation results in underestimation of the bundle stiffness. An incorrect assumption of even stimulation results in an overestimation of the gating swing and an underestimation of the gating spring stiffness. A proper mechanical stimulation of mammalian cochlear hair cells is important to derive correct biophysical parameters of hair cell mechano-transduction.

PS-382

Synchronized Spontaneous Oscillation of Hair Bundles in Bullfrog Sacculus

Tracy Zhang[1]; Dolores Bozovic[2]
[1]University of California, Los Angeles; [2]University of California, UCLA

The active process in the hair cells of the inner ear plays an important role in achieving the high sensitivity and frequency tuning of the auditory system. To study the active process, we focus on the spontaneous oscillation of hair bundles in the frog sacculus. In vivo, the hair bundles are coupled by the overlying structure, and we want to study the effect of coupling on spontaneous oscillations. We used microbeads to couple a few adjacent hair bundles in vitro, and observed synchronization of spontaneous oscillations. Up to four bundles can synchronize, and mode-locking can be either one-to-one or multi-mode. The mean frequency of synchronized oscillations was close to the average of original characteristic frequencies. Moreover, the spread of characteristic frequencies in the group determined how well they can synchronize. Smaller spread corresponded to higher correlation of synchronized oscillations. We also observed improved regularity of oscillations, as the oscillations had higher Q factor when bundles were synchronized. The results could indicate that coupling plays a role in making the system more effective, and our next step is to study how the coupled system responds to outside stimuli.

PS-383

Effect of Calcium on Spontaneous Bundle Oscillations in Saccular Hair Cells

Sebastiaan Meenderink; Patricia Quinones; Dolores Bozovic
University of California, Los Angeles

Introduction

Mechanical perturbations (sounds, vibrations) are transformed into electrical signals (currents) by mechanically gated ion channels within the hair bundle of the sensory hair cell. This mechano-electrical transduction (MET) involves the opening and closing of these channels as well as calcium-dependent adaptation, the interplay of which can lead to limit-cycle oscillations of the hair bundle. Here, we explore the role of calcium in the bundle dynamics.

Methods

For the experiments, we used freshly dissected sacculi from the American bullfrog (*R. catesbeiana*) that were mounted in a two-compartment configuration such that the *in vivo* condition of fluid separation between the apical and basal surfaces was maintained. Hair bundle motion was recorded using a high-speed video camera system, while the hair cell membrane potential was controlled by whole-cell voltage clamp, thus obtaining the MET currents.

Results & Conclusions
We found that the membrane potential controls several properties of spontaneously oscillating hair bundles. For one, the hair bundle transitions from the oscillatory to the quiescent regime at depolarized levels. Also, the steady-state (i.e., resting) position of the hair bundle varies systematically, but nonlinearly, with membrane potential, thus setting the MET open probability at rest. We hypothesize that these dependencies on membrane potential reflect the internal calcium-concentration at the level of the transduction complex, $[Ca^{2+}]_i$.

The instantaneous current-displacement functions from the recordings are well described by a first-order Boltzmann function, from which we can derive the maximum MET current and single-channel gating force as functions of the membrane potential. The former agrees with the MET channel being nonselective for cations; however, we do observe two populations of hair bundles with different MET conductance. We found the gating force to be independent of membrane potential, suggesting that $[Ca^{2+}]_i$ does not directly change the stiffness of the gating spring.

Funding
This work was supported by NIH grant RO1DC011380 to DB.

PS-384

Spontaneous Bundle Oscillations Beyond the Frog Sacculus

Patricia Quiñones; Sebastiaan Meenderink; Dolores Bozovic
University of California, Los Angeles

Introduction
The response of hair bundles to incoming signals has been modeled using nonlinear dynamics. One prediction of these models is that, under specific conditions, hair bundles may move spontaneously in a limit-cycle oscillation. Such spontaneous oscillations have indeed been observed in hair cells from both the frog sacculus and the turtle basilar papilla. In the experiments described here, we searched for spontaneous oscillations in several end organs—which are vestibular and/or auditory in nature—that are found in the frog inner ear.

Methods
The frog ear holds eight end organs, each with its own sensory epithelium holding several to hundreds of hair cells. End organs were freshly dissected from *Rana catesbeiana*. For each of the end organs we studied thus far (i.e. sacculus, utricle, amphibian papilla) we developed a two-compartment recording chamber. Each chamber was optimized for the particular 3D structure of the end organ, to allow appropriate placement and visualization. The two-chamber configuration is important because it allows the separation between peri- and endolymph at the basal and apical surface of the hair cells, respectively, thus, greatly enhancing the presence of spontaneous bundle oscillations in the sacculus. Hair bundles were visualized with an upright microscope and their motion recorded with a high-speed CMOS camera.

Results
We have observed robust oscillations from utricular hair cell bundles, which are qualitatively similar (e.g., amplitude, frequency, calcium-dependence) to oscillations from saccular hair cells. For hair bundles in the amphibian papilla, we have observed spontaneously oscillating hair bundles in the medial region. The frequencies of these oscillations vary greatly between cells, and are either comparable to rates observed in the sacculus, or are at much higher frequencies. We are currently looking across the tonotopic axis of this organ to see whether there exists a correlation between spontaneous oscillation frequency and the papillar location-specific characteristic frequency.

Conclusion
These results suggest that the nonlinear dynamics underlying spontaneous hair bundle oscillations may be ubiquitous in the vestibular and auditory organs among tetrapods.

Funding
This work was supported by NIH grant RO1DC011380 to DB.

PS-385

A Short Splice Form of Xin Actin-binding Repeat Containing 2 (XIRP2) Lacking the Xin Repeats is Required for Maintenance of Stereocilia Morphology and hearing Function

Shimon Francis[1]; Jocelyn Krey[2]; Evan Krystofiak[3]; Wenhao Xu[1]; Bechara Kachar[3]; Peter Barr-Gillespie[2]; **Jung-Bum Shin**[1]
[1]University of Virginia; [2]Oregon Health Science University / Vollum Institute / Oregon Hearing Research Center; [3]National Institute for Deafness and Communications Disorders

Approximately one-third of known deafness genes encode proteins located in the hair bundle, the sensory hair cell's mechanoreceptive organelle. In previous studies, we used mass spectrometry to characterize the hair bundle's proteome, resulting in the discovery of novel bundle proteins. One such protein is Xin-actin binding repeat containing 2 (XIRP2), an actin-crosslinking protein previously reported to be specifically expressed in striated muscle. Because mutations in other actin-crosslinkers result in hearing loss, we investigated the role of XIRP2 in hearing function. In the inner ear, XIRP2 is specifically expressed in hair cells, co-localizing with actin-rich structures in bundles, the underlying cuticular plate, and the circumferential actin belt. Analysis of splice-form representation using peptide mass spectrometry revealed that the bundle harbors a previously uncharacterized XIRP2 splice variant, suggesting XIRP's role in the hair cell differs significantly from that reported in myocytes. To determine the role of XIRP2 in hearing, we applied clustered regularly interspaced short palindromic repeat (CRISPR)/Cas9-mediated genome editing technology to induce targeted mutations into the mouse *Xirp2* gene, resulting in the elimination of XIRP2 protein expression in the inner ear. Functional analysis of hearing in the resulting *Xirp2* null mice revealed high frequency hearing loss, and ultrastructural

scanning electron microscopy analyses of hair cells demonstrated stereocilia degeneration in these mice. We thus conclude that XIRP2 is required for long-term maintenance of hair cell stereocilia, and that its dysfunction causes hearing loss in the mouse.

PS-386

Characterizing the Role of ESPNL in Stereocilia Morphogenesis

Matthew Avenarius; Peter Barr-Gillespie
Oregon Health & Science University

Introduction

We utilized a mass spectrometry approach to identify hair cell proteins of the chick utricle and further described a subset of which were significantly enriched in the hair bundle. To provide a temporal context, we followed expression of these bundle proteins using the newly described transcriptome of the regenerating chick utricular hair cell. One protein that came out of this analysis, ESPN-like (ESPNL), a paralog of the deafness-causing gene *Espn*, is enriched in the hair bundle and demonstrates a localization pattern unique from that of ESPN. Interestingly, expression of *Espnl* precedes expression of *Espn* and overall was one of the first bundle specific proteins to be expressed during the regenerative process. We aim to characterize the role of ESPNL in stereocilia morphogenesis and identify the biochemical function of this protein.

Methods

To define the localization pattern of ESPNL, in utero electroporation was employed to express a GFP-ESPNL fusion construct in hair cells. To characterize the role this gene plays in stereocilia morphogenesis, we utilized the CRISPR/Cas9 system to generate several mutant *Espnl* alleles. Finally, we utilized cultured CL4 cells to understand how ESPNL controls the structure of the actin-rich microvilli.

Results

Using RT-PCR, we showed that *Espnl* expression was restricted to the inner ear. Moreover, the GFP-ESPNL construct, when expressed in hair cells, targeted to the stereocilia. More specifically, in outer hair cell stereocilia GFP-ESPNL localized throughout the second row and to the tips of the third row, while in inner hair cell stereocilia it demonstrated a “thimble-like” pattern. To understand the function of this gene in stereocilia we utilized the CRISPR/Cas9 technology to generated nine independent *Espnl* alleles (108 total alleles screened), a majority of which encoded nonsense mutations. To further characterize the biochemical role of ESPNL we over-expressed GFP-ESPNL in CL4 cells. This hybrid construct localized to the microvilli of CL4 cells and had a lengthening effect on the apical surface microvilli.

Summary

Espnl is expressed early in the regeneration of hair cells and is significantly enriched in immature hair bundles. The localization patterns demonstrated by the GFP-ESPNL construct may either reveal actual ESPNL localization or represent transient, developmental, localization. The newly developed *Espnl* mutant mouse will allow for assessing the requirement of this gene during stereocilia development and provide an opportunity to determine whether ESPNL function has diverged from the stereocilia widening activity of the paralogous gene ESPN.

PS-387

Transforming Asymmetry in the Plane Into a Vertical Asymmetry of Stereocilia Growth

Basile Tarchini; Michel Cayouette
Institut de Recherches Cliniques de Montreal

Hair cells in the cochlea transform sound-induced deflection of stereocilia protruding at their apical surface into electrical impulses relayed to the brain. Since only deflections along the cochlea medio-lateral axis efficiently modulate electric currents, a property known as functional polarity, development of hair cell planar polarity is essential for hearing. Planar polarization is observed at two levels: asymmetry of the cytoskeleton in each cell exemplified by the V-shaped stereocilia bundle, and ‘planar cell polarity’ (PCP) reflected in the uniform orientation of this structure across neighboring hair cells. While the latter requires core PCP signaling, the mechanism generating asymmetry in single cells remains unclear. We focused on an underappreciated region of the hair cell apical membrane that is uniquely devoid of protrusions during development. This ‘bare zone’ hosts the polarized localization of two scaffolding proteins, mInsc and LGN, as well as the Gαi subunit. These proteins collectively create and expand the bare zone while restraining the aPKC kinase to a complementary domain, partitioning the apical membrane to regulate cytoskeleton asymmetry. The interface between lateral mInsc/LGN/Gαi and medial aPKC notably defines the edge of the V-shaped stereocilia bundle. Interestingly, inactivating Gαi but not mInsc/LGN disrupts the uniform orientation of hair cells in the sensory epithelium in addition to cytoskeleton asymmetry in each cell. Therefore, binding between Gαi and LGN is a candidate mechanism to couple population and cell-intrinsic levels of planar polarity. More recently, we uncovered evidence suggesting that mInsc/LGN/Gαi regulate not only the placement of stereocilia, but also their growth and organization in rows of decreasing heights. The resulting staircase-like architecture of the mature bundle is critically important for mechanotransduction, which is triggered by tension on oblique extracellular links that connect a taller with a shorter stereocilium. Our current work thus addresses how mInsc/LGN/Gαi could integrate multiple levels of polarity during organogenesis, including transforming asymmetry in the plane into a vertical asymmetry of stereocilia growth.

PS-388

How do High Frequency Sound and Vibration Activate Vestibular Receptors?

Ian Curthoys[1]; Wally Grant[2]
[1]*University of Sydney;* [2]*Virginia Tech*

Background

Bone conducted vibration (BCV) and air-conducted sound (ACS) are now being used to test otolith function. We suggest that ACS and BCV cause fluid pressure waves which deflect the short, stiff, loosely coupled hair bundles of the type

l receptor cells in the striolar region of both maculae, causing their activation once per cycle, resulting in phase-locked action potentials in the irregular afferent neurons which form calyx synapses on striolar type I receptors.

Methods
Single primary vestibular neurons were recorded extracellularly in guinea pigs anesthetized with Ketamine and Xylazine, and their responses to ACS and BCV were tested before and after a semicircular canal dehiscence (SCD). BCV stimulation was delivered by a Radioear B-71 bone oscillator cemented to the skull. ACS stimulation of up to 140dB SPL was delivered by a TDH-49 headphone.

Results
Neurobiotin labelling showed that activated neurons synapsed on type I receptors at the utricular striola or the crest of the crista. Irregular primary utricular neurons which are activated by both ACS and BCV show phase-locking up to frequencies of >1500Hz. Fluid pressure waves from ACS and BCV would be transmitted through the fluid and deflect hair cells. But such waves will also be conducted to the hair bundles of type I receptors on the crista of the semicircular canals, however in the guinea pig with a normally encased labyrinth, irregular semicircular canal neurons are not activated by ACS or BCV (Curthoys et al 2006). After an SCD, previously unresponsive irregular semicircular canal neurons can be activated and phase-lock up to frequencies of >1000Hz ACS or >700Hz BCV. A damped second order model of hair cell bundles surrounded by endolymph, predicted a very high corner frequency in accord with the evidence of vestibular afferent phase-locking data at high frequencies - frequencies far above the predicted corner frequency of the utricular macula (234Hz).

Conclusion
We propose a dual mode of otolith operation: at low stimulus frequencies the standard otoconial gel-layer mechanical operation is probably dominant. At higher frequencies this conventional mechanical operation is bypassed, and we suggest that fluid pressure waves generated by ACS or BCV can directly activate the short, stiff striola hair bundles up to high frequencies (even 2000Hz), with the result that both ACS and BCV cause phase-locking of irregular primary afferents and so are effective stimuli for tests of otolith function.

PS-389

Cervical Evoked Myogenic Potentials (cVEMP) Tuning in Rats After Gentamicin Induced Vestibulotoxicity

Stefania Goncalves; Esperanza Bas Infante; Suhrud Rajguru; Thomas Van De Water; Simon Angeli
Miami Ear Institute

Objective
To establish if changes in cVEMP tuning is a sensitive measure of gentamicin (GM) vestibulotoxicity.

Methods
20 Wistar rats, divided into 2 groups: Group A (n=10) rats received intratympanic (IT) GM injections in one ear (10mg/40uL) and Group B (n=10) rats received IT injection of saline (40uL) in one ear. The saccular function was tested by tone-burst evoked c-VEMP at different stimulus intensities (i.e., 80, 90, 100 and 110 dB SPL) and sound frequencies (250 - 2000 Hz) before treatment (day 0), one week and one month after treatment was performed. Latency and amplitude values of cVEMP responses were recorded, and intragroup (pre- and post-treatment) and intergroup comparisons were performed. Histological analysis of both saccule and utricle, fluorescent staining and hair cell counts were done.

Results
Animals exposed to IT GM alone showed abnormal vestibular signs after one week of IT injection, compared to animals from the control group which showed normal vestibular signs at at all times (Pearson = 0.038). In pre-treated animals, biphasic cVEMP responses with large amplitude at 500 Hz ('optimal frequency') and a threshold of 80 dB SPL were observed. Animals that received IT GM showed smaller or absent myogenic responses after one week of injection, with responses with a shift towards higher-frequency tuning and thresholds (90 dB SPL) one month after IT GM. All animals receiving IT saline maintained baseline characteristics of cVEMP recordings with same 'optimal frequency' and thresholds.

Saccular and utricular hair cell counts in animals receiving IT GM had significant hair cell loss (55.6%) when compared to those animals belonging to the control group *(p* < 0.001).

Conclusions
Changes in the tuning properties of the cVEMP responses may be an early sign of GM vestibulotoxicity that is more sensitive than the disappearance of the response.

Keywords
Cervical evoked myogenic potentials, tuning and vestibulotoxicity.

PS-390

The Effects of High Intensity Noise on the Peripheral Vestibular System in Rats

Courtney Jernigan[1]; Yue Yu[1]; Xuehui Tang[1]; Jun Huang[1]; Emily Gomez[2]; Adel Maklad[1]; Jerome Allison[1]; David Sandlin[1]; Justin Hyde[1]; William Mustain[1]; Wu Zhou[1]; Hong Zhu[1]
[1]University of Mississippi Medical Center; [2]Base Pair Program, Murrah High School

Background
The vestibular system is exquisitely sensitive to head rotation, translation, and movement with respect to gravity. Because the vestibular end organs are connected to the auditory end organs by a continuous fluid pathway within the membranous labyrinth, they are also impacted by sound stimulation. It has been shown that a large proportion of subjects experiencing noise-induced hearing loss (NIHL) also exhibit signs of vestibular deficiency. The mechanisms of NIHL have been extensively investigated, however, the mechanisms underlying the accompanying vestibular deficits remain to be elucidated. The goal of the current study was to fill this important knowledge gap by examining the effects of noise exposure

on vestibular hair cell morphology and vestibular afferents' sensitivity to head rotation and sound stimulation.

Methods
Male Sprague-Dawley rats were used in the present study. Continuous broadband white noise (0-240kHz) at an intensity of 116 dB sound pressure level (SPL) was delivered via an insert ear phone for three hours under isoflurane anesthesia. Auditory brainstem response (ABR) threshold was recorded before and after exposure to document changes in auditory function. Seven days after exposure, a 45 dB ABR threshold shift was observed in the noise-exposed ears, indicating hearing loss. Seven days following the exposure, single unit recording of vestibular afferent activity was performed on the side ipsilateral to the noise-exposure under pentobarbital anesthesia. Vestibular afferents' responses to sinusoidal head rotations and to broadband click stimulation (duration: 0.1ms; polarity: rarefaction or condensation; intensity: 80 dB SL re ABR threshold) were recorded. For the morphological study, the intact cristae and maculae were dissected out and stained with fluorescence-conjugated phalloidin which labels the F-actin in sensory cilium and cuticular plate of hair cells. Whole-mounts of cristae and maculae were examined with a multiphoton laser scanning microscope.

Results
Morphological analysis showed that noise exposure resulted in substantial sensory stereocilia bundle damage in the saccule, utricle, and semicircular canals. The saccules and utricles showed more damage than the semicircular canals. Preliminary single unit recording analysis revealed that the noise exposure significantly reduced sound sensitivities of otolithic and semicircular canal vestibular afferents.

Conclusions/Summary
To the best of our knowledge, this is the first study that systematically examines the effects of noise exposure on morphology and neurophysiology of all five vestibular end organs in a rat model. The results suggest that noise exposure, which can cause moderate hearing loss, can cause damage in the peripheral vestibular system.

PS-391

Magnetic Field-induced Nystagmus is Dependent on the Presence of Otoconia

Bryan Ward; Dale C; Ethan Naylor; Lani Swarthout; Charles Della Santina
Johns Hopkins University

Background
We previously identified behaviors consistent with peripheral vestibular stimulation in humans, C57BL/6J mice, and *AB* zebrafish while in a strong static magnetic field, and hypothesized that this behavior is due to a Lorentz force acting on the labyrinth. Animal models of magnetic vestibular stimulation can allow exploration of the mechanism. The aim is to determine whether otoconia are important for development of magnetic vestibular stimulation using mice deficient in otoconia.

Methods
Head tilt (*het*, *Nox3* knockout) mice and wild-type C57BL/6J mice were placed within a 4.7T Earth-horizontal magnetic field. Prior to exposure, the mouse's head was secured to a non-ferromagnetic post and positioned so the horizontal semicircular canals were in the approximate earth-horizontal position. Sinusoidal rotations and tilt testing were performed using binocular video-oculography. In the magnet, monocular eye movements were recorded via video camera from the mouse's right eye in darkness with infrared illumination. Mice were positioned in the center of the magnet bore for at least 1 minute in each of several head orientations. Slow-phase nystagmus velocity (SPV) was calculated and an exponential decay was fit to the peak SPV over time. PCR analysis was performed on *het* mice to confirm otoconial absence.

Results
Nox3 knockout mice lacked tilt response, but demonstrated robust horizontal vestibulo-ocular reflex (VOR), similar to C57BL/6J mice. When placed in the bore nose-first, all C57BL/6J mice demonstrated left-beating nystagmus lasting approximately 20 seconds on first entry, with mean peak SPV of six mice was 282°/s and the time constant was 3.62 s (SD 0.39). Nox3 knockout mice had complete lack of magnetic field-induced nystagmus when entering the magnetic field.

Conclusions
Mice exposed to high-strength magnetic fields demonstrate robust magnetic field-induced nystagmus, dependent on the presence of otoconia. According to the Lorentz force model of magnetic vestibular stimulation, this suggests that current density over the utricle is necessary to provide the horizontal nystagmus observed in mice, and potentially humans as well.

PS-392

Characteristics of Vestibular Apparatus and Trauma-induced Otoconia Dislocation in Sprague Dawley Rat

Chunjie Tian; Young Sun Kim; Yeon Ju Kim; Beomyong Shin; Jong Joo Lee; Hye Jin Lim; huh Yi Park; Yun-Hoon Choung
Ajou University School of Medicine

Backgrounds
The mechanism of benign paroxysmal positional vertigo (BPPV) has always been speculated to be the movement of otoconia. Most of studies have focused on clinical findings, but few are related with *in vivo* animal studies. The purpose of the current study was to evaluate the vestibular apparatus of Sprague Dawley (SD) rat, to establish an animal model of trauma-induced BPPV, and to further understand pathophysiology of BPPV.

Methods
Rats were divided into control (CON), 2-time free-fall (2FF), and 4-time free-fall (4FF) groups. Trauma-related BPPV was induced by free fall from 1.5 meters height. Rotarod treadmill and Field-emission scanning electron microscopy (FESEM) were employed for vestibular functional and morphological evaluation, respectively.

Results
The kinocilium height of the crista hair cells was 25.4 ± 2.3 μm, which was significantly longer than that in utricle (9.0 ± 0.6 μm) and saccule (13.8 ± 2.1 μm). The otoconia was significantly larger in the lateral region of utricle (length: 20.2 ± 3.7 μm; width: 9.9 ± 1.9 μm) than the otoconia in the medial region (length: 7.0 ± 1.4 μm; width: 3.7 ± 0.6 μm) and striola (length: 2.5 ± 0.3 μm; width: 1.7 ± 0.2 μm). The size distribution of otoconia in saccule had the same pattern. The average force a single lateral otoconia of utricle produced in the canal and ampulla was about 283 times of the striolar and 22 times of the medial otoconia. The diameter of the ampulla (213.3 ± 33.7 μm) is significantly longer than that of canal (157.9 ± 9.0 μm). The rats in the 4FF group had remarkably shorter stay on rotarod than that in control and 2FF groups. Consistently, the otoconia in the lateral area was dislocated in the rats with shortened stay on rotarod in the 4FF group. The significant dissolution of the otoconia was detected after two-month exposure in artificial endolymph, much slower than that in PBS buffer.

Conclusions
In conclusion, the otoconia in the lateral region of utricle, which is remarkably larger than that in the striolar and medial regions, dislocate in trauma-induced BPPV, and significantly dissolve after two-month exposure in artificial endolymph. These data suggest that the SD rat could be an excellent animal model for investigating BPPV.

PS-393

Effects of Antidepressant on Peripheral Vestibular Disorder-2nd Report

Hiroaki Shimogori[1]; Kazuma Sugahara[2]; Makoto Hashimoto[2]; Yoshinobu Hirose[2]; Hiroshi Yamashita[2]
[1]Yamaguchi University; [2]Yamaguchi University Graduate School of Medicine

Background
Phosphorylation of the transcription factor cAMP responsive element-binding protein (CREB) is thought to play a key role in neurogenesis. In our previous study, phosphorylated CREB (p-CREB) -like immunoreactivities were observed in vestibular ganglion cells after unilateral labyrinthectomy (UL). In addition, another study was reported that, after UL, p-CREB-like immunoreactivities were also detected in bilateral vestibular nuclei. These results indicate that vestibular system may have a potential of neuronal plasticity. It is well known that antidepressant shows its effects by activating CREB-BDNF axis on hippocampal neurons. We thought the possibility that up-regulation of CREB-BDNF axis might facilitate neuronal plasticity in the vestibular system. The aim of the present study was to evaluate the effects of general application of antidepressant on vestibular system by analyzing BDNF and trkB mRNA.

Methods
Hartley white guinea pigs with normal tympanic membranes and normal Preyer reflexes were used in this study. Animals were divided into two groups. In one group, animals were applied normal food for 30 days (control group), and in another group, animals were applied normal food with antidepressant (sertraline hydrochloride) in concentration with 0.01% for 30 days (antidepressant group). After 30 days' feeding, right lateral semicircular canal was transected surgically in all animals. Twenty-four hours after transection, tissues were removed and mRNA was extracted from vestibular nucleus, and vestibular ganglion in each animal. We investigated BDNF and trkB mRNA changes in the vestibular system. RT-PCR was conducted and BDNF and trkB mRNA was analyzed semi-quantitatively.

Results
In the vestibular ganglion cells, BDNF mRNA and trkB mRNA levels of the lesioned side in the antidepressant group were statistically higher than that of the intact side in the control group. In the vestibular nuclei, BDNF mRNA level of the lesioned side in the antidepressant group was statistically higher than that of the intact side in the control group.

Conclusion
Once peripheral vestibular disorder occur, chronic application of antidepressant increased BDNF and/or trkB mRNA levels in the lesioned side in the vestibular system.

PS-394

Response Characteristics of the Vestibulo-Sympathetic Reflex to Linear Acceleration in The Rat

Sergei Yakushin[1]; Theodore Raphan[2]; Bernard Cohen[1]
[1]Icahn School of Medicine at Mount Sinai; [2]Brooklyn College

The Vestibulo-Sympathetic Reflex (VSR) produces an increase in blood pressure (BP) upon arising that counteracts a potential drop in BP to the brain due to pooling of blood in the legs and abdomen. Previous studies in alert and anesthetized animals and in alert humans utilize low linear accelerations in the horizontal plane to study the response of the VSR. The changes in the Gravito-Inertial Acceleration (GIA), the adequate stimulus for the VSR, were small in these studies, potentially allowing other modalities to participate in the response. Here, we used larger linear accelerations in the horizontal plane as well as upward and downward accelerations along the gravitational Z-axis to determine the sensitivity and frequency characteristics of the VSR to linear acceleration. Experiments were performed in six isoflurane-anesthetized, male, Long-Evans rats. The effects of elevation from a prone to an upright position were also determined in alert rats. BP and heart rate (HR) were calculated from systoles recorded from an intra-aortic sensor (DSI). Linear accelerations were sensed by a 3-D accelerometer, and the changes in the GIA were calculated as a vector sum of the equivalent acceleration of gravity. The anesthetized rats were moved about the naso-occipital (Fore-Aft, X-), the interaural (Y-), and the vertical (Z-) axes at 0.2 to 1.8 g. Individual translations forward and upward increased BP, while downward translations decreased BP. The amplitude of the changes in BP were linearly related to the acceleration along these axes with a sensitivity of ≈4 $mmHg*g^{-1}$ in each direction. There were no changes in BP for translations laterally along the Y-axis or backward along the X-axis. To determine the frequency response of the

VSR, the animals were sinusoidally translated in the horizontal plane forward-backward, and side-to-side at frequencies ranging from 0.1 to 5 Hz and at accelerations of 0.2 to 1.8 g. Continuous, sinusoidal X-axis translations induced oscillatory changes in BP that were maximal at low frequencies of 6 to 10 mmHg*g^{-1}. Sensitivities gradually declined to zero at 5 Hz. Bringing the alert animal from a prone to a nose-up position increase BP by 9 mmHg, similar to the values obtained during sinusoidal oscillation along the X-axis at low frequencies. Therefore anesthesia had no apparent effect on the sensitivity of the VSR. This study demonstrates that the VSR has low frequency characteristics and that acceleration along the vertical Z-axis is the adequate stimulus to activate the VSR.

PS-395

Habituation of the Vasovagal Response (VVR) in the Rat

Bernard Cohen[1]; Giorgio P Martinelli[1]; Yongqing Xiang[2]; Theodore Raphan[2]; **Sergei B Yakushin[1]**

[1]Icahn School of Medicine at Mount Sinai; [2]Brooklyn College

Prevention of VasoVagal Syncope (VVS) is a significant medical problem, and there is currently no effective therapy. Habituation with prolonged periods of 60º static tilt was successful in blocking syncope in some studies but not in others, possibly because the habituation procedure was so tedious. We have recently developed a small animal model of the VasoVagal Response (VVR) in the anesthetized rat. In response to sustained sinusoidal Galvanic Vestibular Stimulation (sGVS) and head up tilts, susceptible 'rats developed VVRs in which systolic blood pressure (BP) fell precipitously in conjunction with a drop in heart rate (HR). These VVRs in the rat were essentially the same as the VVRs that produced VVS in humans. In most rats that were initially susceptible to development of VVRs in our earlier studies, repeated stimulation with sGVS caused them to lose this susceptibility. This suggested that the repeated vestibular stimulation had produced habituation of the VVR. Here we determined whether the susceptibility of anesthetized, adult, male, Long-Evans rats that had frequent VVRs from head-up tilt or from sGVS could be reduced by repeated vestibular stimulation. Two rats were exposed either to repeated 30 min periods of 0.025 Hz, 2 mA sGVS, or to 30 min periods of ±70º oscillation in pitch. The animal exposed to repeated sGVS was tested for production of VVRs with 70º head-up tilt (0.91 ***g***). The animal exposed to repeated pitch oscillation was tested with 3 mA sGVS at 0.025Hz. Both animals lost susceptibility to induction of VVRs during the habituating paradigms. Initially, typical VVRs were induced as described above. As repeated stimulation progressed, the drop in BP was counteracted by an increase in HR, suggesting activation of the baroreflex. At the conclusion of the habituation protocol, there was no VVR in response to either sGVS or head-up tilt. However, single pulses and/or sinusoids still induced increases in BP as before, indicating that the Vestibulo-Sympathetic Reflex (VSR) was still functional. Thus, the occurrence of VVRs was reduced by repeated activation of the VSR. A reduction in the occurrence of VVRs in humans with sGVS as in rats could presumably result in a similar reduction in their susceptibility to VVRs and VVS. The results also suggest that activation of the baroreflex may play an important role in the habituation of the VVR.

PS-396

Blood Pressure, Heart Rate and Pulse Pressure Inter-Relationships Through Feedback Mechanisms in the Baroreflex: Modeling Vaso-Vagal Responses

Theodore Raphan[1]; Yongqing Xiang[2]; Sergei B. Yakushin[3]; Bernard Cohen[3]

[1]City University of New York (Brooklyn College and Graduate Center); [2]City University of New York (Brooklyn College); [3]Mount Sinai School of Medicine

Blood Pressure (BP) signals comprised of recurrent systoles and diastoles are generated by the heart. This oscillating system is further controlled to maintain adequate blood flow and orthostasis. In this study, we modeled the periodic behavior of BP to show how the peak to peak amplitudes and frequency of the systoles are interrelated and modulated by vestibular activation. The model implements a relaxation oscillator, which is driven by a signal related to desired BP, a central signal. The periodicity is maintained by multiple feedback loops with a threshold element, causing nonlinear transitions as the feedback signal varies above and below the threshold. The nonlinear element is piecewise linear and it mimicks the threshold and saturation properties of a logistic function that has been used by others to model the physiological properties of the baroreflex. This nonlinearity is critical for implementing the relaxation oscillator, which has been used to simulate the systolic and diastolic behavior of BP. The model also simulates the relationship between BP and Heart Rate as well as the amplitude modulations and pulse pressure observed in the data. These signals are important for maintaining appropriate orthostasis. Through simulations, the model also posits that the baroreflex or other feedback loops implement an integrator function in the feedback loop. A signal related to the vestibular system and the desired BP combine to modulate the systolic level. The study indicates that the vestibular sympathetic reflex (VSR) must be viewed in context of how systolic and diastolic levels of an oscillating system are modulated by vestibular input rather than as an input output system. A sensitivity analysis using changes in the desired BP and threshold indicate that increases in the threshold produce larger pulse pressures to maintain orthostasis, whereas decreases in the desired BP are likely to be responsible for initiating the vaso-vagal responses.

PS-397

Climbing Perception and Eye Movements During Daytime and Nighttime Takeoffs Using a Flight Simulator

Atsushi Tamura[1]; Yoshiro Wada[2]; Naoki Shimizu[2]; Takuo Inui[3]; Takeshi Matsunobu[1]; Akihiro Shiotani[1]
[1]National Defense Medical College; [2]Nara Medical University; [3]Japan Air Self Defense Force

The climbing perception experienced by the pilot during takeoff at nighttime is stronger than that in the daytime. The aim of this study was to investigate this illusion, focusing on eye movements. Eight male subjects participated in this study. We created a simulated aircraft takeoff environment using a flight simulator. We evaluated the maximum slow-phase velocities of vertical eye movements during takeoff. Four of eight subjects reported that their perception of climbing at night was stronger, and the other four reported that there was no difference between day and night. These perceptions were correlated with eye movements; subjects with a small difference in maximum slow-phase velocities of downward eye movements between daytime and nighttime takeoffs indicated that their perception of climbing was the sameidentical under both conditions. We suggest that the climbing perception can be quantitatively evaluated using values calculated from induced eye movements and the pilot can be trained to suppress the vestibulo–ocular reflex to reduce the illusion of this stronger climbing perception at night.

PS-398

Vection, Illusory Motion, and Heading Perception: Does Perceived Motion Influence Heading Perception in the Horizontal Plane?

Steven Rosenblatt; Benjamin Crane
University of Rochester, Strong Memorial Hospital

Introduction

Exposing a viewer to a moving visual field can induce the feeling of self-motion or vection. Illusory motion from static repeated asymmetric patterns creates a compelling visual motion stimulus, however it is unknown if this is perceived as self-motion. In these experiments, human subjects reported the perceived direction of self-motion for sway translation and yaw rotation while viewing illusory motion and moving visual stimuli.

Methods

Subjects were seated on a motion platform with a visual display. Trials were arranged into 5 blocks based on stimulus type: (1) illusory motion with left/right (L/R) translation, (2) moving star field with L/R translation, (3) arrows with L/R translation, (4) illusory motion with L/R rotation, (5) moving star field with L/R rotation. Static arrows were used to evaluate the effect of cognitive suggestion. After each stimulus subjects reported the direction of self-motion as left or right. Each trial had its own control condition; the illusory motion controls were altered versions of the experimental image where the contrasted pairs were changed to a solid gray which removed the illusory motion effect. For the moving visual stimulus, controls were carried out in a dark room. With the arrow visual stimulus, controls were a gray screen. In blocks containing a visual stimulus there was an 8s viewing interval with the motion self-stimulus occurring over the final 1s. When no visual stimulus was present, only the 1s motion stimulus was presented. Eight women and five men, age 22-66 (37 ± 19) participated. All subjects were healthy. Thirteen subjects completed blocks 1-3. Ten completed blocks 4 and 5.

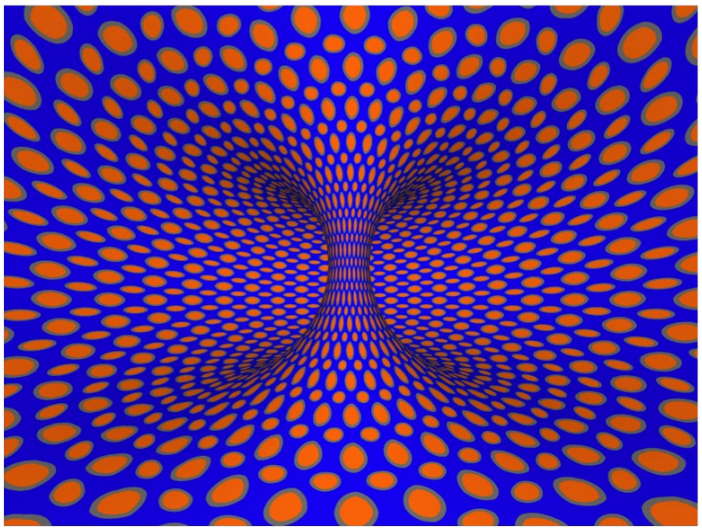

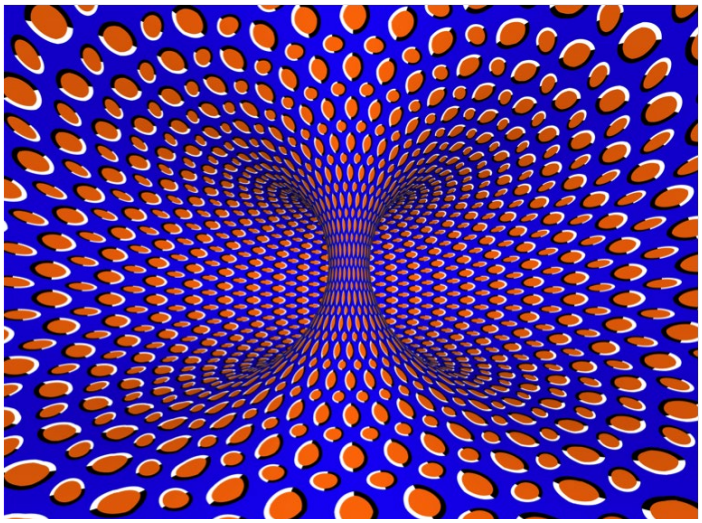

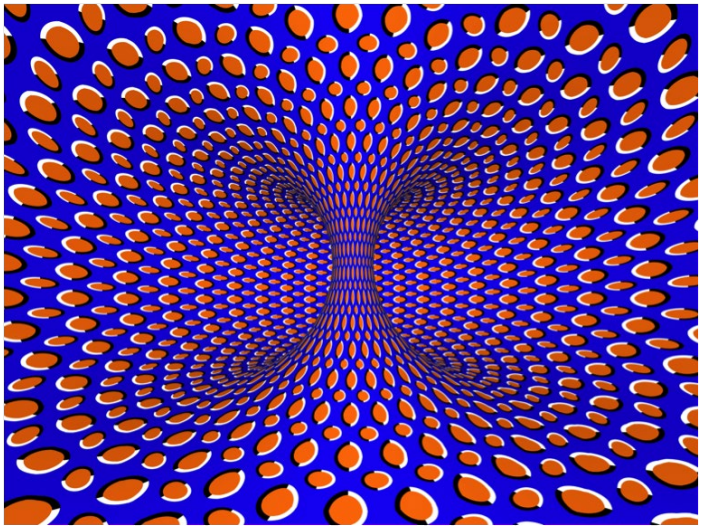

Results

To assess for a shift in the perceived direction of travel, the difference in the means from the L and R staircases were determined and measured in terms of peak velocity (cm/s): Block 1: 0.11 ($p=0.555$), block 2: -0.83 ($p=0.001$), block 3: 0.51 ($p=0.005$), block 4: -0.15 ($p=0.285$), block 5: -3.39 ($p<0.001$).

Summary

No significant shift in the perceived mean was found in illusory motion blocks. A significant difference between the right and left means was noted for both moving visual stimuli. The difference was the greatest with L/R rotation with a moving visual star field. For the arrows, there was a significant shit in the perceived mean opposite to the direction of suggestion, however this effect appears to be driven by a minority of subjects.

PS-399

Binocular Positioning Misalignment as an Assay of Otolith Asymmetry

Kara Beaton; Michael Schubert
Johns Hopkins University

Small, inherent asymmetries between the left and right otolith pathways, resolved on Earth through central compensatory mechanisms, have been correlated with space motion sickness susceptibility in astronauts. Hence, quantifying these otolith asymmetries prior to spaceflight has been proposed as a potential preflight predictor of inflight motion sickness severity. Through a larger NASA-directed project, we have developed a novel approach for inferring otolith asymmetries through simple measures of binocular positioning misalignments using portable equipment. We call these tests Vertical Alignment Nulling (VAN) and Torsional Alignment Nulling (TAN). The purpose of this study was to (1) evaluate our apparatus and methods in the operationally relevant environment of parabolic flight and (2) explore changes in binocular positioning driven by static changes in otolith signaling.

In VAN and TAN, subjects hold a tablet computer displaying red and blue lines while viewing through color-matched red and blue filters; this technique provides separate visual information to each eye. Subjects align the red and blue lines, initially vertically offset from one another in VAN or rotated relative to one another in TAN, until they perceive a single continuous line. Ocular misalignments are inferred from residual offsets in the final line positions. Testing is performed under a shroud to eliminate extraneous visual cues. For this experiment, twelve healthy individuals performed ten trials each of VAN and TAN in the upright, supine, left-ear-down (LED), and right-ear-down (RED) head orientations in 1g, and in the altering 0g and 1.8g g-levels of parabolic flight. Examining eye movements under these head orientations and gravity conditions allowed us to explore their pure, reflexive nature that is typically masked in 1g by central compensation.

Most subjects expressed significant differences in their VAN and TAN responses when upright versus lying supine ($p < 0.05$). All subjects displayed significant differences in VAN and TAN when lying RED versus LED ($p < 0.05$). Parabolic flight-testing revealed that eight subjects showed significant differences in TAN ($p < 0.05$) and seven subjects showed significant differences in VAN ($p < 0.05$) in 0g versus 1.8g. Furthermore, a significant correlation was found between TAN responses inflight and TAN responses on the ground: subjects who showed significant differences in 0g versus 1.8g also showed significant differences in upright versus supine. Together, these data can be attributed to innate otolith asymmetries and suggest that VAN and TAN may have a role in identifying deficits in otolith signal processing.

PS-400

High Density Micromachined Polyimide Electrode Arrays for Vestibular Implants

Peter Boutros[1]; Kristin Hageman[1]; Angela Tooker[2]; Kye Lee[2]; Sarah Felix[2]; Chenkai Dai[1]; Satinderpall Pannu[2]; Charles Della Santina[1]

[1]Johns Hopkins University; [2]Lawrence Livermore National Laboratory

Background

A multichannel vestibular implant that selectively stimulates each vestibular nerve branch could enhance the quality of life for individuals who suffer from bilateral vestibular loss. Multiple stimulation sites within a semicircular canal (SCC) are desired to find the optimal location to selectively stimulate a target branch while avoiding stimulation of non-target neurons. Existing vestibular electrode arrays based on traditional wire/silicone cochlear implant fabrication methods are limited in the number of stimulation sites and the ability to stimulate the ampullary nerve with multipolar configurations.

Methods

We designed, constructed, and tested thin-film polyimide vestibular implant electrode (PVIE) arrays. These microfabricated, polymer-based arrays were designed by referencing microMRI- and microCT-derived 3D anatomical models to choose a range of sites intended to stimulate different branches of the vestibular nerve. Advantages over traditional micro-wire arrays include higher channel count, smaller overall size, and precisely-defined planar geometry that facilitates comparison of empiric data to computational models of current flow in the inner ear.

The PVIE arrays consist of multiple layers of trace metal interleaved between insulating, flexible, polyimide layers. Each array has 30 electrodes evenly distributed on three separate shanks, one for each semicircular canal. The 10 electrodes on each shank are arranged in a tetrode formation, with a minimum center-to-center spacing of 136µm. Electrodes are 101µm in diameter and comprise electrochemically activated iridium-oxide to ensure safe charge injection during stimulation.

PVIE arrays were implanted into the horizontal and superior SCCs of chinchillas (*C. lanigera*), and preliminary experiments were performed to verify the functionality of the devices. We varied the amplitude of 200 pps, 100 ms duration trains of biphasic, 120 µs/phase charge balanced constant-current pulses. We assayed the perceived head rotation 3D axis and velocity by monitoring eye movement responses driven by the electrically-evoked angular vestibulo-ocular reflex (VOR). Results were compared to archival data obtained using traditional wire/silicone electrode arrays.

Results

PVIE devices produced eye movements comparable to standard micro-wire electrode arrays. VOR responses evoked by the PVIE arrays ranged in peak velocity from 15-51º/s, while the minimum angle of misalignment from the intended axis of rotation ranged from 7.39-24.8º.

Conclusion

PVIE arrays facilitate surgical implantation of a large number of stimulating electrodes near each end organ with precisely defined geometry and high density spacing. These devices therefore provide a means to optimize electrode location for vestibular implants intended to restore sensation of balance.

PS-401

Monopolar, Bipolar or Tripolar stimulation Using a MVP in Restoring Vestibular Function in Rhesus

Chenkai Dai; Guoliang Wang; Kristin Hageman; Bryce Chiang; Charles Della Santina

Johns Hopkins University

Background

Patients who have lost vestibular hair cell function in both labyrinths can suffer from debilitating loss of visual acuity and no adequately effective treatment exists rather than rehabilitation exercises. In our lab, a multichannel vestibular prosthesis (MVP) that directly modulates activity of surviving vestibular afferents fibers based on motion sensor input has been developed to improve quality of life for vestibular-deficient individuals. Maximizing the selectivity and efficacy of vestibular nerve branch stimulation is a key goal in development of a MVP and an optimal stimulation strategy (e.g. monopolar, bipolar or tripolar stimulation pattern) must be determined. When performing monopolar stimulation on the ampullary nerve, we observe larger cross-axis eye movements as the stimulation current amplitude increases. Tripolar stimulation should be able to preferentially guide the current in such a way as to decrease spurious activation of the nontarget nerves. We therefore hypothesized that the eye movements in response to tripolar stimulation would be better aligned with the target eye movement than the eye movements in response to either monopolar or bipolar stimulation.

Methods

We measured vestibulo-ocular reflex eye movements in response to monopolar, bipolar and tripolar stimulation in two rhesus monkeys implanted with a MVP. The MVP cross point switch array can connect any of the four cathodic current sources or four anodic current sinks to all electrodes allowing three stimulation paradigms used in this study: I. monopolar pattern between a stimulating electrode and a reference electrode; II. bipolar pattern between neighboring electrodes; III. tripolar pattern between a stimulation and two neighboring electrodes.

Results

Eye movements in response to monopolar stimulation increased off-axis components as the stimulation current is increased (e.g. mean misalignment of 17deg at 100uA, 100 dps, increased to misalignment of 25 deg at 200uA, 100 dps). Eye movements in response to tripolar stimulation, however, exhibited less increase of off-axis components (e.g. misalignment of 14deg at 100uA, 100 dps, increased to 19 deg at 200uA, 100 dps). This supports our hypothesis that tripolar stimulation can result in lower spurious activation of nontarget ampullary nerves by providing different current return paths.

Conclusions
These preliminary data show that tripolar stimulation can achieve better alignment with the ideal eye movement than either monopolar or bipolar stimulation. If these results hold generally true, then tripolar stimulation could be used to minimize cross-axis eye movements while maintaining adequate response amplitude in comparison with monopolar stimulation.

PS-402

Plasticity Within the Vestibulo-Ocular Reflex Circuitry: Implications for Use of Vestibular Prostheses

Diana Mitchell[1]; Charles Della Santina[2]; Kathleen Cullen[1]
[1]McGill University; [2]Johns Hopkins University

Motor learning plays an essential role in fine-tuning the smoothness and accuracy of complex movements as well as in the calibration of simple reflex behaviors. It is mediated by plasticity at localized sites within the neural circuitry that drives the behavior. In order to understand the underlying mechanisms of motor learning, it is necessary to link changes in the patterns of neural activity with specific changes in behavior. The relative simplicity of the vestibulo-ocular reflex (VOR) circuitry and its precise behavioral readout (i.e., eye movements) make it an excellent model system for studying mechanisms of motor learning. Here we utilized a vestibular prosthesis to stimulate vestibular afferents in alert rhesus monkeys using protocols that have been shown to induce synaptic plasticity at the first central vestibular synapse *in vitro* (McElvain et al. 2010) and are similar to stimulation protocols currently used for vestibular prostheses. We simultaneously recorded evoked eye movement and neural responses from VOR interneurons in the vestibular nuclei ipsilateral to the implanted ear to link changes in neuronal activity across different sites within the VOR circuitry with changes in behavioral responses.

Repeated stimulation caused a decrease in the responses of interneurons within the direct VOR pathway receiving monosynaptic input from the vestibular nerve (i.e., type I neurons). When we recorded from the vestibular nerve under these same conditions, we found that the response of single afferent fibers remained unchanged. Thus repeated stimulation targeted to the vestibular nerve in awake behaving primates induced plasticity at the vestibular afferent to central neuron synapse. Repeated stimulation also caused a decrease in evoked eye movements (VOR). Interestingly, however, the sensitivity of direct VOR interneurons decreased by a far greater extent than behavioral responses. Accordingly, we investigated neurons that contribute to commissural vestibular pathways (i.e., type II neurons) to determine if their responses could account for the discrepancy in the behavior and the activity of type I neurons. Strikingly, the response of type II neurons did not change following repeated stimulation targeted to the vestibular nerve. This finding suggests that the weight of vestibular commissural pathways is actually potentiated since type I neurons are the only source of input to type II cells in our unilateral stimulation protocol. Taken together, our results show that vestibular commissural pathways undergo rapid plasticity to compensate for the decreased response of first order VOR interneurons, allowing maintenance of a relatively robust behavioral output.

PS-403

Subcollicular Projections to the Medial Geniculate Body and Collateral Projections to the Inferior Colliculus

Brett Schofield[1]; Jeffrey Mellott[1]; Susan D. Motts[2]
[1]Northeast Ohio Medical University; [2]Arkansas State University, Jonesboro

Behavioral studies have shown that cats can orient to sounds and learn frequency discriminations (with difficulty) even if all projections from the inferior colliculus (IC) to the medial geniculate body (MG) are eliminated (Goldberg and Neff, '61, J Comp Neurol 116:265; Jane et al., '65, J Comp Neurol 125:165; Casseday and Neff, '75, Neurophysiol 38:842). These functions are attributed to an "extralemniscal" auditory pathway that bypasses the IC. Experiments in several species have identified direct projections to the MG from subcollicular auditory nuclei. Moreover, many cochlear nucleus cells that project to the MG send collateral projections to the IC (Schofield et al., 2014, Front. Neuroanat. 8:10). We conducted 3 experiments to characterize projections from subcollicular nuclei to the MG in guinea pigs. For experiment 1, we made large injections of retrograde tracer into the MG. Labeled cells were most numerous in the superior paraolivary nucleus, ventral nucleus of the trapezoid body, lateral superior olivary nucleus, ventral nucleus of the lateral lemniscus, ventrolateral tegmental nucleus, paralemniscal region and sagulum. Additional sources include other periolivary nuclei and the medial superior olivary nucleus. The projections are bilateral with an ipsilateral dominance (66%). For experiment 2, we injected tracer into individual MG subdivisions. Subcollicular projections terminate primarily in the medial MG, with the dorsal MG a secondary target. For experiment 3, we made large injections of different retrograde tracers into one MG and the homolateral IC to identify cells that project to both targets. Such cells were numerous and distributed across many of the nuclei listed above, mostly ipsilateral to the injections. In many of the nuclei, over 50% (and up to 100%) of the MG-projecting cells also projected to the IC. These data indicate close ties between the lemniscal and extralemniscal pathways.

In summary, many brainstem nuclei contribute to extralemniscal projections to the MG, with the largest contributions originating in the ventral cochlear nucleus, ventral nuclei of the trapezoid body, superior paraolivary nucleus, lateral superior olive, sagulum and paralemniscal regions. The variety of projecting nuclei suggest a range of functions, including monaural and binaural aspects of hearing. These direct projections could provide the thalamus with some of the earliest (i.e., fastest) information regarding acoustic stimuli. The prominence of the collateral projections suggests that the same information is delivered to both the IC and the MG, or

perhaps that a common signal is being delivered as a preparatory indicator or temporal reference point.

PS-404

In Vivo Physiological and Anatomical Characterization of Cells in the Gerbil Lateral Nucleus of the Trapezoid Body

Tom Franken[1]; Philip Smith[2]; Philip Joris[3]
[1]KU Leuven; [2]Department of Neuroscience, University of Wisconsin, Madison; [3]Lab. of Auditory Neurophysiology KU Leuven

The lateral nucleus of the trapezoid body (LNTB) is classified as "periolivary" and is located within the population of brainstem auditory nuclei collectively known as the superior olivary complex (SOC). It has been identified in several species including human. Its glycinergic projection to the medial superior olive has placed it in a potentially important position regarding the mechanisms involved in low frequency sound localization. Despite this no *in vivo* data is available on the auditory response features of positively identified LNTB cells.

We utilized in vivo patch recording techniques to successfully record spontaneous and sound-induced sub-threshold synaptic and supra-threshold spike responses from gerbil LNTB cells and subsequently biocytin-labeled and recovered the recorded cell for light and electron microscopy. We also labeled and anatomically evaluated two inputs to cells in LNTB, globular bushy cell (GBC) axon terminals and a previously undescribed projection from LSO cells.

At the E.M. level labeled GBC and LSO axons both provide equally large terminals that synapse on unlabeled LNTB cell bodies or proximal dendrites. In vivo recordings reveal both excitatory and inhibitory spontaneous synaptic events in most neurons, where excitatory events are dominant. EPSPs can be either sub- or supra-threshold and have faster kinetics than ipsps. Action potentials often display a 'double undershoot' as in *in vitro* recordings. EPSP kinetics can vary significantly between neurons. Subthreshold responses to tones vary between cells from individually discriminable EPSPs to summed depolarizations. In response to hyperpolarizing current pulses sometimes a "sag" is displayed indicative of I_H current. In response to depolarizing pulses the cells fire repetitively. We obtained threshold frequency tuning functions to determine the CF. Cells were typically monaural, being excited by ipsilateral stimulation. Short, CF tone-generated PSTHs were typically primary-like-with-notch similar to their GBC inputs. Tones below 1-1.5 kHz result in phase-locked spikes with vector strengths <= 0.8. Ipsilateral clicks result in steep sub- or suprathreshold EPSPs, sometimes preceded by an IPSP. As for tones, ipsilateral broadband noise results in mainly excitatory responses with or without sustained depolarization.

In summary we have obtained the first *in vivo* intracellular recordings from identified LNTB neurons. These cells are monaural and can fire in response by ipsilateral tones, clicks and noise, but the subthreshold responses show inhibitory synaptic potentials as well. EPSP shape varies between neurons. Labeling of afferents shows an unexpected input from LSO neurons.

PS-405

Temporal Properties of Monaural Neurons Recorded in the Trapezoid Body of Gerbil and Chinchilla

Liting Wei[1]; Shotaro Karino[2]; Philip Joris[1]
[1]University of Leuven; [2]University of Tokyo

The trapezoid Body (TB) contains the axonal output of AnteroVentral Cochlear Nucleus (AVCN) neurons. Previous recordings from the TB in cat (Smith et al. 1991,1993; Joris et al. 1994) revealed the presence of enhanced phase-locking and entrainment in axons of bushy cells, relative to the auditory nerve (AN). It is unclear to what extent these properties are present in rodents, which are increasingly used in auditory research. To address this issue and to better interpret recordings from neurons of the superior olivary complex in gerbil and chinchilla, we characterized the basic properties of the monaural inputs to these diverse cell groups, with a focus on temporal coding.

We recorded from TB fibers with high impedance glass electrodes. A threshold tuning curve yielded the Characteristic Frequency (CF), spontaneous rate, and lowest threshold. Short tone bursts at CF were then presented in 5-10 dB SPL steps, covering a wide SPL range, from which we construct the Post Stimulus Time Histogram (PSTH) for physiological classification. We also studied phase-locking in the tuning curve "tail". MNTB cells were studied with low-impedance glass electrodes and were identified based on the presence of a pre-potential and monaural contralateral excitation. The magnitude of phase-locking, measured with vector strength (R), was compared to published AN data for the same species (Versteegh et al. 2011; Temchin et al. 2010), as well as to cat TB data.

The limit of phase-locking in gerbil and chinchilla TB fibers is between 3-4 kHz, which is somewhat lower than in the AN. For CF tones <1 kHz there is an increase in maximal vector strength (R_{max}) values when compared to the AN. However, this enhancement was quantitatively not as striking as in cat, and it was not accompanied by high levels of entrainment. Off-CF low-frequency sound stimulation resulted in large number of high-sync responses when compared to CF tones. "Peak-splitting" was frequently encountered in both gerbil and chinchilla, particularly in response to off-CF tones, unlike in the cat. Overall, enhanced synchronization was more pronounced in the chinchilla than in the gerbil. A number of other differences (e.g. spontaneous rates, distribution of PSTH types) were found between TB responses of gerbil and chinchilla.

We conclude that, as in cat, there is "synchronization enhancement" in the two rodent models studied here. However, the enhancement differs from cat both qualitatively (less entrainment in rodents, more peak-splitting) and quantitatively (less extreme R_{max} values).

PS-406

Serotonergic Modulation of HCN Channels Modifies the Firing Threshold of MSO Principal Neurons.

Kwang Woo Ko; **Kwang Woo Ko**; Nace Golding
University of Texas at Austin

The superior olivary complex is heavily innervated by serotonergic fibers from the dorsal raphe nuclei. These inputs are thought to provide modulatory influences on their targets, signaling changes in motivation or attention. However, the receptors and intracellular modulatory pathways through which serotonin acts are not well understood. Here we show in principal neurons of the gerbil medial superior olive (MSO) that a primary action of serotonin is to modulate hyperpolarization and cyclic nucleotide-gated (HCN) channels both in the soma and dendrites as well as in the axon initial segment (AIS).

To examine the effect of serotonin on HCN channels in MSO neurons, whole-cell voltage-clamp recordings were made from MSO neurons and the properties of Ih (pharmacologically isolated) was compared between control conditions and in the presence of 300 µM serotonin. Serotonin significantly hyperpolarized the activation range of HCN channels by ~10 mV (-60.56 ± 1.96 mV to -71.25 ± 2.34 mV (n=6, p<0.01). In addition, while leak current was consistently maintained, the maximum Ih current was reduced by ~31% in the presence of 5-HT vs. control (-389.77 ± 67.21 pA to -270.39 ± 31.77 pA). Both the change in V½ and amplitude of Ih was blocked extensively by 10 µM WAY-100135, a blocker of 5-HT1A receptors (V½, from -60.62 ± 1.47 mV to -62.06 ± 1.22 mV; Max. Ih, -442.12 ± 33.72 pA to -448.58 ± 27.59 pA, n=7),

Serotonergic modulation of HCN channels in the AIS had robust effects on action potential initiation. Local application of serotonin (300 µM) to the AIS via pressure ejection hyperpolarized the resting membrane potential by only -1.29 ± 0.04 mV ($p < 0.01$, n=7) but negatively shifted spike threshold by -2.29 ± 0.44 mV, ($p < 0.01$, n=7). These effects were eliminated when 20 µM ZD7288, a blocker of Ih, was applied through the recording pipette (ΔVrest = -0.03 ± 0.13 mV, p = 0.82, n=5; (Δspike threshold = -0.08 ± 0.22 mV, p = 0.78, n=5). Finally, strong modulation of Ih and spike threshold could also be induced through stimulation of serotonergic fibers around the MSO.

Together, our results indicate that serotonin acts through 5-HT1A receptors to modulate the amplitude and activation range of HCN channels of MSO neurons. Modulation of HCN channels in the AIS serves as an important mechanism to fine-tune the threshold and sensitivity of spike initiation.

PS-407

Tonotopy in the Turtle Brain Stem

Angeline Johny; Katie Willis; Catherine Carr
University of Maryland

Tonotopy describes the spatial organization of sound frequencies in the brain, and is an almost universal feature of the tetrapod auditory system. Mammals, lizards, fishes, birds, and alligators have auditory nuclei that are organized tonotopically. Tonotopy has not been investigated in the turtle central nervous system. Recent phylogenetic analyses suggest that turtles are a sister group to the archosaurs, whose brain stem nuclei are tonotopically organized. Although the turtle basilar papilla is tonotopically organized (Crawford and Fettiplace, 1980), it is not known whether this tonotopy extends into the brain. To determine whether the tonotopy present in the basilar papilla was preserved in the brain stem, we used neuroanatomical tract tracing experiments. Prior to perfusion, Red-eared Slider turtles (*Trachemys scripta elegans*) were euthanized, then perfused with oxygenated artificial cerebrospinal fluid (ACSF). Fluorescent Neurobiotin (350 and 488 nm) were injected in the apical (low frequency) and basal ends (high frequency) of the basilar papilla, bilaterally. Heads were maintained in oxygenated ACSF for 8-12 hour transport, following incubation in cold 4% paraformaldehyde for 12 hours. Brain stems were cryoprotected and sectioned at 80 um, cleared and imaged using confocal microscopy. Data showed little co-localization between the nerve fibers stained with Neurobiotin 488 and Neurobiotin 350. Terminals were found in both Nucleus Angularis (NA) and Nucleus Magnocellularis (NM). Fibers stained with NB350 and NB488 were observed both in NA and NM, showing that the range of frequencies was represented in NA and NM. There was also evidence of separate terminal fields in NM and NA that supported the hypothesis that tonotopic organization was present in NA and NM. For longer transport times (greater than 12 hours), Neurobiotin crossed synapses and labeled neurons in NA and NM. Using a similar protocol using Neurobiotin injection, we found bouton and varicose terminals in both NA and NM. Terminals were denser on NM neurons than NA. Terminals were found on both the somata and in the neuropil. Demonstration of tonotopic organization in the turtle brain stem indicates that this organization is common to all taxa with tympanic hearing.

PS-408

Differences in axonal conduction speed cancel out cochlear traveling wave delay.

James Sinclair; Conny Kopp-Scheinpflug
LMU Munich

Background

Ford & Grothe (ARO'2012) demonstrated anatomical evidence for specialized myelination patterns of globular bushy cell axons depending on the location of their target cell along the tonotopic axis of the MNTB. These data suggest that due to larger axon diameter and shorter internodes low-frequency axons can conduct incoming signals at a faster speed. Here we are testing this hypothesis using a combination of *in vivo* and *in vitro* recordings of the gerbil MNTB.

Methods

We use in vivo single unit and in vitro patch-clamp recordings of the gerbil MNTB to assess stimulus evoked latencies.

Results

Due to the cochlear traveling wave delay we should expect latency differences of up to 4ms between high-frequency and low-frequency neurons in auditory brainstem neurons (Greenberg et al., 1997; Spencer et al., 2012), with the high frequency neurons having shorter latencies and vice versa. However, in a sample of 180 single units recorded in the MNTB of the gerbil, no significant differences in latency were found between low-frequency and high-frequency neurons (CF_{low}: 3.83 ±0.06ms, n=72; CF_{high}: 3.66 ±0.07ms, n=108; $p \geq 0.05$). This disappearance of the cochlear delay can have two reasons; first, the low-frequency neurons receive inputs from fibers with faster conductance velocities or second, the low-frequency neurons have shorter synaptic delays than the high-frequency neurons. To test for differences in the synaptic delay we analyzed the time between the peak of the calyceal prepotential and the postsynaptic action potential in low-frequency vs. high-frequency MNTB neurons. Again, there was no significant difference in the synaptic transmission delay ($delay_{low}$: 0.44 ±0.01ms, n=13; $delay_{high}$: 0.40 ±0.02, n=28; $p \geq 0.05$). Conduction velocity of single globular bushy cell fibers was measured by whole-cell patch clamp recordings of MNTB neurons along the tonotopic axis while electrically stimulating the trapezoid body fibers. The axonal conduction speed is significantly faster for the axons innervating the more lateral (low-frequency) neurons.

Conclusions

Our data suggest that the MNTB and its input structures serve to provide equally fast inhibition to both, its low-frequency and its high-frequency target cells in the MSO and LSO respectively.

References

Greenberg, S., Poeppel, D., and Roberts, T. (1997). A Space-Time Theory of Pitch and Timbre Based on Cortical Expansion of the Cochlear Traveling Wave Delay. (London: Whurr Publishers).

Spencer, M.J., Grayden, D.B., Bruce, I.C., Meffin, H., and Burkitt, A.N. (2012). An investigation of dendritic delay in octopus cells of the mammalian cochlear nucleus. Frontiers in computational neuroscience 6, 83.

PS- 409

Oligodendrocytes Beyond OPCs are Capable to Generate Na+ Current- induced Action Potentials in the Auditory Brainstem.

Emmanuelle Berret; Jun Hee Kim
University of Texas Health Science Center, San Antonio

The auditory brainstem circuit needs a high density of myelination to process fast, precise, and reliable auditory information. Oligodendrocytes produce myelin sheath, which insulates and protects axons, and is critical for fast saltatory propagation of nerve impulses. In the developing central nervous system (CNS), oligodendrocytes are derived from oligodendroglial progenitor cells (OPCs). Recent studies demonstrated that some OPCs (termed NG2+ cells) could generate an action potential in response to depolarizing current injection (Karadottir et al., 2008; De Biase et al., 2010). Although there is physiological heterogeneity among OPCs in different brain areas, OPCs have been known as a unique cell type to exhibit excitability within the oligodendrocyte lineage. However, it is still to be answered, whether excitable properties are restricted to OPCs or whether oligodendrocytes beyond OPCs can fire action potentials and whether its excitability involves in myelination in developing brain.

To study oligodendrocyte excitability along the oligodendrocytes lineage, we performed patch-clamp recordings and immunohistochemistry from oligodendrocytes in the medial nucleus of the trapezoid body (MNTB) of the auditory brainstem. We found that about 30 % of oligodendrocytes at postnatal days 8-14 (P8-14) were able to generate action potentials with the amplitude of 100 ± 10.5 pA and threshold of -34 ± 8 mV in response to depolarizing current injection of 75 ± 26 pA (n = 24). Our post-recording immunohistochemistry revealed that oligodendrocytes exhibiting action potentials expressed Oligo1 and CNPase, markers for pre-myelinating oligodendrocytes (pre-OLs), but not NG2 protein, indicating that it is not OPCs. These excitable pre-OLs displayed transient Na^+-currents with the peak amplitude of 331 ± 85 pA (n = 16), which were completely inhibited by 1 mM TTX. Our results suggest that voltage-gated Na^+ channels mediated Na^+ influx is sufficient to evoke action potentials in pre-OLs, the stage following OPCs in the auditory brainstem.

Káradóttir R, Hamilton NB, Bakiri Y, Attwell D. Spiking and nonspiking classes of oligodendrocyte precursor glia in CNS white matter. Nat Neurosci. 11(4):450-6, 2008.

De Biase LM, Nishiyama A, Bergles DE. Excitability and synaptic communication within the oligodendrocyte lineage. J Neurosci. 30(10):3600-11, 2010.

PS-410

Energy Utilization During Activity and Rest at the Calyx of Held

Brendan Lujan; **Robert Renden**
University of Nevada, Reno

Maintenance of cellular energy is important in neurons, which are energetically expensive, consuming up to 20% of an organism's energy at rest. The efficient release and recycling of neurotransmitter is critically important to allow chemical transmission between neuronal populations. Mitochondria are the major suppliers of cellular energy, generating ATP via oxidative phosphorylation. However, the specific utilization of energy from cytosolic (glycolytic) and/or mitochondrial respiration at the presynaptic terminal during synaptic neurotransmission is unknown. We used the calyx of Held, a model synapse with ideal synaptic properties for physiological investigation, to test the sources of presynaptic energy utilized to maintain basal and high-frequency neurotransmission, before and after the onset of hearing. Using synaptic vesicle (SV) pool depletion and recovery protocols, we can further estimate how the energy supplied by either glycolysis

or mitochondrial respiration contribute to sustainable synaptic transmission.

We find that mitochondrial sources of energy support synaptic transmission, with little support via glycolysis, at rest or during low frequency stimulation. During bouts of high frequency activity (100-300 Hz), blockade of either mitochondrial respiration or glycolysis both significantly impair synaptic transmission, and this effect is more pronounced in mature terminals after the onset of hearing. During a recovery period following high frequency transmission, blockade of glycolysis, but not oxidative phosphorylation, retards recovery of the readily releasable pool of synaptic vesicles.

Our results indicate that oxidative phosphorylation, powered through presynaptic mitochondria, are responsible for providing cellular energy to support basal and high frequency neurotransmission in the calyx of Held synapse. However, presynaptic recovery from stimuli that deplete the readily-releasable pool of synaptic vesicles depends on extremely local, but lower yield, cellular glycolysis.

PS-411

GIT Proteins Regulate Synaptic Vesicle Availability for Action Potential Evoked Release and Initial Release Probability at the Calyx of Held/MNTB synapse

Samuel Young; Monica Montesinos; Wei Dong
Max Planck Florida Institute for Neuroscience

Introduction

Chemical synaptic transmission relies on a limited number of fusion competent synaptic vesicles (SVs) in the presynaptic terminal, termed the readily releasable pool (RRP); thus sound encoding places great demands on the temporal dynamics of SV release and recycling. Critical to the binaural processing of sound is the calyx of Held, a giant axosomatic glutamatergic presynaptic terminal that arises from the globular bushy cells (GBC) in the cochlear nucleus. The calyx preserves temporal fidelity of the afferent spike train in its patterns of SV release to drive postsynaptic spiking in the principal neurons of the medial nucleus of the trapezoid body (MNTB). The MNTB relays these activity patterns as inhibitory inputs to key binaural cell groups. Due to its experimental accessibility and is representative of several large presynaptic terminals involved at the initial stages of sound, the calyx of Held provides unparalleled opportunities to gain insights into presynaptic mechanisms that support the early stages of auditory processing.

Ultimately, the molecular mechanisms that underlie efficient release and replenishment of SVs underpin synaptic integration and sound encoding. A key step in the pathway that regulates temporal dynamics of SV release and recycling within the RRP is priming, the creation of fusion competent SVs that are tightly coupled to voltage gated Ca^{2+} channels (VGCCs) at the active zone (AZ). It has begun to emerge that central organizing molecules located at the AZ are key proteins regulating SV release and replenishment. In particular, the G-protein-coupled receptor (GPCR)-kinase-interacting protein (GIT) protein family has been implied to have a presynaptic role in synaptic vesicledynamics. GIT1 is a multi-domain scaffolding protein found on both, pre and postsynaptic compartments of the synapses. However, despite of the postsynaptic signaling pathways of these proteins have been well characterized, little is known about the presynaptic function of GIT1.

Methods

We used electrophysiological and biophysical methods, in conjunction with mouse transgenic lines and novel viral vector technology to perturb calyx of Held function to study how loss of GIT proteins affected synaptic transmission and plasticity at the post-natal day 18-21 calyx of Held.

Results

We demonstrate that loss of GIT proteins increase action potential (AP) evoked release and initial release probability and result in slower synaptic vesicle recovery in response to trains of AP stimulation.

Conclusions

GIT proteins are intricately involved in synaptic transmission and plasticity through presynaptic mechanisms at the calyx of Held/MTNB synapse.

PS-412

Impact of Brevican on the Morphology and Ultrastructure of the Calyx of Held.

Mandy Sonntag[1]; Maren Blosa[2]; Carsten Jäger[2]; Solveig Weigel[2]; Johannes Seeger[3]; Rudolf Rübsamen[4]; Markus Morawski[2]
[1]University of Leipzig, Leipzig; [2]University of Leipzig, Leipzig, Paul Flechsig Institute for Brain Research; [3]University of Leipzig, Leipzig, Institute of Anatomy, Histology and Embryology, Faculty of Veterinary Medicine; [4]University of Leipzig, Leipzig, Institute of Biology, Faculty of Biology, Pharmacy and Psychology

Background

Special neurons of the central nervous system are surrounded by a particular composition of extracellular matrix components, which are classified as perineuronal nets (PNs). PNs are suggested to contribute to the stabilization of synapses in adulthood, and might prevent the formation of new synapses after functional connections have been established. Still, to date the exact functions of PNs remain elusive. The medial nucleus of the trapezoid body (MNTB) in the auditory brainstem is characterized by an extraordinarily high density of PN-associated principal neurons, which makes this nucleus a unique model system to study the functions of PNs. In the MNTB, the PNs typically surround the neuronal cell bodies and the calyx of Held synapses. Recently we described that one of the major PN components, the proteoglycan brevican, is characterized by a more specific spatial organization being mainly expressed between the presynaptic membrane and the adjoining postsynaptic membrane. It is assumed that brevican might contribute to sealing the synaptic cleft. To get a better understanding of the role of brevican for the synapse-neuron interaction, we compared the morphology and ultrastructure of the pre- and postsynaptic complex as-

sociated with the calyx of Held in presence and absence of brevican.

Methods
We used transgenic mice deficient for the proteoglycan brevican and performed vGlut1 immunohistochemistry and anterograde labeling of calyx of Held synapses by injection of the lipophilic dye NeuroVue in the ventral cochlear nucleus to study the morphology and fenestration of the calyx of Held. We further used electron microscopy to compare the ultrastructure of the calyx of Held in wildtype and knockout mice.

Results
The results indicate that brevican is accumulated in extended extracellular spaces formed subsynaptically between the calyx of Held and the postsynaptic membrane (i.e. subsynaptic cavities). Such cavities were frequently found between adjacent postsynaptic densities. Electron microscopical analysis in brevican-deficient mice yielded significant reductions in numbers and sizes of the subsynaptic cavities. These marked changes occurred in brevican-deficient mice despite a stable mono-innervation and the typical highly-fenestrated shape of the calyx of Held.

Conclusion
These data indicate that the lack of brevican is specifically associated with ultrastructural alterations at the calyx of Held evidenced by a prominent decrease of subsynaptic cavities the function of which might be the separation of postsynaptic densities from each other. Thus, the role of brevican might be the spatial and functional separation of synaptic compartments at the calyx of Held.

PS-413

A Method to Perform a Ventral Craniotomy for Two-Photon Imaging Experiments in the Ventral Brainstem of Neonate Rats and Mice

Grace Tsui; Daphne Chang; Lingyan Shi; Adrian Rodriguez-Contreras
The City College of New York

The main goal of this work is to illustrate a novel method that facilitates access to the superior olivary complex in the ventral brainstem of anesthetized neonate rodents for two-photon imaging experiments. First, we illustrate the use of this approach in neonate rats by applying a bolus loading procedure to deliver acetoxymethyl (AM) ester calcium indicators and analyzing patterns of ensemble activity before the onset of hearing. Second, we demonstrate that a ventral craniotomy can be used in genetic modified neonate mice expressing different fluorescent reporters to study cellular activity and dynamics in neurons, glial cells and vascular endothelial cells. The use of a ventral craniotomy provides an opportunity to investigate the dynamics of diverse cellular processes in the mammalian auditory brainstem during hearing development in vivo.

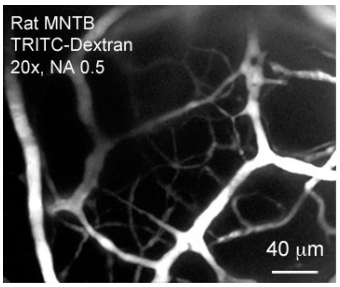

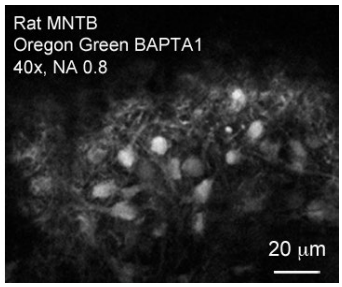

PS-414

Inferior Collicular Input to Olivocochlear Efferents in Hearing and Hearing Loss

Kirupa Suthakar; Hannah Douglas-Kinniburgh; Tan Pongstaporn; Annie Cho; David Ryugo
Garvan Institute of Medical Research

Background
The descending auditory system, which parallels the ascending pathways, consists of long projections and shorter neuronal chains that modulate incoming acoustic signals. The olivocochlear (OC) efferent system is the end point of the descending system, receiving both ascending and descending input, which allows the brain direct control of the peripheral auditory system. Two proposed functions of the OC system are protection from acoustic trauma and modulation of sensory input. Descending topographic projections from the inferior colliculus (IC) to the location of efferent cell bodies in the superior olivary complex (SOC) support the idea of excitatory activation of OC efferents (Vetter et al., 1993; Mulders & Robertson, 2000&2002; Zhang & Dolan, 2006). This study aims to investigate the anatomical nature of descending IC input onto OC efferents in mice with normal hearing, hearing loss, and congenital deafness in order to better understand why impaired speech understanding accompanies hearing loss.

Methods
Adult, hearing CBA/Ca mice received small injections of biotinylated dextran-amine (BDA) into frequency-specific regions of the central nucleus of the IC to study labelled terminals in the SOC, and in some cases also received cholera toxin subunit-B (CTB) injections in the cochlea to visualise OC efferent cell bodies. Connections of normal hearing CBA/Ca mice were compared to those of 'early onset hearing loss' (DBA/2) and 'congenital deafness' (Shaker2) mice. Analysis was directed to identify direct synaptic contact onto OC efferent cell bodies using light and electron microscopy.

Results
Preliminary data confirm that descending IC input is arranged tonotopically. In normal hearing, terminal boutons from lower frequency IC injections appear more laterally located in SOC nuclei. Qualitatively, the terminal bouton fields are all located more laterally in each of the groups; however in congenitally deaf animals the terminal bouton field appears truncated and condensed. Moreover, labelled IC terminal boutons make direct synaptic contact with labelled OC efferent cell bodies. These labelled terminals contain round synaptic vesicles and asymmetric synapses, indicative of excitatory neurotransmission.

Conclusion
Our results indicate that the IC provides excitatory tonotopic input to OC efferents. The IC is ideally situated to provide multi-modal integration for complex filtering tasks at the earliest stages of central auditory processing. Preliminary data suggest that pathological hearing situations may result in reorganisation of descending inputs from the IC to OC efferents. Alterations in the descending auditory projections may contribute to impairment of speech discrimination in noise, which is a common symptom of hearing loss.

PS-415

Neural Response Patterns Recorded from the Guinea Pig Inferior Colliculus to Speech

Claus-Peter Richter; Xiaodong Tan; Nan Xia; Petrina LaFaire; Hunter Young
Northwestern University

Introduction
The maximum achievable repetition rate of action potentials recorded from single units in the central nucleus of the inferior colliculus (ICC) to trains of infrared laser pulses is lower than those evoked by trains of acoustic clicks or electrical pulses. Although the maximum following rate of INS is lower than that of acoustic clicks and electrical current pulses, high repetition rates may not be necessary for cochlear implant coding. Here we demonstrate that the repetition rates for selected units in the inferior colliculus evoked by speech signals are well below 100 Hz for each channel and that the achieved pulse repetition rates with optical stimulation are sufficient to code the acoustic information.

Methods
Word lists obtained from the speech in noise (SIN) test were played to the ear of a guinea pig and corresponding neural responses to the each word were recorded in the contralateral ICC. Recordings were made either with multichannel electrode arrays or with single tungsten electrodes. Spectrograms and peri-stimulus raster plots were created and compared.

Results
Acoustic stimuli increased the rate of action potentials when the frequency in the spectrogram was close to the best frequency of the selected unit. Average repetition rates were typically below 100 Hz even at sound levels above 80 dB SPL. Loudness is well reflected by the sum of the action potentials across the channels.

Summary
In normal hearing animals, average pulse repetition rates in the ICC during speech are lower than 100 Hz in single unit level. The dynamics of optical stimulation appears to be sufficient to encode speech. Loudness seems to be coded by the sum of the activity across the channels rather than the rate increase within a channel.

This project has been funded with federal funds from the NIDCD, R01 DC011855, and by Lockheed Martin Aculight.

PS-416

Neuronal Correlates of Vowel Detection in the Cochlear Nucleus and Inferior Colliculus of Macaques

Chaya Narayan; Margit Dylla; Peter Bohlen; Francesca Rocchi; Ramnarayan Ramachandran
Vanderbilt University

Detection of spectrally complex sound stimuli is a fundamental function of the auditory system. Human vowel sounds are a good example of complex spectra and have been extensively used in literature for studies involving frequency encoding of sound stimuli in the auditory pathway. Previous studies show that detection thresholds for vowels depend on the nature of the vowel (front vs. back etc.). Vowels may be represented by temporal patterns of activity rather than by response magnitude of nerve fibers, but these may be transformed at least somewhat in the cochlear nucleus. Here we investigate the representation of vowels in the subcortical auditory system of awake and behaving macaques and attempt to relate the encoded properties with perceptual metrics.

Four non-human primates (*Macaca mulatta*) were trained to detect vowels in a reaction time Go/No-Go lever release task. The vowel was presented over a 60 – 70 dB range of sound pressure levels in step sizes of 2.5 dB around threshold and larger steps at level further away. Neurophysiological responses from single units in the cochlear nucleus (CN, n=40) and inferior colliculus (IC, n=53) were obtained simultaneously with behavior. The vowel ‘eh’ was used as a stimulus for most units so that we could investigate population encoding for that particular vowel. Psychometric and neurometric functions were created using signal detection theory and ROC analysis. Recorded units had characteristic frequencies between 180 Hz and 4 kHz in both structures, spanning the frequency extent of the vowel. Most units recorded showed monotonic responses as a function of sound level. IC unit responses were seen to fall in two clusters – one with thresholds close to behavioral thresholds (n=32/53), and another group with neurometric thresholds about 20 dB higher than psychometric thresholds (n=21/53). There were no CF-based differences in the clustering of IC units, contrary to expectation. In contrast, CN units were grouped in a single cluster with thresholds centered 21 dB higher than the behavioral threshold. These results suggest the responses of CN neurons may need to be pooled to account for behavioral performance, but the response magnitude of IC neurons was sufficient to account for behavioral thresholds. These results form the baseline for investigations of noise influence on vowel perception, and form the baseline for investigations of mechanisms of complex stimulus perception and encoding after hearing impairment.

PS-417

Neural Correlates of the Detection of Tones in Modulated Noise in the Inferior Colliculus and Cochlear Nucleus of Nonhuman Primates

Justin Watson; **Margit Dylla**; Francesca Rocchi; Peter Bohlen; Ramnarayan Ramachandran
Vanderbilt University

Detection of sounds in noisy environments is an essential function of the auditory system. In natural environments, targets and distractors often show temporal fluctuations that influence the detectability of the target. Previous results show that continuous noise shifts detection thresholds of tones to higher tone levels. Amplitude modulation of noise resulted in reduced tone thresholds. Neuronal responses of inferior colliculus (IC) neurons matched tone thresholds but those in cochlear nucleus (CN) were ~18 dB higher. In continuous noise, neurometric thresholds in IC were shifted by a magnitude that matched behavior, whereas those in CN were shifted by lower amounts, and were accompanied by significant rate compression. Here we report studies of CN and IC responses to tones in modulated noise, specifically investigating the correlation between neuronal responses the IC and the CN and behavioral response metrics.

Five monkeys (four *Macacca mulatta* and one *Macacca radiata*) were trained in a reaction time Go/No-Go lever release task to detect steady tones in sinusoidally amplitude-modulated noise. Single units with characteristic frequencies between 320 Hz and 33 kHz were recorded from the CN (n=44) and from the IC (n=81) separately during behavior. Psychometric and neurometric functions were created using signal detection theory and Receiver Operating Characteristic analyses. Behavioral thresholds in the presence of modulated noise were lower than in steady state noise, consistent with prior findings. Neurometric thresholds in the CN and IC also decreased in the presence of modulated noise relative to steady state noise. Neurometric thresholds in the CN were higher than neurometric thresholds in the IC. Psychometric thresholds decreased by 9.3 dB whereas IC neurometric thresholds decreased by 5 dB relative to steady state noise. CN neurometric thresholds were reduced by 4 dB relative to steady-state noise while with an average psychometric shift of 11.4 dB. The neurometric thresholds in the CN were different from psychometric thresholds, whereas those for IC neurons were not significantly different from behavior. The threshold shifts between modulated and steady state noise in the CN and IC were not significantly different from each other. The results of this study confirm the findings from previous studies that CN responses are transformed by the level of the IC to produce strong neuron-behavior correlations.

PS-418

Distortion Products as a Mechanism for Vocalization Selectivity in the Mouse Auditory Midbrain

Elena Mahrt; Christine Portfors
Washington State University Vancouver

Background

During interactions with females, male mice often produce ultrasonic vocalizations with rapid jumps in frequency. The frequency difference between the two ultrasonic components is usually between 10-30 kHz and the individual components are typically between 50-100 kHz. Interesting, many neurons in the inferior colliculus (IC) respond selectively to jump vocalizations even though they do not respond to pure tones between 50-100 kHz. We have previously shown that neurons tuned to low frequencies respond to combinations of simultaneously presented ultrasonic tones if the difference between the tones matches the frequency tuning of the neuron. We previously suggested that these neurons are responding to distortion products created by the combination of high frequency tones. It is not clear, however, that this mechanism is actually creating selectivity to natural vocalizations in the IC. In this study, we explicitly tested whether neural selectivity to jump vocalizations was due to the frequency jump.

Methods

We recorded single unit responses to tones, frequency jump vocalizations, and the individual components of the vocalizations in the IC of awake, restrained mice. The frequency response area of each neuron was first obtained using pure tones. Responses to the suite of jump vocalizations were then obtained. For each vocalization that evoked a response, the deconstructed components were presented alone, with the natural temporal overlap, and then with increasing temporal separation. We evaluated both spike rate and timing.

Results

Approximately half of the IC neurons responded to one or more of the frequency jump vocalizations. Most of these neurons required the components be overlapped by at least 1 ms, as occurs naturally in the vocalizations. Furthermore, these neurons showed selectivity for particular jump vocalizations that had frequency differences within the most sensitive region of their receptive field. We also found duration to be an important factor, as some neurons were only evoked by vocalizations with component overlaps of specific durations.

Conclusions

These results support the hypothesis that frequency jump vocalizations create low frequency distortion products that fall within the receptive field of low-tuned neurons in the mouse IC. Selectivity for particular jump vocalizations occurs when the frequency difference between the two components falls within the neuron's receptive field. The creation of distortion products due to combinations of high frequency components in vocalizations helps explain how mice can encode some of their ultrasonic vocalizations that would otherwise fall outside of their best hearing range.

PS-419

Neural Correlates of Gap Detection in the Mouse Auditory Midbrain

Rüdiger Land; Alice Burghard; Andrej Kral
Hannover Medical School

Introduction

Humans and mice are able to detect short gaps in an ongoing auditory stimulus. To perform this task, the brain must represent the ongoing stimulus as well as the gap with high temporal precision. Further, this representation must be transmitted along the auditory pathway to affect auditory perception.

Methods

Here we studied the neural representation of auditory gap detection in the mouse auditory midbrain. We recorded local field potentials (LFP) and multiunit activity (MUA) in the inferior colliculus (IC) of isoflurane-anesthetized C57Bl/6 mice (< 6 months). We recorded simultaneous neuronal activity at different depths of the IC with a 16-channel multielectrode array. We measured responses to temporal gaps in white noise, while the gap duration decreased from 10 ms to 0.1 ms. Further, we studied the relationship between the neuronal gap detection threshold and stimulation level. Auditory stimulation was in free field using a calibrated loudspeaker.

Results

Neural activity in the inferior colliculus encoded gaps until a threshold of ~1 ms gap duration. Firing rate and evoked local field potential responses changed with decreasing gap duration. The gap detection threshold was independent of the characteristic frequency at the recording site. However, the minimal gap duration sensitivity decreased with decreasing stimulus intensity, because the neuronal population representing gaps in IC at lower stimulus intensities was reduced. We further compared LFP and MUA as measures of neuronal population activity representing gaps. LFPs conveyed more robust and precise information on the minimal gap representation than MUA. In addition, minimal gap detection threshold could also be determined with non-invasively recorded brainstem responses, however with less precision.

Conclusion

The results show that the mouse midbrain represents temporal gap information with high precision. The neuronal gap detection threshold in the IC defines the limit of behavioral gap detection in mice. Further, the lower precision of stimulus representation at low intensity stimuli can explain reduced perceptual gap detection performance. In conclusion, gap detection in IC is a robust measure for investigating temporal sensitivity of the auditory pathway. In addition, brainstem responses can be used as a non-invasive alternative to measure temporal sensitivity.

PS-420

Meaningful But Passive Sound Exposure Induces Long Lasting and Spatially-Restricted Plasticity in Adult Inferior Colliculus

Hugo Cruces Solis[1]; Zhizi Jing[2]; Nicola Strenzke[2]; Livia de Hoz[1]
[1]Max Planck Institute for Experimental Medicine; [2]University Medical Center Goettingen

Incoming auditory information is filtered by its relevance. To test if passive but meaningful auditory experience affects sound processing at a sub-cortical level, we investigated the plastic changes elicited by behaviourally relevant auditory exposure in the inferior colliculus and cochlear nucleus of mice.

C57BL/6J adult female mice lived in an Audiobox (TSE) that allows continuous monitoring of individual behaviour via an implanted subcutaneous transponder. The Audiobox consists of a home-cage connected by a long corridor to a specialized sound-attenuated corner. Food was available *ad libitum* in the home-cage and water was available in the corner. Visits to the corner were accompanied by the presentation of fixed tone pips in the exposed group and by silence in the control group. A third group (random exposure group) was exposed to the same fixed tone pips but randomly and in the home-cage instead of the corner.

After 7 to 11 days of exposure we recorded sound-evoked neuronal activity in the inferior colliculus of acutely anesthetized mice and characterized tuning curves. The exposed group showed an increase in evoked multiunit activity. The augmented responses were specific to the dorsal part of the central nucleus independently of the exposed frequency (8 or 16 kHz). We also observed a shift in best frequency towards higher values along the tonotopic axis that was stronger when 16 kHz was the exposed frequency. The effect was specific to a meaningful sound since in the random exposed group we observed augmented responses only in the area of the central nucleus where the best frequency matched the exposed frequency and not in the dorsal part. These changes were not due to a general adjustment upstream the inferior colliculus since responses in the cochlear nucleus were comparable in the exposed and control groups. Inactivating the auditory cortex with muscimol during acute recordings subtly increased the responses, but in equal magnitude, for both exposed and control groups.

These results indicate that behaviourally relevant, but not random, sound exposure induces sustained changes in a restricted area of the central nucleus of inferior colliculus. Plasticity takes the form of augmented evoked activity and a shift in best frequencies along the tonotopic axis. Its expression is independent of cortical activity. We conclude that, in adult animals, important sustained plastic changes in sound processing take place at a specific subcortical level that might contribute to the neural substrate of auditory expectations.

PS-421

Can Wiener Kernels Explain Responses to Pure Tones and Amplitude Modulated Tones in the Auditory Midbrain of the Budgerigar?

Kenneth Henry[1]; Erikson Neilans[2]; Mathew Mender[1]; Laurel Carney[1]
[1]University of Rochester; [2]University at Buffalo

Wiener kernels calculated from responses to white noise provide an alternative means of characterizing the spectral and temporal sensitivity of auditory neurons. While the first-order Wiener kernel, or "revcor" function, is the average stimulus waveform preceding a spike, the second-order Wiener kernel is related to the spectro-temporal receptive field (STRF), or mean stimulus spectrogram preceding a spike. While Wiener kernels generally predict responses to tones and frozen noise with good fidelity in the auditory periphery (i.e., predictions approximate observed responses), their ability to predict responses in the central auditory system is less explored.

Here, we evaluate the ability of Wiener kernels to predict responses to tones and amplitude modulated tones in neurons of the avian auditory midbrain. Recordings were made from single cells and multi-cell clusters in awake budgerigars using chronically implanted electrodes. Tones were presented with frequencies ranging from 0.25-8 kHz. Amplitude modulated tones were presented with the carrier frequency set at the cell's characteristic frequency and modulation frequencies ranging from 4-1024 Hz to generate modulation transfer functions (MTFs), which plot mean rate or synchrony as a function of modulation frequency.

Wiener kernels were convolved with tones and amplitude-modulated tone waveforms to generate predicted responses. The kernels were able to predict rate responses to tones (including inhibition) in nearly all cells, as in previous studies of the periphery. Wiener kernels also predicted some aspects of the shape of synchrony-based MTFs in most cells, particularly the roll-off in phase locking with increasing amplitude modulation frequency, but not the shape of rate-based MTFs. Whereas most rate-based MTFs in the midbrain exhibit band-pass modulation tuning, firing preferentially in response to a limited range of modulation frequencies, Wiener kernel predictions were always flat or low-pass in shape.

The results show that Wiener kernels capture some, but not all, aspects of sensitivity to tones and amplitude modulation in the avian auditory midbrain. STRFs seem likely to share the same limitation based on their close relationship to the second-order kernel. The apparent inability to explain rate-based modulation tuning is noteworthy because band-pass modulation tuning is a common feature of auditory midbrain neurons in both birds and mammals, occurring in approximately half of cells. Furthermore, several current models posit that modulation filter banks may play a key role in the processing of complex signals including voiced speech under real-world listening conditions. This work was supported by grants R01-001641 and K99-DC013792 from NIDCD.

PS-422

Notched-Noise Revisited: A Model for Masked Thresholds based on Amplitude-Modulation Sensitivity of Midbrain Neurons

Laurel Carney; Thomas Varner
University of Rochester

Notched-noise maskers (e.g. Patterson, JASA, 1976) have become a standard paradigm for describing auditory filter shapes and nonlinearity in listeners with and without hearing loss. Masked thresholds are typically interpreted based on the power-spectrum model of masking. However, this model fails to explain that thresholds are unaffected by a roving-level paradigm (Lentz et al., JASA, 1999), for which energy cues are unreliable. Here, an alternative model for detection in notched noise is based on amplitude-modulation (AM) tuning of cells in the midbrain. These cells are not driven by amplitude modulations in the *stimulus*, but rather by the low-frequency rate fluctuations that are established in the cochlea and projected to the IC. Because rate fluctuations are envelope-related cues, they are typically robust to the roving-level paradigm.

Models for auditory-nerve (AN) fiber responses and AM-sensitive midbrain (*inferior colliculus*) neurons were used to simulate population responses to notched noises with and without added probe tones. Responses of model AN fibers tuned near edges of the notched noise had fluctuations created by interactions of peripheral filters and the sloping spectrum. When a probe tone was added to the notched-noise masker, responses of AM-sensitive midbrain neurons tuned near the tone frequency were suppressed, because the added tone flattens the envelope of the noise-plus-tone and suppresses neural fluctuation. The differences between model IC responses to noise-alone and noise-plus-tone conditions were used to predict detection thresholds. Threshold values and trends as a function of notch width are similar to those reported for listeners

Preliminary responses recorded for some inferior colliculus neurons in awake rabbit are consistent with model predictions: AM-sensitive neurons with bandpass modulation transfer functions and with characteristic frequencies tuned near the frequency of the probe tone responded well to the notched-noise masker and had reduced responses when a tone was added to the masker.

The model proposed here suggests that notched-noise thresholds depend not only on the bandwidth of peripheral filters, but also on other factors that influence neural fluctuations, such as saturation of peripheral responses, synchrony capture, and synaptic adaptation. Additionally, models for midbrain sensitivity to neural fluctuations involve interactions between excitation and inhibition in the brainstem and midbrain. All of these mechanisms are affected by both hearing loss and aging. The interpretation of notched-noise masked thresholds as a direct measure of peripheral bandwidth must be re-examined, for listeners both with and without hearing loss.

PS-423

Band-Enhanced and Band-Suppressed Rate Modulation Transfer Functions of inferior Colliculus Neurons and a Model: Effect of Duty Cycle and Rise/Fall Slope

Duck Kim[1]; Brian Bishop[1]; Shigeyuki Kuwada[1]; Laurel Carney[2]

[1]University of Connecticut Health Center; [2]University of Rochester

Introduction

Salient features of natural sounds, including speech, can be characterized by their amplitude-modulation (AM) properties (Shannon et al., 1995, Singh and Theunissen, 2003, McDermott and Simoncelli, 2011). Rate modulation transfer functions (MTFs) of inferior colliculus (IC) neurons are band-pass, low-pass, band-reject, and other types (Krishna and Semple, 2000, Joris et al., 2004, Nelson and Carney, 2007). Most studies of AM processing have used sinusoidal envelopes, although some have used non-sinusoidal envelopes (Sinex et al., 2002, Krebs et al., 2008; Zheng and Escabi, 2008). The goal of this study was to determine how IC neurons represent AM stimuli and how duty cycle and rise/fall slope affect the rate MTFs.

Methods

Extracellular single-unit discharges were recorded in the IC of unanesthetized rabbits.The sound source was an octave-band noise centered at the neuron's best frequency. Modulation frequencies ranged from 2 to 512 Hz in doubling steps. Modulation envelopes were sinusoidal, "raised sine" (Bernstein and Trahiotis, 2010), and smooth trapezoid. The trapezoid envelope had a specified duty cycle and smooth rise/fall ramps with specified slopes. A neural circuit model of IC neurons was adapted from Nelson and Carney (2004). The model was extended to include representation of a band-suppressed IC neuron (defined below).

Results

In response to AM sounds, IC neurons had enhanced or suppressed firing rates, relative to the response to the unmodulated sound, over some range of modulation frequencies, referred to as band-enhanced and band-suppressed neurons, respectively. Others showed a mixture of enhancement and suppression over different ranges of modulation frequencies, referred to as hybrid-type neurons. Most IC neurons were sensitive to the duty cycle, with many preferring low duty cycles. Relatively few neurons were sensitive to rise/fall rates. Many neurons had clearer enhanced peaks or suppressed troughs to non-sinusoidal envelopes than to sinusoidal envelopes, often with low duty cycles and, some with higher rise/fall slopes, e.g., "raised sines" with an exponent of 8. The model was able to reproduce both band-enhanced and band–suppressed type MTFs.

Conclusions

When tested with multiple types of AM envelopes, essentially all IC neurons fall into one of three types of rate MTFs: band-enhanced, band-suppressed, and hybrid. The successful model simulation of band-enhanced and band–suppressed rate MTFs supports the view that dynamic interactions between different time courses of excitatory and inhibitory synaptic potentials give rise to tuned rate MTFs.

PS-424

Rapid Task-related Plasticity of Spectro-temporal Receptive Fields in the Auditory Midbrain

Sean Slee; **Stephen David**

Oregon Health and Science University

Previous research has demonstrated that auditory cortical neurons can modify both their spatial and spectro-temporal receptive fields (STRFs) when animals engage in auditory discrimination tasks. Population models suggest that this task-related plasticity produces enhanced neural discriminability between the behaviorally relevant stimuli. Whether this form of task-related plasticity exists in subcortical auditory stations is unknown. We tested this hypothesis by recording neural activity in the inferior colliculus (IC) while ferrets discriminated between a pure tone target and temporally orthogonal ripple combinations (TORCs). To measure task-related plasticity, STRFs measured from responses to the TORCs were compared during behavior and during a passive state before and after behavior. When the target was placed near the best frequency (BF) of the neuron, about half of the STRFs were suppressed relative to the passive state. The size of the suppression (~30-40%) was quantitatively similar in the central nucleus and external nucleus of the IC and occurred throughout the receptive field (a global gain change). The plasticity recovered in some neurons but more often persisted in passive periods after behavior. When the target was placed an octave or more away from the BF, many of the STRFs were less suppressed or enhanced relative to the passive state. The data support a model with tonotopic variation in gain change that enhances neural discrimination of the task stimuli. Taken together, these results suggest that rapid task-related plasticity in the auditory midbrain is quantitatively similar to that described previously in the cortex and demonstrate significant behavioral modulation of the subcortical auditory pathway.

PS-425

Assessing the Contribution of Sub-threshold Synaptic Activity to the Coding of Sound Level in the Auditory Midbrain and Cortex

Jose Garcia-Lazaro[1]; Roberta Donato[1]; Owen Brimijoin[2]; Jessica Monaghan[3]; David McAlpine[1]

[1]University College London; [2]MRC Institute for Hearing Research, Glasgow; [3]University of Southampton

Background

The mammalian auditory system has the remarkable ability to encode sounds that extend over a vast range of intensities. We have previously shown that firing rates of neurons in the inferior colliculus (IC) adapt to the ongoing distribution of sound intensities, improving coding by the neural population around the most-commonly occurring intensities. The neural basis for this "adaptive code" remains as yet unclear. In this study, we use *in vivo* intracellular recordings to investigate the

contribution of subthreshold synaptic activity to the coding of sound level.

Methods
We recorded *in-vivo* intracellular responses to acoustic stimuli from neurons in the IC and primary auditory cortex, in ketamine/xylazine-anesthetized adult Mongolian gerbils (*Meriones unguiculatus*) using sharp glass electrodes. To assess the intrinsic response properties of neurons, we used current steps (100 pA, 400 ms) injected through the recording electrode. Frequency response areas were estimated from the responses to pure tone pips of varying frequencies (250 Hz to 8.192 kHz) and intensities (20 to 80 dB SP) presented once every 150 ms. To investigate the dynamics underlying the coding of sound level, we presented white noise and varied the level every 40 ms. Sound levels (24-96 dB SPL) were drawn randomly from a defined distribution consisting of one or more high-probability regions from which sound levels were selected with an overall probability of 0.8 and the remaining levels with an overall probability of 0.2. In addition, we presented trains of continuous white noise whose level was varied every 40 ms. Stimulus trains were derived by de Bruijn sequences, chosen because of their orderly patterns; they contain a balanced set of all possible level pair, triplet, and quadruplet transitions while retaining a random structure.

Results
Our preliminary results indicate that cortical and midbrain neurons exhibit fundamentally different intrinsic properties. Therefore, we went on to assess the relationship between postsynaptic potentials (PSP) and the number of spikes evoked by our stimuli. The data suggest that only the subset of PSPs with the larger areas (integral) tend to evoke spikes. Sound levels in the de Bruijn sequence preceding evoked spikes differ from those preceding excitatory PSPs not evoking spikes.

Summary
We use *in vivo* intracellular recordings to assess the contribution of sub-threshold synaptic activity to the coding of sound level. Our preliminary analysis suggests that both intrinsic and synaptic properties may underlie the different types of adaptation at these two stages of the central auditory pathway.

PS-426

Insights into the Neural Representation of Speech in Background Noise in the Auditory Midbrain of the Mongolian Gerbil

Jose Garcia-Lazaro; Roland Schaette; David McAlpine; Nicholas Lesica
University College London

Background
The ability to understand speech is one of the most important roles of the human auditory system. In quiet environments, this task is relatively straightforward for normal hearing listeners. Even for listeners whose peripheral auditory system is severely impaired, understanding speech in quiet remains a relatively simple task. However, this changes dramatically once background noise is introduced. While the healthy human auditory system is capable of understanding speech in complex acoustic environments, speech understanding is considerably degraded for those with hearing impairment. Hearing aids provide some, albeit limited benefit by rendering sounds more audible. Nevertheless, audibility does not guarantee intelligibility, i.e., a hearing aid user might be able to 'hear' speech in background noise, but still not be able to understand it. Factors leading to speech-in-noise problems in individuals with hearing impairments are currently not well understood. In this study, we aim to provide insight into the neural representation of speech-in-noise using state-of-the-art electrophysiological recordings in the auditory midbrain of normal hearing Mongolian gerbils and subsequently extend our study to investigate the changes in this representation in hearing impaired individuals.

Methods
We performed *in vivo* electrophysiological recordings in the inferior colliculus (IC), the major auditory nucleus of the midbrain, in ketamine/xylazine-anesthetized adult Mongolian gerbils (*Meriones unguiculatus*) using 32-channel silicon tetrode arrays. To characterize the basic response properties of single units in the IC, we estimated frequency response areas (FRAs) using pure tone pips of varying frequencies (250 Hz to 8.192 kHz) and intensities (20 to 80 dB SPL) presented once every 150 ms. To investigate the neural representation of speech-in-noise, we used neural activity patterns evoked by repeated presentation of 18 different vowel-consonant-vowel (VCV) tokens from an adult female talker presented at 1sec intervals at varying (-12 to 12 dB) signal-to-noise ratios. The overall intensity of both VCVs and background noise was adjusted to either 60 or 75 dB SPL.

Results
Our preliminary results suggest that discriminability of consonants decreases with increasing noise levels. Thus, in the presence of noise, more neurons were required to reach the same discrimination performance than when tested in the absence of noise.

Summary
Assessing neural activity patterns, we investigated the representation of speech in background noise in the auditory midbrain. Our data indicate that spike-timing and spike-rate information are both degraded at high noise levels.

Funded by the Medical Research Council (UK) grant MR/L022311/1 awarded to RS, JAGL and DM.

PS-427

Periodicity Processing is related to Sound-Intensity Processing in the Inferior Colliculus

Peter Baumhoff[1]; Christine Zschau[2]; Andrej Kral[1]; Gerald Langner[2]
[1]Hannover Medical School; [2]Technische Universität Darmstadt

Human listeners assign pitch to harmonic sounds either according to the frequency of temporal envelope or based on its higher order harmonics. Which of those strategies dom-

inates the pitch perception may be based on individual predisposition or the specific signals structure. The temporal envelope of a harmonic signal can also be described as a periodic modulation of a signals sound-intensity ('periodicity'). The inferior colliculus (IC) is known to be an important auditory relay and processing station for periodicity as well as for sound intensity. Here we study the relationship between periodicity- and sound-intensity-processing in the IC to determine whether listening strategy preference might originate in the auditory midbrain.

We recorded multiunit activity from the IC in 5 awake, normal hearing mongolian gerbils. The stimuli were pure tones and sinusoidal amplitude modulated signals (SAMs). For 150 ICC neurons we determined the dynamic range of sound-intensity coding at characteristic frequency (CF). Furthermore we measured modulation transfer functions (MTFs) at modulation frequencies between 30 Hz and ½ CF. In order to determine the best modulation frequencies for rate (rBMF) and for synchronization (sBMF) we calculated the spike rate and the vector-strength of the neural responses.

We classified IC neurons into three categories, according to their sound-intensity processing: wide dynamic range (48%), narrow dynamic range (44%) and dynamic range with sound-intensity optimum (8%). Additionally we classified the neurons based on their response properties to the modulation frequencies of SAMs into band-pass filters (rate: 34%; synchronization: 35%), low-pass filters (rate: 19%; synchronization: 53%), all-pass filters (rate: 13%; synchronization: 2%) and a small group of complex filters (rate: 3%, synchronization: 1%). 31% (rate) and 9% (synchronization) were not specifically tuned. We found that 84 % (rate) and 77 % (synchronization) of all band-pass tuned neurons had wide dynamic ranges. Low-pass tuned neurons mostly had small dynamic ranges (rate 79 %; synchronization 63 %).

Based on their dynamic range for sound-intensity coding neurons of the IC can be divided in ones with broadband and ones with narrowband cochlear input. Our data suggests that neurons with broadband cochlear input commonly serve as band-pass-tuned coincidence detectors. These neurons mainly translate the signal periodicity in a rate code, whereas neurons with narrowband input seem to relay the signal period information mainly by synchronized neural activity in a low-pass fashion. We conclude that both, processing of the temporal envelope and spectral processing, are inherent to nearly equal shares of IC neurons.

PS-428

The Width of the Frequency Channels Determines Stimulus-Specific Adaptation in the Inferior Colliculus of the Rat

Daniel Duque[1]; Xin Wang[2]; Manuel Malmierca[2]
[1]Universidad de Salamanca; [2]Universidad de Salamanca, Auditory Neurophysiology Unit Institute of Neuroscience of Castilla y León

For years, electrophysiological, psychophysical and electroencephalographic studies have tried to disentangle the neuronal basis for intensity coding an intensity deviant detection. Psychophysical forward masking experiments have repeatedly shown how a higher intensity sound masks the subsequent low intensity sound, but electroencephalographic mismatch negativity experiments have proved that pre-attentive deviant detection can be elicited with low intensity deviants sounds embedded in a background of high intensity sounds.

Here we extracellularly recorded 132 single neurons in the inferior colliculus (IC) of 37 adult anesthetized rats to test if there is stimulus-specific adaptation (SSA) for intensity deviants. If we consider two sounds of the same frequency where the low intensity sound presented a low probability of appearance, two scenarios could arise: 1) neurons adjust to stimulus statistics by changing the dynamic range to the high intensity sound or 2) SSA exists for intensity sounds and the neuron presents an enhanced response for the low intensity deviant sound. Then, we calculated the frequency response area (FRA) for each neuron, fixed a low intensity probe sound and evaluated the across-adaptation from different high intensity conditioner sounds to the low intensity probe sound. We used the oddball paradigm to evaluate SSA for frequency, intensity and double deviants for frequency and intensity. We also record 33 single neurons using the novel *rapid adaptation paradigm* to characterize the shape and width of the frequency channels that code for the probe sound.

Our results suggest that there is no SSA for purely intensity deviant sounds in the IC, but the analysis of the across-adaptation data elicited by the double deviants for frequency and intensity show that SSA can be generated if and when the high intensity conditioner is outside the frequency channels that code for the probe sound. Moreover, those frequency channels broaden at higher intensities and are clearly narrower for neurons that show high levels of SSA, strongly suggesting that the frequency-channel theory is explaining SSA in the IC.

PS-429

Neurons in the Inferior Colliculus of the Rat Respond to the Omission of Stimuli.

Blanca M. Aguillon[1]; Javier Nieto[2]; Jonathan Fritz[3]; Manuel Malmierca[2]
[1]University of Salamanca; [2]Institute of Neuroscience of Castilla y León. INCYL University of Salamanca; [3]Department of Electrical and Computer Engineering, Institute for Systems Research, University of Maryland, College Park,

The mismatch negativity (MMN) is a component of the auditory ERP that is elicited when acoustic expectations are violated and has been shown to correlate with behavioral and perceptual measures of deviance detection. Furthermore, the amplitude of the MMN response indexes the magnitude of the expectancy violation. A distinct aspect of the MMN is that the omission of an expected auditory stimulus is often accompanied by elicitation of the omission MMN component (Yabe et al., 1997). This response reveals the predictive activity of the auditory system, since auditory activity can be observed in the absence of any auditory input. Animal studies

have found that some neurons in the auditory cortex (Ulanovsly et al., 2003), medial geniculate nucleus and inferior colliculus (Malmierca et al., 2014) show a specific reduction in their response to repetitive stimuli when stimulated with an oddball paradigm similar to that used in human MMN studies. This phenomenon is termed stimulus-specific adaptation (SSA) and has been suggested to be the neuronal correlate of MMN. However, so far, SSA has been studied in animal models using the simple repetition suppression effect of the classical oddball paradigm and the goal of the present study was to investigate whether single neurons in the rat IC might respond to the omission of stimuli as found in human MMN.

Experiments were performed on female Long-Evans rats anesthetized with urethane (1.5 g/kg). Tungsten electrodes were used to make extracellular recordings of neural responses in well-isolated single units in the IC. Neurons were stimulated using an oddball "omission" paradigm that consisted of trains of 400 pure tone stimuli of variable duration, ISI and rate in fixed blocks in which tones were presented as the standard (90% occurrence); interspersed pseudorandomly with omitted stimuli (silence) as the deviant (10% occurrence).

In preliminary results from an ongoing study, we observed responses to silent oddball "omissions" in ~20% of IC neurons (n=18/99; p≤0.05; Monte Carlo method). These neurons responded to pure tone stimuli, and also exhibited a strong response when expected tones in the sequence were omitted. We explored responses at different rates of tone trains and found that this distinct response to the omitted stimuli only occurred during rapid tone trains, with ISIs <150 ms, as in human MMN. This finding of omission responses in IC confirms that the auditory system does not need an external stimulus trigger to detect a deviation from expectations (Bendixen, et al 2012).

PS-430

Modulation of Auditory Deviant Saliency in the Inferior Colliculus (IC)

Yaneri Ayala[1]; Manuel Malmierca[2]
[1]University of Salamanca; [2]Institute of Neuroscience of Castilla y Leon. University of Salamanca

Auditory neurons adapt to repetitive sounds but retain their excitability to signal the occurrence of a deviant sound. This phenomenon is termed stimulus-specific adaptation (SSA) and has been though to enhance the deviant-stimulus saliency and to reduce the acoustic information redundancy. The inferior colliculus (IC) is a likely structure to exert a dynamic control on the flow of information to facilitate the detection of biological important signals since it integrates massive ascending and descending inputs. Then, synaptic inputs converging on IC neurons may shape their functional response profiles. Here, we explored how the inhibitory local inputs and neuromodulators shape the SSA.

Experiments were performed in anesthetized rats undergoing contralateral acoustic stimulation (pure tones, 75ms). Stimulus were presented using an oddball paradigm which consists in the presentation of a high-probability tone (90%, standard) randomly replaced by a low-probability one (10%, deviant). Single-unit extracellular responses were recorded before, during and after the application of GABAergic- (n=37), glycinergic- (n=24), muscarinic- (n=20) and nicotinic antagonists (n=28) and the agonist acetylcholine (n=105). We also injected a cocktail of GABAergic and glycinergic antagonists (n=6) to test the extend to which adaptation to the standard tone is abolished by the inhibitory blockade.

The general results show that the blockade of inhibition broadens the frequency response areas, shortened the latency and decreased the degree of SSA. The application alone of pre- (n=17) and post-synaptic $GABA_B$ (n=11), as well as of glycinergic antagonists elicited a weak decrease in the SSA. But, this decrement was augmented by the co-application of inhibitory antagonists which increase both, the response to the deviant and standard tones abolishing completely the SSA in some cases (4/6). The modulation exerted by acetylcholine was more delicate and specific, so that only affected neurons with intermediate levels of SSA, affecting mostly the response to the standard tone. This differential effect on a subset of IC neurons was also observed with the blockade of the muscarinic and nicotinic receptors.

In conclusion, SSA occurring at the IC is strongly modulated by the inhibitory and cholinergic inputs. While the inhibition affects both, the response to the deviant and standard tone, the cholinergic modulation affects mainly the response to the standard tone. Also, our cholinergic data suggest that different synaptic inputs converge on IC neurons since not all were homogeneously affected. Thus, synaptic domains with different balance of inhibitory and modulatory inputs can characterized those IC neurons sensitive to deviant sounds.

PD-66

Interaural Phase Modulation Following Responses as a Measure of Binaural Processing

Jaime Undurraga; Nicholas Haywood; Torsten Marquardt; David McAlpine
University College London Ear Institute

Background

Bilateral cochlear implants provide the opportunity for implant users to access binaural cues, potentially increasing performance in spatial listening tasks. However, since implants are inserted and fitted independently, users may have place-mismatched electrode arrays, effectively exciting the same cochlear sites across-ears with information from different frequency channels.

Here, we developed an objective measure to assess binaural processing in human listeners; specifically, we measured the following responses to abrupt interaural phase modulations (IPM-FR) imposed on sinusoidal amplitude modulated (SAM) signals in low- and high-frequency regions of the cochlea using EEG recordings.

Methods
The phase of a 520 Hz carrier signal was manipulated to produce discrete interaural phase switches at certain minima of the SAM cycle. A total of seven Interaural Phase Differences (IPDs), ranging from ±11 to ±135◦, and three IPM rates (3.4, 6.8, and 13.6 Hz) were tested. The carrier was amplitude modulated using several rates (27 to 109 Hz).

In a second experiment, modulated transposed stimuli (carriers between 2 to 5 kHz) were used to measure IPM-FR (at 6 Hz) with bilaterally matched and mismatched carrier frequencies (simulating an electrode mismatch). Transposed tones allowed us to control the envelope shape independently of the carrier rate. In one condition the envelope IPD was modulated from 0 to 180◦ (0/180◦ condition), whilst in a second condition the IPD was modulated at ± 90◦.

Results
Responses to the low-frequency tones could be obtained from all participants. However, the Signal-to-Noise Ratio was largest when the IPM rate was 6.8 Hz and IPDs were between 45◦ and 90◦. Increasing the modulation rate resulted in increased IPM-FR amplitudes.

Responses obtained for the transposed stimuli demonstrated that the magnitude of the IPM-FR was larger for matched than for frequency-mismatched carriers. Moreover, responses were larger for the 0/180◦ IPD condition.

Conclusions
We concluded that IPM-FRs can be used as a reliable objective measurement of binaural processing and may be a suitable measure to match across-ear electrodes.

Higher responses obtained for IPD between 45 and 90◦ suggest that, as shown for small mammals, human MSO neurons are also strongly tuned to this IPD range.

Decreasedresponses to mismatched carriers demonstrated that across ear mismatches can potentially decrease the integration of bilateral information.

Larger responses obtained for the 0/180◦ IPD condition suggest that, at high-frequencies , responses could be indicative of LSO processing.

PD-67

Toward an Understanding of Mechanisms Responsible for Changes in Residual Acoustic Hearing Following Cochlear Implantation

Alexander Claussen[1]; Viral Tejani[1]; Barbara Robinson[1]; Jonathan Kopelovich[1]; Hakan Soken[2]; Murat Salihoglu[3]; Carolyn Brown[1]; Paul Abbas[1]; Marlan Hansen[1]
[1]University of Iowa; [2]Eskisehir Military Hospital; [3]GATA Haydarpaşa Training Hospital

Introduction
Improvements in cochlear implant (CI) design and surgical techniques now allow for preservation of functional acoustic hearing following implantation. However, some patients lose their residual acoustic hearing after implantation; the cause of this hearing loss is not well understood. This study reports results obtained from both mice and humans. In mice, we contrast DPOAE, ABR and histological measures obtained from animals with residual acoustic hearing that were exposed to electrical stimulation. In humans, we report measures of acoustically evoked, intracochlear responses recorded using the neural telemetry system of the Nucleus device.

Methods
CBA/CaJ mice were implanted with platinum electrodes. One group was stimulated for 2 hours at eABR saturation levels. A second group was implanted but not stimulated (sham). One week later ABR and DPOAE testing was performed and cochleae were harvested for immunolabeling of hair cells, synaptic elements and neural fibers. The human data were collected from a group of Nucleus CI users with varying amounts of residual acoustic hearing following surgery. Toneburst stimuli were presented via an insert earphone and the neural telemetry system of the CI was used to obtain intracochlear recordings of the auditory nerve and surviving hair cell responses. Alternating polarity stimuli were analyzed separately and then subtracted or added to emphasize the cochlear microphonic (CM) or neural components in the responses.

Results
In mice, electrical stimulation resulted in a significant increase in ABR threshold versus sham stimulation. Inner and outer hair cell counts were largely preserved while post-synaptic structures and afferent fibers were compromised. The human data demonstrate the feasibility of this testing procedure. The recordings were strongly periodic in nature. Comparison of responses from negative and positive polarity stimuli suggests evidence of both a CM component and a neural response. Isolating the hair cell from the auditory nerve response was problematic.

Conclusions
This mouse model of CI may be used to study exposure to both acoustic and electrical stimulation and the resulting pathophysiology. We further describe a method that may be able to record neural responses from an intracochlear electrode in human CI users, potentially allowing direct comparison of responses from both acoustic and electrical stimulation. Our goal is to use this noninvasive method to assess interactions between acoustic and electrical stimuli at the level of the cochlea and monitor changes over time at both a cochlear and retrocochlear level. Future work comparing results from animals and humans is planned.

PD-68

Comparison of Cochlear Array Insertion Forces with Three Insertion Techniques in Temporal Bone Models

Yann Nguyen[1]; Guillaume Kazmitcheff[1]; Daniele De Seta[2]; Elisabeth Mamelle[1]; Evelyne Ferrary[1]; Olivier Sterkers[1]
[1]Sorbonne University, "Minimally Invasive Robot-based Hearing Rehabilitation", UPMC Univ Paris 06, UMR S 1159, 75005, Paris, France INSERM, "Minimally Invasive Robot-based Hearing Rehabilitation", UMR S 1159, 75018, Paris France; [2]Sensory Organs Department, Sapienza University of Rome, 00100, Rome, Italy

Introduction

In order to achieve minimal trauma to inner ear structures during array insertion, modifications of array design and approaches have proposed. It would be suitable to predict and lower the peak force at the end of the insertion. The aim of this work to compare insertion forces of an array insertion with 3 different techniques: manual insertion with forceps, insertion with a commercial tool, and insertion with a motorized tool into anatomic specimens.

Materials and Methods

Twelve human temporal bone specimens have been prepared in order to expose the basilar membrane to follow the array progression during insertion and visualize scala translocation. Temporal bones have been mounted on a 6-axes forces sensor to collect insertion forces. Each temporal bone has been inserted 3 times in random order with each of the techniques with a 1-J array (Advanced Bionics; Valencia). Peak insertion force values during and at the end of the insertion were studied.

Results

Manual and insertion with the commercial tool generated multiples peaks above 0.1 N during whole insertion length insertion related to fit and start. On the contrary, insertion force with a motorized tool only rose at the end of the insertion. Final peak insertion force was 0.279 ± 0.078 N, 0.331±0.062 N, and 0.227 ± 0.08 N for manual insertion with forceps, insertion with a commercial tool, and insertion with a motorized tool technique respectively.

Conclusion:

No difference between the three techniques considering final peak value was observed. However, a more predictable force profile could be observed with the motorized tool. Such a tool coupled to a force feedback could stop insertion to avoid harmful peak force at the end of the insertion.

PD-69

Animal-to-Human Brain Interface for Cochlear Implants

Petrina La Faire; Xiadong Tan; Nan Xia; Pamela Fiebig; Alan Micco; **Claus-Richter Richter**
Northwestern University

Introduction

By establishing a brain-to-brain interface, sensory information from animals can be transmitted to humans. For deaf individuals, this could mean restoring their hearing to levels far surpassing current cochlear implants.

Method

To investigate the possibility of a brain-to-brain interface, a recording of 53 words from a Speech-in-Noise (SIN) test were played to an anesthetized guinea pig, while neural activity of an identified and stable single neuron unit in the central nucleus of the inferior colliculus were recorded. These recordings and the recordings from the perfectly functioning auditory system of an animal were played to deaf individuals via their cochlear implant. 10 trials were recorded at 20 different single units, each corresponding to a specific frequency, as determined using pure tone acoustical stimulation. The recorded frequencies ranged from 850 Hz to 16000 Hz. The best trial for each unit was selected and a spike train was determined from the recording. The recorded neural signal was used to make a spike train by making a vector of zeros and ones; each one corresponded to the time point when the recorded signal exceeded a threshold level. The spike trains were then played via a system on loan from Advanced Bionics that allows external control of a cochlear implant. Due to limitations of the random access memory of the system, only 10 – 12 channels of the available 16 on the HiRes90 cochlear implant were available. This limited the frequency resolution presented to the patient.

Results

Initial patient trails have shown patients are able to discern length of word and rhythm, despite stimulation with constant current. When patients completed a forced choice test between four words, they were able to identify the correct word 30-40% of the time. Retest reliability was close to perfect. All of the trials occurred with no training of the patient, which could be greatly beneficial in improving accuracy. Further trials are underway.

Conclusions

Initial results show promise that lexical information can be transmitted from an animal to a human auditory system. The approach would allow parallel stimulation at 16 electrode contacts, code 120 dB of acoustical dynamic range, and reduce the power by reducing the average repetition rate at each channel well below 100 Hz. Loudness is not encoded by current level, which can be held constant at stimulation threshold.

PD-70

Swellable Hydrogels to achieve Perimodiolar Electrode Positioning with Encapsulated Perimodiolar Cellular Elements

Elise Cheng[1]; Braden Leigh[2]; Allan Guymon[2]; Marlan Hansen[1]
[1]University of Iowa Hospitals and Clinics; [2]University of Iowa

Introduction

Despite advances in electrode design and sound processing strategies, cochlear implant (CI) performance has plateaued due, at least in part, to the inability to increase the effective number of stimulation channels. Free-fitting CIs typically rest

laterally in the scala tympani, away from the target neural elements in the modiolus. Each channel's stimulation spreads to adjacent spiral ganglion neurons, reducing the number of effective channels of stimulation. Thus the CI is unable to replicate the inherent intimacy of afferent cochlear innervation. To address this problem we propose a two-part approach using swellable photopolymerized polyethylene glycol (PEG) hydrogels to a) achieve perimodiolar positioning and b) encapsulate Schwann cells (SCs) and to guide spiral ganglion neurite extension toward the electrode array.

Methods

We develop two hydrogel systems. One hydrogel system is designed for perimodiolar positioning, with swelling >250% and a compressive modulus of <50kPa. We test for hearing preservation by placing a hydrogel coated electrode array or array substitute into the cochlea of a hearing rat. ABR and DPOAEs are measured prior to insertion, immediately after electrode insertion, and 2 weeks following implantation. Perimodiolar positioning is determined using microCT and histology.

A hydrogel system is also developed for encapsulation of SCs. A 10% PEG photopolymerizable monomer solution is formulated both with and without RGD peptide at 5 mM. SCs are suspended in the solution, which is then polymerized by exposure to UV light at 365nm. Percent cell viability is then determined at two weeks using a dye exclusion assay.

Results

Manipulation of cross-link density and monomer size produced several hydrogel systems with >250% swelling after 24 h and suitable for cochlear implantation in rats. Asymmetric coating of electrode arrays was achieved which allows for perimodiolar positioning upon hydration following implantation. Moderate ABR threshold shifts are observed and DPOAEs are preserved, suggesting that hearing is largely preserved with insertion of hydrogel into the cochlea.

SCs were successfully encapsulated using a photopolymerizable PEG hydrogel system. >50% cell viability was confirmed with both the RGD functionalized hydrogel system as well as with the non-functionalized PEG system, with some morphological differences noted in the RGD functionalized system compared to the non-functionalized system.

Conclusions

Novel hydrogel coatings represent a potential solution to improve the neural:prosthesis interface in CIs.

PD-71

Implantation of the Auditory Nerve via the Middle Ear Cavity in rats with Hearing Preservation

Caroline Guigou[1]; Gaelle Leterme[2]; Bruno Pasquis[3]; Guillaume Tourrel[4]; Lionel Bretillon[5]; Alexis Bozorg Grayeli[6]
[1]Dijon University Hospital, and CNRS UMR-6303 Research Laboratory; [2]Dijon University Hospital and CNRS UMR-6306, Dijon, France; [3]Centre for Science of taste and nutrition CNRS 6265, Burgundy University, Dijon, France; [4]Oticon Medical Neurelec, Valloris, France; [5]Centre of Sciences of taste and nutrition UMR 1324, 6265 CNRS, Burgundy University, Dijon, France; [6]Dijon University Hospital, CNRS UMR-6306, University of Burgundy, Dijon, France

In a previous study we showed the feasibility of transmodiolar implantation of the auditory nerve via middle ear cavities in human (Sobhy Afifi W et al., Audiol Neurotol, in press). The aim of this study was to study the possibility of hearing preservation and to investigate histologic cochlear lesions after the transmodiolar implantation in rats. Nine adult Whistar rats were implanted. The bulla was exposed. Cochlear apex was visualized and a titanium rod (1.55 mm) covered by parylen was inserted in the apex in the direction of the modiolus. The cochlear opening was sealed by a muscle fragment. Auditory brainstem evoked responses (ABR) were recorded before surgery and at postoperative days 0, 2, 15 and 30. Thirty days after surgery, rats were euthanized and cochleae were sampled for histology. Microscopic examination showed 3 implants inside modiolus (33%), one (11%) partially outside, and the remaining 5 (55%) totally outside the modiolar region. Hearing was preserved in all cases. In animals with modiolar implant (n=3), the pre operative average hearing threshold was 35.8 ± 3.18 dB. This threshold increased to 80.0 ± 7.58 dB immediately after surgery, and to 93.3 ± 6.99 dB at Day 2. Subsequently, it decreased to 75.0 ± 7.53 dB at Day 15 and 68.3 ± 8.14 dB at Day 30. The hearing loss was predominant at 2 kHz. This study demonstrated the feasibility of hearing preservation after auditory nerve implantation via middle ear cavities in rats. The hearing improvement with time suggested an acute inflammatory reaction which regressed progresseively.

PD-72

Novel Application of a Computational Model of the Distributed-Diameter Auditory Nerve Population for Modulation Detection Thresholds

Elle O'Brien; Nikita Immenov; Jay Rubinstein
University of Washington

Introduction

Amplitude modulation detection thresholds (MDTs) are a psychophysical measure of temporal sensitivity that correlates with speech and music perception in cochlear implant users. In theory, MDT assessment could evaluate the efficacy of various stimulation strategies, but the testing process is time-consuming. Therefore we aim to develop a computa-

tional model of the auditory nerve fiber (AN) population and discrimination process that replicates key trends in the MDT literature: (1) improved sensitivity at higher stimulus intensity, (2) decreased sensitivity at higher modulation frequencies, and (3) decreased sensitivity at higher carrier pulse rates.

Methods

In this study, we implemented a stochastic biophysical neural population model of 125 myelinated fibers with normally distributed diameters. This model has been previously shown to accurately describe temporal response characteristics of single fibers and predict discrimination of Schroeder-phase stimuli. In each of the three simulations, we presented the model with 60 cycles each of a modulated stimulus and an unmodulated stimulus. We estimated the depth of modulation that could be discriminated 79.4% of the time with a most-likelihood estimation procedure. The temporal binning parameter and number of fibers included in the discrimination process were varied.

Results

(1) The model predicts better discrimination at higher intensities in accord with psychophysical literature. When the entire population is involved in discrimination, MDTs have a plateau shape that eventually tapers off as the dynamic range of the model saturates. However, there are certain fibers that can discriminate with near perfect accuracy at any given intensity. (2) The model predicts worsened discrimination as modulation frequency increases manifested by a lowpass filter shape. The cutoff frequency varies with the temporal binning parameter. This suggests that individual differences in temporal modulation transfer functions could be attributed to an integration constant. (3) For stimuli with approximately equal spike counts, the model predicts enhanced modulation sensitivity at low carrier pulse rates except at the highest intensities.

Conclusions

Our model captures three qualitative trends in MDTs reported in the psychophysical literature, which supports its application to preliminary assessment of novel stimulation strategies. Our study also suggests that varying the temporal binning parameter replicates variability observed in the cochlear implant population, and a distributed diameter population leads to fiber subsets with excellent discrimination abilities at any of our sampled stimulus intensities.

PD-73

Optimization of a Spectral Contrast Enhancement Algorithm for Cochlear Implants based on an Individualized Electrode-Nerve-Interface Model

Waldo Nogueira[1]; Waldemar Würfel[2]; Thilo Rode[3]; Andreas Büchner[3]

[1]Medical University Hannover, Cluster of Excellence "Hearing4all"; [2]Hoerzentrum GmbH; [3]Medical University Hannover

Background

Considerable variation in speech intelligibility outcomes when comparing two sound coding strategies has been seen in many clinical studies. One possible reason that might explain this variability is their individual electrode nerve interface which can impact the spectral resolution they can achieve. Spectral resolution has been reported to be closely related to vowel/consonant recognition in cochlear implant (CI) listeners . One measure of spectral resolution is the spectral modulation threshold (SMT), which is defined as the smallest detectable spectral contrast in the spectral ripple stimulus.

Methods

In this study we hypothesized that an algorithm that improves SMT might also be able to improve vowel recognition, and consequently produce an improvement in speech understanding. With this purpose we implemented an algorithm, termed Spectral Contrast Enhancer (SCE) that is able to emphasize peaks with respect to valleys in the audio spectrum. This algorithm can be configured with a single parameter: the amount of spectral contrast enhancement entitled "SCE factor". Additionally, we would like to investigate whether the "SCE factor" can be individualized to each CI user. With this purpose we developed a peripheral model of cochlear implant neural activity. The model has been individualized to the electrode nerve characteristics of each study participant, for example using information about their cochlear size, electrode position, impedance matrix values and monopolar and bipolar thresholds. Next, the parameters of the model were adjusted using a pattern recognition algorithm to match the SMT of each CI user. Finally, the model was used to predict the performance produced by the SCE algorithm with two different "SCE factors" in a vowel identification task.

Results

In 10 CI users the new algorithm has been evaluated using a SMT task and a vowel identification task. Audio signals were processed with and without the SCE algorithm and presented to the CI users through the nucleus research interface at an equivalent level of 65 dB SPL. The task was performed for SCE factors of 0 (no enhancement), 0.5 and 1. We observed a modest correlation between the SMT task and the improvement in vowel identification scores obtained with an SCE factor of either 0.5 or 1. The mean improvement obtained by the SCE algorithm for the SMT and the vowel/consonant identification task were 1.9 dB and 5% respectively. We show that an individualized cochlear implant electrical model can

be useful to predict the performance of vowel identification scores.

PD-42

Otolith Organization is Mediated by Otogelin

Kenneth Kramer; Kevin D. Thiessen
Creighton University

Otoconia are small biocrystals that link mechanical forces to the sensory hair cells in the mammalian utricle and saccule, a process essential for sensing linear acceleration and gravity as well as maintaining bodily balance. In fish, structurally similar otoliths mediate both balance and hearing. While research across several vertebrates has identified at least seven homologous proteins that are found in both otoliths and otoconia, little is known about how and when these proteins termed otoconins are organized. The goals of this project were to begin to characterize otoconin organization in the zebrafish otolith, determine when otoconin organization occurs during development, and identify some of the cellular and molecular mediators of otoconin organization. Using antibodies that we generated to the otoconins Otoconin-90 and Starmaker, we found that these otoconins initial colocalize in early otoliths. Remarkably, Otoconin-90 and Starmaker expression gradually changed after attachment of the otolith to early tether cells to become complementary by 30 hours post fertilization. When tether cells were ablated, otoconin expression fails to organize; yet otoconin organization eventually occurred in some embryos when tether cells appeared later in development. We further demonstrated that expression of Otogelin in the otolithic membrane is necessary for otolith attachment and otoconin organization since unattached otoconins aggregate in both *otogelin* morphant and mutant embryos. We conclude that zebrafish otolith organization during early development is mediated by Otogelin expression on the tether cell surface.

PD-43

A Systems Genetics Approach to the Study of Vestibular Disorders

Anthony Myint[1]; Joel Lavinsky[2]; Maria K Ho[3]; Amanda Crow[4]; Sarah Kayne[1]; Sherri Jones[5]; Hooman Allayee[4]; Rick Friedman[1]
[1]University of Southern California, Zilkha Neurogenetic Institute, House Research Institute; [2]University of Southern California, Zilkha Neurogenetic Institute, House Research Institute, Federal University of Rio Grande do Sul,; [3]Florida Atlantic University, University of Southern California, Zilkha Neurogenetic Institute, House Research Institute; [4]University of Southern California; [5]University of Nebraska-Lincoln

Dizziness is one of the most common clinical complaints with approximately 55% of such complaints due to vestibular dysfunction. While there is evidence of a genetic contribution to vestibular disorders in humans, these studies are limited by several key factors including statistical power, reproducibility, environmental factors, and coordinating cohorts and genotyping of many individuals.

We propose a novel strategy utilizing mouse Genome Wide Association Studies (GWAS) to explore the contribution of genetics to vestibular dysfunction, to comprehensively define the specific genetic variants involved, and to functionally validate each variant in a mouse model. We use vestibular evoked potentials (VsEP) as our measure of gravity receptor function. Briefly, the VsEP technique uses subcutaneous electrodes to detect electrical impulses in response to mechanically induced linear head jerks in anesthetized mice, thus providing a quantifiable metric for vestibular function. We have demonstrated strong evidence of phenotypic variation in vestibular function across inbred strains of mice, suggesting a similar genetic influence on balance in mice as seen in humans (Analysis of Variance p value <0.001).

Additionally, we have applied this multi-strain phenotypic data to an association mapping approach (Efficient Mixed Model Analysis; EMMA) in combination with the recently developed Hybrid-Mouse-Diversity-Panel (HMDP) to identify candidate loci involved in vestibular functional variation. A preliminary GWAS using 35 strains revealed a significant peak at the *Dcc* locus of Chr18 (p value 4.58E−6), a receptor classically implicated in the pathogenesis of colon cancer but with an essential role in neuronal development as well. Moreover, the DCC-ligand, NETRIN1, plays a key role in the development of inner ear morphology, thus validating the relevance of this peak in vestibular phenotypes.

We are currently in the process of breeding *Dcc* knockout mice to both characterize vestibular function and to define any morphological or molecular changes along the vestibular pathway. In doing so, we hope to validate the role of *Dcc* and other genetic loci identified in our GWAS in the development, physiology, and dysfunction of the vestibular system. In future experiments, we will continue to add mouse strains to our phenotypic library with the ultimate goal of 100 strains, thus expanding the ability of our GWAS to identify more causal variants.

PD-44

Synaptic Ribbon Architectures of mouse Vestibular Hair Cells: a Field Emission Scanning Electron Microscopy and Conical Tomography Study.

Ivan Lopez[1]; Kristopher Sheets[1]; Felix Schweizer[2]; Larry Hoffman[1]
[1]University of California, Los Angeles; [2]University of California

Introduction

We utilized serial section field emission scanning electron microscopy (FESEM) and conical tilt electron tomography to comprehensively investigate the ultrastructure of synaptic ribbons (SRs) within utricular hair cells. These data provide the foundation for ongoing investigations of synaptic plasticity associated with adaptations to spaceflight.

Methods

The specimens for this study were obtained from male C57Bl/6J mice (aged 16 weeks.) that served as controls for

the Russian BION M1 biosatellite mission (April 19 – May 19, 2013). Temporal bones were rapidly infused with mixed aldehyde fixatives. Utricle specimens were microdissected and processed for transmission electron microscopy as described by Terasaki et al. (Cell 154:285, 2013). Ultrathin (40-50nm) sections were obtained for FESEM; thicker (100-150nm) sections were used for conical tomography (Zampighi et al., PLoS One, 6:e16944, 2011).

Results

FESEM enabled serial reconstruction and visualization of entire presynaptic complexes, and revealed SRs that extended up to 1µm into the hair cell with architectural details not previously described. SRs exhibited plate-like and rod-like morphologies, and were observed individually or in complexes of mixed plate and rod-like morphologies (2–5 SRs). Within multiple SR complexes, proximity to the presynaptic membrane was observed for one or two SRs, implying the existence of mechanisms to shuttle vesicles from "distal" ribbons to the most "proximal" ribbons. Synaptic vesicles numbered several hundred associated with either single or multiple SRs. Close apposition of SRs with the presynaptic membrane was very limited, indicating that the area of the active zone was confined despite the extensive architecture of SR-vesicle complexes. Detailed analyses of SRs and synaptic vesicles was enabled by conical tomography and found mean vesicle diameters of 37.5 ± 3.8 nm, without apparent heterogeneity associated with hair cell type or utricular topography.

Conclusions

Results from this study in normogravic conditions allow us to investigate whether utricular hair cell SRs exhibit architectural adaptations resulting from alteration in the ambient gravitational field (i.e. spaceflight or centrifugation). Other features of synaptic ultrastructure, such as SR-vesicle distances and vesicle densities, are being explored for topographic heterogeneities. These analyses are contributing to a more comprehensive understanding of the biology of SRs and the natural adaptive repertoire reflecting *learning* to novel sensory conditions.

PD-45

Acoustic Activation of Vestibular Organs and the Origin of VEMPs: Theory vs. Experiment

Marta Iversen[1]; **Richard Rabbitt**[1]; Hong Zhu[2]; Wu Zhou[2]
[1]University of Utah; [2]University of Mississippi Medical Center

Background

Mechanical activation of vestibular organs by loud sounds was examined with the goal of understanding the origins of vestibular-evoked myogenic potentials (VEMPs). The primary aim was to determine which specific organs are activated by sound [1, 2], and if the stimulus could be tuned to activate a specific organ.

Methods

A morphologically accurate finite-element model (FEM) of the rat bony labyrinth was constructed based on micro-CT data and used to simulate mechanical activation of vestibular organs by sound via acoustic wave propagation in the endolymph. Bone was modeled as rigid and sound was assumed to travel as compressional waves within the fluid. Broadband (100-7000 Hz) 130 dB SPL clicks were delivered to the oval window to simulate VEMP stimuli shown previously to activate vestibular afferent neurons in this species [1]. Mechanical hair bundle displacement was estimated based on FEM simulations for the saccule, utricle and three semicircular canals. Further, natural modes of acoustic resonance were computed to determine if vestibular organs might be preferentially activated by specific sound frequencies.

Results

Acoustic activation of vestibular organs by sound was predicted by the model to be relatively insensitive to frequency for stimuli below 10kHz. The saccule was most sensitive to stimuli, followed by the utricle, lateral canal, anterior canal and posterior canal – with relative mechanical sensitivities of 1, 0.71, 0.31, 0.25, and 0.19 respectively. Results are consistent with afferent nerve recordings of Zhu et al and Curthoys [1, 2], suggesting the relative levels of mechanical activation underlie differences in afferent nerve sensitivities.

Natural frequencies and modes of acoustic vibration were also computed to determine if there might be any stimuli that would selectively activate a specific vestibular organ. The lowest natural frequency was ~11kHz, and 10 natural frequencies occurred below ~75kHz. Some of the natural modes had peaks near specific vestibular organs, but driving the oval window at these natural frequencies was unsuccessful in feeding energy into the modes. Even if modes could be activated by bone conduction, single unit afferent recordings [3] indicate semicircular canal afferents could not phase lock at these high stimulus frequencies.

Conclusion

Results support the hypothesis that the relative activation of vestibular afferent nerves by VEMP stimuli arises from the labyrinth morphology and relative mechanical activation of the organs by sound. Results held true over a broad range of stimulus frequencies, suggesting specifics of the acoustic waveform are unlikely to significantly alter the relative responses.

References

[1] Zhu H, Tang X, Wei W, Mustain W, Xu Y, Zhou W. Input-output functions of vestibular afferent responses to air-conducted clicks in rats. Journal of the Association for Research in Otolaryngology : JARO 2014; 15:73-86.

[2] Curthoys IS, Vulovic V. Vestibular primary afferent responses to sound and vibration in the guinea pig. Experimental brain research 2011; 210:347-352.

[3] Rabbitt RD, Boyle R, Highstein SM. Mechanical indentation of the vestibular labyrinth and its relationship to head rotation in the toadfish, Opsanus tau. Journal of neurophysiology 1995; 73:2237-2260.

PD-46

Pulsed Infrared Neural Stimulation of Vestibular System Evoked Eye Movements

Weitao Jiang; Suhrud Rajguru
University of Miami

Background

Infrared neural stimulation (INS) has been investigated as an alternative neurostimulation modality that does not require direct contact with neural tissue and has been shown to produce significant post-synaptic afferent responses in the vestibular system. In the present study, we investigated the resultant eye movements evoked by pulsed infrared radiation directed at the vestibular organs in mammals.

Method

Eye movements were measured from sprague-dawley rats weighing between 300-550 g. The animals were anesthetized with intraparetonial injections of ketamine (44 mg/kg) and xylazine (5 mg/kg). The animal was placed in a custom-designed modified Kopf stereotaxic frame that allows delivery of head rotations in pitch, roll, and yaw planes tracked using rotary potentiometers. IR stimulation (1863nm, 100-250pps, 250µs, 360-1100µJ) was delivered to the maculae, which were approached by drilling away the dorsal bony wall of the utricle just caudal and medial to the bony casing of the anterior canal ampulla. Eye movements were measured using a video-based eye tracking system (ISCAN inc, Woburn, MA) and a custom MATLAB program was used for analysis. Histological analysis was performed to confirm the site of stimulation.

Results

We observed significant eye movements evoked by INS. The result shows that vestibular neuroepithelium is highly sensitive to direct IR stimulation. IR at 150-300 µJ produced rotational and torsional eye movements in the ipsilateral eye. Eye movement could not be evoked unless the beam directly irradiated the neuroepithelium. The slow component of the eye movement disappeared when the fiber orientation changed even at the maximum energy level. These results suggest that photoacoustic events or indirect heating did not play a role in the IR response.

Conclusions

Results suggest that stimulation of the vestibular system with infrared pulses invoked eye movements following a delay and the magnitude of the slow varied with the incident radiant energy. Further experiments are needed to characterize the evoked responses along with detailing the efficacy and safety of IR stimulation.

PD-47

Altered PACAP Expression in Vestibular Neurons of Aged Rats

Gay Holstein; Victor L. Friedrich Jr.; Giorgio P. Martinelli
Icahn School of Medicine at Mount Sinai

In a landmark contribution, Kodama et al (2012) reported that *Adycap1* is a marker gene for one subtype of excitatory neuron in the mid rostro-caudal region of the mouse medial vestibular nucleus (MVN). They further suggested that *Adycap1*-positive cells may participate in mediating the vestibulo-sympathetic reflex (VSR). *Adycap1* encodes the neuropeptide pituitary adenylate cyclase-activating polypeptide (PACAP). PACAP is involved in a wide range of physiologic functions, including cardiovascular control and neuroprotection. The goal of the present study was to compare PACAP protein expression in neurons of the caudal vestibular nuclear complex (VNC), where VSR cells reside, in young-adult and aged rats.

The study compared tissue from three young-adult (12 mo old) and four aged (minimum age: 20 mo; average age: 24 mo) male Fisher 344 rats. The rats were anesthetized with isoflurane and then euthanized by cardiac perfusion with mixed aldehydes. The entire VNC of each rat was serial-sectioned and the sections were stored at 4°C prior to use. All experiments included concomitant processing of equal numbers of sections from young-adult and aged rats, and the section sets (1 every 250 µm) were matched for rostro-caudal level. PACAP was localized with an antibody against the full 38 amino acid polypeptide (PACAP38; Peninsula Laboratory), visualized using peroxidase-DAB immunocytochemistry or immunofluorescence staining. Adjacent sections were processed for other markers known to be present in the caudal vestibular nuclei (including glutamate, GABA, and IAA-RP) or with secondary antibody combinations but no prior incubation in primary antibodies, as staining controls.

We observed PACAP-specific immunolabeling throughout the VNC of the young-adult rats. Caudally, labeled neurons included small and medium-sized cells scattered throughout the MVN and inferior vestibular nucleus (IVN). More rostrally, there was a higher density of labeled neurons in MVN, and the stained somata in IVN were of larger diameter. In rostral VNC, PACAP-positive neurons were present in some regions of MVN and the superior vestibular nucleus. In contrast, few PACAP-positive neurons were observed in the VNC of any of the aged rats. In addition, most of those neurons appeared to be in the process of degeneration. We conclude that PACAP protein is substantially diminished in the aged rat VNC. Given the neuroprotective function ascribed to PACAP, we speculate that PACAP reduction in the aged rat VNC contributes to neurodegeneration of a specific vestibular cell subpopulation.

PD-48

Comparison of the Vestibulosympathetic Reflex During Dynamic and Static Head-down Rotations

Chester Ray
Penn State University, College of Medicine, Hershey

We have previously reported that static head-down rotation elicits increases in muscle sympathetic nerve activity (MSNA) via activation of the vestibulosympathetic reflex in humans. The purpose of the current study was to compare MSNA responses to dynamic and static head-down pitch rotation. In *Study 1*, 40 subjects performed head-down rotation in the prone position after which the head then remained stationary. The head began in the erect, maximally extended posi-

tion and was passively rotated until the neck was maximally flexed. During head rotation MSNA, expressed as burst frequency and total activity (sum of burst amplitude), increased by 2 ± 0.3 bursts/10 s and 98 ± 13% (P < 0.001), respectively, as compared to baseline. This increase was greater than the observed increase above baseline during the following 60 s of static head-down rotation (Δ 1 ± 0.1 bursts/10 s and Δ 52 ± 6%; P < 0.001). In *Study 2*, 14 subjects performed repetitive dynamic pitch rotation in 10 s cycles for 3 min. MSNA was 2 ± 0.5 bursts/10 s (126 ± 47% total activity) greater when the head was rotated down than up. There was no difference in MSNA when dynamic head rotation was performed in the lateral decubitus position. These results suggest that dynamic pitch rotation in the horizontal axis elicits greater MSNA than static pitch rotation and that the otolith organs and not the semicircular canals appear to mediate these differences. Furthermore, this finding suggests that the vestibulosympathetic reflex does not become desensitized to repeated head movements.

PD-49

Coordinates of vestibular heading perception: Effects of eye and head position.

Benjamin Crane
University of Rochester

While ambulating, a voluntary change in head orientation will change the orientation of the labyrinth relative to the motion stimulus but such changes are generally not disorienting. This finding suggests vestibular perception may occur in body coordinates despite the labyrinth being fixed in the head although this has not been previously been examined. Previously published work on vestibular heading perception has demonstrated that the sway component of headings is often overestimated relative to surge (straight ahead) component, and this offset can be explained by a population vector decoder model in which the majority of units are tuned to be most sensitive to sway (right-left) motion. The current experiments build on this previous work by examining the effect of head and gaze (eye-in-space) position in the horizontal plane (yaw) on human vestibular heading estimation. During each stimulus presentation subjects were translated 15 cm over 2 s then asked to orient a dial toward the direction of perceived motion. During each testing condition, 72 heading directions (360° in 5° increments) were presented in random order. In some trial blocks eye and head positions were varied so that either could be ±30° off center at the start of the trial. Several conditions were tested: head centered/gaze centered (HCGC), head centered/gaze ±30° (HCGV), head ±30°, gaze centered (HVGC), and head and gaze ±30 (HVGV). In conditions were gaze or head position was varied, the ±30° directions were randomly interleaved within a trial blocks to minimize effects of adaptation. Responses were modeled using a simple population vector decoder model with 2 free parameters: the ratio of sway to surge sensitivity and angular offset. Seven healthy subjects (mean age 36, range 20-67) completed all test conditions. The median ratio of sway to surge sensitivity was 1.2 (range 0.86 to 1.5) indicating most (5 of 7) subjects had more sensitivity to detect the sway component of heading that the surge component. Neither gaze or head direction induced any significant angular offset for any of the conditions in which head or gaze direction were varied (p > 0.1, for all) and the offset was usually close to straight head (mean 1.1° right , range -3.6° to 4.6°). These results indicate that vestibular heading perception is unaffected by head or gaze position. In contrast visual headings were strongly biased based on gaze position consistent with retina based coordinates being used for visual heading perception.

PD-50

Brief Restraint Causes Stress and Modulates Neural Responses to Sound in Mouse Amygdala

Jasmine Grimsley[1]; Emily Hazlett[3]; Neil Vallabh[2]; Saloni Sheth[2]; Jeffrey Wenstrup[2]
[1]Northeast Ohio Medical University (NEOMED); [2]NEOMED; [3]NEOMED, Kent State University

Background

There are three main conditions in which neural responses to sound are recorded; anesthetized, awake restrained, or awake free-moving. Although it is well established that long-lasting and repeated restraint (8 hours per day for 21 days) causes stress in mice, most neural recordings from awake mice are conducted under more limited restraint (2-3 hours over multiple days). We hypothesized that even brief, 2-hour periods of restraint over 3 days would induce persistent stress in mice and that neural responses to sound in the amygdala would differ between free moving and restrained mice.

Methods

To assess stress behaviorally, we used a light/dark box, a marble bury test, and rerecorded vocalizations. A total of 16 adult male CBA/CaJ mice were used; half of the mice were restrained for 2 hours on 3 consecutive days, while the other half served as controls. Tests were conducted prior to and following the restraint; vocalizations were recording prior to and during restraint. To assess effects on the amygdala auditory responses, we recorded noise-evoked local field potentials (LFPs) from the basolateral amygdala of 9 adult male mice. Auditory responses were obtained from free moving mice, followed immediately by recording from the same animals during restraint. Signals were transmitted wirelessly from custom multi-electrode implants using a wireless headstage.

Results

Mice spent more time in the dark after undergoing restraint (p = 0.002), indicating increased stress. No change was found in the time control animals spent in dark (p = 0.792). An independent samples t-test confirmed that restrained mice buried more marbles than isolated mice (t (15) = 3.809, p=0.002), indicating increased stress. The mean dominant frequencies of animals ultrasonic vocalizations emitted during restraint were substantially higher than those emitted during mating encounters. Typically the magnitude of the sound-evoked LFP was greater during restraint compared to when the animal was free-moving (6/9 mice, p < 0.001). The recording condition could be determined by computations on the single trial

LFP waveform for an average of 72% of trials (SD = 6, range 66-84%), indicating that restraint caused consistent changes in the neural responses to sound.

Conclusion

Even brief restraint generated long-lasting stress in mice. Neural responses to sound in the amygdala are increased after exposure to restraint comparable to that commonly used in auditory neurophysiology. Since the amygdala connects to auditory centers, this effect of restraint may extend to neural representations of sound in the auditory system.

PD-51

Neural correlates of auditory-tactile integration in meter perception: an EEG study

Juan Huang[1]; Tianxu Wu[2]; Steven Hsiao[1]; Xiaoqin Wang[1]
[1]Johns Hopkins University; [2]Tsinghua University

Previously we reported that auditory and tactile inputs are seamlessly integrated to form the percept of meter in human subjects (Huang, et al. 2012). In this study, we examined the neural correlates of auditory and tactile integration in meter perception using Electroencephalography (EEG) recording. We recorded event related potentials (ERP) from 12 human subjects while they were presented with a unimodal auditory, unimodal tactile, or bimodal sequences. Auditory stimulation was presented through headphones, and tactile stimulation was presented through a tactile vibration stimulator that was placed with subject's left index finger tip. Subjects were also asked to detect whether the last note of some of the sequences (5%) showed changes in amplitude and frequency to assess the attention state of the subject. In the bimodal sequences the auditory or tactile notes signaling whether the meter was duple or triple meter structure were modulated. We report that the EEG signals corresponding to missing notes are similar to those induced by both the metrically important and unimportant notes. The results demonstrate that ERP signals can be induced without actual sensory input (either, auditory or tactile) as long as the "virtual" notes are embedded in a sequence with a valid meter structure. Further more, the EEG components corresponding to bimodal sequences are determined by the modality of the important notes. When the important notes are auditory, the overall EEG waveforms are similar to those induced by unimodal auditory sequences; whereas the EEG waveforms corresponding to bimodal sequences with tactile inputs as the important notes are similar to those induced by the unimodal tactile sequences. The latencies and tonotopical maps of the EEG signals produced by unimodal and bimodal sequences are also modality dependent. Similarities are observed between the signals observed during the unimodal auditory and bimodal conditions when the important notes are carried by the auditory condition, and similarly between unimodal tactile and the bimodal condition with tactile inputs are carrying the important notes. These results suggest that there are neural correlates of auditory and tactile integration of meter perception, which are closely linked to the cognitive aspects of perception and less to the sensory input. The data further suggests that the brain treats inputs from different sensory modalities as uniformed events that are independent of physical properties when the inputs form a regular temporal pattern.

PD-52

Neuronal Response Properties in Mouse Primary Auditory Cortex Change with Anaesthesia

Bettina Joachimsthaler[1]; Marina A. Egorova[2]; **Simone Kurt**[3]
[1]Hertie Institute for Clinical Brain Research; [2]I.M. Sechenov Institute of Evolutionary Physiology and Biochemistry Russian Academy of Sciences, St.Petersburg, Russia; [3]Cluster of Excellence "Hearing4all", Institute of Audioneurotechnology and Hannover Medical School, Department of Experimental Otology, ENT Clinics, Hannover, Germany

The majority of studies that concentrate on questions concerning the neuronal processing of acoustic stimuli in the central auditory system, are conducted on anesthetized animals. It is broadly known, however, that many response properties of neurons can be influenced or even dramatically changed by anesthetic agents.

In this present study we examined the influence of a ketamine/xylazine anesthesia on the neuronal responses of single- and multi-units from the cortical layers III – IV (200- 400 µm depth) in the tonotopically organized primary auditory fields AI and AAF of the house mouse (*Mus musculus*). We presented pure tones (PT) and 100% sinusoidally amplitude modulated (AM) tones to eight weeks old female mice. In line with previous studies on different species, we observed that neurons in both fields of anesthetized animals showed longer response latencies to both PT and AM tone stimulation compared to those in unanaestetized animals. In addition, neurons in anesthetized animals had a considerably lower spontaneous activity and a reduced evoked rate at their best frequency. The effect of the anesthesia was most obvious when comparing the capability of the neurons to synchronize their response to the time structure of the envelope of the AM tones. The neurons of anesthetized animals mostly showed no phase-locked discharge patterns at all or were only able to phase-lock up to modulation frequencies of below or equal 18 Hz. Responses to AM tone stimulation recorded from unanesthetized animals showed phase-locking up to modulation frequencies of about 130 Hz. No significant differences with regard to the effects of anesthesia on neuronal responses were observed between fields AI and AAF. This study provides further evidence that the anesthetic state changes the neuronal responses in the primary auditory cortex in a significant way. Thus neuronal data from anesthetized animals may not provide a relevant basis for studying cortical mechanisms of auditory perception and recognition.

PD-53

Short-term Adaptation of Auditory Cortex Neurons to Changes in the Variance Distribution of Harmonicity Cues in Harmonic Complex Sequences

Astrid Klinge-Strahl; Benjamin Willmore; Andrew King
Oxford University

Neurons at higher levels of the auditory system respond to stimuli in a context-dependent manner. For example, if neurons of the inferior colliculus or auditory cortex were presented with stimuli with varying mean or variance of the level, interaural-level-difference or modulation-depth distribution, they adapted their responses on a short-term basis (e.g. by rapidly changing their firing rate; Dahmen et al. 2010, Rabinowitz et al. 2011, Kvale and Schreiner 2004).

Although harmonicity cues are one of the more important acoustic features in the natural acoustic environment it has not been evaluated whether neurons at higher levels of the auditory system also adapt their responses to varying degrees of harmonicity in harmonic complex stimuli. We presented sequences of harmonic dynamic random chords (hDRCs) to auditory cortex neurons in ferrets. The hDRCs were comprised of a stack of frequencies that were integer multiples of a fundamental frequency. Within a sequence each harmonic component of each hDRC was then multiplied with a random frequency jitter taken from one of two different distributions of variances to create two degrees of harmonicity. The amount of frequency jitter was switched after an adaptation period from low jitter to high jitter or vice versa. To investigate how fast neurons adapt to sudden changes in the variance distribution of harmonicity values we presented the vowels /u/ and /ɛ/ at different temporal positions after a switch in variance distribution of the background hDRC. Based on previous findings one might expect that the neurons would adjust their responses to the current background in order to be able to respond adequately to target sounds. However, it is also possible that neuronal responses are invariant to the different stimulus statistics of the harmonic complex stimuli but show different responses to the vowel in the various background conditions.

We demonstrate that the spike rate in response to the background hDRC sequences shows a transient change immediately after a change in stimulus statistics. Furthermore, the vowel response to either /u/ or /ɛ/ is altered depending on the background they were presented in and depending on the temporal position of the vowel after the switch in stimulus statistics. However, these spike rate changes in response to the vowel appear to be non-systematic. About half of the neurons responded with either an increase or a decrease in the spike rate after a switch in stimulus statistics compared to a no-switch control condition.

PD-54

Left-Ear Advantage in a Monaural Auditory Lexical-Emotional Stroop Task

Liat Kishon-Rabin; Libat Moriya; Osnat Segal
Tel-Aviv University

Background

Dichotic listening of lexical-emotional stroop has been used to assess independently laterality and congruency effects as well as the interaction between them. These studies found a right-ear (RE) advantage for words and a left-ear (LE) advantage for emotion targets. No study, however, investigated whether the ability to selectively attend to the word or the emotional tone is dependent on the ear of presentation when the stimuli are presented monaurally.

Methods

The study included 20 young adults (mean age=24.6 years old).Test stimuli consisted of 80 different words judged as having a sad or happy meaning. Forty of these words were produced with the appropriate (congruent) sad/happy prosody and 40 words were produced with inappropriate (incongruent) happy/sad prosody. Baseline performance of lexical and prosodic emotion recognition was measured with neutral prosody or neutral meaning. Listeners were instructed to either ignore the lexical content and decide whether the tone of voice was happy or sad, or, ignore the prosody and make a lexical decision. For all participants this paradigm was presented monaurally to the right and left ears. Order of presentation was counterbalanced. Performance measures were % correct and reaction time (RT).

Results showed a general congruency effect on both measures. Performance of lexical decisions was better in the congruent condition compared to the incongruent one regardless of ear of presentation (no ear effect). However, RT was shorter for the LE for both congruent and incongruent conditions (congruency effect was similar between ears). For the prosody decisions, a similar congruency effect was found for the two ears in accuracy performance but a larger effect was found in the LE owing to shorter RT in the congruent condition in that ear.

Conclusions

The findings of a LE advantage in the prosodic condition is in keeping with what is known about right hemispheric specialization. The unexpected LE advantage for lexical decisions (shorter RT) is further strengthened by a comparison with another group of adults who performed this task binaurally. RT of the LE group was similar to the binaurals on both tasks but longer in the RE group suggesting that the LE contributed to performance in the binaural listening group. Possible explanations include the influence of the response task on performance and the linguistic-cognitive processing involved in each task. This information has implications for understanding speech processing and selective attention in individuals with hearing in one ear.

PD-55

Passive and Attentive Listening: Transient Cortical Evoked Potentials and Stimulus Induced Oscillations

Andrew Dimitrijevic[1]; Ji-Hye Han[2]
[1]Cincinnati Children's Hospital Medical Center; University of Cincinnati; [2]Cincinnati Children's Hospital Medical Center

Introduction

In this study we examined both transient cortical evoked potentials (i.e., N1/P2) and changes in cortical oscillations in an Acoustic Change Complex (ACC) paradigm. Although there is a rich literature exploring the effects of attention on N1/P2 responses, there has been very little published work examining changes in ongoing EEG oscillations in response to an acoustic stimulus. N1/P2 potentials reflect stimulus attributes while induced cortical oscillations are thought to reflect activation and inhibition of cortical networks and are likely related to "higher order" processing compared to transient evoked potentials.

Methods

Auditory cortical potentials were recorded from 64 scalp electrodes during passive and attentive listening in normal hearing adults. The stimulus consisted of occasional changes of amplitude modulated (AM) white noise in otherwise continuous white noise. The AM lasted 1 sec and varied in both AM rate (4, 40, and 300 Hz) and in AM depth (100, 50 and 25%). In the passive condition, participants watched a closed-captioned movie of their choice while sounds were played in the background. In the attend condition, participants were instructed to press a button when any change was detected in the continuous noise.

Results

AM change stimuli elicited robust N1/P2 responses in both active and attend conditions. N1/P2 responses to both 4 and 40 Hz AM change stimuli were larger than the 300 Hz AM stimulus and resembled the psychoacoustic temporal modulation transfer function. Responses were smaller and later when the AM depth was decreased, or less salient. As expected, N1/P2 responses in the attend condition were larger and delayed compared to the passive listening condition. Stimulus evoked low frequency oscillations (4 to 8 Hz) were apparent in the 120 to 150 ms range representing the N1/P2 response. Alpha desynchronization (7 to 9 Hz) as measured by percent decrease compared to prestimulus baseline was apparent from 500 ms to 1 sec after the AM change in the 100% AM passive and active conditions. With smaller degrees of AM change less alpha desynchronization was apparent in the passive condition whereas in the attend condition, alpha desynchronization was still present. Button presses were associated with beta desynchronization and synchronization (15 to 30 Hz).

Summary

This study demonstrated that alpha desynchronization can be measured during an ACC paradigm. Greater alpha desynchronization was observed during attentive listening compared to passive listening likely indexing a higher degree of neuronal excitability.

PD-56

Autocorrelation Analyses of Magnetoencephalographic Spontaneous Oscillation in Relation to Subjective Impression of Sounds

Seiji Nakagawa[1]; Yoshiharu Soeta[1]; Shunsuke Ishimitsu[2]
[1]National Institute of Advanced Industrial Science and Technology (AIST); [2]Hiroshima City University

Relationships between subjective impression of sounds and the alpha waves, spontaneous cortical activity between 8-13 Hz and thought to play an important and active role in cognitive processing, were investigated.

First, effects of two parameters of sound fields, delay time of a single reflection in reference to the direct sound ($\Delta t1$) and interaural cross-correlation (IACC), having been reported to influence subjective preference, on the alpha waves were investigated. A short speech "piano", which had a 0.35-s duration was used as source sounds. The $\Delta t1$ and IACC were varied at five and three levels, respectively. First, the scale values of the subjective preference of each subject were obtained by the paired-comparison tests. Next, MEG measurements were carried out during combinations of a reference stimulus and test stimuli were presented. The alpha wave evaluated quantitatively using an auto-correlation function (ACF). The results showed that subjective preference for each individual and the effective duration of the ACF, τ_e, representing repetitive features within the signal itself, are linearly related. Also, the maximum value of cross-correlation function (CCF) among channels, $|\phi(\tau)|_{max}$, became larger as the IACC decrease.

Next, the ACF analysis of the alpha waves were also applied to evaluate annoyance of noises. Bandpass noises with a centre frequency of 1000 Hz were used as source signals. To control auditory impression of the noise, the bandwidth of the source signal was varied at 5 levels. The results show that the τ_e became shorter and $|\phi(\tau)|_{max}$ became smaller for an annoying stimulus.

Further, longer and meaningful sounds perceived in our daily life were investigated. Accelerating car engine sounds, which have positive impression like "sportiness" and three musical sounds selected from different genres (classical music, pop song, and rock music) were investigated. No systematic change common to all subjects was observed in the subjective preference test, however, the τ_e became longer in some brain areas for the preferred stimuli of each subject.

The longer τ_e indicates that the brain becomes stable with preferred stimuli and larger $|\phi(\tau)|_{max}$ indicates that wider area of brain synchronized. The results suggest that the brain becomes stable temporally and spatially with preferred auditory stimuli and that the τ_e or $|\phi(\tau)|_{max}$ can be objective indexes of auditory impressions at least in some kinds of sounds. Since clearer results were obtained for short speech

and classical music, it is speculated that the τe reflects the subjective preference associated with “calming” or “healing”.

PD-57

Mechanisms of State Dependent Cortical and Sub-Cortical Auditory Responses

Matthew McGinley[1]; Stephen David[2]; David McCormick[1]
[1]Yale University; [2]Oregon Health and Science University

To assess the state dependence of auditory responses along the auditory pathway, we conducted electrophysiological recordings in the primary auditory cortex (A1), medial geniculate nucleus (MGN) or inferior colliculus (IC) from head-fixed mice on a cylindrical treadmill. Mice were passively exposed to complex noise stimuli (temporally orthogonal ripple combinations; TORCs) or tone pips or engaged in a psychometric discrimination task requiring the mice to detect tones embedded in TORCs while they were free to walk or stand still on the treadmill. The state of the animal was assessed using pupillometry, 16-channel laminar recording of the rhythms in the hippocampus, locomotor activity, and task performance measures.

We find that the diameter of the pupil is highly anti-correlated (~0.8 coherence below ~1 Hz, 180 deg. phase) with fast ripples (100-200 Hz) in the hippocampus and that walking only occurs with large pupil diameter (>~80% max), indicating that pupil diameter is an excellent measure of the state of the animal. In whole-cell recordings in the cortex, membrane potential (Vm) fluctuations were closely related to pupil diameter with a U-shaped relationship. When the pupil was smallest, Vms were depolarized at slow frequencies (2-10 Hz) and extracellular spontaneous unit activity (UA) was high; with intermediate pupil Vms were hyperpolarized and UA was low; and with large pupil (with or without walking) Vms were again depolarized at high frequencies (50-100 Hz) and spontaneous UA was again high. Sound-evoked responses showed the opposite trend (inverted-U). Gain and reliability was largest for intermediate pupil diameters, and reduced with large pupil with or without walking. Incorporating pupil diameter led to an ~50% increase in the ability to explain sound-evoked firing rates, whereas locomotion was about half as affective and its variance was encompassed by the variance explained by pupil.

In the thalamus, sound-evoked UA dependent strongly on locomotion, and had an inverted-U dependence on pupil. However, spontaneous firing rates increased monotonically with pupil diameter and locomotion had a large pupil-independent effect. Overall, locomotion explained more variance than pupil (~50% vs. ~35%). Locomotion also suppressed sensory responses in the IC and increased spontaneous UA. The suppressive effect in IC was not eliminated by bilateral muscimol application to cortex and spontaneous activity in IC persisted after deafening the animal. Taken together, our results suggest that a strong locomotion-related signal enters the auditory system at or below the IC, whereas pupil-indexed arousal has effects along the auditory pathway, but particularly in cortex.

SYM-42

The Encoding of Speech Features in the Human Auditory Cortex

Edward Chang
UC San Francisco

Communication systems generally rely on upon defined organizational schemes for signal generation and sensing. In humans, the production and perception of speech is processed by highly specialized neuroanatomical areas and processes. We have recently identified

important phonetic-level features for vocal tract control during articulation in the speech motor cortex, and for speech sounds in the higher order non primary auditory cortex. I will discuss important similarities and differences in these representational systems with respect to feature organization and dynamics. I will also present related work on auditory-vocal (sensorimotor) integration and transformation in speech.

SYM-43

Cortical Processing of Chinese Phonemes and Tones

Bo Hong
Tsinghua University

A finite set of phonetic units is used in human speech, but how our brain recognizes these units from speech stream is still largely unknown. The revealing of this neural mechanism may lead to the development of new types of speech brain computer interfaces and computer speech recognition systems. In this study, we used electrocorticography (ECoG) signal from human cortex to decode Chinese phonetic units during the perception of continuous speech. By exploring the wavelet time-frequency features, we identified ECoG electrodes that have selective response to specific Chinese phonemes. Gamma and high-gamma power of these electrodes were further combined to separate sets of phonemes into clusters. The clustered organization largely coincided with phonological categories defined by discriminative features, similar as that has been found in English (Mesgarani et al, 2014). These findings were incorporated into a decoding framework of Chinese phonemes clusters and achieved consistent accuracies higher than chance level. Besides phonetic units, in tonal languages, like Chinese, lexical tone also serves as a key feature to provide contrast in word meaning. Behavior studies suggest that Mandarin Chinese tone is categorically perceived (Wang 1976; Xu et al. 2006). However, the neural mechanism underlying Mandarin tone perception is still poorly understood. In this study, an Oddball paradigm was designed by selecting two standard-deviant stimulus pairs with same physical distance but different category labels, among the synthesized tones with continuously varying pitch contours. Using ECoG recording over human auditory cortex, high temporal and spatial resolution cortical neural signals were used for the first time to investigate the cortical processing of lexical tone. Here, we found different neural responses to the two standard-deviant tone pairs, and the difference increased from low to high level along the hierarchy of human auditory cortex. In the two dimensional neural

space, cross-category neural distance of lexical tones is selectively amplified on those high level electrodes. These findings support a hierarchical and categorical model of Mandarin tone perception. Although the Chinese phonemes and tones are likely processed in the same vicinity of superior temporal gyrus (STG) and superior temporal sulcus (STS), it is still a challenge to elucidate how does the speech cortex integrate the phonetic units with lexical tone feature, to give rise to a meaning for each Chinese word. Both the temporal structure and spatial organization of this integration is to be revealed in the future study. (This work is supported by National Science Foundation of China # 61473169)

SYM-45

Invasive Studies of Human Auditory Cortex Functional Organization

Matthew Howard; Kirill Nourski
The University of Iowa

Auditory cognition – "making sense of sounds" – involves hierarchical processing distributed over multiple auditory and auditory-related cortical areas. The roles of different cortical regions in auditory cognition can be addressed with direct intracranial recordings. Using a range of experimental paradigms (target detection, stimulus identification, semantic categorization), we examined neural activity simultaneously recorded from the auditory cortex including Heschl's gyrus (HG), posterolateral superior temporal gyrus (PLST), as well as prefrontal cortex.

Subjects were patients undergoing invasive monitoring for medically refractory epilepsy. Stimuli were speech sounds (clear and spectrally degraded nonsense syllables, words and time-compressed sentences) and complex tones. Neural activity was recorded using implanted depth and subdural grid electrodes and analyzed as averaged evoked potentials (AEPs) and high gamma (70-150 Hz) event-related band power.

Analysis of neural activity demonstrates differential effects of task demands across auditory and auditory-related cortical areas. Activity in posteromedial HG (auditory core cortex) represents stimulus acoustic features on multiple time scales, yet appears minimally modulated by the task. Parsing of temporal acoustic features by evoked cortical activity at this level may be a prerequisite for subsequent phonetic and semantic processing. In contrast, activity within non-core cortex on PLST maintains representation of stimulus acoustic features but is strongly modulated by the level of arousal and task demands. Results from studies using speech stimuli support the role of this area as an intermediate processing stage that subserves transformation of acoustic inputs into phonetic representations. Prefrontal cortex exhibits the most complex activation patterns. Responses here precede the subject's behavioral response, are often selective for target stimuli, and reflect performance accuracy, effort and subject's experience with the task. At all processing levels, information carried by relatively low-frequency evoked components of the neural response (as captured by the AEP) is distinct from and complementary to that conveyed by high gamma activity. Response patterns observed in human auditory and auditory-related cortex confirm and expand relevant animal studies. The observed tiered effects of task demands have translational relevance for enhanced understanding of normal speech processing and its impairments consequential to hearing loss, aging, developmental language disorders and acquired neurological conditions.

SYM-46

Cortical Auditory Response Dynamics: Variability and Adaptation

Dana Boatman
Johns Hopkins School of Medicine

Background

Cortical sensory responses decrease with stimulus repetition, a dynamic response property known as adaptation. Although animal and human studies have demonstrated adaptation of evoked responses to pure tones in primary auditory cortex, it is not known whether adaptation occurs for cortical high frequency (>60 Hz) responses to complex sounds, including speech, processed in higher-level auditory areas of the human brain.

Methods

We recorded electrocorticographic (ECoG) activity from subdural electrode arrays implanted over the lateral temporal lobe (auditory association cortex) of normal-hearing adult epilepsy patients. Auditory stimuli ranged in acoustic complexity from simple tones to speech and were presented in oddball (passive, active) and control paradigms. Time-domain averaged evoked responses were computed for comparison and to identify auditory sites. Time-frequency analysis was performed to measure trial-averaged and single-trial changes in event-related high gamma (HG; 70-150 Hz) power. We measured variability of HG power changes based on test-retest. Connectivity patterns were derived to estimate stimulus and task effects on effective (causal) connectivity among recording sites.

Results

We observed strong adaptation of HG power for simple and complex sounds in responses recorded from left and right auditory association cortex. Single-trial analysis revealed HG response adaptation on multiple timescales (rapid, slow). Test-retest showed robust and reproducible stimulus- and task-specific effects on the time course and connectivity patterns of auditory HG power adaptation.

Conclusions

These results demonstrate that event-related HG responses recorded from human auditory association cortex are highly sensitive to the probabilities of complex auditory events.

Funding

Supported by NIDCD Grant K24-DC010028 and US Army Research Office Grant W911NF-14-1-0491.

PD-58

Pharmacological Reprogramming of Lateral Line Supporting Cells to a Migratory Mesenchyme Capable of Reconstituting Neuromasts and Generating New Hair Cells

Jason Meyers
Colgate University

Introduction

The lateral line is a collection of small sensory organs called neuromasts that run along the body of fish and amphibians. The neuromasts contain hair cells and supporting cells homologous to those in the inner ear, and their accessibility and visibility makes them an attractive model for studying hair cell differentiation and regeneration. The initial deposition of neuromasts occurs from a primordium that begins near the ear and migrates down to the tail between 24-48 hours post fertilization. Cellular proliferation and the deposition of clusters of cells as the primordium migrates are coordinated by Wnt and FGF signaling, and these deposited cells differentiate into hair cells and supporting cells. Wnt signaling is important in controlling proliferation of cells in the neuromasts during initial differentiation, ongoing-growth, and regeneration following lesion. Given the interaction between Wnt and FGF signaling in initial patterning of the primordium and protoneuromast deposition, we have examined whether FGF signaling interacts with the Wnt pathway to coordinate later stages of neuromast development, growth and regeneration.

Methods

We have used pharmacological manipulation of Wnt and FGF signaling in larval zebrafish with time-lapse confocal microscopy, immunocytochemistry, and *in situ* hybridization to examine the fate of progenitor cells within deposited lateral line neuromasts.

Results

Simultaneous activation of Wnt signaling and inhibition of FGF signaling caused supporting cells within the neuromast to revert to a highly proliferative migratory mesenchymal state. The supporting cells lost n-cadherin expression, and the neuromasts lost their compact morphology as the cells migrated bidirectionally along the lateral line. During the dissolution of the neuromasts, hair cells were extruded from the epithelium, and the supporting cells began re-expressing genes associated with the migratory primordium. Notably, upon washout of the drugs, the cells reconstituted neuromasts along the lateral line, and produced new cohorts of hair cells.

Conclusions

These data suggest that Wnt and FGF signaling work together in later stages of neuromast differentiation to maintain the epithelial organization of the neuromast and the balance between proliferation and differentiation. It also indicates that supporting cells within the deposited neuromast can be reprogrammed to an earlier migratory mesenchymal state by manipulating these signals. These reverted cells can subsequently return to an epithelial state, reform neuromasts via a novel mechanism, and initiate hair cell differentiation. Together these results present a new model for studying hair cell and supporting cell differentiation, which has potential implications for therapeutic strategies in humans.

PD-59

Inhibition of Histone Deacetylase Activity Can Modify Pillar Cell Fate in the Perinatal Mouse Organ of Corti

Yassan Abdolazimi; Neil Segil
University of Southern California

Background

Pillar cells, the supporting cells that lie between the inner and outer hair cells are characterized by the expression of transcriptional repressor Hey2. Previous studies have shown the importance of Hey2 for the maintenance of pillar cell fate; downregulation of Hey2 in pillar cells leads to upregulation of hair-cell differentiation factor Atoh1 and transdifferentiation of these cells to hair cell-like cells. Although the inhibitory effect of Hey2 on Atoh1 has been shown, the molecular mechanisms on which this inhibition is based have not been determined. Transcriptional repressors such as the bHLH DNA binding protein Hey2 recruit corepressor proteins including histone deacetylases (HDACs) to form functional repressor complexes. Previous reports revealed that Hey2 relies on both NAD^+-dependent and independent classes of HDACs to inhibit its target genes. In the current study we investigated the mechanism of Hey2 repression of Atoh1 in pillar cells, as well as the role of histone deacetylases in this process.

Methods

Immunohistochemistry, organ culture, FACS purification of supporting cells, in vitro transfection, co-immunoprecipitation and quantitative-PCR were used to investigate the role of Hey2 and HDAC activity in regulation of Atoh1 expression.

Results

Pharmacological inhibition of NAD^+-dependent HDACs and NAD^+-independent HDACs in organotypic cultures led to up-regulation of Atoh1 in pillar cells. The Atoh1-expressing pillar cells gradually lost the expression of supporting cell marker $p75^{NGFR}$ and expressed hair cell marker Myosin VI, indicating their transdifferentiation to hair cell-like cells. We are investigating the identity of the relevant HDACs involved in maintaining pillar cell fate, and characterizing the changes in chromatin that accompany pillar cell transdifferentiation

Conclusion

Our results demonstrate the importance of histone deacetylase activity for maintaining pillar cell fate and suggest that a combination of both NAD^+-dependent and -independent histone deacetylases mediate repression of Atoh1 in pillar cells.

PD-60

Changes in Phosphorylation Dependent Histone Modifications Suggest Dynamic Epigenetic Regulation During the Postnatal Maturation of the Mouse Cochlea.

Bradley Walters; Grace Bailey; Jian Zuo
St. Jude Children's Research Hospital

Epigenetic mechanisms cause changes in gene expression without altering DNA sequence. These include ATP-dependent chromatin remodeling, DNA methylation and acetylation, and histone modifications, most notably, the methylation, acetylation, and phosphorylation of the H1, H2A, H2B, H3 and H4 histone proteins. These epigenetic changes heavily influence gene activation or silencing, and therefore play critical roles in cell fate, proliferation, survival, metabolism, and signaling. Indeed, modifications to the protruding N-terminal tails of histones by the covalent addition of acetyl, methyl, or phosphate groups are particularly important in regulating gene expression. While much attention has focused on correlating histone acetylation and methylation with changes in gene expression, histone phosphorylation may be of equal or even greater importance in epigenetic processes. For example, histone phosphorylation plays key roles in the cellular response to DNA damage, in pro- and anti-apoptotic pathways, in transcriptional regulation, and in chromatin remodeling via the regulation of histone interacting proteins and even the methylation and acetylation of the histones themselves. Despite this, little is known about histone phosphorylation in the mammalian cochlea. Given the important roles played by histone phosphorylation in regulating several key cellular processes, we hypothesized that there may be temporal and cell type specific changes in the phosphorylated state of various histone residues during the maturation of the cochlea. To test this, we examined several specific phosphorylation events on histones H1, H2B, H3, and H4 in the cochleae of FVB mice. As a result, we found that, between postnatal day (P) 0 and P30, an increasing number of cells exhibited the H4phS1 modification, while a decreasing number of cells exhibited H2BphS32, H3phS28, H3phT6, H4phS1, and H4phS47 modifications. Over a similar timeline (P0-P30), we observed no change in the numbers of cells that exhibited the H3phT11 modification. Together these data suggest that the spatiotemporal patterns of several phospho-histone variants are dynamic during the postnatal maturation of the cochlea and that correlating these changes with age or across cell type may provide insight into the functions of these modifications as they pertain to gene expression, cellular processes, and the overall maturation of the cochlea.

PD-61

Expression and Misexpression of the miR-183 Family in the Developing Hearing Organ of the Chicken

Kaidi Zhang; Michelle Stoller; Donna Fekete
Purdue University

Introduction

The miR-183 family consists of 3 related microRNAs (miR-183, miR-96, and miR-182) that are required for the proper maturation of primary sensory cells in both the inner ear and the retina in mammals.

Methods

The developmental expression of these genes was observed in the embryonic chicken inner ear by in situ hybridization. We investigated their functional role in the developing basilar papilla (BP) by overexpressing a GFP-miR-183 family bifunctional plasmid using Tol2 transposase-mediated stable transfection. Plasmids were electroporated into the right otocyst on E2-E3. Either the left ears, neighboring untransfected cells, or pGFP-transfected cells were used as controls, depending upon the analysis. The BPs were evaluated 11-14 days after plasmid electroporation using immunofluorescence and confocal microscopy to detect hair cells, supporting cells and/or ribbon synapses.

Results

The three microRNAs are very similar in their spatiotemporal expression patterns. At E7, miRNA expression in vestibular hair cells is obvious, while the undifferentiated BP shows only a weak radial gradient of miR-182 that is highest on the superior (neural) side. As development proceeds, expression is more robust in the maturing hair cells of both auditory and vestibular organs. At E12-E18, the higher packing density of tall hair cells located on the superior BP suggests the persistence of a radial gradient from surface views, but this is not confirmed at the cellular level in sectioned material. Instead, a longitudinal gradient is observed: levels are higher in the apex compared to the base.

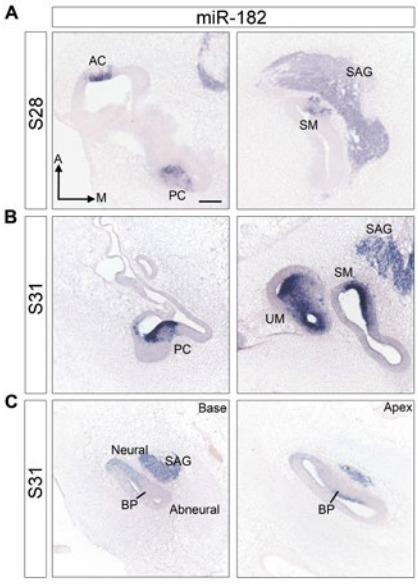

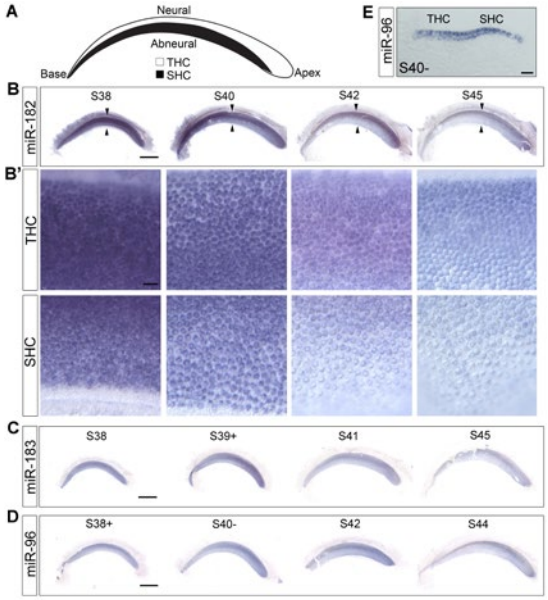

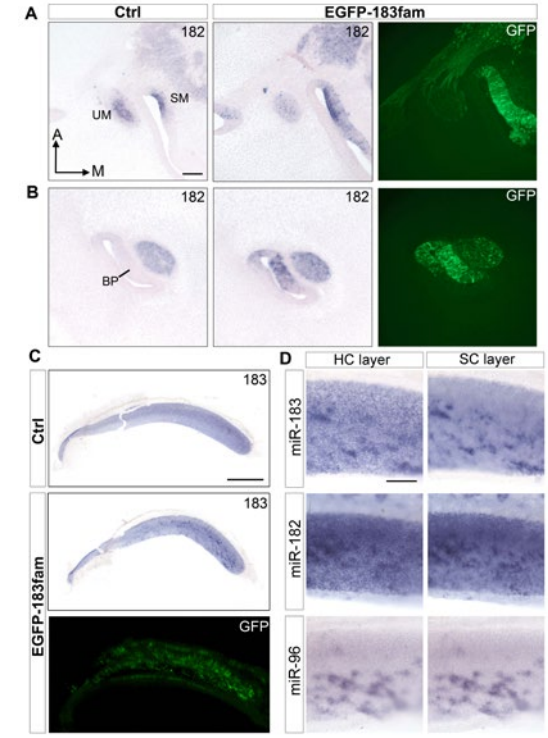

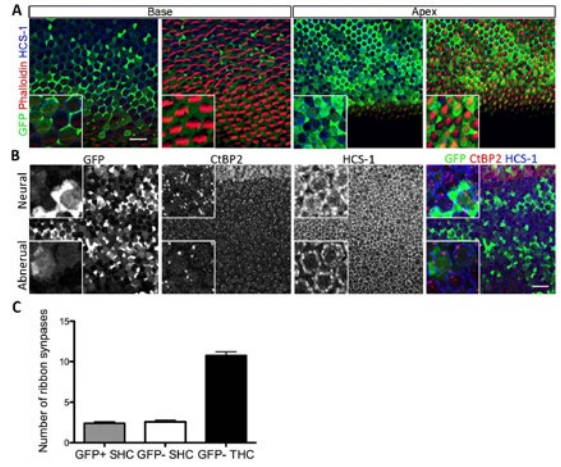

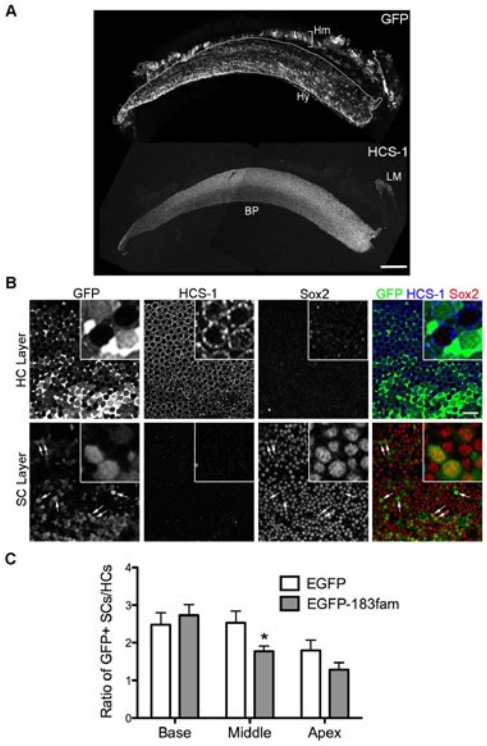

No ectopic hair cells are observed outside the sensory epithelia after the overexpression of miR-183 family. Instead, midway along the longitudinal axis of the BP, miR-183 family-transfected cells, as indicated by GFP, show a higher ratio of transfected hair cells to transfected supporting cells. Therefore, the progenitor cells are slightly biased toward a hair cell fate as compared to cells transfected with control plasmids. However, overexpression of miR-183 family does not perturb hair cell morphologies along the longitudinal axis, nor does it affect the differentiation of tall vs. short hair cells across the radial axis.

Conclusion

While manipulating the levels of the miR-183 family can modestly influence cell lineage decisions, it is insufficient to direct the differentiation of hair cells towards specific radial or longitudinal phenotypes.

PD-62

Lin28b Regulates Developmental Timing within the Mammalian Cochlea Epithelium Through Let-7-Dependent and Independent Mechanisms

Erin Golden[1]; Ana Benito-Gonzalez[2]; Angelika Doetzlhofer[1]
[1]Johns Hopkins University School of Medicine; [2]Johns Hopkins University

The prosensory cells of the mammalian cochlea undergo several critical steps as they progress from undifferentiated progenitor cells to the highly specialized hair cells and supporting cells that comprise the mature organ of Corti. These steps, which include cell cycle withdrawal, cell type differentiation, and maturation, occur in a highly stereotyped order; however, the molecular mechanisms regulating their

timing are largely unknown. We recently identified that the RNA-binding protein Lin28b actively regulates these processes through both let-7 miRNA-dependent and independent mechanisms. Using both lentiviral-infected organotypic cochlea cultures and a doxycycline-inducible transgenic mouse line (iLIN28B) we overexpressed Lin28b throughout the undifferentiated cochlea epithelium and found that its mis-expression was sufficient to deregulate the timing of both cell cycle withdrawal and differentiation of the sensory progenitor cells. This deregulation resulted in the mis-patterning of both hair cells and supporting cells and adversely affected stereocilia formation. Conversely, overexpression of the miRNA let-7g within the undifferentiated cochlea accelerated cell cycle withdrawal but not differentiation, suggesting that Lin28b acts through two separate mechanisms to regulate these processes Finally, we found that re-expression of Lin28b within the differentiated cochlea epithelium increased the capacity for supporting cell trans-differentiation in the absence of Notch signaling, implicating a potential therapeutic effect for Lin28b in hair cell regeneration. The downstream targets mediating Lin28b's regulation of hair cell and supporting cell differentiation have yet to be identified and ongoing experiments addressing these mechanisms will be discussed.

PD-63

cMaf is Required for Development of Spiral Ganglion Neuron Firing Properties and Auditory Function

Wei-Ming Yu[1]; Ye-Hyum Kim[2]; Swetha Murali[2]; Jeffrey Holt[2]; Lisa Goodrich[1]

[1]Harvard Medical School; [2]Children's Hospital Boston, Harvard Medical School

Spiral ganglion neurons (SGNs) play a crucial role in auditory neural circuits by transmitting auditory information from the hair cells to the neurons in auditory brainstem. Understanding how SGNs differentiate to assemble the circuit may help us to design cell-based therapies to repair or rebuild dysfunctional auditory circuitry. To explore the molecular basis of SGN development, we identified the transcription factor cMaf as a potential regulator for development of SGN firing properties. Preliminary studies using SGN whole-cell recordings demonstrate that *c-Maf* conditional knockout mice have decreased evoked potassium currents. cMaf is also required for normal auditory function. *c-Maf* mutant mice show abnormal ABR waveforms, elevated auditory thresholds, and high frequency hearing loss. These findings suggest that c-Maf may induce expression of a specific set of ion channels that endow SGNs with the unique firing properties.

PD-64

Single-cell mRNA-Seq Identifies Supporting Cell Subpopulations in the Mammalian Neonatal Cochlea.

Michael Hoa[1]; Michael C. Kelly[1]; Joseph Burns[1]; Stephen W. Hartley[2]; Jim Mullikin[2]; Robert J. Morell[1]; Matt W. Kelley[1]

[1]National Institute of Deafness and Other Communication Disorders, National Institutes of Health; [2]National Human Genome Research Institute, National Institutes of Health

Introduction

Recent results have suggested that limited conversion of supporting cells to hair cells can occur in neonatal mouse cochleae. These results suggest that the population of supporting cells present in the cochlea in neonates may represent a heterogeneous group of cells with differing developmental potentials. While previous studies have characterized the transcriptional profiles of these cells, limitations in molecular techniques and sequencing technology required large amounts of RNA and therefore large numbers of cells. The subsequent aggregation of RNA from multiple cells resulted in transcriptional averaging that probably masked individual cellular heterogeneity. Recent advances in single-cell sequencing have enabled transcriptome profiling of single cells, which should allow us to characterize cochlear supporting cell subpopulations and provide insights regarding regenerative ability.

Methods

Cochleae were dissected from Tg(Lfng-EGFP) neonatal mice (where most cochlear supporting cells express GFP), dissociated to a single cell suspension, and FACS-purified to enrich the samples for EGFP-positive cochlear supporting cells. Isolated supporting cells were then captured using a Fluidigm C1 microfluidics platform, which sorts single cells into isolated chambers that can then be visualized to confirm occupancy and assess fluorescence intensity. Isolated supporting cells were then lysed, reverse transcribed and amplified within each capture chamber. A total of 113 single cells were captured from four FACS sorts. The amplified cDNA from each cell was then converted to a barcoded Nextera cDNA library and sequenced in 48 cell pools on a single flow cell lane on an Illumina HiSeq. Following mapping and quality assessment relative expression profiles of individual cells were examined by principal component analysis and hierarchical clustering using the Singular Analysis package within R software. Potential supporting cell subpopulations were validated based on expression of both known and newly-identified cell-specific markers.

Results

Analysis of single supporting cells revealed three distinct sub-populations. Correlation with known regional markers suggest that these populations most likely correspond to inner phalangeal cells and border cells, pillar cells and Deiters' cells. However, individual transcriptional profiles within each sub-population were variable, suggesting that there is additional heterogeneity within each group. Moreover, new markers of each subpoulation were also identified.

Conclusion
Single-cell RNA-Seq provides a powerful tool for the characterization of heterogeneity within populations of closely related cells and can hopefully be used to discover the basis for variation in regenerative potential in cochlear supporting cells.

PD-65

Mapping the Transcriptional Programs of Diverse Cell Types of the Developing Cochlear Epithelium by Single-Cell mRNAseq

Michael Kelly[1]; Joseph Burns[1]; Michael Hoa[1]; Stephen Hartley[2]; Jim Mullikin[2]; Robert Morell[1]; Matthew Kelley[1]
[1]NIH/NIDCD; [2]NIH/NHGRI

The cochlear epithelium is composed of a variety of functionally unique types of hair cells and supporting cells that arise during development. While specific cell types can be identified based on relative position within the epithelium at the time of birth, differentiation of unique cell types continues through at least the first postnatal week. The genes involved in directing the divergent differentiation programs of specific cell types are largely unknown. Previous gene expression studies examining the developing cochlear epithelium used either entire tissue preparations comprising diverse cell types or enriched populations thought to be largely homogenous. In either case, averaging of transcriptional profiles likely obscured characteristics of unique cell types. Advancements in single-cell sequencing now allow us to investigate transcriptional profiles of diverse cochlear epithelial cells without the caveat of averaging across numerous cells.

Using transgenic mice with tdTomato-labeled hair cells and Gfp-labeled supporting cells, we isolated cochlear epithelia at specific developmental stages and then mechanically enriched for the organ of Corti and neighboring non-sensory cells. Cells were then dissociated and captured on a Fluidigm C1 microfluidics chip, where cells were lysed and their mRNA was converted to cDNA and subsequently amplified. Single-cell cDNA libraries were prepared and sequenced on an Illumina platform. After sequence alignment and normalization, relative transcriptional profiles of individual cells were examined by principle component analysis and hierarchical clustering. Basic clustering of cell types was validated based on cell type-specific fluorescence documented prior to cell lysis and expression of previously characterized genes.

Not surprisingly, hair cells are significantly different from all other cochlear epithelial cells at all timepoints examined. All hair cells were defined by a unique set of genes, many of which have been the previously described. Furthermore, principle component analysis revealed changes in gene expression consistent with ongoing differentiation. Expression profiles of supporting cells and adjacent epithelial cells reveal large, distinct medial and lateral domains. Cells within each of these domains show considerable diversity, with subpopulations likely representing cells with different fates, from different positions along the basal to apical dimension or in various states of differentiation. Cells from the medial non-sensory region known as Kölliker's organ cluster closely with medial supporting cells, a result that is consistent with the observation that these cells have relatively high competency to generate ectopic sensory cells.

As this dataset expands, it should serve as a valuable resource for the identification and characterization of unique cochlear cell types.

SYM-47

Fundamentals of AUX (AUditory syntaX) and its Use in Research and Education

Bomjun Kwon
Gallaudet University

Recently signal generation and processing for auditory research is increasingly undertaken with software tools without hardware equipment, such as function generators, amplifiers, filters and mixers. Researchers familiar with programing languages such as C++ or MATLAB develop their own software, most of which are often, unfortunately, of limited use to others. Researchers without sufficient or appropriate training often find it difficult to master programming in those computer languages. As an alternative, AUditory syntaX (AUX) has been created as a new scripting language specifically for the generation and processing of auditory signals (Kwon, 2012; Behav Res Methods : 44: 361-373). AUX provides an intuitive and descriptive environment where users focus on perceptual components of the sound. AUX does not require knowledge or experience in computer programming and can be learned and mastered with ease by anyone with working knowledge of psychoacoustics. While the syntax structure of AUX loosely resembles that of MATLAB, AUX offers a number of unique features and operators beyond the scope of MATLAB, for example (here x and y are sounds):

· A time-shift operator adjusts the begin time of a sound by milliseconds. x>>50

· An "append" operator cascade two sounds in sequence. x++y

· An RMS operator sets the scale of sound amplitude by dB. x@-20

· Parentheses and extraction operator specifies a portion of sound by milliseconds. x(30~50)

Most notable point is that in arithmetic or vector operations, e.g., x+y or [x; y] (for a stereo signal), x and y can have different duration, relieving the user of the burden in vector management (one of most tedious tasks in in C++/MATLAB)

Several programs utilizing AUX are available—AUX Viewer, Psycon (psychoacoustic tests), Echo (phoneme identification), Token (word recognition in sentences) and more—in http://auditorypro.com/aux/downloads under Academic Free 3.0 license. AUX is also available as a C library, ready to be adopted by developers to serve custom research needs. Developers are encouraged to participate in the refinement of AUX in its open-source platform.

Researchers or students not proficient with C++ or MATLAB are particularly encouraged to learn AUX as it assists a wide range of needs in speech and psychoacoustic research without substantial overhead effort that is often required in C++/MATLAB. AUX scripts can be easily shared with others, facilitating collaborations. AUX Viewer and Psycon can be particularly useful in classroom teaching for demonstrating various signals and their manipulations and the application in psychoacoustic research.

SYM-48

An Open Platform for Auditory Research

Qianjie Fu
University of California, Los Angeles

A significant portion of research effort is spent on developing stimuli and testing software with which to answer important questions. Our research group has developed many stimuli and computer programs to test and train cochlear implant (CI) users' and normal-hearing (NH) listeners' auditory perception. This effort has contributed greatly to our productivity and, more importantly, has benefitted many of the CI patients who have participated in our research.

In developing the software, we imagined a "wish list" of features that should be available: open- and closed-set testing, an easy-to-use interface, easy configuration of stimuli, response screens, and test procedures, detailed output of stimuli presentation and responses (including tagging and tracking of stimulus features for later analysis), test output that includes many levels of analysis (e.g., percent correct, confusion matrices, feature analyses, etc.), patient data tracking over time, provision of audio-visual feedback, training, and stimulus preview, and an open platform so that software and stimuli could be easily shared and modified by researchers. These features have been implemented within the i-CAST (http://icast.tigerspeech.com) and i-STAR (http://istar.tigerspeech.com) software packages.

The i-CAST software allows for closed-set testing. Phoneme recognition, voice gender recognition, melodic contour identification, digit recognition, and sound source localization are some of the tests currently implemented in i-CAST. The i-STAR software allows for open-set testing. Word or sentence recognition can be measured in quiet or in noise. Speech understanding in noise can be measured at a fixed signal-to-noise ratio (SNR) or adaptively measured by adjusting the SNR according to subject response. A database, stored on the local computer and/or server, tracks all subject responses. Results can be printed after each run and/or viewed over a period of time. Both i-CAST and i-STAR include a real-time CI simulation with which to test NH subjects; a variety of CI signal processing parameters can be simulated (e.g., the number of channels, sinewave or noiseband vocoding, input and output frequency range, etc.).

i-CAST and i-STAR are open-platform research tools, and can be user-configured to test speech perception for different languages, talkers, stimuli, etc. These configurations can be easily shared by researchers to facilitate multi-site testing and collaboration. The software is visually clean and user-friendly, allowing the researcher to concentrate on research projects rather than developing a computer program. As such, the software can accelerate auditory research, which will ultimately accelerate the benefit to hearing-impaired people.

[Development efforts are partly supported by NIH/NIDCD grant R01-DC004993 and R01-DC004792]

SYM-49

APEX 3: a multi-purpose test platform for auditory behavioural experiments

Tom Francart; Astrid van Wieringen; Michael Hofmann; Jonas Vanthornhout; Jan Wouters
KU Leuven

APEX 3 is a software test platform for auditory behavioral experiments. It is built using open technology and standards. Behavioral experiments can be quickly and easily set up without any programming, and are defined in a text file in the XML format.

Examples of experiments that have been successfully conducted with APEX are basic psychophysical detection and discrimination tasks, audiometry, loudness balancing, loudness scaling, pitch and melody identification, sound source localization with a large number of loudspeakers, and speech recognition in quiet and noise with open set, closed set and matrix response options. This is not an exhaustive list, APEX is a generic platform that allows most behavioral experiments to be specified. Features include:

- Constant stimuli, adaptive, training and interleaved procedures are built-in, and custom procedures can be implemented using Javascript or C++.
- Results can be visualized, during and after an experiment. Analysis and visualization is extensible using HTML/Javascript.
- Results are stored in a text file in XML format and can be imported directly into Matlab using the included APEX Matlab Toolbox.
- Support for all sound cards supported by the operating system and various interfaces to cochlear implants. Sound is read from wave files provided by the experimenter.
- Basic sound processing, such as amplification and filtering is available, and can be extended using C++ or Matlab plugins.
- The sound output level can be calibrated using a graphical user interface. Calibration can be conducted automatically using an interface to a sound level meter.
- Speech in noise experiments with an arbitrary number of loudspeakers can be automatically set up with a graphical user interface
- To visually reinforce children down to 2.5 years old, a child mode is available.

APEX 3 is supported under Linux and Windows. Executables and source code are available free of charge under the GPL license. It is currently being successfully used for all behavioral experiments in our lab (ExpORL, Dept. Neurosciences, KU Leuven), and in various other labs around the world. As such, it provides an easy way to collaborate by exchanging experiment and result files. APEX 3 can be downloaded from http://www.kuleuven.be/exporl/apex/

SYM-50

The Eaton-Peabody Laboratories Cochlear Function Test Suite

Kenneth Hancock; Ishmael J. Stefanov-Wagner; Michael Ravicz; M. Charles Liberman
Massachusetts Eye & Ear Infirmary

The Cochlear Function Test Suite (CFTS) is a suite of freeware that controls digital stimulus generation and data acquisition to perform basic assays of cochlear function (URL below). It has been developed through collaboration between investigators and engineers in the Eaton-Peabody Laboratories (EPL) at Massachusetts Eye & Ear Infirmary. The main CFTS modules measure amplitude-vs-level functions of auditory brainstem responses (ABRs), compound action potentials (CAPs), distortion product otoacoustic emissions (DPOAEs) and vestibular evoked potentials (VsEPs). Interfaces allow customization of each stimulus paradigm (stimulus frequency, level spacing, repetition rate, etc.). A higher-level "sequencer" module allows creation of automatic procedures to repeat an arbitrary sequence of cochlear function tests while periodically turning on or off an external "manipulation" (e.g. acoustic noise, electrical pulses, or drug infusion). Additional modules include a CAP threshold procedure that tracks, across frequency, the SPL required to produce a CAP of criterion magnitude, and a utility for simultaneously recording vital signs (e.g. heart rate and body temperature). Data are stored as text files suitable for export to scientific plotting software. The ABR, CAP, and VsEP waveforms can also be ported to a custom peak-finding program, available at the URL below.

The CFTS has evolved in parallel with the EPL Acoustic Assembly, a two-source acoustic system for calibrated sound delivery, with low distortion and high output (>100 dB SPL) to frequencies > 60 kHz. The system uses inexpensive miniature dynamic earphones to generate stimuli and a miniature high-frequency microphone to monitor SPL via a probe tube, all housed in a plastic assembly that can be produced via 3D printing. Designs and assembly instructions are freely available. The CFTS includes subroutines for rapid, densely sampled acoustic calibration, including measuring probe-tube microphone sensitivity against a calibrated microphone in a coupler, and sound pressure produced by each earphone *in situ*.

The CFTS specifically drives National Instruments data acquisition boards, but is flexible with respect to the exact number and types of boards in the system. The executable version of the application requires the LabVIEW Run-Time Engine, a free download from National Instruments. The source code is also included in the distribution, but requires purchase of a LabVIEW license to modify.

http://www.masseyeandear.org/research/otolaryngology/investigators/laboratories/eaton-peabody-laboratories/epl-engineering-resources

Supported by NIDCD P30 DC005209

SYM-51

Neurophysiology Data Acquisition And Analysis with ACQ4

Luke Campagnola; Paul Manis
University of North Carolina at Chapel Hill

We present ACQ4, a general-purpose data acquisition system for experimental neurophysiology. The primary purposes of ACQ4 are 1) to provide a scalable, modular platform that allows rapid development of software to support a wide variety of experiment types, and 2) to provide a set of applications built from that platform to allow easy design and execution of neurophysiology experiments. ACQ4 is open-source (MIT licensed) and built on the open-source tools Python, NumPy, SciPy, and PyQt. We hope to encourage the development of ACQ4 as a collaborative effort in the neurophysiology community. With this system, we emphasize modularity so that each piece of the system supporting a particular device, experiment, or analysis may be reused and recombined in other contexts to reduce the effort in developing new experiments. ACQ4 has been used for several types of experiment including patch-clamp electrophysiology, two-photon laser scanning microscopy, CCD-based calcium imaging, laser photostimulation mapping, and in vivo intrinsic signal imaging. It includes several user interface modules that handle synchronized acquisition and stimulation, imaging, cell patching, and others. Currently ACQ4 supports several types of device, such as National Instruments DAQ devices, Photometrics and QImaging cameras, MultiClamp and AxoPatch amplifiers, galvanometric scan mirrors, and motorized stages. More information is available at www.acq4.org.

SYM-53

Speech Analysis Modification and Synthesis tool STRAIGHT and extended voice morphing

Hideki Kawahara
Wakayama University

STRAIGHT is a set of Matlab functions for analysis, modification and re-synthesis of speech sounds. A set of GUIs are provided for manipulating speech parameters and for preparing stimuli using extended voice morphing procedures. Using STRAIGHT does not require any cost for academic and educational purposes. STRAIGHT and GUI tools can be downloaded from a web site in the restricted access area. The prospective user needs to acquire access key from the author of the tool. For general information about STRAIGHT and its applications, please visit the following site.

http://www.wakayama-u.ac.jp/~kawahara/STRAIGHTadv/index_e.html

STRAIGHT is based on systematic procedures to remove periodic variations in power spectra, instantaneous frequencies and group delay representations enabled flexible and precise manipulation of physical parameters of speech sounds based on so called source-filter model. STRAIGHT decomposes input speech signals into source information (F0 trajectory and aperiodicity map) and filter information (smoothed spectrographic time-frequency representation). Virtually complete removal of periodicity information from filter and aperiodicity parameters enables flexible manipulation of speech parameters without introducing severe quality degradations of menipulated and resynthesized speech sounds. The extended morphing procedure takes advantage of this flexibility and provides temporally variable multi-attribute morphing functionality of arbitrarily many voices.

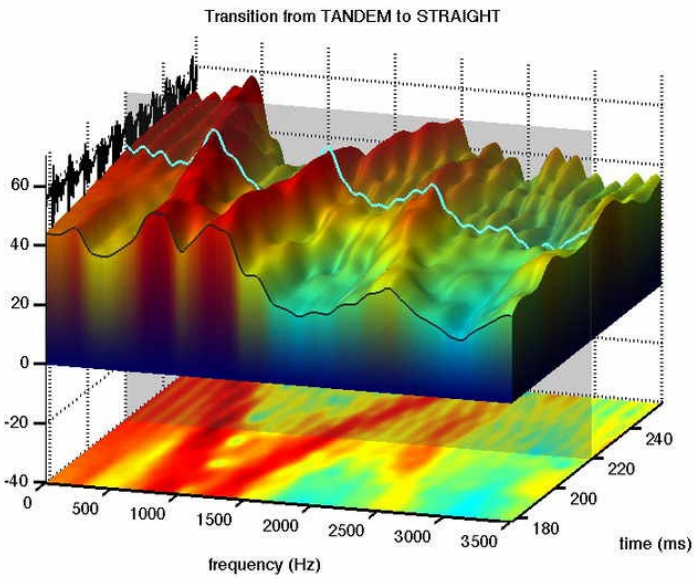

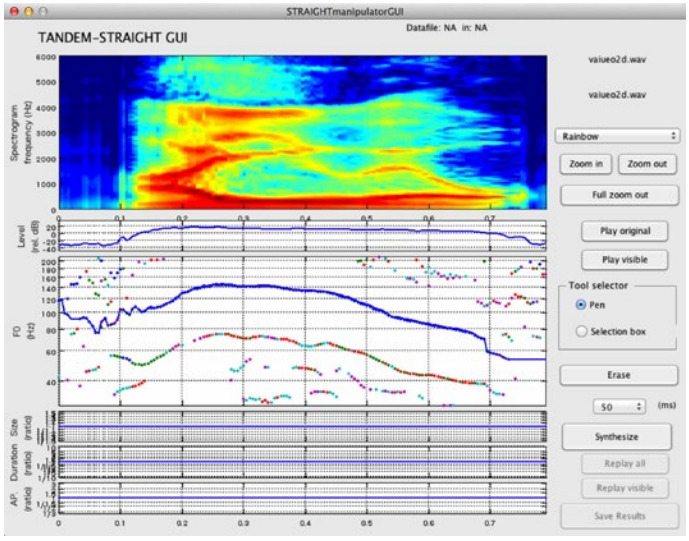

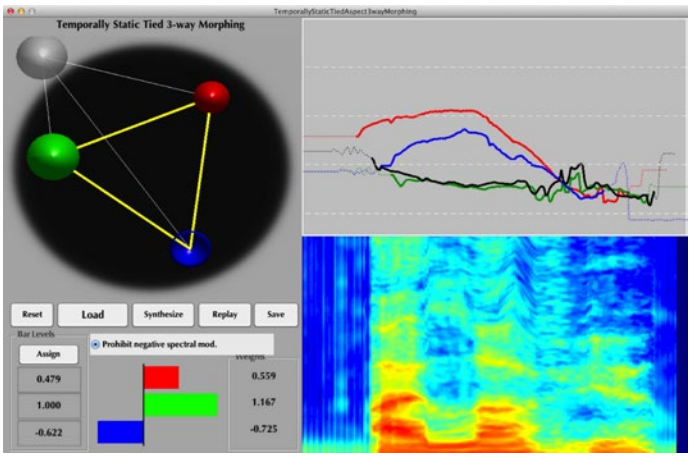

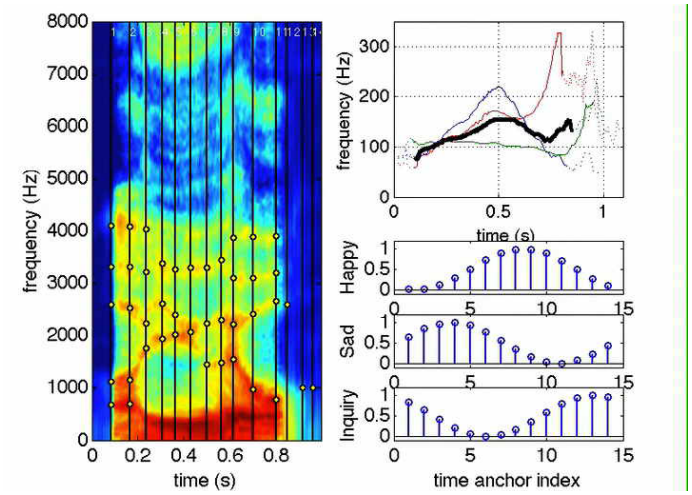

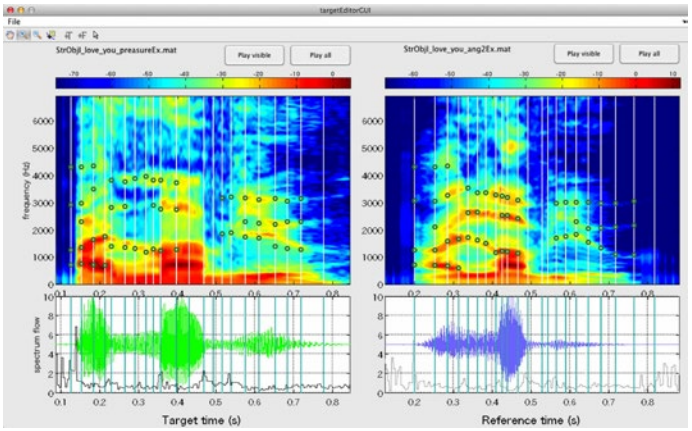

Conceptually simple modular structure of STRAIGHT with Matlab implementation, which does not raly on any machine dependent codes, makes it easy to costomize for specific resarch purpose. For example, modification of re-synthesis functions enabled investigations on effects of inharmonicity in voice source on speech segregation. The spectral analysis component of STRAIGHT is also used in many speech synthesis systems, such as HTS. A freely accessible Matlab tools for speech and auditory education can also be downloaded from the following site.

http://www.wakayama-u.ac.jp/~kawahara/MatlabRealtimeSpeechTools/

This presentation consists of scientific visualizations of speech parameters and morphing demonstrations to illustrate prospective applications of STRAIGHT in auditory perception research. Some of screen shots of such demonstrations are given below.

SYM-54

RBA: Integrated EEG Stimulation and Recording System for Electrical and Acoustical Stimulation

Michael Hofmann; Tom Francart; Jan Wouters
KU Leuven

RBA is a cross-platform integrated EEG stimulation and recording system. It allows for the multi-channel recording of evoked potentials in response to generated acoustical and electrical stimuli and provides facilities for real-time result presentation and analysis. Examples of experiments that have been conducted at ExpORL include the recording of Auditory Brainstem Responses and Auditory Steady State Responses in response to acoustical stimulation. RBA can also be used to record evoked potentials in response to electrical stimulation with cochlear implants (CIs) from Advanced Bionics and Cochlear and Direct Acoustic Cochlear Implants from Cochlear. Some notable features include:

Acoustical and Electrical Stimulation

- Integrated presentation of acoustical and electrical stimuli with direct specification of properties such as amplitude, frequency and stimulus shape
- GUI for the easy calibration of the intensity of acoustical stimuli
- Synchronization with triggers from external stimulator
- Determination of threshold and comfort levels of CI users to protect against overstimulation

Recording

- Recording of preamplified EEG signals as supplied by external preamplifiers such as the Stanford Research Systems SR560 with off-the-shelf sound cards
- Preprocessing steps such as artifact rejection and filtering, storage of raw data so that results can be reanalyzed with different settings
- Output of a trigger signal to synchronize an external recording system, e.g. a Biosemi ActiveTwo
- Support to calibrate hardware properties such as real gain and latency

Real-Time Analysis

- Online presentation of EEG power spectrum and response characteristics in the time, frequency and complex domain
- Statistical evaluation of responses with F and Hotelling T-squared tests
- Interactive result display allows for the saving, reordering and annotation of response waveforms

Session Management

- Storage of metadata in standards-compliant XML+ZIP files and EEG recordings in multi-channel WAV files
- Automatic recording of multiple successive experiments
- Preparation and scheduling of additional experiments while a recording is ongoing

RBA can be used with Linux and Microsoft Windows operating systems. Binaries and source code are available under the GPL under the condition of a research cooperation. For electrical stimulation, distribution is limited by agreements with CI manufacturers and needs to be decided on a case-by-case basis.

SYM-55

Epidemiology of Age-related Vestibular Loss

Yuri Agrawal
Johns Hopkins University School of Medicine

The vestibular system is integral to balance control and locomotion. In this session we will review the evidence showing a decline in both semicircular canal and otolith function associated with aging. We will review data from large-scale epidemiologic surveys and population-based studies that estimate the incidence and prevalence of age-related vestibular loss. We will also review the clinical impacts – with respect to gait, mobility and cognitive function – associated with age-related vestibular loss based on evidence from these epidemiologic studies. This session will set the stage for the magnitude and significance of the problem of age-related vestibular loss, and the need for a carefully laid-out research agenda.

SYM-56

Presbyequilibrium: Characterizing this Geriatric Syndrome

Ilmari Pyykko
University of Tampere Medical School

Background

Dizziness, impaired of balance and fear of falling are common complaints among the older adults. The associations of vestibular symptoms and vestibular findings with accidental falls in the elderly are not well understood. The purpose is to evaluate the presbyequilibrium in the older adults.

Methods

We examined prebyequilibrium among 72 elderly persons from a single residential facility and among 96 active home dwelling older adults. In order to define their complaints, a standardized otoneurological questionnaire was administered that consisted of 98 questions about the subjects' symptoms, medical history and medication. A general health related quality of life measure (QoL-15D) and mini mental status examination (MMSE) were completed. Additionally, records were made of falls. In neurotologal evaluation vestibular findings, their association with posturography and falls were evaluated.

Results

Several terms as vertigo (spinning), dizziness, syncope, floating sensation, fear of falling and visual blurring were used to describe presbyequilibirium. The complaints occurred most commonly in cluster, were age dependent and were present in 42% among home dwelling older adults and in 54% in residential facility living persons. In the latter group persons could show nystagmus in positional testing without experiencing vertigo. The most common complaint was postural instability, with a tendency to fall. “Spinning” vertigo and “floating” sensation had a strong inter-correlation ($p<0.001$) and correlated with habitual falls. The symptoms often occurred in combinations with the most common combination being “poor postural stability” and “gait problems”. Attacks of self-experienced syncope never occurred alone but always in combination with “spinning vertigo” or “tendency to fall”. Presbyequilibrium caused a significant deterioration in the quality of life. Persons living in residential facility benign positional vertigo in Dix-Hallpike’s tet was most common finding (55%) but also vestibular function loss, reduction of gain and phase of vestibulo-ocular reflexes were common. In postural stability the performance was reduced and the elderly used open loop strategy to control their balance.

Conclusion

Vestibular derangement is common among elderly and the complaints are polymorphic and sometimes difficult to associate with vestibular fault. Detailed analysis of presbyequilibrium with vestibular testing provides a potential basis for streamlining diagnostic evaluations and aiding in planning for effective therapy. In oldest old, these problems are magnified, increasing the need for additional expertise in their care, which may be met by training specialized healthcare staff to tailor a vestibular rehabilitation program in that own will and fitness level are individually adjusted.

SYM-57

Recent Research On Falls, Fracture And Effective Interventions

Mans Magnusson
Lund University

Vestibular function contributes to orientation and balance control in the standing human. The vestibular sensors as well as the inate and developed reflexes and central nervous representation, co-operate with proprioceptive, visual afferents and conjugate in a syntheses of orientation and movement control. As the two legged human is dependent on balance and orientation for survival, the importance of tuned balance reflexes is paramount.

There is a continuous recalibration of the human balance system as we age or are exposed to injuries. To meet these requirements the balance system has to be pronouncedly adaptive, and it is. This ability can be used in rehabilitation techniques.

However, also an adapted system will reach its limits. When these limits are surpassed, falls or dizziness may occur. To understand adaptive behavior and its limits as well as the importance of vestibular deterioration in the ageing human considering falls and fractures and possibly to use the adaptive behavior of our balance systems have been a main purpose of the reported research. We have observed the reduction due to ageing of balance function in postural control and correlated that to hip and wrist fractures in elderly. We observe that vestibular asymmetry correlates to falls and side of fracture in both hip and wrist fractures. Recently we have found that a vestibular asymmetry correlates to falls also in subjects that have so called multi sensory deficits. Recently we have seen that also this observed vestibular asymmetry maybe possible to reduce with rehab programs, by simplistic training in elderly, at least in some individuals. We have also observed that normal 70+ years old individuals can be trained to gain a better balance performance assessed with postural control measurements with a combined home based training program, using the adaptive strength of the human balance system. The same adaptivety have been used in the development of the Vestibular PREHAB approach where patients undergoing gentamicin treatment or a re scheduled for posterior fossa surgery, are trained in advance and continuously during gentamicin treatment, causing a vestibular ablation with very little or no subjective symptoms. The congregated knowledge thus points to an paramount importance of the vestibular system and its adaptive capabilities for the postural function, the balance and the integrity of the human being.

SYM-58

Plasticity and Diversity in Central Vestibular Neurons: Implications for Clinical and Basic Science

Sascha du Lac; Takashi Kodama
Johns Hopkins University School of Medicine

The remarkably diverse influences of the vestibular system on cognition, emotional regulation, autonomic functions, skeletomotor control, and eye movements raise fundamental questions of whether the corresponding neural circuits are (1) differentially susceptible to dysfunction in aging or in patients with vestibular impairments, and (2) composed of molecularly diverse neurons that could be specifically targeted via pharmacological and/or rehabilitative clinical therapies. Classically, studies of central vestibular pathways have attributed diversity in neuronal response properties and functions to differences in connectivity, with the assumption that central neurons are otherwise homogenous and generic. More recently, however, cellular and synaptic studies of vestibular nucleus neurons have revealed unappreciated diversity in synaptic properties and receptors, firing properties, and the requirements and mechanisms for intrinsic and synaptic plasticity. To identify the molecular substrates for this functional heterogeneity, our group has performed quantitative, single-cell gene expression profiling of distinct classes of vestibular nucleus neurons in mice (Kodama et al, 2012). Using cell-type specific anatomical marker genes, pathway tracing, and cellular electrophysiology in identified neurons, we have now identified 6 major cell classes in the rostral medial vestibular nucleus, including vestibulo-autonomic, vestibulo-ocular, vestibulo-cerebellar, commissural, and local inhibitory

neurons. Single-cell qPCR and gene array analyses reveal striking differences across the cell types in expression of genes encoding ion channels, neurotransmitters, peptides and receptors, and proteins related to synapses and structural plasticity. These findings set the stage for harnessing modern molecular neurobiological strategies to identify and correct pathway-specific dysfunction across the lifespan in patients experiencing diverse consequences of vestibular impairments.

SYM-59

Basic Science Insights: Vestibular Control of Movement

Robert Peterka
Oregon Health & Science University

The vestibular contribution to the control of movement can be difficult to decipher experimentally due to the parallel contributions of motion information from other sensory systems. This presentation will describe methods that are able to identify the vestibular contribution to movement, and will present results showing that the vestibular contribution is dynamic in that it depends on environmental conditions, on the availability of motion information from other sensory systems, and on the integrity of vestibular function. The vestibular contribution can be identified using a model-based interpretation of body motion evoked by perturbations to standing balance and balance during gait. A relatively simple feedback control model of balance can account for body motion evoked by continuously applied rotations of the stance surface or the visual scene, or by current applied between the mastoids (galvanic vestibular stimulation). Stimulus-evoked body sway is analyzed using Fourier methods to compute frequency response functions (FRFs) that characterized balance control dynamics. Parameters of the model are then adjusted so that model-predicted FRFs optimally match experimental FRFs. The model parameters are physiologically meaningful and include sensory "weights" that represent the relative contributions of sensory systems to balance control [1]. For example, with eyes closed, a low amplitude surface-tilt stimulus (below perceptual threshold) evokes body sway that tends to move the body toward alignment with the surface. The model-based analysis identifies that ~70% of the sensory information used for balance in this condition comes from proprioception and ~30% from vestibular. However, as the stimulus amplitude increases subjects shift toward increased reliance on vestibular information. This shift represents a "sensory reweighting" phenomenon that itself requires dynamic regulation so that rapid changes in environmental conditions produce appropriately rapid changes in sensory weights in order to maintain stability [2]. Vestibular dysfunction affects sensory weighting. Even subjects with well compensated unilateral vestibular loss demonstrate a consistent reduced reliance of vestibular information for balance even though their healthy ear is fully capable of encoding the mild head motions evoked by the test perturbations, and subjects who report being less well compensated show even less use of vestibular information [3]. Subjects with bilateral vestibular loss are obviously unable to utilize vestibular information for balance, but their vestibular loss also affects their ability to regulate the use of proprioceptive and visual information [1].

[1] Peterka, *J Neurophysiol*, 88:1097-1118, 2002.
[2] Peterka and Loughlin, *J Neurophysiol*, 91:410-423, 2004.
[3] Peterka et al., *Front Neurol*, 2:57, 2011.

PD-82

An Integrated Paradigm for Human Hearing Loss Gene Discovery

Jun Shen[1]; James E. Saunders[2]; Sami Amr[1]; Denise Yan[3]; Xue Zhong Liu[3]; David P. Corey[4]; Heidi Rehm[1]
[1]Brigham and Women's Hospital, Harvard Medical School; [2]Dartmouth Hitchcock Medical Center; [3]University of Miami School of Medicine; [4]Harvard Medical School

Introduction

Hearing loss is a genetically heterogeneous condition. Genetic testing of over 70 known hearing-loss genes can only resolve 30-40% of the cases, suggesting that many more genes await discovery. Although next-generation sequencing has expedited the discovery of genetic variants, the large number of variants naturally present in each individual makes it challenging to pinpoint the causative mutations. We aim to identify more genetic causes of hereditary hearing loss by integrating linkage analysis, copy number analysis, exome sequencing, and an inner-ear gene-expression database with comprehensive annotation.

Methods:

We investigated a hearing-loss pedigree from rural Nicaragua. We performed linkage and copy number analyses using high-density single nucleotide polymorphism arrays on all available family members and exome sequencing on the proband. We implemented the Shared Harvard Inner Ear Laboratory Database (SHIELD) to prioritize genetic variants based on inner-ear gene-expression data, domain structures, animal model information, and other auditory research findings.

Results:

We ascertained postlingual progressive non-syndromic sensorineural hearing loss in a Nicaraguan family. The family history was consistent with autosomal dominant inheritance. Genome-wide linkage analysis identified four regions with maximum multipoint LOD scores >2. No copy number variants segregated with hearing loss in the family. Exome sequencing identified over 20,000 variants in the proband. Using the SHIELD, we narrowed them down to only one heterozygous missense variant with potential functional impact in the *TECTB* gene within the linkage intervals. The SHIELD annotation indicates that the mouse homolog *Tectb* is highly expressed in the inner ear and associated with abnormal hearing. *TECTA* and *TECTB* respectively encode alpha- and beta-tectorins, the two major non-collagenous components of the tectorial membrane in the organ of Corti. The tectorins share homology in the zona pellucida (ZP) domain. Missense variants in the ZP domain in *TECTA* are responsible for dominantly inherited hearing loss DFNA8/12. Interestingly, the novel missense variant we identified affects a highly conserved cysteine residue in the ZP domain in *TECTB*. Multiple computational tools predicted it to be deleterious. Sanger

sequencing confirmed its segregation with hearing loss in the family. It was absent from large population studies in public variant databases.

Conclusion:
We identified a novel missense variant in *TECTB* segregating with autosomal dominant non-syndromic hearing loss. Our results associate *TECTB* with human hearing loss for the first time, suggesting 10q25.2 as a new DFNA locus. The integrated paradigm described here represents an efficient approach to hearing-loss gene discovery.

PD-83

Hereditary Hearing Loss: The Use of a High Throughput and Multistep Approach to Identify New Genes

Giorgia Girotto[1]; Anna Morgan[1]; Dragana Vuckovic[1]; Elisa Rubinato[1]; Ilaria Gandin[1]; Mariateresa Di Stazio[1]; Ramin Badii[2]; Diego Vozzi[3]; Paolo Gasparini[4]
[1]University of Trieste; [2]Molecular Genetics Laboratory, Department of Laboratory of Medicine and Pathology, Hamad Medical Corporation (HMC), Doha, Qatar; [3]IRCCS Burlo Garofolo; [4]University of Trieste/IRCCS Burlo Garofolo

The presence of a large genetic heterogeneity and the need to identify new Hereditary Hearing Loss (HHL) genes prompted us to design an extremely powerful algorithm characterized by 2 steps: 1) screening of 113 HHL genes by targeted re-sequencing (TS). In negative cases: data are analysed by 2) whole exome sequencing (WES) to detect causative mutation in new genes and/or copy number variation (CNVs)

TS of 113 different HHL genes was based on Ion Torrent PGM™ (LifeTechnologies) (4.356 amplicons ensuring approximately 92,6 % coverage of 744,38Kb of target region). Genomic variants were annotated by ANNOVAR and filtered according to: a) pedigree pattern of inheritance b) NCBI dbSNP v137, 1000 Genomes Project, ESP6500 databases, c) pathogenicity evaluation by *in silico* predictors tools, d) evolutionary amino-acid conservation (PhyloP, GERP++). As regards to WES protocol (Ion Proton™-LifeTechnologies), after exome enrichment step, library construction, sample sequencing and reads mapping, nucleotide variants and INDELS were called by GATK and annotated/filtered as above described. CNV analysis was carried out by CoNIFER (http://conifer.sourceforge.net/) with a confidence value≥1.5

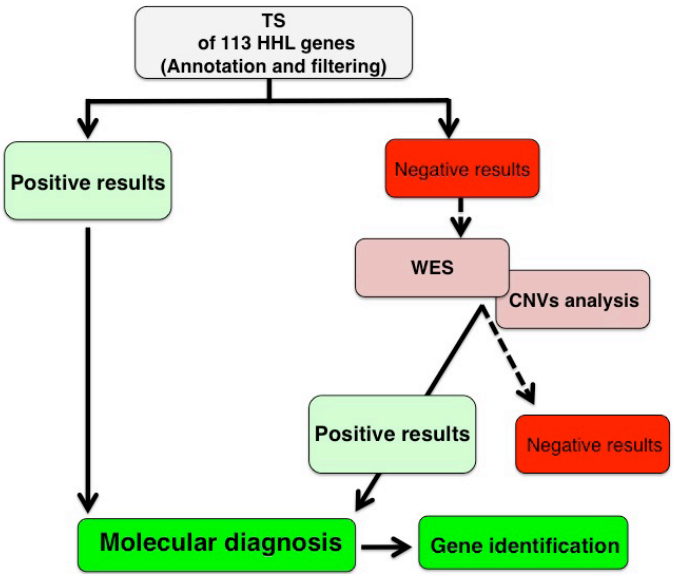

Our algorithm has been successfully applied to 31 families from Italy and Qatar leading to the characterization of many of them as well as to the identification of new HHL genes. In particular, Step 1 (TS) allowed us to characterize 11 families out of 31 (35%) with mutations in known genes (*GJB2*, *TECTA, TMPRSS3*, *TMC1, MYO15A, LOXHD1, WFS1*). Moreover, the analysis by TS of a first series of sporadic cases led to the characterization of half of them. As regards to STEP2, so far, 10 cases entered the WES pipeline. In two cases CNV analysis revealed, a deletion of a region including *STRC* and *CATSPER2* genes in one family and a deletion in *OTOA* gene in the second family in agreement with published data (Shearer A.E. Gen.Med.-2014). Finally, the following new HHL genes were identified: a) *BDP1 and P2RX2* (Girotto G. Plos One-2014; Faletra F. Gene-2013) b) *TBL1Y* carrying a missense mutation (c.A206T; p.D69V) detected in a pedigree resembling a Y-linked form of HHL, c) *PSIP1* carrying a novel frameshift deletion (c.1554_1555del; p. 518_519del). In the remaining 4 cases WES data are still under final validation while the last series of 9 TS cases negative is now under investigation by WES

These findings clearly highlight the importance of NGS technologies as well as the usefulness of our 2 steps strategy to better understand the genetic basis of HHL

PD-84

A New Targeted Re-Sequencing Protocol to Investigate the Genetic Causes of Age-Related Hearing Loss

Anna Morgan[1]; Diego Vozzi[2]; Martina La Bianca[2]; Angela D'Eustacchio[2]; Giorgia Girotto[1]; Paolo Gasparini[3]; Maria Pina Concas[4]; Mario Pirastu[4]

[1]University of Trieste; [2]IRCCS Burlo Garofolo; [3]University of Trieste IRCCS Burlo Garofolo; [4]Institute of Population Genetics, National Research Council of Italy, Sassari, Italy

Background

Age related hearing loss (ARHL) is a degenerative disease that affects millions of elderly people worldwide. It is characterized by a deterioration of the auditory function with a decline of speech understanding. AHRL is a complex disease in which different traits may contribute to define the clinical phenotype. To date, very little is known about the genetics of ARHL. In order to overcome this lack of knowledge, more than 500 patients coming from both inbred and outbred populations were analysed using a custom targeted re-sequencing (TS) panel of 47 ARHL candidate genes.

Methods

TS analyses was performed in 47 different genes using Ion Torrent PGM™ (LifeTechnologies). Briefly, 1942 amplicons ensuring approximately 96,55 % coverage of the target region (a total of 392,89 Kb) were analysed. The selected genes include: i) 13 from already published GWAS data (Girotto G et al. Plos One 2014, Wolber LE et al. Hum Mol Genet. 2014), ii) 34 from animal studies (i.e. expression analysis, ENU mutagenesis in collaboration with UK colleagues such as M.Bowl-MRC, S.Dawson-UCL). Sequencing data have been filtered according to frequency values (all variants with MAF>0,01 have been filtered out), pathogenicity prediction given by several in silico predictor tools (i.e. MutationTaster, Polyphen2, SIFT) and conservation score of mutated residues (PhyloP score).

Results

Results on a first series of 67 cases from 6 villages located in the Northern part of Italy surprisingly revealed a series of interesting mutations in different genes. In particular, a novel heterozygous frameshift deletion, leading to a premature stop codon after five residues, was detected in 3 unrelated cases in a gene recently described as being highly expressed in the hair cells stereocilia (D.Sheffer-HMS-US Personal Communication). Another interesting allele, a missense heterozygous mutation, was detected in another gene that has been recently implicated in presbyacusis in mice models (M.Bowl-MRC Personal Communication). Complete results on the overall series of 500 cases under investigation will be presented and discussed.

Conclusion

These preliminary results were obtained from the sequencing data analysis of 67 out of 500 patients while the remaining ones are now under investigation. The identification of some interesting mutations in ARHL candidate genes further support the role of these genes in causing ARHL and demonstrate the usefulness of our high throughput approach.

PD-85

Genetic Polymorphisms Associated with Noise-Induced Hearing Loss in Marine Recruits during Rifle Training

Yohann Grondin[1]; Magda Bortoni[1]; Rosalinda Sepulveda[1]; Elisa Ghelfi[1]; Adam Bartos[1]; Doug Cotanche[1]; Royce Clifford[2]; Ron Jackson[3]; Rick Rogers[1]

[1]Harvard School of Public Health; [2]Harvard School of Public Health and Naval Medical Center San Diego.; [3]Naval Medical Center San Diego

Background

Noise-induced hearing loss (NIHL) is a significant occupational health issue that affects productivity and safety in all sectors of the workplace. However, not all persons will sustain a hearing loss injury from the same noise exposure.

To identify novel susceptibility loci associated with NIHL in a workforce undergoing their first encounter to occupational noise, we performed a genome-wide association study in a young male population exposed to repeated 157 dB impulse noise over 5 days.

Methods

Subjects were selected from the placebo arm of the Marine Recruit Study "Prevention of Noise-Induced Hearing Loss Using the Antioxidant Supplement, N-acetylcysteine: Impulse Noise Study (NMCSD.2007.0013)". Subjects had no previous exposure to military noise, had normal hearing in both ears and normal tympanometry on baseline and on the day of final hearing test. Noise exposure consisted of 5 days firing 350 rounds of ammunition with a M16 rifle generating 157 dB peak sound pressure level impulse-noise while using foam ear plugs. Thirteen days after, subjects underwent repeat audiograms and saliva sample was collected for genotyping. The IRB-approved study included written informed consent and sample de-identification. Subjects had hearing loss if their average threshold shift over frequencies 2, 3 and 4 kHz over both ears was positive, and had no loss of hearing otherwise.

48 samples randomly selected amongst 110 subjects with threshold shift and 204 without were genotyped on Genome-Wide Human SNP Array 6.0. In total, 41 samples passed the quality controls performed following GWAS standards. Case vs control allelic frequency test was done for all SNPs within 20kb of a gene. The genome-wide significance was set to 5 x 10-7 and suggestive association to 5 x 10-4. Empirical significance levels using permutations were also calculated.

Results

We found one SNP at genome-wide significance, rs7598759, located within the intron of nucleolin gene and 65 other SNPs at suggestive significance. Of particular interest amongst these SNPs are (1) rs7429015, located in the intron of gene KCNMB2 in linkage disequilibrium with previously reported SNP rs4603971, which is also in suggestive associated with

NIHL; and (2) SNP rs2436106, located within gene KCNQ3. Although KCNQ3 has not been previously reported in association with NIHL, other genes belonging to the same family, KCNQ1 and KCNQ4, have been.

Conclusion
Our GWAS data suggest that nucleolin is a potential target for therapeutic intervention. Previously unreported potassium channels associated with NIHL may be of interest as well.

PD-86

DCDC2a Plays a Role in Sensory Hair Cell Kinocilia Length Regulation and is Responsible for Human Deafness DFNB66

M'hamed Grati[1]; Imen Chakchouk[2]; Qi Ma[3]; Mariem Bensaid[2]; Alexandra DeSmidt[4]; Nouha Turki[2]; Denise Yan[3]; Aissette Baanannou[2]; Rahul Mittal[3]; Nabil Idriss[2]; Amjad Farooq[5]; Zhongmin Lu[4]; Xue Zhong Liu[3]; Saber Masmoudi[2]
[1]University of Miami Miller School of Medicine; [2]Laboratoire Procédés de Criblage Moléculaire et Cellulaire, Centre de Biotechnologie de Sfax, Sfax 3018, Tunisia; [3]University of Miami Miller School of Medicine, Department of Otolaryngology, Miami, FL 33136, USA; [4]Department of Biology, University of Miami, Miami, FL 33146, USA; [5]Biochemistry and Molecular Biology, University of Miami Miller School of Medicine, Miami, FL 33136, USA

Introduction
The high prevalence/incidence of hearing impairment (HI) in man makes it the most common sensory defect. The majority of the cases are of genetic origin. Hereditary HI that is not associated to other symptoms classified as non-syndromic deafness, is extremely heterogeneous.

Genetic approach has been instrumental in deciphering genes that are crucial for auditory function and for elucidating molecular pathways related to the development, maturation and function of the auditory system. We have mapped a 16.5-Mb critical region, which segregated in a large consanguineous Tunisian family that is associated with autosomal recessive nonsyndromic hearing impairment (DFNB66), to human chromosome 6p21.2-22.3. Using Sanger sequencing, we excluded the implication of COL11A2, BAK1 and LHFLP5 in DFNB66.

Goal
The identification of the causative gene for DFNB66, and the characterization of the function of the encoded protein.

Methods
We used whole-exome sequencing on patient DNA to identify homozygous variants in genes within the DFNB66 locus that would cause the disease. We performed variant segregation analysis within the family and determined occurrence frequency in Tunisian control population. We used Western blotting on several tissues and whole mount immunofluorescence of rat inner ear preparations to study the tissue and cellular localization of candidate proteins. We used cell lines and organotypic rat inner ear explant cultures to study the targeting properties of wild type and mutant proteins. We used morpholino gene knockdown, live imaging, immunofluorescence, and electrophysiological recordings to study auditory function of the orthologous genes in zebrafish.

Results
We uncovered a point aminoacid substitution in a novel protein, DCDC2a (NP_001182539.1), as the cause of isolated recessive hearing loss DFNB66 in the Tunisian family. We localized DCDC2a to inner ear nonsensory support cells primary cilia, and to sensory hair cells kinocilia that play a crucial role in mechanosensory stereocilia bundle planar polarity and development. In cochlea neuroepithelium, the expression of the uncovered human deafness mutation causes a significant increase in cilia length as well as several cilia defects suggesting a role for DCDC2a in cilia microtubule nucleation, stability and length regulation. In zebrafish, we show that the single ortholog *dcdc2b* is essential for hair cell development, survival, and function.

Conclusions
We present DCDC2a as the cause of DFNB66 form of HI, and the first sensory hair cell protein to be directly implicated in the length regulation of kinocilia.

PD-87

Gene Therapy Restores Hair Cell Stereocilia Morphology in the Whirler Mouse Cochlea

Wade Chien[1]; Kevin Isgrig[2]; Soumen Roy[2]; Inna Belyantseva[2]; Meghan Drummond[2]; Lindsey May[2]; Tracy Fitzgerald[2]; Thomas Friedman[2]; Lisa Cunningham[2]
[1]Johns Hopkins School of Medicine; [2]NIDCD/NIH

Abstract
Background: Whirlin, encoded by *Whrn,* is important for stereocilia elongation. *Whnr*$^{-/-}$ (whirler) mice are born deaf due to a failure in stereocilia elongation. Though stereocilia are short, hair cells in whirler mice persist for approximately 1 month after birth. In this study, we utilize whirler mice to examine the potential therapeutic effects of whirlin gene therapy.

Methods
Homozygous whirler mice and their wild-type littermates were used in this study. AAV8-whirlin was delivered into the cochlea of neonatal mice via the round window. Auditory brainstem-evoked responses (ABRs) were recorded to measure hearing outcomes after whirlin gene therapy. Following ABRs, immunohistochemistry and scanning electron microscopy were used to examine cochlear morphology.

Results
Whirlin expression was restored at stereocilia tips in *Whnr*$^{-/-}$ inner hair cells (IHCs) infected by AAV8-whirlin. In these cells, stereocilia length was increased compared to neighboring non-infected IHCs. Infected IHCs also had fewer supernumerary rows of stereocilia compared to non-infected neighboring *Whrn*$^{-/-}$ IHCs. Whirler cochleas that received whirlin gene therapy retained more IHCs after 1 month compared to the contralateral control ears, suggesting that whirlin gene therapy prolonged IHC survival. There was no improvement in ABR thresholds in whirler mice that received whirlin gene therapy compared to those that did not.

Conclusions

Our data indicate that AAV8-whirlin gene therapy is sufficient to restore stereocilia architecture and prolong IHC survival in the treated whirler ears. This proof-of-concept study demonstrates that cochlear gene therapy can be effective at restoring structural defects in IHCs.

PD-88

Efficient Delivery of Functional Genome Editing Proteins Into Mammalian Inner Ear In Vivo

Yilai Shu[1]; John Zuris[2]; David Thompson[2]; Yong Tao[1]; David Liu[2]; Zheng-Yi Chen[1]

[1]Massachusetts Eye & Ear Infirmary and Harvard Medical School; [2]Harvard University

Introduction

One of the major hurdles to study mammalian inner ear is the lack of efficient delivery of genes and proteins into the inner ear. Study has shown that by fusion or conjugation to cationic molecules, GFP proteins can be made to be super-positively or super-negatively charged. These supercharged proteins can serve as carriers to deliver fused proteins directly into cells. We studied the use of supercharged proteins to deliver genome-editing protein Cre recombinase to mouse inner ear in vivo. We further studied liposomal reagents, developed for DNA and RNA transfection, in Cas9 protein complexed with guideRNA for inner ear delivery and CRISPR-mediated genome editing in vivo.

Methods

Supercharged GFP proteins carrying Cre recombinase, (-30) GFP-Cre and (+36)GFP-Cre, were injected into neonatal Rosa-tdTomato$^{f/f}$ cochlea, with tdT^{+} cells identified by immunolabeling. Gene-editing enzyme Cas9 and guideRNA complexed by liposomal reagents, RNAiMAX and Lipofectamine 2000, were injected to Atoh1-GFP mouse inner ear. Gene editing was assessed by disappearance of signal in the target cells and by new generation sequencing (NGS) to identify indels in the target genes.

Results

Microinjection of (-30)GFP-Cre and (+36)GFP-Cre into P1 Rosa-tdTomato$^{f/f}$ cochlea resulted in tdTomato signal in 30% of hair cells near the injection site. tdT^{+} hair cells survived with intact stereocilia. No tdT^{+} was seen in control cochlea. Comparison of RNAiMAX and Lipo2000 formulations shows that Lipo2000 produced highly efficient Cre protein uptake by hair cells, over 90% of them became tdT^{+}. To study the feasibility of delivering Cas9/gRNA for CRISPR-mediated gene editing, Cas9 and gRNA (against GFP) complexed by Lipo2000 were injected into the Atoh1-GFP mouse cochlea. 20% of hair cells showed disappearance of GFP signal as the result and NGS showed indels in the GFP gene, a demonstration of CRISPR-mediated gene editing in hair cells. All hair cells survived with interact stereocilia. Cas9/gRNA complex was then delivered into hair cells to target the EMX gene, resulting in indels in the EMX gene in the injected animals only.

Conclusion

Supercharged proteins and liposomal formulation can be used to efficiently deliver genome-editing proteins into mouse hair cells *in vivo,* resulting in specific gene editing. This technology should enable the editing of gene mutations to correct genetic deafness, and to study inner ear protein functions. It can be developed to deliver unlimited combinations of proteins for biophysiology study and be used as a protein-based therapy in regeneration in mammalian inner ear.

PD-90

Robust Reporter Activity 8 Weeks After Doxycycline Administration Indicates Persistent Rather than Transient Expression of rtTA Driven Tet-On Transgenes in the Mouse Inner Ear.

Bradley Walters; Jian Zuo

St. Jude Children's Research Hospital

Genetic mouse models provide invaluable tools for discerning gene function *in vivo*. Tetracycline-inducible systems (Tet-On/Off) provide temporal and cell-type specific gene expression, offering an alternative or even complementary approach to existing Cre/LoxP systems. The primary advantage of Tet-On/Off systems over other commonly used methods is that they allow for transient manipulation of genes of interest (GOIs). Specifically, tetracycline, or its more potent derivative doxycycline (Dox), must be present for a given GOI to be expressed (when combined with an rtTA protein) or repressed (when combined with a tTA protein). Here we have characterized a Sox10$^{rtTA/+}$ knock-in mouse line which demonstrates inducible reverse tetracycline trans-activator (rtTA) activity and Tet-On transgene expression in the inner ear following Dox induction at several different ages. These Sox10$^{rtTA/+}$ mice actively drive Tet-On transgene expression in Sox10 positive cells in the inner ear, and do not exhibit any readily observable developmental or hearing phenotypes. Sox10$^{rtTA/+}$ activity was revealed by multiple Tet-On reporters to be relatively ubiquitous in the inner ear following embryonic inductions, and notably absent from hair cells, tympanic border cells, and ganglion neurons following postnatal inductions. Surprisingly, Sox10$^{rtTA/+}$ driven reporter expression in the inner ear persisted for at least 54 days after cessation of neonatal induction, presumably due to the persistence of Dox within the inner ear. Despite the persistent reporter expression that followed neonatal induction, Sox10$^{rtTA/+}$ activity in the inner ear was uninducible in 4-week old mice. Reporter expression could be rescued by co-administration of the loop diuretic furosemide following Dox injection. However, this method also caused significant cochlear hair cell loss. While these findings do suggest that the Sox10$^{rtTA/+}$ mouse line is still a powerful tool for functional genetic studies of the inner ear *in vivo,* they also reveal some important considerations for future studies that may rely upon Tet-On/Off systems. Namely, Dox induced Tet-On gene expression may not be transient in the inner ear, and the induction of rtTA activity in the inner ears of juvenile and adult mice is limited by the inability of Dox to cross the blood-labyrinth barrier. Furthermore, even when Dox is permitted to enter the

cochlear labyrinth, it can have ototoxic effects at concentrations required to drive transgene expression.

PD-74

Unsupervised Parcellation of the Macaque Auditory Cortex from Resting-State fMRI

Eren Gultepe[1]; Jason Gallivan[2]; R Matthew Hutchison[3]; Stefan Everling[1]; Ingrid Johnsrude[1]

[1]Western University; [2]Queen's University; [3]Harvard University

In humans and other animals, resting-state fMRI (rs-fMRI) is now a standard technique used to measure spontaneous patterns of functional connectivity in the brain. Spatial correlations of low-frequency BOLD oscillations are used to characterize broad-scale neural networks and to reveal functionally distinct brain regions [1]. But do parcellations based on rs-fMRI data correspond to those based on anatomical (e.g., cytoarchitectonic) parcellations? In macaques, anatomical parcellation according to cytoarchitectonic criteria is well established [2,3], and so a comparison of anatomical and rs-fMRI parcellation can be performed. Here, we determine whether macaque rs-fMRI data can be used to discriminate six cytoarchitectonically characterized auditory cortical regions: the core areas medial (AKM) and lateral (AKL) auditory koniocortex; and belt areas prokoniocortex (ProK), and caudal (PaAC), rostral (PaAR), and lateral (PaAL) para-auditory areas. Rs-fMRI data were collected on a 7T MRI system from 10 macaque monkeys (7 M. fascicularis; 3 M. mulatta) anesthetized with 1% isoflurane. Registration to the MNI macaque atlas [4] (including both macaque species) and standard rs-fMRI preprocessing [5] were performed. Time-series data from voxels within the ROI (the 6 anatomical areas) were analyzed using spectral clustering, an unsupervised learning algorithm that is able to find non-spherical groupings in data. The clustering results were assessed by determining the overlap accuracy (relative to the anatomical parcellation) and this was compared, across animals, to the clustering performed on the basis of spatial proximity alone (voxel coordinate locations). Accuracy based on spatial proximity was 0.654. Accuracy based on spectral clustering of rs-fMRI was 0.678±0.0195. Clustering based on rs-fMRI data significantly improved the overlap between clusters and underlying anatomical areas ($t(9)=3.89$, $p<0.01$, one-sample t-test). This affirms that rs-MRI signals may contain information related to anatomical structure. Further feature selection rather than direct application to voxel signal may improve clustering performance. These methods may be of great use for the anatomo-functional parcellation of human cortex of humans, even when cytoarchitectonic or other anatomical parcellation data are not available.

References

1. Beckmann M, Johansen-Berg H, Rushworth MFS. J Neurosci. 2009;29:1175–1190.

2. Hackett TA, Preuss TM, Kaas JH. J Comp Neurol. 2001;441:197–222.

3. Paxinos G, Huang XF, Petrides M, Toga AW. The Rhesus Monkey Brain in Stereotaxic Coordinates. San Diego, CA: Academic Press; 2009

4. Frey S, Pandya DN, Chakravarty MM, Bailey L, Petrides M, Collins DL. NeuroImage. 2011;55:1435–42.

5. Murphy K, Birn RM, Bandettini PA. Neuroimage. 2013;80:349-59.

PD-75

Pitch-Responsive Brain Regions are Present in Humans but not Macaque Monkeys

Sam Norman-Haignere[1]; Nancy Kanwisher[1]; Joshua McDermott[1]; Bevil Conway[2]

[1]Massachusetts Institute of Technology; [2]Wellesley College

Introduction

Many real-world sounds are periodic (e.g. voiced speech, many animal calls, music), and evoke a "pitch" percept that varies with the repetition rate. Humans possess stereotyped brain regions, overlapping with and extending anteriorly from primary auditory cortex, that respond substantially more to pitch-evoking sounds than sounds without a pitch (Patterson et al., 2002; Norman-Haignere et al., J. Neurosci., 2013). These regions can be reliably identified in individual participants with fMRI, by contrasting responses to harmonic tones and noise. Currently, it remains unclear whether non-human animals possess homologous regions (Schwarz et al., 1990; Bendor and Wang, 2005; Bizley et al., 2009), because different techniques have been used to assess pitch responses in humans and animals—fMRI in humans and microelectrode recording in animals. In particular, although microelectrode recordings provide cellular resolution, their spatial coverage is more limited than that of fMRI. Here we address the issue by directly comparing fMRI responses measured in macaque monkeys and humans under the same experimental conditions.

Methods

We measured fMRI responses in three awake rhesus macaque monkeys and four human subjects to harmonic tones and frequency-matched noise, each presented in five different frequency ranges. This factorial design allowed us to separately investigate responses to pitch and frequency.

Results

In all of the humans and monkeys tested, we observed fMRI voxels that were selective for different frequency ranges, reflecting cortical tonotopy. All of the human subjects also exhibited voxels that were robustly pitch-selective, responding more to tones than frequency-matched noise. In contrast, we did not observe any voxels in any of the monkeys that responded preferentially to the tones compared with the noise.

Conclusions

These results provide the first direct evidence that the neural organization of human pitch processing differs substantially from another Old-World (Cercopithecidae) primate. These results also provide one of the first examples of a substantial difference in functional organization between the sensory cortices of two primate species.

PD-76

The Contribution of the Core and Belt Regions of the Auditory Cortex to Figure-Ground Segregation: How Do We Hear in Noise?

Sharath Bennur; Yale Cohen
University of Pennsylvania

The ability to detect a behaviorally relevant sound, which is embedded in a noisy background, is a critical function of the auditory system. While this ability has been studied in both anesthetized and passively listening animals, the relationship between cortical activity and an animal's ability to detect a sound in a noisy background has not been fully elucidated. Further, the differential contributions of the core and anterolateral belt regions of the auditory cortex to this figure-ground segregation problem are not known. Thus, the goal of our study was to identify their contributions to figure-ground segregation. To accomplish this goal, we trained rhesus monkeys to participate in two tasks: the 'target-in-noise' and the 'noise-only' task. In the target-in-noise task, a target tone was presented in a background of masking co-modulated noise (bandwidth=0.5-16 kHz). If the monkeys heard the target, they released a lever following target offset and obtained a juice reward. The sound level of the target tone varied between 60 dB SPL and 85 dB SPL in 5 dB intervals, whereas the level of the masking noise was always 60 dB SPL. During the noise-only task, only the masking noise was presented, and monkeys were rewarded for maintaining their grip on the lever; this task generated catch trials. While the monkeys were participating in these tasks, we recorded neural activity in the auditory cortex; the frequency of the target tone was set to the best frequency of the recorded auditory neuron.

We found that the monkeys' performance varied as a function of the level of the tone: as tone level increased, the proportion of correct trials increased. We also found that the activity of belt neurons was not correlated with the physical characteristics of the stimulus (i.e., the sound level of the target relative to that of the masking noise). This finding contrasts with our findings in the core auditory cortex: core neurons, on average, varied smoothly with the relative level of the target. Furthermore, unlike core activity, the activity of belt neurons was modulated by the animal's decision (i.e., behavioral choice) as well as the arrival of the monkeys' reward. In summary, belt neurons encode behavioral responses and outcomes rather than the physical characteristics of the auditory stimulus. These findings are consistent with the hypothesis that the core and anterolateral belt regions of the auditory cortex are part of an information-processing pathway that mediates components of auditory perception.

PD-77

Cross-modal Attenuation of the N1 Peak of the Cortical Auditory Evoked Potential (CAEP) Correlates with Speech in Noise Understanding in Individuals with Hearing Loss

Allison Bradley; Jun Yao; Jules Dewald; Claus-Peter Richter
Northwestern University

Introduction

People with hearing loss vary in their ability to understand speech in background noise. This variance is likely due to differences in central processing, as people with similar peripheral auditory function (as measured by audiograms) can have remarkably different speech in noise (SIN) thresholds. One measure of central auditory processing that has been related to SIN thresholds of cochlear implant users is the attenuation of the amplitude of the N1 peak of the cortical auditory evoked potential (CAEP) to repeated stimuli. CI users with more N1 attenuation had better SIN thresholds. A similar attenuation of cortical potential amplitude with repeated stimuli occurs with visual and somatosensory stimuli, and attenuation can also be induced cross-modally - e.g. an auditory stimulus following a visual stimulus is attenuated.

The goal of this study was to determine if cross-modal N1 attenuation is related to the SIN thresholds of people with mild to moderate hearing loss. We expect participants who have better SIN thresholds to have more attenuation of the N1 peak of the CAEP following a visual stimulus than those with poorer SIN thresholds.

Methods

SIN thresholds of 11 participants with mild to moderate hearing loss were determined with 3 repetitions of the QuickSIN test. CAEPs were recorded in response to 1kHz tone bursts with 32 electrode electroencephalography in the same individuals. Responses were recorded in 3 conditions: auditory with no preceding stimulus (A1), auditory following an auditory stimulus (A2), and auditory following a visual stimulus (Av1; see schematic). The attenuation of the CAEP amplitude following a visual stimulus (Av1 in comparison to A1) and following an auditory stimulus (A2 in comparison to A1) was measured. The relative attenuation in each condition was then correlated with the SIN threshold of each participant.

Results

A correlation of 0.73 was found between the degree of cross-modal attenuation of the N1 peak of the CAEP by a preceding visual stimulus and SIN thresholds, i.e. participants with more attenuation had better SIN perception. A correlation of 0.9 was found between hetero-modal auditory N1 attenuation and SIN thresholds of the same participant group.

Auditory condition:

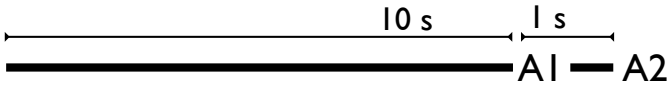

Visual attenuation condition:

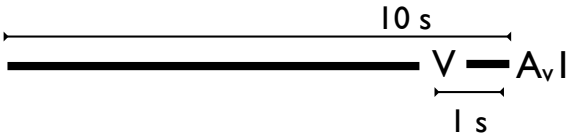

Conclusion

The ability to understand speech in background noise is related to central neural processes that are not specific to the auditory system.

PD-78

Object-related Deviants in Auditory Cortex of the Guinea Pig

Simon Jones; David McAlpine
UCL

Oddball stimulus blocks typically consist of pure tones of either a common standard frequency or a rare deviant frequency and are widely used in human and animal studies . Extensions of this work in humans employ oddball blocks of harmonic complexes, including where one or more components is mistuned. Here, we examined whether guinea pig cortex differentiates between tuned and mistuned complexes presented in oddball blocks. The (human) perception is one of an object 'popping-out' from a harmonic stack when one component of the stack is mistuned. We compared the responses to such pop-out stimuli with responses to stimuli in which each component is mistuned by the same amount to produce an inharmonic stack with the same periodicity.

A 16-channel electrode was implanted through a 16-channel surface electro-corticogram array into A1. Stimuli consisted of two runs of 3 blocks of 500 stimuli; a control with equal numbers of 400ms duration tuned and mistuned harmonics followed by two blocks with a 90-10% and 10-90% division. In one run only a single harmonic component was mistuned. In the other all components were subject to the same numeric shift when mistuned. For all harmonic complexes the fundamental frequency was 200Hz, the first 12 harmonics were used (up to 2400Hz), mistuning was applied to the 400Hz component in the first run which was mistuned to 464Hz (16% mistuning), in the second run all components were mistuned by 64Hz. The presentation period was fixed at 1300ms.

Most A1 sites scored a higher SI for harmonic complexes with a single mistuned component than tuned complexes. This increased difference between standard and deviant was not present for most sites when the entire complex was shifted out of tune.

A1 responds differently to deviant mistuned components than to either deviant harmonic complexes or discordant complexes. Spectral differences between the 400Hz component when tuned and mistuned to 464Hz do not account for this as the difference is abolished when all components are shifted by 64Hz. The context of the other components determines the response. When all components are in tune there is a single harmonic object, when all components are mistuned the discordant set could be interpreted as a single inharmonic object. When only one component is mistuned this single tone can be "heard out" as a second object. It is this difference in the number of objects that accounts for the difference in cortical response.

PD-79

Attention Modulates Adaptation of Human High-Frequency Cortical Auditory Responses

Steven Eliades[1]; Anna Korzeniewska[2]; William Anderson[2]; Deepti Ramadoss[2]; Liana Sanders[2]; Nathan Crone[2]; Dana Boatman-Reich[2]
[1]University of Pennsylvania; [2]Johns Hopkins School of Medicine

Introduction

Cortical auditory responses to repetitive sounds decrease with increasing stimulus probability, a phenomenon known as adaptation. Although adaptation is thought to improve detection of novel or rare sounds, previous studies in animals and humans have relied largely on passive listening paradigms. The effects of attention on the temporal and spatial dynamics of cortical adaptation, therefore, remain largely unknown.

Methods

We investigated effects of attention on cortical high-frequency responses (> 60 Hz) to tones and speech using intracranial electrocorticography (ECoG) recordings from six epilepsy patients with implanted subdural electrode arrays. Subjects engaged in passive and active-attended (button-press) versions of a 300-trial auditory oddball task, consisting of frequently repeated stimuli (tones: 1000 Hz, speech: /ba/) with a second infrequently interspersed stimulus (tones: 1200 Hz, speech: /da/). Time-frequency analysis was used to measure event-related changes in high gamma (70-150 Hz) oscillations under attended and unattended listening conditions. Single-trial analyses were performed to determine the time course of adaptation as a function of stimulus probability. Functional connectivity patterns between ECoG recording sites were computed using event-related causality (ERC), a multichannel technique based on Granger causality to estimate changes in effective connectivity.

Results

We found that attending to an infrequent (oddball) target stimulus 1) enhanced cortical high-gamma responses to the target stimulus relative to passive listening, and 2) delayed and reduced adaptation of responses to the non-target (frequent) stimulus. Target detection was also associated with delayed or long-latency activity, particularly over non-auditory brain areas including frontal and parietal lobes. ERC analyses revealed increased connectivity during attended listening

conditions with repetition-related changes in the balance of inflow and outflow between auditory cortex and other cortical areas, particularly frontal cortex.

Summary
These results suggest that attending to an infrequent target sound modulates the magnitude and time course of cortical auditory response adaptation, as well as the flow of auditory information between cortical areas. The observed changes in connectivity may be a mechanism for selective attentional modulation of adaptation that could enhance detection of infrequent or rare sounds in the setting of regularities in the acoustic background.

PD-80

Cortical Feedback Modulates Adaptive Gain Control in the Midbrain

Daniel Polley[1]; Charles-Henri Vila[2]; Ross Williamson[3]; Kenneth Hancock[1]
[1]Harvard Medical School, Massachusetts Eye and Ear Infirmary; [2]Section of Life Science and Technologies, Ecole Polytechnique Fédérale de Lausanne, Switzerland 1015; [3]Center for Computational Neuroscience and Neural Technology, Boston University, Boston MA 02215

Background
Sound representations at higher levels of the CNS are dynamically maintained by modulatory control systems that vary widely in their mechanisms, forms, and time scales of operation. For example, the neural encoding of sound level can be modulated by stimulus context on relatively short time scales in a manner that matches maximally informative firing rate changes to statistically over-represented sound levels (Dean, Harper, & McAlpine, 2005). Adaptation to stimulus statistics is a general phenomenon that enhances the representational salience of frequently encountered sound features at levels ranging from the auditory nerve to cortex. However, these effects have typically been characterized in the lemniscal feedforward pathway of anesthetized animals, experimental conditions that tend to underestimate the potential involvement of descending corticofugal feedback. This leaves open the question as to whether higher levels of auditory processing might be better at seeing the “forest for the trees”, thereby adapting more rapidly and completely to shifts in stimulus statistics and, in the awake condition, ‘download’ these adjusted models to lower brain areas.

Methods
We explored these ideas by documenting the time course and overall strength of adaptation in the primary auditory cortex (A1) as well as both central and external subdivisions of the inferior colliculus (IC) in awake, head-fixed mice. We characterized dynamic sound level encoding using 50 ms broadband noise tokens that switched every 5s between two distributions that differed in mean level. We used a diode laser in combination with cortical injections of viral constructs encoding ‘Chronos’, an ultra-fast channelrhodopsin, to activate A1 neurons with millisecond precision during extracellular unit recordings.

Results
Firing rates adapted to a steady state within several hundred milliseconds of a switch between sound level distributions. Steeply sloping regions of rate-level functions shifted back and forth to match the mean of each sound level distribution. Because optogenetic activation of A1 neurons with a generic light stimulus produced relatively weak, ambiguous effects on IC units, we used a real time spike feedback optimization algorithm (Chambers et al., 2014) to identify A1 activation patterns that could alternately enhance or suppress sound-evoked unit activity in the IC. Using each type of cortical feedback signal, we then demonstrated that the rate and completeness of IC adaptation to sound level statistics could be bi-directionally modulated according to the temporal patterning of spiking in cortical projection neurons.

Conclusions
These results establish a framework for studying corticofugal modulation in the context of active listening.

PD-81

Spike Timing Error Encodes Sound Envelope Shape in Three Auditory Cortical Fields

Heather Read; Christopher Lee; Monty Escabi; Monty Escabi
University of Connecticut

Animals can discriminate changes in the sound envelope amplitude that create shape temporal cues for perception of loudness and timbre (Irino and Patterson 1996). In primate primary (A1) auditory cortex, sound shapes are represented with a shape-dependent spike rate increase (Wang, Lu et al. 2008). Alternatively, cortical spike rate increase could have a shape-dependent spike-timing error (jitter) as observed in auditory midbrain (Zheng and Escabi, 2008, 2013). Here we ask whether spike-timing error varies systematically to represent sound shape in primary (A1) and ventral non-primary auditory cortical fields in the rat.

Fifty-five unique shaped periodic noise sequences are generated to probe sensitivities to sound shape and modulation frequency. A basis-spline (b-spline) filter function is convolved with a periodic impulse train at a given modulation frequency to generate a shaped periodically modulated sound envelope. The unfrozen noise is then modulated by each periodic envelope to generate a periodic noise sequence. The b-spline frequency cutoff (Fc) is varied from 2 to 64 Hz to generate a range of envelope shapes used to probe neural sensitivities. Sounds are presented through calibrated earbars and single unit responses are recorded in anesthetized rat temporal cortex. Shuffled correlation analyses is used to quantify spike-timing errors (jitter and reliability) (Zheng and Escabi, 2008).

The results indicate that neurons in all three cortical fields respond with an isomorphic increase in spike-timing jitter to systematic changes in sound shape. Reliability does not change appreciably with sound shape in all three fields. In contrast, jitter decreases logarithmically with shape Fc for individual neurons and across neuron populations in A1 and

ventral cortical fields. A1 responses are primarily sound rising envelope of each sound with low spike-timing jitter indicating more precise temporal cue encoding than ventral fields. In contrast, ventral fields have sustained responses following the shape of the periodic noise sequences. Across regional neuron populations, average spike-timing jitter is rank ordered with: A1 < VAF < cSRAF. These differences suggest a functional hierarchy whereby later developing ventral auditory cortical fields respond with greater spike-timing jitter, possibly due to slower temporal integration times or differences in thalamic input pathways. This study supports the notion that spike-timing error is not simply "noise", as it can serve to encode sound envelope shape.

SYM-60

The Role of Planar Polarity Signaling in Directional Neuron Migration

Cecilia Moens[1]; Crystal Davey[2]; Andrew Mathewson[2]
[1]Fred Hutchinson Cancer Research Center; [2]Fred Hutchinson Cancer Research Center and University of Washington

The migration of immature neurons from germinal zones to their functional destinations is an essential step in establishing a functional neural circuit. The facial branchiomotor neurons (FBMNs) undergo a well-characterized migration in the plane of the hindbrain neuroepithelium from rhombomere 4 to rhombomere 6. Rather than identifying chemotropic signals or receptors, forward genetic screens in the zebrafish for FBMN migration mutants have identified mutations in almost all of the core components of the Planar Cell Polarity (PCP) pathway (Vangl2, Fz3a, Pk1b, Celsr3 and Scrib). The PCP pathway is best known as a cell contact-mediated mechanism for transmitting polarity information in the plane of an epithelium. Although components of the PCP pathway have been shown to be essential for a number of cell migratory events, how PCP controls a highly dynamic process like neuronal migration is not understood. FBMNs contact a variety of tissues during their migration including the segmented hindbrain neuroepithelium, the floor plate and other migrating FBMNs. *Where* PCP signaling is required for FBMN migration is controversial. Most studies have identified a cell-non-autonomous role for PCP, but which cells promote FBMN migration, and how they use the PCP pathway to do so, is unknown. We show that PCP signaling is required both within FBMNs and in their rhombomere 4 environment for migration. Focusing on the role for PCP signaling within FBMNS, we reasoned that since cell migration results from the contact-dependent stabilization of cellular protrusions, cellular protrusive activity may be affected in PCP mutant FBMNs. We examined the membrane dynamics of single FBMNs undergoing migration in wildtype and PCP mutant embryos using high-resolution single-cell timelapse microscopy in vivo. Using chimeras we have uncovered opposing cell-autonomous functions for the PCP components Fzd3a and Vangl2 in regulating FBMN protrusive activity: within FBMNs, Fzd3a is required to stabilize filopodia while Vangl2 has an antagonistic destabilizing role. Consistent with a role for Vangl2 in regulating filopodia dynamics, we have found that Vangl2 localizes to the tips of a subset of FBMN filopodia and this localization correlates with retraction events. Together, our findings suggest a model in which PCP signaling between the planar polarized neuroepithelial environment and the FBMNs initiates their directional migration by the selective stabilization of FBMN filopodia.

SYM-61

Assembling and Maintaining Plane-Polarized Sensory Synaptic Connectivity

Hernan Lopez-Schier
Helmholtz Zentrum München

In the zebrafish, two to four postsynaptic afferent axons converge into peripheral mechanosensory organs called neuromasts, which contain hair-cell receptors of opposing planar polarity. Each axon exclusively synapses with hair cells of identical polarity to transmit unidirectional mechanical signals to the brain. The mechanism that governs this exceptionally accurate polarity-selective connectivity remains unknown. We will show that converging axons are mutually dependent for polarity-selective synaptogenesis during development and regeneration, and that a mechanism based on inter-axonal interactions may represent a general solution to maintain coherent synaptic transmission in sensory organs undergoing frequent variations in the number and spatial distribution of receptor cells.

SYM-62

The Border of the Emx2 Expression Domain Within the Macula Determines the Line of Polarity Reversal

Doris Wu; Tao Jiang
NIDCD - NIH

Background

Each sensory organ of the inner ear exhibits a specific pattern of stereociliary bundle orientation. Disruption of the inter- or intra-cellular planar cell polarity (PCP) complex such as Frizzled-Van Gogh-Disheveled and Gai-Inscutable-Par causes stereociliary bundle misalignment, respectively. However, the role of these proteins in coordinating stereociliary pattern specific for each sensory organ is not clear. In the mouse utricle, stereociliary bundles are oriented towards each other across two regions of the organ: the lateral extrastriola (LES) in one and the striola and medial extrastriola (MES) in the other, creating a line of polarity reversal between these two regions. In the *Emx2* null utricle, this line of polarity reversal was reported to be absent and hair bundles in the LES are reversed pointing in the same lateral direction as those in the striola and MES. Our gene expression results indicate that *Emx2*, which encodes a transcription factor, is expressed only in the LES. Therefore, it is possible that the unidirectional hair bundle phenotype reported in the *Emx2* mutants is due to loss of the LES rather than a planar polarity defect in hair cells. To distinguish between these possibilities, we investigated whether the LES is absent in the *Emx2* null utricles by tracing its *Emx2* lineage domain.

Methods
Analysis of *Emx2* lineage in *Emx2* null mutant background was conducted in *Emx2*$^{cre/cre}$*; Rosa*^{tdT} utricles, generated by crossing *Emx2*^{cre} with *Emx2*^{cre}*; Rosa*^{tdT} mouse strains.

Results
Based on the tdTomato reporter activity, the lineage domain of *Emx2* in the *Emx2*$^{cre/+}$*; Rosa*^{tdT} control utricle is located in the LES, consistent with the gene expression results. The border of the lineage domain within the utricle coincides with the line of polarity reversal. We determined that *Emx2*$^{cre/cre}$ homozygous embryos are perinatal lethal that exhibit similar defects in the inner ear, kidney and brain as *Emx2* nulls, suggesting that *Emx2*^{cre} is a null allele. The tdTomato reporter domain in *Emx2*$^{cre/cre}$*; Rosa*^{tdT} mutant utricles is in the lateral utricular region, similar to that of the heterozygous controls (*Emx2*$^{cre/+}$*; Rosa*^{tdT}).

Conclusions
Our lineage results indicate that the absence of *Emx2* causes stereociliary bundle reversal of hair cells in LES. Based on these results and the coincidence of the line of polarity reversal with the border of the *Emx2*-lineage domain in the normal utricle, we propose that Emx2 normally functions to reverse hair bundle orientation in the LES and establishes the line of polarity reversal in the macula.

SYM-63

A Hierarchy of Signaling Mechanisms Initiates and Coordinates Stereociliary Bundle Planar Polarity

Michael Deans
University of Utah

The mechanosensory hair cells of the inner ear have emerged as one of the primary models for studying the development of planar polarity in vertebrates. Planar polarity is the polarized organization of cells or cellular structures in the plane of an epithelium. For hair cells planar polarity is most apparent at the *sub-cellular* level because of the polarized organization of individual stereociliary bundles. However hair cells do not function in isolation and it is clear that a hierarchy of planar polarity signals is required to build the intact, planar-polarized sensory epithelia. This hierarchy appears to be organized along three anatomical scales. Thus in addition to sub-cellular polarization signals, distinct *inter-cellular* planar polarity signals coordinate the orientation of stereociliary bundles between adjacent cells. This signaling pathway is more commonly called Planar Cell Polarity (PCP) and has been described in the greatest detail for auditory hair cells of the cochlea. Mutations in PCP genes result in hair cells with polarized stereociliary bundles that are misoriented relative to neighboring cells. The third level of planar polarity, or *tissue polarity*, is the broadest and is necessary in part to establish the line of polarity reversal (LPR) in the utricle and saccule. The LPR is a cell boundary that lies between two groups of hair cell that have opposite stereociliary bundle polarities. Remarkably PCP proteins are not required to pattern the LPR. Based upon these anatomical observations and the analysis of PCP gene mutants I propose a model in which intercellular signaling via core PCP proteins functions solely to coordinate the orientation of adjacent cells and that other pathways are required to established polarized bundles and align them relative to the geometry of the inner ear. The vestibular maculae are the ideal models for studying these inter-related signaling pathways because the three tiers of the anatomical hierarchy are readily apparent in the same sensory organ.

SYM-64

Molecular Differences Between Tissue Polarity and Translational Polarity in Mammalian Cochlear Epithelium

Mireille Montcouquiol
INSERM - Neurocenter Institute Mireille Montcouquiol Planar Polarity and Plasticity Group, INSERM U862, Neurocentre Magendie, 33077 Bordeaux, France. Université Bordeaux, Bordeaux, 33000, France

The mammalian cochlear epithelium has been branded as one of the best mammalian system to study PCP, and has often been compared to Drosophila wing or eye in terms of mechanisms. One of the major differences between the two systems is that the precise migration of the unique cilium at the apical surface of hair cells in the cochlea (also called translational polarity), defines PCP before the actin-rich bundle has developed and is polarized. This important role of the cilia in hair cells' PCP is in contrast with Drosophila eye or wing cells where cilia do not appear to play major role during PCP establishment. Other important mammalian cell types, such as node cells establishing left-right asymmetry or ependymal cells lining the ventricles of the brain also rely on polarized cilia migration for proper function, and understanding the basis of this difference has raised interest in the recent years (Guirao et al. 2010, Song et al. 2010).

Recent studies have set the stage in the cilia/polarity field by unveiling two important features in ciliated cells: 1/ there is a close relationship between the core PCP genes and the cilium (Jones et al. 2008, Borovina et al. 2010), and 2/ core PCP signaling alone is insufficient to establish asymmetric cortical domains to direct cilia migration within individual cell (Deans et al. 2007). The relationship between the cilium and core PCP remains under scrutiny because still controversial and awaits clarification (Wallingford 2010, Bayly and Axelrod 2011).

I will discuss how these data can be reconciled in mammalian ciliated cells.

SYM-65

Mechanotransduction at Intercellular Junctions Regulates Planar Cell Polarity in the Organ of Corti

XiaoWei Lu[1]; Jianyi Lee[2]; Anna Andreeva[2]; Robert Ross[3]
[1]University of Virginia Health System; [2]University of Virginia; [3]UCSD School of Medicine

During tissue morphogenesis, planar cell polarity (PCP) signaling acts in both epithelial and non-epithelial cells to drive polarized cell behaviors within the plane of the tissue. The

mammalian auditory sensory epithelium, or the organ of Corti, serves as a preeminent model for epithelial PCP. Specifically, the polarized V-shape of the actin-based stereociliary bundles atop auditory hair cells and their uniform orientation are key features of PCP in the organ of Corti. During development, the eccentric positioning of the kinocilium and the associated basal body plays an instructive role in establishing the V-shape of the hair bundle. Recent advances reveal that this is controlled by microtubule cortical capture through a cell-intrinsic machinery including G protein and Rac-PAK signaling. On a tissue level, the core PCP pathway and a novel Protein Tyrosine Kinase 7 (PTK7)-mediated pathway act in concert to mediate the uniform orientation of the hair bundles across the organ of Corti.

PTK7 is a receptor tyrosine kinase-like molecule. To dissect the mechanisms by which PTK7 transduces tissue polarity cues during epithelial morphogenesis, we have taken a multipronged approach including knockout/knockin mouse models, cell and cochlear explant cultures and fluorescence live imaging. We show that PTK7 regulates intercellular tension and actomyosin contractility through Src family kinases (SFKs). We have further identified the Rho-associated protein kinase member ROCK2, as well as Vinculin, a tension-sensitive actin binding protein as in vivo targets of PTK7-SFK signaling. We found evidence that these targets in turn mediate anisotropic junctional tension through regulation of both myosin II and actin dynamics. Our data suggest that PTK7-SFK-mediated mechanotransduction may impinge on the cell-intrinsic polarity machinery both by direct phosphorylation and indirectly through the "tug-of-war" interactions between cochlear epithelial cells, to promote positioning of the kinocilium at the lateral poles of hair cells, thereby orienting hair cell PCP.

SYMK-66

Unreliable Recognition of Noise and Repeating Noise

Trevor Agus[1]; Daniel Pressnitzer[2]
[1]Queen's University Belfast; [2]Laboratoire des Systèmes Perceptifs, UMR 8248, CNRS and Ecole normale supérieure, Paris, France

In order to recognize sounds, we need to pick out re-occurring features from sounds. Agus et al. (2010, *Neuron*) showed that listeners were able to learn re-occurring segments of white noise surprisingly quickly (within 5 trials). A series of subsequent experiments (Agus and Pressnitzer, 2013, *J. Acoust. Soc. Am.*) decorrelated within-trial repetitions and between-trial reoccurrences, making it possible to distinguish effects of repetition detection and recognition.

In a first experiment, normal-hearing listeners were trained to distinguish repeating noises ("RNs"), two identical half-second noise segments without any intervening silence, from non-repeating noises ("Ns"), formed similarly, but with two unrelated noise segments. These Ns and RNs were generated afresh on each trial. In contrast, an arbitrary "reference noise" was fixed across a block of trials, and was used to generate a "reference repeating noise" (RefRN) and a non-repeating noise in which the reference noise was embedded ("Mixed"). Listeners were not told in advance that the RefRN and Mixed stimuli would be included.

The listeners reported repetitions for the RefRN stimuli more often than the RN stimuli, which was interpreted as being indicative of learning of the reference noise. False-alarm rates also differed for the N and Mixed stimuli, showing that listeners were able to recognize the embedded reference noise even without its immediate repetition. Surprisingly, repetitions were (incorrectly) reported more often for the Mixed stimuli than for the N stimuli.

In a second experiment, five of the same listeners repeated the same procedure, this time with full knowledge of the design of the experiment, including the learnable reference noise and the RefRN and Mixed stimuli. The listeners reported fewer repetitions for all stimuli, but the trend to report more repetitions in Mixed than N stimuli was not reversed.

In a third experiment, naïve listeners reported excessive repetitions in a Mixed stimulus in a block of trials that contained no RefRN stimuli. This showed that listeners could learn the reference noise in the absence of immediate repetitions, highlighting a powerful learning mechanism that combines auditory information over non-negligible time spans.

Some of the more counterintuitive features of the results can be explained by models of the psychoacoustical conception of internal noise. They are consistent with listeners finding it easier to recognize the reference noise (d' = 2.0) than detect repetitions (d' = 0.7), confusing the perceptions of the two manipulations to some extent.

SYM-67

Neural Noise and Stimulus Correlations Define Optimal Auditory Representations

Tatyana Sharpee
Salk Institute for Biological Studies

In this talk I will describe a set of theoretical results for how the interaction between stimulus and noise correlations defines the optimal allocation of neurons among different classes, as well as the preferred stimulus features for neurons in each class. These results outline a framework for quantifying how responses of different types of neurons are combined to maximize information transition. While conventionally neuronal classes are defined based on differences in their preferred stimulus features, in the small noise limit, multiple classes of neurons appear that are differentiated by their nonlinear properties, and not by their preferred feature. Theoretical predictions will be tested against neurophysiological recordings from high-level auditory neurons.

SYM-68

Increased Internal Noise Following Juvenile Conductive Hearing Loss

Antje Ihlefeld[1]; Dan Sanes[2]
[1]New Jersey Institute of Technology; [2]New York University

Auditory processing is thought to depend on two types of neural activity: sound driven activity and maintained discharge that is produced within the nervous system, called “internal noise.” Hearing impaired listeners often display auditory performance deficits, and this outcome is commonly attributed to cochlear dysfunction. However, a principal corollary of hearing impairment, sound deprivation, also impacts central nervous system (CNS) function. Developmental sound deprivation can alter membrane and synaptic properties across the entire auditory CNS, and may reduce behavioral sensitivity. The central basis for behavioral deficits in hearing impaired listeners could arise from decreased sound-evoked responses and/or increased internal noise. Here, we asked whether internal noise increases following developmental conductive hearing loss (CHL).

Experiments utilized the Mongolian gerbil (*Meriones unguiculatus*), an animal with excellent low frequency hearing, similar to humans. Internal noise was quantified with the equivalent noise method (EQNM). EQNM theory posits that when external noise is present (e.g., as background noise in a detection task), external noise will raise sensory thresholds if, and only if, external noise intensity exceeds internal noise intensity.

Experiment 1 tested 5 control (CTL) gerbils in an appetitive Go/NoGo task, to detect the presence of a tone (1 s, 1 kHz; 10 ms rise/fall) in a background of continuous noise. The noise had a flat envelope modulation spectrum, and spectrum level was varied across sessions from 13 to 43 dB SPL/Hz. Within each session, the noise intensity was fixed, and tone intensity was varied randomly from trial to trial to determine thresholds with the method of constant stimuli. Experiment 2 tested 3 gerbils that were reared with permanent bilateral conductive hearing loss (CHL), implemented by removal of the malleus at postnatal day 10. Stimuli were identical to Experiment 1, except that sound intensity was adjusted to compensate for the higher audibility thresholds.

Results show that mean 1 kHz audiometric thresholds in quiet were 5.8 dB SPL in CTL and 40.2 dB SPL in CHL. EQNM estimated that internal noise equaled 2.7 dB SPL in CTL, and 29.6 dB SPL in CHL. Thus, in CTL, the audibility threshold for detecting a tone in quiet was 3 dB above the internal noise floor. However, in CHL animals, the audibility threshold was 10 dB above the internal noise floor. Together, results suggest that juvenile sound deprivation can raise internal noise.

[supported by NIH DC014008 to AI; DC009237 to DHS]

SYM-69

Understanding the Network for Top-Down Control of Auditory Representation

Stephen David; Zachary Schwarz
Oregon Health and Science University

Changes in behavioral state allow the brain to detect and discriminate sounds in challenging, noisy conditions. The internal brain state that influences hearing combines many separate behavioral state variables, including selective attention, relative effort, temporal expectation, and reward associations. Each of these variables might provide distinct modulatory influence on auditory neural activity through different top-down circuits.

To contrast the influence of different internal state variables on auditory representations, we developed an auditory discrimination task in which selective attention and overall effort are controlled separately. The task employs a go/no-go paradigm in which head-fixed animals are rewarded for responding to a pure tone target embedded in a continuous stream of vocalization-modulated noise (narrow-band noise modulated by the temporal envelope from a natural vocalization). On each trial, two noise streams are presented simultaneously, centered at different frequencies and from different spatial locations. To manipulate selective attention, the frequency and location of the target tone is matched to one stream and changed between trial blocks. To manipulate effort, the signal-to-noise (SNR) of the target relative to the noise is varied between blocks at a fixed frequency and location. Catch stimuli are included in each block to verify behavioral effects.

We trained two ferrets to perform the task and recorded activity of single neurons in primary auditory cortex (A1) during behavior. For the selective attention manipulation, the target was fixed at the best frequency (BF) of and contralateral to the recorded neuron during one trial block. When attention was directed to BF, evoked activity was weaker than when attention was directed away from BF. Spontaneous spike rate did not change. For the manipulation of effort, on the other hand, we observed changes in evoked and spontaneous activity. Both were smaller during the difficult, low-SNR condition than during the high-SNR condition. Thus these two aspects of behavior state influence neural activity differently, selective attention modulating the gain of auditory responses and relative effort modulating overall firing rate, independent of the stimulus. Ongoing studies are comparing the effects of these behavioral state variables on filter-based models of neural activity (i.e., temporal receptive fields) measured under the different behavior conditions.

SYM-70

Auditory Response Selectivity in Ferret Dorsolateral Frontal Cortex during a Reversal Task

Nikolas Francis[1]; Susanne Radtke-Schuller[2]; Jonathan Fritz[1]; Shihab Shamma[1]
[1]University of Maryland; [2]Ludwig-Maximilians-Universität München

The parameters that modulate neuronal responsiveness in ferret dorsolateral frontal cortex (dlFC) during behavior are poorly understood. Reversal tasks allow comparison of selective responses for stimulus features vs. behavioral meanings, because the stimuli are held constant while their behavioral meanings are reversed. To investigate the modulation of responsiveness in dlFC, we trained two ferrets on a Primed Go/No-Go conditioned avoidance task, with reversals of behavioral meaning for pure-tones. Animals licked freely from a waterspout when a broad-band noise was presented ("go"-stimulus) but avoided licking during certain tones. At the start of each experiment, either low- or high-frequency tones were randomly assigned to be targets, i.e. "no-go" stimuli that instructed the animals to stop licking the waterspout to avoid a mild shock. The noise and non-target tones signaled go-behavior, i.e. an approachable waterspout. Behavior began with a block of "Priming" trials, where only go-signaling sounds were presented. Following a Priming block, a block of Go/No-Go trials occurred, where a randomized sequence of noise, target and non-target tones were presented. After the first Go/No-Go block, the high and low tones' behavioral meanings (i.e. go vs. no-go) were repeatedly reversed during subsequent Primed Go/No-Go blocks. Neuronal activity was recorded using single electrodes in dlFC during task performance. Single-units were sorted offline. Consistent with previous results, we found in both animals that single-unit responsiveness was behaviorally gated, and responses were greatest to (no-go) targets. However, unlike previous findings in dlFC, where no responses were observed to noise (go-signals), in the current reversal task we found strong *suppressive* responses to noise during behavior. Most single-units in dlFC responded to unambiguous go- and no-go-signals with suppression and enhancement, respectively. Nevertheless, despite having the same behavioral meaning as noise ("go"), non-target tone responses were *enhanced* during behavior, though to a lesser extent than target tones. The difference between the noise and non-target responses may have been driven by increased uncertainty about the non-target tones' behavioral meaning caused by interference across reversals. Thus, the range of dlFC responsiveness—from suppression during noise, to mild enhancement during non-target tones, to strong enhancement during targets, may reflect a weighting of uncertainty and valence associated with behaviorally meaningful stimuli. Stimuli with variable vs. fixed behavioral meaning are represented differently, even when their current behavioral meanings coincide. We shall discuss the implications of these results for the hypothesis that top-down control signals from frontal cortex influence task-dependent plasticity in primary auditory cortex.

SYM-71

Neuronal Ensemble Representation of Competing Sounds in Auditory Cortex

Yi Zhou
Arizona State University

The response of a neuron to repeated presentations of a stimulus can be highly variable. This variability increases from periphery to cortex and is thought to reflect noises in ionic channels, synaptic inputs and recurrent network activity. Many studies have investigated the characteristics of response variability in relation to stimulus onset, attention, and brain site. What is less known, however, is whether the response variability also provides information about stimulus saliency, especially in situations with competing sensory stimuli. In this study we examined the variability of spike count in marmoset auditory cortex in response to tone-in-noise stimuli at various signal-to-noise ratios (SNRs).

Single-unit data were collected from primary and caudal-field auditor cortex in three awake adult marmoset monkeys. Best frequency (BF) tones were presented at levels ranging from -10 to 80 dB with or without a background noise. From these responses, we measured trial-by-trial variability of spike count and its mean as a function of BF tone levels. Analyses contrasted the responses of neurons showing linearly increasing rate-level functions (i.e., monotonic neurons) with those showing attenuated rate at high sound levels (i.e., non-monotonic neurons). Neurometric functions were applied to evaluate whether reduction in response variability was correlated with improved signal detection in noise by these neuron groups.

We found that the trial-by-trial variability in spike count scales with the mean spike count. However, the variability-mean relationship often exceeds the Poisson prediction. Interestingly, increasing BF-tone level reduced trial-to-trial response variability for both monotonic and non-monotonic neurons, even though non-monotonic neurons showed no-spiking activity at high stimulus levels. When these neurons were stimulated with additional background noise, the response variability was also reduced regardless of whether noise caused excitatory or inhibitory changes in discharge rate. The reduced variability improves signal detection in noise by preserving spike-time patterns related to BF tone and suppressing those relate to noise.

These results indicate that while the mean firing rate of a cortical neuron fluctuates based on the excitatory and inhibitory nature of a stimuli, the "noise" in its response appears to always decrease with increasing stimulus level. Thus response variability may serve as a useful neural marker in disambiguating the contributions of non-responsive neurons to sensory coding during active suppression and/or suboptimal stimulation.

SYM-72

Unknown Modulatory Inputs: A Large, but Structured Source of Internal Noise for Auditory Neurons

Neil Rabinowitz; Robbe Goris; Eero Simoncelli
New York University / HHMI

The responses of auditory neurons to repeated sounds can be highly variable. This is especially true for neurons further along the processing pathway, such as in auditory cortex. Some portion of this variability arises from fluctuations in modulatory factors that alter neural gain, such as adaptation, attention, arousal, reward, emotion, cognitive state, and local metabolic resource availability. Since these signals change over time, and we generally cannot measure or control all of them, the combined effect of unknown modulatory inputs contributes to the internal noise we measure while exploring neural representations of sound. Here, I shall describe some recent work that breaks this problem apart. We build principled statistical models of auditory neurons' firing patterns as the product of stimulus-driven components, known modulatory inputs, and unknown modulatory inputs, the last of which are constrained to change slowly over time. This modelling approach substantially improves our ability to estimate stimulus-response properties of midbrain and cortical auditory neurons, and also opens up avenues for exploring the sources of internal noise for auditory circuits.

SYM-73

The Cost of Mis-Decoding Correlated Noise in Stimulus Detection, Discrimination and Estimation

Ching-Ling Teng
University of Virginia

Perceptual decision involves interpreting activities from a population of neurons into a categorical choice. Though each neuron may have a unique tuning curve, trial-to-trial variability is shared among neurons, i.e., noise correlation. Previous study has examined the impact of noise correlations on stimulus encoding accuracy. Less is known about how decoding and mis-decoding noise correlation impact perceptual decisions. Particularly, four contexts were considered: stimulus detection, coarse and fine discrimination, and estimation.

We used a linear model to separates sensory representation from population readout and quantified decision errors in decoding correctly or incorrectly about the noise correlation. Specifically, we assume that a scalar-valued stimulus is encoded by a population of neurons with Gaussian-shaped tuning curves corrupted by additive noise. The covariance of the noise is taken to be either stimulus-independent or stimulus-dependent, and we consider a variety of correlational strengths and structures.

Our analysis shows that if noise correlations are present, the optimal decoder is a center-surround linear filter. If noise correlations are absent, the optimal linear decoder has no surround inhibition. Moreover, the optimal decoder for independent responses performs poorly when applied to responses with correlated noise. Thus, it would seem that correlations are important and a decoder – presumably implemented in downstream networks of neurons – needs to know about them. But does a decoder really need to know about the correlation structures? More specifically: is there a decoder that can provide accurate readout regardless of the details of the correlational structure, including no correlations at all? If so, correlations would become unimportant because a decoder would not need to know them to perform near-optimally. Indeed, that is what we found: a center-surround readout is remarkably robust to various correlational structures, including changes in correlational lengths, strengths, and stimulus dependency.

In conclusion, a center-surround readout provides a flexible and effective way to decode both independent and correlated neural populations, including those whose correlation structures can change when driven by factors like attention, arousal, and task demands. Our results suggest that the problem of decoding correlated population activity may be easier than was thought.

PS-431

Behavioral and Electrophysiological Evidence of Central Auditory Processing Deficits in Blast-Exposed Veterans

Frederick Gallun[1]; Robert Folmer[1]; Melissa Papesh[1]; M. Samantha Lewis[1]; Michele Hutter[1]; Heather Belding[1]; Marjorie Leek[2]
[1]Portland VA Medical Center; [2]Loma Linda VA Medical Center

Gallun et al. (2012; JRRD 49(7)) provided behavioral and electrophysiological evidence of central auditory processing deficits in US service members when evaluated within several months of exposure to high intensity blast waves on the battlefield. Here we extend these data to show 1) that these deficits are still measurable when the sample tested is composed of Veterans evaluated up to ten years after exposure, 2) that these Veterans report significant handicap associated with central auditory complaints, and 3) that correlational analyses between and among various behavioral and electrophysiological tests of central auditory function can be used to identify specific patterns of dysfunction even after accounting for potential intervening variables such as attention and memory deficits potentially associated with brain injury and/or PTSD.

Behavioral measures include dichotic listening, temporal processing, and binaural sensitivity as well as tests of potential intervening variables such as auditory selective attention and working memory. Electrophysiological measures include the P300 response to 1000-Hz tone pulses played among 500-Hz tone pulses and the binaural change response to an interaural phase reversal. Further involvement of potential mediating variables was examined by correlating the response to questionnaires designed to evaluate the severity of post-traumatic stress.

Examining the pattern of behavioral and electrophysiological responses for individual listeners, as well as the potential involvement of attention and memory deficits due to brain injury or stress reactions, is a critical step in the long term goal of moving beyond group differences to better identify the nature of the underlying dysfunction leading to the serious impact on auditory processing ability reported by the majority of these blast-exposed individuals. Support provided by VA RR&D.

PS-432

Neurobiochemical, Neuropsychological, Audiological and Psychometric Characteristics of Blast-Induced Tinnitus

Anthony Cacace; John Woodard; Jiani Hu; Yang Huan; Pamela May; Mike Sugerman; Andrea Norman
Wayne State University

Introduction

Understanding the underlying basis of blast-induced tinnitus in humans is a challenging proposition. Contemporary methods in audiology, neurobiology, and neuropsychology are needed to better appreciate those factors associated with this phenomenon.

Methods

Herein, we used single voxel proton magnetic resonance spectroscopy (^{1}HMRS) to study metabolite concentrations in left and right auditory cortical areas (*N*-acetyl aspartate, NAA; choline, Cho; creatine, Cre; glutamate, Glut; myo-Inositol; mI), neuropsychological variables to study cognitive sequalae (vis-à-vis measures derived from the Automated Neuropsychological Assessment Metrics, ANAM, including: throughput scores that combine reaction time and accuracy for simple and choice reaction times, working memory, and mathematical processing measures), audiological measures (averaged 4-frequency audiogram, monosyllabic word recognition in quiet and in noise, and tinnitus loudness estimates based on a magnitude estimation procedure), and selected subscales from the Tinnitus Handicap Questionnaire (THQ; Total score).

Twenty two adults (20 males; 2 females) ranging in age from 28 to 74 (mean age 50.4 $\pm$13.2 years) were studied. Multiple regression analyses were applied to establish relationships among variables that may have predictive value that could provide a better understanding of tinnitus induced by blast exposures and lead to useful treatments. This study was approved by the Institutional Review Board of Wayne State University and signed informed consent was obtained prior to data collection.

Results

Multiple regression analyses revealed that Glu levels in left auditory cortex, pure tone measures of hearing sensitivity, and monosyllabic word recognition performance in quiet for the left ear were significantly related to processing speed and delayed recall memory performance (p's < .001, r^2 = 0.22 and 0.21, respectively). Left auditory cortex Glut levels were also positively related to speeded mathematical processing ($p<.0001$, r^2 = 0.24). Choice reaction time performance was negatively related to mI levels in left ($p<.03$, r^2 = 0.35) and right ($p<.02$, r^2 = 0.132) auditory cortex.

Conclusions

Our findings provide preliminary evidence for tinnitus-related abnormalities at the neural level in auditory cortex that may contribute to neuropsychological deficits on speeded/cognitively demanding tasks. Moreover, monosyllabic word recognition performance in quiet independently predicted processing speed performance.

PS-433

Assessment of Oculomotor, Vestibular and Reaction Time Response Following a Concussive Event

Michael Hoffer[1]; Alexander Kifderman[2]; Alexander Braverman[3]; James Crawfored[4]; Sara Murphy[5]; Kate Marshall[4]; Alexander Braverman[3]; Carey Balaban[6]
[1]University of Miami; [2]Neurokinetics, Inc.; [3]University of Jerusalem; [4]Madigan Army Medical Center; [5]Naval Medical Center San Diego; [6]University of Pittsburgh

Introduction

Mild traumatic brain injury (mTBI) is an increasingly common public health issue that impacts all segments of the population. Some of these cases are seen in the emergency room, but often, affected individuals have no immediate emergency room access and are seen at the site of injury. In both environments diagnosis can be challenging. This is especially true because well established brain injury diagnostic options are not applicable in this group of patients. Moreover, many of the affected individuals have significant neurosensory deficits that don't resolve over time and can produce long-term neurosensory sequelae. As such there is a pressing need for more accurate point of injury diagnosis in these patients.

Goals of the Study

The goals of this study are to examine the oculomotor, vestibular and reaction time responses following a concussive event in individuals with recent onset mTBI and compare these findings to a group of age matched, healthy controls. The chief aim seeks to find a small subset of these tests that are most predictive of mTBI and to miniaturize these onto a portable, objective mTBI diagnostic device.

Methods

Subjects are recruited from the Emergency Departments and Trauma Receiving Departments of two military hospitals and one civilian institution Subjects present to the study site o within 72 hours of head injury and receive a medical exam. Those who meet study criteria and agree to participate undergo a health history questionnaire, a dizziness handicap index (DHI), a functional gait index (FGI), and Trail Making Tests (TMTs). After these assessments the subjects undergo a battery of tests using video-oculography technology (I-Portal® VOG) comprised of a head mounted, high speed and precision infrared eye tracking system on the Neuro-Otologic Test Center (NOTC). The individuals in the study undergo multiple tests including saccades, pursuit tracking, nystagmus, optokinetic, vestibular function, and reaction time.

Results:
We compare the results of 50 mTBI subjects to 100 controls. While no single test was sufficiently predictive to have separation between controls and mTBI subjects, five key variables were highly correlated with mTBI. These key variables including percent of prosaccade error, VOR head impulse gain, saccade latency and phase lag of eye movement, auditory reaction time variability correctly predicted 95.0% for the control group 82.6% for the mTBI group.

Conclusion
These results suggest that NOTC with VOR tests can provide an objective and reliable method of capturing and quantifying abnormal response in patients with mTBI.

PS-434

Optokinetic Fast Phase and Saccade Motor Performance are Depressed in Acute Concussion/Mild Traumatic Brain Injury

Carey Balaban[1]; Alexander Kiderman[2]; Yakov Eydelma[2]; James Crawford[3]; Sara Murphy[4]; Kate Marshall[4]; Michael Hoffer[5]
[1]University of Pittsburgh; [2]NKI; [3]Madigan Army Medical Center; [4]Hearing Center of Excellence; [5]University of Miami

Introduction
Mild traumatic brain injury (mTBI) may result in gross ocular motility disturbances which can indicate the site(s) of disruption in the peripheral motor unit or central nervous system. Particular eye movement velocity analysis may give us a quantitative approach to evaluate brain trauma. Abnormalities of the main sequence velocity of reflective saccade and fast phase optokinetic nystagmus (OKN) (the relation between amplitude and velocity for fast eye movements), were examined initially in the context of saccades for a wide range of diseases. No study to date has evaluated simultaneous fast phase OKN, using high speed and precision infrared eye tracking video-oculography system to determine if the response was sufficiently useful to measure deficit in mTBI patients.

Goals of the Study
The goals of this study are to examine saccade and fast phase optokinetic main sequence following a concussive event in individuals.

Methods
Subjects are recruited from the Emergency Departments and Trauma Receiving Departments of two military hospitals and one civilian institution Subjects present to the study site approximately within 72 hours of head injury and receive a medical exam and undertake a battery of tests using video-oculography technology (I-Portal® VOG) based on of a head mounted, high speed and precision infrared eye tracking system on the Neuro-Otologic Test Center (NOTC) Neuro-Kinetics, Inc., Pittsburgh PA. These tests included standard oculomotor tests and also horizontal random saccade and 20 and 60 degrees per second horizontal optokinetic tests.

Results
For each subject (30 mTBI and 60 age-matched controls), the leftward and rightward main sequences for saccades and fast phases of optokinetic nystagmus were described by parameters from the formula: Peak velocity =A*exp(B*magnitude) +C. The A parameter characterized the size of the peak velocity envelope. The A parameters were tabulated by larger and smaller direction for each movement type. Repeated measures analysis of variance and post-hoc tests showed that the main sequence was depressed in the mTBI group ($p < 0.01$).

Conclusion:
The finding in this study support the potential utility of main sequence analysis of fast phase OKN in assessing potential central dysfunction, provide objective measurements to identify changes consistent with a mTBI and resolution from injury, or absence thereof, and maybe useful in identifying when an individual may be “cleared” to resume prior obligations/activities.

PS-435

Comparing Oculomotor and Optokinetic Findings to Symptoms in Patients with Acute mTBI

Alexander Kiderman[1]; Michael Hoffer[2]; James Crawford[3]; Sara Murphy[4]; Kate Marshall[4]; Liza Oakes[5]; Alexander Braverman[6]; Carey Balaban[7]
[1]Neuro-kinetics Inc.; [2]University of Miami; [3]Madigan Army Medical Center; [4]Hearing Center of Excellence; [5]NKI; [6]University of Jerusalem; [7]University of Pittsburgh

Introduction
Mild traumatic brain injury (mTBI) is an increasingly common public health issue that affects all elements of society. Affected individuals are assessed in a variety of environments including emergency departments, trauma-receiving wards, or at the site of the injury. Since traditional traumatic brain injury assessment techniques fail are not effective or relevant in this patient group there remains an urgent need to effective, objective, and timely testing in this group of patients.

Goals of the Study
The goal of this study is to compare the optokinetic, oculomotor, and vestibular measures obtained in the computerized rotational chair (NOTC device) to a set of predefined symptoms in patients with acute mild traumatic brain injury. This type of comparison will allow us to better define mTBI objective testing and will allow us to correlate this testing to mTBI management and prognosis.

Methods
Subjects are recruited from the Emergency Departments and Trauma Receiving Departments of two military hospitals and one civilian institution.

Subjects present to the study site in each institution within 72 hours of head injury where they receive a medical exam and are assessed for meeting study entrance criteria. Those who meet these criteria and agree to participate in the study undergo a set of examinations to include a health history

questionnaire, a dizziness handicap index (DHI), a functional gait index (FGI), and Trail Making Tests (TMTs). After these assessments the subjects undergo a set of tests in the NOTC device to include gaze, optokinetic, saccade, smooth pursuit, and reaction time tests.

Results

Fifty individuals with recent mTBI are included in this study. Their symptoms on presentation could be clustered into five major areas as follows: Dizziness, headache, cognitive, emotional, and fatigue. The presence, absence, and severity of the symptoms with in each cluster can be correlated with specific findings seen on NOTC testing utilizing principal component analysis and group mean analysis of variance. This analysis creates unique patterns of NOTC outcomes for each major symptom area.

Conclusion

Specific NOTC test abnormalities seem to correlate with symptoms in acute mTBI patients. By analyzing the patterns of response on testing to each symptom both initially and over time a more specific diagnostic and prognostic determination could be made and therapy could be directed to areas with the greatest abnormality.

PS-436

Relationship Between Blast-Induced Tinnitus and Hearing Impairment in Rats

Anika Meggo; Hao Luo; Edward Pace; Jessica Ouyang; Jinsheng Zhang
Wayne State University School of Medicine

Blast, a high pressure impulse noise, is known to induce tinnitus and hearing loss among both military personnel and civilians. However, the neural mechanisms underlying blast-induced tinnitus and hearing loss remain unclear. In the current study, we investigated the relationship between blast-induced tinnitus and hearing loss by exposing rats to a single 22 psi shockwave and evaluating the results at one day, one month and three months. The rats' left ears were blast-exposed while the right ears were occluded. Gap detection and prepulse inhibition were used to assess rats' tinnitus status before and after blast exposure. Auditory brainstem responses were used to evaluate rats' hearing threshold changes before and after blast exposure. In addition, the rats' hearing was also evaluated by measuring the wave 1 amplitude of the auditory brainstem responses. Our results showed that blast induced a temporary threshold shift. At one and three months after blast exposure, significant degradation in wave 1 amplitudes were observed in the blasted rats in comparison to the control rats, but there were no significant difference in the wave 1 amplitudes of rats with tinnitus and without tinnitus. Our data suggest the induced hearing impairment as revealed by the degradation in wave 1 amplitude reliably reflected blast-induced trauma, while the induced chronic tinnitus may be of central origin.

PS-437

Blast-Induced Tinnitus and Neural Activity Changes along the Auditory Axis in Rats

Hao Luo; Xueguo Zhang; Edward Pace; Srinivas Kallakuri; Jinsheng Zhang
Wayne State University

Although blast-induced tinnitus is frequently reported, its underlying neural mechanisms remain unknown. In this study, we used a rat model (n=39) and tested behavioral evidence of tinnitus following a single blast exposure to the left ear. We then investigated neurophysiological changes by simultaneously recording from the dorsal cochlear nucleus (DCN), inferior colliculus (IC) and auditory cortex (AC) at one day, one month and three months after the blast exposure. Our behavior data showed that blast-induced tinnitus occurred at all frequency bands immediately after blast, at high frequency bands one month post-blast, and eventually at a high- and a low-frequency band three months post-blast. Compared to control rats, early onset hyperactivity was found in the DCN of rats with tinnitus, which lasted for a month before shifting to hypoactivity three months after blast. In addition, the low frequency region in the DCN of tinnitus positive rats was more affected than other frequency regions at one day and one month after blast, whereas at three months, the DCN was broadly affected except for the low frequency region. In the IC of rats with tinnitus, hyperactivity exhibited at all frequency regions at one day after blast, and the induced hyperactivity persisted throughout a three month recording period, it was more robust in the middle-frequency loci at one month after blast and in the middle-to-high frequency loci at three months after blast. In the AC of rats with tinnitus, spontaneous activity began increasing at one month after blast and manifested robust hyperactivity at all frequency regions three months post-blast. Overall, these results demonstrated that blast-induced tinnitus does not involve a uniform manifestation of increased spontaneous firing rates (SFR) along the auditory axis. Instead, changes in SFR can happen in different directions and at different levels of the central auditory system. The data also suggest that onset tinnitus may result from hyperactivity in the lower auditory brainstem, whereas chronic tinnitus may be related to high-level auditory centers.

PS-438

Identification of Neurotoxic Tau Variant-Positive Cells in the Hippocampus Following Blast Exposure and Antioxidant Treatment in Rats

Xiaoping Du[1]; Mathew West[1]; Weihua Cheng[1]; Wei Li[1]; Donald Ewert[1]; Robert Floyd[2]; Richard Kopke[1]
[1]Hough Ear Institute; [2]Oklahoma Medical Research Foundation

Background

Traumatic brain injury (TBI) is a serious clinical challenge that negatively impacts millions of people worldwide, which can lead to hearing loss and tinnitus, as well as early onset dementia. Our laboratory previously demonstrated that rats exposed to three successive blast overpressures exhibited

marked somatic accumulation of both normal and neurotoxic variants of the microtubule-associated protein Tau in the hippocampus and that antioxidant treatment (NAC plus HPN-07) significantly decreased this pathophysiological response pattern(ARO 2014 Abstract #PS-270). In the present study, we provide unique insights into the specific subpopulations of hippocampal cells in which these changes are manifested.

Methods
Using a differential immunolabeling approach, we have elucidated the cell types in which somatic Tau (Tau1 antibody), hyperphosphorylated Tau (AT8 antibody), and oligomeric Tau (T22 antibody) accumulate in the brain, following three successive blast overpressure exposures in non-transgenic rats. These analyses were extended to evaluate the therapeutic effects of post-traumatic intraperitoneal injection of the antioxidants 2,4-disulfonyl α-phenyl tertiary butyl nitrone (HPN-07) and *N*-acetylcysteine (NAC) on pathologic Tau accumulation in these cells in a rodent model of blast-induced TBI.

Results
The vast majority of the AT8 or T22-positive cells were co-labeled with an antibody against GluR2/3, a specific marker for Mossy cells, the major excitatory neurons in the hippocampus, while a small subpopulation of these neurotoxic variants accumulated in cells that were co-labeled with calretinin, a specific marker for non-pyramidal γ-aminobutyric acid (GABA)-ergic neurons. Surprisingly, somatic Tau1 accumulation was restricted to oligodendrocytes, a population of hippocampal cells distinct from those in which neurotoxic Tau variants were observed.

Conclusions
Blast exposure induced accumulation of neurotoxic Tau variants in Mossy cells and GABA-ergic neurons and somatic accumulation of normal Tau in oligodendrocytes. The combination of antioxidants HPN-07 and NAC resulted in a significant attenuation of each of these pathophysiological Tau response patterns. Thus, in addition to its ameliorative effects on primary blast-induced hearing loss, this treatment strategy also represents a promising therapeutic approach for reducing progressive Tau-related neurodegeneration and altered patterns of neural signaling in the hippocampus, with important implications for mitigating other neural disorders, such as dementia and tinnitus.

PS-439

Are Envelope Fluctuations Necessary for Binaural Cue Extraction?

Anna Diedesch; G. Christopher Stecker
Vanderbilt University

Reliable coding of a sound source location requires effective processing of binaural differences carried by the sound's envelope and temporal fine structure. Although the envelope characteristics are especially important at high frequencies, envelope features also play a role in localization based on low-frequency cues. For example, the auditory illusion of the Franssen effect demonstrates the importance of cues available near sound onset when later ongoing cues are unreliable (e.g. for pure tones in reverberation). Conversely, the failure of the Franssen effect for noise carriers suggests that ongoing envelope fluctuations may provide better access to binaural information.

Several recent studies demonstrated enhanced sensitivity to binaural cues, including low-frequency fine-structure cues, when they coincide with sound onsets or other positive-going fluctuations of the envelope. The results suggest that binaural-cue extraction might rely heavily on such fluctuations–as are ubiquitous in speech, for example–and therefore partly resolve problems associated with reverberation and competing sounds.

Here, we review and evaluate the results of classic and recent studies that measured binaural sensitivity for sounds with dynamic binaural cues and/or fluctuating envelopes. Across studies, sounds included pure and modulated tones, trains of filtered impulses, and noise bands; acoustic parameters spanned a wide range of spectral and modulation frequencies important for speech. Overall, results support (1) a general emphasis of positive-going envelopes (i.e. sound onsets) during binaural cue extraction, regardless of cue type or carrier frequency, and (2) the importance of fluctuations in the ongoing envelope for the effectiveness of ongoing cues. [Supported by NIH R01-DC011548]

PS-440

Analysis of Internal Noise in the Precedence Effect

M. Torben Pastore; Jonas Braasch
Rensselaer Polytechnic Institute

In reverberant conditions, humans routinely localize sounds based primarily on the binaural cues from the first arriving wavefront – the lead – minimizing the effects of later arriving reflections from the lag – the so-called precedence effect. Within limits, this effect even holds when the reflected sounds contain more energy than the direct sound. In a previous experiment, we investigated the lateral extent of the Precedence Effect for conditions where the level of the lag exceeded that of the lead by 0–10 dB, in steps of 2 dB. A single frozen noise was used as the basis for all stimuli to allow acoustic analysis of the cues present for insight the mechanisms leading to lateralization performance of subjects. Using this frozen noise, we observed that variability increased with lag level for both between and within subjects measures. It is unclear, however, how much of this variability is due to internal noise of the auditory system.

The current research addresses this by using the same stimuli, but with 6 different noise tokens. Stimuli were 200-ms Gaussian noise (500-Hz center frequency, 800-Hz bandwidth) presented dichotically with a programmable amount of temporal overlap (0–5 ms). Listeners indicated the lateralization of their auditory events with an acoustic pointer. Variability is quantified both within and across subjects and a measure of internal noise is deduced from these measures.

For these data, internal noise has a measurable effect on the lateralization of the perceived auditory event, but the general

response pattern from the previous study with frozen noise sample is preserved. The perceptual changes between different noise samples correlate with the noise-specific changes in ILDs that occur in the ongoing portion of the signal due to interference.

PS-441

The Steady-State Evoked Response to Periodic Changes in Carrier IPD – Correlating Response Magnitude with Behavioural Thresholds

Nicholas Haywood; Jaime Undurraga; Torsten Marquardt; David McAlpine
University College London, London, UK

Introduction

If bilateral cochlear implantation is to maximise binaural benefits for hearing impaired listeners, it is essential that objective measures of binaural performance be obtained. Many listeners, especially children, will be unable to report the matching of electrode stimulation across the ears, or the subjective fusion and coherence of binaural sound images. We have developed a clinically viable electroencephalographic (EEG) measure of sensitivity to interaural timing differences for normal hearing by recording a steady-state response evoked by periodic changes to interaural time differences.

Methods

A five -minute sinusoidal amplitude modulated (SAM) tones were presented at 80 dB SPL (carrier frequency = 520 Hz, modulation frequency = 41 Hz). The modulation envelope was diotic, and the carrier tone was presented with an interaural phase difference (IPD; range = 22.5º - 135º). Every six successive modulation cycles (6.8 Hz), carrier IPD was modulated during a SAM minimum to lead in the opposite ear to that previously. This resulted in a stimulus which modulated periodically between right- and left-leading, but for which the overall magnitude of the IPD remained constant. Responses from ten normal-hearing subjects were recorded. Subjects did not attend to the stimuli during the recording session. In a 2I-2AFC psychophysical task, an additional ten subjects identified a target tone with a modulated IPD from a reference tone with an equivalent unchanging IPD. The stimuli were accompanied by a background uncorrelated pink noise, the level of which was varied adaptively to estimate threshold signal-to-noise ratio (SNR).

Results

The periodic IPD switches evoked a robust 6.8 Hz steady-state following response which was detected reliably from background noise. All IPD values tested elicited a following response, but the response magnitude was typically largest when the IPD was set to 90º. Response magnitude decreased at both larger and smaller IPD values tested. This may be attributable to the fact that the ±90º modulation corresponded to an IPD *change* of 180º - the maximal phase difference. In the psychophysical, subjects achieved lowest SNRs for and IPD of 90º, demonstrating a strong correlation between objective and psychophysical performance.

Conclusion

The EEG measure is a reliable indicator of the perceptual salience of the ITD switches. On-going studies are investigating both the effect of carrier frequency and if EEG and behavioural measures correlate amongst individuals.

PS-442

Accounting for Effects of Center-Frequency and Bandwidth on Binaural Detection Measured as a Function of Masker Interaural Correlation

Leslie Bernstein; Constantine Trahiotis
University of Connecticut Health Center

Background

This study was motivated by two previous investigations concerning binaural detection of 500-Hz, Sπ, tonal signals masked by broadband noise. In both, the parameter of interest was the interaural correlation of the masker. The first, Robinson and Jeffress [D. E. Robinson and L. A. Jeffress, J. Acoust. Soc. Am. 35, 1947-1952 (1963)], showed: 1) a steep increase in detection threshold as the interaural correlation of the noise masker (Nρ) was changed from 1.0 to about 0.9 and 2) a more shallow increase in detection threshold as the value of ρ was reduced further toward a value of zero. The second, van der Heijden and Trahiotis [M. van der Heijden and C. Trahiotis, J. Acoust. Soc. Am. 101, 1019-1022 (1997)], accounted for the Robinson and Jeffress (1963) results based on the authors' insight that a masker of arbitrary interaural correlation, ρ, can be expressed as the sum of appropriate amounts of two independent sources of noise, one having an interaural correlation of 1.0 (No), the other having an interaural correlation of -1.0 (Nπ). van der Heijden and Trahiotis postulated that binaural detection thresholds, or their corresponding masking-level differences (MLDs), could be interpreted as reflecting "additive" masking effects produced by the No and Nπ components of the external masking noise having an interaural correlation of ρ. The current study was designed to test the generality of van der Heijden and Trahiotis' additivity approach.

Methods

Using a two-alternative, two-interval forced-choice adaptive task, detection thresholds were measured for 500-Hz or 125-Hz Sπ tonal signals masked by narrow-band Gaussian noise and for the latter stimuli (noise or signal-plus-noise) transposed to 4 kHz. The values of ρ tested were 1.000, 0.998, 0.992, 0.968, 0.874, 0.498, 0.204, -0.262, -0.589, -0.783, and 1.000.

Results and Conclusions

It was found that 1) the patterning of the data did not depend on center frequency; 2) thresholds for transposed stimuli improved relative to their low-frequency counterparts as masker bandwidth was increased; 3) the van der Heijden and Trahiotis (1997) additivity approach accounts well for the data across stimulus conditions but consistently overestimates MLDs, especially for narrowband maskers; 4) a different approach that incorporates *distributions of time-varying ITD-based lateral positions* produced by masker-alone and signal-plus-masker

waveforms improves predictions, but requires more assumptions, parameters, and computational effort.

PS-443

Contribution of Head and Pinnae Growth to the Acoustical Cues to Sound Location in the Developing Guinea Pig (Cavia porcellus)

Kelsey Anbuhl; Nathaniel Greene; Daniel Tollin
University of Colorado- Anschutz Medical Campus

Background

The dimensions and morphology of the head and pinnae shape the spatial-location dependence of the spectral and temporal aspects of sounds that give rise to the acoustical cues to sound source location. During development, the physical dimensions of the head and pinnae grow rapidly; thus, the magnitudes of binaural cues− interaural time (ITD) and level (ILD) differences− are hypothesized to systematically increase until adulthood. Spectral shape cues, the monaural cues to location, are expected to systematically change with pinnae growth. Here, we investigate the cues to location in the developing guinea pig, a precocious species commonly used for developmental studies of the auditory system.

Methods

We computed the cues to location from measurements of the directional components of head-related transfer functions (DTFs) in 19 animals and measured linear dimensions of the head and pinnae from birth through adulthood in 39 animals. DTFs were measured at both ears from 775 locations, with steps of 7.5º in both azimuth and elevation. From the DTF measurements, ITDs, ILDs, and spectral shape cues were computed.

Results

Dimensions of the head, pinnae width and pinnae height increased by factors of 2.01, 1.5, and 1.6, respectively, reaching adult values beginning at ~8 weeks. Maximum ITDs calculated from low-pass filtered (2 kHz cutoff frequency) DTFs increased from ~160 µs at P0, ~180 µs at P28, and up to ~250 µs in adults. ILDs depended on source location and frequency, with maximum ILDs for frequencies >10 kHz of 30 dB at P0, 35 dB at P28, and ~40 dB in adults. Concurrent with increasing head and pinnae size, there was also a shift in the frequency range of ILDs >10 dB from higher to lower frequencies (P0-P28: > 6.5 kHz; adult: > 4kHz). Similar trends were observed for spectral notches, where first notch center frequencies for frontal sources were above 29 kHz at P0 and ranged from 18-26 kHz at P28 to ~10-20 kHz in adults. Removing the pinnae eliminated spectral notches and lowered both ITD and ILD magnitudes.

Conclusions

The increasing dimensions of the head and pinnae in the developing guinea pig are systematically related to generation of spectral shape cues, the spatial- and frequency- dependent distributions of DTF amplitude gain, and the magnitude of ITDs and ILDs. Based on these studies, the guinea pig reaches acoustic adulthood beginning approximately 8 weeks after birth.

PS-444

In Barn Owls Interaural Level Differences Help to Disambiguate Sound-Source Location in the Horizontal Plane

Lutz Kettler; Hannah Griebel; **Hermann Wagner**
RWTH Aachen University, Aachen, Germany

Barn owls determine the location of a sound source from information contained in the interaural time and level differences (ITD and ILD). In these birds the ITD varies with azimuth, while the ILD varies with both elevation and azimuth. ITD is extracted from the signal via a cross-correlation-like algorithm operating in narrow frequency channels. This leads to phase ambiguities. The ambiguity is eliminated through integration over many frequency channels. While broadband sounds carry unambiguous information about the location of a sound source, the information contained in narrowband stimuli is ambiguous, which leads to the localization of phantom sound sources. We speculated that the addition of ILD information might help in disambiguating the sound-source location specified by ITD alone.

To test this hypothesis we performed three experiments with two barn owls:

In experiment 1 the stimuli contained all natural cues and were presented via free-field loudspeakers positioned in the frontal hemisphere at 0° elevation. The owls localized signals of different bandwidths.

In experiment 2 the owls localized the same noise signals as in experiment 1 but the stimuli were now presented via earphones. The different locations were specified by the ITDs corresponding to the speaker positions in experiment 1. The ILD was 0 dB in all cases.

In experiment 3 stimuli filtered with the head related transfer functions (HRTF) measured at the speaker positions used in experiment 1 were presented via earphones. First, we used native HRTFs which contained all natural cues and corresponded to free field stimulation as in experiment 1. In a second step, we fixated the ILD to 0 dB (as in experiment 2) or to the ILD measured at the predicted location of phantom sound sources. All other cues were left normal.

We analyzed the latencies, amplitudes, and direction of head turns, especially with respect to the number of phantom source localizations.

In experiment 1 the owls made localization errors as long as the bandwidth of the narrowband noise was below ~3 kHz. The number of head turns towards phantom sources in experiment 2 was increased compared to the free-field stimulation in experiment 1. The findings with HRTF-filtered stimuli with manipulated ILDs (experiment 3) imply that the ILD is the factor that is responsible for the decrease in phantom source localizations, because with ILDs measured at the location of phantom sources phantom-source locations were increased.

PS-445

Interaural Level Difference Discrimination with a Frequency Mismatch Between the Two Ears

Robert Baudo; Christine L. Williams; Beverly A. Wright
Northwestern University

A primary cue used for sound localization is the difference in sound level that reaches the two ears from the sound source. Such interaural level differences (ILDs) are calculated through the comparison of information between neural channels in each ear that represent the same frequencies. Of interest here is the extent to which listeners are sensitive to ILDs when there is a frequency mismatch between the ears. To investigate this question, we trained two groups of young adult listeners with normal hearing on an ILD-discrimination task using tones of different frequency at each ear. Trained listeners practiced 720 trials per day for 9 days. A control group participated in pre- and post-training tests without intervening training. To determine if listeners were using a monaural-intensity cue rather than an interaural-level cue, we presented two different trial types randomly within each block of two-interval forced-choice trials and followed performance for each trial type using separate adaptive tracks. In one trial type, the overall level was 70 dB SPL for the signal and 60 dB SPL for the standard, while in the other trial type the overall levels of the signal and standard were reversed. For all five listeners who practiced the ILD-discrimination task with a frequency of 4 kHz to the left ear and 6 kHz to the right ear, performance differed markedly for the two trial types and this difference increased across sessions, suggesting that these listeners used a monaural-intensity cue and did not switch to an interaural-level cue even with extensive training. In contrast, for 6 of 8 listeners who practiced the ILD-discrimination task with a frequency of 4 kHz to the left ear and 4.2 kHz to the right ear, performance did not differ significantly for the two trial types and improved across sessions, more so than for controls (n=10), suggesting that these trained listeners used an interaural-level cue despite the frequency mismatch and that their use of this cue improved with practice. These results imply that listeners are sensitive to ILDs with mismatched frequencies between the two ears when the difference in frequency is relatively small, that this sensitivity can increase with training, and that a simple psychophysical technique can be used to reveal whether a listener is using a monaural-intensity as opposed to an interaural-level cue under mismatched-frequency conditions.

PS-446

Temporal Constraints on Neural and Behavioral Sensitivity to Interaural Level Difference Cues to Sound Source Location

Andrew Brown; Daniel Tollin
University of Colorado School of Medicine

Background

In humans and a variety of studied animals, localization of high-frequency sound sources in azimuth depends on sensitivity to interaural level differences (ILDs). In real listening environments, ILDs can be significantly degraded by signal reflections and reverberation, or by superposition of spectrally similar signals from multiple sources. Moreover, in human patient populations, clinical devices (hearing aids and cochlear implants) can cause large distortions of ILD – even in anechoic environments – due to nonlinear automatic gain control algorithms operating independently at the two ears. Critically, such distortions are *time-varying.* Here we examined temporal constraints on ILD sensitivity, with particular attention to ecological conditions that may precipitate reduced sensitivity.

Methods

In physiological experiments, a variety of degraded and control stimuli carrying ILDs were presented to ketamine-anesthetized chinchillas via earphones. Standard extracellular recording techniques were used to measure rate-ILD tuning curves or 2-D "ILD maps" in single neurons of the central nucleus of the inferior colliculus. In parallel with physiological experiments, psychophysical experiments were conducted in normal-hearing human listeners. Psychophysical sensitivity to ILD carried by degraded and control stimuli was measured using a paradigm that simultaneously assessed intracranial lateralization and left-right discrimination.

Results

Results suggest that neural and behavioral ILD sensitivity are most affected by signal degradations such as interaural decorrelation and envelope reshaping (e.g., to simulate nonlinear hearing aid compression) when amplitude envelope fluctuations are relatively low-rate (e.g., 100 Hz). Sensitivity is generally more robust, though not entirely robust, to comparable degradations when envelope fluctuations are higher-rate (e.g., 500 Hz).

Conclusions

Data generally reinforce the view that ILD is processed via integration of excitatory and inhibitory inputs within a relatively long (perhaps ~2 ms) running temporal window. Under some conditions, this long temporal window may result in reduced sensitivity to the ILD associated with the veridical source location due to compulsory integration of source ILDs and spurious non-source ILDs.

PS-447

Modulation Effects on the Auditory Change-Onset Response

Mikaella Sarrou[1,2]; Nicole Richter[2]; Rudolf Rübsamen[3]
[1]*International Max Planck Research School on Neuroscience of Communication (IMPRS NeuroCom), Leipzig, Germany;* [2]*University of Leipzig, Germany;* [3]*Department of General Zoology and Neurobiology, Institute for Biology, University of Leipzig, Germany*

The MOR shows hemispheric-specific differences: low-frequency moving sounds elicit higher cN1 and cP2 amplitudes over the left hemisphere, whereas high-frequency stimulation shows to have bilateral dominance (or shifted to the right hemisphere). The direction of motion does not to have an effect on the amplitude and latency of the MOR components.

Overall, the MOR components have higher amplitudes when the participants are actively engaged in the task.

Research on auditory perception has emphasized the importance of free-field conditions to create a natural sensation of spatial characteristics of auditory stimuli. The current study made use of these advantages to investigate the effects of the mode of auditory stimulation (moving/stationary), on event-related potentials (ERPs) elicited during the perception of moving sounds. The motion-onset response (MOR) is an ERP component which indicates motion-specific brain activity. This is also indicated by the naming of the MOR components, *change*P1-*change*N1-*change*P2 (cP1-cN1-cP2).

The present investigation focuses on the modulation of MOR in either of the two cortical hemispheres depending on motion direction (inward, outward) and the frequency range of the stimuli. The data were acquired from healthy young participants under two conditions: (1) A passive (unattended) task, i.e. the participants were watching a subtitled-movie without sound and were instructed to not pay attention to the presented sounds; (2) An active task, in which the participants are required to listen to the auditory stimuli and indicate, if they perceived a *change* of mode (stationary/moving) within the stimuli. In both conditions identical stimuli were presented consisting of 500ms-long, stationary or moving noise burst uninterruptedly followed by a second 500ms-long stationary or moving noise burst; frequency was constant throughout the 1000ms duration of the stimuli, and it was either low (300 Hz - 1200 Hz) or high frequency (2000 Hz - 8000 Hz).

PS-448

Perceiving Velocity-Changes in Auditory Motion

Shannon Locke; Johahan Leung; Simon Carlile
University of Sydney

Background

Auditory velocity discrimination experiments show that thresholds increase with velocity and that listeners will use displacement cues to improve sensitivity if they are available (Freeman et al., 2014). The majority of these experiments have assessed the perception of spatiotemporally segmented intervals of constant velocity. Here we examined the perception of instantaneous changes in velocity in spatiotemporally contiguous intervals.

Methods:

Stimuli were AM broadband noise (300Hz - 16kHz) presented in virtual space using individualized HRTFs. Trajectories were constrained to +/-90° in the horizontal plane, with velocity changes occurring in the highly localizable region of +/- 15°. Participants discriminated between the sound's initial and final velocity, reporting a target velocity change (increase or decrease) in a yes/no task. In Experiment 1 (n=5), the discrimination thresholds are measured for increases and decreases from reference velocities of 30 and 60°/s. Experiment 2 (n=6) measured the amount of post-transition stimulus necessary for perceiving velocity changes.

Results:

Velocity discrimination thresholds in Experiment 1 were substantially higher than reported previously, indicating that spatiotemporally contiguous intervals disrupt the process or strategy used with discontinuous stimuli. Spatially contiguous intervals separated by 1s of silence, also showed large thresholds, although less than without suggesting that spatial overlap may facilitated discrimination. In all conditions of Experiment 2, the average minimum spatial extent of the post-transition interval required for velocity discrimination was larger than the corresponding MAMA (Chandler and Grantham, 1992). Using thresholds derived from both experiments, the temporal window for discriminating between the two intervals was calculated with a simple temporal averaging model. The temporal window estimates for increases in velocity (30-90 °/s, 60 to 180 and 240 °/s) ranged between 250-310ms. Decreases in velocity (30-10 °/s, 60 to15 and 20°/s), were much larger, (700ms-2.1s).

Conclusion:

Using a velocity change paradigm, we were able to identify additional spatiotemporal factors that influence velocity perception. Surprisingly, the MAMA was unable to predict the amount of post-transition stimulus required for velocity-change perception. By combining the thresholds from both experiments, we were also able to estimate the temporal window required for velocity change detection, revealing large differences between increases and decreases in velocity. These results present further evidence that the auditory system is relatively insensitive to velocity per se, and to velocity change in particular.

References:

Freeman et. al. (2014) *PloSone* 9: e102864
Chandler & Grantham (1992) *JASA* 91:1624-1636

PS-449

Head-Free Gaze Pursuit of Auditory Targets Resembles Head-Fixed Ocular Smooth Pursuit

Justin Fleming; Christina Cloninger; Paul Allen; Gary Paige; William O'Neill
University of Rochester

Background

Accurate perception of self and external motion is crucial for navigation, but the mechanisms underlying auditory motion perception remain poorly understood. Head and eye movements are frequently used to study visual motion processing, particularly velocity-dependent smooth pursuit (SP). Although visual SP has been well-quantified during both head-fixed (*ocular* SP) and head-free (eye+head, or *gaze* SP) conditions, only ocular SP of auditory targets has been demonstrated. Here we address the more natural behavior of auditory gaze tracking, a process that dynamically minimizes inter-aural localization cues while maintaining SP of moving auditory targets.

An added complexity is the vestibulo-ocular reflex (VOR) activated by head movements during gaze SP. Visual gaze SP overcomes the VOR under low frequency and velocity conditions to keep the eyes on target. Low SP gain, as is char-

acteristic of auditory SP, unmasks the VOR, necessitating catch-up saccades to maintain accurate tracking behavior. This study directly compares SP of moving auditory and visual targets under both head-free and head-fixed conditions.

Methods
Normal subjects were presented with moving visual, auditory, and "predictive imaginary" targets in separate blocks under head-fixed and head-free conditions. Free-field targets were presented at 2m distance using an LED or loudspeaker (white noise; 0.2-20 kHz) mounted to a robotic arm. Predictive imaginary trials consisted of a repeated auditory movement, followed by a period with no target during which subjects were asked to recreate the practiced movement. Eye-movements were recorded using a head-mounted El-Mar eye-tracking system. Target motion consisted of ramps with velocities ranging from 10 to 40 deg/sec and excursions ranging between 15 and 60 degrees.

Results
All subjects effectively performed gaze (eye-head) and ocular tracking of moving auditory and visual targets, with small latencies and head undershoot for gaze SP. For both visual and auditory targets, gaze SP closely resembled ocular (head-fixed) SP, with generally lower gain for auditory than visual targets, but greater than that of imaginary tracking. There was substantial inter-subject variability in auditory SP, but subjects with better ocular SP also tended to show better gaze SP.

Conclusions
We demonstrated dynamic head tracking of moving auditory targets (gaze SP) which resembles the properties of ocular SP with the head fixed. Auditory SP generally resembles visual SP but with lower gain. These findings are consistent with a common central mechanism by which auditory and visual motion processing signals drive oculomotor tracking of environmental targets.

PS-450

Smooth Pursuit to Auditory Motion Resembles Visual Pursuit for Prediction and Extinction

Christina Cloninger; Justin Fleming; Paul Allen; William O'Neill; Gary Paige
University of Rochester

Auditory motion perception remains poorly understood. In contrast, visual motion perception has been studied extensively, especially using velocity-dependent smooth pursuit eye movements (SP), making SP an excellent tool for exploring the dynamics of auditory motion. This lab and others have demonstrated that SP occurs when subjects follow moving auditory targets, though with a lower gain than visual SP. This provides direct evidence for motion-specific processing in the auditory system; it is reasonable to hypothesize that audition shares a control mechanism with visual SP. If so, all classic properties of SP should be demonstrable with auditory targets, including prediction. Here, we presented predictable auditory and visual target motion trajectories and unpredictable extinction of these targets to address prediction in auditory and visual SP.

Young human subjects were first presented auditory or visual targets moving in azimuth as velocity triangles of 20°/s at 0.5, 0.25 and 0.125 Hz for six cycles. Targets were presented in the free-field from a loudspeaker (0.2-20 kHz white noise) or LED at 2m distance on a concealed robotic arm. In the second experiment, the same stimuli were used but targets extinguished unpredictably within ±10° of center at some point between cycles three and seven. Eye movements of head-fixed subjects were recorded using a head mounted eye tracker.

As in previous experiments, auditory SP was observed at a lower gain than visual SP. SP improved over trial cycles, typically reaching steady state in 4 cycles, or less for lower frequency targets. In the second experiment, the dynamics of SP extinction revealed that auditory resembled visual SP: roll-offs were roughly exponential, and differences in time-to-stop between auditory and visual extinction were insignificant.

SP of auditory targets closely resembles visual SP, but with lower gain. The resemblance between modalities also holds true for improved performance during SP of predictable stimuli, as well as for brief persistence following target extinction. These findings further support a shared mechanism for sensory motion processing across vision and audition.

PS-451

The Effect of Static and Moving Sounds in Localization for Normal Hearing Listeners and Bilateral Cochlear Implant Users

Keng Moua; Heath Jones; Alan Kan; Ruth Litovsky
University of Wisconsin, Madison

Background
Sound localization typically depends on availability of interaural time and level differences (ITDs & ILDs). Individuals with bilateral cochlear implants (BiCIs) have difficulty with localization due to a number of factors, including degradation of reliable ITDs and ILDs. To date, studies have only measured localization performance for static sound sources. We are interested in the sound localization abilities of BiCI users in conditions with moving sounds. Moving sounds may provide richer context for sound localization with the start and end locations providing anchor points, as well as having the ongoing sound create a window of opportunity for the individual to use the multiple locations in reference to one another. Here we test the hypothesis that moving sounds are localized more easily than static sounds, because the listener is provided with anchoring and perceptual referencing.

Methods
Subjects with normal hearing (NH) and BiCI users were tested in a sound localization task. Two conditions were tested. In the *static* condition, a signal was presented from one of 21 loudspeakers (5˚ intervals, -50˚ to +50˚ azimuth). In the simulated *movement* condition, sound sources spanned a contiguous range of locations and terminated at one of the 21 loudspeaker locations. Stimuli consisted of noise tokens that were high-passed (2-8 kHz), low-passed (<1.5 kHz) and

broadband (100 Hz- 8 kHz) filtered. All noise tokens were pre-measured using KEMAR and presented to subjects during testing, either with ER-2 insert earphones for NH listeners or direct audio input connection to their speech processors for BiCI users.

Results and Discussion

Results will be discussed in the context of testing the hypothesis that moving sounds may provide listeners with ongoing information that can be compared through time, but that may deteriorate as a function of increased velocity. Thus, velocity and resulting stimulus duration may affect the ability of the listener to perceptually compare information across locations, or to improve localization based on spatial context that precedes the end-point location. This finding may help to understand other results to date, which demonstrate poorer localization for BiCI listeners than NH listeners.

PS-452

Sound Source Localization When the Listener Moves: A Multisensory Process

William Yost
Arizona State University

Judgments of the location of sound sources were made by normal hearing listeners (8 to 17) when they and/or the sound sources moved or were stationary. Listeners were rotated in a computer controlled chair and listened to sounds presented from loudspeakers (24 loudspeakers on a 5-foot radius azimuth circle) in a sound-treated listening room. Judgments of sound source localization were made when the listener could and could not use visual cues and when vestibular cues (e.g., semicircular canal cues) were controlled by rotating the listeners at constant velocity or in an accelerating or decelerating manner. Acoustic spatial cues (e.g., interaural differences) determine the sound source location relative to the listeners head in a head-centric reference system (i.e., the acoustic cues change when the listener moves). However, in the real world sound source locations are judged relative to the position of the sound source in the environment in a world-centric reference system (i.e., the perception of sound source location does not change when the listener moves). In order to determine the world-centric location of sound sources, two types of information are required: the head-centric location of the sound source (derived from acoustic spatial cues) and information about the position of the head relative to the world. In our experiments every effort was made to provide only two cues as to head location: visual and/or vestibular cues. Three experimental procedures were used to measure sound source localization when the listener and/or sounds rotated or did not. In all conditions when the eyes were open, sound source localizations were completely determined in a world-centric referent system (e.g., the perception of sound rotation was independent of whether the listener rotated or did not). In most conditions when the eyes were closed (and especially when the listener was rotating at constant velocity), sound source localizations were determined in a head-centric referent system (e.g., the rotation of the listener determined the perception of sound rotation in a predictable manner). Thus, sound source localization in a real world of moving sound sources and/or moving listeners requires the integration of information about acoustic spatial cues and information gleaned from other systems about the location of the head. That is, sound source localization cannot be explained by acoustic cues alone, in that sound source localization is a multisensory process.

PS-453

Detect and Analyze Locomotion Patterns of Marmoset Monkeys in Response to Sound Stimuli

Swarnima Pandey; Yi Zhou
Arizona State University

In natural environments, many animals move around in search for food or to escape from danger in response to an auditory signal. To understand the neural mechanisms underlying the related sensory and cognitive processes, it is important to develop methods that can accurately track the head and body movement of a subject in a 3-D space. In this study, we aim to detect and analyze the fast movement patterns of marmoset monkeys in response to a variety of sounds. We have prototyped an accelerometer based system which is capable of capturing movement data and transmitting it in real time to a remote receiver using radio frequency protocol. The data received is processed by an Arduino Uno and analyzed in MATLAB to obtain acceleration, velocity and position information of mass movement in three dimensions. The transmitter-receiver pair is capable of communicating at the distance large enough to allow remote monitoring of the animal behavior. The sensor part is approximately 1.5”X1.5” and driven by a 5V power supply. We are currently using this prototype to collect the locomotive data from marmosets in response to different sound stimuli. We hope to gain more insights into how animal behaviors change in different listening environments with the help of this device.

PS-454

Auditory Motion Discrimination in the Barn Owl (Tyto alba)

Ulrike Langemann; **Bianca Krumm**; Katharina Liebner; Georg Klump
Animal Physiology and Behavior Group, Department for Neuroscience, School of Medicine and Health Sciences, Oldenburg University

Background

The barn owl, a prime model for studying sound localization, makes use of acoustic motion direction information during prey capture. Neurophysiological studies provided evidence for direction selective motion sensitive neurons in the auditory system of the barn owl inferior colliculus (Wagner & Takahashi 1992). The angular velocity and stimulus duration affected the neurons’ response. Behavioral data on motion perception were lacking. Here we investigate how motion velocity, size of the angle of sound incidence, and stimulus duration affect the behavioral performance. Furthermore, we analyze if the perception of moving stimuli differs when these are presented frontally or laterally.

Methods
Two barn owls were trained in a Go/NoGo paradigm to report a change in stimulus motion direction. Apparent motion was generated by sequentially activating up to 8 free field loudspeakers. Starting point, direction and angular range of the simulated sweep of the sound source were randomized in each trial. Bandpass noise (500 – 6000Hz) presented with different velocities (150 – 2400 °/s) and different durations (30 – 250ms) served as the stimulus. To investigate the effect of stimulus position in auditory space, we divided the range of spatial source locations into 3 sectors (frontal, right, left) each with a width of 28°. We then compared the owl's performance when presented with acoustic motion in the front versus motion in the lateral space.

Results and Conclusion
Stimulus duration and angular range of the simulated sweep of the sound source affected the sensitivity for auditory motion discrimination. If the apparent motion was presented over a large angular range and with a larger duration, the sensitivity index d' was increased. Velocity per se had little effect on the detection of a change in stimulus direction. The owls responded more frequently to a change in acoustic motion in the frontal space compared to the lateral space suggesting that the sensitivity of the birds is higher for auditory motion analysis for frontal than for lateral positions of the sound source. This could be explained by the overlapping representation of the frontal space in the two inferior colliculi that is limited to ±15° (Knudsen, Konishi & Pettigrew 1977).

Funding
The study was funded by a grant from the Deutsche Forschungsgemeinschaft (TRR 31).

PS-455

Sound Segregation Cues in Natural Speech

Sara Popham; Joshua McDermott
Massachusetts Institute of Technology

Background
The short-term spectrum of speech and other natural sounds is frequently harmonic, containing Fourier components at multiples of a fundamental frequency. Harmonic frequency relations are believed to be an important grouping cue for speech and other sounds. However harmonics in speech typically modulate together in frequency as the voiced pitch changes over time. Such common frequency modulation (FM) could in principle also serve as a grouping cue, but previous tests with artificial stimuli have failed to find any evidence for a role in grouping. To test the role of common FM in the segregation of real-world sound signals, we used a speech synthesis method to manipulate the frequency trajectories of the harmonics of otherwise natural-sounding speech tokens. We then measured the ability of human listeners to understand these tokens in isolation and in mixtures with other sounds.

Method
We utilized a modified version of the STRAIGHT methodology for speech manipulation and synthesis [Kawahara (2006), Acoustical Sci. and Tech.], in which a speech waveform is decomposed into voiced and unvoiced vocal excitation and vocal tract filtering. Unlike the conventional STRAIGHT method, we modeled voiced excitation as a combination of time-varying sinusoids. We then manipulated individual components by altering the frequency contour of each component by some (possibly time-varying) amount [McDermott et al. (2012), Proc. SAPA-SCALE Conference]. We first tested the effect of making speech inharmonic by jittering component frequencies up or down by a small amount. We then tested the importance of common FM by adding low frequency Gaussian noise to the frequency contour of each component, with the noise either identical for each component (coherent) or different for each component (incoherent). We presented listeners with individual words and pairs of concurrent words, and asked them to report what was said.

Results
Performance for isolated words was comparable across all conditions. However, for pairs of concurrent words, recognition was worse for inharmonic than harmonic, and for inharmonic with incoherent FM than for inharmonic with coherent FM.

Conclusions
Speech segregation is adversely affected by incoherent FM and by inharmonicity. The results are consistent with the idea that common frequency modulation is an important additional grouping cue for speech.

PS-456

Different Cortical Regions are Modulated by Prior Stimulus and Prior Perceptual Interpretation During Auditory Stream Segregation: Evidence from Functional Magnetic Resonance Imaging

David Weintraub[1]; Faviola Dadis[1]; Claude Alain[2]; Joel Snyder[1]
[1]University of Nevada Las Vegas; [2]Baycrest Centre for Geriatric Care

Introduction
Recent studies of auditory stream segregation have shown that the likelihood of perceptually separating interleaved tones of different frequencies depends on the frequency separation and the perceptual interpretation of the immediately preceding tone pattern, in addition to the frequency separation of the current pattern. The purpose of the current study was to identify areas of the cerebral cortex that might mediate these two context effects, and to determine the extent to which each of the context effects are associated with activity in auditory (i.e., superior temporal gyrus) or association (e.g., frontal or parietal) regions.

Methods
Event-related functional magnetic resonance imaging (fMRI) was performed while normal-hearing participants listened to a context and test pattern, each composed of interleaved low and high tones. The context pattern had a variable frequency separation between the low and high tones (3,6,12 semitones), while the test pattern always had the same frequency separation (6 semitones). After the context and the test, par-

ticipants made judgments as to whether the tones formed a single stream or two separate streams of tones. fMRI signals following the context and test were analyzed depending on the context frequency separation and the perception during the context.

Results

Behavioral data showed more perception of two streams during the context but less perception of two streams during the test when the context frequency separation was larger, consistent with previous studies. There was also a non-significant trend for more perception of two streams during the test when the context was also perceived as two streams, which is the same pattern of results typically found in previous studies. Activity in the superior temporal gyrus was larger during the context and the test when the context frequency separation was larger. In contrast, activity outside of the temporal lobe was larger during the context (precuneus, insula, parahippocampal gyrus) and test (claustrum, middle-frontal gyrus, posterior cingulate, and medial-frontal gyrus) when the context pattern was perceived as two streams.

Summary and Conclusions

During auditory stream segregation, the prior stimulus pattern modulated activity in or near auditory cortex, whereas the prior perceptual interpretation modulated activity in association areas. These findings suggest that distinct representations or processes mediate the two context effects, with the effect of prior frequency separation possibly reflecting sensory-level adaptation and the effect of prior perception possibly reflecting a mechanism that uses high-level categorical information about recent interpretations to stabilize perception of repeating or continuous stimuli.

PS-457

Segregation and Integration in Sound Textures

Shaiyan Keshvari; Joshua McDermott
Massachusetts Institute of Technology

Introduction

Sound information is often ambiguous, and must be integrated over time and frequency to yield a reliable interpretation. However, if information originates from multiple sources, it must be segregated rather than integrated in order for the sources to be accurately estimated. Sound textures present one example of this tension – textures consist of multiple events whose collective properties can be summarized with statistics, be they those of a rainstorm or a swarm of insects. Yet textures are also typically the background to other sound sources, as when a bird is audible over a babbling brook. In order to recognize both the brook and the bird, the auditory system plausibly performs concurrent integration and segregation, averaging across the sound energy belonging to the brook while segregating the energy of the birdcall. We sought to explore the basis of this process in human listeners, using a texture-discrimination task.

Methods:

On each trial, participants heard two "tone clouds" – overlapping sets of pure tone bursts whose frequencies were drawn from a normal distribution, with one cloud higher in average frequency. In one of the tone clouds, one tone was replaced with an "outlier" that could vary in frequency outside the bounds of the tone cloud distribution. Participants were either asked to choose which tone cloud had an outlier, or to choose which tone cloud was higher in average frequency while ignoring the outlier. These two tasks were presented in separate blocks, counterbalanced in order between subjects, after a brief training block. We measured outlier detection performance and the extent to which judgments of the mean frequency were biased by the outlier.

Results:

We found good performance in the outlier detection task when the outliers were more than a few standard deviations from the cloud mean. However, the same outliers strongly biased the perceived average frequency, hurting or helping performance depending on where they were situated relative to the cloud means being discriminated. Observers were thus unable to discount the outliers when making statistical judgments, despite being robustly able to detect them.

Conclusion:

The results suggest that the integration of texture statistics is partially independent of the ability to segregate sound sources. Future work will investigate the generality of this result to other stimulus dimensions, including timbre, envelope shape, and duration. Additionally, we will test responses to stimuli consisting of realistic sound textures with outliers in time-varying statistics.

PS-458

Target-Masker Similarity in Multiple-Burst Multitone Masking Tone Detection

Eric Thompson[1]; Nandini Iyer[2]; Brian D. Simpson[2]
[1]Ball Aerospace & Technologies Corp.; [2]Air Force Research Lab, 711 HPW, RHCB

In simultaneous, multiple burst, multitone masking paradigms, listeners have to detect a sequence of bursts of a fixed frequency target tone that is embedded in a multitone masker, which usually has the same number of bursts as the target. In these paradigms, the spectral variation across multiple bursts of target and masker tones can have a large effect on target detection thresholds [e.g., Kidd, et al. (1994), JASA 95(6), pp. 3475-3480]. When the masker tone frequencies are repeated across the bursts (multiple burst same, or MBS), a fixed frequency target is more difficult to detect than when the masker tone frequencies are independently drawn on every burst (multiple burst different, or MBD). The interpretation of Kidd, et al. (1994) was that the spectrotemporal pattern differences between the target and masker in the MBD condition allowed the target to be perceptually segregated from the masker more easily than in the MBS condition, where the masker and target had more similar spectrotemporal patterns. Thus, target/masker similarity caused an increase in MBS condition thresholds that could not be predicted by target/masker energy ratios. In the present study, the similarity between target and masker was manipulated by changing the number of masker components that had the same frequency across bursts. The target was a series of one to eight 1-kHz tone

bursts with 60 ms duration. Hybrid MBS/MBD maskers with some fixed and some varying components were presented along with the target and comprised of eight simultaneous tonal components that were gated with the target bursts. There was always a protected spectral region around the target frequency to minimize energetic masking effects. As with prior multiple-burst tone-detection studies, large between-subjects variance was observed in detection thresholds, particularly in the MBS condition. For all listeners, increasing the number of fixed-frequency masker components (thereby increasing target-masker similarity), increased the amount of masking. The largest increase in thresholds was obtained from fixing the frequency of one masker component. These data will be compared to data from tone detection experiments where the number of tonal masker components was varied to provide insight into the combined effects of similar and dissimilar maskers on target detection.

PS-459

Informational Masking in Space: A Spatial Analogue to Multiple-Burst Tone Masking

Eric Thompson[1]; Brian D. Simpson[2]; Nandini Iyer[2]; Griffin D. Romigh[2]; Robert H. Gilkey[3]
[1]Ball Aerospace & Technologies Corp.; [2]Air Force Research Lab, 711 HPW, RHCB; [3]Wright State University

When a sequence of target tone bursts, fixed in frequency across bursts, is presented simultaneously with a sequence of multitone masker bursts that vary in frequency across bursts (Multiple Burst Different, MBD), it is much easier to detect the target than when the masker tone bursts are also fixed in frequency across bursts (Multiple Burst Same, MBS) [Kidd, et al. (1994), JASA 95(6), pp. 3475-3480]. It is assumed that the spectral consistency of the target bursts causes the target to “pop out” against a spectrally varying masker background, whereas a spectrally consistent target may be more difficult to segregate from a spectrally consistent masker. The difference in detection thresholds between these masker conditions can be greater than 40 dB, depending on the listener. In the present study, a spatial analogue of these tone detection experiments was conducted, in which the target and maskers were spectrally similar, but spatially distinct. The target stimulus consisted of a sequence of 16 broadband noise bursts (each 90 ms in duration) emanating from a known location (the loudspeaker directly in front of the listener at 0° azimuth, 0° elevation). On each trial, two maskers (with temporal properties identical to the target but drawn from independent noise samples) were presented from loudspeakers in the frontal hemifield outside of a protected spatial region (15° or 45° radius around the target). Four levels of target-to-masker ratio (TMR) were examined (-15, -10, -5, 0 dB); the TMR was randomly varied from trial to trial. The listeners’ task was to detect the presence of the target sound at the known location and to respond whether the target was present or absent. The locations of the maskers were randomly selected for each trial, and were either fixed across the bursts of the trial (MBS-like masker condition), or randomly varied from burst to burst (MBD-like masker condition). The results showed that the listeners were better able to detect the target when the masker locations varied from burst to burst (MBD) than when the masker bursts were fixed (MBS), similar to the results found in the tone-detection studies. However, the listeners’ detection thresholds in the presence of spatially varying MBD maskers was only about 3 dB better than when detecting the target among spatially fixed MBS maskers. This effect was largest when the radius of the protected region was 45°, and the greatest difference in sensitivity was seen with the highest tested TMRs.

PS-460

Interaction of Spatial Source Separation and Vowel Pairing in a Sequential Informational Masking Paradigm

Lena Eipert; Laura Ziegenbalg; Georg Klump
Oldenburg University, Germany

Introduction

The ability to perceive and analyze signals from a single sound source in a cacophony of sounds is reduced, even if these signals are well separated in the auditory periphery from the sounds of other sources. This defines informational masking (IM). IM may emerge in the presentation of sequential sounds (e.g., Watson 2005) in which the temporal separation of masker and target prevents energetic masking in the auditory periphery. IM that causes an elevation of discrimination thresholds is affected by the similarity between target and masker and stimulus uncertainty. Auditory cues that may help to overcome IM in difficult acoustic situations are, for example, pitch or localization differences between target and masker sounds. Here we present results from a sequential IM study investigating the role of the similarity of fundamental frequency and/or vowel type and relative spatial location of target and masker sound sources on level discrimination thresholds.

Materials and Methods

Four gerbils were trained in a sequential IM paradigm adapted from Winkler et al. (2003) to report level increments of target tones in a sequence of level roving distracting tones (maskers) and constant level standard tones. Level discrimination thresholds were determined in a Go/NoGo procedure applying the method of constant stimuli. Different combinations of two vowels (/I/ and /i/) and two fundamental frequencies (101 Hz and 127 Hz) as well as sound source localization (co-located and 90 degrees separated) were presented and the effect of target and masker similarity on IM in a condition of high stimulus uncertainty was determined. In control conditions level discrimination thresholds were determined presenting standards and deviants only.

Results and Conclusions

IM resulting in increased intensity discrimination thresholds was observed if the characteristics of targets/standards and maskers regarding vowel type, fundamental frequency and the location of their sources were the same. IM was reduced if target/standard and masker vowels were presented from separate locations. If target/standard and masker vowel pairs differed either in vowel type or fundamental frequency, this provided a sufficient segregation of the streams of targets/

standards and of maskers that abolished IM completely. Source separation only offers an additional benefit in this sequential IM task, if vowel type and fundamental frequency of targets/standards and maskers are the same.

PS-461

Interaction of Spatial and Non-Spatial Cues in Auditory Stream Segregation by the European Starling

Naoya Itatani; Georg Klump
Carl von Ossietzky University of Oldenburg

Introduction

Auditory object formation relies on the auditory system integrating or segregating sounds based on their acoustic features. Non-spatial cues provided by sound sources such as frequency spectra, temporal fine structure and the signal envelope are important for auditory stream segregation and the role of these cues has been previously studied. For example, auditory streaming based on tone frequency was objectively measured by using an onset time shift detection paradigm (Itatani and Klump 2014). In the natural environment, however, multiple auditory cues are present and they will interact in forming the streaming percept. The purpose of our present study is to behaviorally investigate how two cues, i.e., tone frequency and spatial position of the sound source, affect stream segregation in the European starling (*Sturnus vulgaris*).

Methods

We conducted operant Go/NoGo experiments with a repeated background to obtain an objective measure of stream segregation. Background stimulus was a sequence of ABA- triplets, where A and B represent 40 ms pure tones separated by a 40 ms silent gap and – indicates 120 ms silent period (total duration of one ABA- triplet was 320 ms). For the target triplet, the B tone onset time was delayed by 4, 12, 20, 28 or 36 ms reducing the duration of following silent gap accordingly. Animals were trained to react to the target with a Go response. Time shift detection is easier when the tones are heard as one stream. The non-spatial cue for stream segregation was introduced by varying the frequency difference between A and B tones ($\Delta f = 0$ or $\Delta f = 6$ semitones). For generating varying spatial cues, the A tone was always presented from the front and the B tone position was either the same as the A tone position or shifted to the side.

Results and Summary

Time shift detection thresholds in different stimulus conditions were compared. The results of our first experiments indicate that the time shift detection was worse for Δf of 6 semitones than for $\Delta f = 0$ semitones. When only spatial cues were present (i.e., $\Delta f = 0$), the performance dropped with increasing the distance between the A and B tone positions. This threshold increase with spatial separation was less pronounced for $\Delta f = 6$. Our observation indicates that spatial and non-spatial cues interact in auditory streaming.

PS-462

Reverberation as a Cue for Sequential Streaming

Eugene Brandewie; Andrew Oxenham
University of Minnesota

Background

A physical difference between two stimuli has been known to elicit perceptual segregation when the segregation cue (such as F0) is perceptually salient. Here the use of reverberation as a perceptual cue for sequential streaming is tested using a task involving rhythmic masking release.

Methods

On each trial, listeners were presented with a target stream of sixteen random samples of 50-ms Gaussian noise bursts separated by a minimum of 250 ms silence. Additionally, sixteen identical maskers were presented at random times during the presentation of the target stream. The listener's task was to identify which of two possible rhythms were presented during each trial. Seven conditions were tested that varied in the properties of the target noise bursts: (1) a duration control condition with damped targets to emulate a reverberant decay; (2) simulated diotic reverberation with tail; (3) diotic reverberation with the reverberant tail truncated; (4) dichotic reverberation with tail; (5) dichotic reverberation with tail truncated; (6) dichotic reverberation targets (with tails) with matched-envelope damped maskers, and (7) a dichotic control in which the masker and target streams were presented to opposite ears. Each condition was tested with five effective T_{60} durations, randomly distributed in a block of trials [0, 100, 300, 500, and 1000 ms], determining the duration of the damped tail or reverberation.

Results

When combined with non-reverberant maskers, the reverberation cue on the target did not provide any additional information beyond the increase in duration for the targets due to the reverberant tail. The spectral coloration produced by the reverberation provided only a weak segregation cue, when no temporal envelope (tail) cues were present. However, when the tails were present in both masker and target, performance was high, starting at a T_{60} of 300 ms, based only on spectral and binaural cues present in the reverberation.

Conclusions

The results suggest that binaural and spectral coloration during sound presentation is a relatively weak segregation cue, but that the same coloration in the reverberant tail directly following sound offset can be a significant segregation cue, presumably due to the prominence of the indirect sound in the tails. Overall, differences in reverberation, such as those produced by objects at different distances within a room, can serve as a prominent grouping cue to aid perceptual segregation, provided that the reverberation is binaural and the decaying envelope is available to the listener.

PS-463

Spectral Weighting of Interaural Time- and Level Differences: Effect of Bandwidth and Stream Segregation

Axel Ahrens; **Suyash Joshi**; Bastian Epp
Technical University of Denmark

An important ability of the auditory system is to localize sound sources to improve speech-intelligibility in environments with interfering talkers. The information used by the auditory system for localization in the lateral plane are interaural disparities in time- and level (ITD, ILD), where the sensitivity depends on the frequency of the signal. In the presence of stimulus energy farther from the band with interaural disparity, sensitivity decreases, indicating an across-frequency integration (spectral weighting) of binaural information. This effect is referred to as binaural interference and can be reduced in the presence of auditory streaming. Previous studies used narrowband signals to estimate the spectral weighting for across-frequency integration in binaural processing. Considering that off-frequency information alters sensitivity of an auditory channel to interaural disparities, it can be assumed that across-frequency contributions are different for narrowband- compared to broadband signals.

It is hypothesized that spectral weights derived from broadband stimuli differ from estimates derived with narrowband signals due to presence of binaural interference. It is further hypothesized that the spectral weighting changes in conditions of auditory streaming. The present study estimates across-frequency contributions to the lateralization of a broadband signal consisting of eleven 1-ERB-wide noise bands (442 Hz to 5544 Hz) with 1-ERB-wide spectral gaps. The contribution of each noise band was estimated using regression analysis. In the first experiment, ITD or ILD were applied to each of the eleven noise bands and were roved independently on every trial. In the second experiment, two noise bands on each side of the spectrum were removed to decrease the stimulus bandwidth. In experiment three, noise bands on each side of the spectrum were presented as uncorrelated noise, reducing the effective bandwidth of binaural information. In the fourth experiment, all but the target noise bands were put into a temporal context, forming an auditory stream.

The data show that only the lowest- or highest frequency band received highest weight for ITD and ILD, respectively. In conditions of auditory streaming, streaming of 10 spectral bands significantly enhanced the weight given to the remaining band for ILDs, but not always for ITDs. The spectral weights differed from the weights derived from narrowband stimuli using detection thresholds. In experiment two and three, spectral weighting of binaural cues depended on bandwidth spectral components. The data indicate that the lowest and highest frequencies in the stimulus contribute most to the lateralization of sounds.

PS-464

Temporal Delays between Double-Sounds Enable Single-Target Localization Performance in Elevation

Rachel Gross-Hardt[1]; Peter Bremen[2]; Marc van Wanrooij[2]; John van Opstal[2]
[1]Radboud University, Nijmegen; [2]Dept. Biophysics

Introduction

Synchronously presented sounds from two independent loudspeakers in the median vertical plane result in weighted averaging localization behavior of human listeners. Since temporal onset differences are strong cues for segregating sound sources in a sound mixture, e.g. in the horizontal plane onset differences as small as 5 ms are sufficient for the accurate localization of either of two sound sources, we investigated if asynchronous presentation of two sound sources in the midsagittal plane can also recover accurate single target localization.

Methods

We presented a 140 ms frozen Gaussian white noise (GWN) at either -25, 0, or 25 deg and a 140 ms 50 Hz buzzer (BZZ) at 6 locations (ranging from -55 to 55 deg) in the midsagittal plane. BZZ onset delays re GWN ranged from 0 to 400 ms. As a reference, we also measured localization gain to BZZ alone. We randomized all location and delay configurations within one block and instructed five listeners to localize the BZZ by orienting a head-mounted laser pointer to the perceived sound location.

Results

As in our previous study, synchronous presentation of BZZ and GWN led to a weighted averaging response. With increasing onset delay responses became biased towards the BZZ location. Interestingly, with onset delays >30 ms localization behavior was dominated by the succeeding BZZ. With increasing spatial disparity localization was biased towards the perceived BZZ-alone location at even shorter delays (>10 ms). Interestingly, single-source localization gain was affected by sound duration in a similar fashion as double-sound localization by delay.

Discussion

In accordance with a central tenet of auditory scene analysis, asynchronous presentation of two sound sources can lead to accurate localization of a target sound, indicating that the auditory system is indeed able to disentangle two sound sources based on onset differences. For accurate elevation localization the delay between the two sources had to be >30 ms. The temporal asynchrony needed to segregate two sound sources in azimuth is almost more than an order of magnitude smaller (~5 ms). Differences in task, as well as differences in how the auditory system localizes sources in the vertical and horizontal planes may account for this discrepancy. We address whether a combination of spectral cues or neuronal mechanisms, e.g. adaptation to the leading sound, or the processing time required to map sensory cues to response location, might account for the observed responses.

PS-465

Auditory Grouping in Treefrogs and its Neural Correlates in the Inferior Colliculus

Mark A. Bee; Katrina M. Schrode; Norman Lee
Department of Ecology, Evolution and Behavior, University of Minnesota, St. Paul, MN 55108

Humans exploit environmental regularities in sounds to perceptually bind acoustic energy occurring simultaneously at different frequencies. Such abilities influence vowel perception in speech and timbre perception in music. Other animals solve similar binding problems in the recognition of species-specific acoustic signals. Moreover, they commonly do so using auditory systems that differ in notable ways from that of mammals. This study of two treefrog species investigated temporal and spatial coherence as cues that promote the perceptual binding of two spectral bands emphasized in their acoustic signals. In two-alternative choice tests, females preferred temporally and spatially coherent calls over alternatives in which the onsets/offsets of the two bands were made asynchronous by more than 25 ms or in which the two bands were spatially separated by 7.5° or more. Preliminary single-unit recordings from the inferior colliculus of awake treefrogs have identified potential neural correlates of grouping based on temporal coherence. Neurons that exhibit non-linear facilitation or suppression in response to combination tones also exhibit changes in firing rates to temporal asynchrony that are correlated with changes observed in behavioral experiments with the same species. These results, which suggest temporal and spatial coherence promote across-frequency auditory perceptual binding, are notable given differences in how the two spectral bands are transduced by the anuran auditory system compared with the mammalian auditory system. Sound energy in the high-frequency and low-frequency bands primarily enters the treefrog auditory system via different pathways (tympanum and body wall, respectively) and is encoded primarily by different papillae in the inner ear (basilar papilla and amphibian papilla, respectively). Hence in treefrogs, "across-channel" processing takes on special significance in terms of identifying signal-processing strategies for auditory grouping given the anatomical and physiological bases of auditory channels in these organisms.

PS-466

Speech Reception Benefits of Physiologically Inspired Cochlear Implant Signal Processing

Raymond Goldsworthy[1]; Jayaganesh Swaminathan[2]
[1]Sensimetrics Corporation; [2]Boston University

An approach to developing physiologically inspired cochlear implant (CI) signal processing is described, and perceptual measurements with CI users are reported. These results are discussed in the context of amplitude-modulation analysis that quantifies the effect of noise on speech envelopes. Envelopes were derived from a phenomenological auditory-nerve model (Zilany and Carney, 2010) that has been rigorously tested against physiological responses to simple and complex stimuli. Many of the physiological properties associated with nonlinear cochlear tuning are captured by this model including compression, suppression, and neural adaptation that are known to be critical for representing speech in quiet and noise. For the perceptual measurements, the envelopes were imposed on constant-rate current pulses via a programmable interface. Performance with this "neural" strategy was compared against the listeners' clinical processor as well as a laboratory version of the Advanced Combinational Encoder (ACE) processor. Sentence, consonant and vowel identification were obtained from 5 CI users in quiet and in speech-shaped noise at a 6 dB signal to noise ratio. Overall, performance with the neural strategy was intermediate between that with subjects' clinical processor and that with the laboratory version of the ACE processor. The closeness of results with the neural strategy to those with their personal processor was viewed as promising given that 1) no individual tailoring of parameters were performed, and 2) subjects had no training listening with the neural strategy. To provide context for these results, envelope modulation analysis was conducted to determine the correlation between speech envelopes in quiet and noise at the processor output. The processors examined were the laboratory ACE processor and the neural processor with varying degrees of simulated outer hair cell loss. Preliminary results from this modeling work demonstrate higher correlation of speech envelopes in quiet and noise at the output of the neural processor compared to the standard ACE processor, especially for key speech regions of 3 to 7 Hz (phonemic rate) as well as 80 to 120 Hz (fundamental frequency for the speech analyzed). Future research directions will be discussed that integrate modeling work and perceptual studies towards optimizing this neural strategy.

PS-467

Relative Weight of Temporal Envelope for Speech Perception Across Speech Frequency Regions in Children and Adults

Yingjiu Nie; Alexandra Short; Harley Wheeler; Caleb Harrington
James Madison University

Introduction

Temporal envelopes (TEnv) provide important auditory information for hearing impaired listeners, particularly cochlear implant users. The goal of the current study was to investigate the developmental effect on the use of TEnv for speech perception.

Methods

The relative weight of TEnv for speech perception in each of the eight frequency regions ranging between 72 and 9200 Hz was assessed with children 10-16 years of age and adults with normal hearing. Listeners were tested in quiet and in the presence of steady or amplitude modulated noise at two rates (4 and 16 Hz). The contribution of each region to masking release was also evaluated. An eight-band noise vocoder was implemented to degrade spectral resolution and preserve TEnv cues of Coordinate Response Measure (CRM) speech corpus sentences along with background noise. Speech intelligibility of a given band was assessed by comparing scores in two conditions differing only by the presence or absence of the band of interest; the proportion of the derived score to

the sum across the eight bands was computed as the relative weight.

Results
Preliminary data showed the following,

1. in quiet, similar frequency-weighting pattern for children and adults with higher weight in the mid/mid-high frequency range (bands # 4-6);
2. in noise (presented at 0 dB SNR), for adults, different weighting patterns between steady noise [more weight at mid-high/high frequencies (bands #6-7)] and amplitude-modulated noise [more weight at mid/mid-high frequencies (bands #4-6)]; for children, similar weighting patterns for all types of noise with equivalent weight across mid to high frequencies (bands # 4-7);
3. a large difference between adults and children in frequency-contribution to masking release: positive masking release was observed mainly in the mid frequencies (bands # 4-5) at both AM rates in adults, while negative masking release was seen in children when noise was modulated at 16 Hz in contrast to the positive masking release in noise amplitude-modulated at 4 Hz.

Summary
The study suggests differences between adults and children in making use of TEnv cues for speech perception in noise, which is in line with the psychoacoustic findings that temporal processing does not mature until adolescence.

PS-468

Longitudinal Changes in Perception of Speech and Pitch By a Cochlear Implant User with Different Electrode Array Locations

Mario Svirsky[1]; Alejo Suárez[2]; Valeria Lapilover[2]; Maja Svrakic[1]
[1]NYU School of Medicine; [2]Programa de Implantes Cocleares, Montevideo, Uruguay

Introduction
Human ability to adapt to a modified peripheral frequency-to-place mapping may determine the degree of success of cochlear implantation in postlingually deaf individuals. There are no guarantees that an intracochlear electrode that is mapped to respond to a certain acoustic frequency will stimulate neurons whose characteristic frequency matches the stimulus. In fact, it is common for cochlear implant users to experience basalward mismatch (an electrode stimulates neurons whose characteristic frequency is higher than the acoustic input), and apicalward mismatch also occurs although less frequently. Fortunately, humans have some capacity to adapt to such mismatches. This study examines the perception of speech and pitch in the rare case of an individual who had long term experience with four different electrode array locations, one in the left ear and three in the right.

Methods
Longitudinal changes in speech perception and interaural electrode pitch ranking were examined. The data were interpreted as a function of three factors: the tables used to allocate frequency ranges to each electrode (Frequency Allocation Tables, or FATs), the intracochlear electrode location, and the amount of experience with each frequency-to-place map (which results from a combination of FAT and electrode location). In total, five conditions were assessed due to the use of two different FATs in the left ear and three different electrode array locations in the right ear over the course of seventeen years.

Results
Speech perception scores using a standard FAT (188-7938 Hz) were excellent in the right ear well within a month of electrode insertion, when the angular location of the most apical electrode was either 380° or 290° from the round window. In contrast, an apical electrode location of 220° resulted in very low initial scores with only moderate increases over the course of the following 19 months. Speech perception in the left ear with an apical electrode location of 450° was also modest after several years of experience with the standard FAT but improved significantly over the course of ten months with the use of an alternative FAT (63-5188 Hz). Pitch ranking results changed as a function of experience with different frequency-to-place maps.

Discussion
Depending on the amount of frequency mismatch to be overcome, adaptation to any given frequency-to-place map in the same postlingually deaf individual may be very quick, may take a long time or may even be incomplete despite years of experience.

PS-469

Cochlear Implant Listeners' Performance Improves Beyond Eight Spectral Channels in Some Cases

Kara Schvartz-Leyzac; Teresa A. Zwolan; Bryan Pfingst
University of Michigan

Introduction
Reduced spectral resolution is a limiting factor for cochlear implant (CI) performance. Both electrical current spread and poor neuron survival are thought to contribute to cross-talk between spectral channels. Although multichannel cochlear implants offer up to 22 individual electrodes, evidence to date suggests listeners' performance asymptotes with as few as 4, but no greater than 8-10 spectral channels. However, the literature cited in support of this claim does not necessarily reflect current CI technology and/or current patient populations. For example, processing strategies have evolved, and CI candidacy criteria have expanded to include patients with better pre-operative hearing thresholds compared to several years ago. The current study aimed to revisit the question of how many spectral channels of information are required by CI users to recognize speech.

Methods
Subjects included adults implanted with Cochlear Nucleus® implant systems, using the CP810 speech processor and ACE sound processing strategy. Sentence, consonant and vowel recognition were measured in quiet and speech-

shaped noise, as the number of active electrodes was systematically varied from 4 to 20 while maintaining an even distribution across the frequency spectrum. When the number of active electrodes was reduced, frequencies were reallocated, broadening the allocation to each remaining channel and maintaining the full spectral range across the electrode array. Results were analyzed using a within-subjects design.

Results

Preliminary results show a complex pattern of performance. The number of usable channels varies significantly across listeners, and is also dependent on type of speech. For some listeners, performance seemingly asymptotes with as few as 8 channels, while for other listeners performance continues to improve up to 16 or 20 channels.

Conclusions

The results of this study are in keeping with anecdotal observations in the clinic that deactivating more than a few electrodes has negative consequences for some listeners. The results have important implications for our understanding of cochlear implant processing and the factors that contribute to overall performance with the device. We will explore possible underlying factors, such as cochlear health, that vary across listeners and could help to explain across-subject differences in performance.

PS-470

The Effect of Temporal and Spectral Interactions on Spatial Release From Masking in Simulations of Cochlear Implants for Single-Sided Deafness.

Jessica Wess[1]; Douglas Brungart[2]; Joshua Bernstein[2]
[1]Walter Reed National Military Medical Center, Bethesda, MD University of Maryland, College Park; [2]Walter Reed National Military Medical Center, Bethesda, MD

Communicating in complex, multitalker environments requires listeners to perceptually segregate the speech target of interest from the interfering background. Normal-hearing listeners (NH) are able to capitalize on binaural cues and use spatial separation between target and masker signals to perceptually stream a speaker of interest. Individuals with single-sided deafness (SSD) are therefore at a disadvantage in multitalker situations. Recent results from our laboratory suggest that a cochlear implant (CI) can facilitate speech-stream segregation for individuals with SSD, especially in situations with high informational masking (high confusability between speakers, i.e., same-gender talkers). Nevertheless, the amount of spatial release from masking (SRM) afforded by the CI is limited and variable across individual listeners. One possibility is that the amount of SRM is influenced by the degree of spectral or temporal mismatch across the ears. Temporal mismatch is likely to occur based on the relationship between the CI processing delay and the traveling-wave delay in the NH ear. A spectral mismatch between the ears is likely to occur because the CI electrode does not reach the apex of the cochlea. The goal of this study was to use vocoder simulations to examine how spectral and temporal mismatch across the two ears might limit SRM.

NH listeners participated in a task requiring them to segregate a target talker from two same-gender maskers in the first (normal) ear while listening either to silence or a noise-vocoded mixture containing only the maskers in the second (simulated deaf) ear. This allowed us to test whether listeners could integrate the masker signals across the ears to better hear the monaural target. Experiment 1 varied the number of vocoder channels while frequency-shifting the synthesis filters. We hypothesized that a greater number of vocoder channels (i.e., greater spectral similarity between the masker signals presented to the two ears) would yield more masking release, but that the masking release would also be more susceptible to spectral mismatch. Experiment 2 examined the effect of combined spectral and temporal mismatch on SRM. While previous results suggested that SRM was relatively immune to interaural temporal mismatch between the NH and vocoded ears, we hypothesized that temporal mismatch would have a greater effect when the vocoded stimulus was also spectrally shifted. Implications for fitting strategies for CI users with SSD will be discussed.

PS-471

The Incomplete Role of the Pitch Contour in Voice Emotion Transmission

Anna Tinnemore[1]; Monita Chatterjee[2]
[1]University of Arizona; [2]Boys Town National Research Hospital

Introduction

Acoustic cues that are important for identifying vocal emotion include variations in voice pitch, intensity and duration of utterances. Listeners with cochlear implants (CIs) have limited access to voice pitch (F0). Listeners with hearing impairment have better access to F0 cues than CI patients. However, there is evidence that both groups have deficits in voice emotion recognition. The goal of this study was to ascertain the contribution of the basic acoustic cues of pitch, intensity, and duration alone to vocal emotion recognition by normally-hearing listeners.

Methods

Ten young normal-hearing adults identified voice emotion under various acoustic conditions. Stimuli were 12 sentences (single female talker) expressing five basic emotions: happy, sad, angry, afraid and neutral, spoken in a child-directed manner, i.e. with exaggerated prosody. To isolate the effect of the acoustic cues, we extracted the pitch contours from these recordings with PRAAT software, synthesizing a verbal signal without words containing pitch, intensity and duration information but no phonetic cues and no spectral envelope information (SYNTH).

Pilot testing found reduced emotion recognition in the SYNTH condition. We hypothesized that participants were attempting to identify the lexical content of the original speech, and that this effort detracted from focus on emotion identification. A PRIMED_SYNTH condition tested this hypothesis by preceding each hum with the original sentence spoken in a neutral

tone. Two additional conditions examined the role of phonetic information and simulated the reduced bandwidth in hearing loss by low-pass filtering the original stimuli with corner frequencies of 500 and 353 Hz (LP_500 and LP_353 respectively).

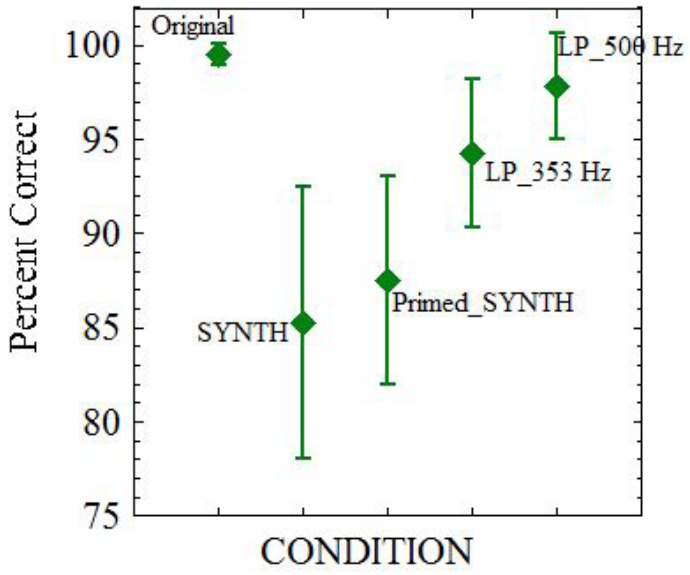

Results
A linear mixed-effect model was used to analyze the data, with speech condition as the repeated, fixed factor and a subject-based random intercept. A significant effect of the speech condition was observed ($p<0.001$). Pairwise, Bonferroni-adjusted comparisons showed that scores in the SYNTH condition were significantly poorer than with original speech ($p<0.001$). No significant benefits of priming were observed. Performances in the LP_500 and LP_353 conditions were significantly better than SYNTH ($p<0.001$ and $p<0.002$ respectively), but not significantly different from performance with original speech, nor from each other.

Conclusion
These results indicate that the acoustic cues of pitch, intensity, and duration alone are not sufficient for best performance on a vocal emotion recognition task. Retaining speech information below 500 Hz appears to provide sufficient information to support excellent performance, pointing to an additional possible role of acoustic phonetic cues in voice emotion recognition.

PS-472

Cochlear Implant Insertion Trauma and Spontaneous Recovery

Deborah Colesa[1]; **Bryan Pfingst**[2]
[1]University of Michigan; [2]Kresge Hearing Research Institute, Department of Otolaryngology, University of Michigan

Introduction
The importance of acoustic hearing preservation for cochlear implant users is widely recognized but the underlying sequence of events that lead to successful hearing preservation are poorly understood. In a guinea pig animal model implanted in a hearing ear, we have observed evidence of insertion trauma and subsequent spontaneous recovery in acoustic detection thresholds over the first month after implantation.

Methods
Subjects were 14 mature adult male pigmented guinea pigs. The animals were trained to perform a simple go-no-go task for measuring psychophysical detection thresholds for pure-tone stimuli. One ear was deafened to allow free field testing of the other ear. Pre-implant baseline acoustic detection thresholds were assessed at frequencies ranging from 250 Hz to 24 kHz. A 6-channel cochlear implant was then inserted into the basal turn of the hearing ear and acoustic pure tone detection thresholds were followed over time for up to 1.8 years after implantation.

Results
Acoustic detection thresholds in the tonotopic region of the implant (24,16 and 8 kHz) measured during the first two weeks after implantation, were elevated by more than 20 dB for one or more test frequencies in 93% of the ears tested. Elevations as high as 75 dB were observed. At lower frequencies (4 kHz to 250 Hz; areas apical to the implant), threshold elevations were similar except in the 500 to 250 Hz range where they were slightly smaller on average. Thresholds then decreased over time toward normal pre-implant levels reaching a relatively stable level by 30 days post implantation in 67% of the cases. Thresholds during the relatively stable period were on average 13.4 dB (S.D. = 16.4 dB) above the pre-implant thresholds. Thresholds remained at these levels in most cases for the duration of the testing period (up to 1.8 years after implantation). However, dramatic increases in thresholds with no recovery were observed in 1 animal and very gradual increases or decreases over time were seen in others.

Conclusions
Guinea pigs implanted in a hearing ear provide a useful animal model for the study of cochlear implant insertion trauma and spontaneous recovery. Similar changes in sensitivity have been observed for electrical detection thresholds as well as ECAP thresholds and amplitude-growth functions in animals implanted in a deaf ear, suggesting that the loss in sensitivity and subsequent recovery might be due to conditions involving the auditory nerve rather than the hair cells.

PS-473

Measuring the Electric Potential Distributions of Different Stimulation Modes in an Implanted Cochlea

Kai Dang[1]; Clair Vandersteen[2]; Nicolas Guevara[2]; Maureen Clerc[3]; Dan Gnansia[4]
[1]Inria / Neurelec - Oticon Medical; [2]Institut Universitaire de la Face et du Cou, Centre hospitalier universitaire de Nice; [3]Inria; [4]Neurelec - Oticon Medical

Background
In cochlear implants, knowing how the electric field is affected by the interaction between the cochlear geometry, the electrode layout and the stimulation modes is important for the optimization of stimulation and the creation of personalized profiles. Until now, such information was acquired mainly

through indirect approaches, such as measuring the spread of excitation, electric field imaging and numerical simulation. In order to have a clear view of how the actual stimulations propagate inside the cochlea, we have designed and conducted an experiment which aims at recording the potential changes at different positions in the cochlea in response to a variety of stimulations.

Methods

We recreated a typical cochlear implantation scenario on a human specimen. A 20 channel straight electrode array was implanted into the scala tympani through a cochleostomy and a reference electrode was placed between the scalp and skull near the cochlea. Stimulations with different waveforms (biphasic square and ramp pulses) and spatial patterns (monopolar, bipolar, tripolar and common ground) were then sent to the implanted electrodes, using various typical durations and amplitudes. During each stimulation, the potential changes on all of the 20 electrodes were recorded by an oscilloscope with 5MHz sampling rate. After the stimulations, a micro-CT scan was applied on the implanted human specimen to determine the cochlear shape and the electrode array positioning.

Results

The stimulation waveforms conducted by the cochlear tissue have been acquired along the scala tympani. Preliminary results confirmed that spatially, tripolar stimulation mode has the best current focusing effect while monopolar mode has the smoothest potential distribution. Some results indicated that the deformation in the recorded waveform observed at a relatively high sampling rate is probably due to the capacitance of the head tissue. The electrodes with insertion issues, such as partially inserted, have also showed different characters in the recorded waveforms.

Conclusion

This experiment provides credible potential distribution data recorded at different locations inside the cochlea. The stimulations being compared in the experiment cover most of the stimulation strategies adopted by current cochlear implant products. The results from it will provide support information for choosing or optimizing the stimulation strategies in the future.

PS-474

Intracochlear Acoustic Receiver for Totally Implantable Cochlear Implants: Concept and Preliminary Temporal Bone Results

Flurin Pfiffner[1]; Lukas Prochazka[2]; Konrad Thoele[3]; Francesca Paris[4]; Joris Walraevens[4]; Jae Hoon Sim[3]; Rahel Gerig[3]; Dobrev Ivo[3]; Dominik Obrist[5]; Christof Röösli[3]; Alex Huber[3]

[1]University Hospital Zurich; [2]Institute of Fluid dynamics, Swiss Federal Institute of Technology in Zurich (ETH), Switzerland; [3]Dept. Otorhinolaryngology, Head and Neck Surgery, University Hospital Zurich, Switzerland; [4]Cochlear Technology Centre Belgium, Mechelen, Belgium; [5]ARTORG Center, University of Bern, Switzerland

Introduction

A cochlear implant (CI) provides electrical stimulation directly to the nerves within the cochlea and is used to treat patients with severe to profound hearing loss. There are substantial unsatisfied needs that cannot be addressed with the currently available partially implantable CI systems. A totally implantable CI system could deliver to recipients significant safety benefits and improved quality of life. An implanted acoustic receiver (IAR) in the inner ear that replaces the external microphone is a crucial step towards a totally implantable CI.

Goals

The overall goal of this project is to develop and validate an IAR that could be included in future totally implantable CI systems.

Methods

1. In a first step different suitable sensor technologies for an IAR have been evaluated on the basis of theoretical modeling as well as experimental testing. Requirements have to meet anatomical cochlea size restrictions, biocompatibility, sensitivity, power consumption and operating environment (fluid).

2. A prototype IAR has been assembled and used to measure the inner ear pressure in prepared human and sheep temporal bones. Acoustic stimulation was applied to a sealed ear canal and recorded as a reference signal near the tympanic membrane. The inner ear pressure measurement position was controlled by a micromanipulator system and verified with a subsequent CT-scan and 3D reconstruction of the temporal bone.

Results

1. The result of the sensor technology evaluation has shown that an IAR on the basis of a MEMS condenser microphone is a promising technology for dynamic pressure measurements in the inner ear. A prototype sensor with a single diaphragm has been assembled.

2. Preliminary results in human and sheep temporal bones confirm that the inner ear pressure can be measured with this prototype IAR. Results show that the inner ear pressure varied depending on stimulation level, sensor insertion depth and access location to the cochlea. Measurement repeatability has been confirmed and prelimi-

nary pressure results are similar to reference values described in literature.

Conclusions
Preliminary results confirm that a MEMS condenser microphone is a promising technology to measure the inner ear pressure. To achieve our overall goal optimal insertion place and sensor design improvements will be needed to improve the signal to noise of pressure measurements.

PS-475

Focused Multipolar Stimulation for Improved Performance of Cochlear Implants: Preclinical Studies

Shefin George; Robert Shepherd; Andrew Wise; Mohit Shivdasani; James Fallon
Bionics Institute

Introduction
The conductive nature of the fluids and tissues of the cochlea can lead to broad activation of spiral ganglion neurons using contemporary cochlear implant stimulation configurations such as monopolar (MP) stimulation. Focusing of the stimulation is expected to result in improved implant performance. We evaluated the efficacy of focused multipolar (FMP) stimulation, a current focusing technique in the cochlea, by measuring neural activation in the auditory midbrain and compared its efficacy to both MP stimulation and tripolar (TP) stimulation. We also explored the efficacy of a stimulation mode that is referred to here as partial-FMP (pFMP) stimulation to achieve lower stimulation thresholds compared to the standard FMP stimulation.

Methods
Following implantation of Cochlear™ Hybrid-L 14 arrays into the acutely (n=8) and long-term deafened (n=8) cochlea of cats, the inferior colliculus (IC) contralateral to the implanted cochlea was exposed. Multiunit responses were recorded across the cochleotopic gradient of the central nucleus of the IC in response to electric (MP, TP, FMP and pFMP) stimulation over a range of intensities using a 32 channel silicon array (NeuroNexus). pFMP stimulation involved varying the degree of current focusing by changing the level of compensation current. The spread of neural activity across the IC, measured by determining the spatial tuning curve (STC), was used as a measure of spatial selectivity. The width of STCs were measured at cumulative *d'*=1 above minimum threshold.

Results
MP stimulation resulted in significantly wider STCs compared to FMP and TP stimulation in animals with normal and severe auditory neuron degeneration (one-way RM ANOVA, $p<0.001$). However, thresholds were significantly higher (one-way RM ANOVA, $p<0.001$) for FMP and TP stimulation compared to MP stimulation. Using pFMP stimulation, the high threshold levels for FMP stimulation was significantly reduced without compromising spatial selectivity (one-way RM ANOVA, $p<0.001$).

Conclusion
The data indicated that FMP and TP stimulation resulted in more restricted neural activation compared to MP stimulation and this advantage of FMP and TP was maintained in cochleae with significant neural degeneration more reflective of the clinical situation. pFMP stimulation would be expected to minimize response threshold of FMP stimulation.

PS-476

Preserving Sensitivity to Interaural Timing Differences in Bilateral Cochlear Implant Listeners: Effects of Rate and Place of Stimulation with Multi-Electrode Stimulation

Tanvi Thakkar[1]; Alan Kan[2]; Heath Jones[2]; Ruth Litovsky[2]
[1]University of Wisconsin-Madison; [2]Waisman Center, University of Wisconsin-Madison

Background
Bilateral cochlear implant (BiCI) listeners experience difficulties in sound localization and speech understanding in noise. One possible explanation is that current speech processing strategies use high-rate electrical pulse trains on ALL channels. While high rates are important for speech recognition, they are unusable for processing important binaural cues, namely interaural timing differences (ITDs). One solution is to preserve high-rate stimulation at some electrodes and present low rates to other electrodes, ideally preserving both speech recognition and sound localization. The goal of this project was to identify a mixed-rate multi-electrode strategy that could preserve sensitivity to ITDs. Furthermore, we examined the effects of multi-electrode stimulation using alternative rate-to-place mappings to evaluate tonotopy regarding ITD sensitivity. We hypothesized that introducing low-rate ITDs at a few electrodes and high-rate ITDs at remaining electrodes would provide sufficient ITD cues, and this strategy may or may not be dependent on specific cochlear locations.

Methods
Using direct electrical stimulation, ITD sensitivity was measured in a two alternative forced choice discrimination task, using three multi-electrode conditions, each with 5 pairs of pitch-matched electrodes (base, mid-base, mid, mid-apex, apex). The three conditions were: (1) 100 pulses per second (pps) stimulation at all 5 pairs; (2) 1000 pps at all 5 pairs; and (3) 1000 pps at 4 pairs and 100 pps on the 5th pair. ITD sensitivity of conditions (1)-(3) were also compared to sensitivities measured at 100 pps at each of the cochlear locations individually. Multi-electrode conditions were aimed at stimulating realistic sets of parameters that could be implemented in future speech processors.

Results
ITD discrimination thresholds, or just-noticeable-differences (JNDs), were higher in the 1000-pps than the 100-pps multi-electrode condition, as expected. However, the introduction of low-rate ITDs on a single-electrode pair (condition 3) led to overall improved ITD sensitivity from condition (2), suggesting that mixed-rate multi-electrode stimulation can convey ITD information. Electrode pairs stimulated with 100-

pps ITDs showed variable ITD JNDs across cochlear locations.

Conclusion
The present data suggests that low-rate ITD cues are persistent under multi-electrode stimulation in the presence of stimulation rates analogous to current speech processors, thus binaural cues for BiCI listeners can be well-represented when stimulating the length of the electrode array with minimal ITD information. Furthermore, it suggests flexibility within the binaural system of BiCI listeners even when unusable high-rate ITD information is presented at the majority of the cochlear locations.

PS-477

Modeling of Across-Frequency Interaural Level Difference Processing in Bilateral Cochlear-Implant and Normal-Hearing Listeners.

Olga Stakhovskaya; Matthew J Goupell
University of Maryland, College Park

Background
For complex broadband sounds presented in the free field, the head produces interaural time differences (ITDs) and interaural level differences (ILDs) that are used to determine the spatial location. When both localization cues are present, sound localization in bilateral cochlear implant (BiCI) listeners is typically dominated by ILDs, which is in contrast to normal-hearing (NH) listeners where sound localization is typically dominated by ITDs. While there are existing models of across-frequency ITD processing, it is presently unclear how the auditory system processes ILDs across frequency. Such a model is particularly necessary for BiCI listeners because inconsistent ILDs might be produced by several factors including mapping procedures, spread of excitation, and across-channel loudness summation. The purpose of this study was to begin developing an across-frequency ILD processing model.

Methods
BiCI listeners were presented monopolar, 1000-pps, 500-ms, constant-amplitude pulse trains at 70-80% of the dynamic range bilaterally on single or multiple electrodes. Lateralization curves were obtained for a range of ILDs from -20 to 20 CUs in 9 BiCI users. NH listeners were presented complexes with inconsistent ILDs across frequency. Laterality at each ILD was modeled with Gaussian distributions. In the summation model, the distributions from all contributing pairs were summed at each ILD value. In the multiplication model, the distributions from all the contributing pairs were multiplied at each ILD value across frequency. Then, either the maximum value or the centroid of the resulting curve was used to predict the extent of laterality at each ILD value. In the average model, the mean lateralization values of all contributing pairs were averaged across frequency to produce response predictions.

Results
For the BiCI listeners, the experiment produced different lateralization at different electrodes, as expected. All three models accounted for 78-87% of variance in the lateralization data when combined across the listeners. The average model and the summation centroid model accounted for the largest amount of variance (85-87%). A significant amount of within- and across-subject variability was observed, ranging from 0 to 87% in some listeners. For the NH listeners, the experiment produced effects of stimulus center frequency. This suggests that the models need to include frequency-dependent weights.

Conclusions:
Models of ILD-based lateralization investigated in this study explained a high percentage of variance in the CI lateralization data and will help us better understand sound localization in BiCI and NH listeners.

PS-478

Increased Incidence of Spontaneous Otoacoustic Emissions in Mice Lacking Otoancorin

Mary Ann Cheatham[1]; Yingjie Zhou[1]; Jonathan Siegel[1]; Guy Richardson[2]
[1]Northwestern University; [2]University of Sussex

Introduction
Otoancorin is an inner ear specific protein expressed in interdental cells of the spiral limbus (Zwaenepoel et al., 2002). Data obtained from otoancorin knockout (KO) mice (Lukashkin et al., 2012) show that this protein is required for limbal attachment of the tectorial membrane (TM). Although mice lacking otoancorin also display a fenestrated lateral edge and lack Hensen's stripe, the TM remains in contact with the tallest of the outer hair cell stereocilia. Based on work using a mouse model lacking Ceacam16 (Cheatham et al., 2014), an important TM protein, we evaluated the otoancorin KO mouse to provide additional information on spontaneous (SOAE) and stimulus frequency emissions (SFOAE), as well as auditory brainstem responses (ABR).

Methods
Distortion product (DP)OAEs were obtained for primaries (F1 and F2) presented at 70 dB and with F2 as the parameter. Input-output functions for various F2 frequencies were also collected and used to extract the level of F1 producing a DPOAE of 0 dB, which was designated as threshold. Spectral averaging without acoustic stimulation revealed any SOAEs, while SFOAEs were acquired for a 30 dB probe tone using the suppression method. ABR thresholds were also recorded using a large number of averages and noting the level at which the ABR waveform disappeared into the noise floor. All data were collected in young mice on a mixed 129/C57BL6 genetic background.

Results
Although there is no frequency region where mice lacking otoancorin have normal hearing, these animals exhibit their largest DPOAEs for low-frequency primary pairs. In addition,

ABR thresholds show an ~50 dB threshold shift above 10 kHz but for lower frequencies the shift is ~25 dB. In spite of the loss of sensitivity, the incidence of SOAEs is enhanced in KOs re: wild-type (WT) controls. SOAEs in KOs predominate in the frequency region around 6 kHz where DPOAEs are also most prominent. Although small, SFOAEs are present in otoancorin KO mice but only in this same frequency region below 10 kHz.

Conclusions

It is remarkable that young otoancorin KO mice with a significant loss of sensitivity display large and multiple SOAEs with frequencies in the region around 6 kHz. In contrast, SOAEs are much less common in WT mice but, when present, they cluster in the frequency region around 23 kHz.

PS-479

Spectral Patterns of Spontaneous Otoacoustic Emissions are Not Dependent on Morphology

Geoffrey Manley[1]; **Christine Köppl[1]**; Christopher Bergevin[2]
[1]University of Oldenburg; [2]York University

Introduction

Spontaneous otoacoustic emissions (SOAE) are highly idiosyncratic in nature: most mammals do not show them, while most non-mammalian groups do. Previously, some obvious similarities have been noted between spectral patterns of SOAE in different groups of animals in which the morphology of the hearing organ varies hugely, raising the question as to the generation mechanisms of SOAE.

Methods

We studied SOAE from a bird, the barn owl (papillar length 11.5mm), and 9 lizard species with papillar lengths from 0.3 to 2.1mm). SFOAEs were also studied in the owl and one lizard species, the green anole, evoked by swept tones and extracted using a suppression paradigm (Kalluri R, Shera CA. J Acoust Soc Am. 2013, 134:356-68.) . All measurements were made in lightly-anesthetized animals in a sound-isolation booth.

Results

In all species, SOAE spectra generally showed many peaks with a quasi-periodic spacing. Median inter-peak distances were 405 Hz for 181 SOAE in the owl, and between 219 and 461 Hz for between 29 and 286 SOAE in the lizards. SFOAE were routinely measurable at stimulus levels of 20 dB SPL and lower (owl) or 30 dB SPL (anole). SFOAE amplitude could exceed that of the evoking stimulus and showed pronounced interactions with SOAEs. Low-level SFOAE phase accumulation between adjacent SOAE peak frequencies in both species clearly clustered around one period and corresponded in total to a delay of > 2 ms.

Conclusions

Together with published results from humans, the present data argue for a common underlying mechanism patterning otoacoustic emissions across very disparate macromorphologies of the inner ear. Despite up to a 40-fold size difference between papillae, SOAE peak spacing was remarkably similar. We suggest that otoacoustic emissions originate from phase coherence in any system of coupled, active oscillators, which is consistent with the notion of coherent reflection but does not explicitly require a traveling wave. The concept of phase coherence ties together our understanding of ears with grossly different morphologies, suggesting that despite some different biomechanical constraints, ears of mammals, birds, and lizards retain fundamental similarities in sound processsing. Wave-based (coherent reflection) and `local oscillator'-based formulations need not be orthogonal notions, but simply reflect differences in inter-element coupling.

PS-480

A Comparison of Psychometric Functions for Tone Detection At and Away from Spontaneous Otoacoustic Emissions

Pim Van Dijk[1]; Glenis Long[2]
[1]University of Groningen, University Medical Center Groningen; [2]City University of New York

Introduction

Tone detection near the threshold of hearing is presumably limited by internal noise in the ear. As a consequence, the threshold is not sharp but the probability of detecting a tone gradually increases from 0 to 1 over a near-threshold range of about 10 dB. The properties of the noise can be inferred from such psychometric functions as it represents the difference between stimuli which are always below the noise, and those that are well above the noise. In the cochlea, spontaneous otoacoustic emissions (SOAEs) affect the threshold of hearing. These cochlear instabilities are hypothesized to modify the internal noise and thus tone detection. To evaluate this hypothesis, psychometric functions for tone detection were obtained from each subject at selected SOAE frequencies and at frequencies at least 85 Hz away from any OAE.

Methods

Psychometric functions for tone detection were measured in 12 normal hearing subjects, of which 10 had detectable SOAEs. Stimulus presentation and SOAE recordings were performed with an in-the-ear probe (Etymotic ER10B). A 3AFC procedure was conducted: a 300-ms tone was temporally aligned with one of three subsequently-lit squares on a computer interface. The subject used a track pad to indicate when they heard the sound. A total of 35 psychometric functions were determined, 16 of these were at the same frequency as a selected SOAE. The psychometric functions were fitted with a curve $y = 2/3 + 1/3*\mathrm{erf}([x-x_0]/\sqrt{2}\sigma)$, consistent with a simple threshold detection model. The parameters x_0 and σ (both in Pascal) are measures of the detection threshold and the RMS level of the internal noise, respectively.

Results

Across subjects and frequencies, the threshold x_0 ranged from 34 µPa to 1.2 mPa (5 to 36 dB SPL), and the rms level s ranged from 55 µPa to 0.49 mPa. The ratio σ/x_0 was relatively stable, at 0.52(±0.06) when measured at an SOAE frequency, and 0.33(±0.06) away from a SOAE.

Discussion/Conclusion

The constancy of the ratio σ/x_0 implies that the threshold of detection is fixed relative to the detector noise. This ratio is presumably determined in the cochlea. The relatively large range of both x_0 and σ suggests that conduction of sound is variable across subjects and frequencies. This conduction through the outer, middle and inner ear will scale x_0 and σ equally. The difference of the ratio σ/x_0 between measurements at SOAEs and away from SOAEs can be interpreted in terms an oscillator model.

PS-481

Measuring Temporal Suppression of Clicked-Evoked Otoacoustic Emissions at High Frequencies

Karolina Charaziak; Christopher Shera
Eaton-Peabody Laboratories

Introduction

When two clicks are presented close together in time, the otoacoustic emission (OAE) evoked by one click (the "test" click) is reduced by the presence of the preceding/following "suppressor" click. This temporal suppression of click-evoked (CE) OAEs is usually expressed as a reduction in the rms amplitude of the CEOAE waveform. In the frequency domain, suppression observed in the CEOAE spectrum varies across frequency. The maximal suppression of low-frequency components tends to occur at longer ICIs, compared to the suppression of higher frequency bands, at least up to the current measurement limit of about 5-6 kHz. Characterizing temporal suppression at higher frequencies faces several technical issues. The principal challenge is to control the click's temporal and frequency characteristics simultaneously at the eardrum (to assure optimal cochlear stimulation across a wide bandwidth) and at the emission probe (to assure adequate temporal separation between short-latency CEOAE components and the stimulus pressures). The goal of this study was to develop methods that permit characterization of CEAOE temporal suppression over a wider range of frequencies.

Methods

A version of a "double-click" paradigm (Kemp and Chum, 1980; Hear Res 2, 213–232) was utilized where responses to the test click and combinations of pairs of clicks separated in time were obtained. Click waveforms were shaped to approximate a flat spectrum at the eardrum. Suppression was calculated as the difference between the time-domain averages of responses to the test click and the pairs of clicks, rather than the rms amplitude reduction of the delayed CEOAE. Thus, the stimulus ringing at the probe resulting from frequency-compensation of the click spectrum subtracts away without the need to window out the early part of the response. In addition, an alternative approach for removing the stimulus artifact was developed in which responses to a higher level click were acquired and used to predict stimulus pressure at the test click level (a modified "nonlinear paradigm").

Results

Preliminary results in humans indicate that successful removal of the stimulus artifact can be obtained with either approach without sacrificing the short-latency CEOAEs. The data reveal patterns of CEOAE suppression across frequency for varying ICIs similar to those observed previously, but with the promise of extending the testable range of frequencies beyond 6 kHz.

Summary:

The proposed approach for extracting changes in CEOAEs due to clicks presented close in time may provide a way to assess temporal suppression of short-latency (i.e., high-frequency) CEOAE components.

PS-482

Measuring DPOAE Area Maps Using Continuously Varying Primary Tones

Stefan Raufer[1]; Carolina Abdala[2]; Radha Kalluri[2]; Sumitrajit Dhar[3]; Christopher Shera[1]
[1]Harvard Medical School; [2]University of Southern California; [3]Northwestern University

Introduction

The striking difference between SFOAE and DPOAE phase slopes measured at fixed *f*2/*f*1 ratios provides evidence for two fundamentally different mechanisms of OAE generation. Whereas DPOAE phase measured with optimal frequency-scaled stimuli (e.g., *f*2/*f*1 ~ 1.2) is essentially constant across frequency, implying a wave-fixed generation mechanism, such as nonlinear distortion; SFOAE phase rotates rapidly, implicating a place-fixed mechanism, such as coherent reflection. Like so many other aspects of cochlear function, this broad understanding of OAE generation mechanisms derives primarily from studies of the basal region of the cochlea. At CFs below 1–1.5 kHz in humans, however, the telling qualitative difference between DPOAE and SFOAE phase slopes characteristic of the base becomes less salient. Whereas SFOAE phase slopes become shallower at low frequencies, DPOAE phase slopes become significantly steeper. Although SFOAE and DPOAE phase slopes change in opposite directions, the effects appear closely related to one another (Abdala et al. 2011). As a step towards understanding the origin of the OAE slope transition and its implications for emission generation and cochlear scaling symmetry in the apical half of the cochlea, our goal here is to develop efficient methods for obtaining high-resolution measurements of OAE magnitude and phase at frequencies extending an octave or more on either side of the apical-basal transition.

Methods / Results

We adapted swept-tone methods (Long et al. 2008; Kalluri & Shera 2013) to obtain high-resolution DPOAE *f*2,*f*1 area maps of the sort pioneered by Knight and Kemp (2001). The desired range of $r = f2/f1$ ratios can be covered either by employing consecutive fixed-ratio sweeps with different *r* or by using an *f*2× r analogue of the "Lissajous" protocol (Neely et al. 2005) developed to efficiently span the *L*1× *L*2 level space using continuous sweeps. One can improve SNRs at low frequencies, where subject and microphone noise are greatest, by using log sweeps and dividing the frequency range into overlapping measurement segments, thereby allowing for a greater number of averages at low frequencies. DPOAE

phase contours and their dependence on stimulus parameters can be derived from the unwrapped phase maps.

Summary
Swept-tone methods provide a promising technique for measuring high-resolution DPOAE area maps with multiple applications, including exploration of the apical half of the cochlea.

PS-483

Extraction of OAEs During Multi-Frequency ASSR Recordings With the Goal to Estimate Peripheral Compression

Bastian Epp; Raul H
Technical University of Denmark

Auditory steady-state responses (ASSR) allow objective assessment of auditory function using electroencephalography (EGG). ASSR receives increasing attention since it is easy to measure and allows frequency-selective testing due to the narrow stimulus bandwidth. The exact mechanisms of ASSR generation and correlates to other objective and subjective measures are, however, still matter of discussion. It was recently proposed to use ASSR-growth functions as estimates of peripheral compression. If peripheral compression is, at least partially, due to cochlear compression, the amplitude of ASSR as a function of level can be assumed to reflect the compressive growth of the cochlear nonlinearity. A recent study (Encina Llamas et al., ARO2014) showed, that compressive input-output functions with slopes similar to proposed compression ratios of cochlear level-growth functions can be found using ASSR obtained by stimulation with multiple sinusoidally-amplitude-modulated (SAM) tones. Comparison with compression estimates using distortion-product otoacoustic emissions (DPOAE) showed larger compression estimates derived from ASSR data compared to DPOAE data, suggesting contributions of both, cochlear and neural mechanisms. Direct comparison between the estimates obtained from ASSR and DPOAE are however challenging due to differences in the used stimuli. The goal of the current study is to investigate the estimation of cochlear compression using the same stimuli as used for ASSR (SAM tones). Estimation of cochlear compression from SAM tones make it possible to obtain information about cochlear compression using the ear canal pressure during stimulation to measure ASSR, without the need of an additional measurement.Signals in the ear canal of human listeners were recorded when stimulated with single or multiple SAM tones using a DPOAE probe. The contribution of sound emitted from the inner ear in response to the stimulus (SAMOAE) was estimated using a compression technique. Epochs of high intensity were compared to epochs of low intensity by scaling of the ear canal signal and subsequent subtraction. The results show, that SAMOAE growth functions are similar to SFOAE growth functions using pure tones for the same listeners. The data also indicate that multiple SAMOAE growth functions can be measured simultaneously by using multiple SAM tones without strong interaction between the stimulus components. It will be discussed in how far this measurement could be used to obtain information about cochlear compression in normally-hearing and hearing-impaired listeners and to which extent the combination of SAMOAE and ASSR might help to identify cochlear and neural contributions to peripheral compression.

PS-484

Cochlear Nonlinearity and Aging: Preliminary Results

Amanda Ortmann[1]; Carolina Abdala[2]
[1]University of Southern California; [2]University of Southern California, Department of Otolaryngology, Neuroscience Graduate Program

Introduction
Distortion product otoacoustic emissions (DPOAEs) provide a metric of cochlear nonlinearity. The level-dependent growth of DPOAEs offers an approximate index of basilar membrane compression, which is important in establishing a normal dynamic range of hearing. Evidence indicates that aging reduces nonlinear distortion emissions more than reflection emissions, suggesting that the ear becomes more linear with age (Abdala and Dhar, 2012). We are interested in studying this aging process using DPOAE amplitude growth as an index of nonlinearity. Here, we establish a protocol in young, normal-hearing ears and present preliminary data in a small group of middle-aged subjects.

Methods
$2f_1$-f_2 DPOAEs were recorded using primary tones swept upward in frequency at 2 s/octave from f_2 = 0.5-4 kHz, and 8 s/octave from 4-8 kHz. A fixed f_2/f_1 ratio was used (1.22) and L_2 varied from 25-80 dB SPL in 5 dB steps. Primary tone level separation was determined by the scissors method. DPOAE estimates were made with a least-squares-fit (LSF) algorithm and an inverse FFT was applied to unmix the DPOAE, isolating the nonlinear distortion emission. Distortion emission input/output (I/O) functions were measured in young adult and middle-aged ears at one-half octave intervals (1.3 – 7.4 kHz) and four features were extracted from a fit to the I/O functions: compression threshold, compression slope, range of compression, and low-level linear growth. These values were compared between age groups to estimate age-related changes in underlying cochlear nonlinearity.

Results
In young normal-hearers, the mean distortion OAE compression threshold was ~40 dB SPL overall. Compression thresholds decreased and the range of compression increased with increasing frequency. In contrast to approximately linear growth at low stimulus levels, the mean compressive growth rate was 0.10 dB/dB at high stimulus levels in these subjects. Our preliminary data suggest that I/O functions from middle-aged ears have higher compression thresholds overall by ~15-20 dB, reduced compression ranges, and a less systematic frequency effect on measures of compression.

Conclusions
DPOAE I/O functions provide a remote gauge of cochlear compression though methodological confounds must be considered. Here, we isolated the distortion component of the DPOAE to generate I/O functions and used a novel fit to characterize the level dependence of the distortion compo-

nent and extract targeted features. Preliminary results suggest that DPOAE

PS-485

Tone Burst-Evoked Otoacoustic Emissions in Different Age Groups of Schoolchildren

Wiktor Jedrzejczak; **Lukasz Olszewski**; Edyta Pilka; Bartosz Trzaskowski; Krzysztof Kochanek; Henryk Skarzynski
World Hearing Center, Institute of Physiology and Pathology of Hearing, Warsaw/Kajetany, Poland

Introduction

Otoacoustic emissions (OAEs) are believed to be good predictors of hearing status, particularly in the 1–4 kHz range. However both click evoked OAEs (CEOAEs) and distortion product OAEs (DPOAEs) perform poorly at 0.5 kHz. Some studies showed that OAEs evoked by tone bursts (TBOAEs) may provide a better estimate of hearing status than those evoked by clicks. The present study investigates the usefulness of responses in the lower frequency range of 0.5–1 kHz evoked by 0.5 kHz tone bursts. The 0.5 kHz TBOAEs were compared with emissions evoked by clicks.

Methods

Measurements were performed for two groups of schoolchildren. Children from grade 1 (age: 7 years) and children from grade 6 (age: 12 years). All children had visual inspection of the ear canal and tympanic membrane of both ears followed by tympanometry, pure tone audiometry, and OAE measurements. Standard click stimuli and 0.5 kHz tone bursts (average amplitude - 80±3 peak dB SPL, nonlinear averaging protocol) were used to evoke a total of 260 OAE responses.

Results

For all subjects OAEs response levels and signal to noise ratios (SNRs) were calculated. As expected, the CEOAE magnitudes were greatest over the range 1–4 kHz, with a substantial decrease below 1 kHz. Responses from the 0.5 kHz TBOAEs were complementary in that the main components occurred between 0.5 and 1.4 kHz. There were some slight differences between OAEs of two groups of schoolchildren. In younger children CEOAEs had higher SNRs in 2-4 kHz range. On the other hand TBOAEs had higher SNRs at 0.7 and 1 kHz for older children.

Conclusion

0.5 kHz TBOAEs can provide additional information about the frequencies up to 1 kHz, a range over which CEOAEs do not usually contain responses above the noise floor.

PS-486

Forward Pressure Referenced Behavioral Thresholds and Otoacoustic Emissions Measured with a Simple Probe

Jonathan Siegel; Xavier Potter; Samantha Ginter
Northwestern University

Introduction

Audiometry using conventional sound sources lacks a way to calibrate for differences in the acoustics of individual ears. We have conducted Thévenin source calibration on a simple acoustic probe intended for performing hearing screenings using otoacoustic emissions (OAEs). Source calibration allows the levels of acoustic stimuli to be specified in terms of the forward-going component of the ear canal pressure, dramatically reducing the influence of standing waves in the ear canal (Souza, et al, J. Acoust. Soc. Am. 136, 2014, in press).

Methods

The acoustic probe from an Etymotic Research Express Probe was configured as a stand-alone probe assembly using a custom-built microphone preamplifier and a Symmetrix 551E parametric equalizer to smooth the frequency response of the internal sound source. The probe's single sound source can produce low-distortion tonal stimuli exceeding 100 dB SPL below 20 kHz with intermodulation distortion low enough to measure OAEs at stimulus levels as high as 70 dB SPL. The Thévenin source pressure and impedance of the probe were measured using a set of cylindrical cavities (Scheperle, et al., J. Acoust. Soc. Am., 124, 288-300, 2008). Békésy tracking behavioral thresholds referenced to forward pressure were measured using custom software written in Visual Basic 6.0, while distortion product otoacoustic emissions (DPOAEs) were measured using two-tone stimuli with f_2/f_1 = 1.2 and L_1 and L_2 presented at 62 and 42 dB FPL, respectively, with f_2 varied in steps from 20 to 1 kHz. The complete set of measurements were performed in each ear of human participants in one test session and repeated approximately one week later. The human subjects protocol was approved by the Northwestern University Institutional Review Board.

Results

The probe source calibrations were stable over repeated measurements made before each test session. Both thresholds and DPOAEs were repeatable in preliminary measurements. A more extensive set of data will be presented and test-retest reliability will be quantified.

Conclusion

We conclude that a simple acoustic probe with adequate performance could allow routine use of forward pressure calibration for audiometry and OAE screening.

PS-487

Cochlear Mechanisms and Distortion Product Otoacoustic Emission Test Performance

Nikki Go; Greta Stamper; Tiffany Johnson
University of Kansas Medical Center

Distortion product otoacoustic emissions (DPOAEs) contain contributions from both a non-linear distortion source and a coherent-reflection source (Shera & Guinan, 1999). It has been suggested that the mixing of energy from the two sources contributes to errors in clinical OAE measures (e.g., Shera, 2004). If source mixing produces errors, those errors will be most pronounced when recording responses from normal-hearing and mild-moderately hearing-impaired ears (Mauermann et al., 1999). Here, we evaluate the influence of controlling DPOAE source contribution on DPOAE test performance. Data were collected from 212

normal-hearing and mild-moderately hearing-impaired subjects. Because previous work suggested that the impact of controlling source contribution differs based on the likelihood of an error in the condition where both sources contribute to the DPOAE (Johnson et al., 2007), we recruited subjects who fell into two general categories based on their DPOAE levels on a screening protocol. Specifically, we enrolled subjects in whom errors were likely, the uncertain-identification group (normal ears with small DPOAEs; impaired ears with large DPOAEs), and in whom errors were unlikely, the certain-identification group (normal ears with large DPOAEs; impaired ears with small DPOAEs). DPOAE fine-structure patterns were recorded by varying f_2 in 1/64-octave steps over 1/3-octave intervals surrounding the f_2 frequencies of 2 and 4 kHz (L_1=L_2+10 dB; f_2/f_1=1.22), with L_2=45 and 55 dB SPL. The reflection-source contribution was reduced by using the Discrete Cosine Transform (DCT) to smooth fine structure. Area under the relative operating characteristic (AROC) curve was used to quantify changes in test accuracy when the source contribution was controlled versus the condition where both sources contribute. When f_2=2 kHz, limiting the source contribution to the distortion source (DCT-smoothed condition) resulted in either no change or small increases in AROC. At this frequency, small increases in AROC were seen for both the certain- and uncertain-identification groups. For f_2=4 kHz, controlling source contribution produced both small increases and small decreases in test accuracy for both identification groups. In general, changes observed at 2 kHz were larger than changes at 4 kHz, although no change exceeded 5%. The present data suggest that reducing the reflection-source contribution had no consistent influence on test accuracy at 4 kHz. Reducing the reflection-source contribution at 2 kHz had a consistently positive influence on test accuracy, but the improvements were small.

PS-488

Changes in the Short- and Long-Latency DPOAE components under Levodopa treatment

Renata Sisto[1]; Valerio Pisani[2]; Arturo Moleti[3]; Stefano Di Girolamo[3]; Sara Mazzone[3]; Teresa Botti[4]; Filippo Sanjust[4]; Paolo Stanzione[3]

[1]INAIL Research; [2]I.R.C.C.S. "Santa Lucia" Foundation, Rome, Italy; [3]University of Rome "Tor Vergata", Rome, Italy; [4]INAIL Research, Monteporzio Catone, Rome, Italy

Objective

Objective of this study is the investigation of cochlear functionality in patients suffering from Parkinson Disease (PD). In particular, the research is aimed at quantitatively evaluating the neurotransmission changes after pharmacological stimulation by measuring Distortion Product Otoacoustic Emissions (DPOAE) as biomarkers of the dopamine effect.

Methods

DPOAE have been measured in a sample of patients affected by PD at their first diagnosis and after pharmacological treatment with levodopa at therapeutic dosage. High-resolution DPOAE spectra have been measured using a swept-tone technique. A suitable time-frequency wavelet analysis has been applied to separate the DPOAE components. The level changes of the short- and long-latency DPOAE components (SL and LL) before and after levodopa assumption have been statistically compared. Both components have been correlated to the audiometric threshold.

Results

A statistically significant enhancement of the DPOAE SL components was found, whereas the difference between the DPOAE LL and SL component levels was rather insensitive to the treatment. The audiometric threshold was slightly improved by the levodopa treatment, particularly at 4 kHz. A high correlation (R^2=0.75) was found between the DPOAE SL component level and the audiometric threshold level before treatment. This correlation underwent some degradation (R^2=0.45) after levodopa assumption. It could be speculated that the levodopa differently affects the strength of nonlinear term and the hearing threshold sensitivity.

Conclusions

This experiment seems to confirm the hypothesis that the dopaminergic signaling in the cochlea also affects the activity of the outer hair cells (OHC). The increase in the strength of the nonlinear term, causing the SL DPOAE level enhancement, does not seem to be highly correlated to the improvement of the hearing threshold.

PS-489

Transiently Evoked and Distortion Product Otoacoustic Emissions in Smoking and Nonsmoking Young Adults

Wiktor Jedrzejczak[1]; Magdalena Koziel[1,2]; Krzysztof Kochanek[1]; Henryk Skarzynski[1]

[1]World Hearing Center, Institute of Physiology and Pathology of Hearing, Warsaw/Kajetany, Poland; [2]Institute of Sensory Organs, Kajetany, Poland

Introduction

There are reports that smoking can influence hearing in negative way. Otoacoustic emissions (OAEs) are known to be indicators of preclinical hearing loss. The changes in OAEs may be apparent even before decline of audiometric thresholds. The present study investigates the usefulness of transiently evoked OAEs (TEOAEs) and distortion product OAEs (DPOAEs) in detecting small changes in hearing of young smoking adults.

Methods

Otoacoustic emissions were compared between two groups of young adults: smoking and nonsmoking. Data was acquired from the ears of 48 young adults (age 20–27 years). The dataset was divided into two groups smoking (24 persons/48 ears) and nonsmoking (24 persons/48 ears). Average amount of smoking was relatively small in comparison to previous studies, it was 3.8 years, and 8.7 cigarettes per day. In each ear three OAE measurements were made: CEOAEs, DPOAEs, and spontaneous OAEs (SOAEs). Pure tone audiometry and tympanometry were also conducted. The datasets did not differ significantly in case of audiometric thresholds. Half-octave-band values of OAE signal to noise ratios

(SNRs) and response levels were used to assess statistical differences.

Results

Average data initially revealed the differences between studied groups only in 1 kHz for TEOAEs. However when datasets were divided into ears with and without SOAEs more differences could be seen both in TEOAEs and DPOAEs. There were no statistically significant differences between evoked OAEs of ears of smokers and nonsmokers that exhibited SOAEs. However in ears without SOAEs the evoked OAEs were higher even by 5 dB in ears of nonsmokers. These differences were most prominent in 1-2 kHz range.

Conclusion

In the present study the decrease of OAE levels was found in some ears even after quite short smoking periods. There was no such evident difference between OAEs of smokers and nonsmokers as reported earlier, for longer times, as some ears, those that exhibited SOAE did not have decrease in evoked OAEs. It appears that smoking does not initially affect the ears with exceptional hearing, those that exhibit SOAEs. However ears without SOAEs even when audiometric thresholds were within norm exhibited some decrease of evoked OAE amplitude.

PS-490

Effects of Short-duration Instrument Practice on the Auditory Peripheral Functions of Violin Players

Sho Otsuka[1]; Minoru Tsuzaki[2]; Junko Sonoda[2]; Shigeto Furukawa[1]

[1]NTT Communication Science Laboratories, NTT Corporation; [2]Kyoto City University of Arts

Background

Recent investigations in animals have revealed that even a moderate-level noise exposure causes neuronal degeneration at the auditory periphery. Some studies reported that musicians, who are exposed to loud musical sounds on a daily basis, show decreased hearing sensitivity. This study aimed to examine whether short-duration exposures to low- to mid-level sounds influence the auditory peripheral function. The subjects of the study were violin players, who were exposed to violin sounds (broadband sounds containing a significant number of high-frequency components) during their regular instrument practice. Pure tone thresholds, distortion-product otoacoustic emissions (DPOAEs), click-evoked otoacoustic emissions (CEOAEs), and the strength of the medial olivocochlear reflex (MOCR) before a practice session were compared with those after it.

Methods

Ten audiometrically normal undergraduates and graduate course students who are majoring in the violin participated in the experiment. Pure tone thresholds were measured at three frequencies (1000, 2000 and 4000 Hz). DPOAEs for 55- and 66-dB pure tones were measured in the frequency range of 793-7996 Hz. CEOAEs were measured by 60-dB (peak-equivalent sound pressure level) clicks. The difference in CEOAE strength with and without contralateral or ipsilateral 60-dB white noise was measured as an index of the strength of the MOCR. The CEOAE level and the strength of the MOCR were computed in two frequency bands (1-2 kHz and 2-4 kHz). Each measurement was conducted bilaterally just before and after a one-hour practice session. The order of the measurements was randomized for each session. The measurement time was approximately thirty minutes.

Results

Significant changes were observed for only the left ears. Significant decreases of the overall DPOAE level and the CEOAE level in the high-frequency band (2-4 kHz) were observed. The strength of the MOCR decreased in the low-frequency band (1-2 kHz) for ipsilateral noise and in both the high- and low-frequency bands for the contralateral noise. A significant elevation of the pure tone threshold was observed at 4 kHz.

Conclusion

This study observed diverse effects of a short-duration violin practice on the auditory periphery, i.e., the function of the outer hair cells and the effect of MOC feedback, which is assumed to play a key role in protecting the ear from acoustic overexposure. The left-ear-specific effects suggest that the degree of exposure related to the proximity of the instruments to the ears could be a decisive factor in musical-sound-induced hearing loss.

PS-491

Characterization of Spontaneous Otoacoustic Emissions in Full-Term Chinese Newborns

Beier Qi[1]; Li Xu[2]; Xiaohua Cheng[1]; Hui En[1]; Yitao Mao[2]; Lihui Huang[1]; Luo Zhang[3]

[1]Key Laboratory of Otolaryngology - Head & Neck Surgery (Ministry of Education), Beijing Institute of Otolaryngology; [2]Communication Sciences and Disorders, Ohio University; [3]Department of Otolaryngology Head and Neck Surgery, Beijing TongRen Hospital, Capital Medical University

Introduction

Spontaneous otoacoustic emissions (SOAEs) are low-level signals measured in the external ear canal in the absence of any acoustic stimulation, and generally regarded as epiphenomena of micromechanical processes in the cochlea. Therefore, it may provide some useful information on the physiological conditions in the cochlea in humans. Previous studies have indicated that the SOAE prevalence and number of SOAEs per ear are related to gender and ear side. There are differences in SOAE characteristics between adults and children, especially between adults and newborn infants. However, discrepancies in SOAE frequency distribution and number per ear exist in the literature. Differences in SOAE characteristics among races have also be demonstrated. Therefore, the purpose of this study was to characterize SOAE prevalence, peak number per ear, frequency, and amplitude in a large sample of full-term Chinese newborns.

Methods

A total of 236 ears from 147 randomly selected full-term Chinese neonates (82 females and 65 males), who had passed the initial newborn hearing screening, were assessed for

SOAEs using the Capella OAE equipment (Madsen, Denmark). The test was performed in a sound booth.

Results

(1) The overall prevalence of SOAE was 56.77% of the ears. The prevalence of SOAEs was significantly higher in females (69.23%) than in males (41.51%, $p < 0.05$), as well as in the right ears (64.17%) than in the left ears (49.14%, $p < 0.05$). (2) The overall mean level of SOAE was 11.78 ± 8.36 dB SPL, with no significant differences between males (11.73 ± 8.25 dB SPL) and females (11.81 ± 8.43 dB SPL) or between the left (11.97 ± 8.56 dB SPL) and the right ears (11.65 ± 8.22 dB SPL). (3) The 25th and 75th percentiles of SOAE frequencies were 2.3 and 4.3 kHz in females and 1.9 and 3.9 kHz in males, which were statistically significantly different ($p < 0.01$). (4) The overall mean number of SOAEs was 3.70 ± 2.75, with no significant differences in females (3.62 ± 2.70) and males (3.86 ± 2.87) or in right (3.70 ± 2.55) and left ears (3.70 ± 3.02).

Conclusions

The prevalence rate of SOAE is significantly higher in females than in males and in the right ears than in the left ears in Chinese newborns. The frequencies of the SOAEs in newborns appeared to be higher than those reported in normal-hearing adults in the literature.

PS-492

Synaptically-Driven Events Recorded in Spiral Ganglion Neuron Somata in an Acute Preparation

Wenke Liu; Robin Davis
Rutgers University, New Brunswick

Background

The postsynaptic terminals of type I spiral ganglion neurons display AMPA-receptor mediated EPSCs with unusually large amplitudes (Glowatzki & Fuchs, *Nat Neurosci*, 2002) that presumably evoke action potentials at proximal heminodes (Hossain et al, *J Neurosci*, 2005; Rutherford et al, *J Neurosci*, 2012). To reach their central targets, these action potentials must first travel through the cell soma, which in spiral ganglion neurons is an obligatory part of the conduction pathway. In order to better understand the consequences of transmission through the soma, we analyzed the firing properties of early postnatal spiral ganglion neurons in acute preparations still attached to their hair cell receptors. Under these conditions we determined that neurons not only exhibited the highly diverse intrinsic membrane properties consistent with previous *in vitro* analysis (Crozier and Davis, *J Neurosci*, 2014), but also displayed electrogenic events driven by synaptic activity.

Methods

Whole-cell voltage and current clamp recordings were made from spiral ganglion in acute preparations of primary auditory afferents still attached to the peripheral endorgan in P0-6 CBA/CAJ mice. In some experiments, 10μM DNQX was included in the extracellular solution.

Results

Consistent with our previous observations in neuronal explant cultures (Crozier and Davis, *J Neurosci*, 2014), recordings obtained from acute, attached preparations displayed three accommodation classes with overlapping interspike interval ranges. Approximately 26% of all recordings fell into the unitary accommodation category by exhibiting only one spike in response to a prolonged step current injection. The remaining neurons were either rapidly accommodating (37%), typically firing 2-8 spikes, or slowly accommodating (36%) firing throughout the stimuli with 9 or more action potentials. Moreover, both invading action potentials and DNQX-sensitive synaptic-like currents were observed in cell somata of spiral ganglion neurons, suggesting that the neuronal somata may be directly affected by synaptic activity during early postnatal developmental stages.

Conclusion

By using an acute preparation of the spiral ganglion with neurons still attached to their peripheral hair cells, we have observed the diverse firing features expected from our studies of isolated neurons in tissue culture and we have also taken the next step to characterize in detail the early stages of sensory coding in the primary auditory afferents.

PS-493

Expanding Clinical Electrocochleography for the Diagnosis of Auditory Nerve Degeneration

Brian Earl; Maggie Schad
University of Cincinnati

Introduction

Electrocochleography (ECochG) is used clinically for the diagnosis of Ménière's disease and for intraoperative monitoring of hair cell and auditory nerve integrity. Another use is to enhance the amplitude of wave I of the auditory brainstem response (ABR), which is particularly relevant given the recent animal research indicating a correlation between the amplitude of wave I and peripheral auditory nerve degeneration. The action potential component of the ECochG response corresponds to ABR wave I and is enhanced when evoked with broadband chirp stimuli as compared to traditional click stimuli. The objectives of this study are to determine the amplitude variability of high-level ECochG recordings and characterize ECochG amplitude growth patterns using a high-pass masking paradigm.

Methods

ECochGs were recorded from normal-hearing adults (ages 18-30; N=7) using a tympanic membrane electrode. Amplitude variability of the responses evoked with chirps and clicks at 106 dB SPL was assessed using the coefficient of variation (standard deviation/mean). ECochG amplitude growth curves for chirp stimuli at 106 dB SPL were constructed using simultaneous white noise that was high-passed in ½ octave intervals between 722 and 8944 Hz. Distortion product otoacoustic emissions (DPOAEs) were measured before and after the ECochG measures.

Results
The amplitude of ECochGs evoked with chirps was 2.2 times larger on average and varied 10% less than those evoked with clicks. The coefficient of variation for the amplitude of masked, chirp-evoked ECochGs ranged from 0.006 to 0.38 with a mean variation of 0.15, which was slightly lower than the mean variation (0.16) for the unmasked recordings. ECochG amplitude growth curves showed a general pattern of increasing amplitude as the high-pass masker cutoff frequency increased. DPOAEs following the masked ECochG procedure were not significantly different than those measured before the procedure.

Summary
These pilot data are consistent with previous research showing a robust ECochG response to chirp stimuli. The low amplitude variability of ECochGs evoked with chirps relative to those evoked with clicks and the relative stability of those evoked during simultaneous masking, point to their potential clinical utility in gauging auditory nerve degeneration. Measuring normalized ECochG amplitude growth is another potential control for the variability of raw amplitude measures across individuals. Data collection is ongoing to further characterize the normative range of ECochG amplitude growth in order to then determine if differences exist in growth curves from individuals with hearing impairment.

PS-494

Effect of Contralateral Stimulation on Cochlear Mass Potentials in Humans

Eric Verschooten[1]; Elizabeth Strickland[2]; Nicolas Verhaert[3]; Philip Joris[4]
[1]University of Leuven; [2]Dept. of Speech, Language, and Hearing Sciences, Purdue University, West Lafayette, Indiana; [3]ExpORL, Univ. of Leuven, Belgium; [4]Lab. of Auditory Neurophysiology, Univ. of Leuven, Belgium

Based on physiological measurements in anesthetized animals (Guinan,2011; Kawase and Liberman,1993; Buño,1978; Liberman,1989; Warren and Liberman,1989; Dolan and Nuttal,1988; Nieder and Nieder,1970) the medial olivocochlear reflex (MOCR) has been hypothesized to enhance speech intelligibility in noise. Several lines of evidence support such a role for the MOCR in humans. Psychophysical paradigms have shown an anti-masking effect that is consistent with MOCR involvement. Also, otoacoustic emissions show suppressive effects by contralateral stimulation (Guinan,2006). To link the observations in humans more directly to the MOCR effects measured in animals, we investigate effects of contralateral stimulation in human volunteers with normal hearing using cochlear mass potentials: compound action potentials (CAP) and cochlear microphonic (CM).

A minimally invasive transtympanic procedure was applied to record mass-potentials from the cochlear promontory or from the niche of the round window in humans. This involved a custom made ear mold to control acoustic stimulation (ER-2 earphone, calibrated in-situ with ER-7 microphone). To assess the MOCR, averaged CAP and CM responses to gated probe tones (100ms) of 4 or 6 kHz with and without contralateral noise (continuous; levels 60 or 70 dB SPL; below threshold of the stapedius reflex) were extracted with a polarity alternating paradigm. In some experiments the probe was preceded by a forward noise masker (>80ms) to investigate the anti-masking effect, similar to that in Kawase and Liberman (1993). The measurements were divided into randomized blocks with intermittent contralateral noise. All subjects were screened for normal hearing (audiogram, tympanogram, threshold stapedius reflex) and psychophysically tested for the presence of a behavioral anti-masking effect (e.g. Strickland,2008; Roverud and Strickland,2010).

In 3 subjects examined so far, we did not find a significant difference in CAP amplitudes between conditions with or without contralateral noise. In some measurements a systematic, small (<8%), amplitude offset could be observed for different probe levels, but these offsets were not within the significance level of 95% and could be positive (enhancement) or negative (suppression) between subjects for the same condition. The same observation was made for the CM (where efferent stimulation classically causes an increase in amplitude).The differences for the CM were sometimes larger (>10%), more systematic but without a clear direction.

We conclude that the effects of efferent activation observed on peripheral mass potentials measured in anesthetized animals (Kawase and Liberman,1993; Buño,1978; Liberman,1989; Warren and Liberman,1989; Dolan and Nuttal,1988; Nieder and Nieder,1970) are not observed in awake humans under the conditions studied here.

PS -495

Characterization of Calcium Currents in Neonatal and Mature Spiral Ganglion Neurons of α2σ3-/- mice

Friederike Stephani[1]; Wenying Wang[2]; Jutta Engel[1]
[1]Saarland University; [2]University of California, Davis

Introduction
Spiral ganglion neurons (SGNs) connect hair cells with central auditory neurons and therefore are indispensable for auditory signal transmission. Type I SGNs, which comprise 95 % of all SGNs, are myelinated and make a precise 1 to 1 connection with inner hair cells (IHCs). Auxiliary $\alpha_2\sigma$ subunits of voltage-gated Ca^{2+} channels (VGCC) control the abundance of VGCCs and shape their biophysical properties. Moreover, the auxiliary $\alpha_2\sigma3$ subunit plays a role for the proper structure and morphology of auditory nerve synapses (Pirone et al., J Neurosci 2014). To investigate the function of the $\alpha_2\sigma3$ subunit for VGCCs in SGN, we analyzed Ca^{2+} currents in SGNs isolated from $\alpha_2\sigma3^{-/-}$ and wild type (WT) mice.

Methods
Patch-clamp recordings of Ca^{2+} currents were performed on enzymatically dissociated spiral ganglion neurons isolated from neonatal (P5) and mature (P20) mice (cf. Lv et al., J Neurosci 2012). SGNs were cultured for 2 days.

Results
Large voltage-activated K^+ currents of SGNs were blocked by TEA (30 mM), 4-AP (15 mM) and linopirdine (100 µM) in the

bath and by 110 mM Cs^+ in the pipette solution. Large voltage-activated inward Na^+ currents were fully suppressed by extracellular NMDG (110 mM). Whole-cell Ca^{2+} currents were reduced in $\alpha_2\sigma3^{-/-}$ SGNs from both, the apical and the basal cochlea at both ages. The contribution of L-type currents was assessed by superfusing SGNs with 10 µM nimodipine. Nimodipine blocked about 30 % of the Ca^{2+} currents in WT SGNs compared with 40 % block in $\alpha_2\sigma3^{-/-}$ SGNs.

The contribution of P/Q-type currents was assessed using 1 µM ω-agatoxin IVA. Preliminary results show that the contribution of P/Q-type currents in WT apical SGNs amounted to 58 %.

Conclusion

Neonatal as well as mature SGN of $\alpha_2\sigma3^{-/-}$ mice showed reduced Ca^{2+} currents compared with WT SGNs. The differential contribution of the different subtypes of Ca^{2+} currents remains to be determined.

PS-496

The Spike Generator of Type I Cochlear Afferents

Kyunghee X Kim; **Mark Rutherford**
Washington University in Saint Louis School of Medicine

Type I spiral ganglion neurons (SGNs) of the cochlea transfer all information from inner hair cells (IHCs) to the central nervous system via action potentials (APs). These APs are propagated from the organ of Corti along the radial fibers in the osseous spiral lamina (OSL), past somas in the spiral ganglion, and along the centrally-projecting axon to the brain stem. Researchers have proposed that APs are generated at the first heminodes of the myelinated SGN fibers near the habenula perforata. However, nodes of Ranvier are electrically nearby in the OSL and the contribution of nodal channels to AP generation relative to heminodal channels has not been studied. Moreover, the organization of voltage-gated channels within nodes and heminodes has not been thoroughly examined in the organ of Corti. With electron microscopy, previous detailed studies have described SGN morphology in a limited number of fibers (Liberman, 1980), however the precise positions and spatial extents of heminodes and nodes have not been measured with molecularly-specific fluorescence microscopy. Here we examined biophysical properties of SGN molecular anatomy with immunohistochemistry in adult rats and mice. Electrophysiological recordings from postsynaptic boutons innervating the modiolar face of IHCs showed a phasic response property, firing only one AP per depolarization no matter how large the injected current (Rutherford, Chapochnikov, and Moser, 2012). However, it is not clear if all SGNs exhibit this phasic property. SGNs innervating opposite faces of the IHCs along the modiolar-pillar axis have been shown to respond differently to sound and have differences in morphology (Merchan-Perez and Liberman, 1996). Thus, we examined whether the properties of SGNs innervating the pillar face differ from those innervating the modiolar face. Immunofluorescence revealed that $Na_V1.6$ was localized to the first heminodes, consistent with Hossain et al. (2005). Immunostaining of $K_V1.1$ was also observed near the first heminodes at a distance from the staining of $Na_V1.6$. $K_V1.1$ appears to exhibit a spatial gradient of staining intensity. Future studies will address the physiological significance of such a gradient by relating positional immunofluorescence data with response properties in electrophysiological recordings.

PS-497

A Model of Synaptic-Vesicle-Pool Depletion and Replenishment Can Account for the Inter-Spike-Interval Distributions and Non-Renewal Properties of Spontaneous Spike Trains of Auditory-Nerve Fibers

Adam Peterson[1]; Dexter Irvine[2]; **Peter Heil**[1]
[1]Leibniz Institute for Neurobiology, Magdeburg; [2]Bionics Institute, Melbourne, Australia

In mammalian auditory systems, the spiking characteristics of each primary afferent (type-I auditory-nerve fiber; ANF) are mainly determined by a single ribbon synapse in a single inner hair cell (IHC), and there is evidence that each transmitter release event evokes a postsynaptic spike unless the ANF is refractory. Therefore, the ANF spike patterns provide information about the release statistics of these synapses. These statistics can be studied in the absence of experimenter-controlled sound because ANFs are spontaneously active. The distribution of inter-spike intervals (ISIs) during spontaneous activity is often modeled as resulting from ANF refractoriness operating on a homogeneous Poisson point process of excitation (release events from the IHC). This model, however, neither describes the ISI distributions accurately nor accounts for non-renewal properties of the spike trains. Heil et al. (*J Neurosci* 2007) demonstrated that the ISI distributions of cat ANFs during spontaneous activity can be much more accurately described as resulting from refractoriness operating on a non-Poisson, stochastic point process of excitation. Here, we first examine whether the discussed mechanism, involving the constrained failure of events from a homogeneous Poisson point process, can also account for the non-renewal properties of these spike trains, manifest as negative serial ISI correlations and reduced spike-count variability over short time scales.

Spikes of 171 individual ANFs were recorded extracellularly from the left auditory nerve in five barbiturate-anesthetized adult cats. Continuous samples of spontaneous activity (between 12.5 and 134.4 s long) were recorded, along with responses to various stimulus protocols.

The previously discussed excitatory mechanism can account for the observed non-renewal properties, but does not offer a parsimonious explanation for certain trends in the data, such as changes in the magnitude of serial ISI correlations with spontaneous rate. We therefore investigate an alternative 3-parameter model of vesicle-pool depletion and replenishment and find that it, combined with refractoriness, accounts for the non-renewal properties, their trends, and the ISI distributions, with only the release probability varying between spike trains. The maximum number of readily releasable units (single vesicles or groups of simultaneously released vesi-

cles) in the pool and their replenishment time constant can be assumed to be constant (~4 and 13.5 ms, respectively).

We suggest that the organization of the IHC ribbon synapses not only enables sustained release of neurotransmitter but also imposes temporal regularity on the release process, particularly when operating at high rates.

PS-498

Model of Auditory Nerve Responses to Electrical Stimulation

Suyash Joshi; Torsten Dau; Bastian Epp
Technical University of Denmark

Cochlear implants (CI) stimulate the auditory nerve (AN) with a train of symmetric biphasic current pulses comprising of a cathodic and an anodic phase. The cathodic phase is intended to depolarize the membrane of the neuron and to initiate an action potential (AP) and the anodic phase to neutralize the charge induced during the cathodic phase. Single-neuron recordings in cat auditory nerve using monophasic electrical stimulation show, however, that both phases in isolation can generate an AP. The site of AP generation differs for both phases, being more central for the anodic phase and more peripheral for the cathodic phase. This results in an average difference of 200 µs in spike latency for AP generated by anodic vs cathodic pulses. It is hypothesized here that this difference is large enough to corrupt the temporal coding in the AN. To quantify effects of pulse polarity on auditory perception of CI listeners, a model needs to incorporate the correct responsiveness of the AN to anodic and cathodic polarity. Previous models of electrical stimulation have been developed based on AN responses to symmetric biphasic stimulation or to monophasic cathodic stimulation. These models, however, fail to correctly predict responses to anodic stimulation.

This study presents a model that simulates AN responses to anodic and cathodic stimulation. The main goal was to account for the data obtained with monophasic electrical stimulation in cat AN. The model is based on an exponential integrate-and-fire neuron with two partitions responding individually to anodic and cathodic stimulation. Membrane noise was parameterized based on reported relative spread of AN neurons. Firing efficiency curves and spike-latency distributions were simulated for monophasic and symmetric biphasic stimulation. The simulations were in line with the average data for firing thresholds and spike latencies for both, monophasic anodic and monophasic cathodic stimulation. The model also correctly predicted the shift in latency as a function of stimulation level.

With the ability to account for the responsiveness to cathodic and anodic phases of electrical stimulation, this model can be applied to account for the response to arbitrary pulse shapes. The evaluation of the neural response to symmetric biphasic pulses helps to estimate the mutual interaction between the two pulse phases. A successful model can be generalized as a framework to test various stimulation strategies and to quantify their effect on the performance of CI listeners in psychophysical tasks.

PS-499

Selective Tonotopic Redistribution of Spiral Ganglion Neuron Timing and Excitability Features by cAMP and H-89 in CBA Mice in vitro

Robert Crozier; Robin Davis
Rutgers University

Background

Spiral ganglion neurons (SGNs) possess a wealth of electrophysiological specializations, many of which are tonotopically organized. These specializations give rise to tonotopic differences in SGN firing including timing features such as action potential (AP) latency, duration and onset t and excitability features such as voltage threshold and accommodation. Timing and excitability properties are graded linearly and non-monotonically, respectively, and these tonotopic differences are regulated largely by the differential distribution of ion channels such as potassium and HCN channels. The activity of these channels is not static but rather can be dynamically modulated by voltage or through second messenger systems. Herein, we have begun to clarify the role of one of the most ubiquitous second messenger systems, the cAMP/PKA pathway, in regulating gangliotopic firing features of the primary auditory afferents.

Methods

Whole-cell current clamp recordings were performed on SGN cultures obtained from the base, middle and apex of postnatal day 6 (P6) CBA mice. One hour before recording, cultures were treated with vehicle (2 µl), 8-Br-cAMP (100 µM) or the PKA antagonist H-89 (10 µM). Constant current injections (240 ms duration) were delivered to assess AP latency and duration, onset t, voltage threshold and accommodation.

Results

Two specific electrophysiological features, voltage threshold (excitability) and onset t (timing), provide a snapshot of our overall results. Under vehicle control, voltage thresholds were most depolarized in the base and non-monotonically distributed: (base (mV): 40.8±0.7, n=19, middle: 47.2±0.6, n=21, apex: 46.5±0.7, n=21). Exposure to cAMP had no effect; however, H89 significantly increased voltage thresholds in all locations such that they transformed into a graded profile (base: 37.7±1.2 mV, n=21, middle: 41.7±0.7, n=21, apex: 43.8±0.8, n=17; $P<0.05$, respectively). Conversely, onset t values were uniformly distributed under vehicle control conditions: (vehicle (in ms): base: 1.4±0.3; middle: 1.3±0.2; apex: 1.2±0.1). In contrast, cAMP, but not H89, significantly sped-up this timing feature for all cochlear locations such that they became graded: (cAMP base (in ms): 0.5±0.04; middle: 0.7±0.1; apex: 0.8±0.1; $P<0.01$, respectively).

Conclusions

The tonotopic redistribution of timing and excitability features indicates that they are mechanistically separable, and supports previous work (Crozier&Davis, *J. Neurosci*., 2014; Liu et al, *Neuroscience*, 2014). The gangliotopic distribution of ion channels, their differential regulation by the cAMP/PKA

pathway and, possibly, tonotopic differences in the second messengers themselves could all participate in this complex signaling process. Thus, our findings suggest an additional level of fine control in SGN encoding of auditory information.

PS-500

Response Properties of Spiral Ganglion Neurons to Shaped Pulses in Electrical Stimulation

Jimena Ballestero[1]; Katie Smith[2]; Daniel Jagger[2]; Laudanski Jonathan[3]; Søren Riis[3]; David McAlpine[2]
[1]University College of London; [2]Ear Institute, UCL; [3]Oticon Medical

Background

Spiral ganglion neurons (SGN) transmit tonotopically organized information from the hair cells to the central auditory system. In severe and profound hearing loss, SGNs can be directly electrically activated through cochlear implants (CI). A critical issue in CI, however, is the spread of electrical current within the cochlea, such that individual contacts on the electrode array excite a broad swathe of the nerve fibres innervating the cochlea. Numerous strategies have been developed to overcome this issue that usually take into consideration the geometry of spread current. Here, we assess the responses of isolated SGNs to a novel electrical pulse shape, designed to take into account their biophysical properties.

Methods

Patch-clamp recordings were made from SGNs in cultured mice (P10-P14). We characterized the biophysical properties of SGNs using current steps to study firing properties, and stimulation with families of voltage steps to study their voltage-dependent conductances. Additionally, we probed their sensitivity to current injections similar to those applied during CI activation. Thus, we applied square current pulses of 100µs duration and with different amplitudes. Finally, we tested a novel stimulation protocol based on the observation that SGNs can be sensitive to the slope of the stimulus input (Oertel 2009). To prove that this principle applies, a family of 100µs stimuli with different slopes were designed.

Summary

We report distinct populations of SGNs with different firing properties (fast adapting, slow-adapting and non-adapting) that varied in their thresholds to square pulses stimulation. By applying a novel stimulation protocol in which electrical pulses are shaped we find that increasing the slope of the stimulus modulate SGN firing in a manner similar to amplitude changes. Our data demonstrate that modulation of the slope of the stimulation current can modify SGN responses in a manner that alters their firing patterns, suggesting that this can be used as tool to modulate SGN responses in the context of electrical stimulation with CIs.

References

Oertel D. (2009) A team of potassium channels tunes up auditory neurons. J Physiol. 587, 2417-8

PS-501

Non-parametric Temporal Probability Density Estimation for Neural Responses

Christopher Boven; Jont Allen; Robert Shepard; Robert Wickesberg
University of Illinois at Urbana-Champaign

Analysis of electrophysiological data often involves the estimation of the probability density function underlying a neuron's response. A common solution is to use the peristimulus time histogram (PSTH) computed from the spike trains that the neuron produces during multiple repetitions of the stimulus. This approach requires the arbitrary selection of a bin width, which may introduce undesirable temporal quantization error, and it may require numerous presentations of the stimulus to reduce noise. An alternative is to average the Fourier transformations of the spike trains, which are represented as temporal sequences of delta-functions. This spectral estimate is particularly accurate because it is an unquantized representation of the data. In the frequency domain, the fidelity of the spectral estimate rapidly increases as more samples are obtained, while the sampling error or noise moves to higher frequencies. Low-pass filtering the spectral estimate where it intersects the noise floor and computing the inverse Fourier transform yields an optimal, non-parametric estimate of the temporal probability density function. This novel method has been used to estimate temporal probability density functions (TPDF) for responses to speech stimuli of individual auditory nerve fibers that were both simulated and recorded *in vivo* from ketamine-anesthetized chinchillas. These TPDFs were compared to the corresponding PSTHs computed using varying bin widths and smoothing parameters. In the simulations, where the underlying probability density function was known, the TPDFs provided significantly more accurate estimates than the PSTHs, even with relatively few repetitions of the stimulus. Comparisons of the TPDFs and PSTHs for the *in vivo* auditory nerve data will also be presented.

PS-502

Detection of "hidden" Auditory Nerve Fiber Loss

Jérôme Bourien; Charlene Batrel; Antoine Huet; Gilles Desmadryl; Jean-Luc Puel
INSERM

Background

Sound-evoked compound action potential (CAP), which captures the synchronous activation of the auditory nerve fibers (ANFs), is commonly used to probe deafness in experimental and clinical settings. Recent studies have shown that substantial ANF loss can coexist with normal hearing threshold and even unchanged CAP amplitude, making the detection of auditory neuropathies difficult. In this study, we took advantage of the round window neural noise (RWNN) to probe ANF loss in the ouabain-induced neuropathy model.

Methods

ANF loss was induced by the application of ouabain onto the round window niche. CAP and RWNN of the gerbil's cochlea were recorded through an electrode placed onto the round

window niche, 6 days after the ouabain application. Afferent synapses count and single-unit recordings were carried-out to determine the degree and the nature of ANF loss, respectively.

Results

Application of a low ouabain-dose into the gerbil RW niche elicits a specific degeneration of low spontaneous rate (SR) fibers, as shown by single-unit recordings. Simultaneous recordings (CAP/single-unit) demonstrate that low-SR fibers have a weak contribution to the CAP amplitude because of their delayed and broad first spike latency distribution. However, the RWMN amplitude decreases with the degree of synaptic loss. The RWNN method is therefore more sensitive than CAP to detect low-SR fiber loss most probably because it reflects the sustained discharge rate of ANFs.

Conclusion

The round window neural noise is a faithful proxy to probe the degree and the SR-based nature of fiber loss. This method could be translated into the clinic to probe hidden hearing loss.

PS-503

Single-Unit and Basilar-Membrane Bases of Latencies of Cochlear-Nerve Compound Action Potentials in Chinchillas

Mario Ruggero[1]; Andrei Temchin[1]; Qin Gong[2]; Quentin Kennedy[3]

[1]Northwestern University; [2]Tsinghua University; [3]Hearing Resource Center of San Mateo

Some studies have attempted to infer traveling-wave delays in human cochleae from latencies of brainstem responses (BSERs) evoked by tone bursts (e.g., Rasetshwane et al., JASA, 133:2803-2817, 2013; Harte et al., JASA 126:1291-1301, 2009). However, as noted long ago (e.g., Teas et al., JASA 34:1438-1459, 1962; Eggermont, JASA 60:1132-1139, 1976), the very nature of traveling waves prevents accurate estimation of cochlear delays from BSERs or compound action potentials (CAPs), since these must include contributions from auditory-nerve fibers (ANFs) innervating large swaths of the cochlea basal to the characteristic place for the stimulus frequency. We investigated the spatial origins of tone-evoked CAPs in chinchilla, the species in which cochlear delays are best known. First, we studied the CAP N1 latencies as functions of stimulus frequency and level and of onset-ramp duration (1, 2 and 4 ms). Second, we compared those latencies with inferred signal-front and group delays of inner hair cells (IHCs) and basilar-membrane (BM) vibrations (Temchin et al., J. Neurophysiol. 93:3635-3648, 2005). This comparison demonstrated that, for stimulus frequencies 1-16 kHz and SPLs ≤ 70 dB, the CAP N1 latencies (regardless of onset-ramp duration) overestimated group delays at the characteristic frequency (CF) of BM and IHC responses at the characteristic places. Third, we compared the CAP N1 latencies with peri-stimulus –time histograms (PSTHs) of ANF responses evoked by similar stimuli. We found that, as previously suggested by Teas et al. and Eggermont (op. cit.), latencies of CAPs evoked by high-level stimuli largely reflect ANF activity at sites basal to the characteristic places corresponding to the stimulus frequency. Furthermore, we demonstrated that for low-level low-frequency stimuli with 2- and 4-ms onset ramps, necessary for place specificity at apical sites, the long latencies of CAPs reflect correspondingly long latencies of ANF PSTHs. This finding is consistent with the conjecture that the very long cochlear latencies inferred from waves V of BSERs evoked by low-level stimuli in humans are introduced at the synapses between ANFs and IHCs (Ruggero and Temchin, JARO 8:153-166, 2007). In conclusion: the basal spread of cochlear excitation and signal-transmission effects at the synapses between ANFs and IHCs jointly prevent the latencies of CAPs from serving as accurate indicators of IHC/BM traveling-wave delays in chinchilla. Probably the same conclusion applies to BSERs recorded in either chinchillas or humans.

PS-504

Spike-Time Coding and Auditory-Nerve Degeneration Best Explain Speech Intelligibility in Noise for Normal and Near-Normal Low-Frequency Hearing

Ian Bruce[1]; Agnès C. Léger[2]; Michael R. Wirtzfeld[1]; Brian C. J. Moore[3]; Christian Lorenzi[4]

[1]McMaster University; [2]University of Manchester; [3]University of Cambridge; [4]Ecole normale superieure, Paris

Background

Léger et al. (JASA 2012) measured the intelligibility of speech that was lowpass filtered at 1.5 kHz in background noise for a group of hearing-impaired (HI) listeners who had normal or near-normal hearing below 1.5 kHz. Compared to a control group of normal hearing (NH) listeners, the HI listeners displayed an overall deficit in speech understanding. However, the improvement in intelligibility obtained by introducing temporal or spectral dips into the masking noise (referred to as "masking release") was similar for the NH and HI groups. It was not possible to explain the patterns of masking release exhibited by the two groups using the extended speech intelligibility index (ESII). Also, the ESII only allows for *ad hoc* implementation of hearing impairment. This motivated the use of a neural-based intelligibility predictor, to see what forms of neural speech coding can explain masking release and what types of cochlear pathology best describe the suprathreshold deficit of the HI listeners while preserving masking release.

Methods

The auditory-periphery model of Zilany et al. (JASA 2009, 2014) was used to obtain predictions of auditory nerve (AN) responses to the stimuli used by Léger et al. (2012). The effects of outer hair cell (OHC) impairment, inner hair cell (IHC) impairment, and degeneration of AN fibers were studied. Two different neural-based predictors were investigated: the Spectro-Temporal Modulation Index (STMI; Elihali et al., Speech Comm. 2003) and the Neurogram SIMilarity index (NSIM; Hines & Harte, Speech Comm. 2012, 2014). Two versions of each of these metrics were assessed, one that depends only on the mean-rate AN representation and another

that depends on the all-information AN representation (i.e., includes spike-timing information).

Results

The mean-rate versions of the STMI and NSIM did not accurately predict the patterns of masking release seen in the human data. The all-information version of the STMI gave somewhat improved predictions of the NH data but over-predicted the effects of impairment for the HI group. In contrast, the all-information NSIM gave accurate predictions of the data for both groups. The best predictions of the deficits in overall intelligibility for the HI group were obtained with mixed OHC/IHC impairment and some degradation of AN fibers.

Conclusions

These results strongly suggest that spike-time coding of speech is required to explain masking release and that some suprathreshold deficits in intelligibility may be caused by AN degradation.

PS-505

Structural and Functional Changes in the Mouse Central Auditory Pathway during Aging

Moritz Gröschel[1]; Nikolai Hubert[1]; Susanne Müller[2]; Arne Ernst[1]; Dietmar Basta[1]

[1]Unfallkrankenhaus Berlin; [2]Charité University Medicine Berlin

Age-related hearing loss (ARHL) represents one of the most common chronic health problems in the aging population and is frequently attended by tinnitus and other psychoacoustic symptoms. In the peripheral auditory system, aging is accompanied by functional loss or degeneration of sensory as well as non-sensory tissue. Beside the degeneration of cochlear structures, the central auditory system is also involved in ARHL. Therefore, our studies should provide insight into the underling mechanisms of aging in central auditory structures. Aged mice (NMRI strain), showing a profound auditory threshold shift, were used in the present experiments. Hearing loss in the animals was measured using ABR recordings. Anatomical changes in the central auditory system were characterized by calculating cell densities in different key structures applying histological standard staining (HE) techniques. Furthermore, physiological alterations in calcium-dependent neuronal activity in central auditory structures have been investigated using non-invasive manganese-enhanced magnetic resonance imaging (MEMRI). The animals showed a progressive hearing loss during aging. Auditory thresholds were increased in all investigated aging groups compared to young controls. Histological data pointed to a strong neurodegeneration in central auditory structures, whereby decrease in cell densities was already present in the middle-aged group at an age of 13 months. Calcium-dependent activity in the central auditory system was highest in middle-aged animals as well but declined later in life. This development suggests an appearance of neuroplasticity with the onset of hearing loss, probably accompanied by long-lasting hyperactivity. The results of our studies give insight into central nervous correlates of age-related decline in auditory processing and perception, which are possibly further related to upcoming psychoacoustic phenomena during aging.

PS-506

Age-Related Changes in BK Channel Composition in the Inferior Colliculus and Auditory Cortex: Modulation Via Phosphorylation and aTargeted Peptide

Bo Ding[1]; Xiaoxia Zhu[1]; Yoshihisa Sakai[1]; Luisa Scott[2]; Joseph Walton[1]

[1]University of South Florida; [2]University of Texas- Austin

The large-conductance BK channel contributes to repetitive firing and the fast after-hyperpolarization in many neurons, including those in the auditory system. The channel exhibits diverse properties that arise from the molecular composition of the channel itself, as well as, the protein complex in which it resides. Protein phosphorylation has been shown to directly regulate the pore-forming α subunit, altering BK channel function. In the central auditory system, the inferior colliculus (IC) and auditory cortex (AC) play important roles in auditory learning, experience-dependent plasticity and processes that change with age. However, how BK channel composition changes in these structures as a function of age is unknown. To probe BK channel expression, the IC and AC were dissected from young (3 mon) and old (30 mon) CBA/CaJ mice. RT-PCR showed that the AC expressed mRNA for α, β1, β2, β3 and β4 subunits. The IC expressed mRNA for all but the β1 subunit. Immunochemistry staining showed that the level of α subunit protein expression *decreased* with age, as did the level of threonine phosphorylation of this subunit. To infer likely subunit combinations expressed in these auditory neurons, α, β1, β2, β3 and β4 subunit isoforms were extracted by PCR from the mouse brain, heart and testes, and cloned to pCDNA 3.1. These subunits were then expressed in mouse embryonic hippocampal cells (Clu195) and an α subunit antibody was immunoprecipitated with cell lysates. Subsequently we found a preferential association between α and β2 or β4 isoforms. Finally, to begin to develop tools for targeting the age-related changes in BK channel phosphorylation, we turned to a designer peptide that has been shown to act as a BK channel closer in heterologously expressed channels. We applied this peptide at 10 μM to Clu195 cells with endogenous expressed BK channels. The dynamic phosphorylation of threonine of the BKα subunit was reduced at 15 min post-treatment, with the maximum reduction observed at 30 min post-treatment. Phosphorylation returned to normal (compared to vehicle-control) at 120 min post-treatment. Together, these data show an *age-related down-regulation* in the BKα subunit expression and phosphorylation in the IC and AC. We have also demonstrated that a novel BK channel peptide modulator transiently reduces threonine phosphorylation. In the future we can use these tools to probe how BK channel phosphorylation contributes to age-related changes in auditory processing.

PS-507

Hormone Replacement Therapy Alters the Acoustic Startle Response in Menopausal CBA/CaJ Mice

Xiaoxia Zhu; Tanika Williamson; Elizabeth Schaefer; Rebecca Henry; Robert Frisina; Joseph Walton
University of South Florida

Background

Our previous studies revealed that hormone replacement therapy (HRT) has detrimental effects on hearing, including audiometry and auditory physiology in postmenopausal women and perimenopausal female CBA/CaJ (CBAs) mice. (Guimaraes et al., *Proc. Nat. Acad. Sci.* 103:14246-9. Price et al., *Hear. Res.* 252:29-36, 2009). The present study's aim was to investigate the behavioral effects of HRT treatment in aging menopausal CBAs.

Methods

Middle-aged (~16 mon) ovariectomized female CBAs were placed into 4 groups based upon treatment: 17β-estradiol (E), progesterone (P), E+P, and placebo (Pb), all administered via slow-release subcutaneous hormone pellets. In addition, a group of age-matched males served as controls. All mice underwent Auditory Brainstem Responses (ABR) including wideband noise (WBN) and the acoustic startle response (ASR); from pre-implantation (baseline) through 6 mon of treatment. ASR input-output (I/O) functions were elicited by 20 msec WBN at random inter-trial intervals (10-20 sec) at intensities ranging from 55-115 dB SPL, in 10 dB increments. Each intensity level was presented 10 times (70 trials total).

Results

The WBN ABR threshold shifted 5~10 dB in all groups, except E at 6 mon treatment, where it remained stable. The ASR I/O function slopes decreased 16~22% at 3 mon treatment relative to baseline in male and female groups except E (32%). There was a 12~15% drop in slope in E+P and E groups between treatment at the 3 mon and 6 mon time points; whereas the drop was less than 5% in the P, Pb and male groups. We found a correlation between bodyweight (BW) and ASR amplitude, from baseline through the 6 mon treatment point; with the E group showing a significant correlation between BW and ASR amplitude. ASR threshold also increased for the P group at 6 mon treatment. Interestingly, the ASR amplitude declined with trial number at 115 dB in E+P and E groups, as compared to the other subject groups after 6 mon of treatment.

Conclusion

ASR amplitude was positively correlated with BW in middle-aged CBAs, and the group E displayed the strongest treatment effects. The E+P and E groups showed reduced startle amplitude following 6 mon of treatment, and a greater decline in the startle amplitude across trial number. These results indicate that ASR I/O functions declined in the E and E+P groups driven by age-related sensorimotor changes and hormone treatments. In conclusion, the E and E+P treatments may modulate the ASR circuitry in aging menopausal mice.

PS-508

Progesterone Impedes Age-Related Hearing Loss for ABR Gap Responses in Female Middle Age Mice

Tanika Williamson; Xiaoxia Zhu; Joseph Walton; Robert Frisina
University of South Florida

Introduction

Most hormone replacement therapy (HRT) studies have found estrogen to be beneficial for hearing. While similar studies have claimed combination hormone treatment, estrogen plus progesterone, to be a catalyst for severe hearing loss. This led researchers to hypothesize that progesterone was the negative component amid the hormone duo, counteracting the protective effect of estrogen. The present study takes a closer look at this hypothesis to gain better insights as to how progesterone affects the auditory system. Progesterone was administered to middle-age female CBA/CaJ mice and auditory brainstem responses (ABR) as well as ABR gap-in-noise (GIN) responses were analyzed.

Methods and Materials

Female, middle-aged (15-18 months) CBA/CaJ mice were ovariectomized and administered subcutaneous, time-released hormone pellet treatments. The subject groups consisted of 17β-estradiol (E), progesterone (P), E+P, and placebo (Pb). The animals underwent ABR and ABR GIN testing to examine the effects, over a 6-month time period. ABR tests covered frequencies ranging from 3 to 48 kHz. Meanwhile, ABR GIN stimuli employed a wide-band-noise (WBN) carrier. For the data analysis, emphasis was placed on the ABR thresholds as well as ABR GIN response amplitude and latency. A male group was also tested to serve as an additional control group.

Results

Coinciding with previous studies, animals treated with E displayed signs of improved peripheral sensitivity. This included decreased latency values and thresholds. ABR GIN recovery ratios also increased as treatment progressed. Meanwhile, in contrast to the hypothesis put forth above, P had consistent ABR GIN recovery ratios and amplitude levels that slowly declined during the treatment period. Animals treated with E+P and Pb had different results, with amplitude levels that drastically declined as soon as treatment began. Signs of age-related hearing loss became apparent at 3 months of treatment for the Pb group.

Conclusions

The results here suggest that progesterone, by itself, is not detrimental to the auditory system. Although hearing is not improved as seen with humans and animals treated with estrogen, progesterone does appear to slow down certain key features of presbycusis when compared to the other subject groups in the study. This finding could provide researchers with a better understanding of how the two hormones interact with one another during treatment and lead to the answer of why E+P has such as negative impact on the aging auditory system.

PS-509

The Harwell Aging Screen Identifies Novel Models of Age-Related Hearing Loss

Michael Bowl[1]; Carlos Aguilar[2]; Susan Morse[2]; Prashanthini Shanthakumar[2]; Ruairidh King[2]; Lauren Chessum[2]; Michelle Simon[2]; Andrew Parker[2]; Giorgia Girotto[3]; Sally Dawson[4]; Paolo Gasparini[3]; Sara Wells[2]; Paul Potter[2]; Steve Brown[2]
[1]MRC Harwell, Oxford; [2]MRC Harwell; [3]University of Trieste; [4]UCL Ear Institute

Introduction

Age-related hearing loss (ARHL), also called presbycusis, is the most common sensory deficit experienced by the elderly. The prevalence of the condition increases significantly with age, and contributes to social isolation, depression, and loss of self-esteem. ARHL is a complex disorder that is not fully understood, but its onset and progression are influenced by environmental factors and genetic susceptibility. To date, little is known of the genes and pathways predisposing to ARHL, and the study of the condition in humans is very limited, due to the genetic heterogeneity within the population, age of onset, and limited access to tissues. Therefore we are using the mouse to investigate the genetics of ARHL.

Aim

Utilize age-challenged mice to elaborate upon the genetic landscape of ARHL. Knowledge of the genetics and molecular mechanisms of ARHL will facilitate the development of therapeutic strategies to ameliorate hearing deterioration.

Methods

At MRC Harwell we are undertaking a large-scale *N*-ethyl-*N*-nitrosourea (ENU) mutagenesis screen to generate mouse models of age-related disease. G3 pedigrees, of ~100 mice, are bred and enter a phenotyping pipeline comprising recurrent assessment across a wide range of disease areas, up to 18 months of age. We are taking advantage of this screen to identify models of ARHL, employing recurrent Clickbox and Auditory-Evoked Brainstem Response phenotyping.

Results

As of August 2014, 140 pedigrees have entered the pipeline, of which 125 have completed auditory screening. To date 27 pedigrees (~19%) have confirmed auditory phenotypes. Of these, 20 pedigrees display early-onset hearing loss, as evidenced by elevated hearing thresholds by 3 months of age, and 7 pedigrees exhibit ARHL with hearing loss evident from 6 months of age. Of the 20 early-onset pedigrees, 11 harbor mutations within known deafness genes and 4 within novel genes. Of the 7 late-onset pedigrees, 6 harbor a mutation within novel genes and 1 within a known deafness gene. Studies to relate mutant gene to phenotype are ongoing, whilst genome mapping and sequencing of the remaining pedigrees are underway.

Conclusions

The Harwell Aging Screen is producing a significant number of novel mutants with age-related auditory phenotypes. The screen provides compelling data to indicate that ageing reveals novel genes and a genetic landscape hitherto not uncovered by the study of congenital/early-onset hearing loss mouse mutants. Investigation of these ageing models, and as yet unidentified pedigrees, promises to increase our understanding of the genetics and pathobiology of ARHL.

PS-510

Progress Report on the Roles of Mitochondrial Isocitrate Dehydrogenase in the Auditory System

Karessa White; Mi-Jung Kim; Chul Han; Logan Walker; Paul Linser; Colleen Le Prell; Shinichi Someya
University of Florida

Backgrounds

Age-related hearing loss (AHL) is the third most common chronic condition among the elderly yet there are no treatments or preventative interventions for this irreversible sensory disorder. However, drugs targeting the NADPH system are a key interest towards treatment. IDH2 (isocitrate dehydrogenase 2) plays a crucial role in the TCA cycle through the conversion of isocitrate to *alpha* ketoglutarate and the reduction of $NADP^+$ to NADPH. IDH2 supplies NADPH for the regeneration of mitochondrial glutathione and thioredoxin for protection against oxidative stress, cell loss and resulting hearing loss. The overall goal of this project is to investigate whether IDH2 plays an essential role in maintaining cochlear and auditory function under normal conditions or during aging in mice.

Methods

To confirm that Idh2 expression is within the mitochondria and not in the cytosol or nucleus of the mouse cochlear cells, we performed co-localization analyses in wild-type mice using confocal-based immunofluorescence microscopy. To determine whether knockdown of Idh2 promotes oxidative stress induced cell death, we performed *in vitro* oxidative stress tests and cell viability tests in mouse inner ear cells (HEI-OC1) transfected with siRNA targeted to IDH2. In order to determine if *Idh2* deficiency results in the loss of spiral ganglion neurons and sensory hair cells in the cochlea, we performed histopathological observations using wild-type and $Idh2^{-/-}$ mice.

Results

Knockdown of Idh2 increased susceptibility to oxidative stress-induced cell death in cultured HEI-OC1 cells. Confocal-based immunostaining analysis revealed that Idh2 immunostaining was detected as a very strong signal similar to the staining for CoxIV in the spiral ganglion. This is consistent with compartmentalization within mitochondria.

Conclusions

Currently, we are investigating whether Idh2 knockdown decreases mitochondrial respiration rates in mouse inner cells, and whether *Idh2* deficiency promotes cochlear degeneration and/or hearing loss in young, middle-aged, and old mice that were backcrossed onto the CBA/CaJ strain. The results of this study will enrich current knowledge of the mechanisms of AHL.

PS-511

Progress Report on the Roles of Glutathione Reductase in the Auditory system

Chul Han[1]; Hyo-Jin Park[1]; Mi-Jung Kim[1]; Karessa White[1]; Logan Walker[1]; Tatsuya Yamasoba[2]; Dalian Ding[3]; Richard Salvi[3]; Paul Linser[1]; Shinichi Someya[1]
[1]University of Florida; [2]University of Tokyo; [3]University at Buffalo The State University of New York

Backgrounds

Glutathione acts as the major small molecule antioxidant and is found mostly in the reduced form (GSH) in healthy cells. During aging, oxidized glutathione (GSSG) accumulates, and hence an altered ratio of GSH:GSSG is thought to be a marker of both oxidative stress and aging. Glutathione reductase (GSR) plays a critical role in preventing accumulation of GSSG and maintaining the appropriate redox environment in cells through regeneration of GSH, thereby enhancing the glutathione antioxidant defense system. We have previously shown that CR (calorie restriction) delays the onset of AHL (age-related hearing loss), reduces oxidative DNA damage and cochlear cell loss, and increases the activity of glutathione reductase and the GSH/GSSG ratio in mouse cochlea. The overall goal of this project is to investigate whether GSR plays an essential role in maintaining cochlear and auditory function under normal conditions or during aging in mice.

Methods

To investigate whether Gsr knockdown promotes oxidative stress-induced cell death, we conducted *in vitro* oxidative stress tests using H_2O_2 and paraquat followed by cell viability tests in mouse inner ear cells (HEI-OC1) or human neuroblastoma cells (SHSY-SY) that are transfected with siRNA targeted to Gsr (Gsr knockdown) or scrambled siRNA (Control). To investigate whether Gsr knockdown affects mitochondrial function, we are currently measuring mitochondrial respiration rates using a mito-stress test in Gsr knockdown cells and control mouse inner ear cells.

Results

Gsr deficiency increased susceptibility to oxidative stress-induced cell death in cultured mouse inner ear cells and human neuroblastoma cells. Currently, we are investigating whether *Gsr* deficiency promotes cochlear degeneration and/or hearing loss in young, middle-aged, and old wild-type, *Gsr* heterozygous knockout ($Gsr^{+/-}$), and homozygous knockout ($Gsr^{-/-}$) mice that were backcrossed onto the CBA/CaJ strain for 6 generations.

Conclusions

These results suggest that GSR may play a key role in protecting cochlear cells against oxidative stress and maintaining auditory function. Currently, we are investigating whether *Gsr* deficiency promotes mitochondrial dysfunction, cochlear degeneration, or hearing loss during aging or under calorie restricted conditions. Knowledge of these molecular mechanisms has enormous potential for improving health outcomes through the discovery/development of novel therapeutics for human AHL.

PS-512

Correlation Between Auditory Brainstem Response and PPI Startle Reflex in Aging Mice on Different Dietary Regimes

Paula Mannström; Karin Pernold; Brun Ulfhake; Mats Ulfendahl
Karolinska Institutet

Introduction

In the current study we investigated if there is a correlation between hearing thresholds and behavioral reflexes in aging mice. We also tested whether this correlation is affected by dietary restriction, previously shown to reduce age-related hearing loss.

Age-related hearing loss is the cumulative effects of aging on hearing. The on-set can be delayed with a restricted diet in several animal models. It has been debated whether the restriction also has an effect when started later in life. Normal aging animals have in preliminary studies displayed lowered behavioral reflexes. Impaired prepulse inhibition (PPI) reflexes are usually seen in neuropsychiatric disorders involving dysfunctional sensory gating function, but can also be caused by poor hearing function.

In a longitudinal study, correlation between increasing hearing thresholds and a decline in the behavioral reflexes was investigated with aging C57Bl/6J mice subjected to restricted diet introduced in mid-life or older age.

Methods

Hearing thresholds were determined using auditory brainstem responses (ABR). The behavioral reflexes were determined by testing the acoustic startle reflex and PPI response. In a pilot study, prepulse stimuli at different intensity levels (110 or 120 dB) were used to determine if the prepulse stimuli itself caused any changes in hearing thresholds in four month old male C57Bl/6N mice (n=11). ABRs were determined before, 24 hours and 2 weeks after the PPI test.

In 10 month old (n=18), 22 month old (n=14) and 27-28 month old (n=9) male C57Bl/6J mice auditory hearing thresholds using ABR were determined as well as responses of acoustic startle and PPI reflexes. The animals aged 10 and 22 month were then subjected either to a restrictive diet (DR; 70% of *ad libitum* (AL) intake) or continued fed AL for six months when they were tested again.

Results

Increased hearing thresholds correlated with lowered acoustic startle responses and PPI reflexes with advancing age of the animals. Results from the dietary restricted feeding regime will be determined later. Neither the 110 nor the 120 dB prepulse stimuli caused any sustainable elevated hearing thresholds.

Conclusion

Aging causes a decline in both auditory function and lowered behavioral reflexes. The results from the dietary regime will reveal whether the restriction has an effect not only on hearing function but also on PPI reflexes in aging animals. The

length and timing for onset of dietary restriction is important for understanding the beneficial effects of the restriction.

PS-513

Mitochondrial DNA Perturbations in the Vestibular Neuroepithelium of Aged Rats

Doug Smith; Gemma Parkinson; Alan Brichta; Mark Bigland

The University of Newcastle

Introduction

As we age our ability to maintain balance becomes increasingly difficult, often leading to falls that require hospitalisation. Impaired vestibular function is thought to contribute to these falls. Whether this is due to the peripheral and/or central components of the vestibular system is not known. In the present study we used a molecular approach to determine how peripheral vestibular organ function may be compromised with aging. Inner ear vestibular hair cells detect head motion and these cells are energetically demanding, in part due to the necessity of continuously removing calcium from the hair cell. Therefore mitochondrial activity is critical for normal hair cell and vestibular system function One essential mitochondrial activity is to encode protein components of the respiratory chain via mitochondrial DNA (mtDNA). Ageing is known to be associated with increased mtDNA alterations including deletion mutations and duplications. These alterations are thought to compromise respiratory chain activity in a number of tissues, including the nervous system. However, it is unknown whether aging alters mtDNA in vestibular hair cells, potentially underlying age-related balance loss. The aim of the present study was to characterise the effect of aging on mtDNA duplications and deletion mutations in rat vestibular hair cells.

Methods

Approximately 300 hair cells were laser microdissected from each of 14 young adult (4-6 months) and 7 old (23-26 months) male F344 rats. DNA was extracted and qPCR analyses carried out to compare the relative abundance of four mtDNA genes and mtDNA copy number between the two age groups.

Results

There was a significant increase in abundance of CytB relative to ND1, ND4 and 12S mtDNA genes ($p<0.001$) in old animals relative to young, indicating specific duplication of the CytB region relative to other parts of mtDNA. However, there was no significant age effect on mtDNA copy number ($p=0.44$).

Conclusions

mtDNA replication and transcription are regulated from the control region of mtDNA adjacent to the CytB gene. Duplication of CytB suggests dysfunction of the control region even though our copy number data suggest replication is unaltered with aging. Taken together these data indicate mtDNA alterations may contribute to age-related changes in vestibular system function. Investigations of potential effects of CytB duplication on mtDNA transcription therefore need to be further characterized.

PS-514

Progress Report on the Roles of Mitochondrial Thioredoxin in the Auditory System

Mi-Jung Kim

University of Florida

Backgrounds

Hearing loss is the third most prevalent chronic health condition in adults and affects more than 40% of people over 65 years of age in the US. Yet, currently there is no treatment or preventative intervention for this common disorder. The overall goal of this project is to investigate the roles of mitochondrial thioredoxin (TXN) in the auditory system under normal conditions and/or during aging. The TXN system is one of major antioxidant defense systems in mitochondria. There are three major players in the mitochondrial TXN system: thioredoxin 2 (Txn2), thioredoxin reductase 2 (Txnrd2), and peroxiredoxin 3 (Prdx3). In mitochondria, NADPH-dependent Txnrd2 regenerates reduced Txn2 ($_{red}$Txn2) from oxidized Txn2 ($_{oxi}$Txn2). Subsequently, $_{red}$Txn2 catalyzes the reduction of oxidized Prdx3 ($_{oxi}$Prdx3) to regenerate reduced Prdx3 ($_{red}$Prdx3) which plays a role in the removal of hydrogen peroxide (H_2O_2), one of the major reactive oxygen species in cells. In this project, we hypothesize that a decline in the mitochondrial TXN antioxidant defense system results in mitochondrial dysfunction which in turn promotes cochlear degeneration and associated hearing loss.

Methods

To investigate whether Txn2 knockdown promotes oxidative stress-induced cell death, we conducted oxidative stress tests using H_2O_2 followed by cell viability tests in cultured mouse inner ear cells (HEI-OC1) which were transfected with Txn2-siRNA or control. We also performed western blotting to measure Txn2 protein levels in the inner ears from 4-6 months old Txn2 heterozygous knockout ($Txn2^{+/-}$) and wild-type mice.

Results

Txn2 knockdown cells were more susceptible to H_2O_2-induced cell death, indicating Txn2 may play an essential role in protecting inner ear cells from oxidative stress. The inner ears from 4-6 months old $Txn2^{+/-}$ mice showed a 60% decrease in Txn2 protein levels in the mitochondria.

Conclusions

We are currently performing colocalization analysis of Txn2 and Txnrd2 proteins in a wild-type mouse cochlea using immunofluorescence confocal microscopy. We are also investigating whether *Txn2* or *Txnrd2* deficiency promotes mitochondrial dysfunction, cochlear degeneration, or hearing loss during aging or under calorie restricted conditions. The results of this project will provide an enhanced understanding of the fundamental molecular mechanisms underlying age-related hearing loss.

Funding

Supported by NIH/NIDCD grants R01 DC012552 (S.S.) and R03 DC011840 (S.S.).

PS-515

Low Level Laser Effects on Auditory Neuron Survival After Ouabain Exposure in Gerbils

Sung-hyen Bae[1]; So-Young Chang[2]; Phil-Sang Chung[2]; Jae Yun Jung[2]

[1]Dankook University Hospital; [2]BLI-Korea

Introduction

Ouabain application through round window is well established method for selective spiral ganglion neuron damage with sparing hair cell injury in guinea pig and Mongolian gerbil. This model mimics auditory neuropathy spectrum disorder in many aspects. This study was designed to investigate whether treatment with low level laser therapy (LLLT) can save hearing loss in selective auditory neuron damage model.

Methods

Selective auditory neuron damage model was made by local application of ouabain (1 mmol/L, 3uL) to the round window membrane in female Mongolian gerbils. For laser group, LLLT treatment was given once a day for 1hour (200mV) during 7days. For sham laser group, laser tip was placed for the same time without turning on the switch for 7 days. The baseline hearing of the animals was evaluated using the auditory brainstem response (ABR) and distortion product otoacoustic emissions (DPOAE). One day and 7 days after ouabain application, ABR and DPOAE were checked in each group (sham laser and laser group). After final audiologic evaluation, animals were sacrificed for morphological analysis to see spiral ganglion neurons (SGNs) and synaptic structures.

Results

Ouabain application resulted in marked ABR threshold increase when tested with 4, 8, 12, 16 ,32 KHz tone pip without DPOAE change. LLLT group showed better result in terms of ABR threshold shift as compared with sham laser group, when tested 7 days after ouabain application. H&E stains of Mid-modiolar section showed the decrease of spiral ganglion cell population, which was more prominent in sham laser group than in laser group.

Conclusions

The results demonstrate that LLLT has potential therapeutic role in ouabain-induced auditory neuron damage.

PS-516

Methionine Sulfoxide Reductase A (MsrA) Mutant Mice Show Early Progressive Hearing Loss and Exacerbated Damage from Acoustic Trauma.

Safa Alqudah[1]; Mark Chertoff[1]; Dianne Durham[1]; Jackob Moskovitz[2]; Hinrich Staecker[1]; Marcello Peppi[1]

[1]University of Kansas Medical Center; [2]University of Kansas

Background

Methionine sulfoxide reductases (MsrA and MsrB), enzymes that protect the biological activity of proteins from oxidative modifications due to methionine oxidation, are important for preventing the biological effects of aging and the onset of age-dependent neurodegenerative diseases. Previously, we showed that MsrA cochlear expression decreased with age (Peppi et al, ARO 2014). However, the role of MsrA in processes leading to hearing loss is unclear in spite of the fact that MsrA is considered to be the major antioxidant enzyme of the Msr system. Our central hypothesis is that depleted levels of cochlear MsrA leads to the damage of neuronal proteins that are important for ameliorating the effect of acoustic overexposure and aging. In this study, we investigated the age-related changes in hearing before and after acoustic overexposure using ABR and DPOAE analysis.

Methods

For auditory recordings, 5-24 weeks old male/female MsrA knockout (MsrA KO) and wild-type (WT) mice were tested. ABRs were elicited by tone pips (5 ms duration delivered at 31.3/sec) at 6 log-spaced frequencies from 5.1 – 26.5 kHz and measurements recorded by placing electrodes in the scalp. DPOAE were recorded as amplitude vs. level functions (L2= L1 – 10) for the same frequencies.

For acoustic overexposure experiments, a broad-band of noise (8-17 kHz) was delivered at 100 dB SPL, for 2 hrs. Exposures were delivered to awake mice placed directly below the horn of the sound-delivery loudspeaker. Seven days following acoustic exposure, ABRs and DPOAEs were recorded.

Results

At five weeks of age, MsrA KO mice had a small threshold elevation in the high frequencies, in comparison to WT cohorts. By 24 weeks, the threshold elevation spread towards the middle and the low frequencies. By eight weeks of age MsrA KO mice showed a decrease in ABR amplitudes and longer Interpeak latencies (V-III and V-I) than WT littermates, suggesting that depletion of MsrA triggers onset of auditory neuropathy. When mice were exposed to a loud noise, five weeks old MsrA KO mice showed more hearing loss compared to WT mice, indicating that MsrA plays a role in protecting neurons from the damaging effect of noise exposure.

Conclusions

The age-related changes in hearing and the exacerbated loss of hearing from noise exposure observed in MsrA KO mice, compared to WT litter mates, support the idea that MsrA might play a role in protecting from the effects of aging and noise induced hearing loss.

PS-517

Histology of the auditory brainstem of aged Mongolian gerbils and its relation to auditory brainstem responses

Sandra Tolnai; Gesa Müller; Genevieve Laumen; Georg Klump

Carl von Ossietzky University Oldenburg

Gerbils' sound localization ability deteriorates with age, e.g. aged gerbils show higher and/or more variable minimal resolvable angles compared to the ones measured in young animals (Maier et al., 2008). Also, the temporal processing is impaired, shown for example by elevated gap-detection

thresholds (Hamann et al., 2004) and increased tone detection thresholds for short sounds (Gleich et al., 2007) in aged gerbils. It has been suggested that anatomical changes in the auditory brainstem of aged gerbils might lie at the heart of the impaired performance in auditory tasks (Maier et al., 2008). We here investigate the brain stem of young and aged Mongolian gerbils histologically and relate those findings to auditory brainstem response measurements.

Brain sections containing the auditory brainstem of Mongolian gerbils, aged between four and forty months at the time of perfusion, were processed using Nissl's staining method and Golgi's method to visualize neuronal somata and fibers, respectively. Brain sections were investigated with respect to the occurrence of spongiform lesions in the lateral and medial superior olives (LSO, MSO) and with respect to the volume of both nuclei. Animals' physiology was assessed by measuring monaural auditory brainstem responses and binaural difference potentials.

We found that the amount of lesions observed in the LSO and MSO was independent of age, although the largest fraction of spongiform lesion was found in an individual with the age of 40 months (on average between 20 and 24% of the surface area in LSO slices). The size of LSO and MSO remained stable throughout age apparent by the lack of significant correlations between age and the total area the nuclei covered. It remains to be investigated if the higher variability of the occurrence of lesions is reflected in more variable hearing thresholds assessed by measuring auditory brainstem responses or mirrored in the amplitudes of those auditory brainstem responses.

The current histological findings confirm observations by Gleich and colleagues (2002, 2004) that spongiform lesions in the auditory brainstem of Mongolian gerbils are prominent in aged animals.

PS-518

A Comparison of Auditory and Vestibular Synaptic Aging in CBA/CaJ Mice

Katharine Fernandez; Sharon Kujawa
Massachusetts Eye and Ear Infirmary

Declines in auditory and vestibular function are common with age, and understanding peripheral contributions to such changes is key to informed diagnosis and therapy. Our prior work in experimental models of cochlear aging and noise exposure shows that loss of synapses between inner hair cells and afferent neurons is a primary event, occurring well before permanent loss of hair cells (Kujawa and Liberman 2009; Sergeyenko et al 2013). Neural response amplitudes decline in proportion to these synaptic losses, even when threshold sensitivity is well preserved. In the case of the vestibular end organs, age-related loss of hair cells and threshold sensitivity is well documented; however, potential synaptopathic and primary neuropathic changes with age have not been explored. Here, we compare vestibular and cochlear synaptic aging in the same ears of an age-graded series of CBA/CaJ mice. Cochlear and vestibular end organ function was characterized using DPOAE-, ABR- and VsEP-based measures of threshold and suprathreshold response growth. Immunostained whole mounts and plastic-embedded sections were studied to quantify cochlear and vestibular hair cells, neurons, and the synapses that connect them. Consistent with previous work in this strain (Mock et al 2011; Sergeyenko et al 2013), sensitivity of both vestibular and auditory evoked response thresholds declined with age. In the current series, vestibular threshold shifts outpaced auditory threshold shifts to roughly 16 months; thereafter, the rate of auditory threshold shift escalated, resulting in comparable threshold shifts in oldest animals. By both ABR Wave I and VsEP P1/N1 metrics, amplitude declines began early and progressed gradually throughout the lifespan; in oldest groups, declines exceeded 60% when compared to young mice. No significant changes in peak latencies were observed. Quantification of age-related changes in hair cells, synapses, and ganglion cells is ongoing. Results will refine our understanding of synaptopathy in the inner ear and guide future efforts to repair what is lost from age or injury.

Research supported by NIDCD: R01 DC008577.

PS-519

Evidence of Age-Related Temporal Processing Deficits in EEG and MEG Recordings

Alessandro Presacco; Jonathan Z Simon; Samira Anderson
University of Maryland

Introduction

Results from both animal and human studies suggest that age-related temporal processing deficits may arise from impairments in central auditory system function. Understanding neural mechanisms underlying age-related changes may be clinically relevant for devising efficient training methods to partially restore age-related degraded temporal processing. In this study we used behavior, and electroencephalographic (EEG) and magnetoencephalographic (MEG) imaging techniques to study how aging affects neural activity at subcortical and cortical levels.

Methods

Participants comprised 8 younger adults (18–30 years old) and 8 older adults (60–69 years old) with normal hearing. Participants' sentence recognition in noise was behaviorally assessed using the Quick Speech-in-Noise test (QuickSIN). Subcortical activity was studied with EEG by recording Frequency Following Responses (FFRs) in response to a 170-ms /da/ speech syllable presented binaurally with alternating polarities in quiet and in single-talker competing speech (0 SNR). Cortical activity was studied with MEG by recording subjects' responses while attending to one of two simultaneously presented speech streams. The MEG responses in the 1–8 Hz frequency band were used to reconstruct the envelope of the two speech streams.

Results

At the subcortical level, noise significantly affects representation of the envelope and fine structure in younger adults, but noise-induced changes are minimal for the older adults. At the

cortical level, the envelope of the target speech stream can be reconstructed from the neural responses of both younger and older adults. The two groups are differentiated, however, by the inability of older adults to efficiently suppress the competing speech, as demonstrated by their reduced contrast in decoding accuracy between the target and competing speech. When comparing subcortical and cortical responses, we found a positive correlation between the extent of noise suppression in the first two harmonics of the envelope and the decoding accuracy difference between target and competing speech in older adults but not in younger adults. We also found that QuickSIN scores were negatively correlated with the MEG decoding accuracy difference in older adults but not in younger adults.

Conclusions

Our findings show a moderate, but significant correlation between subcortical and cortical responses in older adults, suggesting that temporal processing disruption in the midbrain can significantly affect decoding accuracy of the speech stimulus at the cortical level.

PS-520

Differential Modulation of Electrocortical Responses Evoked from Primary and Nonprimary Auditory Cortex by Forward Masking Inducing Residual Inhibition of Tinnitus

Larry Roberts; Daniel Bosnyak; Ian Bruce; Brandon Paul
McMaster University

We compared sound-evoked brain activity (128-channel EEG) in subjects experiencing tinnitus under baseline conditions with that of subjects of similar age and hearing function who reported not having tinnitus. In the same session we subsequently examined how brain activity changed when subjects in both groups were exposed to a forward masking procedure known to induce tinnitus suppression (residual inhibition, RI) in the tinnitus subjects. During the tinnitus baseline the 40-Hz auditory steady-state response (ASSR, localizing to primary auditory cortex, A1) was larger in tinnitus subjects than in controls when evoked by 500 Hz probes (40-Hz AM) below the tinnitus frequency region (TFR) of tinnitus subjects, while the reverse was true for the ASSR evoked by 5 kHz probes in the TFR, revealing frequency-dependence in this response. Frequency dependence was not observed for N1 amplitude which was larger in tinnitus than control subjects at both probe frequencies (N1 localizing to nonprimary auditory cortex, A2). Forward masking by a bandpass noise (CF 5 kHz ±15%, 30 sec, known to induce RI in the tinnitus subjects) altered ASSR and N1 responses, but in different ways. In control subjects masking had no effect on ASSR amplitude evoked by 5 kHz probes but increased ASSR amplitude evoked by 500 Hz probes even though the masking sound contained no energy at 500 Hz. In tinnitus subjects the effects of masking on ASSR amplitude were strikingly reversed, revealing increased ASSR amplitude to 5 kHz probes after masking but no change to 500 Hz probes. In contrast, N1 amplitude was reduced by masking at both probe frequencies in all groups. The frequency dependence of the ASSR but not N1 in our tinnitus groups during baseline compared to controls, and the different effects of masking on ASSR and N1 responses in tinnitus subjects, indicate (1) that ASSR and N1 responses interact differently with the neural changes underlying tinnitus and its suppression in RI, and (2) that the neural changes associated with tinnitus are expressed differently in A1 and A2. We suggest that while disinhibition of neural responses by auditory attention or other mechanisms may occur in both cortical regions enhancing ASSR and N1 amplitude similarly in tinnitus subjects, tinnitus-related hypersynchrony may be confined to the tinnitus frequency region of A1 and is an additional factor affecting ASSR amplitude. Mechanisms for the off-frequency masking effects observed for the ASSR in controls and N1 in both groups are suggested.

PS-521

Dependence of Noise-induced Hearing Loss on Noise Duration in Gerbils and Rats

Lenneke Kiefer[1]; Bernhard Gaese[2]; Manuela Nowotny[2]
[1]Goethe University Frankfurt/Main; [2]Institute of Cell Biology and Neuroscience

Background

Acoustic overstimulation is one of the major causes of tinnitus in humans. Important parameters for the severity of such overstimulation might be the frequency content of the noise, its time course and sound pressure level (SPL). We used animal models to study the influence of these parameters on the time-depended development of noise-induced hearing loss (NIHL). The relationship between NIHL and the duration of acoustic overstimulation up to 2 h was studied in Mongolian gerbils and rats at different time points and at three different frequencies.

Methods

Experiments were performed on 10 adult Mongolian gerbils (*Meriones unguiculatus*) and 10 adult laboratory rats (*Rattus norvegicus*). Hearing ability was investigated by means of auditory brainstem responses (ABRs) measured at 2, 8 and 14 kHz before, during and after intense noise stimulation (noise band of BW 0.5 oct around 8 kHz; 105 dB SPL). The changes in ABR threshold values were measured at different time points during the stimulation procedure including up to 2 h noise duration.

Results

Overstimulation with noise of 105 dB SPL depending on stimulus duration induced a significant decrease in the hearing ability as measured by an increase in ABR threshold values in both, gerbils and rats with a saturation after 60 min and 30 min, respectively. This was found at the induction frequency of 8 kHz as well as at higher frequencies around 14 kHz. At 2 kHz, clearly below the noise band, no significant changes were found. In gerbils, even louder overstimulation (at 115 dB SPL) led to an increase in ABR threshold values at 14 kHz only. In rats, however, this led to an increase in ABR threshold at all frequencies tested. Here, eight weeks after the noise

application the threshold level at 8 and 14 kHz are still significantly increased.

Conclusion
We found a strong noise-induced decrease in hearing ability in the first 30 to 60 min after noise application. Longer durations did not increase the threshold values significantly. An additional, the usage of even louder noise led to a decrease in hearing ability in gerbils only, at the frequency above the applied noise band. However, in rats the hearing ability was decreased at all tested frequencies.

PS-522

First Appearance of Salicylate-Induced Hyperactivity and Plasticity along the Auditory Pathway

Guang-Di Chen; Chen Jiang; Adam Sheppard; Kelly Radziwon; Richard Salvi
University at Buffalo

Sodium salicylate (SS) has been used for decades as a tool to study the neural correlates of tinnitus and recent studies from our lab indicate that salicylate also induces hyperacusis. High dose SS is ototoxic and depresses the neural output of the cochlea, but paradoxically it induces sound-evoked hyperactivity and frequency map reorganization in the auditory thalamus, cortex, amygdala, and striatum. Exactly where SS first initiates neural hyperactivity and plasticity along the auditory pathway is unclear. To address this issue, we recorded sound-evoked responses in the rat cochlea, cochlear nucleus (CN), inferior colliculus (IC), and AC pre- and post-SS (300 mg/kg, i.p.).

SS-treatment greatly reduced sound-evoked responses at low stimulation levels leading to a 20-30 dB threshold shift at the cochlea and higher levels of the auditory pathway. At high intensities, the neural output of the cochlea was dramatically reduced; however, neural responses from the CN were almost normal, indicative of enhanced central gain. Remarkably, suprathreshold responses at higher auditory centers (IC and AC) were larger than normal, neural measurements consistent with our recent behavioral measures of SS-induced hyperacusis. The SS-induced changes were largely independent of frequency/location in the cochlea and CN, but in the IC and AC, suprathreshold hyperactivity was greatest in the mid-frequencies, where our behavioral measures of hyperacusis are greatest. Consistent with our previous measures in the AC and amygdala, frequency receptive fields (FRF) of neurons in the IC shifted/expanded towards the mid-frequency region; an effect not observed in the CN. Figure 1 presents mean FRF of 7 low-frequency IC neurons. The averaged characteristic frequency (CF) of the neurons was ~1.5-2.3 kHz and its threshold ~18 dB. After SS treatment, the response thresholds at frequencies >FRF significantly decreased while thresholds near the CF significantly increased ~20 dB. The changes resulted in a significant right-shift of the FRF, i.e., a high-frequency expansion into the region where suprathreshold hyperactivity is greatest and tinnitus occurs. Taken together, these results indicate that the SS-induced threshold shift originate in the cochlea and propagates centrally. However, at high stimulation levels, major compensatory changes occur along the auditory neuroaxis to compensate for the reduced neural output of the cochlea. Some amplification occurs at the CN, but by reaching the IC and AC responses are larger than normal. These enhanced suprathreshold responses, indicative of enhanced central gain, may be due in part to the frequency map reorganization first seen in the IC.

PS-523

Potassium Agonist Attenuates Salicylate Induced Hearing Loss

Wei Sun[1]; Chao Zhang[1]; Senthilvelan Manohar[1]; Wendy Winchester[2]; Richard Salvi[1]
[1]State University of New York at Buffalo; [2]Pfizer Inc.

High dose sodium salicylate causes moderate, reversible hearing loss and tinnitus. Salicylate-induced hearing loss is believed to arise from a reduction in the electromotile response of outer hair cells (OHCs) and/or reduction of KCNQ potassium currents in OHCs which decreases the driving force for transduction current. Therefore, enhancing OHC potassium currents may prevent salicylate-induced temporary hearing loss. In this study, we tested the effects of ICA-105665, a novel small molecule that opens KCNQ2/3 and KCNQ3/5 channels which can shift the activation voltage of KCNQ channels, in a salicylate-induced hearing loss model. We found that 10 mg/kg of ICA-105665 prevented the salicylate-induced reduction of the amplitude and threshold shift of the compound action potentials. ICA-105665 also prevented the salicylate-induced reduction of distortion products of otoacoustic emission (DPOAE). These results suggest that ICA-105665 partially compensates salicylate induced cochlear hearing loss by enhancing KCNQ2/3 and 3/5 potassium currents in hair cells through enhancing the motility of OHCs.

PS-524

Effects of BK Channel Modulators on Salicylate Induced Tinnitus

Andrea Lowe; Samantha Cresoe; Joseph Walton
University of South Florida

Recent studies have provided preliminary evidence that potassium channels may play a crucial role in the development and/or treatment of tinnitus, including the voltage-gated, Ca+ activated, BK channel. BK channels are found throughout the peripheral and central auditory system, and modulators of this channel have been shown to affect neuronal excitability. This study examined the effects of a BK channel pore blocker (paxilline) and opener (BMS-191011) on young adult CBA/CaJ mice after the induction of tinnitus using sodium salicylate (SS).

All treatments were given systemically via intraperitoneal injections, with baseline measurements followed by assessment of SS alone, and SS+paxilline or SS+BMS on subsequent days. One group was tested for tinnitus using a behavioral measure of gap detection, which utilizes prepulse inhibition (PPI) to a long silent gap imbedded in narrowband noises centered at 6, 12, 16, 20, and 24 kHz. A second

group's peripheral thresholds were assessed using auditory brainstem responses (ABRs), and tinnitus was assayed using long silent gaps in narrowband noise, again centered at 6, 12, 16, 20, and 24 kHz. Previous studies have indicated that SS-induced tinnitus can be characterized by reductions in gap-PPI and increases in the ABR waveform peak 2 (P2)/P1 and P4/P1 amplitude ratios in responses to stimuli in the tinnitus percept region (12–20 kHz). Another tinnitus indicator was the SS-induced decrease of neural recovery to gaps in 16 kHz noise when calculated by taking the P1 amplitude of the response to the second noise burst as a percentage of the response to the first noise burst of the gap stimuli ABR response.

Biomarkers of tinnitus were observed following SS alone; however, treatments with BK modulators + SS revealed conflicting electrophysiological and behavioral responses. Gap-PPI was increased following treatment with paxilline and BMS-191011, but only in the tinnitus percept range (12-16 kHz), indicating elimination of behaviorally measured tinnitus. In contrast, BK modulators did not appear to improve electrophysiological measures of tinnitus or affect peripheral thresholds, but did alter the P1 and interpeak latencies in comparison to SS. This indicates that these drugs may alter temporal processing differently than SS alone. Overall, the differences between the SS+paxilline and SS+BMS effects were minimal, suggesting these seemingly contrasting BK modulators can produce similar outcomes in neuronal activity. Our results indicate that while modulation of SS-induced tinnitus may occur in response to alterations in the BK channel, the associated peripheral measures of hyperexcitability are not reduced.

PS-525

Neurosynchrony Changes in the Auditory Centers of Rats with Noise-Induced Tinnitus

Bin Liu; Xueguo Zhang; Hao Luo; Edward Pace; Jinsheng Zhang
Wayne State University

Introduction

Maladaptive plasticity in auditory centers is considered to be a major mechanism underlying noise-induced tinnitus. It often manifests in the forms of increased spontaneous firing rate, bursting rate, neurosynchrony, and tonotopic map changes within an auditory center. However, the manner in which these neural correlates simultaneously manifest in several auditory centers and the interactive fashion between these centers remains unclear. In this study, we assessed neurosynchrony in the dorsal cochlear nucleus (DCN), inferior colliculus (IC) and auditory cortex (AC) of rats with and without noise-induced tinnitus

Methods

Behavioral tests were performed to verify tinnitus in individual rats following noise exposure (120 dB SPL, 10 kHz for 2-3 hours). Electrophysiological recordings were then simultaneously recorded in the DCN, IC and AC. Neurosynchrony acquired from different electrodes were calculated based on the peak value per 5 ms for each frequency band in each location and compared between noise-exposed rats and naïve controls, and between noise-exposed tinnitus$^{(+)}$ rats and tinnitus$^{(-)}$ rats.

Results

When comparing noise-exposed with control rats, we found an overall decrease in neurosynchrony within the DCN and AC and between all centers. Mixed changes in synchrony occurred in the IC with enhanced synchrony in the low and middle frequency regions, whereas decreased synchrony occurred in the high frequency region. When comparing rats with and without noise-induced tinnitus, we found that tinnitus$^{(+)}$ rats showed increased synchrony in the low and middle frequency regions of the DCN but decreased synchrony in the high frequency region. In the IC, however, tinnitus$^{(+)}$ rats showed decreased synchrony in the low and middle frequency regions. In the AC, tinnitus$^{(+)}$ rats showed decreased synchrony in the middle frequency region and increased synchrony in the high frequency region. In between-structure analysis, similar synchrony changes were found between the AC-DCN and AC-IC, while an overall increase in synchrony was found between the IC-DCN.

Conclusion

Our data demonstrated that neurosynchrony changes occurred in the low to high frequency regions of the DCN, IC and AC of rats with and without noise-induced tinnitus. These data indicated that frequency- and region-dependent maladaptive changes occur in the auditory centers of animals exhibiting tinnitus. Moreover, the changes in different centers are of non-uniformity, demonstrating the complexity of tinnitus-related neural plasticity.

PS-526

Sodium Salicylate Suppresses Rebound Depolarization In Neurons of the Rat's Medial Geniculate Body Through the GABA(B)-GIRK Pathway

Xin-Xing Wang; Yan Jin; Ming Wang; **Lin Chen**
University of Science and Technology of China

Neuronal rebound depolarization (RD) is defined as the offset response to pre-hyperpolarization of the membrane potential. Our previous study shows that sodium salicylate (NaSal), a tinnitus inducer, can drastically suppress the RD in neurons of rat medial geniculate body (MGB) (Su *et al*, 2012, PLoS ONE 7, e46969). The purpose of the present study was to investigate the underlying cellular mechanism by using whole-cell patch-clamp recordings from MGB slices of rats. NaSal (1.4 mM) had no effects on T-type Ca^{2+} or HCN channels, indicating it suppresses the RD not by targeting these channels. Instead, NaSal was shown to hyperpolarize the resting membrane potential of MGB neurons to suppress the RD. NaSal induced an outward leak current that could be abolished by CGP55845, a $GABA_B$ receptor blocker, or by Ba^{2+} and Tertiapin-Q, blockers of G-protein gated inwardly rectifying potassium (GIRK) channels, indicating that NaSal hyperpolarizes the resting membrane potential to suppress the RD through

the $GABA_B$-GIRK pathway. Our study demonstrates that NaSal targets $GABA_B$ receptors to alter the functional behaviors of MGB neurons, which may be implicated in NaSal-induced tinnitus.

PS-527

Tinnitus-Inducing Noise Trauma and D-cycloserine Alter Arc Protein Expression in Amygdalo-hippocampal Circuitry

Michelle Kapolowicz; Peter Assmann; L. Tres Thompson
The University of Texas at Dallas

Background

Tinnitus, a potentially debilitating auditory hallucination affecting 1 in 5 people, is most commonly caused by noise trauma. Poorly understood underlying mechanisms involved in the initiation and maintenance phases make chronic tinnitus difficult to treat. Our lab demonstrated aberrant dorsal hippocampal plasticity in early stages of tinnitus (Goble et al., 2009) and revealed a strong causal linkage within amygdalo-hippocampal circuitry in auditory-linked plasticity (Farmer & Thompson, 2012; Donzis & Thompson, 2013). Our current aims were to further characterize the initial plasticity mechanisms leading to this disorder and to determine if D-cycloserine (DCS), a partial NMDAR-agonist, can reduce or prevent this plasticity. Specifically, our study addressed amygdalo-hippocampal involvement in the early stages of tinnitus and looked at DCS as a potential pharmacological intervention for this disorder in an experimental rat model.

Methods

Young adult male Long-Evans rats (n = 24) were divided into 4 conditions: control, acute high-intensity noise-exposed (16 kHz, 115 dB, for 1 hr), noise-exposed + DCS-injected (6 mg/kg, ip, 15 min pre-noise trauma), or DCS-injected alone. To assess excitatory signaling within the specified limbic regions, Arc (activity-related immediate-early gene) protein expression was evaluated in each group to assess effects of DCS treatment and bilateral exposure to acute high-intensity noise using Western blot analyses and immunohistochemistry via confocal microscopy.

Results

Western blot analyses and immunohistochemistry confirmed Arc expression was significantly up-regulated in both the amygdaloid complex and dorsal hippocampus following noise trauma. DCS prevented up-regulation of Arc expression in the amygdala due to noise trauma, thereby functionally acting as a partial antagonist to reduce NMDA receptor activation in this region. However, DCS alone up-regulated Arc expression within the dorsal hippocampus (see also Donzis & Thompson, 2014) but did not reduce Arc expression from noise trauma, suggesting endogenous hippocampal serine concentrations were not saturated following noise trauma.

Conclusion

These regional differences indicate the need to further study the role of glial release of the endogenous NMDA receptor ligand, serine, in tinnitus-inducing plasticity, and implicate region-specific differences in non-neuronal sources of neural plasticity. Our results corroborate other findings that indicate both the hippocampus and amygdala, non-classical auditory regions, are involved in early neural plasticity underlying tinnitus.

PS-528

Novel KCNQ2/3-specific Channel Activator Prevents The Development of Tinnitus and Suppresses In Vivo Epileptic Activity.

Bopanna Kalappa[1]; Heun Soh[2]; Kevin Duignan[2]; Takeru Furuya[3]; Scott Edwards[3]; Anastassios Tzingounis[2]; Thanos Tzounopoulos[4]
[1]University of Pittsburgh; [2]University of Connecticut, Department of Physiology and Neurobiology; [3]SciFluor Life Sciences LLC; [4]University of Pittsburgh, Department of Otolaryngology and Neurobiology

KCNQ channels are voltage-dependent potassium channels that are activated at subthreshold potentials and therefore provide a powerful break on neuronal excitability at resting potentials. Genetic or experience-dependent reduction of KCNQ2/3 channel activity causes disorders that are characterized by neuronal hyperexcitability, such as epilepsy and tinnitus. Importantly, small molecules that activate KCNQ channels are FDA approved anti-epileptic drugs; however, side effects have limited their therapeutic impact. Therefore, the development of specific KCNQ2/3 channel openers is crucial for the treatment of hyperactivity-related disorders. By introducing a single fluorine atom to retigabine, a KCNQ2-5 channel opener that is an FDA approved anti-epileptic drug, we have synthesized a novel KCNQ activator with improved efficacy and therapeutic index (SF0034). SF0034 is a more potent and selective KCNQ2/3 channel activator than retigabine in vitro; importantly, SF0034 is a more potent and less toxic anti-convulsant than retigabine in vivo. Furthermore, SF0034 prevents the development of tinnitus in mice.

PS-529

Molecular Mechanisms Underlying the Resilience to Noise-Induced Tinnitus

Shuang Li[1]; Thanos Tzounopoulos[2]
[1]University of Pittsburgh; [2]Departments of Otolaryngology and Neurobiology, University of Pittsburgh School of Medicine, Pittsburgh

Our previous studies have revealed that tinnitus-related reduction of Kv7.2/3 (KCNQ2/3) channel activity in principal neurons of the dorsal cochlear nucleus (DCN) is crucial for the induction of noise-induced tinnitus (Li et al., 2013). Here, by investigating the biophysical properties of DCN principal neurons in noise-exposed mice that do not develop tinnitus (non-tinnitus mice), we revealed a reduction in HCN channel activity in non-tinnitus mice. Longitudinal and pharmacological studies indicated the critical role of KCNQ2/3 channel activity in determining both HCN channel activity and the development of tinnitus. Namely, reduction of KCNQ2/3 channel activity happens before the HCN down-regulation, and pharmacological enhancement of KCNQ2/3 channel activity *in vivo* not only prevents the development of tinnitus, but also

leads to decreased HCN currents. Together, our results suggest that recovery of reduced KCNQ2/3 channel activity to normal (pre-exposed) levels is occurring during day 4 to day 7 after noise-exposure, and contributes to the prevention of tinnitus in noise-exposed mice. The decrease in HCN channel activity is a homeostatic response to reduced auditory input, which increases synaptic excitability in noise-exposed mice that do not develop tinnitus.

PS-530

Hyperactivity Due to the Decrease of Inhibitory Neurotransmission in the Auditory Cortex After Intense Noise Exposure

Bin Luo[1]; Chen Jiang[1]; **Guang-Di Chen**[2]; Soroush Sadeghi[2]; Riachard Salvi[2]
[1]Affiliated Anhui Provincial Hospital of Anhui Medical University; [2]University at Buffalo

Noise-induced hearing loss (NIHL) is often accompanied with tinnitus and hyperacusis. While injuries to the cochlea are extensively studied, noise-induced changes in central auditory pathways are less well documented. In the present study, we used *in vivo* and *in vitro* electrophysiology recordings to study changes in responses of auditory cortex (AC) neurons and their inhibitory inputs after NIHL.

Rats were anesthetized with isoflurane and one ear was exposed to a narrowband noise (10-12.5 kHz) at 126 dB SPL for 2 hours, while the other ear was clogged. Histology examination of the noise-exposed cochlea showed complete loss of hair cells in the middle and basal turns and loss of outer hair cells (OHC) in the apical turn. ABR data showed ~30-40 dB hearing loss at low frequencies (<8 kHz) and complete loss of auditory responses at high frequencies (>8 kHz). Two days after noise exposure, changes in the AC were examined.

In vivo, local field potentials and neuronal discharges in the noise-exposed AC (contralateral to the noise-exposed ear) were recorded during acoustic stimulation to the intact ear (ipsilateral to the recording AC). Compared to normal animals, the noise-exposed AC neurons showed lower thresholds and significantly higher response levels to ipsilateral stimulation with values twice as big as control values. Interestingly, the enhancement occurred mainly in the low-frequency region where inner hair cells (IHC) still survived in the noise-exposed cochlea. Thus, our *in vivo* results suggest NIHL-dependent hyperactivity in the AC.

In vitro, whole cell patch clamp recordings were used to measure the changes in inhibitory inputs to pyramidal neurons in layer V of both the ipsilateral and contralateral AC (refer to the noise-exposed ear). The electrical stimulation was provided by a monopolar micropipette placed 100 µm away from the recording neuron. The evoked inhibitory postsynaptic currents (eIPSCs) were produced reliably with stimuli in the range of 50-150 µA, which can be blocked by $GABA_A$ antagonist. The amplitudes of eIPSCs in the noise-exposed AC were significantly smaller than those obtained in the AC of the other side. The results suggest a noise-induced attenuation of inhibitory inputs to the AC neurons.

Overall, our results suggest that responses of the noise-exposed AC are enhanced following NIHL, most likely due to attenuation of inhibitory inputs to these neurons. The NIHL-dependent hyperactivity may be related to noise-induced tinnitus and hyperacusis.

PS-531

Neural Coherence Changes along the Auditory Pathways in Rats with Noise-Induced Tinnitus and Hearing Loss

Jinsheng Zhang; Bin Liu; Xueguo Zhang; Hao Luo; Edward Pace; John Moran
Wayne State University

Tinnitus is considered to result from maladaptive plasticity often in the forms of hyperactivity, increased bursting, hypersynchrony and tonotopic map reorganization. However, it is unclear how coherence, representing synchronized neural connectivity between local and remote brain regions in frequency domains, plays a role in the etiology of tinnitus. We addressed this issue by conducting multi-structural recordings along the auditory axis in noise-exposed rats. These rats were tested behaviorally for tinnitus. First, we found that noise exposure broadly induced increases in coherence activity within and between the dorsal cochlear nucleus (DCN), inferior colliculus (IC) and auditory cortex (AC) in rats. The increases occurred in the frequency bands of theta (4-8 Hz), alpha (8-13 Hz), beta (13-30 Hz) and gamma (30-300 Hz). Power spectrum analysis showed a general increase of power, especially in the gamma band. Second, compared to rats with noise-induced hearing loss only, we found a significantly increased coherence activity in the AC of rats with noise-induced tinnitus and hearing loss, which was accompanied by decreased coherence activity within and between the DCN and IC. Power spectrum analysis showed that, in rats with tinnitus and hearing loss, there was a higher amplitude and rightward-shifted gamma power, which allowed further separation of tinnitus-related activity from hearing-loss-related activity, compared to rats with hearing loss only. The results suggest that the broadly increased coherence activity across different frequency bands throughout the auditory axis may underlie noise-induced hearing loss. In contrast, localized increase in coherence activity at the cortical level along with the decreased interconnectivity at the brainstem and midbrain levels may underlie tinnitus.

PS-532

An mGluR targeted drug controls firing activity in IC neurons

Fuad Alghamdi; Greg Nelson; Ryan Longenecker; Alexander Galazyuk
Northeast Ohio Medical University (NEOMED)

Background

Sound exposure often results in hyperactivity throughout the auditory system. The current consensus is that it plays a role for etiology of tinnitus. Theoretically, pharmacological agents that reduce hyperactivity in auditory neurons could suppress tinnitus. Results of our recent studies suggested that metabotropic glutamate receptors (mGluRs) play a role in controlling

neuronal firing in the auditory system. Therefore it would be logical to test whether systemic injection of these drugs can alter firing of auditory neurons. If so, it would open an opportunity to develop a drug which could suppress tinnitus in humans.

Methods
Adult CBA/CaJ mice were used for the study. Neuronal firing in the inferior colliculus of awake mice was recorded extracellularly before, during, and after systemic injection of group II mGluR agonist LY354740. Injection was performed remotely via an intravenous catheter inserted into the tail vein. Spontaneous firing rates of IC neurons were measured and compared before, during, and after of drug injection. To test whether this drug is affecting general sound processing in the auditory system of mice, the acoustic startle reflex and gap detection performance were also assessed.

Results
The LY354740 injected IV had a quick and dramatic effect on the spontaneous activity in IC neurons. Several seconds after injection the vast majority of IC neurons exhibited near complete suppression of their spontaneous activity lasting several tens of minutes. The magnitude of startle responses was increased at least 20% in 6 out of 7 mice tested. The gap detection performance, however, was not affected by the drug.

Conclusion
LY354740 has the potential to be used as a drug to control tinnitus. Future studies should determine its effect on sound-evoked activity in auditory neurons as well as whether it can suppress behavioral signs of tinnitus in tinnitus animal models.

PS-533

Hyperactivity In The Inferior Colliculus Following Noise Induced Chronic Tinnitus

Antonela Muca[1]; Emily Standafer[1]; Farhan Ahmad[1]; Farhad Ghoddoussi[2]; Mirabela Hali[1]; Sharowynn Wilson[1]; Bruce Berkowitz[1]; Avril Holt[1,2]
[1]Wayne State University School of Medicine; [2]John D. Dingell Veterans Affair Medical Center

Introduction
Tinnitus, the perception of sound in the absence of an external stimulus, is the number one compensated military related disability. Studies have found that tinnitus may be linked to increased neuronal activity in brain regions responsible for hearing, following events causing acoustic trauma, such as exposure to loud noise. Our previous studies have demonstrated tinnitus and increased neuronal activity in a model of permanent threshold shift, 48 hours after tinnitus onset. Therefore, we hypothesize that tinnitus will be present and persist, regardless of hearing status and that the presence of tinnitus will correlate with changes in neuronal activity. We have combined novel and established methodologies to determine the relationship between the persistence of hearing loss, tinnitus and neuronal activity.

Methods
Hearing thresholds were determined in male Sprague Dawley rats (n = 12) randomly divided into three groups: control, temporary threshold shift (TTS), and permanent threshold shift (PTS) using auditory brainstem responses (ABRs). Acoustic Startle Reflex (ASR) testing was used to determine tinnitus across six frequencies (4, 8, 12, 16, 20 and 24 kHz). Changes in neuronal activity were measured using manganese-enhanced magnetic resonance imaging (MEMRI) two months following noise exposure (10 kHz, 118 dB SPL 1/3 octave band, 4 hours - PTS; 16 kHz, 106 dB SPL, 1 hour - TTS) with $MnCl_2$ (66 mg/kg) administered 24 hours prior to imaging. Manganese uptake was assessed in the inferior colliculus (IC), a brain region that plays a significant role in the integration of auditory signals.

Results
Noise exposure resulted in significantly elevated hearing thresholds in the PTS group and normal thresholds in the TTS compared to controls. Generally, the PTS group had a diminished ability to suppress their startle reflex while the TTS group had a heightened ability to suppress their startle reflex. Two months following noise exposure, animals in the TTS group demonstrated significant changes in Mn^{+2} uptake within the IC (dorsal cortex (DCIC) and external cortex (ECIC)), compared to the PTS group.

Conclusions
Neuronal activity was increased in TTS animals as demonstrated by increased Mn^{+2} uptake in the DCIC and ECIC. The increased Mn^{+2} uptake noted in the TTS group may have been observed due to hyperactivity resulting from the induction of tinnitus. Thus, even exposure to loud noise resulting in a TTS can result in tinnitus and persistent changes in neuronal activity.

PS-534

Identification of Biomarkers in a Model of Noise Induced Tinnitus: A Longitudinal Study

Farhad Ghoddoussi[1,2]; Aaron Apawu[1]; Mirabela Hali[1]; Antonela Muca[1]; Nour Arafat[1]; Sharowynn Wilson[1]; Bruce Berkowitz[1]; Avril Holt[1,2]
[1]Wayne State University; [2]John D Dingell VAMC

Introduction
Tinnitus, “ringing in the ears”, is the number one service related disability for Veterans. Currently no objective biomarkers for tinnitus exist and diagnosis is heavily dependent upon patient self-reporting. We have previously demonstrated that both noise and drug induced tinnitus result in deficits in GAP inhibition of the acoustic startle reflex (GiASR) 48 hours following tinnitus generation. In addition, these same tinnitus models result in increased spontaneous neuronal activity (SNA) in the inferior colliculus (IC), a brain region that is key for the integration of auditory signals. Manganese enhanced MRI (MEMRI) uses manganese (Mn^{2+}), a paramagnetic ion, contrast agent and calcium analog, to determine calcium ion regulation and thus neuronal activity. In this longitudinal study of a noise induced tinnitus model, we test hearing (audito-

ry brainstem responses - ABR), tinnitus (GiASR), and SNA (MEMRI) to determine how changes develop over time.

Methods
After baseline images were collected, neuronal activity was assessed in 12 regions of interest (ROIs) using MEMRI (n = 10/group), 24 hours, 4, and 12 weeks following acoustic trauma (16 kHz, 106 dB SPL, 1 hour) in male Sprague Dawley rats. Each animal was administered 66 mg/kg of $MnCl_2$ 24 hours prior to imaging (Bruker 7T scanner). Following a single dose of $MnCl_2$, (n = 4) Mn^{2+}clearance from ROIs was measured after 24 hours, 2, 4, 6 and 12 weeks. *In vivo* and *ex vivo* images (hourly for up to 12 hours) were obtained in the same animal (n = 4). Both T_1-weighted and T_1-mapping images were compared for each ROI. For the duration of the study, Gap detection testing was conducted twice per week, across six frequencies (4, 8, 12, 16, 20 and 24 kHz).

Results
Our data suggest that subdivisions of the IC have differential rates of Mn^{2+} clearance, with the dorsal cortex of the IC clearing most quickly. Manganese levels appear to diminish within the first two hours after euthanasia. In addition, all animals were able to perform during GiASR testing, before and after noise exposure. Even after repeated administration, differential manganese uptake was observed depending upon ROIs. We plan to correlate GiASR with Mn^{2+} uptake at each time point.

Conclusions
Gap detection and MEMRI testing may serve as exciting new tools with translational applicability for both the diagnosis of tinnitus and identification of effective therapeutic agents.

PS-535

Human Primary Auditory Cortex is Hypermetabolic in Bilateral Subjective Tinnitus as Measured by Functional Near Infrared Spectroscopy (fNIRs).

Greg Basura; Silvia Bisconti; Ioulia Kovelman; Paul Kileny
University of Michigan

Background
Tinnitus is the phantom perception of sound in the absence of a physical sound stimulus. The underlying etiology of tinnitus perception is not currently clear, yet basic mechanisms pinpoint hyperactive neuronal activity within the central auditory pathways, including primary auditory cortex (A1).

Objective
The aim of this study was to measure metabolic activity within A1 under conditions of auditory stimulation and silence in patients with subjective bilateral tinnitus as compared to non-tinnitus controls using functional Near-Infrared Spectroscopy (fNIRS).

Methods
Patients with bilateral subjective tinnitus with near normal hearing and non-tinnitus controls were tested during a passive auditory auditory task. Hemodynamic activity was monitored over A1 under episodic periods of auditory stimulation with a 750 Hz or 8000 Hz tone, broadband noise and silence.

Results
Preliminary results demonstrated a greater activation over A1 in patients with tinnitus compared to controls during periods of silence and with auditory stimulation with a 750 Hz tone while less activation was found during broadband noise. No significant differences in the activation were found between the auditory and non-auditory brain areas in patients with tinnitus.

Conclusions
These preliminary data demonstrate A1 is hypermetabolic in tinnitus patients suggesting hat these anatomic areas may be contributing to underlying tinnitus perception. This finding using fNIRs as a non-invasive tool may be an important first step in the diagnosis and management of this pervasive problem.

PS-536

Investigating a New Tinnitus Treatment Using the Auditory Midbrain Implant

Sarah Offutt; Robert J Hughes; Hubert Lim
University of Minnesota

One potential option for tinnitus treatment is to use deep brain stimulation of non-lemniscal auditory nuclei to modulate tinnitus-related activity within the auditory system. The auditory midbrain implant (AMI) is a deep brain stimulator that could provide such stimulation to the dorsal cortex of the inferior colliculus (ICD) to potentially modulate and induce plasticity within the central region (ICC), which in turn has connections throughout the auditory system via ascending and descending pathways. ICD stimulation will be tested during an upcoming AMI clinical trial for hearing restoration in patients with tinnitus. Prior to that trial, we sought to identify electrical stimulation paradigms that produce the greatest amount of neural suppression, which may counteract the central hyperactivity linked to tinnitus.

Multi-site electrode arrays were positioned in the ICC and ICD of ketamine-anesthetized guinea pigs. ICC spike activity in response to broadband noise stimulation was recorded before and after each ICD stimulation paradigm, which included electrical stimulation alone or electrical stimulation paired with acoustic stimulation at specific inter-stimulus intervals (-7 ms to 23 ms, 5 ms steps), and each control paradigm, which included no stimulation and acoustic stimulation alone. Immediate and residual modulatory effects were determined by comparing the changes in ICC spike activity immediately and 30 minutes after each ICD paradigm, respectively, relative to the baseline activity.

We observed more suppressive than facilitatory immediate modulation for all paired paradigms except for the 3 ms delay, which was more facilitatory. Significant residual effects was observed only for the 18 ms paired paradigm and the ICD stimulation alone paradigm that were both predominantly suppressive. Acoustic stimulation alone generally resulted in

more facilitation, while the no stimulation paradigm did not have a dominant effect.

Based on our findings, ICD stimulation alone or paired ICD stimulation with a 18 ms delay could potentially provide lasting suppression of the central hyperactivity associated with tinnitus. Since the AMI will initially be implanted into tinnitus patients that are already deaf, different parameters of ICD stimulation alone can be explored for suppressing tinnitus. If the AMI can be implanted in tinnitus patients with hearing, then paired ICD paradigms may provide greater options for modulating the brain to treat tinnitus. Future studies need to investigate how different ICD stimulation parameters affect the different features and nuclei that have been linked to tinnitus.

PS-537

ABR Waveform Changes 12 Months after Noise Exposure in a Rat Tinnitus Model

Aditi Mohankumar; Deb Larsen; Jeremy Turner
Southern Illinois University School of Medicine

Many people report their first experience with chronic tinnitus in middle or late adulthood. Many of these tinnitus sufferers report “no onset factors” but are very often found to have a noise exposure history indicative of damaging levels of noise earlier in life. Delays in tinnitus development are also seen in laboratory animals, which can be frustrating for researchers trying to develop an efficient tinnitus model. For these reasons, we explored the causal factors that play a role in tinnitus development in rats. We explored the relative impact of noise intensity, duration and frequency by systematically manipulating these variables and tracking the emergence of behavioral evidence of tinnitus over time. Here we report on the relationship between noise exposure parameters and the resulting ABR waveform features and behavioral deficits 12-months later. Fischer Brown Norway (FBN) rats (n=137) were isoflurane anesthetized and unilaterally exposed to 16 kHz, octave-band noise at all combinations of 3 intensities (110, 116, and 122 dB SPL) and 3 durations (30, 60, and 120 min), and 48 additional rats were exposed to either 8kHz, 32kHz, or broadband noise at 110dB for 30 min; 48 rats served as sham-exposed controls. Rats were behaviorally tested for gap and prepulse inhibition of the acoustic startle reflex before noise exposure and monthly for 12 months until they reached middle age (~18 mo). ABRs were then acquired for both ears under ketamine/xylazine at the end of the study. ABR waveform data points were converted to an RMS (root mean square) value for each millisecond epoch in the ABR waveform. The resulting quantitative ABR amplitude and temporal measures (corresponding with approximate wave I-V features) are then used to make statistical correlations with ABR thresholds, startle reflex amplitudes and behavioral evidence for tinnitus and/or hyperacusis. The goals of the analyses are to find features of the ABR waveform that correlate with behavioral evidence of hyperacusis and/or tinnitus. Analyses are ongoing.

PS-538

Increased Levels of Physical Activity Associated with Lower Levels of Tinnitus Severity and Increased Quality of Life.

Jake Carpenter-Thompson[1]; Edward McAuley[2]; Fatima Husain[2]
[1]University of Illinois Urbana-Champaign; [2]University of Illinois

Introduction

Tinnitus, ringing in the ears, is a common disorder that has been shown to be associated with depression, anxiety and decreased quality of life. Physical activity has been shown to decrease depression and anxiety and improve overall quality of life. In this study, we investigated if a relationship between physical activity and tinnitus severity exists. We hypothesized that as physical activity level increased, tinnitus severity and quality of life increases would decrease.

Methods

An online survey was emailed to members of the American Tinnitus Association and past volunteers of the Auditory Cognitive Neuroscience laboratory. A total of 1030 individuals responded to the survey. The survey included a general demographic questionnaire, the Tinnitus Functional Index to measure tinnitus severity, the Godin Leisure Time Exercise Questionnaire to measure physical activity and the SF-36 to measure quality of life. Demographic information was analyzed using descriptive statistics. The relationship between tinnitus severity, physical activity and quality of life was assessed using correlational analysis. To control for confounding factors, hierarchical linear regression was used to analyze the association between tinnitus severity, physical activity and quality of life. Statistical analysis was conducted using SPSS version 22 software.

Results

We found increased levels of physical activity were associated with lower levels of tinnitus severity. Additionally, as physical activity increased, quality of life increased. Similarly, as quality of life increased, tinnitus severity decreased. Using hierarchical linear regression analyses, the beneficial effects of physical activity on tinnitus severity and quality of life were found to be significant when confounding variables were accounted for in the same regression model.

Conclusion

Our results indicate that a small but significant beneficial relationship exists between physical activity and tinnitus severity. Further study is warranted to establish if physical activity may be a potential therapy for tinnitus.

PS-539

Peripheral Coding of Pitch – the Butte Hypothesis

Philip Joris
University of Leuven, Belgium

The study of pitch perception has a long history and extensive literature and has been described as “the heart of hearing theory” (Plomp 2002). Debate regarding the physiological

underpinnings of pitch continues between proponents of various forms and mixtures of spectral and temporal theories, which typically refer to response properties of the auditory nerve (AN). Here, simple properties of the central auditory system are brought into focus. The key proposal is that entrained phase-locking (contracted to "entracking") is a brainstem code to periodicity.

Cariani and Delgutte (1996) observed that there is a robust code for pitch in the pooled AN population interspike interval (ISI) distribution for a wide range of pitch stimuli with fundamental frequencies < 600 Hz. When summed across fibers, the ISI distribution resembles a stimulus autocorrelation representation, with a peak at the fundamental or repetition frequency. A recurring question is how such a representation could be grounded in physiology, as its computation seems to require a combination of coincidence detectors and a range of delays. A physiological basis for long delays (equal to the pitch period) in particular remains an enigma. We dispense with the idea of delays and tuning to a particular period. We propose a scalar rather than vector code of periodicity by virtue of coincidence detectors that translate the dominant ISI directly into spike rate through entracking. Perfect entracking means that a neuron fires one spike per repetition period, so that the firing rate equals the repetition frequency. Key properties of entracking are that it typically improves with increasing SPL and is extremely invariant once perfect entracking is reached; that the number of neurons entracking to a stimulus increases with SPL; and that it occurs in a variety of cell types. The main limitation in this code is the upper limit of firing. Although under some conditions firing rates as high as 1 kHz are achieved, the limit is more typically between 500 Hz and 1 kHz. It is proposed that entracking provides a periodicity tag which is superimposed on a tonotopic analysis. At low SPLs and fundamental frequencies > 500 Hz, a spectral or place mechanism codes for pitch. With increasing SPL the place code degrades but entracking improves and first occurs in the neurons with the lowest thresholds for the spectral components present. The prediction is that populations of neurons extended across CF form plateaus ("buttes") of firing equaling the fundamental frequency.

PS-540

Differential Functional Expression of the α7-type Nicotinic Acetylcholine Receptor in the Developing Auditory Brainstem

Veronika Baumann; Lina Yassin; Ursula Koch
Freie Universität Berlin

Background

In the mammalian brain, the α7-type nicotinic acetylcholine receptor (nAChR) is widely distributed. Anatomical studies described a strong but transient expression of α7-type nAChRs around hearing onset by neurons of the central auditory pathway including the superior olive complex and the ventral nucleus of the lateral lemniscus. Depending on their anatomical distribution, their subcellular expression, their subunit composition and their developmental expression, nAChRs play a critical role in many aspects of brain development. α7-type nAChRs have been implicated to regulate the refinement of neural circuits during the early postnatal period. However, the function of these cholinergic receptors and their modulators like acetylcholine (ACh) remains elusive in the auditory system. Here we investigated the functional expression of the α7-type nAChRs in neurons of the auditory brainstem around hearing onset when major map formation occurs.

Methods

Whole-cell patch-clamp recordings were made from neurons of C57Bl6/J mice at P8, P14 and P22 in acute brainstem slices. Membrane potential changes and inward currents were elicited by locally applying acetylcholine (ACh) with short pressure pulses (200 ms, ~7 psi, 10 s intervals) under constant superfusion of the recording chamber. Atropine was applied throughout the experiments to block muscarinic AChRs. Mecamylamine and methyllycaconitine were used as specific nicotinic receptor antagonists.

Results

In LSO and VNLL neurons, puff application of ACh elicited a small and transient inward current resulting in a transient depolarization of the membrane. The electrophysiological and the pharmacological properties suggested that the ACh-induced current was mediated by at least two different nAChR subunits, putatively the α7-type and a non-α7-type subunit. In contrast to LSO and VNLL, ACh puffs onto somata of MNTB neurons had no effect during the time frame studied. In the VNLL the number of neurons responding to ACh peaked before hearing onset while in the LSO the proportion of neurons showing ACh-induced currents increased after hearing onset.

Conclusion

Here, we show that nicotinic α7-type and non-α7-type AChRs are functionally expressed in auditory brainstem neurons. Furthermore, relative number of neurons sensitive to ACh differs in MNTB, VNLL and LSO during development suggesting different roles for nAChRs in the respective nuclei.

PS-541

Juvenile-To-Adult Auditory Maturation And Improved Hearing-In-Noise Requires CGRP-Mediated Efferent Feedback Signaling

Anne Luebke[1]; Rhiannon Bussey-Gaborski[2]; Paul Allen[2]; Ian Dickerson[2]
[1]University of Rochester Medical Center; [2]University of Rochester

All mammalian hair cell systems contain an efferent innervation. We discovered that the loss of the efferent neurotransmitter calcitonin gene-related peptide (CGRP) decreased sound-evoked activity in the cochlear nerve of mice, yet the loss of CGRP did not influence auditory thresholds or outer hair cell activity (Maison et al. *J Neurophysiol*. 2003). These data suggested that CGRP released from cochlear efferent fibers caused increased sound-evoked activity in the cochlear nerve, which was hypothesized to cause an increase in the dynamic range of sound perception. Similarly, in the CGRP application to the lateral line organ increased afferent firing in adult frog nerve activity but not in juvenile nerves (Bailey & Sewell JARO 2000). We determined there was also a ju-

venile-to-adult delay in CGRP signaling in the mouse model, and determined this delay in CGRP efficacy was due to a delay in formation of functional CGRP receptors. The CGRP receptor consists of three proteins (CLR, RAMP1, RCP) essential for signaling. We used co-immunoprecipitation on tissues from mouse cochlea to detect CGRP receptor protein association, as a measure of formation of functional CGRP receptor complexes. We determined that onset of CGRP efficacy in sound-evoked activity correlates with formation of a functional CGRP receptor complex. In mouse cochlea, CGRP receptor formation was incomplete at 1 month (juvenile), but complete by 3 months (adult), which corresponded to onset of suprathreshold enhancement and improved behavioral-based hearing perception abilities. Moreover, we found that the CGRP receptor was only fully-complexed from the detergent resistant portions of the cell membrane, suggesting that the delay in the forming a functional CGRP complex required sorting to specialized membrane domains such as lipid rafts. These data suggest that the receptor for CGRP is regulated in a developmental pattern that regulates CGRP efficacy in vivo affecting hearing perception, and that signaling through the CGRP receptor is limited by it's subcellular environment.

PS-542

Stresscopin in the Auditory Brainstem

Matthew Fischl[1]; Mihai Stancu[1]; Jan Deussing[2]; Conny Kopp-Scheinpflug[1]
[1]Ludwig-Maximilians University; [2]Max Plank Institute of Psychiatry

Background

Stresscopin, also known as urocortin3 (UCN3), is a peptide that is synthesized and secreted predominantly in the hypothalamus and the amygdala where it plays a key role in the coordination of endocrine and behavioral responses to stress. Interestingly it is also expressed in the neurons of the superior paraolivary nucleus of the auditory brainstem (SPN). UCN3 is part of the corticotropin releasing factor family and binds to the corticotropin releasing hormone receptor type 2 (CRHR2). In the auditory pathway CRHR2s are expressed in the cochlea and have been suggested to be part of a local stress response (for review see Basappa et al., 2012).

Methods

We use immunocytochemistry to examine the expression patterns of the CRHR2 receptor in the auditory brainstem of wild type and UCN3 knock-out (UCN3KO) mice (both C57Bl/6 background). In vivo single unit recordings are utilized to compare the response properties of auditory brainstem neurons in the medial nucleus of the trapezoid body (MNTB), superior paraolivary nucleus (SPN) and lateral superior olive (LSO) in both mouse lines. Additionally we use patch-clamp recordings in vitro to determine differences in intrinsic properties in SPN cells of UCN3KO vs. wild type mice.

Results

We observed positive staining for CRHR2 in both the MNTB and SPN in addition to the areas used as positive controls (e.g. medial nucleus of the amygdala). In vitro patch-clamp recordings from SPN neurons of the UCN3KO show more depolarized resting membrane potentials and higher spontaneous firing activity when compared to wild type mice. We show that our in vivo recordings have the potential to resolve differences in the physiological response properties of auditory brainstem neurons in both genotypes. Preliminary ABR results indicate a trend towards lower thresholds in UCN3KO mice over the range of the mouse audiogram.

Conclusions

Our initial results indicate that UCN3 may be involved in setting the sensitivity levels of the auditory system. Similar to results found in CRHR2KO studies, an increase in the sensitivity of these mice may come at a cost of higher susceptibility to noise induced damage or audiogenic stress. Our results also suggest that this receptor system is present in the brainstem where it could influence neurons that are involved in the efferent feedback to the cochlea.

PS-543

Dynamic Expression of Corticotropin Releasing Factor Receptor 1 in the Developing Cochlear Nucleus

Kathleen Yee[1]; Le'Andrea Mitchell[2]; Douglas Vetter[3]
[1]University of Mississippi Medical Center; [2]Tougaloo College; [3]University of Mississippi Medical Center Department of Neurobiology and Anatomical Center

Extensive literature exists on the morphology and electrophysiological response properties of CN neurons. Molecular analyses have focused predominantly on gene expression *at* and *during* hearing onset as well as association with hearing loss/dysfunction. Less is known about how early developmental gene expression impacts cochlear nucleus maturation.

We are interested in how early gene expression and cell signaling affects maturation of CN structure and function. Corticotropin releasing factor (CRF), a member of a family of related neuropeptides, functions in the systemic stress response and also exhibits modulatory effects over glutamatergic neurotransmission in the nervous system. We have previously shown that CRF is expressed by spiral ganglion (SG) neurons of the cochlea (Graham et al, 2010). Since the CN is the direct target of SG neurons and expression studies have shown that corticotropin releasing factor receptor 1 (CRFR1) is expressed in the adult dorsal and ventral CN, we were interested in examining whether the mature expression pattern of CRFR1 in the CN is mirrored in the developing CN, and if not, whether this might indicate a previously unrecognized role for dynamic neuropeptide expression in maturation of the CN.

A lack of reliable antibodies for CRFR1 led us to exploit a BAC transgenic mouse that expresses GFP under control of CRFR1 promoter and enhancer elements (Justice et al, 2008). Immunohistochemical localization of the GFP transgene in adult animals reveals labeled neurons in the dorsal and ventral subdomains of the CN as reported by Justice et al (2008). We have expanded this characterization by ex-

amining ages ranging from postnatal day (P) 0 through 10 months of age. At P0, GFP localization is broadly expressed in the CN and as postnatal maturation proceeds, strong signal is evident in the molecular and granule cell layers and low expression in the deep regions of the dorsal and ventral subdomains of the CN. Scattered GFP-positive cells are detectable within deep dorsal and ventral CN at P7. Qualitatively, GFP localization in the molecular and granule cell layers declines with maturity but is detectable at least through 4 weeks of age, while scattered cells within deep dorsal and ventral CN are maintained through 10 months of age. These results suggest that CRFR1-mediated signaling is spatially dynamic within subdomains of the maturing cochlear nucleus. Examinaton of CRFR1 null mice is ongoing to examine whether CRF/CRFR1 signaling plays a significant role in CN maturaton.

PS-544

High-Voltage Activated Potassium Channels Regulate Action Potential Time-Coding Properties in the Developing Avian Cochlear Nucleus

Hui Hong; Lisia Rollman; Jason Sanchez
Northwestern University

Introduction

Auditory brainstem neurons fire synchronized action potentials (APs) by "locking" to a specific phase of incoming afferent inputs. This form of neural synchrony depends on specialized time-coding properties found in brainstem neurons and is important for normal auditory temporal processing. Numerous studies have shown that potassium channels contribute to temporal processing abilities in the mature cochlear nucleus. How specific potassium channels regulate AP time-coding properties in the developing cochlear nucleus is lacking. In this study we investigated the development of high-voltage activated potassium channel (K_{HVA}) conductances and quantified how K_{HVA} regulate AP properties in the cochlear nucleus magnocellularis (NM) of chickens.

Methods

Whole-cell voltage and current clamp recordings were obtained from developing chicken embryos before, during, and after hearing onset, corresponding to embryonic (E) days 10-12, E14-E15, and E19-E21, respectively. Voltage and current steps of varying durations, strengths, and frequencies were injected into the soma of NM neurons and potassium conductances and AP properties were recorded before and during application of low-concentration tetraethylammonium (TEA, 1 μM), a K_{HVA} blocker.

Results

Our results show that AP speed, reliability and phase locking firing rates improve with maturation due in part to a significant upregulation in K_{HVA} channel conductances. We observed a nearly 3-fold increase in the total amount of potassium current from E10 to E21 (E10-E12 = 2.9 nA; E14-E15 = 4.4 nA; E19-E21 = 7.6 nA, $p < 0.001$). After hearing onset, ~70% of the total amount of potassium current was mediated by K_{HVA} channels. When TEA-sensitive potassium channels were blocked, APs became significantly slower (AP half-width, control = 0.97 ms, TEA = 1.3 ms, $p < 0.001$), less reliable (AP jitter, control = 0.18 ms, TEA = 0.25 ms, $p < 0.01$), and occurred later in time (AP latency, control = 2.9 ms, TEA = 3.2 ms, $p < 0.001$), resulting in reduced phase locking firing rates with increasing input frequencies.

Conclusions

Our results from the chicken cochlear NM indicate that the maturation of potassium channels – in particular, K_{HVA} conductances – contributes to specialized neural features critical for AP time-coding properties and phase locking abilities. Deficits in auditory brainstem neuron's ability to phase lock and fire fast, reliable, and synchronized APs to afferent inputs are heavily dependent on K_{HVA} channels and may underlie aspects of auditory (dys) synchrony and central auditory processing disorders.

PS-545

Purinergic Modulation During Development is Required for High Freuquency Firing in the Cochlear Nucleus

Tamara Radulovic; Sasa Jovanovic; Rudolf Rübsamen; Ivan Milenkovic
University of Leipzig

Background

In the development of the auditory system, spontaneous neuronal activity arises before the onset of hearing independently of any systemic input. This activity apparently contributes to axonal pathfinding, dendritic morphogenesis and the segregation of axonal terminal arbours. Respective developmental processes contribute to establishment of nuclear tonotopic maps, i.e. the orderly arrangement of neurons according to sound frequency to which they are most sensitive. During this critical developmental period purinergic signaling attunes neuronal activity in the cochlea and in the brainstem. Endogenous release of ATP facilitates action potential generation in the inner hair cells and enhances glutamate-driven firing of bushy cells in the ventral cochlear nucleus (VCN), the first central station along the afferent auditory pathway. In bushy cells, activation of ATP-gated, ionotropic P2X2/3R increases action potential firing through cytosolic calcium signaling and protein kinase C activity. The modulatory effects of ATP diminish with maturity, both in the periphery and in the central auditory neurons.

Methods

We used both in vivo- and acute slice-recordings to determine the contribution P2X2/3R to development of firing properties of bushy cells in the VCN. The data were acquired from $P2X2/3R^{Dbl-/-}$ and corresponding wild type control mice from postnatal days 13-26 (P13-26).

Results

In vivo extracellular recordings during the initial period of auditory experience (P13-16) conducted in combination with iontophoretic drug applications showed P2X2/3R-mediated enhancement of spontaneous and sound evoked neuronal activity restricted to the low-frequency regions of the VCN.

These data were confirmed with slice recordings demonstrating progressive reduction of the area engaged with P2X2/3R signaling during postnatal development. Bushy cells deprived of purinergic modulation (P2X2/3R$^{Dbl-/-}$ mice) had significantly impaired sound frequency selectivity compared to controls. The maximum firing rates evoked by high intensity sound stimulation were lower in P2X2/3R$^{Dbl-/-}$ suggesting either weaker excitatory input or increased inhibitory strength. Corresponding slice recordings excluded the second option by showing no alterations of inhibitory synaptic inputs to bushy cells.

Conclusion

We conclude that purinergic signaling follows a defined developmental pattern related to the topographic position of bushy cells within the ventral cochlear nucleus. By attuning neuronal activity during early postnatal development, P2X-2/3R might be necessary for morphological and/or physiological development of the endbulb of Held-bushy cell synapse. Thus, purinergic modulation during development is probably important to establish a proper stimulus coding in high sound intensity environment.

PS-546

Effects of Noise-Induced Hearing Loss on Coding of Temporal Fine Structure and Envelope in the Chinchilla Ventral Cochlear Nucleus

Mark Sayles; MIchael Heinz
Purdue University, West Lafayette, Indiana

Background

Compared to normal-hearing (NH) listeners, hearing-impaired (HI) subjects struggle to exploit speech-related temporal-fine-structure (TFS) cues, and some show enhanced sensitivity to low-amplitude envelope-modulation (ENV). Previously, our laboratory characterized auditory-nerve-fiber (ANF) TFS and ENV coding after noise-induced hearing loss (NIHL). All ANFs synapse in the cochlear nucleus (CN). Here we examine TFS and ENV coding in ventral CN (VCN) units following NIHL.

Methods

We exposed ketamine-xylazine anesthetized chinchillas to 500-Hz-centered octave-band noise at 116 dB SPL for 2 hours. Following several-weeks' recovery, we confirmed NIHL with evoked-potential and distortion-product otoacoustic-emission audiometry. VCN single-unit responses were recorded extra-cellularly in HI and NH animals, under barbiturate anesthesia.

Results

We recorded spike-train responses to on-CF tones, broadband noise, sinusoidal-amplitude-modulated (SAM) tones and SAM noise, from single units in NH (188 units) and HI (135 units) animals. HI animals had elevated single-unit thresholds, with broadened tuning curves. Units with CFs between 1 and 4 kHz showed the largest threshold elevations and most-broadened tuning; with positive correlation between elevated threshold and broadened tuning. All VCN unit types were found, with no significant difference in unit-type proportions between NH and HI animals [all within-unit-type comparisons between NH and HI, $p>0.05$ (χ^2, Holm-Bonferroni corrected)]. Synchronization to on-CF tones (in quiet) did not differ between NH and HI animals, when considering all unit types (repeated-measures ANOVA main effect of hearing status, $F_{(1,118)}=0.24$, $p=0.628$), or for within-unit-type comparisons of least-squares means (all comparisons, $p>0.05$, Holm-Bonferroni corrected). However, in response to broadband sounds, VCN units with CFs between 1 and 10 kHz responded abnormally to TFS; responses were driven by stimulus frequencies between 0.1 and 0.7 kHz. Neurometric ENV-detection and ENV-discrimination thresholds improved (by ~3 dB) following NIHL in chopper and onset units, but worsened (by ~3 dB) in primary-likes. Background noise worsened ENV-detection and discrimination thresholds more in HI compared to NH animals.

Conclusions

The strength of CF-tone phase locking (in quiet) does not differ, within unit type, between NH and HI animals. However, the degraded *quality* of TFS found in ANF responses is also found in VCN units; broadened tuning results in higher-CF units coding the *wrong* (low-frequency) TFS. The VCN does *not* compensate for the degraded quality of TFS in its inputs following NIHL. *Enhanced detection* of low-amplitude ENV by VCN chopper units may underlie altered ENV processing in HI humans, and likely has implications for their difficulty understanding speech in fluctuating maskers (i.e., in real-world conditions).

PS-547

Brain Changes in the Cochlear Nucleus that Accompany Hearing Loss

Catherine Connelly[1]; Amanda Lauer[2]; Kirupa Suthakar[1]; Tan Pongstaporn[3]; Annie Cho[3]; David Ryugo[1,3]
[1]University of New South Wales; [2]Johns Hopkins University School of Medicine; [3]Garvan Institute of Medical Research

Background

Synaptic features of the central nervous system change as a consequence of alterations in sensory input. Studies of partially deaf cats show atrophic changes in brainstem synaptic morphology and postsynaptic ultrastructure (Ryugo et al., 1998), and congenitally deaf white cats exhibit even more severe brainstem pathologies, such as synaptic hypertrophy (Ryugo et al., 1997) and a redistribution of excitatory and inhibitory synaptic terminals (Tirko et al., 2009). This study aims to identify the sequelae of hearing loss in the central auditory system of mice with hearing loss.

Methods

Three mouse strains (aged 1, 3, and 6 months) representing distinct hearing phenotypes were used: CBA/CaHs with normal hearing thresholds through adulthood; DBA/2s, exhibiting progressive high frequency hearing loss starting at one month of age; and homozygote congenitally deaf *shaker-2s.* Cochlear nuclei from mice of various ages and degrees of hearing loss were immunostained using anti-GlyT2 antibod-

ies. The organization of inputs to bushy cells were analyzed with light and electron microscopy.

Results

Synapses of auditory nerve fibers to bushy cells in CBA/CaH hearing mice are dome-shaped with prominent PSDs, synapses of deaf *shaker-2* mice are elongated and flattened, while synapses of the DBA/2 exhibit synapse morphology that appears graded between the two. With respect to non-primary inputs to the bushy cell, the amount of glycinergic terminals, and terminals containing small round vesicles remains constant from 1 to 6 months of age in the CBA/CaH mouse. However, the deaf *shaker-2* and DBA mice have a reduction in the amount of glycinergic terminals around their bushy cells, whereas the number of terminals with small round synaptic vesicles increases. The amount of change is related to hearing status.

Conclusion

Preliminary data show that congenital and acquired hearing loss result in central auditory pathologies. Loss of inhibitory terminals and proliferation of cholinergic terminals suggest a release of inhibition and expansion of excitation, respectively. These changes may give insight to mechanism that underpin tinnitus. Based on these results, it becomes prudent to determine which abnormalities can be remedied by treatment methods such as sound amplification. Future studies will test the hypothesis that an amplified sound environment prevents of delays the progression of brain pathologies in comparison to that of long-term, unattended hearing loss.

PS-548

Release Probability Changes in the Cochlear Nucleus Following Ear-plugging

Xiaowen Zhuang; Wei Sun; Matthew Xu-Friedman
University at Buffalo, State University of New York

Auditory experience plays an important role in the auditory system. The effects of auditory experience have been mainly studied at the later stages of the auditory pathway, such as auditory cortex, and early stages still remain less examined. However, changes in early stages are particularly important, because they would affect how information is conveyed to higher order areas for sound localization. We examined the effects of auditory deprivation by plugging or ligating the ear canal to reduce activity in the auditory nerve in young mice (p14). Then we examined the properties of auditory nerve synapses onto bushy cells in the AVCN using voltage-clamp recordings in brain slices. These synapses, called endbulbs of Held, normally show strong depression during high rates of activity. We found that after ear-plugging for one week, endbulbs showed even greater depression, reflecting higher release probability. However, there were no differences in quantal size between control and ear-plugged mice. Immunolabeling experiments with VGlut1 indicated that synaptic area decreased for ear-plugged mice. These effects appear to reflect adaptive, homeostatic changes in auditory nerve synapses in response to quiet sound conditions. These results may have implications for pathologies such as otitis media.

PS-549

Effects of Sound Amplification After Hearing Loss on Central Auditory Plasticity

Femi Ayeni[1]; Michael Muniak[1]; Radha Simhadri[2]; David Ryugo[1]
[1]Garvan Institute of Medical Research; [2]Hearing, Tinnitus & Implant Centre, Wollongong

Introduction

Sensory deprivation and/or stimulation modulates the central nervous system through plastic changes. Diminished auditory input caused by hearing loss can disturb the functional and anatomical integrity of structures involved in auditory processing. Peripheral hearing loss is typically treated with hearing aids that amplify acoustic signals, but it is unknown if their use can also mitigate and/or restore changes to central pathways. To address this question, we simulated hearing aid use in DBA/2 mice—a model of progressive peripheral hearing loss—by providing acoustic stimulation specific to the hearing loss profile of each animal. We subsequently examined auditory brain stem responses (ABRs) and the morphology of auditory nerve endings onto bushy cells (endbulb of Held) in the cochlear nucleus.

Method

DBA/2 mice were housed in customised acoustic chambers fitted with overhead speakers. Audiograms were collected weekly from three weeks of age for both experimental and control mice. Animals began stimulation at varying age points, receiving baseline stimulation at 55 dB SPL (RMS). Experimental animals received additional frequency-specific amplification based on the hearing loss profile of weekly audiograms. Stimulation was provided 12 hours nightly for eight weeks and consisted of environmental and synthesized sounds spanning the full hearing range randomly interleaved with equal amounts of silence.

After the study period, each animal received an injection of an anterograde tracer (neurobiotin) into the auditory nerve and was allowed to survive 4-6hrs. Brains were processed to reveal labeled endbulbs of Held using a fluorescent marker. Image stacks were acquired with a confocal microscope (Leica DMI 6000 SP8) using fixed image acquisition parameters. Endbulb stacks were ported to *Imaris* software (Bitplane) for manual thresholding and analysis. The same median filter was applied to all images and the observer was blinded from image acquisition through data analysis.

Results

ABR audiograms suggest that central auditory structures in mice receiving stimulation become more excitable as evidenced by improved response latency and late ABR wave morphology at mid-frequencies (16-32 kHz @ 90dB). Anatomical analyses further suggest that endbulb morphology may be better preserved in mice that commence stimulation at earlier ages.

Conclusion

Our data suggest that the benefits of hearing aids may help to prevent or mitigate synaptic abnormalities in the central auditory system induced by hearing loss. This effect appears

to be more robust if stimulation is provided early, providing an argument for early adoption of hearing aids when hearing loss is detected.

PS-550

Synaptic Transmission at the Endbulb of Held during Age Related Hearing Loss

Ruili Xie[1]; Paul Manis[2]
[1]University of Toledo; [2]University of North Carolina at Chapel Hill

Age-related hearing loss is associated with loss of hair cells and spiral ganglion neurons, which together reduce auditory input to the central nervous system. It remains unclear how the central neural network changes during the process. In the ventral cochlear nucleus, the endbulb of Held is a specialized, multisite synapse that transmits information from the cochlea to the central auditory system, and contributes to the encoding of temporal cues. The basic mechanisms of synaptic transmission have been extensively studied at this model synapse due to its functional specializations. However, most studies used animals during early postnatal development or early adulthood. Little is known about how synaptic transmission changes at the endbulb of Held during natural aging and associated age-related hearing loss.

Synaptic transmission at the endbulb of Held was compared between 2-4 month-old young adult, and 23-26 month-old CBA/CaJ mice. We performed whole-cell patch clamp recording in bushy neurons using parasagittal brain slices containing cochlear nucleus. Evoked EPSCs (eEPSCs) were obtained by electrically stimulating the auditory nerve root with trains of 50 pulses at 100 and 400 Hz. P/Q-type calcium channels were partially blocked in some experiments with 25 nM omega-agatoxin IVA. In other experiments, the brain slices were pre-incubated with 100 uM EGTA-AM to test the effects of adding an exogenous calcium buffer to the synaptic terminals.

We compared spontaneous miniature EPSCs (mEPSCs) and did not observe any significant difference in mEPSC amplitude, frequency, decay time constant, 20 to 80% rise time or half-width between young and aged mice. However, the coefficient of variation (CV) of the mEPSC amplitude was significantly higher in aged mice ($p<0.0001$). Furthermore, neither partial block of P/Q type calcium channels, nor providing additional exogenous calcium buffering with EGTA-AM, affected any of the mEPSC measures. This suggests that excitatory spontaneous quantal synaptic transmission at the endbulb of Held synapse remains largely unchanged during age-related hearing loss, with the exception that quantal size becomes more variable in aged animals. In contrast, evoked transmission during trains of eEPSCs at endbulbs from aged mice showed a decrease in synchronized release and an increase in asynchronous release, which were partially rescued by partial block of P/Q type calcium channels, or by pre-incubation of the slice in EGTA-AM to increase calcium buffering. The results suggest that the compromised synaptic transmission in aged mice is caused by dysfunctional regulation of calcium in the presynaptic terminals.

PS-551

5-HT Excites Fusiform Cells of the Dorsal Cochlear Nucleus

Zheng-Quan Tang; Laurence Trussell
Oregon Health and Science University, Portland

Background

Serotonergic (5-HT) afferents present throughout the auditory system may play diverse roles in the control of auditory processing, and dysfunction of serotonergic system is implicated in tinnitus. The dorsal cochlear nucleus (DCN), one of the first stations of the ascending auditory pathway, is regarded as a possible site for central tinnitus, and also receives a dense serotonergic input. However, it is unclear what 5-HT does in the DCN. The goal of this work is to identify cellular targets of 5-HT and understand how 5-HT influences DCN activity.

Methods

To address the effects of 5-HT on DCN neurons, we used a combined electrophysiological, pharmacological and optogenetic approaches in acute brain slices from P16-49 mice.

Results

After blocking both excitatory and inhibitory inputs with antagonists of glutamatergic, glycinergic and GABAergic transmission, bath application or iontophoresis of 5-HT caused a slow depolarization of fusiform cells, an increase in spontaneous spike activity, and a leftward shift in input-output curves. Under voltage-clamp conditions, 5-HT induced a slow inward current, which could be largely blocked by ketanserin, an antagonist for 5-HT2A/2C receptor. The 5-HT response also could be partially blocked by MDL 11939, SB 242084 and SB 269970, selective antagonists for 5-HT2A, 5-HT2C and 5-HT7 receptors respectively, suggesting that 5-HT2A/2C and 5-HT7 receptors mediate 5-HT responses. Moreover, 5-HT responses could be blocked by Cs^+ or ZD7288, blockers of hyperpolarization-activated channels (Ih or HCN channels), showing that HCN channels are the downstream targets of serotonergic signaling. 5-HT responses could be completely blocked by intracellular dialysis of fusiform cells with 1.5 mM GTP-γ-S, and partially blocked by preincubation of a cell membrane-permeable cAMP analogue 8-bromo-cAMP, or a Src family kinase inhibitor PP2, suggesting that serotonergic regulation of fusiform cell excitability is G-protein dependent and involves both cAMP and Src kinase signaling. Additionally, optogenetic activation of serotonergic axon terminals to induce 5-HT release also generated a slow inward current and increased neuronal excitability.

Conclusion

Our findings demonstrate that serotonergic input to the DCN can enhance excitability of fusiform cells by activating HCN channels through 5-HT2A/2C and 5-HT7 receptors. These results help provide an understanding of how 5-HT modulates cellular and network excitability in the DCN. It will be of interest to explore the role of 5-HT in the enhanced activity of fusiform cells that has been associated with central tinnitus, and whether pharmaceutical treatments for tinnitus may affect the serotonergic system in the DCN.

PS-552

Effect of the Modulation of Kv3 Potassium Channels on Neuronal Excitability of Dorsal Cochlear Nucleus Fusiform Cell, In Vitro

Nadia Pilati[1]; Marcelo Rosato Siri[1]; Giuseppe Alvaro[1]; Charles Large[2]

[1]Autifony Srl; [2]Autifony Therapeutics Limited

Kv3 potassium channels play a major role in determining the pattern and frequency of neuronal firing in several systems. In particular, Kv3 potassium channels are highly expressed in the auditory brainstem where they permit temporal fidelity and high-frequency firing of auditory neurons. The dorsal cochlear nucleus (DCN) is the first relay of the central auditory pathway. This nucleus is involved in the localization of sound in the vertical plane and is also the site of integration between multimodal sensory inputs and auditory information). Within the DCN, fusiform cells (Fcs) showed consistent Kv3.1 expression (Rusznák et al.,2008).

Several studies reported that weeks after acoustic over-exposure (AOE), the cellular excitability of DCN neurons is changed and this is correlated with tinnitus. Recently, we found that after AOE, Kv3-like potassium currents are decreased in Fcs of the DCN, and their firing pattern was altered (Pilati et al., 2012). Thus, loss of Kv3 channel function could contribute to the noise induced changes in the excitability and firing of DCN neurons which has been correlated with tinnitus. Selective action on FCs by pharmacological manipulation of Kv3 channels, could therefore have considerable potential for the treatment of hearing disorders such as tinnitus. We have identified a novel series of small molecules that modulate human and rat Kv3 channels. In this study we investigated the effects of a broad-spectrum potassium channel blocker tetraethylammonium (TEA) and a series of Kv3 modulators (Autifony) on cellular excitability of Fcs by *in vitro* whole-cell recordings in acute brainstem slices. TEA significantly reduced the maximal firing and altered Fc firing pattern by switching the firing from regular to irregular. The Autifony compounds restored the regularity of the firing disrupted by TEA and maintained the firing frequency near control levels. These results suggest that Autifony compounds may be able to restore the physiological activity of DCN neurons by reintroducing action potential timing precision and reducing firing frequency that is increased during tinnitus. Studies in animals previously exposed to noise should be considered.

References.

Rusznák Z, Bakondi G, Pocsai K, Pór A, Kosztka L, Pál B, Nagy D, Szucs G (2008) Voltage-gated potassium channel (Kv) subunits expressed in the rat cochlear nucleus. J Histochem Cytochem 56(5):443-65.

PS-553

Time Course of Cell Death Mechanisms within the Mouse Central Auditory System after Noise Trauma

Felix Fröhlich; Moritz Gröschel; Annekatrin Coordes; Arne Ernst; Dietmar Basta

Unfallkrankenhaus Berlin, Charité Medical School, Berlin, Germany

Background

A noise trauma leads to changes in central neuroanatomy and neurophysiology. Several studies could show an impact on the auditory pathway either by acoustic deprivation or acoustic overstimulation. Our group has found a significant loss of cells in the central structures of hearing after a single noise trauma (Gröschel et al, 2010, JNeurotrauma 27:1499-1507). Apoptosis seems to play a key role in the underlying pathophysiology. We recently showed cell death pathways immediately after a single noise trauma (Coordes et al, 2012, JNeurotrauma 29:1249-1254) as well as after a second noise trauma (Fröhlich et al, Poster at ARO 37th Annual MidWinter 2014) in the auditory brainstem. The aim of the present study was to describe the time course of cell death mechanisms in several structures of the central auditory system after a single or repeated noise trauma and compare the data to our earlier results.

Methods

A broadband noise (5-20 kHz) was applied for 3 hours at 115dB SPL to normal hearing mice (NMRI strain). Cell death mechanisms were visualized via TUNEL-staining (terminal deoxynucleotidyl transferase dUTP nick-end) in brain slices and compared at different time points after a first or a second noise exposure. The focus was put on the ventral and dorsal cochlear nucleus (VCN, DCN), the central nucleus of the inferior colliculus (ICC) and the ventral, medial and dorsal subdivision of the medial geniculate body (vMGB, mMGB, dMGB).

Results

There was a significant increase of TUNEL-positive cells in the basal structures (VCN, DCN, ICC) as well as in the dorsal MGB at different time points within the first 7 days after a single noise trauma compared to normal hearing controls. A second noise trauma elicited significant more TUNEL-positive cells in all subdivisions of the MGB while there were no differences found in the VCN, DCN or ICC.

Conclusion

A single noise trauma seems to induce apoptosis mainly in the basal structures (VCN, DCN, ICC) while the cell death mechanisms found in the MGB were somewhat weaker than in the auditory brainstem and midbrain. An explanation might be that the MGB is protected by inhibitory projections from lower structures during a first noise exposure. This hypothesis is provided by the results after a second noise trauma: mainly the higher auditory structures (MGB) were affected while the impact on the basal structures was diminished compared to the first exposure.

PS-554

Effects of Inhibition Loss on Time and Intensity Coding in the Lateral Superior Olive

Go Ashida; Jutta Kretzberg
University of Oldenburg

Introduction

Interaural time and level differences (ITD/ILD) are major cues for binaural sound localization. Neurons in the mammalian lateral superior olive (LSO), which are excited by ipsilateral sound stimuli and inhibited by contralateral sounds, change their spike rates according to ILD. LSO neurons tuned to low frequencies are sensitive to both ITDs and ILDs. Previous anatomical studies showed age-dependent loss of inhibitory inputs in the auditory brainstem. Electrophysiological recordings, however, found relatively small functional changes in aged LSO. In this study, we constructed a biologically plausible LSO model and examined how loss of inhibitory inputs affects ITD and ILD coding in the LSO.

Methods

We constructed an integrate-and-fire type LSO neuron model with leak and low-threshold potassium conductances. Excitatory inputs from neurons in the anteroventral cochlear nucleus and inhibitory inputs from the medial nucleus of the trapezoid body were modeled as Poisson processes with an intensity function increasing monotonically with the sound intensity at each ear. For low frequency tones, the intensity function was assumed to be periodic, reflecting the phase-locked activity of input neurons. Membrane and synaptic parameters were chosen so that simulated LSO responses resemble previous in vitro results.

Results

Simulated output spike rates of the model neuron smoothly decreased with increasing contralateral sound intensity, resembling ILD tuning found in vivo. For low frequency cases (<800 Hz), simulated spike rates showed periodic changes with the phase difference of ipsi- and contralateral phase-locked inputs, similar to what was found in ITD-sensitive LSO neurons. Next, we changed the number of inhibitory inputs and examined how ILD and ITD tunings of the model neuron were affected. The overall spike rate increased when the number of inhibitory inputs decreased. The modulation depth, defined as the difference between the maximum and minimum spike rates, decreased with the loss of inhibition. However, the modulation depth was only weakly affected when the decreased number of inhibition was compensated by increased amplitudes.

Conclusions

ITD and ILD coding of our model, which reproduced known physiological responses of LSO neurons to sustained sound stimuli, was considerably affected when more than half of the inhibitory inputs were lost. This finding suggests potential effects of aging on sound localization. Amplitude compensation, however, counteracted the loss of inputs of the model, making the system more robust to changes in inhibition. Hence, amplitude compensation may explain the limited aging effects on the LSO function observed in vivo.

PS-555

Three Dimensional Maps and Models of Neurophysiological Responses to Acoustic Stimulation in the Inferior Colliculus

Sarah Offutt; Jessica E Pohl; Kellie J Ryan; Megan L Harris; Hubert Lim
University of Minnesota

Functional maps are useful for understanding and modeling how the brain processes information leading to perception. For this reason, numerous mapping studies have been performed throughout the auditory system for various response features. Specifically for the inferior colliculus (IC), the main auditory processing center in the midbrain, functional mapping studies have examined best frequency, threshold, latency, source localization, and best modulation frequency. To expand upon these studies, we have mapped features across the full extent of the IC with complete histological reconstructions of the recordings locations and used these data to model how the IC responds to acoustic stimulation.

A multi-site array was positioned throughout the IC of three ketamine-anesthetized guinea pigs, resulting in a total of 2945 recording locations spanning the rostral to caudal, medial to lateral, and dorsal to ventral axes of the IC. At each location, spike activity was recorded in response to broadband noise at varying levels (30, 50, 70 dB-SPL) to assess the first spike latency (FSL), FSL jitter, duration, and spontaneous activity. Additionally, responses to pure tones were recorded to evaluate the best frequency, Q-value, and threshold. For each animal, the IC was reconstructed in 3D using histological slices and CAD software. Functional trends for each feature were determined using multiple linear regression and models were fitted to the data.

Our results reveal functional trends across the IC that not only include the central region of the IC, but also expand into the outer cortices. A response gradient exists from the caudal-medial to rostral-lateral regions of IC for FSL, FSL jitter, duration, and spontaneous activity with locations in the rostral-lateral region responding to broadband noise with shorter latencies, more temporal precision, and durations that match acoustic stimulation length as well as higher spontaneous activity. In response to pure tones, no trends were found for Q-value or threshold. Equations were fitted to the data and could accurately predict several response features as a function of IC location.

These functional maps in conjunction with data from previous mapping studies provide further insight into neural processing within the ascending auditory system. The modeling equations derived in this study can be integrated into mathematical models of the auditory system through the IC. Clinically, these maps and models can help guide the placement of electrodes and improve stimulation strategies for central auditory prostheses.

PS-556

Stimulus Specific Adaptation in the Primate Inferior Colliculus to Noise Bursts

Troy Rubin; Eric Young
Johns Hopkins University

Background

The detection of novel stimuli in complex perceptual environments is a fundamental property of neural networks. In its most reduced from, this function known as stimulus specific adaptation (SSA), a reduction in response to a statistically abundant standard stimulus but not to an infrequent deviant stimulus. Auditory SSA has been observed in the cortex, thalamus and the inferior colliculus. However there remains debate as to its properties, given the paucity of data from unanaesthetized preparations with unmodified inhibitory circuits.

Methods

We recorded from single neurons in the inferior colliculus of awake head-fixed marmosets with tungsten microelectrodes. SSA was assessed with spectrally overlapping, nested and band-passed free-field white noise bursts eliciting similar neural firing rates. Stimulus trains compromised abundant (90%, standard), wide band stimuli punctuated quasi-randomly with infrequent (10%, deviant), narrow band noise, followed by the same stimuli with standard and deviant reversed.

Results

The majority of neurons with properties typical of the external (ICX) nuclei showed some degree of SSA. Higher levels of SSA were observed in both wide and narrow band stimuli as changes in both onset and sustained components of the response. Increased SSA often correlated with increases in onset latency and in many instances, the response structure to the standard was altered by changing the deviant spectrum in a manner not correlating with the degree of SSA.

Conclusions

The majority of units showing SSA displayed sustained discharges throughout noisoe presentations with complex consistent banding unique to a given stimulus. The specific adaptation of wide band stimuli by spectrally overlapping narrow band stimuli and vice versa suggests this phenomenon may derive from more complex mechanisms that the adaptation of upstream ascending projections.

PS-557

Patterns of Electrophonic and Electroneural Excitation in the Inferior Colliculus

Mika Sato; Peter Baumhoff; Andrej Kral
Hannover Medical University

Background

Electric stimulation of a hearing cochlea generates hair-cell-mediated response and a direct neural response. It remains unclear whether such electrophonic and electroneural responses appear at the same or separate cochlear regions. Therefore the present study investigated the patterns of excitation in the inferior colliculus with electrical stimulation of a hearing and deafened cochlea.

Methods

Normal hearing guinea pigs were implanted with an cochlear implant through a cochleostomy. A Neuronexus double-shank 32-channel electrode array was stereotactically placed with the inferior colliculus parallel to the tonotopic axis. The stimuli were charge-balanced biphasic electric pulses, 100μs/phase. Threshold, dynamic range, and onset latency were computed from multiunit activity in the midbrain. The cochlea was subsequently deafened with the implant left in place. The responses to electrical stimuli before and after deafening were compared.

Results

The recordings revealed an ordered characteristic frequency (CF) representation along the shanks of the electrode arrays. The thresholds of electrical stimulation increased prominently in the CF region of 3-7 kHz (8.8 ±4.2 dB*). Also the dynamic range in the CF of 3-7 kHz decreased by 8.0 ±5.0 dB* and the onset latencies in the threshold of these CF also decreased by 1.8 ± 0.4 ms after deafening. (*significant at 5% level, Wilcoxon-Mann-Whiteny test)

Conclusion

The low threshold, large dynamic range, and long onset latency at the 5 kHz region and the corresponding change after deafening suggest that this response was predominantly hair-cell-mediated. This electrophonic response appeared at the dominant frequency of the electrical stimulus (5 kHz, period of 200 μs). A direct neural response with short latencies, high thresholds and small dynamic range was observed in the CF region of above 9 kHz (corresponding to the location of the cochlear implant). Consequently, electrical stimulation of a hearing cochlea results in two spatially separate regions of electrophonic and electroneural activation.

PS-558

Development of an MR-based Framework for Localizing Anatomical and Physiological Information in the Inferior Colliculus of the Mongolian Gerbil

Gilberto Graña; Kendall Hutson; Douglas Fitzpatrick
University of North Carolina at Chapel Hill

The development of 3D imaging techniques facilitates comparing different types of data sets within a common digital framework. While such frameworks exist for most common laboratory animals and humans, there is no comparable framework for the gerbil brain, which is an often-studied rodent model for the auditory system due to a low-frequency hearing range similar to that of humans. Magnetic resonance (MR) imaging of a gerbil brain was used as a digital framework to spatially localize anatomical and electrophysiological data. The MR image of the gerbil brain was taken at 7.3 Tesla, producing a stack of images with an isotropic voxel resolution of 21.5 μm. Biotinylated dextran amine (BDA) was injected into the medial geniculate producing retrogradely labeled cells in the IC; this labeling was compared to levels of cytochrome oxidase (CO) activity in alternate 40 μm sections. Electrophysiological measurements of monaural and binau-

ral response properties were made across the inferior colliculus (IC) and localized with lesions in CO-reacted sections. To create a common spatial framework, the image stack of the MR brain was rotated and resliced to match the plane of section of each experimental gerbil brain. The IC in matching MR sections was stretched to align with that of each corresponding histological section. BDA-labeled cells, the locations of physiological recording sites, and CO activity levels were plotted onto the MR sections and stored as image masks. The stack containing the combined information could then be resectioned at any angle or visualized as 3-D renderings, allowing for comparison between the different experimental procedures.

PS-559

3D Model of Frequency Representation in the Inferior Colliculus of the CBA/Ca Mouse

Michael Muniak; Giedre Milinkeviciute; David Ryugo
Garvan Institute of Medical Research

Background

Tonotopy is the dominant organizational principle of the auditory system. The topographic ordering of frequency representation on the organ of Corti is replicated throughout the auditory pathway such that adjacent cell populations receive information about adjacent sound frequencies. Previously, we constructed a 3D model of tonotopy in the mouse cochlear nucleus (CN) based on the projections of physiologically characterized and labeled nerve fibers (Muniak et al., 2013). This model facilitates quantitative testing of hypotheses concerning frequency and location of mapped datasets in the CN. Using similar techniques, we now present a 3D model of tonotopy in the mouse inferior colliculus (IC), a midbrain nexus where nearly all ascending and descending auditory pathways converge.

Methods

Adult CBA/Ca mice received injections of biotinylated and/or fluorescent dextran-amine through a recording micropipette following electrophysiological characterization of the CN or IC. Brains were processed using standard histologic methods to reveal labeled anterograde projections in the IC. Serial sections from each case were photographed, digitally reconstructed using *TrakEM2* software, and segmented in 3D. Aligning and averaging the segmented cases produced a normalized IC template. Individual cases were re-aligned to the template, and the coordinates of frequency-specific anterograde label were extracted using image-processing algorithms. A predictive artificial neural network was then applied to produce a quantitative 3D map of frequency tuning in the IC.

Results

Each injection yielded a pattern of anterograde labeling in the IC consistent with published literature. CN injections predominately produce label in the contralateral IC, whereas IC injections produce bilateral label with an ipsilateral bias. Viewed coronally, each case exhibits a classic “V” shape within the central and external nuclei of the IC that also extends along the rostro-caudal axis to form a largely continuous sheet of label in 3D. Frequency laminae in the central nucleus gradually shift from diagonal to vertical orientations at more rostral locations and are systematically arranged such that lower-frequency laminae are positioned at more dorsal locations. The derived 3D model accurately captures the above details, and demonstrates that the precise orientation of isofrequency laminae is fluid and dependent on position.

Summary

Our study combined physiological and anatomical data to produce a quantitative 3D model that encompasses frequency and anatomical position within the mouse IC. This model can be used to produce virtual reference slices of the IC. More importantly, it provides a standard framework upon which other coordinate-based datasets in the IC can be compared.

PS-560

Squeaks and Growls: Variation in Female Mouse Calls During Courtship and Across The Estrous Cycle

Caitlyn Finton; Sarah Keesom; Laura Hurley
Indiana University

Like many rodents, house mice (*Mus musculus*) emit a diversity of vocalizations during social interactions. During courtship, female mice emit low frequency harmonic calls (“squeaks”), which have been studied to a lesser degree than the copious ultrasonic vocalizations emitted by males. Female calls vary in the extent to which they exhibit nonlinearity (e.g. subharmonics or deterministic chaos), and previous pilot work suggests that this variation is potentially relevant to male receivers, with females producing more nonlinear calls around bouts of mounting. In this study, we expanded this work by recording vocalizations from longer social encounters to more fully capture the time course of female vocal behavior during courtship. Furthermore, we made repeated measures of calls from the same females on different days in their reproductive cycles, allowing us to investigate how female calls vary with receptivity, a potentially significant feature for males. Sexually experienced females were placed with novel males for a period of 20 minutes during which audio and video recordings were taken for later analysis. Multiple parameters of female calls, including fundamental frequency, entropy, and amplitude of different segments within each call, were measured. These measurements were compared to behaviors of both male and female social participants. There was substantial variation in the number of calls produced by individual females across repeated interactions, varying by as much as two orders of magnitude. Across repeated interactions, individual females also varied in the percentage of calls containing nonlinear segments, with an extreme example ranging from 16% to 100% of calls. All females produced calls at timepoints throughout the interaction. However, as with our previous work, females emitted bursts of calls that were relatively more likely to contain nonlinearities, with proportionally longer nonlinear segments. These bursts sometimes corresponded in time to mounting occurrences by males. This work demonstrates that nonlinearities in female calls may have different relationships to male-female interactions during courtship.

This suggests that discrimination between linear and nonlinear segments of female calls is a behaviorally relevant task for the male mouse auditory system.

PS-561

Squeaks and Growls: Discrimination of Harmonic and Nonlinear Components of Female Mouse Calls by Inferior Colliculus Neurons

Miranda Millar[1]; Arianna Gentile Polese[2]; Laura Hurley[2]
[1]New Mexico Institute of Mining and Technology; [2]Indiana University

Ultrasonic courtship vocalizations produced by male mice have been studied extensively, but less is known about audible calls made by female mice in this context. Female mice produce broadband calls that are often paired with kicking at or darting away from males. These calls are harmonically structured, but incorporate transient nonlinear segments likely produced by irregular vocal fold vibration. Nonlinear segments are higher in entropy, and lower in harmonic-to-noise ratio (HNR) than harmonic segments in the same calls. To explore whether auditory neurons can distinguish between harmonic and nonlinear segments, and whether GABAergic inhibition contributes to this process, we recorded action potentials extracellularly from inferior colliculus (IC) neurons of male mice in conjunction with iontophoresis of gabazine. We measured the responses of neurons before, during, and after drug application in response to three types of stimuli: 1) recorded female calls containing harmonic and nonlinear segments, 2) digitally separated harmonic and nonlinear segments from the same calls, and 3) synthesized female calls with varying levels of entropy. A majority of IC neurons showed selectivity for either harmonic or nonlinear segments of the natural female calls. In many cases gabazine decreased this selectivity by unmasking excitatory responses that did not exist in the control condition to either harmonic or nonlinear segments. However, for most neurons, gabazine increased the value of d' between harmonic and nonlinear segments. Thus, gabazine caused neurons to respond more indiscriminately, but increased the statistical distinguishability between call segments. For some neurons presented with synthesized calls, the effect of gabazine varied with the level of entropy. These findings show that IC neurons distinguish between harmonic and nonlinear call components, a process that is refined by GABAergic inhibition. Whether vocal nonlinearities in female mouse calls convey salient behavioral information has not been tested, but in other animals vocal nonlinearities may support individual recognition or the communication of behavioral arousal or estrous state.

PS-562

Modulation of Dopamine Sensitive Neurons in the Inferior Colliculus: Protection from Noise Induced Hearing Loss

Aaron Apawu[1]; Bozena Fyk-Kolodziej[1]; David Dolan[2]; Karin Halsey[2]; Paul Walker[1]; Avril Holt[1]
[1]Wayne State University; [2]University of Michigan

Background

Dopamine (DA), a multi-modal neurotransmitter has been implicated in auditory processes. Data suggest that DA receptors are distributed throughout the inferior colliculus (IC), an area responsible for integration of auditory signals. Additionally, the presence of tyrosine hydroxylase (TH), the rate-limiting enzyme in the production of DA, has been reported within axon terminals in the IC. Our previous data demonstrated that gene expression and immunocytochemistry for TH in the IC decreases significantly following hearing loss. The present work begins to unravel the role of DA neurotransmission in hearing by using pharmacological manipulation of DA D1/D2-like receptors within the IC.

Method

Hearing thresholds were tested in male Sprague Dawley rats (n = 6) before and after (2 and 3 weeks) bilateral stereotaxic cannulae implantation into the IC. Two weeks following surgery, rats were injected with 2 µL of saline (control) or 2 µL of DA D1/D2 receptor (DRDA1/2) antagonists just before sound exposure (16 kHz, 106 dB SPL for 1hr). Hearing thresholds were measured (4, 12 and 20 kHz) at several time points after the exposure (1, 3, 5 hrs, and 3 weeks). To determine sensitivity to sound and tinnitus susceptibility, acoustic startle reflex (ASR) was tested both before and after sound exposure. At the end of the experiment, cannulae placement and spread of DA antagonist within the IC was assessed.

Results

Auditory brainstem responses (ABRs) revealed elevated hearing thresholds (31, 67 and 72 dB) at 2, 12 and 20 kHz, 1 hour following sound exposure. However, when animals were pre-treated with DRDA1/2 antagonists, threshold shift was significantly blunted ($p < 0.05$) compared to controls. Hearing thresholds returned to normal levels by one week. After DRDA1/2 antagonist administration, pre-pulse inhibition of ASR was significantly enhanced. The site of administration and spread of DRDA1/2 antagonists was restricted to the IC.

Conclusion

The present work suggests that DRDA1/2 in the IC mediate noise induced threshold shift and are involved in hearing sensitivity. Our preliminary findings also suggest that DRDA1/2 antagonists can decrease adaptation of distortion product otoacoustic emissions (DPOAEs) at acoustic levels well above hearing threshold. Taken together, our results support a role for DA sensitive IC neurons possibly by modulation of the medial olivocochlear (MOC) reflex. This reflex is postulated to play a role in protecting outer hair cells from noise over-stimulation and enhancing hearing discrimination in noisy environments. Future experiments will evaluate the potential involvement of DA in the MOC reflex.

PS-563

Towards a New Classification Scheme of Cell Types in the Inferior Colliculus: Physiological Response Properties of Neurochemically Classified Neurons

Lauren Kreeger; Michael Roberts; Boris Zemelman; Nace Golding
University of Texas at Austin

Introduction

Neurons in the central nucleus of the inferior colliculus (ICC) have been classified in many species. Anatomical, histochemical, and physiological studies have shown that ICC neurons are heterogeneous with respect to intrinsic membrane properties and expressed neurochemical markers. We aim to identify functional classes of neurons within this heterogeneous population. We postulate that neurons positive for a neurochemical marker and homogeneous with respect to membrane properties may play specific roles within the ICC. A new classification scheme that includes neurochemical markers and physiological properties may be the key to unraveling circuit mechanisms in the ICC.

Methods

Adeno-associated viral constructs that encode for soluble fluorescent proteins were stereotaxically injected into the ICC of Mongolian gerbils. Infected neurons were labeled with the fluorescent marker encoded by the virus, and were later visualized in an acute slice preparation for targeted whole-cell current clamp recordings in gerbils aged P40-49. Voltage responses to current steps were analyzed according to firing pattern, spike shape, and passive membrane properties. The location of neurons in the ICC were confirmed with cytochrome oxidase staining and biocytin labeling of patched neurons. The specificity of each viral vector for the intended neurochemical marker was confirmed with immunohistochemistry.

Results

We have classified neurons based on physiological properties and the presence of neurochemical markers associated with functional circuit mechanisms and their effects on firing properties. We have observed in gerbil ICC firing types consistent with previous reports from other species. Additionally, we have observed a novel firing type that exhibits membrane properties and spiking suited to convey precise timing information. Fluorescent proteins have been successfully expressed using adeno-associated viral constructs with promoters targeting subpopulations of neurons. Viruses were selected based on specificity, density, and reliability of labeling. The specificity of viral expression in the neurochemically targeted population of neurons was verified with immunohistochemistry. Active and passive membrane properties including time constant, input resistance, and firing properties were used to classify neurons within a genetic group.

Summary

We have successfully used viral mediated fluorescent labeling to differentiate between excitatory and inhibitory neurons in the ICC of Mongolian gerbils. We are moving toward an understanding of the functional organization of neurons in the ICC.

PS-564

Connectional and Neurochemical Modularity of the Mouse Inferior Colliculus

Alexandria Lesicko; Daniel Llano
University of Illinois at Urbana-Champaign

Background

The external and dorsal cortices of the inferior colliculus receive a wide range of inputs, including information from both lower and higher-order auditory and somatosensory structures. Previous studies in the rat have demonstrated a modular organization of neurochemical patches within layer 2 of these nuclei. The major afferent projections to these areas have also been shown to terminate in a discontinuous, patch-like fashion. In the present study, we sought to determine whether the shell nuclei of the mouse inferior colliculus also contain neurochemical modules, and how the pattern of inputs to these nuclei relates topographically to their underlying modular organization.

Methods

Bulk injections of a bidirectional tracer, 3,000 MW BDA, were made into the auditory cortex, central nucleus of the inferior colliculus, or the dorsal column nuclei of mice. Following a week survival period, animals were sacrificed and tissue sections were collected at 40 um. The tracer was converted for fluorescence using a streptavidin-conjugated alexa-fluor, and the tissue sections were further processed for GAD-67 immunohistochemistry.

Results

Immunostaining revealed a network of GAD-67 positive modules throughout the rostro-caudal extent of the cortices of the mouse inferior colliculus. These modules were also positive for parvalbumin and NADPH-diaphorase. Overlay images showed that the labeled afferents from the dorsal column nuclei terminate almost exclusively within these modular zones. However, the projections from both the central nucleus of the inferior colliculus and the auditory cortex form clusters that interdigitate with the GAD-positive modules.

Conclusions

The present study reveals that the topography of afferent input to the shell nuclei of the inferior colliculus correlates with the underlying pattern of neurochemical organization. Somatosensory input from the dorsal column nuclei and auditory input from the auditory cortex and central nucleus are segregated into distinct, non-overlapping clusters. This pattern resembles the well-described connectional modularity of the superior colliculus, and could indicate a common organizational theme of these midbrain structures.

PS-565

Somatosensory Inputs to the Lateral Cortex of the Inferior Colliculus Prior to Auditory Experience in Mouse.

Joseph Balsamo; Mark Gabriele
James Madison University

The inferior colliculus (IC) is situated in the midbrain and serves as a primarily auditory relay hub. Well established are the tonotopic arrangement of its central nucleus (CNIC) and the organization of its many converging inputs. Considerably less is known about its external nucleus or lateral cortex (LCIC). In contrast to the CNIC, the LCIC lacks a clear frequency order and receives a multimodal input array. Previous studies in a variety of adult species demonstrate somatosensory inputs to this region arising from the spinal trigeminal nucleus (Sp5) as well as the dorsal column nuclei. These projection distributions, unlike the characteristic layering exhibited by CNIC afferents, appear to target discrete LCIC modular fields. This mature projection arrangement is consistent with certain Eph-ephrin signaling protein expression in LCIC modular and extramodular zones prior to hearing onset. As a first-step in determining the potential roles these guidance molecules play in LCIC circuit formation, the present study examines the development of Sp5 inputs to presumptive LCIC modules prior to auditory experience. Fluorescent tract-tracing approaches in a developmental series of fixed mouse tissue preparations reveal pioneer somatosensory fibers in the nascent IC that preferentially target its lateral cortex. Contralateral projections are particularly robust, as compared with sparse ipsilateral labeling. As early as a week prior to hearing onset, contralateral Sp5 axons exhibit considerable projection specificity, with patchy terminal fields most evident in ventrolateral and rostral aspects of the LCIC. At present it remains unclear whether Sp5 projections target specific Eph-ephrin LCIC domains. Also of interest is the alignment of these developing inputs with previously described LCIC neurochemical modules (e.g. GAD). Understanding LCIC input-output relationships together with corresponding neurochemical signatures should help to elucidate its functional roles. Planned studies pairing tract-tracing and immunohistochemical techniques should provide insights regarding the anatomical substrate of the LCIC and signaling mechanisms that establish its integrative multimodal circuitry.

PS-566

Dopaminergic Inputs to the Inferior Colliculus

Alexander Nevue[1]; Cameron Elde[1]; David Perkel[2]; Christine Portfors[1]
[1]Washington State University Vancouver; [2]University of Washington

Background

How sensory neurons respond to stimuli can be modulated by a variety of factors, including attention, emotion, behavioral context and disorders involving neuromodulatory systems. For example, patients with Parkinson's disease have speech processing problems, suggesting that dopamine alters normal representation of these salient sounds. Understanding the mechanisms by which dopamine modulates auditory processing is thus an important goal. Previous studies have shown that the inferior colliculus (IC) contains nerve terminals immunoreactive for tyrosine hydroxylase (TH), the rate-limiting enzyme in dopamine synthesis. In addition, application of dopamine onto single neurons in the IC alters their response properties. Thus, the IC is a likely location for dopaminergic modulation of auditory processing. However, the sources of dopaminergic input to the IC are unknown.

Methods

In this study we used adult CBA/CaJ mice to determine the dopaminergic neurons that project into the IC. We deposited the retrograde tracer Fluorogold in the central nucleus of the IC in four animals. The location of each deposit was guided by single- and multi-unit recordings. After a survival time of seven days, the brains were sectioned from the brainstem through cortex and stained for TH. We also stained for dopamine beta-hydroxylase (DBH) to differentiate between dopaminergic and noradrenergic inputs in one animal. Retrogradely labeled cell bodies that were TH positive were identified using a Leica DMR fluorescence microscope.

Results

Retrogradely labeled neurons that were positive for TH and negative for DBH were seen bilaterally in the subparafascicular thalamic nucleus, magnocelluar part (SPFm). All other retrogradely labeled neurons were TH negative.

Conclusions

While the function of these dopaminergic neurons is not yet known, these results provide a rich avenue for future studies. Localizing the dopaminergic inputs to the IC can ultimately provide context in understanding the behavioral function of dopamine in auditory processing.

PS-567

Populations of Nitrergic Neurons Distinguished by Expression of GABA and Calcium Binding Proteins in Rat Inferior Colliculus

Bas Olthof; Llwyd Orton; Sasha Gartside; Adrian Rees
Newcastle University

Background

In the brain neuronal nitric oxide synthase (nNOS) catalyses the synthesis of the gaseous signalling molecule, nitric oxide (NO). nNOS expression occurs throughout the auditory pathway, but is most pronounced in the dorsal and lateral cortices of the inferior colliculi (Coote & Rees, 2008). Increased nNOS expression has been reported in the ventral cochlear nucleus in animal models of tinnitus (Zheng *et al.*, 2006; Coomber *et al.*, 2014). Since nNOS activity is closely coupled to intracellular calcium, the calcium binding proteins parvalbumin (PV), calbindin (CB) and calretinin (CR) may influence NO signalling. We determined the distribution of cells expressing nNOS in the IC, determined whether they are GABAergic, and examined whether they express calcium binding proteins

Methods

Adult Lister-hooded rats were perfused with PBS and 4% paraformaldehyde. Brains were cryo-protected in sucrose

and coronal sections (40 µm) were cut on a cryostat. PV, CB, CR, nNOS and GABA were detected using fluorescent immunohistochemistry.

Results
In caudal areas of the IC, nNOS-positive cells were evenly distributed across the subdivisions, while in the rostral two thirds most of these cells were observed in the dorsal and lateral cortices. In the central nucleus, the majority of nNOS-positive cells co-expressed GABA, while in the lateral and dorsal cortices only about half of nNOS-positive cells were GABAergic.

Dense clusters of CR-positive cells were seen in the dorsal and lateral cortices: preliminary evidence suggests that few of these cells co-express nNOS. CB-positive cells were also abundant in the dorsal and lateral cortices and almost all were nNOS-positive.

Most PV expressing cells were observed in the central nucleus. In the caudal IC, nNOS and PV were rarely co-expressed, but in the rostral half of the IC there were many nNOS and PV-positive cells. Most cells co-expressing PV and nNOS were observed in ventro-lateral areas of the central nucleus. Interestingly, although most PV expressing cells also co-express GABA, our preliminary results show that ~15 % of these PV-positive cells are GABA negative.

Conclusions
These data demonstrate that nNOS-positive cells are differentially distributed in the IC and that nNOS is present in GABAergic and non-GABAergic (presumably excitatory) cells. Different populations of nNOS expressing cells can also be distinguished by their co-expression of PV, CB or CR. The neurochemical diversity of cells producing NO in the auditory midbrain suggests multiple roles for NO in modulating sound processing in the IC.

Supported by Action on Hearing Loss.

PS-568

Dopamine Modulates Intrinsic Neuronal Properties in the Mouse Inferior Colliculus

C. Williams[1]; Agata Budzillo[1]; Christine Portfors[2]; David Perkel[1]
[1]University of Washington; [2]Washington State University Vancouver

Background
Auditory processing changes depending on time of day, mood, attention, and other factors. A variety of neuromodulators mediate these changes. One such neuromodulator is dopamine, which is essential for normal motor function, and also plays a role in signaling salience and reward. In addition, dopamine depletion is associated with disrupted auditory processing. One locus of such modulation appears to be the inferior colliculus (IC). Indeed, application of dopamine to IC neurons in mice alters responses to auditory stimuli. Such changes could be mediated through altered electrophysiological properties of individual neurons and/or altered synaptic strengths. Here we asked how dopamine affects the intrinsic electrical properties of IC neurons *in vitro*.

Methods
We made blind or visualized whole cell current-clamp recordings from neurons in the central nucleus of the IC in brain slices prepared from CBA/CaJ or C57Bl6 mice on postnatal day 15-20. Recordings were made at 30-32 °C, and internal solutions were based on potassium methylsulfate. We injected hyperpolarizing and depolarizing current pulses and recorded sub- and suprathreshold membrane potential responses. We applied dopamine (50 µM) in the bath and assessed its effects on resting membrane potential and neuronal excitability.

Results
Intrinsic properties of neurons recorded could be classified into two main categories: those with sustained firing in response to depolarizing current pulses and those that fired only at the onset of a current pulse. A few additional neurons exhibited delayed or intermittent firing, and were categorized as “others”. These neuronal classes were similar to those identified in rats. Application of dopamine caused a depolarization in the vast majority of neurons with sustained firing. In these neurons, dopamine also substantially increased the number of action potentials evoked by current pulses. In neurons with onset or other firing properties, dopamine caused a small hyperpolarization or no change in membrane potential. Together, these results suggest that dopamine acts differentially on different IC neuron types.

Conclusions
In parallel with the diverse effects of dopamine on auditory responses *in vivo* (Gittelman et al. 2013), we find diverse actions of dopamine on intrinsic properties of IC neurons *in vitro*. The differential effect of dopamine on different neuronal types may facilitate future studies of dopamine’s role in modulating auditory processing.

PS-569

Chronic In Vivo Two-photon Calcium Imaging in the Dorsal Cortex of the Mouse Inferior Colliculus

J. Gerard Borst; Aaron Wong; H.-Rüdiger Geis
Erasmus MC

Compared to the central nucleus, the function of the dorsal cortex of the inferior colliculus has been less well characterized. In mice, a large part of the dorsal cortex lies superficially, making it a favorable structure for chronic in vivo two-photon imaging. We expressed the genetically encoded calcium indicator GCaMP6s (Chen et al, 2013) using adeno-associated viruses in C57BL/6J mice and repeatedly imaged sound responses of individual cells through a cranial window during periods exceeding one month. Responses to simple tones of different frequencies and intensities in awake, head-fixed mice showed that frequency response areas (FRAs) were often broad and complex, including areas in which the tones reduced intracellular calcium concentrations, probably as a result of inhibition of spontaneous firing. FRAs of individual cells within the same field of view typically differed considerably, suggesting sparse coding within the dorsal cortex. Re-

peated measurements of FRAs of the same neuron indicated that FRAs were generally stable.

Behavioral work involving lesions in the cat dorsal cortex of the inferior colliculus has provided evidence for a role in auditory attention (Jane et al, 1965). We therefore tested whether the calcium responses to tones depended on behavioral state. Attentional level was monitored by measuring pupil sizes, electrocorticography and lick responses to tones presented in an operant conditioning task. In many cells, calcium responses to sound presentation were modulated by the behavioral state.

The complex tuning properties and the modulation of firing properties by behavioral state suggests that the role of the dorsal cortex of the inferior colliculus in sound processing clearly differs from that of the central nucleus.

PS-570

Neural Correlates of the BK Channel's Role in Temporal Sound Processing Features within the Inferior Colliculus

Elliott Brecht; Joseph Walton
University of South Florida

The slow, Ca^{2+} activated, BK-type channels are responsible for controlling action potential duration, firing frequency, and spike frequency adaptation. BK channels are found in the axon terminal, soma, and dendrites of neurons, and open in response to a rise in intracellular Ca^{2+}. We investigated the effect of applying the general pore blocker, paxilline (PAX), on BK channel function, as measured by the temporal processing properties of inferior colliculus (IC) neurons in a gap-in-noise (GIN) paradigm.

IC recordings were made using a 16-channel vertical electrode-array on tranquilized young adult CBA/CaJ mice. We evaluated pre- and post-drug effects of PAX applied to the exposed IC, at concentrations of 10μM, 1μM, 0.1μM and 0.01μM in 1% DMSO. Temporal coding was assessed using the GIN paradigm by embedding silent gaps, from 1-96ms, 100ms into a 150ms broadband noise-burst presented at 60, 70, and 80dB SPL. Each gap series was presented pseudo-randomly, 50-times, in the contralateral hemifield, from which minimum gap thresholds (MGTs), temporal response patterns (TRPs), and gap functions were measured.

Neural responses to the GIN stimuli exhibited average pre-drug MGTs of 1-2ms. Post-PAX MGTs increased, regardless of concentration level, and were correlated with a systematic drop in driven activity to both the pre- and post-gap carrier over time. The majority of multi-units' temporal response patterns (TRPs) were classified as on-sustained to the noise-burst stimuli, and we found that initially (1-3 hr), the majority of units showed an increase (130 – 200%) in excitatory drive during the sustained portion driven activity. Over time (>4 hr), the driven rate for the majority of units declined to the point where the GIN response ceased, especially for PAX concentrations of 0.1uM and greater.

Previous results suggest a role of BK channels in the formation and maintenance of receptive field properties of IC neurons. Our study demonstrated that blocking BK channels resulted in a 2-stage transformation in the neural coding of gaps, the first being increases in the excitatory drive, consistent with in vitro studies showing that blocking BK results in increased neuronal excitability. The second stage was a loss in driven activity 2-3 hours post-application, with a concomitant loss of gap encoding, possibly related to post-translational changes of the channel. Overall the results implicate the BK channel in the regulation of sustained excitatory drive, which can modulate temporal processing in auditory midbrain.

PS-571

Two Patterns of Cholinergic Inputs to GABAergic Cells in the Inferior Colliculus

Jeffrey Mellott[1]; Nichole L. Foster[2]; William A. Noftz[2]; Brett Schofield[2]
[1]Northeast Ohio Medical University; [2]Kent State University Northeast Ohio Medical University

Acetylcholine affects the responses to acoustic stimuli of most cells in the inferior colliculus (IC). Acetylcholine is also essential for long term effects associated with activation of auditory cortical projections to the IC (Suga, 2013 J Comp Physiol 36:969). Cholinergic effects appear to be mediated largely by direct synaptic activation of GABAergic IC cells (Yigit et al., 2003 Neuropharm 45:504) but in fact the IC cells targeted by cholinergic axons have not been identified. We used immunohistochemistry to identify cholinergic boutons onto GABAergic (and non-GABAergic cells) in the IC.

We labeled cholinergic boutons with antibodies for vesicular acetylcholine transporter (VAChT) and examined the tissue with light and electron microscopy. We also marked GABAergic cells (labeled with anti-glutamic decarboxylase, GAD) and cholinergic boutons with different fluorescent antibodies to identify presumptive cholinergic synapses on GABAergic and non-GABAergic IC cells.

VAChT-immunopositive (VAChT+) boutons were found throughout the IC, with highest densities in the lateral cortex (IClc), dorsal cortex (ICdc) and medial part of the central nucleus. Most VAChT+ boutons were in the neuropil, but a subset showed clear association with neuronal somas. Electron microscopy on a small sample of VAChT+ boutons revealed traditional synapses with round vesicles and asymmetric junctions, consistent with excitatory postsynaptic effects. Double labeling with fluorescence revealed VAChT+ boutons in apparent contact with GAD+ cells and GAD-negative cells in all areas of the IC. We focused on the GABAergic cells given their implication in physiological studies. Over 90% of GAD+ somas were contacted by VAChT+ boutons. These GAD+ cells comprise 2 types. The first type, involving 16% of the contacted cells, has a soma contacted by many (typically >25) VAChT+ boutons. The second type (84%) has a soma contacted by fewer (typically <10) VAChT+ boutons.

We conclude that cholinergic inputs contact a large majority of IC GABAergic cells, with a subset of these GABAergic cells

receiving particularly dense somatic inputs. These inputs are in a position to exert strong effects on the GABAergic cells, suggesting that these cells play a prominent role in cholinergic modulation of collicular function. Cholinergic boutons also appear to contact glutamatergic cells, providing opportunities for varied cholinergic effects on collicular circuits. Finally, the highest density of cholinergic boutons overlaps the regions of the IC (namely, ICd and IClc) that also receive inputs from auditory cortex, supporting the proposal of close interactions between these two inputs.

PS-572

Molecular Markers and Soma Size of Inhibitory Cells: Evidence for Four Subtypes of GABAergic Cells in the Inferior Colliculus

Nichole Foster[1]; Brett Schofield[2]
[1]Kent State University Northeast Ohio Medical University; [2]Northeast Ohio Medical University Kent State University

The inferior colliculus (IC) comprises glutamatergic cells and GABAergic cells that contribute to local circuits and project to the thalamus. In several species (cat, rat, mouse), GABAergic IC neurons are larger, on average, than non-GABAergic neurons. We asked 1) are GABAergic cells larger than non-GABAergic cells in guinea pigs? and 2) how does soma size relate to four subgroups of GABAergic neurons: those surrounded by a perineuronal net (PN), those surrounded by a dense ring of boutons containing vesicular glutamate transporter 2 (VGLUT2), those that have both a net and a VGLUT2-ring, and those that have neither (Foster et al. 2014, ARO Abst 36: 328).

In adult guinea pig IC sections, PNs were stained with *Wisteria floribunda* agglutinin, GABAergic cells were stained with anti-glutamic acid decarboxylase (GAD), VGLUT2+ terminals were stained with anti-VGLUT2, and anti-NeuN was used as a general neuronal counterstain. Stains were distinguished with 4 different fluorescent tags. Using a Neurolucida system, each neuronal soma in the top five micrometers of a transverse section through the IC was outlined and coded based on GAD immunoreactivity and association with PNs and VGLUT2-rings. The results are based on 29,526 neurons distributed across the IC central nucleus (ICc), lateral cortex (IClc), dorsal cortex (ICd), and rostral pole (ICrp) in four animals.

GAD+ neurons make up ~27% of IC neurons and have larger somas than GAD-negative neurons (mean areas of 151 μm^2 and 110 μm^2, respectively). The four subtypes of GAD+ cells differ in soma area: netted/ringed cells are largest (283 μm^2), followed by ring-only cells (197 μm^2), net-only cells (196 μm^2), and cells lacking both markers (126 μm^2). GABAergic subtypes also show a marked difference in distribution: netted cells (with or without rings) are more numerous in ICc and ICrp, while cells lacking both markers are present throughout the IC, but more numerous in ICd and IClc.

Our results show a difference of soma size for GABA vs. glutamatergic IC cells similar to that seen in other species. Further, differences in size and distribution support the distinction of 4 subtypes of GABAergic cells based on the presence or absence of perineuronal nets and perisomatic rings of VGLUT2+ boutons. Given functional implications of soma size (e.g., differences in membrane time constant, input resistance, and axonal conduction velocity), we conclude that the different subtypes of GABAergic cells are likely to perform different functions in the processing of acoustic signals.

PS-573

Pharmacologically Enhanced Kv3.1 Channel Conductances Improves Midbrain Temporal Processing in Mice with Profound Cochlear Neuropathy

Pooja Balaram[1]; Anna Chambers[1]; Jennifer Resnik[1]; Maile Brown[2]; Leonard Kaczmarek[2]; Charles Large[3]; Daniel Polley[1]
[1]Eaton-Peabody Laboratory; [2]Yale University; [3]Autifony

Background

Hearing loss is often associated with deficient neural and perceptual processing of temporal modulation in the sound pressure envelope. While temporal processing deficits have been clearly linked to synaptic dysfunction, less is understood about the contribution of voltage-gated potassium (Kv) channels, which shape spike patterning and are downregulated after hearing loss in the CNS. Here, we test the hypothesis that boosting Kv3.1 channel conductances through systemic administration of an experimental drug, AUT3, can rapidly improve midbrain temporal processing deficits in mice with profound cochlear neuropathy.

Methods

We tested this hypothesis using (1) patch clamp recordings of Kv3.1 currents in transfected Chinese hamster ovary cells (CHO) before and after AUT3 application, and (2) multiunit recordings from the central nucleus of the inferior colliculus (ICc) in awake mice, with unilateral loss of ~95% of Type-1 auditory nerve fibers from round window application of ouabain, before and after systemic injection of AUT3.

Results

Recordings from CHO cells revealed that AUT3 shifted the voltage-dependent activation of Kv3.1 channels to more negative potentials and producing, for example, a 67% increase in current at a test potential of -30mV, where the Kv3.1 channel is normally closed. When administered *in vivo*, we found that AUT3 significantly improved trial-by-trial reliability in the rate and timing of ICc spiking, as indexed by synchronization to broadband pulse trains presented at rates ranging from 5-300 Hz. A computational model that classified temporal modulation rate based on single trial spiking activity indicated that AUT3-mediated neurophysiological changes provided enhanced temporal coding that could be supported by smaller ensembles of midbrain neurons than in the vehicle condition.

Conclusions

AUT3 enhanced Kv3.1 currents in heterologous cell lines by producing an -11mV leftward shift in the voltage-dependence of activation of these channels. AUT3 also rapidly enhanced

the reliability and temporal coding capacities of ICc neurons recorded in awake mice with extensive auditory nerve degeneration. These findings suggest that CNS temporal processing deficits that can accompany hearing loss reflect the combined dysregulation of intrinsic electrical excitability as well as synaptic transmission. Our ongoing studies aim to compare the effects of cochlear neuropathy on Kv3.1 gene expression relative to genes that regulate excitatory and inhibitory neurotransmission. Collectively, these observations support the development of CNS drugs that target the pathophysiological sequelae of cochlear degeneration as a new avenue for therapeutic research, and suggest that AUT3 has potential as a novel treatment for hearing loss.

PS-574

Characterization of the Auditory Thalamotectal Projection in Mouse

Mili Patel; Alexandria Lesicko; Luye Yang; Gehad Taha; Daniel Llano
University of Illinois at Urbana-Champaign

Background

Auditory descending projections have been explored previously by many investigators. However, one pathway which has been evolutionarily highly preserved but not well studied is the auditory thalamotectal pathway. The purpose of this study was to obtain a better understanding of the distribution of thalamic projections to the inferior colliculus and further analyze the chemical and physiological features of these neurons. Therefore, we mapped the distributions of thalamic neurons that project to different sub-nuclei in the inferior colliculus, examined their labeling for three calcium binding-proteins and glutamic acid decarboxylase (GAD) and performed electrophysiological recordings of identified thalamotectal cells *in vitro*.

Methods

Fluorogold was iontophoretically injected in the dorsal cortex, lateral cortex, or central nucleus of the inferior colliculus (IC). For the comparison of reactivity to different calcium binding proteins, larger gelfoam injections were done in the IC with the same tracer followed by immunostaining in the medial geniculate body (MGB) for calbindin, calretinin or parvalbumin. Fluorogold injections were also done in GAD-GFP mice to determine if thalamotectal cells were GABAergic. For physiological studies, brain slices were obtained from red polystyrene Fluosphere-injected animals that contained labeled thalamotectal cells with the retrograde fluorescent tracer. Whole-cell patch clamp recordings were performed and the cells were later filled with biocytin for morphological characterization.

Results

Most cells that projected to the lateral cortex of the IC were derived from the medial and paralaminar MGB. Cells in these regions also projected to the rostral portion of the dorsal cortex of the IC. The dorsal cortex received more projections from the contralateral thalamus than other regions of the IC. The central nucleus of the IC injections labeled very few cells in the thalamus. Further analysis showed that most of the thalamotectal cells (>92%) were negative for any of the three calcium binding proteins or GAD. Thalamotectal cells also did not manifest the typical bursting behavior or the bitufted morphology of thalamocortical neurons.

Conclusions

There are discrete patterns of the thalamic projections to different sub-divisions of the IC. These cells are also disparate from other thalamic cells in terms of their morphology, calcium-binding protein reactivity, and physiology – providing evidence that thalamotectal cells comprise a distinct class of neurons in the auditory thalamus.

PS-575

The Effects of Hidden Hearing Loss on Adaptive Coding in the Mouse Inferior Colliculus

Warren Bakay; David McAlpine; Roland Schaette
University College London

Introduction

It has recently been discovered that noise exposure and aging can cause hidden hearing loss (HHL), i.e. deafferentation of auditory nerve fibres (ANFs) without increasing hearing thresholds (Kujawa and Liberman, 2009; Makary et al., 2011). HHL predominantly affects high-threshold ANFs (Furman et al., 2013), and it could have a particularly detrimental effect on auditory performance in high-level background noise, suggesting an explaination why many people struggle in 'cocktail party' situations even though their hearing thresholds are normal. Moreover, HHL could also lead to distorted central auditory processing, as it is associated with tinnitus (Schaette and McAlpine, 2011) and increased spontaneous firing rates in the auditory midbrain (Hesse et al., 2014). We thus hypothesized that HHL might impair neural mechanisms like adaptive coding (Dean et al., 2005) which could be essential for understanding speech in noise.

Goal

To determine the effect of HHL on the adaptive coding capability of inferior colliculus (IC) neurons in a mouse model.

Methods

Mice were exposed to octave-band noise (8-16 kHz) at 100 dB SPL for 2 hours under anaesthesia. ABRs were measured before and 4 weeks after exposure. Recordings from IC neurons were obtained with Neuronexus tetrode arrays. Adaptive coding was studied using a noise stimulus that changed intensity every 50 ms. Intensities were drawn with 80% probability from a 12-dB range (high-probability region, HPR) centred on either 44, 56, 68, or 80 dB SPL, and with 20% probability from the rest of the intensity range.

Results

ABR measurements 4 weeks after noise exposure showed a reduction of the amplitude of wave I, but no shift of ABR thresholds, thus confirming HHL. IC recordings from control mice demonstrated adaptive coding, the magnitude of adaptation was generally similar to our previous results from guinea pigs (Dean et al., 2005, 2008). In exposed mice, the pattern was more variable, ranging from normal adaptation

magnitude to almost no adaptive coding. In general, there was a tendency towards a smaller degree of adaptation to high intensity background sounds in the exposed group, indicating that HHL could impair the ability of the auditory system to encode acoustic stimuli that are embedded in high level background noise.

Conclusions

HHL could potentially lead to a decrease in the ability of auditory neurons to adapt their responses to noisy situations, which could explain why many people with apparently normal hearing struggle in a cocktail party situation.

PS-576

The Blood-Labyrinth Barrier and its Influence on Endocochlear Potential

Keiko Hirose; Jared Hartsock; Alec Salt
Washington University School of Medicine

Introduction

The blood labyrinth barrier (BLB) separates the contents of circulating blood from the inner ear fluids and is believed to serve a crucial role in normal cochlear function. We have developed a quantitative method to measure the permeability of the blood labyrinth barrier and used this method to study the relationship between BLB integrity and endocochlear potential (EP).

Methods

Mature mice were treated with saline or lipopolysaccharide (LPS, 1mg/kg IP for two days prior to EP measurement). The EP was recorded through the basal turn of the cochlear lateral wall, and subsequently, the mouse was injected with sodium fluorescein IP (0.4ml, 20mg/ml). The otic capsule was sealed, and perilymph was sampled from the posterior semicircular canal 30-40 minutes after sodium fluorescein injection. Blood was also sampled. The ratio of fluorescein in the perilymph to fluorescein in the plasma was calculated in control and LPS-treated mice.

Results

Minor reductions of EP were observed while considerable changes in BLB permeability were observed after LPS treatment. Compromise of the blood labyrinth barrier does not appear to have a large impact on the mouse EP.

Summary

The BLB is thought to play an important role in normal cochlear physiology. However, we do not know if changes in BLB permeability affect hearing function. Contributions of the blood labyrinth barrier to hearing thresholds and to EP maintenance are fundamental questions that are critical to our understanding of the sequelae of cochlear inflammation. Barrier compromise in blood vessels in the perilymph may not correspond to barrier compromise in the intrastrial space. This difference may account for the relatively preserved EP that we detected in mice with BLB barrier dysfunction.

PS-577

Measurements of Endolymphatic K+ Concentrations in the Utricle of Pre- and Postnatal Slc26a4Δ/+ and Slc26a4Δ/Δ Mice.

Fei Zhou; Xiangming Li; Philine Wangemann
Kansas State University

SLC26A4 and the murine ortholog *Slc26a4* encode the anion-exchanger pendrin that is expressed in the inner ear. Mutations of *SLC26A4* cause syndromic or non-syndromic hearing loss associated with a prenatal enlargement of the membranous labyrinth. This enlargement is replicated in the mouse model $Slc26a4^{\Delta/\Delta}$. $Slc26a4^{\Delta/\Delta}$ mice fail to acquire hearing and thereby resemble a phenotype that is more severe than what is seen in most patients. Recent studies have shown that cochlear pendrin expression is not required for the acquisition of normal hearing in mouse models that do not develop an enlargement of the membranous labyrinth (Choi et al 2011; Li et al 2013). These findings suggest that prevention of the enlargement is a strategy to preserve hearing in the absence of functional pendrin expression. A recent study implicated the vestibular labyrinth as the origin for fluid secretion that leads to the enlargement of the entire membranous labyrinth (Kim et al 2010). The goal of the present study was to measure K^+ concentrations ($[K^+]$) in utricular endolymph of $Slc26a4^{\Delta/+}$ and $Slc26a4^{\Delta/\Delta}$ mice during pre- and postnatal development as a first step toward a mechanistic understanding of fluid secretion.

$[K^+]$ and transepithelial potentials (V_{te}) were measured with double-barreled ion-selective electrodes in isolated *in vitro* superfused temporal bones. Although tissues likely experienced anoxia, measurements of $[K^+]$ were assumed to resemble normoxic levels since stable $[K^+]$ have been recorded for as long as 50 min of anoxia (Mori et al 1987). Temporal bones were obtained from perinatal and adult $Slc26a4^{\Delta/+}$ and $Slc26a4^{\Delta/\Delta}$ mice.

At embryonic (E) day 16.5, $[K^+]$ was ~10 mM in both genotypes and V_{te} was -10 mV in $Slc26a4^{\Delta/+}$ mice and -2 mV in $Slc26a4^{\Delta/\Delta}$ mice. $[K^+]$ rose in $Slc26a4^{\Delta/+}$ mice at E17.5. This rise appeared delayed by ~1 day in $Slc26a4^{\Delta/\Delta}$ mice. In adult mice, $[K^+]$ and V_{te} were 150 mM and -22 mV in $Slc26a4^{\Delta/+}$ and 132 mM and -5 mV in $Slc26a4^{\Delta/\Delta}$ mice.

The observations in adult mice of a negative V_{te} in $Slc26a4^{\Delta/+}$ and normal high $[K^+]$ in $Slc26a4^{\Delta/+}$ and $Slc26a4^{\Delta/\Delta}$ mice is consistent with the assumptions that measurements at anoxic conditions resemble normoxic $[K^+]$. Utricular $[K^+]$ were similar to cochlear $[K^+]$ at E16.5. The rise of utricular $[K^+]$ at E17.5 suggests an earlier onset of K^+ secretion and the delay in the rise of $[K^+]$ in $Slc26a4^{\Delta/\Delta}$ mice is consistent with the larger fluid volume.

Supported by NIH-DC012151.

PS-578

Intracochlear Bleeding During Cochleostomy Enhances Cochlear Inflammation and Fibrosis

Sung Tae Seo; Yong-Ho Park
Chungnam National University

Introduction

It has been reported that cochlear fibrosis and ossification could affect delayed hearing loss following cochlear implantation. Cochleostomy as itself might induce intracochlear inflammation and fibrosis because of bone dust and trauma but the effect of intracochlear bleeding is not known well. In this study, we investigated the effect of intracochlear bleeding during cochleostomy on cochlear inflammation.

Materials and Method

Male albino guinea pigs, weighed 250-300g, with normal hearing prior to surgery underwent cochleostomy bilaterally. About 10$\mu\ell$ of blood was injected into the scala tympani through right side cochleostomy site with Hamilton syringe connected micro cannula and left side ear served as control. Auditory brainstem response (ABR) threshold changes from both ears in 8, 16, 32 kHz were evaluated prior to surgery, just after surgery, 1, 4 and 8 weeks postoperatively. Histologic examination and RT-PCR were conducted for the evidence of inflammatory reactions in the cochlea.

Results

ABR threshold shifts (between preoperative and postoperative) were not different in both sides. Inflammatory cytokines were more increased in blood injected side compared to control side in early stage of inflammation. Severe hair cell loss, more extensive fibrosis and ossification were observed in blood injected side than control side, especially in 2-month after blood injection.

Conclusion

Through histologic examination and RT-PCR, we thought that more severe inflammation might be induced by intracochlear blood. We suggest that conservation from bleeding to inside of cochlea during cochleostomy might be important to reduce intracochlear inflammation.

PS-579

Macrophages in the Human Inner Ear

Jennifer O'Malley; Joseph B. Nadol; Michael McKenna
Massachusetts Eye and Ear Infirmary

Background

The innate immune system of the human inner ear is not well understood. Animal studies have demonstrated both cochlear resident and infiltrating macrophages. Mouse studies have shown inflammatory cell migration to the cochlea with both infectious (systemic challenge to lipopolysaccharide) and noninfectious (acoustic trauma) insults. Elucidating such mechanisms in human tissue depends heavily on human otopathology research and our ability to probe human postmortem tissue in a meaningful fashion. To that end, we have been working with mouse postmortem tissue embedded in celloidin to work out details in human postmortem tissue. Our recent findings in human tissue are a product of this effort.

Methods

Archival temporal bone sections (20µm) from 5 presumed normal individuals ranging in age from 52-81 were utilized. Celloidin was removed with a mixture of sodium hydroxide and methanol, rinsed with methanol, rehydrated to water, blocked with 5% normal horse serum, and incubated with a primary antibody against IBA1 (ionized calcium binding adaptor molecule 1). This antibody is reportedly specific for microglia/macrophages. An appropriate secondary antibody followed by avidin-biotin horseradish peroxidase complex was applied. Diaminobenzidine and peroxide was used to colorize the reaction product. The slides were further rinsed, dehydrated, and cover slips applied.

Results

Cells consistent in staining and morphology with microglia/macrophages were identified in the adult human inner ear. Macrophages were present along the eighth nerve, the osseous spiral lamina, the spiral limbus, within the mesenchymal cell layer below the basilar membrane, in the spiral ligament, within the stria vascularis, and within the outer sulcus cells. On occasion, cells could be seen within the organ of Corti. Macrophages were present within the cochlear aqueduct and along the round window membrane. Additionally, the vestibular labyrinth was populated with this cell class. There were macrophages below the saccule, utricle, superior canal ampulla, lateral canal ampulla, and posterior canal ampulla, and within the connective tissue of the rest of the vestibular labyrinth. There were macrophages present within the endolymphatic duct and sac and within the sac lumen.

Conclusion

Temporal bones used in this study were from individuals who had no known otologic problems, so presumably normal for age. Evidence presented here suggests there is a fairly extensive innate immune surveillance system present in the human inner ear. It will be interesting to probe other temporal bones with hearing loss to learn what role the immune system may be playing in well documented cases with known otologic disorders.

PS-580

Imaging of Animal and Human Inner Ears with X-ray Micro Tomography

Rudolf Glueckert[1]; Lejo Johnson Chacko[2]; Martin Gloesmann[3]; Stephan Handschuh[3]; **Anneliese Schrott-Fischer**[2]
[1]Medical University of Innsbruck; [2]Department of Otolaryngology, Medical University Innsbruck, Austria; [3]VetCore Facility for Research, Imaging Unit, University of Veterinary Medicine, Vienna, Austria

Non-destructive 3D imaging of animal and human inner ears are important requirements to quantify anatomical variations or survey developmental steps in embryogenesis. X-ray microtomography (micro-CT) is a versatile tool for mineralized tissues but requires contrast enhancement of soft tissue. In ossified temporal bones we face the problem of high contrasting bone with delicate soft tissue structures of the mem-

branous labyrinth and nerve fibres located within the most compact bone in our body.

We present different techniques suitable for human and animal inner ears. Decalcification of postfixation with osmium tetroxide proved to be most suitable for big human temporal bones to visualize especially nervous tissue within bone. Also membranes and certain tissues provide good contrast. We further tested phosphotungstic acid (PTA), iodine potassium iodine (Lugol's formulation-IKI), elementary iodine in ethanol (I2E), the commercial formulation Gastrografin®, tannic acid and osmium tetroxide (OsO4) before and after decalcification.

IKI turned out to give best contrast for soft tissue while decalcified and osmium treated temporal bones were ideal to trace myelinated nerve fibres.

These techniques provide sufficient contrast for soft tissue in the hard bony capsule and enable non-destructive imaging of inner ear. Data can be used for segmentation of various structures of interest and measured with high accuracy.

PS-581

Conditional Macrophage Depletion by Diphtheria Toxin Affects Distribution of Macrophages in the Cochlear Lateral Wall

Jianping Liu[1,2]; Zachary D. Urdang[1,3]; Meiyan Jiang[1]; Hongzhe Li[1]; Peter Steyger[1]

[1]Department of Otolaryngology, Oregon Health & Science University, Portland, Oregon, USA; [2]Department of Otolaryngology, Eye & Ear Nose and Throat Hospital, Fudan University, Shanghai, China; [3]MD/PhD Program, Oregon Health & Science University, Portland, Oregon, USA.

Objective:

We previously reported that *Diphtheria* toxin (DT) treatment increased fluorescently-tagged gentamicin (GTTR) entry into the stria vascularis and spiral ligament in the CD11b-*Diphtheria* toxin receptor (DTR) mice. We tested that whether macrophage/monocyte depletion varies in different tissues/blood of DTR mice after peritoneal injection of DT.

Methods

Transgenic mice expressing human DTR on macrophages and wild type C57BL/6 mice were treated with DT or PBS. Five days after the initial injection, cochlear lateral wall and kidney tissues were excised, immunolabeled with F4/80 and CD11b and examined by confocal microscopy. Venous blood samples were collected for blood smears or processed for flow cytometry.

Results

Based on blood smears and flow cytometry, DT treatment significantly reduced relative monocyte population and increased granulocytic, especially neutrophil, relative population values in whole blood of DT-treated DTR mice compared to PBS-treated DTR mice. Based on immunofluorescence, DT treatment ablated renal macrophages in DT-treated DTR mice but not PBS-treated DTR mice. CD11b was primarily localized in the spiral ligament but less in the stria vascularis. Macrophage-specific F4/80 was predominantly expressed in the stria vascularis but less so in the spiral ligament. DT treatment ablated $CD11b^+$ macrophages in the spiral ligament, but not $F4/80^+$ macrophages in the stria vascularis, of DT-treated DTR mice. The diameters of strial capillaries varied depending on experimental condition, and were visibly larger in DT-treated DTR mice than in PBS-treated DTR or wild type mice. Only DT-treated DTR mice significantly lost weight.

Conclusion

Using CD11b-DTR transgenic mice, DT treatment depleted macrophages with varying efficacy in different tissues. Additionally, population percentages of differing subtypes of white blood cells to DT treatment in DTR mice varied: specifically monocytes decreased and neutrophils increased, with no change for lymphocytes. Coupled with weight loss and strial capillary vasodilation, these observations collectively suggest that DT-induced depletion of macrophages triggered a systemic inflammatory response.

PS-582

Role of Transient Receptor Potential Vanilloid 1 (TRPV1) in the Cellular Uptake of Aminoglycosides

Meiyan Jiang; Anastasiya Johnson; Takatoshi Karasawa; Allan Kachelmeier; Peter Steyger

Oregon Health and Science University

Background

The aminoglycoside antibiotic **g**entamicin is clinically essential, and is frequently used worldwide, for the treatment of life-threatening bacterial infections. Unfortunately, the nephrotoxic and ototoxic side-effects remain serious complications. Several non-selective cation channels, e.g., TRPV4, are gentamicin-permeant. However, it is not known whether a related non-selective cation channel, TRPV1, that is expressed by hair cells is also gentamicin-permeant and contributes to the cellular toxicity of gentamicin.

Methods

The immunoexpression of TRPV1 in murine cochleae or kidney cell lines was examined by confocal microscopy or western blots. A renal proximal tubule (KPT2) cell line was transfected with TRPV1 or empty vector p-Babe cDNA and tested with GTTR uptake assays. Cell viability was determined by the reduction of 3-(4, 5-dimethylthiazol-2-yl)-2, 5-diphenyltetrazolium bromide (MTT).

Results

TRPV1 immunofluorescence was localized in strial marginal cells of C57BL/6 mice, and, in vitro, in some but not all kidney (KPT2 or KDT3) cell lines. Greater GTTR uptake was present in KPT2-TRPV1 cells than in control KPT2-pBabe cells. The TRPV1 agonists capsaicin and resiniferatoxin (RTX) significantly increased GTTR fluorescence in KPT2-TRPV1 cells than in KPT2-pBabe cells, or KPT2-TRPV1 cells without capsaicin or RTX treatment. Agonist enhanced GTTR uptake in KPT2-TRPV1 cells could be inhibited by calcium. The inert analog of RTX, iodoresiniferatoxin (I-RTX), significantly de-

creased GTTR fluorescence in KPT2-TRPV1 cells compared to cells without I-RTX. KPT2-TRPV1 cells were significantly more susceptible to gentamicin-induced toxicity compared with KPT2-pBabe cells. Capsaicin increased KPT2-TRPV1 cell's susceptibility to gentamicin-induced toxicity.

Conclusions

These data indicate that TRPV1 is likely a gentamicin-permeant channel, and when expressed and activated, facilitates gentamicin entry into cells to increase the risk of toxicity.

PS-583

Abolishing Gastric-Type Proton Pump Fails to Rescue Profound Hearing Loss and Inner Ear Malformations in Slc26a4–defected Mice

Ying-Chang Lu[1]; Chen-Chi Wu[1]; Chung-Wei Yu[1]; I-Shing Yu[2]; Shu-Wha Lin[2]; Xi Lin[3]; Chuan-Jen Hsu[4]

[1]National Taiwan University Hospital, Taipei; [2]National Taiwan University, Taipei; [3]Emory University School of Medicine; [4]Taichung Tzu Chi Hospital

Background

Recessive mutations in *SLC26A4* (protein encoded: pendrin) are a common cause of hearing impairment in children. Acidification of the endolymph in cochlea has been related to the pathogenesis of hearing loss associated with *SLC26A4* mutations. The stability of pH in the endolymph of cochlea is crucial for normal auditory physiology, and is controlled by several proteins in addition to pendrin. For instance, it has been demonstrated that blocking gastric-type proton pump (i.e. the Atp4a H^+, K^+-ATPase) in the inner ear causes prominent reduction of endocochlear potential. We previously established a knock-in mouse model segregating the common *SLC26A4* c.919A>G mutation (*Slc26a4^{tm1Dontuh}*), which revealed phenotypes similar to those observed in humans, including profound hearing loss, pronounced vestibular dysfunction, and inner ear malformations. The purpose of this study is to explore the role of gastric-type proton pump in modulating the phenotypes of *Slc26a4*–defected mice.

Methods

Embryonic stem cells of an *Atp4a* knock-out mouse strain (*Atp4a$^{tm1a(KOMP)Wtsi}$*) were obtained from UC Davis Mouse Biology Program, and then knock-out mice (*Atp4a$^{-/-}$*) were generated and maintained in C57BL/6 background. *Slc26a4-Atp4a* double-mutant mice were generated by intercrossing *Slc26a4^{tm1Dontuh}* and *Atp4a$^{-/-}$* mice. Mice were subjected to audiological assessments, vestibular evaluations, inner ear morphological studies, and electrophysiological examinations.

Results

Atp4a$^{-/-}$ mice showed normal audiovestibular phenotypes and inner ear morphology. On the other hand, the double-mutant mice revealed profound hearing loss, pronounced head tilting and circling behaviors, inner ear malformations including enlarged vestibular aqueduct/sac, atrophy of stria vascularis, and deformity of otoconia, as well as endocochlear potentials close to zero. Detailed data will be presented at the meeting.

Conclusions

There were no significant differences in audiovestibular phenotypes, inner ear morphology, and electrophysiology between the *Slc26a4-Atp4a* double-mutant and the *Slc26a4*–defected mice. These findings indicate that abolishing gastric-type proton pump could not rescue audiovestibular abnormalities and inner ear malformations in *Slc26a4*–defected mice.

PS-584

Controlled Infusion for Drug Delivery to the Inner Ear of Guinea Pigs over Extended Periods.

Woo Seok Kang[1]; Ishmael Stefanov[2]; Evan E Foss[2]; Michael McKenna[1]; Sharon Kujawa[1]; Ernie S. Kimm[3]; Abigail Spencer[3]; Erin Pararas[3]; Vishal Tandon[3]; Keenan Hye[3]; **Mark Mescher[3]**; Jeffery Borenstein[3]; Jason Fiering[3]; William Sewell[1]

[1]MEEI/Harvard; [2]MEEI; [3]Draper Laboratory

Introduction

Techniques for acute delivery of drugs into the inner ear are widely developed and range from direct injection via syringe or micropump to reciprocating fluid delivery (reviewed in Swan et al, 2010). But few options are currently available for a simple, wearable direct infusion system for intracochlear delivery over periods of days to weeks. We developed an infusion system for direct inner ear delivery of drug solutions at variable flow rates and have tested the system for periods of 2 to 8 days. Infusion of a glutamate receptor blocker, DNQX, allowed us to assess both the spatial distribution of the drug (via frequency-specific CAPs and the nonspecific effects (i.e changes in DPOAEs) of the delivery technique.

Methods

The infusion system comprised a commercially available Bartels micropump optimized for very low (<1µl/min) flow rates, a microprocessor that enabled adjustment of run times and intervals between runs, a reservoir made of collapsible latex, which held solutions of 0.3 or 1 mM DNQX dissolved in an artificial perilymph solution, and a lightweight, rechargeable battery. The entire system was placed in 3-D printed pod attached to a post fixed atop the animal's head. The outlet of the infusion system was led into the bulla via narrow bore (50 µm) PEEK tubing, where it attached to Teflon tubing (101 µm id), which was placed into the scala tympani to a depth of 3 mm via a cochleostomy. Frequency-dependent CAPs and DPOAEs were monitored before, during and after drug infusions.

Results

It was possible to deliver drug for at least 8 days after implantation. With acute (hours) delivery of DNQX, effects were largely confined to the frequency regions bathed by the drug (12 to 32 kHz). By 24h, DNQX effects were apparent throughout the cochlea. Effects of DNQX were larger and more widespread when delivered in smaller doses (1 µl of 0.3 mM) more frequently (every 5 min), as compared with 1 µl of 1 mM every 30 min. DPs were unaffected with acute delivery, but after 24h of infusion, we observed a reversible elevation of

DP thresholds in frequency regions (16 -32 kHz) between the tip of the cannula and the cochlear aqueduct.

Conclusions
Controlled drug delivery for extended periods into the scala tympani for animal experimentation has been demonstrated with a simple device constructed from commercially available components.

PS-585

How Long Should Patients Remain in the Supine Treatment Position After Intratympanic Dexamethasone Injection?

Soon Hyung Park[1]; In Seok Moon[2]
[1]Keimyung University College of Medicine; [2]Yonsei University College of Medicine

Objectives
Intratympanic dexamethasone injection (ITDI) is a widely accepted treatment for patientswith sudden hearing loss. We investigated the appropriate patient wait time in the supine treatment position after ITDI.Study Design: Prospective study

Methods
In an *in vivo* animal study, 24 mice were injected intratympanically with dexamethasone. Perilymphatic fluid was sampled at 5, 10, 15, 20, 25 and 30 min post-injection. The dexamethasone concentration was analyzed using high-performance liquid chromatography. In a separate prospective clinical study, 79 patients with refractory sudden hearing loss underwent intratympanic injection. After the injection, patients remained in the supine position with the head rotated 45° to the unaffected side. Patients were divided into two groups according to the wait time in this treatment position postinjection: 30 min (n = 47) and 10 min (n = 32). Final hearing assessments were conducted 2 months after salvage treatment.

Results
In the *in vivo* animal study, the perilymphatic concentration of dexamethasone showed nosignificant increase after 10 min. In the clinical setting, hearing improvement according to Siegel's criteria was similar in the 30-min (14/47) and 10-min (10/32) groups (p = 0.999). No significant differences in relative hearing gain was observed between the two groups (13.80 ± 19.9 dB and 12.57 ± 14.9 dB, respectively; p = 0.766).

Conclusion
We suggest that 10 min is a sufficient time to remain in the supine treatment position after ITDI in patients with sudden hearing loss.

PS-586

Protein Transduction Capabilities Using Cell Penetrating Peptides Into the Inner Ear Via the Round Window

Hiroki Takeda; Ryosei Minoda
Kumamoto University

Background
It is a crucial issue to develop effective and safe drug delivery methods into the inner ear in order to establish treatment modalities of inner ear diseases. We herein report on the successful protein transduction into the inner ear utilizing Cell Penetrating Peptides (CPPs).

Methods
To induce protein transduction, we placed spongel soaked in EGFP or EGFP-9R (EGFP was coupled with nine arginines) at the round window niche of guinea pigs. Firstly, after single application of EGFP (hereinafter referred to as s-EGFP group) or EGFP-9R (s-EGFP-9R group) via the round window niche, we repeatedly assessed the intensity of EGFP expression utilizing modified Labeling Index (mLI) , which was originally reported by H A Lehr, et al. (J. histochem. cytochem. 1997). mLIs were measured at 12 and 24 hours after transductions in s-EGFP group, and at 12, 24, 48 and 72 hours after transductions in s-EGFP-9R group. Secondly, we performed double applications of EGFP-9R (d-EGFP-9R group) at 24 hours after first transductions. mLIs were similarly measured at 48 and 72 hours after first transductions. Auditory function, vestibular function, hair cell counts and spiral ganglion cell counts were assessed at day 28 after the treatments. Additionally, thickness of the round window membranes was measured at 24 hours after in s-EGFP-9R group

Results
In s-EGFP-9R group, EGFP expression was detectable at the stria vascularis (SV), the organ of Corti (OC), and the spiral ganglion cells (SGC). mLIs in s-EGFP group reached their peaks at around 24 hours and return to baseline within 72 hours after the treatments. There were no significant differences between mLIs of non-treated side cochleae and mLIs of treated side cochleae in s-EGFP. Guinea pigs in s-EGFP-9R and s-EGFP groups showed no significant deterioration of auditory and vestibular functions at 28 days. Regarding mLIs at 48 hours and 72 hours after first treatments, the mLIs in d-EGFP-9R group is significantly higher than the mLIs in s-EGFP-9R. In s-EGFP-9R group, thickness of the round window membranes of treated side cochleae was significantly thicker than those of non-treated side cochleae.

Conclusions
The protein transduction method via the round window niche using 9R is safe and effective to delivery drug into cochlea. Repetitive applications may be effective in order to extend protein expression period.

PS-587

Rhesus Cochlear and Vestibular Function are Preserved after Inner Ear Injection of Saline Volumes Sufficient for Gene Therapy Delivery

Chenkai Dai[1]; Mohamed Lehar[1]; Daniel Sun[1]; Lani Swarthout[1]; John Carey[1]; Timothy MacLachlan[2]; Doug Brough[3]; Hinrich Staecker[4]; Alexandra M. Della Santina[1]; Timothy Hullar[5]; Charles Della Santina[1]

[1]Johns Hopkins School of Medicine; [2]Novartis Institutes for Biomedical Research; [3]GenVec; [4]University of Kansas School of Medicine; [5]Washington University School of Medicine

Background

Sensorineural losses of hearing and vestibular sensation due to hair cell dysfunction are among the most common disabilities. Recent preclinical research demonstrates that treatment of the inner ear with a variety of compounds can elicit regeneration and/or repair of hair cells in animals exposed to ototoxic medications; however, injection of volumes required to deliver an adequate dose of a pharmacologic agent could, in theory, cause inner ear trauma that compromises functional outcome. The primary goal of the present study was to assess that risk in rhesus monkeys. Secondary goals were to optimize the delivery route in rhesus and to determine the relative volumes of rhesus, rodent and human labyrinths for extrapolation of results to other species.

Methods

We measured hearing and vestibular function before and 2, 4 and 8 wk after unilateral injection of phosphate-buffered saline vehicle (PBSV) into the perilymphatic space of normal rhesus monkeys at volumes sufficient to deliver an *atoh1* gene therapy vector. To isolate effects of injection, PBSV without vector was used. Assays included behavioral observation, auditory brainstem responses, distortion product otoacoustic emissions, and scleral coil measurement of vestibulo-ocular reflexes during whole-body rotation in darkness. Three groups (N=3 each) were studied. Group A received a 10 µL transmastoid/trans-stapes injection via a laser stapedotomy. Group B received a 10 µL transmastoid/trans-round window injection. Group C received a 30 µL transmastoid/trans-round window injection. Following transcardiac perfusion 8-10 weeks post-injection, we examined 10 um serial sections of each temporal bone. We also measured inner ear fluid space volume via 3D reconstruction of microCT images of adult C57BL6 mouse, rat, rhesus macaque and human temporal bones (N=3 each).

Results

Injection was well tolerated by all animals, with 8 of 9 never exhibiting signs of disequilibrium and one animal exhibiting transient disequilibrium that resolved spontaneously by 24 hrs after surgery. Physiologic results showed that injection was well tolerated, with no animal exhibiting a functionally significant loss of hearing or vestibular function at the 8 week post-injection measurement. Histologic results demonstrated injection site trauma but otherwise corroborated physiologic results. The relative volumes of mouse, rat, rhesus and human inner ears were (mean±SD) 2.5±0.1, 5.5±0.4, 59.4±4.7 and 191.1±4.7 µL.

Conclusions

These results indicate that injection of PBSV at volumes sufficient for gene therapy delivery can be accomplished without destruction of inner ear structures required for hearing and vestibular sensation.

PS-588

Gene Transfer into the Organ of Corti Using the Ad28 Adenovector

Tomoko Takada[1]; Yohei Takada[2]; Lisa Beyer[2]; Donald Swiderski[2]; Min Young Lee[2]; Yehoash Raphael[2]

[1]Kresge Hearing Research Institute; [2]University of Michigan

Background:

Delivering therapeutic reagents into the cochlea for protection or for treatment of hearing loss and/or tinnitus is desirable but challenging. The method of delivery needs to be via a feasible surgical approach and as least invasive as possible, to reduce side effects. Gene transfer is one of the novel approaches for treatment, most efficiently accomplished by viral vectors. Potential routes of viral vector administration that have been tested for inner ear gene therapy include cochleostomy into perilymph or endolymph, trans-round window approach, posterior semi-circular canal and endolymphatic sac. Previous experiments with Adenovirus serotype 5 have shown that following perilymph injections, only mesothelial cells lining the scala tympani are transduced, whereas epithelial cells lining the scala media are not. Here we characterize gene transfection in the organ of Corti using a perilymph approach with a different adenovector serotype, Ad.28.

Methods

The Ad.28 with a GFP reporter (Ad.28-*GFP*) was delivered into the scala tympani via round window in 3 weeks old wild-type mice. Animals were sacrificed 4 days after the injection, and the distribution of GFP assessed using whole-mounts of the sensory epithelium and flanking areas with epi-fluorescence and confocal microscopy.

Results

In 75% of the mice, GFP expression was seen in both mesothelial cells and epithelial components of the auditory epithelium. The most efficient transduction was in the basal and middle cochlear turns, but some GFP positive cells were also seen in the apex. Cell types exhibiting GFP expression in the membranous labyrinth included Deiters, pillar, Hensen and inner sulcus cells. The cochleae appeared clear of inflammation and the mice appeared healthy, with no signs of major side effects.

Conclusions

Unlike Ad.5 which does not infect the auditory epithelium when injected into perilymph of animal models (mouse, rat and guinea pig), we now show that Ad.28-*GFP* can transfect supporting cells and other non-sensory cells in and around the organ of Corti following perilymphatic inoculation. As such, this vector is a good candidate for gene therapy targeting the non-sensory cells. It is necessary to better assess

subtle side effects and to determine why 25% of the animals remained GFP-negative in the auditory epithelium.

PS-589

A Randomized Controlled Clinical trial of Topical IGF-1 Therapy via Gelatin Hydrogels for Refractory Sudden Sensorineural Hearing Loss

Takayuki Nakagawa[1]; Kozo Kumakawa[2]; Shin-ichi Usami[3]; Naohito Hato[4]; Keiji Tabuchi[5]; Mariko Takahashi[6]; Keizo Fujiwara[7]; Akira Sasaki[8]; Shizuo Komune[9]; Tatsunori Sakamoto[1]; Harukazu Hiraumi[1]; Norio Yamamoto[1]; Yasuhiko Tabata[1]; Michio Yamamoto[1]; Juichi Ito[1]

[1]Kyoto University; [2]Toranomon Hospital; [3]Shinshu University; [4]Ehime University; [5]University of Tsukuba; [6]Nagoya City University; [7]Kobe City Medical Center General Hospital; [8]Hirosaki University; [9]Kyushu University

Background

There is no established therapeutic option for sudden deafness refractory to systemic corticosteroids. This study aimed to examine the efficacy and safety of topical IGF-1 therapy using gelatin hydrogels in comparison to intratympanic corticosteroid therapy.

Methods

We randomly assigned patients with sudden deafness refractory to systemic corticosteroids to receive gelatin hydrogels impregnated with IGF-1 into the middle ear (62 patients) or to receive 4 doses of intratympanic injection with dexamethasone (Dex) (58 patients). The primary outcome was the proportion of patients showing hearing improvement. The secondary outcomes included the change in pure-tone average hearing thresholds over time and the incidence of adverse events.

Results

Baseline characteristics including hearing level at the diagnosis, age, time from the onset to test treatments were comparable between the two treatment groups. No significant difference in the proportion of patients showing hearing improvement was found, but the difference in changes in pure-tone average hearing levels over time between the two treatments was statistically significant (P = 0.003). Multiple regression analysis revealed that hearing level at the diagnosis (p<0.001), age (p=0.001), time from the onset to test treatments (p=0.011) and treatment group (p=0.033) were significant variables influencing changes in pure-tone average hearing levels overtime. Tympanic membrane perforation persisted in no patient in the IGF-1 group, but persisted in 15.5% of Dex group patients. The difference in the incidence of tympanic membrane perforation was statistically significant (P = 0.001).

Conclusions

The positive effect of topical IGF-1 application on hearing levels and its favorable safety profile suggest utility for topical IGF-1 therapy in patients with sudden deafness.

Trial Registration. UMIN Clinical Trials Registry Number 000004366.

Funding. Japanese Ministry of Health, Labor, and Welfare.

PS-590

Impedance Changes and Fibrous Tissue Reduction after Cochlear Implantation using a Dexamethasone Eluting Electrode

Verena Scheper[1]; Maciej Wilk[2]; Michael Fehr[3]; Thomas Lenarz[1]; Roland Hessler[4]

[1]Hannover Medical School; [2]Hannover Medical School University of Veterinary Medicine Hannover, Foundation; [3]University of Veterinary Medicine Hannover, Foundation; [4]MED-EL GmbH, Innsbruck

Introduction

The cochlear implant-electrode array mainly consists of platin-iridium and silicone. Both materials have a long tradition as implant materials. Beside the advantages of silicone, with its high flexibility and good processability, is the material recognized as a foreign body. Implantation induces fibrous tissue growth around the implant. In case of cochlear implants (CI) this tissue casing results in increased electrical impedance and may reduce channel separation. Higher impedances cause higher voltages generated across the electrode-tissue interface. This may also lead to a saturation of the current source and may therefore decrease the dynamic range of the stimulation. High electrode voltages lead to increased energy consumption resulting in shorter durability of the implants batteries. These issues have to be addressed especially in view of the economic outcome of a CI. Up to now there exists no pharmacological therapy and no drug delivery system, which allows a localized specific treatment of the inner ear or of the electrode-nerve-interface to reduce the tissue response. No commercial available devices exist to ensure controlled local drug delivery for inner ear treatment which are combinable with the cochlear implant device.

Methods

Guinea pigs were implanted with a monopolar dexamethasone (DEX) eluting electrode devices (10% or 1% DEX loading) or control devices (0% DEX) with two contacts and housed for three month. Acoustically evoked auditory brainstem responses were measured before surgery and after surgery on days 0, 7, 28, 56, and 91. At the same time points impedances were measured. All animals received once weekly a 60 minutes electrical stimulation. A subgroup with 0% DEX electrodes staid fully unstimulated apart from the stimulation during impedance measurement. Fibrous tissue expanse was measured on resin embedded, grinded and stained cochleae.

Results

DEX significantly reduced impedances and fibrous tissue growth after 3 month observation. There is a notable but not statistically detectable difference between the effect of 10% and 1% DEX on impedance development and fibrosis decrease. The fibrous tissue growth detected after 90 days of implantation significantly correlated with the impedance increase over time but did not correlate to the detected hearing loss. Additionally, we observed that impedances were higher at the first electrode, positioned in the region of the round win-

dow niche, than on the second electrode which was located more apical.

Conclusion
DEX eluting CIs are a promising device for impedance and fibrosis reduction in cochlear implant patients.

PS-591

Numerical Modeling of Intracochlear Drug Delivery with Reciprocating Actuation

Marc Weinberg; Erin Pararas; Mark Mescher; **Jeffrey Borenstein**
Draper Laboratory

Introduction
For intracochlear delivery systems, accurate and practical numerical models that account for key physical phenomena such as drug diffusion, convective flow, protein binding, and various clearance mechanisms are needed. These elements determine pharmacokinetic distribution throughout the length of the cochlea, and design of drug delivery devices and the behavior of specific compounds can be optimized through insights gained by application of these models. Here we report on advances in our predictive models for intracochlear delivery involving incorporation of convective effects driven by the reciprocating motion of a microactuator-based system. Initial results of these numerical models predict drug distribution as a function of relevant delivery parameters in both acute and chronic preclinical experiments.

Methods
The numerical model presented here is coded in *Mathematica* (Wolfram Research), a computational environment capable of solving coupled differential equations, which describe multiphysics associated with drug distribution. Earlier implementations described pharmacokinetics by accounting principally for diffusive motion, along with drug binding kinetics, but did not account for the role of convection driven by pulsatile motion of the micropump used to deliver drug to the cochlea. Here we have extended the model to incorporate axially forced convection as the jet of drug exits an implanted cannula and is injected into the scala tympani. Parameters such as the drug diffusion coefficient, binding constants to prevalent proteins in the perilymph, and pump characteristics including the instantaneous flow rate and pulse duration are incorporated into the model.

Results
The primary challenges with solving these systems of equations are the management of boundary conditions and the high Peclet number (ratio of forced convection to diffusion) associated with characteristic parameters for drug delivery. The former obstacle has been dealt with by building a series of three segments in the delivery sequence and matching conditions at each boundary. The latter challenge necessitates very long run times but is overcome by using smoothing techniques and other computational approximations where mass transfer from convection is assumed much faster than diffusion effects. Initial results for times required for drug to reach apical regions of the cochlea are consistent with experimental observations, given the influence of drug binding on attenuation of drug penetration relative to binding-free transport.

Conclusions
A numerical model that accounts for convection as well as drug diffusion and protein binding has been developed and is capable of predicting pharmacokinetic profiles for drug distribution during intracochlear drug delivery. Numerical results will be presented.

PS-592

An Inner-Ear Drug-Delivery Platform Featuring a Microfabricated Micropump Component

Vishal Tandon[1]; Wooseok Kang[1]; Abigail Spencer[2]; Ernest Kim[2]; Erin Pararas[2]; Michael McKenna[1]; Sharon Kujawa[1]; Mark Mescher[1]; Jason Fiering[2]; William Sewell[1]; Jeffrey Borenstein[2]
[1]Massachusetts Eye and Ear Infirmary; [2]Draper Laboratory

Introduction
A key challenge in the treatment of auditory disorders is that therapeutic agents can have undesirable side effects related to non-specific distribution when delivered systemically. Among local delivery methods designed to minimize toxic side effects, direct intracochlear infusion is advantageous because it is capable of highly-controlled pharmacokinetics and is compatible with many drug types. For hair-cell regeneration applications, where delivery of a timed series of agents on a time scale of months to years is likely necessary, a direct intracochlear delivery approach can be used, but requires a portable, self-contained delivery system.

Here we present our progress toward development of a head-mounted microfluidics-based platform for inner-ear drug delivery that utilizes a microfabricated micropump capable of delivering precise, timed doses of drug over extended durations. Our micropump improves on previous-generation systems and commercially-available components in that fluid and drug storage are integrated within the pump, leading to increased miniaturization, robustness, and potential for delivery of multiple agents.

Methods
Our system comprises microfluidic channels, valves, a drug reservoir and fluidic capacitance all patterned in polymer films, along with electromagnetic actuators and control circuitry. We utilize guinea pig models to demonstrate inner-ear drug delivery by using our micropump to deliver artificial perilymph (AP) as a control and DNQX (test drug) via a cannula inserted into a cochleostomy. Our pump is designed to withdraw perilymph from the cochlea, load it with drug, and then infuse the diluted drug. The process can be repeated at determined intervals for acute or chronic delivery. We monitor CAPs and DPOAEs during delivery, as DNQX should affect CAPs but not DPOAEs.

Results
We tested a simplified version of our pump by delivering 1.1-µl doses of DNQX (300 µM in AP) at 5-minute intervals. CAP amplitudes decreased and CAP thresholds increased during DNQX delivery, while DPOAEs did not change. Given the ge-

ometry of intracochlear fluid spaces, DNQX was expected to flow quickly from the cannula toward the base, and to diffuse more slowly toward the apex. Our results are consistent with these expectations, as DNQX effects were first observed at high frequencies near the cannula, and were observed later at low frequencies.

Conclusions

We are developing a head-mountable enclosure for our micropump and miniaturized control circuitry for future chronic drug-delivery experiments. The completed system will be used to examine multi-stage and long-term treatments for auditory disorders.

PS-593

Rescue of Cisplatin Dependent Hearing Loss by a Round Window Drug Delivery Implant

Erik Pierstorff[1]; Mariana Remedios Chan[1]; Yen-Jung Angel Chen[2]; Federico Kalinec[2]; William Slattery[1]

[1]O-Ray Pharma, Inc; [2]UCLA

Introduction

Chemotherapy induced ototoxicity is damage to the inner ear caused by side effects of administered drugs. This can lead to permanent hearing loss and/or tinnitus in the patient. Some of the most common drug classes causing ototoxicity are anti-cancer therapeutics such as cisplatin. Cisplatin is considered one of the more common ototoxic drugs in use, with monitored ototoxicity frequencies commonly ranging from 20-100% depending on the dosage used. The development of an otoprotective treatment to combat chemotherapy induced hearing loss would have significant impacts on patient quality of life. Various compounds have been studied and tested in animal models for protection against cisplatin mediated hearing loss. Among those with some ototoxic activities include antioxidants, sulfur containing nucleophiles, and steroids. Steroids remain attractive candidates as they are well characterized, and have been used extensively for various inner ear indications.

Methods

We previously reported our extended release steroid formulations in various dose-ranges utilizing a sustained release polymer formulation. To test their activity, sustained release steroid formulations were implanted onto the round window of guinea pigs followed by a cisplatin challenge sufficient to induce hearing loss.

Results

Pre- and post- treatment otoacoustic emissions and ABRs were performed to assess hearing. In all cases, significant hearing preservation was observed in ears administered steroid implants.

Conclusion

These results demonstrate otoprotection from cisplatin ototoxicity and form the foundation for the initiation of clinical trials.

PS-594

Peptides with the Ability to Transit the Tympanic Membrane Do Not Influence Middle or Inner Ear Structure or Function

Kerry Beasley[1]; Arwa Kurabi[1]; Kwang Pak[1]; Brian Nuyen[1]; Matthew Ryals[1]; Laura Dreisbach[2]; Stephen Wasserman[1]; Joseph Hardeman[1]; Allen Ryan[1]

[1]University of California, San Diego; [2]San Diego State University

Background

Chronic otitis media (OM) causes acquired hearing loss and is a challenge to treat in third world countries where access to medical personnel is limited. WHO estimates more than half the world's burden of serious hearing loss, ~175,000,000 individuals, is due to under-treated OM. Current treatments include systemic antibiotics and surgery. However, systemic antibiotics cause side effects and increase antibiotic-resistant bacteria. Local drug therapy would avoid side effects and exposure of off-target bacteria and, if simple to apply, could improve outcomes. There are currently no topical treatments that effectively cross the tympanic membrane (TM). Through the screening of 10^{12} genetically engineered bacteriophage, four peptides were discovered (S, W, X, and Y) that actively transport phage across the TM. These peptides could be linked to small drug packages for local middle ear (ME) pharmacotherapy. However, where the particles go once they enter the ME and their sub-sequential effects on the structural and functional integrity of the ME and inner ear (IE) have yet to be established.

Methods

The ME bullae of Sprague-Dawley (SD) male rats were injected with 10 µl containing 10^9 phage particles. To explore any potential functional effects on the ME and/or IE, the hearing sensitivity of SD rats was tested at 24, 48, 72, and 96 hrs post operation through evoked auditory brainstem response utilizing BioSigRP software, for peptide phage and control (saline or wild-type/WT) injections. To examine the possibility of continued transmigration into the IE, perilymph from SD rat ears was harvested after 4-hr or 24-hr ME incubations with phage, and the fluid was titered to determine whether phage particles were present in the IE. To investigate ME and IE structural integrity, ears were harvested after a 24hr ME phage incubation and the ME and IE morphology was evaluated.

Results

Hearing sensitivity of SD rats showed threshold shifts at 24 hrs that were resolved by 96 hrs with saline controls, WT controls, and all 4 peptides (S, W, X, and Y). No significant differences were found between ME or IE sections for WT control ears and SD ears. Examination of the perilymph harvested found that none of the peptides crossed through to the IE at 4-hrs.

Conclusions

The hearing sensitivity findings suggest a presumably conductive hearing loss from the surgical procedure that resolves by 96 hrs. Our results indicate that these peptides are safe for both the ME and IE systems.

PS-595

Cellular and Molecular Mechanisms of Hearing Loss in Type III Usher Syndrome

Didier Dulon[1]; Samantha Papal[2]; Matteo Cortese[2]; Alice Emptoz[2]; Philippe Vincent[3]; Aziz Tlili[4]; Yohan Bouleau[3]; Saaid Safieddine[2]; Paul Avan[5]; **Aziz El-Amraoui[2]**; Christine Petit[6]

[1]Université de Bordeaux/INSERM UMRS1120; [2]Institut Pasteur/INSERM UMRS1120; [3]Université de Bordeaux; [4]Institut Pasteur; [5]Université d'Auvergne; [6]Institut Pasteur/INSERM UMRS1120/Collège de France

Introduction

Usher syndrome (USH) is the major cause of hereditary deaf-blindness in humans. Mutations in the clarin-1 gene cause USH3A, characterized by postlingual progressive deafness and blindness. Clarin-1 is a four-transmembrane glycoprotein that is predicted to be targeted to the plasma membrane. The precise distribution pattern of clarin-1 in the cochlea is still unknown, but *Clrn1* transcripts have been detected, from embryonic day 16 (E16) to adult stages, in both sensory hair cell types (inner and outer hair cells) and in the primary auditory neurons. The role of clarin-1 in these cells is still elusive.

Methods

To elucidate the USH3A pathogenesis, we generated two distinct clarin 1-deficient mouse mutants; one, referred to as *Clrn1*$^{-/-}$, displays a ubiquitous and early gene inactivation of clarin-1, whereas the second, referred to as *Clrn1*$^{fl/fl Myo15\text{-}cre+/-}$, exhibits a delayed, hair cell-specific loss of clarin-1. Audiometric tests (ABR, DPOAEs, CAPs) were used to study the auditory function of *Clrn1*$^{-/-}$ and *Clrn1*$^{fl/fl Myo15\text{-}cre+/-}$ mice. The structural defects in the cochlea of these mice were analyzed by scanning and transmission electron microscopy, and immunohistochemistry and confocal microscopy were used to detect molecular changes. Clarin 1-mediated interactions were analyzed by pull-down and co-immunoprecipitation experiments.

Results And Conclusions

We found that ubiquitous absence of clarin-1 at embryonic stages in *Clrn1*$^{-/-}$ mice causes severe hearing loss, which was attributed mainly to the disruption of hair bundle stereocilia. By contrast, we show that post-natal and hair cell-specific loss of clarin-1 in *Clrn1*$^{fl/fl Myo15\text{-}cre+/-}$ mice leads to a late appearing and progressive hearing loss that mimics the hearing phenotype in USH3A patients. Detailed physiological analyses, along with quantitative molecular and structural analyses, in the hair cells of both inborn and conditional clarin-1-deficient mice provides new insights into the mechanisms by which clarin-1 acts in specific compartments of the auditory hair cells. The impact of our findings on the management of USH3A patients will also be discussed.

PS-596

The Mineralocorticoid Effect of Glucocorticoids in the Ear is More Relevant than Their Immune Suppression Function

Dennis Trune; Jessyka Lighthall; Fran Hausman; Beth Kempton; Carol MacArthur

Oregon Health & Science University

Introduction

While glucocorticoids (dexamethasone, prednisolone, and prednisone) are routinely given for hearing disorders, little is known of their impact on the ear. The rationale for their use is immune suppression, but glucocorticoids also bind to the mineralocorticoid receptor in the ear to control genes for ion and water homeostasis. Thus, the efficacy of glucocorticoids may be due to their impact on these numerous mineralocorticoid-driven processes required for normal ear function.

Goal

To address this question, a review is provided of several of our studies that compare these two functions of glucocorticoids.

Results

Autoimmune Hearing Loss: Hearing loss in autoimmune mice is reversed with the glucocorticoid prednisolone, but also with the mineralocorticoid aldosterone, which has no glucocorticoid receptor binding. Blocking the glucocorticoid receptor does not prevent glucocorticoids from restoring hearing, while blocking the mineralocorticoid receptor does prevent glucocorticoid effects. This suggests they are operating via the mineralocorticoid receptor and affecting mineralocorticoid driven processes. Furthermore, ion homeostasis genes are suppressed by systemic autoimmune disease and glucocorticoids restore them to normal. Conclusion: mineralocorticoid functions more relevant.

Middle Ear Disease: Aldosterone, with no immunosuppression impact, clears middle ear inflammation comparable to glucocorticoids. This lack of an immunosuppression advantage in middle ear inflammation clearance suggests the benefit of glucocorticoids is via the mineralocorticoid receptor to clear effusions and inflammation. Conclusion: mineralocorticoid functions more relevant.

Intratympanic Steroid Delivery: Glucocorticoids delivered intratympanically actually increase inflammation in the inner ear, but also increase mineralocorticoid-driven functions, suggesting immunosuppression simply does not occur in the inner ear with intratympanic delivery. Affymetrix gene chip analysis showed there were more glucocorticoid-driven mineralocorticoid genes than glucocorticoid-driven glucocorticoid genes. Conclusion: mineralocorticoid functions more relevant.

Conclusion

These various findings suggest that it is the mineralocorticoid-driven genes in the middle and inner ear that are being upregulated by glucocorticoids to impact various disease processes. These include clearance of middle ear effusions by sodium and water transport, upregulation of ion transport

genes to restore inner ear endolymph, resealing tight junctions with their respective gene activation, increasing water transport through aquaporin channels, etc. It is critical that these middle and inner ear processes be considered in the explanation of current therapies, as well as developing therapies in the future that target directly the disordered homeostasis processes that underlie the different types of hearing loss.

PS-597

Septin7 Regulates the Formation of Inner Ear during Early Developmental Stage

Hiroko Torii; Juichi Ito; Takayuki Nakagawa; Norio Yamamoto; Atsuhiro Yoshida
Graduate School of Medicine, Kyoto University

Septin proteins are GTP-binding proteins that are evolutionally conserved through eukaryotes except plants. There are 13 and 14 septin genes in mouse and human, respectively. They are divided into 4 subgroups and septin proteins usually exert their effects as a multimeric complex that are composed of 4 septin proteins from each subgroup. The septin complexes can interact with membrane, myosin, and microtubules. Their functions include formation of the cortical rigidity, compartmentalization within plasma membrane, formation of the cellular polarity and neurite extension. Especially Septin7 is a core protein of multimeric septin complex because Septin7 belongs to a subgroup which contains only septin7. Septin7 was expressed in the embryonic cochlea (Yoshida et al., 2012) and Foxg1Cre+-Septin7$^{floxed/floxed}$ (Foxg1Cre cKO) mice showed inner ear hypoplasia by the time of embryonic day 13.5 (E13.5) but sensory epithelial cells develop normally until E18.5 (Torii et al., ARO meeting 2014).

Materials and Methods

To identify the roles of Septin7 in inner ear development, we analyzed the phenotypes of Septin7 cKO mice embryos using two different Cre transgenic lines, Foxg1 Cre and Emx2 Cre lines. Cre recombinase starts to work in inner ears from E8.5 in Foxg1 Cre mice and from E13.5 in Emx2 Cre mice. We performed immunohistochemistry to characterize the cell proliferation, apoptosis, neural development and hair cell differentiation from E8.5 to E18.5. We also investigated the macroscopic morphology of the inner ear by paintfilling.

Results

In Foxg1Cre cKO, inner ear macroscopic morphology was normal until E10.5 but the hypoplasiawas found from E11.5. The elongation of endolymphatic duct was poor and the cochlear duct didn't elongate. The significant promotion of apoptosis was detected by immunohistochemistry at E11.5 and cell proliferation was slightly decreased. The apoptosis promotion was found both in the sensory epithelial and the non-epithelial area. These results indicate that Septin7 inhibit apoptosis to promote the inner ear development.

Emx2Cre+-Septin7$^{floxed/floxed}$ (Emx2Cre cKO) mice, which had Septin7 deletion around E13.5, did not show any gross morphological deformity even at E18.5. We couldn't find any obvious difference in the differentiation of sensory epithelia and the innervation of sensory epithelia from auditory neurons between Emx2Cre cKO and control mice at E18.5. These results indicate that Septin7 determines inner ear gross morphology only in the early embryonic stage.

Conclusion

Our results indicate that Septin7 is involved in the establishment of inner ear gross morphology just after the otocyst formation stage mainly by regulating apoptosis of inner ear epithelia.

PS-598

Roles of Hedgehog Co-receptors in the Developing Mouse Inner Ear

Elaine Y.M. Wong[1]; **Helena H. Caro**[2]; **Boshi Wang**[2]; **Yuchen Liu**[2]; **Mai Har Sham**[2]
[1]*The University of Hong Kong, Hong Kong SAR, China;* [2]*Department of Biochemistry and Centre for Reproduction, Development and Growth, Li Ka Shing Faculty of Medicine, The University of Hong Kong, Hong Kong SAR, China*

Human deafness is a relatively common congenital disorder, with approximately 1 in 800 children born with a serious permanent hearing impairment. Although genes involved in deafness have been reported, a large number of human deafness related genes remain to be identified. The development of the inner ear involves complex processes of patterning, morphogenesis and cell fate specification. *Cdo* (Cell adhesion molecule-related, down-regulated by oncogenes) and *Boc* (Brother of Cdo) are two novel receptors of the Hedgehog (Hh) pathway. Mutations in *Cdo* cause holoprosencephaly, a human congenital anomaly defined by forebrain midline defects prominently associated with diminished Hedgehog pathway activity. *Cdo* and *Boc* function as both components and targets of the Hh signalling and feedback network. *Cdo* and *Boc* enhance Shh signalling by acting as co-receptors with *Ptch1,* or via regulation of *Gli* transcription factors. A proper balance of *Gli* repressor and activators is required to mediate Hh signalling druing inner ear morphogenesis.

Cdo or *Boc* homozygous knockout mice have profound hearing loss. However, the roles of *Cdo* and *Boc* in inner ear development are still unknown. To understand the functions of *Cdo* and *Boc* co-receptors in the modulation of Hh signaling in mammalian inner ear development, we present the differential expression pattern of *Cdo* and *Boc* in the developing mouse inner ear and analyse *Cdo* and *Boc* mouse mutant phenotypes. We found that the expression of *Cdo* and *Boc* at E12.5 marks the prospective organ of Corti, but by E16 *Cdo* and *Boc* are down-regulated in cells that will differentiate into hair cells and becomes restricted to supporting cells, suggest that *Cdo* and *Boc* may have distinct roles in molecular pathways that direct cells towards different cell fates in cochlea. Besides, the otic vesicle-derived inner ear structures are under-developed, with reduced proliferation and premature cell cycle exit during prosensory specification and ectopic hair cells formation in the *Cdo* and *Boc* mutants. It is possible that *Cdo* and *Boc* in Hh signaling are required for inhibiting cells from differentiating into hair cells and specifying progenitor cells to generate the distinctly fated cell populations in the inner ear.

PS-599

Fgf10 and Fgf3 in Otic Morphogenesis

Suzanne Mansour[1]; Xiaofen Wang[1]; Edgar Gutierrez[2]; Shumei Shibata[3]; Takahiro Ohyama[4]; Lisa Urness[1]
[1]University of Utah; [2]University of California, Davis; [3]Kyushu University; [4]University of Southern California

The vertebrate inner ear is a morphologically complex sensory organ comprised of two compartments, the dorsal vestibular apparatus and the ventral cochlear duct, required for motion and sound detection, respectively. *Fgf10*, in addition to *Fgf3*, is necessary for the earliest stage of otic placode induction, but continued expression of *Fgf10* in the developing otic epithelium including the prosensory domain, and later in Kolliker's organ, suggests additional roles for this gene during morphogenesis of the labyrinth. While loss of *Fgf10* was implicated previously in semicircular canal agenesis, we show that *Fgf10* heterozygous embryos also exhibit a reduction or absence of the posterior semicircular canal, revealing a dosage-sensitive requirement for FGF10 in vestibular development. In addition, we show that *Fgf10* null mutant embryos have previously unappreciated defects of cochlear morphogenesis, including a somewhat shortened duct, and, surprisingly, a substantially narrower duct. The mutant cochlear epithelium lacks Reissner's membrane and a large portion of the outer sulcus--two non-contiguous, non-sensory domains. Marker gene analyses revealed effects on Reissner's membrane as early as E12.5-E13.5 and on the outer sulcus by E15.5, stages when *Fgf10* is in close proximity to *Fgfr2b*, but these effects were not accompanied by changes in proliferation or cell survival. These data indicate a dual role for *Fgf10* in cochlear development: to regulate outgrowth of the duct and subsequently as a bidirectional signal that sequentially specifies Reissner's membrane and outer sulcus non-sensory domains. These findings may help to explain the hearing loss sometimes observed in LADD syndrome subjects with *FGF10* mutations.

To assess the functions of FGF10 together with FGF3, the other FGFR2b ligand expressed in the developing inner ear epithelium, we have studied *Fgf3/Fgf10* otic conditional mutants generated using Tg-(*Pax2Cre*) and also induced a dominant-negative form of FGFR2b at various times during otic morphogenesis. Our data indicate that epithelial FGF3 and FGF10 are required redundantly to initiate both vestibular and cochlear morphogenesis and that both play ongoing roles in otic morphogenesis. The results of FGF, BMP and SHH signaling marker analyses will be presented.

PS-600

Electroporation-Mediated Transuterine Gene Transfer into Mouse Otocysts (EUGO) utilizing NEPA21 electoroporator

Ryosei Minoda; Hiroki Takeda; Momoko Ise; Takao Yamada; Eiji Yumoto
Kumamoto University, Graduate School of Medicine

Background

Mouse otocysts are an attractive experimental target for developing treatment modalities for congenital inner ear diseases and for studying inner ear development. There is a paucity of reports on successfully induced gene transfer into the otocysts in vivo. We have previously reported that electroporation-mediated gene transfers of the Cx30 gene into the otocysts of Cx30 knock-out mice successfully prevented putative profound hearing loss (Miwa, Molecular therapy, 2013). We previously utilized a CUY21 EDIT electoroporator (Nepa Gene), which generates a single type of pulses. More recently, it has been reported that the NEPA21 electoroporator (Nepa Gene) induces less collaborate damage to tissue and more efficient expression levels in tissue. NEPA21 pulses consist of two types of pules: poring pulses; and, transfer pulses. We can also adjust those attenuation rates. We herein report on survival rates and expression rates after Gene transfer via the NEPA21 on various conditions.

Materials and Methods

Gene transfer was achieved via Electroporation-Mediated Transuterine Gene Transfer into Otocysts (EUGO) as follows. At 11.5 days post-coitum, the uteruses of pregnant mice were exposed by a low-midline laparotomy, placed on a transparent surgical stage and illuminated from below with a fiber-optic beam to identify the location of the otocysts. EGFP plasmid vectors were microinjected into one side of the otocysts. Utilizing the NEPA21, the plasmid filled otocysts were then electroporated under various stimulation conditions. At E13.5, EGFP expression levels in the inner ears were assessed utilizing cryosectioning.

Results

We performed EUGOs to 29 embryos' otocysts. Overall survival rate of embyos was 58.62%. Overall incidence of EGFP expression in treated otocysts was 20%. The survival rates of embryos which underwent poring pulses of 20V or less were relatively higher: 50-100%. Similarly, embyos which underwent lower transfer pulses showed higher survival rates. Regarding expression rates of the treated otocysts, otocysts which underwent 25V of poring pulses showed highest expression rate: 50%. Expression rates of otocysts with 30V and 10V of poring pulses were 0%.

Conclusions

Changes of poring pulses and transfer pulses had effects on survival rates of treated embyos and expression rates in the otocysts. The NEPA21 gives us a chance to change pulse conditions almost infinitely. Determination of optimal conditions of these parameters is necessary for achieving higher survival rates of the embryos and higher expression rates in the otocysts; our target is to elucidate optimal settings.

Funding

Grants-in-Aid for Scientific Research and Grants-in-Aid for Young Scientists

PS-601

Murine "Mini Ears" for High-Content Screening in Hearing Research

Mirko Jaumann[1]; Aurélie Dos-Santos[1]; Marcus Mueller[2]; Hubert Loewenheim[2]
[1]University of Tübingen Medical Center; [2]University of Oldenburg

Mammalian *in vitro* models to study ototoxicity, otoprotection or otoregeneration have utilized inner ear cell lines, tissue culture and to a certain extent whole organ culture. Tissue cultures have a limited application as a validation tool for the increasing number of potential ototoxic and otoprotective agents that arise from the increasing number of screening efforts using inner ear derived cell lines or the zebrafish lateral line. Since cell lines and non-mammalian models for ototoxicity may behave distinct from primary cells in response to drug treatment, we developed an *in vitro* standardized assay for ototoxic drug screening derived from murine organ of Corti progenitor cells, representing "Mini Ears".

We isolated cells from the postnatal day 0 organ of Corti of NMRI mice that are known to give rise to stem cell derived otospheres (Oshima et al., 2007, J Assoc Res Otolaryngol). From these spheres, differentiated epithelial islands - "Mini Ears" - populated with hair- and supporting cell-like cells can be obtained. Primary cells were cultured in a proliferative environment for 5 days in vitro (DIV). The cells were then plated on 96-well plates for differentiation for 14 DIV. "Mini ears" were fixed, immunohistochemically stained, and analyzed using an ImageXpress Micro XLS High-Content Screening microscope (Molecular Devices).

Varying culture conditions and testing markers for hair and supporting cell–like cells, we found reproducible conditions for the generation of "Mini-Ears". This provides a screening platform to conduct "Mini Ear" based high-content screening for ototoxicity, otoprotection, and otoregeneration.

PS-602

Tetratricopeptide Repeat Domain 21b (Ttc21b), a Ciliary Transport Gene and Negative Modulator of Sonic Hedgehog Signal Transduction, is Required for Inner and External Ear Development.

Marcello Peppi; Pamela V Tran; Hinrich Staecker; Dianne Durham
University of Kansas Medical Center

Background

Development of the inner ear is mediated by Sonic Hedgehog (Shh) signaling and its lack in mice causes absence of the cochlear duct and the vestibular ganglia (Riccomagno et al. Genes Dev. 2002). Primary cilia are antenna-like extensions of the plasma membrane that mediate Shh signaling. So far, primary cilia have not been implicated previously in ear development. *Tetratricopeptide repeat domain 21b* (*Ttc21b*), a ciliary gene frequently mutated in ciliopathies, genetic syndromes with underlying ciliary dysfunction, represses Shh signaling during CNS development (Tran et al, Nature Genetics, 2008). Our central hypothesis is that *Ttc21b* regulates Shh signaling during the development of the inner ear. In this study, we investigated *Ttc21b* expression and inner ear development using a *Ttc21b* developmental mouse mutant, called *alien*.

Methods

To examine expression of *Ttc21b* in the inner ear during mouse development, whole mount LacZ staining was performed at E13.5-E17.5 and 50µm cryostat sections were observed with a light microscope. For histological analysis, 5um serial sections of E13.5 and E17.5 embryo heads were obtained and stained with haematoxylin and eosin (H&E) and observed with a light microscope. For scanning electron microscopy, E17.5 old embryos were fixed in 1.5% paraformaldehyde and 2.5% glutaraldyde, critical point dried, sputter coated, and observed with a high-resolution scanning electron microscope.

Results

By E13.5, *Ttc21b*-LacZ staining was strongly observed in the vestibulocochlear, trigeminal, and glossopharyngeal ganglion. Less intense staining was observed in the cochlear duct in the region of spiral ganglion and below the organ of Corti and in the inner ear capsule. LacZ staining was also observed in the pinna of the ear. H&E serial sections of E16.5 *Ttc21b* mutant embryos showed disorganization of the cochlea, lack of spiral ganglion neurons and organ of corti, and detachment of the neuroepithelium from the cochlear canal wall. Scanning electron microscopy of the external ear revealed a hypoplastic pinna and loss of tissue within the preauricular area near the external auditory meatus.

Conclusions

Our observations demonstrate that *Ttc21b*, which negatively regulates Shh signaling, is required for both inner and external ear development, suggesting that enhanced Shh activity is detrimental to ear development.

PS-603

Hierarchal Interactions between Biochemical and Topographical Physical Cues in Guidance of Neurites from Spiral Ganglion Neurons

Kristy Truong[1]; Braden Leigh[2]; Mark Ramirez[2]; Reid Bartholomew[2]; Allan Guymon[2]; Marlan Hansen[2]
[1]University of Iowa Hospitals and Clinics; [2]University of Iowa

Introduction

Spiral ganglion neuron (SGN) growth cones respond to both biochemical and topographical physical cues, determining the ultimate trajectory of neurite growth. To understand the hierarchal relationships of biochemical and topographic cues on SGN neurite pathfinding, we used the precision afforded by photochemistry to establish precise, competing biochemical and topographic patterns.

Methods

Photopolymerization of acrylate solutions using photomasks of specified periodicities created topographical micropatterns consisting of parallel ridges and grooves. Similarly, photo-induced thiol-ene click chemistry was used to covalently bind

laminin (LN) to acrylate polymer surfaces in precise patterns specified by the photomask. By first creating topographical micropatterns and then rotating the photomask 90 degrees, we created a competition assay with laminin (LN) stripes perpendicular to physical micropatterns. Dissociated rat SGN cultures were plated on smooth substrates with LN micropatterns or on topographical micropatterns with perpendicular LN stripes. We varied the periodicity (10-50 µm) or amplitude (1.5-8 µm) of the micropattern to change the strength of the physical cues to determine the point at which topographical cues prevail over biochemical cues. Neurite alignment was measured as a distribution of angles relative to the horizontal plane of 10 µm neurite segments.

Results

Neurite outgrowth was random on unpatterned surfaces. Micropatterned surfaces of low amplitude and high periodicity induced moderate alignment. On smooth surfaces, neurites strongly aligned to unidirectional LN stripes and were able to partially track complex multidirectional LN patterns of alternating 90-degree angles. On surfaces with competitive LN stripes perpendicular to high periodicity topographical micropatterns, neurites strongly aligned to the LN stripes. As the periodicity of the topographical micropattern decreased, a significantly greater portion of the neurites aligned to the physical features. Likewise, increased amplitude resulted in greater alignment to physical features. Finally, we characterized the point at which a neurite transitions from a feature. We found that 40% of neurites that transition from LN do so at the edge of a ridge and into a groove. In contrast, 25% of neurites transition from a physical feature and follow laminin at the edge of a ridge.

Conclusions

We explored hierarchal relationships between biochemical and physical guidance cues by creating LN stripes perpendicular to topographical micropatterns with varying periodicity or amplitude. Biochemical cues dominate at high periodicity or low amplitude topographical microfeatures. Physical cues dominate neurite pathfinding as the periodicity decreases or amplitude increases.

PS-604

The Regional Organization of Ribbon Synapses in Developing Rat Inner Hair Cells

Radha Kalluri

University of Southern California

Introduction

In adult mice, ribbons opposing low spontaneous rate (SR) auditory afferents are smaller than those opposing high-SR afferents and are regionally organized with larger ribbons located on the basal-modiolar face of the hair cell and small ribbons located on the apical/pillar face. Ribbon size correlates with other properties of auditory neurons and may contribute to the functional distinction between SR groups. As a first step toward understanding the role played by these morphological and other biophysical properties in shaping SR-groups, this study examines whether a regional organization of synaptic ribbons of different sizes is found early post-natal animals before the onset of hearing. Our long-term goal is to understand how the biophysical and anatomical properties of auditory neurons shape their responses.

Methods

Synaptic ribbons were identified by immuno-labeling for c-terminal binding protein 2 (CtBP2) from the middle cochlear turn in post-natal (P) day 3, 6, 9, 12 and 14 rats. In some preparations antibodies to GluR2/3 (labels post-synaptic glutamate receptors) and myosin VI (labels haircells) were also used to further define the relative spatial organization of ribbons and their partner structures. Scan direction, sample mounting direction, and scan duration were carefully varied as methodological controls. Three dimensional reconstructions and volumetric analysis of ctbp2, GluR2/3, and myosin VI fluorescent labels were performed on high resolution confocal z-stacks. The organization of ribbon within inner haircells was analyzed using custom programs in Matlab.

Results

At P3 and P6 most inner hair cell ribbons were segregated towards the modiolar face and densely packed below cell, few ribbons were found on the pillar face. By P9 the average number of ribbons per haircell was reduced and ribbons could be found on both the modiolar and pillar face of the haircell. 3D reconstructions from z-stacks yielded volume estimates for each ribbon. Ongoing volumetric analysis will examine if ribbons are spatially organized according to size.

PS-605

Acrux: Analysis Software for Detecting and Analyzing Hair Cell Planar Polarity Phenotypes

Michael Deans[1]; **Andrew Francl[2]**; Michelle Stoller[1]

[1]University of Utah; [2]Boston College, University of Utah

Hair cell planar polarity is evident in the organization of the stereociliary bundle and the coordinated orientation of bundles between neighboring hair cells. Many key planar polarity genes and signaling pathways have been identified through phenotypic analyses of auditory planar polarity. In contrast, evaluating polarity defects in the vestibular system is more difficult because of the range of bundle orientations that occur throughout the maculae and because vestibular hair cells are not arranged in rows. Current approaches in both systems also lack quantifiable measures of shared alignment that could be used to compare phenotypic severity between mutant lines.

We have developed image analysis software called Acrux that is capable of identifying stereociliary bundle orientation for large-scale, quantitative planar polarity phenotyping. Analysis is based upon immunofluorescent labeling of the hair cell cuticular-plate and basal body of the kinocilium. Acrux adaptively thresholds the cuticular-plate signal to find prominent features and filters these features based on size and shape. The center of each hair cell is then determined based on the image moment, a weighted average of the pixel intensity and location. To detect basal bodies, Acrux creates an image histogram and determines the threshold point that most effec-

tively separates pixel intensities into a bimodal distribution. Objects within the thresholded image are filtered for size and the center of each basal body is identified using minimum spanning circles of the remaining objects.

Acrux annotates stereociliary bundle orientation using a vector extending from the center of the hair cell to the center of the basal body. Bundle orientation is measured using these vectors and user-defined reference lines drawn parallel to the maculae border. This allows individual measurements to be cumulated on circular histograms for different samples, regions or genotypes. Acrux also measures the difference in bundle orientation between nearest-neighbors and uses these pair-wise analyses to calculate an Alignment Coefficient for measuring phenotype severity in individuals or genotypes. The Coefficient is a Sine value ranging from '0' to '1', and is a direct measure of Planar Polarity organization in which an Alignment Coefficient of '1' indicates perfect alignment. Acrux has been validated by analyzing Vangl2 knockouts and can be used to analyze any mutant line. We anticipate that Acrux software will facilitate large-scale phenotyping of vestibular hair cell mutants and provide quantitative measures for assaying genetic interactions between planar polarity candidate genes and signaling pathways.

PS-606

Lgr6 is a Novel Marker of Developing Inner Pillar Cells

Lina Jansson[1]; Renjie Chai[2]; Jessica Shen[1]; Elvis Najarro[1]; Duc-Huy Nguyen[1]; Alan Cheng[1]

[1]Stanford University; [2]Southeast University Nanjing

Introduction

Wnt signaling regulates numerous processes throughout inner ear development, including patterning of otocyst, vestibular morphogenesis and cell fate specification and patterning of the cochlea. This complex pathway mediates cell-cell communication via numerous secreted Wnt proteins. Wnt signaling is also modulated by R-spondins which act as co-activators of the pathways. In particular, R-spondin 2 is expressed in the greater epithelial ridge of the late embryonic cochlea and may play a role in hair cell patterning. The leucine-rich repeat containing G protein (Lgr) coupled receptor subfamily of receptors has three known members that bind R-spondins with different affinities. Among these, Lgr5 broadly marks prosensory cells in the embryonic cochlea in addition to supporting cells and the greater epithelial ridge in the neonatal cochlea. The expression of other members of the LGR subfamily of receptors is currently unknown. The current study aims at characterizing the spatiotemporal expression of Lgr6.

Methods

Cochleae from E14.5 to P8 wildtype CD1 mice were examined as whole mounts and sections. In situ hybridization of oligonucleotide RNA Scope© probes was used to detect Lgr6 mRNA. An Lgr6-EGFP-IRES-CreERT2 reporter mouse was further used to validate the expression pattern together with immunostaining of cochlear hair and supporting cell markers.

Results

In the embryonic cochlear duct, Lgr6 mRNA is localized to developing inner pillar cells in a basal-apical gradient. Its expression co-localizes with the pillar cell marker p75NTR and also supporting cell markers Jagged1 and Sox2. Outside the cochlear duct, gene expression is found in the lateral wall and also in the tympanic border cell region. In the postnatal cochlea from Lgr6-EGFP-IRES-CreERT2 reporter mouse, EGFP remains localized to inner pillar cells, tympanic border cells, and lateral cochlear wall, although EGFP expression was most robust in inner pillar cells. In situ hybridization of wildtype cochlea detected an identical expression pattern of Lgr6 in the postnatal cochlea at P0 and P8.

Conclusion

The LGR family member Lgr6 is dynamically expressed in the embryonic and neonatal cochlea. In the organ of Corti, its expression is specific to the developing inner pillar cells. Thus, using the Lgr6 expression as a marker can facilitate the isolation and cell-specific manipulation of inner pillar cells in the developing cochlea.

PS-607

Expression of Id Genes in Developing Cochlear Epithelium

Susumu Sakamoto[1]; Tomoko Tateya[2]; Yukiko Harima[3]; Juichi Ito[4]; Ryoichiro Kageyama[3]

[1]Kyoto University; [2]Institute for Virus Research; [3]Institute for Virus Research, Kyoto University; [4]Department of Otolaryngology - Head and Neck Surgery, Kyoto University Graduate School of Medicine

The family of inhibitor of differentiation and DNA-binding (Id) proteins, including Id1 to Id4, is a group of evolutionarily conserved molecules, which play important regulatory roles in organisms ranging from Drosophila to humans. Id proteins are small polypeptides harboring a helix-loop-helix (HLH) motif, which are known to mediate dimerization with other basic HLH proteins, primarily E proteins. Because Id proteins do not possess the basic amino acids adjacent to the HLH motif necessary for DNA binding, Id proteins inhibit the function of heterodimers between E proteins and tissue-specific bHLH proteins. The bHLH factor Atoh1 is known to be negatively regulated by Id proteins in developing inner ear. However, the roles of Id proteins in the growth and differentiation of the cochlear epithelium during development are not fully elucidated. The purpose of this study is to clarify the spatiotemporal expression pattern of Id proteins in the developing mouse cochlea as the first step in investigating the functions of Id family members in the cochlea. The expression of Id1-4 in developing cochlear epithelium was examined by in situ hybridization and compared the expression pattern to markers of the prosensory domain (p27kip1, Jag1, Hey2, Fgf10 and Bmp4) and the early hair cells (Atoh1). At E13.5 Id1 and Id3 were expressed weakly in the p27-positive prosensory domain and more intensely in the Bmp4-positive population located more strial to the p27-positive prosensory domain, whereas broad expression of Id2 was observed in both of the greater epithelial ridge and the lesser epithelial ridge. Id1 and Id3 expression

was seen in both of the greater epithelial ridge and the lesser epithelial ridge at E15.5 and diminished at E17.5. At E13.5 Id4 expression was observed in the epithelial cells located more strial to the Bmp4-positive cells and at E15.5 Id4 was expressed weakly on the floor and more intensely on the lateral wall of cochlear duct. The results of this study further consolidate our understanding of bHLH genes and suggest that there are additional, undiscovered roles for Id proteins in cochlear development.

PS-608

Conditional Deletion of ATOH1 in the Mouse Inner Ear Establishes a Novel Model System to Study Therapeutic Gene Transfer to Treat Congenital Deafness

Lingyan Wang; Han Jiang; **John Brigande**
Oregon Health & Science University

Background

Atonal homolog 1 (ATOH1) is a basic helix-loop-helix (bHLH) transcription factor required for sensory hair cell differentiation. ATOH1 knockout mice failed to produce sensory hair cells and misexpression of *Atoh1* in the embryonic and postnatal inner ear generated new hair cells. We conditionally knocked out ATOH1 in the inner ear as a model system to define therapeutic gene transfer strategies to treat congenital deafness. Scleraxis (Scx) is a bHLH transcription factor expressed in the nascent otic vesicle. We generated an ATOH1 conditional knockout mouse (ATOH1 CKO) using transgenic scleraxis Cre (*Tg*(*Scx-Cre*) to delete floxed ATOH1 (*ATOH1$^{f/f}$*) in the inner ear. Electroporation- and virus-mediated gene transfer of *Atoh1* was used to define temporal and spatial constraints on efficacious gene replacement therapy.

Methods

T*g(Scx-Cre)* and *Atoh1$^{f/f}$* mice were bred to produce the ATOH1 CKO mice (*Tg(Scx-Cre)::Atoh1$^{f/f}$*). Histological and immunohistochemical methods assessed inner ear morphology and patterning in the auditory and vestibular sensory epithelia. *In situ* hybridization was performed to assess *Atoh1* expression. Electroporation- and virus-mediated gene transfer of *Atoh1* was conducted at embryonic day 12.5 (E12.5) and inner ear phenotype was evaluated at both embryonic and postnatal time points. Auditory and vestibular function were tested at adult stages.

Results

Tg(Scx-Cre)::Atoh1$^{f/f}$ mice thrive into adulthood and breed; display head bobbing and circling behavior; and have no detectable auditory brainstem response (ABR). The inner ear is grossly morphologically normal though the width of the organ of Corti is reduced. No ATOH1 mRNA was detected by in situ hybridization and no hair cells were identified in the auditory or vestibular sensory epithelia. Spiral ganglion cell loss was observed though neural projections to the putative cochlear sensory epithelium remain.

Electroporation- and virus-mediated gene transfer of *Atoh1* to the E12.5 mutant otocyst produced Myo7A-positive cells with stereociliary bundles in both auditory and vestibular sensory epithelia. Auditory thresholds at 4, 8, 16, and 32 kHz were detected in ATOH1 CKO mice after virus-mediated gene transfer of Atoh1 while vestibular function was not significantly improved.

Conclusion

We have established an ATOH1 CKO mouse that thrives into adulthood permitting quantitative measure of auditory and vestibular function after therapeutic manipulation in utero. Initial gene transfer efforts demonstrate partial restoration of auditory thresholds after virus-mediated gene transfer of *Atoh1* to the E12.5 otocyst. This model system will enable us to address questions involving the necessary cytoarchitecture required to restore auditory function as well as the temporal requirement for Atoh1 efficacy.

PS-609

Cooperation of Islet1 and bHLH Transcription Factors during Inner Ear Development

Iva Macova; Romana Bohuslavova; Tetyana Chumak; Josef Syka; Gabriela Pavlinkova
Academy of Sciences of the Czech Republic, Prague

Introduction

Three precursor populations are generated in the inner ear: neuronal precursors forming only neurons; prosensory precursors forming only sensory epithelia; and neurosensory precursors forming neurons, and also hair cells and supporting cells of sensory epithelia. The kind of cells that are generated depends on the cooperation of transcription factors and their temporal and spatial expression. LIM-homeodomain transcription factor ISLET1 is expressed in the common precursors. However, the role of ISLET1 and its interactions with other specification factors during the development of the inner ear is still unclear. Our primary goal is to analyze the interactions of ISLET1 with basic helix-loop-helix (bHLH) neurosensory specification factors, ATOH1 and NEUROD1. ATOH1 is an important transcription factor for the formation of the sensory epithelia, whereas proneural factor NEUROD1 plays a key role during development of the spiral and vestibular ganglia. *Atoh1* or *Neurod1* deletion causes neonatal death as their expression is essential for postnatal survive of vital organs.

Methods

We used mice with targeted *Cre* recombinase gene into the *Islet1* locus in one allele (Isl1-Cre/+) and *Atoh1* and/or *Neurod1* gene flanked by loxP sites (Atoh1$^{flox/flox}$; Neurod1$^{flox/flox}$) to obtain mice with conditional deletion of *Atoh1* and/or *Neurod1*. Using LacZ staining, immunohistochemistry, *in situ* hybridization, and qPCR methods, we analyzed gene expression during inner ear development in wild type and transgenic mice. We also measured the function of the inner ear by auditory brainstem response (ABR) and distortion-product otoacoustic emission (DPOAE) recording.

Results

The mice with *Neurod1* conditional knockout were viable and indistinguishable from wild type mice; however, they suffered from a mild form of diabetes mellitus. These mice had significantly elevated ABR thresholds compared to the wild type

animals with relatively intact DPOAEs, suggesting primary defect in development of neuronal part of the inner ear. Furthermore, we detected inner ear cell disorganization in the organ of Corti in the mice with *Atoh1* conditional knockout.

Conclusion
Our data suggest that the transcription factor ISLET1 cooperates with ATOH1 and NEUROD1 during inner ear development and that ISLET1 is an important specification factor for neurosensory development in the inner ear.

PS-610

Neurog1, Expressed Instead of Atoh1, Can Differentiate and Maintain Hair Cells

Israt Jahan; Ning Pan; Jennifer Kersigo; Bernd Fritzsch
University of Iowa

Atoh1, a basic helix loop helix transcription factor (bHLH TF), is essential for the differentiation of hair cells (HCs), the mechanotransducers that convert sound into auditory signals in the mammalian organ of Corti (OC). Without Atoh1, the OC becomes a featureless, flat epithelium. Overexpression of Atoh1 causes formation of ectopic HCs in the non-sensory region supporting the importance of Atoh1 for HC development. However, replacing Atoh1 with the fly ortholog *atonal* rescues HC differentiation indicating replacement of Atoh1 by other bHLH genes is possible. We previously showed that replacing Atoh1 with another bHLH TF, Neurog1, cannot rescue hair cell differentiation (Jahan et al. PlosOne, 2012). We now report that Neurog1 insertion in one allele combined with a floxed allele of Atoh1 that is removed using 'self-terminating' Atoh1-Cre (Atoh1-Cre; $Atoh1^{f/kiNeurog1}$) can rescue hair cell differentiation.

The Atoh1-Cre; $Atoh1^{f/kiNeurog1}$ mice lead to significantly increased formation of HCs, both inner (IHCs) and outer (OHCs) in comparison to the more severe and earlier HCs loss in 'self-terminating' Atoh1 conditional null mouse (Pan et al., 2012). In particular, misexpression of Neurog1 maintains and prolongs the longevity of IHCs of the OC. Despite Neurog1 results in quantitative improvement of HCs survival, qualitatively the rescue is incomplete. Fgf8, an essential factor for supporting cell (SC) development, is reduced in this mutant, resulting in topologically inappropriate SCs formation: some Inner Pillar cells are converted into HC demonstrated by ectopic stereocilia in the apical surfaces. Neurog1 misexpression also alters Jag1 and Hes1/5 expression pattern, thereby interfering with cell-cell interactions and disrupting the HCs/supporting cells mosaic. In addition, IHCs develop stereocilia bundles of OHCs indicating a correlation of Fgf8 level with 'IHC' specification, previously demonstrated for Neurod1 mutant mice. Nevertheless, this study shows for the first time that replacement of Atoh1 with the pro-neuronal gene Neurog1 can rescue HCs, but only if combined with a transient expression of Atoh1. These data indicate that HC developing gene networks can be driven by other bHLH TFs'.

Further, we compare the role of Neurod1, as a downstream of Neurog1 in rescuing the HCs by analyzing another complex mutant with Neurog1 misexpression in the absence of Neurod1. It provides a novel approach to molecularly dissect the development of the OC through modulating the intracellular gene network. The outcome of this approach will provide an understanding for the complex intrinsic and extrinsic gene regulation to reconstruct the functionally essential cellular mosaic of the OC.

PS-611

Biochemical and Electrical Coupling in Non-Sensory Cell Networks of the Developing Mammalian Cochlea

Federico Ceriani; Fabio Mammano
Università degli Studi di Padova

Nonsyndromic hearing loss and deafness (DFNB1) is an inherited condition caused by mutations in GJB2 (which encodes connexin26) and GJB6 (which encodes connexin30). Electrical and metabolic coupling mediated by gap junction channels formed by these two protein subunits is fundamental for the development and maintenance of hearing (Anselmi et al. 2008 PNAS 105:18770-5, Schutz et al. 2010 Hum Mol Genet 19:4759–4773, Majumder et al. 2010 Purinergic Signal 6:167–187). However, precise estimates of the degree of coupling and its alterations under DFNB1 conditions are lacking. In this work, we combined large scale optical recordings, single cell electrophysiology and computer simulations to elucidate the mechanisms that underlie intercellular communication in cochlear non-sensory cells from juvenile mice (first postnatal week).

First, we developed a novel technique based on voltage imaging to map the extent and the degree of electrical coupling in cochlear non-sensory cells, which permitted us to rapidly discriminate network connectivity of wild type mice from that of genetically modified connexin30(T5M/T5M) and connexin30(−/−) mice. By comparing our experimental results with numerical simulations, we estimated that cochlear non-sensory cells are already well coupled in the first postnatal week by as many as ~1500 channels per cell pair in wild type animals. In cultures from age-matched connexin30(T5M/T5M) and connexin30(−/−) mice, junctional conductance was reduced respectively by 14% and 91%, and these data account for the increased hearing thresholds exhibited by these animals in the adult stage (Schutz et al. 2010 Hum Mol Genet 19:4759–4773, Teubner et al. 2003 Hum Mol Genet, 12:13–21) .

Furthermore, cochlear gap junction channels and hemichannels have been shown to participate in ATP- and IP_3-dependent intercellular Ca^{2+} signalling (Anselmi et al. 2008 PNAS 105:18770-5 , Majumder et al. 2010 Purinergic Signal 6:167–187). We thus performed Ca^{2+} imaging experiments aimed at elucidating the mechanisms underlying the generation and intercellular propagation of Ca^{2+} signals in cochlear non-sensory cells. We determined that ATP- and IP_3- dependent Ca^{2+} oscillations can occur at constant intracellular IP_3 concentration. We finally combined the information gathered from the different experimental approaches in a mathematical model that (i) correctly reproduces the range and propagation

speed of intercellular Ca^{2+} waves (ii) reproduces the oscillatory behaviour of intracellular Ca^{2+} signals (iii) predicts that ATP release through connexin hemichannels is the primary mechanism responsible for the long range propagation of Ca^{2+} signals in the developing mouse cochlea.

PS-613

The Calcium Activated Chloride Channel TMEM16A Controls Spontaneous Activity in the Developing Auditory System

Han Chin Wang[1]; YingXin Zhang[1]; Rocky Cheung[1]; Jason Rock[2]; Dwight Bergles[1]

[1]Johns Hopkins University School of Medicine; [2]University of California, San Francisco

Before the onset of hearing, inner supporting cells (ISCs) within Kölliker's organ exhibit spontaneous inward currents that are associated with cell shrinkage (crenation). Previous studies have shown that this activity is initiated by the spontaneous release of adenosine triphosphate (ATP) from ISCs themselves, but the molecular mechanisms responsible for generating both the currents and crenations, and the relationship between these two phenomena, have remained elusive. Here we report that both forms of spontaneous activity were reduced when phospholipase C was inhibited or when intracellular Ca^{2+} was chelated, suggesting that these events arise primarily from the activation of metabotropic purinergic P2Y receptors that induce mobilization of Ca^{2+} from intracellular Ca^{2+} stores. Ion substitution experiments revealed that the P2Y receptor-mediated rise in Ca^{2+} activates a Cl^- conductance, and that the resulting Cl^- efflux is responsible for the majority of spontaneous inward currents in ISCs. Using both RT-PCR, *in situ* hybridization and analysis of GFP knock-in mice, we determined that the Ca^{2+}-activated Cl^- channel TMEM16A is expressed by ISCs in the prehearing cochlea and that the developmental sequence of TMEM16A expression closely matches the developmental progression of spontaneous crenations in ISCs. Both spontaneous currents and crenations in ISCs were inhibited by TMEM16A-specific pharmacological inhibitors, and genetic removal of TMEM16A (both conditional: Pax2-Cre;$TMEM16A^{f/f}$ and knockout: $TMEM16A^{-/-}$) markedly reduced both currents and crenations in ISCs, without affecting spontaneous ATP-induced Ca^{2+} transients in Kölliker's organ, indicating that ATP release and purinergic receptor expression were intact. The periodic Cl^- efflux through TMEM16A explains the close link between the ISC currents and crenation, as studies in epithelia have shown that Cl^- flux is accompanied by the movement of water to maintain osmotic balance. TMEM16A also appears to play an essential role in triggering periodic excitation of surrounding inner hair cells (IHCs) by promoting the efflux of K^+, which is released from ISCs to maintain electroneutrality during Cl^- efflux. In TMEM16A null mice, spontaneous inward currents in inner hair cells (IHCs) are substantively reduced and fewer IHCs participate in each spontaneous event. Together, these studies identify the first molecular component of the pathway used by ISCs to control spontaneous activity in the developing cochlea, and provide a new genetic strategy for determining the roles of supporting cell-induced spontaneous activity in the development of the auditory system.

PS-614

Exploring the Neonatal Organ of Corti at Single Cell Resolution

Joerg Waldhaus; Robert Durruthy-Durruthy; Stefan Heller

Stanford University

The organ of Corti harbors an array of highly ordered sensory hair cells and supporting cell types, organized in rows along the baso-apical axis. Although different cell types within the organ of Corti have been classified mainly based on morphology, relative position and function, little is known about their molecular profiles. The aim of this study is to identify and characterize inner and outer hair cells as well as the various sensory supporting cell types using a combination of five different transgenic reporter mice, fluorescence activated cell sorting, and single cell multiplex quantitative RT-PCR using the Fluidigm Biomark HD platform. We used neonatal tissue (P2) and Cre drivers for Fgfr3 and Glast1 in combination with mice expressing GFP under the control of endogenous Sox2 and Lgr5 promoters as well as an Atoh1-enhancer reporter mouse model. Primer pairs for 192 genes represent a preselected array of cell type specific marker genes complemented by signaling pathway related ligand, receptor and effector genes.

Computational mathematic analysis of the resulting mRNA expression profiles of different organ of Corti cells allowed us to reconstruct the neonatal organ of Corti *in silico*. Based on the marker gene expression we successfully identified populations of cells representing inner hair cells, outer hair cells, Deiters' cells, pillar and inner phalangeal cells. Besides confirming cell type-specific expression of known marker genes we identified new markers and highly specific combinatorial gene identifiers for these cell types. Analysis of the single cell type gene expression profiles for various pathways provided insights into cell type specific regulation of Notch-, SHH-, WNT-, FGF- and BDNF-pathways.

The results of this study will add to our understanding of the dynamic regulation of organ of Corti maturation and may help to develop new strategies in the field of hair cell regeneration, particularly in comparison with similar profiling conducted in the adult organ of Corti.

PS-615

Transcriptome Analysis in Developing Otic Neuroblasts in a Mouse Model System

Miho Matakatsu[1]; Akira Imamoto[2]; John A. Kessler[3]; Himanshi Desai[4]; Joel B. Fontanarosa[1]; Akihiro Matsuoka[4]
[1]Northwestern University Feinberg School of Medicine; [2]Ben May Department for Cancer Research, The University of Chicago; [3]Department of Neurology and Pharmacology, Northwestern University Feinberg School of Medicine; [4]Department of Otolaryngology –Head and Neck Surgery, Northwestern University Feinberg School of Medicine

Introduction

While developmental programs that commit a subset of cell types during vertebrate otic neuronal development have been well elucidated over the course of the last 50 years, it is still difficult to define and analyze the precise molecular mechanisms in unique neuronal precursors versus benign cell populations. For this purpose, we used next generation sequencing to characterize gene expression profiles in an early developing otocyst in a mouse model system. Pooled cell genetic analyses mask rare cell type-specific transcriptomes derived from a population of heterogeneous cells. In this study, we used a microfluidic cell isolation technique to conduct a transcriptome analysis at the single-cell level.

Methods

We microdissected and isolated a pair of otocysts from a single embryo at the embryonic age 9.5 (E9.5) and 10.5 (E10.5). The otocyst cells were dissociated in cell dissociation agents and single-suspended cells were captured in the microfluidic integrated fluidic circuit (IFC) on the C1 system (Fluidigm). A 50bp single-end reads RNA-seq was carried out on the Illumina HiSeq 2500 for individual cDNA libraries. A pair of E8.5 otic placodes was used for a cDNA library construction. An RNA-seq experiment was performed similarly.

Results

Our preliminary result indicated that 12 minutes of Accumax + 0.03% Trypsin would yield 93% of surviving cells with Trypan blue staining. We'll discuss a temporal measurement of co-expressing genes in spatially defined neuroblasts.

Conclusions

Discovering regional genetic cell identities with single cell resolution constitutes a useful tool to address subsequent molecular mechanisms in developing neuronal cell populations. The information that we will obtain from this study will provide guidance in re-programming induced pluripotent cells for neuronal differentiation.

PS-616

The Role of the Lin-41/Let-7 Axis in Sensory Progenitor Proliferation and Auditory Hair Cell Differentiation

Lale Evsen; Angelika Doetzlhofer
Johns Hopkins School of Medicine

The auditory sensory organ is required for our ability to hear. This function is mediated by specialized mechanotransducing hair cells (HC) and their associated supporting cells (SC). Proper timing of differentiation is critical for coordinated development and function of the inner ear auditory organ; however, little is known about the molecular mechanisms that regulate growth and differentiation. Here, I am addressing the role of the evolutionary highly conserved heterochronic gene Lin-41 (Trim71) in auditory HC development in both the murine and avian inner ear. Lin-41, as well as its negative regulator Let-7 was initially identified in a screen for heterochronic genes in C-elegans. Let-7 miRNAs are a differentiation-promoting class of miRNAs, whereas Lin-41, an ubiquitin ligase and RNA-binding protein, plays a critical role in stem cell maintenance and proliferation. Based on my preliminary data, I hypothesize that Lin-41 plays an important role in neuro-sensory cell proliferation through opposing Let-7 miRNAs. I conducted Lin-41 and Let-7 gain-of-function studies to determine their function in sensory progenitor proliferation and differentiation. To do so, I conducted in ovo micro-electroporations in chicken combined with in ovo EdU cell proliferation assays. Expression pattern analysis revealed that Lin-41 is expressed at early developmental stages cE4.5 and mE9-mE13.5 in the avian and murine inner ear respectively, specifically within the neural-sensory competent domain of the otic vesicle, in delaminated neuroblasts of the cochleo-vestibular ganglion, the spiral ganglion, and quickly declines upon HC differentiation. This is in contrast to the increasing Let-7 levels in differentiating HC and SC. Over-expressing Let-7b in the avian cochlea leads to decreased sensory progenitor proliferation, loss of the sensory epithelium, and an absence of the spiral ganglion. In contrast, over-expressing Lin-41 leads to increased proliferation with no onset of HC differentiation, and down-regulation of Cath1 (Atoh1). Ongoing experiments are focused on identifying specific molecular mechanisms of the Lin-41/Let-7 axis in regulation of neuro-sensory proliferation and differentiation.

PS-617

Role of the ELMOD Family Members in the Inner Ear Development and Function

Elodie Richard[1]; Sarah E. Mahl[2]; Zubair M. Ahmed[3]; Saima Riazuddin[3]
[1]University of Maryland, Baltimore; [2]Division of Pediatric Otolaryngology Head & Neck Surgery, Cincinnati Children's Hospital Medical Center; [3]Department of Otorhinolaryngology Head & Neck Surgery, School of Medicine, University of Maryland, Baltimore

Background

Recently, our group identified a new mutation in *ELMOD3*, segregating with pre-lingual, nonsyndromic, moderate to profound sensorineural hearing loss, DFNB88. The implication of other ELMOD (Engulfment and cell motility domain) family members in hearing was reported through evaluation of two spontaneous *Elmod1* mutant mice. The purpose of this study is to decipher the role of ELMOD family members in the development and physiology of the inner ear.

Methods

Fluorescently tagged constructs were used to compare the localization of each ELMOD family member, *in vitro*. We also generated knockout mouse models for *Elmod2* and *Elmod3*.

The expression pattern of both genes was determined in the inner ear, using Beta-Gal staining. Auditory evaluation was performed with auditory brainstem response (ABR) and distortion oto-acoustic emission (DPOAE) testing.

Results

In the mouse inner ear, *Elmod2* and *Elmod3* are expressed in all cells of the sensory epithelia. These results contrast with the hair-cell-only expression pattern of *Elmod1*. Fluorescently tagged ELMOD3 protein is targeted to the actin-base structures of hair cells in cochlear explant, while ELMOD2 remains in the cytoplasm of mechanosensory hair cells. Similarly, in CL-4 cells and COS7 cells, ELMOD3 targets to the actin-rich microvilli on the cell surface while ELMOD2 signal is diffused in the cytoplasm. Double and triple transfections of ELMOD1, ELMOD2 and ELMOD3 tagged constructs revealed distinct compartmentalization of all three proteins within MDCK cells. RT-PCR studies demonstrate that the expression of *Elmod3* and *Elmod2* were abolished in the respective mutant mice. ABR and DPOAE testing of the knock out mice showed diverging results compared to the published hearing profile of *Elmod1* mouse model.

Conclusions

Taken together, our *in vitro* and *in vivo* data suggest different roles for the ELMOD family members at the cellular level and more particularly in the hair cells of the inner ear. While the absence of *Elmod1* results in early onset hearing loss in mice, further evaluation of the auditory apparatus of *Elmod3*^{ko} and *Elmod2*^{ko} mouse models is warranted to understand the role of these proteins in the inner ear function.

PS-618

The Toxic Effects of Sphingosine and an Sphingosine Kinase Inhibitor on the Rat Cochlea

Kohsuke Tani; Keiji Tabuchi; Masahiro Nakayama; Chi Le Nguyen Uyen; Akira Hara
University of Tsukuba

The sphingolipid is a generic term of complex lipids, which contain the organic aliphatic amino alcohol such as sphingosine (Sph). Sphingolipids not only act as a cell structure component but play multiple roles in physiological functions, such as apoptosis, cell growth arrest, differentiation, migration, and adhesion. Ceramide (Cer), composed of Sph and a fatty acid, is converted to Sph by ceramidase. Sph is, in turn, phosphorylated to sphingosine-1-phosphate (S1P) by sphingosine kinase (Sk). Based on the previous report, balances between Cer and S1P are thought to be important for determination of hair cell fate. Sk is reportedly over expressed in various cancer cells, therefore pharmacological Sk inhibition has been focused for anti-tumor therapy. In addition, combination of Sk inhibitors and diverse anti-tumor drugs including cisplatin (CDDP) has been attempted in various cancer cell lines to increase toxicity for tumor cells. However the effects of an Sk inhibitor and Sph on cochlear hair cells have not been known. In addition, the effects of co-administration of an Sk inhibitor and CDDP on hair cells have not been investigated. The present study therefore investigated 1) the expression of Sk in the rat cochlea, 2) the effect of CDDP on Sk activity in the cochlea, 3) the effect of an Sk inhibitor or Sph on cochlear hair cells, and 4) the effect of co-administration of an Sk inhibitor or Sph and CDDP on hair cell death. The cochlea was dissected from Sprague-Dawley rats on postnatal days 3 to 5. Basal turn organ of Corti explants were exposed to 5 μM CDDP for 48 h with or without an Sk inhibitor or Sph. Both Sk1 and Sk2 were expressed in the normal cochlea. Compared with non-CDDP exposed samples, 5 μM CDDP significantly increased Sk activity at 48 h. An Sk inhibitor itself caused hair cell loss at a high concentration, and at lower concentrations it enhanced CDDP-induced hair cell loss. Sph itself also induced hair cell death and increased hair cell loss induced by CDDP. An Sk inhibitor and Sph induced the cleavage of caspase 3 in the organ of Corti. On the basis of these findings, it is assumed that hair cell death induced by an Sk inhibitor is related to apoptosis. Sk inhibitors function as increasing ototoxic Sph and therefore potentially cause ototoxicity. Consideration for a possibility of ototoxicity is required in a usage of Sk inhibitors.

PS-619

The Oral Administration of Teprenone Can Protect the Synaptic Ribbons Beneath Inner Hair Cells Against Intense Noise Exposure.

Yoshihiro Okazaki; Kazuma Sugaharaa; Yoshinobu Hirose; Hiroaki Shimogori; Hiroshi Yamashita
Yamaguchi University Graduate School of Medicine

Introduction

In the previous meeting, we reported that heat shock proteins are expressed in the inner ear after intense noise exposure. The expression of heat shock proteins can protect the hearing function in the Noise trauma model of guinea pigs. It is known that teprenone can induce the heat shock response in many kinds of organ. In the present study, we evaluate the effect of oral administration of teprenone on the recovery of synaptic ribbons beneath inner hair cells after intense noise exposure.

Materials and Methods

Hartley male guinea pigs (350 - 400 g) with the normal tympanic membranes and the normal Preyer's reflexes were used in this study. Animals were divided into 2 groups (Noise group, Teprenon+Noise group).

In Teprenone+Noise group, animals were fed with the food containing 0.5% of teprenone before intense noise exposure. In Noise group, animals were fed with normal food. To evaluate the expression of heat shock proteins, the western blot analysis was performed using the extract from the cochleae of the animals.

The animals in both groups were exposed to the intense band noise (130 dBSPL for three hours). Three days later, the temporal bone was removed to evaluate the synaptic ribbon count. To ravel the synaptic ribbon, the immunohistochemistry was performed using the anti-CtBP2 antibody. These samples were observed with the fluorescence microscope.

Results
The density of signals of CtBP2 was lower in both groups than that from control animals. In the Teprenon+Noise group, the significantly higher density of signals for synaptic ribbon was observed than those in Noise group. The result suggested that the heat shock response in the inner ear affect the recovery of synaptic ribbons after noise trauma.

Discussion
We have reported the effect of the heat shock inducer, teprenone in the hearing functional recovery after the intense noise exposure. However, the mechanism of the protective effect of teprenone is unclear. Karunanithi has reported that heat shock proteins protect synapse in Drosophila models. In addition, Bechtold has reported that heat shock proteins were expressed in synapse of the rat brain after heat stress. Therefore, the heat shock proteins induced by teprenone can protect the synapse in the inner ear against the intense noise exposure.

PS-620

Piribedil, Memantine and ACEMg Pretreatment Reduces Noise-Induced Loss of Inner Hair Cell - Auditory Nerve Connections and Reduces Incidence of Tinnitus.

Richard Altschuler; Karin Halsey; Ariane Kanicki; Diane Prieskorn; Susan Shore; Josef Miller; David Dolan
KHRI

Recent studies show noise induced loss of Inner Hair Cell - Auditory Nerve connections can lead to decreased Gap Inhibition of the Acoustic Startle Reflex (Hickox and Liberman, 2014) and are associated with Tinnitus (Singer et al, 2013). We asked whether preventing noise induced loss of connections would decrease the incidence of tinnitus. First, combination of anti-excitotoxic (Piribedil and Memantine) and anti-oxidant agents were administered pre-noise exposure to potentially reduce loss of connections and subsequent incidence of tinnitus. In other studies, the effect of sarcosine (a glycine reuptake inhibitor) on recovery from tinnitus following noise-exposure was tested.

A small arms fire – like noise (50 biphasic impulses over 2.5 minutes at 152 dB SPL) was presented unilaterally. For the prevention studies, Memantine and Piribedil was given i.p. starting 3 days before the noise exposure and continued for 3 days thereafter. A diet enriched in vitamins A, C and E and magnesium (ACEMg) was started 14 days before the noise exposure and continued until termination. Animals were tested for Gap Inhibition and Pre-Pulse Inhibition (PPI) of the Acoustic Startle reflex prior to the noise exposure and 2-3 times a week for 12 weeks until termination. Cochleae were assessed for inner hair cell synapses using CTBP2 immunolabel of ribbons, as well as for hair cell loss. For recovery studies, animals were given Sarcosine i.p. and then in the drinking water, until animal termination at 6 weeks following the noise, cochlea were assessed for synapses and hair cell loss.

Loss of IHC synapses and reduced gap inhibition were observed in approximately half of the noise-exposed rats and reduced gap inhibition with normal PPI (which can suggest tinnitus) in approximately 1/3 of noise exposed animals. Treatment with either Memantine, Piribedil and ACEMg or just Memantine and Piribedil significantly reduced loss of connections and reduced the incidence of reduced Gap Inhibition with normal PPI from 29% in non-treated noise exposed animals to 13% and 19% respectively suggesting reduced incidence of tinnitus. Sarcosine treatment did not change the incidence of tinnitus during the 2 week period after the noise but reduced the incidence by 50% during the remaining 4 week period of assessment, indicating enhanced recovery.

Supported by NIH Grant P30DC05188 and DOD grant W81XWH-10-PRMRP-IIRA

PS-621

Increased Presence of Cells of the Immune System in the Spiral Ganglion in Response to Hair Cell Loss may Promote Spiral Ganglion Neuron (SGN) Death

Erin Bailey; Zarin M Rehman; Steven Green
University of Iowa

Introduction
Hair cells (HCs) are the sole afferent input to SGNs. Following HC death due to aminoglycoside exposure from postnatal day 8 (P8) to P16, rat SGNs degenerate and die over a period of ~3 months (Alam et al. JCN 503:832-52, 2007). The reason for SGN death is not clear. Even after all HCs have been destroyed by aminoglycosides, neurotrophic factors remain expressed in the cochlea and cochlear nuclei (Bailey & Green, J. Neurosci., in press). Perhaps SGN death is an indirect outcome of HC loss, due to inflammatory or degenerative changes in the cochlea initiated by HC loss. We have shown, by gene expression profiling and immunohistochemical labeling, increased presence of cells of the innate immune system, including macrophages and natural killer (NK) cells, in the spiral ganglion at the time when SGNs are dying. Here, we ask what role this immune response has in SGN survival: is it trophic, promoting survival of remaining SGNs? Is it toxic, promoting SGN death? Does this response have no effect on SGN survival?

Methods
Rats were deafened by daily kanamycin injection from postnatal day 8 (P8)-P16. From P21-P60, a period over which ~1/2 of the SGNs die in the basal cochlea, rats were given low-dose dexamethasone (0.25 mg/kg) daily in their drinking water for immune-suppression along with the antibiotic Baytril (23 mg/L) to prevent secondary infection. The rats were euthanized at P60 and the cochleae were isolated, cut into 6 µm frozen sections and labeled with markers for activated macrophages and NK cells to confirm immune suppression and a neuronal marker to quantify neuron survival. These were compared to control deafened and undeafened littermates.

Results
Daily treatment with low-dose dexamethasone was successful in preventing the increased presence of activated macrophages and NK cells normally observed after deafening. This was correlated with increased SGN survival in the basal cochlear region. SGN death was strongly suppressed: the number of surviving SGNs in deafened rats treated with dexamethasone was similar to the number of SGNs in hearing rats.

Conclusions
Following HC loss, an increased presence of cells of the innate immune system, including activated macrophages and NK cells, is observed in the spiral ganglion at the time when SGNs are dying. Preventing increased expression of these cells through immune-suppression increases SGN survival after deafening, suggesting that the innate immune response is toxic and promotes SGN death.

PS-622

Otoprotection using a Combination of L-NAC, Mannitol and Dex in an In vitro model of Inner Ear Trauma

Jeenu Mittal; Mateo Guardiola; Jonathan Roell; Dustin Lang; Esperanza Bas Infante; Carolyn Garnham; Thomas Van De Water; Fred Telischi; Adrien Eshraghi
University of Miami

Background
The inner ear trauma caused by cochlear implant electrode insertion trauma (EIT) initiates multiple molecular mechanisms in hair cells (HCs) or support cells (SCs) resulting in initiation of programmed cell death within the damaged tissues of the cochlea which leads to loss of residual hearing. In earlier studies L-N-acetylcysteine (L-NAC)(an antioxidant), Mannitol(osmotic and diuretic effects) and dexamethasone(-Dex) (a steroid) have been shown independently to protect the HCs loss against different types of inner ear trauma. These 3 molecules have different otoprotective effects. Goal of this preliminary study is to test the efficacy of a different combination of these molecules to enhance the otoprotection of HCs against EIT.

Methods
OC explants were dissected from P-3 rats and placed in serum-free media. Explants were divided into control and experimental groups. Control group: 1) untreated controls 2) EIT. Experimental group: 1) EIT + L-NAC (5, 2 or 1 mM) 2) EIT + Mannitol (100, 50 or 10 mM) 3) EIT + Dex (20, 10 or 5 µg/mL) 4) EIT +L-NAC + Mannitol + Dex. In EIT Groups, a 0.28-mm diameter monofilament fishing line was introduced through the small cochleostomy located next to the round window area, allowing for an insertion of between 110° and 150°. After EIT was caused, explants were cultured in media containing L-NAC alone, Mannitol alone or Dex alone at decreasing concentrations. Concentrations of L-NAC, Mannitol and Dex that showed 50 percent protection of hair cell loss individually were used as a combination in the experimental group 4.

Results
There was an increase of total hair cell (THC) loss in the EIT OC explants when compared with control group HC counts or the tri-therapy cochlea. We defined the dosage of L-NAC, Mannitol and Dex for the survival of 50% protection of hair cells in vitro. Their combination provided close to 96% protection demonstrating a synergistic effect. This combination therapy may be beneficial in other type of inner ear trauma that can result in hair cell loss.

Conclusion
EIT involves oxidative stress and lipid peroxidation early on after the implantation. L-NAC, Mannitol and Dex are effective alone in protecting the sensory cells in vitro at high doses. A cocktail containing L-NAC, Mannitol and Dex at much lower doses of each compound, is effective in protecting sensory cells. The three compounds can be combined with a synergistic effect allowing a decrease in the potential side effects of each of the compound.

PS-623

Endocochlear Potential (EP) Reduction as an Indicator of Noise-induced Reticular Lamina Breach in Mice

Kevin Ohlemiller
Washington University School of Medicine CID at Washington University

We have shown that 3 inbred mouse strains (C57BL/6J, CBA/J, BALB/cJ) present very different responses of the basal turn EP to loud noise (Ohlemiller et al., JARO 2011). Soon after a 2 hr exposure to 110 dB SPL BB or OB noise exposure, B6 mice show little or no EP reduction, while the EP in CBA and BALB is reduced by ~50%. We have further shown that the cellular correlates and genetic bases of EP reduction in CBA and BALB mice are different. We have recently expanded our strain comparisons by constructing comprehensive EP-versus-noise level dose-response relations for mice aged 6 wks - >1 yr. For all 3 strains, 6 wk old mice show acute EP reduction for much lower sound levels than mice >4 mos, suggesting that susceptibility of the cochlear lateral wall is part of the well-known early vulnerability window to noise. For all 3 strains also, noise exposures > 110 dB are associated with a consistent steep decline of the EP to 5-40 mV. This is consistent with a common threshold for catastrophic breach of the reticular lamina, as indicated by Hirose and Liberman (JARO 2003). The threshold for breach may extend to lower noise levels in 6 wk old mice. We are comparing anatomic indicators (light microscopy, immunocytochemistry) with our physiologic data to determine when EP reduction indicates lateral wall pathology, versus when it primarily indicates rupture of the organ of Corti. Both types of events may contribute independently to NIPTS, and probably possess distinct sets of governing and modifier genes.

PS-624

Protection of Cochlear Synapses from Noise-induced Excitotoxic Trauma by Introcochlear Delivery of a Selective AMPA Receptor Antagonist

Ning Hu; Steven Green
University of Iowa

Introduction

Moderate noise exposure can destroy synapses between inner hair cells (IHCs) and spiral ganglion neurons (SGNs) even if hair cells are not lost and there is no permanent threshold shift (PTS). This "synaptopathy" is detectable by histological examination of synapses and, noninvasively, by auditory brainstem response (ABR), as reduced ABR amplitude. Synaptopathy is a consequence of excessive glutamate release from overstimulated IHCs ("excitotoxicity") and Ca^{2+} influx to the postsynaptic bouton. We have found *in vitro* that a blocker of Ca^{2+} permeable AMPA receptors (CP-AMPARs) prevents kainate-induced Ca^{2+} entry into SGNs. We ask here whether such compounds protect cochlear synapses from noise-induced excitotoxic trauma *in vivo*.

Methods

Drugs, dissolved in artificial perilymph (AP), are perfused into cochleae of CBA/CaJ mice via the round window by a minipump/cannula system. The cannula length is such that the minipump contents reach the cochlea 3 days after surgical implantation. Mice are exposed to noise (2 hours, 100 dB SPL, 8-16 kHz octave band) 6 days after surgery. ABRs are measured prior to surgery, 3 and 1 days pre-noise, and 1 and 10-14 days post-noise to obtain the baseline, effect of surgery, effect of the drug, noise-induced temporary threshold shift (TTS) and noise-induced PTS. Ribbons, postsynaptic densities, and HCs, labeled, respectively, with anti-CtBP2, anti-PSD95 and anti-myosin were counted in organ of Corti wholemounts at 8, 16 and 32 kHz locations.

Results

TTS was comparable among nearly all ears regardless of surgery or treatment and PTS was rarely detected in any ears. These data showed that the noise, at the level used, did not destroy hair cells (confirmed by histology) and, importantly, that the drug treatment alone had no significant effect on hearing. In control ears (nonoperated or AP with no drug), ABR amplitude remains reduced even at 10-14 days post-noise, correlated with a loss of ≈20% of synapses on IHCs at 16 kHz. In drug-treated ears, ABR amplitudes recover to pre-noise level by 10-14 days post-noise with no significant loss of synapses relative to control non-noise-exposed ears.

Conclusions

The data show that Ca^{2+} entry via CP-AMPARs plays a major role in noise or excitotoxic trauma to synapses on IHCs *in vivo*, confirming what we found *in vitro*. Blockade of CP-AMPARs *in vivo* has no significant effect on normal hearing but provides considerable protection against noise-induced synaptopathy and consequent reduction of ABR amplitude.

PS-625

Disparities in Auditory Physiology and Pathology between C57BL/6J and C57BL/6N Substrains

Ann Kendall[1]; Jochen Schacht[2]
[1]*University of Michigan;* [2]*Kresge Hearing Research Institute*

C57BL/6 inbred mice are routinely used in biological studies, in part because C57BL/6-derived genetic backgrounds are common in many spontaneous mutant and transgenic mouse strains. Several C57 substrains have evolved with distinct genetic phenotypes and among these, C57BL/6J and C57BL/6N are frequently employed as models in auditory research. C57BL/6J mice were originally bred at Jackson Laboratories in 1948 and then became widely distributed. Such breeding colonies derived from the Jackson strain were designated as the C57BL/6N line. Among other spontaneous mutations, the original C57BL/6J mice acquired a null mutation between 1976 and 1984 in the *Nnt* gene resulting in the absence of an NAD(P) transhydrogenase. This mutation is not found in C57BL/6N mice.

Genetic variation and phenotypic disparities between these two substrains have been extensively investigated, but conflicting information exists about differences in their auditory and vestibular phenotypes. Literature-based comparisons are rendered difficult or impossible because most auditory publications do not designate the substrain used. We therefore evaluated commercial C57BL/6N and C57BL/6J mice for their baseline auditory brainstem response (ABR) thresholds at 3 months of age as well as their susceptibility to noise exposure and aminoglycoside antibiotics. Both substrains have similar thresholds at 4 and 12 kHz, but C57BL/6N show significantly higher baseline thresholds at 24 and 32 kHz. Because of these elevated thresholds, the N substrain is unsuitable as a model for drug ototoxicity, which primarily affects high frequencies. Exposure to 2–20 kHz broadband noise for 2 h at 110 dB produced significantly higher threshold shifts in the J substrain.

The salient point here is the demonstration that commercially available C57BL/6J and C57BL/6N mouse substrains show significant differences in auditory physiology and pathology that preclude interchangeable use or comparisons between them. These results suggest caution in the selection of C57BL/6 substrains for auditory research and indicate the need to specify substrains, age and the breeding source in all publications. Furthermore, our study reinforces the absolute need for using age-matched littermates as controls to ensure valid comparisons when evaluating auditory phenotypes of mutant strains of mice.

PS-626

Role of STAT1 Activation in Mediating Oxidative Stress and Hair Cell Death in the Organ of Corti.

Peng Jiang; **Amrita Ray**; Michael Brenner
University of Michigan

Introduction

STAT1 is a cytoplasmic transcription factor involved in stress-induced inflammation and apoptosis pathways in the inner ear. Stress signals promote rapid phosphorylation of STAT1 at one or both of its conserved residues, tyrosine 701 (Tyr^{701}) and serine 727 (Ser^{727}).STAT1 siRNA knockdown attenuates cisplatin ototoxicity in rats, and utricular hair cells from STAT1-deficient mice are resistant to cisplatin toxicity. Epigallocatechin Gallate (EGCG) is a potent antioxidant and STAT1 inhibitor. To our knowledge, the role for STAT1 and its inhibition has not been studied with aminoglycosides. We hypothesized that STAT1 also mediates aminoglycoside ototoxicity, and we conducted experiments to elucidate the specific pathways involved.

Methods

Effects of gentamicin on STAT1 inhibition and activation were evaluated in neonatal murine organ of Corti explants. Acute gentamicin-treatment conditions (50μM at 4, 8, 16 and 24 hours) were used for induction, and chronic gentamicin treatment (3.5μM or 4μM at 72 hours) for hair cell counts. Gentamicin was given alone or in combination with ECGC (25μM, 35μM and 50μM) or retinoic acid, a STAT1 activator (1μM, 100μM). Explants were stained with Rhodamine and fluorescent labeled Phalloidin and examined under light and confocal microscopy for hair cell counts and STAT1 phosphorylation, respectively. Evaluation included hair cell quantification (cytocochleograms) and immune-labeling of STAT1 phosphorylation at $Tyr^{701}$and Ser^{727}residues.

Results

Outer hair cell loss of 22.23% ± 4.9% in 3.5μM gentamicin-treated explants was decreased to 0.45% ± 0.4% in gentamicin + EGCG 35μM and 0.30% ± 0.4% in gentamicin + EGCG 50μM treatment groups. Hair cell loss was absent in untreated controls.When retinoic acid, an activator of STAT1, was combined with gentamicin, increased hair cell loss was observed (45.59% ± 15.43% in explants treated with 4μM gentamicin alone; 69.65% ± 19.74% in 4μM gentamicin + 1μM retinoic acid; and 80.57% ± 9.89% in gentamicin + retinoic acid 100 μM). The 50μM acute gentamicin treatment increased phosphorylation at the Tyr^{701}residue, but not the Ser^{727}residue, at 4, 8, 16 and 24 hours. Total STAT1 levels remained stable in all conditions.

Conclusion

Inhibition of STAT1 with EGCG protected against gentamicin-induced hair cell loss in a murine organ of Corti culture, whereas retinoic acid potentiated cytotoxicity. Preferential phosphorylation of STAT1 at Tyr^{701}versus Ser^{727}after gentamicin treatment suggests STAT1 mechanism in aminoglycoside-induced injury differs from that observed in cisplatin ototoxicity.

PS-627

Cell-based High-throughput Screens identify Protective Compounds against Cisplatin-induced Hair Cell Death in Mouse Cochlear Explants and the Zebrafish Lateral Line

Tal Teitz; Asli Goktug; Jie Fang; Justine Bonga; Michael Taylor; Taosheng Chen; Jian Zuo
St. Jude Children's Research Hospital

Cisplatin is an effective and common chemotherapeutic drug used to treat various childhood malignancies including neuroblastoma, retinoblastoma, bone tumors, medulloblastoma and sarcoma. Ototoxicity is a major side effect of cisplatin treatment for young children (ages 0-5 years) and more than 50% of pediatric cancer patients suffer from mild to severe hearing loss due to cisplatin regimens. At the concentrations given to patients, cisplatin has been shown to cause death by apoptosis mainly in the cochlear hair cells, spiral ganglion neurons, lateral wall cells in the spiral ligament and stria vascularis. Here we present the results of high-throughput drug screens employing the immortomouse inner ear cell line HEI-OC1 derived from the organ of Corti. We screened libraries of >4,375 unique FDA approved and biologically-active compounds for those that confer protection from cisplatin-induced cell death. The biological assay measured the ability of the tested compounds to inhibit caspase-3 activity induced by cisplatin treatment. The top 157 compound hits of the primary screen were validated in the HEI-OC1 cell line by dose response analysis and viability assays. The best 13 compounds with IC_{50} of 0.04-7.6mM were tested ex-vivo in neonatal (P3) mouse cochlear explant cultures. Ten of the top 13 compounds exhibited protection in the cochlear explants as measured by hair cell viability after 24 hours cisplatin co-treatment. Hair cells' viability was determined by Phalloidin and DAPI staining, FM1-43 dye uptake, and immunohistochemistry with known hair cell markers Parvalbumin and Myo7a. The top 10 compounds that are protective in mouse cochlear explants were further tested in the lateral line of 5 dpf zebrafish larvae; at least 2 of the compounds show protection against cisplatin-induced hair cell loss in neuromasts after 24 hours of co-treatment. These top 10 compounds are currently being tested in medulloblastoma neurosheres and neuroblastoma cell lines to verify they do not compromise the ability of cisplatin to kill the tumor cells when delivered systemically. In summary, we have identified at least 2 compounds that are protective against cisplatin-induced hair cell loss in both mouse cochlear explants and zebrafish lateral lines. We will next test them in mouse and chinchilla animal models for their protection against cisplatin- and noise-induced ototoxicity, determine their *in vivo* toxicity and pharmacokinetics, and perform chemical modifications for ultimate clinical trials in humans.

PS-628

Fluvastatin Protects Against High Decibel Noise Induced Hearing Loss

Donna Whitlon; Hunter Young; Claus-Peter Richter
Northwestern University

Introduction

Exposure to noise levels exceeding 80db SPL can cause hair cell death, degeneration of neurons (synapses, nerve fibers and cell soma), and elevate click and tone evoked ABR thresholds. Currently, no FDA approved drugs are available that have been developed to protect against noise induced hearing loss. We recently reported that the HMG-CoA reductase inhibitor, fluvastatin, promotes neurite elongation in dissociated mouse spiral ganglion cultures. In the course of evaluating the effects of fluvastatin *in vivo*, we applied the fluvastatin at the same time as noise exposure and measured click and tone evoked ABR thresholds.

Methods

To ensure normal hearing, baseline ABR responses were first measured in albino guinea pigs, 500-700g. Animals were then implanted with miniosmotic pumps that delivered 0.25 µl/hr of fluid through a cannula surgically implanted in the scala tympani of the left cochlea. After surgery, animals were exposed to a 4-8 kHz noise band, 120dB SPL, for 4 hours. Fluid was pumped into the cochlea for 28 days; ABR measurements were made weekly. At the experiment's end, cochleas were perfused with fixative, dissected and used for examination by x-ray tomography. Controls for drug application included noise+saline, noise alone, and cannula alone. Nine noise exposed control animals and 15 noise exposed fluvastatin treated animals were used.

Results

Sound evoked ABRs were highly variable in the left cochleas after surgery. Further evaluation using x-ray tomography demonstrated a fibrocytic response to the cannula in the scala tympani. Since this response could conceivably have interfered with sound transfer, the left cochleas were not acceptable for meaningful ABR measurements. On the other hand, the right, unoperated cochlea did not mount that response. Evaluation of ABRs in the right cochlea indicated that fluvastatin injected into the contralateral cochlea exerted effects in the pristine, unoperated, unopened right cochlea. ABR threshold elevation after exposure to clicks averaged 41.7+/12 for noise exposed controls, but was 5.83+/10.7 for noise exposed fluvastatin treated animals. Tone evoked ABRs also demonstrated a protection by fluvastatin treatment.

Discussion

We have demonstrated that 1) drugs injected into one cochlea can exert effects in the opposite cochlea; and 2) fluvastatin protects against high decibel noise induced hearing loss. The mechanisms by which fluvastatin exerts effects on sound evoked ABRs are currently under evaluation, but the results raise the possibility of using a drug class already approved for another purpose by the FDA to protect against noise induced hearing loss.

PS-629

Protective Function of Calcium Channel Blockers Against Noise-Induced Loss of Spiral Ganglion Neurons During Aging

Jianxin Bao[1]; Dan Liu[2]; Jian Tang[3]; Debin Lei[2]; Hui Li[2]
[1]Northeast Ohio Medical University; [2]NEOMED; [3]Shanghai Jiao Tong University School of Medicine

Background

Noise is the most common occupational and environmental hazard. Noise-induced hearing loss (NIHL) is the second most common form of sensorineural hearing deficit. Currently, there are no drug therapies for NIHL. Our previous studies have indicated that calcium signaling may be involved in both NIHL and age-related hearing loss (ARHL).

Method

First we established a extensive noise exposure model which disrupted the organ of Corti using CBA/CaJ mice. In this model, two-month old CBA/CaJ mice were exposed to 120dB octave band noise (8-16k Hz) for two hours which led to ~ 65 dB permanent ABR threshold elevation and nearly total loss of outer hair cell function. Moreover, 35.82% SGNs were lost throughout the cochlea three month after the noise exposure. Then we tested whether calcium channel blockers, zonisamide (a blocker for T-type calcium channels) or diltiazem (a blocker for L-type calcium channels), could protect hearing loss in this type of extensive NIHL. We administrated the drugs before and after the noise exposure. No auditory functions were recovered by drug treatments suggested by ABR threshold shifts and DPOAE. However, a significant protection of spiral ganglion neurons (SGNs) by these drugs was observed three month after the noise exposure.

Conclusion

We identified two existing calcium channels blockers zonisamide and diltiazem which protect SGNs from extensive noise exposure in mice. Since the success of cochlear implants for hearing loss depends on the survival of SGNs, and both of these drugs are already approved by FDA for treating other chronic disease conditions, the translational implication of our finding is significant.

PS-630

Cochlear Pendrin Expression has a Protective Role in Noise-Induced Hearing Loss

Laura Constance; Joel Sanneman; Philine Wangemann
Kansas State University

Mutations of *SLC26A4* lead to progressive hearing loss in humans. The human gene *SLC26A4* and the mouse ortholog *Slc26a4* encode the chloride bicarbonate exchanger pendrin. Pendrin is expressed in the cochlea, the vestibular labyrinth and the endolymphatic sac of the inner ear. A conventional mouse model, $Slc26a4^{\Delta/\Delta}$ that completely lacks pendrin expression, fails to develop hearing, which is a phenotype that is more severe than what is observed in most human patients. Hearing in $Slc26a4^{\Delta/\Delta}$ mice can be fully restored by a transgene that drives pendrin expression in the endolymphatic sac (Li et al 2013). Similar hearing thresholds were

found in Tg(+);*Slc26a4*$^{\Delta/\Delta}$ and Tg(-);*Slc26a4*$^{\Delta/+}$ mice. Both mice expressed pendrin in the endolymphatic sac but differed in the expression of pendrin in the cochlea. These observations suggested that cochlear pendrin expression is not needed for the development of hearing, however, the possibility remained that cochlear pendrin expression provides an advantage in stress situations such as noise. Here we test the hypothesis that cochlear pendrin expression has a protective role in noise-induced hearing loss.

Noise-induced hearing loss was evaluated in Tg(+);*Slc26a4*$^{\Delta/\Delta}$ mice which lack cochlear pendrin expression and Tg(-);*Slc26a4*$^{\Delta/+}$ mice which express pendrin in the cochlea. Hearing thresholds at 8, 16, and 32 kHz were determined from auditory brainstem responses before and two weeks after noise exposure (Gaussian, 14-18 kHz, 109 dB, 2 hrs). Tg(+);*Slc26a4*$^{\Delta/\Delta}$ and Tg(-);*Slc26a4*$^{\Delta/+}$ mice were raised in a mixed background containing alleles from CBA, C57BL6, and 129S6 strains. Tg(+);*Slc26a4*$^{\Delta/\Delta}$ mice were backcrossed into the 129S6 strain for two generations to reduce differences in the genetic background.

Prior to noise exposure, hearing thresholds of Tg(+);*Slc26a4*$^{\Delta/\Delta}$ (n=58) and Tg(-);*Slc26a4*$^{\Delta/+}$ (n=49) mice were similar. After noise exposure, thresholds at all frequencies were elevated in both types of mice. Thresholds at 8 and 16 kHz were higher in Tg(+);*Slc26a4*$^{\Delta/\Delta}$ mice compared to Tg(-);*Slc26a4*$^{\Delta/+}$ mice.

The data demonstrate that hearing in Tg(-);*Slc26a4*$^{\Delta/+}$ mice that express pendrin in the cochlea is more robust compared to Tg(+);*Slc26a4*$^{\Delta/\Delta}$ mice that lack pendrin expression in the cochlea. Although differences between the genotypes could be due to a segregation of background alleles, the data suggest that the greater robustness of hearing in Tg(-);*Slc26a4*$^{\Delta/+}$ mice is due to a beneficial effect of cochlear pendrin expression. This opens the prospect that restoration of pendrin function in the cochlea may slow the progression of hearing loss in humans carrying mutations of *SLC26A4*.

Supported by: NIH-5R01-DC012151-3, NIH-5T32-OD011169-11, NIH-2T35-OD010979-16 and CVM-KSU.

PS-631

Noninvasive Structural Assessment of Cytomegalovirus-Induced Damage in the Cochlea via Delayed Contrast Enhanced MRI

Osama Abdullah; **Ali Almishaal**; Rock Hadley; Craig Goodrich; Elaine Hillas; Matt Firpo; Dennis Parker; **Richard Wiggins**; **Albert Park**
University of Utah

Background

Cytomegalovirus (CMV) infection is one of the leading causes for hearing loss in children in the United States. CMV infection triggers a cascade of deleterious changes in the inner ear such as a progressive loss of the cochlear hair cells (HCs), microvascular degeneration, and sensorineural hearing loss. There is a need for noninvasive imaging techniques that can monitor the damage progression caused by CMV and evaluate potential therapeutic intervention. This work hypothesizes that the degree of signal enhancement in T1-weighted MRI images will reflect the severity of hearing loss caused by CMV.

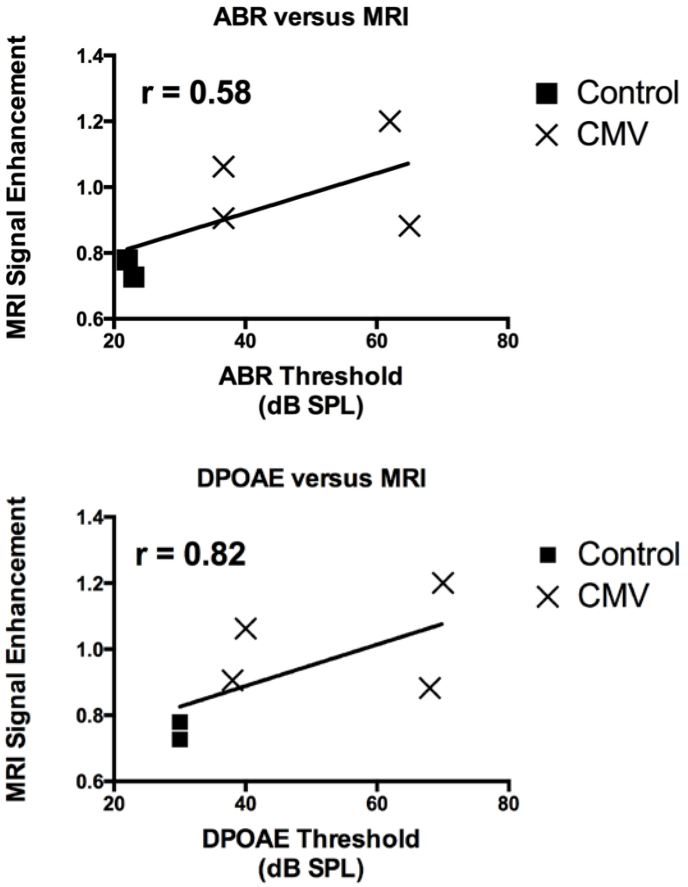

Methods

Two Balb/C mice were infected with murine cytomegalovirus (mCMV-GFP) via intracerebral injection of 2000 pfu at day three of life and imaged with a 7T MRI scanner (Bruker Inc., Ettlingen Germany) 4 weeks post infection. A sham mouse was used as a control. MRI T1 gradient echo images were acquired before and 4-hours after intraperitoneal Gd-DTPA contrast injection (30 micro-liters of Multihance, Bracco Diagnostics, Princeton, NJ). After imaging, auditory function was assessed using both Distortion Product Otoacoustic Emissions (DPOAE) and Auditory Brainstem Response (ABR) studies. Subsequently, the cochleas were harvested for Immunohistochemical Analysis (IHC) to assess viral expression in the cochlea.

Results

Compared to the control mouse, normalized signal intensity in regions of interest (ROIs) in the cochlea taken from the CMV mice were 25% and 43% higher in right and left ears, respectively. The laterality in the measured signal intensity in the CMV infected mice correlated to the laterality of hearing loss. The left ear ABR and DPOAE thresholds for both CMV infected mice were higher than in the right ear. The right ears of the infected mice showed mild hearing loss; the left ears of the infected mice showed severe to profound hearing loss, which is consistent with MRI signal enhancement patterns.

IHC studies showed mCMV-GFP expression in the spiral ganglion and adjacent to the scala tympani. A scatter plot between the MRI-based enhancement score versus the auditory outcomes (2 CMV and 1 control for left and right ears), showed a stronger correlation with DPOAE (Fig. 1) than with ABR (Fig. 2) thresholds (Spearman Correlation, r = 0.82 for DPOAE, and r=0.58 for ABR).

Conclusion

This data showed that increased ROI signal intensity obtained from contrast enhanced MRI correlated with hearing loss in our murine model for mCMV. This imaging modality may provide a useful tool for noninvasive evaluation of CMV induced labyrinthitis.

PS-632

Larval Zebrafish Lateral Line as a Model for Acoustic Trauma

Phillip Uribe[1]; Zecong Fang[1]; Jie Xu[2]; Allison Coffin[1]
[1]Washington State University, Vancouver; [2]University of Illinois at Chicago

Background

Excessive noise exposure leads to permanent hearing loss and there are no effective pharmacological therapies to ameliorate noise damage. To increase the rate of drug discovery, we need an efficient pipeline for the identification of compounds that protect hair cells from acoustic trauma. Larval zebrafish are a tractable model for ototoxicity and otoprotection research, including large-scale drug discovery. Zebrafish posses an externally located lateral line system containing clusters of hair cells which can be rapidly assessed and are homologous to those found in the mammalian inner ear. This project demonstrates the utility of the lateral line system as a model to study hair cell loss associated with acoustic trauma.

Methods

We use underwater cavitation to acoustically stimulate lateral line hair cells. Larval zebrafish were placed in a 24-well plate that was suspended in a water bath, with the plate 20 cm above four ultrasonic transducers that emit a 35 kHz frequency. The ultrasonic field interacts with microbubbles in the aquatic environment resulting in fluctuations in bubble volume that lead to bubble implosion. Bubble implosion generates intense broadband noise including low frequencies within the range of lateral line sensitivity. Following acoustic trauma, hair cell survival was assessed by vital dye staining 0 - 24 hours post noise exposure.

Results

Our results indicate that underwater cavitation produced time- and intensity-dependent hair cell loss in the lateral line. Peak hair cell loss manifests approximately 24 hours post noise exposure. We found that thirty minutes of acoustic trauma results in 50% hair cell loss 24 hours post-exposure whereas no hair cell loss was observed immediately following stimulus cessation. Additionally, surviving hair cells exhibited kinocilial blebbing, a sign of sub-lethal damage.

Conclusions

Our results demonstrate that the lateral line system can serve as a tractable model for the study of acoustic trauma. Future work will employ this model in large-scale drug discovery efforts to identify compounds that protect hair cells from acoustic damage.

PS-633

Abnormal Iron Homeostasis and Oxidative Stress in the Cochlear is Associated with Hearing Loss in Ncb5or Deficient Mice

marcello Peppi; Wenfang Wang; Dianne Durham; Hinrich Staecker; hao Zhu
University of Kansas Medical Center

Background: Altered iron homeostasis in neurons is associated with abnormal neurocognitive and motor functions in neurodegenerative disorders [Zumbrennen-Bullough, et al, PLoS One, 2014]. It is unclear whether iron imbalance in cochlear neurons can trigger degeneration of auditory functions. In this study, we investigate hearing and cochlear oxidative stress and iron status in NADH cytochrome b5 oxidoreductase (Ncb5or) deficient mice. Ncb5or is a potent ferric reductase in vitro [Zhu, et al, J. Biol. Chem, 2004]. In vivo, Ncb5or deficiency causes lipid and iron dyshomeostasis and oxidative stress in association with diabetes [Xu, et al, J. Biol. Chem, 2011; Wang, et al, Biochim. Biophy. Acta, 2011; Wang, et al, Am. J. Hematology, 2011; Wang, et al, in preparation].

Methods

For auditory recording, auditory brainstem responses (ABR) were elicited by tone pips (5 ms duration delivered at 31.3/sec) at 6 log-spaced frequencies from 5.1 – 26.5 kHz and measurements recorded by placing electrodes in the scalp. Distortion product otoacoustic emissions (DPOAE) were recorded as amplitude vs. level functions ($L_2 = L_1 - 10$). Real-time qRT-PCR was performed to measure transcript levels of oxidative stress and iron intake genes in the cochlea of Ncb5or mutant mice and wild-type control. For each sample, the cochleae from both ears were pooled, the bony tissue removed, and the RNA extracted with Trizol reagent. Random primers were used in reverse transcription, and Syber Green dye and the following gene-specific primers in quantitative PCR with ribosomal 18S RNA as an internal control.

Results

By 6 days after birth, Ncb5or mRNA is expressed in the corti and spiral ganglion. At 5 weeks of age, Ncb5or deficient mice show elevated threshold for both ABR and DPOAE along all frequencies tested, suggesting that hearing capability is compromised. These mice also show increased expression of oxidative stress genes, including MT1, HMOX1, GPX, GSTa, GSTm, and PGC1a, when compared to that of age-matched wild type littermates. In parallel, the cochlear of mutant Ncb5or mice have increased transcript levels of ferritin (FTL) whereas expression of genes involved in iron uptake, such as TFR1, DMT1 and ZIP14, decreased. The latter is different from the response in the liver of these animals.

Conclusions
The changes in hearing functionality together with oxidative stress and iron dyshomeostasis in the cochlear of Ncb5or deficient mice demonstrate that Ncb5or may provide a link between iron balances and auditory functions in the cochlear.

PS-634

Critical Role of Ceramide in Gentamicin-Induced Cochlear Hair Cell Death through Ceramide/Sphingomyelin Cycle

Chi Le; Keiji Tabuchi; Mariko Nakamagoe; Kohsuke Tani; Masahiro Nakayama; Bungo Nishimura; Akira Hara
University of Tsukuba

Introduction
Ceramide, a sphingolipid metabolite, regulates diverse cellular processes including apoptosis, cell senescence, the cell cycle, and cellular differentiation. Exogenously administered ceramide reportedly increased cochlear hair cell death due to gentamicin-induced ototoxicity. Ceramide is mainly generated via a ceramide/sphingomyelin cycle by sphingomyelinase and sphingomyelin synthase or via de novo synthesis by serine palmitoyltransferase and ceramide synthase. This study was designed to investigate the possible involvement of neutral sphingomyelinase, sphingomyelin synthase, or serine palmitoyltransferase in hair cell death due to gentamicin.

Methods
The basal turns of the organ of Corti of Sprague–Dawley rats were dissected on postnatal days 3 to 5. Cochlear cultures were exposed to media containing 35 μM gentamicin for 48 hours to assess the effects of GW4869 (a neutral sphingomyelinase inhibitor), 2-hydroxyoleic acid (a sphingomyelin synthase activator), and myriocin (a serine palmitoyltransferase inhibitor).

Results
Hair cell loss was significantly decreased in the presence of GW4869 or 2-hydroxyoleic acid. Myriocin had no significant effects against gentamicin-induced hair cell loss. In addition, neutral sphingomyelinase was activated by gentamicin exposure.

Conclusions
The present findings strongly suggest that the ceramide/sphingomyelin cycle plays an important role in the protection of hair cells against gentamicin-induced ototoxicity.

PS-635

WDR1 Localizes to Golgi Bodies: An Early Model for Functional Reciprocity Between Golgi Bodies and Endoplasmic Reticula

Henry Adler; Brian Carter; Allan Kachelmeier; Peter Steyger
Oregon Health & Science University

Background
WD40 repeat 1 protein (WDR1) is upregulated as part of the stress response to acoustic overstimulation in mammals and birds. We previously reported WDR1 localization to a compact region adjacent to the nucleus of COS7 cells. This WDR1 region was surrounded by, but not colocalized with, peroxisomes. Here, we compared the distribution of WDR1 with fluorescently-tagged gentamicin (GTTR), and with the distribution of either green fluorescent protein (GFP)-conjugated Golgi bodies or endoplasmic reticula.

Methods
COS7 cells were transfected with GFP specific for Golgi bodies or endoplasmic reticula for 18 hours at 37°C, followed by treatment with (or without) 5 mg/mL gentamicin at 22°C for one hour to preclude endocytosis, prior to recovery at 37°C for 0, 1, 3, or 6 hours, fixation, processing for WDR1 immunofluorescence and confocal microscopy. For comparison, COS7 cells transfected with GFP specific for Golgi bodies or endoplasmic reticula were treated with GTTR (5 mg/mL) as above and processed for confocal microscopy.

Results
Confocal microscopy revealed WDR1 fluorescence localized to Golgi bodies in untreated and gentamicin-treated COS7 cells. At 0, 1, 3, and 6 hours post-treatment ± gentamicin, at least 77% of all GFP-labeled Golgi bodies were co-localized with WDR1 fluorescence. Conversely, 50-70% of all GFP-conjugated endoplasmic reticula circumscribed, but did not occupy, the WDR1 fluorescence at 1, 3, and 6 hours recovery (± gentamicin). However, immediately after gentamicin treatment, significantly fewer WDR1 regions were encircled by GFP-conjugated endoplasmic reticula, compared to control cells. In contrast, the level of co-localization between WDR1 and Golgi bodies was significantly higher.

In COS7 cells, GTTR fluorescence was highly similar to that of GFP-conjugated endoplasmic reticula, with a small region of low intensity which appeared to be occupied by GFP-conjugated Golgi bodies.

Conclusion
The high correspondence between Golgi bodies and WDR1 fluorescence indicates that the Golgi body is a primary destination for WDR1, at least in COS7 cells. Also, WDR1 fluorescence is bordered by the endoplasmic reticula. Gentamicin affects WDR1 localization within Golgi bodies as well as its adjacency to the endoplasmic reticula, suggestive of disrupted communications among WDR1, the Golgi bodies and endoplasmic reticula, which may recruit peroxisomes to the WDR1/Golgi body region. Furthermore, the parallel labeling between GTTR and GFP-conjugated endoplasmic reticula as well as the Golgi body localization to the less intense region of GTTR may give insight to how interactions between organelles could contribute to aminoglycoside-induced cytotoxicity and/or protection against cytotoxicity.

PS-636

Early Cell Death Signaling and Oxidative Stress Post Cochlear Electrode Insertion Trauma

Adrien Eshraghi; Jonathan Roell; Mateo Guardiola; Dustin Lang; Carolyn Garnham; Jorge E Bohorquez; Shawn Sinbella; Jeenu Mittal
University of Miami

Background

We described previously, the pattern of hearing loss post cochlear implantation (CI) and electrode insertion trauma (EIT) in animal models. Cochlear implant induced EIT, not only causes direct tissue trauma and cell losses, but also generates molecular events that may initiate programmed cell death (PCD) via various mechanisms such as oxidative stresses, release of pro-inflammatory cytokines; activation of the caspase pathway which can result in apoptosis; generation of pro-apoptotic signal cascades within the damaged tissues of the cochlea which can lead to a loss of residual hearing. Objective of this preliminary study is to dissect the molecular mechanisms involved in oxidative stress of sensory cells post EIT.

Methods

EIT was performed in Guinea pigs by cochleostomy and unoperated contra-lateral ears were used as controls. ELISA for different enzymes involved in oxidative stress and PCD such as SOD, catalase, glutathione reductase or glutathione peroxidase was performed at 6hrs, 12hrs and 24hrs post-EIT.

Results

There was an increase in catalase activity in the trauma ear compared to the control 6 hours after trauma which decreased over time. There was an increase in SOD activity in the trauma ear after 6 hours which remained elevated until 12 hours and then decreased over time. There was no significant change from 6 to 24 hours in neither glutathione reductase nor glutathione peroxidase.

Conclusion

Oxidative damage may result from overproduction and/or lack of clearance of ROS/RNS by the scavenging mechanisms. Enzymatic defenses comprise agents that catalytically remove ROS, such as SOD, catalase, glutathione reductase or glutathione peroxidase. Oxidative stress plays an important role in hearing loss following EIT. A better understanding of the mechanisms involved in oxidative stress can help us determine the best method for preventing hearing loss.

Funding

MED-EL Corporation, Innsbruck, Austria to Dr. AA Eshraghi

PS-637

Feasibility of AAV-Mediated Neurotrophin Gene Therapy in the Cochlea

Patricia Leake[1]; Stephen Rebscher[1]; Chantale Dore'[1]; Lawrence Lustig[2]; Bas Blits[3]; Omar Akil[1]
[1]University of California San Francisco; [2]Columbia University; [3]uniQure biopharma B.V

Background

After deafness, long-term survival of cochlear spiral ganglion (SG) neurons requires both neurotrophic support and neural activity. In early-deafened cats, electrical stimulation (ES) from a cochlear implant (CI) partly prevents SG degeneration. Intracochlear infusion of Brain Derived Neurotrophic Factor (BDNF) further improves SG survival, which is beneficial for CI performance. However, BDNF also elicits disorganized, ectopic sprouting of radial nerve fibers that is potentially detrimental to optimum CI function due to loss of tonotopicity. Further, in initial studies, BDNF was delivered by osmotic pump, which is problematic for clinical application. The current study explores using adeno-associated viral vectors (AAV) to elicit neurotrophic factor (NT) expression by cells in the cochlea.

Methods

AAV2-GFP (green fluorescent protein), AAV5-GFP, AAV2-GDNF (glial-derived neurotrophic factor), AAV5-GDNF or AAV2-BDNF was injected (1 µl) into the scala tympani of FVB mice (1-2 days postnatal) through the round window. Mice were studied 7-21 days later. Additional studies assessed AAV efficacy in transducing cells in the normal and deafened cat cochlea. Kittens were deafened prior to hearing onset by systemic injections of neomycin sulfate. ABRs showed profound hearing loss by 16-18 days postnatal. AAV (10 µl) was injected at 3-4 weeks of age. Animals were studied 4-12 weeks later.

Results

Following AAV2-GFP injections in normal mice, immunohistochemistry revealed strong expression of the GFP reporter gene in inner (IHCs) and outer hair cells (OHCs), inner pillar cells, and also in some SG neurons. With AAV5-GFP, robust transduction of IHCs and many SG neurons was seen, but few OHCs and supporting cells expressed GFP. After injections of AAV2-GDNF, q-PCR demonstrated that human GDNF was expressed at levels about 1500 times higher than endogenous mouse GDNF. AAV5-GDNF elicited even higher levels of GDNF expression.

Injections of AAV2-GFP in normal cats elicited robust expression of GFP in IHCs, OHCs, some supporting cells and SG neurons throughout the cochlea; AAV5 appeared to elicit stronger transduction of more SG neurons than AAV2. However, initial long-term data after deafening showed no neurotrophic effect of AAV2-GDNF on SG survival.

Conclusions

AAV-GFP (both serotypes) elicited GFP expression in IHC and SG neurons in both mice and cats. If AAV-NT similarly elicits SG expression of NTs, as suggested by qPCR in mice, this should directly promote neural survival. Moreover, NT expression in hair cells and supporting cells could attract

resprouting radial nerve fibers, thereby potentially restoring more normal neuroanatomy in ears with hearing deficits due to SG degeneration.

PS-638

Restoration of Hearing by Gene Therapy in Mouse Models of Human Deafness Forms

Alice Emptoz[1]; Anais Meyer[1]; Typhaine Dupont[1]; Sylvie Nouaille[1]; Christine PETIT[1]; Saaid Safieddine[2]
[1]INSERM/Institut Pasteur; [2]CNRS/Institut Pasteur

Hearing impairment is a major concern and a serious burden for Public Health. The early-onset forms of severe or profound deafness are mostly genetic in origin. Current clinical approaches to cure hearing loss include hearing aids, and cochlear implants. These prostheses are still far from ideal especially in noisy environments and to listen to music. Gene transfer technology is thus an attractive *alternative approach* to cure deafness. We used viral gene therapy in deaf mouse mutants established as models for human deafness forms. We chose the adeno-associated virus (AAV) as it is presently one of the most promising gene transfer systems. To date 12 serotypes have been described based on their cell tropism, which can be exploited for targeting different cell types of the inner ear. We treated two mouse models for human profound deafness forms: DFNB9, and Usher syndrome of type IG. DFNB9 results from a defect in otoferlin, a multiple C2 domain protein including a short form (s-Otof) and a long form (l-Otof), composed of three and six C2 domains, respectively. Usher syndrome of type IG results from a defect in the scaffolding protein sans.

First we investigated the tropism of different AAV serotypes for cochlear cells. To this end mice were subjected to the viral cochlear delivery at postnatal day 2. The cochleas were injected with different serotypes (AAV1, AAV2, AAV8, AAV2/1, AAV2/8 and AAV5), encoding the green fluorescent protein GFP as a reporter gene.

We found that the AAV2/8 serotype was the most efficient to target hair cell (about 70% of transfected hair cells). We examined the auditory brainstem responses (ABR) 14 days after viral injection, and found that the ABR thresholds did not differ significantly from those of non-injected cochlea at all tested frequencies. This suggests that the surgery and viral delivery did not prevent the normal post-natal maturation of the auditory system. Next, cDNAs encoding the s-Otof isoform and sans were subcloned into the AAV2 genome and sequenced. Viral particles expressing s-Otof-AAV2/8, or sans-AAV2/8 were produced in the AAV2/8 configuration. Our preliminary results show that hair cell expression of s-Otof and sans in the mutant mice after a single cochlear injection of the recombinant viral particles. The exploration of the restoration of hearing of the treated mice is ongoing. The significance of the re-expression and the subcellular targeting of otoferlin and sans in the auditory hair cells of the treated cochlea will be discussed.

PS-639

Role of p66shc in Noise Induced Hearing Loss and Presbyacusis

Anna Fetoni; Giovanbattista Pani; Sara Eramo; Fabiola Paciello; Gaetano Paludetti; Diana Troiani
Catholic University of Rome

The p66Shc, a member of the ShcA protein family, harbours a unique N-terminal proline-rich domain with a serine phosphorylation site (Ser36) whose phosphorylation is essential in the cellular response to oxidative stress. Accordingly, p66Shc protein has been recognized as an important element of the free radical theory of aging. Namely, p66Shc-induced formation of Reactive Oxygen Species (ROS) in mitochondria promotes apoptotic cell death in response to a variety of pro-oxidant noxious stimuli, and mice lacking the p66 isoform display increased resistance to oxidative stress and delayed aging. However, no study of p66Shc in noise-induced hearing loss (NIHL), a phenomenon linked to oxidative stress, has been previously reported. Thus, the aim of this study was to investigate the role of p66Shc in noise-induced oxidative damage to inner ear and in and in age-related hearing loss.

Mice 126 SvEv wild type (WT) or knock-out (KO) for p66Shc at 2, 7, 12 and 24 months old were used. Auditory function was measured by recording the auditory brainstem responses (ABR) at 6-32 kHz in all age group animals. Acoustic trauma was also induced in animals of 2 months by a continuous pure tone of 120 dB SPL, 10 kHz for 1 hour and 24h after the acoustic trauma auditory function was retested. These NIHL animals were sacrificed, the cochleae were quickly removed and processed for immunofluorescence labelling and western blot analyses to evaluate p66Shc, Ser36-P-p66Shc, SOD2 and superoxide amount.

The functional evaluation illustrated that: (1) At 2 and 7 months old there was no differences in threshold value between KO and WT groups; (2) At 12 months WT animals showed a threshold value of about 25-30 dB higher compared to KO; (3) Two months old WT mice were more vulnerable to acoustic trauma with respect to KO mice. Moreover, the morphological analyses revealed an increase of p66, Ser36-P-p66Shc, SOD2 and superoxide amount in mouse WT cochleae after noise exposure, in particular, in the stria vascularis.

In conclusion, we established that the p66Shc plays a role in both oxidative damage induced by noise and in the presbycusis process.

PS-640

Vascular Degeneration in the Cochlea during CMV Infection in a Mouse Model

Mattia Carraro[1]; Ali Almishaal[2]; Elaine Hillas[3]; Matthew Firpo[3]; Albert Park[4]; Robert Harrison[5]

[1]University of Toronto; [2]Department of Communication Sciences and Disorders, University of Utah, SaltLake City, UT, USA.; [3]Department of Surgery, University of Utah, Salt Lake City, UT, USA; [4]Department of Surgery and Pediatrics, University of Utah, Salt Lake City, UT, USA; [5]Auditory Science Laboratory, Department of Otolaryngology and Program in Neuroscience and MentalHealth, The Hospital for Sick Children, Toronto, ON, Canada

Introduction

Cytomegalovirus (CMV) is an important cause of congenital hearing loss. This virus is estimated to account for at least 20% of sensorineural hearing loss (SNHL) in young children and it is perhaps the only causal agent of SNHL that can be treated.

Since there are no characteristic audiological/otological features unique to CMV, diagnosis is very challenging and more than 60% of these children will have passed their newborn hearing screening.

It is clearly important to determine the pathologic changes resulting from CMV infection. A greater understanding of the underlying mechanisms of CMV induced hearing loss will provide insight into treatment and diagnosis. With this in mind we can use an animal model to investigate the effects of CMV on cochlear vasculature and neural pathways of hearing and potentially identify improved approaches to prevention and treatment.

Methods

We used Balb/C mice inoculated 3 days after birth with murine cytomegalovirus (mCMV-GFP) via intra-cerebral injection of 2000 pfu. At 7 days post injection we performed immunohistochemical analysis to detect the location of the virus within the cochlea and at 4 weeks we tested their auditory function using distortion products otoacoustic emissions (DPOAEs) and auditory brainstem responses (ABR).

In order to evaluate vascular damage after 8-10 weeks, we perfused subjects with the Mercox II polymer, dissected the cochleas, partial corroded and imaged them with scanning electron microscopy (SEM). From these corrosion casts we made detailed assessments of the pathologic effects of CMV infection on blood vessels and capillary networks in different regions of the cochlea.

Results

We have previously demonstrated that a mCMV-GFP signal can be detected in the spiral ganglion and adjacent to the scala tympani a week after infection, and that our measures of auditory function point to a severe to profound hearing loss at 4 weeks.

Our corrosion casts reveal a clear involvement of the stria vascularis, organ of Corti vasculature and spiral ligament vessels. There is not a clear cochlear region where the damage occurs first but the apical turn is affected more frequently than the other ones.

Conclusion

The micro-vasculature of the cochlea is clearly damaged by mCMV infection. Regarding possible progression of pathology, we did not detect any early mCMV-GFP expression near to the organ of Corti however we do observe haircell loss over time. This suggests that the vascular damage is a precursor to the subsequent degeneration of sensorineural elements leading to cochlear hearing loss.

PS-641

High Frequency Hearing Loss In The Pex3 Mouse Mutant

Annalisa Buniello[1]; Christina Abundis[2]; Neil Ingham[1]; Karen Steel[1]

[1]King's College London; [2]University of California

Background

Pex genes encode proteins that are required for normal biogenesis of peroxisomes, which are cellular membrane-bound organelles involved in numerous metabolic pathways including lipid metabolism. There are a number of different *PEX* genes in humans, and mutations in these genes have been found associated with a wide range of disorders such as neurological dysfunction, morphogenetic defects, sensory deficits, liver and digestive problems, and early death. Many of these cases also show hearing impairment. *PEX3* mutations have been found in the most severe form of this spectrum, Zellweger syndrome (Shimozawa *et al.* 2000; Muntau *et al.* 2000) as wells as in infantile Refsum disease (Matsui et al, 2013).

Methods

Auditory Brainstem Response (ABR) was recorded from ketamine/kylazine anaesthetised mice aged 4, 8 and 14 weeks using custom software and TDT hardware. Pex3 cochlear expression analysis was performed by immunohistochemistry and immunofluorescence on 8µm thick paraffin sections from wild type mice. The gross structure of the inner ear of *Pex3* was characterised by inner ear clearing and hematoxylin and eosin staining. The level of knockdown of the *Pex3* allele was measured by qRT-PCR using RNA extracted from cochleae of 4 week old *Pex3* mutants and littermate controls.

Results

Pex3 knockout mice *($Pex3^{tm1a(EUCOMM)Wtsi}$)* were screened for hearing impairment as part of the Wellcome Trust Sanger Institute Mouse Genetics Programme (http://www.sanger.ac.uk/mouseportal/ ; White et al. 2013). ABR measurements showed a large increase in threshold at high frequencies only (from 18 kHz), starting from 4 weeks of age. Immunohistochemistry detected Pex3 expression in sensory hair cells of the organ of Corti and in the stria vascularis, spiral prominence and spiral ganglion in wildtype mice at postnatal day five and at 8 weeks. The gross structure of the inner ear of *Pex3* mutants (4 to 14 weeks old) appeared normal compared to littermate controls. Our qRT-PCR results show presence of 16.5% of *Pex3* mRNA in the mutants' cochleae compared

to littermate controls, suggesting incomplete knockdown of *Pex3* transcription.

Conclusions

Pex3 mutants show high frequency hearing loss at 4, 8 and 14 weeks of age, but normal inner ear morphology. This is of particular interest because in humans with progressive hearing loss it is often the high frequencies that are affected first. We propose to use this new *Pex3* mutant to investigate the role of peroxisomes in hearing impairment and identify new routes to therapies.

PS-642

Isoform-Specific Roles of Whirlin Underlie Distinct Pathophysiologies Associated with DFNB31 and USH2

Seham Ebrahim; Morag Lewis; Neil Ingham; Johanna Pass; Karen Steel

King's College London

Introduction

Mutations in Whirlin (*WHRN)* have been linked to profound deafness DFNB31, and also to Usher syndrome Type 2D (USH2D), an autosomal recessive disorder characterized by heterogeneous hearing and vision deficiencies. *WHRN* contains 12 exons with two dominant splice variants, both expressed in the inner ear. *USH2D* is caused by mutations in exons 1-2, affecting the only long isoform, while mutations linked to DFNB31 are located in exons 10 and 11, affecting both isoforms. We aimed to elucidate the molecular mechanisms underlying the distinct pathophysiologies resulting from different mutations in the *WHRN* gene, and thus also the different roles of WHRN in the inner ear.

Methods

We used RT-PCR to characterize spatiotemporal expression patterns of *Whrn* isoforms across inner-ear sensory epithelia. We also generated a novel mouse mutant, $Whrn^{tm1b(EUCOMM)Wtsi}$, in which only the large isoform was predicted to be affected, compared to the well-characterized *Whirler* mutant, in which both isoforms are affected. We analyzed and compared *Whrn* isoform expression, auditory function using auditory brainstem response (ABR) measurements, stereocilia bundle morphology by scanning electron microscopy (SEM), and localization of known WHRN interacting proteins, in both strains.

Results

Preliminary data show that different isoforms of *Whrn* are expressed in the *Whirler* and $Whrn^{tm1b(EUCOMM)Wtsi}$ mice. As previously reported, *Whirler* mutants presented with early onset, profound hearing loss and overt vestibular abnormalities. Conversely, $Whrn^{tm1b(EUCOMM)Wtsi}$ mice had only elevated ABR thresholds and no obvious vestibular defects. We show that these differences can most likely be explained by intriguing differences in stereocilia bundle morphologies in the two mutant strains: while *Whirler* mice have short stereocilia in all hair cells (HCs), a subpopoulation of HCs in $Whrn^{tm1b(EUCOMM)Wtsi}$ mice have stereocilia of close to normal length. These included stereocilia of inner HCs in the organ of Corti, striolar HCs in the otolithic organs, and peripheral zone HCs of the cristae. The localization of the known WHRN-interacting, actin-regulatory protein, EPS8 was comparable in both mutants.

Conclusion

We show for the first time distinct expression patterns and roles for *Whrn* isoforms in stereocilia length regulation, suggesting that different WHRN isoforms likely have distinct interacting partners locally at stereocilia tips according to HC type and/or location. Variations in vestibular phenotype between the two mutants also highlight differences in the roles of HCs in the central versus peripheral regions of the vestibular organs. These data provide novel insights into the molecular mechanisms underlying DFNB30 and USH2D, and also stereocilia length regulation.

PS-643

In Vitro Molecular Imaging of Cochlear Gap Junction Plaque Composed of Connexins

Kaori Hatakeyama; Ichiro Fukunaga; Katsuhisa Ikeda; Kazusaku Kamiya

Juntendo University

Objectives

The mutations in connexin26 (Cx26), a cochlear gap junction protein, represent a major cause of pre-lingual, non-syndromic deafness, as they are responsible for as many as 50% of such cases in certain population. Recently, we reported that Cx26-dependent gap junction plaque (GJP) disruption occured as the earliest change during embryonic development, results in a drastic reduction in the GJP area and the protein levels in Cx26 mutant mouse models (Kamiya et al., J Clin Invest, 2014;124(4)1598-1607) and Brn4 deficient mice, a model of DFN3 non-syndromic deafness (Kidokoro et al., PLoS One, 2014;9(9) e108216). To elucidate the mechanism of this biochemical change, we developed the molecular live imaging system targeting GJP composed of Cx26 and Cx30. Our final goal is to screen the chemicals to stabilize the cochlear GJPs at the cell borders.

Methods

The cells with the transient expression and stable expression of human wild type Cx26, mutant Cx26 (R75W) and wild type Cx30 untagged and tagged with GFP or mCherry were generated with HEK293 and HeLa cell lines.

Results

With the connexin expressing cells which we newly generated, we observed various types of GJPs as well as Cx26-mutant mouse cochleae. Our system enabled us to analyze the formation, trafficking, membrane integration and degradation of GJPs composed of Cx26 and Cx30 in live cell monitoring.

Conclusions

This imaging system will enable the large scale drag screening targeting GJP stabilization for most typical hereditary deafness, Cx26 associated deafness.

PS-644

The Role of LRBA (LPS-Responsive, Beige-Like Anchor Protein) in Auditory Function

Nicola Strenzke[1]; **Christian Vogl[1]**; Tanvi Butola[1]; Tzu-Lun Wang[1]; Michael Leitner[2]; Natja Haag[3]; Dominik Oliver[2]; Kilimann Manfred[1]; Tobias Moser[1]
[1]Göttingen University; [2]Philipps University Marburg; [3]University Hospital Jena

Introduction

LRBA (LPS-responsive, beige-like anchor protein) belongs to the enigmatic BEACH protein family, members of which were shown to localize to subcellular membranous compartments and to participate in intracellular protein trafficking and pre- and postsynaptic function. LRBA is highly expressed in cochlear inner (IHCs) and outer hair cells (OHCs) and LRBA knockout mice show severe early-onset, progressive hearing impairment.

Methods

To characterize the auditory phenotype resulting from loss of LRBA, we recorded auditory brainstem responses (ABR), distortion product otoacoustic emissions (DPOAE), cochlear microphonic and summating potentials, and responses from single auditory nerve fibers. Moreover, we performed *in vitro* electrophysiological patch clamp recordings to analyze OHC electromotility and IHC presynaptic function, immunohistochemistry and scanning electron microscopy to assess hair cell morphology and live-cell imaging to decipher the localization and function of LRBA in mutant mice and wild-type littermates.

Results

Our data show significantly elevated ABR thresholds alongside reduced ABR Wave I amplitudes and severely attenuated DPOAEs and cochlear microphonic and summating potentials. These findings indicate a major impairment of cochlear amplification, potentially aggravated by additional deficits in sensory receptor function. Electrophysiological recordings of prestin-driven changes in non-linear capacitance in OHCs indicated unchanged electromotility in LRBA mutants. Moreover, IHC presynaptic calcium currents and exocytosis as well as suprathreshold auditory nerve fiber responses remained unaltered despite of LRBA loss. However, morphological studies revealed severe defects in hair bundle morphology accompanied by reduced FM1-43 dye uptake through stereociliary mechanotransduction channels. Finally, we show that LRBA localizes to the kinocilium basal body complex during development, where it might contribute to hair bundle formation and/or maturation.

Conclusions

Our data suggest that LRBA loss impairs hair cell mechanotransduction but argue against a contribution to OHC electromotility or IHC presynaptic function. We propose a role of LRBA in hair cell protein trafficking that is required for normal formation, maturation or maintenance of stereocilia.

PS-645

The Prestin Mutation R130S (DFNB61) Impairs Motor Kinetics

Kazuaki Homma[1]; Satoe Takahashi[1]; Nicole Chen[2]; Mary Ann Cheatham[1]; Jing Zheng[1]
[1]Northwestern University; [2]Stevenson High School

Introduction

A missense mutation, R130S, was recently found in the prestin gene of Japanese patients with moderate to severe hearing loss (DFNB61, Mutai et al., 2013). The objective of this study is to characterize R130S prestin in a heterologous expression system in order to define the pathology of hearing loss induced by this mutation.

Methods

A recombinant gerbil prestin construct harboring the R130S missense mutation was generated and expressed in HEK293T cells. Subcellular localization of the mutated protein was examined by confocal microscopy. Nonlinear capacitance (NLC) of R130S prestin was measured in the whole-cell configuration and the result compared to that of wild-type prestin to assess the effect of the R130S mutation on prestin's motor function.

Results

R130S prestin was targeted to the plasma membrane to confer electromotility on HEK293T cells. The voltage operating point (V-peak) and voltage sensitivity (alpha) of R130S prestin were similar to wild-type prestin. However, the NLC of R130S prestin showed a significant stimulus frequency-dependence compared to wild-type, suggesting that the motor kinetics of prestin is significantly slowed by the R130S mutation.

Summary

Our study demonstrated that the R130S mutation significantly impairs the motor kinetics of prestin, which conceivably underlie the hearing loss associated with this mutation. Our results support the presumed role of prestin as a cycle-by-cycle cochlear amplifier although a potential adverse effect of R130S mutation on OHC function and maintenance needs to be examined in an animal model.

PS-646

Temporal Processing Deficits in a Mutant Mouse Deficient in GluN2D-Containing NMDA Receptors

JoAnn McGee; Alexander Anton; Edward Walsh
Boys Town National Research Hospital

N-methyl-D-aspartate (NMDA) glutamate receptors are heterotetramers consisting of GluN1 and GluN2 subunits. GluN2 subunits A through D are widely expressed in the adult auditory brainstem (Sato *et al.*, 2000) and it has been shown in previous studies that auditory thresholds to click stimuli are elevated in mice lacking the GluN2D receptor subunit, but not GluN2A or GluN2B subunits (Munemoto *et al.*, 1998; Takeuchi *et al.*, 2001). These findings, along with the observation that the GluN2 subunit is a major determinant of the biophysical properties of NMDA receptors, suggest that the GluN2D subunit may play a significant role in auditory system function

in both developing and adult animals. The goal of this investigation was to determine the influence of the GluN2D subunit on the time course of age-related hearing loss, its influence on dynamic frequency- and level-dependent response features of the system, as well as response dependence on stimulus presentation rate, by considering a mouse model lacking the GluN2D subunit. The potential influence of the subunit on recovery from acoustic over-exposure was also assessed. Both auditory brainstem responses (ABRs) and distortion product otoacoustic emissions (DPOAEs) were recorded in GluN2D-null and wild-type (WT) control mice. Evidence supporting diminished temporal processing capacity in GluN2D-null mice relative to WT-controls was observed when ABR Wave V response amplitudes vs. click presentation rate relationships were compared. Outcome differences in this test of temporal processing capacity were observed primarily at lower simulation levels, even though NMDA receptors commonly operate at higher stimulation levels. Threshold differences were not observed, nor were response feature differences associated with level and frequency dependence. Likewise, the time course of recovery from noise-induced hearing loss was normal in GluN2D subunit deficient mice. Thus, based on outcomes of this battery of physiological tests, deficits associated with loss of the GluN2D subunit appear to be limited to the realm of temporal processing in higher brainstem regions, a finding supporting the view that the subunit influences the kinetic properties of the receptor. Supported in part by the National Science Foundation/Nebraska EPSCoR Program.

PS-647

Role of Synj2 in High Frequency Progressive Hearing Loss

Elisa Martelletti; Johanna C. Staines; Annalisa Buniello; Neil Ingham; Karen Steel
King's College London

Introduction

Synaptojanin 2 (Synj2) is a phosphatidylinositol phosphatase which removes the 5-position phosphates from phosphoinositides, such as PIP_2 and PIP_3. It is a key enzyme in the phosphoinositide signalling cascade and in clathrin-mediated endocytosis. We are interested in exploring the effect of *Synj2* mutation on the development and function of inner hair cell synapses. In 2011 another mouse mutant for *Synj2* was reported and showed progressive hearing loss (Manji *et al.*, 2011).

Methods

A targeted mutation of *Synj2* (*Synj2*$^{tm1a(EUCOMM)Wtsi}$) was generated and screened using auditory brainstem responses (ABR) at 14 weeks old as part of the Sanger Institute Mouse Genetics Project (White *et al.*, 2013). Following deletion of critical exons of *Synj2* (generating the *Synj2*$^{tm1b(EUCOMM)Wtsi}$ allele), ABR measurements were made from ketamine/xylazine anaesthetised mice at 2, 4, 6, 8, 12 and 14 weeks old in response to click stimuli and tone pips ranging from 6-42kHz. The morphology of the nerve endings in the organ of Corti was studied in whole mount preparations labelled with anti-neurofilament antibody and CtBP2 antibody was used to label ribbon synapses. Specimens (*Synj2*$^{-/-}$ n=5, control n=4) were examined at 10% intervals along the length of the cochlear duct using a Zeiss LSM 710 confocal microscope.

Results

Synj2^{tm1a} mutant mice showed normal ABR thresholds, which might be due to incomplete inactivation of transcription in this allele. Therefore, we crossed the *Synj2*^{tm1a} mutant mice to CMV-Cre mice in order to delete the critical exons (9-11) of the *Synj2* gene and generate the *Synj2*^{tm1b} mutant allele. ABR recordings performed on *Synj2*^{tm1b} mutant mice at different ages (4, 6, 8, 12 and 14 weeks) showed progressive increase of ABR thresholds for frequencies higher than 30 kHz in comparison to littermate controls. Mutant mice tested at 2 weeks old had normal threshold sensitivity. In order to understand whether the loss of high frequency sensitivity is caused by an innervation defect in the organ of Corti, we investigated the morphology of nerve terminals in 4 week old *Synj2*^{tm1b} mice. We observed swelling of auditory nerve fibres under inner hair cells in mutant mice.

Conclusions

ABR measurements showed that *Synj2*^{tm1b} mutant mice have normal thresholds at 2 weeks, while they lose high frequency sensitivity from 4 weeks onwards. This suggests that some defects occur during that window of time. The *Synj2*^{tm1b} mice are a useful tool to improve our knowledge of mechanisms underlying high frequency progressive hearing loss.

PS-648

Capillary Density Does Not Contribute to Cochlear Hypoxic Miroenvironment.

Edward Doyle, III; Alexis Varvares; Kara Emery; MIchael Anne Gratton
Saint Louis University

Introduction

Autosomal recessive Alport syndrome is a genetic disorder of type IV collagen that leads to aberrant basement membranes. Alport syndrome is associated with glomerulosclerosis and progressive sensorineural hearing loss. The cochlea of an Alport mouse is a hypoxic microenvironment. Previously we have shown that Alport mice have an increased expression of hypoxic inducible factor-1α (HIF-1α), are susceptible to noise-induced hearing loss, and have a reduction in endocochlear potential when exposed to noise. Based upon these findings we hypothesize that this microenvironment is due to a thickening of the strial capillary basement membrane (SCBM), which inhibits the diffusion of energy substrate from the stria vascularis (SV) to the organ of Corti. However, we have suspected a qualitative difference of the capillary bed within the SV of Alport mice when compared with wild-type (WT) littermates. This has led us to investigate if reduced capillary density or strial area of an Alport mouse contributes to the hypoxic environment.

Goal: To investigate whether a difference in capillary density or strial area exists in the stria of Alport vs. WT littermates.

Methods

9 wk old 129Sv/J Col4α3 KO and WT mice were anesthetized with Urethane (1.5mg/kg BW). Cochleae were isolated,

round window was pierced, the stapes removed, and the cochleae perilymphatically perfused with fixative. Each cochlea was immersion fixed for 30 minutes before washing with phosphate buffered saline. The cochleae were perilympathically perfused with 3,3'-diaminobenzidine and 3% H_20_2. Both cochleae were immersed in this solution for one hour to allow for endogenous reaction with endothelial cells and red blood cells. The lateral wall of the cochlea was microdissected from apex to base and flat mounted in glycerin. Care was taken to mount the SV upward. Serial images of the stria, focused on the capillaries, were captured in an apex to base sequence at 20x magnification. The capillary density of the stria was calculated by using Volocity (Perkin Elmer). The data were analyzed with a Student's t-test using Sigma Plot.

Results
No significant difference was found between the mean capillary density ($t(8)=0.0859$, $p=0.934$) nor the area of the SV ($t(8)=0.0604$, $p=0.562$) of the KO and WT groups.

Conclusions
The lack of difference in capillary density and strial area between the WT and Alport mouse supports our prior hypothesis that a thickening of SCBM is the primary cause of a hypoxic microenvironment in the Alport cochlea.

PS-649

Proteome Analysis of the Human Perilymph

Heike Schmitt[1]; Merve Wollweber[2]; Martin Höhl[2]; Uwe Morgner[2]; Andreas Pich[3]; Giorgio Lilli[4]; Günter Reuter[4]; Thomas Lenarz[4]
[1]Hannover Medical School, Hanover; [2]Centre for Optical Technologies, Leibniz University Hannover, Hanover; [3]Core facility proteomics, Hannover Medical School, Hanover; [4]ENT Department, Hannover Medical School, Hanover

Introduction
The composition of human perilymph and its pathophysiological alterations due to inner ear diseases is largely unknown so far. This project is focusing on the identification of protein biomarkers characterizing inner ear function. The main goal of the project is the improvement of diagnostics for different types of inner ear diseases applying at first an invasive method for the analysis of human perilymph. The analysis of human perilymph by mass spectrometry coupled with liquid chromatography (LC-MS) should enable the identification of protein composition of perilymph per se and changes of perilymph composition significant for sensorineural hearing loss. Based on this analysis, a non-invasive method is being developed.

Methods
Pathophysiological relevant markers for different inner ear diseases and therefore especially the proteins of human perilymph are analyzed. The sampling of human perilymph was performed during inner ear surgeries like cochlear implantations. It is crucial to avoid contamination of the samples and to gain a sufficient volume of perilymph (>2 µl). The proteins of perilymph samples are identified by shot-gun proteomics including data-dpendent analysis and in parallel an optical method (Raman spectroscopy) for non-invasive protein analysis will be validated.

Results
An appropriate sampling method for sampling of human perilymph was developed. Microglasscapillaries were modified and used for taking human perilymph. Sampling of perilymph occurs during surgeries through the round window membrane by capillary forces directly before insertion of the cochlear implant electrode. Up to now we took 41 perilymph samples from patients of various ages during cochlear implantations and four samples during acoustical neurinoma surgeries with transcochlear approach. The perilymph-sample volumes are 2-10 µl. By mass spectrometric analysis, we identified approximately 300 different proteins per sample. Altogether more than 1000 different proteins were found in all perilymph samples.

Conclusions
Indepth comparison and verification of proteins identified by LC-MS and information from literature and databases is necessary in order to compile a detailed protein map of human perilymph. Analysis of this protein database is then used to identify proteins that are specific for certain diseases of the inner ear leading to inner ear hearing loss.

PS-650

Scala Tympani Delivery of Adeno-associated Virus Vectors to the Mouse Inner Ear

Andrew Breglio; Kevin Isgrig; Lisa Cunningham; Wade Chien
National Institutes of Health

Background
Development of viral-based therapies for gene delivery to the inner ear requires evaluation of the cellular tropisms and infection efficiencies of potential viral vectors. We examined the inner ear infection pattern following trans-round window injection of three different Adeno-associated virus (AAV) serotypes.

Methods
Neonatal (P3) and adult (2-5 months) tdTomato mice were used in this study. These mice are heterozygous for a loxP-flanked STOP cassette preventing transcription of the tdTomato reporter at the Gt(ROSA)26Sor locus. AAV (serotype 1, 2, or 8) expressing Cre recombinase under control of a CMV promoter was administered via round window injection. Cochleas and utricles were dissected 3 weeks postoperatively and analyzed by confocal microscopy. The contralateral (non-operative) ears were used as controls. Auditory brainstem evoked responses (ABRs) were used to evaluate surgically- and virally-induced hearing loss.

Results
Overall, 42% (8/19) of adult mice and 42% (5/12) of neonatal mice showed infection following surgery. Across ages and viral serotypes the efficiency of infection was greatest in the basal 1/3 of the cochlea. AAV2 was the only viral serotype observed to infect hair cells, and it exclusively infected inner hair cells in adult mice. In neonates AAV2 did not infect hair

cells, but rather infected supporting cells and other cell types. In adults and neonates, AAV1 and AAV8 infected a number of different cell types including spiral ganglion neurons and cells located within the lateral wall and spiral limbus. Interestingly, only neonatal mice showed Cre-mediated tdTomato expression in the contralateral, non-surgical cochlea, albeit at levels much lower than the associated surgical cochlea. Neonatal mice were also the only mice to show infection in the utricle. Surgery resulted in a high-frequency hearing loss of moderate severity in all mice, including sham surgery animals that did not receive virus.

Conclusions

Our results illustrate the infection patterns achieved in the cochlea and utricle using three different AAV serotypes via the round window approach. AAV2 was most effective as a viral vector for targeting inner hair cells.

PS-651

Hair Cell Loss, Spiral Ganglion Loss, and High Frequency Hearing Loss in Fvb/Nj Mice with Slc44a2 Deletion

Bala Naveen Kakaraparthi; Trey T. Thomas; **Thankam S. Nair**; Pavan Kommareddi; Irina Laczkovich; Ariane Kanicki; Lisa Kabara; Catherine A. Martin; David Dolan; Thomas E. Carey

University of Michigan

SLC44A2/CTL2 (**s**o**l**ute **c**arrier **44a2**) (**c**holine **t**ransporter-**l**ike protein **2**)was discovered in the inner ear and is implicated in immune-mediated hearing loss. Exons 3-10 of mouse *slc44a2* were deleted in the C57BL/6 strain. C57BL/6 *slc44a2* wild-type (WT) mice strongly express *slc44a2* mRNA and protein. *Slc44a2* KO mice fail to express detectable protein, exhibit significant hair cell loss and have progressive high frequency hearing loss. Sequence analysis of cDNA from C57BL/6 KO mice revealed an out-of-frame transcript leading to early stop codons. This strain exhibits age-related hearing loss secondary to the *Ahl* $Cdh23^{753A}$ mutant allele, complicating analysis of *slc44a2*-related effects. Therefore the C57BL/6 knockout (KO) was repeatedly backcrossed (BC) to FVB/NJ strain ($Cdh23^{753G}$) and hearing was evaluated in this genetic context and compared to results found in the initial background strain. We found a 99% match between the *slc44a2* nucleotide sequences in C57BL/6 and FVB/NJ backgrounds. The *slc44a2* KO transcript in the FVB/NJ KO mouse was confirmed to be identical to the out-of-frame transcript in the C57BL/6 KO. Auditory brainstem response (ABR) testing in 99% FVB/NJ (BC7) background showed that KO mice display progressive hearing loss and high frequency (32 kHz) loss beginning from approximately five months, while WT mice maintain normal hearing thresholds through more than eight months of age. Histological assays of offspring from BC7 intercross mouse group included seven WT, nine HET, and 14 KO mice. Cochlear whole-mount images and cytocochleogram analysis of seven WT, four HET, and seven KO mice harvested at eight months of age revealed extensive outer hair cell (OHC) loss at all turns, particularly at the middle turn, in KO mice compared to WT and HET littermates. Inner hair cell (IHC) loss was variable and scattered throughout the cochlea in KO mice but was less extensive than loss of OHCs. HET mice were comparable to WT mice, but showed slightly more OHC loss at the apex/base. Cochlear cross-section images of five WT, five HET, and seven KO mice depicted extensive damage to the spiral ganglia of KO and HET mice at the base whereas little damage occurred in WT mice. These results confirm the previous findings in C57BL/6 mice. Confirmation of these results in the *Ahl* resistant FVB/NJ background demonstrates that the *Slc44a2* gene is critical for maintenance of normal hearing.

PS-652

Immunocytochemical markers for otosclerosis

Kumiko Hosokawa; Seiji Hosokawa; **Ivan Lopez**; Gail Ishiyama; Akira Ishiyama; Fred Linthicum

David Geffen School of Medicine, University of California, Los Angeles

Background

Otosclerosis is a localized hereditary disorder affecting enchondral bone of the otic capsule that consists of one or more localized foci where there has been repeated resorption and remodeling of osseous tissue. Histopathological studies of otosclerosis have been well documented. The molecular mechanisms of otosclerosis are beginning to be elucidated. In the present study we investigated the expression of several proteins in the human otic capsule from patients with histological otosclerosis using immunohistochemistry.

Methods

Formalin-fixed celloidin-embedded (FFCE) human temporal bone sections were immunoreacted with antibodies against nidogen, UBA52, laminin and collagen IX. Temporal bones of 8 otosclerosis patients (2 male and 6 female) ranging from 55 to 87 years of age, with an average age of 69.1 years old, and temporal bones with 4 normal auditory function, 5 other otological diseases were used for this purpose.

Results

A differential immunoreactivity pattern was detected in the otosclerotic region. Nidogen-immunoreactivity (IR), UBA52-IR, and laminin-IR was seen mainly in the sclerotic portion (verified by polarized light and examination of hematoxylin and eosin stained adjacent section). Immunoreactivity for these three proteins was seen between the anterior part of the stapedial footplate, the processus cochleariformis and the bulge of the promontory. The spongiotic (area, characterized by numerous areas of fibrous tissue containing monocytes, macrophages, and enlarged capillaries) showed almost no immunoreactive signal. Mild collagen IX-IR was seen in the whole otosclerotic region. Non significant immunoreactive pattern was seen for all the antibodies tested in the temporal bones with normal auditory function, Meniere's disease, and other otological diseases of the cochlea.

Conclusion

Nidogen, and laminin two extracellular matrix and basement membrane proteins highly expressed in the sclerotic region, previously thought to be inactive, suggests a remodeling process of bone. UBA52 is an ubiquitin protein that plays a

fundamental role in mediating selective protein degradation was also highly expressed in the sclerotic foci. These results suggest that these proteins maybe therapeutic targets for the treatment of otosclerosis.

PS-653

The Activation of Stem Cell Homing Factors Highly Induces the Cochlear Invasion of Bone Marrow Mesenchymal Stem Cells.

Ichiro Fukunaga[1]; Kaori Hatakeyama[1]; Osamu Minowa[2]; Katsuhisa Ikeda[1]; Kazusaku Kamiya[1]
[1]Juntendo University; [2]RIKEN, BioResource Center

Objectives:

Congenital deafness affects about 1 in 1000 children and more than half of them have genetic background such as Connexin26 (Cx26) gene mutation. The strategy to rescue such heredity deafness has not been developed yet. Recently, a number of clinical studies for cell therapy have been reported and clinically used for several intractable diseases. Inner ear cell therapy for sensorineural hearing loss also has been studied using some laboratory animals, although the successful reports for the hearing recovery accompanied with supplementation of the normal functional cells followed by tissue repair, recovery of the cellular/molecular functions were still few. Previously, we developed a novel animal model for acute sensorineural hearing loss due to fibrocyte dysfunction and performed cell therapy with bone marrow mesenchymal stem cells (MSC) as supplementation of cochlear fibrocytes functioning for cochlear ion transport.

In this study, we examined the new treatment to enhance the MSC induction to cochlear tissue to improve this strategy.

Methods

We applied the inner ear MSC transplantation to Cx26 deficient mice which we developed as a model for hereditary hearing loss (Kamiya *et al.,* 2014, *J Clin Invest* **124 (4)**, 1598-1607). We transplanted the MSCs to the lateral semicircular canal after the induction of stem cell homing factors (stromal cell-derived factor-1: SDF-1, monocyte chemotactic protein-1: MCP-1) in the host cochlear tissue, and their receptors in transplant MSCs.

Results

To enhance MSC invasion to cochlea tissue, we developed a novel transplant strategy by induction of SDF-1 /MCP-1 expression in host cochlear tissue and enhanced expression of their receptors, chemokine (C-C motif) receptor 2 (CCR2) and C-X-C chemokine receptor type 4 (CXCR4) in MSC.

Conclusions

With this strategy, we induced efficient invasion of MSC to inner ear tissue and differentiation to form gap junctions with Cx26 among transplanted MSCs in Cx26-deficiente mouse inner ear.

PS-654

Tricellulin Knockout Mice, a Model of DNFB49, Show Severe Hearing Loss with Cochlear Hair Cell Apoptosis

Toru Kamitani[1]; Hirofumi Sakaguchi[1]; Takenori Miyashita[2]; Ryuhei Inamoto[2]; Reitaro Tokumasu[3]; Yuji Yamazaki[3]; Atsushi Tamura[3]; Nozomu Mori[2]; Sachiko Tsukita[3]; Yasuo Hisa[1]
[1]Kyoto Prefectural University of Medicine; [2]Kagawa University; [3]Osaka University

Introduction

Tricellulin is a protein which localizes mainly at tricellular tight junctions. It is reported that the tricellular junction was disorganized and that the barrier function was decreased in *tricellulin* knock-down cell lines. However, the function of tricellulin *in vivo* has not been elucidated. On the other hand, mutation of *tricellulin* causes human nonsyndromic deafness DFNB49. The pathophysiology of DFNB49 has not been elucidated although it has been reported recently that *tricellulin* "knockin" mice show alteration of tight junction architecture and hair cell degeneration (Nayak et al. 2013). We generated *tricellulin* knockout mice and investigated their phenotype.

Methods

We generated *tricellulin* knockout (*Tric*$^{-/-}$) mice and examined their hearing ability by ABR. We assessed the histological phonotype by immunofluorescence microscopy, scanning electron microscopy, and transmission electron microscopy. We detect apoptosis of hair cells by the TUNEL method. We preformed the organotypic culture of organ of Corti from postnatal day 4 (P4) for 12 days to investigate the influence of the extracellular environment of the hair cells. We also examined the endocochlear potential.

Results

Tric$^{-/-}$ mice showed deafness . Immunofluorescence microscopy revealed rapid cochlear hair cell generation from P14, although any other apparent alterations were not observed by scanning and transmission electron microscopy. The degenerating hair cells were TUNEL positive. Many hair cells from *Tric*$^{-/-}$ cochlea survived *in vitro*, as well as hair cells from *Tric*$^{+/+}$ cochlea. This suggested that the degeneration of hair cells are caused by extracellular environment rather than by intrinsic factors. The EP of *Tric*$^{-/-}$ cochlea was maintained normally.

Conclusion

Tricelluin knockout mice showed severe hearing loss as an only phonotype as well as DFNP49 patients. Therefore *Tric*$^{-/-}$ mice can be regarded as a model of DFNB49. Rapid hair cell degeneration occurred in *Tric*$^{-/-}$ cochleae from P14. The degeneration coincided with the rapid elevation of EP. Although no apparent structural alteration was observed by immunofluorescence microscopy, scanning or transmission electron microscopy, it is assumed that the permeability of tight junction at reticular lamina is increased in *Tric*$^{-/-}$ cochlea. The peameability of the stria vascularis should be maintained because the EP was unaffected. It is probable that the EP maturation causes leakage of K^+ from the scala media to the

cortilymph. The elevated K^+ ion concentration is considered toxic to hair cells and it leads to apoptosis and hearing loss.

PS-655

Accumulated Caveolins in the Models of Connexin26 Associated Deafness

TAKASHI ANZAI; KAZUSAKU KAMIYA; KATSUHISA IKEDA
Juntendo University School of Medicine

Introduction and Purpose:
The mutations in connexin26 (Cx26), a cochlear gap junction protein, represent a major cause of pre-lingual, non-syndromic deafness. Recently, we showed that Cx26 mutation resulted in a drastic reduction in the gap junction plaque (GJP) and caveolins associated with the GJP disruption.(Kamiya et al. J. Clin. Invest. 2014;124(4)1598-1607).Caveolins are integrated plasma membrane protein and structural component of caveolae membranes. Recent studies showed that the over expression or abnormal localization of caveolins associated with delayed wound healing or cellar aging in several organs. The purpose of this study is to investigate the association of caveolins in the pathology of Cx26 related hearing loss

Method
We analysed the protein expression and localization of Caveolin-1 or Caveolin-2 in two types of the models of GJB2 associated deafness, Cx26R75W-Tg (dominant negative) and Cx26cKO (protein deficient).

Conclusion
Interestingly, we observed significantly increased the expression of CAV1 and CAV2 in Cx26 mutant cochleae. Although, only a diffused labelings of caveolins were observed in the control mice, there were accumulations of caveolins in the organ of Corti in both Cx26 mutant mice. Especially, these accumulations were notably observed in the outer hair cells (OHCs), Deiter's cells and pillar cells. The Cells with abnormally accumulated caveolins were significantly increased in the both Cx26 mutant mouse. Furthermore, it was also revealed that CAV1 and CAV2 protein levels were significantly increased in Cx26 mutant cochleae.

In this study, we suggested that caveolins in cochlea may play a crucial role in the pathogenesis of GJB2 associated deafness.

PS-656

Vestibular Pathology in the Npc1-/-mouse, a Model of Niemann Pick Disease Type C

Karen Pawlowski; Joyce Reppa
University of Texas Southwestern Medical Center

Introduction
Early onset hearing loss and cochlear pathology have recently been demonstrated in humans and in animal models (due to genetic inactivation of the *Npc1* gene) of the debilitating cholesterol storage disease, Niemann Pick disease type C (NPC, King K, et al. Hearing loss as an early consequence of Npc1 gene deletion in the mouse model of Niemann-Pick disease, Type C. JARO 15(4):529-41, 2014). Cerebellar and vestibular dysfunction has also been observed in this condition in both humans and animal models. Voikar and colleagues demonstrated deficits in vestibular/motor coordination in male *Npc1*$^{-/-}$ mice as early as P28 (Voikar V, Rauvala H, & Ikonen E. Cognitive deficit and development of motor impairment in a mouse model of Niemann-Pick type C disease. Behav Brain Res 132:1-10, 2002). The authors suggest these early changes could be central or peripheral in origin. However, the condition of the peripheral vestibular system of this model has yet to be described.

Methods
Npc1$^{-/-}$ and wild type mice at 20, 30, 50 and 70 days of age were euthanized, both inner ears quickly perfused with, and fixed in 2.5 % glutaraldehyde in PBS. Tissues for light microscopic imaging were processed and embedded in JB-4 and tissues for electron microscopic imaging processed and embedded in Embed-812 according to published protocols (King, et al. JARO, 2014). Light microscopic serial sections were analyzed for the occurrence of histological changes within the vestibular system. Transmission electron microscopy was used to more closely analyze cellular changes within the epithelia.

Results
Histological changes were seen in serial sectioned tissue from *Npc1*$^{-/-}$ mice compared to the wild type littermate controls. Changes seen include swelling of neural endings and nerve fibers within or in close proximity to the sensory epithelia of the utricle, saccule and semicircular ducts. The earliest histological changes occurred within the sensory epithelia. Details of onset, differences in onset for male and female mice, and ultrastructural findings will be discussed.

Conclusions
The results of this study indicate that like the auditory system, there is a peripheral vestibular phenotype that develops early in disease progression in the *Npc1*$^{-/-}$ mouse.

SYM-74

Chromodomain Protein Regulation of Sensory Placode and Central Nervous System Neural Stem Cell Proliferation and Fate

Donna Martin[1]; Ethan Sperry[1]; Jennifer Skidmore[1]; Donald Swiderski[1]; Lisa Beyer[1]; Peter Scacheri[2]; Yehoash Raphael[1]
[1]The University of Michigan; [2]Case Western Reserve University

Transcriptional regulation of gene expression is critical for proper function of embryonic and neural stem cells. Epigenetic regulators including histone modifying proteins have recently emerged as dynamic modulators of gene expression, especially during development. In addition, chromatin remodeling protein members of the SNF2 superfamily, including the Chromodomain Helicase DNA-binding (CHD) family use the energy of ATP to regulate access of transcription factors and other epigenetic modifiers to promoter and enhancer regions throughout the genome. We have sought to understand the roles of CHD proteins in otic and olfactory placodes and in the central nervous system, with a focus on CHD7, a member of the 3rd subfamily of CHD proteins.

CHD7 forms large protein-protein complexes with other transcription factors (e.g. SOX2), methyltransferases (e.g. SETDB1), and PBAF complex proteins, and preferentially binds to methylated histones at promoter and enhancer sites. We have generated and studied mice with germline and conditional loss of *Chd7* function to identify basic epigenetic mechanisms involved in neuronal development. Studies with *Foxg1-Cre;Chd7f/f* mice showed that *Chd7* is essential for proliferation of progenitors in the neurogenic domain of the mouse otocyst, and that reduced *Chd7* leads to hypoplasia of the statoacoustic ganglion. Other studies with germline *Chd7$^{Gt/+}$* and *Ubc-Cre;Chd7f/f* mice revealed a requirement for *Chd7* in olfactory neuroblasts that generate olfactory sensory neurons and GnRH-positive neurons. More recently, we learned that *Chd7* is critical for formation of neural stem cells in the embryonic and postnatal subventricular zone, an area that gives rise to olfactory bulb neurons via the rostral migratory stream.

We have also identified several genes whose expression depends upon CHD7. These include *Tbx1, Otx2,* and *Fgf10* (inner ear), *Otx2, Bmp4, Fgf8* and *Fgfr1* (olfactory placode), and *Rarb*, *Rxrg*, and *Neurod1* (subventricular zone). Other studies have indicated *Sox4/11* as downstream targets of CHD7 in the forebrain (Feng et al., 2013). Together, these results implicate retinoic acid, Fgf, Bmp, and Tgfb signaling in CHD7-dependent neural development. Interestingly, in the inner ear, genes in some signaling pathways appear unaffected by loss of *Chd7*, including *Eya1* and Notch (*Lfng*), suggesting specificity of CHD7 function.

Identification of CHD7 protein partners in embryonic neural stem cells is limited to SOX2 (Engelen et al., 2011). We are using RNA-seq and ChIP-seq on microdissected embryonic inner ear tissues to identify binding sites at CHD7 targets. Preliminary data suggest that CHD7 promotes loss of pluripotency via changes in occupancy of specific promoter and enhancer histone modifications.

SYM-75

c-Myc Transcriptionally Amplifies Sox2 Target Genes to Regulate Self-Renewal in Multipotent Otic Progenitor Cells

Kelvin Kwan
Rutgers University

Sensorineural hearing loss is caused by the loss of sensory hair cells and neurons of the inner ear. Once lost, these cell types are not replaced. Two genes expressed in the developing inner ear are c-Myc and Sox2. Using only these two factors, we created induced multipotent otic progenitor (iMOP) cells, a fate-restricted cell type, by transient expression of c-Myc in Sox2-expressing otic progenitor cells. This activated the endogenous c-Myc and amplified existing Sox2-dependent transcripts to promote self-renewal. Global analysis of the transcriptome and transcription-factor-binding sites revealed that c-Myc and Sox2 occupy over 85% of the same promoters. c-Myc and Sox2 target genes include cyclin-dependent kinases that regulate cell cycle progression. iMOP cells continually divide but retained the ability to differentiate into functional hair cells and neurons in vitro. We propose that Sox2 and c-Myc regulate cell cycle progression of these cells, and that downregulation of c-Myc expression following growth factor withdrawal serves as a molecular switch for differentiation. Our findings on c-Myc and Sox2 in iMOP cells will accelerate efforts for auditory regeneration.

SYM-76

EYA1-Six1 transcriptional complex in inner ear neurosensory development

Pin-Xian Xu
Icahn School of Medicine

In mammals, cochlear hair cells and their associated neurons do not regenerate, resulting in irreversible deafness. Currently, we do not yet have a definitive strategy for auditory regeneration. We recently found that reprogramming of cochlear nonsensory cells toward a hair-cell or neuronal fate can be induced by a set of inner ear neurosensory cell-specific transcription factors EYA1/SIX1 in combination with different cofactors and chromatin remodeling complexes. Furthermore, overexpression of this set of factors in combination with chromatin-remodeling complex in fibroblast cells can convert the cells to neurons. Our study indicates that EYA1 and SIX1 are key transcription factors in initiating the neuronal or sensory developmental program and represents a major step forward to reprogramming or transdifferentiation in the auditory field.

SYM-77

Transcription Factors and Pioneer Factors in Inner Ear Induction

Andrew Groves[1]; Sunita Singh[1]; Onur Birol[1]; Takahiro Ohyama[2]
[1]Baylor College of Medicine; [2]University of Southern California

The mammalian inner, middle and outer ears have different embryonic origins, yet the development of each component of the auditory apparatus must be precisely synchronized in space and time. Understanding the mechanisms that regulate and co-ordinate the development of these structures is of central importance in understanding the basis of the many birth defects that affect hearing. We have identified a Forkhead transcription factor, Foxi3, that is expressed at very early stages in the embryonic head. Foxi3 mouse mutants made in our lab lack all components of the inner, middle and external ears. Our preliminary evidence suggests that one of the first steps in inner ear induction– the formation of the otic placode – does not occur in Foxi3 mutants. Moreover, the neural crest-derived mesenchyme of the first and second branchial arches that generate the middle ear ossicles, tympanic ring and pinna begins to form in Foxi3 mutants, but quickly succumbs to massive cell death.

To our knowledge, Foxi3 is the only gene that causes a complete developmental failure of the entire mammalian inner, middle and outer ears when mutated by itself. We are therefore extremely interested to understand how Foxi3 orchestrates development of the auditory apparatus at both the cellular and molecular levels. Preliminary evidence from our lab

and others suggests that Foxi3 may act as a "pioneer" transcription factor – its main function in addition to initiating transcription is to epigenetically organize genomic loci containing ear-specific genes in a transcriptionally competent state. We are addressing the function of Foxi3 in inner ear induction by analyzing the effect of Foxi3 mutation on the developmental steps from naïve ectoderm to pre-placodal ectoderm to otic ectoderm, which forms in the presence of FGF. In addition, we are using an ES cell model of inner ear induction to characterize the transcriptional and epigenetic roles of FOi3 in ear induction.

SYM-78

Transcriptional Control of Sensory Progenitor Specification in the Inner Ear

Kathryn Cheah[1]; Keith K.H. Leung[1]; Michael Hang Kwong[1]; Ben Niu[1]; Anna Pelling[1]; Israt Jahan[2]; **Robin Lovell-Badge**[3]; Bernd Fritzsch[2]

[1]University of Hong Kong; [2]University of Iowa; [3]MRC National Institute for Medical Research, London, UK

Development of the inner ear requires coordination of early specification, in the correct location, of specific cell types: sensory hair cells, non-sensory supporting cells and sensory neurons that innervate the hair cells. These cells are essential for hearing and balance, acting as mechanosensors for the detection of sound, gravity and acceleration which are transmitted to the central nervous system. Sensory and non-sensory structures in the functional inner ear are specified early in development, before any overt structure can be seen, according to the spatial location of progenitors within the epithelium of the otocyst. It is thought that the six sensory organs in the inner ear develop from common progenitors in the otic epithelium.

We previously studied two allelic mouse mutants with recessive deafness and balance-impairment, Light coat and circling (*Lcc/Lcc,* completely deaf) and Yellow submarine (*Ysb/Ysb*, severely hearing impaired) and discovered that *Sox2* is essential for the prosensory and sensory precursors in the inner ear starting from the otocyst stage. In *Lcc/Lcc* inner ears, all six sensory regions were absent, neither hair cells nor supporting cells differentiate, while the sensory epithelium was severely disrupted in *Ysb/Ysb.* These phenotypes are due to the severely reduced *(Lcc/Lcc)* or reduced *(Ysb/Ysb)* expression of *Sox2*, specifically within the developing inner ear. We asked whether Sox2 is also essential for specifying the progenitors for the sensory neurons that innervate the hair cells. We found a temporal and dose-dependent requirement for *Sox2* in the specification of and/or maintenance of the otic neuroblasts during neurogenesis. Our studies implicate *Sox2* as the master specifier for progenitors of the three lineages (sensory neurons, hair cells and supporting cells). How is sensory versus non-sensory fate was controlled in the inner ear? Transcriptome analyses of purified presumptive prosensory cells $Sox2^{EGFP/+}$ and $Sox2^{EGFP/Lcc}$ showed upregulation of BMP/TGFβ signaling with loss of Sox2 function. By contrast loss of BMP/TGFβ signaling results in ectopic sensory development. We propose a model whereby Sox2 and BMP/TGFβ signaling function antagonistically to coordinate development of sensory and non-sensory structures in the correct location in the inner ear.

SYM-79

Mechanisms of Transcriptional Control of Atoh1 Gene Expression During Inner Ear Development and Maturation

Neil Segil[1]; Yassan Abdolazimi[1]; Zlatka Stojanova[1]; Tao Kwan[2]; Litao Tao[1]

[1]University of Southern California; [2]House Research Institute

Hearing loss is predominantly caused by death of auditory hair cells. The *Atoh1* gene is necessary and sufficient for sensory hair cell formation and is a potential therapeutic target for hearing regeneration. The goal of our research is to analyze the mechanisms of *Atoh1* gene regulation in the mammalian organ of Corti during development and maturation of hair cells, as well as during the induced transdifferentiation of supporting cells to hair cells following inhibition of Notch signaling.

An important mode of transcriptional regulation is through a variety of reversible post-translational modifications of histone N-terminal tails some of which are permissive for expression and some are not. To decode the epigenetic contribution to Atoh1 regulation, we have developed tools for studying the epigenetic status of genes in the purified cell types of the embryonic and perinatal organ of Corti, using small numbers of cells for "micro"-chromatin immunoprecipitation (μChIP) from FACS-purified hair cells and supporting cells.

We found that the Atoh1 locus in sensory progenitor populations is "bivalently" marked, and that this "poised state" is resolved at the time of Atoh1 up-regulation in nascent hair cells. Interestingly, this poised state is maintained in differentiating perinatal supporting cells, consistent with their continued transdifferentiation potential. In addition, appearance of the permissive histone modification, Histone H3 acetylation at lysine K9 (H3K9ac) at the *Atoh1* locus also correlates with Atoh1 transcriptional regulation, and blocking ongoing acetylation blocks progression of hair cell differentiation.

In separate studies, we have investigated the mechanisms of Notch-mediated inhibition of *Atoh1* in perinatal supporting cells. We and others have previously observed that in the perinatal organ of Corti, inhibition of Notch signaling leads to the up-regulation of Atoh1 in supporting cells, and subsequent transdifferentiation into hair cell-like cells. These studies focus on an analysis of Hes/Hey transcription factor activity at the Atoh1 locus, and epigenetic changes potentially associated with this activity. We are currently employing genome-wide methods (μChIP-seq) to investigate several other epigenetic changes involved in hair cell differentiation and supporting cell transdifferentiation. These studies will contribute to a better understanding of how expression of the *Atoh1* gene is controlled, and potentially how it could be manipulated at the epigenetic level, with the hope of identifying novel methods for treating hair cell loss.

SYM-80

The Role of Notch and SOX2 in the Neurosensory Lineages

Amy Kiernan; Aleta Steevens
University of Rochester

Otic neurons and sensory hair cells arise from a common region of the otic vesicle, although in mammals their production is largely temporally distinct. Previous studies in different vertebrate models have demonstrated the likelihood of three distinct progenitors for these cell types: those that give rise to hair cells and supporting cells; those that give rise to cochleovestibular (CVG) neurons; and those that give rise to both sensory cells and neurons. Previous studies from our lab and others have demonstrated that the Notch signaling pathway and the HMG transcription factor SOX2 are required for the establishment of the sensory progenitors. Overexpression studies have shown that Notch likely acts to specify the sensory progenitors, as activation of the Notch receptor in different vertebrate models including mammals causes ectopic sensory regions to form. It is clear that at least one of the functions of Notch is to activate or maintain SOX2, since SOX2 is immediately upregulated in response to Notch activation. However, at least in mammals, unlike Notch activation, ectopic expression of SOX2 does not lead to robust ectopic sensory formation, leaving the exact role of SOX2 in sensory progenitor formation unclear.

In contrast to sensory progenitor formation, it has been demonstrated that Notch and SOX2 play opposite roles in neural progenitor specification. Overexpression experiments have shown that SOX2 can robustly induce neuron formation, through the activation of Neurogenin1. In contrast, activation of Notch prevents neuronal specification. Indeed, studies have shown that late activation of Notch in the neural progenitors diverts them from the neural fate to the sensory fate, leading to ectopic hair cells and supporting cells in the CVG. Here, we discuss the roles of Notch and SOX2 in the neurosensory lineages, and include recent fate-mapping and deletion studies to help clarify their roles. As loss or dysfunction of critical cell types arising from these sensory/neural progenitors underlies a large proportion of hearing and balance disorders, establishing how these progenitors form is critical for therapies aimed at replacing or regenerating these cell types.

SYM-81

The Histone Demethylase LSD1 in Otic Progenitor Cell Differentiation

Eri Hashino
Indiana University School of Medicine

Pax2 is a member of the paired box family of DNA-binding proteins and required for morphogenesis and cell fate specification during inner ear development. Little, however, is known about how Pax2 promotes sensory development in the inner ear. Accumulating evidence indicates that Pax2-mediated transcription is regulated by epigenetic modifications of chromatin conformational changes at its target gene loci. Lysine-specific demethylase 1 (LSD1) demethylates specifically histone H3K4 and is essential in decommissioning enhancers during cellular differentiation. Based on our observation that LSD1 is expressed in the majority of Pax2-expressing cells in the mouse otocyst, we hypothesized that the transcriptionally active H3K4 marks at Pax2-binding loci might be silenced by histone demethylase activity in otic progenitor cells. To determine if Pax2 interacts with LSD1, we made use of a mouse ventral-otocyst cell line (VOT-N33), which constitutively expresses Pax2 and gives rise to beta-tubulin expressing bipolar neuron-like cells under a differentiation condition. Our immunoprecipitation analyses revealed that Pax2 binds LSD1 in nuclear fractions of undifferentiated VOT-N33 cells. Moreover, we detected an association of Pax2 and LSD1 with components of the NuRD repressor complex, including MTA1 and Mi-2. In contrast, no interaction was detected between Pax2 and components of the CoREST/CtBP complex. To characterize the nature of these protein-protein interactions, we generated a VOT-N33 cell line stably expressing a Pax2-integrated reporter construct (PRS4-EGFP). This construct contains five copies of the Pax2-binding elements inserted upstream of a minimal TK promoter driving EGFP, providing a robust and reliable readout of Pax2 responsiveness. Chromatin immunoprecipitation assays were carried out with VOT-N33-PRS4-EGFP cells to reveal that all known components of the LSD1/NuRD complex occupy the Pax2 responsive elements, suggesting that transcription of Pax2 target genes is suppressed, at least in part, by demethylation of H3K4 at the Px2-binding loci. Moreover, the expression levels of Ngn1, NeuroD, and Brn3a in undifferentiated VOT-N33 cells significantly increased after these cells were treated with the specific small molecule LSD1 inhibitor LSD1-C12. These results reveal a previously unrecognized role for LSD1 in Pax2-mediated chromatin remodeling and transcriptional repression, and suggest that LSD1 can be used as a target for promoting prosensory cell differentiation. Investigation is currently underway to test the effects of LSD1-C12 on otic progenitor cell differentiation using stem cell-derived inner ear organoids.

SYM-82

The Representation of Surprise in Auditory Cortex

Israel Nelken
Hebrew University of Jerusalem

Neurons in the auditory system are highly context-sensitive - they respond to a stimulus not only as a function of the stimulus itself, but also in relation to the sequence of stimuli that just preceded it, emphasizing the responses to rare stimuli. Context-sensitivity occurs as early as the inferior colliculus, but in cortex, it acquires a number of additional properties that may contribute to processing music. Cortical context sensitivity cannot be accounted for by adaptation of the responses to the expected sounds only. In particular cortical responses to sound may depend on tens to hundreds of preceding stimuli presented over tens of seconds, and on an extremely fine-grained representation of these sounds. Furthermore, while in the inferior colliculus the adaptation underlying con-

text-sensitivity is largely frequency-specific, in cortex neurons are selective to complex spectro-temporal structures. In consequence, in response to oddball sequences that contain two spectrally-balanced random chords, which would give rise to similar frequency-specific adaptation, neurons in inferior colliculus fail to detect the rare chord while cortical neurons do. I will then discuss how these processes may participate in the processing of musical surprises.

SYM-83

Harmonic Organizations of Auditory Cortex

Xiaoqin Wang
Johns Hopkins University

A fundamental structure of sounds encountered in the natural environment is the harmonicity. Harmonicity is an essential component of music found in all cultures. It is also a unique feature of vocal communication sounds such as human speech and animal vocalizations. Harmonics in sounds are produced by a variety of acoustic generators and reflectors in the natural environment, including vocal apparatuses of humans and animal species as well as music instruments of many types. Given the widespread existence of the harmonicity in many aspects of our hearing environment, it is natural to expect that it be reflected in the evolution and development of the auditory systems of both humans and animals, in particular the auditory cortex. Recent neuroimaging and neurophysiology experiments have identified regions of non-primary auditory cortex in humans and non-human primates that have selective responses to harmonic pitches. Accumulating evidence has also shown that neurons in many regions of the auditory cortex exhibit characteristic responses to harmonically related frequencies beyond the range of pitch. Together, these findings suggest that a fundamental organizational principle of auditory cortex is based on the harmonicity. Such an organization likely plays an important role in music processing by the brain. It may also form the basis of the preference for particular classes of music and voice sounds.

SYM-84

From Perception to Pleasure: Music and its Neural Substrates

Robert Zatorre
McGill University

Music has existed in human societies since prehistory, perhaps in part because it allows expression and regulation of emotion, and evokes pleasure. In this lecture I present findings from cognitive neuroscience that bear on the question of how we get from perception of sound patterns to pleasurable responses. First I identify some of the auditory cortical circuits that are responsible for encoding and storage of tonal patterns; I will then discuss evidence that cortical loops between auditory and frontal cortices are important for maintaining musical information in working memory, and for the recognition of structural regularities in musical patterns which then lead to expectancies. I will then review evidence concerning the mesolimbic striatal system and its involvement in reward, motivation and pleasure in other domains. Recent data from our lab indicate that this dopaminergic system mediates pleasure associated with music; specifically, that reward value for music can be coded by activity levels in the nucleus accumbens, whose functional connectivity with auditory and frontal areas increases as a function of increasing musical reward. We propose that pleasure in music arises from interactions between cortical loops that enable predictions and expectancies to emerge from sound patterns, and subcortical systems responsible for reward and valuation.

SYM-85

Correlates of Musical Structure and Behavioral Experience in the Prefrontal Cortex of Homo sapiens

Petr Janata
University of California, Davis

The technological advancements and decrease in cost for methods that measure gene expression on a genomic scale, such as microarray and RNA-seq, resulted in popularization of these tools to address biological questions. A growing recognition of the importance of cell type-specific measurement of gene expression, combined with development of tools to apply these analyses to the ear (e.g. cell sorting, genetic models and single cell gene expression analysis), result in a multitude of transcriptomic datasets generated by a variety of labs. These data include inner ear gene expression values from selected groups of cells of wild type or mutant animals derived from diverse species. While the data are deposited in the Gene Expression Omnibus, their utilization for cross comparisons and integrative analyses is both technically and conceptually challenging. Here we present the gEAR portal, an interactive website for query and analysis of cell type-specific gene expression across datasets. This novel tool, currently implemented for the ear field, could be adapted for a variety of tissues. Data are displayed in dynamically colorized anatomical maps/cartoons, presented in absolute and relative values, and cross dataset queries will be possible (e.g. identify transcripts that are enriched in the hair cells of the newborn mouse cochlea and the zebrafish lateral line). Because gene expression data by individual investigators are often generated several years before publication, researchers have the option of depositing their data in a way that is visible to them only. They can then view their data alongside the rest of the publically available data in the portal. This helps with analyzing individual datasets in context, and asking questions in functional genomics through cross comparisons with existing datasets. We believe that the gEAR will prove to be an exciting tool for the inner ear research community. Here we present the beta-version. We call investigators who wish to contribute to the beta-version to contact our group directly. We anticipate the release of the full-featured version, allowing private user uploads, by ARO 2016.

PD-91

α1 nAChR Expression in the Inner Hair Cells Parallels the Onset of Cholinergic Efferent Synaptic Function but is Not Necessary for Efferent Synapse Formation

Isabelle Roux[1]; Jingjing Wu[1]; J. Michael McIntosh[2]; Elisabeth Glowatzki[1]

[1]Johns Hopkins School of Medicine; [2]University of Utah, Salt Lake City

Background.

Little is known of the molecules and mechanisms involved in the formation of the cholinergic efferent synapses which modulate the activity of both inner hair cells (IHCs) (transiently) and outer hair cells (OHCs) in the mammalian cochlea. In hair cells (HCs), the acetylcholine response and efferent synaptic activity are mediated by activation of α9/α10 nicotinic acetylcholine receptors (nAChRs) (Elgoyhen et al. 1994, 2001). Intriguingly, Scheffer et al. (2007) additionally detected the expression of α1 and γ nAChRs subunits in developing HCs.

Methods

We combined mouse genetic approaches, immunohistochemistry, electrophysiology and pharmacology to study the expression pattern and a possible role of α1 nAChR in the cochlea.

Results

Using a reporter mouse in which a *lacZ* coding sequence preceded by an IRES replaces the exon 4 of *Chrna1,* the gene encoding the α1 nAChR subunit, we charted the onset and developmental expression of α1 in HCs. Using whole-cell voltage-clamp recordings from IHCs in acutely excised preparations, we showed that acetylcholine response and efferent synaptic activity start to be detectable in the mouse apical cochlea in the same time window as α1 expression (P0 to P4). In IHCs, which lose their efferent innervation around hearing onset, α1 expression is maintained for at least several months. On the contrary, in OHCs, which maintain their efferent innervation through adulthood, α1 expression is only transiently detectable (P4-P12). As α1 is classically found in 'muscle type receptors', we tested agonists of the muscle nAChRs which do not or poorly activate α9 and α9/α10 nAChRs (Verbitsky et al. 2000, Elgoyhen et al. 2001). Neither anatoxin A, epibatidine, DMPP nor nicotine induced a response in IHCs at P4 or P8, arguing against α1 being part of a functional 'muscle type receptor' in IHCs, in addition to α9/α10 nAChR. We next tested whether α1 is necessary for the formation of functional nAChRs and efferent synapses in IHCs. Using a knockout approach, we showed that both acetylcholine response and synaptic activity are present in the absence of α1, indicating that α1 is not necessary for assembly and membrane targeting of the nAChRs nor for synapse formation.

Conclusions

α1 expression in HCs parallels the onset of cholinergic efferent synaptic function but is not necessary for synapse formation. Further experiments are under way to localize this receptor subunit in HCs and understand its possible roles in efferent synapse formation.

PD-92

Efferent Innervation of Outer Hair Cells in BKα-/- Mice

Kevin Rohmann[1]; Eric Wersinger[1]; Jeremy P. Blaude[2]; Sonja Pyott[2]; Paul Fuchs[1]

[1]Johns Hopkins University School of Medicine; [2]University of North Carolina Wilmington

Background

Medial olivocochlear (MOC) efferent neurons from the auditory brainstem form synapses on outer hair cells (OHCs) of the mammalian organ of Corti to regulate cochlear function. This cholinergic synapse is inhibitory in nature due to the well-documented coupling of nicotinic acetylcholine receptors with small conductance calcium activated potassium channels (SK2) at the post-synaptic membrane. More recent studies have identified the post-synaptic expression of large conductance calcium activated potassium (BK) channels in OHCs of the higher frequency (basal) range of the rodent cochlea. To further explore the possible contribution of BK channels to efferent synaptic function and structure we compared MOC synaptic anatomy and physiology in BKα-/- versus wild-type BKα+/+ littermates.

Methods

Whole cell recordings were performed on mid-apical (6-12kHz) OHCs from BKα-/- mice on an FVB/NJ background (Meredith et al., 2004), which lack expression of the pore-forming α-subunit of BK channels. Wild-type littermates served as controls. All physiology and analysis was conducted blind to genotype. Efferent synaptic release was accelerated with application of 40mM potassium and IPSCs were recorded. Immunofluorescent staining was performed using anti-BK and anti-synapsin I antibodies and imaged with confocal microscopy. Efferent synaptic ultrastructure was measured by 3D reconstruction of transmission electron micrographs of serial ultra thin (65nm) sections.

Results

IPSC waveform was significantly slower (tau decay 50.67±0.68 msec) in the BKα-/- OHCs compared to IPSCs recorded from wild-type littermates (tau decay 39.41±0.43 msec, $p<0.0001$). These results concur with previous experiments on rat OHCs which showed that IPSCs involving a combination of BK and SK channels have faster kinetics than those served by SK channels alone, reflecting the relative gating kinetics of these two channel types. Immunofluorescence and electron microscopy studies revealed that efferent synapses of BKα -/- mice are smaller than those of BKα+/+ littermates and the post-synaptic cistern of knockouts were proportionally smaller still.

Conclusion

Both BK and SK channels are co-expressed at efferent synapses in high frequency OHCs. BK channels shape efferent synaptic physiology, primarily the time constant of decay. BK channel expression occurs days later than the onset of efferent synaptic function and continues to increase with age.

Loss of BKα expression results in altered presynaptic (terminal size) and postsynaptic (cistern size) morphology. Together, our studies show BK channels play a role in the physiology as well as the structural development of efferent synapses on OHCs.

PD-93

Mechanisms of Cholinergic Efferent Synaptic Inputs to Vestibular Type II Hair Cells

Zhou Yu[1]; Soroush Sadeghi[2]; J.Michael McIntosh[3]; Elisabeth Glowatzki[4]

[1]Johns Hopkins University; [2]Center for Hearing and Deafness, University at Buffalo; [3]Deartment of Biology; Department of psychiatry, University of Utah; [4]Department of Otolaryngology-Head and Neck Surgery and Department of Neuroscience, The Johns Hopkins University, School of Medicine

In the mammalian vestibular epithelium, efferent fibers form cholinergic synapses onto type II hair cells (HCIIs) and afferent fibers. Stimulation of the efferents in mammals results in an increase in resting discharge and a decrease in sensitivity of afferent responses (Reviewed in Holt et al., 2011). To understand the cellular mechanisms underlying the function of efferent circuitry, we focused our study on the efferent to HCII inputs.

Whole-cell patch clamp recordings were performed in excised preparations of rat cristae, postnatal days 13-29. HCIIs were identified by their morphology, membrane resistance and channel conductances. Micropipettes were placed underneath the epithelium to provide monopolar electrical stimulation to efferents.

Spontaneous efferent-mediated currents were rarely observed during recordings (4/45), suggesting that the efferents have little influence at rest. When efferents were activated electrically or by high potassium external solution, most HCIIs showed synaptic currents (43/45). Electrically evoked synaptic currents had amplitude of 17.4 ± 0.6 pA (n = 23, Vh = -90 mV); and were reversed ~ -70 mV (n = 2), similar to efferent currents in cochlear HCs. However, at a slow stimulation rate, 1-2 Hz, the efferents showed a low probability of release (P-release = 0.07, n = 10). Although synapses were not efficient when efferents fired sparsely, the synaptic strength could be potentiated during paired-pulse experiments, where two closely spaced stimuli were applied. With a stimulus interval of 20 ms, the second pulse triggered ~2-fold larger responses due to short-term facilitation (n = 5). Moreover, when efferents were stimulated with trains of high frequency pulses, responses could be augmented even more dramatically (e.g., 80 pA at 80 Hz stimulation), due to the continuous potentiation of release probability and the summation of synaptic responses.

To identify the postsynaptic receptors in HCIIs, we tested specific antagonists on responses induced by 1 mM acetylcholine (ACh). Results suggested that ACh responses were mediated by α9* nicotinic ACh receptors (revealed by 600 nM α-conotoxin RgIA block) and associated SK channels (revealed by 300 nM apamin block). Furthermore, 200 nM strychnine reversibly blocked synaptic currents.

Our results demonstrate that the efferents can powerfully modulate the activity of HCIIs when activated at high rates. Because of the negative reversal potential, efferent effects on HCIIs can be excitatory or inhibitory. Future studies on afferents, which are also targets of efferent inputs, will provide additional knowledge and result in a more complete understanding of efferent function.

PD-94

The Synaptic Protein Neuroplastin-65 Is Required For Inner Hair Cell Functional Differentiation And Essential For Hearing

Michael Bowl[1]; Leanne Carrott[2]; Carlos Aguilar[2]; Stuart Johnson[3]; Susan Morse[2]; Andrew Parker[2]; Alun Barnard[4]; Sara Wells[2]; Walter Marcotti[3]; Steve Brown[2]

[1]MRC Harwell, Oxford; [2]MRC Harwell; [3]University of Sheffield; [4]University of Oxford

Introduction

At MRC Harwell ENU-mutagenesis coupled with auditory phenotyping is utilised to generate new mouse models of hearing loss. This approach led to the discovery of *pitch*, a recessive model of profound sensorineural deafness. Mapping studies identified a critical region on chromosome 9 and prioritized candidate gene sequencing identified a coding mutation in *Neuroplastin* (*Nptn*). Through alternative splicing *Nptn* encodes two protein isoforms, Np55 and Np65, which are transmembrane glycoproteins able to mediate a broad range of cellular processes including the genesis, maintenance and plasticity of synapses. Currently, there are no human diseases attributed to the loss of Nptn.

Aim

Utilize the *pitch* mutant to explore the role of Nptn in the function and maturation of the auditory system.

Methods

Undertook a comprehensive characterization of the *pitch* mutant including: *in vitro* analyses to investigate the effect of the mutation on protein function; qRT-PCR and immunolabelling studies to determine the temporo-spatial expression of Nptn transcripts and protein; ultrastructural and histological analyses to assess the organ of Corti; and, electrophysiology studies to assess the function and maturation of the sensory hair cells.

Results

Our studies have found the *pitch* mutation causes substitution of a highly conserved structural cysteine residue (Cys315Ser), leading to loss-of-function. In wildtype mice Np65, but not Np55, is strongly up-regulated in the cochlea from around postnatal day 12 (P12), which corresponds to the onset of hearing in mice. We also found that the physiological development of *pitch* inner hair cells is arrested at around P12, preventing their biophysical differentiation into mature sensory receptors. The maturation of the hair cell synaptic machinery and potassium currents fails to occur in *pitch* mutants. Moreover, assessment of pre-synaptic ribbons and post-synaptic

densities (RIBEYE- and GluR2-positive puncta, respectively) demonstrated a significantly reduced number of matched puncta in mutant mice.

Conclusions
We conclude that Np65 regulates the physiological and morphological differentiation of cochlear inner hair cells at the onset of hearing and as such coordinates one of the most distinctive functional refinements of the mammalian auditory system. These data also demonstrate that *Nptn* is a new deafness-related gene.

PD-95

Vesicular Replenishment in Cochlear Inner Hair Cells Operates Without Munc13 and CAPS Priming Proteins

Christian Vogl[1]; Benjamin Cooper[2]; Jakob Neef[3]; Sonja M. Wojcik[2]; Kerstin Reim[2]; Ellen Reisinger[4]; Nils Brose[2]; Jeong-Seop Rhee[5]; Tobias Moser[6]; Carolin Wichmann[7]
[1]InnerEarLab; [2]Department of Molecular Neurobiology, Max Planck Institute of Experimental Medicine Goettingen; [3]InnerEarLab, Department of Otolaryngology, University Medical Center Göttingen; [4]Molecular Biology of Cochlear Neurotransmission Group, Department of Otolaryngology, University Medical Center Göttingen; [5]Neurophysiology Group, Department of Molecular Neurobiology, Max Planck Institute of Experimental Medicine Goettingen; [6]InnerEarLab, Dept. of Otolaryngology and Collaborative Research Center 889, University Medical Center Goettingen; [7]Molecular Architecture of Synapses Group, Department of Otolaryngology, University Medical Center Goettingen

Cochlear inner hair cells (IHCs) encode sound with high temporal precision, a process that requires tight regulation of presynaptic vesicle release. Recent data show that the molecular composition of IHC active zones differs substantially from conventional glutamatergic synapses. Hence, fundamental steps of the synaptic vesicle cycle – such as vesicular tethering, docking and priming – have to be revisited in these cells. In neurons, neuroendocrine and immune cells, vesicular release critically depends on priming factor proteins of the Munc13 and Ca^{2+}-dependent activator protein for secretion (CAPS) families. In the present study, we tested whether Munc13 and CAPS proteins also regulate exocytosis in mouse IHCs, in which another C_2 domain protein, otoferlin, is critical for priming and fusion of vesicles. We combined auditory systems physiology, IHC patch-clamp recordings and immunohistochemistry in Munc13 and CAPS mouse mutants to probe for potential roles of these proteins in IHC exocytosis. We show that IHC Ca^{2+}-currents and exocytosis as well as auditory brainstem responses remained largely unchanged in Munc13 and CAPS deletion mutants. Moreover, we provide evidence for complete absence of Munc13-like proteins from adult IHC ribbon synapses but instead detected local clustering of otoferlin in the presynaptic membrane below the ribbon. In otoferlin mutants, we observed a dramatic reduction of exocytosis and, using electron microscopy, a significant increase in synaptic vesicle tether length, both indicative of impaired vesicular priming and attenuated fusion competence. In conclusion, our data indicate that IHCs do not rely on Munc13-like priming factors but instead use a priming machinery that critically depends on otoferlin.

PD-96

Fusing the Intravesicular Domain of Otoferlin with GFP Reveals Its Role in Sustained Exocytosis at the Inner Hair Cell Ribbon Synapse

Jacques Boutet de Monvel[1]; Didier Dulon[2]; Philippe Vincent[2]; Yohan Bouleau[2]; Sylvie Nouaille[1]; Adeline Mallet[1]; Anna Sartori-Rupp[1]; Marc Guillon[3]; Marcel Lauterbach[3]; Christine Petit[1]; Saaid Safieddine[4]
[1]Institut Pasteur; [2]University of Bordeaux II; [3]University of Paris Descartes - Paris 5; [4]CNRS/Institut Pasteur

Otoferlin, a six C2-domain transmembrane protein of synaptic vesicles (SVs) defective in a genetic form of human deafness, is essential for calcium-triggered exocytosis at the ribbon synapses of inner hair cells (IHCs). Deaf mice defective for otoferlin lack both the fast and sustained components of synaptic exocytosis, despite a normal synaptic structure. To shed further light on the role of otoferlin in the IHC synaptic vesicle cycle, we engineered a knock-in mouse model in which EGFP is fused to the intravesicular carboxy-terminal domain of otoferlin. Using a range of techniques including high resolution imaging, 2-photon FRAP and electrophysiological recordings, we characterized ribbon synapse morphology and function, as well as the distribution and mobility of GFP-tagged SVs, in IHCs from homozygous *Otof-GFP/Otof-GFP* mice and heterozygous *Otof*/*Otof-GFP* mice. Expression of otoferlin-GFP protein occurred with the expected developmental time course, with a subcellular distribution similar to that of native otoferlin. Using STED microscopy in *Otof-GFP* IHCs to resolve individual SVs double-stained with antibodies against otoferlin-GFP and vGlut3, we found that otoferlin-GFP molecules are associated with a significant fraction of SVs in these cells. Furthermore, post-embedding immunogold electron microscopy showed that otoferlin-GFP is present in ribbon-associated SVs. 3D electron tomography reconstructions of ribbon synapses in both heterozygous and homozygous IHCs indicated normal synapse maturation. The number of SVs surrounding ribbons was similar to those of wild-type IHCs in *Otof*/*Otof-GFP* IHCs, but larger in *Otof-GFP/Otof-GFP* IHCs. Before postnatal day 8, *Otof-GFP/Otof-GFP* IHCs displayed normal Ca^{2+} inflow and membrane capacitance changes upon depolarisation applied by whole-cell patch clamp, indicating normal synaptic exocytosis. However, SV exocytosis was significantly impaired in these IHCs from P8 onward. Mobilization of the readily releasable pool (RRP) was normal, but the sustained component (SRP) was nearly abolished, and recovery of the RRP between pulse pairs was strongly reduced. Using two-photon FRAP experiments, we found that the mobile fraction of otoferlin-GFP-tagged SVs was larger in *Otof-GFP*/*Otof-GFP* IHCs than in *Otof*/*Otof-GFP* IHCs. In both types of IHCs this fraction increased at the basal IHC region upon depolarization by K^+, but this increase was less pronounced in the *Otof-GFP*/*Otof-GFP* IHCs. To-

gether, our results indicate that vesicle dynamics balance is perturbed in IHCs from *Otof-GFP*/*Otof-GFP* mice, likely due to lack of sustained exocytosis. We conclude that the intravesicular otoferlin domain is essential for the maintenance of sustained exocytosis in IHCs.

PD-97

A Mouse Model for Human Temperature Sensitive Auditory Neuropathy to Study the Role of Otoferlin in Synaptic Function

Ellen Reisinger[1]; Rituparna Chakrabarti[2]; Hanan Al-Moyed[2]; Alexandra Mueller[2]; Tina Pangrsic Vilfan[2]; Sandra Meese[3]; Gerhard Hoch[2]; Nils Brose[4]; Tobias Moser[2]; Nicola Strenzke[2]; Carolin Wichmann[2]

[1]University Medical Center Goettingen; [2]Dept. of Otolaryngology, University Medical Center Goettingen; [3]Dept for Molecular Structural Biology, School of Biology, University of Göttingen, Germany; [4]Molecular Neurobiology Group, Max-Planck-Institute for Experimental Medicine, Göttingen, Germany

Hearing relies on neurotransmitter release from inner hair cells, the sensory cells of the inner ear. Exocytosis and vesicle replenishment are thought to be regulated by otoferlin, a multi-C2 domain protein. Most mutations in otoferlin lead to profound prelingual deafness in humans and mice. Remarkably, few point mutations in human *OTOF* were found to cause a mild hearing impairment at normal body temperature but a severe to profound hearing loss at slightly elevated body temperature. We generated a knock-in mouse mutant with one of these mutations and studied the effect of elevated temperature on hearing, otoferlin protein levels, synaptic morphology and - function. Auditory brainstem response thresholds in these mice were moderately elevated, yet ABR wave I only showed a mild linear decrease in amplitude upon local heating of the temporal bone. Otoferlin immunofluorescence levels in inner hair cells were 50% lower in mutants and were further reduced with increasing temperature. Patch clamp recordings of inner hair cells revealed that exocytosis of the readily releasable pool was normal in mutants, but sustained exocytosis, elicited by depolarization steps of 50 ms or longer, was reduced. Analyses of synaptic ultrastructure with electron microscopy revealed larger vesicles around the ribbon and close to active zone membranes in mutant inner hair cells at elevated body temperature, indicating a potential defect in regenerating proper sized synaptic vesicles. Together with vivo-electrophysiological and behavioral analysis of hearing impairment performed in the group of N. Strenzke, our data serve to understand the pathomechanism of temperature induced hearing loss and propose a new role for otoferlin in synaptic vesicle regeneration at the inner hair cell ribbon synapse.

PD-98

Ribbon Synapse Numbers across the Tonotopic Gradient in Barn Owl and Chicken Basilar Papilla

Christine Koeppl[1]; Andrew Affleck[2]; Mirka Jordan[1]; Roksana Stachowiak[1]

[1]Carl von Ossietzky University; [2]Neuroscience Research Australia

Introduction

All afferent connections with hair cells, whether vestibular or auditory, are of the specialized ribbon synapse type. In the plesiomorphic (ancestral or default) case, several synaptic ribbons occupy one afferent terminal. Mammalian inner hair cells are the exception; these typically show a strict 1:1 relationship between ribbons and afferent terminals, and many afferent terminals on each IHC. The barn owl shows a similar increase in numbers of afferent terminals on the tall hair cells in the high-frequency regions of its basilar papilla (Fischer, 1994, Hear Res 73:1-15). The aim of this study was to examine whether the ratio of synaptic ribbons to terminals is unusual in the owl, perhaps related to its high-frequency specializations. We determined the number and distribution of ribbon synapses along the tonotopic gradient and across the width of the basilar papilla in the barn owl and, for comparison, in the unspecialized chicken.

Methods

Serial cross-sections of basilar papilla were immunohistochemically labelled for Na^+-K^+-ATPase (labelling all neural structures), CtBP2 (synaptic ribbons) and otoferlin (hair cells). Quantitative counts of ribbons and, where possible, neural terminals, were derived from confocal image stacks. Individual hair cells from different locations along and across the papilla were systematically sampled. All basilar papillae were from young adult owls; chickens were 3 weeks or older.

Results

In both species, the number of ribbons per hair cell declined from neural to abneural, consistent with a known decline of afferent innervation density from tall to short hair cells. Intriguingly, we observed labelled ribbons even in very basal-abneural hair cells, where no afferent terminals are present (Fischer, 1994, Scan Micr 8:351-364). Focusing specifically on tall hair cells (the analog of mammalian inner hair cells), both species showed a similar decline of the number of ribbons per hair cell from low to high characteristic frequencies. Preliminary data suggested a typical ratio of 2-4 ribbons per terminal for tall hair cells, regardless of characteristic frequency.

Conclusions

The number of synaptic ribbons and the ratio of synaptic ribbons to afferent terminals were not different in the barn owl and the chicken. This is in contrast to previous reports of a drastically increased afferent innervation density of the high-frequency regions of the owl basilar papilla. Furthermore, the consistent observation of CtBP2 label in very basal-abneural short hair cells suggests the presence of non-functional ribbon structures, similar to some lizard hair cells (Chiappe et al., 2007, J Neurosci 27:11978-11985).

SYM-86

The Successes and Tribulations of Using Non-Coding RNAs as Therapeutics: From the Bench to the Bedside

Andrea Kasinski[1]; Frank Slack[2]; Andreas Bader[3]; Esteban Orellana[1]

[1]Purdue University; [2]BIDMC Cancer Center/Harvard Medical School; [3]Mirna Therapeutics

MicroRNAs are small non-coding molecules that can function as powerful therapeutic entities assuming that a well-defined, relevant biological role for the miRNA has been revealed. Indeed, for many diseases aberrantly expressed miRNAs have been determined, target mRNAs have been identified, and clear phenotypes have been associated with altered miRNA expression. Undeniably, the most advanced miRNA studied, in terms of its biological role being elucidated and its translation into the clinic, is miR-34. Using miR-34 and cancer as a model I will discuss how our studies have been instrumental in translating this miRNA from the bench to the bedside and the approaches we are currently taking to capitalize on the promising Phase I data (NCT01829971). Our initial studies revealed that lentiviral delivered miR-34a robustly prevents the onset and progression of non-small cell lung cancer (NSCLC) in *Kras;p53* mouse models through targeting multiple highly relevant oncogenes that are often overexpressed in tumor tissue. Clinical utility was reinforced in a second series of studies through the use of a delivery vehicle already in clinical practice. When NSCLC mice were treated systemically with lipid-encapsulated miR-34a (MRX34) life span increased by over 40%, something not easily achievable in this model. Nonetheless, tumors still progressed and animals ultimately died of disease, suggesting that more robust approaches centered on miR-34a replacement should be explored. To enhance the miR-34a effect, and identify tumors that may be refractory to miR-34a treatment we are identifying miRNAs that synergize with or antagonize miR-34a activity. The data obtained from this very timely work will distinguish synergistic pairs of miRNAs with exceptional clinical promise to move forward therapeutically, as well as miRNAs, that when overexpressed in a tumor, may impair miR-34a activity. The later of which will signify tumors that might be refractory to the miR-34a therapy currently in the clinic. These studies are being performed in a semi-high-throughput cell-based screen by combining miR-34a with every miRNA (based on miRBase v20) and evaluating effects on cellular proliferation. Data from this screen will be presented, as will our attempts to bring miRNA combinatorial therapeutics to the clinic based on these findings. Although these studies are focused on cancer therapeutics, they provide a platform for other models and disease systems to build on with regard to translating miRNAs into routine clinical practice. Our successes and challenges will be discussed with the hope of streamlining future miRNA-based therapeutics for cancer and other diseases.

SYM-87

MicroRNAs and Regeneration in the Avian Utricle.

Michael Lovett

Imperial College, London

Damage to inner ear hair cells is a major cause of hearing and balance disorders. Mammals have little or no hair cell regenerative capacity. However, lower vertebrates, such as birds, have a robust regenerative program. The stem cells for this are the supporting cells within the sensory epithelia which share a developmental lineage with hair cells. We have explored avian hair cell regeneration in a series of genome-scale studies, most recently at the mRNA (protein coding) transcriptome level and have identified interesting patterns and programs of mRNA expression for testing in regenerative models. MicroRNAs represent particularly attractive candidates for therapeutic manipulation, since altered expression of just a few miRNAs can have wide-ranging effects upon cell differentiation and fate. Here we report the entire spectrum of miRNAs expression during hair cell regeneration in the sensory epithelia of the avian vestibular utricle. We employed next generation sequencing to derive miRNA expression profiles over a 168-hour regenerative time course at 24 hour intervals following *in vitro* aminoglycoside treatment. Forty four separate miR libraries were sequenced. 750 miRNAs are detectably expressed across this time course and 73 show patterns of differential expression. Among these, several show positive temporal correlations with phenotypic conversion of supporting cells to hair cells, with initiation/end of cell cycle, and with the differentiation of hair cells from regenerative proliferation. We chose five miRs (gga-miR-7, gga-miR-34c, hsa-mir-143-3p, gga-miR-183 and hsa-miR-96) to functionally test in greater detail. We specifically knocked down or overexpressed these miRNAs using anti-miRs and pre-miRs in dissociated cultures of supporting cells and measured the effects upon regenerative proliferation. All showed significant effects upon proliferation, indicating that four of the miRs normally inhibit cell cycle whereas hsa-mir-143-3p appears to up-regulate these processes (in agreement with our expression profiles). We also explored the specific mRNA targets of these 5 miRs in avian supporting cells by conducting mRNA-seq on all miR knockdown and overexpression cultures. This resulted in the identification of a subset of putative mRNA targets. These include, for example, components of Notch signaling and cell cycle entry/exit as being targets of the miR34 family during utricle hair cell regeneration.

SYM-88

The gEAR Portal: a Gateway to gene Expression for Auditory Research

Joshua Orvis[1]; Beatrice Milon[2]; Amiel Dror[3]; Ran Elkon[4]; Anup Mahurkar[1]; **Ronna Hertzano[1,2]**
[1] Institute for Genome Sciences, University of Maryland School of Medicine, Baltimore, USA; [2]Department of Otorhinolaryngology Head and Neck Surgery, University of Maryland School of Medicine, Baltimore, USA; [3] Department of Human Molecular Genetics and Biochemistry, Sackler Faculty of Medicine, Tel Aviv University, Tel Aviv, Israel; [4]The Netherlands Cancer Institute, Amsterdam, Netherlands

Non-coding RNAs play key roles in regulation of gene expression, cell survival and differentiation. In the ear, non-coding RNAs such as micro RNAs (MiRs) are not only differentially expressed, but also are necessary for hearing and balance. For example, MiR96, which is expressed in the developing inner ear hair cells, is essential for hearing and hair cell differentiation both in human and in mouse. Others have shown that genes associated with hair cell differentiation are downregulated in the MiR96 mutant mice. However, the critical direct targets of this MiR in hair cells are still largely unknown. One conceivable explanation would be that if MiR96 functions to downregulate genes normally expressed in supporting cells which surround and outnumber the hair cells, expression analysis of whole sensory epithelia would not detect changes in target gene expression due to signal averaging. We recently undertook a cell type-specific approach for global analysis of gene expression of newborn mouse inner ears using a variety of wild type and mutant mice. We present our initial findings from cell type-specific analyses of the MiR96 mutant ears revealing a novel mechanism leading to the hair cells maturation arrest. These data underscore the importance of cell type-specific approaches in deciphering the roles of regulatory genes in the mouse inner ear. Next, we describe differential cell type-specific expression of long non-coding RNAs (lncRNA) in the wild type newborn mouse inner ears. Finally, we discuss comparisons of deep sequencing of hair cell transcriptomes and translatomes as a tool to further our understanding of inner ear cell type-specific genome biology.

SYM-89

Role of the Mir96/182/183 Family in Hearing and Deafness

Karen Steel; Jing Chen; Morag Lewis
King's College London

MicroRNAs are small non-coding RNAs that bind to specific sites in the 3'UTR of target mRNAs, inducing transcript destabilisation and translational inhibition. They allow rapid control of gene activity and have been shown to be important in multiple developmental programs. The miR-96/182/183 family is expressed specifically and strongly in hair cells and also in auditory neurons. A single point mutation in the seed region of miR-96 (*Mir96^{Dmdo}*), a region critical for target recognition, causes deafness and vestibular dysfunction in homozygote mice, and progressive deafness in humans (Lewis *et al*, 2009, Mencia *et al*, 2009). Correct targeting by miR-96 is required for correct maturation of cochlear hair cells; in *Mir96^{Dmdo}* mutants, hair cells retain juvenile characteristics and never reach functional maturity (Kuhn *et al*, 2011).

miR-96 appears to have wide-ranging effects on many genes. Four particularly interesting genes which were markedly downregulated in *miR96^{Dmdo}* homozygotes are *Slc26a5*, *Ocm*, *Pitpnm1* and *Ptprq*. All four are expressed specifically in hair cells, and two were previously known to be important for hearing. We have compared the phenotype of mice carrying knockout alleles of each gene with *Mir96^{Dmdo}* mutants, using confocal microscopy, auditory brainstem response, immunohistochemistry, scanning electron microscopy and transcriptome analysis, and found that *Slc26a5*, *Ocm* and *Ptprq* appear to contribute to specific aspects of the *miR96^{Dmdo}* phenotype.

Another notable downstream target of miR-96 is *Gfi1*, a transcription factor also known to be critical for hair cell development. However, *Gfi1* is not a direct target; it is downregulated in *MiR96^{Dmdo}* homozygotes, and direct targets should be upregulated. It is likely to be one of many regulators ultimately controlled by miR-96 to regulate maturation of the hair cells. In order to discover the links between miR-96, intermediate factors like *Gfi1*, and the eventual endpoint genes such as *Ptprq* and *Slc26a5*, we have carried out several different network analyses to identify important pathways and genes. We have made use of protein-protein interaction networks, regulatory networks and gene set enrichment analyses to approach the question from multiple angles. In addition, we have begun analysis of a knockout of miR-182 and a double knockout of miR-96 and miR-183, which also demonstrate raised thresholds, although not as severe as that seen in *miR96^{Dmdo}* homozygotes.

Understanding the networks of genes controlled by these regulators in hair cells will lead to a better understanding of hair cell maturation and potentially to therapeutic targets for treating progressive hearing loss.

SYM-90

The Role of miR-96 in the Central Auditory System

Hans Nothwang[1]; Tina Schlüter[2]; Elena Rosengauer[2]; Karen Steel[3]
[1]Neurogenetics group, Center of Excellence Hearing4All, School of Medicine and Health Sciences, Carl von Ossietzky University Oldenburg; [2]Neurogenetics group, School of Medicine and Health Sciences, Carl von Ossietzky University Oldenburg; [3]King´s College London

MicroRNA-96 (miR-96) is part of the microRNA-183 cluster (miR-183, miR-92 and miR-182) and shows abundant expression in sensory cells such as photoreceptors and hair cells. It was the first microRNA associated with a human mendelian disorder (Mencia et al. 2009). Point mutations in this gene result in deafness due to arrest of hair cell development and subsequent degeneration of these cells. We recently reported an increase in miR-96 expression in the developing mouse brainstem (Rosengauer et al., 2012). Using RNA *in-situ* hy-

bridization, we also observed prominent expression of miR-183/miR-96 in the chicken auditory brainstem. To explore whether miR-96 is involved in development of central auditory structures, we characterized homozygote *dmdo* mice. These mice harbor a point mutation in miR-96, which causes peripheral deafness. Quantitative anatomical analyses of Nissl-stained brainstem sections containing the cochlear nucleus complex and the superior olivary complex revealed a significant volume reduction of auditory nuclei in young-adult (P25-P30) *dmdo* mice, ranging from 25% to 35%. In contrast, no volume difference was observed in neonatal *dmdo* mice, whereas 4 days old mice showed an intermediate reduction. To investigate whether the volume reduction was restricted to the auditory brainstem, we also determined the volume of the nucleus of the 7th nerve, a non-auditory brainstem structure. This nucleus showed only a slight volume decrease of 7.5% in young-adult *dmdo* mice. To estimate the contribution of peripheral deafness to the volume reduction in the auditory brainstem of *dmdo* mice, we included deaf *claudin14*$^{-/-}$ mice in our analysis. These animals show a cochlear phenotype similar to *dmdo* mice, yet no volume reduction of auditory nuclei was observed. This indicates that the disturbed anatomy in *dmdo* animals is caused by an on-site role of mutated miR-96 in the auditory brainstem. Cell counts and determination of cross sectional area identified reduced cell size as the major contributor to the observed volume decrease. In summary, our data reveal that mutation in miR-96 affects postnatal development of the auditory brainstem. The gene therefore adds to the growing list of peripheral deafness genes with functions in the central auditory system as well. Furthermore, the expression pattern in the avian brainstem points to an evolutionary conserved role of miR-96 in central auditory structures across different vertebrate groups.

SYM-91

MicroRNAs in Hair Cell Development and Maintenance.

Garrett Soukup; Marsha Pierce; Isha Pandya; Michael Ebeid; Colby Bradfield
Creighton University

MicroRNAs (miRNAs) represent one class of non-coding RNAs that fine-tune gene expression in specific cell types including hair cells of the inner ear. Of particular interest are the importance of hair cell-specific miR-183 family members (miR-183, miR-96, and miR-182), among which mutations in *miR-96* have been shown to underlie hearing loss in both mouse and human. We have used various models to explore the function of miRNAs in mouse hair cell development and maintenance. These models include conditional knockout of *Dicer1* in hair cells to preclude small RNA processing and function (miRNA and siRNA), conditional knockout of *Dgcr8* in hair cells to preclude miRNA processing and function, and knockout of specific miR-183 family members (*miR-183/96* knockout and *miR-182* knockout). Each of these models demonstrates substantial hair cell loss preceded by defects in proper stereocilia formation or maintenance. The models show that small RNA fine-tuning of gene expression in hair cells is crucial to proper hair cell development and function; the epitome being deafness that results from miRNA dose-dependent effects in heterozygous *miR-183/96* knockout mice. A considerable challenge remains in attributing effects on hair cells to specific miRNA-target gene interactions. Toward this goal, analyses of small RNA and gene expression profiles of inner ears and hair cells from various models, and effects of miR-183 family members in embryonic stem cell differentiation are combined with bioinformatic predictions of miRNA target genes and pathways. Together, these studies explore the subtle but requisite regulation of gene expression that miRNAs fulfill in hair cell development and maintenance, and provide insight into miRNA-regulated processes that might be manipulated to therapeutically effect hair cell maintenance or regeneration.

SYM-92

Competing Endogenous RNAs--Regulating the miRNA Regulators

Donna Fekete
Purdue University

Hundreds of microRNA (miRNA) genes are found in the typical mammalian genome. Also present are thousands of genes for long non-protein-coding RNAs (lncRNAs), as well as pseudogenes (the latter initially thought to be evolutionary remnants). Many non-coding RNAs and many miRNAs are misregulated in various types of tumors and cancer cell lines.

In 2011, Salmena et al., from the laboratory of Pier Paolo Pandolfi, postulated a novel functional role for non-coding RNAs that involved their ability to interfere with the interactions between microRNAs (miRNAs) and their protein-coding target transcripts. By sharing common miRNA binding sites (also called microRNA response elements or MREs) with protein-coding targets, the non-coding RNAs could serve as “sponges” for the miRNAs. These regulators were dubbed “competing endogenous RNAs” or ceRNAs. By competing for the binding of the miRNAs through their MREs, ceRNAs can protect the protein-coding targets from RISC/miRNA-mediated translational repression. A phenomenon like that of the ceRNA sponges had previously been reported in plants, where it was called “target mimicry”. This idea has expanded to include both coding and non-coding transcripts as potential ceRNAs, provided their 3’ UTRs have the appropriate MREs. Specifically, it is now thought that RNAs can actively regulate each other via competition for miRNA binding.

A prominent example of ceRNA activity is found in the regulation of the tumor-suppressor protein, PTEN. The PTEN transcript has a large 3’ UTR with many predicted MREs (miRNA binding sites), and this 3’ UTR can be targeted by miRNAs that are upregulated in tumor cells. A number of ceRNAs for PTEN have recently been identified that are either downregulated or mutated in cancer cells. The absence of such ceRNAs should exacerbate the miRNA-mediated repression of PTEN. Logically, then, ceRNAs that share MREs with PTEN normally serve to buffer PTEN transcripts from miRNA targeting, allowing this tumor-suppressor protein to accumulate in healthy cells.

The detailed cataloging of lncRNAs expressed in inner ear tissues will pave the way for studies designed to ask whether ceRNAs play regulatory roles in inner ear development and disease.

SYM-94

Factors Affecting Access to Adult Rehabilitation

Donna Sorkin
American Cochlear Implant Alliance

Learning to listen and access spoken language and environmental sounds is an accepted (and often required) element of the process of providing a hearing impaired child with cochlear implant(s) or hearing aid(s). At the same time, there is considerable variability in whether and how rehabilitation is offered to adults. In many instances, adults are not actively encouraged to participate in a formal rehabilitation program and consequently there is an assumption that it is: (1) not necessary; (2) not covered by health insurance; and/or (3) not provided by rehabilitation professionals in the hearing health field. All of these assumptions are false. These factors all contribute to a lack of awareness about hearing rehabilitation strategies for adults. This presentation will focus on factors 2 and 3 above.

While it is true that rehabilitation after fitting of a hearing aid is not covered by most health insurance policies (nor is the hearing aid itself), rehabilitation for an adult post cochlear implantation *is* typically part of insurance coverage for the intervention just as it is for any rehabilitative procedure such as a hip or knee replacement. Insurance policies do not distinguish between children and adults in coverage of such services. The more significant barrier for adult rehabilitation is accessing appropriate rehabilitative professionals who will work with adults. Mobile and web training apps that allow for home practice are appropriately included in an auditory therapy program provided by a professional with a specialty in the discipline.

This paper will: (1) Review specifics of health insurance coverage and reimbursement relative to adult rehabilitation; (2) Share findings from a survey of adult cochlear implant recipients on their experiences in accessing auditory therapy; and (3) Discuss perspectives of cochlear implant clinics on therapy for adults, including mobile and web apps.

SYM-95

Personal Experiences with Auditory Training After Cochlear Implantation

Tina Miller
N/A

Overview

My hearing loss was first diagnosed when I was about 12 years old, and likely to have been from birth. I used hearing aids shortly thereafter. I was completely mainstreamed and never received any support. Over time, my hearing deteriorated to the extent that my ability to use the telephone was greatly diminished. I relied on lip-reading and could not understand speech unless I faced the speaker. At age 53 years old, I had a CI on my left ear in May 2011 at GBMC. I then attended auditory training sessions every other week for six months.

Methods

Right from activation, I was hearing new sounds, but had difficulty "translating" many of them. Two weeks later, I began auditory training. The therapist was impressed with my progress - I was already understanding words on the car radio - so I started at a higher level than the norm. Techniques included covering her face and having me repeat back words, then sentences, then paragraphs. At first she gave me clues as to what words to listen for, but eventually stopped giving clues. We also practiced with both digital background noise and with live background noise by going to the hospital cafeteria. We worked on the phone whereby the therapist called me from another room. Also between sessions I worked at identifying sounds that I heard and naming them as a way of helping my brain to recognize and understand sound.

Results

After about six months, the therapist and I felt there really wasn't much more she could do. I was able to clearly hear and understand what was said in all types of situations and was able to use the phone. Since then, my phone skills have increased to the point that I can have clear conversations without the captioning service I used in the past. Friends and colleagues comment on how well I hear and understand in situations that in the past I was unable to carry on a conversation, such as in a car, in noisy environments, or when the speaker's face was not in my line of vision.

Summary

The sessions were essential to my success with the CI. I also used a CD software for auditory training at home, but found it to be not as helpful as the sessions with the therapist.

SYM-96

Development of Computer-Assisted Speech Training to Help Cochlear Implant Patients

Qian-Jie Fu
University of California, Los Angeles

For more than 30 years, much research has been directed at understanding the large variability in cochlear implant (CI) patient outcomes; some CI patients perform very well soon after initial activation, while others have great difficulty even after years of experience with their device. Postlingually deafened CI users must adapt to electric stimulation in light of previous experience with acoustic hearing. Prelingually deafened patients, especially children, learn to hear exclusively with electric stimulation. In both cases, "passive" learning drives much of the neural plasticity that has made CIs so successful. However, much research has shown that active auditory training can greatly improve CI users' speech performance, even for patients with years of experience with their device. These improvements are comparable to, and often exceed, those associated with recent developments in CI technology. Unfortunately, auditory rehabilitation for CI users is not widely available, due to limited financial and time resources. Less

than 10% of practicing audiologists currently offer CI patients a comprehensive auditory training program.

To address this issue, our research group has been developing computer-assisted speech training techniques specifically targeted to CI users. The specialized software provides a wide range of auditory rehabilitation tools that can be used by patients at home or in conjunction with a clinical speech pathologist. Because there is a wide range of speech capabilities among CI users, the software targets users' specific rehabilitation needs, which can be assessed and re-assessed during training. Training tasks range from simple discrimination of non-speech sounds (e.g., pure tones), to phoneme identification using monosyllable words, to speech understanding in noise, to music perception, to sound source localization. CI users with different needs can thereby focus on appropriate tasks and stimuli, which contribute to the efficiency and effectiveness of the training.

During the development, many lessons have been learned. First, translational research requires deep understanding of the target population and a strong desire to help these people. Second, scientific validation is important to verify the effectiveness of the approach. Third, collaboration is needed for commercial development. Fourth, acceptance and continued interest from patients is essential for initial success and further development. Despite the tremendous effort required, we truly believe this has been an important and worthwhile endeavor for universities, investigators, and patients. Currently, the "Angel" series of computer-assisted speech training software is freely distributed by Emily Fu Foundation: http://angelsound.emilyfufoundation.org.

[Development efforts partly supported by NIH/NIDCD grant R01-DC004792]

SYM-97

Auditory Training as Portable Games

Dennis Barbour
Washington University

Continual advances in hearing-assist hardware make hearing correction feasible for an increasing number of individuals. Lagging behind the hardware developments that compensate for ear pathology, however, are the rehabilitation strategies for training the brain to use these devices most effectively. Research into auditory training for challenging hearing-in-noise scenarios, for example, has revealed multiple strategies that might be effective in improving the listening performance of at least some individuals. Major challenges of exploiting these findings for therapeutic benefit include high capital costs of audiology equipment, high personnel costs of implementation, longitudinal subject engagement, retention of gains and transfer of gains to novel scenarios. One way to counter these limitations involves implementing successful strategies from the cognitive and skill acquisition literature in the form of portable video games played on widely available hardware.

We have developed games that engage players in large numbers of unique auditory training exercises over an extended period of time at their convenience. We have designed these games for the Android family of touch-screen devices. This novel platform provides the launching point for delivering unsupervised training materials optimized by being 1) naturally spaced in time, 2) naturally variable in content and 3) variable in feedback to players.

The games we have developed are successful at implementing the targeted training exercises and logging all aspects of player interaction. Adaptive procedures maintain engagement while still delivering trials near performance threshold, thus ensuring time on task is spent on challenging, relevant activities. Game-like tasks create an intrinsic motivation for subjects to proceed with training. The platform enables training modifications to be pushed to players as ongoing results reveal the nature of successful training elements.

Packaging of auditory training strategies into a platform readily available to a large population in an engaging, user-friendly format opens up new possibilities for auditory training research and therapy. Longer total training times with greater numbers of unique trials enables more ready evaluation of training task effectiveness. Wholly automated procedures and portability allow training to occur with minimal constraints on the patient. Engaging game environments encourage continued participation in training exercises for extended periods of time. Collectively, these strategies incorporated into auditory training research from the beginning increase the chances of identifying successful interventions that can scale up to population-wide applicability.

SYM-98

Standards For Speech and Hearing Mobile and Web Applications

Ray Goldsworthy
Sensimetrics Corporation

This presentation will outline differences between mobile and web applications, and will describe how the two application types are generally combined. Applications developed at Sensimetrics Corporation will be reviewed, but the presentation will focus on standards for mobile and web applications that improve the connectivity of applications while providing safeguards for managing personal information. The argument will be made that there are no existing *technological* obstacles for the development of mobile and web applications targeting speech and hearing training and assessment. Modern mobile and web applications have already demonstrated technologies that can combine streaming video, real-time signal processing, and secure data transfer. Consequently, focus is now on the *scientific* challenges for defining the most relevant training and assessment procedures for speech and hearing applications. The scientific basis for applications that include low-level psychoacoustics as well as high-level speech reception using audio and video will be reviewed.

SYM-99

Speech Banana – A Modular Ipad App for Auditory Training for Adults with Hearing Loss

Tilak Ratnanather
Johns Hopkins University

Introduction

An ipad application for auditory training (AT) to enable adults with hearing loss benefit from amplification provided by cochlear implant (CI) or hearing aid (HA) has been developed. AT is necessary to exploit brain plasticity or development. However, adults are literally "left to their own devices" since private or public insurance in US and UK respectively will cover part of or limit regular sessions of AT. Thus what is the point of covering the cost for CI and not learning how to use it? Indeed in the US, clinics absorb costs and/or raise funds to pay for AT. While adult AT should be classified as rehabilitation or habilitation not "educational" so that it is medically equivalent with therapy covered for physical injuries, "time is money" since adults need to balance with work and home. Weekly sessions in the clinic are ideal but attended by few adults. Software for AT exists but tablet applications are limited by focus on words or phrases for adults and children and by computers used for comprehension.

Method

The ipad app consists of word-based exercises and sentence-based quizzes from "Auditory Training for the Deaf" by Monsees and Whitehurst (1952). The modular structure is designed with each exercise consisting of thematic sets of single words allowing the user to play the word one or more times. The exercise is followed by a quiz of several sentences using these words with options for repetition. Progress can be monitored after completion of quizzes.

Results

A beta version with 10 exercises was implemented and a basic version with all 38 exercises has just been released. Positive and favourable feedback was obtained from several users. However improvements especially with regard to scoring are needed.

Summary

It should be possible for adults with hearing loss who have sufficient amplification via CI or HA to comprehend speech at least in quiet. Real-time data of auditory plasticity can be recorded and used to justify private and public insurance funding. Future implementation should involve i) different speakers, ii) feedback based on phonemes, vowels and consonants, iii) adaptive training i.e. jumping to increased levels of difficulty, iv) send results to clinics, v) extend tablet app template for other languages. Thus rather than just a few people having weekly session at the clinic, more could have monthly sessions. Hence there could be improved cost coverage and feedback for clinics.

SYM-100

Adult Cochlear Implant Aural Rehabilitation

Kristin Ceh
Johns Hopkins University School of Medicine

Adult aural rehabilitation has been defined as the reduction of hearing-loss-induced deficits of function, activity, participation, and quality of life through sensory management, instruction, perceptual training and counseling. (Boothroyd, 2007) The Listening Center's adult cochlear implant rehabilitation program approaches this undertaking by providing an intervention model that focuses on counseling, auditory training and instruction in communication management. Services extend beyond the individual to include family members and significant others.

Insurance reimbursement, patient compliance and carryover of skills newly acquired through the individualized rehabilitation program are a few examples of challenges to clinicians working to maximize the auditory potential of those receiving cochlear implants.

Despite these challenges, individual auditory rehabilitation remains an essential component in the cochlear implant process.

PD-99

Investigating Bottom-Up Auditory Attention in the Cortex

Emine Kaya; Mounya Elhilali
Johns Hopkins University

A key component of auditory scene analysis is shifting the focus of attention to events of interest, either due to a task at hand or the inherent saliency of events in the scene. Previous studies have employed electroencephalography (EEG) to establish common markers in the event-related potentials (ERP) of the neural response for deviants in a stream of regularly repeating simple tones. While this paradigm sheds light on neural processes underlying processes of deviance detection and regularity tracking, it does not directly tie these mechanisms to cortical processes underlying auditory salience in complex acoustic scenes. This work employs overlapping complex sound events to create natural soundscapes; while preserving some acoustic and temporal regularity to take advantage of information available from the ERPs. The detection of salient notes is confirmed with the mismatch negativity (MMN) marker. Further, we use spectro-temporal response functions (STRFs), two-dimensional transfer functions between the acoustical attributes of the stimulus and overall brain response, to decode the representations of regular and salient events as they emerge in the cortex. The results reveal mismatch negativity components elicited by these complex sound events. An analysis of the spectro-temporal brain functions reveal variable cortical responses to regular and salient events and demonstrates changes in neural tuning during events that grab our attention in a busy scene.

PD-100

Atypical Auditory Attention by Children with Moderate Hearing Loss Revealed by ERPs during Multi-talker Listening

Emma Holmes[1]; Padraig Kitterick[2]; A. Quentin Summerfield[1]

[1]University of York; [2]NIHR Nottingham Biomedical Research Unit

Background

Individual differences in multi-talker listening could arise from differences in either central attention or peripheral transduction. We aimed to isolate differences in attentional processing between normally-hearing and hearing-impaired children, based on a procedure devised by Hill and Miller (2010, *Cerebral Cortex*). During the presentation of acoustical stimuli (which we refer to as the 'Selective Phase'), we expected to observe differences in brain activity between normally-hearing and hearing-impaired children as a result of differences in peripheral processing of speech. Differences before the onset of acoustical stimuli ('Preparatory Phase') were expected to show differences in the control of attention without being confounded by differences in transduction.

Methods

Participants were 24 normally-hearing children and 13 children with moderate sensorineural hearing loss, all aged 7-16 years. We recorded brain activity using 64-channel electroencephalography (EEG). On each trial, two sentences spoken by adult talkers (one male, one female) were presented simultaneously from loudspeakers at two spatial locations (one left, one right of fixation). A third 'child' talker was presented from straight ahead. Participants were cued, in advance of the acoustic stimuli, to either the location (left/right) or the gender (male/female) of the target talker. The task was to report key words spoken by that talker. A control condition, in which the visual cues did not have implications for attention, allowed cortical activity evoked by the configurational properties of the cues to be distinguished from activity evoked by attentional processes.

Results

Normally-hearing children displayed significant differences in event-related potentials (ERPs) between the Test and Control Conditions. These differences started early after the visual cue was revealed and were sustained throughout the Preparatory Phase. In contrast, hearing-impaired children did not show significant differences between the Test and Control Conditions during the Preparatory Phase. Furthermore, a signifiniant interaction between the amplitude of ERPs recorded from normally-hearing and hearing-impaired children provided evidence for atypical ERPs. Hovever, hearing-impaired children showed significant differences between the Test and Control Conditions during the Selective Phase, similar to normally-hearing children. This result demonstrates that atypical ERPs during the Preparatory Phase did not result from insufficient statistical power.

Conclusions

We interpret atypical ERPs during the Preparatory Phase as evidence that children with hearing loss do not utilise location or gender information to prepare their attention for an upcoming talker. This deficit may contribute to their difficulty understanding speech in noisy environments.

PD-101

Attentional Modulation of Cortical Networks in a Dynamic Auditory Scene

Inyong Choi; Hannah Goldberg; Hari Bharadwaj; Barbara Shinn-Cunningham

Boston University

Introduction

To communicate in social settings, we focus selective attention on one voice while simultaneously monitoring novel voices that unexpectedly arise from other locations. This study investigates the behavioral and neural consequences of "social monitoring" during selective auditory attention. We hypothesized that when a specific location is the focus of attention, sensory inputs from other locations are strongly inhibited, but that when listeners anticipate having to reorient to unexpected events, inhibition is weaker, degrading the ability to focus on the original target.

Method

Listeners heard either two or three spatially separated sequences of syllables spoken by the same talker. Both a center stream and a concurrent distractor stream on the left (-700 μs or -100 μs interaural time difference or ITD) were always played. In 2/3 of trials, a stream on the right (+700 μs or +100 μs ITD) started at a random time after the second syllable of the center stream. On each trial, a visual cue 2s before the auditory stimulus denoted whether the trial was "Fix" or "Switch." On "Fix" trials, listeners had to report the syllables from the center stream. On "Switch" trials, listeners had to report the syllables from the delayed, right steam if it occurred (2/3 of trials), but report the center stream on other trials (1/3). Throughout, cortical neural activities were measured using magnetoencephalography. Oscillatory power from the whole cortical surface as well as the evoked responses from auditory cortices were analyzed.

Results

We compared behavioral performance for Fix and Switch conditions in the trials where no right stream was present (i.e., physically identical trials with only center and left streams, report center). Performance was significantly better in the Fix condition, revealing the behavioral cost of social monitoring. During the preparatory period (after the fix/switch cue, but before the sound), alpha-oscillation over intraparietal sulcus (IPS) of right hemisphere (contralateral to the to-be-ignored right stream) was larger for Fix than for Switch trials. Moreover, the right stream onset response evoked from auditory cortices was weaker for Fix than for Switch trials, even though the timing of the right stream onset was unpredictable.

Conclusion

Our results suggest that IPS processes auditory space; alpha oscillations from IPS are associated with inhibition of audito-

ry inputs from to-be-ignored locations. In addition, listeners pay a cost to enable dynamic switching of attention to new events, presumably the result of reducing the inhibition that focuses selective attention.

PD-102

The Roles of Harmonicity and Temporal Pitch in the Perception of Speech in Noise: A Study of Intelligibility and Listening Effort

Matthew Winn; Ruth Litovsky
University of Wisconsin-Madison

Introduction

Pitch cues are thought to benefit the perception of speech in noise. In question is whether that benefit arises because of the pitch information itself, or because of the harmonic structure of voiced speech, which can serve as a stream segregation cue. Because speech in noise is notoriously difficult for people with cochlear implants (CIs), much effort is dedicated to exploring the restoration of pitch information in CI processors, primarily in the form of temporal pitch. This study was designed to investigate the relative contributions of temporal and harmonic pitch information in the perception of speech in noise.

Accuracy scores alone are likely not sensitive enough to capture the effects of pitch because there are few words that should be perceived correctly with pitch information that would not be perceived correctly without pitch information (at least in non-tonal languages). Therefore, the effect of pitch cues was evaluated using measures of listening effort, which might more robustly reveal the extent to which temporal fine structure and harmonicity aid the speech perception process.

Methods

Listeners heard and repeated sentences in modulated noise. The sentences were presented normally or with pitch cues neutralized in one of three ways. First, pitch contours were flattened with harmonicity preserved. Second, harmonic pitch cues were eliminated by using a vocoder that preserved spectral detail but disturbed temporal fine structure, resulting in an inharmonic whisper-like sound. Finally, temporal pitch cues in the form of transient pulses were added to the inharmonic signals so that pitch information could be conveyed temporally instead of spectrally.

Cognitive load during sentence recognition was measured using pupillometry; larger pupil dilation was an index of greater listening effort. Pupil dilation was modeled using multilevel growth curve analysis, where differences in effort were quantified mainly by linear slopes and overall level/intercept.

Results

F0 neutralization via pitch flattening yielded a modest increase in listening effort compared to the normal speech. Inharmonic sounds required relatively greater effort than harmonic sounds, suggesting the importance of harmonicity in speech-noise segregation. Addition of temporal pulses to inharmonic sounds provided inconsistent benefit. Intelligibility scores were generally unaffected for harmonic sounds but were lower for inharmonic sounds.

Conclusion

The contribution of pitch information can be revealed through measures of pupil dilation in ways that are not captured by accuracy scores alone. The evaluation of new F0-driven signal processing technology for CIs can be enhanced by pupillometric measures of sentence processing.

PD-103

Auditory Stream Segregation of Sequential Speech Sounds Based on Differences in Fundamental Frequency

Marion David[1]; Andrew Oxenham[1]; Mathieu Lavandier[2]; Nicolas Grimault[2]
[1]University of Minnesota; [2]University of Lyon

Introduction

Speech intelligibility in complex environments relies on our ability to perceptually separate competing voices. Differences in fundamental frequency (F0) between voiced sounds are known to be a strong cue for stream segregation; less is known about the perceptual organization of unvoiced sounds, such as consonants. In this study, we used naturally uttered consonant-vowel pairs and played them in a sequence with alternating F0 values, measuring the ability of listeners to perceive the sequence as one or two streams as a function of the F0 difference (ΔF0).

Methods

The speech sounds used consisted of naturally uttered pairs of unvoiced fricative consonants and voiced vowels. A set of 45 such sounds were recorded and their pitch contours were flattened and then artificially manipulated. Listeners were presented with sequences of alternating F0s (ABA sequences) with the speech tokens selected randomly for each presentation. The F0 of the As was constant and the F0 of the Bs was set ΔF0 (0-9) semitones above A. In half of the presentations, selected at random, a consecutive repetition of a speech token was introduced either across or within the streams. Performance was predicted to improve in the within-stream task when listeners were able to segregate the sequence into two streams, and to improve in the across-stream task when listeners were able to integrate the sequence into a single streams.

Results

The results were expressed in terms of sensitivity (d-prime) as a function of the ΔF0 between the streams. Sensitivity increased as ΔF0 increased for the within-stream measure, suggesting that stream segregation became easier as the F0 difference between the streams increased. Sensitivity also tended to decrease with increasing ΔF0 in the across-stream measure, indicating that the integration became harder as the F0 difference increased. The fact that F0 differences in the voiced portions of the stimuli assisted in segregation or integration onf the entire speech sound suggests that the unvoiced portions were successfully integrated with the correct voiced portions.

Conclusions
Sequential segregation of speech sounds was possible based on F0 differences in the voiced parts, despite the lack of explicit cues in the unvoiced segments. The paradigm introduces the use of real speech sounds into streaming experiments that have usually used artificial stimuli, and provides a basis for the exploration of further cues to perceptual organization of natural sounds.

PD-104

Source-Separation Strategies Based on Allocation of Time-Frequency Units Using Interaural Differences: The Role of High-Frequency Components

Jing Mi; Steven Colburn
Boston University

This study aims to explore how our brains separate multiple speech sources. Although the functional roles of multiple cues (including spatial cues, pitch, onset/offsets, etc.) have been studied for years, the principles of how we integrate the information from these cues remain unclear. We are exploring this problem from a frequency-analysis perspective, considering time-frequency (T-F) units generated from sets of simultaneous stimuli. Because of the complex phase relationships between stimuli, the combined T-F units are difficult to decompose into the original stimulus components.Therefore, selection of T-F units which mainly contain information from single sources may be an efficient route to stream segregation. If information dominated by one source is collected through relatively “clean” T-F units, predictions can be made for the missing components, using knowledge of the characteristics of speech, for example; then, combined T-F units can be tested for compatibility with the predictions. As an early exploration of this hypothesis, the functional role of high-frequency components in speech is being studied. High-frequency components are much sparser than low-frequency components in human speech. As a consequence, in multiple speech mixtures, there are more “clean” T-F units in the high-frequency range than in the low-frequency range. From preliminary psychoacoustic experiments, it appears that high-passed speech can be recognized easily and is critical for speech segregation. To further test the functional role of high-frequency components in speech segregation, a speech segregation algorithm based on sound localization is implemented. In that algorithm, estimates of the interaural time difference and the interaural level difference are extracted from each T-F unit of binaural stimuli. Then, k-means clustering is applied in this binaural feature space. Based on the clustering results, each T-F unit is classified as being dominated by one of the competing sources. When this algorithm is tested on speech (using the CRM speech corpus), it shows better segregation performance with high-passed mixtures compared with low-passed mixtures. This result supports the hypothesis that, at least from a spatial perspective, that high-frequency components play a more important role than low-frequency components in speech segregation tasks.

PD-105

Can We Choose to Integrate or Segregate? Effects of Task Instruction on Subjective and Electromagnetic Measures of Auditory Streaming

Alexander Billig; Matthew Davis; Robert Carlyon
MRC Cognition and Brain Sciences Unit, Cambridge

To form an accurate model of the auditory world we must establish whether incoming energy arises from existing or new sound sources, and allocate it to corresponding perceptual representations (auditory streams). For a large range of stimulus parameters, repeated ABA- patterns of pure tones are initially heard as a single source but after several seconds typically split into two streams, each consisting of tones of one frequency. The percept then switches bistably between “integrated” and “segregated” forms. The relative likelihood of these percepts depends on the between-tone frequency and temporal separation, but can also be affected by attention and context. Using subjective reports and neural measures we investigate another top-down factor: the extent to which listeners can deliberately influence what they perceive (intention).

Twenty-four participants with normal hearing listened to 150-second ABA- sequences (A tones four or six semitones higher than 1017-Hz B tones, 600-ms triplet onset asynchrony) while continuously reporting their percept. Cortical activity was recorded with simultaneous electro- and magneto-encephalography. Participants heard ten sequences for each frequency separation. In four sequences they listened neutrally, while in others they attempted to perceive integration or segregation (by attending to the whole pattern, or to the high A or low B tones exclusively).

Listeners reported more segregation for the larger frequency separation. This factor did not interact with intention but influenced the initial (integrated) phase duration as well as subsequent phases during bistability. Participants reported segregation approximately 40%, 50%, and 65% of the time in the “integrate”, “neutral”, and “segregate” listening conditions, respectively. These differences occurred because subjects lengthened the phases of the intended percept and shortened those of the unintended percept; both approaches were more effective when trying to segregate than when trying to integrate. Our findings differ from those of a previous study in which volitional control was asymmetric with respect to intended versus unintended phase durations, rather than with respect to integrated versus segregated percepts.

Event-related potentials/fields elicited by tone triplets in the neutral condition will be analysed to validate/reconcile previously reported signatures of integration versus segregation. Data from the trials in which listeners tried to influence their percept will be compared to these neutral signatures to establish the extent to which subjective reports reflect true intentional control over low-level auditory responses, rather than response biases. In this way we aim to further characterise the nature of top-down influences on perceptual organisation.

PD-106

Monitoring Changes in Complex Auditory Scenes by Normal and Hearing Impaired Listeners

Julie Cohen[1]; LaGuinn Sherlock[1]; Danielle Zion[1]; Hector Galloza[1]; Sridhar Kalluri[2]; Douglas Brungart[1]
[1]Walter Reed National Military Medical Center; [2]Starkey Hearing Research Center

Background

In order to maintain spatial awareness in realistic environments, listeners must be able to detect and identify changes in complex auditory scenes containing multiple competing sound sources. Most previous research on spatial hearing has focused on how well listeners are able to localize sound sources in isolation or in combination with other competing sounds. However, many real-world situations require listeners not only to identify the locations of new sound sources that emerge in an acoustic scene, but also to detect and identify changes in the long-term characteristics of those sources. The purpose of this experiment was to evaluate how well normal and hearing impaired listeners were able to monitor changes in a complex scene involving multiple simultaneous competing talkers.

Methods

This study used a paradigm that requires listeners to detect four types of changes to the sound environment: the addition of a new sound source; the deletion of an existing sound source; a change in the voice characteristics of an existing talker; and a change in the sentence topic of an existing talker. In all cases, the sound sources consisted of continuous streams of sentences that were randomly selected from a single topic area in the CUNY corpus and spoken by the same talker from a fixed location in a 27 loudspeaker array. At the start of each trial, the listeners were cued which kind of change to expect and, when the change in the sound scene was noted, they were asked to press a button to indicate perception of the change and then use a wand to select the speaker location where the change occurred . Some trials were foils where no change occurred, and the number of active sources increased or decreased over time as additions and deletions occurred. Listeners completed the Speech, Spatial and Qualities of Hearing Scale (SSQ), which assessed their reported spatial hearing ability in everyday situations.

Results

As expected, preliminary results indicate that hearing impaired listeners have greater difficulty than their normal hearing counterparts in detecting changes in complex acoustic scenes, both for unaided and aided listening.

Conclusions

The results of this study will be used to develop optimized parameters for evaluating spatial awareness in hearing impaired listeners. Once these parameters are established, it is our hope that this testing procedure can be used to evaluate the impact that different hearing aid processing algorithms might have on spatial awareness in complex scenes.

SYM-101

Stimulus- and Task-dependent Spatial Processing in the Human Auditory Cortex

G. Christopher Stecker[1]; Nathan Higgins[1]; Susan McLaughlin[2]; Suvi Talja[3]; Teemu Rinne[3]
[1]Vanderbilt University Medical Center; [2]University of Washington; [3]University of Helsinki

The importance of spatial processing in the auditory cortex (AC) is highlighted by two key findings in the literature. First are observations of binaural tuning in a majority of AC neurons. Second are profound disruptions of sound localization by AC lesions in both human and animal listeners. Together, these observations suggest that populations of AC neurons participate in the representation of auditory space and link such representations to behavior. However, the specific nature of spatial processing in AC–and especially human AC–is not well understood. Current debates revolve around the nature of spatial coding by neural populations, the degree to which spatial processing varies across AC regions, the sensitivity to specific cues such as interaural time and level differences (ITD and ILD), and the potential impacts of task-related factors.

This presentation highlights several results of recent studies using functional MRI to investigate these questions in human listeners. In the first set of studies, we attempted to quantify changes in sound-evoked responses as a function of ITD and ILD in presented sounds. Clear tuning to ILD could be observed throughout large regions of human AC including Heschl's gyrus (HG) and posterior regions in planum temporale (PT) and superior temporal gyrus (STG). Consistent with animal data, more robust ILD tuning was observed in these regions than anterior to HG. ILD tuning functions typically favored contralateral ILD values but demonstrated clear non-monotonicity consistent with opponent-channel representations of auditory space. Across studies, tuning to ITD was much weaker, limited in both the degree of response modulation and the extent of AC in which it could be observed.

Other studies focused on the influence of task features on spatial processing, contrasting auditory spatial, auditory non-spatial, and non-auditory tasks involving sensory discrimination and sensory memory judgments. Across studies, sound-evoked responses were enhanced during auditory as compared to visual tasks, especially in regions of posterolateral STG implicated previously in studies of auditory attention. However, we observed little to no evidence for feature-specific modulations, such as sharper AC tuning to ITD or ILD or specific response enhancements, during auditory spatial tasks. In contrast, some regions of the inferior parietal lobule outside of AC proper showed spatial sensitivity during auditory but not visual tasks, suggesting that cortical processing of auditory space extends beyond AC when behaviorally relevant.

SYM-102

Processing Streams and Internal Models in the Cerebral Cortex

Josef Rauschecker
Georgetown University

An ethological view of the brain, comparing the same or similar functions in different species, offers a number of advantages. In particular, it allows separating the computational purpose of a model structure in the service of behavior from its implementation in specific brains. Comparing auditory and visual cortex in the same species is similarly advantageous as it reveals neural processing mechanisms that the two systems have in common. Examples at the receptive field level are FM and direction selectivity, bandwidth and size selectivity, as well as simple- and complex-like receptive fields based on the segregation of on- and off-sub-regions. This may ultimately lead to a generalized understanding of canonical structure in cortical modules of any kind.

On a larger scale, dual processing pathways have been envisioned as representing the two main facets of sensory perception in both the auditory and visual cortical systems: identification of objects, and processing of stimuli in space. However, the analogy is even more far-reaching and, by further expanding this view in terms of control theory, may offer an overarching model of cortical function.

Hierarchical processing of increasingly complex features has been shown to occur along the ventral stream of both auditory and visual cortex and is now widely accepted. The expanded view of dorsal-stream function in primates (Rauschecker 2011) defines a generalized role of the dorsal pathway in sensorimotor integration and control. For instance, the production, storage and anticipation of sounds resulting from action sequences seems to be mediated by the dorsal stream through its close relationship to sensorimotor structures in parietal and premotor cortex and in the basal ganglia. Expressed in terms of control theory, dorsal-stream function may subserve the encoding of actions as “forward models” informing sensory structures of actions that are about to occur, i.e. as internal models that produce a predicted sensation (sound). Conversely, dorsal-stream function also relates to the programming of motor structures by sensory information as “inverse models”. In this case, the motor system (“controller”) receives the desired sensation as input and must find actions that cause actual sensations to be as close as possible to desired sensations (sounds) (Jordan and Rumelhart 1992).

Models of audio-motor function have obvious relevance for the understanding of communication and its evolution (Rauschecker 2012). Language and music in humans are two cognitive functions that are highly evolved but are likely based on similar mechanisms (Bornkessel-Schlesewsky et al., 2014).

SYM-103

The Cortical Analysis of Speech-Specific Temporal Structure: Evidence from Sound Quilts

David Poeppel
NYU

Speech contains temporally structured information that the brain must analyze and apprehend to enable linguistic processing. To investigate the neural basis of this analysis, we used a new form is signal: sound quilts – stimuli constructed by shuffling segments of foreign speech, approximately preserving speech properties at short timescales while profoundly disrupting them at longer scales. We manipulated the extent of natural speech structure by varying the quilt segment length. Using fMRI, we identified bilateral regions of the superior temporal sulcus whose responses to speech quilts systematically increased with segment length. This effect did not occur for various non-speech quilts, suggesting tuning to speech-specific temporal structure. When examined parametrically, the response to speech quilts plateaued at segment lengths of ~500 ms. Quilts made from time-compressed speech yielded a similar plateau despite the increase in stimulus structure per unit time. Our results identify a locus of speech analysis in bilateral human auditory cortex with a hypothesized intrinsic temporal limit roughly between 1-2 syllables.

SYM-104

Phonetic Feature Representation in Human Superior Temporal Gyrus

Nima Mesgarani[1]; Connie Cheung[2]; Keith Johnson[3]; Edward Chang[2]
[1]Columbia University; [2]University of California San Francisco; [3]University of California Berkeley

During speech perception, linguistic elements such as consonants and vowels are extracted from a complex acoustic speech signal. The superior temporal gyrus (STG) participates in high-order auditory processing of speech, but how it encodes phonetic information is poorly understood. In this study, we used high-density direct cortical surface recordings in humans while they listened to natural, continuous speech to reveal the STG representation of the entire English phonetic inventory. At single electrodes, we found response selectivity to distinct phonetic features. Encoding of acoustic properties was mediated by a distributed population response. Phonetic features could be directly related to tuning for spectrotemporal acoustic cues, some of which were encoded in a nonlinear fashion or by integration of multiple cues. These findings demonstrate the acoustic-phonetic representation of speech in human STG.

SYM-105

Ultra-high Field fMRI Investigations of Natural Sound Encoding in Human Auditory Cortex

Michelle Moerel[1]; Federico De Martino[2]; Roberta Santoro[3]; Kamil Ugurbil[1]; Essa Yacoub[1]; Elia Formisano[2]
[1]University of Minnesota; [2]Maastricht University; [3]Universite de Geneve

We combine ultra-high field functional MRI (7T) with computational modeling to investigate the mechanisms of cortical analysis relevant for human listening in natural environments. First, we show that auditory cortical processing is well represented as the frequency-specific analysis of and combined spectral and temporal modulations present in natural sounds. Throughout the human auditory cortex, neuronal populations with similar acoustic feature preference cluster together creating large-scale maps. Second, we show that within the well-known large-scale map of frequency preference (i.e. tonotopy), each neuronal population (i.e. fMRI 'voxel') - when stimulated with complex sounds - prefers specific combination of frequencies. That is, approximately 60% of auditory populations display sensitivity to multiple frequency bands. Within these populations selected combinations of frequency bands may be amplified, which could serve to detect complex sound features and aid in segregating sounds of interest in noisy auditory scenes. Finally, we collect fMRI responses to natural sounds at sub-millimeter resolution to examine the origin of tuning to acoustic feature combinations. Specifically, we zoom in to human primary auditory cortex and explore both the stability of feature tuning within cortical columns and changes in feature tuning from granular input layers to supragranular output layers.

SYM-106

Active Mechanisms in the Auditory Cortex based on Direct Electrical Recording in Humans: Figure-Ground Segregation and Auditory Working Memory

Timothy Griffiths
Newcastle University

I will describe direct recordings of human local field potentials carried out in collaborative experiments with colleagues at Iowa University. Recordings were carried out from depth electrodes in human core and belt homologues and surface grids over the temporal convexity in two series of patients. Recordings were made during the abstraction of complex auditory figures and the maintenance of tones in auditory WM. The figure-ground data show induced activity from non-core auditory cortex in the gamma range as a correlate of the percept. The working memory data show low frequency delta and theta activity from auditory cortex during tone maintenance. Ongoing work examines how these observations inform systems models of auditory cognition based on constructive mechanisms involving brain areas remote from conventionally defined auditory cortex. Figure-ground analysis requires a system that includes the intraparietal sulcus whilst working memory for tones requires a system that includes the hippocampus and inferior frontal gyrus. The work emphasises that the functional organization of the auditory cortex cannot be considered in isolation. Fundamental aspects of auditory cognition require organised systems well beyond classical auditory cortex for which precise models can be tested incorporating the nodes in the network and the effective connectivity between those nodes.

SYM-107

Auditory Cortex is Highly Tuned to Patterns in Rapid Sound Sequences

Maria Chait; Nicolas Barascud
UCL

This talk will describe recent work in our laboratory, involving functional brain imaging (MEG and fMRI) and behavioural experimentation aimed at revealing how human listeners discover patterns and statistical regularities in sound sequences, a task that is fundamental to sensory processing, in particular in the auditory system, and a major component of the influential 'predictive coding' theory of brain function. Supported by growing experimental evidence, the 'predictive coding' framework suggests that perception is driven by a mechanism of inference, based on an internal model of the signal source. However, a key element of this theory - the process through which the brain acquires this model, and its neural underpinnings - has largely eluded investigation. Our work focuses on this crucial missing link, using a new paradigm that affords a unique opportunity to observe these processes within the auditory system. The method, based on measuring behavioural and brain responses to rapid tone-pip sequences governed by specifically controlled rules along a variety of feature dimensions, enables us to uncover (1) how the brain discovers patterns in sound sequences, (2) which neural mechanisms are involved and (3) to what degree the process is automatic or susceptible to attentional state and behavioural goals of the listener. The results reveal that Listeners are remarkably sensitive to the emergence of complex regular patterns within rapidly evolving random tone-pip sequences, in many cases exhibiting performance similar to that of an ideal observer model with perfect memory. Source localization and connectivity analysis suggests that the process of regularity detection is subserved by an automatic network comprised of an interplay between 'early' - primary auditory cortical sources and sources in frontal cortex (inferior frontal gyrus).

SYM-108

Responses to Natural Sounds Reveal the Functional Organization of Human Auditory Cortex

Sam Norman-Haignere; Joshua McDermott; Nancy Kanwisher
MIT

Auditory cortex is critical to speech recognition, music perception, and the ability to infer useful information from acoustic scenes. However, the functional organization of auditory cortex remains poorly understood compared with earlier stages of the auditory system. This is in part because most studies only test a small number of hypotheses about auditory

cortical organization, limited in part by the constraints of using relatively modest numbers of stimuli. To overcome these limitations, we measured cortical responses with fMRI to diverse collection of 165 individual natural sounds. We then took a data-driven approach to explore whether there was organization in the measured responses to these sounds. The response of each voxel to the 165 sounds was modeled as a weighted combination of an unknown number of canonical response profiles, each potentially representing the selectivity of an underlying neuronal sub-population. We used independent components analysis (ICA) to recover these components, and then explored the function of each component by correlating its response profile with acoustic measures and category labels (e.g. speech, music). The analysis revealed five components that collectively explained all of the replicable variance. These components had surprisingly distinctive and interpretable response profiles despite the lack of functional or anatomical constraints imposed by the analysis. The response profiles of three components were strongly correlated with acoustic measures of either frequency or spectrotemporal modulation, and did not respond selectively to any of the categories tested. In contrast, two other components exhibited pronounced category-selectivity, one for speech and one for musical sounds, and weak correlations with our acoustic measures. These two components occupied distinct regions of non-primary auditory cortex, and their response profiles that could not be explained by standard acoustic features. Our method thus identifies a set of dominant selectivities underlying cortical responses, and reveals separable neural pathways for the analysis of music and speech.

PD-107

Modulation of Wnt/β-catenin Signaling Enhances Mitotic Hair Cell Regeneration from Damage-recruited Lgr5+ Cells

Grace Kim; Renjie Chai; Tian Wang; Nicole Pham; Duc-Huy Nguyen; Alan Cheng
Stanford University

Background

The canonical Wnt/β-catenin pathway is one of the most essential signaling pathways involved in tissue homeostasis by directing the self-renewal of stem cells. Tissue injury in numerous mammalian organ systems upregulates Wnt signaling, which can function to promote tissue repair. Unlike the mammalian cochlea, the utricle has a limited capacity to regenerate lost hair cells *in vitro* and *in vivo*. Our recent work shows that the Wnt target gene Lgr5 marks a subset of supporting cells in the neonatal utricle after hair cell damage in vitro and in vivo. While these Lgr5-expressing supporting cells can regenerate hair cells to a limited degree, the effects of overactivating Wnt signaling on the extent of hair cell regeneration is unknown. The current study is designed to examine the effects of stabilizing β-catenin, the central mediator of canonical Wnt signaling, on hair cell regeneration.

Methods

To further examine the effect of β-catenin stabilization on Lgr5-positive supporting cells, we first generated a triple transgenic Pou4f3$^{DTR/+}$; Lgr5$^{EGFP\text{-}CreERT2/+}$; Catnb$^{flox(exon3)/+}$ mouse, which allowed us to temporally control hair cell damage and the activation of β-catenin stabilization. In this set of experiments, diphtheria toxin (DT; 6.25 ng/g) was administered at postnatal day 1 (P1) to ablate hair cells, tamoxifen (0.075 mg/g) given at P3 to activate Cre recombinase in Lgr5+ cells, and the thymidine analog EdU (25 mg/kg) given daily at P4-6 to label proliferating cells. Finally, the utricles were examined at P30.

Results

With DT-induced damage alone, there was an increase in EdU-labeled supporting cells (95.7±21.7 vs. 0.7±0.4) and hair cells (14.0±13.6 vs. 0) in the striolar region of the utricle in comparison to undamaged tissues (per 20,000 μm^2). Tamoxifen-mediated β-catenin stabilization after damage significantly increased the number of EdU-labeled supporting cells and hair cells in the striolar region compared to damage alone (113.2±16.4 and 29.6±4.6, respectively). In addition, damaged organs with stabilized β-catenin contained larger sensory epithelia (46.2±15.6 and 64.7±4.9% relative to undamaged controls, respectively) as well as a 70% increased hair cell density.

Conclusions

Prior work shows that the Wnt target gene Lgr5 marks damage-recruited hair cell progenitors in the mouse utricle. These progenitors contribute to both mitotic and non-mitotic regeneration of hair cells *in vivo*. Our results suggest that β-catenin stabilization stimulates the proliferation of damage-activated Lgr5+ supporting cells and mitotic hair cell regeneration.

PD-108

Time-Lapse Imaging Of Spontaneous and Notch-inhibited Supporting Cell-Hair Cell Transition in Mouse Utricle

Tian Wang[1]; Nicole Pham[1]; **Jiayi Luo**[1]; Lina Jansson[1]; Lindsey May[2]; Lisa Cunningham[2]; Alan Cheng[1]
[1]Stanford University; [2]NIH/NIDCD

Background

Hair cell regeneration in the avian inner ear organs and the zebrafish lateral line can be attributed to both mitotic regeneration and direct transdifferentiation. The two mechanisms differ in that the latter is characterized as a direct phenotypic conversion of a supporting cell to a hair cell without intervening mitosis. In the regenerating mammalian utricle, almost no mitotic regeneration occurs, and hair cell regeneration occurs predominantly via direct transdifferentiation. Previously, we have demonstrated expression of the Wnt target gene Lgr5 in striolar supporting cells after neomycin-mediated damage to the neonatal mouse utricle in vitro. In addition, our lineage tracing data showed that Lgr5+ supporting cells gave rise to new hair cell-like cells *in vitro*. The current study utilizes time-lapse imaging to characterize the morphologic and positional changes during supporting cell-hair cell transition both with and without suppression of Notch signaling.

Methods

Utricles from postnatal 3- to 5-day-old (P3-5) Lgr5-EGFP-CreERT2; ROSA26R-tdTomato transgenic mice were iso-

lated and cultured as whole organs. Neomycin was used to ablate hair cells and 4OH-tamoxifen to activate Cre-recombinase. A spinning-disc confocal microscope system (Zeiss and Olympus) coupled to a culture chamber was used for time-lapse imaging. Images were acquired with MetaMorph software and then analyzed with Volocity and ImageJ softwares.

Results

Lgr5 expression is normally absent in the P3 utricle. After neomycin damage, Lgr5-EGFP appeared predominantly in supporting cells in the striolar region. Quantitative PCR and in situ hybridization of damaged, wildtype utricles showed increased Lgr5 expression and transcripts regionalized to the striolar region. Fate-mapping experiments showed that traced, tdTomato+ cells from the Lgr5 lineage expressed the hair cell marker Myosin7a 3 days post neomycin treatment, and the number of tdTomato/Myosin7a+ cells had increased 8 days later. Co-treatment with the thymidine analog EdU fails to label traced, Myosin7a+ cells. Time-lapse imaging for 4-6 days post neomycin treatment showed that most tdTomato+, Lgr5-traced cells retained a columnar shape throughout the imaging period, while a subset demonstrated morphologic change involving the basal connection narrowing to a thin, elongated process. Finally the cells took on a flask shape and detached from the basement membrane. Inhibition of Notch signaling did not alter Lgr5 expression, but increased the frequency with which traced cells acquiring hair cell-like morphology, a lumenal position and also Myosin7a expression.

Conclusions

Damage to the neonatal utricle induces Lgr5 expression in striolar supporting cells, which can directly acquire a hair cell fate *in vitro* in a Notch-regulated manner.

PD-109

Resolution of Cellular Heterogeneity in the Newborn Mouse Utricle Using Single Cell RNA-Seq

Joseph Burns; Michael Hoa; MIchael Kelly; Stephen Hartley; Jim Mullikin; Robert Morell; Matthew Kelley
NIH

Introduction

The sensory regions within the auditory and vestibular organs of the inner ear contain exquisite arrays of supporting cells (SCs) and mechanosensitive hair cells (HCs). However, our understanding of the diversity of cell types within each of these broad categories remains limited, in large part because of the relatively small number of each particular cell type. High throughput transcriptional profiling methods, such as RNA-Seq, should accelerate the pace of discovery; however, the averaging of results that occurs in pooled populations typically masks single cell heterogeneity. Profiling the transcriptomes of single cells should eliminate this complication, facilitating the identification of similarities and differences between individual cells.

Methods

Utricles were dissected from newborn Lfng-EGFP; $Gfi1^{Cre}$; $ROSA26^{CAG\text{-}tdTomato}$ mice. In these mice, 99% of utricular HCs express tdTomato, and all extra-striolar SCs express Egfp. Sensory epithelia were isolated from underlying stroma with thermolysin, and dissociated to a single cell suspension. The cells were then loaded onto a Fluidigm C1 microfluidics platform, which captures single cells in isolated chambers and performs lysis, oligo-dT-based reverse transcription, and cDNA amplification. A total of 159 single cells were captured, each of which was imaged by fluorescence microscopy prior to lysis. The amplified cDNA from each cell was converted to a barcoded library. Libraries from 48 cells were pooled and sequenced together on a single flow cell lane of an Illumina Hi-Seq to an average depth of $2.26x10^6$ reads per cell. Reads were quantified using Tuxedo Suite tools. Statistical analysis was performed with the Singular Analysis package within R software.

Results

Unbiased cluster analysis identified seven distinct populations of cells in the newborn mouse utricular epithelium: non-sensory epithelial cells outside the macula, extra-striolar SCs and HCs, striolar SCs and HCs, and progenitor cells within and outside the macula that were in the process of differentiating into HCs. The identity of each cell was validated based on pre-lysis fluorescence. Cells from each of these populations reliably expressed previously identified genes, as well as new markers that were validated by immunocytochemistry. Finally, using Monocle, an algorithm that orders multidimensional samples by similarity, we were able to construct the progression of differentiation from progenitor cell to hair cell in our sample set.

Conclusions

Transcriptional profiling of individual, genetically labeled cells by RNA-Seq reveals heterogeneity within the early postnatal utricular sensory epithelium. In particular, despite limited morphological and/or physiological differences, distinct striolar and extra-striolar populations of HCs and SCs are already present.

PD-110

Supporting Cell and Hair Cell Populations Are Dynamic in Adult Mouse Utricles

Stephanie Furrer Bucks[1]; Brandon Cox[2]; Brittany A. Vlosich[1]; Tot Nguyen[1]; Remy Pujol[3]; Jennifer Stone[1]
[1]University of Washington; [2]Southern Illinois University School of Medicine; [3]INSERM Institute of Neuroscience

Throughout adulthood in mammals, the established vestibular hair cell (HC) and supporting cell (SC) populations are assumed to remain relatively unchanged except in cases of age-related HC loss. Recently, we discovered that HCs are phagocytosed in undamaged adult mouse utricles, suggesting mammalian vestibular HCs undergo cell turnover similar to non-mammals. In this study, we further characterized HC addition and clearance in whole-mounted utricles from adult mice. Utricles were labeled with antibodies to detect HCs (myosin VIIa, calretinin, Pou4f3, or Sox2) and immature HC ste-

reocilia bundles (protocadherin15-CD2). Phalloidin was used to visualize filamentous actin in stereocilia and phagosomes. For fate-mapping, we used transgenic mice with SC-specific inducible Cre activity (Plp-CreER^{T2}) to drive expression of a fluorescent reporter (tdTomato) in SCs. Tamoxifen was injected at 6 weeks of age to label SCs, the presumed HC progenitors, and track their fate over 15 weeks.

In adult Swiss Webster (SW) utricles, up to 20 stereocilia bundles per utricle were labeled with the immature bundle marker protocadherin15-CD2. We also observed an average of 50 actin-labeled phagosomes per utricle, of which ~11 (22%) appeared to be targeting a myosin VIIa+ HC. These findings suggest that HCs may be undergoing addition or clearance at any time in adult SW utricles. To confirm SC to HC conversion and begin to elucidate the rate of HC addition, we used Plp-CreER^{T2}:ROSA26$^{CAG\text{-}tdTomato}$ mice (on a mixed background) to label SCs at 6 weeks of age, and we traced the labeled cell population up to 15 weeks later. We discovered that tdTomato-labeled SCs can convert into HCs by 16 weeks of age. Preliminary data suggest that 3-4 new HCs are added per week while at a single timepoint, 20 phagosomes exist per utricle in Plp-CreER^{T2}:ROSA26$^{CAG\text{-}tdTomato}$ mice. These observations suggest HC turnover occurs at a slower rate than in SW mice. We are seeking further evidence of HC turnover using transmission electron microscopy and semi-thin sections analyzed with light microscopy. We have found what appears to be SC nuclei transitioning from the SC to the HC layer. We also observed HCs that seem to be undergoing cell death (e.g., condensed chromatin). Our findings support the hypothesis that a slow rate of HC turnover occurs in the undamaged utricles of adult mice. Characterizing the molecular mechanisms governing continual HC addition throughout adulthood in mammals may allow the development of novel therapies to boost HC regeneration in a damaged system.

PD-111

Screening and Identification of Reprogramming Compounds in Hair Cell Regeneration

Yong Tao[1]; Shibing Tang[2]; Angela Song[3]; Weijia Kong[4]; Sheng Ding[2]; **Zheng-yi Chen**[5]

[1]Harvard Medical School, Boston; [2]Gladstone Institutes, UCSF; [3]Harvard University; [4]Department of Otolaryngology, Union Hospital, Tongji Medical College, Huazhong University of Science and Technology, Wuhan, China; [5]Eaton-Peabody Laboratory, Department of Otolaryngology Massachusetts Eye & Ear Infirmary Harvard Medical School

Introduction

In contrast to mammals, non-mammalian vertebrates have the capacity to spontaneously regenerate hair cells after hair cell loss. While the mechanisms underlying hair cell regeneration are largely unknown, it is likely that reprogramming of differentiated supporting cells is involved, which leads to cell cycle re-entry and transdifferentiation into hair cells. Screening of reprogramming small molecule compounds using hair cell regeneration model such as zebrafish could be an efficient way to identify the compounds with key function in hair cell regeneration. Further, the identified “hit” compounds could be directly tested in mammalian inner ear for their relevance in regeneration of mammalian hair cells.

Methods

Using zebrafish neuromast hair cell regeneration model, we screened a group of reprogramming compounds and identified those with positive effects on proliferation and regeneration of hair cell. The identified hits were subsequently tested in cultured mouse cochlea for the effects on mammalian hair cell regeneration. In addition, mechanistic studies of how the hits work were pursued by immunolabeling, lineage tracing, and qRT-PCR.

Results

By studying proliferation rate and hair cell regeneration in a zebrafish lateral line neuromasts, we screened over two dozens of reprogramming compounds. Several hits were identified, which increased proliferation and the number of hair cells after neomycin induced hair cell death. Using neonatal mouse cochlea explant culture, we tested the hits in mammalian hair cell regeneration. By co-culture for 5 days, one of the hits (SD19) dose-dependently led to a significant increase in the outer hair cell number from middle turn to apex. In contrast to the zebrafish model, SD19 treatment does not induce proliferation. By lineage tracing, new hair cells were demonstrated to be primarily derived from transdifferentiation of supporting cells. During the course of transdifferentiation, up-regulation of Atoh1 and down-regulation of Hes5 were seen. By qRT-PCR and western, both STAT3 and its pathway gene Jak1 were shown up-regulated. Furthermore, a STAT3 inhibitor S3I-201 blocked the increase in hair cell number by SD19.

Conclusion

Screening of reprograming compounds using zebrafish model followed by direct testing their function in mammalian inner ear is an efficient strategy to identify hits promoting hair cell regeneration. We identified such compound SD19 that promotes hair cell regeneration in both zebrafish and mammalian inner ear. We provide strong evidence that SD19 activates STAT3 pathway and promotes transdifferentiation of supporting cells into hair cells.

PD-112

Micropatterned Chemotactic and Topographical Cues Direct Neurite Growth from Spiral Ganglion Neurons

Kristy Truong[1]; Reid Bartholomew[2]; Braden Leigh[2]; Linjing Xu[2]; Allan Guymon[2]; Marlan Hansen[2]

[1]University of Iowa Hospitals and Clinics; [2]University of Iowa

Introduction

The distance between cochlear implant (CI) electrodes and spiral ganglion neuron (SGN) elements that are stimulated represents a major limitation of current CI technology. Precise guidance of SGN axon regrowth into proximity of CI electrodes would likely improve performance. Neurite pathfinding is determined by both biochemical chemotactic signals and physical topographical features. Here we compare the ability of micropatterned biochemical and topographical

guidance cues, singly and in combination, to direct SGN neurite growth.

Methods

Photopolymerization was used to create methacrylate polymer films with micropatterned surface topographic features consisting of unidirectional parallel lines or multidirectional 90° angle turns. Microcontact printing methods were used to create comparable protein micropatterns. Methacrylate polymer stamps with the same spacing as the topographical features were "inked" with laminin and used to imprint polymers lacking topographical features to assess the contribution of laminin patterns alone to directed neurite growth. We also applied laminin to an unpatterned polymer stamp to print onto the ridges of a topographical micropattern, thereby producing materials with both topographic and biochemical micropatterns. Dissociated rat spiral ganglion cultures were plated on topographically and/or biochemically patterned substrates and neurite alignment to the micropatterns was quantified. Neurite preference for specific microfeatures (e.g. ridge vs groove vs laminin) was also assessed.

Results

SGN neurites aligned strongly to both surfaces with unidirectional laminin or topographical micropatterns compared to surfaces lacking micropatterns. SGN neurites preferentially grew on laminin-coated stripes and in grooves of topographical micropatterns. In addition, biochemical and topographic cues were combined to determine the effects on alignment. Coating laminin in the grooves enhanced alignment whereas printing laminin on the ridges significantly disrupted alignment. The percentage of neurite length on a microfeature was measured to determine whether combining biochemical and topographic cues affects the preference for a given feature. The highest percentage of neurite length is found in depressed microfeatures in polymers with laminin coated in these grooves.

Conclusions

Microprinting biochemical cues that promote neurite growth, such as laminin, onto the grooves of microtopographical surfaces results in the best alignment of SGN neurites, while microprinting growth promoting biochemical cues on the ridges disrupts alignment. These data suggest that biochemical and topographical cues interact to improve or disrupt neurite alignment depending on the specific arrangement of the micropatterns.

PD-113

Cloning and Characterization of Full-Length Chicken Atonal Homologue 1

Joanna Mulvaney[1]; Yutaka Amemiya[1]; Stephen Freeman[2]; Raj Ladher[2]; Alain Dabdoub[1]

[1]Sunnybrook Research Institute; [2]RIKEN Center for Developmental Biology

Introduction

Atoh1, a vertebrate basic helix-loop helix transcription factor, is essential for formation, maturation and survival of mechanosensory hair cells of the inner ear, neurogenesis, differentiation of the intestine, homeostasis of the colon and is implicated in cancer progression. The predicted sequence of chicken Atoh1 (cAtoh1) shares identity with mammalian Atoh1 homologues only in the basic helix-loop-helix domain and a portion of the carboxy tail. We hypothesized that cAtoh1 could have differing protein binding affinity and active phosphorylation sites to mammalian Atoh1 that might confer functional differences to its activity. In this study we set out to obtain a full sequence of the cAtoh1 open reading frame, and to assess its behavior in the developing inner ear of the chicken and mouse.

Methods

cAtoh1 was cloned directly from genomic DNA by inverse PCR and an antisense morpholino was designed against the 5' untranslated region near the kozak site. Gain- and loss-of-function experiments were performed in chicken, and over expression studies conducted in mouse. Plasmids were electroporated into the chicken otic vesicle, which was then maintained *in ovo,* while morpholinos were eletroporated into chicken basilar papilla explant cultures. Mouse cochlear explant cultures were electroporated with expression constructs and maintained *in vitro.* Samples were analyzed using immunofluorescence via confocal microscopy to determine cellular phenotype.

Results

cAtoh1 was necessary and sufficient to drive hair cell differentiation in the developing chicken ear. We then compared the behavior of cAtoh1 and human Atoh1 (hAtoh1) in embryonic mouse cochlear explants, showing that cAtoh1 was a potent inducer of hair cell differentiation and induced supporting cell identity in neighboring untransfected cells. Furthermore, while cAtoh1 and hAtoh1 were similarly affected when co-transfected with Notch1 intracellular domain (NICD), cAtoh1 overcame Sox2 mediated repression of hair cell differentiation more effectively than human Atoh1 when co-transfected.

Conclusions

We generated the full-length sequence of the cAtoh1 open reading frame and confirmed that cAtoh1 is required for avian mechanosensory hair cell differentiation. We showed for the first time that cAtoh1 interacts with the Sox2 mediated transcriptional cascade differently to mammalian Atoh1. This variation is likely due to the non-conserved 5' region of the open reading frame.

PD-114

Notch Inhibition Increases the Proliferation and Transdifferentiation Mediated by Beta-catenin and Atoh1 in Lgr5+ Supporting Cells in Postnatal Mouse Cochlea

Bryan Kuo[1]; Wanda Layman[1]; Makoto Taketo[2]; Jian Zuo[1]

[1]St. Jude Children's Research Hospital; [2]Graduate School of Medicine

Supporting cells (SCs) expressing the stem cell marker Lgr5 has been of interest for regeneration because they could represent the progenitor/stem cells of the postnatal mouse inner ear with potential for hair cell (HC) regeneration. Although

there is no HC transdifferentiation in the b-catenin-mediated proliferating Lgr5+ SCs, there is a synergistic proliferation and differentiation response in these cells to the combined ectopic expression of b-catenin and Atoh1 in postnatal mouse cochlea. Although new hair cells are generated from this combined genetic manipulation, they remain immature. Given the importance of Notch signaling during cochlear/HC development, we hypothesize that Notch signaling might be impeding the maturation of the newly generated HCs from our genetic manipulation. We describe the effect of Notch1 conditional deletion in the Lgr5-EGFP-IRES-CreER;Rosa-floxed-stop-beta-catenin; CAG-flox-STOP-flox-Atoh1-HA+ mouse following tamoxifen induction at P0-1 and analysis at various postnatal ages for HC maturation. Our results show that the deletion of Notch signaling results in an increase proliferation response in Lgr5-EGFP-IRES-CreER;Rosa-floxed-stop-beta-catenin mouse with resulting clusters of cells abutting the inner hair cells (IHCs) remaining at P21 (they were previously absent in the b-catenin ectopic expression model at this age). In Lgr5-EGFP-IRES-CreER;Rosa-floxed-stop-beta-catenin; CAG-flox-STOP-flox-Atoh1-HA+; Notch fl/fl mice, we observe an increased generation of new IHCs that remain at least at P21; however, these new HCs still remain immature. We conclude that Notch inhibition increases the proliferation and differentiation of neonatal cochlear Lgr5+ SCs in response to b-catenin and Atoh1ectopic expression.

SYM-109

Cochlear Hair Cell Mechanotransduction is Specialized for Speed by by Eliminating Calcium Dependent Adaptation while Incorporating a Novel Lipid Based Mechanism for Modulating Resting Open Probability

Anthony Ricci; Anthony Peng; Thomas Effertz
Stanford University

Across vertebrate species, inner ear organs, both vestibular and auditory, share a common pathway of signal processing where the sensory hair cells serves as the transducer of mechanical energy and the conveyor of information to the central nervous system. Deflection of the sensory organelle, the hair bundle, regulates the open state of mechanically gated channels that drive the hair cell receptor potential. To date, it is assumed that the mechanisms regulating the mechanotransduction process are ubiquitous across sensory organs. We are suggesting that the mechanotransduction process of mammalian cochlear hair cells is specialized for speed. Scanning electron microscopy shows that hair bundle morphology is very different in cochlear hair cells as compared to lower frequency systems. Electrophysiological recordings of mechantransducer currents in response to high speed mechanical deflection of the hair bundle demonstrate that both activation and adaptation kinetics are much faster in mammalian cochlea hair cells. High speed calcium imaging reveals that channel localization may be different between hair bundle types (mammalian vestibular compared to auditory). Most recently we demonstrated, again using electrophysiological measurements and high speed mechanical stimulation, that mammalian hair bundles show little or no slow motor adaptation and that the remaining adaptation does not require calcium entry. The loss of calcium sensitivity is posited to underlie the faster kinetics measured in mammalian cochlear hair cells. We have identified and characterized a novel mechanism regulating the resting open probability of the cochlea hair cell mechanotransduction channel. This mechanism may operate via the lipid membrane and is sensitive to both external divalent ions and membrane potential. Evidence supporting a role for the lipid bilayer include sensitivity to the gating modifier GsMTX4, cholesterol/lipid depletion and the insertion of lipids with different geometries and charge. Together these data support a hypothesis that mechanotransduction in mammalian cochlea hair cells is specialized to operate at higher frequencies and does this by optimizing pathways that are not rate limiting and limiting those that are. Data also suggests that hair cell mechanotransduction may be more similar to other mechanosensory modalities than previously suspected.

This work was supported by grants: RO1 DC003896 to AJR, F32 DC109752 to AWP, K99 DC013299 to AWP, DAAD (German academic exchange service) to TE and core grant P30-44992,

SYM-110

Multifunctional Calcium Channels in Mammalian Inner Hair Cells: Composition, Functions and Developmental Aspects

Jutta Engel
Saarland University

Voltage-gated Ca^{2+} channels (VGCCs) are protein complexes composed of an α_1 pore-forming subunit and auxiliary subunits β and $\alpha_2\delta$. VGCCs of cochlear inner hair cells (IHCs) are mainly composed of the L-type pore-forming subunit $Ca_v1.3$ (contributing to ~90% of I_{Ca}; Platzer et al., Cell 2000) and the auxiliary subunit β2 (contributing to ~70% of I_{Ca}; Neef et al., J. Neurosci. 2009). Lack of either $Ca_v1.3$ or β2 causes deafness in mice, and humans with a glycine insertion mutation in the pore region of $Ca_v1.3$ suffer from deafness and sinoatrial node dysfunction (SANDD syndrome, Baig et al., Nat. Neurosci. 2011). Transcript analysis revealed $\alpha_2\delta2$ as the dominating $\alpha_2\delta$ subunit. Ducky mice with a mutation in $\alpha_2\delta2$ (functional $\alpha_2\delta2$ null mice, du/du) showed moderate hearing loss, reduced Ca^{2+} currents and exocytosis, and altered biophysical properties of the Ca^{2+} currents, indicating that $\alpha_2\delta2$ is part of the $Ca_v1.3$ channel complex.

VGCCs of IHCs serve multiple functions: They provide the Ca^{2+} influx that triggers depolarization-induced vesicle fusion and transmitter release in IHCs before and after the onset of hearing. In mature IHCs, $Ca_v1.3$ channels exclusively cluster at the ribbon synapses. Before hearing function, they further serve the generation of Ca^{2+}-based action potentials that help in the final differentiation of the IHC itself and that of the afferent auditory pathway. To this end, the peak Ca^{2+} current amplitude undergoes a developmental maximum around postnatal day 6 (P6). The transient supernumerary Ca^{2+} channels are partially localized extra-synaptically and vanish by the end of

the second postnatal week. This up- and downregulation is thoroughly controlled by thyroid hormone acting through thyroid hormone receptors (TR) TRα and TRβ.

Proper expression of $Ca_v1.3$ channels in development is essential for expression of several genes, such as the KCNMA gene encoding the BK channel α subunit, because this protein is not expressed in constitutive $Ca_v1.3$ knockout mice. It will be interesting to test whether hair cell-specific deletion of $Ca_v1.3$ after the phase of spontaneous activity will generate a similar phenotype.

Funded by DFG (SFB 894-A8, and Saarland University.

SYM-111

Cellular Functions of CaBPs in the Auditory System

Amy Lee
University of Iowa

CaBPs are a family of Ca^{2+} binding proteins with high similarity to calmodulin (CaM), and are enriched in the brain, retina, and cochlea. Like CaM, CaBPs have 4 EF-hand Ca^{2+} binding domains, the second of which is non-functional. CaBPs can interact with effectors that are regulated by CaM, but with distinct functional consequences. For example, while CaM promotes Ca^{2+}-dependent inactivation (CDI) of voltage-gated $Ca_v1.3$ Ca^{2+} channels, CaBPs strongly oppose CDI. The mechanism may involve both competitive displacement of CaM from the channel by CaBPs, as well as allosteric modulation by CaBPs from a distinct binding site in the channel. In the cochlea, 4 CaBP family members are expressed: CaBP1, CaBP2, CaBP4, and CaBP5. By quantitative PCR, CaBP1 and CaBP2 are the primary CaBPs expressed in mouse cochlea. Alternative splicing gives rise to three CaBP1 and CaBP2 splice variants. The largest of the CaBP1 variants, caldendrin, is strongly expressed in the spiral ganglion, while lower levels of the shorter CaBP1 variants are found in cochlear hair cells. The largest of the CaBP2 variants is expressed in hair cells but not in the spiral ganglion. While CaBP1 expression increases two-fold from postnatal day 7 to postnatal day 21, that for CaBP2 remains constant during this period of development. In transfected HEK293T cells, both CaBP1 and CaBP2 suppress CDI of $Ca_v1.3$ channels. These effects may be important for prolonged presynaptic $Ca_v1.3$ Ca^{2+} signals that support tonic glutamate release at the inner hair cell synapse. Consistent with this hypothesis, a mutation in CaBP2 that causes autosomal-recessive hearing impairment impairs the ability of CaBP2 to suppress CDI of $Ca_v1.3$ channels. Our results indicate partially overlapping, yet distinct cellular and developmental functions of CaBP1 and CaBP2 in the cochlea.

SYM-112

Quantitative Nanophysiology of Synaptic Calcium Influx

Tobias Moser[1]; Tzu-Lun Wang[1]; Jakob Neef[1]; Nicolai Urban[2]; Thomas Frank[1]; Mark Rutherford[3]; Fabian Göttfert[2]; Stefan Hell[2]; Katrin Willig[2]
[1]University Medical Center Göttingen; [2]Max-Planck-Institute for biophysical Chemistry; [3]Washington University St. Louis

The ribbon-type synapses between auditory inner hair cells and spiral ganglion neurons encode acoustic information with remarkable precision, reliability, and dynamics, demonstrating very high rates of vesicle release and resupply.

Understanding the anatomy and physiology of the active zone (AZ) at the nanometer scale is crucial to understanding the mechanisms employed to accomplish this challenging task. Stimulated Emission Depletion (STED) imaging of immunolabeled Ca^{2+} channels and AZ scaffolds and electron tomography indicated that membrane proximal (most likely readily releasable) vesicles are tethered in nanometer proximity to stripe-like $Ca_V1.3$ cluster at the AZ. STED Ca^{2+} imaging revealed presynaptic Ca^{2+} nanodomains often also assuming a stripe-like shape. We have utilized laser scanning and spinning disk confocal in order to quantify the number of Ca^{2+} channels at the AZ.

Specifically, we counted the number of Ca^{2+} channels by optical fluctuation analysis and by quantifying the reduction of whole-cell Ca^{2+} current during imaging-controlled specific abolition of Ca^{2+} influx at a single AZ.

Both methods converged on a range of approximately 20-250 channels per AZ. These approaches allow us to improve the accuracy of our biophysical modeling and thus promise to further our understanding of AZ Ca^{2+} signaling and Ca^{2+} influx-exocytosis coupling.

SYM-113

Short-term Plasticity at Auditory Hair Cell Synapses

Soyoun Cho; Henrique von Gersdorff
Vollum Institute, Oregon Health & Science University

Background

Ca^{2+} influx across the plasma membrane of hair cells triggers glutamate release at ribbon-type active zones. We have shown previously that residual Ca^{2+} build-up by a pair of short-duration pulses with a short inter-stimulus interval results in EPSC facilitation. By contrast, vesicle pool depletion causes paired-pulse depression with longer depolarizing pulses. Hair cell synapses can thus exhibit both paired-pulse facilitation and depression. To manage an uninterrupted flow of auditory signals, hair cell synapses must continuously release glutamate. Vesicular glutamate transporters fill synaptic vesicles with glutamate using an electrochemical proton gradient. We have studied the effects of released glutamate and protons using bullfrog auditory hair cell synapses. We find that the exocytosis of protons can alter significantly the short-term plasticity of hair cell synapses.

Methods
Amphibian papillae were carefully dissected from adult bullfrogs. Semi-intact preparations of hair cells and their connecting afferent fibers were obtained and paired whole-cell voltage-clamp recordings were performed.

Results
When hair cells are held at -60 mV, a potential close to the physiological resting membrane potential of *in vivo* hair cells, and depolarized to -30 mV, the Ca^{2+} current showed a transient block. The transient block results from a block of Ca^{2+} channels by protons released from fused synaptic vesicles. The transient block in Ca^{2+} current was removed when the concentration of the external pH buffer (HEPES) was increased to 40 mM. We measured EPSCs from the postsynaptic afferent fibers by depolarizing hair cells using a train of 1 ms-long pulses from -60 mV to -30 mV at 400 Hz. Removing transient block with 40 mM HEPES altered the paired-pulse ratio (PPR; $EPSC_2/EPSC_1$) and the recovery kinetics of depression. When we applied 40 mM glutamate in presynaptic pipette solution, the amplitude of transient block became significantly larger. To examine the effect of additional glutamate on PPR, we compared EPSCs within 2 minutes after break-in (as a control) and after more than 4 minutes of whole-cell configuration (to allow extra time for glutamate to diffuse into the hair cell and be transported into vesicles). We stimulated hair cells using a pair of 20 ms-long pulses from -60 mV to -30 mV with 20 ms inter-stimulus interval. PPR was significantly increased by 40 mM internal glutamate.

Conclusions
The concentration of vesicular glutamate, and the release of protons during exocytosis, can alter short-term plasticity at adult bullfrog auditory hair cell synapses.

Funding sources: DRF and NIDCD grants. (.+)

SYM-114

Calcium Signaling at the Hair Cell's Efferent Synapse

Paul Fuchs
Johns Hopkins University School of Medicine

Cholinergic inhibition of hair cells results from the activation of calcium-dependent potassium channels that hyperpolarize and shunt the membrane. The time-course and voltage-dependence of efferent synaptic currents are consistent with activation of potassium channels by calcium entering through the ionotropic ACh receptor. The postsynaptic calcium signal is constrained by a thin near-membrane cistern (14 nm separation) that is aligned with the efferent terminal contacts. The postsynaptic cistern plays an essential role in cholinergic calcium signals, serving as sink or source depending on ongoing activity and the extent of buffer saturation. Equally importantly, the cistern segregates calcium signals that mediate inhibition from those that trigger transmitter release at nearby ribbon synapses. Finally, calcium crosstalk between afferent and efferent synapses may mediate activity-dependent maturation of cochlear inner hair cells, when afferent and efferent synapses first proliferate, then disappear (efferent) or are refined (afferent) prior to the onset of hearing.

SYM-115

Exocytosis and Endocytosis at an Auditory Synapse

Ling-Gang WU
National Institute of Neurological Disorders and Stroke

The calyx of Held synapse in the auditory brainstem is a relay synapse that faithfully relays action potentials from the presynaptic neuron to the postsynaptic neuron. It is involved in sound location. Here I will provide an overview of our recent progresses towards the understanding of how exocytosis and endocytosis take place at this synapse to ensure relay of action potentials from the presynaptic to the postsynaptic neuron at various frequencies of firing. Exocytosis mediates transmitter release, whereas endocytosis recycles exocytosed vesicle for the second round of exocytosis. There are three modes of exocytosis: 1) full-collapse fusion, in which vesicles open a fusion pore to release transmitter, followed by collapse of the vesicle into the plasma membrane, 2) kiss-and-run, in which fusion pore opens and closes without vesicle collapse, and 3) compound exocytosis, in which vesicles fuse with each other to form a compound vesicle which then undergoes exocytosis. These three exocytosis modes are followed by three endocytosis modes, 1) classical endocytosis involving reformation of vesicles from the plasma membrane, 2) kiss-and-run, and 3) bulk endocytosis, which retrieves vesicles much larger than a regular vesicle. Here we will review the supporting evidence for each exo- and endocytosis mode found at the calyx of Held nerve terminal.

SYM-116

Calcium-dependent Regulation of Neurotransmitter Release in the Cochlear Nucleus

Matthew Xu-Friedman
University at Buffalo, State University of New York

Synaptic transmission is highly sensitive to calcium, and small changes in presynaptic calcium can have major consequences. We consider this issue from a functional standpoint, by examining the synapse formed by auditory nerve fibers on bushy cells in the cochlear nucleus. This synapse is a major gateway for auditory information entering the brain, so changes in calcium there can influence what information is available to the rest of the auditory pathway. We have found that neuromodulation of presynaptic calcium influx reduces synaptic strength, which weakens the fidelity with which the auditory nerve drives bushy cell spiking. This fundamentally changes the computational properties of the synapse. In addition, calcium lingering in the nerve terminal can drive considerable asynchronous release. Despite this, bushy cells resist imprecise spiking through a developmental increase in potassium channels to suppress excitability. Finally, we have found that the probability of neurotransmitter release from auditory nerve fibers is regulated by sound-driven activity. We propose that this novel form of homeostasis may result from

modulation of the efficacy with which calcium drives neurotransmitter release.

SYM-117

Regulation of conduction velocity in auditory brainstem circuits

Armin Seidl[1]; Andres Barria[2]; Edwin Rubel[2]
[1]University of Washington Virginia Merrill Bloedel Hearing Research Center; [2]University of Washington

The processing of auditory information in the brain relies on precise timing of signal propagation. Recent studies on the auditory system of birds and mammals present examples of conduction velocity regulation in the brainstem binaural processing circuits that require precise temporal regulation to encode interaural time and intensity differences between the two ears, as required for for sound localization and auditory scene analysis. Our studies of the avian brainstem revealed that precise regulation of action potential velocity contributes to the computation of microsecond arrival differences of sound at the two ears, so called interaural time differences (ITDs). Collaterals of a single axon in the chicken auditory brainstem calibrate their signal propagation velocities individually to achieve the specific conduction times required for sound localization. In mammals, ITDs are encoded by coincidence detector neurons in the medial superior olive (MSO). MSO neurons receive input from the two ears via the anteroventral cochlear nucleus (AVCN) on each side of the brain. A single AVCN axon projects to both the ipsilateral and the contralateral MSO. The binaural inputs to MSO must be timed correctly to enable coincidence detection. We analyzed internode lengths of both the ipsilateral and the contralateral branches of AVCN axons innervating MSO in gerbils. Both collaterals are heavily myelinated. The ipsilateral axon branch has significantly shorter internode lengths compared to the contralateral branch (52 µm and 95 µm, respectively). These data suggest that signal propagation in the axon branch projecting to the ipsilateral MSO is about 50% slower than the contralateral input, a value that compensates for the length difference of the AVCN axon collaterals reaching the ipsilateral and contralateral MSO. Taken together, our data suggest a conserved mechanism for adjusting conduction velocity of axon collaterals to achieve binaural coincidence detection at the level of the brainstem. Furthermore, our findings suggest that local interactions at the level individual axon segments with oligodendrocytes establish the appropriate conduction velocity. Future studies involving these systems will provide further insight into how specific conduction times in the brain are established and maintained during development.

SYM-118

Action Potential Conduction Velocity in Low- and High Frequency Globular Bushy Cell Axons Measured In Vivo

Annette Stange; Benedikt Grothe; Michael Pecka
Ludwig-Maximilians-University Munich

The timing of inputs in microcircuits plays a crucial role in information processing. The relative arrival time of inputs is largely determined by the relative conduction velocity of action potentials along individual axons. The conduction velocity, in turn, is effectively shaped by the axon diameter, the myelin thickness and the myelination pattern of the axon, which is the internode length. Traditionally, it has been thought that axon diameter and internode length are uniformly correlated with each other. However, recent data from our lab has revealed that the ratio of internode length and axon diameter deviates significantly in axons of low- and high frequency regions of globular bushy cell (GBC) axons in the antero-ventral cochlear nucleus (AVCN). Nevertheless, both the extent and the mechanisms by which the differences in internode length and axon diameter can actually contribute to adjust conduction velocity remain obscure.

Here, we investigated the structure-function relationship of axon morphology and conduction velocity. To this end, we measured the action potential conduction velocity in GBC axons in adult Mongolian gerbils *in vivo*. The measurements were performed by electrically stimulating GBC somata in the AVCN and simultaneously recording single cells extracellularly in the medial nucleus of the trapezoid body (MNTB). The precise measurement of the time period between the stimulation artifact and the initiation of the action potential allows for the calculation of the axonal action potential propagation latency between the GBC soma and the GBC-MNTB synapse.

Our experiments show that action potentials in the AVCN can be electrically elicited and simultaneously recorded in the MNTB *in vivo*. Thus, these recordings for the first time allow for the evaluation of the conduction velocity of morphologically characterized axons over a distance of as long as 5 mm *in vivo.* To relate the differences in axon morphology between low- and high frequency tuned GBC axons to axonal conduction properties, current work is concentrating on a frequency-specific characterization of conduction characteristics. Furthermore, comparing the latencies of electrically and acoustically evoked action potentials will give insight into the role of cochlear delays in shaping input timing.

SYM-119

Developing MNTB Neurons Excite Each Other Via Inter-Axonal GABA Spillover

Catherine Weisz; Maria Rubio; Karl Kandler
University of Pittsburgh

The lateral superior olive (LSO), an auditory nucleus involved in horizontal sound localization, receives tonotopically organized inhibitory glycinergic inputs from the medial nucleus of the trapezoid body (MNTB). The MNTB-LSO pathway undergoes refinement before hearing onset through synaptic strengthening and silencing. In addition to glycine, developing MNTB neurons also release glutamate and GABA, but their function is poorly understood. Here, we investigate a possible role for GABA.

Whole-cell voltage-clamp recordings were performed from LSO neurons in brain slices from P3-P14 C57BL/6J mice. Electrical stimulation of MNTB axons elicited post-synaptic currents (PSC) in LSO neurons.

In about half of recordings an unusual PSC occurred characterized by two distinct components following a single stimulus. We term these responses "doublets". In doublets, the second component did not occur without the first, but the first could occur without the second. The reversal potential of both components (~-20 mV, 60 mM Cl^- internal) suggests inhibitory neurotransmitter release from MNTB neurons. The short latency from the first to the second component (~3 ms) is faster than MNTB neurons can release neurotransmitter at these ages (300 Hz stimulation), suggesting that the two components are elicited by different populations of axons. Our results suggest that doublets are the result of GABA spillover between MNTB axons: 1) The probability of recording a doublet increased with stimulus strength (increased neurotransmitter release). 2) The second component in a doublet was blocked by the $GABA_AR$ antagonist gabazine (30 μM), without loss of the first component (n = 14 of 24 cells). 3) Doublet occurrence was enhanced by the GABA reuptake blocker guvacine (30 μM, 2 of 7 cells). 4) Higher frequency stimulation increased the occurrence of doublets in ~20% of cells. Postembedding immunogold labeling for GABAb2/3 localized $GABA_AR$ to MNTB axon terminals. To test the presynaptic excitatory action of GABA on MNTB axons, current-clamp recordings were performed from MNTB somata. Dye-filled axon terminals were visualized with 2-photon imaging. Focal pHP-GABA (200-500 μM) uncaging at the MNTB axon terminals in the LSO depolarized the soma ~5 mV (>500 microns distant) indicating direct axonal excitation by GABA (n=11). This depolarization increased the MNTB soma excitability in response to current injection(n=6), and in some cells an action potential was elicited (n=4).

We suggest that GABA spillover excitation of neighboring MNTB axons may play a role in the refinement of tonotopic projections from the MNTB to the LSO.

Support: NIDCD grants R01DC004199(KK), 1R01DC013048-01(MER), T32DC011499-01(CW), F32DC013207-01(CW).

SYM-120

Fast Neurons in the Inferior Colliculus: Substrates for Temporal Coding?

Michael Roberts; Lauren Kreeger; Nace Golding
The University of Texas at Austin

Background

Precise temporal coding is critical for the processing of low frequency sounds in the auditory brainstem. Binaural neurons in the medial superior olive (MSO), for example, encode interaural time differences with microsecond-order precision. These and other auditory timing specialists project to the central nucleus of the inferior colliculus (ICC), but previous studies suggest that ICC neurons lack the biophysical and synaptic properties needed to utilize such fast temporal information. Here, we describe a novel class of neurons in the low frequency region of the ICC that appears to be specialized for rapid temporal processing.

Methods

Acute slices containing the ICC were prepared in a plane parallel to the isofrequency lamina from P21-59 Mongolian gerbils. Whole cell current clamp recordings were targeted to neurons in the low frequency lamina where inputs from the MSO are concentrated.

Results

Among a cohort of neuron types similar to those previously described, we identified an additional class of ICC neurons that express robust hyperpolarization-activated currents, have input resistances < 30 MOhm, and membrane time constants <1 ms. Spontaneous and stimulus-evoked EPSPs in these neurons have rapid kinetics, with 10-90% rise-times < 1 ms and half-widths < 3 ms. We call these neurons strong adapters because they exhibit powerful spike frequency adaptation in response to suprathreshold current steps. Despite this, strong adapters were able to fire rapidly, exhibiting instantaneous firing frequencies >1 kHz and firing an average of 450 action potentials (SEM = 130) at the peak of input-output curves generated in response to 1 second current steps. These biophysical and synaptic specializations suggest that strong adapters possess the speed necessary for processing the temporal content of synaptic events arriving at high frequencies.

Conclusions

We propose that strong adapters provide a neuronal substrate for temporal coding in the auditory midbrain and thus may play an important role in the processing of low frequency sound information in the ICC. Using viral techniques for expressing fluorescent markers and optogenetic tools, we are determining whether strong adapters are inhibitory or excitatory and ultimately aim to test hypotheses about the sources of input to these neurons.

Funding

This work was supported by NIH DC006877 to NLG and NSF Graduate Research Fellowship DGE-1110007 to LJK.

SYM-12

Synaptic Inputs to Inferior Colliculus (IC) Neurons Underlying Coding of Interaural Level Differences in Mouse.

Munenori Ono; Douglas Oliver
University of Connecticut Health Center

Background

Interaural level difference (ILD) is an important cue used to localize a sound source. The IC receives and integrates ILD information from more than one source in the brainstem. However, the synaptic basis for this integration in the IC is unclear. Here, we used *in vivo* whole cell voltage clamp recordings to study the synaptic responses of IC neurons to ILD stimuli presented in a closed sound field.

Methods

Thirty seven GAD67-GFP knock-in mice of either sex (Postnatal day 26 – 42) were used for this study. We used voltage clamp and whole cell recordings to isolate and investigate EPSCs and IPSCs in IC neurons *in vivo* in response to mon-

aural or binaural sound. The EPSCs and IPSCs were isolated by clamping the cell at reversal potentials of IPSCs (-65 mV) and EPSCs (0 mV), respectively. The resting potentials *in vivo* were pharmacologically validated. In some neurons, the sound evoked extracellular spike responses were recorded in a giga-seal configuration before a break-in. We used stimuli in which ILD varies around a constant average binaural level (ABL) to approximate sounds on the horizontal plane.

Results
We found that the most IC neurons had both EPSCs and IPSCs to the sound stimuli in either the contralateral or ipsilateral ear. Most IC neurons showed balanced excitatory and inhibitory inputs to the change of ILD in average binaural level constant stimuli. The temporal properties of monaural responses were well matched, suggesting connected functional zones with matched inputs. The EPSCs had three patterns in response to ABL stimuli, preference for the sound field with the highest level stimulus: (1) contralateral; (2) bilateral highly lateralized; or (3) at the center near 0 ILD. EPSCs and IPSCs were well correlated except in center-preferred neurons. Summation of the monaural EPSCs predicted the binaural excitatory response but less well than the summation of monaural IPSCs. Binaural EPSCs often showed a nonlinearity that strengthened the response to specific ILDs. Extracellular spike and intracellular current recordings from the same neuron showed that the ILD tuning of the spikes was sharper than that of the EPSCs.

Conclusion
Our results suggest that the synaptic process underlying ILD coding in the IC is a complex mixture of excitatory and inhibitory inputs driven by both ears. The balanced excitatory and inhibitory inputs to the IC maybe a general feature of synaptic coding for many types of sound processing.

Funding
NIH grant R01-DC000189 (DLO)

SYM-122

Neural Encoding and Decoding of Sound Source Location in the Face of Changes in Sound Level

Mitchell Day; Bertrand Delgutte
Massachusetts Eye and Ear

Background
The mammalian central auditory system contains neural circuits that allow accurate localization of a sound source whether it is soft or loud, yet the firing rates of central auditory neurons, such as those in the inferior colliculus (IC), change with both sound level and source location. We ask the following questions: 1) How does tuning to source location in individual neurons change with sound level? 2) How does information on sound source location encoded in the firing rates of IC neurons change with sound level? 3) How might source location be decoded from the response of a neural population when individual neural responses change differentially with sound level?

Methods
To answer these questions, we recorded the firing rates of single neurons in the IC of awake rabbits in response to broadband noise bursts presented at each of 13 different azimuths in the frontal horizontal plane (15 degree spacing) in a virtual acoustic space and at each of three different sound levels (35, 50 and 65 dB SPL). We then analyzed these data using information theory and maximum-likelihood estimation of source location based on neural population responses.

Results
The mutual information between firing rate and source azimuth changed greatly with sound level for individual neurons, and could either increase or decrease with increasing sound level. On the other hand, there was little to no change in the accuracy of maximum-likelihood estimation of source azimuth with changes in sound level, indicating little to no change in the amount of azimuthal information encoded in the population of IC neurons. Azimuth tuning functions of individual neurons at different sound levels were highly correlated with each other, indicating a linear transformation with level. We trained a linear, maximum-likelihood decoder of source azimuth (assuming Poisson statistics) on population responses at 65 dB SPL, incorporating sound level-dependent weights and biases. The performance of the decoder was similar when tested on population responses at either 35, 50 or 65 dB SPL, indicating accurate cross-level decoding of source azimuth.

Conclusions
We conclude that, for IC neurons, azimuthal information encoded in the population changes little with sound level, azimuth tuning functions undergo linear transformations with sound level, and a neural population decoder can accurately estimate source azimuth using knowledge of the linear transformations.

Funding: NIDCD-NIH R03 DC013388, R01 DC002258 and P30 DC005209.

SYM-123

Source segregation by spectra and space

Peter Bremen[1]; John Middlebrooks[2]
[1]Radboud University Nijmegen; [2]University of California at Irvine

Psychophysical signal detection in complex listening environments is vulnerable to masking by competing sounds, even if the maskers are remote in frequency from the signal. This phenomenon is called informational masking (IM) and is thought to reflect a breakdown in the formation of discrete signal and masker auditory objects. Here, we sought evidence of IM in primary auditory cortex (A1) of anesthetized cats.

Stimuli were presented from calibrated free-field speakers arranged in the horizontal plane. We fixed the signal at contralateral 40 deg and varied masker locations. Stimuli were four pure-tone pulses repeated at 2.5, 5 and 10 pulses per second. Each pulse contained 4 masker components and (on half the trials) one signal component. We set signal frequency and level to the unit's characteristic frequency and to vari-

ous levels above threshold. Masker frequencies were held constant or randomized across pulses. We defined a ±1/3, ±1/2, or ±1 oct band centered on the stimulus. Within-band maskers had all components within this band, whereas out-of-band maskers contained frequencies outside of the band. We presented individual masker tones at 40 dB above unit threshold and gated them either synchronously or asynchronously with the signal.

Interestingly, we observed masking by components outside the reported critical band of auditory nerve fibers. Frequency-tuning curves in A1, however, are considerably broader than peripheral critical bands, and masker components that produced appreciable masking generally fell within A1 tuning curves. As a result, neuronal thresholds for signal detection were lower for 1) out-of-band compared to within-band maskers, 2) for asynchronous compared to synchronous maskers, and for 3) random re constant frequency maskers. Furthermore, we found that spatial separation (~80 deg) of the signal and masker sources led to mild improvements in signal detection. These observations roughly mirrored results from human psychophysics.

We found no indication of IM or across-frequency auditory object formation in anesthetized A1 aside from that accountable by broad central tuning curves. We deem three explanations possible: 1) IM is a form of energetic masking at the level of A1; 2) IM and auditory object formation arise outside of A1; and 3) they are a product of cortico-cortical feedback loops, which are effectively silenced under anesthesia. We plan to address these possibilities with future studies in awake-behaving animals.

SYM-124

Emphasis of Spatial Cues in the Temporal Fine-Structure during the Rising Segments of Amplitude Modulated Sounds III: Influence of Stimulus Level, Depth of Modulation, and Carrier.

Mathias Dietz
Universität Oldenburg

Background

Interaural temporal fine-structure disparities are the most potent sound localization cue for normal hearing listeners in common listening environments. The temporal weighting of these disparities is critical for sound localization coding. Dietz et al. (Proc. Natl. Acad. Sci., 2013; J. Neurophysiol. 2014) reported that for sinusoidally amplitude modulated tones the temporal fine-structure disparity is read-out only during a short “glimpse” (on the order of 10 ms) early in the modulation cycle, while binaural information during the remaining time is only weakly encoded in the brainstem and the auditory cortex. In human behavioral experiments employing a tonal 500-Hz carrier it was found that the modulation frequency influences the modulation cycle position that has the strongest weighting (4 Hz: 37°; 64 Hz: 115°). The current study investigates how, in comparison to the previous study, the weighting is influenced by (I) carrier frequency, (II) reduced modulation depth, (III) reduced signal level, and (IV) low-pass filtered noise carriers.

Methods

The psychoacoustic procedure is identical to that described in Dietz et al. (2013): The target stimulus is an amplitude modulated binaural beat (AMBB). The amplitude modulation frequency and the binaural beat frequency are both set to 16 Hz, resulting in a fixed relation between modulation cycle position and interaural phase difference (IPD). A pointer stimulus with adjustable IPD was used to match the intracranial percept of the AMBB. With the assumption that the matched pointer IPD is a measure of the instantaneous IPD with the maximum weighting, the dominant cycle position is determined.

Results

All conditions revealed clear rising slope dominance. Carrier frequencies of 750 and 256 Hz resulted in a slightly earlier and later read-out position, respectively, as compared to the 500-Hz reference. Reduced modulation depth, reduced level, and using noise instead of a tonal carrier all resulted in a later read-out, but still well before the amplitude maximum.

Conclusions

Adaptation prior to binaural interaction facilitates a mechanism of “glimpsing”, by which listeners strongly weight IPDs during the rising segment of ongoing envelopes. The effect has a strong contribution to a listener’s ability to localize speech in reverberation (Haas effect). The current study mimics more realistic stimuli employing non-tonal carriers, imperfect depth of modulation, and different overall levels. The persistence of the rising slope dominance, albeit some reduction, suggests it has an important role in sound localization in complex environments.

PD-115

Cochlear Ultrastructural High-frequency Hearing Adaptations in Toothed Whales

Maria Morell[1]; Marc Lenoir[2]; Robert E. Shadwick[3]; Marina A. Piscitelli[3]; Sonja Ostertag[4]; Stephen Raverty[5]; Thierry Jauniaux[6]; Willy Dabin[7]; Lineke Begeman[8]; Marisa Ferreira[9]; Iranzu Maestre[10]; Eduard Degollada[11]; Gema Hernandez-Milian[12]; Andrew Brownlow[13]; Chantal Cazevieille[14]; José-Manuel Fortuño[15]; Wayne Vogl[16]; Jean-Luc Puel[2]; Michel André[17]

[1]University of British Columbia, Vancouver, Canada; [2]Inserm U. 1051, Institut des Neurosciences de Montpellier, France; [3]Zoology Department, University of British Columbia, Canada; [4]Department of Fisheries and Oceans, Canada; [5]Animal Health Center, Canada; [6]Pathologie Vétérinaire, Université de Liège, Liège, Belgium; [7]Centre de Recherche sur les Mammifères Marins, Université de la Rochelle, France; [8]Department of Pathobiology, Faculty of Veterinary Medicine, Utrecht University, The Netherlands; [9]Sociedade Portuguesa de Vida Selvagem/CBMA, Departamento Biologia, Universidade do Minho, Portugal; [10]AMBAR. Sociedad para el Estudio y la Conservación de la Fauna Marina/Itsas Faunaren Ikerketa eta Babeserako Elkartea, Bilbao, Spain; [11]Asociación EDMAKTUB para el estudio y divulgación del medio acuático, Barcelona, Spain; [12]School of Biological, Environmental & Earth Sciences, University Colleague Cork, Ireland; [13]Scottish Marine Animal Stranding Scheme, SAC Veterinary Services, Inverness, UK; [14]Centre Régional d'Imagerie Cellulaire (CRIC), France; [15]Institute of Marine Sciences (CSIC), Barcelona, Spain; [16]Department of Cellular and Physiological Sciences, University of British Columbia, Canada; [17]Laboratori d'Aplicacions Bioacústiques, Universitat Politècnica de Catalunya. Vilanova i la Geltrú, Spain

Morphological studies of the organ of Corti in toothed whales together with studies of possible structural alterations in the organ associated with damage from sound exposure, represent key conservation approaches to assessing the effects of acoustic pollution on marine ecosystems. By collaborating with stranding networks from several European and North American countries, over 100 ears from 13 species of toothed whales were collected and analyzed by scanning (SEM), transmission (TEM) electron microscopy and immunofluorescence. Based on our analyses, we first describe and compare toothed whale cochlear structures and second propose a diagnostic method to identify inner ear alterations in stranded individuals. Despite possible autolytic artifacts due to technical and experimental constraints, the SEM analysis allowed us to describe unique cuticular plate features (Fig. 1a-c) and detect the presence of scarring processes resulting from the disappearance of outer hair cells from the epithelium, possibly as a result of sound overexposure. The two species analyzed by TEM (harbor porpoise and striped dolphin) showed numerous morphological features in the lower basal turn of the organ of Corti that are characteristic of high-frequency hearing species (Fig. 1d)

These features include 1) short outer hair cells (OHCs), 2) thick cuticular plates in OHCs, Deiters cells and outer pillar cells, 3) robust cup formation of the Deiters cell bodies, 4) well developed cytoskeleton in Deiters and pillar cells, and 5) thick basilar membranes. Such morphological characteristics, also present in horseshoe bats, suggest that there has been convergent evolution of sound reception mechanisms amongst echolocating species.

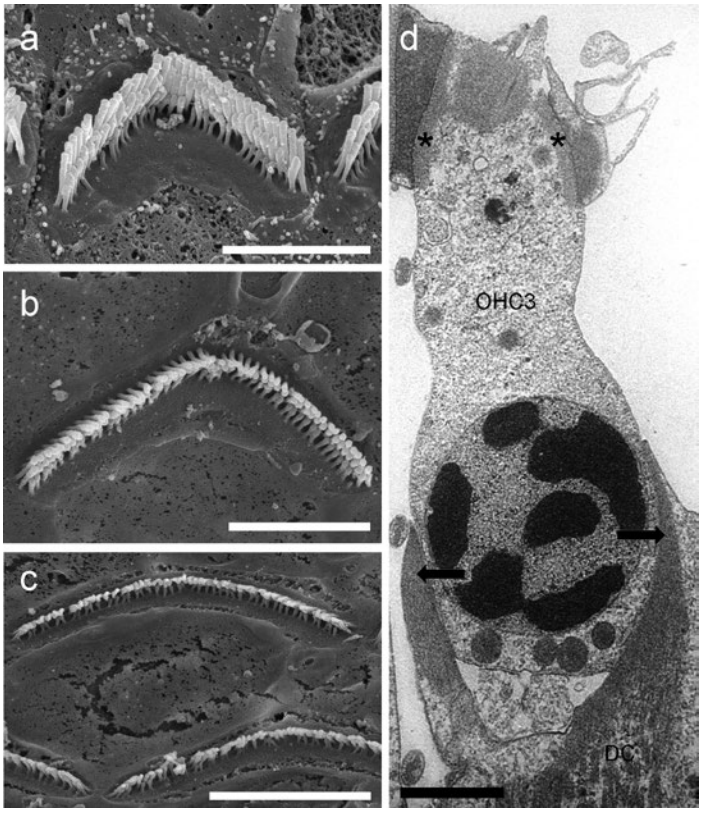

Fig. 1. Scanning electron microscopy images of outer hair cells (OHCs) of beluga whale from the apical (a), upper basal (b) and lower basal turn (d) of the cochlea. d) transmission electron microscopy image of an outer hair cell from the lower basal turn of the cochlea of a harbor porpoise. Black arrows indicate Deiters cell (DC) cup attachment with the lower bodies of OHCs. Asterisks highlight a large zone of contact between OHCs cuticular plate and Deiter cells phalangeal process. Scale bars: 3 µm (a and b), 4 µm (c) and 2 µm (d).

PD-116

Deep Sequencing Analysis of Transcriptomes in Immature and Mature Inner and Outer Hair Cells

Nicolas Michalski[1]; Sébastien Chardenoux[1]; Christine Petit[2]

[1]Institut Pasteur, INSERM, UPMC; [2]Institut Pasteur, INSERM, UPMC, Institut de la Vision, Collège de France

The identification of molecular complexes in mammalian hair cells by biochemical approaches has been impeded by the very small number of these cells within the cochlea. In contrast, the study of inherited forms of deafness led to the discovery of several essential proteins of cochlear hair cells,

which are currently used as entry points to decipher the associated molecular complexes. However, the identification of molecular components of the mechano-electrical transduction machinery in the hair bundle and of the inner hair cell ribbon synapses are incomplete. Similarly, very few proteins specific to either cochlear hair cell types, inner hair cells (IHCs) or outer hair cells (OHCs), have been uncovered by the genetic approach. By using next generation sequencing techniques, we first sequenced unamplified mRNA extracted from whole organs of Corti of mice either at postnatal day 7 (P7) or at embryonic day 16.5. This approach provided us with a comprehensive list of the genes expressed in the cochlea, with a robust relative quantification. By using the latest bioinformatics tools, we could make relative predictive quantifications at the isoform level. To identify the most relevant proteins for hair cell function, we then combined next generation sequencing techniques and our expertise in sampling single hair cells. We adapted single cell mRNA amplification techniques to samples containing 20 hair cells, either IHCs or OHCs. We sequenced these samples for three different age groups, P2, P7, and P16, in addition to a control P7 set containing spiral ganglia and associated glial cells. By using gene ontology databases or by making reasonable assumptions such as, for example, a channel subunit should contain a transmembrane domain, and by comparing the different datasets obtained, we could produce lists of strong candidate proteins involved in hair cell function, notably potential new mechano-electrical transduction channel subunits.

During the talk, I will review our deep sequencing results. I will focus on their contribution to our molecular understanding of hair cell maturation, mechano-electrical transduction, synaptic transmission, and OHC versus IHC molecular specification.

PD-117

The Cello Mouse Model of Early-Onset Hearing Loss Identifies a Novel OHC-Specific Transcription Factor Expressed During OHC Functional Maturation

Lauren Chessum[1]; Beatrice Milon[2]; Stuart Johnson[3]; Walter Marcotti[3]; Ronna Hertzano[2]; Steve Brown[1]; Michael Bowl[1]
[1]MRC Harwell; [2]University of Maryland; [3]University of Sheffield

Background

Cochlear inner and outer hair cells (IHCs and OHCs) develop from common sensory progenitor cells, which then diverge morphologically and physiologically to become functionally mature. A fundamental but still largely unknown question in auditory research is how the functional maturation of the mammalian cochlea is regulated at the molecular level. In particular, we still know very little about the molecular mechanisms underlying the onset of functional maturation of the IHCs and OHCs, which occurs during pre-hearing stages of development. Our characterisation of *cello*, an ENU-induced mouse model of early-onset hearing loss, has identified a novel OHC-specific transcription factor critical for hearing. Importantly, expression of this transcription factor in OHCs is coincident with their postnatal functional maturation.

Aim

We investigated the *cello* mice to fully characterize the functional and physiological requirement of this transcription factor for hearing.

Methods

We have undertaken a comprehensive characterization of the *cello* mutant including: *in vitro* analyses to investigate the effect of the mutation on protein function; qRT-PCR and immunolabelling studies to determine the temporospatial expression of the *cello* transcript and encoded protein product; ultrastructural and histological analyses to assess the organ of Corti; qRT-PCR and luciferase studies to determine transcriptional target genes; and, electrophysiology studies are underway to assess the function and maturation of the sensory hair cells.

Results

cello mice harbour a missense mutation in a novel OHC-specific transcription factor. *In vitro* studies show the mutant protein can still localize to the nucleus, but has an impaired ability to homodimerize - a prerequisite for DNA-binding. The *cello* protein is expressed in OHC nuclei from P4 onwards, and whilst the hair cells appear normal up to 1 month of age, they then begin to degenerate. At P8, two key OHC genes *Prestin* and *Oncomodulin* show greatly reduced expression in *cello* mutants compared to wildtype mice. In addition, luciferase studies demonstrate wildtype *cello* protein is able to transactivate the *Prestin* promoter, whereas mutant *cello* protein cannot.

Conclusion

Our data suggest the *cello* protein plays a major role in cochlear development and function by controlling the expression of genes specifically within OHCs. Further investigation of *cello* will increase our understanding of the genes and pathways required for OHC functional maturation and elaborate upon the mechanisms underlying early-onset hearing loss.

PD-118

Coordination of ATP-gated P2X2 Receptors with Prestin Reduces Hearing Sensitivity to Attenuate Environmental Noise

Yan Zhu; Hong-Bo Zhao
University of Kentucky Medical Center

Background

The P2X2 receptor is an ATP-gated ligand (ionotropic) ionic channel and plays important roles in many physiological and pathological processes. Recently, it has been found that P2X2 mutations can induce autosomal dominant nonsyndromic hearing loss (DFNA41) and increase susceptibility to noise stress (Yan et al., 2013). However, the cellular mechanisms underlying increase in noise susceptibility and deafness remain unclear. We previously demonstrated that ATP can activate P2X receptors to regulate outer hair cell (OHC) electromotility and active cochlear amplification (Zhao et al., 2005; Yu and Zhao, 2008). We also reported that dom-

inant deafness P2X2 mutations have no dominant effect on wild-type (WT) P2X2 activity. In this study, we investigated the effect of P2X2 deficiency on active cochlear mechanics and whether P2X2 dominant deafness mutations have trans-dominant effect on prestin activity.

Methods

P2X2 knockout (KO) mice were used to assess the effect of P2X2 deficiency on active cochlear mechanics. Auditory brainstem response (ABR) and distortion product otoacoustic emission (DPOAE) were recorded. OHC electromotility as measured by nonlinear capacitance (NLC) and ATP-evoked responses were also recorded by patch clamp recording. Prestin, P2X2 WT and deafness mutant p.V60L (c. 178G -> T) and p.G353R (c. 1057G -> C) clones were further used and transfected into HEK 293 cells to assess the effect of P2X2 deafness mutations on prestin activity and ATP responses.

Results

In the absence of noise stress, P2X2 KO mice have normal hearing. Under general environmental noise, P2X2 KO mice had moderate hearing loss in middle and high frequencies. DPOAEs in P2X2 KO mice were reduced in low-frequency region (< 8kHz) but paradoxically increased in middle and high frequency regions (>16 kHz); the increase was significant in middle and low intensities (<50 dB SPL). OHCs in P2X2 KO mice retained a normal bell-shape of NLC but lacked the response to ATP. In transfected cells, prestin itself had no response to ATP stimulation but ATP could mediate Prestin activity in the co-transfection with WT P2X2 receptors as that in native OHCs. However, co-transfection with P2X2 deafness mutation V60L shifted prestin activity to the left in the hyperpolarized direction and eliminated the response to ATP stimulation.

Conclusions

P2X2 deficiency can compromise OHC electromotility regulation, which may result in over-activity of active cochlear mechanics under environmental noise stress to enhance noise-induced impairments leading to hearing loss. P2X2 V60L dominant deafness mutation diminishes ATP responses and has trans-dominant negative effect on prestin activity.

PD-119

Functional Analysis of Clarin-1 using a Transgenic Mouse Model of Hearing Loss in Usher Syndrome III and Preservation of Hearing in that Model by AAV-mediated Gene Therapy.

Ruishuang Geng[1]; Akil Omar[2]; Suhasini Gopal[1]; Daniel Chen[1]; Astra Dinculescu[3]; David Furness[5]; William Hauswirth[3]; Lawrence Lustig[4]; **Kumar Alagramam[1]**

[1]Case Western Reserve University, Cleveland, OH; [2]University of California, San Francisco, CA; [3]University of Florida, Gainesville, FL; [4]University of California, San Francisco, Columbia University, NY; [5]Keele University, Keele, UK

Background

Usher syndrome III (USHIII) is an autosomal recessive disorder caused by mutations in the human clarin-1 gene, characterized by progressive loss of hearing and vision. Previously, we showed that, in the mouse, 1) clarin-1 is expressed during pre- and postnatal periods, and its expression is restricted to ganglion and hair cells of the inner ear, 2) clarin-1 mutant mice show hair cell defects as early as postnatal (P) day two, and 3) clarin-1 mutants are deaf by P25. In this project, we tried to answer the following questions: Is the expression of clarin-1 in spiral ganglion and hair cells necessary for hearing? Is the ear dependent on postnatal expression of clarin-1? Can we develop a mouse model to mirror the progressive hearing loss phenotype observed in USHIII patients? If so, can we preserve hearing in that model by viral vector-mediated gene therapy? Answers to these questions will help us understand the role of clarin-1 in the ear and develop therapies for USHIII patients.

Method

A transgenic line, termed TgAC1, was generated to limit expression of clarin-1 to hair cells during embryonic stages and few days after birth. We then generated mice carrying TgAC1 in the clarin-1 knockout (KO) background, termed 'KO-TgAC1'. Hearing and hair cell morphology were evaluated in KO-TgAC1 mice at various time points. In separate experiments, adeno-associated viral vectors (AAV) type 2 or 8 carrying mouse clarin-1 cDNA were delivered to cochlea of KO-TgAC1 and control mice at P1-3 to prevent onset of hearing loss. Hearing and hair cell morphology were evaluated at various time points.

Results

KO-TgAC1 mice displayed wild-type hearing function at P21-P25. However, longitudinal evaluation (P22 to P100) showed progressive loss of function, starting around P30 and most KO-TgAC1 mice were deaf by P90. At a young age (<P20), hair cell bundle structure from the KO-TgAC1 mice is comparable to wild-type hair cells. The hair bundles begin to show signs of degeneration starting around P25, consistent with the phenotype observed in KO-TgAC1 mice. Lastly, cochlear delivery of AAV2 or 8-clarin-1 showed preservation of hearing and hair bundle structure at P90 and beyond in a majority of the treated KO-TgAC1 mice.

Conclusion
Postnatal expression of clarin-1 in hair cells is necessary for maintenance of hair bundle structure and hearing in the adult mouse. In addition, successful preservation of hearing in an USHIII-mouse model of hearing loss can be achieved using AAV-mediated gene therapy.

PD-120

Passive Nature of Mammalian Hair Bundle Adaptation

Kuni Iwasa[1]; Anthony Ricci[2]
[1]NIH; [2]Stanford University

It has been widely believed that hair bundles are all alike and that every phenomenon identified in one vertebrate hair bundle is shared with hair bundles of all other vertebrate hair cells, including mammalian, avian, reptile, and amphibian. This belief was contradicted by the recent finding that Ca influx is not associated with fast adaptation (<~0.1 ms) (Peng et al. Neuron, 2013), which is closer to the time scale of the operating frequency, in sharp contrast with slower Ca-dependent adaptation in hair bundles of frogs and turtles. This observation further suggests that adaptation process in mammalian cochlear hair cells is not based on an active process in this time scale because Ca signaling is usually indispensable for activities of myosins. Instead, it is consistent with viscoelastic relaxation, a mechanical energy-dissipating process. If that is the case, hair bundles cannot function as an amplifier in mammalian hearing. Here we examine whether or not viscoelasticity is consistent with the experimental data of Kennedy et al. (Nature, 2005), which appear the most suggestive of active process, showing negative stiffness and negative force. We found that negative stiffness can be produced by introducing either a nonlinear dashpot into a Maxwell model, in which a dashpot and a spring are connected in series, or a nonlinear spring into a Kelvin-Voigt model of viscoelasticity, where the connection is in parallel. Negative force can be explained by a combination of resting stress and a reduction in the hair bundle stiffness by the stimuli. Thus we do not need an active process for explanation. We also observe that the absence of a second messenger is advantageous for producing fast responses. For example, to be compatible with the mammalian auditory frequencies, Ca diffusion imposes a rigid constraint on hair bundle organization. These examinations suggest that the mammalian ear is specifically adapted for high frequency hearing with second messenger-free adaptation and prestin-based piezoelectricity in the cell body of outer hair cells for amplification.

PD-121

Whirlin Different Regions have Unique Functions in the Inner Ear and Retina

Pranav Mathur; Junhuang Zou; Tihua Zheng; Ali Almishaal; Deepti Vashist; Yong Wang; Albert Park; Jun Yang
University of Utah

Background
Mutations in different regions of *WHRN* gene cause either Usher syndrome or non-syndromic recessive deafness. The molecular basis underlying this phenomenon remains unknown.

Methods
Whrn$^{neo/neo}$ and *Whrn*$^{wi/wi}$ mice were used, which harbor a mutation in the *Whrn* 5'- and 3'-region, respectively. ABR, DPOAE and rotarod tests were performed to assess moue hearing and vestibular functions. Scanning electron microscopy and confocal scanning laser microscopy were conducted to examine hair bundle morphology. RT-PCR, immunoblotting and immunostaining were utilized to study *Whrn* expression and its protein localization.

Results
In *Whrn*$^{wi/wi}$ mice, a truncated *Whrn* transcript was found, which could be translated into a protein fragment with N-terminal two PDZ domains and save the retina from degeneration. *Whrn*$^{wi/wi}$ mice had more severe hearing and vestibular dysfunctions than *Whrn*$^{neo/neo}$ mice. In cochlear hair cells, *Whrn*$^{wi/wi}$ mice had disorganized and shortened stereocilia, while *Whrn*$^{neo/neo}$ mice had only disorganized stereocilia. In vestibular hair cells, *Whrn*$^{neo/neo}$ stereocilia were as short as *Whrn*$^{wi/wi}$ stereocilia during postnatal development, but grew longer in adult. In the *Whrn*$^{neo/neo}$ inner ear, a C-terminal short WHRN protein fragment/isoform (C-WHRN) was found at the stereociliary tip.

Conclusions
N-terminal two PDZ domain region of full-length (FL) WHRN is sufficient for retinal survival. In the inner ear, the N-terminal region of FL-WHRN is essential for stereociliary organization, whereas the FL-WHRN C-terminal region and C-WHRN are crucial for stereocilia elongation. Therefore, disruption in different WHRN regions caused by *WHRN* mutations is probably the reason underlying different disease manifestation.

PD-122

Effects on the Different Types of Sudden Hearing Loss in 897 Chinese Patients: Based on the Data of Randomized Trial Controlled Multi-Center Study in 33 Clinics in China

Li-sheng Yu[1]; Ruiming Xia[2]; Jie Chen[2]; Dong-yi Han[3]; Wei-yan Yang[3]; **Shi-ming Yang[3]**
[1]People's Hospital of Peking University.; [2]Department of Otorhinolaryngology, People's Hospital of Peking University; [3]Department of Otorhinolaryngology Head and Neck Surgery, Chinese PLA Medical School, Chinese PLA General Hospital, Beijing 100853, China; Chinese sudden hearing loss multi-center clinical study group, Chinese Assocaition of Otorhinolaryngology Head and Neck Surgery, Chinese Medcal Association, China

To investigate the effects on the different types of sudden hearing loss.

We used the standardized clinical research methods with unified design and unified program in the prospective clinical multi-center study. Collect the sudden deafness patients between 18 to 65 years old, the course in less than two weeks, and without any medical treatments, then divided into four

types according to the hearing curve: A, type of acute sensorineural hearing loss in low tone frequencies; B, type of acute sensorineural hearing loss in high tone frequencies; C, type of acute sensorineural hearing loss in all frequencies; D, type of total deafness. Each type had four different treatment programs, based on the unified design randomized table; randomly select a program for treatment.

Tally, 897 cases with single side sudden deafness were collected in the study by 33 hospital in China during August 2007 to October 2011, including male for 432 cases (48.20%), while female 465 cases (51.80%). The average age was 41.08±12.73 years old. Left ear 485 cases (54.07%), right ear 412 cases(45.93%). By classification of audiogram, 897 cases including 174 cases with the type in low tone frequencies(19.40%); 123 cases with the type in high tone frequencies (13.71%); 341 cases with the type in all frequencies(38.02%); 259 cases with the type of total deafness (28.87%). The curative effects of different types were showed, the type in low tone frequencies had the highest rate of 89.66%, the type in all frequencies was 82.11%; the type of total deafness was 70.27%; the type in high tone frequencies had the lowest rate of 66.67%. It had significant difference of the effective rate between different types ($\chi 2=211.94$, P=0.000). The curative results of the 897 cases was that, 332 cases were recovery (37.01%), 205 cases were excellent better (22.85%), 163 cases were better (18.17%), however 197 cases.

Different type of the hearing curve of sudden deafness had different curing effect, it indicating that different type should get different treatments. It's important that sudden deafness should be cured according to the type of the hearing curve. The type in low tone frequencies had the best curative effect; the type in all frequencies took the second phase. It was not good of the curative effect of the type in high tone frequencies and the total deafness type.

PD-123

The Vestibular Implant: Vestibulo-Ocular-Reflex Characteristics when combining VI-input with residual vestibular function in humans

Raymond Berg[1]; **Raymond van de Berg**[1]; Nils Guinand[2]; Herman Kingma[1]; Jean-Philippe Guyot[2]; Robert Stokroos[1]; Angelica Perez-Fornos[1]

[1]Maastricht University Medical Center; [2]Geneva University Hospital

Introduction

Patients with bilateral vestibular hypofunction (BVH) can still have some residual vestibular function. This study investigated the interaction between residual vestibular function and VI-input, when both inputs were combined.

Methods

Four vestibular electrodes in 3 BVH-patients with a modified cochlear implant were selected. Electrodes with different electrically evoked vestibulo-ocular reflex (eVOR) alignments were tested: 2 electrodes with a near horizontal alignment and 2 electrodes with a relative cross-axis alignment with respect to the horizontal axis. Four conditions were tested at 1Hz using 60-cycle trials of sinusoidal electrical stimulation, 60-cycle trials of whole-body rotations in a rotatory chair, or both combined. Residual vestibular function and vestibular implant (VI) input were separately measured first (condition 1 and 2 respectively) and then combined in conditions where both inputs would hypothetically collaborate (condition 3) and counteract (condition 4) in case of a horizontally aligned eVOR.

Results

Three types of interaction between residual function and VI-input were found for total peak eye velocity (PEV): 1. VI-input was significantly the most dominant factor for PEV (3 cases); 2. Residual vestibular function was significantly the most dominant factor for PEV (1 case); 3. VI-input and residual function cooperated together without one input significantly dominating the other (4 cases). Regarding effects of vector-alignment, angle values of condition 3 and 4 were significantly different from condition 1 and 2 in all sessions, implying a combined interaction between both inputs. When vectors of residual vestibular function and VI-input conflicted, the resulting vector was in the direction of the strongest stimulus in all cases. No cross-axis adaption was observed in the acute phase of stimulation. Linear vector summation was only present in 3 out of 8 sessions for (e)VOR-vector alignment, but never for PEV. Phase could be significantly improved in the horizontally aligned electrodes.

Conclusion

In the acute phase of stimulation, the combination of residual vestibular function and VI-input elicits an interaction between both inputs in which they contribute differently to the resulting (e)VOR-characteristics. Probably influenced by the relative difference in force of both inputs, one input significantly dominates the other or both inputs interact significantly, to create a combined (e)VOR. Our data also suggest that the VI could potentially serve as a vestibular pacemaker in case of fluctuating residual vestibular function. The results in this study present again more arguments for feasibility of a VI, providing a foundation for clinical use in the future.

PD-124

Direct Acoustic Cochlear Stimulation for Therapy of Severe to Profound Mixed Hearing Loss: Codacs Direct Acoustic Cochlear Implant System

Thomas Lenarz; Hannes Maier; Eugen Kludt; Burkhard Schwab

Hannover Medical School

Objective

Implantable hearing aids have become a valid option for the therapy of various forms of hearing loss. The Codacs Direct Acoustic Cochlear Implant System is the first vibratory implant available for patients with severe to profound mixed hearing loss (MHL). By directly coupling sound energy into the perilymph, a very high maximum power output (MPO) is achieved over a broad frequency range. Via a conventional stapedotomy, the vibratory energy of the electromagnetic ac-

tuator is transferred directly to the perilymph through the oval window.

Patients And Methods
This article describes the technical principle, basic surgical aspects and audiological outcomes of two clinical studies. Additional coupling procedures and extensions to the spectrum of indications are also discussed. Surgically, the two-component system can either be implanted via a purely transmastoid approach with posterior tympanotomy, or additionally via transmeatal access to the stapes footplate. Pre- and postoperative audiological results of patients wearing conventional hearing aids and with severe to profound MHL, who were implanted with the Codacs system at the Medical University Hannover, were compared.

Results
Significant improvements over conventional hearing aids could be achieved with initial bone conduction thresholds between 44 and 63 dB HL (O 54 dB HL) and an air-bone gap between 19 and 51 dB HL (O 34 dB HL) in patients with MHL caused by advanced otosclerosis or tympanosclerosis and an intact posterior wall of the auditory canal. The mean functional gain was 50 +/- 9 dB (0.5 - 4 kHz) and the monosyllabic word score was 85 % at 65 dB presentation level compared to conventional hearing aids with 25 %. Speech intelligibility in noise (S0N0) improved by 7.1 to O 0.3 dB SNR with Codacs. The mean bone conduction threshold remained unchanged or showed a minimal increase in the low-frequency range.

Conclusion
The CODACS system provides an effective new treatment for patients with severe to profound MHL for the first time.

PD-125

Musician Effect on Speech and Music Perception in Normal Hearing Children with Cochlear Implant Simulations– Preliminary Results

Rolien Free; Like Schepel; Deniz Baskent
University of Groningen, University Medical Center Groninginger

Introduction
Normal hearing (NH) musician children seem to have advantages over NH non-musician children regarding speech and music perception. Due to musical experience, NH musician children are able to hear more subtle pitch cues in both speech and music, and they have better rhythm perception. For children with a cochlear implant (CI), music perception and understanding speech in noisy environments is difficult. Musical experience might help them develop the advantages that NH musician children have. In this study, we test NH musician and non-musician children with CI simulated tests related to speech and music perception, to explore if the musician effect could potentially help children with a CI. We expect that the results in children may even be more robust in comparison to adults because of the strong development of the brain when children start musical training around the age of 7 or younger.

Methods
Musician and non-musician children, age 11 to 13 years, are recruited. Four speech and music-related tests are used; identification of words and sentences (in different noise conditions, including speech on speech), emotions, and melodic contours, with normal acoustic and with CI simulated stimuli. In addition to the behavioural tests, participants are also asked to fill in a questionnaire.

Results
The preliminary data of 8 participants, 4 musicians and 4 non-musicians, showed that there might be a positive effect of musical experience on speech and music perception in children; musician children performed better than non-musicians in identification of words and melodies in unprocessed conditions, and in all four tests in CI-simulated conditions. However, the group difference in the sentence identification test was small overall.

Conclusion
While data collection has not been finalized yet, the preliminary data indicate a positive effect of musical experience. The effects observed in the word identification test seem to be stronger than in adults, as was reported in a similar study by Fuller et al (2014, Frontiers in Neuroscience). This indicates that in children the transfer from musical experience to speech comprehension could be more robust. Hence, musical training may be beneficial for identification of speech in noise, melodies and emotions in pediatric CI users. If more data support such enhancements, this may lead to the recommendation of implementing musical training for the rehabilitation of pediatric CI users.

PD-126

Improvement in Balance with Hearing Amplification

Timothy Hullar; Adham Karim; Kavelin Rumalla
Washington University in St. Louis

Falls are the leading cause of accidental deaths in older Americans older than 65. There is a correlation between hearing loss and the risk of falling among older people, but this relationship is not understood. One possibility is that the correlation reflects global functional loss in the entire labyrinth. Another possibility is that the lack of auditory input leads to imbalance through loss of available external “auditory landmarks” normally used to maintain equilibrium. The vestibular, proprioceptive, and visual systems are known to contribute to postural stability, but the contribution of audition to maintaining balance has not yet been determined.

Balance was assessed using the Romberg on foam test and the tandem stance test in a group of experienced hearing aid users greater than 65 years old. Patients heard a point-source broadband white-noise sound (0-4 kHz) in both unaided and aided conditions in the dark. Postural stability was significantly better in the aided than unaided condition ($p = 0.005$ for both tests). No statistically significant relationship between improvement in postural stability and hearing was identified.

Hearing aids are a novel treatment modality for imbalance in older adults with hearing loss and suggest that wearing hearing aids or other assistive devices such as cochlear implants may offer a significant public-health benefit for avoiding falls in this population.

PD-127

Exploring Cerebral Hemodynamics with Transcranial Doppler during Computerized Dynamic Posturography

Julie Honaker[1]; Jessie Patterson[2]; Max Twedt[2]; Edward Truemper[3]; Gregory Bashford[2]
[1]University of Nebraska-Lincoln; [2]University of Nebraska-Lincoln, Lincoln, NE; [3]Children's Hospital & Medical Center, Omaha, NE

Transcranial Doppler (TCD) is an ultrasonic blood flow measurement technique that measures continuous cerebral blood flow velocities. This non-invasive technique is most commonly performed through the transtemporal window to localize middle and posterior cerebral arteries. Recent evidence suggests that changes in cerebral hemodynamics occur during clinical vestibular measures, with and without fixation. This technique has not been applied to postural control evaluation, given previous time limitations with TCD application to monitor changes in cerebral hemodynamics. This research is the first step exploring the feasibility of combining TCD and dynamic balance conditions to understand changes in cerebral hemodynamics in association with balance perturbation responses. We collected combined Doppler and Computerized Dynamic Posturography data (CDP: Sensory Organization Test, Motor Control Test, and Adaptation Test) from 25 healthy adults (mean age = 22.9, range = 20-32 years). Of these individuals, 7 wore a TCD fixation device with transducer focused on the middle cerebral artery (MCA), 5 with TCD transducer focused on the posterior cerebral artery (PCA), 5 with TCD transducer focused on the basilar artery (BA), and 8 with combined MCA and PCA transducers positioned on contralateral sides. Three hemodynamic parameters (peak systolic velocity, end diastolic velocity, and mean velocity) and two cerebral blood flow indices, (resistance index (RI) and pulsatility index (PI), were obtained during all CDP conditions.

Our results show that there are differential effects in cerebral hemodynamics during testing that induces motor balance challenges compared to vestibular balance challenges in both the MCA and PCA. In the adaptation test, the resistivity index decreased in the MCA by 5% and increased in the PCA by 2% ($p = 0.05$). No significant changes have been found in the BA. The patterns of flow responses during different challenges suggest that the mechanisms that govern alterations in cerebral blood flow to maintain balance are complex. The differential changes in cerebral hemodynamics may be a useful adjunct to current balance testing procedures to determine if alterations in cerebral blood flow autoregulation contribute to the pathophysiology of balance disorders.

PD-128

Non-steroidal Anti-inflammatory Medications are Cytostatic Against Human Vestibular

Sonam Dilwali; Shyan-Yuan Kao; Konstantina Stankovic
Massachusetts Eye & Ear Infirmary

Introduction

Vestibular schwannomas (VSs) are the most common tumors of the cerebellopontine angle. Significant clinical need exists for pharmacotherapies against VSs. Motivated by previous findings that immunhistochemical expression of cyclooxygenase 2 (COX-2) correlates with VS growth rate, we investigated the role of COX-2 in VSs and tested COX-2 inhibiting salicylates against VSs.

Methods

Freshly-harvested human specimens of sporadic VSs and great auricular nerves (GANs) were collected from indicated surgeries. The study protocols were approved by Human Studies Committee of the Massachusetts Eye and Ear and Massachusetts General Hospital. The specimens were divided for protein, RNA, histologic or culture work. Expression and activity of COX-2 was measured in VSs versus GANs using qPCR, immunohistochemistry of tissue sections, western blot analysis and measurement of prostaglandin E2 in tissue lysates. Because COX-2 inhibiting salicylates, such as aspirin, are well-tolerated and frequently clinically used, we assessed their repurposing for VS. Changes in proliferation and cell death were assessed in primary VS and Schwann cell cultures treated with aspirin, sodium salicylate (NaSal) or 5-aminosalicylic acid (5-ASA).

Results

Immunohistochemistry and Western blot results showed that COX-2 was aberrantly expressed in human VS and primary human VS cells in comparison to control human nerve specimens and primary Schwann cells (SCs), respectively. Levels of prostaglandin E2, the downstream enzymatic product of COX-2, correlated with primary VS culture proliferation rate. Salicylates significantly reduced proliferation in primary human VS cultures; 5 mM aspirin, 1 mM NaSal and 5 mM 5-ASA reduced average proliferation to 19%, 18% and 55% of non-treated cells, respectively. These drugs did not increase VS cell death nor affect healthy SCs. The cytostatic effect of aspirin *in vitro* was in concurrence with our previous clinical finding that VS patients taking aspirin demonstrate reduced tumor growth.

Conclusions

Overall, this work suggests that COX-2 is a key modulator in VS cell proliferation and survival, and highlights salicylates as promising pharmacotherapies against VS.

PD-129

Walking with the Geneva-Maastricht Vestibular Implant: Normalization of Dynamic Visual Acuity in Patients with a Bilateral Vestibular Loss.

Nils Guinand[1]; Raymond van de Berg[2]; Marco Pelizzone[1]; Robert Stokroos[2]; Herman Kingma[2]; Jean-Philippe Guyot[1]; Angelica Perez Fornos[1]

[1]University Hospitals Geneva; [2]Maastricht University Medical Centre

Introduction

Patients with a bilateral vestibular loss (BVL) lack a properly functioning vestibulo-ocular reflex (VOR), which impairs gaze stabilization abilities. This results in an abnormal loss of visual acuity (VA) in dynamic situations. For instance, while walking, BVL patients' ability to read signs or recognize faces is severely limited. Nowadays it is still not possible to treat efficiently this handicapping condition. Promisingly, our group has previously demonstrated that the VOR can be artificially restored with the Geneva-Maastricht Vestibular Implant (GM-VI). This study was designed to investigate whether this restoration results in an improvement of dynamic VA.

Methods

Five BVL patients, unilaterally or bilaterally deaf, were fitted with the Geneva-Maastricht vestibular implant (GM-VI). This device consists in a modified cochlear implant (MED-EL, Innsbruck, Austria) providing extracochlear electrodes for "vestibular" stimulation. Motion sensors fixed to the patient's head, controlled the amplitude of electrical stimulation delivered through "vestibular" electrode to the posterior or to the superior ampullary nerve. VA was determined using Sloan letters displayed on a computer screen, in four conditions: (1) with the patient standing still without moving (static), (2) while the patient was walking on a treadmill at constant speed with the GM-VI turned off (system OFF), (3) while the patient was walking on a treadmill at constant speed with the GM-VI turned on providing coherent motion information (system ONmotion), and (4) while the patient was walking on a treadmill at constant speed with the GM-VI turned on but providing aberrant motion information (i.e., electrical noise; system ONnoise). VA values in each condition were normalized to those obtained in the static condition. A one-way repeated measures analysis of variance (ANOVA) was conducted to compare VA differences across conditions.

Results

Individual and group results are presented in Figure 1. The ANOVA analysis revealed a statistically significant difference between conditions ($F(3,12) = 30.04$, $p<0.0005$). Post hoc tests using the Bonferroni correction revealed a significant decrease ($p<0.05$) in VA in the system OFF and in the system ON_{noise} conditions when compared to the static and the system ON_{motion} conditions (asterisks in Fig. 1).

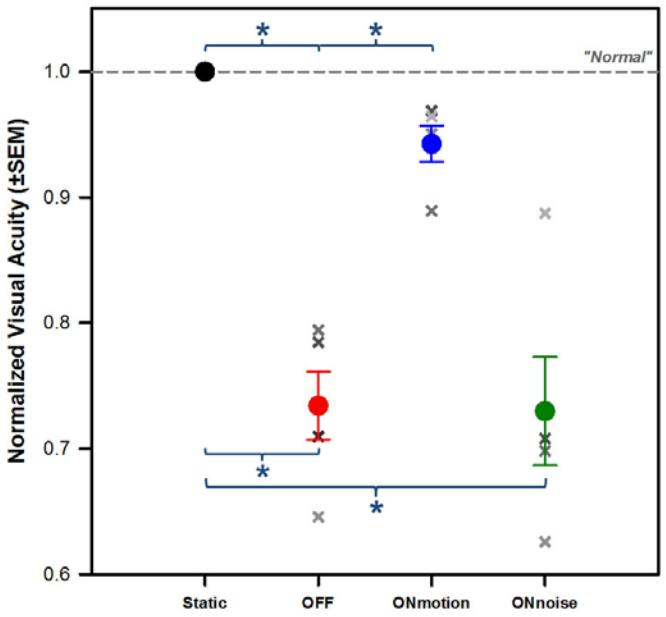

Figure 1: Comparison of VA results in four conditions: static (subjects standing still), system OFF (subjects walking on a treadmill at fixed velocity and with the GM-VI turned off), system ON_{motion} (subjects walking on a treadmill at a fixed velocity while motion information is used to modulate electrical currents delivered via the GM-VI) and system ON_{noise} (subjects walking on a treadmill at a fixed velocity while "aberrant" information is used to modulate the electrical currents delivered via the GM-VI). Individual results are presented as gray crosses. Filled circles represent mean values (± standard error of the mean, SEM) in each condition. Statistically significant differences in post-hoc pairwise comparisons are marked as asterisks.

Conclusions

In BVL patients, motion-modulated electrical stimulation of the vestibular nerve allows a significant improvement of the dynamic visual acuity while walking. This demonstrates that the GM-VI can significantly improve gaze stabilization by artificially restoring the vestibular function. For the first time it offers a promising therapeutic alternative to patients with a BVL.

PS-657

Development of Auditory Sensitivity in Barn Owls

Caitlin Baxter; **Alayna Hendrix**; Beth Brittan-Powell; Catherine Carr

University of Maryland

The auditory brainstem response (ABR) was used to track the development of auditory sensitivity in barn owl chicks from P2 to 10 weeks of age. Responses were first obtained from P5 chicks at high stimulation levels at frequencies at or below 2 kHz, showing that barn owls do not hear well at hatch, and consistent with cochlear microphonic and compound action potential measures (Koppl and Nickel, 2007). Over the next 2 months, ABR thresholds improved markedly, and responses were obtained for almost all test frequencies throughout the

range of hearing by 4 weeks (between 500 Hz and 8 kHz). By 2 weeks post-hatch, birds' best sensitivity shifted from 2 to 4 kHz, and the morphology of the ABR became similar to that of adult owls. Responses to the highest frequencies, 10-12 kHz, appeared around 5-6 weeks of age, at about the same time as ear canal and ruff feather growth stabilized. ABR audiogram development was consistent with previous cochlear microphonic and compound action potential measurements (Koppl and Nickel, 2007).

PS-658

Early Postnatal Noise Exposure Affects The Pattern Of Age-Related Hearing Loss In Rats.

Natalia Rybalko[1]; **Tetyana Chumak[2]**; Josef Syka[2]
[1]The Institute of Experimental Medicine, Academy of Sciences of the Czech Republic; [2]Institute of Experimental Medicine

Noise exposure during the critical period of development results in adult rats in changes of the function of the auditory system. In the present study we assessed the impact of early postnatal acoustic trauma on the state of the rat auditory system during the lifespan.

Long Evans rats were exposed to 125 dB SPL broad band noise (BBN) either for 8 min (BBN8) or 25 min (BBN25) on the 14th postnatal day, i.e. when the onset of hearing occurs. Post exposure changes in the auditory system were assessed starting from the day after exposure up to 2.5 years of age using electrophysiological, behavioral and histological methods. Hearing sensitivity (the thresholds of auditory brainstem responses, ABRs) and behavior in response to loud sounds (amplitude-intensity functions of the acoustic startle response, ASR) were monitored to assess the state of the hearing function. Information about the state of the inner ear was obtained from cochlear whole mount preparation, analyzing number of outer hair cells (OHC), inner hair cells (IHC) and IHC ribbon synapses. The data obtained from exposed rats was compared with age-matched control animals.

Both noise exposed groups of animals showed ABR threshold elevation after exposure, although, for BBN8 animals the threshold shift was transient while changes in BBN25 rats were permanent. Major recovery of ABR thresholds occurred during the first two weeks after exposure. In adult (2 month old) BBN8 rats hearing thresholds were similar to controls. In agreement with this the number of ribbon synapses in BBN8 animals did not differ significantly from the control levels in most frequencies, whereas in BBN25 rats we observed relatively high IHCs ribbon loss. In both exposed groups, noise exposure led to hyper-reactivity to loud acoustic stimulation that was manifested by increased ASR amplitude compared to control rats. The enhancement of ASR amplitude was transient and practically disappeared by the second week after exposure. In adult noise exposed rats the startle reactivity was weaker than in control animals. All groups of animals showed an age-related decline in auditory function, though to a different extent. In spite of the signs of hearing recovery after noise exposure, BBN8 rats showed faster age-related deterioration of electrophysiological and histological parameters than controls.

The results suggest that the effects of early moderate (BBN8) noise trauma, although leading to recovery of hearing thresholds, leaves the auditory system more susceptible to age-related deterioration.

PS-659

A Comparison of the Binaural Difference Potential of the Auditory Brainstem Response in the Young and Old Mongolian Gerbil (Meriones unguiculatus)

Genevieve Laumen[1]; Daniel Tollin[2]; Georg Klump[3]
[1]Oldenburg University, Germany; [2]Department of Physiology and Biophysics, University of Colorado School of Medicine; [3]Cluster of Excellence Hearing4all, Animal Physiology and Behavior Group, Department for Neuroscience, School of Medicine and Health Sciences, Oldenburg University

Background

The auditory brainstem response (ABR) is a clinical non-invasive tool for the investigation of hearing abilities (e.g. auditory thresholds) and the determination of hearing loss. The binaural difference potential (BDP) of the ABR, yields information about binaural interaction within the brainstem. To study the influence of age on physiological mechanisms underlying binaural hearing, BDPs of young and old gerbils were measured for different interaural times (ITD) and level differences (ILD).

Methods

ABRs and associated BDPs of ketamine-anesthetized young (<1 year;n=10) and old (>3 years;n=9) gerbils were measured at ~30dB above threshold using flat frequency spectrum (1-14 kHz) click stimuli presented monaurally and binaurally with ITDs ranging from ±2000 µs and ILDs ranging from ±30 dB. Needle electrodes were placed at vertex and neck. The amplitudes and latencies of DN1, and the corresponding binaurally-evoked ABR wave IV were determined.

Results

The so-called DN1 peak of the BDP correlates in its latency with wave IV of the ABR indicates an inhibitory-reduction in the binaural ABR amplitude. For both young and old gerbils, an increase in latency with increasing ITDs was observed for both the DN1 and binaural wave IV, while different ILDs had no effect on the latency of these responses. With increasing ITDs the amplitude of the DN1 and binaural wave IV decreased in both age groups. However, older animals showed overall lower DN1 amplitudes than younger animals. Moreover, the amplitude of the DN1 decreased with increasing ILDs in both age groups with lower amplitudes in old gerbils. In contrast the amplitude of the binaural wave IV increased with increasing ILDs in the young group whereas ILD had only little effect on the binaural wave IV for old individuals.

Conclusion

The binaurally-evoked ABR was smaller in amplitude than the sum of monaurally-evoked ABRs. Therefore, the results suggest that the BDP arises from IE-type neurons in the lateral superior olive (LSO) or dorsal nucleus of the lateral lemnis-

cus (DNLL). The decreased amplitude and longer latency of the DN1 component might be due to shifts in the timing of excitatory/inhibitory inputs from both sites and delays of these inputs, respectively. The reduction in the DN1 amplitude for old individuals might be explained by a reduced inhibitory input into the LSO. This could originate from a decrease in inhibitory neurotransmitter and/or response synchrony in older individuals.

PS-660

Effects of Neuropathy on Auditory Brainstem Response Wave-V latency in Noise

Golbarg Mehraei[1]; Hannah Goldberg[2]; Ann Hickox[3]; M . Charles Liberman[4]; Barbara Shinn-Cunningham[2]
[1]Massachusetts Institute of Technology and Harvard University; [2]Boston University; [3]Purdue University; [4]Massachusetts Eye and Ear Infirmary and Harvard Medical School

Introduction

Listeners with normal hearing thresholds (NHT) who report difficulty communicating in noisy environments have long been assumed to suffer from central rather than cochlear deficits. However, animal studies show that noise-induced loss of auditory nerve fibers (ANFs) reduces auditory brainstem responses (ABRs) without affecting hearing thresholds. In addition, human studies suggest that reduced ABRs are correlated with perceptual deficits in NHT listeners. Although noise-induced neuropathy affects the growth of ABR amplitude with level, ABR latencies have not been thoroughly investigated. We have suggested that the change in latency of ABR wave-V with increasing background noise could be a sensitive measure of ANF survival. We showed, in NHT human listeners, that wave-V latency shift correlates with psychophysical performance: listeners with poor sensitivity to envelope interaural timing showed a small latency shift with increasing noise, consistent with neuropathy.

Methods

Here, we measured click- ABR wave-I in quiet at click levels of 60-100 dB pSPL (10 dB step) in NHT listeners. In the same listeners, we obtained masked-ABR wave-V latency changes using click (80 dB pSPL) in broadband noise (42-82 dB SPL). In addition, we analyzed masked-ABRs in CBA/CaJ mice measured using 32kHz tone-bursts against a background broadband noise varying from -5-85 dB SPL. We studied three groups of mice: 1) controls, 2) exposed to octave-band noise (8-16kHz at 94 dB SPL) designed to cause only transient threshold elevation and no ANF loss (non-neuropathic) and 3) exposed to the same noise at 100 dB SPL that causes transient threshold elevation and marked degeneration of ANFs.

Results

Results show a significant correlation between the wave-I amplitude growth in quiet and wave-V latency change with noise level in NHT listeners. In the mice, a significant reduction of wave-IV latency change with noise level is observed in the neuropathic group compared to the control and non-neuropathic animals. This change in wave-IV latency in mice was uncorrelated with distortion product otoacoustic emission thresholds, supporting the idea that wave-IV latency depends on the loss of ANFs rather than changes in cochlear mechanics that can affect ABRs.

Conclusions

These results suggest that measures of how ABR wave-V latency changes in noise may be used as a clinical test to diagnose ANF loss in NHT listeners.

PS-661

Development of a Web-Based System for Analysis of Auditory Brainstem Response (ABR) Data

Samuel Kirkpatrick[1]; David Ryugo[2]; Zenon Chaczko[1]
[1]University of Technology, Sydney; [2]University of New South Wales/Garvan Institute of Medical Research

Background

The auditory brainstem response (ABR) is a widespread, non-invasive measure of hearing status used both in the clinic and in hearing research. ABR recording and analysis techniques vary greatly between research labs, which can pose a problem for testing the validity of assumptions made about hearing status in an experimental setting. ABR data represent a collection of time series which theoretically can be compared and aggregated based on supporting metadata. This project focused on the development of an online ABR analysis tool—'*Open ABR*'—along with a common online data structure to improve the comparability of ABRs between researchers and laboratories. The outcome may reveal subtle anomalies with recordings and lead to new discoveries.

Methods

A web-based system was created to collect ABR data to identify pertinent metadata for developing analysis vectors. The program computes and quantifies waveform features for comparisons across and between experimental animals. The system was initially launched as *Open ABR* and piloted by a single lab. Its usage was monitored over a period of 12 months during which it iteratively evolved with a variety of new functions and features.

Results

Open ABR allows for the collection, independent storage, retrieval, and analysis of ABRs. All ABRs uploaded are coalesced into the common data format and a copy of the original file is always retained. The ABRs are organised by subject but can be blinded to investigators if required. Analysis techniques include visual inspection of the waveform, comparison to other waveforms, automatic determination of hearing thresholds for click and tone responses, graphing of threshold values against subject age, peak mapping, and calculation of latency and amplitude of the peaks. These tools are complemented by a query system that allows for the comparison of results based on metadata; for example, the average N1 peak latency can be examined under different anaesthetic doses and/or different anaesthetics.

Conclusions

Open ABR provides a valuable, standardised waveform analysis tool for researchers who utilise ABRs as a core parameter in their research. Within the field of auditory research, *Open ABR* can provide a quick, concise, and accurate means of analysing new and/or archived data, and finding extra value in it. The system is designed to be extensible and will continue to evolve with new technology and improved tools.

PS-662

Multichannel Recordings of the Human Brainstem Frequency-Following Response: Scalp Topography, Source Generators, And Distinctions from the Transient ABR

Gavin Bidelman

University of Memphis

Objective

Brainstem frequency-following responses (FFRs) probe the neural transcription of speech/music, disorders, and plasticity in subcortical auditory function. Despite clinical/empirical interest, the response's neural basis remains poorly understood. Here, we characterized functional properties of the human FFR (topography, source locations, generation).

Methods

Speech-evoked FFRs were recorded using high-density electrode montages. Source dipole modeling localized response generators. Transient auditory brainstem responses (ABRs), recorded in the same listeners, were used to predict FFRs based on the long-held assumption that the sustained potential reflects a series of overlapping onset responses.

Results

FFRs were maximal at frontocentral scalp locations with oblique sources in the inferior colliclus (IC). Comparisons between derived and actual recordings revealed the FFR is not repeated ABR wavelets. Temporal recordings showed larger and higher frequency amplitudes than vertex sites (Fz, Cz).

Conclusions

FFRs reflect sustained neural activity in the brainstem IC, generated by distinct neurophysiological mechanisms from those producing the ABR. Temporal electrodes reflect FFRs generated more peripherally (auditory nerve) than measurements at frontocentral scalp locations revealing the importance of choice in reference electrode location for FFR interpretation.

Significance

We provide non-invasive evidence that: (i) sources of the human FFR are likely located in the rostral brainstem; (ii) FFRs are functionally distinct from the onset ABR.

PS-663

Musical Training Orchestrates Coordinated Neuroplasticity in Auditory Brainstem and Cortex to Counteract Age-Related Declines in Categorical Speech Perception

Gavin Bidelman[1]; Claude Alain[2]

[1]University of Memphis; [2]Rotman Research Institute

Musicianship in early life is associated with pervasive changes in brain function and enhanced speech-language skills. Whether these neuroplastic benefits extend to older individuals more susceptible to cognitive decline and for whom brain plasticity is weaker, has yet to be established. Here, we show that musical training offsets declines in auditory brain processing that accompanying normal aging, preserving robust speech recognition late into life. We recorded both brainstem and cortical neuroelectric responses in older adults with and without modest musical training as they classified speech sounds along an acoustic-phonetic continuum. Results reveal higher temporal precision in speech-evoked responses at multiple levels of the auditory system in older musicians who were also better at differentiating phonetic categories. Older musicians also showed a closer correspondence between neural activity and perceptual performance. This suggests musicianship strengthens brain-behavior coupling in the aging auditory system. Lastly, "neurometric" functions derived from unsupervised classification of neural activity established that early cortical responses could accurately predict listeners' psychometric speech identification and more critically, that neurometric profiles were organized more categorically in older musicians. We propose that musicianship offsets age-related declines in speech listening by refining the hierarchical interplay between subcortical/cortical auditory brain representations, allowing more behaviorally relevant information carried within the neural code, and supplying more faithful templates to the brain mechanisms subserving phonetic computations. These findings imply that robust neuroplasticity conferred by musical training is not restricted by age and may serve as an effective means to bolster speech listening skills that decline across the lifespan.

PS-664

Rapid FFR: A New Technique to Rapidly Collect the Frequency Following Response

Tim Schoof; Stuart Rosen

University College London

Background

Frequency following responses (FFR) are typically recorded to stimuli with a duration of 40 – 170 ms. Since the acquisition of a robust response requires approximately 3000 repetitions of the stimulus, recording the FFR can take quite some time. A new technique is proposed, the rapid FFR, which can significantly reduce recording times by presenting the stimulus continuously (i.e. without an inter-stimulus-interval) and averaging across a single cycle of the response. In addition, a new set of stimuli is developed which contain spectrotemporal modulations crucial for speech perception.

Methods
First, FFRs were recorded in response to a steady-state harmonic complex using the standard and rapid techniques. The primary aim was to determine whether the rapid FFR is equally sensitive to inter-individual differences as the standard FFR. Subsequently, FFRs were recorded to a new set of stimuli which were based on a steady-state vowel whose properties were modulated at a speech appropriate rate in either fundamental frequency, overall amplitude, or first formant frequency. The possibility of introducing modulations of some combination of 2 or 3 properties and yet analyse their neural representations separately, thus saving measurement time, was also explored. All FFRs were recorded in response to positive and negative polarity stimuli separately.

Results
The data showed that, when responses to the positive and negative polarity steady-state harmonic complexes were added, there was a significant correlation between response measures of the rapid and standard FFRs across listeners. When polarities were subtracted, however, response measures were not significantly correlated. We furthermore expect to find that the rapid technique is well suited to record FFRs to dynamic stimuli with a combination of spectrotemporal modulations crucial for speech perception.

Conclusions
For the steady-state stimulus, recording times were reduced from approximately 2.5 minutes to 35 seconds using the rapid technique. The rapid technique provides a reliable measure in terms of the opposite-polarity added FFR, although cannot currently reliably be used to assess higher frequency spectral components thought to reflect temporal fine structure. For dynamic stimuli, averaging must occur over the period of the modulation. However, eliminating silent intervals in the stimulus presentation still means a much quicker measurement time than using the standard technique.

PS-665

Single-Trial Activity in Inferior Colliculus Reveals a Neural Basis for Human Auditory Processing

Travis White-Schwoch; Trent Nicol; Catherine Warrier; Evan C. Davies; Nina Kraus
Northwestern University

Auditory-evoked potentials are classically defined as the summations of synchronous firing along the auditory neuraxis. Individual differences in neural synchrony, as reflected in the auditory brainstem response to complex sounds (cABR; sometimes referred to as the frequency-following response), have been implicated in human auditory processing. For example, in middle-aged adults with normal audiograms, intertrial phase locking is linked to selective auditory attention abilities. In children, the trial-by-trial consistency of neural responses to speech is systematically correlated to reading skills. However, the local mechanisms underlying this (dys) synchrony are poorly understood. To that end, we undertook a comparative study of auditory subcortical function, contrasting near field multi-unit activity (central nucleus of inferior colliculus, ICc) and far field epidural recordings in guinea pigs to scalp recordings in humans.

Responses were elicited by speech syllables presented in quiet and noise, and identical stimuli were used across species. ICc recordings had sufficient signal-to-noise ratio to analyze single trial activity, allowing for a direct assay of intertrial variation. To evaluate synchronous processing, each trial was correlated against every other trial in a stimulus condition. The timing difference between all possible pairs of trials was also computed. This trial-by-trial timing variation (i.e., jitter) drove neural synchrony—lower intertrial timing jitter was associated with higher intertrial correlations. These correlations were highest for responses to sustained portions of speech, such as vowels, and lowest for transient features, such as onset bursts and consonant transitions. Noise disproportionately degraded intertrial correlations for responses to these transients. These effects were observed across multiple tonotopic sites in ICc. Importantly, this pattern of results was mirrored in simultaneous epidural recordings and in human scalp recordings—in fact, all effects were statistically equivalent across species.

These results demonstrate that robust neural synchrony relies on precise timing in ICc across tonotopic sites. With respect to human auditory perception, these results explain why certain populations (listeners with auditory processing disorder, older adults, etc.) have difficulty understanding acoustic transients in noise. ICc likely has a chief role in this phenomenon, as part of an integrated auditory circuit. The driving mechanism of this poor processing appears to be variability in time of neural coding. Taken together, these results provide a neural basis for individual differences in human auditory processing.

PS-666

Binaural Interaction Component of the Auditory Brainstem Response in Veterans with Type II Diabetes

Laura Coco[1]; Marilyn Gilli[2]; Garnet P. McMillan[2]; Dawn Konrad-Martin[2]
[1]University of Texas, Austin; [2]National Center for Rehabilitative Auditory Research, Portland VA Medical Center, Portland OR

Diabetes Mellitus (DM) is a metabolic disease that can lead to microvascular and neuronal complications like heart disease, stroke and neuropathy. Hearing loss is twice as common in adults with DM versus adults without the disease (Bainbridge et al., 2008), although the effects of DM are not limited to the periphery. Individuals with DM also show prolonged neural conduction times within the brainstem even after controlling for peripheral hearing loss (Diaz de Leon-Morales, 2005; Konrad-Martin et al., 2010). Further, Frisina and colleagues (2006) demonstrated that diabetics performed more poorly understanding speech in noise than individuals without the disease, even in the easier condition of noise spatially separated from speech. This suggests that DM impacts binaural hearing. Since binaural comparisons occur at the level of the brainstem, we investigated the difference between monaural and binaural Auditory Brainstem Responses (ABR) to eval-

uate the effect of DM. By calculating the difference between the sum of the two monaural ABRs and the binaural ABR, we extracted a distinctly binaural potential known as the Binaural Interaction Component (BIC), representative of neural activity underlying central auditory processing of binaural stimuli.

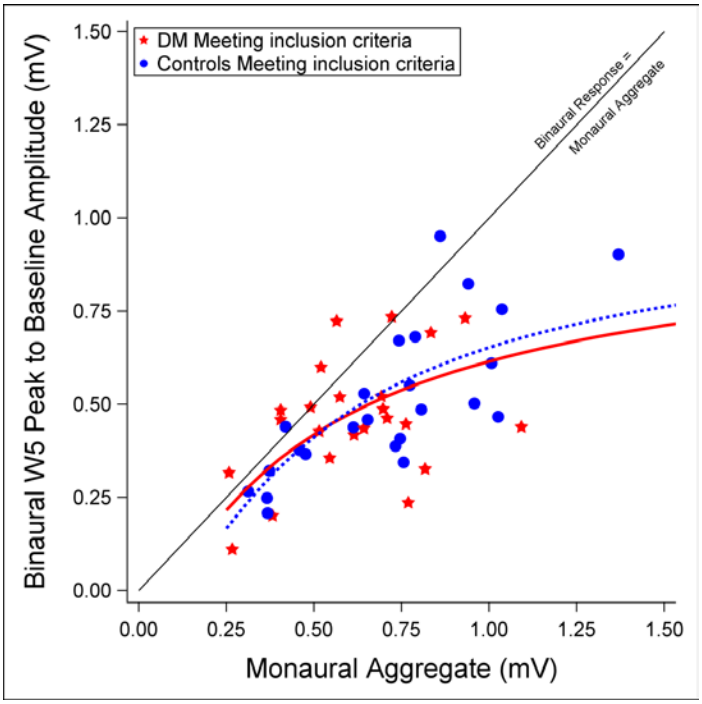

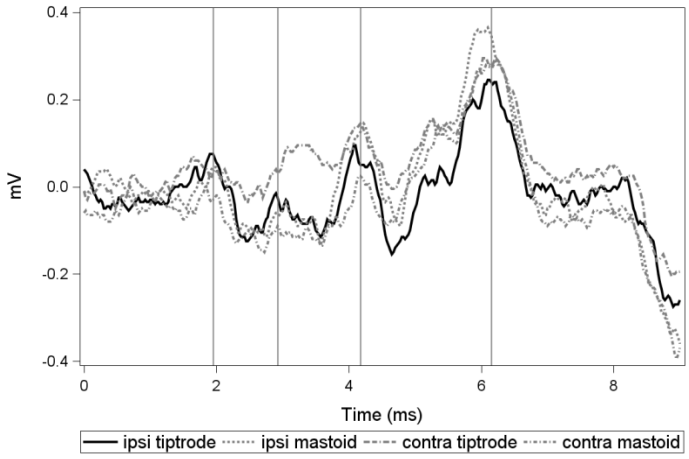

The goal of this research is to evaluate binaural function in the brainstem for Veterans with DM compared with non-diabetic controls. ABR waveforms were obtained from 81 Veterans with DM and no DM based on medical diagnosis, as well as severity and control of the disease. The binaural response was subtracted from the aggregate of the two monaural responses (L + R) from wave V of the ABR to elicit the BIC. We measured the peak amplitude and area under the curve of each monaural, binaural and BIC waveform, and calculated amplitude ratios as BIN/(L+R). A regression model was used to identify group differences in BIC after adjusting for potential confounders of age, hearing, noise exposure history and other factors.

We demonstrated three different ways to measure Binaural Interaction. There was no statistically significant difference in Binaural Interaction between DM and Controls in each model, but trends suggest if more subjects were added, a difference might be apparent among those with poor control of the disease and those without the disease. We demonstrated a curved line is the best fit to describe Binaural Interaction, suggesting the binaural auditory brainstem response depends more heavily on the response of the monaural aggregate than was previously assumed.

PS-667

The Effect of Type 1 Diabetes on the Neural Representation of Temporal Envelope and Temporal Fine Structure.

Arwa AlJasser; Christopher Plack; Kai Uus; Richard Baker
University of Manchester

Diabetes mellitus (DM) is associated with a variety of complications. Neuropathy is one of the more common complications in DM, affecting around 50% of patients. The investigation of the relation between DM and disorders of the auditory system has been going on for over a century, however the association remains controversial. By far the most commonly used techniques when exploring the association between DM and the auditory system are pure tone audiometry (PTA), measurement of otoacoustic emissions and measurement of the auditory brainstem response. Results of all three measures have been inconsistent. Very little attention has been given to neuropathic complications in DM involving the auditory nerve and central neural pathways. These are likely to result in subclinical auditory dysfunction due to temporal processing difficulties leading to perceptual difficulties in challenging acoustic environments despite normal audiometric thresholds. The current study investigated the effect of type 1 DM on the neural representation of temporal envelope and temporal fine structure (TFS) in the electrophysiological frequency-following response (FFR). The FFR, reflecting sustained neural activity in the brainstem synchronized (phase locked) to the stimulus, was measured for 21 young normal-hearing participants, 11 type 1 DM participants and 11 age-sex-and PTA-matched healthy controls. Participants were presented with five amplitude-modulated stimuli. Each stimulus consisted of three simultaneous equal-amplitude pure-tone components. The central component had a frequency of 590 Hz and additional components were positioned either side separated from the central component by 95-135 Hz in 10 Hz increments. In order to enhance the FFR to either the cochlear envelope or TFS, each presentation window contained two stimuli with the onset polarity of the second stimulus in the pair inverted 180 degrees with respect to the onset polarity of the first stimulus. By adding and subtracting responses to the two polarities, an estimate of phase locking to the stimulus envelope and TFS was produced respectively. Signal-to-noise ratios (SNRs) were calculated to estimate the strength of the target frequency representation in the FFR relative to background activity. Results showed significantly lower SNRs calculated for responses to the added and subtracted polarities in the diabetic group compared to the control group. The

results suggest that type1 DM can affect phase locking to the temporal envelope and TFS in diabetic participants in the absence of a reduction in hearing sensitivity measured by PTA.

PS-668

Subcortical Neural Encoding of Speech in SNHL: Attenuation and Distortion Effects

Saradha Ananthakrishnan
Towson University

Speech perception deficits in listeners with sensorineural hearing loss (SNHL) arise from a combination of attenuation (i.e. decreased signal audibility due to elevated audiometric thresholds) and distortion (i.e. abnormal neural representation of the signal) effects. In addition, several recent behavioral studies examining perception of specific speech acoustic cues such as envelope and temporal fine structure (TFS) suggest that diminished TFS perception in SNHL may be attributed to distortion effects such as reduced phase-locking. However, there are few electrophysiological studies examining *neural* correlates of speech perception deficits in SNHL. The Frequency Following Response (FFR), a scalp recorded sustained potential reflecting phase-locked activity from a population of neural elements in the rostral brainstem, offers an objective, non-invasive window to investigate neural encoding of speech in SNHL. Previous FFR experiments (Ananthakrishnan, S., 2013) have established that sub-cortical neural responses are degraded in SNHL for both envelope and TFS encoding; further, such degradation persists at higher stimulus presentation levels in listeners with SNHL. Since restoring signal audibility does not *entirely* restore normal neural encoding in SNHL, these findings suggest that the neural response in SNHL is determined by both attenuation and distortion related effects. However, none of the prior FFR studies examine the specific contributions of attenuation and distortion effects to the degraded neural response. In order to answer this question, we first evaluate brainstem neural phase-locking by recording the FFR in normal hearing (NH) listeners in response to a steady state speech sound presented an intact, quiet condition and a low-pass filtered condition. The low-pass filtered condition reflects elevated audiometric thresholds in high frequency hearing loss; in other words, the effects of attenuation alone. Both stimulus conditions were presented at multiple sound pressure levels in order to observe neural response growth with intensity. Stimulus-response spectral correlations, autocorrelation functions, spectrograms and correlograms were used to describe the FFRs. Next, by comparing the neural response in NH listeners in the quiet and low-pass filter (attenuation only) conditions to previously obtained FFR data in listeners with high frequency SNHL (attenuation and distortion), we are able to tease apart the relative roles of attenuation and distortion in speech encoding in SNHL.

PS-669

Olivocochlear Efferent Effects on Neural Temporal Coding of Sounds in Humans

Hari Bharadwaj[1]; Coralie Pardo[2]; Christopher Shera[3]; Barbara Shinn-Cunningham[1]
[1]Boston University; [2]Amherst College, Amherst; [3]Massachusetts Eye and Ear Infirmary

Introduction

The olivocochlear efferent system is thought to improve hearing in noise by modulating the input to the ascending auditory system. Although much is known from direct neural recordings about how efferents affect afferent responses in small laboratory animals, much less is known in humans. This is particularly true for conditions most relevant to everyday listening. For example, how do efferents affect neural population encoding of broadband sounds at moderate to high sounds levels? Here, using subcortical steady-state responses (SSSRs) and otoacoustic emissions (OAEs), we attempt to bridge this gap.

Methods

In Experiment 1, we measured the effects of a contralateral white noise “elicitor” (75 dB SPL rms) on distortion product (DP) and stimulus frequency (SF) OAEs to establish whether the elicitor is effective in activating the efferent system and to measure the time-course of the effects. In Experiment 2, we measured the effects of the same contralateral noise elicitor on SSSRs to short (300 ms), relatively high level (70 dB SPL) modulated (331 Hz, 80% depth) broadband (2-8 kHz) noise “probes”. The onset time and duration of the elicitor was manipulated relative to the timing of the probe. In addition, several supporting OAE and SSSR measures were included to aid in the interpretation of the results.

Results

Both DPOAE and SFOAE measures revealed efferent effects with overall onset and offset time constants of the order of 150-250 ms. Supporting measurements were used to exclude subjects for whom the dominant effects were attributable to middle-ear muscle reflexes. When the contralateral elicitor began 500 ms before the probe, the SSSR was significantly enhanced, showing an average magnitude increase of about 3.5 dB . In contrast, when the elicitor began simultaneously with the probe, the SSSR magnitude remained unchanged, consistent with the onset time-course of efferent effects on OAEs. When the elictor had an early onset but was turned off just before the probe onset, the efferent effect on the SSSR was smaller, averaging about 2 dB, but still significant, consistent with the finite decay time of the efferent effect.

Conclusions

Our data provide evidence that olivocochlear efferents significantly enhance neural temporal coding under conditions akin to everyday listening in noise.

PS-670

Attention (Still) Does Not Affect the Brainstem EFR

Lenny Varghese; Barbara Shinn-Cunningham
Boston University

Numerous earlier findings indicate that the auditory brainstem response (ABR) and the steady-state brainstem envelope following response (EFR) are insensitive to cognitive demands. However, a few recent and not-so-recent studies have reported that selective auditory attention or modality-specific attention (e.g., paying attention to a visual stimulus while ignoring auditory stimuli) affects these scalp-recorded responses in humans. A closer examination of these findings reveals that the reported effects of attention on these measures across listeners are rather small (in the case of modality-specific attention) or inconsistent (in the case of selective attention). Recent studies presented at ARO (Varghese and Shinn-Cunningham, 2013; Ruggles et al., 2014) have upheld the negative findings for an effect of selective attention on the EFR. Here, we examined whether attending to a different stimulus modality (visual stimuli) affects the brainstem EFR in a consistent way, while also collecting additional data on intramodal selective attentional effects on the EFR.

Electroencephalographic (EEG) activity was recorded at 4 kHz from 13 native English-speaking listeners with normal audiometric thresholds while they heard spoken digits (1-5). The fine time structure of the speech tokens was replaced with a click train (F0 = 113 Hz or 97 Hz). Listeners were presented with a continuous stream of digits either on-screen or over headphones, and were asked to identify the presence of two consecutively increasing digits in the stream presented in the attended modality. There were three conditions of interest: 1) monaurally presented digits while the listener attended to the auditory stimuli (attend auditory); 2) monaurally presented digits while the listener attended to the digits presented on-screen (ignore auditory); and 3) dichotically presented digits (113 Hz in one ear, 97 Hz in the other) while the listener attended to the digits in a single ear (selectively attend auditory). Response strength was quantified using the phase-locking value (PLV) obtained via a frequency-domain PCA (Bharadwaj and Shinn-Cunningham, *Clinical Neurophysiology*, 2014).

Behavioral performance and cortical EEG data recorded simultaneously from these same listeners suggests that listeners were, in fact, modulating attention to perform the task. EFRs showed significant, strong phase-locking at the click train F0 and at the first and second harmonics across listeners. However, we found no consistent effects of either modality-specific or selective auditory attention on EFRs. These findings agree with older literature on the topic, and aid in validating the EFR as a measure of peripheral auditory processing insensitive to ongoing cognitive activity.

PS-671

Generation of the Mismatch Negativity Requires Perceptual Awareness of the Standard Stream

Andrew Dykstra; Alexander Gutschalk
University of Heidelberg

The mismatch negativity, or MMN, is one of the most well-studied components of the auditory evoked response. Elicited by any violation of an otherwise regular stimulus sequence, generation of the MMN has long been thought to be automatic and preattentive, even subconscious. By embedding classical auditory oddball sequences in a multi-tone informational-masking stimulus, we show instead that generation of the MMN occurs only when listeners are perceptually aware of the standard stream prior to the occurrence of the MMN-eliciting deviant stimulus. Deviants occurring during unperceived standard streams failed to elicit an MMN despite clear representation of both standards and deviants in primary auditory cortex. The results strongly suggest that the MMN reflects violations of the regularity of conscious or attended stimulus representations in non-primary auditory cortex.

PS-672

Effect of Noise Type on the Processing of Words: An AERP Study

Katharine Fitzharris[1]; Jeffrey S. Martin[1,2]; Ross Roeser[1,2]
[1]The University of Texas at Dallas, Richardson, TX; [2]Callier Center for Communication Disorders, School of Behavioral and Brain Sciences

Background

The detrimental effects of background noise on communication abilities have been well documented with behavioral measures. Several AERP studies have illustrated the effects of stimulus effects on SIN performance, e.g., signal and masker type, but there are very few studies which have used whole word stimuli, which is the standard in behavioral testing. The aim of this study was to use AERPs to evaluate the interaction between SNR levels (based on behavioral performance) and type of background noise using whole word stimuli in young adults.

Methods

Twenty young adults (10 male) with normal hearing and middle ear function were tested. All participants were right-handed native English speakers and reported no history of middle ear disease, neurological, language, or learning disorders.

AERPs were collected to monosyllabic words in a semantic-categorization oddball paradigm. Words were presented from a single front loudspeaker in quiet, babble, and speech-shaped noise; noise was presented at two SNRs representing behavioral accuracy levels of 60% (poor) and 100% (good). Participants were instructed to press a YES button if they heard a word in a predetermined semantic category and to press a NO button if the word they heard was not in the specified category. Participants were cued as to the semantic category prior to each listening block; the SNRs were mixed within each block.

AERPs were analyzed relative to the N1, P2, and P3 components; amplitude and latency measures were normalized to the same components in the quiet condition. Two-factor repeated measures ANOVAs were used to evaluate differences in mean amplitude and latency between the noise types and SNR. Post hoc paired t-tests were used to examine significant main effects and interactions in the ANOVA.

Results

Preliminary data analysis yielded measurable differences in the latency and amplitude measures in the P3 component across noise types and SNR. The greatest amount of processing (longest latencies; smallest amplitudes) arose in the babble-poor condition whereas the least amount of processing (shortest latencies; largest amplitudes) occurred in the noise-good condition. Differences in N1 and P2 components were measured across SNR, but not noise type. Collection of data is ongoing.

Summary

Preliminary results indicate that even when behavioral accuracy is controlled for across participants, the understanding of speech-masking-word-signals requires more processing resources than noise-masking-word-signals. These results agree with previous research utilizing syllable stimuli.

PS-673

Investigating the Influence of Temporal Context on Vowel Discrimination in Noise: Behaviour and Neural Mechanisms

Stephen Town; Tara Etherington; Katherine Wood; Jennifer Bizley
University College London

Our ability to organize an auditory scene is crucially dependent on the temporal context in which sounds arrive at the ear. For example, onset asynchrony is a potent cue in sound source separation. Here we ask what the role of temporal context is when hearing in noise, and specifically whether synchronous onset of signal and noise impairs sound discrimination and its underlying neural mechanisms.

We trained 14 humans to discriminate artificial vowel sounds in a two-alternative forced choice task. Discrimination was then tested when vowels (40 to 60 dB SPL) were presented in white noise (70 dB SPL) that occurred either continuously in the background, or within a restricted time window occurring only during the vowel presentation. Subjects demonstrated better performance when vowels were presented in continuous rather than temporally restricted noise (mean ± s.e. change in threshold: 3.06 ± 0.89 dB [calculated at 70.7% correct]).

To investigate the neural basis of this behavior, we trained six ferrets in an analogous vowel discrimination paradigm and found again that performance was better in continuous than temporally restricted noise. We then asked whether primary auditory cortex (A1) was necessary for vowel discrimination in noise by reversibly inactivating A1 using cooling. In one ferret, bilateral cooling impaired task performance when vowels were presented in temporally restricted noise but not when vowels were presented in silence. Current experiments are investigating the effects of cooling on vowel discrimination in continuous noise. Two animals tested with unilateral A1 inactivation did not show a performance deficit for vowel discrimination in silence or noise.

We next asked how noise affected the responses of neurons in auditory cortex by bilaterally implanting three animals with microelectrode arrays. We recorded 214 sound-responsive units during task performance with vowels presented alone or in noise. In a preliminary analysis, we identified 131 units that discriminated between vowels during a fixed time window (0 – 350 ms after vowel onset). Of these units, 90 showed responses that were modulated by noise type (One-way ANOVA). On-going analysis is focused on quantifying the information about vowel identity present in auditory cortical responses and how noise modulates this.

These findings suggest that the time-course of background noise can influence discrimination of vowel sounds in both human and non-human listeners, and such effects are – at least in part – mediated by auditory cortex.

PS-674

Deep Neural Networks Trained on Speech Tasks Predict Auditory Cortex Responses to Natural Sounds

Alexander Kell; Daniel LK Yamins; Sam Norman-Haignere; Joshua McDermott
MIT

Background

In the last five years, convolutional deep neural networks [DNNs] have suddenly achieved remarkable performance on difficult perceptual tasks such as speech recognition. If the set of possible solutions to such demanding auditory problems is small, then these high-performing networks could plausibly converge on similar representational schemes to those implemented in the brain. Thus, DNNs may be a useful tool to understand the auditory system – e.g., to parcellate auditory cortex into functional regions, and to examine which tasks different regions of auditory cortex may be optimized to perform. Here we explore whether DNNs optimized for speech tasks converge on representations similar to those in human auditory cortex.

Method

Using fMRI, we measured the functional response of thousands of voxels to 165 natural sounds in the auditory cortex of ten humans. Separately, we trained a deep neural network to identify words, using millions of excerpts from labeled speech corpora. We selected the network's architecture using hierarchical modular optimization [Yamins, et al. NIPS 2013] and trained the weights using backpropagation. Crucially, the network was trained on the speech task; it was not optimized to predict neural activity. Once training on the speech task was complete and the network parameters fixed, we measured the network's ability to predict fMRI responses in auditory cortex. We first presented the 165 natural sounds to the net-

work and recorded each model unit's activity. We then used regularized regression to learn a linear mapping between the model units' responses and each voxel's response profile to the 165 sounds. We quantified predictive power via cross-validated explained variance.

For comparison, we tested how well auditory cortical responses could be predicted by conventional auditory models, including cochleagrams and a spectrotemporal filter bank [Chi, Ru, & Shamma 2005]. Additionally, we tested the contribution of speech training by comparing speech-trained DNNs with two types of control networks: [1] a DNN optimized for visual object recognition; and [2] dozens of "random" DNNs with randomized filters and/or randomized network architecture.

Result
Speech-trained DNNs predicted auditory cortex responses substantially better than conventional auditory models and both kinds of control networks.

Conclusion
Speech-trained convolutional DNNs share representational similarities with human auditory cortex. Our work suggests that deep neural networks may be a useful tool to examine the functional organization of auditory cortex. Future work will examine whether different cortical regions may be best predicted by networks optimized for different tasks.

Authors AK&DY contributed equally.

PS-675

EEG Evidence of Temporal Coherence in Streaming of Alternating and Synchronous Tone Sequences

Lakshmi Krishnan; **Shihab Shamma**
University of Maryland, College Park

Background
Mechanisms behind perceptual organization of incoming sound sequences into auditory streams are not yet well understood. One hypothesis for the formation of these perceptual streams is the temporal coherence principle. In this study, we test this hypothesis using EEG by presenting alternating and synchronous tones as stimuli. We study the effects of attending to a target tone in the presence of concurrent or alternating distractor tones at other frequencies. We hypothesize that competitive interactions between the alternating (incoherent) sequences reduce the overall response power compared to the synchronous sequences. Furthermore, when selectively attending to one of the sequences, the competitive interactions in the alternating case significantly facilitate suppression of the distracting sequence compared to when the tones are synchronous.

Methods
Tone sequences centered at 1000Hz and 420 Hz were presented as either alternating or synchronous sequences. The 1000Hz tone sequence was amplitude modulated(am) at 40Hz to facilitate segregation and to quantify the measured EEG response in terms of 40Hz steady state power. Subjects were asked to attend to either the high frequency stream or low frequency stream during the selective attention task. Oddball tokens (4dB higher) were presented occasionally, and subjects were instructed to report oddballs in the attended stream by key press. During the global attention task, subjects were asked to report the presence of oddballs in both streams with a key press. Three different frequency separations of 6, 9 and 15 semitones were tested for the global attention condition.

Results
The results of this study are consistent with previous studies indicating that the neural response to a tone is stronger when the tone is the attended tone compared to when the tone is the distractor. However, this difference in response is significantly reduced when the distractor tones and target tones are synchronous.For the global attention condition, response power to a post-task tone was larger when the preceding stimulus was synchronous than when it was alternating. Moreover, a systematic shift in latency of the response as a function of the frequency separation between the tones is observed when the post-task tone is preceded by alternating tones.

Conclusion
These results support the hypothesis that a listener detects temporal coherence in the incoming sound sequence and exploits it to bind all coherent features of the sequence. At the same time, temporally incoherent sequences compete with each other to form separate auditory streams, with the significant winner being the attended sequence.

PS-676

Psychophysiological Correlates of Listening Effort in Theta-Band EEG

Matthew Wisniewski
Air Force Research Laboratory

Introduction
Attempts to identify physiological correlates of listening effort have mainly focused on peripheral measures (e.g., pupillometry) and auditory-evoked/event-related potentials (AEP/ERPs), with greater amplitude responses associated with greater effort. Although non-auditory studies suggest that frontal midline θ dynamics in EEG (Fmθ; 4-7 Hz) correlate with domain-general mental effort, little work has characterized θ during effortful listening. In the current experiments, Fmθ and AEP/ERP features were investigated concurrently in listening tasks having varying degrees of difficulty.

Methods
EEG was collected while listeners heard speech in different signal-to-noise ratios (SNRs) under active (Experiment 1) or passive (Experiment 2) listening conditions. In Experiments 3 and 4, listeners performed an auditory-oddball task in which sequentially presented tones varied in frequency (30% high tones). Levels of SNR (Experiments 1 & 2) and frequency difference (Experiments 3 & 4) were blocked. Relationships between EEG, performance, and self-reports of effort were assessed.

Results
In experiment 1, Fmϴ power increased with decreasing SNR and was positively correlated with reports of effort. Increased Fmϴ power was present before speech onset and during speech presentation. Although speech-recognition accuracy varied across SNRs, a significant effect of SNR on Fmϴ remained when analyzing only trials in which 100% correct recognition was achieved. No effect of SNR was observed during passive listening (Experiment 2). In Experiments 3 and 4, Fmϴ was greater in conditions where frequency differences were small (<1 semitone) relative to conditions in which differences were large (>12 semitones). As in Experiment 1, Fmϴ effects were not dependent on differences in performance (Experiment 4). In all experiments, Fmϴ was best accounted for by equivalent current dipoles in medial prefrontal brain regions at or near the anterior cingulate cortex. In contrast to previous studies, N1, P2, and P3 components of AEP/ERPs appeared to decrease in amplitude as listening became increasingly difficult (Experiments 1, 3, & 4).

Conclusions
Results suggest that frontal cortical networks play a larger role when listening conditions become increasingly difficult. These networks do not appear to be specifically recruited for speech, but may rather reflect domain-general attention and/or working memory processes. Fmϴ and other time-frequency features in EEG may usefully supplement previously employed measures of effortful listening. They may be especially useful in investigations of listening in the absence of a stimulus (e.g., anticipatory listening), and in situations in which stimulus- and effort-related effects on AEP/ERPs are difficult to parse.

PS-677

Detection of Appearing and Disappearing Objects in Acoustic Scenes is Supported by Distinct Neural Representations: Evidence from MEG

Ediz Sohoglu; Maria Chait
University College London

Change detection is a critical computation in hearing and underlies our capacity to perceptually organize the auditory scene (Fishbach et al., 2001). However, the precise brain mechanisms by which change detection is accomplished, particularly in complex ongoing scenes, remain unknown. In the current MEG study, we test the hypothesis that changes in acoustic scenes are represented in fundamentally different ways depending on whether the change involves an appearing or disappearing object in the ongoing scene.

Listeners were presented with scenes containing four or ten auditory objects, formed from rapid pure-tone sequences that each had a unique carrier frequency and amplitude modulation rate. On some trials, one of these objects appeared at a variable time relative to scene onset while on other trials one object disappeared from the scene. An additional control condition involved scenes without a change. While MEG was collected, listeners were required to actively detect the changing objects.

Our results show that listeners are quicker and more accurate in detecting appearing rather than disappearing objects. Underpinning this behavioral difference are change-evoked neural responses that are not only significantly larger and earlier for appearing objects but are also fundamentally different: the first observable responses to appearing and disappearing objects (peaking at ~50 ms and ~150 ms, respectively) associate with distinct spatial patterns of MEG activity. Furthermore, we show that these change-evoked responses not only code for changes in stimulus power but also the behavioral outcome (accuracy and speed of detection).

These results suggest that detection of appearing and disappearing objects is supported by distinct neural representations. One possible reason for this asymmetry is because detecting disappearing objects is a computationally harder problem, necessarily requiring the prior representation of the acoustic scene (Cervantes Constantino et al., 2012). In ongoing work, we are using a similar paradigm to investigate how the temporal patterning of scene objects influences change detection.

PS-678

Cortical Time-Frequency Representation: Effect of Stimulation Mode and Experience

Prasandhya Yusuf; Peter Hubka; **Andrej Kral**
Medical University Hannover, Hannover, Germany

Background
Neuronal activations and interactions are often manifested as oscillations in extracellular recordings. Here we evaluated time-frequency representations of local field potentials (LFP) recorded simultaneously from primary auditory cortex (A1) and posterior auditory field (PAF). Responses elicited with acoustic and electric stimuli (through cochlear implants) were compared.

Methods
LFP were recorded from eight isoflurane-anaestehtized cats using two multielectrode arrays in the fields A1 and PAF simultaneously. Stimuli were click trains and charge-balanced pulse trains (through a cochlear implant). Time-frequency representations (TFR) of total, evoked and induced power, and inter-trial phase locking factor (PLF) were calculated using wavelet analysis. Powers of TFRs in alpha (7-15 Hz), beta (16-30 Hz), low gamma (31-60 Hz), and high gamma (61-120 Hz) bands were compared.

Results
PAF showed larger ongoing activity than A1, however total power of responses were stronger in A1 than PAF in all analyzed frequency bands. Compared to electric stimulation, acoustic responses in A1, but not in PAF, contained less energy. At longer latencies (>100ms) more energy was observed for acoustic stimuli. At threshold, evoked gamma response at early latencies (< 100 ms) was appeared and increased for both stimulation modes. Both synchrony (PLF) and ener-

gy (evoked power) increased correspondingly with stimulus levels.

Induced signals were, as expected, weaker than evoked signals. Furthermore, a stronger suppression following the early response was observed in the induced signals than in the evoked signals In contrast to evoked signals, there was a weak induced suppression of the alpha band activity at early latencies. Electric stimulation recruited significantly less late activity in all bands compared to acoustic stimulation. In total, whereas evoked signals showed similarities between both stimulation modes, induced signals indicated differences in their spectral content.

Finally, contralateral, ipsilateral and bilateral stimulation showed similar spectral signatures, indicating that in all these stimulus combinations, similar neuronal processes are activated.

Conclusion

A1 and PAF were differently affected by stimulation mode: A1 showed stronger responses by electrical stimulation, whereas PAF showed same or stronger responses by acoustical stimulation. A consistent finding was the reduced power at longer latencies elicited by electrical stimulation. As induced responses at longer latencies are subject of corticocortical interactions this finding is likely a consequence of the artificial nature of the electrical stimulus.

PS-679

Endogenous Oscillatory Lateralization For Speech Perception in Noise

Elaine Thompson; Kali Woodruff Carr; Travis White-Schwoch; Adam Tierney; Trent Nicol; Nina Kraus
Northwestern University

Speech perception in noisy environments is important for young listeners, as childhood is a critical period for learning and classrooms tend to be noisy (Bradley and Sato, 2008). Hemispheric lateralization of speech processing has been largely understood through the Asymmetric Sampling in Time framework (Poeppel, 2003), which hypothesizes left and right hemispheric specialization for processing speech at different time scales: phonemic information and syllabic rate, respectively. Endogenous cortical oscillations, the ongoing neural activity recorded in an individual at rest, are measured using electroencephalography (EEG) in the absence of stimulation. Left hemisphere-specific oscillatory activity has been linked to specialized processing of acoustic regularities in speech, particularly the spectro-temporal rhythms important for phonemic perception (Giraud et al., 2007). We reasoned that if the left hemisphere preferentially encodes the fast-moving properties of speech, we might find a leftward shift in endogenous brain oscillations at higher frequencies, such as gamma. We further reasoned that the more lateralized the left hemisphere is at rest, the better equipped the brain would be to process phonemic aspects of speech, particularly in the presence of background noise.

We evaluated speech-in-noise perception using a pediatric words-in-noise task (the CRISP; Litovsky, 2005), and collected endogenous brain activity in the absence of sound in 55 preschool-aged children (3-5 years old). Overall, as oscillations increased in frequency, over a 2 to 55 Hz span, they became more left-hemisphere lateralized. This pattern was more pronounced in children who better perceived speech in noise. In this age group, performance on the CRISP has been linked to phonological awareness, the auditory manipulation and recognition of language sounds. The observed connection between endogenous left-lateralized cortical activity in phonemic-relevant frequencies and speech perception in noise is consistent with known left auditory cortex specialization. We suggest that young children's left-lateralized endogenous oscillatory activity facilitates speech processing in challenging listening environments.

PS-680

Cortical Electrophysiological Markers of Language Abilities in Children with Hearing Aids: A Pilot Study

David Bakhos[1]; Helene Delage[2]; John Galvin[3]; Emmanuel Lescanne[1]; Sylvie Roux[1]; Frederique Bonnet-Brilhault[1]; Nicole Bruneau[1]
[1]Université François-Rabelais de Tours, CHRU de Tours, UMR-S930, Tours, France.; [2]Laboratoire de Psycholinguistique Expérimentale, Faculté de Psychologie et des Sciences de l'Education, Université de Genève, 40 boulevard du pont d'Anne, 121 Genève, Suisse.; [3]Department of Head and Neck Surgery, David Geffen School of Medicine, University of California Los Angeles, Los Angeles, California, United States of America.

Objective

In case of moderate hearing loss in childhood, hearing aids can improve speech audibility and facilitate language development, assuming that the auditory cortical areas are functional. However, individual variation in language performance has been observed in children with mild to moderate sensorineural HL.The aim of this study was to use cortical auditory evoked potentials (CAEPs) to investigate cortical auditory processing in regards to pediatric HA users with different levels of language ability.

Subjects and Method

We included 11 children (age: 8-12 years old) with symmetrical bilateral sensorineural hearing loss fitted with hearing aids and 11 age-matched, normal-hearing (NH) children. Aided and unaided pure tone average (PTA) thresholds (averaged across audiometric frequencies 0.5, 1, 2, and 4 kHz) were < 20 dB for pediatric hearing aid users and normal hearing participants. Spoken language and literacy skills were assessed using a set of standardized, computerized French language tests. CAEPs were measured in 11 pediatric hearing aid users with moderate bilateral sensorineural hearing loss (HL); participants were classified according to language ability. CAEPs were also measured for the control group (normal hearing children). The stimuli were presented at four different inter-stimulus intervals: 700 (i1), 1100 (i2), 1500 (i3), and 3000 (i4) ms.

Results
Hearing loss children without language impairment exhibited normal CAEPs. Hearing loss children with language impairment exhibited atypical temporal CAEPs, characterized by abnormal temporal responses with the absence of N1c. No significant effect of inter-stimulus interval was found for the amplitude and latency of the successive peaks recorded at temporal sites. A significant effect of inter-stimulus interval was observed on N1b amplitude for all groups except for the hearing loss children with language impairment.

Conclusion
Results suggest that abnormal temporal responses may underlie language impairment pediatric hearing aid users with moderate sensorineural hearing loss. These findings need to be confirm with arger sample of children.

PS-681

The Effect of Visual Load on Auditory Figure-Ground Segregation

Katharine Molloy[1]; Timothy Griffiths[2]; Nilli Lavie[3]; Maria Chait[4]
[1]University College London; [2]Institute of Neuroscience, Newcastle University; Wellcome Trust Centre for Neuroimaging, University College London; [3]Institute of Cognitive Neuroscience, University College London; [4]Ear Institute, University College London

It is well established that perception is limited in demanding conditions of high load which overwhelm perceptual capacity (e.g. Lavie, 1995). The effects of perceptual load have typically been studied within sensory modality, especially within vision, but less work has explored whether high perceptual load in one modality can limit processing in another. Recent work demonstrates that under conditions of high visual load, participants fail to hear pure tones which are audible under low visual load (Raveh & Lavie, in press). Magnetoencephalography (MEG) data indicate that this is because increased visual load leads to a reduction in neural responses to sound from as early as 150ms post stimulus (Molloy et al. in prep). Here, we use psychophysics and MEG to investigate whether visual processing load can also impair auditory figure ground segregation.

Participants performed a visual search task of either low or high visual load, comprised of a 100ms search display followed by a 100ms mask, with 200ms auditory stimuli presented concurrently. The auditory scenes were formed by a background (chords of random frequencies which changed every 25ms) and on 50% of trials an additional 'figure' comprised of multiple frequency components repeating throughout the stimulus (Stochastic Figure-Ground, SFG, stimuli; Teki et al., 2011). These stimuli are designed so that the figure can only be formed based on temporal coherence cues. In the behavioural study a dual task paradigm was used to gage conscious awareness of the auditory figure, whereas in the MEG sessions, neural responses to the auditory stimuli were passively recorded while participants engaged solely in the visual load tasks.

In the behavioural task, participants showed significantly poorer detection sensitivity for the figure under high visual load compared to low). Preliminary MEG data (n=8) suggest that under high visual load the amplitude of the auditory M100 response is reduced for both figure and no-figure sounds, with a small reduction also occurring for the later peak at ~200ms, in line with previous findings. Further, the response to the figure (a negativity from ~170-320ms) is reduced under high visual load compared to low.

These data suggest that high demands on the visual system can impair auditory figure-ground segregation. This indicates that the integration of temporal coherence cues over time, a process previously suggested to be automatic (Teki et al. 2011), may be modulated by the availability of modality-general attention resources.

PS-682

Electrophysiological Examination of the Triplet Digit in Noise Test

Andrew Dimitrijevic[1]; Michael Smith[2]; Stephanie Sieswerda[2]; David Moore[2]
[1]Cincinnati Children's Hospital Medical Center; University of Cincinnati; [2]Cincinnati Children's Hospital Medical Center

Introduction
Limitations of pure-tone audiometry for predicting speech perception, particularly among hearing impaired listeners in challenging environments, are becoming increasingly apparent and important. Examples of recently developed speech-in-noise tests include the Digit Triplet Test (DTT), Matrix Sentence Test, Coordinate Response Measure, Listening in Spatialized Noise (LiSN-S), and Enhanced QuickSIN. However, behavioral tests provide only a final outcome measure, the performance on a particular task. Although some clinical populations may show similar behavioral responses, the underlying mechanisms may differ. For example, people with both auditory neuropathy and presbyacusis may show similar difficulties with speech-in-noise hearing, but these populations can be differentiated on the basis of electrophysiology. The overall purpose of this study was to characterize the brain's response to a speech-in-noise test, the DTT. The specific aim was to separate sensory and cognitive components of the cortical auditory evoked potential (CAEP) that may be useful in differentiating disorders associated with listening difficulties, such as auditory processing disorder.

Methods
Listeners performed two DTT conditions. In each condition, a custom Matlab program presented blocks of 25 trials, each of three randomly chosen, successively presented monosyllabic digits (0to9, excluding 7), spoken by a US English female talker in the presence of a fixed level, speech (digit) shaped noise. In Condition 1, the level of the digits (signal) varied. The signal to noise ratio (SNR) needed to identify all three digits in a trial 50% of the time (speech reception threshold, SRT) was determined adaptively. In Condition 2, 64 channel EEG recording was performed while the listener performed the DTT at three fixed signal levels: SRT, SRT+5dB, and SRT+10dB. Trial blocks of each signal level were repeated 5

times, yielding 125 trials per SNR. EEG activity was averaged across trials, yielding CAEPs for each digit position across the three different SNRs. EEG oscillatory activity was also examined.

Results
Pilot data from normal hearing adults showed identifiable N1/P2 responses at each digit position. The amplitude of the N1/P2 response was larger and earlier at the highest SNR level and decreased across successive digits within each triplet. Event-related alpha desynchronization was greatest at the lowest SNR.

Summary
A new, US English DTT was developed. SRTs were comparable to those measured using other DTTs. Physiological data showed clear CAEPs in response to each digit. The N1/P2 response may represent sensory encoding of the digits whereas the alpha desynchronization may represent cognitive processing related to auditory attention.

PS-683

Investigating Stream Segregation and Spatial Hearing Using Event-Related Brain Responses

Le Wang; Scott Bressler; Barbara Shinn-Cunningham
Boston University

Several studies have used auditory mismatch negativity (MMN) to study auditory stream segregation. Few of these studies, however, focused on stream segregation that involves spatial hearing. Here, we used MMN to examine spatial effects on stream segregation.

All subjects in both experiments had pure-tone thresholds within 20dB of normal hearing level in both ears. In Experiment 1, traditional oddball streams were presented in a passive listening paradigm, either in isolation or in the presence of an interfering stream. Interfering streams were either spectrally distant from or close to the oddball stream, and were also spatially separated from the oddball stream. The deviant stimuli differed from the standards only in simulated spatial location. In Experiment 2, similar stimuli were presented, but in a task-based MMN paradigm. The standards and the interfering stream were fixed in space while the spatial location of the deviants was randomized from trial to trial. Subjects were asked to attend to the oddball stream and to press a button every time a deviant was detected.

In Experiment 1, the MMN was strongest when the oddball stream was presented in isolation, less strong but present when the two streams were spectrally separated, and not observable when the streams were spectrally close. In Experiment 2, results depended on whether the streams were distinct in spectral content. When the interfering stream was spectrally distant from the oddball stream, deviant detection was poor when deviants were spatially close to the standards, and was accurate for all other deviant locations. In these cases, the MMN was present for all deviant locations except the location that was closest to the standards. In contrast, when the interfering stream was spectrally close to the oddball stream, the deviant detection was accurate when the deviants came from the midline location between the standards and the interfering stream, and deteriorated for deviants that were spatially closer to either the standards or the interfering stream. The MMN was present only for the midline deviant locations, not when the deviant location was near either the standard or interfering stream.

These results demonstrate the feasibility of using the MMN to measure spatial stream segregation in both passive and task-based experiments. The results from Experiment 2 provide behavioral and neural evidence that the detection of spatial discontinuities within a sequence of tones strongly depends on how well those tones are segregated from the competing tones at other locations.

PS-684

Aligning Anatomic and Physiologic Divisions of Rat Auditory Cortical Fields

Douglas Storace[1]; Kelsey Dutta[2]; Deborah Bishop[3]; Nathan Higgins[4]; Douglas Oliver[3]; Heather Read[2]
[1]Yale University; [2]University of Connecticut; [3]University of Connecticut Health Center; [4]Vanderbilt University

In the rat, six auditory fields with distinct topographic organization of responses to sound frequency have been identified using multi-unit, micro-encephalographic and intrinsic optical imaging (IOI) techniques. It is unclear whether these functional fields correspond to primary and secondary processing stages and/or to anatomically defined fields including: temporal areas 1, 2 and 3 (i.e. Te1, Te2 and Te3, respectively). In other mammals, primary and secondary sensory cortices are distinguished by the laminar and areal distributions of SMI-32, a subclass of neurofilament proteins, and type 2 vesicular glutamate transporter (VGLUT2). Here, we located primary (A1), ventral (VAF) and suprarhinal (SRAF) auditory fields with IOI and examined the laminar and areal organization of SMI-32 and VGLUT2 immunoreactivity in these physiologically defined fields.

Our results show that SMI-32 labeled laminar patterns changed with the ventral progression from Te1 to Te3, and with the posterior progression from Te1 to Te2. SMI-32ir was high in layers 3, 5 and 6 in Te1, but was restricted to layers 5 in Te2 and Te3. VGLUT2ir was concentrated in layers 3 and 4 in Te1, Te2 and Te3, consistent with prior studies indicating that VGLUT2 is primarily expressed in glutamatergic auditory thalamocortical terminal fields. Alignment with our functional map confirmed that A1, VAF and SRAF were all located within the regions containing a tri-laminar SMI-32ir pattern that is typical of primary sensory cortices in other mammals. These results suggest that SMI-32 can be used to define the posterior and ventral borders of Te1 cortex, and that multiple frequency organized auditory cortices exist within Te1.

PS-685

Projection-specific Mechanisms of Layer 5B Neurons Underlie Activity-dependent Fractionation of Layer 2/3→5B Excitation in Mouse Auditory Cortex

Ankur Joshi[1]; Jason Middleton[2]; Katharine Borges[3]; Benjamin Suter[3]; Gordon Shepherd[3]; Thanos Tzounopoulos[4]

[1]University of Pittsburgh; [2]Department of Cell Biology and Anatomy LSUHSC School of Medicine; [3]Department of Physiology, Feinberg School of Medicine, Northwestern University; [4]Departments of Otolaryngology and Neurobiology, University of Pittsburgh School of Medicine

Auditory cortex (AC) layer (L) 5B contains two major classes of cortical projection neurons represented by corticocollicular neurons, a type of pyramidal-tract (PT) neuron projecting to the inferior colliculus, and corticocallosal neurons, a type of intratelencephalic (IT) neuron projecting to contralateral AC. Although distinct response properties to sound have been ascribed to IT and PT neurons in AC, little is known about the underlying intrinsic and synaptic mechanisms. To investigate these mechanisms, we recorded in brain slices of mouse AC from retrogradely labeled corticocollicular and neighboring corticocallosal neurons in L5B. Corticocollicular neurons had lower input resistance, greater hyperpolarization-activated current, depolarized resting membrane potential, faster action potentials, initial spike doublets, and less spike frequency-adaptation. Paired-recordings from single presynaptic L2/3 neurons connected with a single postsynaptic L5B projection neuron revealed an absence of synaptic depression during short trains of inputs for L2/3 connections to corticocollicular neurons, but the presence of depressing L2/3 connections to corticocallosal neurons. Our findings indicate that sustained activity dynamically fractionates the L2/3→5B pathway to generate more sustained (tonic) firing in corticocollicular neurons and more transient (phasic), frequency-dependent firing in corticocallosal neurons. These findings are consistent with the differential response properties to sound observed in IT and PT neurons in AC. In this context, the present results contribute to the development of integrative models of AC function that bridge cell-specific mechanisms and network properties.

PS-686

Information Transfer Between Auditory Thalamus and Cortex in Rats

Hirokazu Takahashi; Hiroyuki Nagata; Tomoyo Shiramatsu; Ryohei Kanzaki

The University of Tokyo

Background

The interaction between the auditory cortex and thalamus plays an important role in the neural computation along the auditory pathway. To investigate the thalamo-cortical interaction, we measured the auditory evoked activities simultaneously in the auditory cortex and thalamus in anesthetized rats and estimated the information transfer between these nuclei on the basis of information theoretical analyses.

Methods

Wistar rats were anesthetized with isoflurane during experiments. The depth microelectrode array was used to measure click- and tone-evoked local field potentials (LFPs) simultaneously at the auditory thalamus (medial geniculate body (MGB)) and the primary auditory cortex (A1). In addition, layer-specific responses were characterized in the auditory cortex. The shank of array was 6 mm long with an inter-electrode distance of 500 μm. Each shank had 15 recording sites for the thalamus and 17 for A1. Transfer entropy in both the thalamus-to-cortex and cortex-to-thalamus directions was estimated with time delays ranging from 5 and 200 ms in 5-ms increments.

Results

In MGB, the recording site exhibiting the largest auditory evoked response was chosen as a test site. In A1, the recording site exhibiting the largest response was chosen as a test site at the 4th layer, and 300 um below from the 4th layer was also investigated as the 5/6 layer. In each neural pathway and direction, significant information transfers were observed in specific time delays: from MGB to the 4th layer in A1, the information tended to best transfer with a time delay of around 200 ms, i.e., the theta band; from MGB to 5/6th layer, the gamma band; from the 4th layer in A1 to MGB, the alpha band; and from the 4th layer in A1 to MGB, the beta band.

Conclusions

Our results suggest that the frequency band used to transfer information between the auditory thalamus and cortex is pathway-specific.

PS-687

Cortical Encoding of Frequency Glides

Wen-Jie Wang[1]; Brett Martin[1]; Glenis Long[1]; Chin-Tuan Tan[2]

[1]Graduate Center, City University of New York; [2]New York University, School of Medicine

Introduction

Cortical encoding of frequency change was investigated using the N1 component of the acoustic change complex (ACC) evoked by a frequency glide. Magnitude of frequency change, rate of change and glide duration all affect N1 latency, but these variables can be difficult to disassociate. These potential sources of ACC elicitation were disentangled by using quadratic glides with fixed frequency change but different durations. Varying glide duration permitted separation of the contribution of instantaneous frequency change and instantaneous rate of change. It was hypothesized that longer glides would elicit longer ACC N1 latency delay relative to onset N1 latency. However, if ACC elicitation is primarily associated with the instantaneous frequency change, the estimated instantaneous frequency change based on the ACC N1 latency delay would be independent of glide duration. In contrast, if ACC elicitation is associated with the instantaneous rate of change, then the estimated instantaneous rate of change would be independent of glide duration.

Methods
Auditory evoked potentials to frequency glides following a steady tone were recorded from eight normal hearing listeners. The glides either increased or decreased in frequency by 200 Hz as a quadratic function of time, and the instantaneous frequency was $f(t) = f_{initial} + nkt^2$, where $k = 200\ Hz / (glide\ duration)^2$ and n = 1 or -1 for upward or downward glides, respectively. Glide duration was 50, 100 and 200 ms and initial frequency was 500 and 1000 Hz. The rate of change increased linearly with time: $r(t) = 2kt$.

The impact of both instantaneous frequency change (kt^2) and the instantaneous rate of change ($2kt$) potentially associated with the ACC elicitation was estimated using the delay in ACC N1 latency relative to onset N1 latency.

Results
Based on this latency delay, the estimated instantaneous frequency change was independent of glide duration, but the estimated rate of change was higher for shorter glides. When both the initial frequency and the estimated instantaneous frequency of glides were mapped onto position along the basilar membrane, the associated place shift was essentially constant across glide conditions.

Conclusion
ACC N1 latency is primarily associated with the instantaneous frequency change of a glide and thus the shift of frequency-place position along the basilar membrane. There was no clear evidence that the ACC N1 peak was dependent solely on the instantaneous rate of change or the duration of glide.

PS-688

Time-Constrained Neural Decoding From Multiple Auditory Cortical Areas

Krishna Puvvada; Jonathan Z. Simon
University of Maryland, College Park

Sensory signals are processed cortically in a hierarchical fashion: results of neural computations performed in a primary sensory area are relayed to secondary and tertiary cortical areas. In this way, sensory information is represented at different levels of abstraction in different hierarchical areas. For non-invasive neurophysiological recordings, however, sensor activity is typically a linear combination of responses from several neural sources, making neural source separation difficult, or even ill-posed. An experimental byproduct of cortical hierarchical processing, however, is that separate responses to the same stimulus, but from different neural sources in the processing hierarchy, add together with different latencies. In auditory cortex, for example, earlier latency responses such as the P1/M50 originate from Heschl's gyrus, whereas and longer latency responses such as the N1/M100 are dominantly from planum temporale.

We show that these latency differences can be utilized within neural decoding algorithms to separate sources whose neural signals are otherwise so strongly mixed at the sensor level that they cannot easily be separated using spatial methods. Standard neural decoding algorithms integrate information over sensors and time. When sources have different latencies, however, by constraining integration time-window boundaries we can temporally isolate the neural responses from different sources. This method is effective when different neural sources are non-overlapping/minimally overlapping in time and as such is well-suited for high temporal resolution recording techniques such as electroencephalography (EEG) and magnetoencephalography (MEG).

The utility of this method is demonstrated in the context of neural decoding of continuous speech in a multi-speaker environment. Neural activity is recorded using 157-channel MEG. Using a linear model, the envelope of target and competing speech streams are decoded from both early latency and later latency responses. Reconstruction results show that, in neural sources with early latency responses, both target and competing speech streams are equally well represented. For neural sources with later latency responses, however, reconstruction results show that the envelope of the attended speech is represented with significantly greater fidelity than that of competing speech.

PS-689

Auditory Network Optimized for Noise Robust Speech Discrimination Predicts Auditory System Hierarchy

Fatemeh Khatami; Monty Escabi
University of Connecticut

Sound recognition, including speech recognition, is accomplished by multiple hierarchical neural processing levels. Starting with the cochlea, sounds are decomposed into frequency components and subsequent auditory levels (e.g, cortex and midbrain) further decompose sound into spectro-temporal components. This multi-level nonlinear processing scheme produces a robust neural representation enabling sound recognition in acoustically challenging environments (e.g., high noise levels or multiple subjects). Yet how this high performance is accomplished is poorly understood. Here we develop a biologically inspired computational auditory network consisting of multiple hierarchical levels of spiking neurons and test its performance in a speech recognition task.

The proposed network contains three primary stages. The first stage consists of a cochlear model that transforms speech into spike trains for multiple frequency channels. Stage two consists of a biologically inspired neural network of spiking neurons designed simulate the central auditory pathway. The network contains 6 network layers containing 100 biologically realistic *spiking* neurons per layer and biologically motivated architecture that contains *excitatory* and *inhibitory* connections between layers. The final stage consists of a statistical classifier that reads the output spike trains from the network to categorize and identify speech words.

Upon optimizing the network architecture to maximize discrimination performance for speech words (i.e., maximize the sensitivity index: d'), the network achieves high performance even under variable conditions (e.g., multiple speakers). Furthermore, the optimal network shares several structural and

functional properties of the mammalian auditory system. The integration time constants of the optimal network configurations increase systematically across the network layers such that the early layers are fast and most central layers are substantially slower, analogous to transformation for temporal processing in the auditory system. At the early network layers, connections between layers are largely restricted to nearby frequencies. Connectivity becomes progressively more divergent from layer-to-layer and across-channel interactions are much more prevalent for the deep network layers, analogous anatomical transformations in connectivity observed between the auditory periphery and cortex. Finally, selectivity increases and spike rates decrease systematically across the network layers analogous to response trends observed in the auditory system. Compared to a constrained network that lacks these structural features (time constants and interconnections are constant across layers), the optimal network outperforms it in acoustically variable conditions (e.g., multiple speakers). Thus, the hierarchical organization and functional transformations derived from the optimal network, and possibly the auditory system as a whole, are critical for achieving robust performance in variable acoustic conditions.

PS-690

Spike Timing Precision for Discriminating Temporal Sound Cues in Three Cortical Fields

Ahmad Osman; Christopher Lee; Monty Escabi; Heather Read
University of Connecticut

Animals can discriminate changes in the sound envelope amplitude that create shape temporal cues for perception of loudness and timbre (Irino and Patterson 1996). Sound shapes can be represented with a shape-dependent spike rate increase in primary (A1) auditory cortex (Wang, Lu et al. 2008). In addition, shape can be represented with spike timing error (jitter) in auditory cortex (Lee et al., 2014). Here we ask whether cortical neuron spike-timing patterns in primary and secondary auditory fields of the rat can be used to discriminate sound shape.

Spike distance metrics are used to estimate neural discrimination indices for pairwise discrimination of neural responses to shaped periodic noise sequences. Layer 4 single neuron responses are acquired in anesthetized rats in response to dichotic presentation of 55 unique noise sequences composed of N=11 modulation frequencies (Fm) and N=11 shape parameters (Fc) (N*(N-1) / 2 total combinations). Recordings are obtained from primary (A1), ventral (VAF) and caudal suprarhinal (cSRAF) auditory cortical fields of the rat (Polley et al., 2007). To compare time scales for shape representation to those needed for sound discrimination, shuffled autocorrelograms are computed and fit to estimate spike timing jitter for responses to each variation in sound shape (Zheng Escabi 2007). Next, spike times for multiple response trials are convolved with an exponential kernel having a time constant, tc, to compute a spike distance metric and a discrimination index (d-prime) (van Rossum 2001; Gai and Carney 2008) for discriminating pairs of sounds with different shapes. For each, pair-wise comparison, the time constant is varied between 1 and 1024 ms to determine the optimal d-prime (i.e., the maximum d-prime) and time constant (tc,opt).

In all fields, jitter decreases as sound shape Fc increases (Lee et al., 2014). The best discrimination, optimal d-prime, is obtained for Fm=2Hz and Fc=2Hz for the set of sounds examined. Optimal d-prime decreases with increasing Fm and Fc. For discrimination of Fc, the optimal time constant varies from 2-200ms reflecting the change in jitter over the same sound conditions. A rank order increase in tc yielding optimal d-prime is observed with: A1 < VAF < cSRAF. This parallels a rank order increase in jitter observed for these same cortical fields. These results support a framework where shape discrimination is constrained by spike timing precision and corresponding time scales for responding in primary and secondary ventral auditory cortical fields.

PS-691

Gentamicin Alters the Sensitivity of GABAA Receptors in Cultured Auditory Cortex Networks

Kevin Hamilton; Kamakshi Gopal; Ernest Moore; Guenter Gross
University of North Texas

Background

Aminoglycoside antibiotics, such as gentamicin, are commonly used clinically, experimentally, and agriculturally to combat aerobic gram-negative bacteria. Gentamicin treatment is widely linked to cochlear and vestibular toxicity; but not much is known regarding the effect of gentamicin on auditory neuro-function. Goal: The goal of this study was to determine if spontaneously active auditory neuronal networks growing on microelectrode arrays (MEAs) exhibit changes in neuropharmacological responses when exposed acutely to gentamicin. Methods: Auditory cortex tissue was extracted from E16 Balb-C/ICR murine embryos, and cells were dissociated and seeded onto MEAs. Seventeen auditory cortex networks (ACNs) that were at least 21 days *in vitro* (div) were used in this study. All cultures underwent electrophysiologic recording of spontaneous extracellular activity in the native condition, as well in response to a dose titration of the $GABA_A$ agonist, muscimol. Ten of the 17 cultures were pre-treated with 100-μM gentamicin (the recommended concentration for cell culture) for 0.5-1.0 hour prior to muscimol titration. Spike rate based EC_{50} values and action potential waveforms were statistically analyzed (α = 0.05) between ACNs with (n = 10) and without (n = 7) gentamicin pretreatment. Results: Sigmoidal fit concentration response curves (CRCs) generated a muscimol EC_{50} ± SD of 0.12 ± 0.04 μM without gentamicin and 0.08 ± 0.02 μM with gentamicin. Statistical analyses of the derived EC_{50} values resulted in a significant ($p < 0.05$) decrease of muscimol EC_{50} in the presence of 100-μM gentamicin. Furthermore, action potential waveform analyses suggested reduced K^+ conductance in neurons exposed to gentamicin. Conclusion: The significant reduction of EC_{50} value for muscimol under gentamicin suggests that gentamicin modulates and alters the sensitivity of $GABA_A$ receptors.

PS-692

Subunit Composition of Neuronal Nicotinic Receptors in the Medial Geniculate Body: Impact of Aging

Brandon Cox; Lynne Ling; Evgeny Sametskiy; Sarah Sottile; Donald Caspary
Southern Illinois University

Background

In sensory thalamus, including the medial geniculate body (MGB), the neurotransmitter, acetylcholine (ACh), plays a critical role in attention and in establishing the salience of important stimuli. High levels of neuronal nicotinic cholinergic receptors (nAChRs) are found in MGB, yet much remains to be learned about their subunit composition and the impact of aging on this system. nAChR subunit composition determines the affinity and efficacy of ACh released from brainstem and forebrain cholinergic inputs onto MGB, while potentially providing novel pharmacologic targets for the treatment of a subset of individuals with age-related hearing loss.

Methods/Results

Our initial receptor binding studies in MGB using [^{3}H]epibatidine confirmed previous studies showing high levels of heteromeric nAChRs composed of alpha (α) and beta (β) subunits. These findings were supported by competition binding studies using Iodo-A-85380, a ligand with high affinity for β2-containing nAChRs and low affinity for β4-containing nAChRs, to compete with [^{3}H]epibatidine which has a similar affinity for all heteromeric nAChR subtypes. These competition binding studies found that 95+% of nAChRs in young MGB contained the β2 subunit with less than 5% of β4-containing nAChRs. Preliminary competition binding studies with Iodo-A-85380 in aged MGB found a significant decrease in the number of β2-containing nAChRs, with an age-related increase (up to 45%) in β4-containing nAChRs. β4-containing nAChRs have been shown to possess lower affinity for ACh than β2-containing nAChRs which was reflected in preliminary patch clamp recordings from young and aged MGB slices. Puffing ACh onto patched MGB neurons in the presence of the muscarinic antagonist atropine, showed a *mecamylamine* (nAChR antagonist) sensitive presynaptic potentiation of miniature IPSCs and a postsynaptic excitatory response, also blocked by *mecamylamine*. Pre- and postsynaptic ACh-evoked responses were reduced in recordings from aged MGB neurons.

Conclusions

These findings suggest that nAChRs in MGB undergo age-related changes in subunit composition, which in combination with the previously identified loss of extrasynaptic $GABA_A$ receptors could underpin a loss of normal functioning of these circuits in attention/arousal and sleep.

PS-693

Acoustic-trauma-induced Desynchronization of Steady-state Activities in the Auditory Cortex in Rats

Naoki Wake; Tomoyo Shiramatsu; Ryohei Kanzaki; Hirokazu Takahashi
The University of Tokyo

Introduction

Maladaptation of auditory central pathway after peripheral acoustic trauma can be a cause of tinnitus and hyperesthesia. We hypothesized that spontaneous activities among neural population in the auditory cortex altered due to the adaptation after trauma, which may lead to tinnitus and hyperesthesia. Specifically, we focused on phase synchrony in steady-state activities in the present study.

Methods

Male Wistar rats at postnatal week 7-11, with a body weight of 200-300 g, were used. A microelectrode array with a grid of 96 recording sites recorded local field potentials (LFP) from the fourth layer of the auditory cortex under isoflurane anesthesia. The auditory brainstem response (ABR) was first measured in response to click stimuli. The onsets of tone-evoked LFPs were then characterized on the basis of decoding accuracy to confirm that the cortical activities represented test tones. Phase locking values (PLV) of LFPs during steady state activities were quantified. To characterize PLV, 9 pure tones (4, 6.3, 10.1, 12.7, 16, 20.2, 25.4 and 32 kHz, 60 dB SPL) were presented for 30 seconds, each of which was interleaved with a silent block of 30 seconds. From the recorded LFPs, we calculated PLVs in 5 bands (theta, 4 - 8 Hz; alpha, 8 - 14 Hz; beta, 14 - 30 Hz; low gamma, 30 - 40 Hz; high gamma, 60 - 80 Hz). After the first recording, the rat was exposed to intensive pure tone (16 kHz, over 95 dB SPL) for 1 hour. After the exposure, the neural activities were recorded again using the same sound stimuli.

Results

After the intensive tone exposure, ABR exhibited reduced amplitude and prolonged latency, and tone-evoked LFPs resulted in deteriorated decoding accuracies around 16 kHz, i.e., exposed tone frequency, suggesting that partial hearing loss was induced. During the intensive tone exposure, PLV decreased over time. For both spontaneous and tone-induced PLV became smaller after the exposure than before. These changes were not observed in a control group, i.e., no exposure group.

Conclusions

Intensive, prolonged tone exposure desynchronized neural population in the auditory cortex, possibly due to the adaptation mechanism. These results support our hypothesis that the steady-state phase synchrony in the auditory cortex can be used as a neural signature of acoustic disturbances such as tinnitus and acoustic hyperesthesia.

PS-694

Contributions of Brain Noise, Phase Locking, and Spectral Power to Auditory-Evoked Cortical Activity

Kelly Harris; Kenneth Vaden; Judy Dubno
Medical University of South Carolina

Background

The N1-P2 is an obligatory cortical response that can reflect the representation of spectral and temporal characteristics of an auditory stimulus. Traditionally, mean amplitudes and latencies of the prominent peaks in the averaged response are compared across experimental conditions and participant groups. However, peaks in the averaged response reflect only a subset of the information contained within the EEG signal. We used single-trial analyses to determine the contributions to P2 amplitudes of variability in non-evoked endogenous EEG activity, or 'brain noise', neural synchrony, and spectral power, and characterize how these features may differ for younger and older adults. This information can provide support for interpreting cortical responses and understanding age-related neural pathologies.

Methods

EEGs were recorded from 25 younger and 25 older adults with normal hearing. Model testing and linear regression were used to determine the extent to which individual differences in brain noise, estimates of neural synchrony using phase-locking values (PLV), and spectral power (4-8 Hz) uniquely predicted P2 amplitudes and varied by age group.

Results

P2 amplitudes, PLV, and spectral power were significantly larger in younger than older adults, whereas brain noise did not differ significantly between age groups. Multiple regression and model testing revealed that brain noise and PLV, but not spectral power, were unique predictors of P2 amplitudes. The lack of an association of power and P2 amplitudes may relate to ERP generation, which was triggered by the offset of the noise rather than the onset of a new stimulus, and is supportive of a phase-resetting hypothesis for the generation of P2. Model fit was significantly better in younger than older adults, suggesting that relationships among EEG variables may not be stable across age group.

Conclusions

The current results provide additional evidence that age-related declines in neural synchrony contribute to smaller P2 amplitudes in older adults, even those with normal hearing. Moreover, individual variability in timing and power across trials may help explain how larger P2 responses have previously been linked to both improving and declining task performance. Neural characteristics such as brain noise, neural synchrony, and spectral power can further our understanding of mechanisms underlying brain plasticity associated with development, auditory training, and experience, as well as changes in neural mechanisms underlying age-related declines in auditory processing.

Work supported by NIH/NIDCD

PS-695

Spatial Stream Segregation by Neurons in the Ascending Auditory System

Justin Yao; Peter Bremen; John Middlebrooks
University of California, Irvine

Background

Spatial stream segregation (SSS) aids a listener in hearing out sounds of interest amid competing sounds. A recent study in our laboratory demonstrated that cortical neurons exhibit SSS by synchronizing preferentially to one of two sequences of noise bursts that alternate in location (Middlebrooks and Bremen, J Neurosci 33(27):10986-11001, 2013). Here, we examine the derivation of SSS along the ascending auditory pathway.

Methods

Extracellular recordings were made in anesthetized rats at three levels of the lemniscal auditory pathway: the central nucleus of the inferior colliculus (ICC), the ventral division of the medial geniculate body (MGBv) and the primary auditory cortex (A1). Stimuli consisted of interleaved sequences of 5-ms noise bursts that alternated between A and B source locations. The A bursts were presented from contralateral (C) 40°, 0°, and ipsilateral (I) 40°, whereas B bursts were presented from C80° to I80° in 20° steps. Aggregate A/B burst rates were 5 or 10 bursts per second (bps), such that the difference in A and B onset times was 200 or 100 ms, respectively. Burst rates were extended to 40 bps for MGBv and ICC units. For each unit we measured the mean rate of spikes synchronized to A and B bursts as a function of A and B source locations.

Results

SSS strengthened along the ascending auditory system. For 5- and 10-bps conditions, neurons in the ICC showed little evidence of SSS, whereas a subpopulation of neurons in the MGBv and all A1 neurons displayed SSS. For example, at the 10-bps aggregate rate, mean spike rates synchronized to A bursts located at C40 increased by only 8% in the ICC when the B source was shifted from C40 to I40, whereas they increased by 45% in A1. Also, sharpening of spatial sensitivity due to the addition of a competing source (AB versus B-alone) was greatest in A1 and in the subpopulation of MGBv neurons, with spatial sensitivity narrowing by ~50°. SSS was seen in the ICC only at the highest tested burst rate, 40 bps, which is considerably higher than the rate at which SSS is reported in psychophysical studies.

Conclusion

Neural SSS is absent in the ICC, it appears in a subpopulation of MGBv neurons, and it becomes dominant in A1. Overall, the strengthening of SSS reflected both increased spatial sensitivity and increased forward suppression at successively higher levels of the lemniscal auditory pathway.

PS-696

Understanding the Octave Illusion

Anahita Mehta[1]; Andrew Oxenham[2]; Ifat Yasin[1]; Shihab Shamma[3]

[1]University College London; [2]University of Minnesota, Minneapolis, Minnesota, USA; [3]University of Maryland, College Park, USA & Ecole Normale Supérieure, Paris, France

Introduction

This study investigates the neural correlates and processes underlying the ambiguous percept produced by a stimulus similar to that termed Deutsch's "octave illusion" (Deutsch, D., 1974, Nature 251:307-9), where each ear is presented with a sequence of alternating pure tones of low and high frequencies. The same sequence is presented to each ear, but in opposite phase, such that the left and right ears receive a High-Low-High… and a Low-High-Low… pattern, respectively. The illusion is that subjects often hear an alternating pattern of low and high tones, with all the low tones lateralized to one side and all the high tones lateralized to the other side. The current explanation is that the illusion occurs because of illusory conjunctions of pitch and location values. Here we test this and alternative hypotheses involving concurrent and sequential stream segregation, and study potential neural correlates of the illusion by combining psychophysical and EEG measures.

Methods

A series of psychophysics and EEG experiments were conducted to discover which of the four tones in the sequence contribute to the percept of alternating low and high tones. Subjects were cued to focus on a particular frequency and side, as indicated by a priming sequence of tones presented at a single frequency and ear. This cuing elicited different percepts for the same stimulus. The psychoacoustic experiments manipulated one of the four tones, and asked subjects whether the manipulated tone belonged to the perceived sequence of alternating low-high tones. The EEG experiments employed a method of differentially tagging the individual tones in the sequence with different modulation frequencies.

Results

Results from the psychoacoustic experiments consistently suggested that the perceived illusory alternating percept arises from the cued tone and the tone that is presented *concurrently* with it. This outcome suggests that the illusory percept might arise from misattributions of the stimuli in *time*, rather than *location*, as has been previously assumed. Preliminary EEG results are consistent with this interpretation.

Conclusion

Overall, we found that the illusion of alternating tones seems to arise from concurrent, rather than sequential tones, suggesting that the illusion arises from a misattribution of time across perceptual streams, rather than a misattribution of location within a stream. These results provide potentially new insights into the mechanisms of bilateral streaming and concurrent sound segregation.

PS-697

Direct Electrical Recordings of Neural Activity Related to Auditory Figure-Ground Segregation in the Human Auditory Cortex

Phillip Gander[1]; Sukhbinder Kumar[2]; Kirill Nourski[1]; Hiroyuki Oya[1]; Hiroto Kawasaki[1]; Matthew Howard[1]; Timothy Griffiths[2]

[1]University of Iowa; [2]Newcastle University

The ability to detect a relevant sound by filtering out irrelevant sounds in the environment is crucial in day-to-day listening. This ability requires that the features of the relevant sound be grouped together as a single source (figure) and segregated from the features of other competing sounds in the environment (background). How the auditory system performs this task is not completely understood. In the current experiment we recorded local field potentials from human subjects undergoing invasive monitoring for pre surgical localization of epileptic foci. The subjects were implanted with depth electrodes in auditory cortex along the axis of Heschl's gyrus (HG) and subdural grids covering the superior temporal gyrus (STG).

The subjects listened to a stimulus in which the salience of the figure was varied systematically against a background. We used a stochastic figure-ground (SFG) stimulus developed in our lab that has been previously characterised using psychophysics and modelling. The SFG consisted of a sequence of simultaneously presented tones that were randomly distributed in log frequency space and varied from one 25 ms time frame to the next. During one time segment, a certain proportion of the tones remained the same over several consecutive time frames. This caused a figure to emerge from the background in which the salience was determined by the number of tones kept fixed (coherence) and the number of timeframes over which this occured (duration). In the current experiment, the first part (700 ms) of the stimulus consisted of only the background with no figure, and in the second part the coherence of the figure was varied systematically between 1, 2, 4 and 8. The overall duration of the figure was 24 25 ms time frames (700 ms).

We measured event-related potentials (ERPs) and carried out single-trial time-frequency analysis using a wavelet transform. In HG no significant ERPs or power change were observed in response to the figure when compared to the acoustically matched background. We observed a sustained power change in the high gamma band (60-120 Hz) that peaked at around 200 ms and varied with the coherence of the stimulus on STG for all tested subjects.

The data demonstrate a neural correlate of auditory figure-ground segregation in the form of high-frequency local oscillations in human non-primary auditory cortex.

PS-698

Neural Correlates of Auditory Pattern Processing in Humans

Nicolas Barascud[1]; Timothy Griffiths[2]; Karl Friston[1]; Maria Chait[1]
[1]University College London, UK; [2]Newcastle University Medical School, UK

Background

Our ability to detect regularities, or patterns, in ongoing sensory input is an important function of perception, and serves to facilitate the prediction of future events. We used functional magnetic resonance imaging (fMRI) and dynamic causal modelling (DCM) – a measure of effective connectivity that allows for investigating how brain areas interact during different experimental conditions – to study the cortical network underlying listeners' sensitivity to the emergence and violation of complex acoustic regularities (characterized by repeating spectro-temporal patterns) in ongoing sound sequences.

Methods

Stimuli were sequences of 50ms pure tones arranged according to two different frequency patterns: **REG** – a regularly repeating pattern of 10 tones (a new pattern was generated for each stimulus), and **RAND** – a sequence of tones of random frequencies. Also included were periods of silence (scanner noise). Stimulus duration was randomized between 4 and 10 seconds, allowing ample time to detect the repetitions in **REG** sequences. A single, long sequence was built by presenting abutting sequences of **REG**, **RAND**, and 'Silence' periods, in a randomized fashion. In this way, the nature and the timing of the transitions were completely unpredictable. 16 naïve participants participated in the study. They performed an incidental visual (n-back) memory task while passively listening to the different auditory sequences.

Results

Our results revealed a network consisting of auditory cortical sources (primary auditory cortex A1, and planum temporale bilaterally; extending in the left hemisphere along the superior bank of the superior temporal gyrus) and inferior frontal gyrus, demonstrating an interplay between early sensory processing and 'higher level' frontal mechanisms in the course of regularity extraction, even in the absence of directed attention. Preliminary DCM and Bayesian Model Selection (BMS) results suggest that the detection of regular patterns is mediated by recurrent dynamics within a hierarchical network comprising temporal and frontal sources. Furthermore, we show that modulation of both forward and backward connections, as well of intrinsic connections within primary auditory cortex, are necessary to explain the data. Overall, our results suggest that the regular behaviour of sound sources, even in the absence of directed attention, influences connectivity both within and between hierarchically organized areas.

PS-699

Physiologically Based, Spatial Sound-stream Segregation Using Stimulus Reconstruction: Proof-of-concept

Junzi Dong; Steven Colburn; Kamal Sen
Boston University

We present a physiologically based, computational network model of spatial sound-source segregation in the auditory cortex, and show preliminary work using the outputs of this model to segregate mixed-source acoustic speech stimuli. The model is based on a previous study in the zebra finch, where neurons in Field L, the analog of mammalian primary auditory cortex, showed increased spatial sensitivity to target sounds in the presence of a competing masker as compared to single-source stimulation (Maddox et al., 2012, PLoS Biology). When a single sound source is presented in space, the model responds broadly to all spatial locations. However, when the model is presented with multiple sound sources from different spatial locations, it generates a neural response that mainly represents a single acoustic source from the selected direction. This model suggests a possible mechanism through which spatial information is reorganized at the cortical level. With the outputs of this model, one can perform spatial sound-source segregation of a desired source location by using stimulus reconstruction to convert this neural response back to the acoustic domain. Here, we show that the sound segregation model matches a population of recorded neurons, and present the preliminary steps taken towards using the output of the model to segregate multi-source speech stimuli. We present a proof-of-concept study where we reconstruct the neural outputs of a peripheral Jeffress-type localization model—a simple model that preferentially responds to one direction. This peripheral model serves as input to the cortical model, and the reconstruction of the peripheral model outputs is a proof-of-concept test. We then quantitatively and qualitatively assess the quality of spatial sound-source segregation by comparing it to the non-segregated equivalent and listening to the reconstructed stimulus.

PS-700

Using Cortical Auditory Evoked Potentials to Predict Speech Feature Discrimination in Infants

Barbara Cone; Spencer Smith; Diane Cheek
University of Arizona

Introduction

There are no clinical methods to assess speech-feature perception in infants, making it difficult to determine how infants with hearing loss access the information in speech during a crucial period of language and speech development. The goal of this research was to identify cortical auditory evoked potential (CAEP) markers of vowel perception that could be translated into a clinical tool to predict infant speech perception abilities.

Methods

Twenty-seven normally hearing infants (aged 4-12 months) participated in this study. For the CAEP measurements, 500

ms synthesized speech tokens (/a/ /i/ /o/ /u/) were presented an odd-ball paradigm via loudspeaker. CAEP component amplitudes and latencies were measured in response to each token when it was used either as a standard (75% probability) or as a deviant (25% probability). The odd-ball sequences were presented at 1 and 2/s. CAEPs were obtained from the infants while they were awake and engaged in passive play. The infant's ability to discriminate vowel tokens was measured in another session using observer-based psychophysical methods. Infant-and-observer pairs underwent a brief training in which behavioral responses (typically, a head turn) to the "change" token were reinforced with a visual display. During testing, reinforcers were available only for a correct detection of the vowel change token.

Results

CAEP latency and amplitude varied with respect to the vowel contrasts, the order in which they were presented and the rate of stimulation. These differences reflected the underlying acoustic differences between the contrasting tokens, the effect of direction of spectral change in vowel formants, and the influence of neural adaptation. Significant differences in CAEP amplitudes for a vowel contrast were obtained at higher rates than perceptual responses for the vowel token change, although there were modest correlations between CAEP parameters and perceptual performance found for some vowel contrasts.

Conclusions

CAEPs for vowel contrasts is an indicator of the underlying neural capacity to encode spectro-temporal differences in vowel sounds. This technique holds promise for translation to clinical methods for evaluating speech perception.

PS-701

Cortical Encoding in Juvenile Animals During a Psychometric Task

Melissa Caras; Dan Sanes
New York University

The relationship between neural activity and perceptual performance in adult animals increasingly has been addressed by simultaneously measuring behavioral and electrophysiological responses while animals actively engage in a perceptual task. This approach often reveals a subset of neurons with neurometric properties that can account for psychophysical thresholds. However, developing animals generally display poorer perceptual sensitivity than adults, suggesting that the neural representation might also be degraded. To explore this possibility, recordings were made from the auditory cortex of freely moving juvenile gerbils as they performed an amplitude modulation (AM) detection task. Using a Go-Nogo paradigm, hit and false alarm rates were obtained as animals detected a range of AM depths, and a metric of perceptual sensitivity (d') was fit to obtain a psychometric function for each testing session. Single and multi-unit activity was recorded telemetrically from chronic microelectrode arrays on a trial-by-trial basis during task performance. Firing rates and harmonic power (at the AM rate of 5 Hz) were quantified and used to calculate d' neurometric functions. Neural and perceptual performance were tracked across at least 10 consecutive days, often from the same recording site. We found that the neural sensitivity of individual sites could not account for the perceptual performance of juvenile gerbils. This finding suggests that during development, AM depth perception may rely on coordinated activity amongst a larger network.

PS-702

Relating Behavioral and Electrophysiological Measures to Spatial Release from Masking in Individual Subjects

Ross Maddox; Adrian KC Lee
University of Washington

In realistic conditions, a listener often attempts to focus on one sound in a mixture of many with distinct spatial origins. While we are remarkably adept at performing this feat, it is a fragile ability that depends on a healthy auditory system capable of coding and interpreting fine temporal cues. Listeners with elevated audiometric thresholds are understandably less able to listen selectively, but they are not the only ones who struggle—even some listeners with normal hearing as measured by clinical tests report significant difficulty. Recent work has related impoverished brainstem frequency-following response with poor performance in speech understanding tasks. These results suggest that poor monaural temporal coding may drive some listeners' difficulties, but they do not account for downstream processing issues, particularly in midbrain nuclei that are critical to binaural spatial processing. We sought to improve our understanding of the role of spatial processing integrity in listening ability in noise.

We recruited subjects with normal hearing thresholds with and without self-identified difficulty listening in noise or locating sounds. In four sessions, we collected self-report data from the SSQ Questionnaire, behavioral data from a number of established psychoacoustical tasks of spatial release from masking as well as more basic binaural and monaural tasks, and electrophysiological measurements from EEG recordings using stimuli designed to test binaural and monaural coding fidelity. We related the results across individuals to determine how different levels of auditory processing affect listening ability and perceived listening difficulty.

While we are only part way to the full planned sample ($N \approx 40$), some correlations have emerged. The importance of monaural temporal coding for binaural processing was confirmed, but it does not fully explain performance variations in speech-on-speech listening task.

Listening to speech in noisy conditions is a complex process that depends on accurate coding of stimuli, binaural processing, and higher order attentional and cognitive mechanisms. The present study will shed some light on the variation of these processing stages across the population and how each contributes to individuals' listening abilities.

PS-703

Sensitivity to interaural time differences in envelope and fine structure, individually and in combination

Agnes Leger[1]; Michael G. Heinz[2]; Louis D. Braida[3]; Brian C.J. Moore[4]

[1]University of Manchester; [2]Department of Speech, Language, and Hearing Sciences, Purdue University, West Lafayette, IN, USA; Weldon School of Biomedical Engineering, Purdue University, West Lafayette, IN, USA; [3]Research Laboratory of Electronics, Massachusetts Institute of Technology, Boston, MA, USA; [4]Department of Experimental Psychology, University of Cambridge, Cambridge, UK

Two types of temporal information occur in sounds: slowly varying overall amplitude – the temporal envelope (ENV) – and more rapidly varying short-term fluctuations, the temporal fine structure (TFS). Hearing loss and/or age do not greatly affect the processing of ENV, but tend to reduce the ability to process TFS (even at frequencies with normal audiometric thresholds). Here, binaural processing of ENV and TFS cues was investigated for normal-hearing (NH) and hearing-impaired (HI) listeners by measuring thresholds for detecting different types of interaural time difference (ITD) in low-frequency amplitude-modulated sinusoidal carriers. All listeners had normal audiometric thresholds at the test frequencies. Listeners with a wide age range (19 to 71 years for NH) and (20 to 78 years for HI) were tested, but the mean age was greater for the HI than for the NH listeners.

For the first test, ITD detection thresholds were measured when the ITD was present either in the modulator (ENV-ITD), with the carrier in-phase at the two ears, or in the carrier (TFS-ITD), with synchronous modulators at the two ears, or in both the modulator and the carrier phase. TFS-ITD detection thresholds were also measured for an unmodulated carrier. For the second test, the trading of ENV-ITD and TFS-ITD cues was evaluated by presenting stimuli with the ENV-ITD and TFS-ITD values corresponding to the respective detection thresholds measured previously for each listener in a given condition. Those two ITDs were either congruent (same lateralization) or incongruent (different lateralization). For both tests, the comparison stimulus was diotic.

The HI listeners had higher TFS-ITD thresholds than the NH listeners, despite normal audiometric thresholds at the test frequency. This effect may have been driven by age. Across all listeners, mean TFS-ITD thresholds were significantly correlated with age. ENV-ITD thresholds were similar for the two groups. Thresholds for detecting an ENV-ITD were much higher than those for detecting a TFS-ITD (when expressed in units of time). For both groups, trading results suggest a super-additivity of ENV- and TFS-ITDs for congruent lateralization, and incomplete cancellation for incongruent lateralization, suggesting that those cues were processed independently.

Overall, these results support the hypothesis of a deficit specific to TFS processing in the aging/impaired auditory system.

PS-704

Assessing Temporal Fine Structure Processing Indirectly: Combining AM detection with BMLD

Nicolas Wallaert[1]; Marine Rambaud[2]; Dan Gnansia[3]; **Christian Lorenzi**[4]

[1]Ecole normale superieure, Paris; [2]DEC, UMR CNRS LSP, Ecole normale superieure, France; [3]Neurelec - Oticon Medical; [4]UMR CNRS LSP, Departement d'Etudes Cognitives, Ecole normale superieure

Several studies suggest that ageing and sensorineural hearing loss (SNHL) impair the processing of temporal fine-structure (TFS) cues while sparing the processing of temporal-envelope (E) cues. However, this deficit in TFS processing may partly result from reduced "processing efficiency". This raises the need to design tasks assessing TFS-processing capacities while limiting the contribution of reduced processing efficiency. We designed a novel psychophysical task aiming to assess TFS-processing capacities indirectly. We assessed TFS-processing capacities via an amplitude-modulation (AM) detection task, where efficiency was assumed to be normal for both elderly and SNHL listeners. Here, the audibility of the AM was controlled by the magnitude of the Binaural Masking Level Difference effect, BMLD, which in turn was controlled by the accuracy of TFS encoding in the auditory periphery (and known to be reduced normal for both elderly and SNHL listeners). The goal of this pilot study was to determine whether cochlear damage alters AM detection because of degraded TFS encoding.

All stimuli were presented binaurally. The task consisted in detecting a slow (20 Hz) sinusoidal AM applied to a low-frequency (0.5kHz) pure-tone carrier. This tone was always presented against a narrowband noise masker centered at 0.5kHz, and its audibility (and thus, the audibility of the superimposed AM) was altered by changing its interaural phase (its TFS). The SNR was fixed at: 0, +3 or +6dB The target tone was presented diotically (NoSo condition) and dichotically (NoSπ condition). It was reasoned that reduced BMLD (caused by poor TFS encoding) would result in poor AM detection, whereas large BMLD (caused by good TFS encoding) would result in good AM detection.

AM detection threshold were measured in normal-hearing (NH) and hearing-impaired listeners (HI) with mild-to-moderate SNHL at 0.5kHz. Normal or better-than-normal AM detection in quiet and in noise (NoSo condition) was found for HI listeners, supporting the hypothesis that processing efficiency for E perception is normal despite SNHL. Reduced BMLD for AM detection was found for HI listeners at +3dB SNR. The deficit was mild but significant.

These results suggest that a TFS-processing deficit affects indirectly the ability to detect AM in noise for HI listeners. This is consistent with the notion that HI listeners have reduced ability to use TFS cues, and that this deficit is not due to reduced processing efficiency for TFS perception.

PS-705

Assessing Temporal Fine-Structure Processing: "Derived Measures"

Nicolas Wallaert[1]; Amandine Grousseau[2]; Dan Gnansia[3]; Christian Lorenzi[2]

[1]Ecole normale superieure, Paris; [2]Ecole normale superieure, Paris, UMR CNRS LSP, Dept d'Etudes Cognitives, Institut d'Etude de la Cognition; [3]Neurelec

Several studies suggest that ageing and cochlear damage degrade the ability to use temporal fine-structure (TFS) cues. However, these deficits may partly result from reduced "processing efficiency". The latter reflects high-level (i.e. cognitive) factors such as the ability to concentrate, the fidelity of the short-tem memory, and the ability to make an optimal decision. Here, we assessed the effect of changing (center) audio-frequency on perceptual scores in several auditory tasks in order to separate sensitivity to TFS and processing efficiency for normal-hearing (NH) and hearing-impaired (HI) listeners. If processing efficiency is the same for extraction of TFS information at two (low) frequencies, then the effect of efficiency should cancel out when subtracting perceptual scores measured at each frequency, leaving only the temporal factor. It was reasoned that derived scores (estimated for each task) should be affected by cochlear damage and/or ageing if the latter affects the roll-off of phase locking to TFS cues in auditory-nerve fibers.

Psychoacoustic measures of sensitivity to TFS were obtained at two low centre frequencies of 0.5 and 1 kHz. We measured: i) thresholds for detecting a sine frequency modulation (FM) of 5 Hz (a masking sine AM (5 Hz) was added to the FM tone to disrupt excitation-pattern cues), (ii) thresholds for detecting a change in interaural phase (IPD), and iii) the "binaural masking level difference" effect (BMLD) which involves detection of a pure tone in noise, in diotic and dichotic conditions. Psychoacoustic measures of sensitivity to temporal-envelope cues were also obtained at the same centre frequencies by measuring thresholds for detecting a 5-Hz, sine amplitude modulation (AM). In each task, the derived score was computed by subtracting perceptual thresholds at the two center frequencies. Two groups of young and elderly NH and HI listeners participated in this study.

Preliminary results showed that only the derived measures assumed to rely on the fidelity of TFS encoding (FM, IPD, BMLD tasks) were affected by cochlear damage and ageing. These pilot data are consistent with the notion that cochlear damage and ageing degrade the accuracy of neural phase locking to TFS cues.

PS-706

Using Individual Differences to Test the Role of Temporal and Place Codes in the Representation of Frequency Modulation

Kelly Whiteford; Andrew Oxenham

University of Minnesota

Background

Whether frequency and frequency modulation (FM) is coded by peripheral place (tonotopy) and/or time (phase-locking) cues is a classic and ongoing debate. It is generally believed that FM detection at low rates (< 10 Hz) and low carrier frequencies (< 4 kHz) is assisted by phase locking to temporal fine structure (TFS), whereas FM at higher rates and carrier frequencies may be coded primarily via phase-locking to temporal envelope cues, reflecting cochlear frequency selectivity. We compared FM detection at low and high rates with tasks thought to reflect phase-locking (binaural FM disparity detection) and frequency selectivity (forward masking patterns). We predicted that sensitivity to interaural time differences should predict FM detection at low rates, whereas the slopes of the forward-masking patterns should predict FM detection at high rates.

Methods

Several psychophysical tasks were used to measure sensitivity to TFS cues, envelope cues, and frequency selectivity in 30 normal-hearing listeners, using adaptive threshold tracking. To isolate TFS cues with a 500-Hz carrier, slow FM tones (f_m = 1 Hz) were presented with different starting phases in the two ears, creating a moving, lateralized percept. An analogous task was completed for fast FM (f_m = 20 Hz), slow amplitude modulation (AM), and fast AM. Detection thresholds were also measured for diotic slow FM, fast FM, slow AM, and fast AM. Frequency selectivity was estimated via a forward-masking pattern produced by a 500-Hz pure-tone masker.

Results

Correlations between and within FM and AM thresholds were generally high (i.e., r = .6 for dichotic vs. diotic slow AM). Thresholds for slow dichotic FM tones were substantially and significantly better than slow FMDLs, confirming the role of phase-locking to low-frequency TFS in binaural interaural discrimination. Fast dichotic FM thresholds were similar to their diotic counterpart. Preliminary analyses suggest a lack of support for either of the main hypotheses, as masking-pattern slopes did not correlate significantly with fast (or slow) FM. In addition, measures designed to isolate phase locking from binaural processing did not correlate with similar monaural measures, even at the slow FM rate. Principal components analysis revealed 60% of the variance across all tasks could be explained by a single extracted component.

Conclusions

Across our group of normal hearing listeners, there was a tendency for people who performed well in one task to perform well in other tasks. Little remaining variance could be explained in terms of phase locking or frequency selectivity.

PS-707

Performance of Naive Listeners on Auditory Tasks

Daniel Shub
University of Nottingham

In studies of perceptual learning, there is a relationship between how much subjects learn and their initial performance. To provide insight into perceptual learning, this study investigated if performance of naive individuals is limited by a general auditory/cognitive ability, the perceptual saliency of auditory cues, or the efficiency of task relevant neural populations. Ninety seven naive young healthy listeners were divided into three groups with listeners from each group being measured on two tasks: frequency and level discrimination, interaural time difference (ITD) and interaural level difference (ILD) discrimination, and N_0S_0 and N_0S_π tone-in-noise detection. Two estimates of threshold were made with an adaptive staircase with both low (0.5 kHz) and high (4 kHz) frequency tonal signals in every tasks except for ITD discrimination where only the low frequency signal was used.

The average performance of the naive subjects in all tasks is much worse than previous reports with highly experienced subjects. There are large individual differences in the measured performance, but the range is consistent with reports of initial performance in studies of perceptual learning. While there is no evidence of within session learning, there is a statistically reliable correlation between the first and second runs in all tasks except for the ITD discrimination task. The correlation between frequency and level discrimination is not statistically reliable suggesting a limited role of general auditory/cognitive ability in the performance of naive listeners. The correlation in performance across the two signal frequencies is consistently reliable across all the measured tasks suggesting that either the relative neural efficiency does not vary within an individual or that the efficiency of neural populations has limited influence on performance of naive listeners. There is a relatively low correlation between ITD and ILD discrimination where the perceptual cue is nominally similar and a relatively high correlation between N_0S_0 and N_0S_π detection performance where the perceptual cue is nominally different. The generally poor performance on ILD discrimination task, however, means that loudness may have provided an additional informative perceptual cue in ILD discrimination that is absent in ITD discrimination. Further, with the low frequency signal there was no binaural masking level difference suggesting that both detection tasks may have been based on the same perceptual cue. Overall, the pattern of correlations suggests that the perceptual saliency of cues varies across individuals and may be a good predictor of naive performance.

PS-708

In Search for the Cochlear Neuropathy Component of Audiometric Hearing Loss

Sarah Verhulst[1]; Frauke Ernst[2]; Steven van de Par[2]
[1]Oldenburg University; [2]Cluster of Excellence "Hearing4all", Dept. of Medical Physics and Acoustics

The finding that cochlear neuropathy can greatly reduce the number of auditory nerve-fibers available to encode sound while leaving auditory thresholds intact, has significantly changed our views on hearing loss. Human perceptual consequences of cochlear neuropathy are likely related to coding fidelity of supra-threshold sound, and more pronounced in noisy scenarios where redundancy in auditory information coding is important. Recent studies have focused on isolating this component of hearing loss in normal-hearing listeners and reported correlations between EEG metrics and psychoacoustic tasks targeting temporal coding precision, that were uncorrelated to audibility. However, it is not known how cochlear neuropathy interacts with the well-studied outer-hair-cell-loss component of hearing loss, or whether cochlear neuropathy is equally important.

This study tries to find answers through the design of psychoacoustic tasks with various types of masking noise to target performance either to be limited by the auditory filter width (broadband noise), or by temporal coding fidelity (narrowband noise). We tested both clinically normal-hearing listeners and listeners with mild-to-moderate losses, and correlated our results with a metric of pre-neural performance (DPOAE growth), and one of brainstem coding fidelity (ABR and EFR).

In the broadband noise condition, signal-to-noise ratios for pure-tones at fixed stimulus levels were dominated by the audiometric losses. The higher the loss, the smaller the decrease of performance as stimulus level increased, consistent with the idea that the increase of the amount of noise entering auditory filters as stimulus level increases is less pronounced for subjects that already have wider filters at lower stimulus levels. In the narrowband conditions, people with elevated thresholds often outperformed normal-hearing listeners. Cochlear neuropathy, as a loss of redundancy of coding within a single auditory filter, may be counteracted by cochlear compression loss leading to effective modulation depth enhancement at the output of the individual filter for listeners with elevated thresholds, compared to normal-hearing listeners that don't have this compression loss benefit. We are currently further analyzing these results in relation to the recorded otoacoustic emission and brainstem EEG metrics to see whether individual differences in performance are caused by differences in cochlear mechanics, or whether reduced coding fidelity at the auditory brainstem can explain these results.

PS-709

Comparing Behavioral and Physiological Measures in Chinchillas Before and After Moderate Noise Exposure

Ann E. Hickox; Sandra Carbajal; Michael K. Walls; Amanda C. Maulden; Kelton M. Verble; Michael G. Heinz
Purdue University

Until recently, the recovery of audiometric thresholds following noise exposure was generally taken as an indication of a recovered cochlea and auditory system. However, a myriad of recent animal studies show that moderate-level acoustic overexposure can lead to permanent loss of cochlear synapses, or synaptopathy, while thresholds remain normal. This raises the question of how the central auditory pathway and perception may be altered by this disruption of primary auditory-nerve signaling. Recent studies in humans suggest that this kind of disruption may impair temporal coding in the auditory brainstem and impair ability to use temporal cues. In both animal and human studies, auditory brainstem response (ABR) wave-1 amplitude reduction in the absence of threshold shift is taken as a measure of cochlear synaptopathy. Here, we examine auditory behavior in chinchillas exposed to moderate noise levels shown to produce ABR wave-1 amplitude decrement and recovered thresholds, suggestive of cochlear synaptopathy. This behavioral model of "hidden hearing loss" will allow us to evaluate directly the perceptual consequences of this subclinical hearing impairment.

Adult male chinchillas were trained using a positive-reinforcement operant-conditioning paradigm to perform tasks of auditory detection and discrimination. Animals initiated trials by pressing and holding a lever, then released the lever to indicate that a sound was either detected or was different from a standard stimulus played during the hold time. Parameters were varied to build psychometric functions from which detection/discrimination thresholds were calculated in three different tasks: 1) tone-in-quiet detection; 2) masked tone-in-noise detection; and 3) amplitude-modulation-depth discrimination. All three tasks are measured both before and after acoustic overexposure designed to induce cochlear synaptopathy with normal cochlear thresholds (assessed by ABRs and by distortion-product otoacoustic emissions). Behavioral and physiological measurements made at frequencies with more vs. less ABR wave-1 decrement provide a further intra-animal control of the effects of putative cochlear synaptopathy vs. other noise-exposure effects.

By comparing pre- and post-exposure behavior in the same animals, along with physiological assessments of cochlear threshold and auditory-nerve health, we aim to correlate supra-threshold perceptual abilities with indicators of cochlear synaptopathy. Furthermore, by comparing results from a test comparable to a clinical audiogram (tone-in-quiet) with more challenging perceptual tests (tone-in-noise and amplitude-modulation-depth discrimination), we aim to provide further evidence for which clinical tests may be most useful in diagnosing noise-induced hidden hearing loss.

PS-710

Normal Thresholds but Poorer Hearing in Noise in Rats Following a "Deafferenting" Noise Exposure

Edward Lobarinas; Christopher Spankovich; Colleen Le Prell
University of Florida

Noise exposures that generate robust temporary threshold shifts (TTS) but fail to produce permanent threshold shift (PTS) can produce damage to afferent auditory fibers; this afferent loss has been suggested to result in a latent form of hearing loss. The functional correlates of this "hidden" hearing loss have been speculated to potentially include hearing in noise problems or perhaps tinnitus. Here, we explicitly assessed the relationship between a robust TTS and listening in noise deficits. We first assessed thresholds in adult SASCO rats using both electrophysiolological [auditory brainstem response (ABR)] and behavioral (pre-pulse inhibition paradigm) techniques. We determined thresholds for narrowband signals in the presence of competing broadband noise by varying the signal to noise ratio (SNR) between 0-40 dB. Animals were then bilaterally exposed to an 8-16 kHz octave band of noise at 109-dB SPL for two hours under ketamine anesthesia. Both ABR thresholds and distortion product otoacoustic emission (DPOAE) amplitudes showed results consistent with a robust 30-40 dB TTS 24 hours post exposure. We observed complete recovery of ABR thresholds and DPOAE amplitudes at two weeks post exposure. However, some animals showed reduced ABR wave I amplitudes despite complete recovery of thresholds. When animals were re-evaluated behaviorally, the subjects with incomplete recovery of ABR Wave I amplitude showed poorer thresholds in noise but no evidence of threshold shift in quiet. Behavioral deficits were not observed in animals with complete recovery of Wave I amplitude. The data suggest that poorer hearing in noise may correlate with reduced wave I ABR amplitudes even when thresholds in quiet remain unaffected.

PS-711

Simulating Speech Understanding in Noise for Hearing Impaired Listeners

Jessica Monaghan[1]; Arkadiusz Stasiak[2]; Ian Winter[2]; Matthew Wright[1]; Stefan Bleeck[1]
[1]University of Southampton; [2]University of Cambridge

Understanding speech in noise is challenging for hearing-impaired (HI) listeners, and hearing aids can provide only limited benefit. As well as elevated thresholds for hearing, supra-threshold deficits such as loudness recruitment and reduced frequency and temporal resolution contribute to difficulties experienced by HI-listeners in complex listening environments. Recent experiments in our laboratory suggest that intelligibility of speech in noise in moderate-to-severely HI listeners is lower than would be predicted by simulations of hearing loss. Here, we assess a simulation of speech-in-noise performance for HI listeners in which spectral smearing is used to simulate reduced frequency selectivity (Baer and Moore, 1993), the effects of deafferentation (Lopez-Poveda

and Barrios, 2013) and broadening the temporal integration window were included in the simulation. We also investigated whether increases in intelligibility for HI listeners provided by speech enhancement algorithms could be reproduced in simulated conditions.

Appropriate parameters for the different simulation conditions were determined by measuring the masking release obtained by adding either a temporal or spectral notch when detecting a tone in a band of noise. Data from normal-hearing (NH) participants listening through the simulation were compared with data from HI listeners. Speech recognition scores for sentences in noise were measured for HI listeners and for NH listeners listening under simulations of hearing impairment. To determine whether simulation can be used to predict any benefit provided by speech enhancement algorithms, scores were also measured for noisy speech processed by a Wiener filtering algorithm known to improve intelligibility of speech in noise for HI listeners.

Preliminary data indicate that a large degree of spectral smearing (five times normal) is sufficient to simulate the performance of very mild-to-moderately HI listeners, but that temporal degradation may be necessary to simulate the effects of more severe hearing loss, particularly at low frequencies. Simulation with spectral smearing alone was unable to reproduce the improvements found for HI listeners when speech enhancement was used. However, when temporal smearing was applied similar improvements were seen with speech enhancement.

Spectral smearing alone was sufficient to simulate the effects of very mild-to-moderately hearing loss on speech-in-noise intelligibility. However, preliminary results indicate that simulation of degradation of temporal processing may be necessary to simulate some aspects of listening in noise for HI people particularly for those with greater levels of hearing impairment.

References

Baer T, Moore BCJ (1993) J. Acoust. Soc. Am. 94, 1229-1241.

Lopez-Poveda, EA, Barrios P (2013) Frontiers in Neuroscience 7 (online)

PS-712

Cortical Mechanisms of Sound Localization in the Pallid Bat

Khaleel Razak[1]; Stuart Yarrow[2]; Dustin Brewton[1]
[1]University of California, Riverside; [2]Edinburgh University

The auditory cortex is required for sound localization behaviors, but how the cortex represents spatial information is unclear. A common feature of auditory cortex is the presence of binaural clusters. A recent study of the pallid bat auditory cortex showed that the intrinsic organization of a binaural cluster contains a substrate for systematic changes in the extent of active cortex with sound azimuth (Razak, 2011, J. Neurosci.). This suggests that azimuth location is represented by changes in the area (extent) of activated cortex. The main goal of the present study was to determine how the elevation of the sound source influences the extent of active cortex.

Pallid bats hunt terrestrial prey by passively listening to prey-generated noise. The auditory cortex of the pallid bat contains a tonotopic region with characteristic frequency (CF) between 5-35 kHz and selectivity for broadband noise that mimics prey-generated noise. Single unit recordings were obtained from pentobarbital-anesthetized pallid bats. The 2D spatial receptive field (SRF) of each neuron was determined by presenting broadband noise transients at multiple azimuths (spanning 75^o on either side of midline) at 15^o resolution and multiple elevations (spanning 60^o on either side of 0^o elevation) at 30^o resolution. Polar plots of the 2D SRFs were generated and the centroid, together with the polar radius of gyration about the centroid, was calculated for each SRF. SRFs were determined for at least two different intensities between 10-40 dB above threshold.

The radii of gyration of the SRFs measured at different intensities changed by less than 0.4^o/dB indicating relative stability of SRF extent with intensity. The azimuth angles of the centroids were distributed across the contralateral sound field and showed no relation to the CF. This indicates that each isofrequency band has access to the same range of azimuth centroids as any other band. The elevation angle of the centroid, however, was correlated (r^2=0.49, $p<0.0001$) with the CF, with high CF (20-35 kHz) neurons showing sensitivity to upper elevations and low CF (8-15 kHz) neurons showing sensitivity to lower elevations. These data indicate the systematic spread of cortical activity with azimuth will be constrained by the elevation of the sound. The computational rule for this constriction will be guided by the overlap of tonotopy with binaural clusters. These data are consistent with known effects of bandwidth on localization in the elevation plane and suggest a possible mechanism of elevation coding in the auditory cortex.

PS-713

Fine Spatial Representation of Interaural Level Differences in the Auditory Cortex: a Two-Photon Imaging study.

MARIANGELA PANNIELLO; ANDREW KING; JOHANNES DAHMEN; KERRY WALKER
University of Oxford

Introduction

Hearing research has been revolutionized by the recent introduction of in vivo two-photon (2P) calcium imaging, thanks to the high spatial sampling rate of this technique. The topographic representation of sound frequency, recognized as the main organizational principle of primary auditory cortex (A1), has been shown to be absent at a fine spatial scale (within tens of micrometers) in mice. Here, we used 2P calcium imaging in mouse A1 to investigate the spatial arrangement of neuronal responses to sound level differences between the two ears (Interaural Level Differences; ILD) at a much higher spatial resolution than has previously been possible. Previous extracellular recording studies have described bands or clusters of neurons with similar binaural interaction proper-

ties, and the only evidence for a topographic organization of ILD sensitivity across the auditory cortical surface has been reported in bats.

Methods
Stereotaxic injections of an AAV vector carrying GCaMP6m, a genetically encoded calcium indicator, were performed in A1 of mice aged 6-7 weeks. 2P imaging of auditory cortical activity was carried out 3-6 weeks later in anesthetized animals. During imaging, we presented binaural noise bursts over a 0-30 dB ILD range (average binaural levels: 60, 80 dB SPL), monaural bursts and pure tones (2-50 kHz, 4 attenuation levels).

Results
Among the responsive neurons, the majority responded to ILD noise bursts and not to pure tones. We found a patchy arrangement of binaural preferences. In cortical fields as small as 200 μm², neurons usually showed high heterogeneity in their ILD preferences. However, some imaging fields showed clusters of neurons with common ILD preferences. These were often found adjacent to clusters with very different ILD tuning, which together sometimes spanned both contralateral and ipsilateral locations. Noise correlation between pairs of neurons decreased as the distance between the cells increased, suggesting the presence of local subnetworks. We did not find evidence for binaural bands in the mouse AC.

Conclusions
These results are in accordance with previous electrophysiology studies that propose a poorly ordered spatial representation of ILD in the AC at a large spatial scale. However, the dense spatial sampling of 2P imaging demonstrated that locally clustered ILD preferences exist among neighboring auditory cortical neurons.

PS-714

The Effect of "Awake and Behaving" on Cortical Processing of Binaural Spatial Cues

Nathan Higgins; G. Christopher Stecker
Vanderbilt University

Measurement of brain activation in awake and behaving subjects is ideal for understanding functional processing and resulting behavioral responses. Separating out the independent contributions of sensory processing, task-related attention, and the motor response prior to behavior can be difficult, particularly with fMRI, an imaging modality with limited spatial and temporal resolution. Previous studies on human auditory cortex (AC) have revealed modulation effects of task-related attention, and AC is known to send projections to motor cortex and striatum. However, many unanswered questions regarding the interaction of stimulus features, task-related activation, and behavioral responses remain.

To further explore this topic, continuous event-related fMRI was used to measure cortical responses to trials of amplitude-modulated noises varying parametrically in interaural level (ILD) or time (ITD) differences. Participants engaged in a task, varying across epochs of 10 trials each of which potentially carried a target of any type: location (change in ILD or ITD), pitch (change in burst rate), or visual (change in brightness). Subjects indicated the direction of each target when cued. Following preprocessing, functional data were subjected to a standardized hemodynamic regression analysis and parcellated into regions of interest (ROIs) using Freesurfer.

Analysis of cortical activity in two well known auditory ROIs (Heschl's, and Superior Temporal Gyrus) revealed increased response magnitude for trials associated with a response (button press) versus no-response trials. This result was observed in both left and right hemisphere, despite a right-hand only button press by participants. Comparison of correct versus incorrect-responses showed a trend towards increased magnitude in correct responses, and a greater contralateral dominance for ILD and ITD, the conventional response profile for BOLD tuning to horizontal positions. Finally, cortical activation during no-response/non-target trials was significantly increased for the auditory tasks (location and pitch) compared with the visual task. This effect was independent of non-target stimulus changes presented in each block and provides support for modulation of cortical sensitivity as a function of task-related attention.

This study provides evidence that auditory cortex is engaged in generation of an appropriate behavioral motor response. The increased BOLD activation on response trials tends to obscure tuning to binaural cues, creating a noisy response across the binaural stimulus range. A similar trend was observed as greater activation associated with correct versus incorrect responses, suggesting the auditory cortex plays a pivotal role in attending, detecting, evaluating, and initiating behavior as a result of auditory stimulation.

PS-715

Spike-Frequency Adaptation in the Barn Owl's ICX

Roland Ferger; Natalja Ciganok; Hermann Wagner
RWTH Aachen University

Adaptation has been observed in many nuclei of the auditory pathway. One aspect of adaptation is that a neuron's response may decrease during an ongoing stimulus. This kind of adaptation is called spike-frequency adaptation. We investigated spike-frequency adaptation as a function of the bandwidth of a stimulus in the external nucleus of the inferior colliculus (ICX) in the barn owl. This bird is a specialist in sound localization. For localizing sound sources in the horizontal plane it relies primarily on the interaural time difference (ITD). An auditory space map is formed in ICX by combining binaural cues for azimuth and elevation and integrating across frequency channels.

Extracellular recordings were obtained from neurons in ICX. The stimuli (each 300ms duration, 5ms onset/offset ramps, combination of most effective binaural cues) were presented via earphones. The stimulus level was chosen to elicit 50% of the saturating response. Broadband noise as well as band pass filtered noise of one octave or one third octave width and pure tones served as stimuli. Band pass filtered nois-

es and tones were centered at the neuron's best frequency. Peri-stimulus time histograms (PSTH) were assembled from responses to 200 repetitions for each condition.

We observed four different response types in ICX: Most neurons respond "phasic-tonic" (or primary like) to broadband stimuli, i.e. with a strong onset peak followed by a sustained response over the whole stimulus length. The other types were "pure phasic" (only an onset peak and no sustained response) "pure tonic" (no onset peak but a constant response) and "pauser" (onset peak followed by a short pause and then a sustained response). Responses were more phasic for tones than for broadband noise. Similarly, response latency was shorter for pure tone stimuli than for broadband noise. We quantified the response patterns by fitting the decay slope of the phasic-tonic PSTHs. The best fitting function was a double exponential function, resulting in two distinct time constants, one below 5 ms and one in the range of several hundred milliseconds.

Neurons in the barn owl's ICX exhibit spike-frequency adaptation. Phasic-tonic responses were best fitted by a double-exponential function. The delay was shorter and the decay constant of the phasic response was faster for tones than for broadband noise.

PS-716

Experimental and Modeling Study on the Effect of Envelope Shape on the Sensitivity to Interaural Time Difference in the Inferior Colliculus

Le Wang[1]; David Greenberg[2]; Torsten Marquardt[2]; David McAlpine[2]; Mathias Dietz[3]

[1]Boston University; [2]University College London; [3]University of Oldenburg

The auditory system is sensitive to interaural time differences (ITD) in the fine structure and the envelope of sounds. Both human psychoacoustic data (Klein-Hennig et al. JASA, 2011) and the activity of single neurons in the inferior colliculus (IC) of guinea pigs (Greenberg et al. ARO 2014) revealed that the ongoing envelope-ITD sensitivity is dominated by the steepness of the amplitude modulation (AM) rise and by the pause duration prior to each modulation onset.

Single neuron activities of the IC in guinea pigs were recorded in response to 17 differently amplitude-modulated tones as the ITD of the stimulus was varied (data from Greenberg et al. ARO 2014). In the present study, four exemplary IC neurons were chosen to represent the range of response patterns seen in the IC population of this study. An IC model driven by inputs from a lateral superior olive (LSO) model was developed in the present study to reproduce the responses of the four example neurons. For each envelope shape, period histograms were computed for all ITDs, forming 17 2-D histograms per neuron. Contralateral and ipsilateral influences to the IC neurons were inferred from the 2-D histograms (e.g., onset vs. sustained, excitatory vs. inhibitory), and were used to determine the inputs to the LSO model. The membrane property of the IC and LSO model was fixed and the synaptic parameters of the LSO model were varied for each model neuron to fit the experimental data of the four exemplary neurons.

The detailed 2-D histogram analysis of the experimental data revealed that the envelope-ITD sensitivity of most IC neurons in this study stems from E-I type binaural interaction, which is likely to be inherited from the LSO. The variety of envelope shapes in this study allowed for disambiguation between alternative explanations and offers stronger constraints on the model than simple sinusoidal envelope shapes. By using different types of inputs and different synaptic parameters, the IC model was capable of reproducing the response patterns in all four example neurons with high accuracy.

The results demonstrate the utility of varying stimulus parameters (e.g., envelope shape) in single cell recordings for determining underlying neural mechanisms. Based on binaural inputs that were estimated for each individual cell, the IC model captures the main effects of the envelope shape on the ITD-sensitivity in the IC, i.e., the steepness of the AM attack and the pause duration prior to each AM attack.

PS-717

Intrinsic and Synaptic Properties of Dorsal Nucleus of the Lateral Lemniscus Neurons in the Avian Interaural Level Difference Coding Circuit

Rebecca Curry; Yong Lu

Northeast Ohio Medical University, Kent State University

Background

The central auditory system computes horizontal sound location through encoding binaural cues such as interaural level difference (ILD). In birds, the first central auditory nucleus encoding ILD is the dorsal nucleus of the lateral lemnsicus (LLD; formerly VLVp, the nucleus ventralis lemnisci lateralis pars posterior), and is functionally equivalent to the lateral superior olive (LSO) in mammals. Previous *in vivo* and histological studies have shown that LLD neurons receive excitatory inputs from the contralateral cochlear nucleus, as well as inhibitory inputs from the other LLD. However, little is known about the specialized morphological and physiological properties of LLD neurons that enable them to encode ILD.

Methods

Brainstem slices (300 μm) were prepared from late chick embryos (E17-E18) and early hatchlings (P0-P3). Whole-cell current and voltage clamp experiments were used to measure intrinsic and synaptic properties of LLD neurons at 35 °C. Cell morphology was revealed through biocytin and Lucifer yellow staining.

Results

Firing patterns of LLD neurons were broadly classified as either onset or tonic firing neurons, with further classification applied to tonic firing neurons, such as adaptive, pauser, or buildup. A rebound depolarization at hyperpolarized potentials was present in most onset neurons, but its presence and amplitude varied among tonic firing neurons. Onset firing neurons were less commonly encountered and generally had

few, short dendrites, while tonic firing neurons had either bipolar or multipolar dendrites. Tonic firing neurons appeared to receive matched excitatory and inhibitory synaptic inputs, whereas onset firing neurons received powerful excitatory inputs, but relatively weak inhibitory inputs. EPSCs were completely blocked by DNQX, an antagonist for glutamate AMPA receptors. IPSCs were completely blocked only with a combination of gabazine and strychnine, respective antagonists for $GABA_A$ and glycine receptors. Strikingly, stimulation of the one LLD elicited postsynaptic currents in neurons in the other LLD, with a mean delay of 8.5 ms (±1.6 ms, n = 4, distance ~4 mm). These currents were largely blocked by a combination of gabazine and strychnine, indicating reciprocal inhibitory connections between the two LLDs.

Conclusion

The LLD is composed of a heterogeneous neuron population. Subpopulations of the neurons may contribute to different aspects of ILD coding. The tonic firing neurons may encode ILD through integration of excitatory and inhibitory inputs from the contralateral cochlear nucleus and other LLD, respectively. The onset firing neurons in one LLD may provide inhibitory inputs to ILD-coding neurons in the other LLD.

PS-718

Pre and Postsynaptic Roles for α7 Nicotinic Acetylcholine Receptors in the Gerbil Medial Superior Olive

Sonia Weimann; Elise Esposito; R. Michael Burger
Lehigh University

The α7 nicotinic acetylcholine receptor (nAChR) has broad distribution throughout the mammalian brain (Dominguez et al. 1942; Marks et al. 1996; Morley et al. 1977). The functional properties of this receptor can vary based on it cellular location and developmental expression. Presynaptic expression of α7 nAChRs is known to facilitate neurotransmitter release due to it's high calcium permeability (Albuquerque et al. 1997; McGehee et al 1995) while postsynaptic expression can have broad effects including the regulation of gene expression, neuron survival, and the mediation of excitatory currents. Happe and Morley (2004) showed that, the α7 nAChR is richly expressed in the superior olivary complex (SOC). However, physiological relevance within nuclei involved in the computation of sound location has yet to be determined.

We examined the expression of the a7 nAChRs and VAChT within the MSO using immunohistochemistry (IHC). IHC was performed on paraformaldehyde (PFA) fixed tissue from gerbils aged p9-p60 (a7 nAChR: mouse monoclonal; 1:400; Sigma; cat. #M220; VAChT: rabbit polyclonal 1:500; Synaptic Systems; cat. #139103). The tissue was counterstained with MAP2 (chicken;1:1000; Neuromics; cat. #CH22103). Tissue was examined using confocal microscopy. The functionality of α7 nAChRs was examined using in vitro whole-cell patch clamp on brain stem slices obtained from gerbils age P9-15. Measurements of sEPSC amplitude and frequency were taken during application of agonist, acetylcholine (ACh) and antagonist, methyllycaconitine (MLA) for evidence of the synaptic location of α7 nAChR activity. Additionally, carbachol, a cholinergic agonist, was applied using a 250 mS puff while other drugs were bath applied.

Our results demonstrate that α7 nAChRs are expressed in the gerbil MSO across development. Furthermore, IHC indicates the presence of VAChT positive sites apposing MSO principal cell somata and dendrites. These data combined show evidence for classical cholinergic signaling with the MSO. Bath application of ACh caused an increase in both the frequency and amplitude of sEPSCs indicating both pre and postsynaptic α7 nAChRs. Furthermore, puff application of carbachol evoked inward currents that were blocked by the α7 specific antagonist MLA. These data combined demonstrate the presence of functional α7 nAChRs on pre and postsynaptic sites within the MSO and that cholinergic signaling via α7 nAChRs does have physiological relevance in the mammalian sound localization pathway. This suggests that cholinergic signaling may contribute to the development of the sound localization circuitry or mediate excitatory currents involved in the precision of temporal coding.

PS-719

In Vivo Intracellular Responses of MSO Neurons to Binaural Amplitude-Modulated Beats

Tom Franken; Philip Joris
KU Leuven

Binaural amplitude-modulated beats (BAMB) have been used recently as a tractable stimulus to examine how sound localization can be effective in conditions of reverberation. For these stimuli, the amplitude modulation (AM) frequency is equal to the beat frequency, so that one AM cycle contains all IPDs, and each IPD is fixed at a specific phase of the AM cycle. IPDs during the rising slope of the AM cycle dominate perception, even though this does not reflect the acoustically dominant IPD. Extracellular recordings in IC and MSO confirmed a dominance of rising slope IPDs for most neurons. A model suggested that adaptation before binaural interaction was responsible for this phenomenon.

To investigate the mechanism of dominance of the rising slope, we recorded intracellular *in vivo* responses from gerbil MSO neurons to BAMB. Carrier frequency was near the best binaural frequency. AM frequency was between 4Hz and 32 Hz. Binaural beat sign was alternating positive and negative. Stimuli were interaurally in phase at the maximal amplitude of the stimulus. Furthermore, responses were collected for monaural AM tones and unmodulated binaural beats.

For most neurons, binaural spike rates to BAMB were higher for the beat sign for which the best IPD to unmodulated binaural beats was in the rising part of the AM cycle. The average membrane potential showed phaselocking to the carrier frequency as well as to the modulation frequency. In agreement with adaptation of the excitatory inputs, we observed skewing of the monaurally driven average membrane potential towards the rising part of the AM cycle. Within an AM cycle, the number of monaural EPSPs as well as the average EPSP amplitude were usually larger for the rising part of the

cycle. However, monaural action potentials usually showed more pronounced skewing towards the rising part of the AM cycle than the subthreshold responses, suggesting that postsynaptic mechanisms enhance the response to the rising part of the cycle.

To conclude, we successfully obtained *in vivo* intracellular responses of MSO neurons to BAMB and monaural AM tones. Consistent with a previous report, binaural spike rate was higher when the best IPD occurred during the rising rather than the falling phase of the AM cycle. Skewed subthreshold responses towards the rising part of the cycle directly showed adaptation of the inputs, and combine with postsynaptic processes to produce the dominance of the rising slope.

PS-720

Binaural Response Prediction from Monaural Inputs in the Gerbil Medial Superior Olive

Andrius Plauška[1]; Marcel van der Heijden[2]; J. Gerard Borst[2]

[1]Erasmus MC, University Medical Center Rotterdam; [2]Department of Neuroscience, Erasmus MC, University Medical Center Rotterdam

Background

The Medial Superior Olive (MSO) is a binaural nucleus in the mammalian auditory brainstem that plays a prominent role in the localization of low-frequency sounds. MSO cells are specialized to detect the coincident arrival of inputs from both ears. Each MSO cell responds maximally to a particular interaural time difference ('best ITD'). Differences in the internal delay between sound arrival at either ear and arrival of the input at the MSO are thought to be important for ITD tuning, but it is not yet known to which extent the binaural responses can be predicted from the monaural responses to both ears. We made juxtacellular recordings in the gerbil MSO to test to how well binaural responses to broadband stimuli can be predicted by cross-correlation of monaural responses.

Methods

Juxtacellular recordings from principal neurons of the MSO were made from anesthetized Mongolian gerbils using a ventral approach, as described previously (van der Heijden et al, 2013). Closed-field auditory wideband tone complex stimuli were generated using MATLAB algorithms. Analysis was restricted to cells showing binaural responses.

Results

Juxtacellular recordings allowed us to measure the subthreshold response of individual MSO neurons to sound presentation at a single ear. We then cross-correlated both monaural responses to get a prediction of the expected ITD response of each cell and compared it with the recorded spike rates to binaural sound presentation. For the cells which passed the criteria, the predicted and measured best and worst ITDs correlated well ($r > 0.8$), with occasional differences in general shape of predicted and measured ITD responses.

Conclusion

Monaural responses provide enough information to predict not only best ITD but also in many cases the overall shape of ITD tuning of neurons in the gerbil MSO. This suggests that the binaural responses of MSO cells are well described by a straightforward coincidence detection of the monaural inputs, and the contribution of local preprocessing of the inputs is limited.

PS-721

In Vivo Recordings from Low-frequency Nucleus Laminaris in the Barn Owl

Nicolas Palanca-Castan[1]; Christine Köppl[2]

[1]Carl von Ossietzky University, Oldenburg; [2]University of Oldenburg

Introduction

Humans and animals with good low-frequency hearing make extensive use of interaural time differences (ITDs) to locate the origin of sounds. The first stage that processes ITDs is the nucleus laminaris (NL) in birds and the medial superior olive (MSO) in mammals. Both are tonotopically organized. At high frequencies (>3 kHz), the barn owl's NL conforms to a delay-line model in which arrays of systematically arranged cells create a representation of auditory space, with different cells responding maximally to specific ITDs. However, recent studies suggest that the low-frequency regions could use a different system (Harper and McAlpine, 2004, *Nature* 430:682-686). Here, we address this question and present the first extensive dataset from the low-frequency region of barn owl NL.

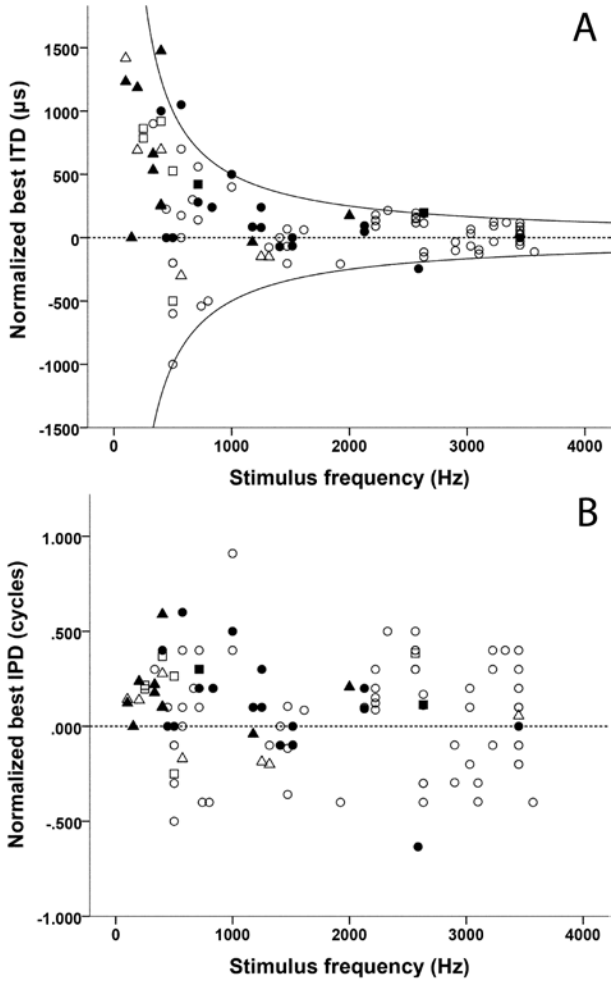

Methods
We recorded responses (single units and neurophonics) from the low-frequency NL of anesthetized owls. Best frequency (BF), best ITD, best interaural phase difference (IPD) and, for a subset of recording sites, characteristic frequency (CF), phase (CP) and delay (CD) were determined using pure tones. Selected sites were anatomically confirmed by placing a fluorescent label.

Results
The recorded responses showed a contralaterally biased distribution of best ITDs, distributed homogenously across the entire range at each frequency (supporting figure). The best IPD distribution was also homogeneous, with no clustering around specific values. Histological data revealed a frequency gradient and a best ITD gradient along the mediolateral axis of the low-frequency region of NL, as well as a weak frequency gradient along the rostrocaudal axis.

Discussion
The homogeneous distribution of best ITDs and IPDs is in agreement with previous studies on high-frequency NL and high- and low-frequency inferior colliculus in the barn owl (Wagner et al., 2007, Journal of Neuroscience 27(15): 4191-4200). It suggests an organization consistent with a delay-line model, for both low- and higher-frequency regions in the owl. Our data also suggest that the low-frequency region of owl NL contains a tonotopic organization similar to that of high-frequency regions (Carr and Konishi, 1990, *Journal of Neuroscience* 10(10): 3227-3246). Furthermore, we obtained evidence for a topographic organization of best ITD, similar to that in chicken NL (Köppl and Carr, 2008, *Biological cybernetics* 98(6): 541-559). In summary, these results argue against any significant change in ITD processing at lower frequencies in barn owl NL.

PS-722

Properties of Short-term Synaptic Plasticity in vivo in the Nucleus Laminaris of the Barn Owl

Thomas McColgan[1]; Paula T Kuokkanen[1]; Hermann Wagner[2]; Catherine Carr[3]; **Richard Kempter**[1]
[1]Humboldt-Universität zu Berlin; [2]RWTH Aachen; [3]University of Maryland

Short-term plasticity in early auditory synapses plays important roles in the processing of transient and ongoing stimuli, such as gain normalisation and enhancement of coincidence detection (Tsodyks et al, 1998; Cook et al, 2003). Recent in-vitro studies (Cook et al, 2003; Oline et al, 2014) have shown depressing excitatory synapses in avian auditory brainstem nuclei. We here present evidence from an in-vivo study of the barn owl nucleus laminaris.

The input to nucleus laminaris from the preceding nucleus magnocellularis has a high spontaneous firing rate (~200 spikes/s) and responds to tone bursts with a sharp increase of firing rate (~430 spikes/s, Peña et al, 1997). The spikes are strongly phase locked to the stimulus. The highly organised temporal structure of this input to the nucleus gives a rare opportunity to perform study of short-term plasticity in vivo.

To isolate synaptic contributions to the extracellular field potential, we recorded extracellularly from the nucleus laminaris while we acoustically stimulated the neural circuit using short binaural tone bursts. Then we applied pharmacological synaptic blockers and subtracted the responses after application from the baseline response. By comparing the time courses of different frequency ranges of the response, we were able to separate the synaptic adaptation effect from the spike-rate adaptation effect in the previous nuclei. We also manipulated the interaural time difference of the stimulus, allowing us to exclude possible postsynaptic effects.

The recorded responses showed an extracellular field-potential signature consistent with a model of synaptic short-term depression (Tsodyks et al, 1998), in which each action potential reaching a synapse releases a certain percentage of the available vesicles, and the vesicle reserve is replenished over time. The average over a large number of synapses then allows the derivation of the synaptic extracellular field potential response. We were able to fit the model to the responses and thus infer the properties of the adaptation, namely the percentage of synaptic vesicles released on every spike and the time constant of the replenishment of the vesicle reserve.

The findings allow us to compare the observed time constants and utilisation factors to results from previous in-vitro studies and gain a better understanding of the effects of synaptic depression under more lifelike conditions.

PS-723

Perforated Patch Clamp Revealed Kv Modulation by Metabotropic Glutamate Receptors in Chicken Nucleus Laminaris Neurons

William Hamlet; Yong Lu
Northeast Ohio Medical University

Background
Intrinsic neuronal properties are subject to modulation by second messenger systems via G-protein-coupled receptors (GPCRs) such as metabotropic glutamate receptors (mGluRs). Such a modulation regulates cellular excitability, spike timing, and signal processing. Nucleus laminaris (NL) neurons of the chicken brainstem encode the location of sound in horizontal space. Strong voltage-gated K+ (Kv) currents in these neurons are essential for their temporal processing. Group II mGluRs are expressed in NL neurons, likely on both presynaptic and postsynaptic loci. Using perforated patch clamp recording, which allows electrical access to the neuron without disrupting intracellular components of GPCR signaling cascades, we aimed to determine whether group II mGluRs modulate Kv currents and consequently alter firing properties of NL neurons.

Methods
Brainstem slices (250-300 µm) were prepared from late chick embryos (E17-E19). Whole-cell and perforated patch clamp experiments were performed on neurons in the low frequency region of the NL at room temperature. Control experiments revealed that it is possible to obtain stable perforated patch

clamp recordings using perforating substance nystatin. Pharmacological agents targeting mGluRs were bath applied.

Results
Under perforated but not conventional whole-cell voltage clamp recordings, pharmacological activation of group II mGluRs by DCG-IV increased the amplitude of Kv current. At the commanding potential of -15 mV the current increased dramatically, whereas at -50 mV the current remained unchanged, indicating that the high-threshold but not the low-threshold Kv component was modulated by group II mGluRs. No modulation of Kv currents was observed when cells were pretreated with a group II mGluR blocker LY341495. Under perforated current clamp recordings, activation of group II mGluRs enhanced outward rectification, sharpened action potentials evoked by somatic current injections, and improved the ability of NL neurons to follow train stimulations at high frequency.

Conclusion
Postsynaptic group II mGluRs enhance Kv currents and consequently modulate action potential firing properties in NL neurons in a way that improves the precision for timing coding.

PS-724

Synaptic Integration and Modulation in Chick Nucleus Laminaris Neurons with and without Hearing Loss

Yu-Wei Liu; Yong Lu
Northeast Ohio Medical University

Background
Neurons in the nucleus laminaris (NL) receive bilaterally segregated excitatory inputs from cochlear nucleus magnocellularis, via morphologically symmetrical dorsal and ventral dendrites. The bilateral excitatory inputs are physiologically symmetrical in both extracellular responses to sound stimuli and intracellular EPSCs and EPSPs evoked with synaptic stimulation. Such symmetry provides a unique opportunity to determine the effect of unilateral hearing loss with within-cell control. The excitatory transmission is subject to modulation by metabotropic glutamate receptors (mGluRs). However, there exist conflicting results regarding the subtypes of mGluRs involved as well as the differential modulation in different frequency coding regions of the NL. More importantly, it remains unknown whether the bilateral inputs are equally modulated, and to what extent unilateral hearing loss affects this symmetry.

Methods
Brainstem slices (250-300 μm thick) were prepared from chick embryos (E15-21) and early hatchings (P0-5) of both sexes. For hearing loss model, unilateral cochlea removal was performed in P1-3 animals. Voltage-clamp experiments were performed with an AxoPatch 200B amplifier. Bilateral extracellular stimulations were performed using two concentric bipolar electrodes, with one being placed on the ipsilateral NM, the other on the fiber tract ventral and medial to NL.

Results
The bilateral excitatory inputs to NL neurons had similar synaptic strength, kinetics, and short-term plasticity. The two excitatory inputs onto singe NL neurons were largely but not completely segregated, and integration of the inputs was sub-linear. More importantly, EPSCs in low frequency neurons were modulated by group I and II, but not III, mGluRs, and the degree of modulation was identical between the ipsilateral and contralateral inputs. None of the mGluR agonists had significant modulation on the glutamatergic transmission in middle and high frequency NL neurons, regardless of animal ages tested. Unilateral cochlea ablation tremendously reduced the excitatory transmission on the deprived dendritic domain of NL, measured at 24 hrs after the surgery. Interestingly and somewhat surprisingly, EPSCs evoked at the deprived domain were more strongly modulated by mGluR II than EPSCs evoked at the counterpart domain that received intact input.

Conclusion
mGluR subtype-dependent modulation of EPSCs in NL neurons is symmetrical between the bilateral excitatory inputs, which ensures balanced bilateral excitation and preserves the symmetry in synaptic strength under modulatory conditions. Unilateral hearing loss (24 hrs) reduced synaptic excitation and yet increased group II mGluR-mediated modulation of EPSCs, pointing to possible anti-homeostatic plasticity of excitation at this time point after sensory deprivation.

PS-725

Test-Retest Reliability of the Binaural Interaction Component (BIC) of the Auditory Brainstem Response (ABR) in Guinea Pigs (Cavia porcellus)

Alexander Ferber; Daniel Tollin
University of Colorado - Anschutz Medical Campus

The binaural interaction component (BIC) is the residual auditory brainstem response (ABR) after subtracting summed monaurally-evoked from binaurally-evoked ABRs. The β peak is the first negative peak of BIC, and it may have diagnostic value: altered β amplitudes and latencies in children and adults have been shown to correlate with and predict long-term behavioral binaural processing deficits. β amplitude also depends systematically upon binaural cues to location, exhibiting maximal amplitude for interaural time differences (ITDs) of zero (midline sources), and is often undetectable outside the physiological range. Using absolute BIC amplitude for diagnostic purposes may be challenging due to ABR and β amplitude variability within and across subjects.

Investigating BIC test-retest reliability in guinea pigs, we conducted five ABR/BIC measurements per animal in 3 adult animals under ketamine/xylazine anesthesia on different days. At minimum, three viable re-tests were completed per animal. Recordings were made with needle electrodes at the apex (active), nape (reference) and hind leg (ground) using click stimuli (rate: 33/sec) at 80 dB SPL (~40 dB SPL re: threshold). 500 repetitions (excluding EKG artifact rejections) per

monaural and binaural condition were recorded across an ITD range spanning ± 2000 μsec, bandpass filtered (0.1-3kHz) and averaged. BIC was calculated (described above) for each ITD. β amplitude variability, potential sources, and mitigation strategies were assessed.

ABR and β amplitudes varied between and within subjects across recording sessions, despite consistent ABR thresholds. Within subjects, β amplitudes varied by up to ~50%; similarly, ABR wave amplitudes (e.g. Wave III) varied by up to 35% or more. Within-animal correlation analysis revealed that β amplitudes varied across tests proportionally with parent ABR amplitudes, suggesting that common experimental factors (e.g. electrode depth, contact quality, precise electrode location, earphone placement) and other factors that generally reduced signal to noise ratio likely account for variability in both waveforms. While monaural and binaural absolute amplitudes changed concordantly between tests, the overall shape of β amplitude dependence on ITD did not, suggesting that the binaural system could still be reliably probed, even under non-optimal recording conditions. Several normalization strategies to facilitate comparisons between different-amplitude recordings were considered.

Care must be taken to minimize variability when measuring BIC for individual diagnosis or across-subject comparison. Despite such efforts, test-retest variability can persist. However, binaural characteristics of BIC were retained across tests despite variance in absolute amplitude of monaural and binaural ABRs. Accordingly, we discuss relevant parameters and strategies for BIC comparison.

PS-726

Effects of Cochlear Implant use on Binaural Processing

James Fallon; Sam Irving; Andrew Wise; Dexter Irvine
Bionics Institute

Introduction

Bilateral cochlear implantation is increasingly common, particularly for young children, and results in an increase in performance for both sound localization and speech discrimination in noise compared to unilateral implantation. However, the improvements are small and performance remains inferior to that of normal listeners. Animal and psychophysical studies have shown that long-term deafness from a young age degrades processing of interaural time differences (ITDs) but not interaural level differences (ILDs). The effects of chronic bilateral cochlear implant use on binaural processing are less clear; therefore we examined the effects of chronic bilaterally cochlear implant use on ITD and ILD sensitivity in long-term neonatally deafened animals.

Methods

Three groups of cats were used: two normal hearing controls (NHC), two neonatally profoundly deafened unstimulated cats (NDUS) and four neonatally profoundly deafened cats that received approximately 6 months of bilateral intra-cochlear electrical stimulation from clinical cochlear implants and speech processors (NDS). Single-unit responses (n= 110, 60, 86 for the NHC, NDUS and NDS groups respectively) to electric binaural stimulation with a range of ITDs and ILDs were bilaterally recorded from both central nuclei of the inferior colliculus using 32-channel silicon arrays (NeuroNexus).

Results

ITD sensitivity was significantly poorer in both the neonatally deafened groups compared to the normal hearing animals (Kruskal-Wallis test, $p < 0.05$), and there was no difference between the stimulated and unstimulated groups ($p > 0.05$). ILD sensitivity was not different between the groups ($p > 0.05$).

Conclusions

The use of bilateral clinical cochlear implants does not prevent/reverse the degradation in ITD processing that occurs following long-term deafness from a young age. Whether experience with appropriate ITD cues would improve ITD processing still needs to be examined. ILD processing is largely unaffected by either long-term deafness or chronic stimulation.

We thank Nicole Critch, Amy Morley, Damian Robb for technical assistance.

PS-727

The Role of Spectral and Temporal Cues in Binaural Fusion

Corey Shayman; Julia Stelmach; Akila Prasad; Deepa Suneel; Justin Aronoff
University of Illinois, Urbana-Champaign

Introduction

There is a growing population of individuals with single sided deafness (SSD) that have a cochlear implant in their deaf ear. These patients receive an acoustical signal in their hearing ear and an electrical signal in their deaf ear from their cochlear implant. Although these patients do eventually develop binaural abilities, those abilities are considerably slower to develop than they are for individuals receiving bilateral cochlear implants. This study investigated whether unilateral spectral and temporal compression may play a role in diminishing binaural abilities by preventing binaural fusion and whether bilateral temporal cues can help restore that fusion.

Methods

Two experiments measured normal hearing listeners' binaural fusion by asking them to determine if they heard the same sound in both ears (fused) or a different sound in each ear. For Experiment one, twelve individuals with normal hearing were presented with vocoded speech stimuli where one ear was spectrally or temporally compressed. The spectral compression mimicked what occurs when mapping an acoustic signal onto the relatively short cochlear extent covered by an implant array. The temporal compression was akin to what occurs in the electrically stimulated ear without the cochlear traveling wave delay. For Experiment two, participants were given nonsense stimuli that were spectrally reversed in one ear with or without a bilaterally matched temporal cue.

Results
In Experiment one, as expected, when both ears received the same signal, participants perceived a fused sound (96% fusion). In contrast, the perception of a fused sound was greatly reduced when there was unilateral spectral (2%) or temporal (54%) compression. In Experiment 2, adding bilateral temporal cues increased fusion from 2% to 52%.

Conclusion
The results from Experiment 1 indicated that unilateral spectral and temporal compression, both of which occur with SSD patients, reduce binaural fusion. However, as indicated from the results from Experiment 2, using bilateral temporal cues can foster binaural fusion, potentially providing a means to improve these patients' binaural abilities.

PS-728

Impaired Recognition of Musical Sound Quality Deterioration in Cochlear Implant Users: Sample Rate and Comb-Filtering

Judy Doong; Alice He; Patpong Jiradejvong; Charles Limb
Johns Hopkins University

Music perception mediated by cochlear implant (CI) remains limited for most CI users, with significant impairments in pitch and timbre perception, as well as reductions in sound quality. The factors that are responsible for reductions in sound quality remain poorly understood. In this study, we sought to quantify the impact of specific manipulations in sample rate and comb-filtering on sound quality for CI users and normal hearing control subjects. We hypothesized that CI users would demonstrate impairments in their ability to recognize sound quality deterioration introduced through sample rate or comb-filtering manipulations. We used CI-MUSHRA (Cochlear Implant-Multiple Stimulus with Hidden Reference and Anchor), a sound quality assessment method, to examine sound quality ratings based on sample rate and comb-filtering. Two sets of stimuli were created from real-world musical stimuli to investigate sample rate and comb-filtering separately. Sample rate modifications were created with the reference at 44.1-kHz, and sample rates of 22.05-, 16-, 11.025-, 8-, 4-, and 1-kHz (anchor) for stimuli versions. Comb-filtering manipulations attenuated a set of harmonically related frequencies by creating notches with equal bandwidths of 0.033 normalized frequencies from original reference sound samples. Stimuli versions were created by attenuating 10, 20, 30, 40, 50, and 60 notches (anchor), equally spaced over the interval of [-1, 1] normalized frequency. For both tests, a labeled and unlabeled reference (hidden reference), the altered versions, and anchor were presented to the listener simultaneously under the CI-MUSHRA paradigm. Listeners rated the stimuli from 0 to 100 based on sound quality differences perceived between the stimuli. Twenty-five musical stimuli (5s duration) were presented for both sample rate and comb-filtering manipulations. Compared to normal hearing listeners, CI users were generally worse at differentiating sound qualities between stimuli as a function of both sample rate and comb-filtering. Normal hearing listeners were able to significantly differentiate between each stimulus for both tests, while CI users could not. Specifically, for comb-filtering, CI users could not significantly differentiate between the reference, stimuli with 10, 20, 30, and 40 notches of frequencies attenuated. For sample rate, they could not significantly differentiate between the reference, 22.05-, 16-, 11.025-, and 8-kHz sampling rate. CI users have an impaired ability to detect sound quality deterioration based on sample rate and comb-filtering manipulations. These factors should be considered in the development of CI technology and sound processing strategies specifically directed towards improvement of music perception in CI users.

PS-729

Mandarin Tone Identification in Cochlear Implant Users Using Exaggerated Pitch Contours

Alice He[1]; Judy Doong[2]; Patpong Jiradejvong[2]; Charles Limb[2]
[1]Johns Hopkins University; [2]Johns Hopkins University School of Medicine

Background
Cochlear implant (CI) users demonstrate significant impairment in pitch perception. This impairment is particularly evident in tonal languages, such as Mandarin Chinese, in which meanings of words are encoded by pitch contours. In this study, we sought to determine the impact of exaggerated pitch contours on Mandarin tone identification. In particular, we wanted to determine the minimum difference in pitch range needed for normal hearing (NH) listeners and CI users to identify tone contours modeled after Mandarin tones. We hypothesized that CI users would exhibit significantly greater differences in minimum pitch range than normal.

Methods
Nine NH listeners and 6 CI users were tested for their ability to correctly identify tone of sound stimuli from a 5-alternative forced-choice paradigm in which the pitch range of each contour sweep was decreased successively. The five contours were: flat, rising, dipping, falling, peaking. We used Praat to create two series of pure tone pitch contours (centered around 150Hz for male and 250Hz for female versions). Participants also took another version of the test using pre-recorded words from native Mandarin speakers. These stimuli were subsequently compressed (smaller interval) or exaggerated (larger interval) about the median frequency of each word. Four alternatives were offered here. Participants were presented with free field sound stimuli and asked via touchscreen to identify the tone that best represented the sound heard. The pitch range covered by each stimulus was decreased until participants could no longer consistently identify tones with >70% accuracy.

Results
For tests using pure tones, CI users demonstrated a 41.72Hz (SD=31.1) interval requirement to attain >70% accurate tone discrimination, while NH listeners required a 3.98Hz (SD=1.6) interval ($p<0.001$). In the modified versions, CI users required a 59.58Hz (SD=44.3) pitch range, also significantly higher than NH listeners' threshold of 5.06Hz (SD=9.0) ($p<0.001$). There was no difference in performance within groups using

male vs. female stimuli. NH listeners performed significantly better at pure tone identification ($p<0.05$), while CI user performance did not vary between pure tone and voice identification ($p>0.05$).

Conclusions
Compared to NH participants, CI users required significantly greater pitch ranges to identify pitch contours modeled after Mandarin tones. These results demonstrate markedly impaired ability for CI users to identify tonal contours, and suggest that the use of exaggerated pitch contours may be helpful for tonal language perception. These findings may have useful implications for future CI sound processing strategies directed specifically towards improving tonal language perception.

PS-730

The Relationship between Insertion Angles, Default Frequency Allocations, and Spiral Ganglion Place Pitch with Cochlear Implants

David Landsberger[1]; Maja Svrakic[2]; J. Thomas Roland[2]; Mario Svirsky[2]
[1]New York University; [2]New York University School of Medicine

Introduction
Commercially available cochlear implant systems attempt to deliver frequency information going down to a few hundred Hz, but the electrode arrays are not designed to reach the most apical regions of the cochlea which correspond to these low frequencies. This may cause a mismatch between the frequencies presented by a cochlear implant electrode array and the frequencies represented at the corresponding location in a normal hearing cochlea. In the following study, the mismatch between the frequency presented at a given cochlear angle and the frequency expected by an acoustic hearing ear at the corresponding angle is examined for the cochlear implant systems that are most commonly used in the United States.

Methods
The placement of each of the electrodes on four different electrode arrays (MED-EL Standard, MED-EL Flex28, Advanced Bionics HiFocus 1J, and Cochlear Contour Advance) is examined in 92 ears. For the angular location of each electrode on each electrode array, the predicted spiral ganglion frequency was estimated. The predicted spiral ganglion frequency was compared with the center frequency provided by the corresponding electrode using the manufacturer's default frequency-to-electrode allocation.

Results
Differences across devices were observed for frequencies below 650 Hz. Longer electrode arrays (i.e. the MED-EL Standard and Flex28) demonstrated smaller deviations from the spiral ganglion map than the other electrode arrays. For insertion angles up to approximately 270 Hz, the frequencies presented at a given location were typically approximately an octave below what would be expected by a spiral ganglion frequency map, while the deviations were larger for angles deeper than 270 Hz. For frequencies above 650 Hz, the frequency to angle relationship was very similar across all four electrode models.

Conclusions
A mismatch was observed between the predicted frequency and default frequency provided by every electrode on all electrode arrays. The mismatch can be reduced by changing the default frequency allocations, inserting electrodes deeper into the cochlea, or allowing cochlear implant users to adapt to the mismatch.

PS-731

The Sung Speech Corpus (SSC): A Database/ Task to Measure Speech in Music Perception

Joseph Crew[1]; John Galvin[2]; Qian-Jie Fu[2]
[1]University of Southern California; [2]University of California - Los Angeles

Pitch and timbre contribute differently to speech and music perception. Typically, pitch and timbre perception are measured independently in music and/or speech, even though everyday listening includes both pitch and timbre cues (e.g., prosody, vocal emotion). While normal hearing listeners might be able to combine or segregate these cues, hearing impaired individuals have greater difficulty. Interventions such as combined acoustic-electric hearing may improve access to both pitch and timbre cues. However, the relative contributions of acoustic and electric hearing have been typically evaluated with independent speech and music tests, using very different stimuli and methods which may emphasize or de-emphasize the contribution of pitch and timbre cues to the perceptual task. It may be desirable to test speech and music perception using a single database that contains musical pitch, timbre and speech information. To address this issue, we have recorded and evaluated the Sung Speech Corpus (SSC).

The SSC consists of sung monosyllable words. Each word was sung at all thirteen fundamental frequencies (F0) between A2 (110 Hz) to A3 (220 Hz) in semitone steps. The words were chosen to fit in a Matrix Sentence Test with the following syntax: "name" "verb" "number" "color" "article of clothing." E.g., "Bob sells three blue ties." Each category consists of ten words; given a total of five categories, the SSC contains a total of 100,000 possible unique sentences. After recording, all productions were normalized to have the same duration and amplitude; minor pitch adjustments were applied to each the exact target F0. Natural speech utterances were also produced for each word.

Word and sentence recognition can be evaluated with the SSC using a closed-set task in which there are ten possible response choices within each category (5 x 10 matrix). Pitch contour perception can also be measured with the SSC stimuli in the same way as the Melodic Contour Identification task. The semitone spacing for the pitch contours can be varied from 1 to 3 semitones for some measure of pitch resolution. In either task, pitch or speech perception is measured with changes in timbre and pitch respectively across the se-

quence. The SSC stimuli provides both lexical information as well as some melody information, and results in a more complex perception than is typically measured in speech or music perception tasks. These stimuli better represent the complex pitch and timbre cues present in everyday listening.

PS-732

A MEMS Based Stimulating Cochlear Implant with Integrated Microfluidics for Drug Delivery

Eric Kim; Hongen Tu; Michael Chen; Jinsheng Zhang; Yong Xu
Wayne State University

Cochlear implant technology over the past three decades has provided a powerful modality for the restoration of hearing in patients with sensorineural hearing loss. The basic structure of these implants includes a flexible probe with electrodes along its length that can be inserted and coiled around the curved structure of the cochlea. Recently, micro electrical mechanical systems (MEMS) technology has been employed to produce microfluidic drug delivery systems targeting the inner ear for the treatment of cochlear and auditory nerve degenerative processes; however these systems so far have lacked electrical stimulation capabilities. Using a novel MEMS fabrication process, we have successfully produced an parylene-polymer silicon hybrid cochlear implant device with integrated microfluidics capable of both electrical stimulation and precise fluidic drug delivery via individually addressable fluidic channels. Fabrication relies on a layering approach which produces microchannels below the layer of the device that includes the microelectrodes, interface pads, and electrical communications. For the first layer, an isotropic XeF2 gas etch method is used to etch silicon in a pattern and produce continuous trenches that act as hard molds that shape the walls of sealed micro channels after the deposition of a second layer of parylene-C. On top of this second parylene-C layer gold contact pads, microelectrodes, and communicating wires are formed. To insulate the electric metal components and provide a final encapsulation layer, a third layer of parylene-C is deposited and patterned to open holes exposing micro electrodes, contact pads, and the end of microfluidic channels to act as fluidic exit ports. Finally, silicon of the device is etched away in specific regions to free the flexible parylene-C probe and to shape a rigid interface chip. After device packaging, the gold microelectrodes are electro-plated with iridium oxide to improve the stimulating capabilities of the device. The final device is a hybridization of a rigid silicon interface chip and a flexible parylene-C polymer probe region with iridium oxide coated microelectrodes along the probe's length and parylene-C microchannels traveling underneath the electric layer. Thanks to the design flexibility of the fabrication process, microelectrodes and microfluidic exit ports can be positioned at any location in the device. In our current prototypes, we have microfluidic exit ports, each with an individual microchannel, immediately adjacent to microelectrodes to optimize targeting of drug delivery to the area of greatest effect.

PS-733

A Novel Cochlear Implant for Electrical Stimulation in the Rat via a Minimally-Invasive Postauricular Approach

Michael Chen[1]; Eric Kim[2]; Yong Xu[2]; Jinsheng Zhang[1]
[1]Wayne State University; [2]Wayne State College of Engineering

Introduction

Cochlear implants for hearing restoration in humans often produce variable degrees of tinnitus suppression, yet there is no existing animal model to study these effects. We have developed a custom microfabricated device with electrochemical interfaces designed for chronic implantation in the rat. In the current study, we described a safe and reliable surgical approach to cochlear implantation in the rat via a post-auricular incision and confirmed *in vivo* stimulation.

Methods

The cochlear implant was assembled at Wayne State University using microelectricomechanical systems (MEMS) technology and packaged for chronic implantation. The intracochlear probe contained 4 thin-film electrodes. A postauricular surgical approach was adapted to expose the round window using minimal dissection to preserve normal anatomy and maximize residual hearing. Tympanostomy locations, including mean distances from surface landmarks, were recorded in six adult male Sprague-Dawley rats. One rat was implanted unilaterally. Pre- and post-implant auditory brainstem responses (ABR) were performed to compare hearing thresholds. Post-implant electrical ABR (EABR) between 25 uA and 2000 uA was performed to confirm delivery of electrical stimulation to auditory nerve fibers.

Results

Identification of the tympanic bulla was routinely achieved via postauricular soft tissue dissection with preservation of the facial nerve and cartilaginous ear canal. The tympanostomy was performed on the tympanic bulla with mean distances of 5.1 ±0.4 mm superior to the mastoid tip, 2.8 ±0.3 mm posterior to the stylomastoid foramen, and 2.6 ±0.5 mm posteroinferior to the temporal line. The stapedial artery was frequently encountered and required electrocautery for hemostasis. The mean depth of the round window from the lateral wall of the tympanic bulla was 10.3 ±0.6 mm. Post-implant EABR using biphasic pulses delivered by the cochlear implant demonstrated identifiable auditory waveforms at a threshold of 400 uA. Pre- and post-implant click ABRs showed a hearing threshold shift from 5 to 45 dB in the implanted ear following the procedure.

Summary

The post-auricular surgical approach provides direct and minimally-destructive exposure of the round window in the rat. Our method of implantation appears to be feasible and preserves hearing. Future studies will investigate chronic implantation in additional animals to confirm long-term viability, and cochlear implant stimulation strategies to suppress tinnitus.

PS-734

Myographic Recordings of the Electrically and Acoustically Elicited Stapedial Reflex with a Chronically Implanted Recording Electrode

Dietmar Basta; Moritz Gröschel; Rolf Battmer; Arne Ernst
University of Berlin

Introduction

It is well-known that the electrically elicited stapedial reflex threshold (ESRT) correlates very well with the maximum comfortable level (C- or M-Level) and thus, is a viable tool with which to set upper stimulation limits when fitting cochlear implant (CI) recipients. Therefore, in many CI programs, ESRT is obtained intraoperatively by observing the stapedial muscle contraction. Postoperative evaluation of the muscle response using an impedance bridge is very time consuming and in many cases not possible due to middle ear disturbances of the contralateral ear. The aim of this study was to investigate the feasibility of making a myographic recording via a chronically implanted intramuscular micro needle electrode in guinea pigs.

Methods

Different recording electrodes were developed to suit the anatomical requirements and to easily penetrate the stapedial muscle. The ideal electrodes were prepared from a silicone coated Pt/Ir-wire which was uninsulated for 1mm and sharpened at the tip to 5µm. The reflex was elicited intraoperatively by either, contra-lateral acoustic stimulation, or by an ipsilateral dual biphasic pulse from a cochlear implant electrode. The recording electrode was left in place for 3 months. After 3 months the measurements were repeated and the muscle were removed for histological investigation.

Results

Myographic recordings of the stapedial reflex could be obtained in the monopolar and bipolar setup intraoperatively as well as after 3 months of chronic implantation. No migration of the electrode or macroscopic damages of the muscle were observed. Microscopic changes could be detected mainly at the insertion site as the result of healing.

Conclusion

The present study demonstrate that myographic signals can be reliably recorded via a chronically implanted electrode placed into the stapedial muscle. However, more work is required to improve signal strength and stability by stimulus optimization.

PS-735

Characterization of Middle Ear Effusion Proteins from Children with Chronic Otitis Media and Their Biological Effects on Human Middle Ear Epithelial Cells.

Stéphanie Val; Christie Demason; Samita Goyal; Kristy Brown; Yetrib Hathout; Mary Rose; Diego Preciado
Children's National Medical Center

Otitis Media (OM) is one of the most common conditions characterized by middle ear inflammation that leads to persistent mucoid effusions, characteristic of chronic OM. This study aims at characterizing the proteome of middle ear effusions (MEEs) from children having chronic OM and to further investigate the presence of MUC5B, MUC5AC and pro-inflammatory cytokines. The potency of MEEs to sustain OM was assayed using an *in vitro* model.

Six MEEs were collected from children undergoing myringotomy with tube placement at Children's National Medical Center (Washington, DC) for proteomics analysis using a liquid chromatography tandem mass spectrometry (LC-MS/MS). 16 other samples were collected for mucin Western Blot analysis and cytokine multiplex assay for pro-inflammatory cytokines, and used to expose human middle ear epithelial cells (HMEEC) to assay mucin and pro-inflammatory response by RT-qPCR.

Among the proteins identified by proteomics, 15 were common to all the samples. The mediators of the innate immunity complement proteins C3 and C4-A; the immunoglobulin Ig alpha/gamma/lambda/kappa/mu chain C and the antibacterial proteins lactotransferrin and serotransferrin, and MUC5B were detected in all the samples. Other proteins implicated in innate immunity and inflammation but less studied, such as long palate lung and nasal epithelium carcinoma associated protein 1 (PLUNC family), deleted in malignant brain tumors 1 protein, alpha 1 antichymotrypsin and protein S100-AS were also found by mass spectrometry and would need to be further studied for their implication in OM. The mucoid MEEs (14/16) were all positive for MUC5B but not MUC5AC by Western Blot analysis. The cytokine array assay showed very high average concentration for IL-8 (more than 30 ng/ml) and a moderate average level of TNF-α (max 0.1 ng/ml). The exposure of HMEEC to MEEs showed the potency of MEEs to sustain inflammation and mucus production, demonstrated by RT-qPCR.

This work shows an extensive study of MEEs proteins by mass spectrometry, and confirms the importance of the mucin MUC5B and the pro-inflammatory cytokine in COM. Their effect on HMEEC demonstrated the importance of MEE composition as it is able to sustain inflammation and mucus production. This study finally aims at investigating the implication of unknown proteins in COM development.

PS-736

A Paradoxical Effect of NTHi Lysates on Microtubule Dynamics of Middle Ear Epithelial Cells

Jeong-Im Woo; Sung-Hee Kil; Yoo Jin Lee; David Lim; Sung Moon
University of California, Los Angeles

Nontypeable *Haemophilus influenzae* (NTHi) is an opportunistic human pathogen, which usually results in localized mucosal infections such as otitis media and sinusitis. Recently, it has been reported that NTHi is able to cause invasive infections such as meningitis and sepsis. An alarming increase in the incidence of invasive NTHi infections has been observed due to the pathogenic shift associated with *H. influenzae* type b vaccination, making it a public health concern today. Here,

we aim to determine the role of innate immunity in the pathogenesis of invasive NTHi infections, focusing on antimicrobial peptides and microtubule dynamics, which may influence NTHi penetration of the epithelial barrier, an essential step for invasive infections. Bacterial transmigration assays showed that NTHi R2866, an invasive NTHi strain, transmigrates across the epithelial cells more than NTHi 12. The *htrB* mutant (B29), which is susceptible to DEFB4, appeared to transmigrate less across the epithelial cells than the parent strain. Viability assays showed that NTHi R2866 is more resistant to DEFB4 than NTHi 12. In contrast, the *opsX* mutant (R3743) was more sensitive to DEFB4 than the parent strain. "Live NTHi" is known to enhance microtubule polymerization of host cells *via* intergrin-mediated signaling, resulting in potentiation of NTHi invasion. On the contrary, "NTHi lysates" (i.e. bacterial components derived from dead NTHi) were found to paradoxically destabilize microtubules in the middle ear epithelial cells. Interestingly, we found that epithelial microtubules are destabilized in response to DEFB4-treated NTHi, but not to untreated NTHi. Stathmin, a microtubule destabilizer, appeared to be up-regulated upon exposure to the NTHi lysate. Gentamicin protection assays showed that epithelial invasion of NTHi is inhibited by indibulin, a microtubule destabilizer. Indibulin was found to up-regulate stathmin expression. Taken together, our results suggest that epithelial cells are able to attenuate NTHi invasion through modulation of microtubule dynamics mediated by defensin-induced release of bacterial components.

PS-737

The Pneumococcal PspA Protein is Essential for Formation of Neutrophil Extracellular Traps in Chinchillas with Otitis Media

Patricia Schachern[1]; Nicole Kwon[1]; Steven Juhn[1]; David Briles[2]; Patricia Ferrieri[1]; Sarah Goetz[1]; Sebahattin Cureoglu[1]; Michael Paparella[3]; Vladimir Tsuprun[1]
[1]University of Minnesota; [2]University of Alabama; [3]University of Minnesota & Paparella Institute

Introduction

Surface proteins of *Streptococcus pneumoniae* have been considered as vaccine candidates against pneumococci-induced otitis media. Our previous studies have shown that pneumococcal surface protein A (PspA) of *S. pneumoniae* strain D39, serotype 2 (D39) was less viable and virulent in chinchilla ears than its wild-type parent strain. The middle and inner ears present a challenge to the host defense system for containment of bacteria in a large air and/or fluid filled space, making neutrophil extracellular traps (NETs) a likely part of host response. We compared the presence of NETs in chinchilla middle and inner ears inoculated with D39 and its isogenic mutant ($PspA^-$).

Methods

Middle ears of 6 chinchillas that were inoculated with 0.5 ml of 10^6 CFU of D39 and 5 with 10^6 CFU of $PspA^-$ were killed two days later and middle ear effusion taken for CFU counts. Bullae were removed, fixed in 10% buffered formalin, decalcified, paraffin embedded, sectioned, stained with hematoxylin and eosin and examined by light microscopy, for the presence of bacteria and neutrophils embedded within a fibrous network (NETs) and other histopathological findings. Slides with NETs were stained with propidium iodide for DNA. Additional sections were immunostained with anti-fibrin antibodies. Because NETs were not seen 2 days after inoculation in any ears inoculated with $PspA^-$, we further studied if they may have formed earlier, but resolved prior to 2 days, inoculating the bullae of 26 additional chinchillas with 0.5ml of 10^6 CFUs of $PspA^-$ and killing them at 6,12,18,24,30, and 36 hours post-inoculation.

Results

Two days after inoculation, we observed bacteria and neutrophils within an extended fibrous network in 6/6 middle ears from the D39 wild-type strain, but in 0/5 ears inoculated with $PspA^-$ mutant. Although effusion CFU counts were 2 logs higher than inoculum levels in ears inoculated with D39, no bacteria were found in effusions of $PspA^-$ inoculated ears. No NETs were observed at any time period from 6 to 48 hours following inoculation with $PspA^-$, even though bacteria were found in some effusions up-to 30 hours post-inoculation.

Conclusion

NETs were observed in all ears inoculated with D39 at 2 days post-inoculation. They were not observed in any ears inoculated with PspA-, from 6 hours to 2 days. Although we currently do not understand the mechanism(s) involved in NET formation, PspA protein appears to play an essential role in their formation in experimentally induced pneumococcal otitis media.

PS-738

Targeting the Tympanic Membrane Identifies a Biological Mechanism of Active Transport to the Middle Ear

Arwa Kurabi; Kwang Pak; Andrew Baird; Allen Ryan
UCSD

Background

Otitis media (OM) is a serious disease, especially in developing countries where the burden of mortality or hearing loss is severe. Systemic antibiotics are often used to treat OM; however, recently this has been challenged due to their side-effects including antibiotic resistance and gastrointestinal disorders. While local treatment would avoid these issues, the tympanic membrane (TM) prevents drug penetration unless surgically breached. We hypothesized that the TM might harbor innate biological mechanisms that could mediate trans-TM transport.

Methods

We used M13 bacteriophage display biopanning to search for mediators of trans-TM transport. Aliquots of a phage library displaying 10^{10th} 12mer peptides were applied onto the TMs of rats undergoing OM, for 1 hr. The middle ear (ME) contents were harvested and amplified for additional rounds of selection. For recovered phage, transport rates, temperature/O2 dependence and competition with free peptide were determined.

Results
Several unique peptides were recovered from the TM screens. All peptide-bearing phage exhibited ME recovery significantly greater than that of wild-type (WT) phage, with transport rates of the best peptides being 10^{5th} to 10^{6th} above that of WT phage. Temperature and oxygen dependence indicate an active transport mechanism. Transport block by free peptide suggests involvement of a specific binding site.

Conclusions
Historically, the TM has been viewed as an impermeable barrier. However, our studies reveal that it is possible to translocate small particles across the TM. The identified mechanism offers a new platform drug delivery into the ME. Future aims include identifying the transporter and enhancing transport rates.

Funding Source/Disclosures
Supported by grants from the NIH/NIDCD (DC000129, DC012595), Action on Hearing Loss and the VA Research Service (BX001205).

Email: akurabi@ucsd.edu

PS-739

Human Middle Ear Morphology: New Data from MicroCT and PTA Staining

Daniël De Greef; Jan Buytaert; Johan Aerts; **Joris Soons**; Joris Dirckx
University of Antwerp

Introduction
In human middle ear (ME) morphologic research, some topics are still debated, while others can benefit from new quantitative data. New knowledge in these areas can potentially improve ME finite element modeling and surgery. Here, various morphological properties of ME components were studied.

Methods
Six human temporal bones were scanned using mCT, then stained using phosphotungstic acid (PTA) and scanned again. The mCT reconstructions were segmented and converted into surface models (Amira® 5.3; Figure 1). The ossicle joint angles before and after staining were measured.

Figure 1: surface models of ME structures

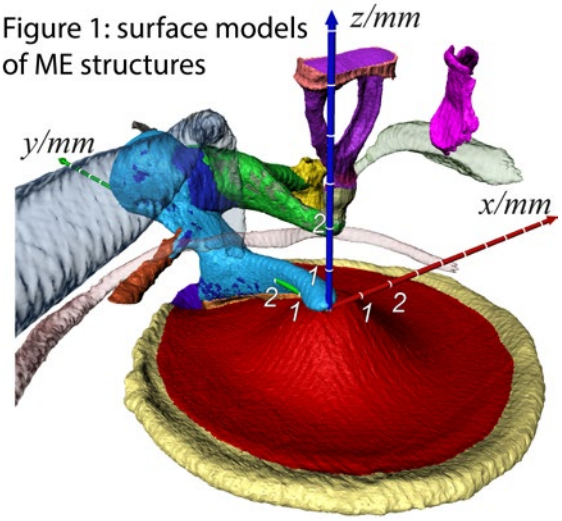

Figure 2: ME ossicular chain with surrounding mucosa (transparent) and ligaments (red)

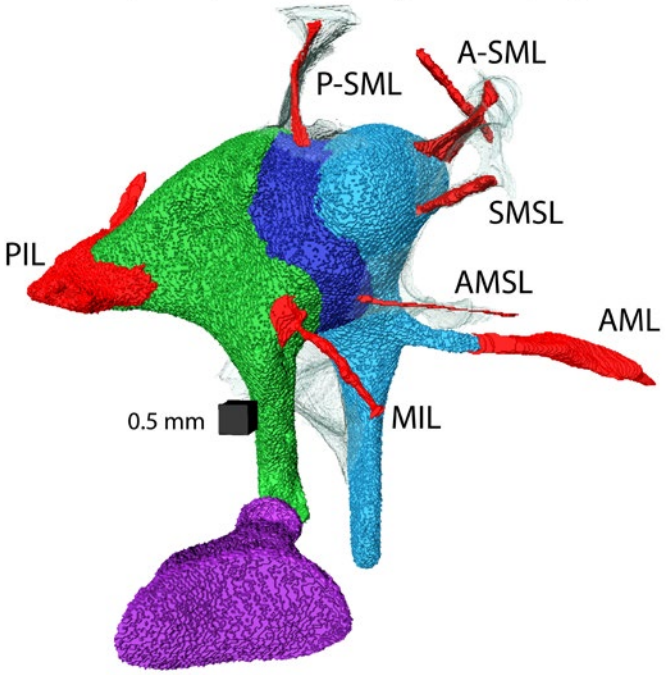

Figure 3: bony pedicle of the lenticular process of the incus in all samples.

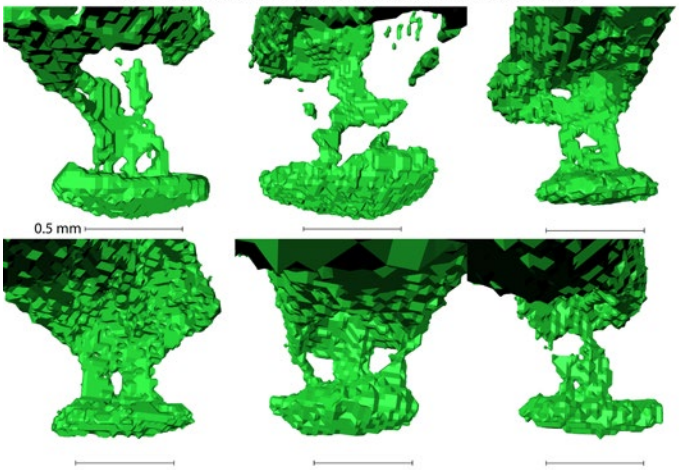

Results
The magnitudes of the ossicle joint angle differences between recordings were small (incudomallear: (1,10±0,67)°; incudostapedial: (1,3±1,0)°) and the direction of change was not consistent. Therefore, we conclude that the use of PTA staining does not decrease the validity of morphometric results.

Three ligaments (malleus: anterior(AML), lateral; incus: posterior(PIL)) were found in all samples, while eight were only present in some samples (malleus: anterior suspensory(AMSL), superior suspensory(SMSL), anterior superior(A-SML) and posterior superior(P-SML); incus: medial(MIL) and lateral; incudomallear joint capsule: medial; stapes: superior). The superior stapedial ligament has not been reported before. Figure 2 provides an impression of the ligaments in one sample.

The principal moments of inertia (PMI) and principal axes of rotation of the individual ossicles were calculated, both with and without inhomogeneities to account for internal blood canals. The influence of the canals on these parameters was shown to be insignificant, so solid ossicles in mechanical models are justified. It was furthermore calculated that the PMI of the incudomallear complex for rotation around the anatomical rotation axis (anterior mallear ligament – posterior incudal ligament) could be (37±7)% smaller if its center of mass was coincident with the anatomical axis.

The ratio of ossicular lever arms - defined by the respective distances from the umbo of the malleus and the lenticular process of the incus to the anatomical axis - was calculated to be (1,30±0,11).

The shape and dimensions of the bony pedicle, connecting the incus to its lenticular process, had large variations among individuals, but the bony connection between the incus and the process was nowhere interrupted (Figure 3), thus undermining the existence of a fourth ossicle.

Summary
The presented results are a step towards the resolution of debated topics in ME morphology and confirm large inter-individual variations of the dimensions and presence of some ME components. These and other results will be reported in detail in a soon-to-be-submitted manuscript.

PS-740

Photodynamic Effect of Visible Light in Pneumococcal Otitis Media

Geeyoun Kwon[1]; Marnie Peterson[1]; Karunya Kandimalla[1]; Patricia Schachern[1]; Vladimir Tsuprun[1]; Sebahattin Cureoglu[1]; Michael Paparella[2]; Kevin Landgrebe[3]; Jack Lai[3]; Steven Juhn[1]
[1]University of Minnesota; [2]Paparella Ear Head and Neck Institute; [3]3M company

Otitis media is one of the most common bacterial infections affecting approximately 80% of children. *Streptococcus pneumoniae* is one of the main pathogens associated with otitis media, others including *Haemophilus influenza* and *Moraxella catarrhalis*. With emerging problem in antibiotic resistance, new treatment strategies are being sought such as non-antibiotic therapy. Photodynamic therapy is a therapeutic modality extensively used in treatment of cancer and other diseases. It involves injection of a photosensitizer (PS) and activation of the PS with proper wavelength of light source. Irradiation of a PS generates singlet oxygen species and other reactive oxygen species, which have selective cytotoxic effect on target cells.

In this study, we investigated antimicrobial effect of visible light on pneumococcal otitis media both *in vitro* and *in vivo*. The light-emitting diode (LED) visible light source of two different intensities was directed onto *Streptococccus pneumoniae*, serotype 19 cultured in 96-well plates. *In vivo* study was conducted using an optical bioluminescent imaging method to monitor infection dynamics and antimicrobial effect of the visible light source. Chinchillas were inoculated with 100 CFU of the bioluminescent *Streptococcus pneumoniae* serotype 3 (Xen 10, Califer Life Science). Three days after the inoculation, when infection of Xen-10 was confirmed, illumination using the LED light source was conducted.

The photodynamic effect of the visible light in elimination and suppression of bacterial growth was observed both *in vitro* and *in vivo*. *In vitro* data showed higher intensity light killed bacterial population faster. Further studies involving both functional and histopathological testing are required to clarify selective efficacy of the visible light against pneumococcal otitis media.

PS-741

Stenting the Eustachian Tube with a Commercial Coronary Stent to Treat Chronic Otitis Media - a Feasibility Study in Sheep

Friederike Pohl; Robert Schuon; Felicitas Miller; Andreas Kampmann; Eva Bültmann; Christian Hartmann; Thomas Lenarz; **Gerrit Paasche**
Hannover Medical School

Chronic otitis media in humans severely decreases quality of life of affected people. If not treated, it can lead to irreversible local destruction of the middle ear and its neighboring structures leading to hardness of hearing or hearing loss.

The objectives were to: 1) develop a model of induced aseptic otitis media in the sheep; and 2) evaluate the efficiency of a temporarily implanted commercial coronary stent to maintain the patency of the *Eustachian tube* (ET) to promote ventilation of the middle ear.

Three healthy adult blackface sheep were bilaterally implanted with bare metal cobalt-chrome alloy coronary stents of two sizes: 2.75 x 26 mm (left) and 2.0 x 20 mm (right). The ET was assessed endoscopically via a nasopharyngeal approach. Stent implantation was performed with a commercial expandable balloon catheter which was also used to instill inflammatory mediators: 10^{-5} mol/l prostaglandin E_2 (PgE_2) and 10^{-5} mol/l platelet activating factor (PAF; delivered as single treatment of 1 ml once at the beginning and in doubled concentration at the end of the study). Daily checks on clinical health status and periodical endoscopic examinations of the ears were done. After 12 weeks, the animals were sacrificed and CT scans of the head, as well as histological examinations were done with a focus on stent location and expansion, as well as inflammation in the ET.

All animals consistently had only minor signs of inflammation throughout the entire study. The method for induction of an acute otitis media with effusion needs further development, since hardly any sign of triggered tympanic effusion was detected. Notwithstanding, based on the absence of severe inflammation, we inferred that stenting the *Eustachian tube* could be done without severe complications, and in general , the stents remained where they had been placed. The observed inflammatory reaction was moderate and middle ear ventilation was apparent in the CT scans, even if the stent

was filled with secretion. However, based on an overgrowth of the proliferative tissue with respiratory epithelium, we inferred there was normal movement of secretions. Later atraumatic stent removal appeared unlikely, due to the stable integration into the tissue.

The *Eustachian tube* could easily be stented, and the patency of the Eustachian tube could be maintained making the blackface sheep a promising in vivo model to test stents for the ET. However, explantation of the stents ought to be avoided.

PS-742

Anatomical Reference for Otic Structures in Common Laboratory Animals

Andrea Koch; Matthew Abernathy; Amber Doan; Kelly Fill; Kevin Steffer; Rachel Konieczka; Joshua Yoder; Tyler Robinson; Rachel Tapp; Theodore Baird
MPI Research

The Food and Drug Administration requires that drugs in development for otic use be assessed for systemic absorption and ototoxicity. Of greatest importance when conducting these experiments is the characterization of the drug in an animal model that will produce translatable data for human use. Currently, there is no comprehensive data set comparing relative anatomical features of external, middle, and inner ear structures of research-relevant laboratory animal species to aid in model selection. The objective of this study was to compile a comprehensive set of anatomical measurements of the major auditory structures in commonly utilized laboratory species to serve as a historical reference aiding future drug development efforts. Following necropsy and perfusion fixation using 4% paraformaldehyde, otic tissues were collected, finely dissected, and measured in Sprague Dawley rats, Albino Hartley guinea pigs, and Domestic Short Hair felines. Structures evaluated include the volume (mL) of the external auditory canal and tympanic cavity; the diameter (mm) of the tympanic membrane, oval and round windows, and otolith organs; the length (mm) of the ossicles and organ of Corti; and the total hair cell counts of the organ of Corti and otolith organs. The mean values, with variability estimates of each metric evaluated were compiled to generate a comprehensive dataset. Experimental data may be used as a reference for species-specific dose volume selection and drug formulation for auditory canal and transtympanic drug administration during study design development. The relative size of the tympanic membrane, and the round and oval windows measured in this experiment may aid in predicting drug absorption into the middle and inner ear for each species. Total hair cell counts and physical data on middle and inner ear structures assists in the identification and characterization of potential adverse, treatment-related effects.

PS-743

The Hannover Coupler: Round Window Stimulation with the Floating Mass Transducer at Static Contact Forces up to 90 mN

Mathias Müller; Rolf Salcher; Thomas Lenarz; Hannes Maier
Medical University Hannover

Introduction

When the ossicular chain of the middle ear is absent or destroyed the floating mass transducer (FMT) of the MED-El Vibrant Soundbridge has proven to be an efficient way to stimulate the round window (RW) of the cochlea. However, RW stimulation still suffers from large variability in clinical outcomes. The goal of this study was to reduce the variability using a specially designed coupler that allows vibration of the FMT in combination with a static force preload to the RW to increase coupling efficiency.

Methods

Experiments were performed in fresh human temporal bones compliant to the ASTM standard (F2504.24930-1). The Hannover coupler prototype consists of a prosthesis with a spherical tip (d=0.5 mm) and a hook shaped spring attached to the FMT that allows mobility of the FMT in combination with a static preload. Round window stimulation was performed with the coupler tip perpendicular to the RW at variable forces (0 – ~90 mN). The coupler/FMT position was displaced relative to the RW using a micromanipulator connected to the spring element. The resulting static preload was determined with a force cell. Under varying static load the stapes footplate (SFP) response to FMT stimulation of the RW and sound stimulation of the tympanic membrane was measured using a Laser Doppler Vibrometer. SFP responses to sound and to FMT stimulation at nominally 1 V_{RMS} input voltage were compared to estimate the equivalent sound pressure level (eq. SPL). From the SFP response to FMT stimulation and the FMT vibration the transfer function was calculated.

Results

Five temporal bones fitting the acceptance range of the ASTM standard were included in the analysis. The displacement amplitudes of the SFP response to actuator stimulation, equivalent sound pressure levels and transfer functions were highly dependent of the applied RW force. Increase of the static force lead to a monotonic increase of eq. SPL from approx. 89 ± 6 (MV ± SD) dB eq. SPL at forces <1 mN to 111 ± 9 (MV ± SD) dB eq. SPL at ~90 mN in the mid-frequency range (avg. 1 – 4 kHz).

Summary

Static force preload applied to the RW proves to be an important factor for transmission efficiency. From contact forces below 1 mN up to ~90 mN SFP responses and eq. SPLs show a pronounced monotonic increase in amplitude.

PS-744

Bone conduction pathway through non-osseous contents

Christof Roosli[1]; Jae Hoon Sim[2]; Rahel Gerig[2]; Stefan Stenfelt[3]; Alex Huber[2]

[1]University Hospital Zurich; [2]Department of Otolaryngology, Head and Neck Surgery, University Hospital Zurich, Switzerland; [3]Linkoping University, Sweden

Background

Bone conduction hearing aids (BCHAs) are commonly used for patients with conductive or mixed hearing loss who cannot wear conventional hearing aids, or for patients with single sided deafness. Whereas several BC pathways have been revealed, recent studies proposed direct stimulation of the cochlea via non-osseous pathways such as brain and cerebro-spinal fluid (CSF). While some studies argue that stimulation on non-osseous sites such as the eye and neck generates BC propagation mainly through non-osseous pathways, contribution of these pathways to hearing and their interaction with osseous pathways are still controversial. This study investigates on roles of non-osseous pathways in BC hearing. Non-osseous cranial contents are excited by direct stimulation on the dura in cadaver heads.

Methods

Measurements were performed in human cadaveric heads. A bone conduction hearing aid (Bonebridge, Med-El) was attached to the dura after craniotomy, and stepped-sine signals in the frequency range of 0.1 – 10 kHz were delivered directly to the transducer. Motions of the cochlear promontory were measured using a Laser Doppler Vibrometer (OFV-3001, Polytec) system and intracranial pressure change was simultaneously recorded with a hydrophone (Type 8103, Brüel & Kjær) placed within the cranial space. Then, the relative magnitudes of the two measured values were compared in the frequency domain for stimulation at the dura and at the mastoid.

Results

Intracranial pressure change and promontory motion were measurable for direct stimulation on the dura. The intracranial pressure change maintained flat magnitudes up to 1.4 kHz, and then the magnitudes decreased with frequency. The phase was also flat up to 1.4 kHz, and decreased with frequency. The promontory motion showed the maximum magnitude around 1.4 kHz, and the magnitude decreased with frequency at higher frequency range. The phase decreased with frequency uniformly along the entire considered frequency range of 0.1 – 10 kHz.

Conclusion

The intracranial pressure changes show comparable magnitudes and phases to vibrations of the cochlear promontory above 1.4 kHz, suggesting the non-osseous contents interact with bone vibrations in this frequency range. Comparison of the results with stimulation on dura with ones with stimulation on bony sites is expected to show contribution of pathways via non-osseous skull contents to BC hearing more clearly.

PS-745

Human Middle- and Inner-Ear Impedances

Darcy Frear[1]; Christof Stieger[2]; John Rosowski[3]; Hideko Nakajima[3]

[1]Harvard University; [2]University Hospital Basel; [3]Harvard Medical School

Introduction

Current models of the human inner ear rely on the two-window hypothesis for various methods of sound stimulation. The hypothesis assumes the oval window (OW) and round window (RW) act as the only significant areas of pressure release within the cochlea. Although this hypothesis generally holds for air conduction (AC), during alternative cochlear stimulation modes, such as mechanical RW stimulation, we showed evidence that at least another “window” in the cochlea allows for volume velocity flow and plays a role in sound transduction. To fully understand the flow of volume velocity during cochlear stimulation, the impedances of middle ear, cochlear partition (basilar membrane), RW, OW, and other leakage points (i.e. third window) need to be identified and quantified. We used data from AC and RW stimulation to create a model of the impedances in the cochlea.

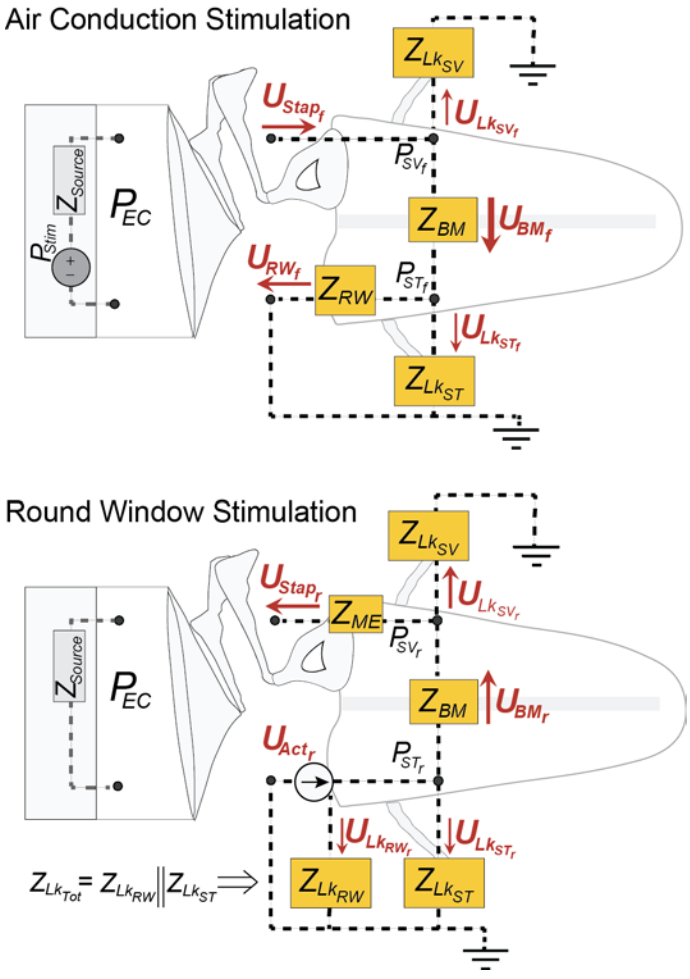

Methods

Pressure sensor measurements in scala vestibuli (SV) and scala tympani (ST) and velocities of the stapes and RW actu-

ator were analyzed. The figure shows a representation of the model in consideration.

Results

In forward AC stimulation, the impedance across the basilar membrane, $Z_{BM,}$ was calculated using the pressure difference of the scalae (P_{SV} - P_{ST}) divided by the stapes volume velocity (U_{Stap_f}). The volume velocity across the basilar membrane was considered almost equivalent to that of the OW, therefore $U_{Stap} \approx U_{BM}$ during AC. We assumed Z_{BM} was equivalent during AC and RW stimulation. In RW stimulation, Z_{ME}, Z_{BM}, and reverse stapes velocity (U_{Stap_r}) allowed us to find the leakage in the scala vestibuli (U_{Lk_SV}). The leakage from the RW (due to inefficiency of the actuator interface) and ST (due to a physiological window) were calculated together (Z_{Lk_Tot}) using the volume velocity of the actuator (U_{Act_r}), U_{BM}, and Z_{BM}. Subsequently, impedances and volume velocities were found for the basilar membrane and the SV and ST leakage areas.

Conclusion

Analyses of intracochlear pressures in SV and ST, as well as velocities of the middle ear, enables us to quantify the frequency-dependent impedances in the middle ear and cochlear system. Our analyses also further the understanding of AC and RW stimulation by quantifying the volume velocities of various paths of sound during different stimulation modes.

PS-746

Effects of Perforations on Vibration Patterns of Tympanic Membrane and Middle-Ear Sound Conduction

Nima Maftoon[1]; Jeffrey Tao Cheng[1]; Cosme Furlong[2]; John Rosowski[1]

[1]Massachusetts Eye and Ear Infirmary, Harvard Medical School; [2]Worcester Polytechnic Institute, Department of Mechanical Engineering

Although perforations of the tympanic membrane (TM) represent a common middle-ear pathology, their effect on middle-ear sound conduction is controversial. Work by Voss et al. *(JASA 2001; 110: 1432-44)* suggests the effects of perforations and slits on middle-ear sound conduction are independent of their location, whereas a study by O'Connor and Puria *(Laryngoscope 2008; 118:483-9)* concludes that slits made circumferentially in the TM have larger effects than radial slits. We investigate how perforations and slits change the vibrations of the TM and the sound conduction characteristics of the middle ear. Measurements are made in temporal-bone preparations with closed middle-ear cavities in an open sound field. Probe microphones measure the sound pressure near the TM on the lateral side and inside the middle ear cavity. The TM and stapes vibrations are measured with near simultaneous stroboscopic laser holography and laser Doppler vibrometry. Measurements are made on an intact TM and then repeated after making progressive perforations on the TM. Measurements are made when the perforations are open and when they are patched. Preliminary results show that with low-frequency sound stimulation unpatched slits cause an increase in the sound pressure in the middle-ear cavity, change the vibration pattern of the TM local to the perforation site and decrease the stapes velocity. At high stimulus frequencies with circumferential slits, located approximately midway between the manubrium and the annulus, patching restores the middle-ear pressure and the stapes velocity to near the intact condition but not the TM vibration patterns. This study has implications for selecting proper materials for more successful tympanoplasty.

PS-747

Effects of Three Frequencies(226Hz, 678Hz, 1000Hz) on Tympanograms of the Children: Who are Typically Developing and who Need Special Care at the School-age Stage

Chun hyeok Kim[1]; Jinsook Kim[2]

[1]Hallym University; [2]Division of Speech-language Pathology and Audiology

It has been reported that the 1000 Hz tympanometry is useful in neonates having normal hearing as well as Down syndrome. Usually, the frequencies of 226Hz, 678Hz have been used to conduct tympanogram and there have been few studies about tympanometry measurement with school-aged children especially who are typically developing and who need special care at the school-age stage. Thus, this study investigated frequency impact on the tympanometry, especially focusing on 226Hz, 678Hz, 1000Hz and ages at the school-age stage in order to find the more efficient tympanometry measurement for children at this age.

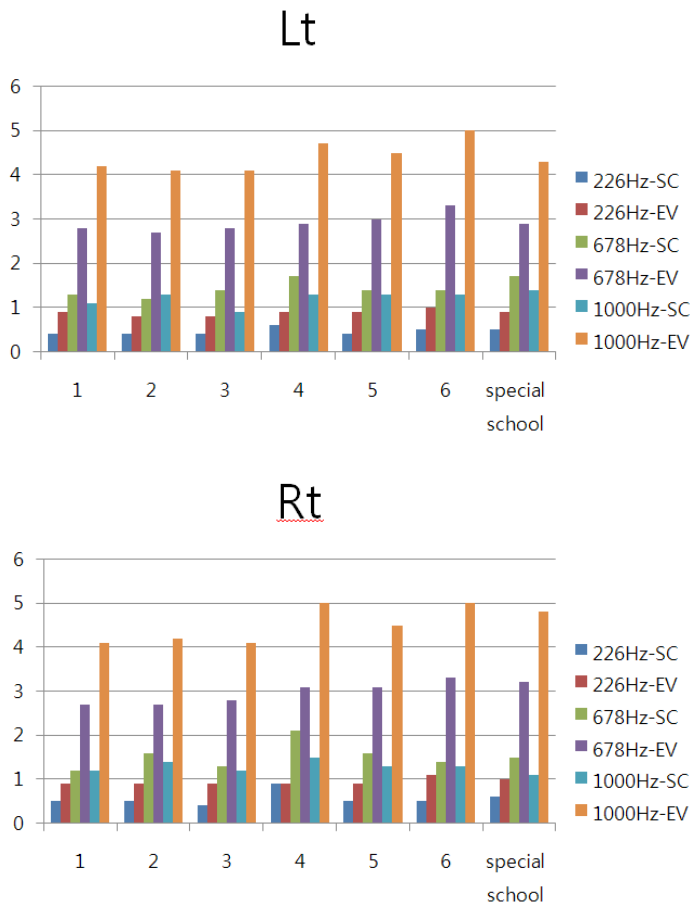

A total number of 182 children participated in this study. Of the subjects, 152 were typically developing children educated in public elementary school, and 30 recruited from special education program with 93 male and 89 female. The participants were tested with tympanometry, DPOAE, and otoscopy. The tympanometry measurement was conducted at three frequencies; 226Hz, 678Hz, and 1000Hz. Statistical analysis was carried out with SPSS version 21.

The average of tympanometry measurement at 226Hz was SC 0.5 and EV 0.9 for typically developing children, and SC 0.6 and EV 1.0 for children who need special care. There was no statistically significant difference on the SC and EV from the tympanometry measurement at 226Hz between children who are typically developing and who need special care, as well as at 678 Hz, and 1000Hz. However, there was a significant difference for SC and EV across three tested frequencies, 226Hz, 678Hz, and 1000Hz.

The result of this study showed that the 1000Hz tympanometry was not sensitive to the middle ear function for school-aged children although it has been reported to be sensitive for neonates regardless of special care. This study was limited in number of children who need special care. Further study should explore the usefulness of the tympanometry measurement with more children with or without special care.

PS-748

HIV Infection Impairs Cochlear Function

Jay Buckey[1]; Abigail Fellows[1]; Jiang Gui[1]; Isaac Maro[2]; Odile Clavier[3]
[1]Geisel School of Medicine at Dartmouth; [2]Dar Dar Programs; [3]Creare Inc

Introduction

Our previous work shows significantly lower DPOAE magnitudes in HIV+ individuals compared to HIV- controls, regardless of whether the patients receive anti-retroviral therapy (ART). To confirm that ART does not affect cochlear function we measured DPOAEs on a cohort of HIV+ individuals before and after starting ART.

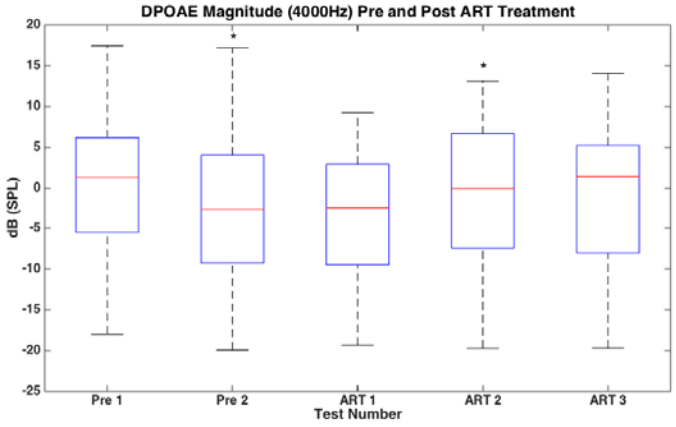

Methods

DPOAEs were acquired at f2 values of 1500, 1700, 2000, 2200, 3000, 3200, 4000, 4200, 6000, 6200, 7800, and 8000 Hz with an f2/f1 ratio of 1.2 and L1/L2 values of 65/55. Data were collected at approximately 6-month intervals. First, data were analyzed from individuals who had completed 5 visits (i.e. 33 individuals with data from 2 visits before starting ART and 3 visits after starting ART plus 142 HIV+/ART+ individuals and 30 HIV+/ART- with 5 visits). Average DPOAE magnitude from both ears was analyzed using a repeated measures model. Data were also analyzed for individuals who had completed 3 visits (77 starting ART (1 visit before and 2 after), 233 HIV+/ART+, 43 HIV+/ART-, and 57 HIV-) using a linear mixed effect model with adjustment for age, gender, ear drainage history and abnormal tympanometry.

Results

Starting ART did not decrease DPOAEs significantly at any frequency. In the 5-visit group, there was tendency for DPOAEs to increase during the first year after starting ART, which was significant at 3200 and 4000Hz ($p<0.04$, Figure 1). For the 3 visit groups, the linear mixed model showed a significant interaction between ART start group and the HIV+/ART+ group at 3000, 3200, 4000, and 4200 Hz with the HIV+/ART+ group showing reduced DPOAE magnitudes over time compared to the ART start group.

Conclusions

Several studies have shown that HIV+ patients on ART still develop signs of neurological deterioration, likely due to continued inflammation in the central nervous system produced by HIV. This may happen in the cochlea as well. The fact that the cohort starting ART showed either increased or stable DPOAE magnitudes, compared to a gradual decline in the HIV+ group with established ART treatment, suggests that ART was improving cochlear function at the beginning of the treatment, compared to the gradual decline in the HIV+/established ART group. The combined data from our cross-sectional and longitudinal studies suggest that the cochlear findings are due to HIV infection and its consequences and not ART.

PS-749

Effect of Sepsis and Systemic Inflammatory Response Syndrome on Neonatal Hearing Screening Outcomes following Gentamicin Exposure

Selena Liao; **Campbell Cross**; Anna-Marie Wood; Olivia Ettinger; Lindsey McEvoy; Johnathan Galati; Art Riddle; Zachary Urdang; Nicholas Vigo; Christopher Hart; Lauren Moneta; Troy Lubianski; Noe Coopersmith; Priya Srikanth; Jess Mace; Angela Garinis; Heather Durham; Carol MacArthur; William Martin; Peter Steyger
Oregon Health & Science University

Rationale:

Hearing loss rates in neonatal intensive care units (NICU) run at 2-15% compared to 0.3% in full-term births, and the etiology of this discrepancy remains unknown. The majority of NICU admissions receive aminoglycoside therapy for presumed sepsis that is discontinued upon confirmed absence of infection. Endotoxemia and inflammation can increase cochlear uptake of aminoglycosides in mice. We tested the hypothesis that an association between sepsis or systemic

inflammatory response syndrome (SIRS) and intravenous gentamicin exposure may contribute to increased hearing loss rates in NICUs.

Methods
Prospective data was collected from 91 subjects enrolled at OHSU Doernbecher Children's Hospital Neonatal Care Center. Distortion product otoacoustic emissions (DPOAE) were obtained to determine auditory performance prior to discharge. To pass the DPOAE screen, normal responses in >6 of 10 frequencies in both ears were required; otherwise the subject was considered a "referral" for a diagnostic hearing evaluation after discharge. Cumulative dosing data and the prevalence of neonatal sepsis or SIRS was obtained from OHSU's electronic health record system. The data were analyzed using Stata 13.1 to obtain risk and odds ratios.

Results
Using the DPOAE screening criteria described above, 37 (41%) of 91 subjects would be referred. Among the 91 subjects, 74 (81%) had intravenous gentamicin exposure. 20 (22%) had ≥4 days of gentamicin, and 71 (78%) had <4 days. Comparing these two groups, the risk ratio of referral with ≥4 days of gentamicin is 1.92 (p=0.012); and an odds ratio of 3.63 (p=0.015). There were 7 subjects with sepsis, and 11 meeting neonatal SIRS criteria, for a total of 18 (20%) out of 91 patients with clinical evidence of systemic inflammation, 9 of whom had ≥5 days of gentamicin and a DPOAE referral risk ratio of 3.5 (p=0.018), and odds ratio of 12.25 (p=0.027) compared to the other 82 subjects. Comparing sepsis/SIRS patients with ≥4 days of gentamicin (11/18) to the rest of the cohort was not statistically significant. Combining subjects with either vancomycin or furosemide overlap with gentamicin treatment yielded an almost significant risk ratio (1.77, p=0.05).

Conclusions
We demonstrated an increased risk of referral with DPOAE screening for those receiving ≥4 days of intravenous gentamicin administration that may contribute to the increased hearing loss rates observed in the NICU. We propose an expanded study to gather a larger cohort of subjects, including those with sepsis and neonatal SIRS, to increase the statistical power of these findings.

PS-750

Quantifying the Effects of Medication Dosage and Age on Hearing in Cystic Fibrosis Patients Receiving Obligate Intravenous Antibiotic Treatments

Angela Garinis[1]; Patrick Feeney[1]; Douglas Keefe[2]; Lisa Hunter[3]; Daniel Putterman[1]; Campbell Cross[1]; Priya Srikanth[1]; Peter Steyger[1]
[1]Oregon Health and Science University; [2]Boys Town National Research Hospital; [3]Cincinnati Children's Hospital

Background
Aminoglycosides and glycopeptides are cochleotoxic antibiotics that are clinically essential to treat life-threatening infections in chronic diseases such as cystic fibrosis (CF). CF patients receive large cumulative intravenous doses of these antibiotics over their lifespan, yet some develop hearing loss whereas others do not. It remains unclear whether the effects of medication dosage and/or age play a role in the incidence of hearing loss in these subjects.

Methods
We evaluated the effects of cumulative intravenous aminoglycoside (tobramycin and/or amikacin) and/or glycopeptide (vancomycin) doses on hearing in 76 subjects (mean age= 26; 43 males and 33 females) recruited at Oregon Health & Science University CF centers. Hearing was assessed across the standard clinical frequency range (0.25-8kHz) and an extended high-frequency range (9-16kHz) that often exhibits the initial effects of cochleotoxicity. Cumulative dosing for intravenous aminoglycoside, with and without vancomycin treatment, were calculated for each subject. Subjects were categorized into four groups ranging from low (0.5-3 doses) to high exposure (63.25-399.5 doses) for analyses. Subjects were also classified into a normal hearing (≤ 25dB HL for 0.25-16kHz) or hearing loss group (>25dB HL at any audiometric frequency) for either ear. Logistic regression modeling using STATA 13 was conducted to assess the effect of medication dosage on hearing loss after adjusting for age at the hearing test.

Results
Of the 76 subjects enrolled, 33 had normal hearing bilaterally and 43 subjects showed some degree of sensorineural hearing loss between 0.25-8kHz (1%), 9-16kHz (65%) or 0.25-16kHz (34%). There was a significant effect of age between the normal hearing (mean age=22) and hearing loss (mean age=30) groups (p=.0012). Subjects in the highest antibiotic exposure groups were 7.24 times (95% CI: 2.25, 23.32) more likely to have hearing loss than those in the lowest exposure groups after adjusting for age at the hearing test. There was also a significant trend of increasing risk of hearing loss with higher dosing (p=0.002). Excluding vancomycin attenuated the result, yet findings remained significant, as patients with more aminoglycoside doses were still 3.76 times (95% CI: 1.31, 10.78) more likely to have hearing loss compared to those with fewer doses (p = 0.003).

Conclusions
There was a significant effect of cumulative intravenous aminoglycoside doses (with or without glycopeptides) on hearing loss in CF patients after accounting for age. Subjects taking these medications were 3.76 to 7.24 times more likely to develop hearing loss with higher medication exposure.

PS-751

Electrocochleography During and After Cochlear Implantation

Adrian Dalbert; Jae Hoon Sim; Flurin Pfiffner; Rahel Gerig; Christof Roosli; Alexander Huber
University Hospital of Zurich

Introduction
Much of the mechanisms causing loss of residual hearing after cochlear implantation are poorly understood so far. Acute trauma during electrode insertion as well as delayed events

such as foreign body reaction and excitotoxicity due to electrical stimulation are discussed.

Electrocochleography (ECoG) can be used to assess cochlear function. Therefore, our goal was to monitor the cochlear status during and after cochlear implantation by ECoG and thereby evaluate mechanisms underlying loss of residual hearing.

Methods
ECoG signals from an extracochlear site near the round window were recorded before and after insertion of the cochlear implant electrode (n=20). Intraoperatively and during follow-up consultations further recordings from inside the cochlea using the cochlear implant electrode as recording electrode were obtained (n=9). Sinusoid tone bursts with a frequency of 250, 500, and 1 kHz were used as acoustic stimuli.

Results
90% (18/20) of cochlear implant subjects had measurable ECoG responses. Repeatability of extracochlear recordings was assessed by recordings under unchanged conditions. Mean difference between these recordings was 0.23 dB (n=16).

94% (17/18) of subjects showed no changes indicating acute cochlear trauma in the extracochlear recordings during cochlear implantation. One patient showed large decreases in all frequencies. This was associated with a complete hearing loss 4 weeks after surgery (mean presurgical low frequency hearing 78 dB HL).

Mean difference in ECoG signal amplitude between extra- and intracochlear recordings was 13.9 dB with usually larger signals from the intracochlear recording site. In two cases intracochlear responses at 1000 Hz were smaller. Changes in threshold and amplitude of ECoG signals in follow-up consultations showed a correlation to pure tone audiogram findings. At 250 Hz there was a trend toward slightly larger ECoG signals in recordings from more apical located electrodes, whereas no consistent trend could be detected at 500 and 1000 Hz. No deterioration of ECoG signals after the beginning of the electrical stimulation was shown.

Conclusion
ECoG recordings from an extracochlear site seem to be a reliable tool to assess cochlear function during cochlear implantation. A decrease in multiple frequencies represented acute cochlear trauma associated with loss of residual hearing. However, especially moderate threshold shifts seem to be caused by postoperative mechanisms or cochlear trauma not detectable by ECoG.

Using cochlear implant electrodes for intracochlear ECoG recordings could be used to monitor cochlear function following cochlear implantation and to assess the proximity of different electrodes to intact cochlear structures.

PS-752

Children With Autism Have Reduced Otoacoustic Emissions (OAEs) In Speech Frequencies

Anne Luebke; Paul Allen; Jessica Keith; Loisa Bennetto
University of Rochester

Filtering auditory information in background noise is required for a person's social communication abilities, and impairment of such filtering abilities is one of the key features of autism spectrum disorders (ASD). A potential physiological basis for filtering relevant auditory information is caused by descending regulation by the brain onto cochlear activity—the olivocochlear efferent feedback systems. The olivocochlear efferent systems consist of two components whose cell bodies are found in the superior olivary complex: a medial olivocochlear (MOC) system projecting primarily to cochlear outer hair cells (OHCs); and a lateral olivocochlear (LOC) system projecting primarily to the dendrites of cochlear afferent neurons in the region beneath inner hair cells. The contractile activity of the OHCs can be evaluated in human subjects, because contractions of the OHCs generate acoustic signals (otoacoustic emissions; OAEs), which can be recorded in the external ear canal, making it possible to directly measure baseline and MOC efferent feedback processes at the cochlear periphery. It has previously been shown that adolescents and children with ASD have reduced MOC efferent feedback strength using either transient OAEs (TrOAEs) or distortion-product otoaacoutic OAEs when compared with typical controls. Moreover, some studies have found differences in baseline OAEs in ASD, while other studies have found no such differences. Our objective was to specifically measure efferent feedback strength and baseline otoacoustic emissions in children with ASD with normal audiometry when compared with matched, typically developing controls. Children with ASD (n=36) and typically developing controls (n=43), ages 6 through 17, participated in this study. Groups were rigorously characterized via ADI-R and ADOS, and matched on age, gender, and verbal ability. High-functioning children and adolescents with ASD have greatly reduced DPOAE responses in the 1 kHz speech frequency range (~6 dB SPL, f_2=1 kHz, $p<0.001$), yet have comparable DPOAE responses at 0.5 and 4-8 kHz regions. These differences were not due to differences in middle ear muscle activity. No differences were found between high-functioning children and adolescents with ASD and TD controls on overall baseline click TrOAE emissions, yet an analysis of the spectral features of the TrOAE baseline measures revealed similar decreased emissions in 1.0 and 1.5 kHz regions. However, there were no differences in TrOAE suppression between children and adolescents with ASD and TD controls. In conclusion, non-invasive measures of cochlear function may serve as an early physiological biomarker for ASD.

PS-753

Correlation between Bone Mineral Density and Hearing Thresholds in Older Adult Population

Eun Jin Son; **Kyoung Jin Roh**; Ah Young Park; Yun Seok Seo; Kyoung Hwa Han
Yonsei University, College of Medicine

It has been proposed that decreased bone mineral density (BMD) may pose additional risk for sensorineural hearing loss. In this study, we investigated the association between BMD and hearing thresholds in adults over 50 by using data from a large population–based survey. Data from the Korea National Health and Nutrition Examination Survey included a total of 28009 subjects over the period of 2009-2011. Records of 3507 subjects with complete data for BMD and audiologic evaluation were analysed. A pure-tone audiogram and physical examination of the ear were performed, and bone mineral density was measured by dual-energy X-ray absorptiometry (DEXA) scanning. The results were obtained after adjustment for age, sex, body mass index, menopause and exposure to occupational and explosive noise. The average of pure tone thresholds in 500-6000Hz were 7.9dB higher in osteoporosis(T-score≤-2.5) group($p<0.01$) and 3.5dB higher in osteopenia(-2.5<T-score<-1.0) group($p<0.01$) than Normal T-score group(T-score≥-1.0). BMD scores did not show any correlation with hearing results($P>0.05$). Our data suggest that osteoporosis is related to higher incidence of sensorineural hearing loss in older adult population. In addition, low bone mineral density may be associated with increased hearing thresholds although there was no statistically significant difference.

PS-754

Effects of Amplification on Auditory Evoked Responses

Kimberly Jenkins; Alessandro Presacco; Samira Anderson
University of Maryland, College Park

Introduction

Older adults often have difficulty understanding speech in noise, even with the use of digital amplification technology. The current method of hearing aid verification, probe-microphone measurement, does not address the effects of amplification beyond the tympanic membrane. An understanding of amplification effects at higher levels of the auditory system may inform amplification algorithms or strategies and thus improve the success of hearing aid fittings. Few studies to date have assessed the effects of amplification on auditory evoked responses. Billings et al. (2007, 2011) found no differences in response amplitudes of cortical evoked responses between aided and unaided conditions, but cortical responses can be used to demonstrate audibility for speech sounds in infants and others who are difficult to test (Glista et al., 2012). The purpose of this study is to assess the effects of amplification on frequency following response (FFRs) and cortical evoked responses to a speech syllable, as a first step in determining if these measures can be used to assess efficacy of the hearing aid fitting.

Methods

Fifteen older adults with mild to severe hearing loss and no prior hearing aid experience were fitted with Widex Dream 440 receiver-in-the-canal hearing aids bilaterally. The fittings were verified using probe-microphone measurements. FFRs and cortical evoked responses to the syllable [ga] were obtained in the sound field in aided and unaided conditions: quiet (65 dB SPL and 80 dB SPL) and four-talker babble (80 dB SPL, +10 signal-to-noise ratio). For the FFR, responses to two stimulus polarities were added to assess responses to the envelope and subtracted to assess responses to the temporal fine structure.

Results

In the FFR, amplification resulted in an amplitude reduction in response to the stimulus envelope but an amplitude enhancement in response to the temporal fine structure across the three presentation conditions, with the greatest effects seen in the quiet condition at 80 dB SPL. No differences in amplitude were noted between aided and unaided cortical evoked responses across presentation conditions, consistent with the findings of Billings et al. (2007).

Conclusions/Summary

The FFR can be used to assess amplification effects on distinct speech features, suggesting potential future uses for evaluating changes in processing associated with different settings or algorithms and for assessing overall hearing aid benefit.

PS-755

Another Behavioral Assay for Tinnitus in Laboratory Rats

Aikeen Jones; Bradford May
Johns Hopkins University

Behavioral screening procedures remain a contentious issue for animal studies of tinnitus. Most paradigms are based on the assumption that tinnitus-positive animals confuse the “sound” of tinnitus with objective auditory stimuli. Therefore, animals with tinnitus will fail to hear silent gaps in ongoing sounds, or will emit behaviors in silence that were previously elicited only by sound stimuli. When tinnitus screening involves repetitive testing, animals may cease to exhibit these behavioral signs because they eventually learn to distinguish their own subjective tinnitus experience from objective sounds. Our behavioral assay avoids these stability issues by using tinnitus as a discriminative stimulus. Consequently, positive test results can be maintained through differential reinforcement of the tinnitus percept. Initially, the rats are trained to obtain water rewards by licking a spout during periods of silence and to escape shocks by avoiding contact with the spout during presentations of noise or tonal stimuli. Rats learn these behaviors quickly and are then unilaterally sound exposed to induce tinnitus. Post-exposure training is limited to the discrimination of silence versus noise. If the rats are experiencing tinnitus, they are actually learning to discriminate the tinnitus pitch that they hear in silence versus noise. This training selectively extinguishes the suppression response for tonal stimuli that match the tinnitus pitch because

the pitch is now associated with water rewards. After a few weeks, the rats are probed with the full set of discrimination stimuli. Rats with a high-pitch tinnitus are expected to show high rates of licking during presentations of high-frequency tones. Rats with a low-pitch tinnitus are expected to show the opposite response bias. Rats without tinnitus will maintain pre-exposure suppression because they have not experienced extinction during post-exposure training. The stability of these response patterns is confirmed by continuing training with silence versus noise and then probing with tonal stimuli at 1 – 2 week intervals. This presentation will provide examples that document the efficiency of our training procedure, the accuracy of suppression behavior, and the reliability of probe tests. Although our findings relate specifically to laboratory rats, conditioned suppression is a robust behavioral phenomenon that can be adapted to most animal models of tinnitus including laboratory mice.

PS-756

A New Measure to Detect Tinnitus in Guinea Pigs?

Amarins Heeringa[1]; Martijn Agterberg[2]; Pim van Dijk[1]
[1]University Medical Center Groningen; [2]Radboud University Nijmegen Medical Centre

Introduction

Tinnitus is the perception of a sound that cannot be attributed to an external acoustic source. Many people suffer from tinnitus and to date, there is no common treatment to provide alleviation. Animal models have proven to be useful to study tinnitus neuropathology and will be essential to develop treatments. However, it is of great importance to reliably determine whether an animal perceives tinnitus or not. Available models are based on the assumption that tinnitus impairs their ability to detect silence. The aim of the current study was to evaluate a new possible measure to determine tinnitus in guinea pigs, which involves studying the spontaneous behavioral activity during intervals of noise and silence.

Methods

Anesthetized guinea pigs were either sham exposed or unilaterally exposed to an 11-kHz pure tone of 124 dB SPL for one hour. The next day, the animals were placed in a shuttle box (46 x 23 x 23 cm). Spontaneous behavior was observed in the presence of alternating intervals of noise and silence with a random duration between 30 – 120 s.

Results

Sham-exposed, normal-hearing guinea pigs were primarily immobile during silence (on average 98 % of the time), which differed significantly from their immobility during noise (66 % of the time). By interpreting immobility as a signature of perceiving silence, we hypothesized that the presence of tinnitus would reduce immobility in silence. Indeed, a subset of the exposed animals was significantly more active in silence. However, exposed animals were also more active in noise, as compared to the control group.

Conclusions

It is possible that the increased mobility of the affected animals in the exposed group represents tinnitus, as tinnitus would impair the ability to perceive complete silence. However, this group of animals also moved more in noise, implying that the observed behavior could have also derived from an overall increase in general activity. Therefore, conducting several validation experiments is very important before accepting this method as a new measure to detect tinnitus. These validation experiments must further elucidate the origin of the increased mobility in both silence and noise after sound exposure.

PS-757

Improving Effectiveness and Reliability of Startle-based Tinnitus Characterization in Rodents

Natalie Steube; Manuela Nowotny; **Bernhard Gaese**
Goethe University Frankfurt

Background

Gap-prepulse inhibition (gap-PPI) measurements of the acoustic startle response (ASR) is the common method for objective tinnitus assessment in laboratory animals. Repetitive startle measurements are required for tracking long-term changes of trauma-induced alterations related to the formation of tinnitus. Thus, it is necessary to be able to ensure reliable results that can be compared over an extended period of time. For that purpose, we tested important stimulus parameters that influence gap-detection measurements and investigated the reliability of motor responses in Mongolian gerbils (*Meriones unguiculatus*) and Sprague Dawley rats, two established animal models in tinnitus research.

Methods

Besides standard measurements for startle-based tinnitus assessment we tested gap-PPI with gap durations of 50, 200, 500 and 1000 ms in background noise for different frequency-ranges (8, 10, 12, 18 kHz +/- 0.25 oct and broadband noise, BBN). Further, we analyzed the influence of measurement timing and background noise on ASR amplitude and spontaneous motor activity in both species (n=8, each).

Results

Regarding optimal stimulation, we found that gap-PPI was more stable for all measured frequencies with a gap duration of 500 ms than with 50 ms gaps. Longer gap durations might be more suitable to detect faint perceptions such as trauma-induced tinnitus.

The amplitude of the ASR motor response is the one important measure for tinnitus assessment. One additional influence that might interfere with this is the frequency content of stimulation. While ASR amplitude was always high for broadband (1.5 – 20 kHz) background noise, ASR amplitude decreased in gerbils from low (4 kHz) to high frequency (18 kHz; 0.5 oct background noise), while rats showed now frequency-dependency of the amplitude. Possibly interfering long-term habituation was not observed which indicates comparable startle measurements over a long period.

The spontaneous activity of gerbils was nearly two-fold higher than of rats and was higher in gap paradigms with either BBN or NBN (0.25 oct) background noise. This could cause misleadingly low inhibition values.

Conclusions

Taken together, gap-PPI-based tinnitus assessment can further be improved by optimizing stimulation parameters such as gap duration or test frequency. Comparability between the necessarily repeated measurements over an extended time of tinnitus development can be ensured by tracking ASR amplitudes and spontaneous motor activity.

PS-758

Gap-Detection Behaviour in the Naïve and Monaurally Impaired Adult Ferret: A Possible Model of Lesion-Induced Tinnitus

Joshua Gold; Fernando Nodal; Andrew King; Victoria Bajo
University of Oxford

Tinnitus is characterised in its subjective form by the patient-reported perception of sound in the absence of a corresponding environmental acoustic source. A key step in the development of a reliable animal model of tinnitus is to identify the presence of an abnormal auditory percept in animals exposed to a peripheral insult that is akin to those insults that might be responsible for tinnitus induction in human patients. We aimed to characterise gap-detection behaviour in adult ferrets, prior to and at multiple time points following the introduction of a selective unilateral lesion of the spiral ganglion (SG), intended to replicate the peripheral pathology observed in certain tinnitus cases. Animals (N = 9) were trained, under positive operant conditioning, to discriminate between either uninterrupted noise ("no-gap"), or the same sound in which gaps were embedded ("gap"; four interleaved gaps, varying between 3-270 ms from trial-to-trial). Stimuli comprised noise-bursts generated trial-to-trial and bandpassed between 500 Hz – 30 kHz (broadband noise; BBN), or as octave bandwidths centred at 1-, 4-, or 16 kHz (narrowband noise; NBN). In addition to measuring approach-to-target performance, we also recorded response times from stimulus onset and head-orienting responses to lateralised response locations. Single-session behavioural performance was analysed using a bootstrap inference-based technique to extract psychometric functions and derived measures of single animal performance (including gap length at d' = 1, psychometric function slope, false alarm rate, and maximum d'). Cohort performance across multiple measures, in particular detection thresholds and psychometric function slopes, was universally poorer for NBN stimuli compared with BBN, in line with previously reported gap detection data in ferrets and other mammals. Following the introduction of SG lesions by mechanical curettage, a proportion of animals (3/7) displayed frequency-specific changes in certain measures of performance, including increases in d' threshold, that were stable over time (>6 months). In an effort to modulate neural activity potentially underlying tinnitus, a subset of lesioned animals underwent behavioural testing during randomised unilateral optogenetic silencing of auditory cortical activity, following region-specific expression of the archaerhodopsin construct ArchT. Preliminary analyses indicate mixed effects in this cohort, depending upon their post-lesion behavioural phenotype. In conclusion, gap-detection behaviour may be a useful tool for characterising a tinnitus-like percept in ferrets.

PS-759

Evaluation of Behavioral Measures of Tinnitus-related Anxiety in Rats

Gail Larkin; Bradford May; **Amanda Lauer**
Johns Hopkins University School of Medicine

Up to 20% of tinnitus patients experience a strong adverse emotional response to tinnitus, termed tinnitus-related distress. High tinnitus-related distress is typically associated with more severe tinnitus. Despite the prevalence of tinnitus-related distress and the serious impact on quality of life, the mechanisms underlying tinnitus distress remain poorly understood. Our objective is to develop a behavioral model of the emotional response to tinnitus in rats. Adult rats were exposed to salicylate or acoustic overexposure. Exposed and control rats were screened for anxiety/distress using open field tests of exploratory activity and social interaction tests. Behaviors consistent with high-anxiety phenotypes were verified independently in rats exposed to stressful conditions. Salicylate exposure induced high-anxiety phenotypes for all doses and animals tested, whereas control animals showed low-anxiety phenotypes. A subset of salicylate-exposed animals maintained high-anxiety phenotypes weeks after cessation of salicylate injections. Sound-exposed animals showed a range of anxiety phenotypes, but most animals showed behavioral patterns consistent with low anxiety. Despite the general lack of high-anxiety phenotypes in exposed animals, expression of tryptophan hydroxylase 2 (TPH2) neurons in the dorsal raphe nuclei was higher in some exposed animals, suggesting abnormal activation of the serotonergic pathways. Standard behavioral screening procedures designed to measure anxiety in groups of rodents may not be sensitive to individual levels of tinnitus-related anxiety except for extreme phenotypes. These high-throughput behavioral tests can identify very strong effects of acute anxiogenic manipulations, but more sensitive measures are required to probe emotional effects in models of chronic tinnitus. Identification of appropriate phenotyping measures will facilitate future studies of the physiological and anatomical substrates of the emotional response to tinnitus.

PS-760

Conditioned Licking Suppression: A New Behavioral Test for Tinnitus

Edward Pace; Michael Bobian; Ajay Panekkad; Xueguo Zhang; Jinsheng Zhang
Wayne State University

Introduction

Numerous behavioral tests to assess tinnitus in animals have been proposed and used over the years. However, each paradigm possesses its own strengths and limitations. Consequently, there is a need to further improve behavioral protocols in order to enhance tinnitus testing. Our lab has recently developed a conditioned licking suppression procedure to examine noise-induced tinnitus in rats. We sought to devise a paradigm that achieves consistent behavioral performance and frequency specific tinnitus detection in short testing periods.

Methods
Rats were water-deprived and allowed to receive water during daily 30-min testing sessions. They learned to access water by constantly licking a spout during sound trials (6-8, 10-12, 14-16, 22-24, or 30-32 kHz, or BBN), but were punished with a mild electrical shock (0.25-0.75 mA) if they continued to contact the spout during silent trials. Suppression of silent trial licking to criterion levels was achieved within 10 training days for BBN sounds and within 6 additional training days for tonal sounds. Upon completion of baseline training, rats were noise exposed (8-16 kHz, 105-110 dB SPL, 2h) and routinely tested for tinnitus development. ABRs were conducted before and after noise exposure.

Results
All rats exhibited a significant increase at broad frequencies in silent trial licking immediately after noise exposure, suggesting robust noise-like tinnitus. Only certain rats, however, exhibited lasting tinnitus behavior, which typically manifested during silent trials following mid-to-high frequency sound trials. As expected, licking activity during sound trials remained unchanged following noise exposure. ABR hearing threshold shifts were transient and demonstrated no significant differences between the tinnitus positive and negative groups. This suggests that our behavioral data specifically result from tinnitus perception as opposed to hearing loss.

Conclusion
Our conditioned licking suppression paradigm provides a relatively fast and consistent method for screening behavior in rats. The tinnitus-related behavior exhibited by our rats is comparable to other tests and matches clinical data in that only certain subjects maintained tinnitus following acoustic trauma. This paradigm may be used to reliably screen tinnitus in animals, which is important to mechanistic studies and treatment development.

PS-761

Untangling the Effects of Tinnitus, Hearing Loss, and Hypersensitivity to Sound in the Gap Detection Test

Rony Salloum[1]; Gwendolyn Dillman[1]; Joshua Niforatos[1]; Christopher Yurosko[2]; Lia Santiago[1]; Sharon Sandridge[1]; James Kaltenbach[1]
[1]Cleveland Clinic; [2]Ohio University

Introduction
In recent years, there has been increasing use of the gap detection method to demonstrate induction of tinnitus in animals. Animals with tinnitus show weakened gap detection ability for background noise that matches the pitch of the tinnitus due to the tinnitus 'filling in the gap'. This interpretation has recently been questioned on the grounds that humans with tinnitus show weakened gap detection at all background noise frequencies, not just those matching the tinnitus pitch. We address here the possibility that altered gap detection may result from a second problem often associated with tinnitus, namely enhanced sensitivities to the startle stimulus and/or background noise. We hypothesize that such alterations can affect gap detection because they can change the ratio of response amplitudes to startle stimuli preceded by background noise with and without gaps.

Methods
Hamsters were tested in 2 groups, those exposed to intense sound and those serving as unexposed controls. To titrate out the optimal conditions that minimize the effects of hearing loss and alterations of sound sensitivity, exposure tones (10 kHz) were varied in level across groups from 80 to 120 dB SPL and in duration from 1 to 4 hours. Measures of ABR thresholds and/or prepulse inhibition (PPI) were obtained at two time points: shortly after exposure, then again at varying times after exposure (2-6 weeks post-exposure). Following recovery from hearing loss, gap detection tests were performed.

Results
The results showed that for many exposure conditions, altered gap detection abilities were observed, but could be at least partially explained as consequences of hyper-responsiveness to either the startle stimulus or to background noise. However, for some exposure conditions, animals displayed weakened gap detection abilities that were most likely due to tinnitus because hearing loss and altered sound sensitivities were negligible or the heightened response to the startle stimulus was counterbalanced by heightened suppression of the startle stimulus by background noise. That is, there was a major weakening of gap detection ability in exposed animals without any difference in startle amplitudes evoked by startle stimuli preceded by noise without gaps.

Conclusion
These results demonstrate that not only hearing loss but also changes in sensitivity to background noise or to startle stimulus itself are potential confounds that can underlie changes in gap detection irrespective of tinnitus. However, our results also indicate that such confounds can be largely reduced or eliminated with appropriate choice of exposure conditions.

PS-762

Functional Integrity of Outer Hair cells in Usher Mice

Abhilash Ponnath[1]; Hamilton Farris[2]; Frank Rigo[3]; Michelle Hastings[4]; Jennifer Lentz[2]
[1]LSU Health Sciences Center, New Orleans; [2]Department of Otorhinolaryngology and the Neuroscience Center of Excellence, LSU Health Science Center, New Orleans; [3]Isis Pharmaceuticals, Inc.; [4]Department of Cell Biology and Anatomy, Chicago Medical School, Rosalind Franklin University of Medicine and Science

Introduction
Usher syndrome is a genetic disorder with hearing, vision and vestibular defects. Patients are classified as type I, II or III based on the severity and age of onset of the symptoms of the disease. Acadian patients suffer from type I due to a cryptic splice mutation (c.216G>A) in the *USH1C* gene. Using a knockin mouse model of type I Usher syndrome containing the c.216G>A mutation, it was shown that hearing and vestibular function can be rescued with a single systemic dose of antisense oligonucleotides (ASOs) given a few days after

birth (Lentz et al 2013). However, whether rescue of hearing by ASOs is mediated by rescue of outer hair cell function is not known. This study addressed this gap by measuring outer hair cell function in treated and control-treated Usher mice.

Methods
Distortion product otoacoustic emissions (DPOAEs) were used to measure OHC function in response to simultaneous primary tones, F1 and F2, in one month old Usher mice treated systemically with a single dose of ASOs five days after birth and control mice.

Results
The signal to noise ratio of the distortion product suggests that outer hair cell function was not rescued at the primary tones tested.

Conclusions
These results suggest that a single systemic treatment of ASOs restores hearing by rescuing IHC, but not OHC, function. Thus, to determine if OHC function can be affected by ASOs, different protocols using earlier treatments, multiple doses and / or different delivery routes may be required.

PS-763

Susceptibility of Outer Hair Cells to Cholesterol Manipulation is Prestin-Dependent

Satoe Takahashi; Yingjie Zhou; Vincent Mui; Mary Ann Cheatham; Jing Zheng
Northwestern University

Cholesterol is a key component of biological membranes and plays important roles in many physiological processes by regulating membrane properties, membrane protein function, and signal transduction. In the inner ear, membrane cholesterol levels are intimately linked to outer hair cell (OHC) physiology, as modulation of membrane cholesterol using cyclodextrins (CDs) has been demonstrated to alter ion channel function as well as the motor protein, prestin (Rajagopalan et al., 2007). Recently, it has been reported that Hydroxypropyl b-cyclodextrin (HPbCD), a relatively benign and more soluble derivative of CDs, induced hearing loss in mice (Crumling et al., 2010). Because OHCs seem to be the only cells affected by this cholesterol-chelating agent, we wondered if this vulnerability might depend on prestin. This OHC specific motor protein is abundantly expressed in the OHC's lateral membrane (LM) and our previous data suggested that prestin directly binds to cholesterol *in vitro* (Duan et al., ARO 2012). It is, therefore, conceivable that OHC death in response to cholesterol manipulation may result from disruption of the cholesterol-prestin interaction. In order to investigate this possibility, we treated wild-type (WT) and prestin-knockout (KO) mice with HPbCD and analyzed their organs of Corti using immunofluorescence microscopy on cochlear whole-mount preparations. Consistent with the report by Crumling and colleagues, extensive OHC death was observed in WT mice. In contrast, OHCs from prestin KO mice, harvested at an early age to minimize OHC loss, were preserved. This observation suggests that a prestin-dependent mechanism underlies HPbCD ototoxicity. It is, however, paradoxical that the cholesterol levels in the OHC's LM are generally thought to be low yet OHCs containing prestin are specifically affected when a cholesterol chelator is administrated. Additional experiments are, therefore, required to learn if the commonly-used cholesterol dye, filipin, underestimates cholesterol levels in OHCs. Currently, we are investigating the possibility that cholesterol evades detection by virtue of the fact that it binds to prestin and forms a complex within the OHC's LM. In parallel, we are also investigating the functional consequences of a direct interaction between cholesterol and prestin in order to define the molecular mechanisms underlying OHC maintenance. As HPbCD and CD-containing formulations are attracting interest in the field of drug delivery, understanding the consequences of this cholesterol-prestin interaction is required in order to minimize adverse effects on cochlear OHCs.

PS-764

Intracellular Calcium Affects Outer Hair Cell Turgor Pressure

Lei Song[1]; Joseph Santos-Sacchi[2]
[1]Yale University, New Haven; [2]Yale University

The outer hair cell forms the basis of cochlear amplification. Second messengers may provide gain control of amplification. The recent identification of a calmodulin binding site within prestin's C-terminus indicates that calcium can significantly alter prestin's operating voltage range as gauged by the Boltzmann parameter V_h (Keller et al., J. Neuroscience, 2014). We reasoned that those experiments may have identified the molecular substrate for the protein's tension sensitivity. In an effort to understand how this may happen, we evaluated the effects of turgor pressure on such shifts produced by calcium. We find that the shifts are induced by calcium's ability to reduce turgor pressure during whole cell voltage clamp recording. Clamping turgor pressure to 1kPa, the cell's normal intracellular pressure, completely counters the calcium effect. Furthermore, following unrestrained shifts, collapsing the cells abolishes induced shifts. We conclude that calcium does not work by direct action on prestin's conformational state. The possibility remains that calcium interaction with prestin alters water movements within the cell, possibly via its anion transport function.

PS-765

An Un-bleachable YFP-based Chloride Sensor

Sheng Zhong; Dhasakumar Navaratnam; Joseph Santos-Sacchi
Yale University School of Medicine

Prestin (SLC26A5), the protein responsible for electromotility in the mammalian outer hair cell, remains incompletely characterized. We are interested in the protein's transporter/channel-like behavior. Clearly, the functional analysis of many chloride-related membrane proteins, such as channels/transporters/receptors, would benefit from a genetically encoded chloride sensor with reliable properties. Recently we developed an YFP-based chloride sensor, mCl-YFP (Zhong et al., PLoS ONE 2014, 9(6): e99095), with chloride K_d of 14 mM and pK_a of 5.9, as well as 15-fold better photostability than wild-type EYFP. Using this chloride sensor, we demonstrated

enhanced dynamic flux of chloride in the mM range into HEK cells expressing the fused protein of prestin and mCl-YFP. In order to avoid photobleaching interference during long exposure measurements, a new chloride sensor was developed with 80-fold better photostability than wild-type EYFP by stabilizing the chromophore structure via hydrogen-bond network. Other characteristics are similar to the original sensor we developed. We are currently testing the new sensor's sensitivity to other anions that typically exist in cells. We expect that this sensor will provide more detailed information on the transporter function of prestin, as well as other membrane proteins.

PS-766

On the Area Motor Model of Outer Hair Cell Electromotility: Interactions of Salicylate and Chloride

Joseph Santos-Sacchi; Lei Song
Yale University

The outer hair cell (OHC) is electromotile, its membrane motor identified as the protein SLC26a5 (prestin). An area motor model, based on 2-state Boltzmann statistics, was developed about two decades ago and derives from the observation that OHC surface area is voltage-dependent (Kalinec et al., 1992). Indeed, aside from the nonlinear capacitance (NLC) imparted by prestin's voltage sensor charge movement, linear capacitance (C_{lin}) also displays voltage dependence as motors move between expanded and compact states. Naturally, motor surface area changes alter membrane capacitance. Unit linear motor capacitance fluctuation (dC_{sa}) is on the order of 140 zF. A recent 3-state model of prestin (Homma and Dallos, 2011) provides an alternative view, suggesting that voltage-dependent linear capacitance changes are not real but only apparent because the two component Boltzmann functions shift their midpoint voltages (V_h) in opposite directions during treatment with salicylate, a known competitor of required chloride binding. We show here using manipulations of NLC with both salicylate and chloride that an enhanced area motor model, including augmented dC_{sa} by salicylate, can accurately account for our novel findings. We also show that while the 3-state model implicitly avoids measuring voltage-dependent motor capacitance, it registers dC_{sa} effects as a byproduct of its assessment of C_{lin}, which increases during salicylate treatment as motors are locked in the expanded state. The area motor model, in contrast, captures the characteristics of dC_{sa}'s voltage-dependence, leading to a better understanding of prestin.

PS-767

An Electrical and Cable Model Inspection of Outer Hair Cell Properties.

Joseph Santos-Sacchi; Lei Song
Yale University

The cylindrical outer hair cell (OHC) of Corti's organ drives cochlear amplification by a voltage-dependent activation of the molecular motor, prestin, in the cell's lateral membrane. The voltage dependent nature of this process leads to the troublesome conclusion that the membrane RC filter could limit high frequency acoustic activation of the motor. The unique 30 nm width compartment (ECS) formed between the cell's lateral membrane and adjacent subsurface cisternae (SSC) could further limit the influence of receptor currents on lateral membrane voltage. Here we use dual perforated/whole cell and loose patch clamp on isolated OHCs to sequentially record currents resulting from excitation at apical, middle and basal loose patch sites before and after perforated patch rupture to establish traditional whole cell mode. We find that generated current transients are always single exponential, in contrast to expectations from previous modelling efforts (Halter et el., 1997). Furthermore, the timing of currents is fast and uniform only prior to whole cell pipette washout following perforated patch rupture, suggesting little voltage attenuation along the length of the lateral membrane. Prior treatment with salicylate, a disrupter of the SSC, shows no differences following perforated patch rupture. Finally, a cable model of the OHC indicates that the SSC poses a minimal barrier to current flow across it, thereby facilitating rapid delivery of voltage excitation to the prestin-embedded lateral membrane.

PS-768

PKA Activation Results in Increased BK Channels Expression on the Surface of the Cell

Jun-Ping Bai[1]; Iman Moeini-Naghani[2]; Joseph Santos-Sacchi[3]; Dhasakumar Navaratnam[2]
[1]Yale University, New Haven; [2]School of Medicine, Department of Neurology; [3]School of Medicine, Department of Surgery

Background

BK channels are expressed in increasing concentration on the surface of chick hair cells along the tonotopic axis of the basilar papilla. Their increasing expression in high frequency hair cells is thought to be a contributor to electrical resonance. Since mRNA levels of the alpha subunit of BK channels (Slo) decrease along the tonotopic axis the existence of post-translational control of protein expression is likely. We have previously demonstrated the importance of CDK5 and PKC in the expression of BK channels in hair cells.

Method

We used FACS analysis of HEK cells expressing the Slo subunit to ascertain how activation of PKA affected its surface expression. In addition, we used site directed mutagenesis using phosphodeletional and phosphomimetic mutations to determine if PKA produced its effects by direct phosphorylation of the protein. Finally, we used immunofluorescence of chick cochlea cultures to ascertain of PKA activation affected Slo expression on the surface of hair cells.

Result

We confirm PKA activation resulted in increased surface expression of Slo. Both forskolin and 8-Br-CAMP increased surface expression of Slo. We also determine that the effects of surface expression are due to direct phosphorylation with synergism between different phosphorylation sites. Thus multiple specific single phosphodeletional mutants were un-

responsive to PKA activation, while their corresponding phosphomimetic mutants demonstrated robust responses to PKA activation. Initial experiments suggest that these effects are in part due to reduced internalization of Slo after PKA activation. Our preliminary data suggest that these effects of PKA on surface expression of Slo also extend to hair cells.

Supported by NIH/ NIDCD R01DC 007894

PS-769

Pigmentation Increases Maximum Electrical Gain of Outer Hair Cells in a Guinea Pig Animal Model

Varun Sreenivasan; Christian Corbitt; Federica Farinelli; **Brenda Farrell**
Baylor College of Medicine

Outer hair cells (OHCs) amplify sound by producing an electrical and mechanical gain to mitigate the losses incurred by sound waves in the cochlea. The potential where the maximum gain is poised is expected to be nearly coincident to the silent membrane potential *in vivo* for a mammal to fully benefit from amplification. The maximum electrical gain for OHCs is the peak charge density and is the product of two measurable components: the maximum voltage sensitivity, (α(Vpeak)) at the membrane potential, (V≡Vpeak), and the charge density, (σ). We measure the electrical gain with isolated OHCs extracted from sexually immature and mature albino and pigmented guinea pigs by monitoring the voltage-dependent capacitance with admittance techniques. Experiments were conducted at room temperature, at constant pipette pressure (0 ± 0.1 kPa) and in the presence of a specific KCNQ channel blocker (> 30 μM XE991) to ensure robust voltage clamp. After interrogating a relatively large number of cells (n: 135) we report that α(Vpeak) is strongly dependent upon phenotype; cells originating from pigmented guinea pigs exhibit values of 8.45 V^{-1} (n: 74) compared to cells extracted from albinos

7.6 V^{-1} (n: 61, P-value < 0.0001). For OHCs isolated from pigmented animals the α(Vpeak) is significantly higher (P-value < 0.0001) at the basal region of the cochlea (9 V^{-1}) compared to the apical region (8 V^{-1}) with no spatial gradient detected for cells originating from albinos. In contrast, we observe no detectable difference between phenotypes for σ and Vpeak. After adjusting the measurements for physiological temperature we report that Vpeak varies with position at -0.070 (± 0.025) V for cells originating from turn 1 and -0.047 (± 0.022) V for cells originating from turn 3. The voltage of maximum sensitivity is within the scatter of the *in vivo* measurements for the silent membrane potential at -0.077 (± 0.018) V for cells from turn 1 and

0.056 (± 0.018) V for cells from turn 3. There is evidence that melanin and its precursors help alleviate age and noise-induced hearing loss by maintaining the magnitude of the endocochlear potential. This shows a pigmented phenotype increases the maximum electrical gain of OHCs by up to 20% and reveals an additional cellular mechanism to explain how skin color may affect hearing health.

PS-770

Mammalian Cochlear Inner Hair Cells Show Intrinsic Membrane Tuning

Stuart Johnson
University of Sheffield

The mammalian auditory system is specialised for detecting a wide range of sound frequencies and intensities. Each component along the auditory pathway has to faithfully encode and relay auditory information with remarkable speed and precision in order to detect minute differences in timing and intensity of sounds arriving at the two ears. This largely depends on the speed and accuracy of the sensory inner hair cells (IHCs) that are the primary site for the conversion of sound into neural activity. Although the biophysical properties of IHCs are generally suited for rapid signalling, they are believed not to be intrinsically tuned to encode a particular frequency or component of sound, which differs from the hair cells of lower vertebrates.

Apical (low frequency) and basal (high frequency) IHCs in acutely dissected mature gerbil cochleae were patch-clamped at body temperature and voltage-clamp recordings were made of mechanotransducer and basolateral membrane currents. Some experiments were performed in a solution containing an endolymph-like low-Ca^{2+} concentration (40 μM) to simulate *in vivo* conditions. Current clamp recordings were performed to see how the underlying membrane biophysics controlled the cells voltage responses to steps and sound-like stimulation.

Low and high frequency IHCs had substantially different biophysical characteristics that would make the resting potential of apical IHCs more depolarised *in vivo*, resulting in a shorter membrane time constant but smaller responses than in basal cells. When IHCs were stimulated with a protocol mimicking *in vivo* sound stimulation at different frequencies and amplitudes, the more rapid kinetics of apical cells allowed them to accurately follow the phasic component of sound. On the other hand, basal IHCs were suited for encoding sustained graded responses.

These findings represent the first evidence for intrinsic tuning in mammalian IHCs that is likely to specialise them for precise frequency-following (low frequency) or intensity-following (high-frequency) responses to sound. This ensures that the predominant component of their *in vivo* receptor potential is as accurate as possible, which correlates with the different strategies used to localise low and high frequency sounds using interaural time or level differences.

PS-771

Interaction of Syntaxin-1 with Receptor-Like Protein Tyrosine Phosphatase

Neeliyath Ramakrishnan; Dennis G. Drescher
Wayne State University

Background

Syntaxin-1, widely expressed in neuronal and neurosensory synapses, is thought to mediate vesicle fusion. Protein-protein interactions involving syntaxin-1 at the hair cell pre-syn-

aptic membrane are not clearly understood. The present study reflects our approach to identifying the synaptic-junction protein complex of hair cells.

Methods

We employed a yeast two-hybrid assay using trout syntaxin-1B as bait and a trout hair-cell cDNA library as prey. Equivalent regions of rat sequences corresponding to candidate prey sequences were further tested in yeast two-hybrid co-transformation experiments. GST pull-down experiments involving GST-syntaxin-1 fusion protein and total rat brain protein were performed to confirm these results in vitro.

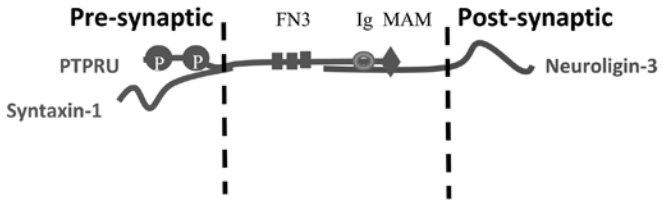

Results

In trout hair-cell yeast two-hybrid experiments, we found a binding partner that has sequence identity with receptor type protein tyrosine phosphatase (PTPRU, also known as PTP λ), a single pass transmembrane protein with two carboxy-located phosphatase domains (P) in the cytoplasmic region and an extracellular region consisting of fibronectin type III domains (FN3), one immunoglobulin-like domain (Ig) and a Meprin/AS/μ (MAM) domain (see illustration). We confirmed the interaction of syntaxin-1 and PTPRU using rat sequences: GST pull-down experiments, with anti-PTPRU antibody, verified the yeast two-hybrid results. Similarly, we observed interaction between PTPRU and neuroligin-3 by yeast two-hybrid analysis, followed by GST pull-down experiments utilizing specific antibodies.

Conclusion

Many receptor-type PTPs localized to the pre-synaptic membrane interact via their extracellular domains with post-synaptic proteins (Lim et al., EMBO J 28: 3564-3578, 2009) such as neuroligin and neurexin (Takahashi and Craig, Trends Neurosci 36: 522-534, 2013). PTPRs, in general, play crucial roles in cell signaling (Tonks, Nat Rev Mol Cell Biol 7: 833-846, 2006) and interact with many proteins, including cell-junction and synaptic-junction proteins, to regulate active zone assembly (Ziv and Garner, Nat Rev Neurosci 5: 385-399, 2004). In this light, our results point to a possible molecular complex formed between syntaxin-1 and PTPRU on the pre-synaptic side and neuroligin-3 on the post-synaptic side. Further experiments will help to establish the importance of these interactions at the hair-cell afferent synapse.

PS-772

A Membrane Guanylyl Cyclase Pathway in Hair Cells

Marian Drescher; Dakshnamurthy Selvakumar; Dennis G. Drescher

Wayne State University

Background

CNGA3, a highly Ca^{2+}-permeable, pore-forming cation-channel mediating sensory transduction in photoreceptors, primary olfactory neurons and chemosensory receptors, has been identified in both vestibular and cochlear hair cells, localized to the stereocilia and demonstrated to interact with myosin VIIA and cadherin 23 +68 (Selvakumar et al., Biochem. J. 443: 463-476, 2012; J. Biol. Chem. 288: 7215-7229, 2013). The existence of cGMP-gated CNGA3 in hair cells would require a cGMP pathway for functionality. Sensory transduction in other modalities utilizes specific membrane guanylyl cyclases (GCs) and their associated pathways mediating Ca^{2+} influx, as opposed to utilizing soluble GC which couples to NO and PKG phosphorylation of targeted proteins such as VGCC inhibiting Ca^{2+} influx.

Methods

Hair cell mRNA sequence crossing introns has been obtained and deposited in GenBank for the teleost purified saccular hair cell preparation with corresponding proteins immunolocalized in mammalian cochlear sensory epithelium. Yeast two-hybrid protocols, pull-down assays, and surface plasmon resonance (SPR) were used to determine kinetic constants and calcium-dependency of protein-protein interactions. Scanning electron microscopy (SEM) facilitated morphological analysis of stereociliary arrays for the cpfl1 (PDE6C) mutant.

Results

A membrane GC, with identity to both retinal GC2 and GC1, is expressed in saccular hair cells (GenBank Accession No. KM603484). Further, guanylyl cyclase-activating proteins which activate GCs in photoreceptors at low $[Ca^{2+}]i$ and inhibit at high $[Ca^{2+}]i$ are expressed: guanylyl cyclase activating protein 2 (GCAP2) and guanylyl cyclase activating protein 1 (GCAP1) (GenBank Accession Nos. KM603483 and KM603486, respectively). Guanylyl cyclase inhibitory protein (GCIP) (KM603485), inhibiting retinal-GCs at high $[Ca^{2+}]i$, is expressed in hair cells. CNGA3, a target of the membrane guanylyl cyclase pathway, interacts with intraflagellar transport protein 20 (IFT20), and IFT20 in turn couples to opsin. SPR analysis indicated Ca^{2+}-dependent binding of CNGA3 to AP2mu1, another targeted protein. PDE6C, the phosphodiesterase catalyzing degradation of cGMP, regulates cGMP-gated CNGA3. SEM has revealed defects in stereociliary arrays of the PDE6C mutant, cpfl1, morphologically similar to those observed in mutants of myosin VIIa, a tight binding partner of CNGA3.

Conclusion

Given that transcript for PDE6C was previously identified in saccular hair cells with PDE6C protein localized to stereocilia of saccular and cochlear hair cells, and that PDE5/6 inhibitors (and cGMP itself) initially elevate $[Ca^{2+}]i$ in cochlear OHC, the

predicted outcome of cGMP-activation of highly Ca^{2+}- permeable CNGA3, we suggest the new results support the existence of a membrane GC pathway in saccular/cochlear outer hair cells regulating cGMP-gated CNGA3.

PS-773

In Vivo Biophysical Properties of Hair Cells from the Mature Zebrafish Lateral Line.

Jennifer Olt; Stuart Johnson; Walter Marcotti
University of Sheffield

Introduction

Hair cells convert sound or balance cues from the environment into neuronal activity in the inner ear and vestibular system with remarkable precision and fidelity. We do not fully understand the mechanisms underlying these physiological processes, mainly because the experimental approaches required to achieve them *in vivo* are currently not feasible in mammals. Thus, an alternative animal model is needed to fully understand hair cell function. Although the zebrafish represents an ideal model for *in vivo* studies (Nicolson 2005 Ann Rev Genet 39:9-22), its exploitation is currently restricted by the limited understanding of hair cell physiology and how comparable they are with mammals. Recently investigations have characterized the biophysical properties of hair cells from immature larval zebrafish (Ricci et al.2013,JNeurosci,33:3131;Olt et al.2014,JPhysiol,592:2041). However, *in vivo* information from hair cells of the fully mature zebrafish lateral line is still lacking.

Method and Results

In the present study we have developed an experimental approach to perform electrophysiological recordings from hair cells of the functionally mature zebrafish lateral line. We have established the experimental conditions required to maintain healthy >20 days post-fertilization zebrafish using an appropriate anaesthetic that did not affect the biophysical properties of hair cells (the commonly used MS-222 is not suitable: see Olt et al. 2014). We found that benzocaine was able to anaesthetise fish to an adequate depth, causing muscle relaxation without nociception, whilst allowing viable electrophysiological recordings from hair cells. We are also developing a method to intubate the zebrafish in order to guarantee gill oxygenation. Experiments were licensed by the UK Home Office under the Animals Act 1986.

Conclusions

This study provides a crucial methodological advance that will allow *in vivo* recordings to be performed on hair cells of the mature zebrafish lateral line to investigate mechano-electrical transduction, synaptic transmission and afferent recordings.

PS-774

Clarin-1 is Involved in Vesicle Trafficking Regulation in Zebrafish Hair Cells.

Marisa Zallocchi; Oluwatobi Ogun
Boys Town National Research Hospital

Introduction

Clarin-1 is a four transmembrane protein expressed by hair cells and photoreceptors. Mutations in its corresponding gene are associated with Usher syndrome type 3, characterized by late onset and progressive hearing and vision loss in humans. Mice carrying mutations in the clarin-1 gene have hair bundle dysmorphology and a delay in synapse maturation. Here we examined the expression and function of clarin-1 in zebrafish hair cells.

Methods

Immunohistochemistry, FM1-43 incorporation, immunoprecipitation and co-localization with different markers were some of the techniques used to study clarin-1 function in zebrafish morphants and in morphants co-injected with full length or truncated forms of the clarin-1 transcript.

Results

Clarin-1 localized below the cuticular plate and at the point of insertion of the kinocilium in neuromast and inner ear hair cells. Cross-sections also showed the presence of clarin-1 at the base of the neurosensory epithelia. Knockdown of the protein by the generation of morphants resulted in inhibition of both fast and slow FM1-43 incorporation which suggests clarin-1 is regulating mechanotransduction channel activity and vesicle recycling. Co-localization and co-immunoprecipitation studies demonstrated an *in vivo* association between clarin-1 and Pcdh15a at the apical aspect of hair cells. In the clarin-1 morphants, the lack of clarin-1 results in Pcdh15a re-distribution/absence from the hair bundle correlating with mechanotransduction channel impairment. Morphants also showed a reduction in rab11a/b-positive vesicles. These phenotypes were fully prevented by co-injection with clarin-1 transcript, requiring its carboxyl-terminal tail.

Conclusion

Altogether our results suggest clarin-1 vesicle trafficking regulation is the underlying mechanism by which clarin-1 modulates hair cell function and provide new insights into a more detailed investigation by which clarin-1 affects vesicle recycling and how other Usher proteins might be also playing a part in this pathway.

PS-775

Inner Ear Formation and Hair Cell Function Depend on the Presence of Integrin a8 in Zebrafish

Marisa Zallocchi[1]; Oluwatobi Ogun[1]; Dominic Cosgrove[2]
[1]Boys Town National Research Hospital; [2]Boys Town National Research Hospital University of Nebraska Medical Center

Introduction

Although the expression of integrin a8b1 (itga8) in mouse hair cells has been demonstrated more than 10 years ago, very little is known regarding its role during inner ear development and function. Itga8 localizes to the hair cell apical surface along with its ligand, fibronectin, and one of its downstream effectors, focal adhesion kinase (FAK). Previous studies of homozygous mice for itga8 showed mis-localization of both fibronectin and FAK and defects in stereocilia morphology in utricular hair cells. The present work addresses the role of

itga8 during hair cell development using zebrafish as a model and the interaction of this integrin with Usher proteins.

Methods
Expression of itga8 was analyzed by immunohistochemistry and western blot. Itga8 morphants were generated to study the effect of this integrin in neuromast and inner ear hair cells. Usher protein association with itga8 was determined by co-immunoprecipitation, co-localization, and proximity link assay (PLA) studies.

Results
We developed two peptide antibodies against different regions of itga8 that allowed us to discriminate between variants. We observed localization of Itga8 in the hair cell bundles and in a subset of cells at the basolateral membrane. The absence of Itga8 protein in the specific zebrafish morphants led to absence FAK and defects in FM1-43 uptake. There was also a delay in placode cavitation and in the corresponding formation of the otic vesicle. Otolith formation was also abnormal. Because previous experiments from our laboratory demonstrated an interaction between itga8 and some of the Usher proteins in mice, we examined the possible existence of an Usher/itga8 complex in zebrafish. Co-localization and co-immunoprecipitation studies showed an association between itga8, clarin-1 and Pcdh15a. The formation of this complex was confirmed by PLA.

Conclusion
Similar to what it was observed in the mouse, itga8 is necessary for inner ear and hair cell development and/or maturation in zebrafish, with some of these functions being regulated through the formation of an Itga8/Usher complex. In this regard, by associating with itga8, clarin-1 and Pcdh15a might have the capacity to modulate hair cell function in response to external cues, establishing for the first time a link between Usher proteins and an integrin signaling cascade.

PS-776

The Ush2a Protein Product is Involved in Kinocilia Formation and Synapse Maturation in Zebrafish Hair Cells.

Marisa Zallocchi; Oluwatobi Ogun
Boys Town National Research Hospital

Introduction
Usher syndrome (USH) is the most common genetic cause of combined deaf/blindness. Mutations in the *USH2A* gene are responsible for the majority of the USH cases. Two variants have been described for the ush2a protein. The short variant is a secreted protein and a component of the extracellular matrix in different tissues including ear and eye while the long variant of ush2a is a transmembrane protein. Ush2a is expressed by hair cells and photoreceptors. Together with GPR98, ush2a forms the transient ankle links that maintain hair bundle cohesion during stereocilia development. Ush2a also localizes at the ribbon synapses. Because it has been localized at or near the true cilia in both photoreceptors and developing hair cells, a role associated with that sub-cellular compartment has been suggested for ush2a.

Methods
The expression and function of ush2a protein was analyzed in wild type and *ush2a* mutant zebrafish. Distribution of apical and basal hair cell structures was analyzed by immunohistochemistry with specific markers. Fast and slow FM1-43 uptake was used to study ush2a effect on mechanotransduction channel activity and vesicle recycling, respectively.

Results
Neuromasts hair cells from 5-7dpf ush2a mutants showed a significant shortening of the kinocilia. In the inner ear, kinocilia were also shorter or absent with the otolith resting directly over the hair cell bundle. At the basal aspect of the hair cells we observed a decrease in the number of ribbons, determine by ribeye b immunostaining. At the synapses ush2a heterozygous animals dual immunostained for ribeye b and MAGUK showed the characteristic juxtaposed synaptic bouttons. Conversely, ush2a mutants not only have a reduced number of ribeye b puncta but also the pre- and post-synaptic bouttons are diffuse and not well defined. FM1-43 incorporation through endocytosis was also altered in the mutants.

Conclusion
Ciliary defects have previously been described for ush2a morphants in Medaka fish. Here we not only observed kinocilia defects in hair cells but also abnormalities in synapse formation/maturation and function. Because the mutants display vesicle recycling impairments we propose that ush2a regulates the formation of these hair cell-specific structures by the modulation of vesicle recycling and endocytosis in the neurosensory epithelia.

PS-777

Characterization and Kinetic Analysis of ATPase activity of P2X2

Rahul Mittal[1]; M'hamed Grati[1]; Fenghua Yuan[1]; Qing Chang[2]; Denise Yan[1]; Xi Lin[2]; Amjad Farooq[1]; Yanbin Zhang[1]; XueZhong Liu[1]
[1]University of Miami-Miller School of Medicine; [2]Emory University

Background
Hearing loss is a sensory deficit afflicting humans. We and others have demonstrated that p.V60L and p.G353R mutations in P2X2 cause dominant progressive hearing loss in humans. P2X2 is an ATP-gated trimeric ion channel that plays an important role in sound transduction and auditory neurotransmission in the inner ear. ATP binding to the extracellular loop of the channel is believed to cause conformational changes that trigger channel pore opening and cation internalization. The aim of the present study is to characterize the molecular mechanism by which P2X2 channel acquires activation energy to open its pore.

Methods
Wild-type (WT) and mutant forms of P2X2 were overexpressed and purified. Organ of Corti organotypic cultures were established from 2-3 day old rat pups. WT and mutants forms were expressed in HEK293 cells. ATPase activity was determined using commercially available kits. We examined the effect of cations on the ATPase activity of P2X2. The ef-

fect of mutations on ATP binding capability of P2X2 was determined by structural modeling. The permeability of mutant and WT forms of P2X2 was evaluated by patch-clamp recordings of HEK293 cells.

Results

We found that WT P2X2 and p.G353R hydrolyzed ATP in time-dependent manner whereas p.V60L did not show significant ATPase activity. This ATPase activity was also demonstrable in organ of Corti explant cultures and HEK293 cells. Interestingly, we observed no significant effect of K+, Na+, Ca++ on the ATPase activity of P2X2. Kinetic analysis showed that P2X2 has strong affinity for ATP. This ATPase activity was abolished in the presence of inhibitors confirming the specificity of this reaction. Radioactive and fluorescent ATP binding assays revealed that p.V60L is unable to bind ATP compared to WT and p.G353R. These results were corroborated by computer modelling which demonstrated that p.V60L caused a conformational change in the structure of P2X2 preventing ATP binding and hence hydrolysis, Electrophysiological recordings also showed that p.V60L failed to generate ATP-evoked membrane current. On the other hand, p.G353R mutation in the channel gate affected its ionic permeability without altering its ATP binding or hydrolysis properties.

Conclusions

We demonstrate that P2X2 is capable of hydrolyzing ATP *in vitro* and in hair cells, following a first order reaction, and relies on its ATPase activity to operate its pore. We characterized all the enzymatic parameters related to this ATPase activity. We also shed light on the molecular mechanisms by which P2X2 catalyzes the degradation of ATP.

PS-778

Subcellular Distribution of a Non-classical Spectrin, Beta V, in the Amphibian and Mammalian Hair Cells

Matteo Cortese[1]; Samantha Papal[1]; Christine Petit[2]; Aziz El-Amraoui[1]

[1]Institut Pasteur, Genetique et Physiologie de l'Audition, INSERM UMRS1120; [2]Institut Pasteur, INSERM UMRS1120, Collège de France

Usher syndrome is the major cause of dual hearing and visual impairment. The proteins responsible for Usher syndrome of type I (USH1) — myosin VIIa (USH1B), harmonin (USH1C), cadherin-23 (USH1D), protocadherin-15 (USH1F) and SANS (USH1G) — play key roles in the proper organization and functioning of the hair bundle, the sound receptive structure. We have shown that in photoreceptor cells, spectrin bV, the mammalian non-classical b spectrin (which is almost twice the length of classical b spectrins), interacts with myosin VIIa, SANS and harmonin.

Consistent with its cytosolic distribution from the Golgi apparatus to the base of the photoreceptor outer segment, we found that spectrin bV also binds to rhodopsin and to two subunits of the microtubule-based motor proteins, kinesin II and the dynein complex. A failure of the spectrin bV-mediated coupling between the actin-based motors and opsin molecules probably accounts for the opsin transport delay in myosin VIIa-deficient mice. In the mouse inner ear, we found that the distribution of spectrin bV differs according to the type of hair cells. In the auditory hair cells, this spectrin, which exist as heteromers of aII and bV subunits, is abundant along the plasma membrane of the outer hair cells (OHCs), contributing to the spectrin-based cytoskeleton that provides these cells with the flexibility required for electromotility. In the inner hair cells, aII and bV subunits are restricted to the neck region around the cuticular plate. In vestibular hair cells, spectrin bV did not colocalise with spectrin aII; instead, spectrin bV immunolabeling showed a punctate cytoplasmic pattern that overlaps with Golgi structures. Notably, in amphibian inner ears, all the sensory hair cells display the same spectrin bV labeling, mainly located in the apical cell region, at the level of the cuticular plate and nearby the apical junctional complex. Likewise, in drosophila, the b-Heavy spectrin, the equivalent of mamalian spectrin bV, has been detected in the apical cell region of all eipthelial cells.

Our results illustrate how during evolution, the spectrin βV spatial distribution displays an inter- and intra-species pattern varying according to the specific needs of specialized membrane domains in sensory cells. The spectrin βV-mediated network adapts to the cell type, contributing either to cytosolic trafficking as in photoreceptor and vestibular hair cells, or sustaining the plasma membrane domain organization as in OHCs.

PS-779

Localisation of LHFPL5 in Hair Cells of the Mouse Cochlea, and the Effects of Lhfpl5 Knockout on Hair-Bundle Morphology.

Carole Hackney[1]; Shanthini Mahendrasingam[2]; David Furness[2]

[1]University of Sheffield; [2]Keele University

Hair cells are the mechanosensors of the cochlea where they convert the mechanical vibrations caused by sound into electrical signals to be carried along the auditory nerve to the brain. Deflections of the stereocilia on hair cells are believed to place a strain on these channels which then open, letting through K^+ ions which result in cell depolarisation. The molecular components of the mechanotransduction channels of the hair cells are still under investigation. Recently, mechanotransduction has been shown to be impaired in mice lacking a tetraspan membrane protein, TMHS (also known as LHFPL5*)*. Immunofluorescence suggests this protein is found near the stereociliary tips (Xiong et al., Cell, 151, 1238-1295). Here we have utilized post-embedding immunogold labelling and stereological analysis to refine and more precisely localize this protein in P5 mice, and examined the effect of loss of LHFPL5 on stereociliary bundle morphology in P12 KO. Our data confirm the suggested stereociliary tip localization but they also shows LHFPL5 in lower levels in the cytoplasm as well as in the membranes, suggesting that during development, this protein is being shipped to the membranes from the manufacturing areas of the cell. In P12 mice, the short

and intermediate stereocilia of the bundle are reduced in number and height. As mutations of the *Lhfpl5* gene lead to deafness and because it may show the precise anatomical position of the mechanotransduction channels, we believe that ultrastructural localization could provide further clues to its function. Immunogold postembedding labelling gives a way of doing this, particularly if combined with quantitative analysis of precise localization.

PS-780

The Effect of Harmonin Expression on Usher Proteins in a Mouse Model of USH1C

Suzanne Smart[1]; Frank Rigo[2]; Michelle Hastings[3]; Jennifer Lentz[4]

[1]Louisiana State University Health Science Center, New Orleans; [2]Isis Pharmaceuticals, Inc.; [3]Department of Cell Biology and Anatomy, Chicago Medical School, Rosalind Franklin University of Medicine and Science; [4]Department of Otorhinolaryngology and the Neuroscience Center of Excellence, Louisiana State University Heath Science Center

Introduction

Usher syndrome is the leading genetic cause of combined deafness and blindness. Type 1 Usher syndrome is characterized by profound hearing impairment and vestibular dysfunction at birth and the development of retinitis pigmentosa in early adolescence. Approximately 6–8% of type 1 Usher syndrome cases are caused by mutations in the *USH1C* gene, which encodes the protein harmonin. Mice homozygous for the *Ush1c* c.216G>A mutation (216AA), responsible for Acadian Usher syndrome type 1C, show severe vestibular dysfunction and deafness with disorganized inner and outer hair cell rows, abnormal hair bundle morphogenesis and mis-localization of harmonin protein. We have developed an antisense oligonucleotide (ASO) targeting the 216AA mutation and have recently shown that treatment within the first week of life rescues hearing function, improves hair bundle morphology and harmonin protein expression. Harmonin has been suggested to play an important scaffolding role in the development of hearing through protein-protein interactions. The purpose of this study was to determine the effect of harmonin mis-localization and correction with ASOs on the expression and localization of other Usher proteins known to interact with harmonin in cochlear hair cells.

Methods

Immunohistochemistry with antibodies against Sans, Protocadherin 15, and Cadherin 23 was used to analyze localization within cochlear hair cells in ASO treated and control-treated 216AA mutant and control mice during post-natal development.

Results

Localization of Sans appears abnormal within the hair cell bundles of *Ush1c* 216AA mutant mice, however, treatment with 216A-targeted ASOs shows localization more similar to wild type mice. Expression of the tip-link proteins, Cadherin 23 and Protocadherin 15, are currently being evaluated.

Conclusion

Correct localization of Sans, a protein suggested to play a structural role in the sensitivity to mechanical stimulation, may require intact expression and localization of harmonin protein to localize to the upper tip link density of hair cell bundles.

PS-781

Hair Cell Loss and Stereocilia Defects in miR-183 Family Knockout Models

Marsha Pierce[1]; Jennifer Kersigo[2]; Bernd Fritzsch[2]; David Nichols[1]; Garrett Soukup[1]

[1]Creighton University; [2]University of Iowa

Background

MicroRNA-183 family (miR-183, miR-96, and miR-182) is highly conserved and coordinately expressed in neurosensory cells. Mutations in *miR-96* lead to hair cell (HC) loss and profound deafness in both humans and mice. *miR-183/96* and *miR-182* knockout (KO) mice were assessed to investigate miR-183 family member loss of function (LOF).

Methods

miR-183/96 KO and *miR-182* KO mouse lines were generated by and acquired from the Sanger Institute. Behavioral observations and evaluation of Preyer's reflex were used to grossly assess HC function. HC loss and stereocilia defects in mice ranging from P0 to P180 were examined by immunofluorescence microscopy (IFM) detection of MyoVIIa, scanning electron microscopy (SEM), and phase contrast microscopy (PCM) of plastic embedded sections through organ of Corti.

Results

In *miR-183/96* KO mice, SEM showed delayed stereocilia development at P0 and gross stereocilia disorganization at P16. PCM of sectioned organ of Corti revealed basal HC loss at P21, and IFM detection of MyoVIIa displayed substantial middle turn and basal HC loss at P30. Accordingly, *miR-183/96* knockout mice failed to exhibit Preyer's reflex at any age and furthermore diplayed head bobbing and circling behavior beginning ~P90.

Interestingly, *miR-183/96* heterozygous mice showed an age-related loss of Preyer's reflex beginning ~P60, and IFM detection of MyoVIIa displayed subtle HC disorganization and punctate HC loss.

In *miR-182* knockout mice, IFM detection of MyoVIIa showed HCs present in the apex and middle turn at P180. However, SEM revealed inner HC stereocilia fusion and some outer HC disorganization. Correspondingly, *miR-182* knockout mice displayed an age-related loss of Preyer's reflex.

Conclusions

Results demonstrate that miR-183 family LOF leads to stereocilia defects and HC loss that contribute to hearing and balance deficits, suggesting that each family member is requisite for HC maintenance and survival. Additionally, analysis of *miR-183/96* heterozygous mice suggests that miRNA concentration or "dose" is crucial for HC function and survival. Moreover, behaviors consistent with profound vestibular defects are observed only in *miR-183/96* knockout mice,

suggesting that vestibular HCs are less sensitive to miR-183 family expression levels than auditory HCs. Understanding miR-183 family effects on target genes and pathways is expected to provide insight to approaches for preventing HC loss or stimulating regeneration of neurosensory cells.

PS-782

Differential Small RNA Expression in Hair Cells of Dgcr8 and Dicer1 Conditional Knockout Mice.

Isha Pandya[1]; Garrett Soukup[1]; Colby Bradfield[1]; Sharalyn Steenson[2]; Marsha Pierce[1]
[1]Creighton University; [2]University of Nebraska Medical Center

Background

Small RNAs including endogenous small interfering RNAs (siRNAs) and canonical microRNAs (miRNAs) transcriptionally and post-transcriptionally regulate gene expression, respectively. Canonical miRNA processing requires proteins encoded by both *Dgcr8* and *Dicer1*, whereas siRNA processing requires only *Dicer1*. Conditional knockout (CKO) of *Dgcr8* versus *Dicer1* in hair cells (HCs) of the inner ear (IE) has different effects on HC development and maintenance. *Dgcr8* CKO shows disorganized HC stereocilia and mild HC loss in the base of the cochlea from mice aged 1-2 weeks old, whereas *Dicer1* CKO exhibits little or no stereocilia aberrations or HC loss in mice aged 2 weeks old. The earlier demise of HCs following *Dgcr8* CKO is hypothesized to result from greater changes in miRNA expression and/or gene expression.

Methods

HC-specific *Dgcr8* CKO and *Dicer1* CKO mice were generated using *Atoh1-Cre.* Total RNA was isolated from IE of two biological replicates from each of three groups including *Dgcr8* CKO, *Dicer1* CKO, and control (lacking *Atoh1-Cre*). Small RNA content in each sample was examined by Illumina small RNA sequencing (RNA-Seq). Normalized reads were analyzed to determine miRNAs and potential siRNAs that exhibited differences in abundance between groups of at least three fold.

Results

Small RNA-Seq analysis indicated there was relatively little change in miRNA expression in *Dgcr8* CKO IE compared to control. *Dicer1* CKO IE however exhibited a large number of downregulated miRNAs that included known sensory epithelial and HC-specific miRNAs. Potential siRNAs derivative of repetitive regions were less affected in *Dgcr8* CKO IE than *Dicer1* CKO IE, where potential siRNAs were largely upregulated. Potential siRNAs derivative of specific loci were relatively unperturbed in *Dgcr8* CKO IE, but largely downregulated in *Dicer1* CKO IE.

Conclusion

Analysis of small RNAs alone fails to provide insight into the HC phenotype of *Dgcr8* CKO mice. Dgcr8 might be associated with other RNAs including mRNAs to effect changes in gene expression and earlier HC demise. Examination of mRNA content in the *Dgcr8* CKO model is warranted to further explore the effect on HCs. *Dicer1* CKO in HCs largely leads to an expected depletion of both miRNA and potential siRNA content in the IE. Further examination of depleted small RNAs might reveal novel HC and sensory epithelial-specific miRNAs and siRNAs that contribute to HC maintenance.

PS-783

Do Auditory and Vestibular Cell Culture Techniques Vary?

Mirko Manojlovic Kolarski; Juzer Kakal; Desmond Nunez
University of British Columbia

Introduction

The inner ear cells processing auditory and balance stimuli are co-located and share common extracellular fluid compartments. In vitro models of the inner ear are an effective method of studying these organs. Several models have been described, but no comparison between auditory and vestibular cells has previously been attempted. We summarize current knowledge and techniques in inner ear cell culture, compare relative yields and viability, and determine the optimal culture method with regards to tissue source, harvesting technique, growth conditions, and cell characterization.

Goals of Study

To compare and contrast the optimal tissue sources and methods used to establish auditory and vestibular cell cultures. The aim was to compare culture techniques, viability, and yields of these sites.

Methods

A comprehensive search of MEDLINE (1946-2014) and Embase (1976-2014) was undertaken using the search terms “primary cell culture” and “inner ear”. Only English language articles reporting the results of cell culture of non-neuronal tissue derived from inner ear sites were included. Studies were divided by inner ear site. Studies reporting auditory or vestibular cell cultures derived from stem cells were included for media conditions and cell characterization.

Results

32 studies met the inclusion criteria. These studies exclusively used fresh tissue, primarily harvested from mice (50%), rats (15.7%), and guinea pigs (12.5%). There was little variation in tissue harvesting techniques. 84.4% of studies used auditory cells and 6.3% used vestibular. Anditionally, endolymphatic sac cells were used in 9.3%. Culture techniques were divided into four categories: standard adhesive, free-floating stem cell, immortalized cell (by virus or cell line), and stem cell differentiation. Hair cells were the primary target cell grown (59.4%). The cell type targeted for culture correlated with the culture media used. Immunocytochemistry was the predominant method of phenotypic characterization. There was variation in use of growth assays and functional assays. Maximal culture duration ranged from 5 hours to 36 weeks.

Conclusions

Characteristic inner ear cells can be cultured by several methods. There is insufficient data regarding yield and cell function for comparison of these methods. The majority of

studies to date have used auditory cells and further studies are needed to compare non-auditory sources. Specific phenotypic markers for hair cells have been established, but not for most other inner ear cells. Methods to maintain long-term culture growth and conserve phenotypic characteristics over time are lacking.

PS-784

Regional Specialization of Posterior Lateral Line Efferent Neurons in the Hindbrain of Larval Zebrafish

James Liao; Cat Smith; Melanie Haehnel-Taguchi; **James Liao**
The Whitney Lab for Marine Bioscience

The lateral line efferent system is thought to protect fishes from desensitization during motion-induced self stimulation and improves signal to noise levels. The hair cells contained in the neuromasts of the flow-receptive lateral line system in fishes are directly innervated by two populations of efferent neurons. Efferent cell bodies are located in the octavolateralis efferent nucleus (OEN) and are subdivided into rostral and caudal efferent neurons (REN and CEN, respectively) without knowledge of their post-synaptic targets. Our goal was to investigate which posterior lateral line neuromasts the RENs and CENs are connected to, and to do this we electroporated fluorescent dyes into efferent terminals at specific neuromasts. First, we labeled each neuromast in the trunk posterior lateral line (n = 5 fish), and found that only one REN and two CEN innervate about a dozen neuromasts. We next labeled pairs of neuromasts with two fluorescent dyes of different wavelengths to look at their position relative to each other in the hindbrain. We found that 57.7% of the most rostrally located neuromasts (L1, n = 26 neuromasts) are connected to the REN, while 80.8% were connected to a single CEN. In contrast, L2 (n = 10) and L5 (n = 13) neuromasts were not innervated by the REN but always connected to one or both CENs. By showing that the REN exclusively innervates one rostral trunk neuromast, while one of the CENs specifically innervates more caudal neuromasts, we demonstrate a regional hindbrain specialization of the efferent lateral line system based on peripheral neuromast location in larval zebrafish.

PS-785

Interactomes in the Sensory Epithelium of the Developing Cochlea

Lancia Darville; Bernd Sokolowski
University of South Florida, Morsani College of Medicine

Background

The sensory epithelium of the inner ear contains specialized receptors known as hair cells, which are necessary for the transduction of sound. In mouse, the onset of hearing occurs at approximately postnatal days (P) 12-14, while the inner ear continues developing through P30. We previously identified a number of proteins in the cochlear sensory epithelium in the young and mature mouse. In the present study, we wish to understand their function and how they are involved in normal cochlear development and disease. However, proteins do not function independently, but rather form complexes with other proteins. Therefore, we used an analysis tool to determine protein interactions that compose different functional interactomes.

Methods

Ingenuity Pathway Analysis (IPA) was used to determine networks of differentially expressed proteins from cochlear sensory epithelia of 3-, 14- and 30-day-old mice and to observe their biological processes. IPA identified the most significant biological functions of these differentially expressed proteins and the top five were categorized and reported based on their P values. A Fisher's exact test was used to calculate P values to determine the significance of input proteins with their biological functions. Network analysis was computed with IPA using the Ingenuity Pathways Knowledge Base as a reference.

Results

For proteins exclusively expressed on P3 relative to P30, we analyzed networks containing a maximum of 35 molecules. The highest scoring network contained 32 proteins associated with RNA post-transcriptional modification, cell morphology, and cell function and maintenance. Of particular significance was a network that contained 23 proteins associated with renal disease, since the kidney and cochlea have similar cellular attributes. For proteins downregulated on P3 relative to P14, we considered a maximum of 140 molecules in the network. IPA identified a network of 27 proteins associated with nervous system development and function, cellular development, and skeletal development and function. For proteins upregulated on P3 relative to P30, we also used a maximum of 140 proteins. The highest scoring network included proteins in development and hereditary disorders, and inflammatory disease. Among the proteins in this network were those associated with deafness and hearing, such as Myo6 and Myh9.

Conclusions

This study identified a number of interactomes relevant to early postnatal development. Within these networks are pathways that direct the function of deafness-related proteins, thereby providing insights to interacting signals relevant to hearing loss.

PS-786

Increased Apoptotic Response to Nucleolin Downregulation following Cisplatin Treatment in HEI-OC1 Cochlear Hair Cells

Magda Bortoni; Yohann Grondin; Elisa Ghelfi; Adam Bartos; Rosalinda Sepulveda; Archana Swami; Rick Rogers
Harvard School of Public Health

Background

Our GWAS identified Nucleolin as a potential candidate for susceptibility to NIHL. In this study, we asked if Nucleolin has an effect on oxidative stress response in cochlear cells. Nucleolin is a multifunctional protein that translocates to the cytoplasm under cellular stress. Its involvement in DNA metabolism and mRNA stabilization and translation play an important role in stress response and regulation of apopto-

sis. Moreover, our protein network association studies have shown that nucleolin is also involved in reactive oxygen species (ROS) response.

Goal
To identify the effect of nucleolin downregulation in the cellular response of cochlear hair cells exposed to cisplatin-induced stress in vitro.

Methods
We silenced nucleolin gene from cochlear hair cell line HEI-OC1 with either siRNA or shRNA, using non-target sequences as control. Silencing was confirmed with RTqPCR and Western Blot. Overnight exposure to 5µg of cisplatin was used as a challenge. Immunocytochemistry was performed on fixed permeabilized cells. Apoptosis was measured by flow cytometry using Annexin V / PI stain and by luminescence using CaspaGlo 3/7 from Promega. Intracellular ROS and nitric oxide (NO) was measured by Flow Cytometry using live dyes DCF-DA (2',7'-dichlorofluorescin diacetate) and DAF-FM 4-amino-5-methylamino-2′,7′-difluorescein, respectively.

Results
Cisplatin induced a dose-dependent apoptotic response in HEI-OC1 cells. Silencing of Nucleolin resulted in its downregulation by 35% at the protein and mRNA levels. Remaining Nucleolin protein in the cells was functional as evaluated by nucleolin diffusion in the nucleoplasm under cisplatin stress. Nucleolin downregulation decreased cellular viability and significantly increased early apoptosis ($p<0.05$), with cells showing significantly higher intracellular ROS ($p<0.05$) and NO ($p<0.05$) under cisplatin stress.

Conclusions
In accordance to our previous studies suggesting nucleolin's role in resistance to stress, these results demonstrate that nucleolin downregulation increases intracellular oxidative stress and early apoptosis during cisplatin challenge, increasing cellular susceptibility to stress.

PS-787

Endoplasmic Reticulum Stress is Involved in Cdh23 Mutant Mice Hearing Loss

Bo Li[1]; Xiaolin Zhang[2]; Juan Hu[2]; Jing Yuan[2]; Eileen Chen[2]; Tihua Zheng[3]; Heping Yu[2]; Maria Hatzoglou[4]; Qingyin Zheng[2]
[1]Binzhou Medical University; Case Western Reserve University; [2]Department of Otolaryngology-HNS, Case Western Reserve University; [3]Transformative Otology and Neuroscience Center, Binzhou Medical University; [4]Department of Pharmacology, Case Western Reserve University

Introduction
The mutations in the CDH23 gene are considered crucial for hearing loss due to disruption of hair cell (HC) in the cochlea and the vestibule during late embryonic/early postnatal development. Hearing loss was associated with HC loss and induction of apoptosis. But data are limited regarding the clear molecular mechanism that lead to the development of hearing loss. Endoplasmic reticulum stress (ER stress) may play a role in hearing impairment. Using *erl/erl* mutation mice, we hypothesis that ER stress resulting from the accumulation of mutant CDH23-ERL protein is the initial pathway that leads to HC death. This provides a new target to explore for protective therapies for USH/DFNB12 and age-related hearing loss.

Methods
We examined the ER stress marker genes and proteins in *erl/erl* and *v2J/v2J* mice cochlea tissue by Real-Time PCR, western blot and immunohistochemistry.

Results
In *erl/erl* CDH23 mutation mice, we found progressive loss of CDH23 expression and tip-link degeneration. CDH23-ERL protein are accumulated in the ER of cochlear hair cell area and induce ER stress then apoptotic cell death. ER stress responses are up-regulated in *erl/erl* and *v2J/v2J* mice.

Conclusions
ER stress might be a possible mechanism for auditory hair cell degeneration and cell death.

PS-788

Medial Olivocochlear Mappings: A (Blurry) Edge of CFs Recorded from a Point along the Cochlea

M. Christian Brown
Harvard Medical School

Introduction
Medial olivocochlear (MOC) neurons provide an efferent innervation to outer hair cells, but their mapping onto the cochlea is incompletely known. Differences between activation of the OC reflex in response to ipsilateral vs. contralateral sound (Lilaonitkul and Guinan, 2009) suggest different mappings for the two reflexes but these have not worked out because of the difficulties of intracellular labeling. Here, extracellular recordings were made at a site in the basal turn corresponding to a cochlear position of about 16 kHz. By this point in their spiral course, MOC axons innervating the most basal parts of the cochlear have already spun off from the OC bundle and are not sampled, resulting in an edge of characteristic frequencies (CFs) in the distribution of the remaining, sampled neurons.

Methods
In anesthetized guinea pigs, recordings were made using "sharp" electrodes and CFs were obtained from the unit's tuning curves. Other experiments made extracellular, focal injections of horseradish peroxidase.

Results
MOC units (n=631, in 133 guinea pigs) had a broad distribution of CFs from low to high, up to a high-CF edge equal to that of the highest-CF auditory-nerve fiber recorded at the site (about 16 kHz). Extracellular injections into the recording site labeled many MOC axons with endings also having a broad distribution, extending basally to an edge corresponding to the location of the labeled auditory-nerve fibers. There were exceptions that make the observed edges blurry. A few

MOC units (15 or 2.4%) had CFs just above (< 1/2 octave) the nerve-fiber CFs. Correspondingly, some anatomical cases had a basal extension of scattered MOC endings up to 1.5 mm, about 8% cochlear distance. The proportion of response types (which ear drove the unit) with CFs near and above the edge was similar to the proportion overall (60.4% Ipsi, 27.2% Contra, 12.4% Either Ear).

Conclusions

The correspondence of the CF edge of MOC units with the CF of the nerve fibers at the site suggests a mapping alignment at this site, similar to previous labeling studies (Robertson and Gummer, 1985; Liberman and Brown, 1986; Brown, 2014). The exceptions that blur the edge may be MOC axons recorded within their branching spans, and the basal extension up to 1.5 mm suggests a MOC axonal span consistent with previous studies. There were no clear differences in response types near the edges, suggesting that the Ipsi and Contra MOC response types are mapped similarly.

PS-789

Mechanical and Electrical Tuning in the Auditory System of Bushcrickets

Jennifer Hummel[1]; Stefan Schöneich[2]; Berthold Hedwig[2]; Manfred Kössl[1]; Manuela Nowotny[1]

[1]Goethe University; [2]University of Cambridge

Introduction

The hearing organ (*crista acustica*, CA) of bushcrickets is located within the tibiae of the forelegs and processes frequencies from about 3 to 80 kHz. Earlier studies on the sound-induced mechanical and electrical activity in bushcrickets revealed a frequency-dependent representation of response maxima along the CA, providing a tonotopy. However, details about the mechano-electrical transduction (MET) process within the CA and its tuning mechanisms remain unknown.

Methods

To investigate the acoustic signal transduction *in vivo*, we analyzed in a first step the sound-induced mechanical tuning using laser-Doppler vibrometry in the tropical bushcricket species *Mecopoda elongata*. In a second step, we measured the resulting neuronal response performing intracellular recordings of sensory cell activity.

Results

The mechanical and neuronal frequency-tuning curves (FTCs) confirmed the tonotopy along the organ with low stimulus frequencies represented at the proximal end and high frequencies represented at the distal end of the CA. However, since mechanical displacement amplitudes induced by frequencies below 30 kHz were generally larger in magnitude than those induced by frequencies above 30 kHz, even the distal region was highly deflected by the extensions of the low-frequency induced motion. Therefore, frequencies that led to the most sensitive mechanical responses (characteristic frequency, CF) and those that led to the highest amplitudes in response to all applied frequency-level-combinations (best frequency, BF) were restricted to values below 30 kHz in the distal region. Intracellular recordings of the distal cells, however, revealed CFs and BFs of at least 50 kHz in the neuronal FTCs. Comparing the mechanical and neuronal tuning at different regions along the CA, normalized and averaged mechanical FTCs were tuned less sharply (~6 to 30 dB/oct) than neuronal FTCs (~21 to 90 dB/oct).

Conclusions

The neuronal response of the CA is tuned sharper than the mechanical reaction induced by the same frequencies and the CF differs strongly in the mechanical and neuronal tuning of the distal region. Therefore, we suggest that the neuronal tuning of the CA depends on additional intrinsic tuning mechanisms that go beyond simple signal transduction.

Funding

Jürgen Manchot Foundation, DFG (NO 841/1-2) and Hanne and Torkel Weis-Fugh Fund.

PS-790

Acid-Sensing Ion Channel Characterization and Functional Expression in Cochlear Afferent Neurons

Antonia Gonzalez-Garrido[1]; Rosario Vega[2]; Francisco Mercado[3]; Ivan Lopez[4]; Enrique Soto[2]

[1]The University of Chicago; [2]Instituto de Fisiologia-BUAP; [3]Instituto Nacional de Psiquiatria Ramon de la Fuente Muñiz; [4]Department of Head and Neck Surgery, David Geffen School of Medicine at UCLA

Acid-sensing ion channels (ASICs) are activated by an increase in the extracellular proton concentration. There are four genes (ASIC1-4) that encode six subunits. ASIC subunits have been localized to sensory neurons of the somatosensory and visual systems. Also, ASIC2 and 3 subunits have been studied in spiral ganglion (Peng et al., J Neurosci, 2004; Hildebrand et al., Hearing Res, 2004). Here we studied the four subunits and characterized the ASIC currents of primary culture spiral ganglion neurons (SGNs) using whole cell patch clamp and identify contributing subunits.

The proton-gated current in SGNs is primarily carried by Na^+, has transient and sustained components and is blocked by amiloride, indicating that this current is an ASIC current. The aminoglycosides neomycin and streptomycin reduced the desensitization rate of the ASIC current in SGNs, indicating that ASICs may contribute to the ototoxic action of aminoglycosides. Although only a few SGNs exhibited action potential firing in response to an acidic stimulus, protons in the extracellular solution modulated SGN activity that was evoked by sinusoidal current injections. Greater acidity depolarized the membrane and reduced ongoing AP activity, possibly by a depolarization block.

To determine which subunits contribute to ASIC currents in SGNs, we applied selective pharmacological tools to the currents and investigated mRNA expression with RT-PCR. Gadolinium and acetylsalicylic acid reduced the SGN ASIC currents, and FMRFamide, zinc (at high concentrations) and N,N,N',N'–tetrakis-(2-piridilmetil)-etilendiamina (TPEN) increased them, indicating that functional ASICs in SGNs include the subunits ASIC1a, ASIC2a and ASIC3. Real-time

RT-PCR of the spiral ganglion revealed the expression of all ASIC subunits. In summary our data show that ASIC1, 2 and 3 contribute to SGN currents, not only ASIC2 as previously proposed (Peng et al., J Neurosci, 2004).

In eighth-nerve afferents, ASIC channels may be activated by mechanically-evoked proton release from hair cells, via vesicular release of protons along with glutamate (intravesicular pH is 5.7).

PS-791

Visualization of Vestibular Systems in Slc26A4 Mutant Mice Using Optical Coherence Tomography

Yosuke Tona[3]; Tatsunori Sakamoto[2]; Akiko Taura[2]; Takayuki Nakagawa[2]; Juichi Ito[2]

[2]Department of Otolaryngology-Head and Neck Surgery, Graduate School of Medicine, Kyoto University; [3]Kyoto University

Introduction

Although importance of abnormalities of the vestibular system have been widely recognized in clinical medicine, the ability of available imaging modalities is limited to the detection of malformations of the bony labyrinth. Optical coherence tomography (OCT) has been demonstrated to visualize normal and abnormal internal structures of rodent cochleae, such as Reisner's membrane, the tectorial membrane, and the basilar membrane. However, the feasibility of OCT for vestibular systems has not been elucidated.

Gene mutation of *Slc26A4* is known to result in the anomalies of the vestibular systems including giant and dislocated otoconia and dilation of the endolymphatic sac and duct. In this study, we visualized the abnormal vestibular structures using *Slc26A4* mutants by OCT.

Goals of the study

To examine the feasibility of OCT to detect structural abnormalities of mouse vestibular systems.

Methods

OCS1300SS OCT system was used for imaging. The harvested inner ears of *Slc26A4* KO mice and wild type (WT) controls were used after fixation at postnatal day 1 (P1) and in the adult stage. Samples were placed under the OCT probe, and visualized from the cranial side to obtain cross-sectional images of vestibular systems. The inner ears were then prepared for paraffin sections, and stained with hematoxylin and eosin. The inner ears from adult mice were decalcified before embedding in paraffin.

Results

In *Slc26A4* KO samples, OCT cross-sections demonstrated small high intensity spots in the saccule and the utricle at both postnatal and adult stages. The paraffin sections from P1 mutants also revealed large and dislocated otoconia in the utricle and the saccule. The histology of adult mutant inner ears failed to show corresponding minerals; faint amorphous stains were found, instead. This is well explained by the degradation of otoconia after decalcification. In WT samples, OCT detected the strong signals indicating normally assembled otoconia. In *Slc26A4* KO samples, the dilation of the endolymphatic duct and sac was demonstrated. In WT samples, the endolymphatic duct was identified as a narrow bony canal.

Conclusions

The anomalies of both otoconial membranes and the endolymphatic duct and sac were visualized using OCT. OCT possesses the potential to be used for the morphological evaluation of the vestibular systems.

PS-792

Evaluation of Cochlear Structures Using Hard x-ray Tomography

Hunter Young[1]; Amanda Vo[1]; Sonja Richter[1]; Whitney Liddy[1]; Stuart Stock[1]; Xianghui Xiao[2]; Donna Whitlon[1]; Claus-Peter Richter[1]

[1]Northwestern University; [2]Argonne National Laboratory

Introduction

Classical histology is often used to study cellular structures in normal cochleae as well as in cochleae after insult or genetic alterations. However, experimental progress is often limited by time-consuming histologic methodology, which can take weeks to months to complete. In an effort to reduce processing time, we introduce a novel imaging method using coherent hard x-rays, combined with computer-aided analyses that can dramatically reduce the time for anatomical study.

Methods

Cochleae of adult mice and guinea pigs were harvested immediately after death and fixed in paraformaldehyde for at least 24 hours. Cochleae were decalcified using 10% ethylenediaminetetraacetic acid (EDTA) in phosphate-buffered saline (PBS) over 2 or more weeks, then post fixed in osmium tetraoxide. Coherent x-rays were used to scan the cochleae at Argonne National Laboratory (ANL) using a 5x lens. Scans were reconstructed using a custom written phase imaging algorithm and spiral ganglion neurons (SGNs) were counted from the reconstructions using custom written SGN counting software. For comparison, the scanned cochleae were embedded in araldite epoxy and manually sectioned at 5μm. SGNs were then stereotatically counted in the plastic and reconstructed sections manually and the numbers were compared with those calculated by the SGN counting software. Custom written frequency place mapping software determined frequency place representations of the x-ray reconstructions.

Results

Reconstructed x-ray scanned cochleae allowed viewing selected structures from any angle. Soft tissue structures, including the basilar membrane, tectorial membrane, pillar cells, supporting cells, and hair cells could be identified. SGN numbers, counted either by hand from the x-ray reconstruction, by computer from the x-ray reconstruction, or by hand from the histologic sections differed by no more than 5.2%. The calculated resolution of the tomographic reconstruction was 1.45 μm/pixel. The resolution of the tomographic reconstruction determined from using a sharp edge was ~4 μm.

Discussion

We have validated a novel method to greatly reduce the time needed for gross anatomical analysis of the guinea pig and mouse cochleae. In classical histology, fixation, decalcification, dehydration, slicing, staining and image capturing is needed for analysis. Using coherent X-rays and the custom software used for this study, only fixation, decalcification, scanning, and reconstruction is needed. Current scanning and reconstruction methods at ANL typically take a total of 60 minutes for one scan. For a guinea pig cochlea two scans are required to capture the entire field of view.

PS-793

Deletion of Shank1 has Minimal Effects on the Molecular Composition and Function of Glutamatergic Afferent Postsynapses in the Mouse Inner Ear

Jeremy Braude[1]; Sarath Vijayakumar[2]; Katherine Baumgarner[3]; Rebecca Laurine[4]; Timothy Jones[2]; Sherri Jones[2]; **Sonja Pyott[5]**

[1]University of New South Wales; [2]University of Nebraska-Lincoln; [3]University of South Carolina Upstate; [4]University of North Carolina Wilmington; [5]University Medical Centrum Groningen

Shank proteins (1-3) are considered the master organizers of glutamatergic postsynaptic densities in the central nervous system, and the genetic deletion of either Shank1, 2, or 3 results in altered composition, form, and strength of glutamatergic postsynapses. To investigate the contribution of Shank proteins to glutamatergic afferent synapses of the inner ear and especially cochlea, we used immunofluorescence and quantitative real time PCR to determine the expression of Shank1, 2, and 3 in the cochlea. Because we found evidence for expression of Shank1 but not 2 and 3, we investigated the morphology, composition, and function of afferent postsynaptic densities from defined tonotopic regions in the cochlea of Shank1$^{-/-}$ mice, which presumably lack all three Shank isoforms. Using immunofluorescence, we identified subtle changes in the morphology and composition (but not number and localization) of cochlear afferent postsynaptic densities at the lower frequency region (8 kHz) in Shank1$^{-/-}$ mice compared to Shank1$^{+/+}$ littermates. However, we detected no differences in auditory brainstem responses at matching or higher frequencies. We also identified Shank1 in the vestibular afferent postsynaptic densities, but detected no differences in vestibular sensory evoked potentials in Shank1$^{-/-}$ mice compared to Shank$^{+/+}$ littermates. This work suggests that Shank proteins play a different role in the development and maintenance of glutamatergic afferent synapses in the inner ear compared to the central nervous system.

PS-794

The Hearing Level Change of the Versatile Gene Modulation Mouse (NKCC1-tetO mouse)

Takahisa Watabe[1]; Masatsugu Masuda[2]; Kaoru Ogawa[3]

[1]Keio University; [2]Department of Otolaryngology, School of Medicine, Kyorin University; [3]Department of Otolaryngology, School of Medicine, Keio University

The Na^+-K^+-$2Cl^-$-co-transporter 1 (NKCC1) is expressed on the basolateral membrane of the stria vascularis. It has been demonstrated that the transporter plays an important role in the formation of the endocochlear potential that is essential for normal hearing. For example, NKCC1-deficient mice were deaf with the collapsed Reissner's membrane and the loss of supporting and hair cells. Moreover, it is known that intraperitoneal injection of bumetanide, a NKCC1 inhibitor, causes reversible hearing loss using animals.

In this study, we used a versatile gene modulation mouse (NKCC1-tetO mouse) to reveal the influence of NKCC1 dysfunction in the stria vascularis on the inner ear function. The mouse allows us to knockdown and upregulate the NKCC1 expression with temporal specificity by doxycycline (DOX). In other words, the gene expression is maintained at the normal level when the mouse is given DOX, but is downregulated when the mouse is not given DOX. The mice were classified into three groups according to the time point of the conditional knockdown start by removal of DOX: group I. embryonic day 0 (E0), group II. postnatal day 0 (P0), group III. P35. The hearing levels were evaluated using ABR four or eight weeks after the initiation of the gene knockdown.

In the group I, 7/14 mice showed catastrophic hearing loss with equilibrium disturbance, and 7/14 mice showed severe hearing loss without equilibrium disturbance. Mice of group I showed the loss of hair cells regardless of the presence or the absence of equilibrium disturbance. However, the Reissner's membrane was normal unlike NKCC1-deficient mice. In the group II, mice showed moderate hearing loss without equilibrium disturbance. Hearing levels did not improve even after NKCC1 expression was returned to the normal level by giving the mice DOX again. In the group III, mice showed mild to moderate hearing loss at eight week after the initiation of NKCC1 knockdown, although they did not showed hearing loss at four week after the initiation.These results demonstrate that chronic dysfunction of NKCC1 in the stria vascularis resulted in the loss of hair cells and irreversible hearing loss.

Acknowledgement: We thank Dr. Junichi Nabekura and Dr. Miho Watanabe for kindly providing the mutant mice and Dr. Kenji Tanaka and Dr. Xu Ming for supporting this research.

PS-795

Ototoxicity of 2-hydroxypropyl-β-cyclodextrin (HPβCD) in Mice

Young Ho Kim; Min Young Lee; Lisa Beyer; A Lin; R. Keith Duncan; **Yehoash Raphael**
University of Michigan

Cyclodextrins are sugar compounds showing ability to complex with hydrophobic molecules. The specific cyclodextrins 2-hydroxypropyl-β-cyclodextrin (HPβCD) is known to have an ability to mobilize cholesterol. HPβCD is considered as a safe therapeutic agent for treatment of Niemann-Pick Type C disease, but a recent study found that it causes hearing loss in mice and widespread injury to outer hair cells (OHCs) (Crumling et al., PLoS One, 2012). In the present study, we further investigated the auditory function and cochlear histology in mice after subcutaneous injection of HPβCD. We also assessed the effects of the antioxidant agent Ebselen on HPβCD ototoxicity, to indirectly determine if oxidative stress plays a role in the mechanism of HPβCD-induced hearing loss.

Mice were divided into 4 groups: control (n=3), Ebselen (n=3), HPβCD (n=6), and HPβCD + Ebselen (n=6). Auditory brainstem response (ABR) thresholds at 12 and 24 kHz were recorded in the left ears before and one week after treatment. One day after intraperitoneal injection of Ebselen (16 mg/kg), HPβCD (8,000 mg/kg) was injected subcutaneously. As control, normal saline (IP) was injected intraperitoneally. One week after HPβCD injection, cochleae were harvested and prepared for immunofluorescence with antibodies to prestin and ZO-1, and with phalloidin.

ABRs demonstrated threshold shifts (mean; 49.6 and 53.1 dB at 12 and 24 kHz, respectively) in 10 of 12 HPβCD-injected mice. Hearing was unaffected by HPβCD in approximately 15% of the subjects. Pretreatment of Ebselen showed no protective effect, suggesting that oxidative stress may not be the mechanism of action of HPβCD. Cochlear histology showed symmetric bilateral OHC loss, starting at the cochlear base and extending to the mid-apical turn. Scars in the area of OHC loss were formed by outer pillar and Deiters cells in the typical pattern, suggesting that supporting cells were not affected by the ototoxin.

We conclude that HPβCD ototoxicity includes a symmetric loss of OHCs with inner hair cells and supporting cells surviving. Lesion is progressive from base to apex and hearing loss reflects the loss of OHCs. One in six animals is unaffected, as reported in the previous study (Crumling et al., PLoS One, 2012). The absence of protective effects of Ebselen against HPβCD ototoxicity indirectly suggest that the mechanism of toxicity does not involve oxidative stress.

PS-796

Antisense Oligonucleotides for the Treatment of Usher Syndrome

Michelle Hastings[1]; Francine Jodelka[1]; Abhilash Ponnath[2]; Frederic Depreaux[1]; Anthony Hinrich[1]; Mette Flaat[2]; Mette Flaat[2]; Frank Rigo[3]; Jennifer Lentz[2]
[1]Rosalind Franklin University of Medicine and Science; [2]Louisiana State University Health Science Center; [3]Isis Pharmaceuticals

Usher syndrome (Usher) is the leading genetic cause of combined deafness and blindness. Type 1 Usher (Usher 1) is the most severe form of the disease and is characterized by profound hearing impairment and vestibular dysfunction from birth, and the development of retinitis pigmentosa (RP) in early adolescence that progresses to blindness. We developed antisense oligonucleotides (ASO) to target two different mutations in USH1C that cause Usher syndrome in humans. One mutation is the Acadian Usher syndrome mutation c.216G>A (p.V72V), and the other is c.238-239insC (p.R80fs). The ASOs block the deleterious effects of the mutations and partially restore USH1C gene expression in vitro and in vivo in transgenic mice engineered to have the Ush1c.216G>A mutation. These mice have profound hearing impairment, circling behavior indicative of severe vestibular dysfunction and retinal dysfunction early in life. Mice treated with a single dose of ASO shortly after birth had normal vestibular function and could hear for more than six months of age. Remarkably, systemic delivery of progressively lower doses of ASO, which yielded minimal recovery of gene expression in the cochlea, was sufficient for phenotypic rescue, and hearing thresholds were shifted in a dose-dependent manner at 1, 3 and 6 months of age. Threshold values in response to low, mid and high frequency stimulation were stable at 1 and 3 months of age for all doses tested. However, at 6 months of age hearing thresholds were elevated for all frequencies and doses tested. By 9 months of age, only the highest dose continued to show rescue of hearing in response to low frequency stimulation. These results demonstrate that the ASOs are a promising drug platform for the treatment of auditory and vestibular disorders.

PS-797

Neurotrophic Encapsulated Cell Device for Co-Implantation with Cochlear Implants: Electrical Stimulation in vitro

Wiebke Konerding[1]; Malte Hoffmeister[1]; Jenny Ekberg[2]; Anandhan Dhanasingh[3]; Thomas Lenarz[1]; Jens Tornøe[2]; Verena Scheper[1]
[1]Medical School Hannover; [2]NsGene Denmark; [3]Medel

Introduction

Recent developments in cochlear implant (CI) research rely on a functional auditory nerve. To prevent the degeneration of spiral ganglion neurons, as is common in sensorineural hearing loss, treatment with neurotrophins has been shown to be effective both *in vitro* and *in vivo*. To apply neurotrophic factors (NTF) to the human inner ear a safe and long-term stable release method has to be found. A promising method is the

delivery of NTFs by encapsulated cells. A first step in developing an integrative NTF treatment together with a cochlear implant is the generation of a cell-line which produces stable amounts of NTF also under normal CI electrical stimulation.

Methods

We tested *in vitro* the NTF productivity of the retinal ARPE-19 cells. This cell line is genetically engineered to produce either glial cell line-derived neurotrophic factor (GDNF), brain-derived neurotrophic factor (BDNF) or cerebral dopamine neurotrophic factor (CDNF). The cells were injected into a cylindrical encapsulated cell device (EC device: 7 mm long, 0.7 mm diameter; NsGene) clipped onto a three-contact CI, custom made for this study (MED EL), and stimulated electrically via a research interface (RIB) box, according to common CI processor activation (biphasic pulses: 25 µs phase duration, 1000 pulses per second, 1200 µA) for a total duration of twelve hours. For analysis of NTF production by ELISA, medium was sampled (4 h) the day before and after electrical stimulation, as well as three times during electrical stimulation (4, 8 and 12 h). Electrically stimulated EC devices and non-stimulated controls were run in parallel.

Results

Results indicate that electrical stimulation applied in this study has no negative effect on the productivity of ARPE-19 cells transfected for production of BDNF, GDNF or CDNF.

Conclusions

These data qualify the tested encapsulated cell device for *in vivo* studies on long-term stability and safety.

This project is funded by the EC project NeuEar: Neurotrophic Cochlear Implant for Severe Hearing Loss.

PS-798

Perfecting the "Stem Cell Niche": the Use of Nanogels for Morphogen Delivery and Human Pluripotent Stem Cell Differentiation in the Inner Ear.

Zafar Sayed; Augusta Fernando; Eric Berns; Nick Stephanopoulos; Tammy McGuire; Omotara Sulyman; John Kessler; Samuel Stupp; Akihiro Matsuoka
Northwestern University

Introduction

Despite recent advances, the potential clinical use of human pluripotent stem cell (hPSC) based therapies for regeneration of spiral ganglion neurons is hindered by several critical hurdles - namely the long term survival of transplanted hPSCs and their subsequent neuronal differentiation. Using a variety of nanofiber based gels including peptide amphiphiles, we aimed to re-create a specific "stem cell niche" in order to promote their viability and neuronal differentiation at the time of transplantation.

Methods

In vitro cell viability and EdU proliferation assays were performed on cultured hPSCs in a variety of nanogel matrices in order to examine their effect on differentiation towards otic neural progenitors. *Ex vivo* human cadaveric temporal bones were used to test the feasibility of using nanogels in a future clinical setting. The resultant vestibulocochlear nerve complex was then harvested for transmission electron microscopy in order to examine the self- assembled nanofiber structure.

Results

Cell viability assays in all nanogels demonstrated adequate hPSC viability at 1-2 weeks with subsequent Nestin positivity supporting hPSC maturation into a neuronal phenotype. Following intracochlear injections of IKVAV-PA into cadaveric temporal bones, fluorescence corresponding to both tagged nanogel and hPSCs was noted along the internal auditory canal. Electron microscopy of the corresponding nerve sections demonstrated an aligned nanofiber arrangement conducive for neurite outgrowth.

Conclusions

Recreating a "stem cell niche" by providing nanogels to hPSCs in the inner ear is technically feasible and may promote neuronal differentiation by assisting in morphogen delivery following transplantion as well as creating a biophysical framework for outgrowth.

PS-799

Cochlear Spiral Ganglion TRPC3 Ion Channels Contribute to BDNF-mediated Neuritogenesis

Ann CY Wong[1]; Alan Ng[1]; Lutz Birnbaumer[2]; Allen Ryan[3]; Gary D. Housley[4]
[1]UNSW Australia, Sydney; [2]NIEHS/NIH, Research Triangle Park, NC, and IIB-INTECH, Univ Nacional de San Martin, Prov Buenos Aires, Argentina; [3]Departments of Surgery & Neuroscience, University of California San Diego, and Veterans Administration Medical Center, La Jolla, CA; [4]Translational Neuroscience Facility/ Department of Physiology, UNSW Australia

Background

Transient receptor potential (TRP) ion channels are known for their role in sensory transduction. The canonical TRP (TRPC), ion channels are non-selective cation channels that promote BDNF-mediated neurite outgrowth in cultured cerebellar granule cells (Li et al. 2005, Nature 434, 894). Immunohistochemical analyses have shown TRPC3 protein expression in neonatal spiral ganglion neurons (Phan et al. 2010, Histochem Cell Bio 133, 437). Here, we investigated the potential contribution of TRPC ion channels to BDNF-mediated neuritogenesis in a cochlear spiral ganglion neuron (SGN) explant model with TRPC3-null and background mouse strains.

Methods

Spiral ganglion neurons dissected from postnatal day 5 TRPC3KO and C129/SvEv WT mouse cochleae were spatially separated by apical, mid and basal turns, and cultured in neuron maintenance medium supplemented with BDNF (0 – 100 ng/ml) for 48 hours. Neuritogenesis was visualized by Neurofilament 200 immunolabelling. Neurite outgrowth density, average neurite length, and total neurite number were assessed with NeuronJ/ ImageJ (NIH).

Results
BDNF-mediated neuritogenesis in the WT SGN explants was dose- and region of origin dependent: 10 ng/ml BDNF was sufficient to induce neuritogenesis in the apical and mid turn, but ≥ 25 ng/ml BDNF was required for basal SGN neurite outgrowth. BDNF also induced neuritogenesis in TRPC3KO SGN explants, but the effect was substantially reduced. Total neurite number of KO mid-turn SGN explant was 8.3 times less than their WT counterpart. The reduction in TRPC3KO SGN neuritogenesis was most evident in mid- and basal- turn explants.

Conclusion
TRPC3 ion channels likely contribute to the development of afferent neuritogenesis of the cochlea mediated by BDNF-TrkB-PLC signaling.

PS-800

Intercellular Calcium Waves in Supporting Cells of the Adult Gerbil Cochlea

Dylan Chan; Stephanie Rouse
University of California, San Francisco

Introduction
Intercellular Ca^{2+} signaling (ICS) waves are critical for cochlear development and inner-hair-cell maturation. They propagate through a coordinated system of ATP release, Connexin hemichannel and gap-junction conductance, and Ca^{2+} second messengers. Through analogy to well-characterized networks in glial cells as well as limited observations in organotypic cochlear cultures, these ICS waves have been implicated in downstream MAPK pathways involved in cell proliferation, differentiation, and apoptosis. In the cochlea, ICS waves have been characterized only in neonatal cultures and explants; once spontaneous ATP release ceases at the onset of hearing, ICS waves are no longer observed. In this study, we sought to determine whether ICS occurs in the hearing ear by performing ratiometric Ca^{2+} imaging in an explant model of the adult gerbil cochlea shown previously to support acoustically stimulated microphonic potentials and active cochlear amplification.

Methods
The middle turn of an adult gerbil cochlea was dissected and mounted in a two-chamber recording apparatus, with artificial endolymph bathing the apical surface of the sensory epithelium and artificial perilymph against the basilar membrane. Cells were loaded with the ratiometric FURA-2 Ca^{2+} dye, and fluorescence imaging was performed to quantitatively determine Ca^{2+} concentrations in individual supporting cells of the organ of Corti. Ca^{2+} levels were measured in response to external stimuli, including focal ATP delivery and acoustic overstimulation in the presence or absence of gap-junction blockers. Identical experiments were conducted in organotypic cultures from neonatal mice.

Results
Under physiologic conditions, the adult middle cochlear turn exhibited intercellular Ca^{2+} waves that propagated longitudinally over a distance of 200 µm primarily along the inner pillar cells, but also into adjacent supporting-cell regions. The wavefronts propagated at a rate of 7 µm/sec, which is comparable to the ICS wave velocity seen in neonatal cochlear cultures. Application of carbenoxolone, a broad-spectrum gap-junction inhibitor, suppressed ICS waves in both adult and neonatal cochleae.

Conclusions
This study demonstrates that gap-junction-dependent ICS occurs in the adult cochlea. Whereas neonatal ICS waves have been implicated in cochlear development, the role of adult ICS waves is unknown; one possibility is involvement in the cochlear response to acoustic overstimulation. ICS propagation requires functional Connexin 26; human Connexin 26-associated hearing loss is frequently progressive, and sensitivity to noise-induced hearing loss has been suggested among Connexin 26 heterozygotes. Disruption of ICS waves and subsequent aberrant activation of downstream MAPK pathways could represent a pathophysiological mechanism for progressive Connexin 26-associated hearing loss.

PS-801

Chloride Sensitive Electrodes for the Detection of Round Window Membrane Perforation

James Stevens[1]; Joseph Wazen[2]; Hirobumi Watanabe[2]; Jeffrey Kysar[2]; Anil Lalwani[3]
[1]Columbia University College of Physicians and Surgeons; [2]Columbia University; [3]Columbia University Medical Center

Introduction
The human round window membrane (RWM) is a common target for the delivery of medication into the cochlea, to treat inner ear disorders such as sudden sensorineural hearing loss (SSNHL) or Ménière's disease. While currently available techniques utilize the natural diffusion of liquids or gels applied topically across an intact membrane, our lab has focused on the creation of microneedles to perforate the RWM. Such perforations can assist in faster and more consistent delivery of medications, bypassing the significant intra and inter-person variability in membrane permeability and therefore allowing for the creation of effective dosing regimens in time-sensitive clinical scenarios. However, the RWM is often partially obscured during surgical or clinical intervention, and the exact moment of membrane perforation is quite difficult to visualize. Imperforate membranes lose the benefit of increased medication permeability, while needles injected too far into the cochlea can easily contact the walls of the scala tympani, with possible damage to the patient's fragile hair cells or auditory nerve. Here we introduce a novel technique for the detection of membrane perforation, utilizing microneedle electrodes to measure the voltage spike at the moment of penetration in both artificial and animal model RWM's.

Methods
0.2 mm diameter stainless steel Minutien pins were electroplated with 10 nm thick copper, followed by 10 nm thick silver. These pins were then soaked in sodium hypochlorite solution for 24 hours to complete oxidation of the silver to make a silver chloride layer. Initial experiments were performed using 5-µm pore synthetic membranes for perforation, with fol-

low-up experiments using dissected animal RWM's embedded in an acrylic adapter. The ionic solutions were separated by placing the membranes in a 3ml vertical Franz diffusion cell. 1%, 2%, 3%, 4%, or 5% saline solutions were placed in the donor chamber (middle ear) side, with an artificial perilymph solution occupying the receptor chamber. Voltages were constantly recorded through the process of membrane penetration. Results were compared with voltages from Ag/AgCl wire as a control.

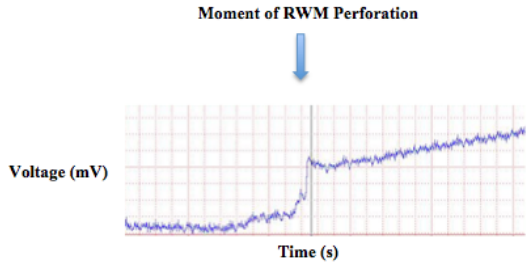

Figure 1. Voltage measurement through the process of RWM penetration, detected by Ag/AgCl coated microneedle electrode with the use of an artificial membrane sample.

Results

The silver-plated needles were able to detect a change in voltage when traversing the membranes from a test solution into the perilymph. For each saline solution testing artificial membranes, measurements were within 7 mV of the theoretical value and 3 mV of the control values on average.

Conclusion/ Summary: Ag/AgCl microneedle electrodes are an effective means of detecting the moment of penetration across semi-permeable membranes.

PS-802

Optical Stimulation of Spiral Ganglion Neurons In Vitro for Laser Pulse Durations in the µs to ms Range

Alexander Rettenmaier; Thomas Lenarz; Günter Reuter
Hannover Medical School

It has been shown that the inner ear can be stimulated in vivo by laser pulses resulting in cochlear potentials corresponding to auditory evoked signals [1]. Optical stimulation can be very site specific which coincides, due to the tonotopy of the cochlea, with a very frequency specific stimulation, possibly overcoming the limitations of conventional hearing aids as well as of electrical cochlea implants. To investigate the basic effects and mechanisms of the optical stimulation of the cochlea, single cell measurements were performed for different laser parameters.

Spiral ganglion neurons, isolated from the cochleae of P3 - P6 Sprague Dawley rats, were stimulated with laser pulses. Their electrophysiological reactions to different laser parameters such as pulse duration and optical peak power were detected by means of the whole cell patch clamp technique. Pulse durations from 10 µs up to 20 ms and optical peak powers from 50 mW up to 500 mW were investigated. Additionally, the corresponding temperature change was analyzed.

The irradiated cells show inward currents at resting potential, depending linearly on the peak power of the laser light. These reactions are clearly elicited by the laser beam and can be observed in voltage clamp measurements as current changes. For pulse durations of at least 200 µs the reaction saturates for all peak powers. For shorter pulse durations the cell reaction decreases. Corresponding current clamp measurements show only slight depolarizations of the membrane potential which are not sufficient to generate action potentials. The laser-induced temperature change depends highly on the employed laser parameters, namely pulse duration and optical peak power whereas the cellular response seems to depend mainly on the optical peak power, provided that the pulse duration is long enough.

The results show that the thermal effects of laser irradiation with pulse durations in the µs to ms range lead to cellular responses, but do not suffice to generate action potentials. In combination with in vivo experiments demonstrating positive stimulation results, performed with similar laser parameters, this suggests that direct stimulation of spiral ganglion neurons is not the main mechanism of optical cochlear stimulation. The results rather support the theory that the optical stimulation of the cochlea is based on an optoacoustic effect.

[1] Wenzel et al. Green laser light activates the inner ear. J. Biomed. Opt. 144, 044007 (2009)

PS-803

The Effect of Oriental Herbal Medicine and Calorie Restriction on the Age-related Hearing Loss of TSOD Mouse

Takeshi Hori; Kazuma Sugahara; Junko Tsuda; Yoshinobu Hirose; Makoto Hashimoto; Hiroaki Shimogori; Hiroshi Yamashita
Yamaguchi University Graduate School of Medicine

Introduction

A frequent thing that hearing loss in diabetes is shown in past epidemiologic studies. However, the cause is still unknown. Recently, it was reported that TSOD (Tsumura-Suzuki-Obese-Diabetes) male mouse presented metabolic abnormality such as obesity and hyperlipidemia, high blood pressure, diabetes with aging. We reported that hearing loss progressing with aging and the narrowing of the blood vessel in the inner ear were accepted in TSOD mice in the last meeting. For metabolic syndrome, there are some reports that Chinese medicine is effective recently. In the present study, we evaluated the effect of Kampo medicine (Bofutsushosan and Daisaikoto) and the calorie restriction on the age-related hearing loss in TSOD mice.

Materials and Methods

TSOD male mice used in study were derived from the Tsumura Research Institute. Animals were divided into four groups (Normal food group; NF group, Bofutsushosan group; BF group, Daisaikoto group; DS group and Calorie restriction group; CR group). The Chinese medicine mixed 3% into the normal foods in BF group and DS group each other. The mice had the every other day feeding in CR group. We measured

the weight and blood glucose level and auditory brainstem response thresholds in 7, 9, 11 month of age. In addition 11 months aged TSOD mice were dissected for histological examination.

Results

The body weight and the blood glucose level were lower in CR group than in the NF, BF and DS groups. The ABR thresholds were elevated in each group with age. However, the threshold tended to rise more gently in the BF group, DS group and CR group than in NF group. Furthermore, the diameter of blood vessel in the stria vascularis was significantly larger in DS group compared with those on the other groups.

Conclusion

The result suggested that Chinese medicine prevented the hearing loss of the diabetic by preventing the narrowing of the blood.

PS-804

Efficacy and Safety of Nanoparticle-mediated Steroid Delivery to the Cochlea Following Acoustic Trauma

Didier Depireux; Bharath Ramaswamy; Sandip Kulkarni; Benjamin Shapiro; Mika Shimoji
University of Maryland, College Park

Over the last few years, we have developed a technology that uses magnetic forces to precisely and effectively deliver drugs to the inner ear, and in particular the cochlea. In a rat model of noise-induced tinnitus and hearing loss, we have previously shown that delivery of steroids (in particular prednisolone) to the cochlea post-trauma can prevent tinnitus and reduce severe hearing loss even when administered several weeks post-trauma. We have also demonstrated our ability to use the magnetic nanoparticles as a platform to deliver a variety of other drugs.

The use of magnetically pushed nanoparticles into the cochlea has been shown by us to result in micromolar levels of steroids in the cochlear fluids within an hour of treatment. The drug distribution is much more uniform than that obtained by passive drug diffusion, and the binding of the drug to the nanoparticle coating allows for a controlled drug elution resulting in a clinically relevant concentration for several days. Preliminary studies, including the use of auditory brainstem response, gap pre-pulse inhibition of the startle reflex and immunochemistry have shown no obvious signs of long-term toxicity from either the method or the particles.

In the present study, we report on a detailed preclinical safety assessment of the nanoparticle treatment on healthy rats, including negative and vehicle (nanoparticle alone) controls, with and without magnetic push. Drug levels, nanoparticle concentration and cytokine levels, measured days and weeks following treatment, will be presented, in the cochlea, the blood, the brain, and other major organs. We observe a transient but no permanent shift in hearing thresholds, and no significant histological changes in the middle and inner ear tissues.

Thus, the use of magnetic nanoparticle-mediated delivery of steroids and other drugs is a non-toxic, safe and controlled method to achieve a sustained, clinically significant drug concentration in the cochlea.

PS-805

Planar Relationships of the Cochlea, Facial Nerve, and Posterior Semicircular Canal

Anita Deshpande[1]; Bruno Soares[2]; N Wendell Todd[3]
[1]Emory University School of Medicine; [2]Department of Radiology, Emory University School of Medicine; [3]Department of Otolaryngology – Head and Neck Surgery, Emory University School of Medicine

Cochlear orientation (or angular position), which is variable among individuals, is important at surgery and can be characterized on imaging. We sought to quantitatively describe cochlear orientation, both within the temporal bone and within the head relative to the plane of the horizontal and vertical portions of the facial nerve (FN), the plane of the posterior semicircular canal (PSCC), and relative the sagittal, coronal, and Frankfort horizontal planes. We also assessed the association of planar relationships with the extent of mastoid pneumatization.

From 41 bequeathed anatomically ear-normal cadaveric cranial specimens, utilizing a custom cephalostat, high-resolution CT images were obtained for the five crania with the largest and the five with the smallest mastoids. Nine points in 3-dimensional Cartesian space (3 each to define the plane of the basal turn of the cochlea, the plane of the horizontal and vertical portions of the facial nerve, and the plane of the posterior semicircular canal) were appointed and studied with the software program FIJI.

The median angle values (and ranges) between planes are as follows: Cochlea-FN 15° (2-19) right, 13° (5-20) left; Cochlea-PSCC 57° (35-64), 53° (37-68); Cochlea-Sagittal Plane 52°(47-61), 50°(44-57); Cochlea-Coronal Plane 39°(29-44), 41°(33-47); Cochlea-Frankfort horizontal plane 84°(79-89), 82°(79-89); PSCC-Sagittal Plane 52°(49-62), 50°(47-59); PSCC-Coronal Plane 41°(34-45), 40°(38-46); PSCC-Frankfort horizontal plane 74°(71-83), 74°(70-83). Bilateral symmetry was found for the relationships between the planes of the cochlea and PSCC, the plane of the cochlea and the coronal plane, and the plane of the PSCC and Frankfort horizontal plane. There was no association of any planar relationship with mastoid pneumatization.

Local phenomena likely control the position of the horizontal and vertical portions of the facial nerve. In the temporal bone, the orientation of the cochlea presumably relates to the more recent evolution of the cochlea relative to the semicircular canals, and packing the cochlea into a small space.

PS-806

Hearing and Histologic Changes Induced by Intratympanic Capsaicin Injection in Wistar Rats

Ji Won Lee[1]; Jong Woo Chung[2]; Hong Ju Park[2]
[1]Asan Medical Center, University of Ulsan; [2]Department of Otolaryngology, Asan Medical Center, University of Ulsan

Background

This study aimed to identify functional and morphological changes of cochlear by intratympanic capsaicin injection. Developing an animal model of TRPV1 receptor agonist over the inner ear function is expected to possibly estimate the inner mechanisms which lead to recurring symptoms such as dizziness associated with migraine and verify the effects of new drugs.

Methods

Male Wistar Rats with normal Prayer's reflexes were used. Click-ABR was recorded at 2 hour, 1 day, 2, 3 and 7 days after the right ear of the rat was injected with 1 μM capsaicin solution (capsaicin group). Same procedures were done with vehicle only (control group) and mixed solution of capsaicin and capsazepine, which is a TRPV1 receptor antagonist (combination group). To determine the morphological changes of cochlea, we used plastic tissue sections and observed the histological changes.

Results

All three groups showed the deterioration of threshold about 26.3-28.3 dB in 2 hours after injection, which might be caused by middle ear effusion. Threshold recovered to the pre-treatment range after a week in control group. But capsaicin group showed also improvement of hearing, but didn't recover to the pre-treatment level. The capsaicin group showed significantly more hearing loss compared to the control and combination groups at 1d, 3d, and 1 week after the injection and there was no significant difference of hearing level between the control and combination groups. Histologic examination did not show any significant changes and there was no difference among the three groups.

Conclusion

There was the temporary threshold shift by intratympanic capsaicin injection, but the significant threshold recovery was shown when the capsazepine, a competitive antagonist of capsaicin, was administered in combination with capsaicin. This indicates that capsazepines cause the complete and specific block of capsaicin's effect, suggesting the TRPV1 receptor can play a role in causing temporary hearing loss in animal models. There was no gross histologic abnormality and further morphologic and functional studies are needed.

PS-807

Protection of Auditory Function with T Type Calcium Channel Antagonist in the Cdh23 Mice

Weijun Ma; Eileen Chen; Tihua Zheng; Hui Chen; Heping Yu; **Qing Zheng**
Case Western Reserve University

Introduction

Cadherin 23, the constituent of the hair cell tip link in the organ of Corti, is associated with age-related hearing loss. We reported a new mouse model for age-related hearing loss, which was characterized by onset hearing impairment at postnatal 4 weeks and progressing to total deafness at postnatal 12 weeks. Genetic and sequencing analysis demonstrated a 208 T>C transition leading to an amino-acid substitution (S70P), which affected the secondary structure of the protein (Han et al., 2012). What we had done suggested that apoptosis played a crucial role in the hearing impairment of the mouse model. Nevertheless, we had demonstrated that a pan-caspase inhibitor and erythropoietin can preserve hearing effectively in the model (Han et al., 2012, Han et al., 2013). Here we show that the T-type calcium channel antagonist ethosuximide can delay the hearing impairment and OHCs loss in *cdh23*$^{erl/erl}$ mice. Our findings implicated that T-type calcium channels and calcium ions may have an important effect on the mechanism of deafness. This result may provide a possible treatment for patients with age-related hearing loss in the future.

Methods

Ethosuximide was obtained from Sigma Chemical Co. (St. Louis, MO). Dosages of 10mL/kg of body weight for saline and 10mg/kg of body weight for ethosuximide intraperitoneally every other day at the age of 7 days. Administration lasted to the age of 8 weeks. ABR and DPOAE were evaluated at 4, 6 and 8 weeks for all mice in each group. Cochlear surface preparation and hair cell counts were performed.

Results

Increase ABR thresholds and decrease of DPOAE amplitudes in ethosuximide-treated *cdh23*$^{erl/erl}$ mice (n=12) were significant delayed comparing to those of saline-treated *cdh23*$^{erl/erl}$ mice (n=12)

Conclusions

Ethosuximide was found to offer significant otoprotection against hearing loss, as determined by auditory brainstem response and distortion product oto-acoustic emission. Quantitation of hair cells suggested that preservation of outer hair cells is obligated to the observed protection. Immunocytochemistry and RT-PCR suggested that the protection involves the caspase apoptosis pathway in the cochlea.

PS-808

Characterizing Strial Capillary Dilation in Mouse Models of Sound-Enhanced Intra-Cochlear Aminoglycoside Trafficking

Hongzhe Li; Jianping Liu; Peter Steyger
Oregon Health & Science University

Introduction

Acoustic overstimulation potentiates the intra-cochlear trafficking of aminoglycoside antibiotics, serving as a potential mechanism of ototoxic synergy between sound and aminoglycosides, such as gentamicin. Along with this potentiation, we observed dilated strial capillaries in fixed tissues. Post-mortem analysis of capillary diameters has been questioned, as fixation may alter capillary tension and fail to faithfully preserve the anatomical diameter of capillaries and their endothelial structure. Using confocal images, we systematically quantified the diameter of strial capillaries from sound-treated and control mice to assess if meaningful physiological correlatives can be derived from such measurement and comparison.

Methods

Adult C57Bl/6 mice were exposed to wideband noise (WBN) at moderate and intense sound levels, then intraperitoneally injected with fluorescently-conjugated gentamicin (GTTR) to track gentamicin trafficking. Thirty or sixty minutes later, animals were cardiac-perfused, first with saline, then 4% paraformaldehyde. Fixed cochlear lateral walls were processed and whole-mounted for confocal microscopy. Individual focal plane(s) representing strial capillary beds were identified, and 50+ measures were acquired from apical, middle and basal cochlear locations, using NIH Fiji software.

Results

Intense GTTR fluorescence was typically observed in the endothelial cells of strial capillaries, allowing easy determination of capillary diameters using Fiji line profile function. The diameter was respectively defined either by the distance of intensity peaks, or by the width of an intensity plateau, whether the lumen was identifiable or not. Without sound treatment, strial capillaries from the cochlear base present larger diameters than the cochlear apex, whilst strial capillaries from the mid-cochlear coils present the smallest diameters. After moderate and prolonged WBN (96 dB SPL, 18 hour) exposure, capillary diameters are significantly increased ($p<0.05$). In contrast, shorter, more intense WBN (110 dB, 2 hour) exposure did not dilate strial capillaries.

Conclusions

Here we confirmed sound-induced capillary dilation in paraformaldehyde-fixed cochlear tissues. To our knowledge, the amount of dilation surpassed previously-documented sound-induced capillary dilation *in vivo*, suggesting other pathological phenomena, e.g., inflammation, or fixation artifacts. The dilation was specific to sound conditions that enhanced cochlear uptake of GTTR. This finding is in accordance with the observation that vasodilation is associated with elevated aminoglycoside uptake and exacerbated ototoxicity in other situations beyond acoustic overstimulation.

PS-809

AAV5-Mediated Expression of GDNF in the Mouse Cochlea

OMAR AKIL[1]; Lawrence Lustig[2]; Bas Blits[3]; Patricia Leake[4]
[1]UCSF; [2]Dept. of Otolaryngology-HNS, Columbia University; [3]uniQure biopharma B.V.; [4]Dept. of Otolaryngology-HNS, University of California San Francisco

Background

Hearing loss is the most common sensory disorder in the US. Mechanisms underlying the degeneration of sensory cells and neurons in the cochlea include mechanical stress, toxic insults, ischemia, and many others. Survival of neurons in the cochlea is dependent on a delicate balance of neurotrophic factors and calcium influx elicited by depolarization. Many studies have shown that GDNF, BDNF and NT-3 are capable of rescuing neurons following insult. The aims of the current studies are to determine whether adeno-associated viral vector serotype 5 (AAV5) encoding either GFP or GDNF can transduce cells in the mouse cochlea and to define the optimum therapeutic dose(s) for transfecting both hair cells and SG neurons.

Methods

1µl of virus, either AAV5-GFP (1.4E14GC/ml) or AAV5-hGDNF (1.8E14GC/ml) was injected into the scala tympani of P1-3 FVB mice through the RWM. Mice were studied at P16-18. In animals injected with AAV5-GFP, immunofluorescence was performed for GFP detection. Because there is no good antibody for assessing the distribution of hGDNF, quantitative PCR (qPCR) data was employed to demonstrate the relative levels of expression of hGDNF and endogenous mouse GDNF(mGDNF). Additional studies assessed hGDNF expression following injections of 1µl of AAV5-hGDNF diluted to 1/10 and 1/20.

Results

Following AAV5-GFP injections, strong expression of GFP was observed in IHC and SG neurons throughout the cochlea, with modest expression in OHC and supporting cells. However, after undiluted AAV5-hGDNF injections, mice displayed neurological symptoms (tremors, poor coordination, ataxia, malformed tails) at P12, which became lethal starting at P16. qPCR data showed that hGDNF was expressed at extremely high levels, roughly 300,000 to 3 million times higher than the endogenous mGDNF. In contrast, mice injected with the diluted AAV5-hGDNF showed no neurological symptoms (except a minor tail deformity with the 1/10 dilution) or mortality. The qPCR data again revealed high levels of expression of hGDNF relative to mGDNF, on the order of 500,000 to 750,000 times for the 1/10 dilution and 46,000 to 100,000 times for 1/20.

Conclusions

From these findings we conclude that the high titer and efficient transduction of these AAV5 viral vectors elicited extremely high levels of transgene expression in the cochlea. Moreover, the over-expression of hGDNF in newborn mice can cause severe neurological symptoms, possibly due to cerebellar pathology. However, it is important to note that no

symptoms occurred in mice injected with diluted virus, suggesting that extremely high levels of transgene protein expression should be avoided.

PS-810

Responses of Deafness Genes to Acoustic Overstimulation

Qunfeng Cai; Shuzhi Yang; Bohua Hu
State University of New York at Buffalo

Introduction

Genes that cause deafness can contribute to auditory dysfunction. Thus far, hundreds of deafness genes have been identified. Because these genes have a role in the maintenance of cochlear function, we hypothesized that these genes are able to respond to acoustic overstimulation and potentially contribute to noise-induced hearing loss. The current study was designed to profile the constitutive expression of deafness genes in the mouse cochlear tissue and to determine their response to acoustic overstimulation.

Methods

C57BL/6J mice were used for this study. The animals received a baseline measurement of the thresholds of the auditory brainstem response (ABR). Then, noise-group mice were exposed to a broadband noise at 120 dB (SPL) for 1 hour. At 1 day post-noise exposure, the ABR test was repeated and then the animals were sacrificed. Two types of cochlear samples were collected. One contains the sensory epithelium and lateral wall tissues (S-L samples) and the other sample contains the sensory epithelium tissue only (SE samples). The S-L samples were used for qRT-PCR analysis and the SE samples were used for RNA-seq analysis. Based on the current knowledge on gene function, expression profiles and developmental roles, a total of 92 genes were selected for transcriptional analyses. The control group subjects received the same treatment except for the noise exposure.

Results

Among the 92 genes examined, 85 were detected in S-L samples, and 63 were detected in SE samples in the normal condition, suggesting that these genes are constitutively expressed in the cochlear tissues. The acoustic overstimulation caused an average ABR threshold shift of 43.13 ± 12.14 dB at 1 day post-noise exposure. The qRT-PCR analysis of the S-L tissue revealed up-regulation of two genes (*Ndp*, *Smpx*) and down-regulation of 4 genes (*Col4a4*, *Tmc1*, *Tprn* and *P2rx2*). By contrast, the RNA-seq analysis of the SE tissue revealed down-regulation of two genes (*Col9a1* and *Ndp*). The disagreement in these transcriptional changes suggests that the expression responses of deafness genes due to acoustic overstimulation are site-dependent. However, the difference in the techniques used for the analyses may also contribute the disagreement. Functional analysis of these genes revealed the diverse functional relevance including chemical signaling, conversion of acoustic energy to nerve impulses, auditory neurotransmission, outer hair cell electromotility, inner ear gap junctions, and K(+) recycling, the basement membrane and ion channel gated by extracellular ATP.

Conclusion

Deafness genes participate in the process of noise induced cochlear injury.

PS-811

Protective Effect of Unilateral and Bilateral Ear Plugs on Noise-Induced Hearing Loss: Functional and Morphological Evaluation in Animal Model

Shi Nae Park
The Catholic University of Korea, College of Medicine, Seoul, Korea

The aim of the following study is to evaluate immediate protective effect of ear plug from noise morphologically and functionally. An 1-month aged 29 male C57BL/6 mice. Subjects were divided into four groups as normal control(G1), bilaterally plugged group (G2), unilaterally plugged group (G3) and noise control group (G4) and later 3 groups were exposed to 110 sound pressure level white noise for 60 min. Immediately after noise exposure, audiologic tests were performed and cochlear morphology and expression levels of a-synuclein in the cochlea were investigated. There were no functional changes in G2 and plugged ears of G3 after noise exposure, whereas unplugged ears of G3 and G4 showed significant hearing loss. In morphological study, there were a significant degeneration of the organ of Corti and mean number and diameter of efferent buttons, in unplugged ears of G3 and G4. Plugged ears of G3 also showed mild changes in morphological study. Reduction of a-synuclein was observed at the efferent terminals or cochlear extracts after noise exposure. The protective effect of ear plug on noise exposure was proven morphologically and functionally in the animal model of noise-induced hearing loss. Further study on cellular or ultrastructural level with ear plug will be needed to reveal more precise mechanism.

PS-812

Ultrastructural Changes in Type I Spiral Ganglion Neurons and their Glial Cells in the Deafened Guinea Pig Cochlea

Andrew Wise[1]; Remy Pujol[2]; Thomas Landry[1]; James Fallon[1]; Robert Shepherd[1]
[1]Bionics Institute; [2]INSERM

Introduction

Sensorineural hearing loss is commonly caused by damage to the sensory hair cells within the cochlea. Hair cells are sensitive to various insults including exposure to aminoglycoside drugs. After hair cell damage the type I spiral ganglion neurons (SGNs) that extend peripheral fibres to form synaptic connections with the inner hair cells gradually degenerate. We have examined the timecourse of changes in type I SGNs and their satellite glial cells at the ultrastructural level in the deafened guinea pig.

Methods

Adult pigmented Dunkin–Hartley guinea pigs were used (n=14). Eleven guinea pigs were anaesthetised and deafened via an intravenous injection of frusemide (130mg/kg)

followed by a subcutaneous injection of kanamycin (420mg/kg). Deafened animals exhibited an increase in the click-evoked auditory brainstem response thresholds of at least 50 dB p.e. SPL. Three deafness durations (two, six and 12 weeks) were examined in this study. Following fixation, cochlear tissue was prepared for examination on a transmission electron microscope (TEM).

Results

At basal cochlear location, where all hair cells have degenerated, we report a progressive decrease in SGN density and size. At any one time point few SGNs were observed undergoing degeneration suggesting that the mechanism of cell death was rapid. Over the time course of the study significant SGN loss was observed. The surviving SGNs, even three months after deafening, appeared relatively normal with few overt signs of atrophy. However, a prominent feature of the surviving SGNs was alterations to their shape. Neurite protrusions out of the soma and cellular interaction with de-differentiated glial cells were likely to be key factors in the altered SGN morphology. Degeneration of the peripheral fibres, occurred prior to the degeneration of the SGN cell body, and was characterised by retraction of the axoplasm within the myelin lumen. Often, seemingly normal myelin lumen devoid of any axoplasmic content was observed, suggesting that fibre demyelination was not a primary mechanism of degeneration in this deafness model.

Conclusions

The relatively normal ultrastructure of surviving SGNs is consistent with electrophysiological studies showing few function changes in SGNs in deafened cochleae in response to electrical stimulation.

PS-813

Influences of Chronic Alcohol Intake on Hearing Recovery of CBA Mice From Temporary Noise-induced Threshold Shift

Myung Hoon Yoo[1]; Ji Won Lee[2]; Jong Woo Chung[3]; Joong Ho Ahn[3]

[1]Asan Medical Center, University of Ulsan College of Medicine; [2]As an Institute of Life Science; [3]Asan Medical Center

Background

The effects of chronic alcohol on hearing is not conclusive, and showed conflicting results in previous studies. Alcohol might play some role in the recovery from noise-induced temporary threshold shift (TTS) by influencing protective mechanisms from oxidative stress.

Objective

To investigate the effects of chronic alcohol intake on hearing recovery of CBA mice from noise-induced TTS.

Methods & Materials

We divided CBA mice with normal hearing into 2 groups; control (n=6), 1 g/kg alcohol group (n=13). In alcohol group, ethanol was administrated intragastrically via feeding tube daily for 3 months. In control group, normal saline was administrated for 3 months. TTS was induced by 1-hour exposure of 110 dB broad band noise. Hearing thresholds were checked with click ABR, before noise exposure, just after exposure, and 1,3,5,7,14 days after exposure. Anatomical findings with immunohistochemical study and western blots for HIF1-α were also evaluated.

Results

In alcohol group, average hearing thresholds were significantly higher than control group after 3 months before noise exposure in 4, 8, 16 kHz. But after noise exposure, alcohol group showed no significant difference of hearing recovery at all tested times when compared with control group. HIF1-α expression was decreased in alcohol group compared with control group before and after noise exposure.

Conclusion

Low dose chronic alcohol provoked elevated thresholds before noise exposure in CBA mice. However chronic alcohol intake didn't influence the recovery from TTS.

PS-814

The Role of Complex I in Mitochondrial Reactive Oxygen Species Formation in Cochlear Sensory and Supporting Cells During Aminoglycoside Exposure

Heather Jensen Smith; Danielle Desa; Michael G Nichols

Creighton University

Background

Aminoglycoside antibiotics are used to treat numerous gram-negative bacterial infections. Unfortunately, aminoglycosides also damage cochlear sensory cells, resulting in permanent hearing loss. These studies evaluate putative mitochondrial dysfunction and excess reactive oxygen species (ROS) formation during acute antibiotic exposures. Low levels of ROS, primarily superoxide, are produced at electron transport chain complexes I and III during normal metabolism, yet increase when mitochondrial metabolism is altered. We assessed endogenous and ototoxic aminoglycoside-induced differences in NADH metabolism, mitochondrial membrane potential, mitochondrial ROS production and pro-apoptotic signaling. A complex I-specific inhibitor was used to determine the role of electron transport chain complex I in ROS formation during acute ototoxic insult.

Methods

These studies were conducted using acutely-cultured (18-24 h) cochlear explants from mice (postnatal day 6 ± 1 d). Fluorescence intensity-based measurements of the metabolic intermediate, nicotinamide adenine dinucleotide (NADH), were used to detect changes mitochondrial metabolism during acute (1 hour) exposures to gentamicin (GM, 300 mg/mL), a representative ototoxic aminoglycoside antibiotic. Relative amounts of superoxide and hydrogen peroxide produced during acute GM exposure were measured using MitoSox Red and Dihydrorhodamine 123, respectively. GM-induced changes in mitochondrial membrane potential and pro-apoptotic signaling were measured using Tetramethylrhodamine and apoptosis-inducing factor (AIF) labeling, respectively.

Results
GM increased NADH fluorescence intensity in low- and high-frequency sensory cells. The complex I inhibitor rotenone (250 nM) significantly increased superoxide, not hydrogen peroxide, in low- and high-frequency sensory cells ($p < 0.01$). GM significantly increased superoxide and hydrogen peroxide formation in low- and high-frequency sensory cells ($p < 0.05$). Rotenone increased GM-induced superoxide formation but decreased GM-induced hydrogen peroxide formation. This effect was greatest in high-frequency sensory cells.

Conclusion
AG ototoxicity is a multifactorial process involving both acute and long-term metabolic alterations. Acute GM significantly increased complex I superoxide formation in high-frequency sensory cells indicating fundamental differences in ROS formation in high- and low-frequency sensory cells exposed to ototoxic antibiotics. This project provides a base for understanding the underlying mechanisms of rapid mitochondrial ROS production in cochlear cells during acute exposures to ototoxic antibiotics.

PS-815

Cisplatin-induced Cytotoxicity is Associated with Down-regulation of LMO4 in Organ of Corti Cell Cultures

Rajamani Rathinam; **Samson Jamesdaniel**
Wayne State University

Introduction
The efficacy of cisplatin, a crucial life-saving drug used to treat solid tumors, is limited by its major side-effects, namely, ototoxicity, nephrotoxicity, and neurotoxicity. LMO4, a transcriptional regulator, appears to be a key player in mediating the cochlear pathology in cisplatin ototoxicity, as it can control cellular responses by modulating the formation of transcriptional complexes. We reported that cisplatin nitrates LMO4 and decreases LMO4 protein levels in the cochlea to facilitate ototoxicity in Wistar rats. However, a robust cell culture model is required to further delineate this signaling mechanism in cisplatin ototoxicity. This study aims to determine whether organ of Corti cell lines are good models for investigating LMO4 signaling in cisplatin-induced ototoxicity.

Methods
UB/OC1 cell line, that has important features of early hair cell differentiation, was used in this study. UB/OC1 cells were treated with either 5 or 10 μM cisplatin and cultured for 24 h to determine cisplatin-induced changes in LMO4 protein levels and cytotoxic effects. In addition, HK2 cells and SH-SY5Y cells were used to determine whether cisplatin-induced cytotoxic effects in UB/OC1 cells were comparable to those observed in the renal and neuronal cells that are susceptible to cisplatin toxicity. LMO4 expression was determined by immunoblotting with anti-LMO4, while associated cytotoxicity was determined by a count of viable cells after trypan blue staining.

Results
Cisplatin induced a dose-dependent decrease in the number of viable cells in the auditory, renal, and neuronal cell cultures. In UB/OC1 cell cultures, the count of viable cells decreased from $8.33\pm1.03 \times 10^4$ cells in the controls to $3.16\pm0.68 \times 10^4$ ($p<0.01$) and $2.16\pm0.25 \times 10^4$ ($p<0.01$) cells after 5 and 10 μM cisplatin treatment, respectively. Similarly, in HK2 and SH-SY5Y cell cultures, treatment with 5 μM cisplatin decreased the number of viable cells by 55 and 59%, while 10 μM cisplatin decreased it by 76 and 90%, respectively. More importantly, immunoblots indicated that the LMO4 protein levels decreased significantly after 5 μM cisplatin treatment in UB/OC1 cell cultures. The data was analyzed by one-tailed t test and the results are expressed as mean ± standard deviation.

Conclusion
The findings of this study demonstrate a potential correlation between cisplatin-induced down-regulation of LMO4 and cytotoxic responses in UB/OC1 cell cultures. In addition, the cytotoxic response was comparable to other cell types that are sensitive to cisplatin suggesting that UB/OC1 cell line could be employed to investigate LMO4 signaling pathways in cisplatin ototoxicity.

PS-816

In Vivo Protective Effect of Qter Against Styrene Ototoxicity and Acoustic Trauma: A Functional and Morphological Study in a Model of Noise Induced Hearing Loss (NIHL).

Anna Fetoni[1]; Rolando Rolesi[2]; Fabiola Paciello[2]; Sara Maria Letizia Eramo[2]; Diana Troiani[2]; Gaetano Paludetti[2]
[1]Catholic University of Rome; [2]Catholic University

In the western world the chemical processing industry is the third largest industry counting, only in Europe, about 1,2 million workers. The study of risk factors related to occupational exposures in this context assumes a relevant significance and the health effects caused by organic solvents have long been investigated. Among them styrene is an organic compound widely used in the industrial production of plastics and resins, currently classified as an ototoxic agent and a possible carcinogen in humans. A progressive increase of Reactive Oxygen Species (ROS) and a redox defenses imbalance have been demonstrated to play a significant role in noise induced hearing loss (NIHL) as well as in styrene induced ototoxicity. In this study we evaluated the synergistic effect between exposure to styrene and chronic acoustic trauma on the pattern of cochlear cell damage and the protective effect of the water soluble Coenzyme Q_{10} (Q-ter), molecule known to have antioxidant properties.

Wistar rats were exposed to styrene by gavage (400mg/Kg) and to chronic noise exposure (97 dB SPL, 10 kHZ, 60 min/day). The animals were exposed to an acoustic trauma and to styrene for 3 weeks, 5 consecutive days/week. Two groups were simultaneously treated with the antioxidant Q-ter (100mg/Kg) over the same period. The induced hearing loss in treated groups was functionally assessed by auditory brainstem responses (ABRs) and distortion product otoacoustic

emissions (DPOAEs). We also studied the immunostaining for redox imbalance in the outer hair cells, supporting cells, spiral ganglion neurons and stria vascularis.

Our results demonstrate that hearing loss and cochlear damage by styrene exposure are increased by the concomitant exposure to noise and Q-ter treatment can reduce the cochlear damage caused by chronic exposure to noise and styrene.

Based on our results, we speculate that the association between noise and organic solvent exposure in industrial working represent a risk factor for the health workers and the antioxidant treatment provides a promising preventive approach.

PS-817

The Pathogenesis of Sensorineural Hearing Loss During Virus Infection of the Cochlear Sensory Epithelium

Yushi Hayashi[1]; Koji Onomoto[2]; Mitsutoshi Yoneyama[2]; Kimitaka Kaga[3]; Takashi Fujita[4]; Nobuyuki Tanaka[5]
[1]Institute of Clinical Research (Sensory Organs) National Hospital Organization Tokyo Medical Center, Nippon Medical School; [2]Chiba University, Kyoto University; [3]Institute of Clinical Research (Sensory Organs) National Hospital Organization Tokyo Medical Center; [4]Kyoto University; [5]Nippon Medical School

Background

Although there are some diseases of the cochlea which are possibly related to viral infection such as sudden hearing loss, Meniere's disease and congenital sensorineural hearing loss, there were no reports which clarify the relationship between viral infection and inner ear diseases. We have reported so far that not auditory hair cells but supporting cells produce type I interferon (IFN) that is an anti-viral cytokine through retinoic acid inducible gene-I (RIG-I) like receptor (RLR) signaling cascade against viral infection. The aim of this research is to investigate the pathogenesis of sensorineural hearing loss induced by viral infection more deeply.

Methods

We used ex vivo system of the cochlear sensory epithelium infected with Theiler's murine encephalomyelitis virus (TMEV). The time of cultivation with TMEV was prolonged and the degree of cochlear hair cell injury was estimated using immunohistochemistry. Moreover the expression change of Noxa, Puma and Bim which are pro-apoptotic genes during virus infection was estimated using qRT-PCR.

Results

When cochlear sensory epithelia were cultivated with TMEV for 9 hours, almost all outer and inner hair cells were preserved. As the time period of exposure to virus was lengthened up to 24 hours, only outer hair cell number was decreased, which is statistically significant. However, almost all inner hair cell bodies were preserved at least. qRT-PCR analysis for pro-apoptotic genes revealed that Puma and Bim expression is significantly up-regulated when cultivated in medium including virus.

Conclusions

Only outer hair cells but not inner hair cells were damaged during virus infection in our experimental system. Up-regulation of pro-apoptotic genes in this condition indicates the possibility of apoptosis involvement in outer hair cell injury.

PS-818

Elucidating Otoprotective Mechanisms of Steroids by Systemic Application of the Selective Glucocorticoid Receptor Agonist Compound A

Chengjing Zhu[1]; **Lukas Landegger**[1]; Clemens Honeder[1]; Hanna Schöpper[2]; Elisabeth Engleder[3]; Franz Gabor[3]; Wolfgang Gstoettner[1]; Christoph Arnoldner[1]
[1]Medical University of Vienna; [2]University of Veterinary Medicine, Vienna; [3]Department of Pharmaceutical Technology and Biopharmaceutics, University of Vienna

Introduction

After decades of research, glucocorticoids still represent the only clinically available therapeutic option for many inner ear disorders, although their otoprotective mechanism of action is poorly understood and some of the concomitant side effects can lead to severe health complications (e.g. hyperglycemia or osteoporosis). Selective glucocorticoid receptor agonists (SEGRAs) are a novel class of drugs that prevent the dimerization of target receptors and directly act via the monomeric form, which is thought to reduce side effects and demonstrate similar pharmacological potency. Promising preliminary results have shown therapeutic success (e.g. in inflammatory bowel and neurodegenerative disease), but to our knowledge, no research has been performed related to the otoprotective capacities of these substances. Therefore, we aim to directly compare the effects of a potent steroid, dexamethasone, and one of the first commercially available SEGRAs, Compound A, in an animal model of noise trauma.

Methods

40 adult pigmented guinea pigs were divided into four equivalent cohorts, which received an intraperitoneal injection once daily on ten consecutive days. Administered experimental agents included Compound A (1 mg/kg or 3 mg/kg), dexamethasone (1 mg/kg) as gold standard and the same amount of water for injection as negative control. After five applications, each animal was exposed to broadband noise (8-16 kHz) at 115 dB for three hours. Hearing thresholds were determined by the recording of auditory brainstem responses (ABRs) to clicks and noise bursts between 1 and 32 kHz. This was performed a week prior to and immediately after acoustic trauma, as well as on post-exposure day 1, 3, 7, 14, 21 and 28. After euthanasia, ears were extracted and either analyzed as cochlear whole-mounts under the confocal microscope or histologically embedded and sectioned.

Results

Compared to the control group and dexamethasone, the two dosage regimens of the novel compound failed to preserve auditory thresholds after noise exposure with statistical significance. Additional findings at the histological level (hair cell and spiral ganglion neuron counts) confirm the ABR data.

Conclusions
The current study revealed that Compound A does not seem to have the same otoprotective capacities as dexamethasone, which – although unfruitful for clinical practice – gives interesting insights into the function of glucocorticoids: apparently, the dimerization of the receptor is important for their mechanism of action in the inner ear.

PS-819

Blockade of PI3K/Akt Signaling Increases Sensitivity to Noise-Induced Hearing Loss

Haishan Long; Jun Chen; Yuan Hu; Kayla Hill; **Su-Hua Sha**
Medical University of South Carolina

Introduction
Considerable evidence has demonstrated that a decrease in phosphoinositide-3 kinase/protein kinase B (PI3K/Akt) signaling pathways is associated with hearing loss and hair cell death following a variety of insults and stimuli. Here, we investigated the involvement of PI3K and Akt in noise-induced hearing loss (NIHL) under both permanent threshold shift (PTS)- and temporary threshold shift (TTS)-noise models, in combination with p85α-siRNA techniques using adult CBA/J mice at an age of 12 weeks and C57BL/6J Akt1-knockout mice at an age of 8 weeks.

Methods
Broadband noise (BBN) from 2–20 kHz for 2 hours at 98 dB SPL was used to induce permanent threshold shifts (PTS) or at 96 dB SPL to induce temporary threshold shifts (TTS) Anti-phospho-Akt (S473), anti-phospho-Akt (T308), anti-p85α, and anti-p110α antibodies were applied to cochlear surface preparations to determine the expression of PI3K/Akt signaling molecules in outer hair cells (OHCs) and to total cochlear tissue homogenates in response to both PTS and TTS noise exposure. Auditory brainstem responses were used as the measure of auditory thresholds. OHC losses were quantified following myosin VII labeling and then DAB staining of surface preparations. Delivery of p85α siRNA to the round window via intra-tympanic injection 72 hours before noise exposure was utilized to assess the effects of PI3K inhibition on both PTS and TTS. Finally, C57BL/6J Akt1-knockout mice were examined for their sensitivity to both TTS- and PTS- conditions.

Results
The levels of the PI3K regulatory subunit p85α and phosphorylation of Akt on serine 473 (p-Akt S473) were down-regulated in both outer and inner hair cells as well as in supporting cells of the organ of Corti 1 hour after PTS noise, but not after TTS noise. In contrast, the PI3K catalytic subunit p110α and phosphorylation of Akt on threonine 308 (p-Akt T308) did not change with either PTS or TTS noise. Additionally, mice pretreated with p85α siRNA had decreased expression of p-Akt1 (S473) in OHCs and increased sensitivity to TTS. Finally, Akt1-knockout mice showed enhanced sensitivity to TTS, but not to PTS.

Conclusions
This study suggests that PI3K/Akt signaling is an intrinsic protective mechanism of the inner ear. Blockade of PI3K/Akt signaling pathways increases the sensitivity to TTS-noise-induced hearing loss.

PS-820

Cisplatin Impairs the Phagocytic Response of Supporting Cells both In Vitro and In Vivo in Mouse

Elyssa Monzack[1]; Lindsey May[1]; Soumen Roy[1]; Jonathan Gale[2]; Lisa Cunningham[1]
[1]National Institutes of Health; [2]University College London

Introduction
Sensory transduction requires both mechanosensory hair cells and the surrounding glia-like supporting cells. Many factors can lead to hair cell death, including aging, noise overexposure, and clinical treatments with ototoxic side effects. Aminoglycoside antibiotics and the antineoplastic drug cisplatin are examples of such therapies. While both classes of drugs are known to kill hair cells, their effects upon supporting cells are less well understood. Last year, we reported that hair cell corpses are cleared by supporting cells in the mature mouse inner ear, and that this phagocytic activity is robust when hair cells are killed by aminoglycoside antibiotics but is impaired when hair cells are killed by cisplatin.

Methods
Adult mouse utricles from Atoh1-Cre x Rosa26-tdTomato transgenic mice were cultured for up to 48 hours in 3 mM neomycin, 30 µg/ml cisplatin, or control medium. In live imaging experiments, the interactions between hair cells and supporting cells were recorded using spinning disk confocal microscopy. For *in vivo* experiments, mice received systemic injections of kanamycin, cisplatin, or saline.

Results
During live imaging with neomycin, we observed supporting cells constrict the dead/dying hair cell, separating the apical portion (stereocilia bundle and cuticular plate) from the cell body to form a scar at the reticular lamina. Upon cisplatin treatment, we observed fewer constrictions during live imaging. In addition, phalloidin staining of fixed tissue revealed many dead hair cells in the cisplatin-treated sensory epithelium that were not sealed by supporting cell scars. This was in contrast with neomycin-treated utricles, in which nearly every dead hair cell was sealed by a scar. This defect in supporting cell scar formation was supported by *in vivo* experiments, in which scars in the kanamycin-damaged cochleas were thicker and composed of more actin than the scars observed in cochleas from cisplatin-treated mice. Together, these data point to a broader defect in the ability of the cisplatin-treated supporting cells to maintain an intact reticular lamina.

Conclusions
Our data show that cisplatin impairs the supporting cell response to hair cell death both *in vitro* and *in vivo*, suggesting that these drugs have differential effects on critical interactions between stressed hair cells and the surrounding supporting cells. The data suggest that supporting cells could be specifically targeted in the future development of therapies aimed at preventing hearing loss.

PS-821

Screening for Ototoxic Potential of Natural Products in the Zebrafish Lateral Line

Nicole Smith; Sarah Neveux; Allison Coffin
Washington State University, Vancouver

Introduction Several drugs, including aminoglycosides and platinum-based chemotherapy agents, are well known for their ototoxic properties. However, the ototoxic potential of most therapeutic compounds is unknown. FDA-approved drugs are not routinely tested for ototoxicity, so their potential to affect hearing often goes unrecognized. This issue is further compounded for natural products, where there is a lack of FDA oversight and the manufacturer is responsible for ensuring the safety of their products. Natural compounds such as herbs, vitamins and minerals, and plant derivatives are easily accessible and commonly used in the practice of traditional Eastern and alternative medicine. Here, we performed a natural products screen to identify new compounds that may cause ototoxicity.

Methods
We conducted a blind drug screen using larval zebrafish, whose externally located hair cells provide an excellent model for hearing research. We screened the Enzo Natural Products library for compounds with ototoxic potential during a 24 hr exposure period. Initial screen "hits" were validated in triplicate, then further studied with dose- and time-response analyses.

Results
We found nine natural products (1.8%) that demonstrated significant ototoxicity in our initial screen and were validated in follow-up experiments. Two compounds, the flavonols quercetin and kaempferol, are both extracts of ginkgo biloba and several other plants. Both of these compounds showed considerable lethality to hair cells even with shorter exposure times as well as causing sub-lethal damage such as kinocilial blebbing.

Conclusions
This research provides future avenues for investigation into hair cell interactions with natural products, and thus broadens the library of potential ototoxins. These findings may also imply preventative measures for human hearing loss as educated consumers can limit their consumption of ototoxic natural compounds.

PS-822

Effects of Histone Deacetylase Inhibitors on Aminoglycoside Ototoxicity

Chao-Hui Yang[1]; Jochen Schacht[2]
[1]*University of Michigan;* [2]*Kresge Hearing Research Institute*

Histone modifications are major post-transcriptional mechanisms to modulate gene expression during differentiation, aging or in response to environmental conditions. Epigenetic changes also play a role in changing cell physiology into pathology in a variety of diseases. In addition, auditory trauma may affect the cochlear epigenome. As a case in point, we have previously reported (Chen *et al*., J. Neurochem. 2009) deficient histone acetylation in aminoglycoside-treated organ of Corti explants. Conversely, restoration of histone acetylation by histone deacetylase (HDAC) inhibitors trichostatin A or sodium butyrate could rescue the hair cells from aminoglycoside toxicity.

More recently, several HDAC inhibitors have undergone or are currently undergoing clinical trials in other contexts; some have already received FDA approval. In a step to translate our earlier findings of ototoxic protection into a potential clinical application, we chose three clinically relevant HDAC inhibitors (vorinostat, belinostat and panobinostat) and tested their efficacy in vitro and in vivo. In vitro, we employed 72-h incubations of organ of Corti explants of the early postnatal mouse in which micromolar amounts of gentamicin produce loss of outer hair cells in a dose-dependent base-to-apex gradient. All three HDAC inhibitors exhibited protective capability with different efficacies but also potential toxicity to hair cells. Two μM vorinostat, 0.4 to 1 μM belinostat or 15 nM panobinostat completely protected hair cells from gentamicin-induced damage. However, toxic effects (disorganization or loss of hair cells) were found when exposing the explants to slightly higher concentrations of the inhibitors alone in the absence of gentamicin. The safety margin (protection vs. toxicity) is an important factor in vivo and is being tested in a guinea pig model of aminoglycoside ototoxicity.

PS-823

Attenuation of Histone Acetylation Contributes to Noise-Induced Outer Hair Cell Death

Xianren Wang; Jun Chen; Kayla Hill; **Su-Hua Sha**
Medical University of South Carolina

Introduction
Post-translational modification of histones is an important form of chromatin regulation. By altering their interactions with DNA and nuclear proteins, modifications of histones impact the activation of gene transcription, including those related to stress response and cell fate. Histone acetylation is regulated by histone acetyltransferases (HATs) and histone deacetylases (HDACs) and HDAC inhibitors have been studied for the treatment of cancer and neurodegenerative diseases. In addition, the involvement of histone acetylation in aminoglycoside-induced outer hair cell (OHC) loss both *in vitro* and *in vivo* suggests a role for histone acetylation in inner ear insults. Here, we investigated histone acetylation in OHC nuclei of adult CBA/J mice in a model of noise-induced permanent threshold shift (PTS noise) in combination with the HDAC inhibitor suberoylanilide hydroxamic acid (SAHA).

Methods
Broadband noise from 2–20 kHz at 98 dB SPL for 2 hours was used to induce permanent threshold shifts (PTS). Anti-acetyl-histone H3 Lysine 9 (H3K9ac), anti-HDAC2, and anti-p300 antibodies were employed to label cochlear surface preparations and cryosections in order to determine the expression of p300, HDAC2, and H3K9ac in OHCs, spiral ganglion neurons, and the stria vascularis. Auditory thresholds were measured by auditory brainstem responses. OHC losses were quantified after myosin VII labeling and DAB staining

on surface preparations. Treatment with the HDAC inhibitor SAHA via intra-peritoneal injection was utilized to assess potential protective effects of HDAC inhibition on NIHL.

Results
The levels of H3K9ac were decreased in OHC nuclei in the basal region of the cochlea 1 hour after noise exposure. In addition, levels of HDAC2, an enzyme that removes acetyl groups, were increased in noise-exposed OHC nuclei in the basal region. In contrast, p300, which adds acetyl groups, was unchanged. Finally, treatment with the HDAC inhibitor SAHA altered the distribution of H3K9ac in OHC nuclei and attenuated NIHL and OHC death.

Conclusions
These findings suggest that histone acetylation is involved in the pathogenesis of noise-induced OHC death. HDAC inhibitors may protect against NIHL.

PS-824

Prevention of Hearing Loss using Dietary Supplements

Colleen Le Prell; Christopher Spankovich; Karessa White; Edward Lobarinas
University of Florida

Background
Data from Kujawa and Liberman suggest that noise exposures that do not cause any lasting hearing loss at the time of the exposure can induce significant, accelerating hearing loss during aging, as a result of progressive long-term neural degeneration throughout the lifespan. The long-term changes are presumably initiated by the rapid, extensive loss of synaptic contacts between hair cells and nerve fibers within 24 h of noise exposure. In this investigation, we explored the potential prevention of both age-related and noise-induced decreases in ABR amplitude, as well as their synergistic interaction.

Methods
Immediate and long-term post-noise function was assessed using ABR wave I thresholds and amplitudes. In brief, C57Bl6J mice were maintained on a nutritionally complete diet (TD.07213), a diet supplemented with beta-carotene, vitamins C and E, and magnesium (TD.120071; ACEMg), or a diet supplemented with vitamins C and E, and magnesium (TD.120072: _CEMg) from 8-weeks of age until 8 months of age. Thresholds were assessed at 2, 4, 5, and 8 months of age. There were no reliable differences in the degree of hearing loss observed at 8-months of age when animals assigned to different diets were compared. Subsets of each group were exposed to an 8-16 kHz octave band noise at 102 dB SPL for 90 minutes, or 2 hours. Exposures were completed at 4.5 weeks of age, and temporary threshold shift (TTS) was calculated as the difference between the 4-month old thresholds, and the 24-hr post-noise thresholds.

Results
TTS was reduced by the supplemented diets when the exposure was 90 minutes in duration, but not when the exposure was 2-hours. Threshold tests were then repeated at 5-months of age; there was no evidence of permanent noise-induced threshold shift in any of the dietary groups.

Conclusions
The noise-induced acceleration of age-related hearing loss that has been described in CBA/CaJ mice and guinea pigs was not observed in the C57Bl6J mice used in this study. However, the average threshold shifts in this study were 20-30 dB across all groups. The average TTS in other earlier studies reporting permanent deficits was greater, with 40-50 dB TTS observed. Because the exposure used here did not result in ABR-amplitude decreases or long term functional (threshold) deficits, our findings draw into question the specific conditions under which TTS results in long-term progressive harm.

PS-825

Analysis of the Protective Effect of Aminothiol PrC-210 on Irradiated Inner Ear of Guinea Pig – a Pilot Study

Arnaud Giese[1]; Jessica Guarnascelli[2]; Jonette Ward[3]; Saima Riazuddin[4]; Daniel Choo[3]; Zubair M. Ahmed[4]
[1]University of Maryland, Baltimore; [2]TriHealth Cancer Institute; [3]Division of Pediatric Otolaryngology Head & Neck Surgery, Cincinnati Children's Hospital Medical Center; [4]Department of Otorhinolaryngology Head & Neck Surgery, School of Medicine, University of Maryland, Baltimore

Background
Radiation therapy is often used in patients to treat tumors located in the head, neck and central nervous system. When the inner ear is within the radiation field, in many cases it can result in post-irradiation sudden deafness (PISD). Irradiated patients commonly experience moderate to profound sensorineural hearing loss as well as balance disorders. Recently, PrC-210, a new orally active aminothiol radioprotector, has been shown to prevent cell death by scavenging radiation-induced reactive oxygen species (ROS). The purpose of this study was to investigate whether PrC-210, administered to guinea pig inner ear protects against radiation-induced inner ear damages and hearing loss.

Methods
To evaluate the protective effect of PrC-210 on PISD, guinea pigs were treated with an intra-peritoneal or intra-tympanic dose of PrC-210 prior receiving a 3000 cGy dose of gamma radiation in each ear. Auditory brainstem responses were recorded 1 week and 2 weeks after the radiation and compared with non-treated animal group. Finally, the morphological changes of guinea pig inner ear were analyzed by cryosectioning and immunofluorescence techniques, two weeks after the radiation.

Results
This pilot study revealed that ABR thresholds of guinea pigs that received an intra-peritoneal dose of PrC-210 were significantly better than the non-treated control animals at 1 week post-irradiation. However, the radio-protective effect of PrC-210 was abolished 2 weeks post-irradiation. Intra-tympanic injection of PrC-210 did not protect the hearing of irradiat-

ed guinea pigs. The morphological analysis of the inner ear showed that the sensory hair cell loss induced by the radiation in the organ of Corti was low two weeks post-irradiation. However, the radiation induced an inflammation and a degeneration of the cochlear nerve. These damages were reduced when animals were treated with an intraperitoneal dose of PrC-210.

Conclusions

This provisional study revealed that Prc-210 increases the survival of neurons of the cochlear nerve when injected intraperitoneally. These results warrant further investigation.

PS-826

STAT3: Protector or Enemy of Outer Hair Cell Health?

Teresa Wilson; Sarah Foster; Alfred Nuttall
Oregon Health & Science University

Background

Signal transducers and activators of transcription 3 (STAT3), part of Janus kinase/signal transducer and activator of transcription (JAK/STAT) signaling pathway, is a mechanism for transducing extra-cellular signals into a transcriptional response. Additionally, ischemia and oxidative stress modulate STAT3 activities through oxidation-reduction mechanisms and increasing evidence points to an important regulatory role for STAT3 in mediating cellular oxidative stress injury. Mitochondria-based STAT3 activities include maintenance of optimal complex I and II activity and regulation of mitochondrial permeability transition pore opening. Here, we generated outer hair cell (OHC)-specific STAT3 knock-out mice to better understand the function of STAT3 in OHCs as well as its role in the noise-induced stress response.

Methods and Results

Floxed STAT3 mice were crossed with prestin-CreER^{T2} mice for several generations to produce STAT3$^{fl/fl}$ x prestin-CreER$^{T2+/-}$ (STAT3$^{fl/fl}$) mice. Tamoxifen treatment resulted in STAT3 deletion specifically in OHCs (STAT3$^{OHC\Delta/\Delta}$). The OHCs of 8 week old STAT3$^{OHC\Delta/\Delta}$ mice appeared morphologically normal and a full complement of OHCs was present. Additionally, the STAT3$^{OHC\Delta/\Delta}$ mice had normal ABR and DPOAE thresholds relative to STAT3$^{fl/fl}$ and wildtype C57Bl/6 mice. The mice were exposed to a loud sound protocol of 96 dB SPL, 8-16 kHz for 1 hour. At 1 hour (temporary threshold shift, TTS) and 2 weeks post noise exposure (permanent threshold shift, PTS), auditory brainstem response (ABR) and distortion product otoacoustic emission (DPOAE) levels were assessed revealing contrasting effects of OHC-specific STAT3 deletion on TTS and PTS levels.

Summary

We found that STAT3$^{OHC\Delta/\Delta}$ mice possessed normal hearing thresholds indicating that STAT3 activity is not required for normal OHC function. However, exposure of STAT3$^{OHC\Delta/\Delta}$ mice to loud sound revealed that STAT3 performs both protective and deleterious roles in OHCs under stressful conditions. These opposing effects on hearing sensitivity are likely due to the multiple and diverse activities of STAT3 including those of a transcription factor, protector of mitochondrial function, and mediator of oxidative stress injury.

PS-827

Diptheria Toxin Ablation Of Monocytes/ Macrophages in a Transgenic Mouse Does Not Induce Sustained Cochlear or Serum Expression of Acute Phase Innate Inflammatory Markers

Zachary Urdang[1]; Jianping Liu[2,3]; Hongzhe Li[2]; Peter Steyger[2]
[1]Oregon Health and Science University; [2]Oregon Hearing Research Center, Department of Otolaryngology; [3]Eye & Ear Nose and Throat Hospital, Fudan University, Shanghai, China

Background

Macrophages and monocytes in transgenic mice expressing the human *Diphtheria* toxin receptor (DTR) can be selectively ablated using low-dose *Diphtheria* toxin (DT). DT-induced monocyte/macrophage ablation is reported to diminish the integrity of the blood-labyrinth barrier (BLB). DT-induced monocyte/macrophage ablation can also increase cochlear lateral wall uptake of fluorescent gentamicin. Furthermore, DT-mediated ablation of monocytes/macrophages in DTR- mice causes weight loss (~10% over 4 days) suggestive of systemic illness, including Systemic Inflammatory Response Syndrome (SIRS). We tested the hypothesis that ablation of monocytes/macrophages in DTR-mice induces a systemic and/or cochlear inflammatory response that enhances cochlear uptake of aminoglycosides.

Methods

To test our hypothesis we measured cochlear and serum levels of inflammatory markers in four groups of mice: (A) DTR mice treated with low dose DT on days 1, 3 and 4; (B) vehicle-treated DTR mice; (C) DT-treated C57BL/6 mice; and (D) vehicle-treated C57BL/6 mice. Whole cochlear homogenates and sera were assessed using multi-plex ELISA and qRT-PCR for a panel of acute phase innate inflammatory markers (TNFα, IL-1α, IL-1β, IL-6, IL-8, IL-10, MIP-1α, and MIP-2α).

Results

None of the 8 acute phase innate inflammatory markers in our panel were significantly elevated 24-hours after the last DT/vehicle injection in any of the groups. This was true for both cochlear and serum samples.

Conclusions

Non-significant elevation of acute phase innate inflammatory markers 24 hours after the final DT injection suggests that there is minimal active acute phase inflammation at this time point, 96 hours after the initial DT injection. However, this result does not preclude an ongoing later phase innate inflammatory response, or an acute phase innate inflammatory response occurring after the initial DT injection. Thus, ongoing acute phase innate inflammation is not directly responsible for the observed enhanced aminoglycoside uptake following DT-ablation of monocytes/macrophages, despite clinical evidence that these mice are systemically and acutely ill. Fur-

ther studies are warranted to determine if acute phase innate inflammation at earlier time points (which could have lasting effects on cochlear physiology), and/or late-phase innate inflammatory processes contribute to the enhanced cochlear uptake of aminoglycosides observed in DT-treated DTR mice.

PS-828

Points, Strands and Donuts: The Mitochondria Dynamics of Cochlear Cells

Alfred Nuttall; Sarah Foster; Yuan Zhang; Teresa Wilson
Oregon Health & Science University

Background

The generation of reactive oxygen species (ROS) is one of the underlying causes of noise-induced damage to tissues in the inner ear. The exact mechanisms that initiate this process are not well understood, but are thought to include ischemia/reperfusion injury as well as metabolic overstimulation, in both of which excessive superoxide radicals are produced by the mitochondria. Mitochondria are highly dynamic organelles that are maintained by the opposing processes of fusion and fission, events which alter mitochondrial morphology, biogenesis, and energy metabolism. In this study, our goal was to characterize mitochondrial morphology in auditory hair cells under normal and stress conditions and to examine the role of the key fission regulator, dynamin-related protein 1 (DRP1).

Methods and Results

Immunolabeling of HEI-OC1 cells for Tom20 and subsequent confocal imaging revealed that these cells possess a highly interconnected mitochondrial network structure under normal growth conditions. To examine alterations in mitochondrial dynamics under oxidative stress conditions, HEI-OC1 cells were treated with the complex III inhibitor, antimycin A, in the presence or absence of either a DRP1 inhibitor or DRP1 siRNA. Treatment with antimycin A increased fission processes resulting in a shift from a primary population of tubular and intermediate length mitochondria to punctate and donut-shaped mitochondria. Inhibition of DRP1 activity effectively reduced mitochondrial fission and ROS production and increased cell survival. Super-resolution imaging of Tom20 immunolabeled mitochondria in organ of Corti cells from adult mice showed primarily punctate mitochondria in OHCs, a mixed population of punctate and intermediate length mitochondria in IHCs, and tubular mitochondria in Deiters cells.

Summary

Excessive ROS is generated in OHCs as a byproduct of aerobic respiration following loud sound exposure. Even under ambient noise conditions, it is likely that these cells place high energy demands on their mitochondria. Examination of mitochondria in OHCs revealed a punctate mitochondrial morphology suggesting that the balance of fission and fusion processes are altered, potentially due to a higher oxidant environment being present in these cells.

PS-829

Evaluation of a Cochlear Implant Insertion Tool in Combination with Dexamethasone in Situ Gel Delivery

Elisabeth Mamelle[1]; Naila El Kechai[2]; Yann Nguyen[3]; Amélie Bochot[2]; Florence Agnely[2]; Evelyne Ferrary[3]; Olivier Sterkers[3]
[1]Sorbonne University, "Minimally Invasive Robot-based Hearing Rehabilitation", UPMC Univ Paris 06, UMR S 1159, 75005, Paris, France INSERM, "Minimally Invasive Robot-based Hearing Rehabilitation", UMR S 1159, 75018, Paris France 4 Sensory Organs Department, Sapienza University of Rome, 00100, Rome, Italy; [2]Institut Galien, university Paris sud; [3]Otolaryngology Department, Unit of Otology, Auditory Implants and Skull Base Surgery, Hospital Pitié Salpêtrière, 47-83 boulevard de l'Hôpital, Cedex 13, 75651 Paris, France Sorbonne University, "Minimally Invasive Robot-based Hearing Rehabilitation", UPMC Univ Paris 06, UMR S 1159, 75005, Paris, France INSERM, "Minimally Invasive Robot-based Hearing Rehabilitation", UMR S 1159, 75018, Paris France 4 Sensory Organs Department, Sapienza University of Rome, 00100, Rome, Italy

Auditory rehabilitation of patients with profound hearing loss can be provided by cochlear implants. During surgery, the electrode insertion, performed with no visual feedback beyond the entry into the cochlea, generates cochlear cell damages that could account of worse auditory performance. However the relationship between the quality of the array insertion, the cochlear damages, and the postoperative hearing is not clearly demonstrated. Furthermore, few local therapies for the inner ear are available to limit intracochlear damages.

In this study, our goal was to evaluate, in guinea pigs, the impact on postoperative hearing on the one hand, of a new electrode insertion technique with a mechatronic tool and, on the other hand, of a hyaluronic acid gel formulation bearing liposomes encapsulating an anti-inflammatory,

The potential ototoxicity of the gel was studied measuring auditory brainstem responses (ABR) at D-0, and at D-2 and D-7 after its injection in the middle ear (n=21). The round window loading of the gel (n=7), and biodistribution (n=4) in perilymph samples were evaluated at the same time-points, and at D-15. Guinea pigs were implanted with manual technique (n=6), or with an in-house mechatronic tool (n=15), with a 4-mm electrode length (Neurelec). A 6-axis force sensor, placed under the animal head, recorded the insertion forces. At the end of the procedure, hyaluronic acid (2,28%) gel (120 µl) containing liposomes (80 mM) encapsulating, or not, DexP (15 mg/ml), was injected. ABR thresholds were recorded at D-0, D-2 and D-7 after the cochlear implantation.

Implanted animals with our mechatronic insertion tool had better hearing thresholds at D-7 compared with that observed after the manual insertion procedure ($p<0.001$). We did not find any correlation between insertion forces parameters and postoperative hearing thresholds. The gel was not ototoxic and its components were detected in the perilymph samples.

The recovery after the initial loss observed at D-2 was enhanced when DexP was administrated ($p<0.05$).

This study has validated a new animal model of electrode cochlear implantation with our mechatronic tool. It allows better postoperative hearing. In addition, we showed the interest of an original hyaluronic acid gel containing liposomes encapsulating DexP, to prevent endocochlear trauma. Further studies are needed to confirm long-term benefit of DexP treatment on hearing after cochlear implantation.

PS-830

Evaluation of Multiple Methods of RNA Extraction from Mouse Cochlear Hair Cells and QPCR Analysis of Notch Target Genes Induced By Kanamycin and Furosemide Treatment

Geraldine Cabrera; **Paul Medina**; Yiwei Li; Thomas Jon Seiders; Daniel Lorrain; Peppi Prasit; Karin Stebbins
Inception Sciences

Introduction

Common approaches to RNA extraction from challenging samples like mouse cochleae involve flash freezing, mortar pestle, and Trizol. These techniques tend to be troublesome and sacrifice the quantity and quality of RNA needed for QPCR analysis. There are multiple commercially available kits on the market that allow for quick and easy RNA extraction from common tissues, however, none specifically to deal with limited challenging samples like mouse cochlear hair cells.

Methods

Mice were challenged with Kanamycin and Furosemide to induce changes in gene expression and cochleae were collected. In one study, mice were pretreated with a potent gamma secretase inhibitor. To address degradation that occurs upon collection and storage, three different methods were evaluated - liquid nitrogen, dry ice, and ice with RNALater. RNALater proved to be sufficient and preferred substitute for liquid Nitrogen collection and storage. Three commercially available kits were evaluated in conjunction with collection and storage in RNALater - Qiagen Rneasy Mini Kit, GE illustra RNAspin Mini Kit, and 5 PRIME - PerfectPure RNA Tissue kit. A hybrid method was also developed using Trizol extraction using 5 PRIME™ Phase Lock Gel™ tubes for lysis and Qiagen Rneasy Kit for washing and elution. Complete homogenization was achieved using Next Advance Bullet Blender. Following RNA extraction, QPCR was performed on the samples to assess changes in various notch target genes.

Results

All commercially available kits tested showed poor recovery and quality of RNA with an inability to obtain a QPCR profile of notch target genes upon deafening with aminoglycosides. The developed Trizol-Rneasy method provided the most consistent, highest quality and quantity of RNA recovery. A QPCR profile was obtained using this extraction method showing elevated notch target genes Hes5 and Hey1 in aminoglycoside/loop diuretic challenged mice. Pretreatment of gamma secretase inhibitor prevented the induction of notch genes Hes5 and Hey1 compared to vehicle treated mice.

Conclusion

Storage and collection in Qiagen RNALater, homogenization with Next Advance Bullet Blender and RNA extraction with the Trizol-Rneasy method provides the most consistent RNA quality and quantity recovery from mouse cochlear hair cells.

PS-831

Hearing Threshold Shift and Reduced Responses of the Central Auditory System in a Model of Blast-induced Traumatic Brain Injury

Jesyin Lai; Nicholas Race; Jordan Addison; Gavin Kuziel; Riyi Shi; Edward Bartlett
Purdue University

Background

Blast injuries resulting in hearing loss and tinnitus have been well-documented. Recent investigations have also revealed that blast-induced traumatic brain injuries (bTBI) may increase spontaneous activities in rat auditory nuclei. However, neurophysiological changes in the brainstem and midbrain to sustained, temporally modulated sounds are undocumented. Furthermore, no attempt has been made to separate acoustic trauma from the damage of the blast shock wave. We hypothesize that, in addition to middle and inner ear injuries, blast-induced neuronal injury can affect temporal processing in the central auditory system. This study investigates the acute and longer-term impact of blast exposure on the peripheral and central auditory systems.

Methods

Sprague-Dawley rats (3-4 months) were tested pre-blast (baseline), two-weeks post-blast, and one-month post-blast. Sham animals were exposed to similar levels of blast-noise but not blast-pressure (shock wave). 150kPa shock wave injury with 1.5 ms overpressure duration (mild injury – no overt deficits) was administered via an open-ended shock tube. Distortion product otoacoustic emissions (DPOAEs) input-output functions (35-80 dB SPL) were recorded at 2, 4, 8 and 12 kHz. Auditory brainstem responses (ABRs) were obtained with clicks and tone-pips of 2, 4, 8, 12, 16, and 32 kHz (15-95 dB SPL). Noise carrier or 8 kHz tone carrier modulated at 16-2048 Hz with 100% modulation depth were used for envelope-following response (EFR) stimuli. Sound intensity was at both 80 dB SPL and the intensity that stimulated wave I amplitudes similar to those of pre-blast sessions at 40 dB sensation level (dB SL). Clicks at 80 and 70 dB SPL and brief 8 kHz tones at 80 dB were used to measure middle latency responses (MLRs).

Results

Compared to noise-exposed shams and pre-blast session, blast-exposed rats at two-week post-blast had: (1) Higher hearing thresholds at high frequencies (16 and 32 kHz); (2) Decreased ABR wave I amplitude at 30 SL and 80 dB SPL; (3) Reduced EFR amplitude at low amplitude modulations (16-128 Hz); and (4) Smaller MLR amplitudes evoked by

click or 8k Hz tone. No major differences were observed in DPOAE input-output functions.

Conclusion

Elevated hearing thresholds and decreased ABR wave I amplitudes indicate damage of auditory nerve in blast-induced rats. Even with wave I compensation to pre-blast levels, reduced EFRs and MLRs also reflect degradation of auditory processing in the brainstem, midbrain and thalamus. These neurophysiological measurements can serve as biomarkers to distinguish human with bTBI from noise-overexposure.

PS-832

Protection of Cochlear Synapses From Excitotoxic Trauma In Vitro

Steven Green; **Catherine Kane**; Sepand Bafti; Ellayna Wiedow; S.M. Mirghorbani
University of Iowa

Introduction

Moderate noise exposure can destroy synapses between inner hair cells (IHCs) and spiral ganglion neurons (SGNs). This "synaptopathy" is a consequence of excessive glutamate release from overstimulated IHCs ("excitotoxicity") and resulting Ca^{2+} influx to the postsynaptic bouton. Synaptopathy can be mimicked in vitro by adding the excitotoxic glutamatergic agonist kainic acid (KA) to organotypic cochlear explant cultures that possess intact synaptic connections between hair cells and SGNs (Wang & Green, J. Neurosci. 31:7938-49, 2011). This allows a rapid assessment of compounds that can protect cochlear synapses against excitotoxic trauma in vitro and noise trauma in vivo. Here we optimize this approach by titration of the dose of KA to match synapse loss in vitro to quantitatively match noise-induced synaptopathy in vivo. We test the role of glutamate receptor blockers under these assay conditions.

Methods

Cochleae were dissected from postnatal day 5 rat pups and a portion of the organ of Corti (middle turn) with the associated portion of spiral ganglion isolated and cultured on polyornithine/laminin-coated coverslips (Wang & Green, 2011). After allowing one day for recovery and attachment, the culture medium was replaced with experimental or control conditions. KA exposure is for two hours with a 30 min pretreatment with putative protective agents. After allowing 8 h for affected postsynaptic densities (PSDs) to degenerate, the cultures were fixed and labeled to image hair cells (anti-myosin 6/7a), presynaptic ribbons (anti-CtBP2), and PSDs (anti-PSD95). A synapse was defined as a PSD co-localized with a ribbon. Synapses, as well as "orphan" PSDs and ribbons, were counted in confocal image stacks. Quantitation can be facilitated by a new ImageJ plug-in we are developing that recognizes and counts PSDs and ribbons, as well as indicating colocalization between them.

Results and Conclusions

We have previously shown that a two hour exposure to 0.5 mM KA results in destruction of >90% of IHC-SGN synapses. Glutamate receptor blockade in this case does not completely protect the synapses. This is unexpected because such blockade does prevent Ca^{2+} entry into cultured SGNs. However, exposing CBA mice to noise (2 hours 100 dB SPL, 8-16 kHz) results in loss of <30% of synapses. A dose response assay for KA in vitro shows that [KA] ~0.05 mM results in synapse loss in vitro comparable to that in vivo and a suitable platform for drug testing.

PS-833

The Effect of the ngr1 Gene Knockout on Threshold and Suprathreshold Measures of Mearing.

Lisa Zhang; Lei Song; Dhasakumar Navaratnam; Stephen Strittmatter; Joseph Santos-Sacchi
Yale University

Recent studies have shown rapid and irreversible loss of synapses in the cochlear within 24 hours postexposure to moderate noise levels. This neuropathy progresses over months even after outer hair cells recover to normal threshold levels (Kujawa and Liberman, *J. Neurosci* 2009). Our ultimate aim is to study the effects of moderate noise exposure and aging on cochlear neural degeneration and recovery in *ngr1*-knockout mice.

The *ngr1* gene encodes for the NgR1 receptor and with other neurite growth inhibiting factors is responsible for limiting axonal growth and neurological recovery (Wang et al., *Ann Neurol* 2011). Recent studies show that knockout of the *ngr1* gene in mice suffering from spinal chord injury have increased sprouting of hippocampal axons and dendrites as well as up-regulation of growth associated genes in the brain (Schwab and Strittmatter, *Curr Opin Neurobiol* 2014). We hypothesize that *ngr1*-knockout mice will show higher resilience towards neuropathy as a result of age-related and noise-induced hearing loss. To this end, NgR1 -/- mice (age = 90 ± 0 days) were used in this study and compared to control C57Bl6 mice (age = 103 ± 19 days). Auditory brainstem responses (ABR) were recorded and compared for threshold levels, peak I amplitude, peak I latency period, and interpeak interval II-I. Analyses show that NgR1 -/- mice have significant reductions of the ABR Wave I amplitude at stimulus levels greater than 50 dB. While we did observe a prolonged peak I latency and interpeak interval II-I in NgR1 -/- mice, the difference did not approach significance. Ongoing analysis with ABR, emissions and histochemistry is underway. We would also like to explore the neural response of NgR1 -/- mice under noise-exposed conditions and observe recovery of cochlear neurons after noise exposure.

PS-834

JNK Isoforms Play Different Roles in Noise-Induced Hearing Loss

Joseph Hardeman[1]; Kwang Pak[2]; Matthew Ryals[2]; Eduardo Chaves[2]; Laura Dreisbach[3]; Stephen Wasserman[2]; Kerry Beasley[2]; Allen Ryan[2]

[1]University of California, San Diego; [2]UCSD; [3]San Diego State University

Background

The organ of Corti is susceptible to damage from high-level auditory inputs. While the signaling pathways responsible for damage to the auditory system are not fully understood, intracellular stress and apoptotic signaling have been implicated. Mitogen-activated protein kinases (MAPKs) have been shown to be involved in cellular death and damage, including Jun-N-terminal Kinase (JNK). There are three isoforms of JNK, each encoded by a separate gene: *jnk1*, *jnk2* and *jnk3*. While there is evidence to link JNK signaling to hair cell damage and hearing loss, the roles of the JNK isoforms are not yet established.

Methods

Young adult mice were exposed to a two-octave band of noise with a peak sound pressure level (SPL) of 105 dB centered at 8 kHz for thirty minutes. Immediately after noise exposure (TTS) and at two weeks (PTS), frequency-specific auditory brainstem responses (ABRs) were recorded. The responses of mice deficient in different JNK isoforms were compared to those of congenic, wild-type (WT) controls.

Results

For mice deficient in JNK2, significantly lower PTS was observed when comparing ABR thresholds to those in WT controls at 8, 16 and 32 kHz and TTS at 32 kHz. JNK1 deficiency resulted in significant reductions in TTS when compared to WT control mice at 8, 16 and 32 kHz and in PTS at 32kHz. TTS and PTS in JNK3 knockout mice were similar to those for controls.

Conclusions

Our results indicate that JNK1 and JNK2 contribute differentially to noise-induced hearing loss. JNK2 plays a greater role in PTS, while JNK1 contributes more to TTS, at the noise exposure conditions tested. The data suggest that the cellular signaling pathways leading to permanent versus temporary noise-induced hearing loss are distinct, with JNK2 signaling preferentially leading to irreversible cochlear damage.

PS-835

Neuronal Retraction Bulbs in the Cochlea

Donna Whitlon; Lyubov Czech; Hunter Young; Claus-Peter Richter

Northwestern University

Introduction

Throughout the nervous system, retraction bulbs characterize axonal injury. They are thought to be caused by damage to the axonal cytoskeleton, resulting in aberrant protein and organelle transport to and from the damaged end of the fiber, resulting in abnormal swelling at the end of the fiber. Although they share certain characteristics with neuronal growth cones, retraction bulbs differ in structure. Retraction bulbs in the cochlea have been noted in several reports, but have not been examined in depth.

Methods

Albino guinea pigs of both sexes, 500-700g were used. Retraction bulbs were examined in cochleas from ongoing experiments carried out for other purposes. Cochleas were derived from normal (unexposed) animals, and animals exposed to 116-120 dB SPL broadband noise (4-8 kHz or 8-16 kHz). Baseline thresholds for ABRs were determined before the study to ensure normal responses to sound. Throughout the study, ABRs were measured weekly. At the conclusion, animals were perfused with fixative. The bullas were harvested, opened and placed into 4% paraformaldehyde for another 1-2 hours at room temperature. After decalcification in 10% ethylenediaminetetraacetic acid (pH=7.4), cochleas were dissected into half turns, and the pieces were immunolabeled as whole mounts for the hair cell marker myosin VIIa, or with two different antibodies against neurofilaments. Only the region around the inner hair cells was evaluated.

Results

Large spheres of neurofilament, some more than 10 microns in diameter, were present in all animals, even in the control group. Cochleas with considerable damage to the organ of Corti also had many more retraction bulbs. All bulbs were immunoreactive to a phosphorylation independent neurofilament antibody. Most of the bulbs had a core that was immunoreactive to an antibody that recognizes a phosphorylated epitope of neurofilament. Retraction bulbs could get so large that they caused a disorganization in the row of adjacent inner hair cells. Holes between inner hair cells, in the shape of adjacent retraction balls were sometimes found.

Discussion

Guinea pigs show highly variable ABR threshold changes following acoustic insult. Retraction bulbs in their cochleas are no less variable. Even control cochleas have retraction bulbs, but in varying degrees, suggesting that despite normal tone and click thresholds, some animals may already be undergoing degenerative events even before we begin our experiments. The physical interaction between retraction bulbs and their adjacent inner hair cells raises the possibility that retraction bulbs may be one cause of hair cell damage.

PS-836

Cellular Mechanisms of Noise Otoprotection with Antioxidants

Jose Juli

University of Castilla-La Mancha

Ñas Ñ Poiv

PS-837

Optimization and Characterization of Migration Inhibitory Factor Induced Differentiation of Mouse Embryonic Stem Cells into Spiral Ganglion Neuroprogenitors.

Angela Dixon; Yadah Ramirez; Tiffany Anthony; Derek Esty; Kathryn Haengel; Katharine Barald
University of Michigan

Embryonic stem cells provide a potential promising therapeutic approach for inner ear regeneration, specifically by replenishing depleted otic cells such as spiral ganglion neurons (SGNs). Macrophage migration inhibitory factor, MIF, has been identified as a crucial cytokine that is involved in the development of the inner ear, which contains spiral ganglion neurons, along with other sensory cells. Here we showcase a dual-approach study that focuses on 1) qualitatively and quantitatively characterizing the formation of SGNs progenitors from mouse embryonic stem cells (mES) exposed to varying concentrations of MIF and 2) the development of a microfluidic inner ear model in which to assess regeneration potential of mESC derived neurons.

We established optimal cell plating densities and refined medium formulations to promote neuronal differentiation with MIF. Visualization of a fluorescence tagged pan-neuronal marker was used to confer the ability of MIF to direct mESCs towards a neuronal phenotype. We monitored temporal changes in cell morphology over a 16 day period, and neuronal differentiation was evident early as 4 days in culture. Real time qPCR will be used to quantify expression of SGN specific proteins and receptors.

We also detail the use of a contemporary compartmentalized device to culture mouse embryonic stem cells (mESCs) and differentiate them with a defined neuronal medium into process-extending “neurons” that traverse a set of microgrooves from one compartment containing cell bodies to another that is devoid of cell bodies. This device allows spatial isolation of medium and cell parts, and contains a series of microgrooves that guide the paths of neuronal processes.

The anticipated outcome of this dual-approach study is that MIF can guide the differentiation of mESCs into neuronal precursors that give rise to spiral ganglion neuroprogenitors, possessing uniform biochemical and electrophysiological characteristics. We will also use the new microfluidic culturing approach to determine how various soluble factors or tissue targets might influence neuronal differentiation during inner ear development.

This study’s findings may be useful in better informing treatments for medical conditions that involve hearing loss, by providing mES derived SGNs, as a replacement for depleted inner ear cells.

PS-838

Polarized Innervation during Formation of the Calyx of Held

Paul Holcomb[1]; Kartik Motwani[1]; Thomas Deerinck[2]; Mark Ellisman[2]; George Spirou[1]
[1]West Virginia University; [2]University of California San Diego

Neuronal polarity—the arrangement of both intracellular organelles (intrasomatic polarity) and cellular structures such as axons and dendrites—plays a key role in the differentiation, migration, and maturation of the central nervous system. However, the role of polarity during terminal formation and refinement is poorly understood. Recently, a qualitative examination of the principal cells of the medial nucleus of the trapezoid body (MNTB) in mice suggested a polarized relationship between the developing calyx of Held (CH) terminal and the eccentric location of the cell nucleus. We hypothesize that eccentric nuclear position influences terminal placement by establishing an intrasomatic polarity defining two cellular poles: a nucleus-free “cytoplasmic” pole amenable to terminal formation, and a nucleus-containing “nuclear” pole where terminal formation is less likely. To examine this hypothesis, we utilized the novel approach of serial block-face scanning electron microscopy (SBEM) and 3D reconstruction of neurons and associated structures at key time points during CH development (P2, P3, P4, P6). Segmentation of cells from SBEM images was accomplished by hand, and 3D reconstructions were aligned across ages using the cell center, nucleus center and location of the basal body of the cilium as reference points. The eccentric position of the nucleus was significant in all cells (average distance of nuclear center from cell center = 2.878 μm, $p < 0.05$) and nuclear distance from the cell membrane was found to be stable across all ages studied (average distance = 0.569 μm, $p = 0.2742$). Terminal apposed surface area (ASA)—the contact between the terminal and the cell body—was compared to nuclear position by binning each cell into 1 μm sections (20 bins/cell) oriented orthogonally to the vector between the cell and nucleus centers. Area of ASA and volume of nucleus within each bin was quantified. This analysis showed a high degree of structural polarity, with terminals and cell nuclei positioned opposite one another with very little overlap (average overlap of largest input and nucleus on each cell = 25.57%). Overlap decreased as development proceeded from P2 (26.7%) to P6 (21.4%), despite a significant increase in largest terminal size ($6.545 \mu m^2$ (P2) to $232.767 \mu m^2$ (P6)). These data indicate that terminal placement and growth both occur preferentially on the cytoplasmic pole of the cell, as established by nuclear position. Further studies will be necessary to determine both the necessity of nuclear placement for terminal growth and the intrinsic and extrinsic mechanisms mediating principal cell polarity.

PS-839

Comparison of Superior Olivary Complex Glycinergic Network Development in Normal Mice and Mice Lacking the Medial Nucleus of the Trapezoid Body

Stefanie Altieri; Stephen Maricich; Tianna Zhao
University of Pittsburgh

Glycinergic inhibitory inputs to the superior olivary complex (SOC) play important roles in sound localization. Normally, the majority of these inputs arise in the medial nucleus of the trapezoid body (MNTB). However, extensive glycinergic innervation to the SOC is also present in mice that lack MNTB neurons. We used glycine transporter type 2 (GlyT2) immunohistochemistry to study the development of glycinergic innervation to the lateral superior olive (LSO) and superior paraolivary nucleus (SPN) in normal mice and mice lacking the MNTB. We found that mice lacking the MNTB showed decreases in glycinergic innervation of the LSO across postnatal ages, while the SPN simply showed a delay in reaching adult levels. We found no differences in the dendritic localization of glycinergic boutons between controls and mice lacking the MNTB. Adult mice lacking the MNTB showed reductions in GlyRα1 expression in the LSO but not the SPN. Current work is underway to determine the origin of non-MNTB-derived glycinergic innervation to the LSO and SPN. These data contribute important information about the development of glycinergic pathways to the SOC and highlight the ability of this system to compensate in the absence of the MNTB.

PS-840

Gene Expression Changes Reflect Cellular Diversity in the Developing MNTB

Douglas Kolson[1]; **Ashley Brandebura**[1]; Jun Wan[2]; Jiang Qian[2]; Peter Mathers[1]; George Spirou[1]
[1]West Virginia University; [2]Johns Hopkins University

Neuronal development and maturation are complex processes involving the execution of precise genetic programs, and the role of glia in mediating these events is still poorly understood. To begin deciphering these developmental processes, we conducted an extensive microarray study, utilizing the early postnatal medial nucleus of the trapezoid body (MNTB) as our model system. The MNTB offers several advantages for this study, as it contains predominantly one neuronal subtype, the principal neuron. The large presynaptic nerve terminals onto MNTB neurons, the calyces of Held, grow very quickly between postnatal day (P)2 and P4, and MNTB neurons exhibit significant maturation of biophysical properties within the same narrow time window. The calyces of Held and MNTB principal neurons are also well studied at juvenile ages and in adult animals, such that their functional properties are aligned with established roles in binaural hearing, including localization of sound. For this study, we first performed microarray analyses on microdissected MNTB tissue at seven different developmental time points (P0, P1, P2, P3, P4, P6, and P14) and found 541 genes that are significantly changing between P0 and P6. These genes were clustered into eight groups based upon their expression profiles, and quantitative real-time PCR confirmed the validity of genes from each of the profile groups with correlation co-efficient values over 0.90. Many of the monotonically increasing transcripts were associated with glia, while the monotonically decreasing transcripts were associated with neurons. Gene Ontology (GO) analysis identified numerous dynamic processes within this early maturational time window, including perineuronal net (PNN) formation, myelination, axon guidance, and calcium buffering. Protein localization for Hapln1, aggrecan, and brevican revealed that PNNs begin forming in the MNTB by P6 and are prevalent by P14. This study provides a genetic framework for future research investigating nerve terminal development and maturation.

PS-841

Laminar Distribution of Neurogranin-immunopositive Cells during Early Postnatal Development in Mouse Auditory Cortex and Influence of Maternal Thyroid Hormone Deficiency

Minzi Chang; Hikaru Kubota; Hideki Kawai
Soka University

Thyroid hormone is necessary for normal development in the auditory system. Deafness is one of the risks in certain developmental thyroid disease, such as hypothyroidism. Whether and how hypothyroidism alters the development of auditory cortex is not well understood. Thyroid hormone regulates expression of many genes, including a protein kinase C substrate called neurogranin, which is located in neuronal dendritic spines and soma and is known to contribute to synaptic plasticity in excitatory neurons. In this study, we analyzed the distribution of neurogranin-immunopositive neurons in auditory cortex during early postnatal development. We will also look into the effect of maternal thyroid hormone deficiency on the formation of cortical lamination.

In control mice (FVB strain), two phases of expression pattern of neurogranin-immunopositive neurons were observed. Before postnatal day (PD) 10 from birth (PD 0), when corticogenesis is actively forming cortical layers, neurogranin-positive soma were located in the lower layers that were immunolabeled with anti-Ctip2 antibody, a marker for layer 5. On PD 10 and onwards, when cortical lamina has already formed, the expression of neurogranin-positive somata segregate into the lower layer and the upper layers (presumed layers 2 and 3), as the immunofluorescence intensity became stronger in the upper layers. The middle layer had little neurogranin-positive neurons, while layer 6 identified with anti-FoxP2 antibody began to express neurogranin-positive cells around PD 15.

In parallel experiments, where pregnant mothers were treated with methimazole, an antithyroid drug that inhibits a thyroid hormone synthesizing enzyme thyroperoxidase, starting at embryonic day 10 and continued until newborns were sacrificed for experiments, a different pattern of expression was observed especially on PD 10. The distribution of neurogranin-positive cells was wider in layer 5 in hypothyroid-treated mice compared to non-treated control mice as they shifted

upward along with Ctip2-immunopositive neurons, indicating that hypothyroidism alters the distribution of layer 5 neurons.

Our studies show that cortical laminar-dependent expression of neurogranin-positive excitatory neurons in auditory cortex and that maternal hypothyroidism affects distribution of the neurons during the early postnatal development.

PS-842

Control of Inner Hair Cell Innervation in the Cochlea by Neuropilin-2 and Semaphorin-3F

Thomas Coate[1]; Kevin Isgrig[2]; Matthew Kelley[2]
[1]Georgetown University; [2]NIH/NIDCD

The mouse cochlea provides an excellent model for investigating molecular mechanisms associated with sensory organ innervation. To establish appropriate hearing function in the cochlea, type I spiral ganglion neurons (SGNs) must synapse with mechanosensory inner hair cells (IHCs), whereas type II SGNs must synapse with outer hair cells (OHCs). In addition, low-spontaneous rate (low-SR) SGNs target the medial side of IHCs, whereas high-SR SGNs target the lateral side of IHCs. To better understand cochlear innervation, we developed a live imaging model in which sparse numbers of SGNs express tdTomato, while all hair cells express GFP. Using this, we have visualized how supernumerary type I SGNs project to the OHCs around E15, but then retract to the IHCs through P0. These data support the hypothesis that cues within the hair cell environment direct different SGN subtypes to different hair cell regions.

Cells within the OHC region express the axon guidance factor Semaphorin-3F (Sema3F) while the SGNs express its receptor, Neuropilin-2 (Nrp2). To characterize the role of these factors with high optical resolution, we combined *Nrp2* mutants with our imaging model and documented the projection of each labeled SGN. *Nrp2* deletion leads to significantly higher numbers of type I SGNs in the OHC region, but does not alter the arrangement of low- and high-SR type I SGNs. In addition, loss of *Nrp2* also leads to type I SGNs with greater branching, suggesting that Nrp2 activation normally limits SGN outgrowth. We also found that treating cultured cochleae with exogenous Sema3F causes SGN branches to collapse, suggesting Sema3F normally acts as a chemorepellant. Finally, *Sema3F* knockout mice also show enhanced projection of type I SGNs into the OHC region, similar to the *Nrp2* mutants. These data support a model whereby Sema3F within the cochlear epithelium activates Nrp2 on type I SGNs to sequester them at the IHC. We are currently examining how processing of the co-receptor Plexin-A3 dictates differential targeting by SGNs. Funding by NIDCD to MWK and TMC.

PS-843

Activity-dependent Integration of Spiral Ganglion Neurons in the Developing Cochlea

YingXin Zhang; Amit Agarwal; Dwight Bergles
John Hopkins School of Medicine

Spontaneous neural activity is a common feature of developing sensory systems and has been implicated in controlling the survival, maturation and wiring of their respective brain circuits. In the developing auditory system, spontaneous activity is initiated within the cochlea through interactions between supporting cells and inner hair cells (IHCs), which induce IHCs to fire periodic bursts of Ca^{2+} spikes, leading to bursts of action potentials in spiral ganglion neurons (SGNs). Here, we investigated the role of this sound-independent activity in regulating the formation and refinement of synapses between IHCs and SGNs, which experience a striking transition from multiple to single innervation during the prehearing period. When glutamate release from IHCs was abolished using vGluT3 knockout mice, SGN dendrites remained highly branched, suggesting that spontaneous synaptic activity is required for refinement of connectiosn between IHCs and SGNs. We explored whether activation of NMDA receptors (NMDARs), which have been shown to play an important role in synaptic maturation in the CNS, are involved in this process. We determined that functional NMDARs are expressed by SGNs during the prehearing period, are activated at IHC-SGN synapses, enable glutamate-mediated Ca^{2+} influx, contribute substantially to the excitation of individual SGNs by reducing their repetitive firing in response to each IHC Ca^{2+} spike, and promote synchronous activation among groups of SGNs. To test whether activation of NMDARs affects SGN development, we pharmacologically blocked these receptors in cochlear explant cultures, and genetically removed GluN1 (NR1) from SGNs *in vivo*. Loss of NMDAR signaling in SGNs reduced the survival of SGNs and impaired the refinement of IHC-SGN synapses. Together, these studies indicate that establishing the exquisite unitary connections between IHCs and SGNs requires activation of NMDARs in SGN dendrites through spontaneous activity during the prehearing period.

PS-844

Speech Intelligibility Deficit in Energetic, Modulation and Informational Masking in Dyslexic Children

Axelle Calcus[1]; Cécile Colin[1]; Paul Deltenre[2]; Régine Kolinsky[1]
[1]Université Libre de Bruxelles; [2]Hopital Brugmann, Université Libre de Bruxelles

Introduction

Understanding speech in typical cocktail-party situations is a complex task for most adult listeners, and even more so for children. Recently, several researches have revealed important difficulties in speech intelligibility in noise in dyslexic children that could lead to difficulties acquiring phoneme to grapheme conversion, and hence induce reading impairment. However, other studies failed to show such impairment. This apparent contradiction might be due to differences in the na-

ture of the interference induced by different background noises. Therefore, this project aimed at systematically investigating pure energetic (EM), modulation (MM) and informational masking (IM) in dyslexic children.

Methods

We compared consonant identification performance of 14 dyslexic children (mean age: 10;1 years) to both chronological age matched (n = 14; mean age: 10;1 years) and reading level matched (n = 14; mean age: 9;1 years) controls. Target tokens were presented in three different background noises: sinusoids (inducing primarily EM), speech-shaped noise (inducing primarily MM) and babble noise, composed of one, four or eight interfering speakers (inducing primarily IM). Additionally, dip listening was investigated by comparing EM and MM in stationary and fluctuating situations.

Results

Our results point to a general impairment in all three types of interference induced by most ecological auditory environments (EM, MM and IM) in dyslexic children. However, that deficit was only observed in comparison to their age matched controls, but their performance was similar to that of younger, reading level control children. Interestingly, when present, dyslexic children experienced dip listening similarly to their controls. Finally, despite performing significantly lower than their age matched controls in all IM backgrounds, they were not differentially affected by the increasing number of interfering speakers.

Summary

Our results confirm previous evidence suggesting speech intelligibility deficits in dyslexic children, and specify their nature. Indeed, it seems that dyslexic children are impaired whatever the nature of the interference induced by the background noise (EM, IM or MM). However, that deficit was only observed when comparing their performance to age matched, but not reading level matched controls. Further research is thus needed to determine whether dyslexic children's auditory difficulty stems from a maturational delay or from their impairment in reading acquisition.

PS-845

Expression of Pou4f1 Defines a Potential Subtype of Spiral Ganglion Neurons

Hanna Sherrill; Matthew Kelley
National Institute on Deafness and Other Communication Disorders

The transmission of auditory information to the brain relies on the proper development and innervation of the first neuronal relay of sound information: the spiral ganglion neurons (SGNs). The spiral ganglion (SG) is comprised of two main types of SGNs, characterized by their morphology and pattern of innervation. Type I SGNs, which comprise 90-95% of the total, make a single synapse with one inner hair cell (IHC), while type II SGNs (remaining 5-10%) cross the tunnel of Corti and extend towards the base of the cochlea before synapsing with 10-20 outer hair cells (OHCs). SGNs are generated from Neurogenin1 (Ngn1)-positive neuroblasts that delaminate from the otocyst from E9-E13.5. As the neuroblasts divide, immature neurons begin to express Pou4f1 (Brn3a). a class IV Pou domain containing transcription factor that is highly expressed throughout the developing peripheral nervous system including the SG, the dorsal root ganglion and the trigeminal ganglion. In the dorsal root and trigeminal ganglia, Pou4f1 plays a role inthe specification of neuronal subtypes but its role in the SG remains unknown.

To examine the role of Pou4f1, expression was profiled over developmental time. By P0, a majority of SGNs have ceased expression of Pou4f1; however, ~30% of SGNs maintain expression into adulthood. Pou4f1-positive SGNs show a significant distribution gradient from base to apex with 26.2% of neurons at the base and 37.6% of neurons at the apex expressing the transcription factor. Since SGN response characteristics change along the tonotopic axis the gradient suggests that Pou4f1 could play a critical role in specification of a subtype of SGN. To explore this possibility, sparse-labeling of SGNs using $Ngn1^{creErt2}$;$R26R^{tdTomato}$ reporter mice was combined with anti-Pou4f1 immunofluorescence to reveal neuronal morphologies of Pou4f1-positive SGNs. Results indicate that post-natal Pou4f1-positive SGNs are exclusively type Is, and that most of these neurons preferentially synapse on the medial side of the IHC. Medially-located SGN synapses are thought to be associated with lower spontaneous rates of activity and tuning to lower frequencies, suggesting a possible role for Pou4f1 in the specification of a subset of low frequency neurons. To explore this hypothesis, we are in the process of generating tissue-specific, temporally regulated, Pou4f1 mutant mice. In summary, Pou4f1 is expressed in nearly every SGN embryonically but in the post-natal and adult periods is maintained in only approximately 30% of the neurons. Sparse labeling suggests that Pou4f1 expression may correlate with a functional subset of SGNs.

PS-846

Asymmetric Development of Speech Envelope and Fine Structure Encoding in Early Childhood

Kali Woodruff Carr; Travis White-Schwoch; Nina Kraus
Northwestern University

Background

Speech comprises acoustic information that unfolds across multiple timescales, requiring the listener to simultaneously process slow temporal modulations (such as syllables and word boundaries) and fast temporal information (such as formant transitions). Neural encoding of these signals can be assessed by the frequency following response (FFR). Balanced neural encoding of the stimulus envelope and temporal fine structure is critical for robust speech perception, especially in noisy environments. The developmental trajectory of envelope and fine structure feature encoding remains unknown in early childhood. Here, we aim to delineate how temporal processing of speech develops at ages critical for language learning.

Methods
We analyzed temporal features of preschoolers' (ages 3-5) auditory brainstem responses to the syllable [da], presented in quiet and in noise. Neural processing of the envelope and stimulus fine structure was distinguished by adding or subtracting responses to stimuli presented in opposite polarities, respectively, an approach shown to separate the neural responses to these orthogonal signals.

Results
We discovered that neural processing of slow temporal information (i.e., envelope encoding) develops rapidly during early childhood. There were no effects of age for encoding the fine structure of the stimuli.

Conclusions
There is a selective developmental trajectory of FFR encoding for slow information, but not faster frequencies in preschool children. Temporal fine structure encoding remains stable, and likely develops later in childhood. Taken together, these findings suggest different developmental trajectories for auditory processing at slower and faster timescales.

PS-847

Adolescent Development of Temporal Processing in ACx of Awake Gerbils

Jennifer Gay[1]; Merri Rosen[2]
[1]The Northeast Ohio Medical University (NEOMED); [2]Northeast Ohio Medical University

Many studies of neural development only examine early time periods where developmental changes are both rapid and dramatic. Human studies have identified a number of perceptual skills that do not reach adult-like performance until relatively late in development. Despite this, little work has been done to examine continued neural development into the juvenile period. While some skills are quick to mature there is a great amount of variability in the developmental time course of different auditory tasks. Temporal processing seems particularly slow to develop in humans, with some tasks not yielding adult-like levels of performance until late adolescence. Since the peripheral auditory system has been shown to have adult-like function fairly early in development, this leads to the hypothesis that a slower development of central mechanisms may underlie some of the age-dependent performance for perceptual tasks.

Some evidence exists that the central auditory system does continue to develop long into the juvenile period. Behavioral studies have shown immature temporal processing for sAM modulation detection in juvenile animals. For some cell types at the level of cortex, neurophysiological evidence shows a prolonged developmental trajectory in IPSC amplitudes and decay rates. The present study aimed to explore temporal processing in the auditory cortex of awake Mongolian gerbils using single- and multi-unit extracellular recordings. Several simple stimuli that underlie more complex auditory tasks were used to explore the difference between juvenile (P23-33) and adult (P65-120) cortical processing. These included signals that varied in rise time, duration, and bandwidth. The population responses of both adult and juvenile units were then compared to examine differences in sound-evoked responses across stimulus parameters. Our results indicate several neural mechanisms that may underlie perceptual difficulties in temporal processing seen throughout late development. Compared to adults, juvenile responses to signals with varying rise times suggest a difficulty with temporal integration over long time windows. Additionally, immature responses to signals of short durations or large bandwidths suggest either a delay in recruitment or a reduced amplitude of inhibitory inputs, or a lack of maturity in inhibitory circuitry. The prolonged time course of adult-like cortical responses to these simple stimuli is consistent with immature adolescent performance on temporal integration tasks and suggests potential neural substrates for immature perception.

Support: R01DC013314 to Merri J. Rosen

PS-848

Intracortical Sources of Glutamatergic inputs to GABAergic Interneurons during Neonatal Development

Rongkang Deng; Patrick Kanold
University of Maryland, College Park

γ-Aminobutyric acid (GABA) signaling is important in cortical development and can play diverse roles in neuronal migration, synapses formation and synchrony of network activity. Moreover, the maturation of GABAergic signaling during the first few weeks (in rodents) of postnatal life is thought to be important in controlling critical period plasticity. Thus, controlling the amount of GABAergic signaling is an important regulator in cortical development. In GABAergic interneurons, neuronal activity could regulate synthesis of GABA by controlling glutamic acid decarboxylase (GAD) expression. Therefore, controlling GABAergic interneurons' activity could serve as a major mechanism for regulating cortical development. Glutamatergic input to GABAergic interneurons is a major source of excitatory neural activity but the presynaptic neurons providing glutamatergic inputs to GABAergic neurons are still unknown. We here utilized gad2cre transgenic mice to label GABAergic interneurons in the auditory cortex and used laser-scanning photo stimulation (LSPS) combined with whole cell patch clamp recording to identify the presynaptic cells that provide glutamatergic input to GABAergic interneurons during the first 2 weeks of postnatal development in mice. By comparing α-amino-3-hydroxy-5-methyl-4-isoxazolepropionic acid (AMPA) receptors mediated input and N-methyl-D-aspartate (NMDA) receptors mediated input, we found GABAergic interneurons receive extensive glutamatergic inputs mediated by NMDA receptor only synapses in neonatal mice (<P7). In contrast, AMPA receptor mediated input was low in neonatal mice (<P7), but increased rapidly during the second postnatal week. Presynaptic cells providing glutamatergic input were located within the cortical plate and the cortical subplate. Since early cortical activity is dominated by spontaneous and sensory evoked activity bursts our findings suggest that glutamatergic signaling via NMDA receptors from subplate and intracortical sources might play a major

role in mediating the excitation and maturation of GABAergic interneurons and thereby cortical development and plasticity.

PS-849

Characterization of MyosinVIIa in the Cochlear and Vestibular Ganglia of the Developing Chick

Kristi Nguyen; Jennifer Rowsell
Washington College

The cochlear vestibular ganglion (CVG) comprises a cluster of undifferentiated neurons that delaminate from the otocyst beginning around embryonic day 2 (E2). The CVG will then divide into two separate populations; the cochlear and vestibular ganglion by (E7). The mechanisms that specify auditory versus vestibular neurons within the vertebrate inner ear are for the most part unknown. The motor protein myosinVIIA has been shown to play an important role in the function of the sensory hair cells during the process of hearing (Hasson, 1999). Individuals with Usher's syndrome lack myosinVIIA expression, and consequently suffer from deafness and blindness. While previous studies in mice show restricted myosinVIIA expression to sensory hair cells, we have data indicating that myosinVIIA is also present in the inner ear neurons in chicks. This study characterizes the spatiotemporal expression of myosinVIIA during the differentiation of otic neurons. We utilized immunohistochemistry to characterize the expression of myosinVIIa in the developing chicken inner ear neurons from E3 - E7. The onset of Myosin7a expression was detected at E3 (HH20) in a subset of neuronal precursors in the anterior-lateral portion of the CVG, a region which previous studies associate with presumptive vestibular neurons. Expression becomes restricted to vestibular neurons at E5 and persists in this population as late at E7. Our results indicate that MyosinVIIa may be playing a role in the differentiation of inner ear neurons, specifically vestibular neurons.

PS-850

Evaluation of A Binaural Asymmetric Directional Microphones with Automatic Switching Mode for Better Noise Reduction

Jinryoul Kim[1]; Il-Joon Moon[2]; Yang-Sun Cho[2]; In Young Kim[3]; Sung Hwa Hong[2]
[1]Hanyang University, Seoul; Samsung Medical Center, Sungkyunkwan University School of Medicine, Seoul; [2]Department of Otorhinolaryngology-Head & Neck Surgery, Samsung Medical Center, Sungkyunkwan University School of Medicine; [3]Department of Biomedical Engineering, Hanyang University, Seoul

Background

Even though many aspects of digital technology have been implemented into recent digital hearing aids, there are still difficulties in noise reduction. One of several methods for improving speech intelligibility in noise is to use the directional microphone (DM). However, data regarding real world effectiveness suggested that it would be limitedly beneficial with directional microphone. Recently, the asymmetric directional microphone fitting, a fixed DM on the left and an omni-DM on the right side, was introduced and confirmed that it had partial benefit when the noise was from the same side of the fixed DM. However, there was no benefit if the noise was from the opposite side of the fixed DM, meaning further technology improvement is needed.

Methods

Authors developed a new binaural asymmetric DM algorithm to overcome the limitation of the previous asymmetric DM fitting strategy with fixed DM and omni-DM positions. This algorithm was designed to measure a position of a specific dominant noise (DN). Then, the DM mode is automatically switched between fixed DM and omni-DM by dependent the position of the DN. If there is the DN on right side, the microphone mode of right side is automatically switched to fixed DM and that of left side is switched omni-DM. The microphone mode of each ear is implemented by two omni-DM. The fixed DM is obtained as a difference between the front omni-DM and a delayed rear omni-DM. Overall algorithms were implemented using MATLAB and Simulink.

Using KEMAR, authors recorded and evaluated the output (Signal-to-Noise Ratio, Perceptual Evaluation of Speech Quality, Hearing-Aid Speech Quality Index) through the artificial ear. Authors also measured by Comparison Mean Opinion Score (CMOS) in normal hearing subjects.

Results

Results with KEMAR demonstrated that the performance of the previous algorithm was seriously deteriorated when the fixed DM and the DN were not placed in the same side as expected; in contrast, the performance of the proposed algorithm was consistently maintained regardless of the directional variation of the DN. In normal hearing subjects, there was a slight, but limited improvement of CMOS.

Conclusion

The proposed algorithm demonstrated improvement of speech quality and intelligibility in noise when KEMAR was used. It suggested there would be a possibility of better noise reduction with this algorithm. However, further clinical studies with hearing impaired subjects are needed for evaluation of the effect of this algorithm in the real world.

PS-851

Electrophysiological Measures of Masking Period Patterns in Children

Heather Porter; John Grose; Emily Buss; Lori Leibold
University of North Carolina at Chapel Hill

Introduction

The ability to detect a signal in a fluctuating background depends, in part, on susceptibility to temporal masking. These forward and backward masking effects are well represented in masking period patterns (MPPs). Psychophysical MPPs are constructed from estimates of behavioral threshold for brief pure tone signals as a function of the temporal location of the signal within the modulation cycle of a fluctuating masker. Comparing 6.5 to 10 year-olds and adults, the child/adult difference was greater for backward than forward masking under some conditions (Buss et al, 2013), suggesting that inefficiency cannot entirely account for child-adult differences

in temporal processing. The objective of this project is to assess the feasibility of using cortical auditory evoked potentials to derive an electrophysiological MPP (eMPP), wherein characteristics of the evoked response reflect susceptibility of the encoded signal to temporal masking effects. The hypothesis is that larger temporal masking effects are present in the eMPP of children than adults, in parallel with behavioral results.

Methods

Cortically-evoked eMPP responses are obtained for children (ages 8-10 years) and adults with normal hearing using a 20-ms, 1000-Hz pure tone signal, presented monaurally at 60 dB SPL at a rate of 0.3 Hz, within specific temporal positions in masker modulation minima. The wideband masker (500 to 7000 Hz) is square-wave modulated at a 5.1-Hz rate, alternating between 30 and 65 dB SPL. Evoked responses are collected from surface electrodes at Fz (active/non-inverting), nape of neck (reference/inverting), and Fpz (ground). At least 200 artifact-free responses are averaged in each condition while participants rest quietly in a reclining armchair watching a silent video.

Results

Preliminary data indicate an N1 response (adults) or N2 response (children) to the signal presented in quiet, with reduced amplitude in all modulated noise conditions, and no response in the presence of noise alone. Relative to signal presentation alone, average N1 latency (adults) appears most delayed for signals presented early in masker modulation minima, whereas average N2 latency (children) appears most delayed for signals presented late in masker modulation minima. Finally, normalized individual child N2 latencies for signals presented late in masker modulation minima decrease as a function of age.

Conclusions

These preliminary data support the feasibility of obtaining eMPPs using cortical auditory evoked potentials. Specifically, response latency for the N1 (adult) or N2 (child) component appears to depend on signal temporal position within the modulated masker.

PS-852

Disruption of the Earliest Auditory Cortical Circuits in the Valproic Acid Model of Autism

Daniel Nagode; Xiangying Meng; Patrick Kanold
University of Maryland, College Park

Autism is thought to be of neurodevelopmental origin, but its causes are unclear. Recent brain imaging studies have revealed significant abnormalities in the way that autistic individuals process speech and sound. Specifically, temporal (including auditory) cortical areas exhibit different patterns of activation compared with typically developed individuals, suggesting that improper “wiring” in these areas during development might contribute to problems in speech perception or interpretation. Such faulty wiring could result from abnormal development of the thalamocortical-corticothalamic loop in primary auditory cortex, though this hypothesis has never been tested.

In the fetal cortex, the first functional circuits are formed by subplate neurons (SPNs). SPNs are crucially involved in key steps of cortical maturation, particularly in the functional maturation of thalamocortical and intracortical wiring and in critical period plasticity.

Prenatal exposure to the antiepileptic drug valproic acid (VPA), increases the incidence of autism in humans, and is also an established rodent model of autism with auditory processing deficits. The vulnerability window for VPA exposure coincides with the peak generation window of SPNs; thus, SPN disruption might lead to later cortical dysfunction in this model.

Therefore, we are investigating the functional connectivity of SPNs in slices of developing primary auditory cortex from VPA-exposed mouse pups, using in vitro laser scanning photostimulation (LSPS) of caged-glutamate, and whole-cell patch clamp electrophysiology. Our preliminary results indicate that inter-laminar connectivity to SPNs in VPA-exposed mouse pups is altered. Specifically, SPNs show increased excitatory input from the deeper layers of the cortical plate. Most notably, we detect these changes on postnatal days 1-6, thus before the formation of thalamocortical synapses, the maturation of layer 4, and the onset of hearing. Our results provide direct evidence that the earliest cortical auditory circuits are already disrupted in models of autism, and suggest that dysfunction in transient SPN circuits in the developing brain might play a key role in the etiology of autism spectrum disorders.

PS-853

Development of Gap Detection in Mongolian Gerbils as Assessed by Pre-Pulse Inhibition of the Acoustic Startle Reflex

David Green; Jocelyn Ohlemacher; Alexander Galazyuk; Jianxin Bao; **Merri Rosen**
NEOMED

The majority of developmental animal research has focused on changes that occur in early life. Human psychophysical studies, however, show that percepts of temporally varying sounds have developmental time courses that can extend into late adolescence. In order to measure the neural substrates that subserve the maturation of these percepts, it is necessary to clarify the time periods over which these percepts mature in our animal model, the Mongolian gerbil. We thus assessed the development of gap detection over the full course of development, from hearing onset through adolescence to adulthood. Assessing perceptual abilities across this range requires a measure that can be applied equally well to very young and adult animals. To this end, we determined gap detection thresholds using pre-pulse inhibition of the acoustic startle reflex.

We measured the perceptual ability of gerbils to detect a gap in a broadband noise background. Acoustic startle responses

to a loud noise (110dB SPL, 20 ms) were measured using an accelerometer. This startle stimulus was preceded by 2-10ms gaps in a 60dB SPL background noise. Reduction in startle amplitude was interpreted as perception of the preceding gap. Animals were tested every 4 days over a 16 day period. Ages at the start of testing were separated into early developmental (P12, 13, 14 and 16), mid-developmental (P26), late development (P38) and adult (P73).

Four early developmental groups were not significantly different from one another in their ability to detect gaps of different lengths. These ages are known to cover a period of developmental plasticity during which the auditory cortex is sensitive to manipulations of auditory input and auditory skills are likely to mature rapidly. Additionally, and in concurrence with human performance, within-group variability was larger for younger animals, progressively reducing with age. Finally, we measured performance over the 5 testing sessions to assess whether repeated exposure affected performance. Only the late developmental group showed improved performance over sessions. This suggests that at this age range either gap detection thresholds are developing rapidly, or that animals are particularly susceptible to being shifted toward adult thresholds with experience.

Given what is known of the early maturation of the peripheral auditory system, the timeline of gap detection between mid-development and adult is likely to reflect central auditory development. These data will inform our future electrophysiological research to elucidate the neural correlates of the development of this perceptual ability.

Support: R01DC013314

PS-854

Auditory Brainstem Development: Insights from Expert and Disordered Populations

Erika Skoe[1]; Nina Kraus[2]
[1]University of Connecticut; [2]Northwestern University

Background

Auditory brainstem structures have been long considered to develop precociously. However, recent evidence indicates that development extends into adolescence, as seen through the auditory brainstem response (ABR). We recently reported that latency and amplitude measures of the ABR are matched to the adults at age 3 (Skoe et al., 2014). However, this adult-like state is temporary. After age 3, response latencies continue to decrease and amplitudes continue to increase until mid-childhood, when the developmental trajectory changes slope and gradually returns to the adult value.The window during which ABR latencies are earlier than the adult value and amplitudes are larger is termed the "overshoot" period (~5-14 years old). In this study, we use our normative sample as a canvas for studying ABR development in expert and disordered populations.

Methods

We recorded ABRs from normal-hearing individuals between the ages 0.25 to 70 years. Participants were classified into four groups: typically-developing (TD), musician, dyslexic, autistic. We use musicians as a model for how enriched auditory experiences interact with developmental processes. We integrate data from populations with reading disabilities and Autism Spectrum Disorders to examine deviations in ABR development associated with neurodevelopmental disorders.

ABRs were recorded to a click stimulus and the speech syllable "da". Stimuli were presented monaurally to the right ear at suprathreshold levels. We measured the latency of each prominent peak in the speech- and click-ABR. We also measured frequency encoding across the response spectrum, in addition to gauging the trial-by-trial consistency of the response.

Results

We find that experience-dependent plasticity is amplified during periods when developmental changes are underway, with the effect being greatest during the overshoot period. Our analysis of developmental disorders indicates that the shape of the developmental trajectory is similar to the TD group, such that both typical and atypical development includes an overshoot period. However, the atypical populations we have surveyed appear to have a different developmental baseline than the TD sample.

Conclusions

By expanding our dataset to include larger samples of atypical populations, we hope to document the auditory correlates of neurodevelopmental disorders across the lifespan and to undercover the ages at which the gap between typical and atypical systems is greatest. Through ongoing longitudinal experiments, we also seek to understand when deviations between typical and atypical populations first emerge in life and whether it might be possible to see deviations in the developmental trajectory before the disorder presents behaviorally.

PS-855

The Longitudinal Analysis of Aquaporin Expression Levels and Localizations during Inner-Ear Development and Maturation

Takushi Miyoshi[1]; Norio Yamamoto[1]; Taro Yamaguchi[2]; Yosuke Tona[1]; Kiyokazu Ogita[2]; Takayuki Nakagawa[1]; Juichi Ito[1]
[1]Graduate School of Medicine, Kyoto University; [2]Faculty of Pharmaceutical Sciences. Setsunan University

Introduction

Aquaporins (AQPs) are water channel proteins, playing major roles for water regulation. AQP family has 13 subtypes in mammalian, and previous reports have described their localizations in the inner ear. However, few reports focused on the longitudinal changes of each AQP subtype through development and maturation. We applied quantitative reverse transcription polymerase chain reaction (qRT-PCR) to inner-ear samples of various developmental and postnatal stages, and revealed the transitions of expression levels.

Our objective is elucidating the exact contribution of each AQP subtype to the water homeostasis in the inner ear. For this purpose, we also performed immunohistochemistry (IHC) for several subtypes, and traced the localization changes. In our presentation, we compare the data of qRT-PCR and IHC, and discuss the contribution of each AQP subtype.

Methods

Whole inner ears were dissected from C57BL6/J mice at embryonic days (E) 10, 13 and 18, and at postnatal days (P) 3, 10 and 21. Total mRNA was extracted and the expression level of each AQP subtype was determined by qRT-PCR. The frozen sections of inner ears (E10 – P21) were subjected to IHC using anti-AQP2, 4 and 5 antibodies (Millipore), and anti-AQP6 and 9 antibodies (Abcam).

Results

The expression level transition of each AQP subtype was classified into 4 patterns: constant (AQP4 and 11), increase (AQP0, 1 and 9), peak at E18 (AQP2, 3, 5 and 7), and decrease (AQP6, 8 and 12) patterns. Among increase pattern subtypes, the AQP9 expression level increased drastically. It changed 70-fold from P3 to P21. IHC revealed that the AQP9 was gradually expressed around endolymphatic space after P3, suggesting that AQP9 is involved in the development of endolymphatic potential. AQP2 and 5 expressions became limited to subtype-specific sites after P3. In addition, AQP5 expression in the sensory epithelium expands from the basal turn at E13.5 to the apical turn at E18.5. Its expression became limited to outer sulcus cells. Considering that outer sulcus cells are included in the potassium recycling pathway, the expansion of AQP5 expression may represent the maturation of potassium recycling function.

Conclusions

Subtypes of increasing expression level indicate their contribution to the establishment of inner ear function. Especially, the location and the time-course of AQP9 increase may be related to the establishment of endolymphatic potential. Limited localization of AQP2 and 5 in the cochlea suggest that AQP subtypes with peak formation pattern are related to the differentiation of the sensory epithelium.

PS-856

Pseudo-Immortalization Of Postnatal Cochlear Progenitor Cells Yields A Scalable Cell Line Capable For Hair Cell Differentiation Studies

Fei Zheng; Shiyong Diao; Brandon Walters; Bradley Walters; Wanda Layman; Jian Zuo
St Jude Children's Research Hospital

Hearing loss affects about 360 million people worldwide, and primarily results from the loss/dysfunction of mechano-sensory hair cells (HCs). To develop HC regeneration therapies, a critical step is to understand the HC development and identify key regulators during its differentiation. However, the factor-identification study benefits little from many powerful high-throughput screening techniques (e.g. RNA-seq, ChIP-seq, etc), partly because of the limited number of HCs (about 5,000 HCs in each mouse sensing cochlea and all are post-mitotic). Meanwhile, none of the existing otic cell lines is ideal to study terminal HC differentiation. To overcome this disadvantage, we developed "Conditionally Reprogrammed Otic Stem Cells" (CR-OSCs). In the CR-OSCs, we use small molecules and a feeder cell layer to bypass the senescence inherent to cochlear progenitor cells without genetically altering the cells. CR-OSCs can be passaged for more than 25 passages and one single cochlea can generate more than 15 million cells. Notably, CR-OSCs can be differentiated, allowing for the up-regulation of both early and terminal HC maturation genes (including Myo6, Myo7a and prestin). Moreover, CR-OSCs can respond to known HC cues, including up-regulation of early HC genes in response to Atoh1 overexpression, and up-regulation of prestin expression after thyroid hormone application. Recent efforts including to grow the cells under "feeder-free" conditions and to pre-select the progenitor cell populations simplified the culture environment and uniformed the cell population, which makes the CR-OSC adaptable for future high-throughput screening.

PS-857

Posttranslational Modifications Affect ATOH1 Activity in the Developing Cochlea

Weise Chang[1]; Karen Avraham[2]; Matthew Kelley[3]
[1]National Institute of Health; [2]Department of Human Molecular Genetics, Tel Aviv University, Tel Aviv, Israel; [3]Laboratory of Cochlear Development, NIDCD, NIH

The development of an ordered pattern of hair cells and supporting cells from cochlear prosensory cells is critical for normal auditory function. Previous studies had shown that disruption of an FGF20-FGFR1signaling interaction results in decreased numbers of hair cells and significant cochlear patterning defects. To determine the factors that might regulate these effects, changes in gene expression were assayed following disruption of FGF20-FGFR1 signaling in cochlear explants using a function- blocking antibody against FGF20. As previously reported, we observed loss of sensory hair cells and down regulation of several genes including *Sox2, Cdkn1b, Prox1, Pea3*, *Jag1*, and *Atoh1*. The change in *Atoh1* expression was particularly interesting as *Atoh1* mRNA levels decreased to17 times less than control within six hours of initiation of the treatment. In fact, subsequent experiments indicated significant decreases in *Atoh1* mRNA started within 30 min of inhibition of FGF20. The speed of this change suggested that FGF20-FGFR1 signaling might disrupt the Atoh1 positive feedback loop through post-translational modification of ATOH1 protein. To test this hypothesis, we analyzed the ATOH1 peptide sequence for potential MAPK-mediated phosphorylation sites and identified several potential sites including Amino Acid (AA) 32, AA64, AA 339, AA342, and AA347. Site-directed mutagenesis was performed to modify each candidate residue to a constitutively active or constitutively inactive form. In addition, we tested two constructs: one in which the carboxy-terminal 12 amino acids, including four serines, were eliminated, and another with a frame-shift which preserved the full length of the protein but eliminated the final four serines. To test the effects of each modification, mutated forms of ATOH1 were expressed in primary mouse cochlear

explant cultures or the OC1 cell line. Ectopic expression of all mutant constructs successfully generated additional sensory hair cells in cochlear cultures based on expression of Myo6. However, the efficiency of some constructs appeared to be reduced based on the time required for onset of Myo6 expression. Similarly, some *Atoh1* mutant constructs displayed decreased levels of ATOH1 protein when expressed in OC1 cells. Subsequent assay of the Atoh1 protein expression revealed that proteasome dependent Atoh1protein degradation was compromised in some of these mutants. The results of these studies suggest that post-translational modulation of ATOH1 through the FGF signaling pathway could play a role in regulating Atoh1 activity within the developing cochlea.

PS-858

Co-expression of Atoh1 and miRNA 183 Family in Pluripotent Stem Cells to Promote Inner Ear Hair Cell Fate

Michael Ebeid; Prashanth Sripal; Jason Pecka; Timothy Hallman; Kirk Beisel; Garrett Soukup
Creighton University

Introduction

A barrier to hearing restoration after hair cell (HC) loss is the inability of mammalian auditory HCs to spontaneously regenerate. Guiding pluripotent stem cells (PSCs) toward a HC fate represents a potential method for HC regeneration that might be achieved by overexpressing factors known to be crucial for HC development. Atoh1 is widely accepted to be necessary and contextually sufficient for driving HC fate. Furthermore, the miRNA-183 family is known to be expressed at the time of HC differentiation. We propose that using a combination of factors controlling both transcriptional and post-transcriptional gene expression can drive HC fate in PSCs.

Methods

We have developed plasmid vectors (pVs) co-expressing various combinations of miR-183 family, Atoh1, and red fluorescent protein (RFP) from a single transcript. HEK293 cells were used to validate protein expression by western blot analysis, RFP expression by flow cytometry, and miRNA expression by quantitative RTPCR. Mouse embryonic stem cells (mESCs) were transfected with pVs, and RFP-positive cells were sorted 48 hours post-transfection using fluorescence activated cell sorting. Gene expression profiling (GEP) was assessed using Affymetrix Mouse Gene ST Arrays. Transfected mESCs were used to generate embryoid bodies (EBs) in suspension culture, and subsequent cryosectioning and immunostaining was performed to examine effects on cell morphology and differentiation.

Results

In HEK293 cells, vectors functioned as expected by yielding Atoh1, RFP and miRNA expression. GEP of mESCs transfected with control vector expectedly showed down-regulation of pluripotency markers (oct3/4, nanog & klf4) and up-regulation of neuronal progenitor markers (Otx2, Msi1 & Sox1) compared to mESC. Expression of Atoh1 caused further down-regulation of pluripotency markers, and up-regulation of cerebellar granule cell progenitor markers (Meis1,2 & Zic2), notch signaling pathway markers (Hes6 & Dll3), and multiple transcription factors (Snai2, Foxi3, Id1, Id2, Lbh & Pou3f1). miRNA-183 family repressed the expression of some Atoh1 up-regulated genes including Cdkn1c, Mmp11, Hoxa5, Mtx2 & Myh9. EB analysis showed Myo7a-positive cells on the exterior of 5 & 9 days old EBs across all conditions including control. After 13 days, less myo7a positive cells were detected populating the interior of EBs. These cells were not associated with F-actin enrichment and likely represented neuronal precursors known to transiently express Myo7a.

Conclusion

Our analysis indicated numerous targets for Atoh1 in PSCs, some of which can be associated with HC development. miR-183 family had relatively less effect on PSC transcriptome, but appeared to fine-tune Atoh1-mediated changes in gene expression.

PS-859

Multi-Trait Genome-wide Association Studies (GWAS) to Investigate Hearing Function and Interactions with BMI, Blood Pressure and Glycaemia

Dragana Vuckovic[1]; Valentina Iotchkova[2]; Giorgia Girotto[1]; Nicole Soranzo[3]; Paolo Gasparini[4]
[1]University of Trieste, Italy; [2]Wellcome Trust Sanger Institute - EMBL-EBI; [3]Wellcome Trust Sanger Institute; [4]University of Trieste, Italy - IRCCS Burlo Garofolo

Introduction

Recently, considerable progress has been made in identifying mutations/genes involved in hereditary hearing loss (HHL), but still little is known about the genetic basis of complex traits such as Normal Hearing Function (NHF) and Age-Related Hearing Loss (ARHL). Single-trait GWAS meta-analyses on hearing thresholds already identified and replicated a number of candidate genes for both NHF and ARHL (Girotto et al. JMG 2011 & PLOS ONE 2014, Vuckovic et al. in submission). Considering that many other factors are known or hypothesized to interact with the auditory system, these analyses lacked the necessary ability to analyze several traits in parallel. Here, for the first time, we present a multivariate GWAS, analysing: 6 hearing thresholds simultaneously and the association between auditory function and Body Mass Index (BMI), Blood Pressure (BP) and Glycaemia.

Methods

A multivariate linear mixed model regression was performed using GEMMA software (Zhou&Stephens, Nat.Met. 2014). A total of 1597 subjects from isolated cohorts located in Italy and Central Asia were analysed. After adjusting for sex, age and relatedness, the following traits were tested: (a) 6 hearing thresholds (HT) (0.25, 0.5, 1, 2, 4, 8 kHz); (b) HT and BMI; (c) HT and BP; (d) HT and Glycaemia. These results were then combined in a multivariate meta-analysis based on inverse-variance weights; a novel method that has been previously successfully tested on other traits from the UK10K project (Vuckovic et al. personal communication).

Results
Preliminary data for analyses (a) and (b) revealed a positive association within two loci (located on chromosomes 5 and 6, p-value<10E-07) and both hearing phenotypes and BMI. Very interestingly, these findings, for the first time, demonstrate a possible genetic link between these 2 phenotypes and might explain epidemiological data from cross-sectional and prospective studies, in which higher BMI, larger waist circumference, and lower physical activity have been associated with poorer hearing. In order to validate our findings, a replication step is now in progress in two outbred cohorts from Finland and UK (FITSA and B58C). Moreover, additional analyses are ongoing for the remaining phenotypes (c and d). Up-to-date results will be presented and discussed.

Conclusions
The multivariate approach is particularly important when dealing with complex and correlated traits such as hearing thresholds. It allows for detection of novel associations by increased power as well as thorough investigation of interactions between related traits. Present findings could lead towards a better understanding of the molecular mechanisms underlying hearing function.

PS-860

A Genome-Wide Association Study Defining the Genetic Architecture of Hearing in Inbred Mouse Strains.

Rick Friedman[1]; Amanda Crow[2]; Aldons Lusis[3]; Hooman Allayee[2]; Eleazar Eskin[3]; Juemei Wang[2]
[1]Keck Medical Center of USC; [2]University of Southern California; [3]University of California, Los Angeles

Age-related hearing loss is characterized by a symmetrical sensorineural decline most commonly in the high frequencies and is the most common sensory abnormality in the world. Heritability studies have shown that the sources of the variability in hearing with age are both genetic and environmental with roughly 50% accounted for by heritable factors. A limited number of large-scale genome wide association studies (GWAS) for age-related loss have been undertaken in humans, to date. In an initial study, we and our collaborators reported on an association in GRM7 and have subsequently demonstrated the highly polygenic nature of this disease in a more detailed follow up study. There are several limitations to GWAS for hearing traits in humans including the need for large well characterized cohorts and the inherent difficulty in controlling for environmental exposures. Additionally, most GWAS in humans fails to identify a significant amount of the total heritability of most traits. Buoyed by the prospects of and successes of human GWAS, several groups, including ours, have proposed mouse GWAS. The mouse has several advantages including tight control of environmental exposures, replication of phenotypic measurements in genetically identical animals, and a higher proportion of the variability being explained by genetic variation due to the greater effect sizes seen in mice in comparison to humans. Utilizing the Hybrid Mouse Diversity Panel, we have, for the first time, completed an association based analysis of hearing loss in mouse strains with correction for population structure. Our results have identified a number of genetic loci, with high resolution, containing candidate genes that in each instance are novel with no overlap with existing Mendelian genes/loci. Furthermore, our physiological/genetic analysis demonstrates a tonotopic architecture to the genetics of hearing loss in these strains.

PS-861

Genome-wide Association Study and Systems genetics approach identifies Nox3 as a Critical Gene for Susceptibility to Noise-Induced Hearing Loss.

Joel Lavinsky[1]; Calvin Pan[2]; Amanda Crow[3]; Ksenia Aaron[3]; Anthony Myint[3]; Maria K. Ho[3]; Qingzhong Li[4]; Pezhman Salehi dermanaki[3]; Jake Lusis[2]; Hooman Allayee[5]; Rick Friedman[6]
[1]University of Southern California, Federal University of Rio Grande do Sul; [2]University of California, Los Angeles; [3]University of Southern California; [4]Eye & ENT hospital of Fudan Universtiy; [5]USC Keck School of Medicine; [6]University of Southern California, Department of Otolaryngology-Head & Neck Surgery, Keck School of Medicine

Background
The genetic basis of noise-induced hearing loss (NIHL) has been demonstrated as different susceptibilities have been seen in different inbred stains of mice. Based on this variation, genome-wide association studies (GWAS) and co-expression network analysis were used for the first time in the recently described Hybrid Mouse Diversity Panel (HMDP) to identify and characterize novel genes related to NIHL.

Methods
Approximately three female mice (5 weeks old) for each HMDP strain were evaluated by ABR (auditory brainstem responses) and 2 weeks after noise-exposure (10 kHz octave band noise for 2 hours at 108 dB SPL). Knockout mice of varying $Nox3^{het}$ genotype ($Nox3^{het}/Nox3^{het}$ and $Nox3^{het}/+$) and wild-type (C57BL/6JEiJ strain) were evaluated by the same procedure. The Efficient Mixed-Model Association (EMMA) algorithm was applied to each hearing phenotype separately. Network analysis was performed using the WGCNA (Weighted Gene Co-Expression Network Analysis) R package.

Results
Post noise exposure GWAS revealed 5 significant (P=4.1 x 10-6, -log10P=5.39) associations and implicated a total of 27 candidate loci. However, the goal was to prioritize NADPH oxidase *Nox3* as a candidate gene (Figure 1) for validation based on its cochlear expression QTL profiles and its high expression in the inner ear. The involvement of *Nox3* gene in NIHL was confirmed by the observation that $Nox3^{het}/Nox3^{het}$ mutant mice were more susceptible to noise measured by ABR permanent threshold shifts (PTS) specifically at 8 kHz tone-burst stimuli (Figure 2). Distortion product otoacoustic emissions and ABR wave 1 amplitudes indicated that the mechanism of the $Nox3^{het}/Nox3^{het}$ mutant mice susceptibility resided in the spiral ganglion neurons. Immunohistochemis-

try demonstrated a significantly higher density of synaptic ribbons in wild-type mice (Figure 3) without a difference in outer hair cell loss count. To understand the mechanism through which *Nox3* influenced NIHL, a gene co-expression network was created using cochlear gene expression microarray data from HMDP strains. *Nox3* was identified as a member of a co-expression turquoise module (Figure 4) enriched for genes involved in the sensory organ development (Figure 5).

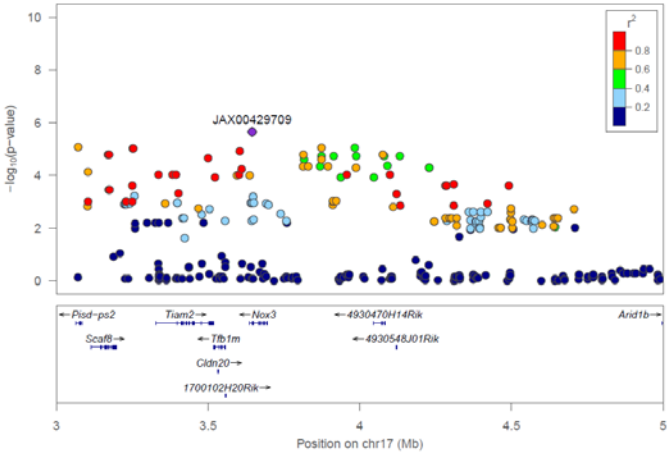

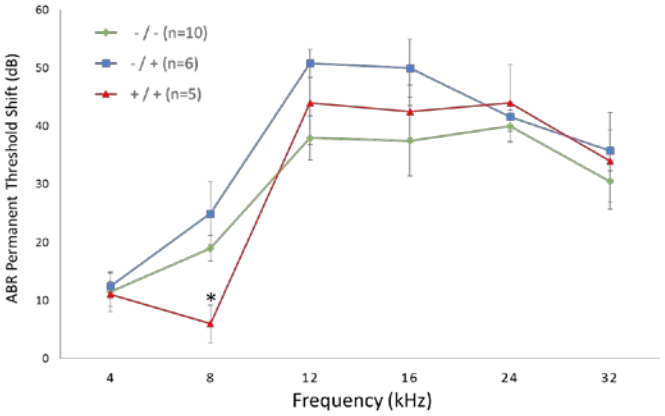

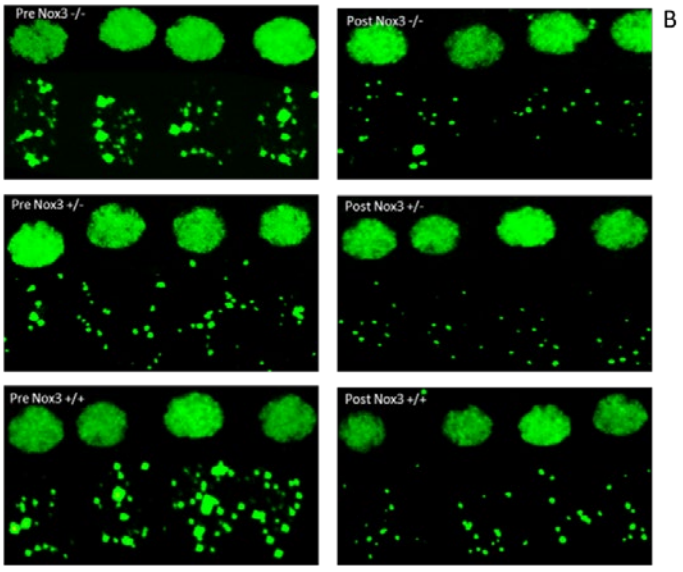

B

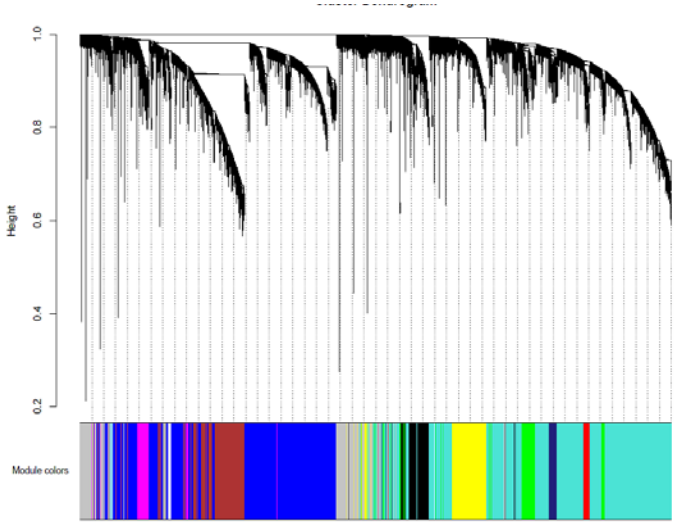

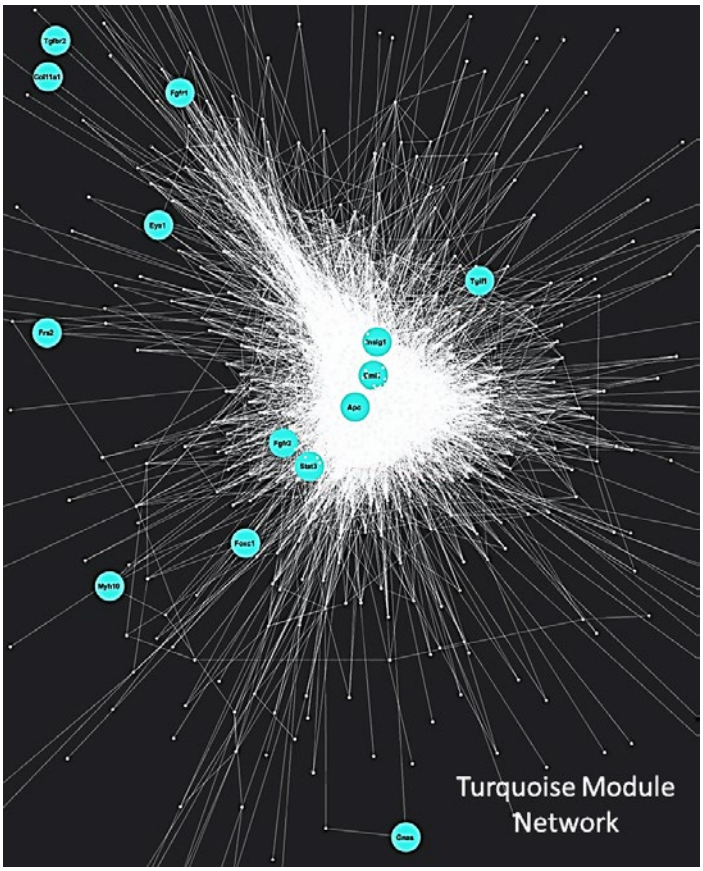

Conclusions

We have demonstrated the first functional validation of a gene of the auditory system arising from GWAS, showing that the *Nox3* gene is related to NIHL, the absence of *Nox3* is involved in susceptibility to noise. This finding was remarkable at the frequency of 8 kHz, especially at the synaptic afferents. Also, based on the co-expression network *Nox3* may play a role in inner ear development.

PS-863

Mining the Genetic Mouse Library Identifies Critical Regions for the Chronic Otitis Media Phenotype in Down Syndrome

Mahmood Bhutta[1]; Steve Brown[2]; Michael Cheeseman[3]; Yann Herault[4]; Yuejin Yu[5]

[1]UCL Ear Institute; [2]MRC Harwell; [3]Roslin Institute; [4]ICS Starsbourg; [5]Roswell Park

Aim

Chronic otitis media (OM) is prevalent in Down syndrome (DS), but the cause is unknown, although often hypothesized to be due to craniofacial deformity. A previous study of Eustachian tube morphology failed to show any difference in children with DS. We set out to define a critical genetic region responsible for the OM phenotype by screening the library of engineered mouse models carrying partial trisomy for regions syntenic to human chromosome 21.

Methods

Through a collaboration of MRC Harwell (UK), ICS Strasbourg (France) and Roswell Park (USA), cadaveric specimens of almost the entire reported library of DS mouse models were obtained: Ts65Dn, Ts1Cje, Ts2Yah, Ts1Rhr, Dp16(1)Yey, Dp10(1)Yey, Dp17(1)Yey, and Tc1 adult mice. Heads were sectioned and assessed for histological presence of chronic OM, and compared to wild-type littermates.

Results

532 ears were analysed. The Dp16(1)Yey mouse line develops chronic OM, with a phenotype penetrance of 0.73 (19 of 26 ears) and disease onset at age 2 months. Mice displayed thickened mucoperiosteum, neutrophil and macrophage infiltration, and an effusion of variable cellularity. No OM was found in the Dp(17)1Yey mouse or the Dp(10)1Yey mouse, suggesting disease loci are located only on MMU16. The Ts1Cje, Ts1RhR, and Ts2Yah, trisomies and the transchomosomic Tc1 mouse did not develop OME. We failed to confirm previous reports of highly penetrant OM in the Ts65Dn line.

Conclusion

Susceptibility to chronic OM is determined by a critical region of genes on mouse chromosome 16 (MMU16) that are sytenic to human chromosome 21 (HSA21). However, the failure to demonstrate OM in mice with shorter-segment trisomy within this region implies complex aetiology, with important gene-gene or gene-environment interactions. Based upon our data, in a model of gene-gene interaction we propose interaction between the regions Rh46998-D21s11 and Ifngr2-Rh123045. In a gene-environment interaction model we propose triggering through respiratory pathogens reflecting differing housing conditions of laboratory mice.

Further analysis of mouse models, integrating hypothesised phenotype modifiers or engineering of custom genetic mutant mouse models, may enable us to refine our model of chronic OM aetiology in Down Syndrome.

PS-864

A Novel Mutation in NLRP3 Causes Nonsyndromic Dominant Hearing Loss DFNA34

Hiroshi Nakanishi[1]; Yoshiyuki Kawashima[2]; Kiyoto Kurima[3]; Julie Muskett[3]; Ivona Aksentijevich[4]; Jae Jin Chae[4]; John Butman[5]; Seema Patel[6]; Daniel Kastner[4]; Raphaela Goldbach-Mansky[6]; Andrew Griffith[3]

[1]NIH; [2]Tokyo Medical and Dental University; [3]NIDCD, NIH; [4]NHGRI, NIH; [5]Clinical Center, NIH; [6]NIAMS, NIH

Background

NLRP3 encodes cryopyrin, a key component of the NLRP3 inflammasome that is activated by injury, toxins or microorganisms. The activation of the NLRP3 inflammasome triggers the maturation and secretion of interleukin 1β (IL-1beta), a potent proinflammatory cytokine. Gain-of-function mutations of *NLRP3* are known to cause cryopyrin-associated periodic syndromes (CAPS) that can include recurrent fever, episodic skin rash and sensorineural hearing loss (SNHL). Peripheral blood mononuclear cells (PBMCs) from CAPS patients show increased IL-1beta secretion at rest or in response to lipopolysaccharide stimulation. Here, we report that a novel mutation in *NLRP3* also causes nonsyndromic SNHL, without systemic autoinflammatory symptoms, at the DFNA34 locus.

Methods

We ascertained a North American family, LMG113, segregating autosomal dominant SNHL. None of the affected family members had symptoms of CAPS. We performed linkage and nucleotide sequence analyses of peripheral blood genomic DNA. PBMCs from one affected patient were cultured and IL-1beta concentration was measured in the supernatant. The therapeutic response to anakinra, an IL-1beta receptor antagonist used to treat CAPS, was evaluated in this patient.

Results

A genome-wide linkage analysis yielded a maximum two-point LOD score of 3.15 with short tandem repeat markers on chromosome 1q44. This is a novel DFNA locus designated as DFNA34. Fine-mapping narrowed the DFNA34 interval to 3.93 Mb that included 36 genes. One of these genes was *NLRP3*. Dideoxy sequencing of *NLRP3* detected a heterozygous missense substitution, c.2753G>A (p.R918Q). p.R918Q co-segregated with SNHL in the family and was not present in 574 ethnically matched control chromosomes. Massively parallel sequencing of DNA samples from 3 affected members of LMG113 identified no other probable pathogenic variants in the DFNA34 interval. The patient's erythrocyte sedimentation rate, C-reactive protein and fibrinogen levels were all elevated or borderline elevated. The level of IL-1beta secreted from PBMCs from this patient was elevated. Pathologic enhancement of the cochlea was identified on postcontrast FLAIR MRI, similar to that observed in CAPS patients. Six months of treatment with anakinra did not change her audiometric test results, but her inflammatory markers were normalized.

Conclusion

The p.R918Q of *NLRP3* causes DFNA34 hearing loss without symptoms of systemic autoinflammation. Abnormal acti-

vation of the NLRP3 inflammasome is therefore a potential cause of isolated SNHL.

PS-865

Novel Mutations in DTNA and FAM136A Genes in Autosomal Dominant Familial Meniere's Disease

Teresa Requena[1]; Sonia Cabrera[1]; Carmen Martin-Sierra[1]; Lidia Frejo[1]; Steven D Price[2]; Anna Lysakowsky[2]; **Jose A Lopez-Escamez**[1]

[1]Center for Genomics and Oncology Research (Genyo), University of Granada; [2]Dept. of Anatomy and Cell Biology, University of Illinois at Chicago

Background

Familial Meniere's disease (MD) is found in 5-15% of cases in European population, suggesting that MD may have a genetic component. Although genetic heterogeneity is observed, most of the families have an autosomal dominant pattern of inheritance with incomplete penetrance (1).

Methods

DNA was isolated from human peripheral blood and whole exome sequencing (WES) was carried out in a SOLiD 5500xl platform in a family with three affected women in consecutive generations to identify rare variants. Bioinformatic analyses were used to filter and prioritize variants according to their effect on the protein structure and phylogenetic conservation, and phenotype, obtaining seven candidate variants that were validated by Sanger sequencing. These variants were filtered by WES data from familial controls and 2386 European genomes. Morphological and functional studies including immunohistochemistry, gene expression, and immunoblotting were carried out to confirm the pathological effect of the candidate variants.

Results

We have identified two novel single nucleotide variants so far: a heterozygous nonsense mutation in the FAM136A gene chr2:70527974C>T which truncates the protein by 62 AA and a second heterozygous missense mutation in DTNA chr18:32462094G>T generating a novel splice-site which skips exon 21 (Fig. 1)

FAM136A encodes a membrane protein of unknown function associated with mitochondria. Two FAM136A mRNA transcripts and their protein products were confirmed in patient lymphoblasts. Carriers of FAM136A mutation showed a significant decrease in the expression levels of both transcripts in lymphoblastoid cell lines (p=0.002).

DTNA encodes alpha-dystrobrevin, an essential membrane protein involved in the formation and stability of synapses and the preservation of brain-blood barrier (3). The DTNA splice-site effect was evaluated in lymphoblasts and a new mRNA isoform, missing 49 nucleotides in exon 21, was confirmed.

In rat cristae ampullares, we have found that FAM136A protein co-localizes with the mitochondrial marker COX IV in the basal pole of vestibular hair cells. Moreover, alpha-dystrobrevin was located in supporting cells, close to the stromal region.

Conclusions

1. Novel mutations in FAM136A and DTNA genes are probable causal variants in familial MD.
2. A decrease in expression of coding transcripts in patient lymphoblasts, leading to haploinsufficiency of FAM136A, and the generation of a novel splice-site in DTNA gene, skipping exon 21, suggest a functional role for both mutations in familial MD.

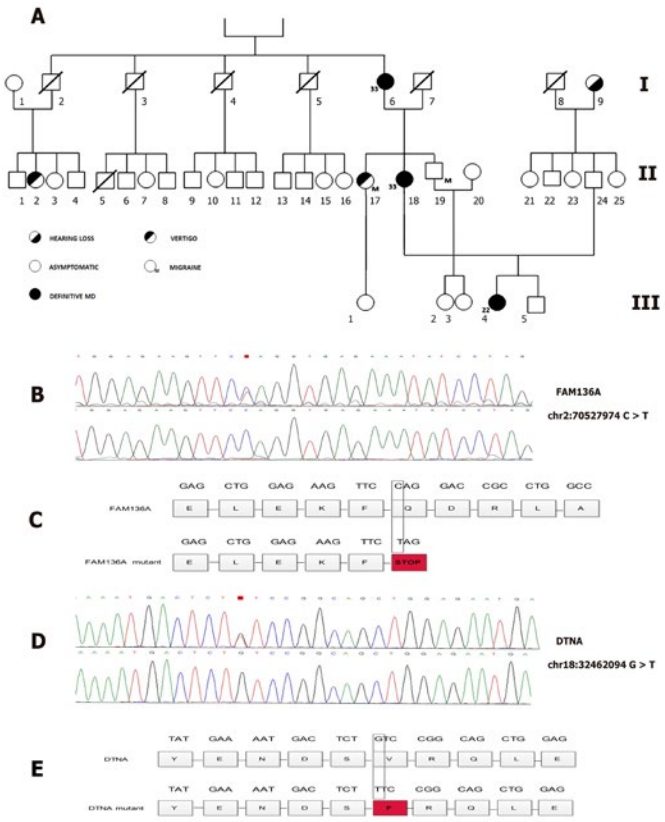

3.

References

[1] Requena T, Espinosa-Sanchez J, Cabrera S, et al. (2014) Familial clustering and genetic heterogen-eity in Meniere's disease. Clin Genet 85:245-52.

PS-866

Achieving Genetic Diagnosis in Hearing-impaired Patients with "Non-confirmative" or "Genotype-phenotype Mismatched" GJB2 Mutations Using Massively Parallel DNA Sequencing

Chen-Chi Wu[1]; Yin-Hung Lin[2]; Yi-Hsin Lin[3]; Ying-Chang Lu[3]; Pei-Lung Chen[2]; Chuan-Jen Hsu[4]

[1]National Taiwan University Hospital; [2]Graduate Institute of Medical Genomics and Proteomics, National Taiwan University College of Medicine; [3]Department of Otolaryngology, National Taiwan University Hospital; [4]Department of Otolaryngology, Taichung Tzu Chi Hospital

Background

Recessive mutations in the *GJB2* gene are the most common genetic cause of sensorineural hearing impairment (SNHI) in humans. However, in 10%~50% patients, only 1 recessive *GJB2* mutation can be detected, resulting in "non-confirmative" genetic diagnosis. Another dilemma in interpreting the genetic results lies in the "mismatch" between the *GJB2* genotypes and phenotypes. For instance, the common *GJB2* p.V37I mutation has been associated with mild-to-moderate SNHI, yet occasionally patients with severe-to-profound SNHI are found to segregate two p.V37I alleles. In these patients, we hypothesize that there might be undetected mutations in: (1) the non-coding region of *GJB2* (such as untranslated exons, introns, promoter or enhancer) leading to compound heterozygous inheritance; (2) other gap junction genes leading to digenic inheritance; or (3) other causative or modulating deafness genes.

Methods

We designed a massively parallel sequencing (MPS) panel which target the whole *GJB2* gene and the exons of 129 deafness genes (including all gap junction genes), and applied this panel to two different cohorts: (1) 12 patients with only 1 recessive *GJB2* mutation detected by conventional Sanger sequencing of the *GJB2* coding region [the "single *GJB2* mutation" cohort]; and (2) 22 patients homozygous for *GJB2* p.V37I whose hearing levels ranged from mild to profound SNHI [the "V37I" cohort]. Variants detected by MPS were then subjected to bioinformatic data filtering, Sanger sequencing, and segregation pattern analyses to confirm their pathogenicity.

Results

In the "single *GJB2* mutation" cohort, causative mutations in other deafness genes were identified in 4 patients, including *SLC26A4* mutations in 2 patients (genotypes: p.K369X/p.T410M and p.P8T/p.P8T, respectively), *KCNQ4* mutation in 1 patient (genotype: p.F182L/wt), and *MYO15A* mutations in 1 patient (genotype: p.W58C/c.8596-1G>C). A splicing site mutation (IVS1+1G>A) in *GJB2* was detected in 1 patient, contributing to compound heterozygosity of *GJB2* mutations. Of note, we also found ~67% mosaicism of *GJB2* c.235delC in another patient which was difficult to be identified by Sanger sequencing alone. Similarly, in the "V37I" cohort, we identified causative mutations in other deafness genes in 2 patients with severe-to-profound SNHI (genotypes: *TMC1*, p.P128L/p.320_320del and *CDH23* p.V856I/p.R962Q, respectively).

Conclusions

By using an MPS panel, we confirmed genetic etiologies in 6 patients with single recessive *GJB2* mutation, as well as 2 patients homozygous for the mild p.V37I mutation but showed severe-to-profound SNHI clinically. Our results demonstrated the utility of MPS in achieving genetic diagnosis in hearing-impaired patients with "non-confirmative" or "genotype-phenotype mismatched" *GJB2* mutations on conventional genetic examinations.

PS-867

Next-Generation Sequencing for Deafness Gene Discovery in the Middle East

Meirav Sokolov[1]; Zippora Brownstein[2]; Amal Abu Rayyan[3]; Ofer Isakov[4]; Maria Birkan[2]; Fábio T.A. Martins[2]; Nada Danial-Faran[2,8]; Moshe Frydman[2,5]; Hagit Baris-Feldman[6]; Reuven Sharoni[7]; Stavit Shalev[8]; Noam Shomron[4]; Moein Kanaan[3]

[1]Tel Aviv University, Tel Aviv, Israel; Meir Medical Center, Kfar Saba, Israel; [2]Department of Human Molecular Genetics and Biochemistry, Sackler Faculty of Medicine, Tel Aviv University, Tel Aviv, Israel; [3]Department of Biological Sciences, Bethlehem University, Bethlehem, Palestine; [4]Department of Cell and Developmental Biology, Sackler Faculty of Medicine, Tel Aviv University, Tel Aviv, Israel; [5]Danek Gartner Institute of Human Genetics, Sheba Medical Center, Tel Hashomer, Israel; [6]Genetics Institute, Rambam Health Care Campus, Haifa, Israel; [7]Genetic Institute, Meir Medical Center, Kfar Saba, Israel; [8]Genetics Institute, Ha'Emek Medical Center, Afula, Israel

The combination of targeted genomic capture and massively parallel sequencing (MPS) has become an optimal tool for detecting novel and known mutations involved in hereditary hearing loss and for solving many cases in a rapid and cost-effective manner. While hundreds of mutations in more than 70 genes are associated with hearing loss, for many individuals with hereditary defects, the etiology remains unknown. In many cases, the causative mutation might be in a known gene that is not screened routinely due to practical limitations. Until recently, the large reservoir of known deafness genes, as well as their large size, precluded comprehensive genetic diagnosis. Alternatively, mutations in new genes may be solved by whole exome sequencing (WES). We performed MPS using a targeted genomic capture approach with 284 genes, including 121 human genes and 163 human orthologues of mouse deafness genes in 150 hearing impaired unrelated individuals from Israeli Jewish and Palestinian Arab families. Variants were validated by Sanger sequencing. Our results doubled the number of identified mutations in these populations, with new mutations discovered in the genes *POU4F3, MYO6, MYO7A, MYO15A, LOXHD1, USH2A, SLC26A4, TECTA, OTOF, PCDH15* and more. As a result, the etiology of a significant portion of our population has been solved. The challenges, however, remain, when more than one apparently pathogenic variant is present in

a patient or when there are as yet undefined and potential regulatory variants present. Finally, will gene discovery help our patients?

Funding
NIH/NIDCD R01-DC011835 (KBA and MK)

PS-868

Mutations in the Mitochondrial tRNA Synthetase Cause Nonsyndromic Deafness DFNB94 or Leigh Syndrome

Mariella Simon[1]; Elodie Richard[2]; Xinjian Wang[3]; Mohsin Shahzad[2]; Vincent H Huang[3]; Tanveer A. Qaiser[4]; Prasanth Potluri[5]; Sarah E. Mahl[6]; Antonio Davila[7]; Sabiha Nazli[4]; Shaheen N. Khan[4]; Ronghua Li[3]; Min-Xin Guan[3]; Thomas Friedman[8]; Doris Wu[9]; Vincent Procaccio[10]; Sheikh Riazuddin[11]; Douglas C. Wallace[5]; Zubair M. Ahmed[2]; Taosheng Huang[3]; **Saima Riazuddin[2]**
[1]University of California, Irvine; [2]Department of Otorhinolaryngology Head & Neck Surgery, School of Medicine, University of Maryland, Baltimore; [3]Division of Human Genetics, Cincinnati Children's Hospital Medical Center; [4]National Center for Excellence in Molecular Biology, University of the Punjab, Pakistan; [5]Center for Mitochondrial and Epigenomic Medicine, Children's Hospital of Philadelphia Department of Pathology and Laboratory Medicine, University of Pennsylvania; [6]Division of Pediatric Otolaryngology Head & Neck Surgery, Cincinnati Children's Hospital Medical Center; [7]Smilow Center for Translational Research, University of Pennsylvania; [8]Laboratory of Molecular Genetics, National Institute on Deafness and Other Communication Disorders, National Institutes of Health, Bethesda; [9]Section on Sensory Cell Regeneration and Development, National Institute on Deafness and Other Communication Disorders, National Institutes of Health, Bethesda; [10]National Center for Neurodegenerative diseases, Department of Neurology, Charcot section, CHU Angers, France; [11]Jinnah Hospital Complex, Allama Iqbal Medical College, University of Health Sciences, Pakistan

Background
The emergence of genome enrichment arrays followed by massive parallel sequencing (next-generation sequencing, NGS) technologies have accelerated gene discovery for hearing loss (HL). To date the genetic basis of only half of the identified deafness loci has been elucidated.The goal of our study was to identify a new gene responsible for hearing impairment in Human.

Methods
We enrolled a large consanguineous Pakistani family, PKDF406, segregating pre-lingual, recessively inherited, nonsyndromic, profound hearing loss (DFNB94) and a Caucasian family, LS06, with Leigh syndrome including congenital auditory neuropathy. Whole exome sequencing followed by Sanger sequencing was performed using DNA from some of the affected individuals of both families. Sub-cellular localization of the tagged mutant protein was examined. Fibroblast cell line derived from affected patient of family LS06 was used to assess mt-RNA steady state levels and mitochondrial respiratory chain functions.

Results
In this study, we identified three mutations in a mitochondrial tRNA synthetase, as the underlying cause of Leigh syndrome with congenital auditory neuropathy in family LS06 and nonsyndromic hearing loss (DFNB94) in a Pakistani family PKDF406. Whole-exome sequencing revealed novel compound heterozygous mutations [c.969T>A; p.Tyr323*]; [c.1142A>G; p.Asn381Ser] in family LS06 and a novel transition mutation (c.637G>T, p.Val213Phe) in PKDF406. All the newly described mutations are located in the putative catalytic domain of the protein. *In situ* hybridization assays showed expression in the sensory and non-sensory epithelia of the inner ear as well as the spiral ganglion and brain tissues of the mouse. Transient expression of GFP- tagged protein demonstrates mitochondrial localization, which is not altered by the missense mutations. Co-immunoprecipitation assays have shown that p.Asn381Ser variant alters its ability ti dimerize. Decreased steady-state levels of mt-tRNA were found in the fibroblasts from affected patient of family LS06, without aminoacylation defect. In these cells, impaired oxygen consumption rate and OXPHOS deficiency were also observed. In contrast to the wild-type protein, over-expression of p.Val213Phe mutant protein in patient-derived fibroblast cell line was unable to rescue the mitochondrial respiratory chain defect.

Conclusions
These results demonstrate that tRNA synthetase mutations are responsible for Leigh syndrome in family LS06 and DFNB94 in family PKDF406. Our *in vitro* studies validate that the protein of mitochondria respiratory chain is essential for hearing within the inner ear.

PS-869

Advanced Next-Generation Sequencing Unveils Hearing Loss Genes

Benjamin Currall[1]; Vamsee Pillalamarri[2]; Kristen Wong[1]; Tammy Kammin[1]; Shahrin Pereira[1]; Michael Talkowski[2]; Cynthia Morton[1]
[1]Brigham and Women's Hospital; [2]Massachusetts General Hospital

De novo balanced chromosomal aberrations (BCAs) occur in 1 in 2,000 newborns, resulting in specific nucleotide lesions that can disrupt or dysregulate essential genetic regions. These lesions can lead to many forms of congenital disorders including hearing loss. Traditionally, BCAs have been diagnosed through cytogenetic techniques (*e.g.,* karyotyping), which rarely identify specific genes involved without additional expensive and time-consuming molecular assays. Through the Developmental Genome Anatomy Project (DGAP, www.dgap.harvard.edu), we have developed paired-end next generation sequencing (NGS) techniques that can identify BCA breakpoints at nucleotide resolution in as few as 10 days. Of the nearly 300 subjects enrolled in DGAP, more than 50 have a hearing loss and/or language development delay phenotype of which 3 cases have been recently solved through

this advancement in NGS and are described here. In the first subject with hearing loss and *café-au-lait* spots, application of NGS revealed a more complex chromosomal aberration (*i.e.*, chromothripsis) leading to the loss of *KIT*, an established hearing loss gene. In the second subject with non-syndromic high frequency hearing loss, NGS revealed disruption of *ESSRG*, a gene that has only recently been associated with hearing loss through genome-wide association studies (GWAS). In the third subject with "cookie bite" hearing loss, NGS identified disruption of a novel gene, named *ADGB*, which has no known function. These cases demonstrate both the research potential and clinical utility of paired-end NGS in determining genetic etiology of congenital hearing loss.

PS-870

Miami Otogenetic Program: From Basepairs to Bedside

Xue Zhong Liu; Denise Yan; Demet Tekin; Arpit Mehta; Susan Blanton; Mustafa Tekin

University of Miami-Miller school of Medicine

Background

Inherited deafness demonstrates extreme heterogeneity, making single gene testing inefficient. Therefore, a target enrichment/next generation strategy is more time and cost-efficient for the translation of research data into clinical care.

Methods

We have established the Miami Otogenetic Program, combining the research and the clinical components. Our multidisciplinary otogenetics team utilizes a variety testing algorithms when evaluating patients with sensorineural hearing loss (SNHL).The Miami Otogenetic Program has developed a unique platform to carry out translational research on delivering genetic services to deaf patients.

Results

We have developed a custom capture panel, the MiamiOtoGenes, composed of 180 known deafness genes with a target size of approximately 1.327 MB (Agilent Sure Select DNA Design). The genes were identified by searching databases, including Hereditary Hearing Loss Homepage, RefSeq, Ensembl, The Human Genome Mutation Database (HGMD), and Online Mendelian Inheritance in Man (OMIM) and most recent peer-reviewed publications related to the genetics of deafness. The design covered all coding exons, UTRs and 25 bases of intronic flanking sequences for each exon. The overall *in silico* coverage of the design was 97.47%. The mitochondrial genome with 16.520 kbp was also blended into the design. The Genomes Management Application (GEMapp; https://genomics.med.miami.edu/) was applied for data analysis. Our study with positive controls has proven the accuracy and reliability of the MiamiOtoGenes system. This custom panel is being used for determining the molecular epidemiology of hereditary deafness in a multi-ethnic cohort of 200 deaf probands. Causative mutations for the enrolled individuals are stored in the HL Genotype Database. To analyze the genotype-phenotype relationship, we have created a web-based resource GeneHeal, which links auditory phenotypic information of the deaf patients enrolled in the study to the respective pathogenic genomic variants. Both databases are accessible through the Miami Genetics of HL Resource (GeneHeal) at http://hihg.med.miami.edu/deafness/geneheal and are open for researchers who would like to contribute their data. It provides search capabilities to end users making it an efficient data repository and query tool for the researchers around the world.

Conclusion

The multidisciplinary team approach is an effective way to bring the sequencing data to clinical practice for the clinical diagnosis and management of deaf and hard-of-hearing families.

PS-871

Identification of a Novel Truncation Mutation of EYA4 in Moderate-Degree Hearing Loss by Targeted Exome Sequencing

Hyun Seok Choi[1]; Ah Reum Kim[2]; Shin Hye Kim[2]; Byung Yoon Choi[3]

[1]Seoul National University; [2]Seoul National University Hospital; [3]Seoul National University Bundang Hospital, College of Medicine, Seoul National University; Sensory Organ Research Institute, Seoul National University Medical Research Center

Introduction

The *EYA4* gene encodes a 640-amino-acid protein that serves as a transcription factor. This protein contains a highly conserved Eya domain (eya-HR) and a variable domain (eya-VR). Mutations of this gene are known to cause postlingual and progressive sensorineural hearing loss (SNHL), either as non-syndromic (DFNA10) or syndromic hearing loss, depending upon the location of the truncation of the mutant protein.

Table 1. Overview of EYA4 mutations.

No. of exons	Nucleotide change	Amino acid change	Reference
12	c.1028_1029insAA	p.(Cys344Thrfs*61)	Wayne et al. (2001)
19	c.1759C>T	p.(Arg587*)	Wayne et al. (2001)
13	c.1118_1119insTTTG	p.(Trp374Leufs*6)	Pfister et al. (2002)
4	c.581_804del	p.(Asp194Glyfs*30)	Schonberger et al. (2000, 2005)
12	c.1048_1049dupAA	p.(Arg352Profs*53)	Makishima et al. (2007)
14,15	D6S133833847	Splice site	Hilderbrand et al. (2007)
11	c.863C>A	p.S288X	Baek et al. (2012)
11	c.C909G	p.F03L	Choi et al. (2013)

Supplemental table 1. List of candidate genes after basic filtering.

Chr	Ref Pos	Gene Name	Ref Seq	Called Seq	Depth	P not ref	Q call	SNP %	GERP Score	Classification	Contig Pos	Genotype	Protein Change	Type
1	6500867	ESPN	A	G|A	82	98.55%	18.342	21.95%	3.84	Non-synonymous, splice	6500897	Hetero. Ref.	E286E, E286G	
2	131414737	POTEJ	A	G|A	47	100.00%	60	46.80%		Non-synonymous	131415402	Hetero. Ref.	M802M, M802V	
2	131414975	POTEJ	A	T|A	43	99.99%	41.022	23.25%		Non-synonymous	131415640	Hetero. Ref.	Y881Y, Y881F	
2	131415008	POTEJ	T	T|C	42	99.99%	43.462	23.80%		Non-synonymous	131415673	Hetero. Ref.	M892T, M892M	
2	132021237	POTEE	C	T|C	44	93.09%	11.3	18.18%		Non-synonymous	132021906	Hetero. Ref.	R737R, R737C	
2	132021684	POTEE	C	C|A	46	99.99%	44.006	23.91%		Non-synonymous	132022353	Hetero. Ref.	P886T, P886P	
2	132021781	POTEE	A	T|A	47	81.05%	6.314	17.02%		Non-synonymous	132022450	Hetero. Ref.	Y918Y, Y918F	
2	132021888	POTEE	C	T|C	40	99.99%	58.041	27.50%		Non-synonymous	132022557	Hetero. Ref.	R954R, R954W	
6	133827246	EYA4, LOC101928164	T	T|-	111	100.00%	60	48.64%		Frameshift [EYA4]; Change, non-coding RNA [LOC101928164]	133827905	Hetero. Ref.	D350D, D350fs [EYA4]	Indel
17	72915874	USH1G	C	T|C	44	100.00%	60	40.90%	4.34	Non-synonymous	72916308	Hetero. Ref.	D353N, D353D	
22	38119758	TRIOBP	C	C|-	125	100.00%	60	46.39%		Frameshift	38119909	Hetero. Ref.	R399R, R399fs	Indel
NC_012920	8537	ATP8, ATP6	A	G	357	100.00%	60	96.63%	3.69	Non-synonymous [ATP8]; Non-synonymous [ATP6]	8549	Homo. Variant	I58V [ATP8]; N4S [ATP6]	
unplaced	1646665	LOC101928511	T	T|G	43	100.00%	60	37.20%		Non-synonymous	1646793	Hetero. Ref.	K74K, K74Q	

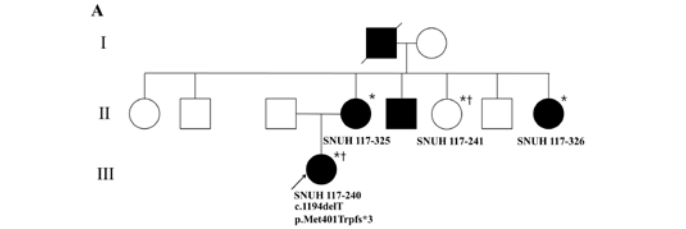

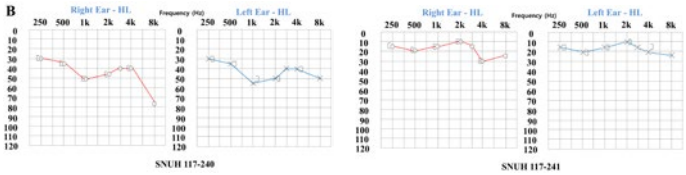

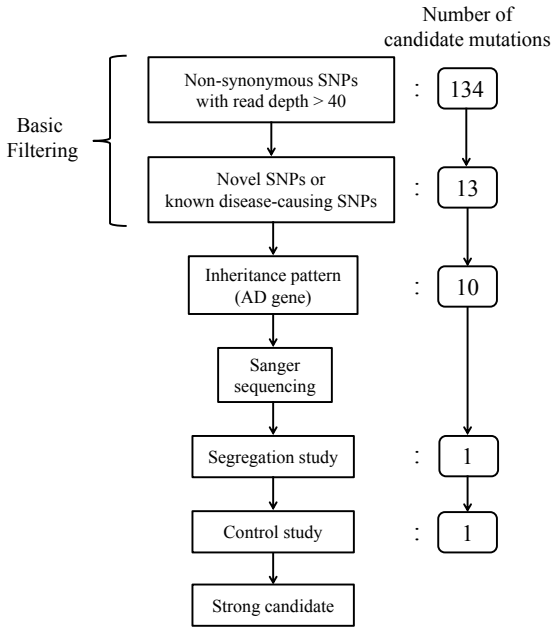

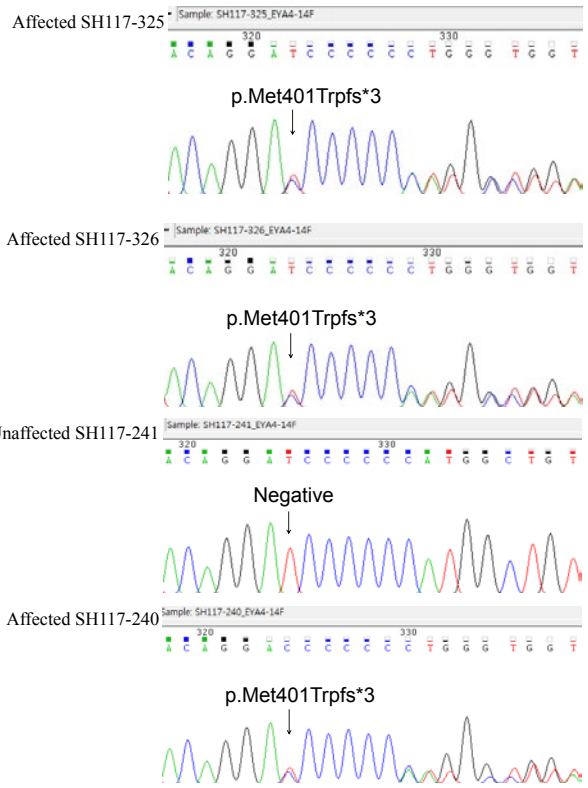

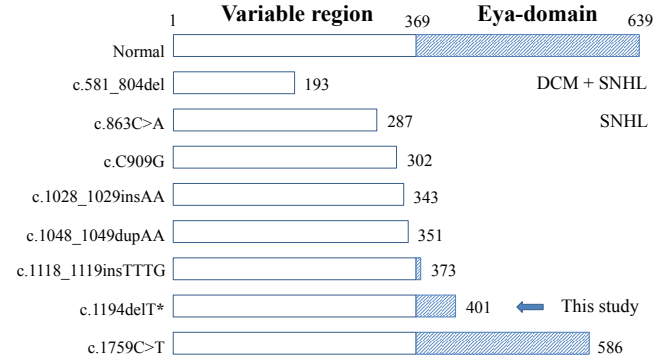

Method

Since out previous report, we have recruited 14 families segregating autosomal dominant moderate SNHL. A thorough medical history and physical examination including evaluation of heart problems ruled out any syndromic features in these families. Screening of *EYA4* was performed by targeted exome sequencing (TES) of 134 known deafness genes (TES-134) from the probands.

Result

After basic filtering of the variants, we identified one proband who carried a novel truncation mutation, c.1194delT (p.Met401TrpfsX3) of *EYA4*, making the frequency of DFNA10 to be 7.14% (1/14) in Koreans. The variant co-segregated perfectly with a slightly down-sloping, moderate degree of SNHL in the family (SH117), and was not detected in any of the 276 normal control chromosomes. This variant most likely generated protein products that were truncated just downstream of the eya-VR domain. None of the three

affected family members showed any syndromic features, including cardiac problems, which was compatible with a previous genotype-phenotype correlation.

Conclusion

The identification of a novel *EYA4* truncation mutation associated with DFNA10, rather than syndromic hearing loss, supports a previously reported genotype-phenotype correlation in this gene. Considering the relative high detection rate, *EYA4* mutations should be suspected in hereditary moderate hearing loss with a corresponding audiologic configuration, and a cardiac examination should be included in the initial evaluation.

PS-872

Functional Analysis of Mutant DIAPH1 Formin Proteins Associated with Hearing Loss

Bong Jik Kim[1]; Jessica Winkels[2]; Ah Reum Kim[3]; **David Kohrman[2]**; Byung Yoon Choi[4]

[1]Dankook University Hospital; [2]University of Michigan Medical School; [3]Seoul National University Hospital; [4]Seoul National University Bundang Hospital

Background

Formin proteins, through regulatory effects on cytoskeletal remodeling, impact a range of cellular processes, including cell division, organelle trafficking, and the formation of specialized cytoskeletal structures (Chesarone et al., Nat. Rev. Mol Cell Biol. 11:62-74, 2010). The *DIAPH1* gene encodes a diaphanous-type formin protein and it is the first gene reported to cause autosomal dominant nonsyndromic hearing loss (*DFNA1*; Lynch, et al., *Science* 278:1315–1318, 1997). Recent next generation sequencing strategies have identified a number of potential causative mutations in *DIAPH*-type formin genes that are associated with progressive, sensorineural hearing loss in humans (e.g., Baek, J.-I., et al., *Orphanet J. Rare Diseases* 7:60, 2012). Through similar studies, we have uncovered a novel heterozygous nonsense variant (c.C3145T) in *DIAPH1* in an individual with progressive hearing loss. This variant is expected to truncate the DIAPH1 protein within its central FH2 domain (p.R1049X), resulting in loss of the C-terminal Dia autoregulatory domain (DAD). To investigate the cellular and molecular effects of this variant and its potential relationship to cochlear dysfunction, we have begun to evaluate the effects of this and additional *DIAPH1* variants in cultured cells and in cochlear explant cultures.

Methods

We used *in vitro* mutagenesis of a wild type human *DIAPH1* cDNA clone to generate the c.C3145T variant. Plasmids expressing the wild type and/or the variant cDNA were transfected into cultured fibroblast (human 293T and mouse 3T3) and epithelial (pig LLC–PK1–CL4) cells, and DIAPH1 protein stability and localization were evaluated by Western and immunocytochemical approaches.

Results

Western analysis of protein lysates derived from transfected cells indicates that the p.R1049X variant protein has stability comparable to that of wild type DIAPH1. Cytoplasmic localization of wild type and p.R1049X DIAPH1 also appears similar in fibroblast and epithelial cells. Interestingly, the R1049X protein induces a neuron-like morphology in transfected 3T3 cells, a phenotype not observed following transfection with wild type DIAPH1.

Conclusions

The stability of p.R1049X DIAPH1 and the altered morphology associated with its expression in cultured cells is consistent with a causative role for this variant in hearing loss. In addition, these results suggest a neomorphic or hypermorphic gain of function mechanism of the truncated DIAPH1 protein. Further investigation of the impact of the mutant DIAPH1 on actin filament and microtubule architecture, as well as vesicle trafficking, should provide greater insight into the mutational mechanism of *DIAPH1* underlying human deafness.

PS-873

Identification of Promoter and Enhancer Regions for Known NSHL Genes in the Mouse Inner Ear

Paul Ranum; Seiji Shibata; Hide Moteki; Richard Smith

University of Iowa

Introduction/Background

Recent advances in genetic testing platforms make possible simultaneous screening of all coding exons of all genes implicated in non-syndromic sensorineural hearing loss (NSHL). Based on statistics compiled by HGMD and extrapolating their data to OtoSCOPE®, our diagnostic platform, we estimate the prevalence of causative variants in regulatory elements of NSHL genes to be ~14%. We seek to define promoter and enhancer regions in developing mouse cochlea and isolated populations of hair cells. We aim to identify temporal gene expression patterns using ChIP-seq and RNA-seq. These data will be queried against a NSHL population enriched for likely non-coding deafness-causing genetic variants.

Methods

Antibodies against H3K4Me3 and H3K4Me1 marks will be used to identify active promoters using ChIP-Seq on p1 and p14 wild type Balb/c mouse cochlea and pure hair cell populations; RNA-seq will be carried out on the same tissues and time points. Toward the identification of noncoding causative variants in hearing loss patients we will utilize targeted genomic enrichment and massively parallel sequencing (TGE+MPS). Using a TGE+MPS platform, OtoSCOPE®, we have sequenced all known NSHL genes in patients with autosomal recessive NSHL and enrolled into the study individuals segregating only one causative variant in an autosomal recessive NSHL-causing gene.

Results

To date, we have identified H3K4Me3 marked histones at promoter regions in p1 and p14 in whole cochlear tissue from mice using ChIP-Seq and have completed RNA-seq to map RNA expression levels in whole mouse cochlear tissue at these developmental time points.

Conclusions

This study has identified promoter regions and gene expression levels at pre (P1) and post (P14) hearing developmental

stages in the mouse cochlea. We are expanding these data using additional histone marks and manually isolated pure populations of inner and outer hair cells at the same two time points. In aggregate, these experiments will define noncoding genetic elements and allow us to investigate the prevalence of genetic variants in these regions in a carefully selected patient cohort segregating NSHL.

PS-874

Hearing Loss Diagnostics in the Era of Genomic Medicine: Perspective from Iowa

Hela Azaiez; Amanda Bierer; Ann Black-Ziegelbein; Kevin Booth; Terry Braun; Thomas Casavant; Sean Ephraim; Kathy Frees; Jori Hendon; Diana Kolbe; Yingyue Li; Carla Nishimura; Paul Ranum; Todd Scheetz; Eliot Shearer; Allen Simpson; Christina Sloan; Kyle Taylor; Donghong Wang; Amy Weaver; Richard J.H. Smith
University of Iowa

Hearing Loss (HL) is the most frequent sensory deficit in humans. It affects 1 in 500 newborns and 50% of octogenarians and in aggregate affects 360 million people worldwide. The genetic heterogeneity of HL made comprehensive genetic screening using Targeted Genomic Enrichment and massively Parallel Sequencing a mandatory approach for molecular diagnosis. Therefore, our laboratory has developed OtoSCOPE ®; a next-generation sequencing platform that simultaneously screens 90 genes known to cause non-syndromic HL (NSHL) as well as some syndromic forms. Data analysis is performed using a customized local installation of Galaxy. OtoSCOPE ® combines single nucleotide variant detection, indel detection and CNV identification simultaneously. Results are discussed at a multidisciplinary meeting attended by clinical experts, research scientists, bioinformaticians and genetic counselors. OtoSCOPE® has been a fully operational clinical diagnostic test since January 2012. To date, our Clinical Diagnostic Services has received 1,400 requests for OtoSCOPE® testing.

Using OtoSCOPE® as a streamline genetic test for deafness enabled us to offer genetic diagnosis for ~ 30% of patients. The solve rate depended on the inheritance mode, ethnicity and type of HL. For patients with identified deafness-causing variants, we were able to provide important answers and information regarding recurrence risk for future children, prognosis and best method of treatment. Patients with no causative variants are invited to participate in ongoing novel gene identification projects using Customized Targeted Genome Panels and Whole Exome Sequencing. We have also shown that CNVs are a major contributor to hereditary HL, comprising nearly one in five of all diagnoses.

In order to aid researchers, clinician-scientists and patients alike, we have developed a set of tools to determine the clinical significance of genetic variations. We have created the Deafness Variation Database (DVD), an interface that provides an accurate annotation and evaluation of genetic variants for pathogenicity by integrating data from popular pathogenicity prediction algorithms and published allele frequencies. We have also designed AudioGene, a software system employing machine-learning techniques that utilizes phenotypic information derived from audiograms to predict the genetic cause of HL in persons segregating autosomal dominant NSHL. This tool is also valuable for the identification of audiometric outliers for each genetic locus.

As personalized genomic medicine is becoming more common, our designed tools are being increasingly useful as phenotypic and genotypic filters to assess pathogenicity of variants identified by massively parallel sequencing.

PS-875

A Novel Splicing Mutation in COL11A1 as a Cause of Dominant Progressive Nonsyndromic Hearing Loss

Shelley Smith[1]; Zohreh Talebizadeh[2]; Eudy James[1]; Judith Kenyon[1]; James Askew[1]; Hoover Denise[1]; Jeff Kittrell[1]
[1]University of Nebraska Medical Center; [2]Children's Mercy Hospital

Introduction

Heterozygous mutations in *COL11A1* cause dominantly-inherited Stickler Syndrome Type II and Marshall Syndrome which have been associated with craniofacial and skeletal anomalies and high frequency hearing loss. Missense, nonsense, and splice site mutations causing these syndromes have been reported in the helical domain of the protein, with a "hotspot" around exon 50 (Acke et al., 2014). We previously reported a large 4-generation family with dominant progressive nonsyndromic sensorineural hearing loss (DPHL) which showed genetic linkage to the region of the *COL11A1* gene located at 1p21. This DPHL locus received the preliminary designation of DFNA37. Sequence analysis of fibroblast-derived cDNA of the candidate genes, including *COL11A1,* using PCR and Sanger sequencing did not detect a mutation (Talebizadeh et al., 2000). Follow-up whole exome sequencing was performed to identify the causal mutation in this family.

Methods

The family was ascertained as part of a study of genetic causes of dominant progressive hearing loss. Audiograms, medical information, and blood samples for DNA extraction were obtained from participating family members. Serial audiograms were obtained when available. Several family members were examined by a clinical geneticist to rule out syndromic features, and a skin biopsy for fibroblast culture was obtained from one affected family member. Hearing loss was detected as early as 5 years of age, starting in the midfrequency range and progressing to include low and then high frequencies by middle age, resulting in a moderate hearing loss. DNA samples from 4 family members with hearing loss and one unaffected family member were used for whole exome sequencing on an Illumina Hi-Seq DNA Analyzer.

Results

Exome sequence analysis identified a single base substitution in *COL11A1* near the beginning of the helical region which appears to affect a splice acceptor site between exons 4 and 5. PCR-amplification and Sanger sequencing demon-

strated that the mutation segregated with the hearing loss in the rest of the family.

Conclusions

A novel splice site mutation in *COL11A1* can cause dominantly inherited nonsyndromic hearing loss. This was apparently missed in the original PCR-based screening of cDNA from fibroblasts and may result in an altered transcript with greater significance in the inner ear. The mutation identified in this study is located much more toward the proximal part of the helical domain than the previously reported mutations causing syndromic hearing loss, which may account for the audiologic and phenotypic differences.

PS-876

Stonedeaf: A novel Mutation in S1pr2 Causes Rapid and Progressive Hearing Loss Associated with Impairment of the Endocochlear Potential

Neil Ingham[1]; Francesca Carlisle[2]; Selina Pearson[2]; Morag Lewis[1]; Annalisa Buniello[1]; Jing Chen[1]; Rivka Isaacson[1]; Johanna Pass[2]; Karen Steel[1]

[1]King's College London; [2]Wellcome Trust Sanger Institute

Introduction

Mice carrying targeted mutations of single genes undergo a broad range of phenotyping tests, including auditory brainstem response (ABR) measurements, as part of the Wellcome Trust Sanger Institute Mouse Genetics Project. However, spontaneous mutations causing deafness also arise, and we can detect these when a deafness phenotype does not segregate with the targeted knockout allele. One such hearing-impaired mutant mouse line was established (stonedeaf, *stdf*) which showed autosomal recessive inheritance.

Methods

The stonedeaf mutation was mapped using linkage analysis of backcross mice and exome sequencing was used to identify the causative mutation. We measured ABRs and endocochlear potentials (EP), examined the organ of Corti by scanning electron microscopy and the lateral wall using confocal microscopy, and used immunohistochemistry to reveal distribution of S1pr2 protein in the inner ear.

Results

The stonedeaf mutation mapped to proximal chromosome 9. Analysis of exome sequence showed the mutation was a C>G point mutation producing a Thr289Arg substitution in a predicted transmembrane domain of Sphingosine-1-Phosphate Receptor-2 (*S1pr2*). This mutation produced a rapidly progressive hearing loss. *S1pr2*$^{stdf/stdf}$ mutants aged 2 weeks had comparable hearing sensitivity to littermate controls. At 4 weeks, some *S1pr2*$^{stdf/stdf}$ mutants had normal hearing, but most showed mild to severe hearing impairment, which had become severe or profound in all mutant mice by 14 weeks. Gross anatomy of the middle and inner ears was normal in *S1pr2*$^{stdf/stdf}$ mutants. Scanning electron microscopy indicated a progressive loss of cochlear hair cells from age 5-9 weeks. Measurements of EP at 2 weeks old were comparable in *S1pr2*$^{stdf/stdf}$ and littermate controls. However at 4 and 8 weeks old, EP was reduced in the mutants. . Immunohistochemistry showed S1pr2 was expressed in the stria vascularis and hair cells of wildtype and stonedeaf mutant mice, suggesting the missense mutation produced impaired function rather than a loss of S1pr2 protein. Phalloidin staining of the stria vascularis indicated morphological changes in the cell boundaries between strial marginal cells.

Summary

The origin of the deafness pathology in *S1pr2*$^{stdf/stdf}$ mice likely resides within the stria vascularis and the loss of hair cells is probably a secondary degenerative process. Three additional alleles of *S1pr2* have been described previously, but this is the first time that a reduced EP has been reported.

PS-877

Transcription Factors Expressed in the Cochlear Inner and Outer Hair Cells of Adult Mice

Yi Li[1]; Huizhan Liu[2]; Lidong Zhao[2]; Kirk Beisel[2]; Shusheng Gong[1]; David He[2]

[1]Beijing Tongren Hospital; [2]Creighton University

A transcription factor (TF) is a protein that binds to specific DNA sequences, thereby controlling the rate of transcription of genetic information from DNA to messenger RNA. TFs play important roles in virtually every cellular process. Previous studies have identified a number of TFs that are critical for hair cell development and functions. In the present study, we examined the expression profiles of TFs in inner hair cells (IHCs) and outer hair cells (OHCs) using the hair cell transcriptome datasets from adult mouse cochleae. 806 and 842 known TFs are expressed in IHCs and OHCs, respectively. 791 are expressed in both populations. We examined the uniquely and differentially expressed TFs in IHCs and OHCs. The top 10 differentially expressed TFs include *Bcl6, Tbx2, Jun, Id1, Etv5, Egr1, Nfib, Klf5, Hivep2, Nr1d1* in IHCs, and *Ikzf2, Six2, Zfp687, Zfp319, Lm07, Atf1, Zfp618, Sox8, Arid3b, Cebpg* in OHCs. The top uniquely expressed TFs include *Maf, Zfp932, Ptfl1, Hoxa4, Npas1, Foxe3, Bcl11a, Tfcp2l1 Zbtb16, Pou3f1* in IHCs and *Tfec, Stat1, Ttf1, Ascl3, Tcf15, Nr4a2, Hmgb2, Casz1, Arid5b, Pparg* in OHCs. We also compared TFs between hair cells and supporting cells (pillar and Deiters' cells). Our analysis holds important information about the molecular mechanisms underlying hair cell morphology, function, pathology, and cell-cycle control.

PS-878

Auditory Characteristics in Mouse Model of the Sclerosteosis

Jong Sei Kim; Il Joon Moon; Ki Ryung Kim; Dong-Kyu Jin; Sung Hwa Hong

Samsung Medical Center, Sungkyunkwan University School of Medicine

Objectives

Sclerosteosis, caused by a mutation of the sclerosteosis gene (SOST, 17q12-21), is a very rare autosomal-recessive disorder characterized by progressive bone overgrowth. Although otolaryngologic manifestations in sclerosteosis patients in-

clude progressive hearing loss, the auditory characteristics of sclerosteosis have not been well known. Thus, we aimed to evaluate the auditory characteristics of the sclerosteosis using SOST knock-out (KO) mice.

Methods
The SOST-KO mouse model was developed by Dr. Jin DK. Auditory brainstem response, micro-computed tomography (CT) scans of the temporal bone, and histologic analysis of the cochlea were performed in 19 SOST knock-out and SOST wild type (WT) mice (B6/129) from 5 to 25 weeks of age.

Results
The SOST-KO mice showed clear discernable phenotype compared with the SOST-WT mice, including short stature, curved spine, and syndactyly. The hearing thresholds for the SOST-KO mice were significantly elevated compared to the SOST-WT mice after 9 weeks of age. Both skull bone thickness and temporal bone volume were significantly increased in the SOST-KO mice at 25 weeks of age. Histologic findings indicated that inner ear structures, such as organ of Corti, spiral ganglions, and stria vascularis, were intact in the SOST-KO mice. However, proliferation of osteoblast in periosteal layer and subsequent new bone formation was observed around the stapes footplate in the SOST-KO mice. Furthermore, cellular proliferations in the malleoincudal joint were also found in the SOST-KO mice.

Conclusions
The SOST-KO mouse can be a useful model in understanding auditory features of sclerosteosis. Ossicular fixation caused by increased osteoblastic activities may be responsible for conductive hearing loss in sclerosteosis.

PS-879

Hearing Loss and Ossicle Anomaly in a Mouse Model for Osteogenesis Imperfecta Type IV

Donald Swiderski[1]; David K. Barton[1]; Terese Jenks[1]; Joan Marini[2]; Kenneth M. Kozloff[1]; Michelle Caird[1]; Yehoash Raphael[1]
[1]University of Michigan; [2]NIH

Introduction
Osteogenesis imperfecta (OI, brittle bone disease) is one of several bone development disorders with a potential to impair hearing. OI is genetically heterogeneous, arising from diverse mutations affecting collagen synthesis. The Brtl/+ mouse is heterozygous for a single codon substitution of cysteine for glycine [Gly349Cys] in the *col1a1* gene, replicating the genetic defect in an OI type IV patient. This substitution results in a heterogeneous mixture of mutant and normal type I collagen in the extracellular matrix, leading to a skeletal phenotype of weakened, brittle bones and a reduced body size, characteristics of OI type IV. The purpose of this study was to investigate the association of hearing loss with OI in the Brtl/+ mouse.

Methods
Six week old Brtl/+ and wild-type mice were tested for ABR thresholds at 4kHz and 24kHz, sacrificed immediately afterward, decapitated and scanned by nano-computed tomography. 3D reconstructed volumes were generated to assess morphological anomalies in middle ear ossicles. Gross dissection of ossicles provided corroboration of features seen in scans.

Results
Wild-type mice exhibited only a partial high frequency hearing loss in one ear (+50dB at 24kHz). Most Brtl/+ mice had moderate low frequency hearing loss (+25-45dB at 4kHz) in at least one ear and a less severe high frequency loss (+15-30dB). Ossicles of Brtl/+ mice were thinner and more fragile in general, especially the stapedial crura and the pedicle supporting the lenticular process on the long arm of the incus – structures most often disrupted in human OI patients. Gross signs of displaced fractures were absent. Fixation of the stapedial footplate was observed in some affected ears. Changes in ossicle shape were most evident in the stapes, with unusual curvatures of the crura and relatively flat footplate.

Conclusion
The middle ear ossicles of Brtl/+ mice show structural anomalies similar to those seen in limb and vertebral elements. These features are consistent with an elevated risk of fracture in the most delicate components of the ossicular chain, which also are the features most often disrupted in human OI patients. Some Brtl/+ mice also exhibit fixation of the stapedial footplate, a feature that is invariably associated with conductive hearing loss in human OI patients. These results demonstrate that Brtl/+ mice are a valid model for investigating mechanisms and potential therapies for hearing loss in OI and related skeletal syndromes.

PS-880

Loss of MAP3K1 Kinase Domain Results in Early-Onset Hearing Loss and Supernumerary Outer Hair Cells in Mice Inner Ear

Rizwan Yousaf[1]; Qinghang Meng[2]; Robert B. Hufnagel[3]; Ying Xia[2]; Zubair M. Ahmed[4]; Saima Riazuddin[4]
[1]University of Maryland, Baltimore; [2]Department of Environmental Health, University of Cincinnati; [3]Division of Human Genetics, Cincinnati Children's Hospital Medical Center; [4]Department of Otorhinolaryngology Head & Neck Surgery, School of Medicine, University of Maryland, Baltimore

Background
MAP3K1 belongs to the serine/threonine kinase class that participates in the regulation of the MAPK signaling cascade. MAP3K1 is activated in response to a number of different stimuli such as growth factors, microtubule disruption, cell shape disturbance, pro-inflammatory cytokines and other physiological stresses. Once activated, MAP3K1 exerts its effect through the JNK, ERK1/2 and p38 MAPK pathways. MAP3K1 protein has two functional domians, one regulatory and the other is a kinase domain, which is important for the transduction of signal along the pathway. In humans, disruption of *MAP3K1* causes 46, XY gonadal dysgenesis and is associated with cancer as well. However, in the case of *Map3k1* mutant mice until recently, the only reported pheno-

type is open eyelids at birth. Here, we determined the role of MAP3K1 in the mouse inner ear development and function.

Methods
To understand the role and function of *Map3k1 in vivo*, mutant mouse model was generated in which the kinase domain of the protein was replaced with the bacterial LacZ gene (*Map-3k1^{tm1Yxia}*), resulting in the formation of a MAP3K1-β-galactosidase fusion protein. The hearing function of the mice was assessed using ABR and DPOAE. The inner ear tissue from homozygous mutant as well as wild type control mice were also isolated to look at the morphology and cytoarchitecture of the organ of Corti (OC), by immunoflorescence using different markers as well as scanning electron microscope. Moreover, we used qRT PCR to assess the effect of MAP3K1 disruption on downstream targets.

Results
Analysis of homozygous *Map3k1^{tm1Yxia}* mutant mice revealed early-onset profound hearing loss accompanied by progressive degeneration of outer hair cells (OHC). In the mouse inner ear, MAP3K1 has punctate localization at the apical surface of the supporting cells in close proximity to basal bodies. Although the gross cytoarchitecture, neuronal wiring and synaptic junctions in the organ of Corti are preserved, *Map-3k1^{tm1Yxia}* mutant mice have supernumerary functional OHCs and Dieter's cells. Loss of MAP3K1 function resulted in the dysregulation of FGF-pathway genes

Conclusions
Taken together, these results indicate critical role of MAP3K1 in the development and function of the mouse inner ear and hearing.

SYM-125

Consequences of Chronic and Acute Sound Exposure on Behavior and Auditory Brainstem Responses

Amanda Lauer
Johns Hopkins University School of Medicine

Phenotyping approaches used to assess hearing deficits after noise exposure in animal models typically employ auditory brainstem response (ABR) thresholds, sometimes in combination with distortion product otoacoustic emissions. Experimenters may miss important discoveries if only traditional ABR and emissions paradigms are used. This is especially true if the phenotypes involve changes to complex auditory processing tasks that are not easily related to peripheral damage patterns. Following the seminal work of Kujawa and Liberman demonstrating ribbon synapse loss in the absence of ABR threshold shifts, many investigators have begun to quantify changes to wave 1 of the ABR in noise-exposed animals in addition to threshold shifts. This shift in data collection procedures will no doubt lead to important new insights, but there are many aspects of hearing deficits that may not be detected with these measurements. Recent experiments demonstrating how more sophisticated phenotyping measures can reveal novel effects of chronic and acute exposure to noise will be reviewed. We have investigated the phenotypic consequences of noise exposure using modified ABR procedures, acoustic startle response modification, and conditioned lick suppression techniques. Animals with increased susceptibility to noise can show extreme temporal processing abnormalities even when traditional ABR measures show no effect. Exposed animals also sometimes show abnormal behavioral response profiles that are not well predicted by traditional ABR measures. The techniques reviewed can also be adapted to test the effects of background noise on hearing in non-exposed animals. While behavioral techniques require a larger time commitment compared to rapid ABR measurements, experimenters can implement previously optimized procedures to increase efficiency. Use of these measures can help characterize central auditory processing in genetically engineered animals and animals exposed to oto-protective substances.

SYM-126

Homeostatic Changes in Auditory Nerve Synapses in the Cochlear Nucleus

Matthew Xu-Friedman[1]; Tenzin Ngodup[1]; Jack A. Goetz[1]; Brian McGuire[2]; Wei Sun[1]; Amanda Lauer[2]
[1]University at Buffalo, State University of New York; [2]Johns Hopkins University

Sound-driven activity leads to changes in high-order areas of the auditory pathway, such as inferior colliculus and cortex. However, lower-order areas have received less attention, although they could potentially have an out-sized impact on the information that is relayed to the rest of the auditory pathway. We examined this issue by studying effects of sound-driven activity on the first synapse in the central auditory pathway, the endbulb of Held, which is formed by auditory nerve fibers onto bushy cells in the anteroventral cochlear nucleus. These synapses normally show strong depression during extended activity. However, after rearing animals in loud noise for a week, the synapses become less depressing, and many even facilitate. This reflects a decrease in the probability of neurotransmitter release. Furthermore, the number of release sites increases, such that the initial synaptic current does not change. These changes appear to be homeostatic responses that maintain synaptic fidelity in the face of continuous high activity. Indeed synapses recover to near normal depression when animals are returned to quiet sound conditions. This mechanism could contribute to hyperexcitability when noise exposure ceases.

SYM-127

Stimulus-specific Response Adaptation in the Lateral and Medial Superior Olive

Michael Pecka; Annette Stange; Andrea Lingner; Helge Gleiss; Benedikt Grothe
Section of Neurobiology, Biocenter of the LMU Munich

In mammals, information about the location of azimuthal sound sources is computed by the lateral and medial superior olive (LSO and MSO, respectively) by binaural comparison. Specifically, to localize a high-frequency sound source, LSO neurons detect differences in the intensity level at the two ears (interaural level differences, ILDs) that are generated by

the head. MSO neurons, on the other hand, detect differences in the arrival time of a low-frequency sound at the two ears (interaural time differences, ITDs) that are generated by the interaural distances.

Until recently, it had canonically been assumed that the brain's representation of the location of sound sources is hard-wired and thus encodes for absolute positions in space. However, recent experimental findings from our and other groups strongly contradict this assumption. These findings instead suggest a relative representation of auditory space. Specifically, psychophysical tests revealed that the perceived location of a stationary sound source can shift substantially depending on the prior acoustic experience. Neurophysiological findings demonstrated that these perceptional shifts could be explained by neuronal adaptation mechanisms at early stages in the auditory pathway. In particular, we have recently demonstrated the existence of pronounced response adaptation in both LSO and MSO that depends on the composition of the presented stimulus. Two distinct functional mechanisms seem to be involved in this stimulus-specific adaptation: on the one hand, dedicated $GABA_B$-mediated inhibitory feedback circuits exist for both MSO and LSO that control the output gain in the respective nuclei. On the other hand, neurons in the auditory system exhibit a generic adaptation mechanism: the dynamic range of responses is continually shifted to match the intensity distribution of the concurrent stimulus. Such stimulus-statistic dependent shifts have been reported already of the level of the auditory nerve, hence for the monaural inputs upstream to the LSO and MSO. Notably, for large ILDs, auditory nerve fibers at the left and right ear will consequently be adapted to drastically different intensity levels. Yet, it is unknown to what extend binaural computation is affected by the dissimilar dynamic range adaptations of the two monaural inputs. We performed *in vivo* extracellular single-cell recordings in anesthetized Gerbils to investigate stimulus-specific processing in LSO and MSO. We find that $GABA_B$-mediated adaptation and adaptation of monaural inputs to stimulus-statistics have distinct consequences for binaural processing. Together, these effects give rise to a relative representation of space that is modulated by stimulus context.

SYM-128

Effects of Noise-Induced Hearing Loss on Temporal Coding in the Auditory Nerve and Ventral Cochlear Nucleus

Michael Heinz
Purdue University

Recent perceptual studies have suggested that poor speech intelligibility for listeners with sensorineural hearing loss may result from suprathreshold deficits in temporal coding. Specifically, psychoacoustic studies suggest that listeners with cochlear hearing loss have a deficit in their ability to use rapidly varying temporal fine-structure cues, but that slowly varying temporal-envelope cues remain normal or are even slightly enhanced. The translational implications of these perceptual results depend on their physiological bases; e.g., whether they result from a simple deficit in temporal-coding strength originating in auditory-nerve (AN) responses, or from a deficit that emerges centrally due to reduced convergence of peripheral fibers, altered peripheral coding across the tonotopic axis, and/or from an altered balance of excitation and inhibition. Our recent work has examined some of these questions by comparing temporal coding in spike-train responses recorded from anesthetized chinchillas with normal hearing and those with permanent noise-induced hearing loss. Hearing status was characterized with otoacoustic emissions, auditory-brainstem responses, compound action potentials, and single-unit responses from either AN fibers or ventral-cochlear-nucleus (VCN) neurons. Temporal coding was characterized both in terms of *quantity* (i.e., overall strength of fine-structure and envelope coding) and *quality* (e.g., tonotopic representation, or relative timing across CFs) based on responses to pure tones, modulated tones, broadband noise, and speech stimuli. Overall, our data suggest that noise exposure does not degrade the fundamental ability of AN fibers or VCN neurons to phase lock to temporal fine structure in quiet, but that quantitative peripheral deficits do emerge in background noise. Furthermore, physiological deficits in AN temporal coding appear to be most prominent: 1) for broadband sounds (rather than narrowband sounds), 2) in terms of the balance between envelope and fine structure (rather than fine structure alone), and 3) in terms of the quality of temporal coding (rather than quantity). Central effects also appear to play a role because significant differences were seen in the effect of noise exposure on modulation detection/discrimination thresholds in background noise across different VCN cell types. Overall, our data do not support a simple interpretation of these psychoacoustic deficits as resulting from a reduction in phase-locking strength at the level of AN or VCN. Rather, physiological deficits emerge primarily for complex sounds, which suggests the importance of considering the relative balance between envelope and fine-structure coding, temporal-coding quality in addition to quantity, and differences between quiet and noisy listening conditions. Supported by NIH grant R01DC009838.

SYM-129

Noise Exposure Induces Neuromodulatory Plasticity in the Auditory Midbrain

Laura Hurley[1]; Melissa Papesh[2]; Adam Smith[1]
[1]Indiana University; [2]National Center for Rehabilitative Auditory Research U.S. Department of Veterans Affairs

Neurochemical modulatory systems regulate central auditory circuitry according to important factors such as behavioral context. There is increasing evidence that hearing loss triggers plasticity in these regulatory systems and intrinsic auditory circuitry in parallel, creating the potential to disrupt context-dependent auditory modulation. The serotonergic system is a well-characterized neuromodulatory network that innervates many auditory regions including the inferior colliculus (IC), where serotonin increases during exposure to some types of stressors as well as during social interaction in CBA/J mice. Following exposure to tonal acoustic trauma, this system shows plasticity at multiple levels, including in the density of serotonergic fibers and the expression of serotonin

receptors. Monaural trauma causes a bilateral imbalance in serotonergic fibers over a period of several weeks, with relatively lower fiber densities in the colliculus contralateral to the traumatized ear. This bilateral imbalance occurs in all 3 major subdivisions of the IC. Trauma also affects the serotonergic pathway downstream of release, increasing the expression of serotonin receptors by auditory neurons intrinsic to the inferior colliculus relative to a sham trauma group. These increases are selective in that some receptor types, notably the 5-HT1B receptor, show larger increases than others. Together, these studies illustrate that acoustic trauma has pervasive effects on the infrastructure of a non-auditory neuromodulatory system within the auditory midbrain. The functional consequences of trauma-associated plasticity in fiber density and receptor expression are largely unexplored, but one possibility is that they alter the relationship between external context and neuromodulatory regulation of auditory processing.

SYM-130

Getting More for Less: Enhanced Central Gain with Cochlear Hearing Loss

Richard Salvi[1]; Guang-Di Chen[2]; Kelly Radziwon[1]; Chen Jiang[1]; Dalian Ding[1]; Senthilvelan Manohar[1]; Adam Sheppard[1]

[1]University at Buffalo; [2]Center for Hearing and Deafness

Exposure to intense noise or ototoxic drugs not only causes hearing loss, but also depresses the neural afferent output of the cochlea. While a reduced neural input to the auditory brain might be expected to cause **hypo**acusis (muted sounds), loudness paradoxically grows abnormally rapidly before reaching normal levels (recruitment) or becoming excessively loud (**hyper**acusis). The neural substrates for loudness recruitment and hyperacusis are poorly understood, but there is growing evidence that weakened neural signals leaving a damaged cochlea are amplified at multiple stages along the central auditory pathway so that by time they reach the inferior colliculus (IC) or higher levels of the auditory pathway, neural responses can equal or even exceed those measured prior to cochlear damage. In the case of noise-induced permanent threshold shift in chinchillas, local field potential (LFP) amplitudes in the IC were, at high intensities, nearly normal in the region of hearing loss but surprisingly, were greatly enhanced (increased gain) below the region of hearing loss. To identify when and where these changes were occurring, LFPs were recorded from the cochlea, cochlear nucleus (CN) and IC following a 2 h, 105 dB SPL, 2.8 kHz noise exposure. LFP amplitudes were depressed in the cochlea and CN 1 day post-exposure, but were enhanced in the IC. At 2 h post-exposure, LFPs from the IC were initially depressed, but were slightly larger than normal 8 h post-exposure, indicating that central gain changes occur rapidly. Carboplatin, a drug that induces inner hair cell (IHC) lesions in chinchillas also reduced the output of the cochlea. However, suprathreshold LFP amplitudes from the IC were normal; behavioral thresholds were also normal for IHC losses of up to 85%. Sodium salicylate, an ototoxic drug, also greatly reduced the neural output of the cochlea; however, LFP amplitudes in the CN were nearly normal at high intensities whereas LFP amplitudes in the IC were much larger than normal. These results suggest that the CN partially compensates for the reduced cochlear output and that further gain increases occur as neural transmission ascends to the IC. Importantly, the salicylate-induced enhancement of LFP amplitude was strongly correlated with behavioral measures of hyperacusis, suggesting that excessive central gain may be the neural correlate of hyperacusis. While enhanced central gain allows weak cochlear signals entering the brain to be “heard” too much amplification may lead to tinnitus and hyperacusis. Supported by ONR (N000141210731) and NIH (R01DC011808)

PS-130

Evidence Against Power Amplification of the Cochlear Traveling Wave

Marcel van der Heijden[1]; Corstiaen Versteegh[2]

[1]Erasmus MC, Rotterdam; [2]The Rockefeller University

Background

The inner ear of mammals mediates sound-induced traveling waves that peak at a frequency-dependent location. It is widely assumed that active processes inject extra power into this wave, thereby enhancing sensitivity, but the power delivered by this cochlear amplification is unknown.

Methods

We analyzed local wave propagation in the gerbil cochlea by recording basilar membrane motion at two adjacent locations using a laser vibrometer and comparing the amplitude and phase across the two locations.

Results

At low intensities, the waves slowed down abruptly when approaching their peak, causing an energy densification that quantitatively matched the amplitude peaking, similar to the growth of sea waves approaching the beach. At high intensities, the deceleration became more gradual and the peaking became smaller and disappeared. Thus we found no local power amplification of soft sounds, and strong local attenuation of intense sounds.

Conclusions

The most parsimonious interpretation of these findings is that cochlear sensitivity is not realized by amplifying acoustic energy, but by spatially focusing it, and that dynamic compression is realized by adjusting the amount of dissipation to sound intensity.

PD-131

The Outer Hair Cell, Phalangeal-Process and Deiters cell Y-shaped building block and the relation to cochlear amplification

Joris Soons[1]; Charles Steele[2]; Sunil Puria[2]

[1]University of Antwerp; [2]Stanford University

Background

The organ of Corti (OoC) cells are highly organized, with a 3D arrangement which is important for cochlear function. Deiters cells (DCs) are connected to basally tilted outer hair cells (OHCs) and apically oriented phalangeal processes (PhPs).

Together they form a lattice of 'Y-shaped' structures that is sandwiched between the basilar membrane (BM) and reticular laminar (RL). We hypothesize that the morphometry and material properties of this Y-shaped structure has a profound effect on cochlear amplification.

Methods

To test the hypothesis, an explicit mechanical finite element (FE) model of a mouse cochlea, based on its morphometry and material properties, is developed and solved in the frequency domain using COMSOL multi-physics. Linearized Navier-stokes equations for the fluids are coupled with shell elements for the membranes (BM; RL; round window) and beam elements for the OoC cytoarchitecture. As a first approximation, a single row of 600 overlapping Y-shaped elements was considered. OHC somatic motility was incorporated as an expansion force proportional to the pressure difference across the BM. The influence of PhP stiffness and inclination on BM and RL responses are reported for the passive and active cochlea.

Results

BM peak response in the nominal passive model (20kHz) was 36dB, re the stapes. The RL gain was slightly higher (37dB). Decreasing the PhP stiffness, reduces the RL gain (26dB in the limit where there are effectively no PhPs), while the BM response stays similar. Increasing the OHC stiffness makes the RL response similar to the BM, but not higher.

In the active nominal model, the BM and RL gains increase to 60dB and 65dB, respectively. The RL peak is shifted 30um more apical than the BM peak (qualitatively similar to Chen et al. 2011). In mouse the PhP span is 3 OHC. Decreasing the PhP length in our model reduces the BM gain, while longer PhPs cause little change in the gain. At lower frequencies, however, this transition occurs at larger length spanning (4 OHCs for 10 kHz). In addition, reducing PhP stiffness decreases BM response to the passive case, while the RL gain stays approximately the same but its sharpness decrease (at minus 10dB, from 0.3mm to 3mm).

Conclusions

The PhP connection is needed to explain the shift between RL and BM peak. The FE model approach indicates that the length span of Y-shaped OoC structure is place dependent with shorter spans necessary for higher frequencies.

PD-132

Mechanics of the Chicken Cochlea

John Oghalai[1]; Anping Xia[1]; Patrick Raphael[1]; Brian Applegate[2]; **John Oghalai**[1]
[1]Stanford University; [2]Texas A&M University

The bird cochlea is unique in that it has similarities to both the mammalian cochlea as well as the auditory papillae of other non-mammalian species. Like mammals, it has a vibratory basilar membrane and two types of hair cells; like frogs, turtles, and lizards, it has hair cells with electrical tuning and a non-differentiated supporting cells layer. To understand how these similarities and differences impact the physiology of the bird cochlea, we used volumetric optical coherence tomography vibrometry (VOCTV) to image the P5-8 chick cochlea *in vivo*. Using a ventral approach, we were able to visualize most of the length of the cochlea although the region underneath the stapedial artery was inaccessible. We then measured sound-induced vibrations non-invasively. Traveling waves propagated from base to apex. The basilar membrane was tuned tonotopically, with characteristic frequencies ranging from 650 Hz at the base to 350 Hz at the apex. The Q10dB was ~1.6 at both the base and the apex. Basilar membrane displacement varied linearly with the stimulus intensity. The fibrocartilaginous plate under the tall hair cells vibrated in synchrony with the basilar membrane, although with a reduced magnitude. Along any given cross-section, there was no evidence of frequency-dependent phase gradients within any of the vibratory tissues. Together, these findings indicate that the chicken cochlea has substantial differences from the mammalian cochlea. It is not mechanically tuned to cover the full frequency range covered by its auditory nerve fibers (roughly 0.15-3 kHz). The vibratory response of the chicken cochlea is not as sharply tuned as its auditory nerve responses (mean Q10dB 3.2, range 0.8-10.2). Lastly, it does not have sharply-tuned phase gradients within the vibratory epithelium. Therefore, in contrast to the mammalian cochlea where frequency tuning within the auditory nerve derives from the vibratory characteristics of the organ of Corti, these data are consistent with the long-postulated concept that frequency tuning in birds derives from the electrical characteristics of the hair cells.

PD-133

Energy Flow in a Passive and Active 3D Cochlear Model and Power Output of Outer Hair Cells

Yanli Wang; Sunil Puria; Charles Steele
Stanford University

Introduction

It has been suggested by Lighthill that energy flow should be an essential criterion for cochlear models. The energy, however, has primarily been discussed qualitatively in the previous literature. Ever since the discovery of the active mechanism of outer hair cells (OHCs), there have been substantial arguments on whether the active cochlea provides power gain. Many experiments have been conducted; however direct measurements of energy are difficult since velocity and pressure are required simultaneously. Estimating the pressure by measuring velocity using assumed impedance can be misleading. Dong and Olson (2011) used an innovative method to approximate the basilar membrane (BM) displacement using the estimated pressure gradient. In the present work, a formulation for energy calculation is developed. Moreover, to provide insight to experimental measurements, the accuracy of the approximation of BM displacement from pressure gradient is simulated.

Method

The formulation of energy calculation is based on conservation of energy. Power done on cross section of the cochlea are calculated by numerical integration of the product of pressure and velocity, which are obtained from a 3D cochlear model

using WKB method. For the active process, the feed-forward/feed-backward (FF/FB) mechanism is adopted, which incorporates the cytoarchitecture of the organ of Corti. The power gain from the OHCs, power on the cross sections along the cochlea, and the energy dissipated by fluid damping are calculated.

Results

For the passive cochlea, the power monotonically decreases from the base to the apex, corresponding to the energy loss from fluid damping. For the active cochlea, the result shows positive energy input basal to the best frequency location, which is consistent with the negative damping in the previous literature. The energy dissipated is comparable to the energy gain from the OHCs. The peak power provided per OHC at 10 and 60 dB SPL are estimated to be 3*10E-17 and 10E-15 Watts respectively. Secondly, our simulation of Dong and Olson's approximation of BM displacement shows that their method slightly underestimates the actual displacement, and it is not sensitive to experimental errors.

Conclusions

A comparison between the power gain per OHC and the independent estimation of the energy supply (VxI = 1 mV x 100 pA =10E-13 Watts) of OHC from the electrical system supports the validity of the proposed model. The formulation for the energy calculation developed in this work is applicable to any cochlear model, and it would provide insight into the validity of the model.

PD-134

Sound Evoked Movements of the Tectorial Membrane

Pierre Hakizimana; Anders Fridberger
Linköping University

The tectorial membrane (TM), an acellular gel-like structure overlying the auditory epithelium, is mainly composed of collagen as well as proteoglycans and negatively charged glycoproteins. Several genetic manipulations of the TM proteins have shown that this structure is critical for hearing, but little is known about its mechanical role in sound transduction. Many studies have suggested that the shearing motion of the TM deflects the stereocilia in the stimulatory direction. However, few direct measurements on the TM in situ are available due to the fact the TM is highly transparent, which makes it almost 'invisible' for interferometry and other laser-based techniques commonly used for investigating the dynamic behavior of the hearing organ during sound stimulation.

Thanks to an increased sensitivity of newer generations of confocal microscopes, we have now overcome the TM's 'invisibility' problem for time-resolved confocal imaging of the hearing organ in the temporal bone preparations from guinea pigs. Bright clusters of the positively charged dye RH795 formed in the upper surface of the TM when the dye was released by electrophoresis through a glass pipette in the scala media. These dye clusters were then used to investigate the dynamic behavior of the TM during sound stimulation by time-resolved confocal imaging. Preliminary results show that the motion amplitude of the TM above the hair cell region was 5 times higher than in the limbal region (258 vs 54 nm, $p<0.01$, $n= 8$ and 4 respectively). Furthermore, the frequency tuning for the TM in the hair cells region and the tip of the tallest OHC stereoclia were highly similar while the TM movement in the limbal region exhibited a poor tuning. Comparison of the motion trajectories for the TM in the hair cells region and the tips of the tallest OHCs stereocilia showed that the motion direction was similar. However the motion amplitude was significantly higher for the tip of the tallest OHC stereocilia ($p<0.01$). If the TM movement were initiated by the stereocilia, the lower movement amplitude at the upper surface of the TM could be a result of attenuation by the TM compliance.

The results give a preliminary insight into the dynamic behavior of the TM during sound transduction and show that it is now possible to investigate the mechanical role of this elusive key structure using laser-based techniques.

PD-135

Modeling Wave Propagation on Isolated Tectorial Membrane Segments

Julien Meaud[1]; Jaehyun Yi[1]; Ali Bouattour[2]
[1]Georgia Institute of Technology; [2]ENSTA ParisTech

In recent years, experiments with genetically modified mice have demonstrated that the tectorial membrane plays a critical role in mammalian cochlear mechanics. Observation of wave propagation on isolated tectorial membrane segments have been used to characterize the material properties of the TM of wild-type and genetically modified mice. In order to determine the material properties of the TM, these experiments were interpreted using a simple one-dimensional shearing wave theory. In this work we investigate the effect of the finite dimensions of the TM segments on wave propagation using analytical and finite element models. We demonstrate that, due to the finite length of the TM segments, reflection of the waves at the boundaries is significant. Furthermore, we show that the shearing wave theory is only appropriate for TM segments of very large width compared to the wavelength of the waves. We derive the equations for bending waves using Timoshenko and Euler-Bernoulli theories. For TM segments of small width compared to the wavelength, finite element models converge to the bending wave theories. At realistic width for basal and apical TM segments, the simulated results fall somewhere in between the bending and shearing theories. Our computational results demonstrate that the material properties of the TM cannot be found using one-dimensional wave theory; inverse modeling using finite element models is required. However, qualitative interpretation of these experiments and comparison between wild-type and mutant TM segments might be appropriate.

PD-136

Round Window Membrane: a Saddle Roof of the Inner Ear Immobilizing the Perilymph Movement

Hirobumi Watanabe; Anil Lalwani; Jeffrey Kysar
Columbia University

The round window membrane (RWM) is a boundary separating two phases: gas and liquid. The air-filled middle ear allows the smooth movement of tympanic membrane as well as the ossicle chains to conduct vibratory energy. In the inner ear, the two types of lymph maintain the ionic environment for the hair cells to transduce the vibratory energy into neuronal signals. The RWM bears the load from the inertia caused by the density difference of the air and water. Thus, the RWM is responsible for securing these two compartments and preventing leakage of liquid in the middle ear or gas in the inner ear. At the same time, the RWM releases the sound pressure wave from the oval window by oscillating in the opposite phase. These two functions demand the RWM to satisfy two opposite mechanical objectives: 1) strength to bear the load from perilymph inertia and 2) flexibility to release the sound pressure. It has been an accepted fact that the RWM is just a thin membrane made of soft tissues including collagen fibers that passively releases the sound pressure. However, the other aspect of the RWM has not been well studied in any perspectives. In this study, we analyzed the unique structure of the RWM that has the geometric form of a hyperbolic paraboloid (HP). The existence of dual curvatures: concave and convex, in the RWM has been known and dubbed as “Pringles Potato chips®.” The shape of the potato chips was designed to prevent breakage during transport. The HP has been extensively applied in architecture to maximize the structural stability of a thin shell or a membrane structure. Herein, we performed finite element modeling to demonstrate the advantage of the HP shape of the RWM compared to a flat one. As a measure of a structural reliability, the compliance of the RWM was defined and calculated as the displacement rate of the RWM with pressure change. The compliance of a HP was low across the physiological pressure range. But, the compliance of a flat surface showed a spike at the zero pressure due to a singularity. Because a flat membrane exerts only in-plane stress, there is no vertical component that allows the membrane to withstand pressure change. Thus, the RWM must be modeled as a HP to model a system for the physical study of inner-middle ear dynamics.

PD-137

A Comparative Study of Human Auditory Periphery Models

Amin Saremi[1]; Sarah Verhulst[2]; Mathias Dietz[2]; Rainer Beutelmann[3]; Jutta Kretzberg[4]
[1]Oldenburg University; [2]Medizinische Physik and Cluster of Excellence “Hearing4all”, Department of Medical Physics and Acoustics, University of Oldenburg; [3]Animal Physiology and Behavior and Cluster of Excellence “Hearing4all”, Department for Neuroscience, University of Oldenburg, Germany.; [4]Computational Neuroscience and Cluster of Excellence “Hearing4all”, Department for Neuroscience, University of Oldenburg , Germany.

Introduction

For over seven decades, auditory models have been developed and used to sharpen our understanding of the hearing system. Here six recently-published models, that can cover the mainstream approaches in modern auditory modelling, are selected to be studied: four filter bank models (Irino and Patterson, 2006; Lyon, 2001; Lopez-poveda and Meddis, 2001), one transmission-line model (Verhulst *et al.*, 2012) and one biophysical model (Saremi and Stenfelt, 2013). These chosen models are extensively used today in various applications ranging from biological studies to cochlear mechanics, otoacoustic emission generation and applications within digital industry. Nevertheless, it is often unknown how these models respond to stimuli they were not designed for, or how well they compare to other auditory models. This study compares the performances in response to a fixed set of stimuli in order to quantitatively explore their respective advantages and limitations.

Methods

The responses of the models to pure tones and to narrow-band noise stimuli with center frequencies of 0.5, 1, 2 and 4 kHz and at intensities ranging from 30 dB SPL to 85 dB SPL are simulated. The spectral responses and the shapes of the resultant filters are compared in terms of amplitude, compression and slopes. This procedure is repeated for clicks between 0 and 90 dB SPL, as well. Moreover, each model’s capability in predicting the outcome of the psychoacoustic experiments is evaluated by simulating the pulsation thresholds, that had been reported by Plack and Oxenham (2001).

Results

Although the filter models are to some extent based on similar modelling principles, they process the incoming stimuli differently due to their underlying differences in generating the cochlear nonlinearity, compression and tuning. For example, the preliminary results demonstrate that the double resonator nonlinear filter model (Lopez-poveda and Meddis, 2001) produces a transmission delay as well as high levels of distortion: two fundamental issues that can impose serious limitations to real-life applications of this particular model.

Summary

The auditory models are widely used in hearing machines, speech processors and hearing aid designs. We plan on sys-

tematically comparing all six models in this study to discuss the advantages as well as limitations of each approach. The outcome of this study is important for those modelers seeking the best model for their specific application.

PD-138

Temporal Integration in Sound Texture Perception

Richard McWalter[1]; Joshua McDermott[2]
[1]Technical University of Denmark; [2]Massachusetts Institute of Technology

Background

Many aspects of auditory perception require integrating sound information over time, but the underlying mechanisms remain poorly understood. The perception of sound textures – relatively stationary signals resulting from large numbers of acoustic events, as in rain, fire, or swarms of insects – present a potentially simple but largely unstudied example of integration. Prior research suggests that textures are represented with statistics that capture their average acoustic properties, raising the question of the window over which the averaging occurs. We probed the averaging process underlying texture perception using "texture gradients" – signals synthesized such that their statistical properties changed gradually over time. We hoped to measure how far back in time the stimulus history would exert biasing effects on texture judgments.

Method

The statistical synthesis method of McDermott and Simoncelli (2011) was extended to allow the synthesis of texture gradients that gradually morphed from one set of statistics to another. On each trial, subjects heard a texture gradient followed by a probe texture with constant statistical properties that varied across trials. Subjects were instructed to compare the end of the gradient stimulus to the probe, and to determine which was closer to a standard reference texture. We compared performance for gradients that started or ended at different points in the space of statistics, and for gradients that concluded with a constant segment of different durations. Because subjects were instructed to base their judgments on the end of the stimulus, we expected the gradient to bias judgments only if it fell within the averaging window. For each type of gradient we obtained a psychometric function (performance vs. the position of the probe statistics).

Results

Psychometric functions differed for gradients that ended at the same point in the space of statistics but that had different starting points, indicating that the stimulus history was included in subjects' estimates of the texture statistics. The biasing effects were also present for gradients that concluded with a one-second segment of constant statistics, but were not evident when the concluding constant segment was extended to 2.5 seconds.

Conclusion

The results suggest that texture perception is based on statistics that are averaged over windows greater than 1 second and less than 2.5 seconds in length. Future work will compare human performance to that of ideal observer models on the same task.

PD-139

Analysis of Auditory Signal Processing Via Synthesis of Environmental Sounds

Jan Brümmerstedt; **Richard McWalter**; Torsten Dau
Technical University of Denmark

Background

Temporal envelope fluctuations, or modulations, have a crucial role in auditory perception. The sensitivity and selectivity of the auditory system to the temporal envelope of acoustic signals has been characterized by the temporal modulation transfer function and functionally modeled by a modulation filter-bank. In addition, auditory models to evaluate speech reception and sound texture perception have been successfully developed by combining spectral processing of the peripheral auditory system with temporal processing (Jørgensen et. al 2013, McDermott et. al 2011). In this study, we present an auditory model to account for the perception of environmental sounds. Firstly, we used synthetic sound textures generated by measuring time-averaged statistics from an auditory model in order to investigate spectro-temporal processing in the auditory system. The model was then extended to account for dynamic and unique events common in environmental sounds using a multi-resolution approach in the modulation domain.

Method

Synthetic sounds generated from several models of the auditory periphery were used to evaluate the perception of environmental sounds. The models were comprised of frequency and modulation selective filtering and accompanying marginal moments and pair-wise correlation statistics (McDermott et. al 2011). In the first experiment, listeners were presented with synthetic sound textures generated from auditory models with various modulation-processing stages and asked to evaluate the similarity to a corresponding original sound texture. The second experiment used the multi-resolution framework to synthesize temporally complex environmental sounds. Listeners were, again, asked to evaluate the similarity of the synthetic sound to an original instance.

Results

Auditory models derived from psychophysical and physiological experiments were preferred in all conditions. The perception of sound textures relied on a set of time-averaged statistics measured from a biologically inspired auditory model. Environmental sounds generated with the multi-resolution framework showed a strong similarity to the original sounds. Interestingly, the multi-resolution modulation analysis allowed for a reduced set of statistical measures as compared to the sound texture synthesis system. We observed that short-time analysis in the modulation domain could account for the coding of temporally complex acoustic features.

Conclusion

Auditory perception of environmental sounds can be accounted for by using models of the auditory periphery that include modulation-selective filtering. Environmental sounds syn-

thesized with a multi-resolution framework were subjectively similar to the originals, suggesting the auditory system could use modulation selectivity as a tool in sound identification. Lastly, we demonstrated the effectiveness of sound synthesis in the investigation of fundamental auditory perception.

PD-140

Auditory Enhancement as a Gain Control Function

Ningyuan Wang[1]; Andrew Oxenham[2]
[1]University of Minnesota; [2]Department of Psychology

Introduction

The auditory enhancement effect (EE) refers to the observation that a single component within a complex tone tends to "pop out" as a separate perceptual object if it is preceded by the same complex tone with that target component removed (the precursor). Contextual effects such as EE may help "normalize" the incoming sound and produce perceptual constancy in diverse acoustic environments. However, the neural mechanisms underlying EE remain unclear. The present study investigated EE as an effective change in perceptual level, or loudness. Explanations based on various combinations of target enhancement and masker inhibition were tested in a series of psychophysical experiments in normal-hearing listeners.

Methods

In the first experiment, the 500-ms precursor, consisting of an inharmonic complex with 0.3-octave logarithmically spaced components extending from 250 to 8000 Hz, was followed by the 200-ms target or masker alone with a gap of 50 ms, the loudness of which was compared with the same stimulus presented 2 s later. In the second experiment, the spectral and temporal properties of the stimuli were exactly the same, but the masker and target were presented simultaneously, preceding the comparison signal by 2 s. In the third experiment, the precursor and masker were replaced with narrow-band noise, so that the target tone could be heard out more easily to facilitate direct comparisons.

Results

The results from the first experiment suggested that the precursor did not significantly affect the loudness of either the target or the masker alone. The results from the second experiment showed that the loudness of the target in the presence of the masker was enhanced by the precursor, whereas the loudness of the masker remained unaffected. A "release from inhibition" was observed in the third experiment with increasing precursor duration and/or decreasing gap duration between the precursor and target.

Conclusions

The results from all experiments are consistent with the idea that the target component is usually inhibited by surrounding masker components, but that this inhibition is "released", perhaps through adaptation, in the presence of a precursor. The outcomes therefore support the "adaptation of inhibition" explanation first proposed by Viemeister and Bacon [J. Acoust. Soc. Am. 71:1502-7 (1982)].

PD-141

Different Adaptation Mechanisms for Binaural Localization Cues

Marko Takanen[1]; Nelli Salminen[2]; Bernhard Seeber[3]
[1]Technische Universität München; [2]Aalto University, Department of Biomedical Engineering and Computational Science; [3]Technische Universität München, Audio Information Processing Group

Human sound localization relies on the binaural cues between the ear canal signals. For horizontal sound localization, the most important cues are interaural time and level differences (ITDs and ILDs, respectively). Exposure to adaptor stimulus carrying specific localization information is known to bias lateralization of the target stimulus: potentially because the adaptor suppresses the activation of the ITD/ILD channel tuned to that side. Here, a psychoacoustical experiment was conducted to test whether the ITD channel is less prone to adaptation, reflecting the emphasized role of low-frequency ITD in localization.

First, white noise signals and measured head-related transfer functions (HRTFs) of a human subject were used to generate HRTF, ITD and ILD target stimuli that had the frequency-dependent ITD and/or ILD cues. Specifically, the ITD and ILD targets were designed to share the phase and magnitude responses of the HRTF corresponding to horizontal angles in the range from -15° to 15° with a 5° resolution. Subsequently, left-right discrimination of such stimuli was investigated to acquire psychometric functions for laterality before and after exposure to an adaptor sequence. Two adaptation paradigms were employed following Phillips and Hall (Hear. Res., 202, 2005): One asymmetric having an ILD adaptor on one side and an ITD adaptor on the other, and the other symmetric having an ITD adaptor on both sides of the midline. In both paradigms, the adaptors (pink noise bursts) were presented in an alternating sequence having directional cues corresponding to ±60°.

The preliminary results (eight normal-hearing volunteers) show that the asymmetric adaptor shifts the psychometric functions of all target stimuli towards the ILD adaptor. Hence, it seems that the ILD adaptor on the left suppresses the activation of the ILD channel of the right hemisphere substantially more than the ITD adaptor on the right affects the ITD channel of the other hemisphere. As a consequence, sound events are lateralized more to the right when the spatial location is determined by analyzing the relative activation rates of populations at the two hemispheres. On one hand, symmetric adaptation reduces the slope of the psychometric function but only in the case of the ITD target. This implies that the ITD channel is not immune to adaptation either. Consequently, the results bolster the idea that the adaptation mechanisms for the binaural cues are indeed different. In other words, ITD provides a more robust cue for localization, which correlates well with the existing psychoacoustical literature.

PD-142

Auditory Distance Perception with Congruent and Incongruent Cues

Jana Eštočinová[1]; Jyrki Ahveninen[2]; Samantha Huang[2]; Stephanie Rossi[2]; Norbert Kopčo[1]
[1]P. J. Šafárik University; [2]Harvard Medical School/ Massachusetts General Hospital

Introduction

The estimates of auditory distance are typically dominated by the overall received stimulus intensity. However, distance processing can also be guided by intensity-independent cues. Specifically, the *interaural level differences* (ILDs) provide distance information for lateral stimuli and, in reverberant space, the *direct-to-reverberant energy ratio* (DRR) cue provides distance information for sources from all directions. In the absence of the intensity cue, listeners use these cues to estimate nearby-source distance [Kopčo et al. (2012) PNAS, 109, 11019-11024]. In the current study, we examined how the ILD and DRR cues are combined and weighted to create an auditory distance percept, and how previous experience influences this weighting.

Methods

We performed a series of behavioral experiments in a virtual reverberant environment in which we simulated sound sources presented at a varying distance (15-100 cm) from directly in front or to the side of the listener. To explore the listeners' weighting of the cues, we manipulated the availability and congruency of the cues. Specifically, we compared performance with the ILD or DRR eliminated, presented congruently, or presented incongruently. Stimuli were either binaural, monaural, or diotic. We also examined the effect of the preceding listening experience on cue weighting.

Results

Incongruent DRR-ILD stimulation caused a weaker distance percept (inaccurate estimates of source distance) compared to the congruent presentation. Individual cue weighting critically depended on previous experience. Very low weight was put on DRR after the subject was exposed to stimuli with congruent ILD and intensity cues. On the contrary, after stimulation with DRR-based DRR, DRR weighting increased dramatically. Finally, diotic DRR-based performance was found to be better than monaural DRR-based performance even though the directional percept was more consistent with a realistic listening situation in the latter condition.

Conclusions

The weighting of ILD and DRR cues in judging distance of nearby sources is strongly adaptive, depending the previous room exposure. This result is consistent with the hypothesis that the brain dynamically updates its model of the acoustic environment, preferring the most reliable cue combination in each room. Future studies will need to examine the properties of this process and the underlying neural mechanisms.

PD-143

Auditory Memory for Time-Domain Information

HiJee Kang[1]; Trevor Agus[2]; Daniel Pressnitzer[3]
[1]Ecole Normale Supérieure; [2]Sonic Arts Research Centre (SARC), School of Creative Arts, Queen's University Belfast, Northern Ireland, UK; [3]Laboratoire des Systèmes Perceptifs (CNRS UMR 8248), École normale supérieure, France

Perception requires recognizing and identifying patterns, for instance to associate a voice or a face with an acquaintance. For the auditory modality, a series of studies have hinted at rapid and robust learning process: listeners can display perceptual learning for Gaussian noises samples, just after a few repeats of those samples (e.g. Agus et al., 2010). In all of the available data, however, it is unclear what listeners were able to learn from the noise. In particular, listeners could have used frequency patterns or time patterns, as both are available in noise. Here, we focused on auditory learning of purely time-domain information.

Stimuli were sequences of energy bursts (click trains) with stochastically distributed time intervals between clicks. Three types of click trains were included in an experimental block. Random click trains (C) consisted of a sequence of clicks with random time intervals between clicks (uniform distribution), for a nominal duration of 1s. Repeated click trains (RC) consisted of a random click train of 0.5s, immediately repeated for the next 0.5s. Reference click trains were generated exactly as RCs, but the exact same sequence of time intervals re-occurred on several trials within a block. High-pass filtering and low-pass masking noises were added to remove any frequency-domain cues. Five conditions were run, with different maximum gaps between clicks, from 25 ms to 400 ms. Results showed that listeners were able to distinguish RC from C, with performance improving for the sparser sequences (longer maximum gaps). Moreover, just as for the noise experiments (Agus et al., 2010), performance was better for RefRC than RC. This suggests there was learning of the specific temporal patterns within a given RefRC.

The click trains are especially well suited for neuro-imaging, for instance with EEG, as each burst of energy triggers a synchronized cascade of neural events and hence large population responses. Moreover, click trains bear a reasonably close relationship to spike trains within single neurons, at several levels of the auditory hierarchy, so the paradigm could be used to probe computational models of neural plasticity.

References

Agus, T. R., Thorpe, S. J., & Pressnitzer, D. (2010). Rapid formation of robust auditory memories: Insights from noise. Neuron, 66, 610-618.

PD-144

Differential Effects of Attention and Stimulus Strength for the Auditory Streaming Paradigm

James Rankin; John Rinzel
New York University

The auditory streaming paradigm (van Noorden 1975), in which alternating high- A and low-frequency tones B appear in a repeating ABA- pattern, has been shown to be perceptually bistable for extended presentations (order of minutes). Pressnitzer and Hupe (2006) showed that auditory and visual bistability share common traits of exclusivity, randomness and inevitability using such ABA- sequences and visual motion plaids. In each modality there are alternations between a grouped percept (a single galloping ABA-ABA- stream; coherent pattern motion) and a split percept (segregated streams A-A-A-A- and -B---B--; drifting transpent motion). They further investigated the effect of volitional control at equidominance (where the durations for each percept are equal) and found that attending to one percept (grouped or split) reduced the mean dominance durations of the unattended (weaker) percept. Moreno-Bote et al. (2010) investigated three bistable visual stimuli and generalized Levelt's proposition II (Levelt 1968) that describes the effect of stimulus strength manipulations around equidominance: ``the mean dominance duration of the stronger percept changes more than that of the weaker percept''. These findings are incompatible with Pressnitzer and Hupe (2006) if one assumes, as in (Chong et al 2005), that attention increases the strength of the targeted percept.

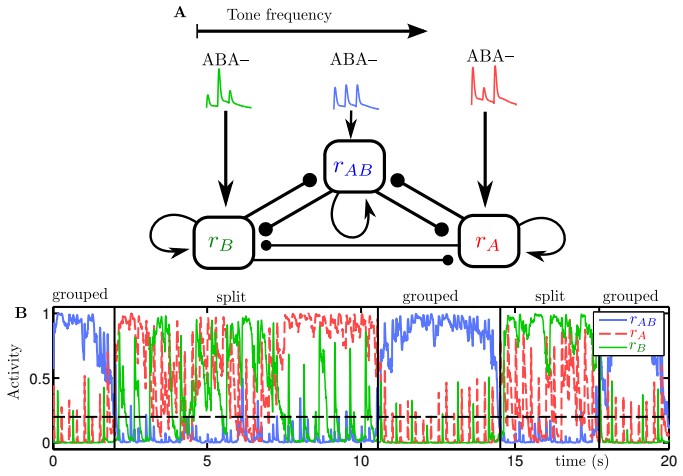

FIG. 1. **A:** Tonotopically organized populations r_A, r_{AB} and r_B have best frequencies A,$(A+B)/2$ and B, respectively. Input profiles mimic A1 responses from Fishman et al (2001) and Micheyl et al (2005); our network is assumed to be in a higher perceptual competition area that takes input from A1. Each populations has intrinsic adaptation (not shown), self inhibition (not shown) and recurrent NMDA excitation; there is mutual inhibition between the units. **B:** Activity time course where central population encodes the grouped percept and the peripheral populations encode the split percept.

We present a three population tonotopically organized model that is motivated from physiological studies of cortical responses to streaming stimuli; see FIG. 1A. FIG. 1B shows a model time course where the central population encodes the grouped percept and the peripheral populations encode the split percept. Mutual inhibition, adaptation and noise are incorporated, which are important mechanisms to account for the dynamics of perceptual bistability (Shpiro 2007). The inclusion of slow NDMA recurrent excitation was necessary to deal with the periodic nature of the streaming inputs. The model has been developed alongside concurrent psychoacoustics experiments. The statistics of the switching durations from our experiments and the known perceptual organization from van Noorden (1975) are used to constrain the model's parameters. The validated model provides a platform to show that a proposed state-dependent, top-down attention mechanism can resolve the apparent conflict between input strength and attention in auditory streaming.

PD-145

Integrated Sensory Predictions of Both What and When in Beta Band Oscillation: Unexpected Pitch in Rhythmic Entrainment

Andrew Chang[1]; Daniel Bosnyak[2]; Laurel Trainor[2]
[1]McMaster University; [2]Department of Psychology, Neuroscience & Behaviour, McMaster University

The neural basis of predicting *what* (predictive coding) will occur next and *when* (predictive timing) it will occur have typically been investigated separately. Beta band (15-25 Hz) oscillations in auditory cortex reflect predictive timing in that fluctuations in the power of beta band activity (BBA) predict the expected onset timing of the next beat during rhythmic entrainment. However, BBA also reflects predictive coding in that the power and phase of BBA increases following a mismatch between a perceived event and its expected content. Therefore, we hypothesized that BBA might reflect an integrated sensory prediction system crossing both what and when domains. In a series of experiments, we recorded EEG while subjects passively listened to an auditory oddball sequence with a fixed inter-onset interval (IOI) of 500 ms, in which 80% or 90% of the tones were a standard pitch (262 Hz) and 20% or 10% were a deviant pitch (494 Hz). We performed wavelet time-frequency decomposition to the source waveforms from right primary auditory cortex. In Experiment 1, the deviant tones were randomly dispersed in the sequence (and therefore not predictable). In addition to replicating the BBA power fluctuation predicting onset timing, the unexpected deviant tones induced a low-beta band (15-20 Hz) power increase after the deviant tones that was not present after the standards. This BBA increase was larger when the occurrence rate of deviant tone was lower (10% vs. 20%). In Experiment 2, we compared a predictable version (every fifth tone was a deviant) to an unpredictable version. We found that the power increase in BBA after the deviant tones was larger when the deviant tones were unpredictable than predictable. In contrast, the phase consistency of BBA was increased more following deviant than standard tones, but it was not modulated by predictability of the deviants. In Experiment 3, we presented the sequence of Experiment 1 at two additional tempos (390 and 610 ms IOI). The prelimi-

nary results of experiment 3 replicate previous work showing that the prediction of *when* the next tone is expected follows the tempo (IOI). However, a BBA increase following deviant tones remained for all tempos. Our results to date suggest that BBA power reflects top-down sensory prediction of upcoming auditory events, while BBA phase reflects bottom-up responses to rare events. In general, we have shown that beta band oscillation activity in auditory cortex is co-modulated by sensory prediction of both *what* and *when*.

SYM-131

Estrogens as Modulators of Audition: Rapid Brain Estrogen Signaling Guides Auditory Physiology and Behavior in Songbirds

Luke Remage-Healey
University of Massachusetts

Neuroendocrinologists have come to appreciate that the brain can synthesize its own supply of steroid hormones such as estrogens, much in the way of classical neuromodulators. In a variety of vertebrate species, 'neuroestrogen' synthesis enzymes are particularly concentrated in auditory regions, including within human temporal cortex. There is now growing interest in the influence of estrogens on audition, ranging from peripheral auditory encoding to central auditory-motor integration. We have developed methods to measure and manipulate neuroestrogen signaling within the auditory forebrain circuits of songbirds. Our initial findings indicate that social interactions between adult males and females can drive acute fluctuations in neuroestrogens within the auditory cortex. A combination of unit recordings in awake and anesthetized birds as well as whole-cell patch clamp recordings in vitro have provided greater insight into the mechanism and functional significance of neuroestrogen modulation of audition. This work suggests that social stimuli can influence the firing properties of auditory cortical neurons in part via local fluctuations in neuroestrogens. We have also begun to explore the influence of song tutoring on neuroestrogen signaling in the auditory cortex of juvenile songbirds. This work takes advantage of the compelling developmental and neuroanatomical parallels for vocal learning between songbirds and humans. During the sensory critical period for song acquisition in juvenile songbirds, we have observed that neuroestrogens within the auditory cortex are elevated following brief tutoring events, consistent with a role for estrogens in enhancing the representation of recent social experiences. Lastly, transient inhibition of neuroestrogen signaling in the auditory cortex of awake behaving males impairs their ability to express social preferences for familiar songs. Together, these findings are consistent with the hypothesis that acute and local estrogen synthesis within the auditory cortex is driven by social interactions and is a key regulator of auditory physiology and behavior.

SYM-132

Cortical Plasticity for Salient Social Vocalizations

Robert Liu
Emory University

The functional role of the auditory cortex in processing sounds has been a question of long-standing interest for the auditory community. The idea that it is simply a bank of filters decomposing a complex acoustic environment is being refined. There is growing evidence that the auditory pathway from periphery to cortex transforms a sound's neural representation from being acoustically accurate to being more perceptually biased, with experience-dependent plasticity within auditory cortex playing a key role in shaping this. Plasticity is presumed to allow the emergence of salient sound categories based on prior experience, so that downstream areas can more robustly facilitate an organism's behavioral response. While this plasticity mechanism and its putative function have been extensively explored in the context of laboratory training paradigms involving synthetic cues and/or operant responses, much less is known about the form such plasticity takes in more natural learning paradigms. This is especially true of sound learning in social contexts, which is the main way that the meaning and salience of species-specific vocalizations are naturally acquired (e.g. speech for humans, or ultrasounds for mice). Does auditory cortical plasticity manifest in the same way for natural vocal categories as they do for conditioned pure tones? Does plasticity improve the functional processing of vocalizations? Work from our lab and others have been investigating these questions in the context of a robust natural "learning" paradigm wherein maternal mice acquire the behavioral significance of ultrasonic vocalizations emitted by pups isolated from the nest, and respond by searching for and retrieving the lost pups. Using behavioral and electrophysiological methods, we have found that the form of plasticity observed when ultrasound pup calls become salient to a female is not what would be predicted from simple conditioning paradigms. In contrast to the usually reported expansion in the tonotopic map for a conditioned tone frequency, we see no plasticity in the spatial map of best excitatory frequencies in the ultrasound range, or for natural ultrasounds themselves. Instead, inhibitory plasticity in lateral frequency bands and excitatory plasticity in a specific, physiologically delineated subset of late-onset putative pyramidal neurons combine to enhance the detection, discrimination and downstream ability to categorize the pup ultrasonic category of calls. Our results suggest that plasticity mechanisms to bias the representation of salient signals manifest on a finer scale within core auditory cortex than might have been previously thought.

SYM-133

Sensory Attunement vs. Perceptual Salience: Explaining Hypersensitivity in Autism Spectrum Disorders

Gordon Ramsay
Marcus Autism Center, Children's Healthcare of Atlanta & Department of Pediatrics, Emory University School of Medicine

Autism is a devastating neurodevelopmental disorder of early onset defined by core deficits in social communication and restricted interests/repetitive behaviors. Individuals with autism often report hypersensitivity to sensory stimulation as a symptom of the disorder, yet paradoxically most studies of sensory acuity in autism have failed to find any systematic difference in basic mechanisms of sensation. Instead, research has shown that it is rather the deployment of those sensory mechanisms in actively seeking out relevant task-dependent information in the environment that seems to be derailed in autism soon after birth.

Typically developing infants naturally learn to attune their senses to pick up salient information in the world around them, and are exquisitely sensitive to those aspects of sensory input that signal social responses from caregivers. From the first hours of life, infants orient reflexively towards face- and voice-like stimuli in ways that seem to reflect the social function of the stimulus rather than its visual or auditory properties. Infants with autism do not display these patterns of selective attention to social agents, but seem to focus on physical properties instead.

How might the social deficit in autism explain claims of hypersensitivity? Any theory of perception and action inevitably hinges on a comparison between on-line predictions an organism makes about the world with corrections based on sensory feedback received from the environment. The relative weighting between internal prediction and external sensation depends implicitly on the information each is believed to contain about the task in hand. Without the ability to make context-appropriate predictions, an organism will be forced to over-weight the importance of sensory information instead. Thus, hypersensitivity in autism may well be a natural consequence of an inability to predict the social world, and the atypical biasing of sensory input that must result from this.

We demonstrate this principle using a mathematical model of perception derived from estimation theory, and illustrate the theoretical development with examples drawn from a longitudinal study of infants at risk of autism, from birth to three years of age. The results have implications for reconsidering imbalances in the central efferent modulation of peripheral afferent pathways as a potential mechanism of developmental derailment in complex disorders such as autism.

SYM-134

Contextual Modulation of Responses to Social Vocalizations in the Bat and Mouse Amygdala

Jasmine Grimsley; Jeffrey Wenstrup
Northeast Ohio Medical University (NEOMED)

Human and animal vocal communication requires the recognition and interpretation of the meaning of sounds. The listener must evaluate the contextual cues surrounding the vocalization to accurately interpret its valence. The brain evaluates context with reference to preceding sounds, information from other sensory modalities, and internal state based on neural and hormonal signals. One of the primary structures of the limbic system, the amygdala, is highly responsive to speech, or social vocalizations in animals. We postulated that amygdalar neurons may interpret information about social vocalizations with reference to specific contextual cues and internal states.

Behavioral paradigms were used to demonstrate that the social vocalizations of bats and mice carry contextual information from the caller to the listener. Complimentary electrophysiological studies in awake animals were conducted to investigate whether this contextual information is represented by amygdala neurons. These studies show that the amygdala encodes a broad range of contextual information pertaining to social vocalizations.

Bats emit different vocalizations in social interactions associated with low, medium, and high aggression and appeasement. Playbacks of these sounds have differential effects on the heart rate of the listener, indicating that they evoke different arousal states. Neurons within the amygdala of bats predominantly encode the valence of these vocalizations using a temporal code. In mice, females emit the same vocalization during mating and in response to fear. Although the female "caller" may be in some distress in both contexts, a male "listener" uses non-auditory cues to interpret the valence of this vocalization. Amygdala neurons of awake, free-moving male mice code for the valence of this vocalization in their spike discharge patterns. In restrained mice, the vocal repertoire and spectral characteristics of syllables are altered. Although it is well established that restraint causes stress in mice, most neural recordings from awake mice are conducted whilst the mouse is restrained for 2-3 hours over multiple days. We show that this restraint induces stress, and that neural responses (both LFP and single unit responses) to sound in the amygdala are amplified when animals are restrained.

Taken together, these studies provide evidence that the amygdala encodes both the external sensory context and internal state associated with the reception of social vocalizations.

PD-154

Ectopic expression of Emx2 inverts hair cell polarity in the mammalian maculae

Tao Jiang[1]; Doris Wu[2]
[1]NIDCD/NIH; University of Maryland, College Park; [2]NIDCD/NIH

Introduction

A unique feature that distinguishes the otolithic organs, maculae, from other sensory organs of the inner ear, is the presence of a line of polarity reversal (LPR), across which stereociliary bundles of hair cells are pointing in opposite directions to each other. For example, hair bundles point toward each other in the mouse utricle across the LPR, whereas they point away from each other in the saccule. Previously, it was reported that the LPR is absent in the maculae of *Emx2* knockout mouse embryos. Compared to hair bundles that point medially in the lateral extrastriolar region of the wildtype utricle, stereocilia orientation in this region of the mutant is reversed pointing toward the lateral edge of the macula. However, hair bundles in the striolar and medial extrastriolar region do not appear to be affected, pointing toward the lateral edge similar to the wildtype. To address the role of Emx2 in establishing hair bundle orientation, we generated a mouse model in which ectopic *Emx2* expression in the sensory organ can be spatially and temporally regulated.

Methods

We generated a transgenic mouse strain,*Rosa*$^{Emx2\text{-}GFP}$ (Rosa-lox-STOP-lox-Emx2-*t2A-GFP* and crossed this strain to *Sox2*^{CreER} mice to ectopically express *Emx2* in the prosensory domains of the developing inner ear.

Results

Sox2^{CreER}*; Rosa*$^{Emx2\text{-}GFP}$ utricles at embryonic day (E) 18.5 that received tamoxifen at E12.5 and E13.5, showed stereociliary bundle reversal in the medial region of the macula where *Emx2* is not normally expressed. Ectopic *Emx2* also affected the otoconia formation and expression of striolar-specific markers, oncomodulin, suggesting that the identity of the medial utricular region is compromised. Similar results were observed in the saccule. Stereociliary bundle orientation was reversed in the peripheral region of the mutant saccule where *Emx2* is not normally expressed.

Conclusion

Our results suggest that ectopic expression of *Emx2* in the maculae is sufficient to change the regional identity of the maculae and reverse the orientation of the stereociliary bundles located within. Future studies will focus on whether *Emx2* is sufficient to invert hair bundle polarity in a cell autonomous fashion.

PD-155

Temporal Manipulation of the Wnt Pathway Influences Radial Patterning in the Developing Mouse Cochlea

Vidhya Munnamalai; Donna Fekete
Purdue University

There is growing interest in Wnts for their potential to regenerate sensory cells in a damaged cochlea. These regeneration studies will be informed by a better understanding of how Wnt-mediated gene regulatory networks function during cochlear development. By activating the Wnt pathway using the GSK-3 inhibitor, CHIR99021 (CHIR) in a temporal manner, we can tease apart the immediate Wnt target genes from the secondary genes involved in other signaling pathways, as well as identify potential feedback and feed forward loops.

We temporally manipulated the pathway *in vitro* in E12.5 murine cochleas by adding CHIR on different days and analyzed effects on cell fate and patterning after the 6th day. The drug was washed out the following day and replaced with DMSO control media. For all other days, cochleas were kept in DMSO control media. Cochleas were immunolabeled for Sox2, Prox1 and Myo6 to monitor the status of sensory formation. We performed RT-qPCR and in-situ hybridization (ISH) to assess changes in gene expression levels and expression patterns.

Profoundly different phenotypes are observed based on the timing of Wnt activation. CHIR treatment on day 1 of the 6-day culture paradigm generates an organ of Corti composed of only the medial domain, with little or no hair cell formation. Day 2 treatment leads to a drastic increase in inner hair cells (IHCs) along with a medial expansion of Sox2. In these earlier time points, some medial genes (e.g., Jagged1) were up-regulated and/or expanded while lateral genes (e.g., Bmp4) were down-regulated when evaluated 6 hours after CHIR treatment by RT-qPCR or ISH. Day 4 treatment decreased outer hair cell (OHC) differentiation, while the underlying Prox1-expressing supporting cells were unchanged. Day 6 treatment triggers a modest increase in OHCs that apparently transdifferentiate from supporting cells.

The observed changes in the appearance and size of sensory subdomains upon Wnt activation hint at the different genes important in the specification of various cell types or domains. Our data suggest that precise Wnts signaling activity regulates the specification and size of the medial (IHC) domain before it influences the lateral (OHC) domain. In conclusion, as prenatal cochlear development progresses, the downstream response to Wnts is changing and this serves to pattern the radial axis.

PD-156

Live Imaging of Convergence and Extension and Dynamic Cellular Activity in the Developing Mammalian Cochlea

Elizabeth Driver; Zoë Mann; Matthew Kelley
National Institute on Deafness and Other Communication Disorders, NIH

The mammalian organ of Corti (OC) consists of a mosaic of highly ordered rows of mechanosensory hair cells (HCs) and several types of supporting cells (SCs), which extends along the length of the cochlea. The proper formation of this mosaic of cells is critical for auditory function. In early cochlear development, the domain of cells of the prospective OC is much shorter and broader than is found in the mature OC. As the cochlea grows, the OC becomes longer and narrower. This type of cellular rearrangement has been observed in many developmental contexts, and is often achieved via the process of convergent extension (CE). Cellular rearrangements in the cochlear duct are also thought to occur through CE, but the actual movement of cells within the embryonic cochlear epithelium has never been directly observed. Using mouse cochlear explant cultures with individual fluorescently labeled cells, we have visualized the movement of cells within the developing epithelium *in vitro*. Time-lapse videos generated at various times between embryonic day 14 and birth show movements of cells that are consistent with CE. Both migrating HCs and SCs exhibit protrusive activity, suggesting that this movement is an active process, but the activity of SCs is much more dynamic, indicating that SCs may provide the driving force in the rearrangement of OC cells. Moreover, as presumptive HCs continue to differentiate, they become rounder and detach from the basement membrane, while SCs continue to send out cellular extensions along the basement membrane. Observation of cell movements over several days indicate that most convergent cell migration occurs prior to embryonic day 16, but that extension continues until at least the equivalent of post-natal day 1. Epithelial cell migration occurs whether explants are established together with their underlying cochlear mesenchyme or directly onto an artificial substrate, demonstrating that the signals and mechanisms for migration are intrinsic to the epithelium. Both the protrusive activity of OC cells and their migration are dependent on non-muscle Myosin II, as inhibiting its activity causes cells to retract cellular extensions and to stop moving. This study is the first to visualize the migration of living cells within the developing cochlea and indicates that active cell movements are necessary for cochlear development and patterning.

PD-157

β-Catenin Controls Sensory Progenitor Proliferation and Differentiation in the Developing Inner Ear

Fuxin Shi[1]; Lingxiang Hu[2]; Bonnie Jacques[3]; Joanna Mulvaney[4]; Alain Dabdoub[4]; Albert Edge[5]
[1]Massachusetts Eye and Ear/Harvard Medical School; [2]Xinhua Hospital/ Shanghai Jiaotong University School of Medicine; [3]University of California San Diego; [4]University of Toronto; [5]Massachusetts Eye and Ear Infirmary, Harvard Medical School

Introduction

Differentiation and patterning of cochlear hair cells occurs in a precise order. Although the differentiation of hair cells requires *Atoh1*, the upstream signals that initiate *Atoh1* expression remain obscure. Wnt signaling was suggested to play a role, because *Atoh1* is a direct target of the Wnt pathway. More importantly, *Lgr5*, a protein that both potentiates and is regulated by Wnt activity, is expressed in the prosensory cells of the developing sensory epithelium and in supporting cells that differentiate into hair cells after postnatal stimulation of Wnt. In this study, we investigated the role of canonical Wnt pathway mediator, *β-catenin*, in hair cell differentiation in the cochlea.

Methods

We assessed the role of *Wnt/β-catenin* in gain- and loss-of-function models in mice during establishment of sensory progenitor cells and differentiation of hair cells between E12.5 and P0. *β-catenin*$^{flox(exon2-6)}$ and *β-catenin*$^{flox(exon3)}$ mutant mice were crossed to Cre mice to create conditional double-mutants that would overexpress or delete *b-catenin* in all cells *(CMV-CreER)*, sensory progenitors *(Sox2-CreER)*, or hair cells (*GFi1-Cre)*. Cre-induced deletion of exons 2– 6 of *β-catenin* results in a *β-catenin*-null allele, and deletion of *β-catenin:exon3*, containing sites that signal for degradation, increases β-catenin levels. Cre activity was induced by administration of tamoxifen.

Results

β-catenin expression changes induced by Cre became evident 24 – 48 h after tamoxifen. Cochleae with *β-catenin* deletion initiated at E11.5 had no apparent change in number of Sox2-positive progenitors but did not contain Atoh1-expressing hair cells when examined at E14.5. Fewer inner hair cells and no outer hair cells developed in *β-catenin* knockout mutants initiated in sensory progenitors at E12.5 and examined at E15.5 or at E18.5. Inner pillar cells were absent in these ears, and no expression of pillar cell markers, Prox1 and p75. However, cochlear structure was unaffected after conditional deletion of *β-catenin* in cochlear hair cells; cochlear function (ABR and DPOAE) was also normal. Overexpression of β-catenin at E12.5 resulted in a wider sensory epithelium in the mid-basal region, with a lack of elongation along the cochlear axis. When overexpression was initiated one day later (E13.5), the sensory epithelium continued to extend toward the apex. Activation of Wnt decreased the expression of adhesion molecule, E-cadherin. Application of R-spondin1 to

E13.5 cochlear explants resulted in an increase in the number of inner and outer hair cells.

Conclusions
Our data demonstrate that β-catenin controls sensory progenitor division and hair cell differentiation in the developing inner ear.

PD-158

Notch Signaling Plays an Instructive Role in Supporting Cell Development and is Critical for Supporting Cell Survival

Dean Campbell; Angelika Doetzlhofer
Johns Hopkins University School of Medicine

The sensory epithelium of the cochlea is a specialized structure responsible for the perception of sound. While much is understood about the development of the mechanosensory hair cells found within this epithelium, little is known about the development of the glial-like supporting cells. The Notch signaling pathway has already been shown to be important in cochlear differentiation by limiting a subset of sensory progenitor cells from adopting a hair cell fate; however, here we hypothesize that the Notch signaling pathway actively promotes a supporting cell fate by regulating additional genes that are indispensable for proper supporting cell development. Transcriptional profiling of organotypic cultures in which Notch signaling was acutely inhibited, identified over 50 novel Notch-regulated genes within the differentiating cochlea. Based on the diverse function of these genes we reason that Notch signaling controls differentiation, homeostasis and survival of supporting cells. Canonical Notch signaling activates target gene expression through the Rbp-j/ Mastermind-like1 transcriptional complex. We used two genetic strategies to evaluate the consequences of disrupting canonical Notch signaling. The first strategy was to overexpress the dominant negative mastermind like 1 (DNMAML1) transgene, which resulted in a Notch hypomorph. Although some ectopic hair cells are produced, supporting cells are largely retained in this mutant. Expression levels of the novel Notch-regulated genes are greatly reduced in this hypomorph mutant, thus validating their Notch regulation. Furthermore, examination of sequential early postnatal stages within this mutant revealed that outer supporting cells slowly degenerate. The second strategy we used was conditional deletion of Rbp-j to completely disrupt canonical Notch signaling during supporting cell differentiation. This mutant model did not show any ectopic hair cells but showed rapid degeneration of supporting cells, indicating that Notch signaling is required for supporting cell survival. Overall our study indicates that Notch signaling instructively regulates supporting cell development. We show that reduced or complete loss of Notch signaling results in supporting cell degeneration, thus demonstrating that Notch signaling is indispensable for supporting cell survival.

PD-159

Investigation and Modeling of Otic Sensory Lineage Development with Fbxo2 Reporter Mice and Stem Cell Lines

Byron Hartman[1]; Stefan Heller[2]
[1]Stanford University School of Medicine; [2]Stanford University School of Medicine, Department of Otolaryngology - Head and Neck Surgery

The otic lineage harbors unique progenitors that give rise to neural, sensory, and non-sensory populations. Beginning early in development, unique transcriptional and structural features distinguish this lineage from the myriad other fates of embryogenesis. We aim to better understand how transcriptional states and cellular identities specific to otic sensory development are initiated and maintained. Two complementary model systems, mouse embryo and directed stem cell differentiation, offer approaches to investigate and manipulate the otic sensory lineage.

Here we investigate developmental mechanisms and transcriptional regulation in the lineage of the highly otic-specific gene *Fbxo2*, which encodes F-box 2 (Fbx2), a ubiquitin ligase subunit required for cochlear homeostasis. Previous studies have shown that Fbx2 is robustly and specifically expressed in the otic sensory lineage from early otic vesicle cells to mature hair cells and supporting cells, and that lack of *Fbxo2* results in cochlear degeneration. These results suggest that *Fbxo2* activation is a specific transcriptional feature of the otic sensory lineage and dedicated machinery for early and ongoing protein quality control is essential for inner ear function.

We aim to characterize, isolate, and propagate otic progenitors based on *Fbxo2* expression in order to study mechanisms of otic lineage development. Thus we have engineered mouse and stem cell lines with a multifunctional tricistronic reporter cassette targeted to the *Fbxo2* locus. The *Fbxo2-VenusHC* reporter expresses H2BVenus (a bright nuclear YFP), a hygromycin resistance gene (for drug selection of *Fbxo2* expressing cells), and CreERt2 for lineage tracing. Current experiments include characterization of Venus as a reporter for *Fbxo2*, tracing the *Fbxo2* lineage with tamoxifen injections and propagation of otic progenitors from embryos and stem cells. We seek to enable a stem cell model of otic sensory development using *Fbxo2-VenusHC* for lineage reporting/selection coupled with experimental manipulations in signaling pathways and transcription factor expression to test developmental hypotheses. We are also using *Fbxo2-VenusHC* fibroblasts to access the potential for transcription factor based reprogramming approach to convert non-otic cells to an otic sensory fate.

Another set of experiments seeks to identify mechanisms regulating *Fbxo2* expression in the otic sensory lineage. Phylogenetic and transcription factor binding site analyses suggest that one or more cis-regulatory modules may regulate *Fbxo2* by integrating activity of multiple transcription factors. We have generated transgenic mice with the tdTomato reporter gene under the control of several candidate regulatory

elements and are now closer to identifying the minimal elements required to recapitulate *Fbxo2* expression.

PD-160

Induced Neurod1 Misexpression Provides Novel Insights into Progression of Inner Ear Neurosensory Specification

Ning Pan; Israt Jahan; Jennifer Kersigo; Bernd Fritzsch
University of Iowa

Introduction

Mammalian inner ear neurosensory precursor cells undergo highly regulated proliferation and differentiation to develop neurons and hair cells. Three proneural basic helix-loop-helix (bHLH) transcription factors (Atoh1, Neurod1 and Neurog1) play crucial roles in these processes. Early studies of loss-of-function (LOF) mutant mice suggested a simple scheme of Neurog1 driving neuronal development and Atoh1 driving hair cell development. However, more detailed studies have demonstrated extensive cross-regulations among the three bHLH genes, which form part of a complex gene regulatory network that controls the neurosensory cell fate determination. In particular, Neurod1 inhibits both Atoh1 and Neurog1 through negative feedback loops and appears to play a central role in the regulatory network.

Methods

To further elucidate the functions of Neurod1, we generated an inducible Neurod1 misexpression mouse model to evaluate the effects of 'gain-of-function (GOF)' mutations in the ear. We used three different Cre lines (Atoh1-Cre, Foxg1^{Cre}, and Pax2-Cre) to drive Neurod1 misexpression in different populations of neurosensory precursors and characterized the effects on the ear development.

Results

When induced by Atoh1-Cre in differentiating hair cell precursors that have exited the cell cycle, Neurod1 misexpression has little consequences and the ear neurosensory development appears normal. In contrast, when Neurod1 is misexpressed in Foxg1^{Cre}-expressing presumptive otic vesicles, inner ear formation seems to be completely disrupted, indicating that the precursors at this early stage are unable to respond to Neurod1 with differentiation. A slightly later misexpression of Neurod1 using Pax2-cre results in various alterations in neurosensory development, including shortening of the cochlea, loss of horizontal canal crista, greatly diminished neurons, reduced hair cells, and complete loss of hair cells in the base of the cochlea. Most surprisingly, ectopic hair cells form in the ganglia of Neurod1 misexpression mutants, which is similar to the Neurod1 LOF phenotype (Jahan et al., 2010). This seemingly contradictory result suggests that the spatiotemporal expression of Neurod1 plays important roles in the complex interplay that defines ear neurosensory specification.

Conclusions

Our results show that the altered Neurod1 expression in these novel GOF mouse mutants affects neurosensory cell fate commitment differently. We propose that Neurod1 acts to drive differentiation at whichever state of decision making a cell is in. Therefore, the state of decision making ultimately determines the outcome elicited by Neurod1. These data provide novel insights into molecular mechanism underlying cell fate determination of the neurosensory precursors in the inner ear.

PD-161

Activated Caspase-3 in the Developing Chick Auditory Brainstem

Sarah Rotschafer; Michelle Allen-Sharpley; Jamiela Kokash; Karina Cramer
University of California, Irvine

Caspases are a group of cysteine proteases that are sequentially activated during apoptosis. Caspase-3 is an essential effector caspase and is necessary for programmed cell death during normal brain development. To test for the presence of caspase-3 within the developing auditory system, we stained for activated caspase-3 in embryonic day (E) 6, 7, 9, 10, 11, 12, and 13 chicks. At the earliest days of development tested (E6 and E7), we detected activated caspase-3 expression along the dorsolateral aspect of the VIIIth cranial nerve near the nerve entry point. Centrally, expression was seen in the VIIIth nerve projection regions toward auditory brainstem nuclei. By E9, activated caspase-3 expression was found in fibers emanating from n. magnocellularis (NM) directed toward n. laminaris (NL). NL is composed of well-defined glial, neuropil, dendritic, and neuronal layers. At E10-13 expression was evident in the neuropil surrounding the layer of NL cells. To test whether caspase-3 activation is necessary for auditory brainstem development, we cultured developing chick embryos *ex ovo* and injected them in the fourth ventricle daily from E6 to E9 with either 50 µg/mL Z-DEVD-FMK in 1xPBS (a caspase-3 inhibiting compound; n = 30), vehicle in 1xPBS (control condition; n = 17), or 1xPBS (sham condition; n = 11). We then assessed auditory brainstem morphology and neural connections. Brains were collected at E10 and injected at the midline with rhodamine dextran amine to assess axonal targeting of crossed NM fibers. Brain sections were stained with bisbenzamide to examine the distribution of cells within NL. The portion of NL that showed clear lamination was calculated as a percentage of the total nucleus length. We compared Z-DEVD-FMK, control, and sham groups. When caspase-3 activity was inhibited in developing chick brains, NL lamination was significantly reduced. However, despite expression of activated caspase-3 in axons at the time projections form, inhibition of caspase-3 did not seem to impair overall axonal targeting toward NL. Caspase-3 is expressed along the auditory pathway during the early stages of auditory brainstem development, and loss of caspase-3 function disrupts the formation of the NL. Disorganization within the NL may result from excess neurons and glia and/or from a loss of signaling that generates boundaries around this nucleus.

PD-146

Functional Interactions and Co-localization of Prestin (Slc26a5) and Slc26a6 in Outer Hair Cells

Xiao-Dong Zhang; Wei Chun Chen; Choong-Ryoul Sihn; Jeong-Han Lee; Hannah Ledford; Yi-Nuo Zhang; Valeriy Timofeyev; Padmini Sirish; Nipavan Chiamvimonvat; **Ebenezer Yamoah**
University of California, Davis

The mammalian hearing organ has exquisite sensitivity and frequency selectivity which surpasses any sensory system in the body. An important technical quality of outer hair cells (OHCs) is their high-gain mechanical amplification of sound. The key molecule involved in this amplification is prestin (or slc26a5), a molecular motor protein expressed almost exclusively in the OHCs of the cochlea. Prestin is a direct voltage-to-force converter and mediates the membrane potential–dependent OHC length changes termed electromotility. As a result, sound-evoked responses are amplified in the inner ear to generate acoustic emissions. Indeed, dysfunction of prestin results in hearing loss in both human and mouse models. Prestin belongs to slc26 solute carrier gene family with diverse functions. Prestin is distinct in this family because of its molecular motor function in contrast to the anion transport functions of other family members. Recent studies suggested that slc26 proteins may form dimers or tetramers by homo-oligomerization. Based on the sequence and structural similarity as well as the expression pattern of slc26 proteins in OHCs, we hypothesized that prestin may co-assemble or interact with slc26a6 to form heteromeric proteins or functional complex with distinct functions in OHCs. We used direct electrophysiological measurement to demonstrate that prestin is indeed, a weak anion transporter compared with a member of its family, slc26a6. Moreover, co-expression of prestin and slc26a6 generates membrane proteins with distinct anion exchanger functions and nonlinear capacitance properties. The voltage-dependence of the nonlinear capacitance of the new complex is shifted to more hyperpolarized potentials compared to prestin alone. Immunofluorescence confocal microscopy and qPCR analyses demonstrated that slca6a6 is highly expressed and co-localized with prestin in OHCs. Our results support that prestin interacts with slc26a6 in OHCs and the sensitivity of OHC motor not only depends on prestin but also on its interaction with slc26a6.

PD-147

Silent Synaptic Degeneration is a Hallmark of Progressive Hearing Loss

Jeong-Han Lee; Wenying Wang; Hyo Jeong Kim; Ebenezer Yamoah
University of California, Davis

Age-related hearing loss (AHL) is the most common sensory deficit in the human population. A substantial component of the etiology stems from sensory and/or non-sensory pathological changes in the cochlea. In contrast to previous reports that ascribe hair cell loss as the primary defect followed by secondary neuronal degeneration, we demonstrate that hair cell loss is preceded by latent neurite retraction at the hair cell-auditory neuron synapse, which was first observed in afferent inner hair cell synapse followed by type II neuronal cell body degeneration. Loss of postsynaptic densities was the inaugural event before any outward manifestation of hair bundle disarray and hair cell loss. Simultaneously, we have identified profound alterations in type I neuronal membrane properties, including reduction in input membrane resistance, prolonged action potential latency and decrease in excitability. The resting membrane potential of the aging type I neurons in the AHL model was significantly hyperpolarized, and analyses of the underlying membrane conductance showed a massive increase in K^+ currents. We propose that attempts to alleviate AHL should target primary “silent” neural degeneration as opposed to the long-held notion that it is secondary to hair cell loss.

PD-148

Radiant Energy at the Target of Cochlear Infrared Neural Stimulation (INS)

Xiaodong Tan[1]; Nan Xia[1]; Hunter Young[1]; Claus-Peter Richter[1]; Xianghui Xiao[2]; Claus-Peter Richter[1]
[1]Northwestern University; [2]Argonne National Laborotory

Introduction

Infrared Neural Stimulation (INS) has been successful in different brain structures with the merit of improved spatial selectivity when compared to electrical stimulation. This is potentially beneficial for clinical applications such as cochlear implantation, a neural prosthesis of which the bottleneck is the number of perceptual channels. Yet, controversy remains over the mechanism and the target structures for INS. We have previously shown the direct stimulation of spiral ganglion neurons (SGNs) with acoustic-on-light masking. In this study we provide more decisive evidence that the target of INS is SGNs rather than auditory hair cells. We also provide measurements of the radiant energy, radiant power, and radiant exposure at the target tissue that are effective for stimulation of the auditory neurons in guinea pigs.

Methods

A combination of custom-designed angle polished fibers and microCT imaging was used in this study. Flat and angle polished fibers were both inserted into scala tympani to deliver infrared light. The angle polished fiber allowed to change the orientation of the radiation beam by rotating the optical fiber, so that the laser could target different structures of the cochlea. INS-evoked compound action potentials (CAPs) and single unit responses in the central nucleus of inferior colliculus (ICC) were measured. At the conclusion of the experiments the angle polished fiber was cemented in the cochlea using dental acrylic. MicroCT scanning was performed afterwards and the beam path and the target structures were identified from 3D reconstruction.

Results

The radiant exposure required to evoke CAP or ICC responses was on average 17.2±13.9 or 14.1±8.1 mJ/cm^2, respectively. Changing the orientation of the optical beam resulted in a change of the evoked responses. Maximum response cor-

responded to an orientation of the beam towards the SGNs, whereas response diminished when the beam was directed away from the spiral ganglion. No ICC response was detected while the beam path was facing the hair cells even in normal hearing animals.

Conclusions

The results indicate that the response to INS is from direct stimulation of SGNs, but not hair cells. These results will be a critical guide for future applications of INS in auditory prosthesis.

PD-149

Scanning Electron Microscope Observations of the Decellularized Mouse and Human Cochlea

Peter Santi; Robair Aldaya; Sebahattin Cureoglu
University of Minnesota

Decellularized tissues have been used to investigate the extracellular matrix (ECM) in a number of different tissues and species. Decellularized matrix has also been used as a scaffold for tissue transplantation by the implantation and proliferation of stem cells within the matrix. Santi and Johnson (2013) recently described detergent decellularization of the inner ear in the mouse, rat, and human using scanning thin-sheet laser imaging microscopy (sTSLIM). The purpose of the present investigation is to examine the decellularized cochlea at higher resolution using scanning electron microscopy (SEM). Fresh, harvested cochleas were removed from mice and a human and processed for decellularization using two different detergent extraction methods and examined by SEM. Decellularization removed all of the cell components while preserving the bone and ECM. Cell removal allowed for detailed examination of the 3D geometry of the ECM. The spiral limbus appeared as columnar plates with notched apical projections. The internal sulcus surface appeared smooth and we interpreted this as the continuous sheet of type IV collagen of the basal lamina. This smooth sheet was interrupted holes of the habenula perforate and extended further laterally until a spirally directed line of septa-like structures was observed. These septa-like structures lie between Hensen and Boettcher cells. These novel structures were short and reduced in mice, but tall and extensive in the human. Further lateral in mice were large and small holes which housed the external sulcus cell root processes. We were unable to find these holes in the human. Attached at the apical and basal portion of the spiral ligament were profiles of the capillaries of the stria vascularis. These capillary nets appeared to be “floating” within the endolymphatic space since the cells surrounding them and attaching them to the spiral ligament were removed. The spiral ligament appeared to have a flat mat of fibrous material, which we assume, consists primarily of collagen type II. The spiral ganglion contained empty spheres that previously housed the spiral ganglion neuron cell bodies and tubes of basal lamina that surrounded their corresponding nerve fiber processes. Reissner’s membrane consisted of a smooth sheet of basal lamina. Examination of decellularized cochlear tissues not only allows for a better understanding the cochlear ECM and the recognition of a novel basilar membrane structure, but may also be a first step in producing an acellular ECM that could be used to direct stem cells toward an auditory lineage for tissue transplantation.

PD-150

Aminoglycoside Increases Permeability of Osseous Spiral Laminae of Cochlea by Interrupting MMPs balance

Deng-ke Li[1]; Jian-he Sun[2]; Wei Sun[3]; Li-dong Zhao[2]; Wei-wei Guo[2]; **Shi-ming Yang[4]**
[1]Chinese PLA Medical School, Chinese PLA General Hospital; [2]Department of Otolaryngology, Head & Neck Surgery, Institute of Otolaryngology,Chinese PLA Medical School, Chinese PLA General Hospital, Beijing 100853, China; [3]Department of Communicative Disorders & Sciences, Center for Hearing andDeafness, the State University of New York at Buffalo, Buffalo, New York 14214, United States; [4]gwent001

Survival and function of the spiral ganglion neurons (SGNs) in profound hearing loss individuals are critical for cochlea implant. Delivery of exogenous neurotrophic factors, genes and stem cells can enhance the residual SGNs. However, since SGNs are separated from the scala tympani (ST) by the osseous spiral laminaes (OSLs), delivery of small molecules and stem cells to the SGNs are inefficient. Previous studies have found small pores which allow small molecules migrate from the ST to the SGNs in the OSLs. However, details about these passages and how to enhance the passages for migration has not been studied. In this study we found that intercellular perforations of bone lining cells on OSLs become significant wider in amikacin treated cochlea. Intracochlear perfusion of Evans Blue in the amikacin treated cochlea showed significant increase of dye migration into the area of SGNs compared to the untreated cochlea. These results suggest that a passage may exist between the ST and the area of SGNs and permeability of the passage increase in amikacin treated cochlea. Since amikacin treatment can increase the expression of matrix metalloproteinases (MMPs), which cleave most components of the extracellular matrix, we speculate that MMPs may be mediated in the enlarged perforation of bone lining cells on OSLs. Indeed, we found that treatment of amikacin with oxytetracycline, an inhibitor of MMPs, significantly reduced the migration of Evans Blue to the SGNs. These results indicate that inhibition of MMPs can reduce the permeability of OSLs in amikacin treated cochlea. In conclusion, treatment of amikacin which increases MMPs can enhance the permeability between the ST and SGNs. Increase the permeability of bone lining cells on OSLs may be beneficial for small molecules and stem cells delivery to SGNs via the ST.

PD-151

Round Window Membrane Vibration May Increase the Effect of Intratympanic Dexamethasone Injection

Jin Young Seo; Jung Min Kim; In Seok Moon
Yonsei University College of Medicine

Objectives/Hypothesis

We investigated whether the round window membrane (RWM) vibration can facilitate dexamethasone perfusion via the RWM in patients with sudden hearing loss.

Study Design

Prospective study.

Methods

We first performed an in vitro study using a semipermeable membrane. In the subsequent in vivo study, 20 mice were randomized into two groups: an intratympanic dexamethasone injection (ITDI)-only group, and an ITDI with RWM vibration group. Concentration of dexamethasone was investigated using high performance liquid hromatography. Third, we performed a prospective clinical study. Fifty-five refractory sudden hearing loss patients were divided into two groups: those who received ITDI only (n536) and those who received ITDI with RWM vibration (n519). Final hearing assessments were conducted 2 months after salvage treatment.

Results

In the in vitro study, the concentration of dexamethasone increased with vibration time with the peak concentration observed at 3 minutes of vibration. In the in vivo study, ITDI with RWM vibration resulted in a significantly higher perilymph concentration of dexamethasone (7.686+/-3.13 mg/ml) than that in the ITDI-only group (2.666+/-1.73ug/ml). In a clinical setting, the overall improvement in hearing was similar between the two groups. However, when we compared the speech discrimination score between the two groups, we found that the relative discrimination gain in the ITDI with RWM vibration group (18.11623.54%) was higher than that in the ITDI-only group (7.00615.54%) (P50.042).

Conclusion

RWM vibration can enhance the effect of intratympanic dexamethasone injection and is a viable treatment option for sudden hearing loss.

PD-152

Glucocorticoids Stimulate Endolymphatic Water Reabsorption in Inner Ear Through Aquaporin 3 Regulation.

jerome nevoux[1]; Say Viengchareun[1]; Ingrid Lema[1]; Anne-Lise Lecoq[1]; Evelyne Ferrary[2]; Marc Lombès[1]
[1]Paris Sud University; [2]Paris Diderot University, Inserm U867

Introduction

Menière's disease is linked to an increase in endolymph volume, the so-called endolymphatic hydrops. Since dysregulation of water transport could account for the generation of this hydrops, we investigated the role of aquaporins (AQP), the water channel proteins assembled in tetramers to constitute a pore allowing transmembrane water transport, in endolymph homeostasis. Glucocorticoids that are frequently used to treat sudden deafness, and that are known to regulate water and electrolytes transport in human body, could be a therapeutic option in Menière's disease. The aim of the present study was to investigate the role of AQP3 in water transport into endolymph, and its regulation by glucocorticoids,

Methods

EC5v murine inner ear cell line that exhibits functional properties of vestibular dark cells, and primary cells culture of human utricule (harvested during vestibular schwanomma surgery) were used. AQP3 was localized in these cells and mouse inner ear tissues by confocal fluorescence and standard microscopy, respectively. The stimulatory effect of dexamethasone upon AQP3 expression was assessed in EC5v cells and *in vivo* in mice at the mRNA (RT-PCR), and protein (Western blot) levels. AQP3 promoter activity was analysed by a transient transfection of a plasmid construct in different cell types (EC5v, KC3AC1 and HEK293). Transepithelial water transport was studied by means of $^{3}H_2O$ in EC5v vestibular cells cultured on filters, treated or not with dexamethasone (10^{-7} M).

Results

The different AQP subtypes 1 to 9 were identified in inner ear mice by RT-PCR, but only AQP3, 6 and 7 were identified in EC5v cells. AQP3 was unambiguously detected in human utricle, and was expressed in both endolymph secretory structures of the mouse inner ear, and EC5v cells. We demonstrated that water reabsorption, from the apical (endolymphatic) to the basolateral (perilymphatic) compartments, was stimulated by dexamethasone in EC5v cells. This was accompanied by a glucocorticoid-dependent increase in AQP3 expression at both mRNA and protein level, presumably through glucocorticoid receptor-mediated AQP3 transcriptional activation.

Conclusions

We show for the first time that glucocorticoids enhance AQP3 expression in human inner ear, and stimulate endolymphatic water reabsorption. These findings should encourage further clinical trials evaluating glucocorticoids efficacy in Menière's disease.

PD-153

Transfecting Ability of Nano-hydroxyapatite in Inner Ear Can Be Enhanced via Surface Modification

Hong Sun; **Fengjun Wang**; Xuewen Wu
Central South University

Background

Hydroxyapatite nanoparticles (HAP) are known to have excellent biocompatibility, and have attracted increasing attention as new candidates of nonviral vectors for gene therapy. But there are still many obstacles on the application of hydroxyapatite as gene carriers. The key issue is to improve the dispersion stability of nano-hydroxyapatite and its ability of

both carrying gene and transfection. In this study, we synthesized and surface-modified a new kind of nano-hydroxyapatite, then investigated its transfection efficiency as well as its potential for gene therapy in inner ear.

Methods

Hydroxyapatite nanoparticles were made from $Ca(NO_3)_2 \cdot 4H_2O$ and $(NH_4)_2HPO_4$ through a hydrothermal process. PEG-PEI copolymers were synthesized by conjugating methoxy poly(ethylene glycol) (mPEG) to branched polyethylenimine (PEI). PEG-PEI-HAP/DNA/PEI-PEG and PEI-HAP/DNA/PEI-PEG colloid were prepared with different weight ratios of HAP and DNA via ultrasonic dispersion and mechanical stirring. Then we measured and compared the sizes, zeta potentials, DNA binding capacities and cytotoxicity of them. Finally we examined their transfection efficiency in HeLa and 293T cell lines as well as the cochleae of Sprague-Dawley rats.

Result

1. Naked HAP nanoparticles are short rods, with diameter and length ranging from 20-30nm and 50-80nm. Their zeta potentials are between -10mv-10mv. And it is common to find serious congregations in the prepared samples.

2. Either modified by PEI or PEI-PEG, the dispersion of HAP nanoparticles has been significantly enhanced, while the average zeta potential of them has been elevated up to more than 30mv and their sizes were the same as naked HAP.

3. Both PEI-HAP and PEG-PEI-HAP can bind DNA completely at a HAP/DNA ratio of 12.5, after adding PEG-PEI soultion,no obvious cytotoxicity was revealed in working concentrations (HAP was no more than 250ug/ml) of both of them by MTT (3-(4,5)-dimethylthiahiazo(-z-y1)-3,5-di-phenytetrazoliumromide) experiments.

4. Both PEG-PEI-HAP/DNA/PEI-PEG and PEI-HAP/DNA/PEI-PEG showed very high transfection efficiencies in cell line experiments of which nearly 50% of the Hela or 293T cells were transfected, And these efficiencies can be expected in cultured cochlea in which SGNs and supporting cells were also transfected, while PEI-HAP/DNA has little transfenction in these cells.

Conclusion

The application of an additional outer layer of PEG-PEI around the PEI-HAP/DNA or PEI-PEG/DNA can produce higher transfection rates with almost intact complete cell viability, these copolymers can be potential vectors for gene therapy of inner ear diseases.

PD-162

Inflammaging and Age-Related Hearing Loss

Carl Verschuur; Akosua Agyemang-Prempeh; Tracey Newman
University of Southampton (UK)

Introduction

Age-related hearing loss (ARHL) is a common condition that causes significant disability among the elderly. Inflammaging, a state of low-grade chronic inflammation associated with the aging immune system, has been shown to contribute to a number of age-related pathologies, including frailty, Alzheimer's disease and cardiovascular disease. We have previously shown an association between chronic inflammation and hearing level among two cohorts of elderly individuals, supporting the hypothesised link between inflammaging and ARHL. However, these studies were based on available data sets and did not allow an evaluation of longitudinal data or a more detailed characterisation of inflammatory status or hearing function over time. We present preliminary data from a new longitudinal study, the main aim of which was to determine the extent to which inflammatory status predicts hearing deterioration with age.

Method

60 individuals in the age range 65-75 underwent detailed testing of inflammatory markers and auditory function at three time points over three years. Auditory function testing included pure tone audiometry from 250-12000 Hz and both transient and distortion product oto-acoustic emissions. During the first year of the study, detailed characterisation of inflammatory profile over time was undertaken using inflammatory markers derived from monthly urine samples. General health and hearing history information was captured using a questionnaire.

Results

Among those in the age range 70-75, there was a significant association between white blood cell count and hearing level ($p < 0.05$) which was independent of age, noise exposure, hypertension and chronic disease. Using a cut-off value derived from previous research, subjects with higher white blood cell counts had an average hearing level that was approximately 4 dB worse than the hearing level among subjects with lower white blood cell counts. Only preliminary analysis of cross-sectional data was available at time of writing, but additional data will be presented to show detailed inflammatory profile information in relation to hearing.

Conclusions

Preliminary results from a new longitudinal study of inflammatory status and hearing among older adults provides further evidence of the association between inflammaging and ARHL, further to our recently published studies from analyses of existing data sets, and highlights the exciting possibility of modifying ARHL through pharmacological and lifestyle intervention directed at chronic inflammation.

PD-163

Are Age-related Changes in ITD Coding Due to Changes in the Binaural Opponent-channel Mechanism Associated with Down-regulation of Neural Inhibition?

Erol Ozmeral; David A Eddins; Ann Clock Eddins
University of South Florida

Introduction

Converging evidence indicates that binaural processing declines with age and is exacerbated by age-related hearing

loss. Research in young, normal-hearing mammals (including humans) indicates that interaural time difference (ITD) coding is governed by an opponent-channel (OC) mechanism rather than an internal delay line mechanism as has previously been thought. Under the OC model, the sensitivity to changes or shifts in ITD can be predicted based on the initial ITD and the direction and magnitude of the shift, where large, outward shifts are predicted to cause a greater neural response than small and/or inward shifts. Only recently have studies looked at potential changes in ITD coding with age. It is possible that age-related changes in ITD coding reflect changes in the OC mechanism, perhaps due to reduced neural inhibition or a more general reduction in temporal precision. The purpose of this study was to determine the effects of aging on the OC mechanism of ITD coding.

Method

Spatial tuning in the context of the OC model was investigated with electroencephalography (EEG) in normal hearing younger and older adults using a change-detection paradigm, where a single stimulus "trial" was defined by a long standard ITD stimulus immediately followed by a short deviant ITD stimulus. Stimuli were band-pass Gaussian noise (500-750 Hz) with standard and deviant ITDs at 0 μs, 250 μs and 500 μs (both left and right leading ITDs were tested). Magnitudes of cortical evoked responses (P1-N1-P2) elicited by the ITD change were analyzed with regard to degree of ITD shift, direction of shift (toward or away from midline), and listener group.

Results

Data and modeling work support an OC mechanism of ITD coding for both younger and older adults. Moreover, in older adults, smaller evoked responses at the P2 latency and reduced overall hemispheric asymmetries suggest a more limited temporal precision and a down-regulation of neural inhibition in ITD coding with age.

Discussion

The present study provides needed groundwork to understanding the nature of and mechanisms underlying age-related changes in ITD tuning. Complementary behavioral data from the same subjects are reported for correlation analyses. Future work will evaluate simultaneous behavioral and electrophysiological measures to investigate the factors responsible for auditory spatial processing deficits in older listeners and to identify potential diagnostic methods and remediation targets.

PD-164

Gene Expression Profiling of the Aging Mouse Cochlea by RNA-Seq

Anne Giersch[1]; Jun Shen[1]; Nahid Robertson[2]; Cynthia Morton[1]

[1]Brigham and Women's Hospital, Harvard Medical School; [2]Brigham and Women's Hospital

Background

Age-related hearing loss is the most common sensory deficit in the aging population. Its social impact will only become more pronounced as life expectancy continues to increase. Despite the discovery of many deafness genes, pathophysiology of progressive hearing impairment due to the normal aging process remains elusive. We have undertaken extensive gene expression profiling of the mouse cochlea with advancing age in order to characterize important pathways and molecular mechanisms of age-related hearing loss and to inform potential target selection for prevention and treatment.

Methods

We performed gene expression profiling of mouse cochlea by next-generation sequencing (RNA-Seq) using cochlear tissue from mouse strains with good hearing past one year of age (CBA/CaJ and C57BL/6J.CAST-Cdh23^{Ahl+}). Cochlear tissue was collected at discrete ages ranging from one week through late adulthood. Polyadenylated mRNAs were purified and fragmented and the derived cDNA samples were indexed, pooled, amplified and sequenced using an Illumina HiSeq. Biological replicates were used for all strains and time-points. Analyses of expression levels of all transcripts and of differential gene expression were performed.

Results

We have obtained gene expression profiles of the mouse cochlea at various ages by RNA-Seq. With total reads of at least 30 million, more than 16,000 genes were detected in each sample, and expression levels were highly reproducible. We detected significant systematic differences in gene expression profiles between C57BL/6J.CAST-Cdh23^{Ahl+} and CBA/CaJ strain backgrounds, regardless of age. Hundreds of genes show significant temporal changes in expression levels on both genetic backgrounds. This postnatal to adult cochlear gene expression dataset will be added to the publicly accessible Shared Harvard Inner Ear Database (SHIELD: https://shield.hms.harvard.edu).

Conclusions

We have surveyed gene expression in mammalian cochlea by RNA-Seq and have identified genes that show age-related differential expression. Systematic differences exist between different genetic backgrounds. Temporal gene expression profiles in the cochlea may suggest candidate targets for prevention and treatment of age-related hearing loss.

PD-165

Premature Age-related Hearing loss (ARHL) in Fus1 KO Mouse Model of Mitochondrial dysfunction

Alla Ivanova[1]; Alex Hewko[2]; Joseph Santos-Sacchi[1]; Lei Song[1]

[1]Yale University; [2]SUNY

Ample evidence exist linking oxidative stress/mitochondrial dysfunction with age-related neurodegenerative diseases and neurosensory hearing loss (ARHL). Yet, the molecular mechanisms of how oxidative stress and/or mitochondrial dysfunction lead to hearing loss during aging remain unclear, and currently there is no treatment for this age-related disorder.

We developed a mouse model of mitochondrial dysfunction via targeted inactivation of one of the mitochondrial proteins called Fus1/Tusc2 (Ivanova et al., 2007). Loss of Fus1 leads to increased mitochondrial ROS production along with insufficient activation of anti-oxidant defense resulting in systemic chronic oxidative stress (Uzhachenko et al., 2012; Yazlovitskaya et al., 2013). Among other mitochondrial pathologies we found decreased rate of calcium accumulation in mitochondria resulting in perturbed calcium signaling, compromised mitochondrial fusion, and low respiratory reserve (Uzhachenko et al., 2012; Uzhachenko et al., 2014). Applying this mouse model to age-related studies was substantiated by our *in silico* analysis that shows age-associated decrease of Fus1 expression in human tissues (unpublished).

We used this mouse model to investigate the impact of mitochondrial dysfunction/oxidative stress on ARHL. Using Auditory Brainstem Response (ABR) test we showed that hearing in young (2 mo old) Fus1 KO mice was undistinguishable from WT mice. A slight but significant threshold elevation was detected in 4-6 mo old Fus1 KO mice. Noteworthy, at the age of 9-12 months Fus1 KO mice exhibited a profound hearing loss at all frequencies while WT mice showed only a minor hearing decline. Histopathological analysis showed no severe signs of auditory system degeneration in older Fus1 mice. However, using a specific macroglia/macrophage marker Iba-1 we identified increased numbers of infiltrated cochlea macrophages in the Fus1 KO mice indicating that oxidative stress/cytokine-induced damage may be the cause of Fus1 loss-mediated ARHL. Analysis of ABR latency interpeak intervals (IPI) also suggested that the pathology of ARHL in Fus1 KO mice is not limited to the inner ear but could also involve the auditory ascending pathway.

Based on the analysis of ABR in Fus1 KO mice and ample evidence of involvement of chronic systemic oxidative stress and age-related inflammatory changes in the pathogenesis of the auditory system, we suggest that premature age-related hearing loss in these mice is the result of mitochondrial dysfunction followed by oxidative stress and chronic inflammation. We also propose that preventive systemic alleviation of oxidative stress by ROS scavengers targeted to mitochondria will reduce oxidative stress and delay the onset of hearing loss.

PD-166

Age-Related Differences in Consonant Perception in Real and Simulated Cochlear-Implant Users

Casey Gaskins; Maureen Shader; Sandra Gordon-Salant; Samira Anderson; Matthew Goupell
University of Maryland, College Park

Introduction

Cochlear-implant (CI) users experience poor spectral resolution and rely mostly on temporal cues to understand speech. However, temporal processing slows with age. Previous studies have assessed the speech perception of CI users, but there are few studies explicitly investigating the effects of age on speech perception in older CI users, which was the purpose of this study.

Method

Twelve younger normal-hearing (YNH; 23.2±4.7 yrs), four older normal-hearing (ONH; 61.8±7.3 yrs), six younger cochlear-implant (YCI; 51.5±12.9 yrs), and six older cochlear-implant (OCI; 74±11.1 yrs) listeners were presented with the "Dish/Ditch" word pair. The closure duration of the silent interval between the fricative and the vowel of each word was varied on a seven-step continuum between 0 and 60 ms. Listeners were asked to identify whether the sound they heard was "Dish" or "Ditch." All listeners were presented with unprocessed speech. YNH and ONH listeners were also presented sine-vocoded speech, varying in spectral channel (N=1, 2, 4, 8, 16) and low-pass filter cutoff of the temporal envelope (f=50 or 400 Hz). Stimuli were presented monaurally at 75 dB(A) for NH listeners over an insert earphone or at a comfortably soft level using direct connect for CI listeners.

Results

Identification of the unprocessed endpoint stimuli, "Dish" and "Ditch", was highly accurate; however, the ONH listeners needed a significantly longer silent interval than the YNH listeners to perceive the word "Ditch." The YCI and OCI listeners performed similarly to the YNH listeners. For the vocoded conditions, there was no difference in performance for unprocessed and vocoded stimuli with eight or more vocoder channels. Four vocoder channels resulted in fewer "Ditch" responses, particularly when the envelope was low-pass filtered at 50 Hz. Compared to the YNH listeners, the ONH listeners had a reduced ability to hear the word "Ditch" when fewer than four channels with a low-pass filter cutoff at 400 Hz.

Conclusions

This study supports previous evidence showing that age-related differences in consonant perception occur when NH listeners rely on temporal cues. Although CI listeners only use temporal cues to discriminate between consonants, the effects of age are not as apparent. From the vocoder conditions, the age-related temporal processing differences between groups are more evident when there are four or fewer channels. Therefore, the vocoder conditions may partially explain why there were no age-related differences in the CI listeners, because CI listeners typically have more than four perceptual channels.

PD-167

Evidence of a New Class of Age-Related Hearing Disorders Defined by Deficits in Temporal Processing

Jianxin Bao[1]; Hui Li[1]; Kyle Nakamoto[1]; Mike Hewit[1]; Megan Kobel[1]; Brent Spehar[1]; Nancy Tye-Murray[2]
[1]NEOMED; [2]Washington University in St. Louis

Background

Age-related hearing loss (presbycusis) is the most common neurodegenerative disease, afflicting nearly half of the population over 75 years of age. Based on the assumption that

presbycusis is caused by peripheral hearing loss, current treatment options, which only a fraction of older adults with presbycusis receive, are primarily limited to hearing aids and cochlear implants, which often fail to restore optimal auditory function. It is currently controversial whether age-related central auditory deficits can occur independently from peripheral age-related hearing loss. This issue has important implications for the following two main reasons: (1) If it exists, it would suggest urgent clinical needs for developing specific auditory screening tests, new auditory rehabilitation, and new guidelines to treat this disorder,; (2) For basic research, it would lead to a new focus for genetic and regenerative medicine studies.

Method

Participants consisted of a total of 863 individuals from two cohorts (recruited from 1997 to 2013): 101 participants from the St. Louis area and 762 participants from the Rochester, New York greater metropolitan area, all of whom provided informed consent for their inclusion in the study. The hearing ability of each subject was measured by a battery of auditory tests: pure tone audiogram, supra-threshold gap detection, speech recognition thresholds and Hearing in Noise Test. For the St. Louis cohort, participants completed additional lip reading tests. Factor analysis and mixed effects regressions were used to identify the statistical relationships among these measures.

Results

Strong evidence for age-related temporal processing deficits, which occur independent of peripheral hearing loss, was seen by focusing on gap detection in elderly with “golden ears” (e.g. elderly who have do not have clinically defined hearing loss on their pure tone audiograms). Vision and memory function were also monitored by lip reading tests to determine the possible influence of cognitive function. We found temporal deficits in elderly participants with normal audiograms, which is a strong indication of an independent aging processes for peripheral and central presbycusis.

Conclusion

Our results revealed a subclass of elderly individuals who have age-related temporal processing deficits, despite having clinically normal peripheral hearing. The presence of this subclass deserves more clinical and basic research in the future.

PD-168

Cochlear Hair Cells Depend on Innervation for Long Term Viability

Jennifer Kersigo; **Bernd Fritzsch**
University of Iowa

Hair cells are essential for hearing and orientation in space. Age related hearing decline correlates with loss of neurosensory elements and similar changes occur in the aging vestibular system. Genetic predisposition and environment combine to trigger such decline. Why individual hair cells may survive remains unclear. Age related neuronal loss is mediated through intercellular interactions through trophic support changes that can affect one cell sparing the neighbor. Hair cells can develop independently of any innervation in mice that never form any sensory neurons (Ma et al., JARO 1:129; 2000). Likewise, multiple lines of evidence seem to support that hair cells do not require innervation for hair cell viability. However, on closer examination, these claims are difficult to interpret based on the data. For example, in Walsh et al (J Neurosci 18:38591998) loss of efferents caused ‘minimal hair cell loss’ (abstract) but a ‘significant lesions of all three OHC’s rows in some animals (p3862)’ was also found. In contrast, a recent paper cutting the efferent bundle reports no loss of OHCs but a functional decline of OHCs (Liberman et al., J Neurosci 34: 4599; 2014). In another paper, Sugawara et al., (JARO 6: 136; 2005), the auditory nerve was cut unilateral with postoperative survival times ranging from 45-413 days. This paper found loss of hair cells in one case, but claimed no HC loss in several other cases with variable degree of remaining innervation. Nevertheless, some of the data show variable loss of OHC and IHCs. Obviously, surgically eliminating innervation in postnatal animals may not result in the desired complete loss of all afferent and efferent innervation in time to probe for their effects on HC survival. Moreover, hair cell viability effects of innervation may be restricted to a critical phase comparable to the critical phase of afferent input on viability of cochlear nucleus neurons and neurotrophin effects on afferents (Rubel and Fritzsch, Ann Rev Neurosci, 25:51; 2002). To sidestep these potential technical and conceptual problems we generated mice with targeted deletions of both neurotrophins using Pax2-cre and loxP flanked BDNF and NT3. BDNF and NT3 are essential to support all afferent innervation in the embryonic ear (Yang et al., Her Res 278: 21; 2011). We show a progressive lossof all OHC and most IHC within a few months after complete perinatal denervation. Minor residual innervation results in a progressive loss of OHCs followed by IHCs after 8-10 months.

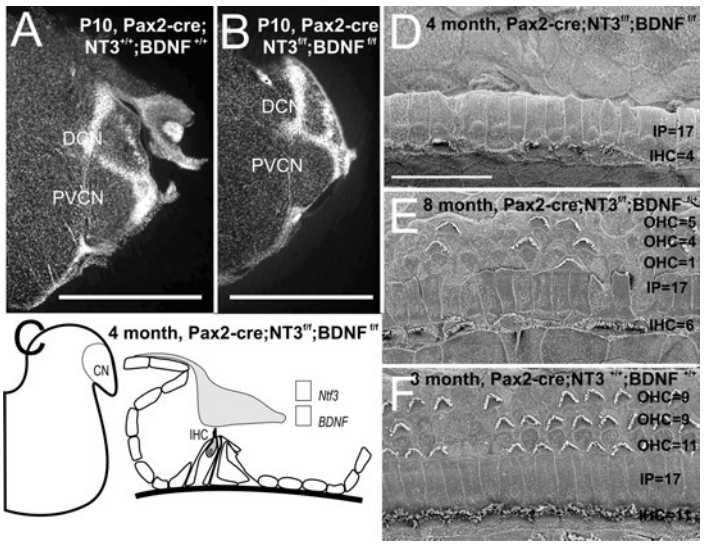

Author Index

BALTIMORE MARRIOTT WATERFRONT
700 Aliceanna Street
Baltimore, Maryland 21202
Phone: 410.385.3000
BaltimoreMarriottWaterfront.com

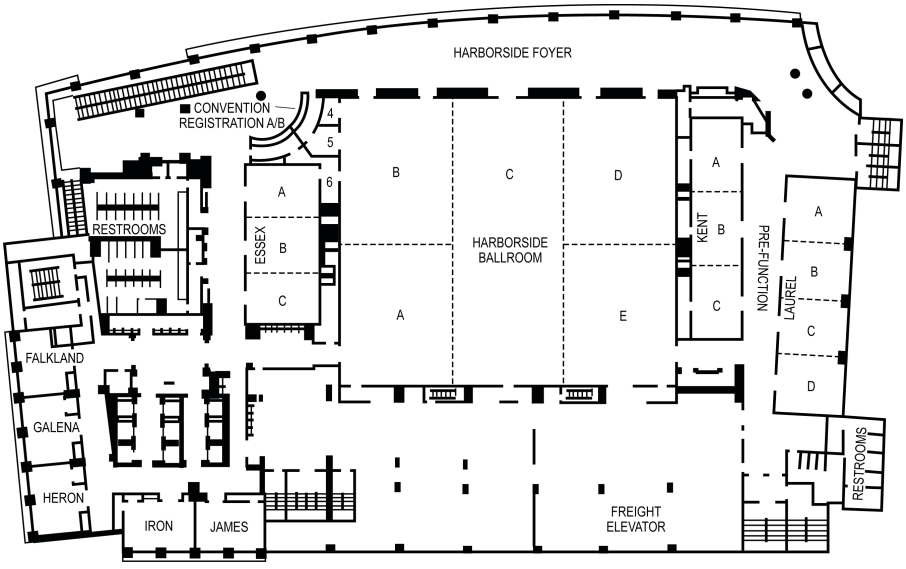

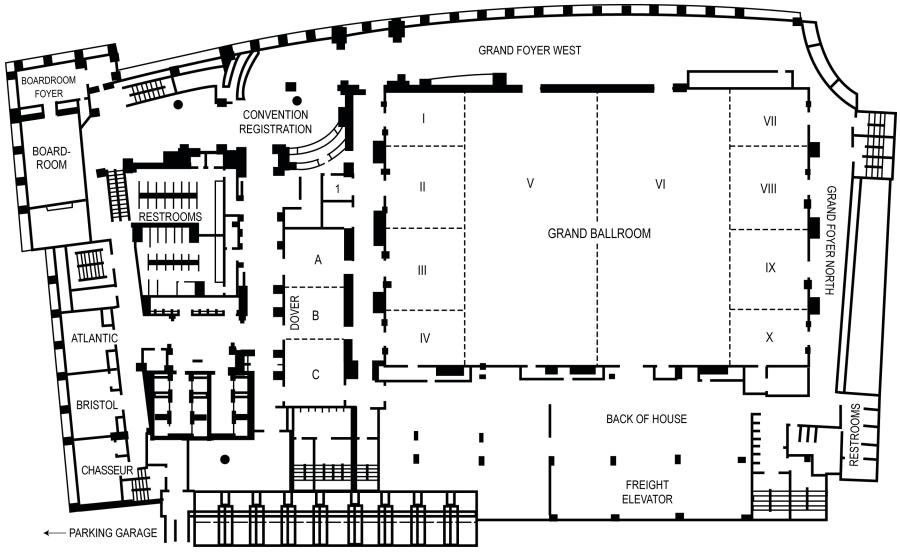

SAVE THE DATES

February 20-24, 2016
39th Annual MidWinter Meeting
Manchester Grand Hyatt
San Diego, California, USA

February 11-15, 2017
40th Annual MidWinter Meeting
Baltimore Marriott Waterfront
Baltimore, Maryland, USA

February 10-14, 2018
41st Annual MidWinter Meeting
Manchester Grand Hyatt
San Diego, California, USA

February 9-13, 2019
42nd Annual MidWinter Meeting
Baltimore Marriott Waterfront
Baltimore, Maryland, USA

Association for Research in Otolaryngology
19 Mantua Road
Mt. Royal, NJ 08061
www.aro.org